

# **Selective C–H Activation by Ruthenium(II) Carboxylate and Nickelaelectro-Catalysis**

Dissertation

for the award of the degree

“Doctor rerum naturalium” (Dr.rer.nat.)

of the Georg-August-Universität Göttingen

within the doctoral program of chemistry

of the Georg-August-Universität School of Science (GAUSS)

Submitted by

Shoukun Zhang

From Puyang (China)



Göttingen, 2021





### **Thesis Committee**

Prof. Dr. Lutz Ackermann, Institute of Organic and Biomolecular Chemistry

Prof. Dr. Shoubhik Das, ORSY Division, Department of Chemistry, Universiteit Antwerpen, Antwerpen, Belgium.

### **Members of the Examination Board**

Reviewer: Prof. Dr. Lutz Ackermann, Institute of Organic and Biomolecular Chemistry, Göttingen

Second Reviewer: Prof. Dr. Shoubhik Das, ORSY Division, Department of Chemistry, Universiteit Antwerpen, Antwerpen, Belgium.

### **Further members of the Examination Board**

Prof. Dr. Manuel Alcarazo, Institute of Organic and Biomolecular Chemistry, Göttingen

Prof. Dr. Dietmar Stalke, Institute of Inorganic Chemistry, Göttingen

Jun.-Prof. Dr. Johannes C. L. Walker, Institute of Organic and Biomolecular Chemistry, Göttingen

Dr. Michael John, Institute of Organic and Biomolecular Chemistry, Göttingen

**Date of the Oral Examination:** 11.01.2021



## Contents

1. Introduction.....	1
1.1 Transition Metal-Catalyzed C–H Activation.....	1
1.2 Ruthenium-Catalyzed Selective C–H Activation.....	6
1.2.1 Ruthenium-Catalyzed <i>ortho</i> -C–H Activation.....	6
1.2.2 Ruthenium-Catalyzed Remote C–H Activation.....	10
1.3 Nickel-Catalyzed C–H Activation.....	14
1.3.1 Nickel-Catalyzed C–H Activation for C–C Formation.....	15
1.3.1.1 Nickel-Catalyzed C–H Arylation.....	15
1.3.1.2 Nickel-Catalyzed C–H Alkynylation.....	18
1.3.1.3 Nickel-Catalyzed C–H Alkylation.....	20
1.3.2 Nickel-Catalyzed C–H Amination.....	23
1.3.3 Nickel-Catalyzed C–H Alkoxylation.....	27
1.3.4 Nickel-Catalyzed C–H Phosphorylation.....	31
1.4 Oxidative C–H Activation by Metalla-Electrocatalysis.....	34
1.4.1 Pallada-Electrooxidative C–H Activation.....	34
1.4.2 Rhoda-Electrooxidative C–H Activation.....	37
1.4.3 Ruthena-Electrooxidative C–H Activation.....	39
1.4.4 Irida-Electrooxidative C–H Activation.....	40
1.4.5 Cobalta-Electrooxidative C–H Activation.....	41
1.4.6 Cupra-Electrooxidative C–H Activation.....	43
1.4.7 Ferra-Electrooxidative C–H Activation.....	44
1.4.8 Mangana-Electrooxidative C–H Activation.....	45
2. Objectives.....	46
3. Results and Discussion.....	49
3.1 Selective <i>ortho</i> -C–H Activation by Ruthenium Catalysis.....	49
3.1.1 Optimization and Scope.....	49
3.1.2 Removal of Silyl Group.....	50
3.1.3 Mechanistic Studies.....	51
3.1.4 Proposal Catalytic Cycle of <i>ortho</i> -C–H Alkynylation.....	52
3.2 Selective <i>meta</i> -C–H Activation by Ruthenium Catalysis.....	53
3.2.1 Optimization and Scope of Ruthenium-Catalyzed <i>meta</i> -C–H Mono- and Difluoromethylation.....	53
3.2.2 Optimization and Scope of <i>meta</i> -C–H Alkylation by Arene-Ligand-Free Ruthenium Catalysis.....	56
3.3 Nickela-Electrocatalyzed C–H Amination.....	59
3.3.1 Optimization Studies.....	59

3.3.2	Scope of Nickela-Electrocatalyzed C–H Amination .....	61
3.3.3	Mechanistic Studies .....	63
3.3.3.1	Competition Experiments .....	63
3.3.3.2	Experiments with Isotopically Labelled Solvent .....	64
3.3.3.3	Reaction Profile.....	64
3.3.3.4	KIE Studies .....	65
3.3.3.5	H <sub>2</sub> –Detection.....	66
3.3.3.6	Cyclic Voltammetry.....	66
3.3.4	Proposed Mechanism.....	67
3.4	Nickela-Electrocatalyzed C–H Alkoxylation with Secondary Alcohols.....	68
3.4.1	Optimization Studies.....	69
3.4.2	Testing of Secondary Alcohols Following Reported Methods.....	72
3.4.3	Scope of Nickela-Electrocatalyzed C–H Alkoxylation.....	74
3.4.4	Mechanistic Studies .....	77
3.4.4.1	Competition Experiments Between Distinct Arenes .....	77
3.4.4.2	Competition Experiments Between Different Nucleophiles .....	77
3.4.4.3	Experiments with Isotopically Labelled Solvent .....	78
3.4.4.4	KIE Studies .....	79
3.4.4.5	Headspace GC-Analysis.....	80
3.4.4.6	Radical Trapping Experiments .....	80
3.4.4.7	Switch On-Off experiments .....	81
3.4.4.8	Isolation and Characterization of Nickel(III) Intermediate .....	82
3.4.4.9	DFT Calculations .....	84
3.4.5	Proposed Mechanism.....	85
3.4.6	Removal of the Directing Group .....	86
3.5	Nickela-Electrocatalyzed C–H Phosphorylation .....	87
3.5.1	Optimization Studies.....	87
3.5.2	Scope of the Nickela-Electrocatalyzed C–H Phosphorylation.....	90
3.5.3	Mechanistic Studies .....	94
3.5.3.1	Competition Experiment Between Phosphite and Amine .....	94
3.5.3.2	Experiments with Isotopically Labelled Solvent .....	94
3.5.3.3	KIE Studies .....	95
3.5.3.4	Headspace GC-Analysis.....	95
3.5.3.5	Switch On-Off Experiments.....	96
3.5.3.6	Radical Trapping Experiment .....	96
3.5.3.7	Monitoring of the Electrocatalytic Reaction.....	97
3.5.3.8	DFT Calculations .....	99
3.5.3.9	Synthesis, Characterization, and Catalytic Performance of Nickel(II) and Nickel(III) .....	100

---

3.5.4 Proposed Mechanism.....	102
4. Summary and Outlook .....	104
5. Experimental Section .....	107
5.1 General Remarks .....	107
5.2 General Procedures.....	111
5.3 Experimental Procedures and Analytical Data.....	114
5.3.1 Ruthenium-Catalyzed <i>ortho</i> -C–H Alkynylation.....	114
5.3.1.1 Characterization Data.....	114
5.3.1.2 Radical Trapping Experiment .....	117
5.3.1.3 Removal of Silyl Group .....	117
5.3.2 Ruthenium-Catalyzed <i>meta</i> -C–H Mono- and Difluoromethylation .....	118
5.3.2.1 Characterization Data.....	118
5.3.2.2 Hydrolysis of Ethyl Ester <b>103</b> .....	123
5.3.3 Ruthenium-Catalyzed <i>meta</i> -C–H Alkylation.....	125
5.3.3.1 Characterization Data.....	125
5.3.4 Nickela-Electrocatalyzed C–H Amination .....	131
5.3.4.1 Characterization Data.....	131
5.3.4.2 Competition Experiment.....	144
5.3.4.3 Experiments with Isotopically Labelled Solvent .....	145
5.3.4.4 Reaction Profile.....	146
5.3.4.5 KIE studies .....	147
5.3.4.6 H <sub>2</sub> –Detection.....	148
5.3.4.7 Cyclic Voltammetry.....	149
5.3.5 Nickela-Electrocatalyzed C–H Alkoxylation .....	151
5.3.5.1 Characterization Data.....	151
5.3.5.2 Mechanistic Studies .....	180
5.3.5.3 Isolation and Characterization of Nickel(III) Intermediate .....	190
5.3.5.4 Gram-Scale Experiment.....	194
5.3.5.5 Traceless Removal of the Directing Group .....	195
5.3.5.6 Cyclic Voltammetry.....	197
5.3.5.7 Studies on the Potential Racemization of <b>107u</b> .....	199
5.3.6 Nickela-Electrocatalyzed C–H Phosphorylation .....	200
5.3.6.1 Characterization Data.....	200
5.3.6.2 Mechanistic Studies .....	223
5.3.6.3 (Electro)synthesis of Nickel(II) and Nickel(III) Complex.....	235
5.3.6.4 Catalytic and Stoichiometric Reaction Performance of <b>Ni<sup>III</sup>-M1</b> .....	239
5.3.6.5 Gram-Scale Experiment.....	242
5.3.6.6 Studies on the Potential Racemization of <b>110y</b> .....	242
5.3.6.7 Cyclic Voltammetry .....	244

## Contents

---

6. References .....	246
7. NMR Spectra.....	258
7.1 Ruthenium-Catalyzed <i>ortho</i> -C–H Alkynylation.....	258
7.2 Ruthenium-Catalyzed <i>meta</i> -C–H Mono- and Difluoromethylation .....	264
7.3 Ruthenium-Catalyzed <i>meta</i> -C–H Alkylation.....	281
7.4 Nickel-Electrocatalyzed C–H Amination.....	296
7.5 Nickel-Electrocatalyzed C–H Alkoxylation .....	320
7.6 Nickel-Electrocatalyzed C–H Phosphorylation .....	369
Acknowledgement.....	417
Curriculum Vitae.....	419

**List of Abbreviations**

Ac	acetyl
acac	acetyl acetate
Ad	1-Adamantane
Alk	alkyl
AMLA	ambiphilic metal-ligand activation
aq.	aqueous
Ar	aryl
atm	atmospheric pressure
BDMAE	bis(2-dimethylaminoethyl)ether
BHT	butylated hydroxytoluene
BIES	base-assisted internal electrophilic substitution
Bn	benzyl
Boc	<i>tert</i> -butyloxycarbonyl
bpy	2,2'-bipyridyl
BQ	1,4-benzoquinone
Bu	butyl
Bz	benzoyl
calc.	calculated
<i>cat.</i>	catalytic
CCE	constant current electrode
CMD	concerted-metalation-deprotonation
cod	1,5-cyclooctadiene
conv.	conversion
Cp	cyclopentadienyl
Cp*	1,2,3,4,5-pentamethylcyclopenta-1,3-diene
Cy	cyclohexyl
Cyp	cyclopent
$\delta$	chemical shift
d	doublet
DBN	1,5-diazabicyclo[4.3.0]non-5-ene
DBU	1,8-diazabicyclo[5.4.0]undec-7-ene
DCE	1,2-dichloroethane
DCIB	dichloro- <i>iso</i> -butane
dcype	1,2-bis-(dicyclohexylphosphino)ethane
dd	doublet of doublet

## List of Abbreviations

---

DFT	density functional theory
DG	directing group
DME	dimethoxyethane
DMA	<i>N,N</i> -dimethylacetamide
DMAP	4-dimethylaminopyridine
DMF	<i>N,N</i> -dimethylformamide
DMPU	1,3-dimethyltetrahydropyrimidin-2( <i>1H</i> )-one
dppbz	1,2-bis(diphenylphosphino)benzene
dppe	1,2-bis(diphenylphosphino)ethane
dppf	1,1'-bis(diphenylphosphino)ferrocene
dppp	1,3-bis(diphenylphosphino)propane
dt	doublet of triplet
D <i>t</i> BEDA	<i>N,N</i> -di- <i>tert</i> -butylethane-1,2-diamine
dtbpy	4,4'-di- <i>tert</i> -butyl-2,2'-bipyridine
EI	electron ionization
equiv	equivalent
ES	electrophilic substitution
ESI	electrospray ionization
Et	ethyl
Fc	Ferrocene
FG	functional group
g	gram
GC	gas chromatography
GVL	$\gamma$ -valerolactone
h	hour
Hal	halogen
Het	heteroatom
Hept	heptyl
Hex	hexyl
HFIP	1,1,1,3,3,3-hexafluoro-2-propanol
HPLC	high performance liquid chromatography
HR-MS	high resolution mass spectrometry
Hz	Hertz
<i>i</i>	<i>iso</i>
IPr•HCl	1,3-bis-(2,6-diisopropylphenyl) imidazolium chloride
IR	infrared spectroscopy
IES	internal electrophilic substitution



<i>J</i>	coupling constant
KIE	kinetic isotope effect
L	ligand
<i>m</i>	<i>meta</i>
m	multiplet
M	molar
[M] <sup>+</sup>	molecular ion peak
Me	methyl
Mes	mesityl
mg	milligram
MHz	megahertz
min	minute
mL	milliliter
mmol	millimole
M.p.	melting point
MQ	6-methylquinoline
Ms	Mesyl
MS	mass spectrometry
<i>m/z</i>	mass-to-charge ratio
NBA	nitrobenzoic acid
NBE	norbornene
NMO	<i>N</i> -methylmorpholine oxide
NMP	<i>N</i> -methylpyrrolidinone
NMR	nuclear magnetic resonance
n.r.	no reaction
<i>o</i>	<i>ortho</i>
OPV	oil pump vacuum
<i>p</i>	<i>para</i>
PAHs	<i>polycyclic aromatic hydrocarbons</i>
Ph	phenyl
Phen	1,10-phenanthroline
PIP	2-(pyridin-2-yl)- <i>iso</i> -propyl
Piv	pivaloyl
ppm	parts per million
Pr	propyl
Py	pyridyl
Pym	pyrimidine

## List of Abbreviations

---

PyO	2-aminopyridine 1-oxide
q	quartet
Q	quinoline
RT	room temperature
s	singlet
sat.	saturated
SCE	saturated calomel electrode
SPS	solvent purification system
<i>t</i>	<i>tert</i>
t	triplet
T	temperature
TBAA	tetrabutylammonium acetate
TBAB	tetrabutylammonium bromide
TBAI	tetrabutylammonium iodide
TBHP	<i>tert</i> -butyl hydroperoxide
TEMPO	2,2,6,6-Tetramethylpiperidine-1-oxyl
Tf	triflate
TFE	2,2,2-trifluoroethanol
THF	tetrahydrofuran
TIPS	triisopropylsilyl
TM	transition metal
TMA	tetramethylammonium
TMEDA	<i>N,N,N',N'</i> -tetramethylethane-1,2-diamine
TMG	tetramethylguanidine
TMS	trimethylsilyl
Ts	<i>para</i> -toluenesulfonyl
TS	transition state

## 1. Introduction

During the past century, tremendous progress has been achieved in the field of organic synthesis, with considerable contributions to pharmaceuticals, crop-protection agents, and functional materials, among others. Nevertheless, the influence of organic synthesis on the environment in terms of pollution, chemical waste, toxic reagents, etc. is non-negligible. Therefore, the application of novel, green and cost-effective protocols in organic chemistry emerged as a major goal for chemists. In 1988, the 12 principles of green chemistry were introduced by Anastas and Warner as a guideline to minimize the ecological footprint of synthetic transformations.<sup>[1]</sup> Moreover, the application of catalysis in organic chemistry without stoichiometric metals is important to increase the economic benefits and reduce waste formation.

### 1.1 Transition Metal-Catalyzed C–H Activation

Since the early contributions of chemists in the 1970s, transition metal-catalyzed cross-couplings,<sup>[2]</sup> as exemplified by the Nobel Prize in chemistry in 2010, have become one of the most powerful strategies for modern molecular synthesis.<sup>[3]</sup> Thus far, predominantly palladium-catalyzed cross-couplings, represented by Mizoroki–Heck,<sup>[4]</sup> Suzuki–Miyaura,<sup>[5]</sup> Migita–Stille,<sup>[6]</sup> Negishi,<sup>[7]</sup> Sonogashira–Hagihara,<sup>[8]</sup> and Hiyama–couplings,<sup>[9]</sup> have found widespread applications in pharmaceutical and agrochemical industries as well as polymer sciences for the construction of C–C bonds. Additionally, transition metal-catalyzed cross-couplings, such as Buchwald–Hartwig,<sup>[10]</sup> Ullmann–Goldberg,<sup>[11]</sup> and Chan–Evans–Lam-couplings,<sup>[12]</sup> were exploited for C–Het bond formations.

Despite indisputable achievements, cross-coupling reactions are associated with significant inherent drawbacks, such as the formation of stoichiometric amounts of metal waste. Besides the necessary prefunctionalized organic (pseudo)halides, organometallic coupling partners, e.g. Grignard reagents, organostannanes, organozinc and organolithium compounds are employed, which are typically sensitive and require multistep synthetic procedures (**Figure 1.1.1a**).<sup>[13]</sup> Moreover, the

production of toxic byproducts results in hazardous pollution and waste. Therefore, atom-<sup>[14]</sup> and step-economical processes<sup>[15]</sup> have been becoming increasingly attractive to chemists.

In contrast, transition metal-catalyzed site-selective C–H functionalizations<sup>[16]</sup> have obvious advantages since they avoid pre-functionalization steps to construct C–C and C–Het bonds (**Figure 1.1.1b**), thereby providing outstanding levels of resource-economy.<sup>[17]</sup> Thus, the influence of organic synthesis on the environment were considerably decreased. Although cross dehydrogenative couplings (CDC) with molecular hydrogen as the sole byproduct in principle constitute the most sustainable concept (**Figure 1.1.1c**),<sup>[18]</sup> chemical oxidants, such as expensive silver and copper salts, are indispensable to realize these transformations, which in fact compromises the resource-economy. Despite the utilization of one prefunctionalized organic electrophile in the direct C–H functionalization, these conditions refrain from expensive and toxic chemical oxidants and the substrates, such as most commonly used organic halides and phenol derivatives, are easy to obtain on large scale in industries (**Figure 1.1.1b**).<sup>[19]</sup>

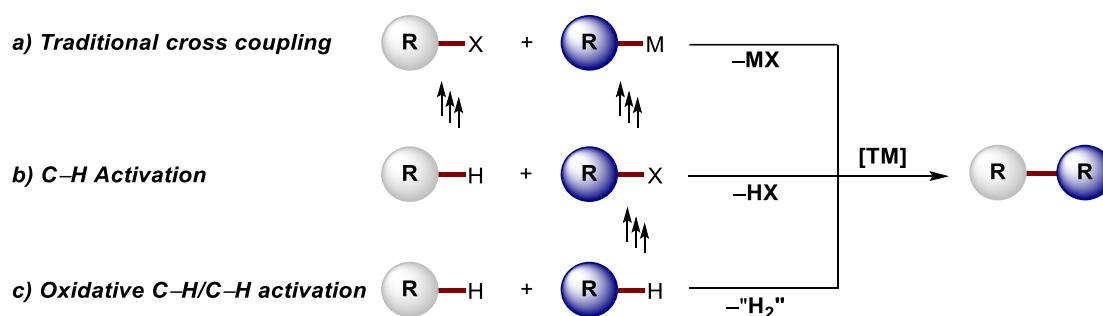
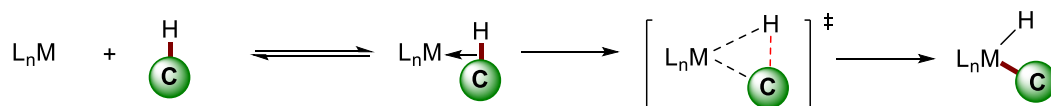


**Figure 1.1.1.** Comparison of classical cross-coupling reactions with C–H activation and oxidative C–H/C–H activation.

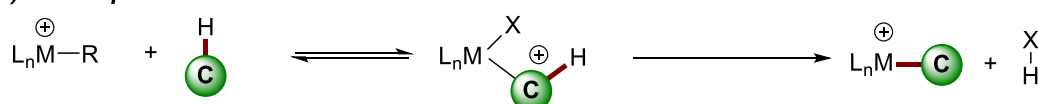
The foremost foundation for developing transition metal-catalyzed C–H functionalization is the elucidation of the reaction mechanism. Thus, numerous studies have focused on the key C–H activation step, resulting in several mechanistically distinct pathways being identified depending on the electronic properties and nature of the metal catalyst (**Figure 1.1.2**). Without considering outer-sphere/radical-type mechanisms,<sup>[20]</sup> five reaction modes are proposed in general.<sup>[19c]</sup> Oxidative addition

was mostly observed for electron-rich late transition metals in low oxidation states.<sup>[21]</sup> Electrophilic substitution was proposed for late transition metals in higher oxidation states involved an electrophilic attack of transition metal to the carbon.<sup>[22]</sup>  $\sigma$ -Bond metathesis is a common pathway for early transition-metals, as well as lanthanides and actinides which are difficult to change oxidation states.<sup>[23]</sup> In addition, 1,2-addition of C–H bonds to unsaturated M = X bonds, such as metal imido complexes, is favored.<sup>[19c, 24]</sup> Closely related to electrophilic substitution, a base-assisted C–H activation event<sup>[19c, 25]</sup> is proposed to go through an electrophilic attack of the metal and deprotonation by carboxylate or carbonate ligands. Within this mechanistic manifold, the cleavage of C–H bond and the formation of C–M occurs simultaneously.

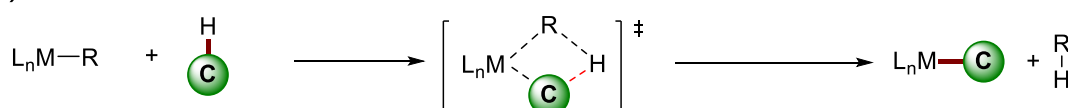
**a) Oxidative addition**



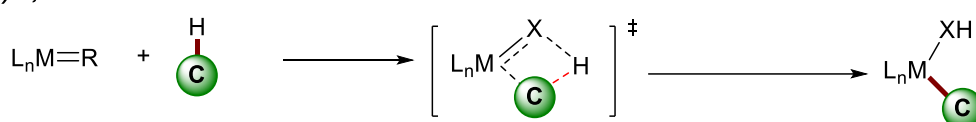
**b) Electrophilic substitution**



**c)  $\sigma$ -Bond metathesis**



**d) 1,2-Addition**



**e) Base-assisted metalation**

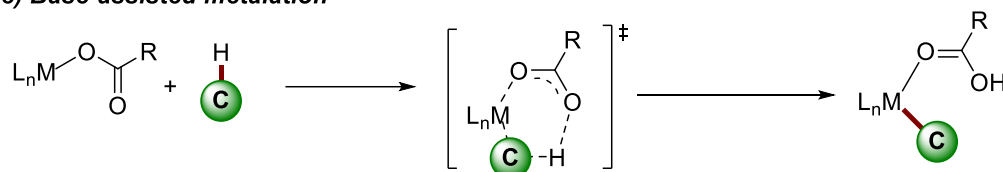


**Figure 1.1.2.** Mechanistic pathways for C–H activation.

In recent years, the base-assisted mechanism was investigated in detail, unveiling the important role of an internal base for the C–H cleavage processes. Based on the distinct transition states, base-assisted C–H metalation processes could be further categorized (**Figure 1.1.3**). While the term concerted metalation-deprotonation (CMD) was coined by Fagnou/Gorelsky,<sup>[26]</sup> an agostic interaction between transition metal and

the C–H bond was proposed by Macgregor/Davies, being named ambiphilic metal-ligand activation (AMLA).<sup>[27]</sup> Both mechanisms involving metalation and deprotonation steps proceed through a six-membered transition state and are favorable for electron-deficient substrates with high kinetic C–H acidity. On the contrary, the base-assisted internal electrophilic substitution (BIES) was uncovered by Ackermann for electron-rich arenes with acetate or carboxylate ligands and proceeds *via* an electrophilic substitution-type pathway.<sup>[28]</sup>

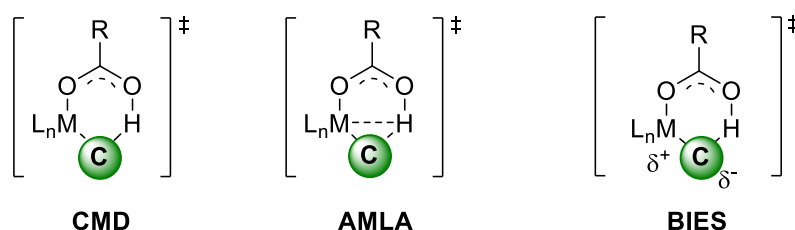


**Figure 1.1.3.** Distinct transition state models for base-assisted C–H metalation.

Due to the omnipresence of C–H bonds and their similar dissociation energies, site-selectivity control is a major challenge in direct C–H functionalization.<sup>[29]</sup> Several typical strategies have been introduced to overcome the selectivity issue (**Figure 1.1.4**). Distinct C–H bonds in heterocycles possess inherent differences in their acidities and bond dissociation energies, which result in a selective activation of specific C–H bonds (electronic bias) (**Figure 1.1.4a**).<sup>[19f, 30]</sup> Another approach is the installation of a bulky substituent, resulting in a steric control by preventing access to the adjacent C–H bonds (steric bias) (**Figure 1.1.4b**). However, both electronic bias and steric bias have intrinsically limited applications owing to the requirement for particular substrates. A more widely-used strategy is the introduction of Lewis-basic directing groups, which coordinate to the metal center and bring it in close proximity to the desired *ortho*-, *meta*- or *para*-C–H bond (**Figure 1.1.4c**).<sup>[31]</sup> Recently, transient directing groups that can be reversibly installed *in situ* and removed in the catalytic C–H scission possess have the potential to decrease the number of laborious synthetic operations (**Figure 1.1.4e**).<sup>[29e]</sup> The transient directing group, installed *in situ* through the reaction of the substrates with a catalytic amount of external ligand, can coordinate to the metal center, achieve the position-selective C–H activation and finally release the transient ligand. For

remote *meta*-selective C–H activation, one key strategy is the ruthenium-catalyzed  $\sigma$ -activation (**Figure 1.1.4d**).<sup>[29f, 31a]</sup> The generated *ortho*-substituted cycloruthenated complex activates the remote *para*-C–H bond with respect to the ruthenium center by strongly influencing the electronic properties of the aromatic ring. An alternative method for *meta*-C–H functionalization is to exploit carboxylic acids as traceless directing groups, that can be removed in a traceless fashion after the carboxylic acid-directed C–H activation (**Figure 1.1.4f**).<sup>[29g, 32]</sup> Palladium/norbornene (NBE) cooperative Catellani-catalysis has emerged as a useful approach to accomplish selective C–H activation (**Figure 1.1.4g**).<sup>[29a]</sup> During this transformation, the *ortho*-C–H activation takes place in the presence of NBE to provide a palladium-norbornene species, which can further activate the adjacent C–H bond to selectively achieve the remote selective *meta*-C–H bond functionalization.

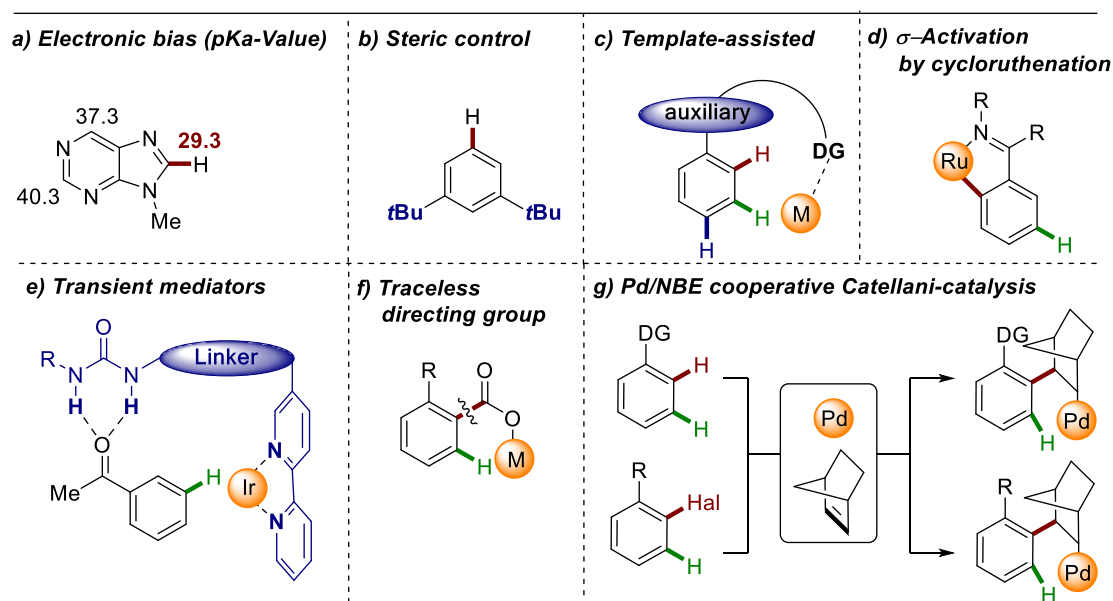


**Figure 1.1.4.** Different strategies for selective C–H functionalizations.

## 1.2 Ruthenium-Catalyzed Selective C–H Activation

During the last decades, C–H functionalization has achieved enormous success employing noble metal catalysts, especially palladium, rhodium or ruthenium. Due to the significantly lower price of ruthenium, which is only 13% of the price of palladium and 3% of rhodium (Figure 1.2.1), the application of ruthenium catalysts for the molecular construction is highly desirable.<sup>[33]</sup>

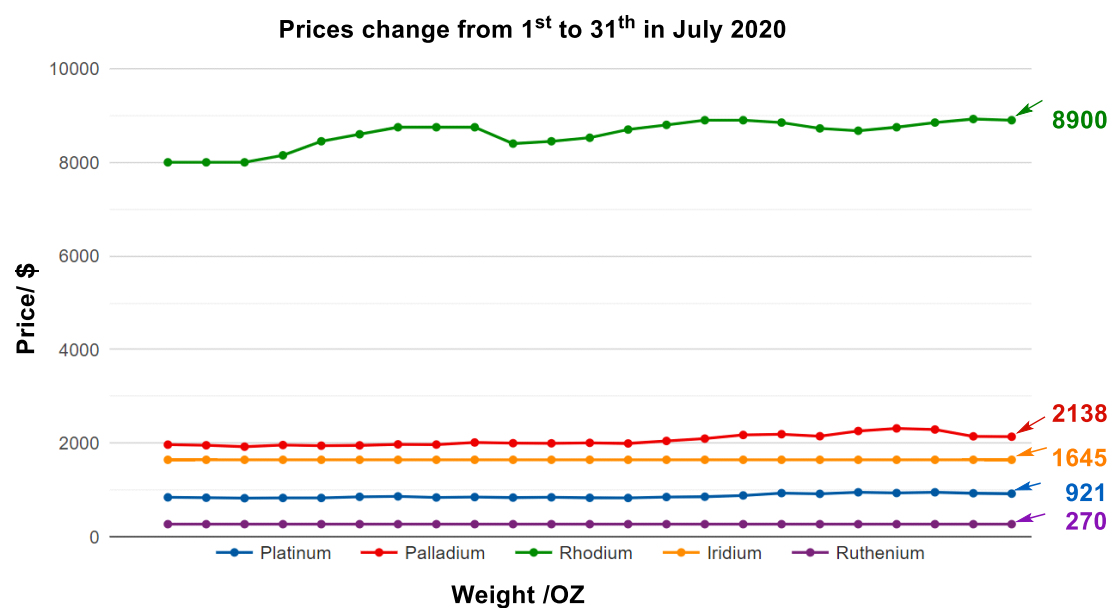


Figure 1.2.1. The price of 4d and 5d precious metals.

### 1.2.1 Ruthenium-Catalyzed *ortho*-C–H Activation

In 1965, Chatt and Davidson described the ruthenium-mediated C–H activation, in which an *in situ* generated ruthenium(0)-phosphine complex was employed to achieve the C–H cleavage of sodium arene **2** for the generation of hydride-ruthenium(II) complex **3** (Figure 1.2.2).<sup>[34]</sup>

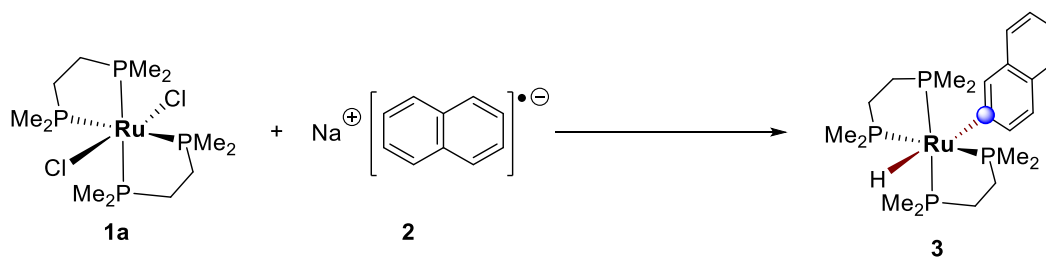


Figure 1.2.2. Ruthenium-mediated C–H activation.



Approximately 20 years later, the first regioselective catalytic C–H alkylation of phenols employing ruthenium complex **7a** and KOPh as the cocatalysts was reported by Lewis and Smith, in which the ruthenium complex was obtained from a phosphite derived from phenol **4a** (Figure 1.2.3).<sup>[35]</sup>

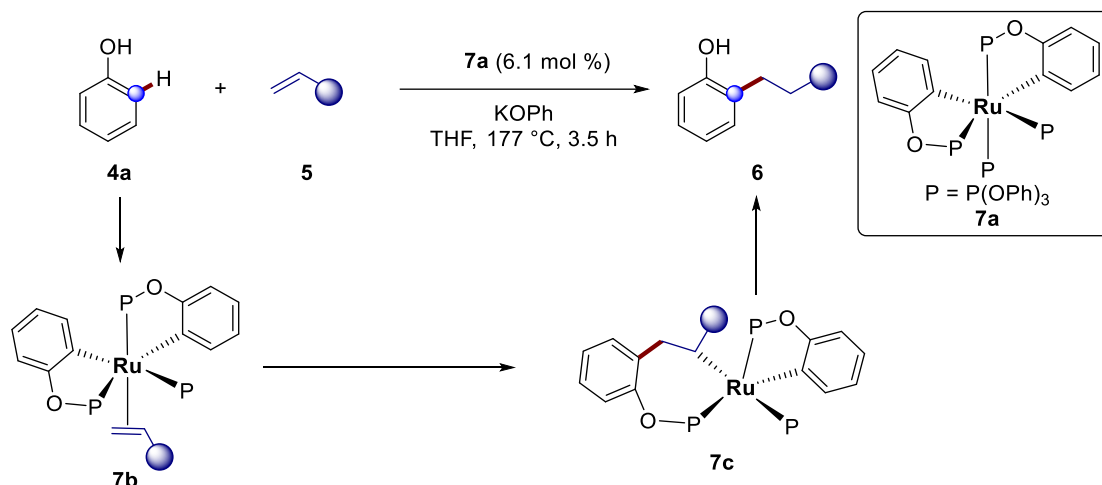


Figure 1.2.3. Ruthenium-catalyzed C–H alkylation.

A ruthenium-catalyzed highly site-selective C–H alkylation of aromatic ketones **8** with a wide range of olefins was discussed by Murai/Chatani in 1993 (Figure 1.2.4).<sup>[36]</sup> Remarkably, the use of chelation assistance to form the cyclometalated ruthenium-hydride **10** proved crucial for C–H cleavage. Then, insertion of the alkene **5** into the Ru–H bond (or Ru–C bond, the author did not clarify this) provides the desired product **9** through reductive elimination (Figure 1.2.4).

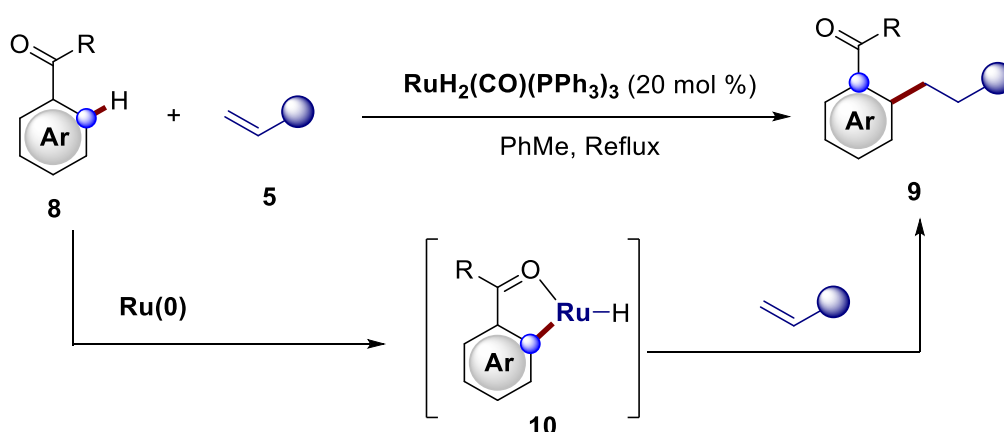


Figure 1.2.4. Ruthenium-catalyzed C–H alkylation of aromatic ketones.

In 2001, Milstein and coworkers introduced the ruthenium-catalyzed oxidative coupling of olefin **5b** with arene **11a** to furnish aryl alkene **12a**, using molecular oxygen (Figure 1.2.5).<sup>[37]</sup>

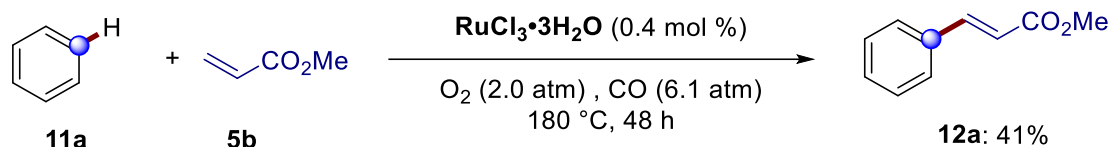


Figure 1.2.5. Ruthenium-catalyzed oxidative coupling.

In the same year, the first *ortho*-selective C–H mono- or di-arylations with a ruthenium(II)-phosphine complex as the catalyst were reported by Oi and Inoue (Figure 1.2.6).<sup>[38a]</sup> An increased amount of aryl bromide **14a** and base was beneficial for the formation of the diarylated product **15a'**. However, the protocol was not fully reproducible.<sup>[38b]</sup>

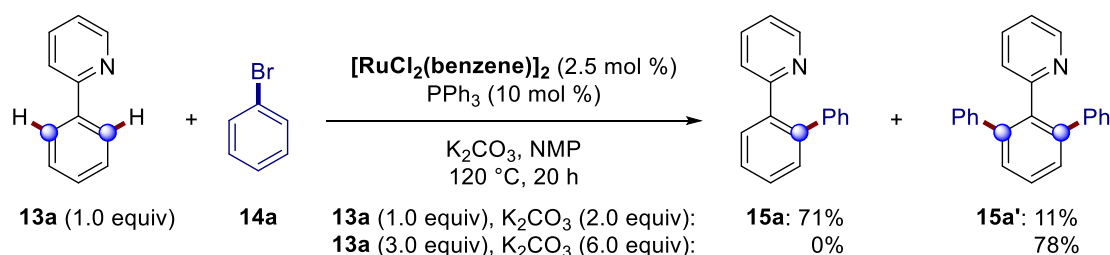


Figure 1.2.6. Ruthenium-catalyzed *ortho*-selective C–H arylation.

In 2008, the Ackermann group developed carboxylate assistance for the first ruthenium(II)-catalyzed C–H activation, involving the possible generation of a six-membered ruthenium-carboxylate species (Figure 1.2.7).<sup>[39]</sup>

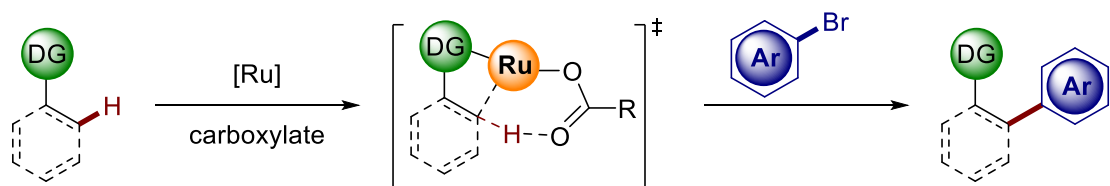
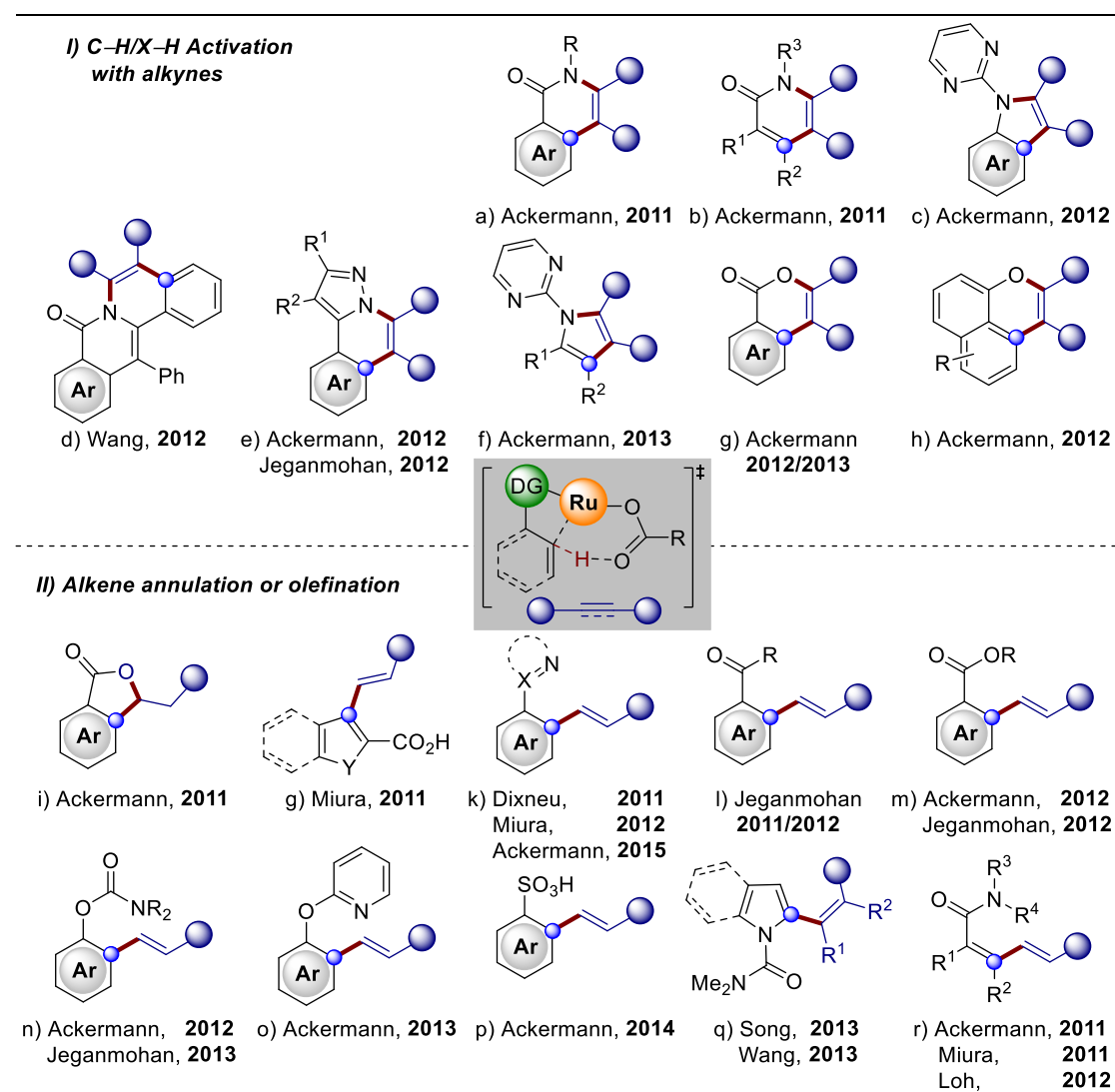


Figure 1.2.7. Ruthenium-catalyzed C–H arylation under carboxylate assistance.

Subsequently, this novel method was widely applied in ruthenium-catalyzed oxidative C–H/N–H<sup>[40]</sup> and C–H/O–H bond<sup>[41]</sup> annulations of heteroarenes and olefins with alkynes in the presence of copper(II) oxidants by Ackermann and others, providing access to various heterocyclic molecules (Figure 1.2.8a–h).<sup>[42]</sup> In addition, ruthenium-

catalyzed oxidative alkene annulations of aromatic acids to access 5-membered lactones was introduced by Ackermann (**Figure 1.2.8i**).<sup>[43]</sup> Employing ruthenium catalysis by carboxylate assistance, selective oxidative C(sp<sup>2</sup>)-H olefinations of heteroarenes and olefins were accomplished to deliver the desired aryl alkenes (**Figure 1.2.8j-r**). Various directing groups were explored for these transformations, for instance, carboxylic acids,<sup>[44]</sup> oxazoles/triazoles,<sup>[45]</sup> ketones/aldehydes,<sup>[46]</sup> esters,<sup>[47]</sup> carbamates,<sup>[48]</sup> 2-pyridyloxys,<sup>[49]</sup> sulfonic acids,<sup>[28b]</sup> *N*-dimethylcarbamoyls<sup>[50]</sup> and amides.<sup>[51]</sup>



To avoid the use of problematic metal oxidants, such as copper(II) salts, an oxidizing directing group was employed by Wang and Ackermann for the ruthenium-catalyzed

C–H/N–O functionalization with alkynes **16**, leading to the formation of bioactive isoquinolones **19** and isoquinolinones **20** (Figure 1.2.9a, b).<sup>[52]</sup> Moreover, this strategy proved also efficient for the olefination or alkene annulation of *N*-methoxybenzamides **17A** by Li and Wang (Figure 1.2.9c).<sup>[53]</sup>

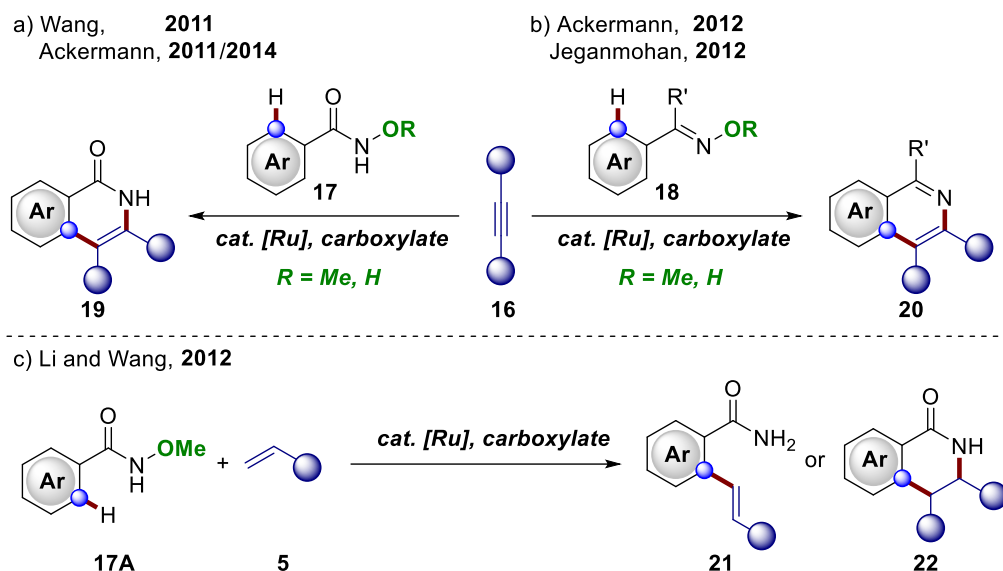


**Figure 1.2.9.** Ruthenium-catalyzed C–H/N–O functionalization with alkynes and alkenes with an oxidizing directing group.

Among the pioneering contributions, the Ackermann group introduced ruthenium-catalyzed *ortho*-C(sp<sup>2</sup>)–H alkylation by carboxylate assistance utilizing electrophilic primary and secondary alkyl halides **24** (Figure 1.2.10).<sup>[54]</sup>

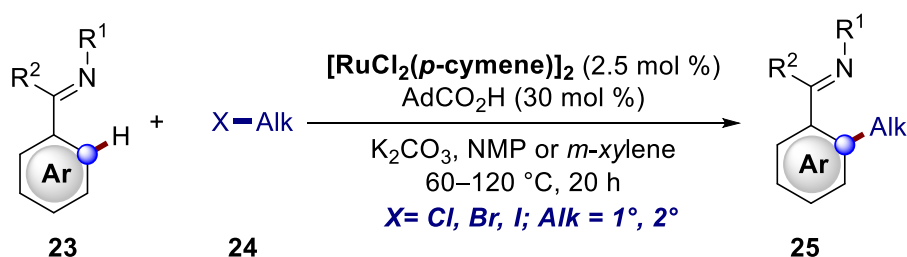


**Figure 1.2.10.** Ruthenium-catalyzed C–H alkylation by carboxylate assistance.

## 1.2.2 Ruthenium-Catalyzed Remote C–H Activation

As mentioned in **chapter 1.1**, a strategy for achieving remote C–H activation by ruthenium catalysis is represented by the  $\sigma$ -activation through cyclometallation. Herein, the development of ruthenium-catalyzed remote C–H activation based on this mechanism will be discussed.

In 1994, Roper reported this strategy of ruthenium-mediated  $\sigma$ -activation, in which the *para*-C–H nitration of a ruthenium-benzene complex **26a** was realized, although in low yield (**Figure 1.2.11a**).<sup>[55]</sup> Afterwards, van Koten reported another stoichiometric *para*-C–H activation of a ruthenium-arene complex **26b**, providing the homo-coupling complex **27f** as well as the chlorinated product **27g** (**Figure 1.2.11b**).<sup>[56]</sup> These results evidenced that the position-selectivity of C–H activation could be controlled by the formed C–Ru bond *via* the electronic influence of the arene ring.

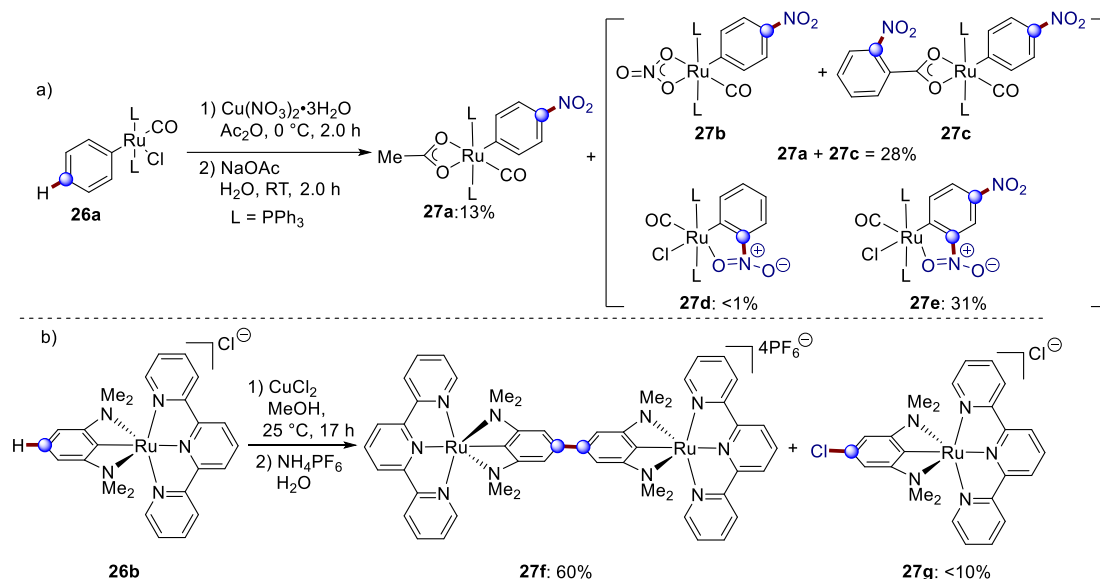


**Figure 1.2.11.** C–H activation of cyclometalated ruthenium complexes.

In 1998, Coudret and coworkers reported the electrophilic C–H bromination of phenylpyridine-ruthenium complex **26c** at the *para*-position with respect to the Ru–C  $\sigma$ -bond with *N*-bromosuccinimide (NBS) in excellent yield and regioselectivity (**Figure 1.2.12a**).<sup>[57]</sup> One year later, Roper and Wright described the electrophilic *para*-C–H bromination of phenylpyridine-ruthenium complex **26d** using  $\text{PyHBr}_3$  as the halogenating reagent (**Figure 1.2.12b**).<sup>[58]</sup> These two examples showed that the formal cyclometalated ruthenium complex could be identified as a Friedel-Crafts-type *ortho/para* directing group for the *para*-C–H activation of Ru–C bond.

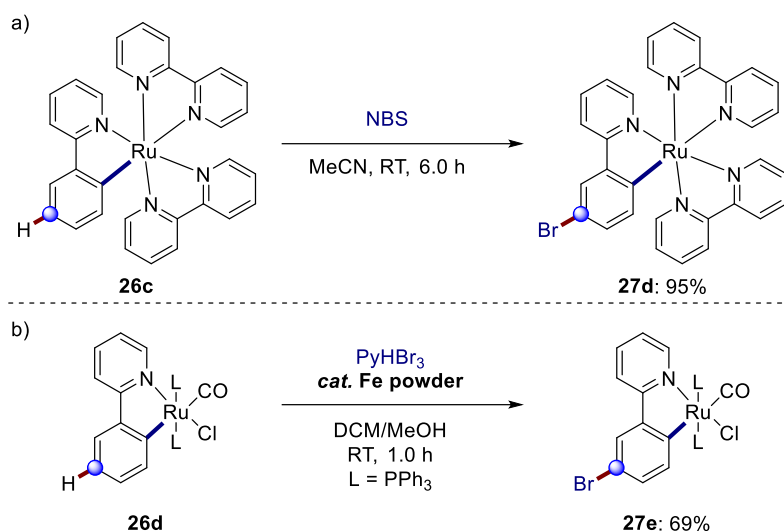


**Figure 1.2.12.** Remote C–H bromination of cycloruthenium complexes.

This strategy was utilized as a useful tool for the selective C–H activation with a catalytic amount of ruthenium in 2011. In a pioneering contribution by the Ackermann group, the first ruthenium-catalyzed *meta*-C–H alkylation was reported, albeit with low yield (**Figure 1.2.13**).<sup>[59]</sup>

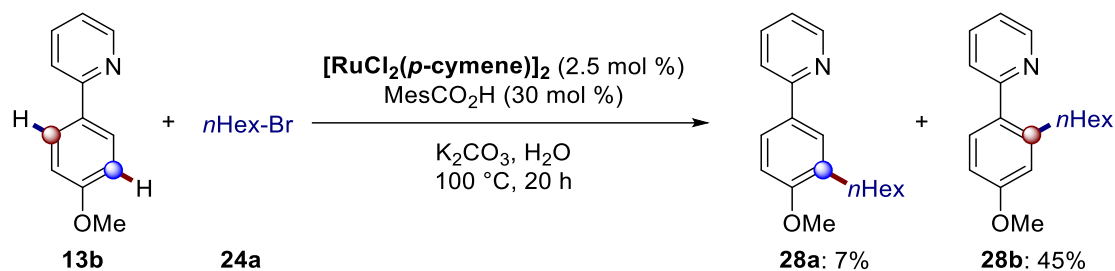


**Figure 1.2.13.** The first ruthenium-catalyzed *meta*-C–H alkylation.

Later, in the same year, the Frost group reported the ruthenium-catalyzed *meta*-C–H sulfonation of unactivated arene derivatives (**Figure 1.2.14a**).<sup>[60]</sup> The *ortho*-cyclometalated phenylpyridine species was prepared and demonstrated to be a catalytically competent intermediate. Using pyridines as the directing group (**Figure 1.2.14c, g–i**), a variety of ruthenium-catalyzed *meta*-C–H activations, such as primary, secondary and tertiary alkylations,<sup>[61]</sup> benzylations,<sup>[62]</sup> brominations<sup>[63]</sup> and nitrations were described.<sup>[64]</sup> Remarkably, Ackermann reported the *meta*-C–H bromination of aryl-substituted purines using a heterogeneous ruthenium catalyst, which set the stage for direct nucleobase fluorescent labeling (**Figure 1.2.14j**).<sup>[65]</sup> In 2013, ruthenium-catalyzed carboxylate-assisted *meta*-C–H alkylations with secondary alkyl halides

using a removable directing group were disclosed by the Ackermann group (**Figure 1.2.14b**).<sup>[66]</sup> Subsequently, various removable directing groups were developed as a tool to activate remote C–H bonds of anilines,<sup>[62c]</sup> azoarenes,<sup>[67]</sup> phenols,<sup>[68]</sup> and ketones,<sup>[69]</sup> providing the desired *meta*-substituted products (**Figure 1.2.14d–f, k**).

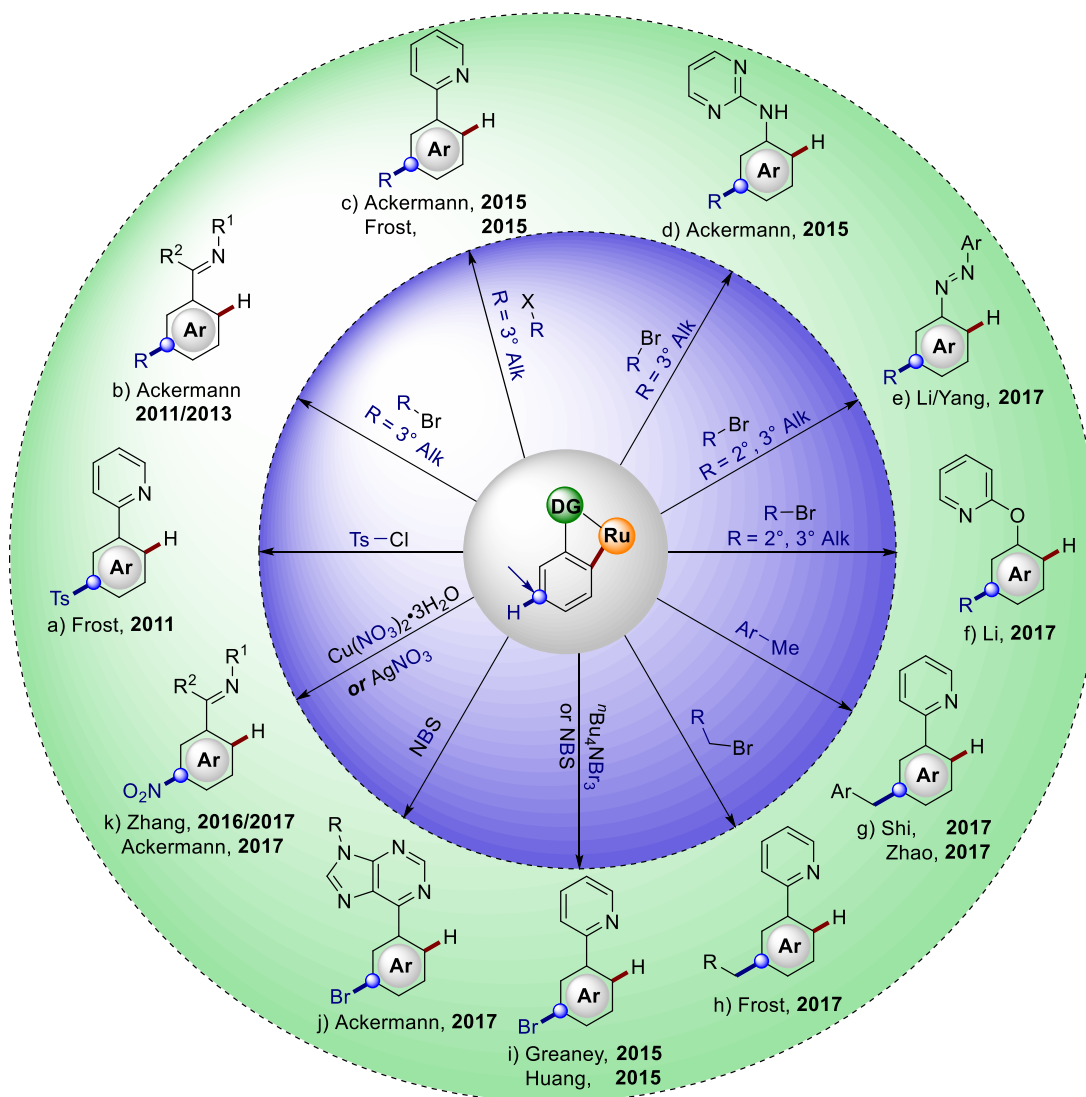


**Figure 1.2.14.** Ruthenium-catalyzed selective *meta*-C–H activation in the presence of nitrogen-containing directing groups.

### 1.3 Nickel-Catalyzed C–H Activation

Nickel as an earth-abundant 3d metal is less expensive and less toxic than commonly used 4d and 5d transition metals, like palladium, and is thus highly desirable for the synthetic transformations. Furthermore, the relatively more electropositive property of nickel is advantageous in the process of the oxidative addition with less reactive coupling partners.<sup>[70]</sup> Additionally, nickel bearing 10 *d-electrons* in a neutral nickel(0) species displays different oxidation states from the common lower oxidation states nickel(0), nickel(I), and nickel(II) to the relative rare higher oxidation states nickel(III) and nickel(IV), which allows unusual mechanistic pathways.<sup>[71]</sup> Although the tremendous progress in cross-coupling reactions has been achieved, for instance, Suzuki-Miyaura, Negishi, Kumada cross-couplings,<sup>[72]</sup> nickel-catalyzed C–H functionalizations are more attractive in consideration of economic and ecological advantages for modern organic synthesis.<sup>[73]</sup>

In 1963, the successful synthesis of an *ortho*-cyclometallated nickel species **31a** employing the azo moiety as directing group was generally recognized as the first example of nickel-mediated C–H activation (**Figure 1.3.1a**).<sup>[74]</sup> Forty years later, an early example of nickel(0)-catalyzed C–H alkylation of imidazolium salts with olefins was described by Cavell using a Ni(cod)<sub>2</sub>/PPh<sub>3</sub> cooperative system (**Figure 1.3.1b**).<sup>[75]</sup> In 2006, a C–H nickelation of unactivated benzene **11a** with an air-stable pincer-nickel(II) complex **30b** in the absence of chelation assistance was reported by Liang (**Figure 1.3.1c**).<sup>[76]</sup>



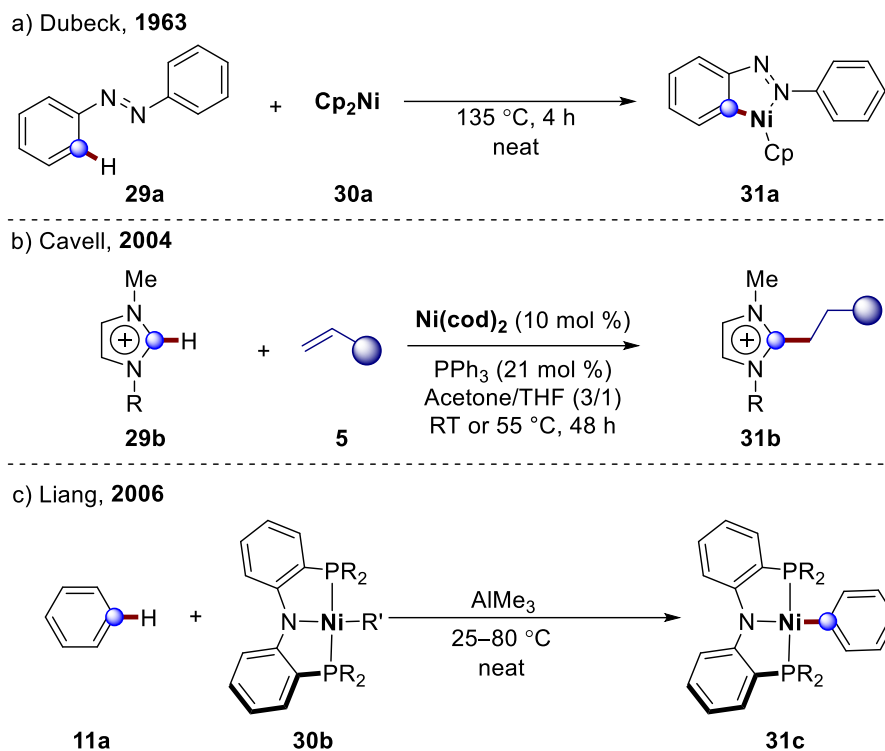


**Figure 1.3.1.** Early contributions of nickel-catalyzed C–H activation.

Thereafter, tremendous progresses on nickel-catalyzed C–H functionalizations have been achieved for synthetic transformations, especially the formation of C–C bonds like arylations, alkylations, alkenylations, alkynylations and hydroarylations of alkynes and allenes.<sup>[73]</sup> Herein, I provide details on C–H arylations, alkynylations and alkylations.

### 1.3.1 Nickel-Catalyzed C–H Activation for C–C Formation

#### 1.3.1.1 Nickel-Catalyzed C–H Arylation

In 2009, Itami and Miura independently reported the nickel-catalyzed direct C–H arylation of azole derivatives **32** bearing an electronically activated C–H bond with aryl halides **14** (**Figure 1.3.2**).<sup>[77]</sup> In both approaches, the strong base LiOtBu was necessary to give the desired arylated products **33**. Subsequently, a modified protocol was introduced by Itami in 2011, employing  $\text{Mg}(\text{OtBu})_2$  as an alternative base to achieve this molecular transformation.<sup>[78]</sup>

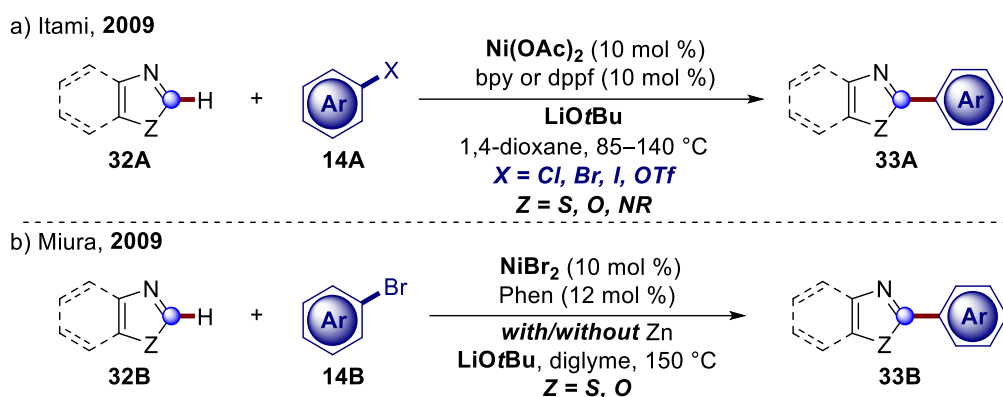


**Figure 1.3.2.** Nickel-catalyzed C–H arylation with aryl halides **14A**, **14B**.

In addition to aryl halides, arylsilanes **14C** were firstly employed by Miura for the nickel-catalyzed C–H arylation in the presence of copper(II) oxidant (**Figure 1.3.3a**).<sup>[79]</sup> Other arylating reagents, namely, arylboronic acids **14D** and Grignard reagents **14E** also displayed high-efficacy with different oxidants like, O<sub>2</sub> or 1,2-dichloroethane, to obtain the corresponding biaryl products **33D**, **33E** (**Figure 1.3.3b, c**).<sup>[80]</sup> In 2009, Tobisu and Chatani reported the C–H arylation with arylzinc reagents **14F** as the arylated reagents (**Figure 1.3.3d**).<sup>[81]</sup>

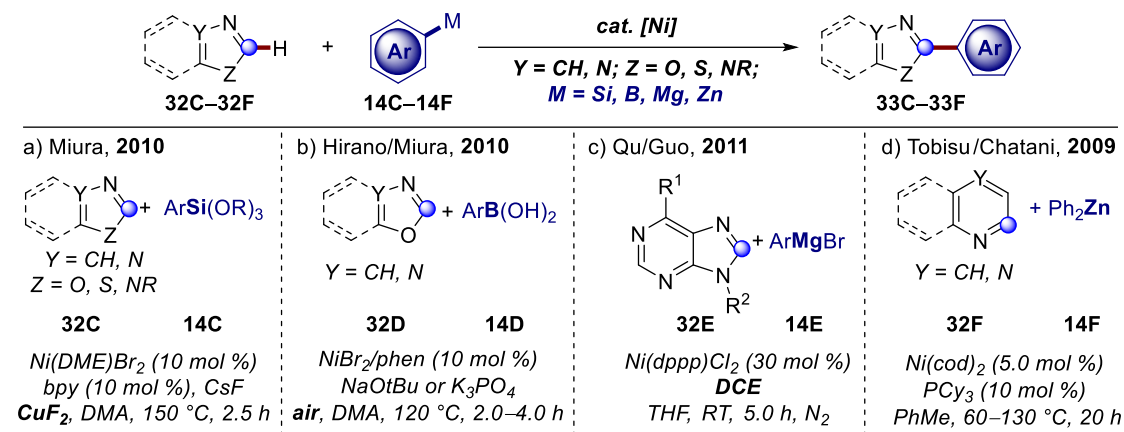


**Figure 1.3.3.** Nickel-catalyzed oxidative C–H arylation with organic nucleophiles **14C–14F**.

Ackermann early uncovered the C–H/C–O coupling of heteroarenes by palladium and cobalt catalysis.<sup>[82]</sup> In 2012, Itami described the first nickel-catalyzed C–H/C–O coupling of azoles **32B** and phenol derivatives **14G** using the Ni(cod)<sub>2</sub>/dcype catalytic system (**Figure 1.3.4a**).<sup>[83]</sup> Mechanistic studies including the isolation and elucidation of the key intermediate arylnickel-dcype pivalate **34**, kinetic studies and the determination of the kinetic isotope effect, revealed the C–H activation as the rate-

limiting step (**Figure 1.3.4b**).<sup>[84]</sup> The same group improved the protocol employing air-stable  $\text{Ni}(\text{OTf})_2$  as the catalyst for both C–H alkenylations and arylations of imidazoles, thiazoles and oxazoles (**Figure 1.3.4c**).<sup>[85]</sup> The key to obtain the desired products was the use of the tertiary alcohol *t*AmylOH, while aprotic solvents and secondary alcohol likewise *i*PrOH failed to give the product. Nickel-catalyzed decarboxylative C–H arylation of azole derivatives was successfully introduced using aryl esters **14I** and benzoic acids **14J** (**Figure 1.3.4d, e**).<sup>[86]</sup> Recently, Kalyani and coworkers described the nickel-catalyzed C–H arylation of azoles **32G** with benzonitriles **14K**, in which the Lewis acid  $\text{BPh}_3$  was found to be beneficial to decrease the catalyst loading (**Figure 1.3.4f**).<sup>[87]</sup>

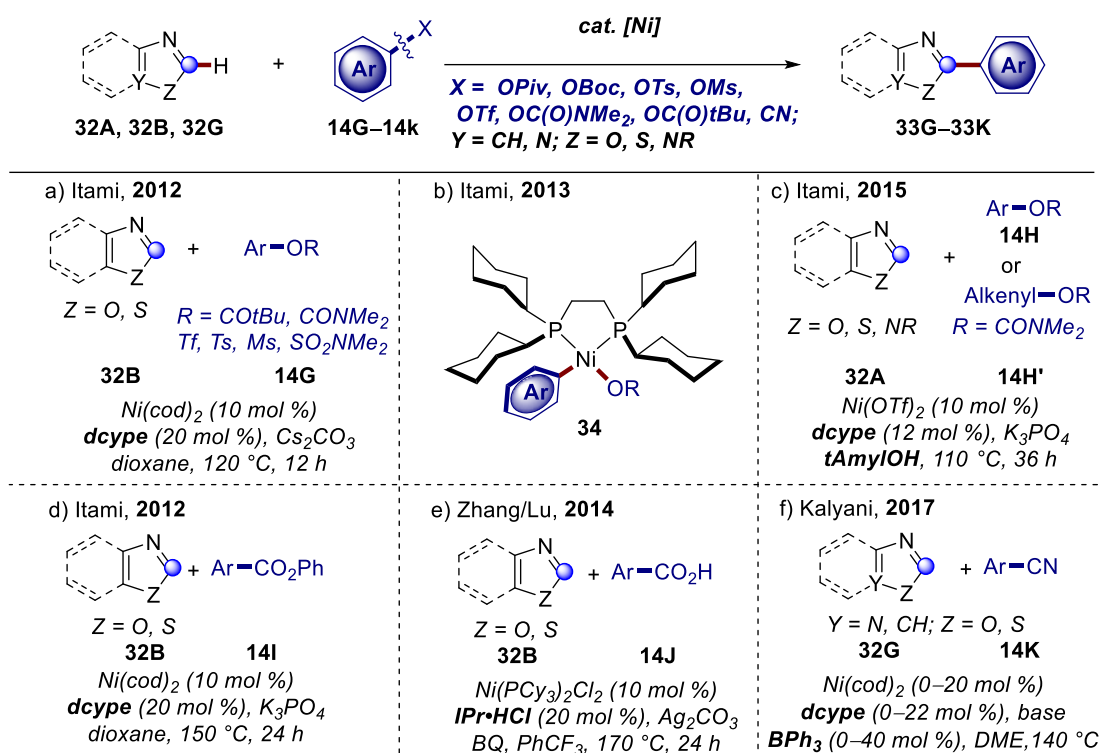


**Figure 1.3.4.** Nickel-catalyzed redox-neutral C–H arylation with unconventional coupling partners **14G–14K**.

Most known methods focused on the use of electronically activated substrates, like pyridine and azole derivatives, containing an acidic C–H bond. However, C–H functionalizations of unactivated arenes were thus far undeveloped. Among the strategies for the cleavage of inert C–H bonds, the installation of monodentate or bidentate directing groups to substrates has become as one of the most powerful and

useful tools.<sup>[88]</sup> In 2014, Chatani reported the nickel-catalyzed C–H arylation with aryl iodides **14L** with AQ (8-aminoquinoline) as the directing group.<sup>[89]</sup> Subsequently, diverse *N,N*- and *N,O*-bidentate directing groups (2-pyridinylisopropyl (PIP) and pyridine 1-oxide (PyO)) were utilized to accomplish the transformations with different arylated coupling partners including aryl boronic acid esters **14M**,<sup>[90]</sup> silanes **14N**,<sup>[91]</sup> carboxylates **14O**<sup>[92]</sup> and halides **14P** (Figure 1.3.5a–e).<sup>[93]</sup> In 2016, an oxidative cross-dehydrogenative-coupling (CDC) between two heteroarenes was demonstrated by You group, delivering the target biaryl products **39**, in which the expensive silver oxidants could be recycled up to three times without decreasing the efficacy (Figure 1.3.5f).<sup>[94]</sup> In 2017, Punji reported a solvent-free C–H arylation using a mono-chelation assistance and Ni-pincer catalyst **30c** (Figure 1.3.5g).<sup>[95]</sup>

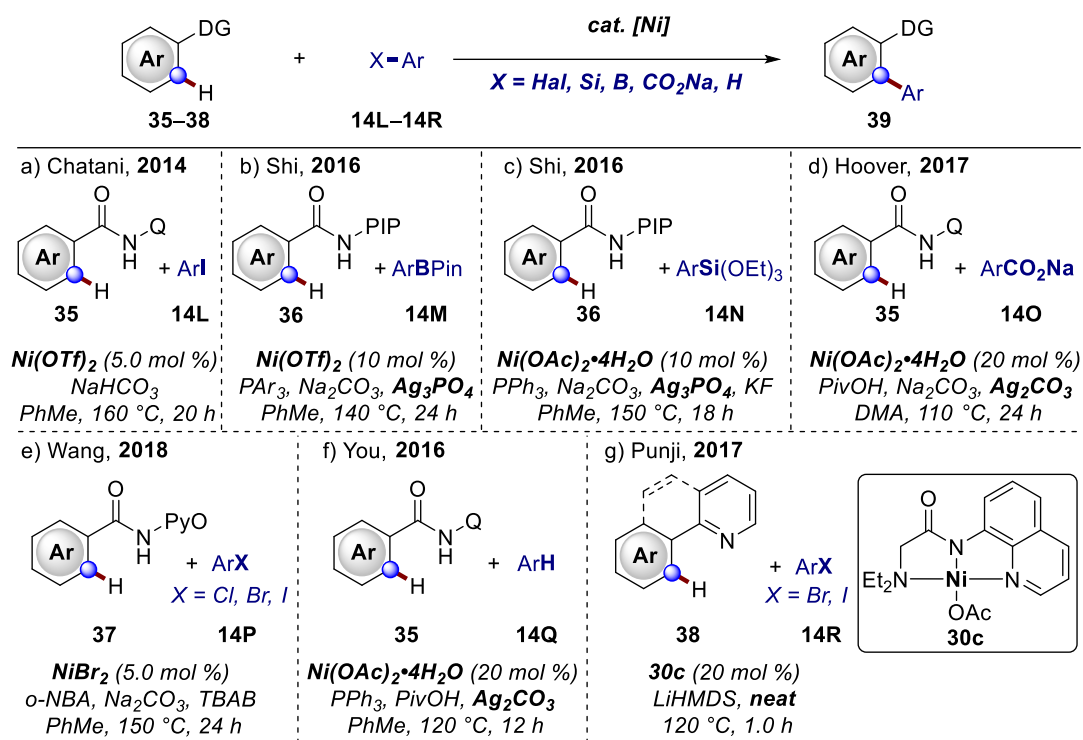
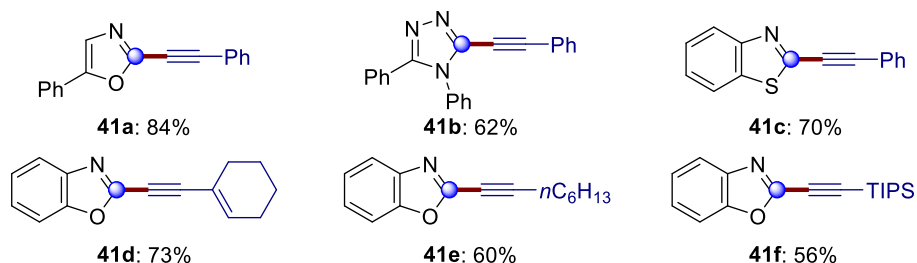
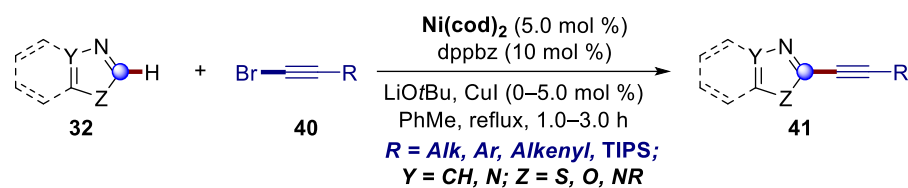


Figure 1.3.5. Nickel-catalyzed C–H arylation with diverse chelation assistances.

### 1.3.1.2 Nickel-Catalyzed C–H Alkynylation

In 2009, Miura reported the C–H alkynylation ofazole derivatives **32** with alkynyl bromides **40A** with a nickel-based catalyst, in which a catalytic amount of CuI was crucial for various substrates, like benzimidazoles and benzothiazoles (Figure 1.3.6).<sup>[96]</sup>



**Figure 1.3.6.** Nickel-catalyzed C–H alkylation of azoles **32**.

With bidentate chelation assistance, catalytic C–H arylations of unactivated arenes were also proven to be highly-efficient by the group of Shi and Balaraman, respectively (**Figure 1.3.7a, b**).<sup>[97]</sup> In 2016, the first nickel-catalyzed C–H functionalization on anilines and purine nucleobases using a monodentate directing group was achieved by the Ackermann group (**Figure 1.3.7c**).<sup>[98]</sup> One year later, the monodentate chelation assistance was also employed by Punji to provide access to the alkynylated indoles **44** (**Figure 1.3.7d**).<sup>[99]</sup>

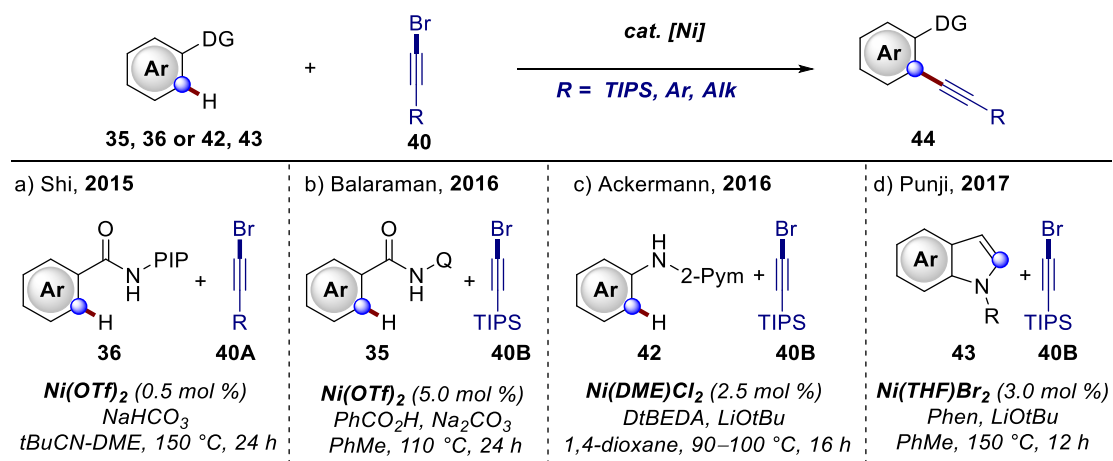


**Figure 1.3.7.** Nickel-catalyzed C–H alkylation of unactivated heteroarenes **25–43** via chelation assistance.

Nickel-catalyzed oxidative C–H alkylation with terminal alkynes **40C**, **40D** was also described independently by Miura and Shi group, providing the aryl alkynes **45**, **46** without requiring pre-functionalization of the substrates (**Figure 1.3.8**).<sup>[100]</sup> In 2010,

Miura and coworkers reported a nickel-based catalyst for the activation of acidic C–H bonds using molecular oxygen as the oxidant (**Figure 1.3.8a**).<sup>[100b]</sup> Subsequently, Shi developed a base-free protocol for the direct oxidative C–H alkylation of unactivated arenes **36** using O<sub>2</sub> as the oxidant and PIP as the bidentate directing group (**Figure 1.3.8b**).<sup>[100a]</sup>

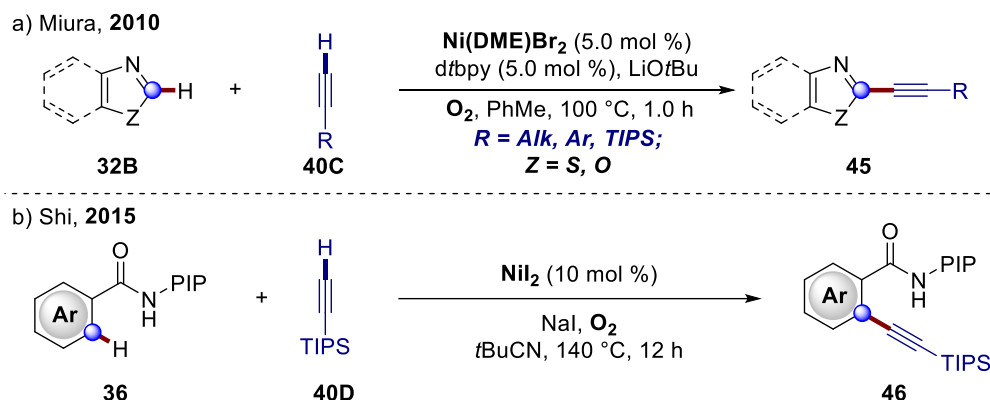


**Figure 1.3.8.** Nickel-catalyzed oxidative C–H alkylation.

### 1.3.1.3 Nickel-Catalyzed C–H Alkylation

Generally, C–H functionalization using non-activated alkyl halides is underdeveloped because the alkylmetal species, generated from the oxidative addition, is prone to undergo  $\beta$ -hydrogen elimination.<sup>[31e, 101]</sup> In 2010, the Hu group reported the C–H alkylation of 1,3-azoles **32H** with alkyl halides **24A** containing  $\beta$ -hydrogen atom using a pincer nickel catalyst **30d** and a co-catalytic amount of CuI (**Figure 1.3.9a**).<sup>[102]</sup> In the same year, Miura and coworkers demonstrated the Ni(DME)Cl<sub>2</sub>/terpyridine **49** catalyst also worked efficiently in suppressing the  $\beta$ -hydrogen elimination, thus accomplishing the alkylative transformation (**Figure 1.3.9b**).<sup>[103]</sup> In 2011, an efficient nickel-catalyzed C–H alkylation of heteroarenes **32B** was achieved by Ackermann using a nitrogen ligand-free Ni(DME)Cl<sub>2</sub>/diglyme catalyst (**Figure 1.3.9c**).<sup>[104]</sup> Two years later, Miura and Hirano described another approach to bypass the  $\beta$ -hydrogen elimination employing *N*-tosylhydrazone **24C** as the alkylating reagent (**Figure 1.3.9d**).<sup>[105]</sup> Diazo compound **51a**, derived from **24C**, could react with the arylnickel species **51b** to deliver **51c** that underwent a faster proto-demetalation or ligand exchange in comparison with the conceivable  $\beta$ -hydrogen elimination to afford the C–H alkylated product **50** (**Figure 1.3.9d**).<sup>[105]</sup>

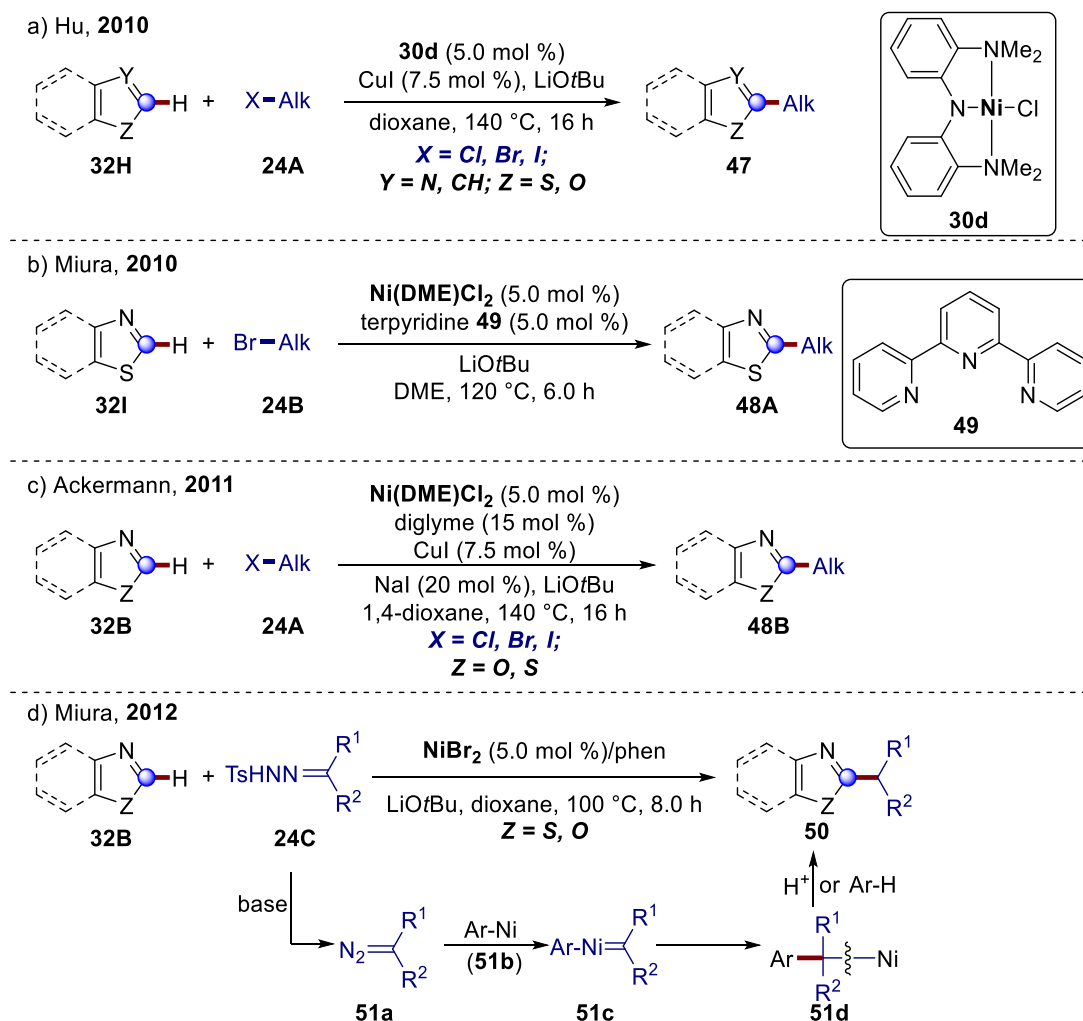


**Figure 1.3.9.** Nickel-catalyzed C–H alkylation of azole derivatives **32**.

In 2012, Qu and Guo reported the first oxidative C–H alkylation of purine and imidazole derivatives **32E** with alkyl Grignard reagents **24D**, using DCE as the oxidant at ambient temperature (**Figure 1.3.10**).<sup>[106]</sup>

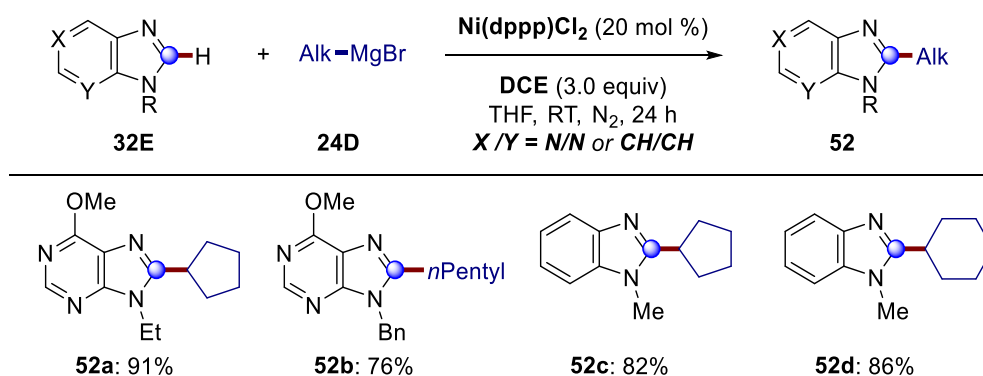


**Figure 1.3.10.** Nickel-catalyzed oxidative C–H alkylation with Grignard reagents **24D**.

In 2013, with the assistance of AQ, the Chatani group reported the nickel-catalyzed C–H alkylation of arenes and olefins with primary alkyl halides **24E** (Figure 1.3.11a).<sup>[107]</sup> One year later, with the assistance of bidentate directing group, the Ackermann group reported the much challenging secondary alkylation and trifluoroethylation by nickel catalysis (Figure 1.3.11b).<sup>[108]</sup> In 2016, Chatani successfully realized the aromatic C–H methylation using dicumyl peroxide **24G** as the methylating reagent (Figure 1.3.11c).<sup>[109]</sup> Recently, the strategy of introducing mono-chelation assistances to arenes was proven to be highly efficient for alkylative transformation by Punji and Ackermann, respectively (Figure 1.3.11d, e). A C-2 alkylation of indoles **43** in the presence of a well-defined nickel-pincer catalyst **30c** with pyridine or pyrimidine as the monodentate directing group was fulfilled by the group of Punji (Figure 1.3.11d).<sup>[110]</sup> In 2017, Ackermann reported the nickel-catalyzed C–H alkylation of purine nucleobases **53**, providing access to crucial structural motifs of various bioactive compounds **54** (Figure 1.3.11e).<sup>[111]</sup>

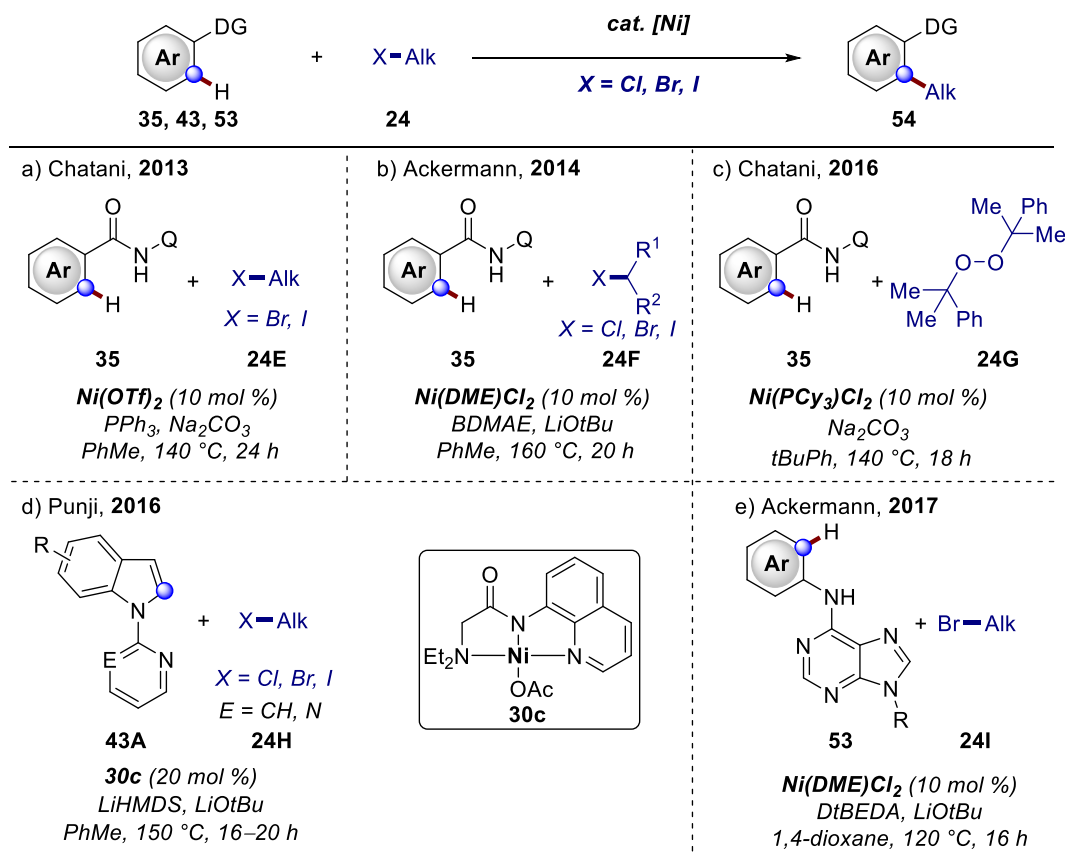


Figure 1.3.11. Nickel-catalyzed C–H alkylation of arenes **35**, **43**, **53** with chelation assistance.





less developed. However, nitrogen-containing molecules are the key structural fragments in natural products, biological molecules and pharmaceutical agents.<sup>[112]</sup> Thereby, the construction of C–N bonds has attracted increasing attention. Recently, C–H aminations have been well developed by transition metals, including iridium, ruthenium, rhodium, palladium, copper and cobalt.<sup>[113]</sup> Nickel as an Earth-abundant and less-toxic 3d metal was relatively less explored in the amination reactions.

In 2012, the nickel-catalyzed C–H amination of benzoxazoles **32J** with secondary amines **56** was introduced by Li and Duan.<sup>[114]</sup> The electronically activated C–H bond was prone to cleavage by the use of Ni(OAc)<sub>2</sub>·4H<sub>2</sub>O as the catalyst and TBHP as the oxidant (**Figure 1.3.13**).

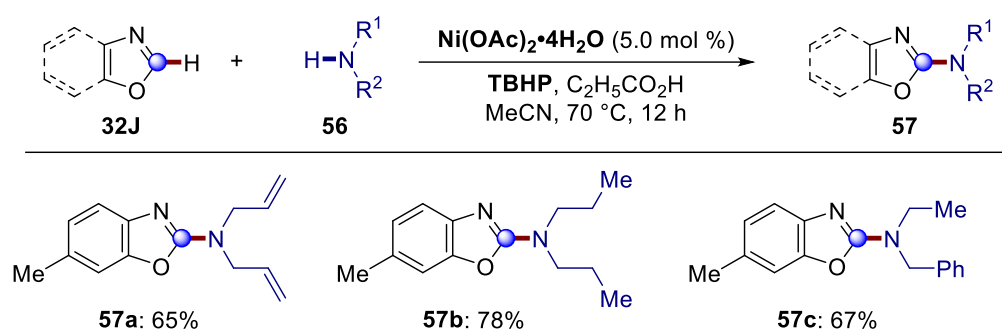


**Figure 1.3.13.** Nickel-catalyzed C–H amination of benzoxazoles **32J**.

In 2015, Zhang reported the nickel-catalyzed C–H transformation of unactivated arenes **35** with secondary amines **56** in the presence of a nickel/silver catalyst and a bidentate directing group, furnishing various arylamines **58** (**Figure 1.3.14**).<sup>[115]</sup> After extensive mechanistic studies, they proposed a catalytic cycle involving nickel(II/III/I) (**Figure 1.3.14**).<sup>[115]</sup> With the assistance of a base, the irreversible C–H activation took place to deliver nickel(II) species **59c** from amide-nickel species **59b**. Cyclometalated nickel complex **59c** underwent oxidative addition to generate the amine-nickel intermediate **59d** (**59d'**), which was confirmed by MAIDIL-TOF-MS spectrum. C–N bonds were formed through reductive elimination, followed by protonation to obtain the desired product **58** and nickel(I) species **59f**. The catalytically active nickel(II) **59a** was finally regenerated by silver(I) carbonate and O<sub>2</sub>.

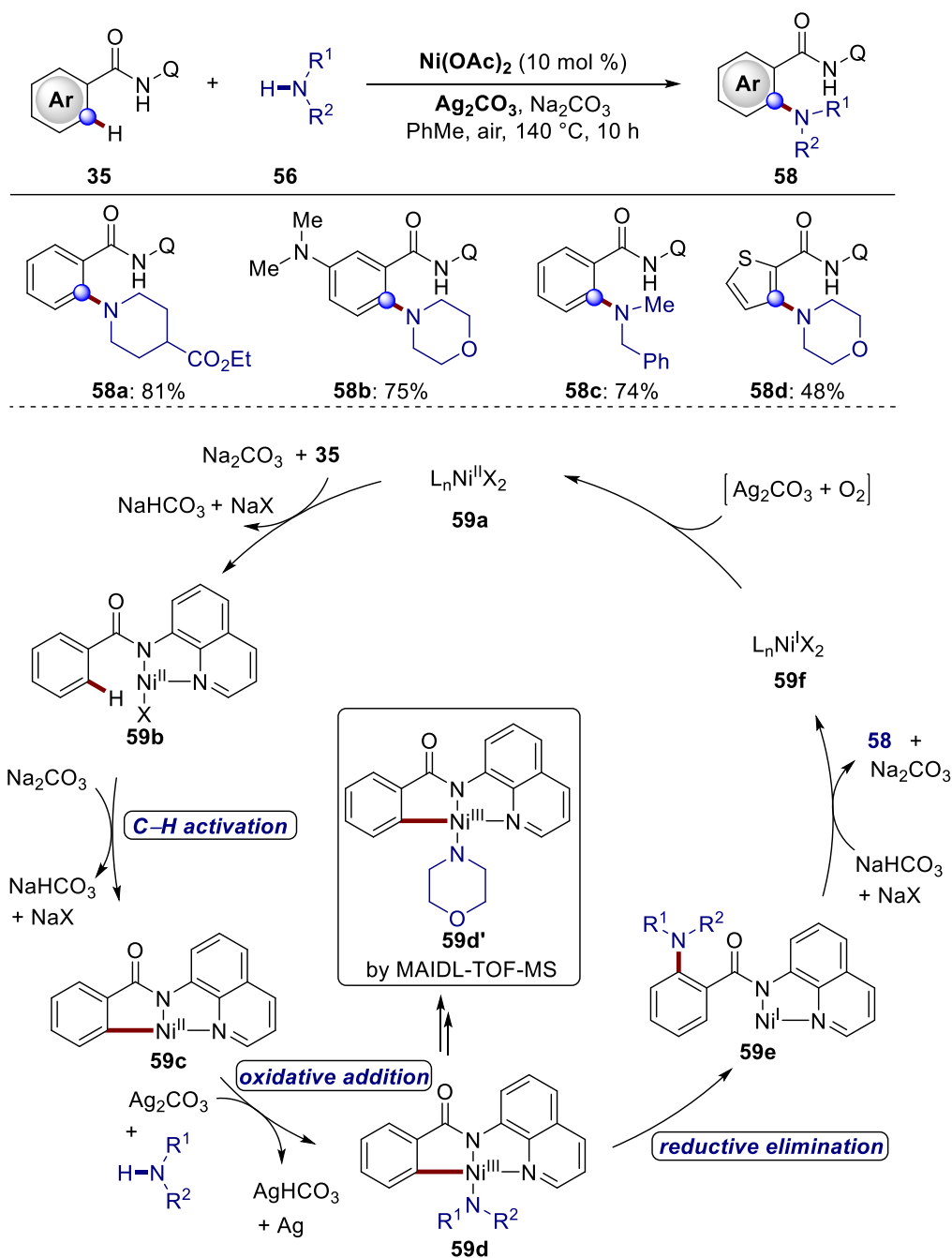


**Figure 1.3.14.** Nickel-catalyzed C–H amination of arenes and its mechanism.

Nickel-mediated C–H amination of arenes and olefins **35A** with sodium azide **60** in the presence of an 8-aminoquinoline directing group was firstly described by Tan and coworkers, providing access to primary anilines **62A** (Figure 1.3.15a).<sup>[116]</sup> One year later, the same group realized this transformative amination utilizing ammonia **61** as a cost- and atom-economical amino source under similar conditions (Figure 1.3.15b).<sup>[117]</sup>

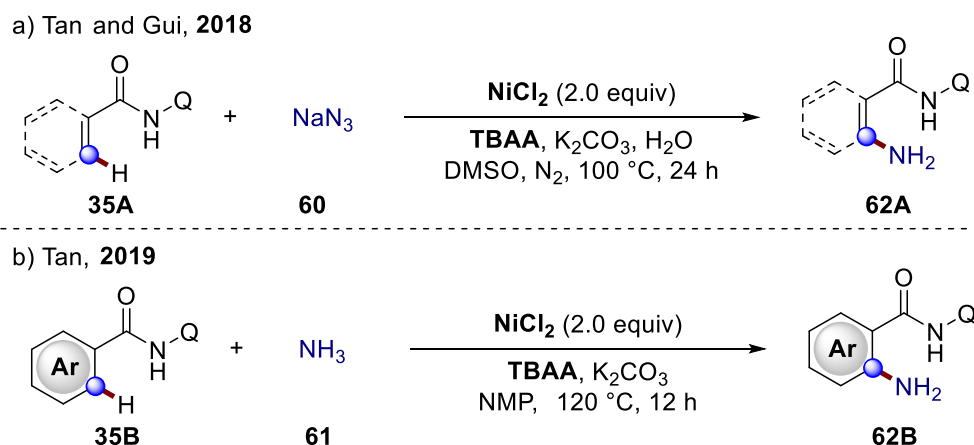


**Figure 1.3.15.** Nickel-catalyzed C–H amination for the synthesis of primary anilines **62**.

In 2014, Ge described a nickel-catalyzed intramolecular dehydrogenative C(sp<sup>3</sup>)–H amidation by 8-aminoquinoline assistance, gaining access to various  $\beta$ -lactams **64** (**Figure 1.3.16**).<sup>[117]</sup> The reaction showed a preference for activating the C–H bond of  $\beta$ -methyl groups, compared to the C–H bond of  $\beta$ -methylene and  $\gamma$ -methyl groups (**64a**) as well as the aromatic C–H bond (**64b**). Additionally, this protocol could achieve the selective activation of benzylic secondary C(sp<sup>3</sup>)–H bonds, albeit the more reactive  $\beta$ -methyl C–H bonds (**64c, d**).

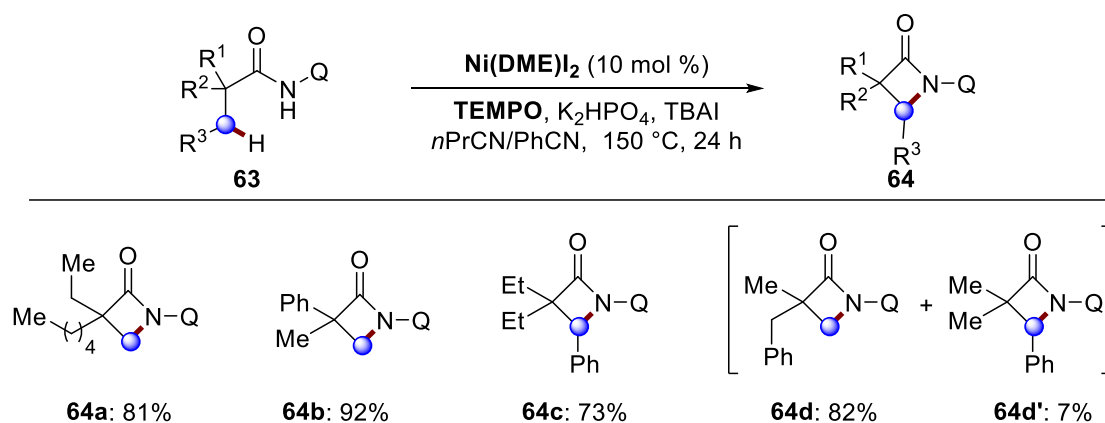


**Figure 1.3.16.** Nickel-catalyzed C–H amidation for the synthesis of  $\beta$ -lactams **64**.

### 1.3.3 Nickel-Catalyzed C–H Alkoxylation

C–O bond formations play a crucial role for the synthesis of pharmaceutical agents,<sup>[118]</sup> functional materials,<sup>[119]</sup> and natural products.<sup>[120]</sup> Classical cross-couplings like Buchwald–Hartwig,<sup>[10]</sup> Ullmann–Goldberg<sup>[11]</sup> and Chan–Evans–Lam reactions<sup>[12]</sup> have been well developed for the synthesis of various aryl ethers. The inherent drawbacks of cross-coupling reactions, e.g., the requirement of prefunctionalized substrates were already discussed in **chapter 1.1**. In the past decades, C–H activation as a step-economy and atom-economical synthetic strategy has gained tremendous achievements for the C–O formation.<sup>[121]</sup> Numerous studies mainly focused on the C–H acetoxylations,<sup>[122]</sup> hydroxygenations<sup>[123]</sup> and phenoxylation,<sup>[124]</sup> but the C–H alkoxylation was relatively underdeveloped due to the concomitant competition  $\beta$ -hydride elimination or overoxidation of alcohols. During the transition metal-catalyzed C–H alkoxylation, palladium, copper and cobalt were frequently explored as the catalysts with the strategy of installing chelating assistances, which were shown in **Figure 1.3.17–1.3.19**.

Diverse monodentate directing groups containing oxygen and nitrogen atoms were successfully designed by many groups for the palladium-catalyzed oxidative C–H alkoxylation of unactivated arenes with primary or secondary alcohols, providing various aryl ethers (**Figure 1.3.17a–r**).<sup>[125]</sup> In most cases, alcohols were employed as the solvents, and only primary alcohols or several simple secondary alcohols, such as *i*PrOH and HFIP were converted smoothly. In contrast to the considerable achievements by palladium catalysis, copper was less investigated for the C–H alkoxylation (**Figure 1.3.17s, t**).<sup>[126]</sup>

## 1. Introduction

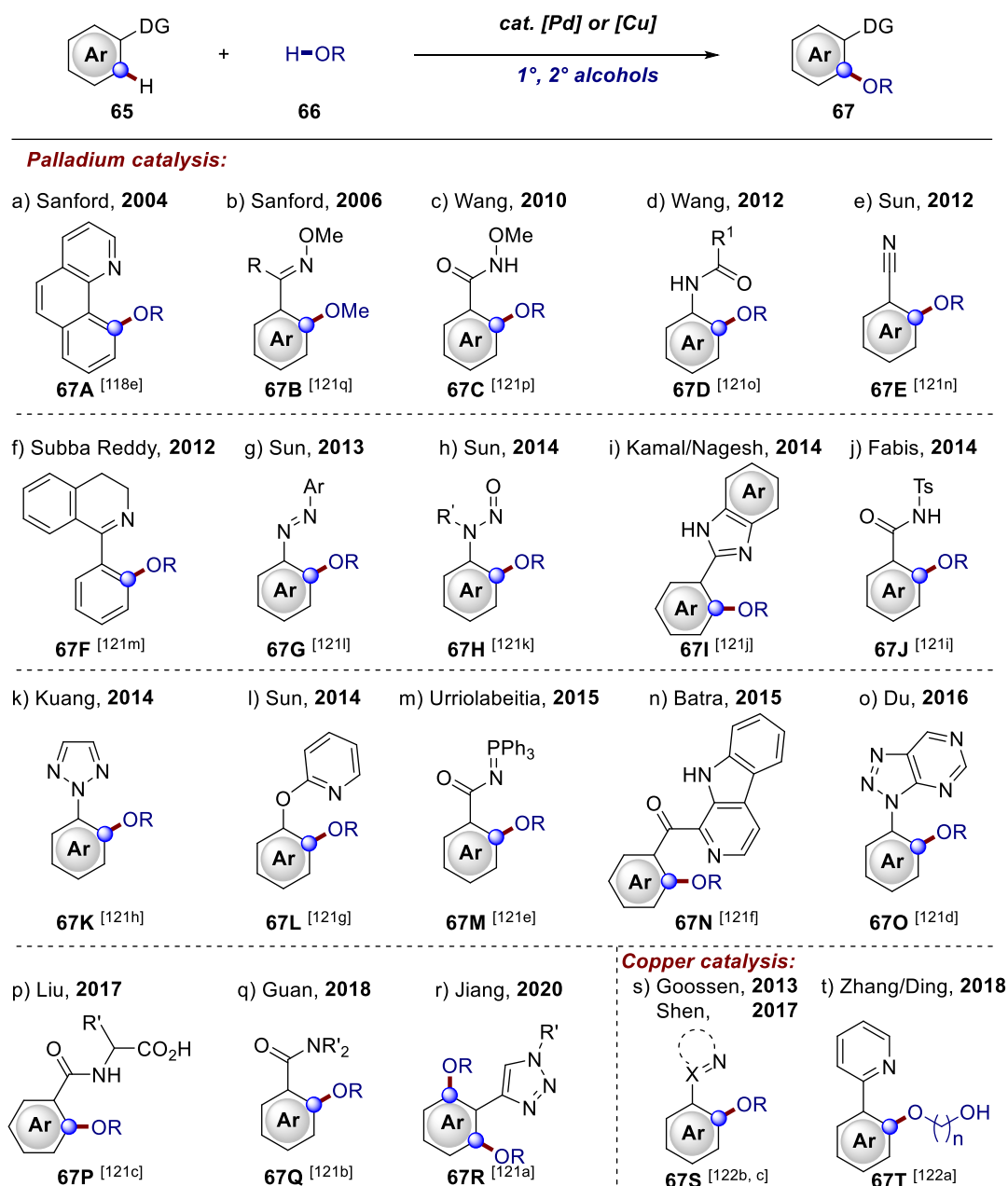
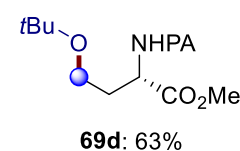
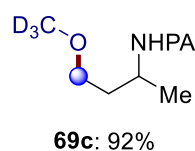
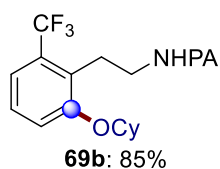
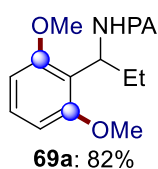
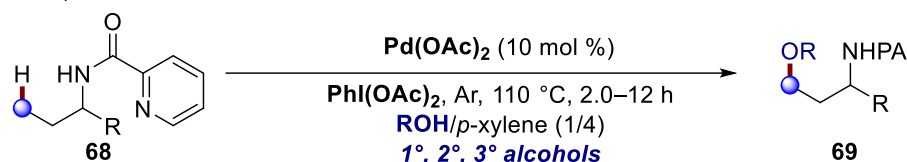


**Figure 1.3.17.** Palladium, and copper-catalyzed C–H alkoxylation with alcohols **66** using various monodentate directing groups.

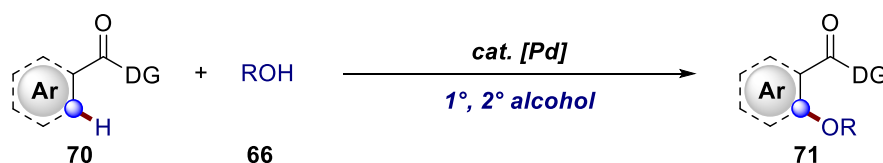
Compared to monodentate chelation assistances, bidentate directing groups were more useful and powerful for the C(sp<sup>2</sup>)–H and C(sp<sup>3</sup>)–H alkoxylation without affecting the resulting molecular structures, since they were readily removable (**Figure 1.3.18**).<sup>[127]</sup> In 2012, Chen employed picolinamide **68** as a *N,N*-bidentate directing group to synthesize alkyl ethers **69** via palladium-catalyzed C(sp<sup>2</sup>)–H and C(sp<sup>3</sup>)–H activation with primary, secondary and even tertiary alcohols (**Figure 1.3.18a**).<sup>[127d]</sup> In 2013, the PIP auxiliary was successfully developed by the Shi group for functionalizing

C(sp<sup>2</sup>)-H and C(sp<sup>3</sup>)-H bonds of carboxylic acid derivatives, thus furnishing the desired products **71A** (Figure 1.3.18b).<sup>[127c]</sup> Later, AQ was exploited by Rao and coworkers to achieve palladium-catalyzed C(sp<sup>3</sup>)-H alkoxylation using cyclic hypervalent iodine reagents **72a** or **72b** as oxidants for the synthesis of symmetric and unsymmetric acetals **71B**, **71C** (Figure 1.3.18c, d).<sup>[127a, 127b]</sup>

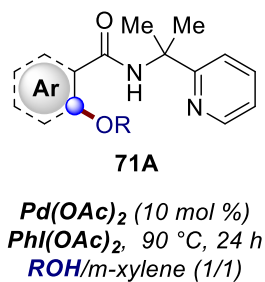
Amines: a) Chen, 2012



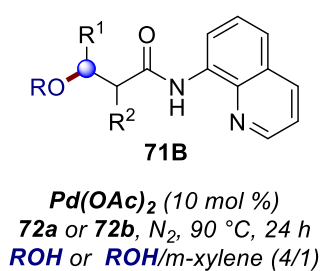
Carboxylic Amides:



b) Shi, 2013



c) Rao, 2013



d) Rao, 2014

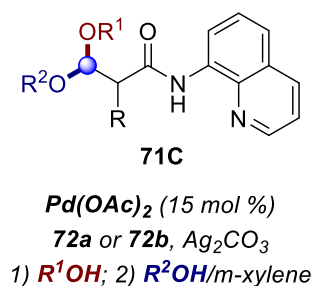


**Figure 1.3.18.** Palladium-catalyzed C(sp<sup>2</sup>)-H and C(sp<sup>3</sup>)-H alkoxylation using removable bidentate directing groups. **72a** = 1-methoxy-1,2-benziodoxole-3(1H)-one, **72b** = 1-acetoxy-1,2-benziodoxole-3(1H)-one.

Not limited to precious 4d transition metals, inexpensive and Earth-abundant 3d transition metals, for example, copper<sup>[124b, 128]</sup> and cobalt<sup>[129]</sup> were also utilized to catalyze oxidative C(sp<sup>2</sup>)-H alkoxylation with the assistance of bidentate auxiliaries (Figure 1.3.19a–h). Notably, Song and Niu reported the first cobalt-catalyzed C–H alkoxylation of olefins under mild condition (Figure 1.3.19d).<sup>[129e]</sup>

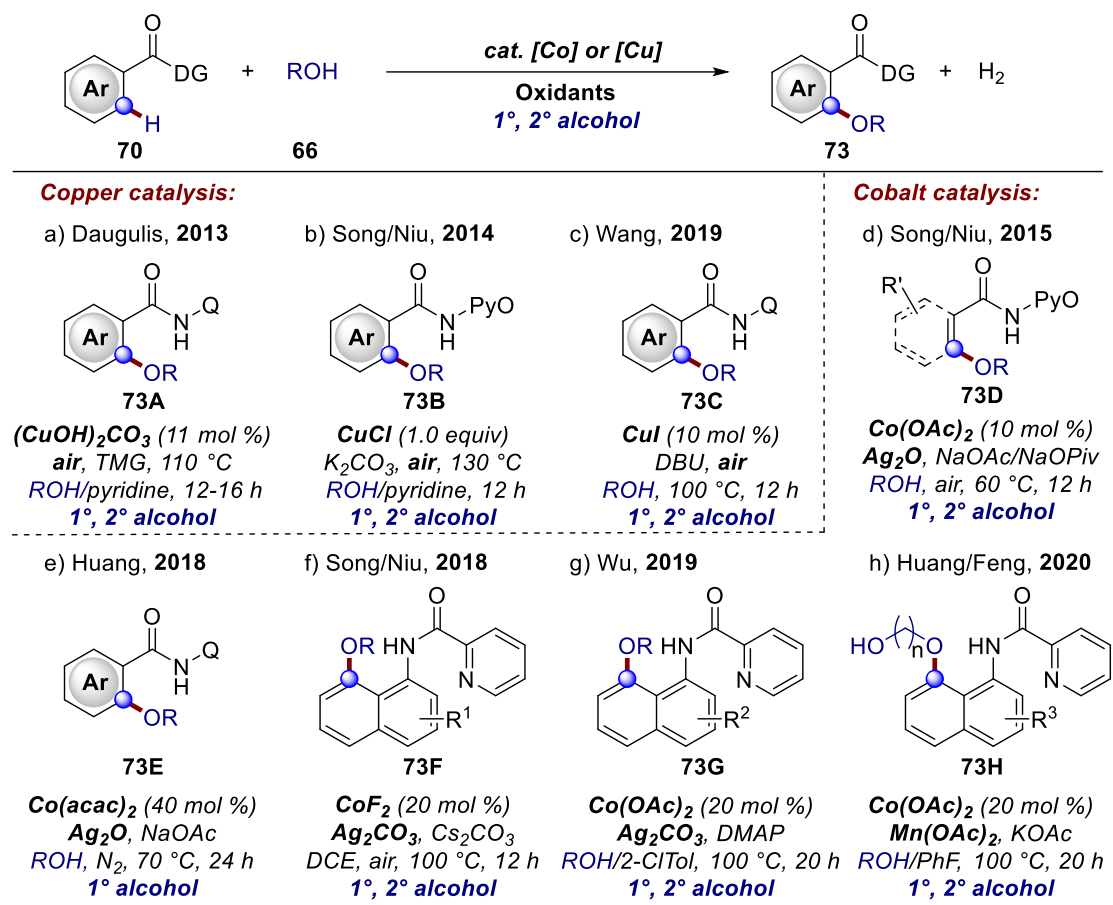


**Figure 1.3.19.** Copper or cobalt-promoted C(sp<sup>2</sup>)-H alkoxylation using bidentate directing groups.

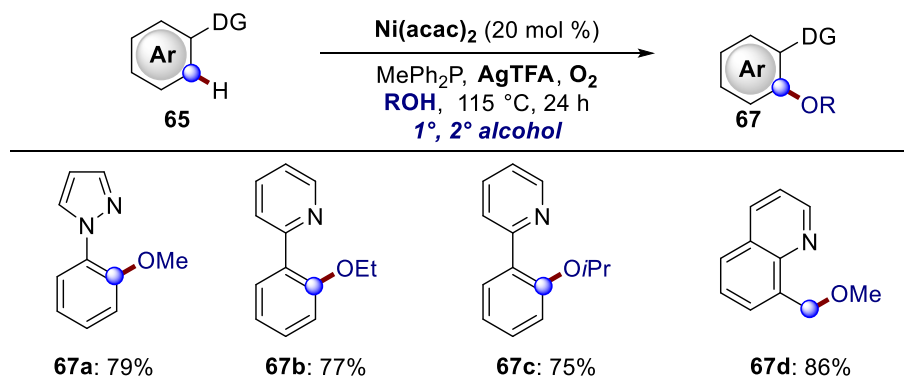
In comparison to the progress that palladium, cobalt and copper have achieved, nickel-catalyzed C-H alkoxylation continued to be scarce, and so far only two examples were reported (**Figure 1.3.20**).<sup>[130]</sup> In 2019, Cai reported the nickel catalyzed C-H alkoxylation of arenes with primary alcohols and one secondary alcohol *i*PrOH in the presence of monodentate chelation assistance (**Figure 1.3.20a**).<sup>[130a]</sup> Additionally, other C-O formations, like acetoxylations and acyloxylations were also realized with slightly modified conditions.<sup>[130a]</sup> Sundararaju described a bidentate-assisted nickel-catalyzed C-H alkoxylation of unactivated arenes **35** with primary alcohols employing the stoichiometric amounts of silver(I) oxidants, providing an alternative approach for the synthesis of aryl ether **73E** (**Figure 1.3.20b**).<sup>[130b]</sup>

Although considerable improvements on C-H alkoxylation have been achieved by transitional metals, these C-O transformative synthesis were limited to use primary alcohols or simple less-bulky alcohols and required the over-stoichiometric amounts of



alcohols, commonly used as solvents, to increase the catalytic efficiency.

a) Cai, 2019



b) Sundararaju, 2018

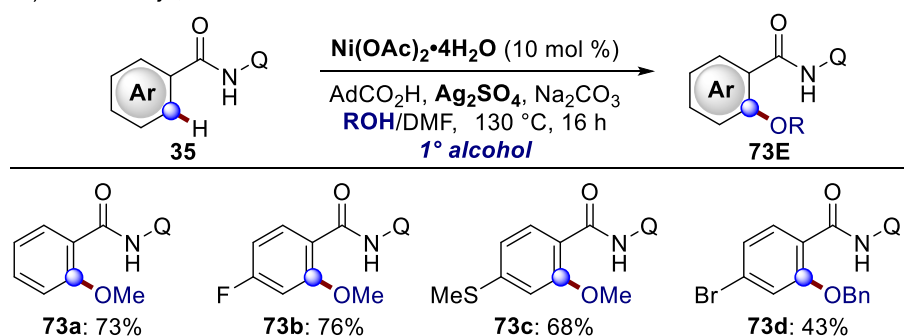


Figure 1.3.20. Nickel-catalyzed C–H alkoxylation using chelation assistance.

### 1.3.4 Nickel-Catalyzed C–H Phosphorylation

Arylphosphonate derivatives are widely used in pharmaceutical and agrochemical industry,<sup>[131]</sup> material chemistry,<sup>[132]</sup> and ligand design.<sup>[133]</sup> Although significant advances have been made from the early contribution by Hirao<sup>[134]</sup> for the synthesis of organophosphorus compounds, C–H phosphorylation avoiding prefunctionalized materials was highly desirable due to its consistency with the concept of green chemistry. The strong coordination property of organophosphorus molecules that could easily poison a transition metal catalyst resulted in the fact that C–H phosphorylation remained so far underdeveloped.<sup>[135]</sup> Therefore, developing new methodologies were very significant and attractive.

In 2013, Yu and coworkers described the palladium-catalyzed intermolecular C–H phosphorylation of unactivated arenes **13** with *H*-phosphonates and diaryl phosphine oxides **74**, which were added slowly by a syringe pump to minimize the deactivation of

the catalyst (**Figure 1.3.21**).<sup>[136]</sup> In addition, AgOAc and BQ were mandatory for accomplishing this C–P transformation.

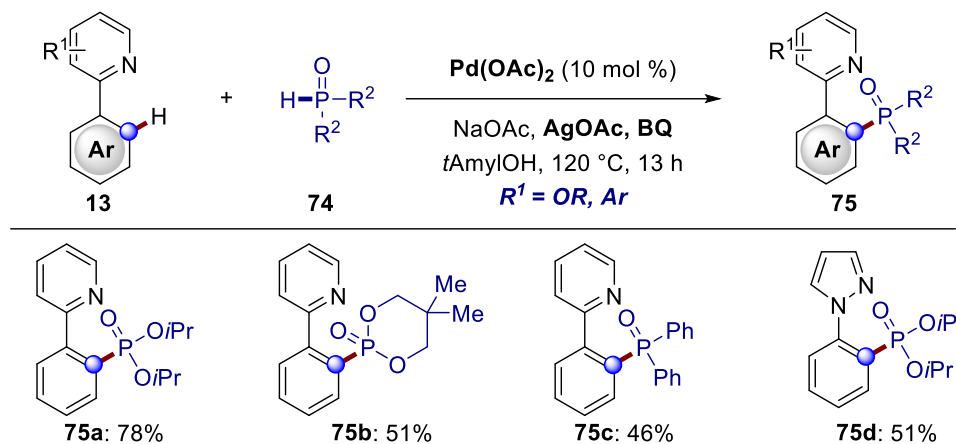
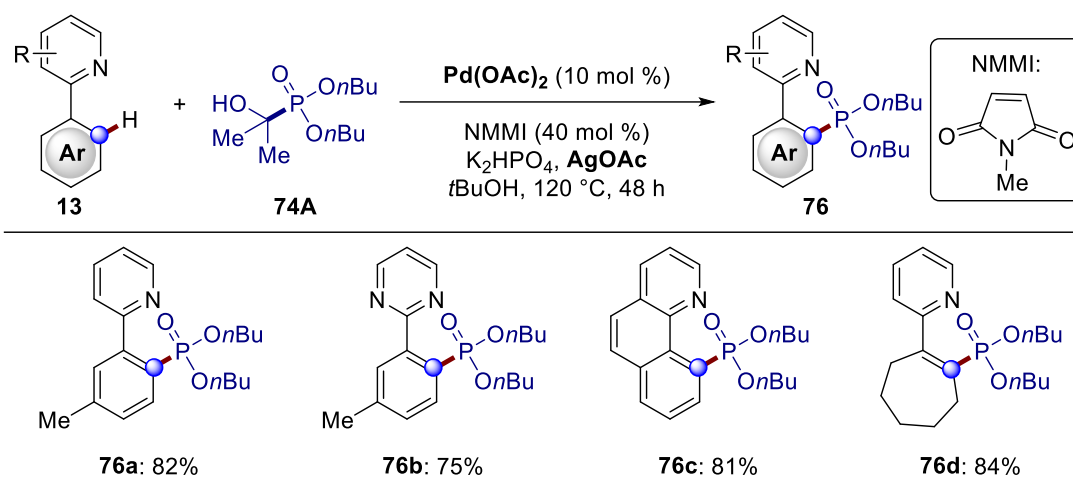


**Figure 1.3.21.** Palladium-catalyzed C–H phosphorylation with slow addition of phosphonating reagents **74**.

At the same time, Murakami introduced a one-pot method to obtain the arylphosphonates **76** in the presence of palladium-silver catalytic system by a masked, slow-releasing phosphonating reagent hydroxyalkylphosphonate **74A**, which could avoid palladium catalyst being poisoned (**Figure 1.3.22a**).<sup>[137]</sup> In 2016, Hong successfully developed this strategy of a masked, slow-releasing phosphonating reagents for rhodium-catalyzed C–P transformations with the assistance of silver(I) oxidants, providing access to the corresponding arylphosphonates **78** (**Figure 1.3.22b**).<sup>[138]</sup> The substrates bearing distinct nitrogen-coordinating groups, including late-stage functionalized substituents were well investigated.

In 2014, Chen and Yu reported a copper-catalyzed C–P formation of arenes **35** through the sequential addition of *H*-phosphonates **74C** (**Figure 1.3.23**).<sup>[139]</sup> The construction of arylphosphonate derivatives **79** was accomplished employing silver salts and *N*-methylmorpholine oxide as co-oxidants and the AQ moiety as a directing group.

a) Murakami, 2013



b) Hong, 2016

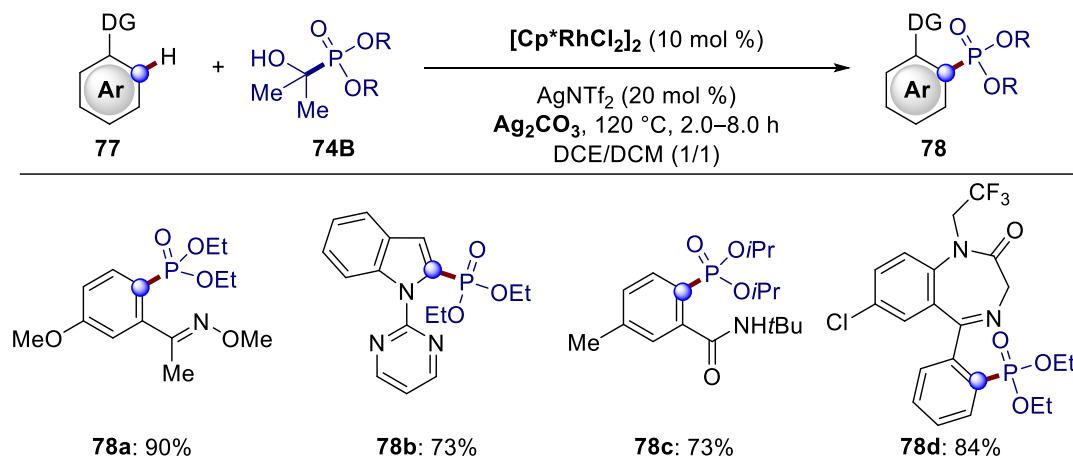


**Figure 1.3.22.** Palladium and rhodium-catalyzed C–H phosphorylation with masked phosphorylation reagents **74A**, **74B**.

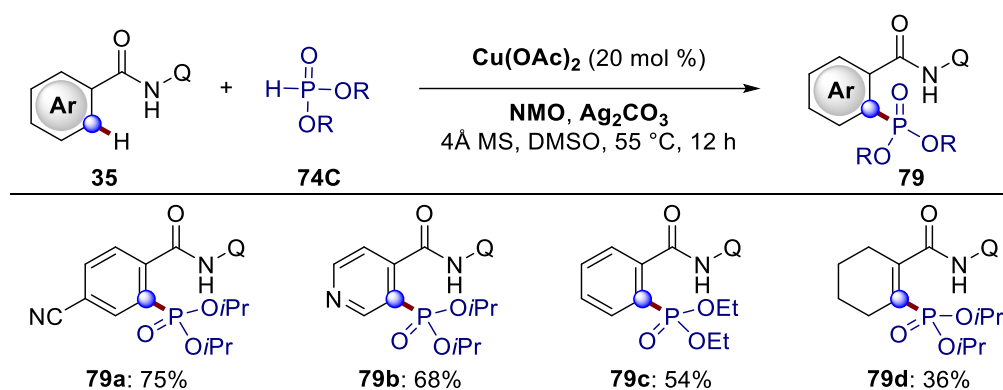


**Figure 1.3.23.** Copper-catalyzed C–H phosphorylation by sequential addition of *H*-phosphonates **74C**.

## 1.4 Oxidative C–H Activation by Metalla-Electrocatalysis

Oxidative C–H/C–H and C–H/Het–H activation reactions have obtained considerable advances due to the use of non-prefunctionalized starting materials.<sup>[18]</sup> However, oxidative C–H activations generally required stoichiometric amounts of expensive and toxic metal oxidants, such as copper and silver salts for the regeneration of the active metal catalyst, which compromised the overall sustainable nature of organic synthesis. Since early contributions from Volta,<sup>[140]</sup> Kolbe,<sup>[141]</sup> and Faraday,<sup>[142]</sup> electrosynthesis with inexpensive and waste-free electricity as a viable redox equivalent has recently experienced a renaissance, holding the huge potential to accomplish excellent levels of oxidant and resource economy.<sup>[143]</sup> Compared with the classical substrate-controlled electrosynthesis, metalla-electrocatalysis sets the stage for transition metal-controlled position-selective oxidative C–H activations.<sup>[144]</sup>

At the outset of this thesis, electrocatalytic C–H activation by nickel catalysis was so far unknown.<sup>[145]</sup> The next part will provide an introduction about electrooxidative C–H activation by other transition metals.

### 1.4.1 Pallada-Electrooxidative C–H Activation

In 2007, Amatore and Jutand made a pioneering contribution on the electrooxidative C–H activation by palladium catalysis (**Figure 1.4.1**).<sup>[146]</sup> They successfully modified the Fujiwara-Moritani-type reaction<sup>[147]</sup> with electric current as a redox equivalent to replace expensive silver(I) and copper(II) oxidants, albeit with a limited scope.

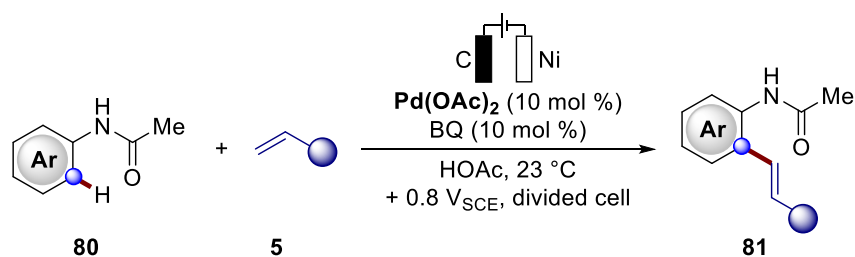


**Figure 1.4.1.** Pallada-electrochemical C–H olefination.

During the last decade, the powerful pallada-electrocatalysis was well developed with the assistance of distinct directing groups to achieve C–H activation for carbon–carbon formation<sup>[148]</sup> like arylation, alkylation and olefination, as well as carbon–heteroatom formation, represented by halogenation, phosphorylation and acetoxylation (**Figure 1.4.2**).<sup>[149]</sup> The pyridine-assisted electrocatalytic C–H halogenation with HX or I<sub>2</sub> was described by Kakiuchi and coworkers (**Figure 1.4.2a, b**),<sup>[149h, 149i]</sup> and this protocol was further developed under bidentate directing groups by the Kakiuchi and Mei with distinct halogenating reagents (**Figure 1.4.2h, k**).<sup>[149b, 149d, 149g]</sup> The versatility of pyridine chelation group was not only explored for C–H halogenation of arenes by pallada-electrocatalysis, but also for electrocatalytic intermolecular C–H arylation,<sup>[149e]</sup> phosphorylation<sup>[149e]</sup> and alkylation (**Figure 1.4.2c, d, j**).<sup>[149e]</sup> Moreover, pyridine was also developed for the intramolecular C–H amination by Lei in 2020 (**Figure 1.4.2i**).<sup>[149e]</sup> Noteworthy, in 2017, Mei reported the palladium-catalyzed electrochemical C(sp<sup>3</sup>)–H oxygenation under mild conditions in a divided cell, providing various oxygen-containing molecules (**Figure 1.4.2e**).<sup>[149e]</sup> To accomplish the C–O formation, oxime was employed as the directing groups, which was subsequently employed for the C–H acetoxylation<sup>[149e]</sup> and alkylation by the same group (**Figure 1.4.2f, g**).<sup>[149e]</sup> Another example of electrooxidative C(sp<sup>3</sup>)–H oxygenation of 8-methylquinoline with TMAOAc was introduced by the Sanford group (**Figure 1.4.2i**).<sup>[149c]</sup>

Rather recently, the first asymmetric electrochemical C–H olefination with palladium catalysis was described by the Ackermann group *via* a transient directing group, offering an expedient access to enantioenriched BINOLs, dicarboxylic acids and helicenes **84a–84c** (**Figure 1.4.3**).<sup>[148a]</sup>

# 1. Introduction

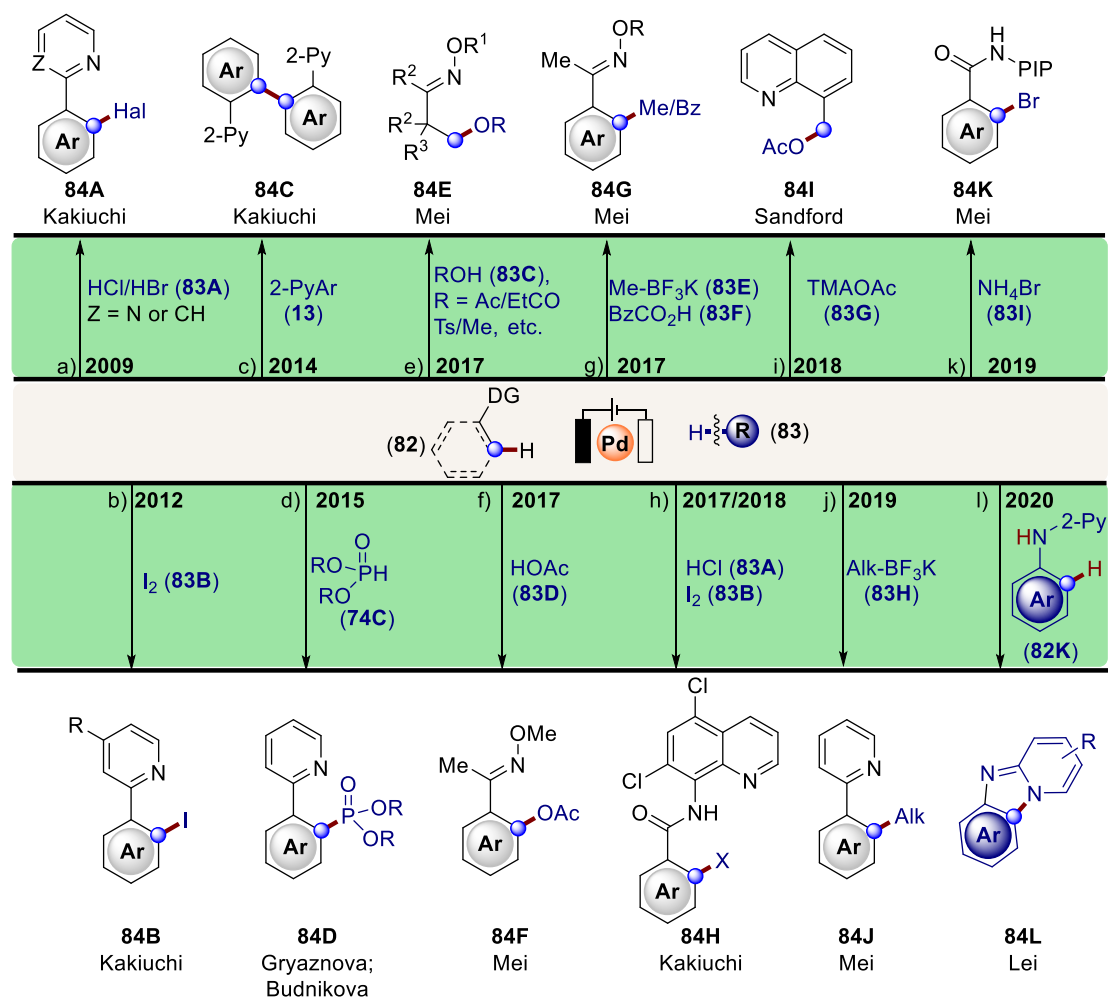


Figure 1.4.2. Pallada-electrooxidative C–H activation.

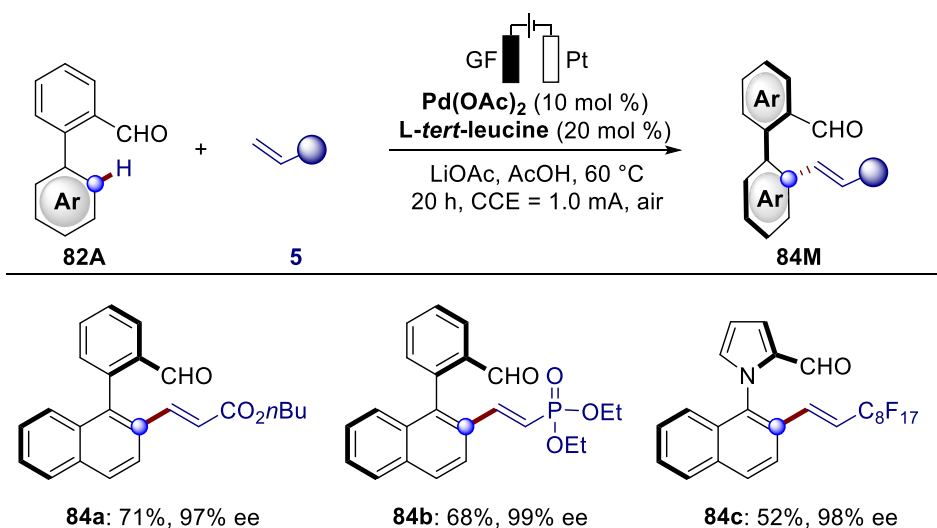
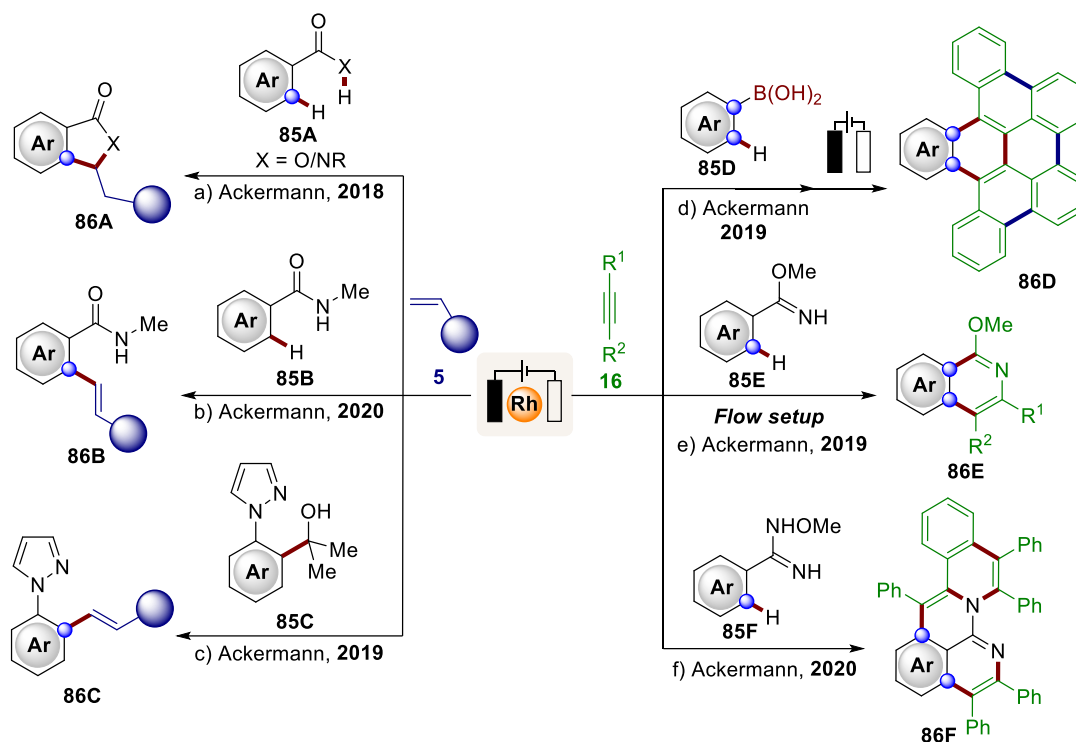


Figure 1.4.3. Asymmetric pallada-electrooxidative C–H activation.

## 1.4.2 Rhoda-Electrooxidative C–H Activation

During last three years, rhoda-electrooxidative C–H activations has been well investigated by Ackermann (**Figure 1.4.4**). The weak coordination was found to be efficient for rhoda-electrocatalytic C–H transformations. In 2018, an air-stable Cp\*Rh(III) was firstly employed as electrocatalyst by Ackermann for the C–H/O–H alkene annulation of weakly coordinating benzoic acids **85A** with ample scope in a dehydrogenative manner (**Figure 1.4.4a**).<sup>[150]</sup> The direct cross-dehydrogenative couplings between olefins **5** and benzamides **85B** bearing both electron-rich and electron-poor substituents were also established with rhodaelectro-catalyst by the same group in 2020 (**Figure 1.4.4b**).<sup>[151]</sup> Not limited to electrocatalytic C–H activation, the challenging electrooxidative C–C cleavage for the synthesis of aryl alkenes **86C** under electricity was achieved with the versatile rhodium catalysis manifold by the Ackermann group, producing molecular hydrogen as the sole byproduct (**Figure 1.4.4c**).<sup>[152]</sup>

The very recent rhoda-electrocatalysis by the same group for the synthesis of structurally diversified polycyclic aromatic hydrocarbons (PAHs) in the absence of directing groups through cascade C–H annulations showed an outstanding level of chemo-selectivity (**Figure 1.4.4d**).<sup>[153]</sup> This transformation allowed the diverse novel nonplanar substituted PAHs being prepared from the easily accessible alkynes **16** and boronic acids **85D**. In 2020, a modular assembly of nitrogen-doped polycyclic aromatic hydrocarbons (aza-PAHs) **85F** was introduced by the same group through a combination of rhodium-catalyzed electrochemical cascade C–H activation and alkyne annulation (**Figure 1.4.4f**).<sup>[154]</sup> In 2019, a flow-rhodaelectro-catalyzed C–H functionalization of weakly coordinating imidates **85E** with alkynes was firstly established, which showed the potential for scale up in industries (**Figure 1.4.4e**).<sup>[155]</sup>



**Figure 1.4.4.** Rhoda-electrooxidative C–H activation.

Rhoda-electrocatalysis was employed not only for the C–C formation, but also for construction of C–Het bonds.<sup>[156]</sup> In 2019, Xu group elegantly reported a rhodium-catalyzed electrooxidative aryl C–H phosphorylation with different types of phosphorylating reagents **74D**, providing a convenient access to bioactive arylphosphonates **87a–87g** (**Figure 1.4.5**).<sup>[156]</sup> Various nitrogen-containing directing groups, like pyridazine, pyridine, pyrazole, purine and aminopyridine were put into practice and in a dehydrogenative fashion. Moreover, hundred gram-scale experiments were performed well, with a huge potential for the synthesis in industry, albeit with a decreased yield (**75c**).



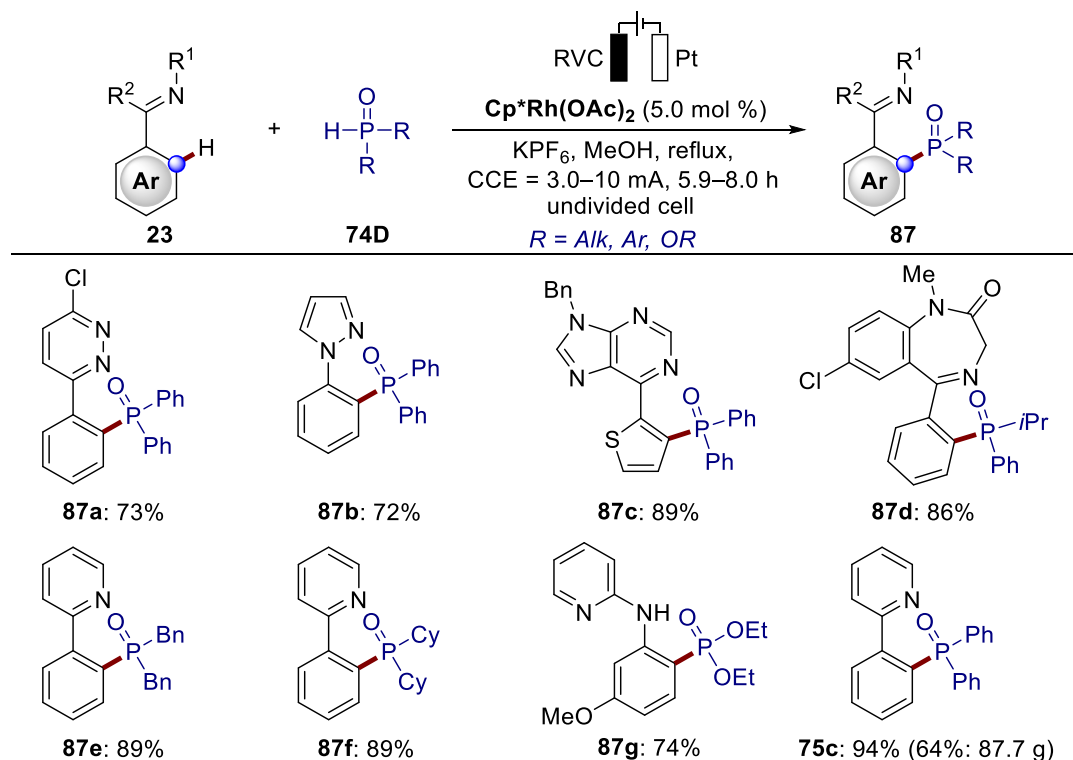


Figure 1.4.5. Rhoda-electrooxidative C–H phosphorylation.

### 1.4.3 Ruthena-Electrooxidative C–H Activation

Pioneering contributions on ruthena-electrooxidative C–H activation were made independently from Xu and Ackermann.<sup>[157]</sup> In 2018, Xu and coworkers employed electricity as redox reagent to promote the ruthenium-catalyzed C–H/N–H activation for alkyne annulation, leading to the cost-effective preparation of indole derivatives **89A** (Figure 1.4.6a).<sup>[157a]</sup> Concurrently, Ackermann reported the first weak O-coordinated ruthenium-catalyzed electrooxidative C–H/O–H activation/alkyne annulations of accessible benzoic acids **88B** as well as benzamides **88B'**, furnishing the desired six-membered heterocycles **89B** (Figure 1.4.6b).<sup>[157b]</sup>

This strategy proved to be broadly applicable for ruthenium-enabled electrooxidative C–H activation of phenols or aromatic carbamates **88C**, benzylic alcohols **88D** and imidazoles **88E** with alkynes **16** (Figure 1.4.6c–e).<sup>[158]</sup>

In 2019, Tang described a ruthena-electrocatalyst enabled dehydrogenative double C–H/N–H functionalization of benzoylamide **88F** with internal alkynes to gain polycyclic isoquinolinones **89F** (Figure 1.4.6f).<sup>[159]</sup> This electrocatalytic transformation was performed with high regioselectivity through the generation of intermediate **89F'**.

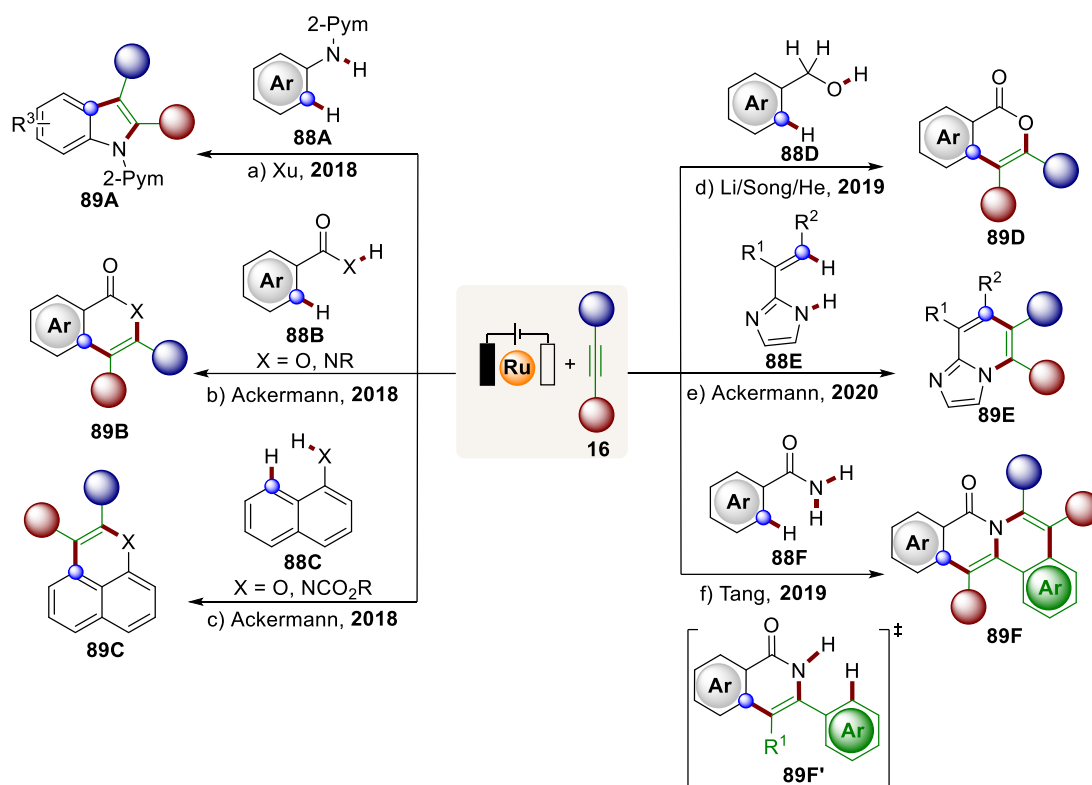


Figure 1.4.6. Ruthena-electrooxidative C–H/X–H annulation. (X = N, O).

In general, these C–H/N–H or C–H/O–H activations for alkyne annulations were accessed with outstanding levels of chemo- and site-selectivity, providing an alternative procedure for various useful heterocycles in a resource-economical fashion.

#### 1.4.4 Irida-Electrooxidative C–H Activation

5d Transition metal iridium also proved to be particularly effective for the electrocatalytic C–H activation. In 2018, Ackermann made a pioneering contribution on the irida-electrocatalysis for C–H alkenylation of weak coordinating benzoic acids **85B** with alkenes **5**, producing a series of 5-membered heterocycles **90A** (Figure 1.4.7a).<sup>[160]</sup> Remarkably, the chemo-selectivity was improved by the use of benzoquinone as a redox mediator. One year later, the Mei group demonstrated the iridium-catalyzed electrooxidative vinylic C–H annulation with alkynes **16** by an

undivided cell setup, affording various  $\alpha$ -pyrones **90B** in a cross-dehydrogenative and resource-economic manner (Figure 1.4.7b).<sup>[161]</sup> Very recently, the direct iridium-catalyzed electrooxidative C–H alkylation of arenes **23** with terminal alkyne **40D** was achieved by Xie and Shi, providing diverse aromatic alkynes **90C** (Figure 1.4.7c).<sup>[162]</sup>

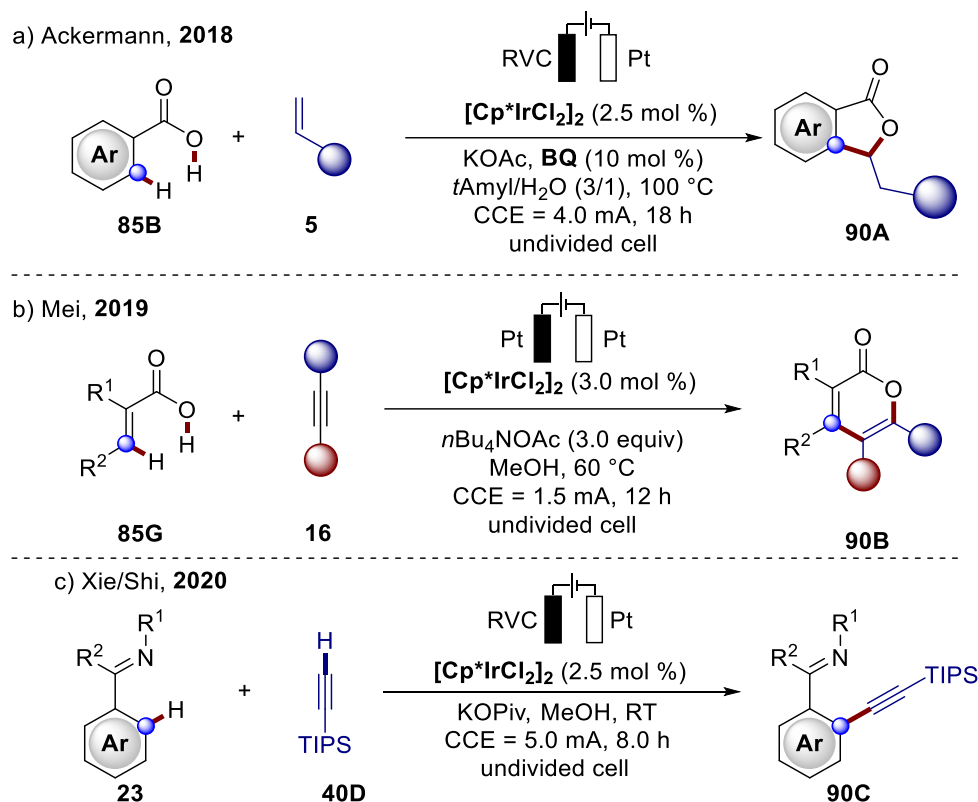


Figure 1.4.7. Irida-electrooxidative C–H/O–H annulation.

### 1.4.5 Cobalta-Electrooxidative C–H Activation

In comparison with the precious 4d and 5d transition metals, the development of less toxic, Earth-abundant and cost-effective 3d metals in the electrocatalysis is more challenging.

The first 3d metalla-electrocatalysis for C–H activation was achieved with cobalt catalysis by the group of Ackermann in 2017, which was actually reported before many other transition metals except palladium.<sup>[163]</sup> The cobalta-electrooxidative C–H alkoxylation with primary alcohols **66** using a *N,O*-bidentate auxiliary could be performed at ambient temperature, producing molecular hydrogen as the sole waste and avoiding stoichiometric amounts of silver(I) or copper(II) salts (Figure 1.4.8).<sup>[163]</sup>

Not limited to aryl C–H oxygenation, alkenes were also identified as highly-effective substrates for the construction of alkenyl ethers **73** (Figure 1.4.8).

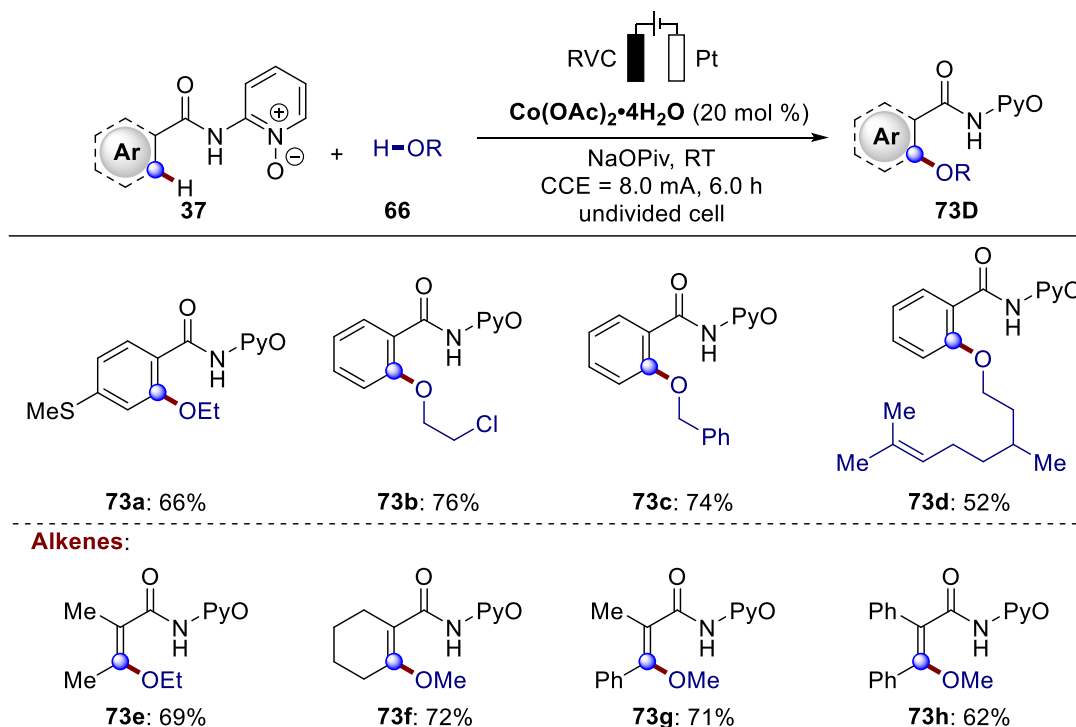


Figure 1.4.8. Cobalt-electrooxidative aryl and vinylic C–H oxygenation.

During the last 3 years, considerable advances on cobalt-electrocatalyzed C–H activations for the construction of C–C<sup>[164]</sup> and C–Het bonds<sup>[165]</sup> were gained by Ackermann and other groups (Figure 1.4.9). Cobalt-electrocatalysis was extremely effective for the C–H/N–H annulation of arene and olefin derivatives **91** with alkynes,<sup>[164d, 164f, 164i]</sup> alkenes,<sup>[164g]</sup> allenes,<sup>[164a, 164h]</sup> carbon monoxide or isocyanides<sup>[164c, 164e]</sup> to obtain biorelevant heterocycles (Figure 1.4.9a–c, f–g, i–k). The robust cobalt catalysis also electrochemically enabled the C–H allylation with inert alkenes **92D** for the C–C bond construction (Figure 1.4.9i).<sup>[164b]</sup> In 2018, Ackermann and Lei group reported the cross-dehydrogenative coupling between arenes **91** and secondary amines **56** with different directing groups (*N,O*- or *N,N*-coordinating auxiliaries) for the C–Het formation (Figure 1.4.9d, e).<sup>[165b, 165c]</sup> One year later, Ackermann described a cobalt-catalyzed the C–O formation for electrochemically promoted C–H acyloxylation (Figure 1.4.9h).<sup>[165a]</sup>

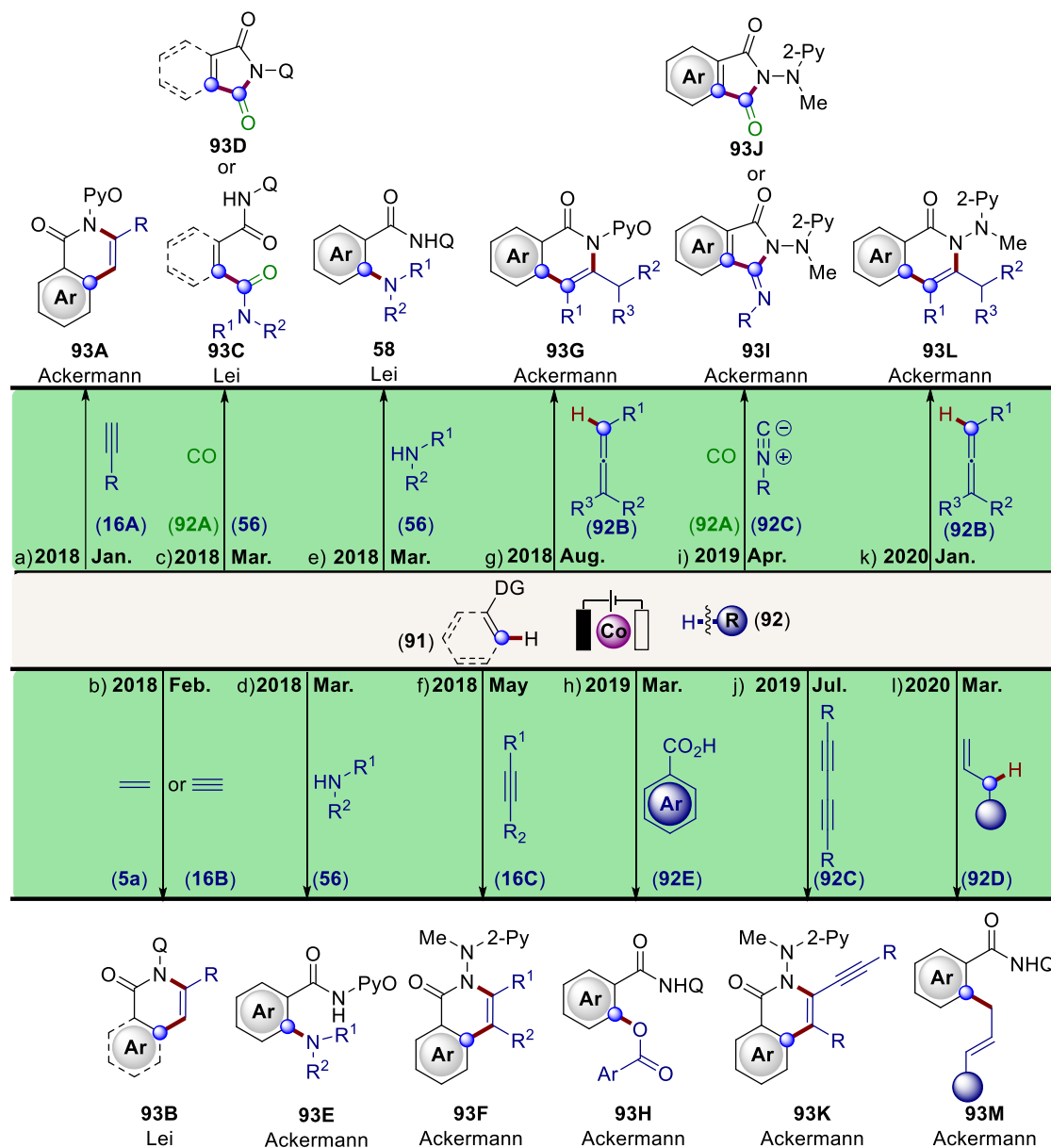


Figure 1.4.9. Cobalta-electrooxidative C–H activation.

In general, a bidentate chelation assistance is essential for accomplishing the selective C–H transformation by cobalta-electrocatalysis.

### 1.4.6 Cupra-Electrooxidative C–H Activation

The first electricity-mediated C–H activation by copper catalysis was reported by Mei and coworkers in 2018.<sup>[166]</sup> Using a strategy of installing a directing group, the copper-catalyzed electrooxidative C–H amination of anilines **94** was achieved with a mild condition for the synthesis of aromatic amines **95A** in an atom- and step-economical fashion (Figure 1.4.10a).<sup>[166]</sup> A redox mediator-free condition was applied by Nicholls

for the cupra-electrooxidative C–H amination of benzamides **35** with AQ as a directing group, producing the molecular hydrogen as the sole and benign byproduct (**Figure 1.4.10b**).<sup>[167]</sup>

Recently, the group of Ackermann established the first cupra-electrochemical C–H/N–H alkyne annulation to gain the bioactive five-membered isoindolones **95B** in both dehydrogenative and decarboxylative manner (**Figure 1.4.10c, d**).<sup>[168]</sup>

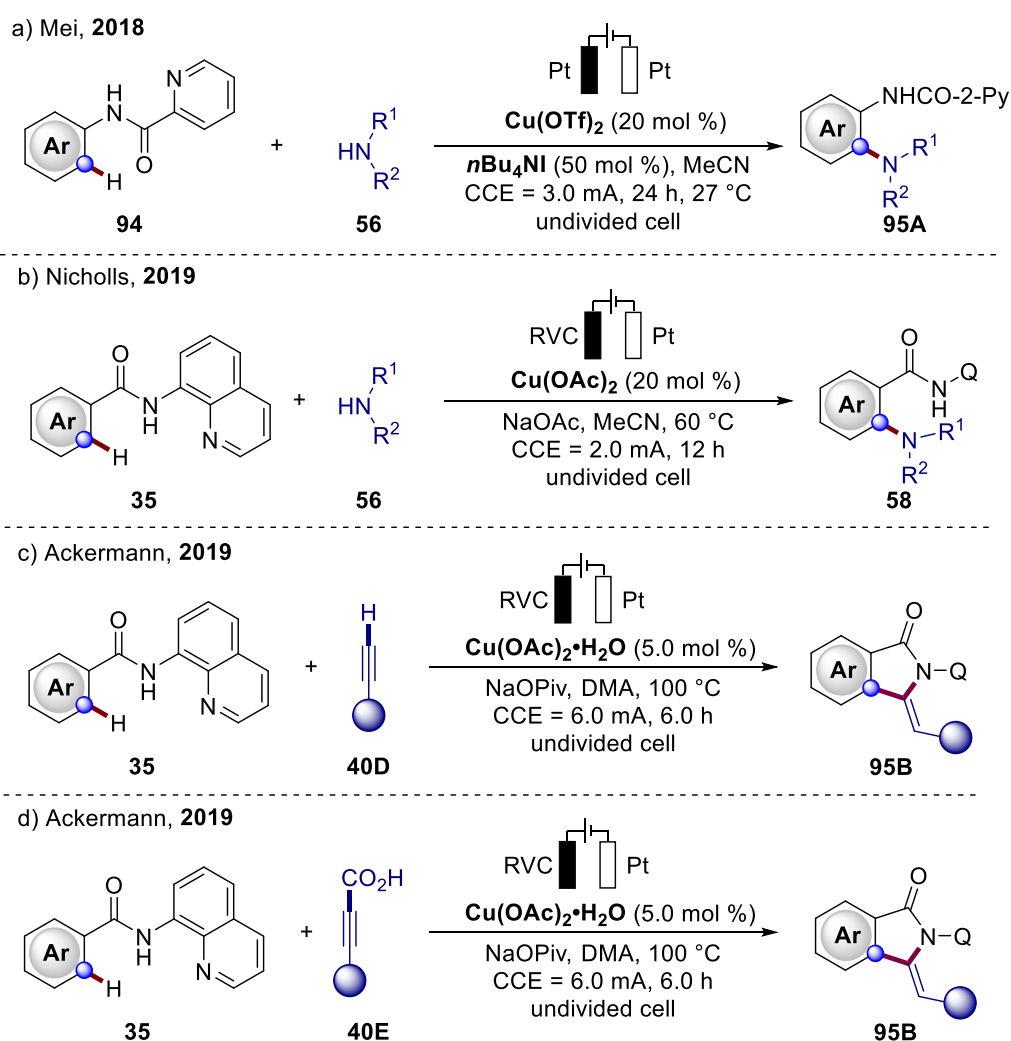


**Figure 1.4.10.** Cupra-electrooxidative C–H activation.

### 1.4.7 Ferra-Electrooxidative C–H Activation

Iron is the most naturally abundant transition metal, explored by Ackermann group in 2019 for the electrochemical C–H transformation.<sup>[169]</sup> They described a ferraelectrocatalyzed C–H arylation with Grignard reagent **15E** for the synthesis of biaryls **97A**,

which avoided the use of cost-intensive dichloro-*iso*-butane (DCIB) as oxidant (**Figure 1.4.11**).<sup>[169]</sup>

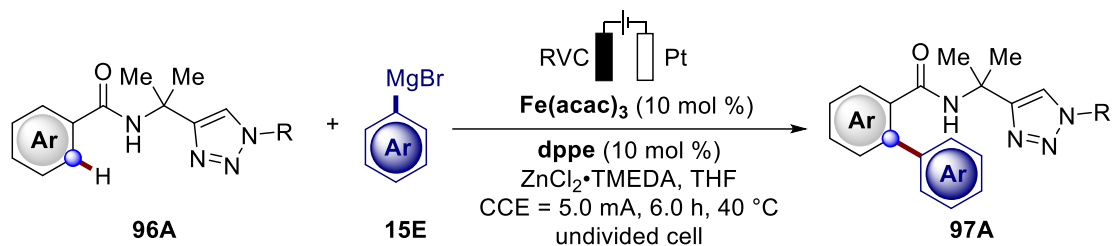


**Figure 1.4.11.** Ferra-electrooxidative C–H activation.

### 1.4.8 Manganese-Electrooxidative C–H Activation

Having established the C–C formation by ferra-electrocatalysis, Ackermann group found that the non-toxic  $\text{MnCl}_2$  was effective for the transformative C–H arylation of picolinic acids under a slightly modified conditions (**Figure 1.4.12**).<sup>[169]</sup>

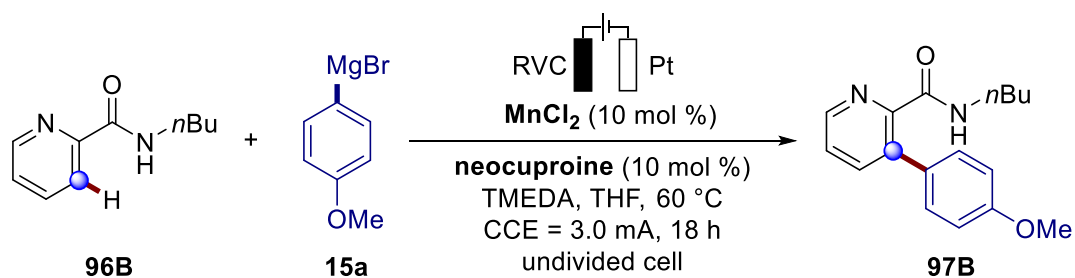


**Figure 1.4.12.** Manganese-electrooxidative C–H activation.

## 2. Objectives

During the last decades, transition metal-catalyzed C–H functionalization<sup>[16]</sup> has emerged as a powerful tool for the construction of C–C and C–Het bonds due to their outstanding levels of atom-<sup>[14]</sup> and step-economy.<sup>[15]</sup> C–H bonds are omnipresent in organic compounds, therefore, site-selective functionalization of C–H bonds is challenging and extremely important. Compared with other 4d transition metals, such as palladium and rhodium, cost-effective ruthenium catalysis<sup>[33]</sup> is highly desirable for the selective *ortho*- or *meta*-C–H activation.

In this context, with ruthenium as the catalyst, the *ortho*-C–H alkylation of benzoic acids **98** via weakly-O-coordination should be explored (Figure 2.1). Moreover, in the presence of strong chelating nitrogen assistances, the highly selective remote *meta*-C–H activation for the construction of C–C bonds through the  $\sigma$ -activation of the cycloruthenium intermediate is possible to occur and should be investigated with the use of the alkylation, mono- and difluoromethylating reagents (Figure 2.1).

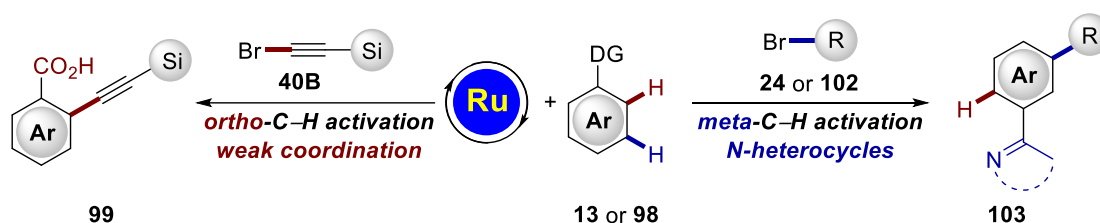


Figure 2.1. Ruthenium-catalyzed selective C–H activation with diverse chelating assistances.

Recently, the elegant merger of metalla-electrocatalyzed oxidative C–H functionalization without expensive and toxic metal oxidants holds the unique power for the resource-economical and environmentally-benign molecular construction.<sup>[144]</sup> Considerable developments have been achieved by precious 4d and 5d transition metals as well as the base metal cobalt. However, cost-effective and Earth-abundant 3d transition metal nickel for electrocatalytic C–H activation remain so far underdeveloped. Therefore, another main objective of the thesis was the C–H activation by nickel electro-catalysis.



Nitrogen-containing compounds are important structural fragments in natural products, biological molecules and pharmaceutical agents. The established nickel-catalyzed C–H amination with stoichiometric amounts of expensive silver(I) or copper(II) salts is inconsistent with the real nature of atom-economy.<sup>[121]</sup> Thereafter, we wish to develop a green and inexpensive electricity-promoted nickel-catalyzed C–H transformation in a dehydrogenative manner without producing stoichiometric metal waste, which could provide an accessible synthetic path to a variety of diverse arylamines **58** (Figure 2.2).

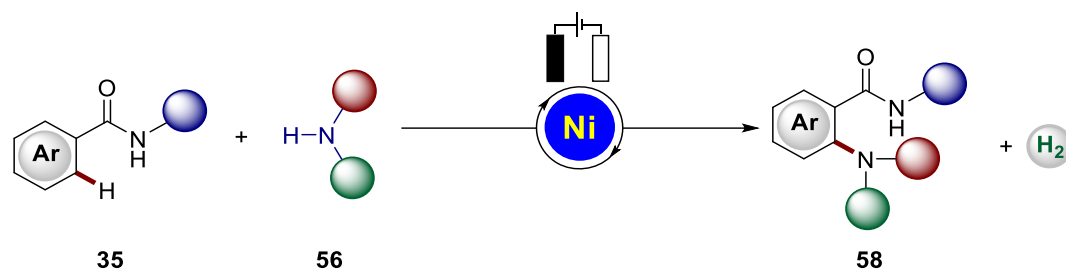


Figure 2.2. Nickela-electrocatalyzed C–H amination with amines **56**.

Despite considerable achievements on the traditional metal-catalyzed C–H activation for constructing C–O bonds, the C–H alkoxylation were relatively scarce due to the possible  $\beta$ -elimination or overoxidation of alcohols.<sup>[121]</sup> Moreover, the sterically encumbered secondary alcohols are even less investigated in the C–H activation using both chemical- and electro-oxidants. Therefore, the nickela-electrooxidative cross-dehydrogenative couplings of unactivated arenes **106** with the challenging secondary alcohols **66** for the synthesis of biorelevant aryl ethers **107** should be further explored (Figure 2.3).

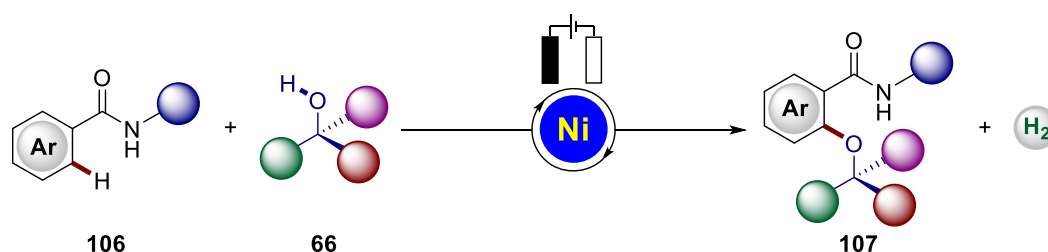


Figure 2.3. Nickela-electrocatalyzed C–H alkoxylation with secondary alcohols **66**.

## 2. Objectives

---

The synthesis of arylphosphonate derivatives also has a very important role for pharmaceutical and agrochemical industry, <sup>[131]</sup> <sup>[130]</sup> <sup>[130]</sup> <sup>[130]</sup> material science, and coordination chemistry. However, the construction of C–P bonds encounters a major challenge, because the phosphorus-containing reagents are inherently strongly-coordinating molecules,<sup>[135]</sup> resulting in less developed transition-metal-catalyzed C–H phosphorylations.<sup>[121]</sup> Scarce reports on C–P formation were so far restricted to the electrosynthesis with precious 4d metals or the methodologies of using a masked coupling partner or adding phosphonating reagents slowly or sequentially in the presence of stoichiometric silver(I) oxidants. Hence, the cost-effective 3d transition metal should be explored for the challenging electrooxidative C–H phosphorylation by an operationally-friendly setup to gain useful arylphosphonates **110** (Figure 2.4).

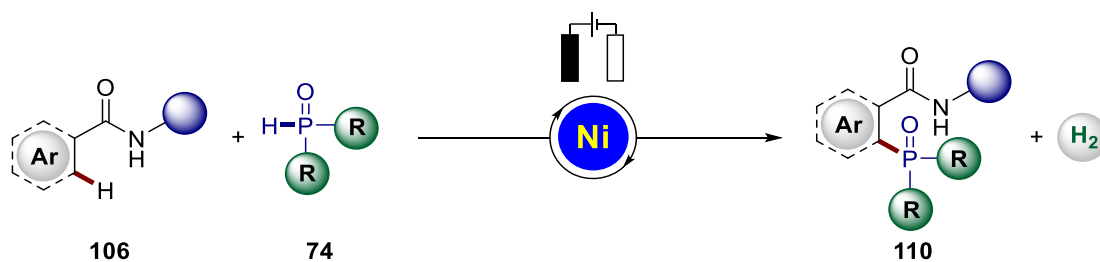


Figure 2.4. Nickela-electrocatalyzed challenging C–H phosphorylation.

## 3. Results and Discussion

### 3.1 Selective *ortho*-C–H Activation by Ruthenium Catalysis

Recently, the versatile ruthenium(II)-carboxylate catalyst has shown its power for *ortho*-C–H functionalizations with diverse electrophiles.<sup>[33a-c]</sup> Although considerable achievements have been made, ruthenium(II)-catalyzed C–H transformations with weakly-O-coordinating assistance remain scarce, with only recent investigations on C–H arylations<sup>[33c]</sup> and olefinations.<sup>[33a]</sup> However, the direct C–H alkylation of benzoic acids by ruthenium catalysis has so far proven elusive.

#### 3.1.1 Optimization and Scope

Optimization studies on the ruthenium(II)-catalyzed C–H alkylations were done by Dr. Ruhuai Mei<sup>[170]</sup> and after testing various bases and solvents, catalytic reaction conditions comprised of  $[\text{RuCl}_2(p\text{-cymene})]_2$  (5.0 mol %),  $\text{K}_2\text{CO}_3$  (2.0 equiv) in 1,4-dioxane or NMP at 120 °C for 16 h were identified as optimal. With the optimized conditions in hand, the scope of the ruthenium-catalyzed C–H alkylation of benzoic acids was investigated (**Figure 3.1.1**). The aromatic C–H transformations were not limited to mono-C–H alkylations (**99a–99d**), but also furnished the di-alkylated product **99e**, when 2.5 equivalents of alkylated bromides **40B** were used.

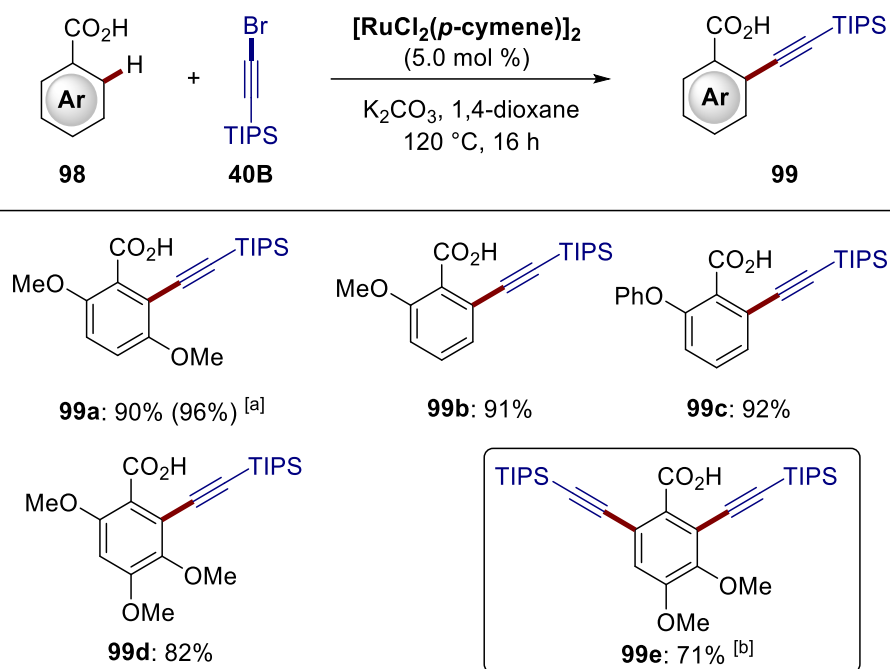


**Figure 3.1.1.** Scope of ruthenium-catalyzed C–H alkyneation of benzoic acids **98**.  
<sup>[a]</sup>  $\text{Ru}(\text{O}_2\text{CMes})_2(\textit{p}\text{-cymene})$  (10 mol%). <sup>[b]</sup> **40B** (2.5 equiv).

### 3.1.2 Removal of Silyl Group

The silyl group was easy to be removed in the presence of  $n\text{Bu}_4\text{NF}$ , providing the corresponding terminal alkyne **100d** (Figure 3.1.2), which could be employed for further transformations, like Sonogashira–Hagihara cross-couplings.<sup>[8]</sup>

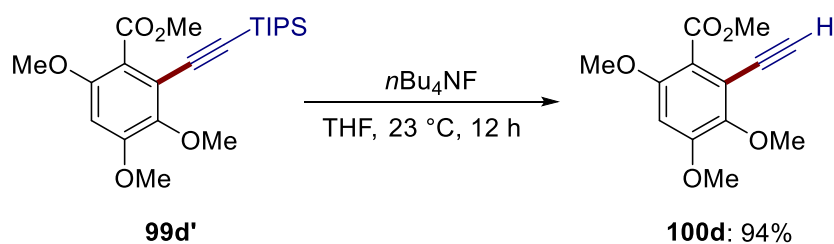


**Figure 3.1.2.** Traceless removal to access terminal alkyne **100d**.

## 3.1.3 Mechanistic Studies

A series of mechanistic studies was carried out to understand the reaction mode of the ruthenium catalysis. A significant H/D exchange was observed by the reisolated substrate  $[D_n]$ -**98f**, when using deuterated cosolvent  $CD_3OD$  for the C–H alkylation, revealing the reversibility of C–H activation (**Figure 3.1.3a**). Typical radical scavengers, such as TEMPO and BHT, failed to prevent the C–H transformation, ruling out a radical mechanism (**Figure 3.1.3b**). In addition, an intermolecular competition experiment between electronically distinct arenes **98** demonstrated that the electron-donating arene **98b** was more reactive, suggesting a facile base-assisted internal electrophilic substitution-type (BIES) C–H activation.<sup>[28]</sup>

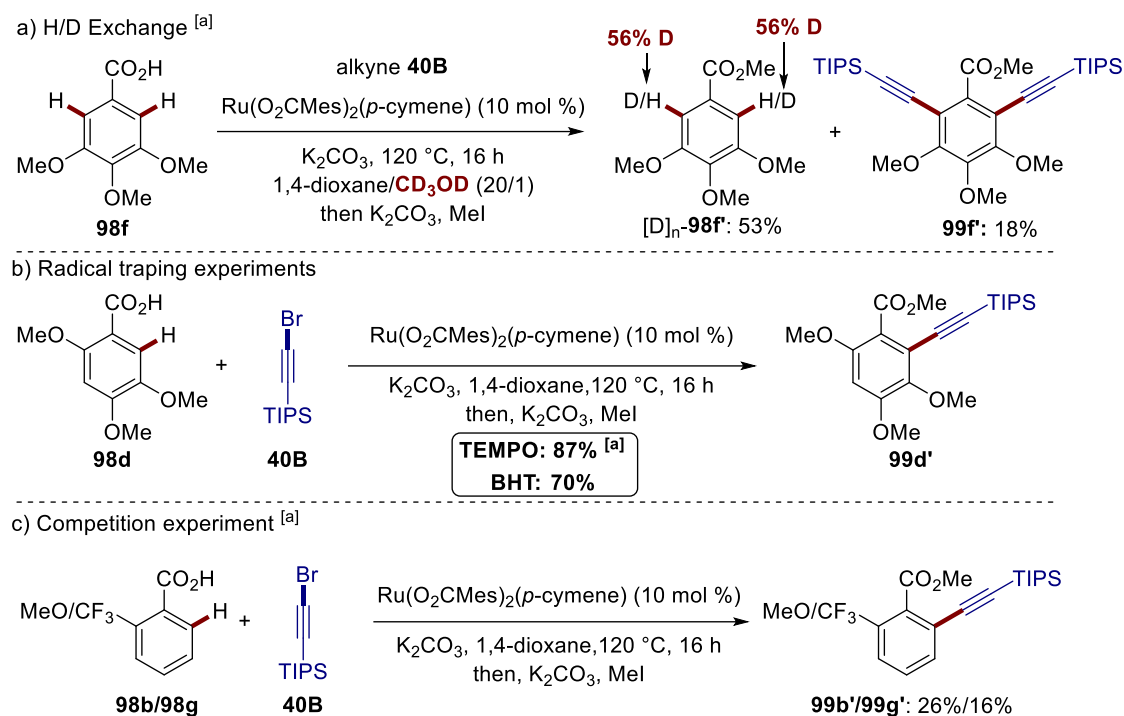


**Figure 3.1.3.** Mechanistic studies. <sup>[a]</sup> Performed by Dr. Ruhuai Mei.

### 3.1.4 Proposal Catalytic Cycle of *ortho*-C–H Alkynylation

On the basis of these results, a catalytic cycle was proposed as shown in **Figure 3.1.4**. The initial C–H cleavage occurred with the assistance of carboxylate to deliver ruthenium(II) complex **101c**, followed by a coordination and oxidative addition to generate ruthenium(IV) intermediate **101e**. The final product **99** was obtained through reductive elimination, together with the regeneration of ruthenium complex **101a**.

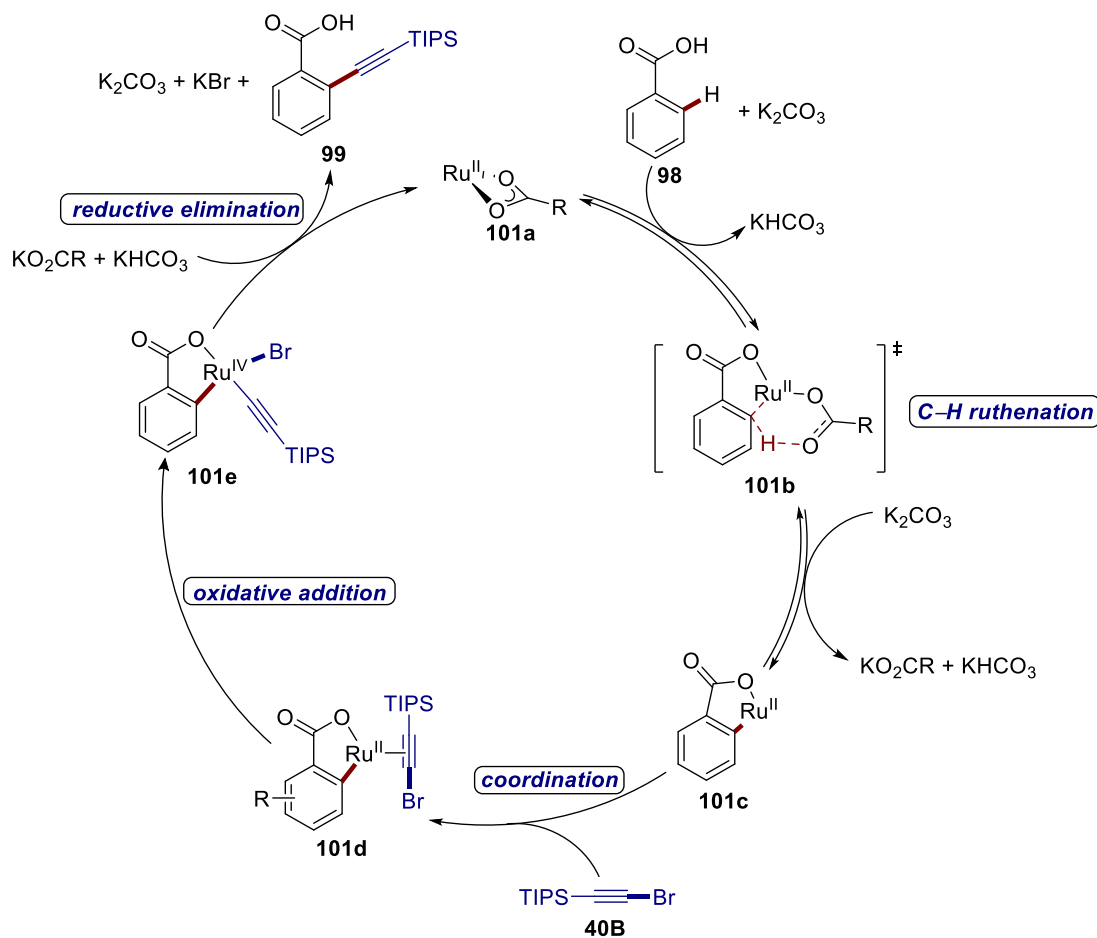


**Figure 3.1.4.** Proposed catalytic cycle for *ortho*-C–H alkynylation by ruthenium catalysis.

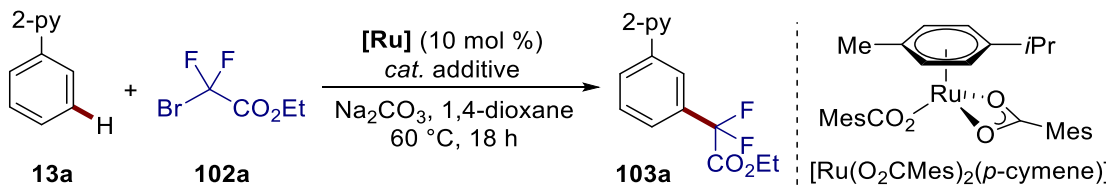
### 3.2 Selective *meta*-C–H Activation by Ruthenium Catalysis

The control of site-selectivity is of key significance for the development of molecular transformation.<sup>[16]</sup> Compared with the tremendous progress of chelation-assisted proximity-induced *ortho*-C–H functionalizations,<sup>[19]</sup> remote *meta*-C–H transformation was so far less explored.<sup>[29c]</sup>

#### 3.2.1 Optimization and Scope of Ruthenium-Catalyzed *meta*-C–H Mono- and Difluoromethylation

The optimized conditions were established by Dr. Zhixiong Ruan in the Ackermann group, as shown in the **Table 3.2.1**. After diverse nickel cocatalysts were tested, Ni(PPh<sub>3</sub>)<sub>2</sub>Cl<sub>2</sub> was found to be beneficial to the ruthenium-catalyzed *meta*-C–H transformation (entries 1–4). Further studies revealed that the phosphine ligand was the crucial additive for the carboxylate-assisted *meta*-C–H activation (entries 5–19).

**Table 3.2.1.** Optimization of ruthenium-catalyzed C–H difluoromethylation [a, c]



Entry	[Ru]	Additive	103a [%]
1	[Ru(O <sub>2</sub> CMes) <sub>2</sub> ( <i>p</i> -cymene)]	-	< 5
2	<b>[Ru(O<sub>2</sub>CMes)<sub>2</sub>(<i>p</i>-cymene)]</b>	<b>Ni(PPh<sub>3</sub>)<sub>2</sub>Cl<sub>2</sub></b>	<b>72</b>
3	[RuCl <sub>2</sub> ( <i>p</i> -cymene)] <sub>2</sub>	Ni(PPh <sub>3</sub> ) <sub>2</sub> Cl <sub>2</sub>	---
4	-	Ni(PPh <sub>3</sub> ) <sub>2</sub> Cl <sub>2</sub>	---
5	[Ru(O <sub>2</sub> CMes) <sub>2</sub> ( <i>p</i> -cymene)]	NiCl <sub>2</sub>	< 5
6	[Ru(O <sub>2</sub> CMes) <sub>2</sub> ( <i>p</i> -cymene)]	NiCl <sub>2</sub> + PPh <sub>3</sub>	71
7	[Ru(O <sub>2</sub> CMes) <sub>2</sub> ( <i>p</i> -cymene)]	PPh <sub>3</sub>	62
8	[Ru(O <sub>2</sub> CMes) <sub>2</sub> ( <i>p</i> -cymene)]	PCy <sub>3</sub>	12 [b]
9	[Ru(O <sub>2</sub> CMes) <sub>2</sub> ( <i>p</i> -cymene)]	IPr•HCl	---
10	[Ru(O <sub>2</sub> CMes) <sub>2</sub> ( <i>p</i> -cymene)]	P(Ad) <sub>2</sub> nBu	< 5

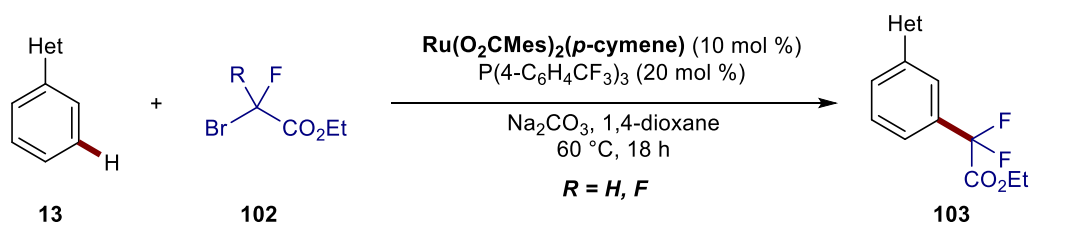
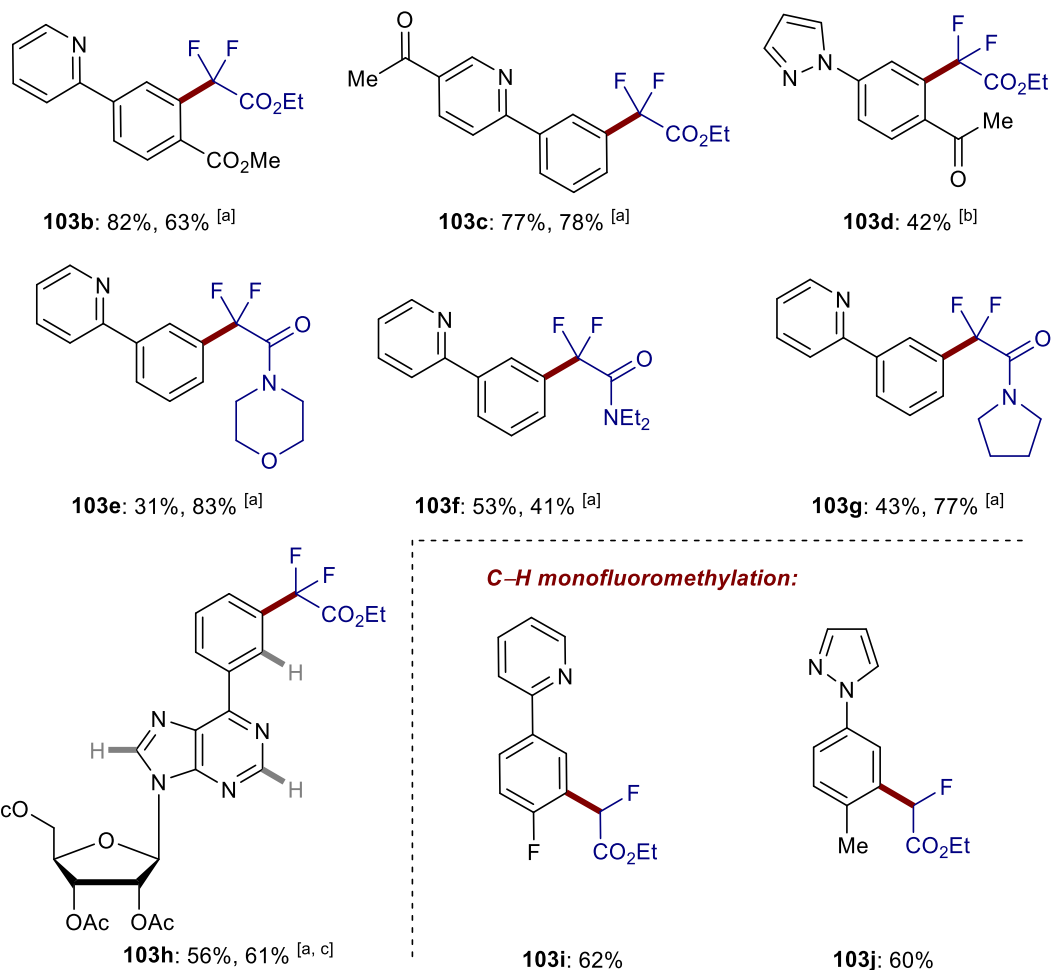
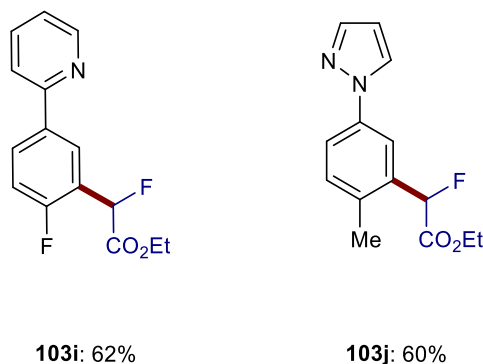
### 3. Results and Discussion

11	[Ru(O <sub>2</sub> CMes) <sub>2</sub> ( <i>p</i> -cymene)]	P( <i>n</i> Bu) <sub>3</sub>	7
12	[Ru(O <sub>2</sub> CMes) <sub>2</sub> ( <i>p</i> -cymene)]	P(OEt) <sub>3</sub>	---
13	[Ru(O <sub>2</sub> CMes) <sub>2</sub> ( <i>p</i> -cymene)]	XPhos	---
14	[Ru(O <sub>2</sub> CMes) <sub>2</sub> ( <i>p</i> -cymene)]	P(4-MeC <sub>6</sub> H <sub>4</sub> ) <sub>3</sub>	< 5
15	[Ru(O <sub>2</sub> CMes) <sub>2</sub> ( <i>p</i> -cymene)]	Ph <sub>2</sub> P(O)H	---
<b>16</b>	<b>[Ru(O<sub>2</sub>CMes)<sub>2</sub>(<i>p</i>-cymene)]</b>	<b>P(4-C<sub>6</sub>H<sub>4</sub>CF<sub>3</sub>)<sub>3</sub></b>	<b>71</b>
17	[Ru(OAc) <sub>2</sub> ( <i>p</i> -cymene)]	P(4-C <sub>6</sub> H <sub>4</sub> CF <sub>3</sub> ) <sub>3</sub>	63
18	[RuCl <sub>2</sub> ( <i>p</i> -cymene)] <sub>2</sub>	P(4-C <sub>6</sub> H <sub>4</sub> CF <sub>3</sub> ) <sub>3</sub>	---
19	[RuCl <sub>3</sub> •(H <sub>2</sub> O) <sub>n</sub> ]	P(4-C <sub>6</sub> H <sub>4</sub> CF <sub>3</sub> ) <sub>3</sub>	---

<sup>[a]</sup> Reaction conditions: **13a** (0.5 mmol), **102a** (3.0 equiv), [Ru] (10 mol %), additive ([Ni]: 10 mol % or [P]: 20 mol %), Na<sub>2</sub>CO<sub>3</sub> (2.0 equiv), 1,4-dioxane (2.0 mL), 60 °C, 18 h, isolated yield. <sup>[b]</sup> Conversion was determined by <sup>19</sup>F NMR using C<sub>6</sub>F<sub>6</sub> as the internal standard. <sup>[c]</sup> Performed by Dr. Zhixiong Ruan.

Having established the optimized conditions, we explored the robustness of the ruthenium catalysis in the *meta*-C–H activation with various arenes **13** (Figure 3.2.1). With the distinct nitrogen-containing directing groups, arenes **13** bearing both electron-rich and electron-poor substituents were converted to the desired *meta*-C–H mono- or difluoromethylated products **103b–103j** with excellent site-selectivity. Various functional groups were well tolerated, for instance, ester, halo and ketone substituents. Besides the bromodifluoroacetate **102a**, the corresponding amides were as well efficiently transferred (**103e–103g**). In select cases, the use of Ni(PPh<sub>3</sub>)<sub>2</sub>Cl<sub>2</sub> resulted in a high turnover towards products **103**, which could either be because of a low concentration of the free phosphine or a heterobimetallic regime. Notably, the outstanding level of high regioselectivity was demonstrated using the bioactive purine substrate bearing acidic C–H bonds and the DG-proximity-induced *ortho*-C–H bond, furnishing only the *meta*-C–H activated product **103h**.



**C–H difluoromethylation:****C–H monofluoromethylation:**

**Figure 3.2.1.** Scope of *meta*-C–H mono- and difluoromethylation by ruthenium. [a] Ni(PPh<sub>3</sub>)<sub>2</sub>Cl<sub>2</sub> (10 mol%) instead of P(4-C<sub>6</sub>H<sub>4</sub>CF<sub>3</sub>)<sub>3</sub>. [b] 70 °C. [c] Performed by Dr. Zhixiong Ruan.

Finally, the successful removal of the ester moiety<sup>[171]</sup> provided a potential alternative to difluoromethylated compounds (**Figure 3.2.2**).

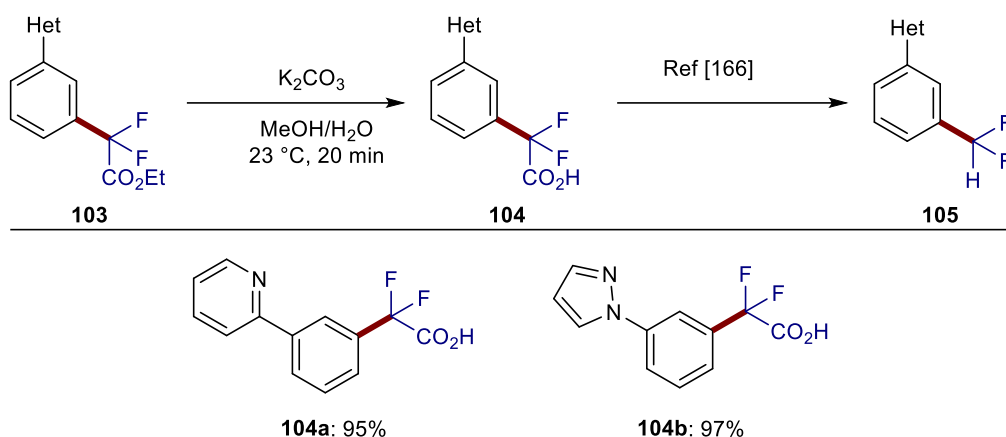


Figure 3.2.2. Removal of ester **103**.

### 3.2.2 Optimization and Scope of *meta*-C–H Alkylation by Arene-Ligand-Free Ruthenium Catalysis

Despite the notable progress on remote C–H functionalization by carboxylate-assisted ruthenium catalysis,<sup>[60–69]</sup> transformative syntheses have been largely limited to the use of arene-ruthenium complexes. Moreover, C–H alkylation of purine derivatives continued to be elusive, considering their significant roles in biochemistry.<sup>[172]</sup>

After considerable optimizations of ruthenium complexes, bases and solvents by Fernando Fumagalli in the Ackermann group, a catalytic system containing arene-ligand-free  $Ru(OAc)_2(PPh_3)_2$  (10 mol %),  $K_3PO_4$  (2.0 equiv) in 1,4-dioxane at  $100\text{ }^\circ\text{C}$  for 18 h was identified as the model reaction condition.

With the optimized single-component  $Ru(OAc)_2(PPh_3)_2$  catalysis in hand, we probed its versatility of *meta*-C–H alkylations of decorated arenes **13** with alkyl halides **24B** (Figure 3.2.3). Different directing groups bearing a nitrogen-coordinating atom, including pyrazole, pyridine, pyrimidine, oxazole and purine, facilitated the C–C formation with an outstanding level of chemo- and position-selectivity (**103k–103x**). Remote *meta*-C–H alkylation was achieved with diverse alkyl halides, such as bromodifluoroacetate, tertiary and secondary alkyl bromides, providing corresponding *meta*-products **103v–103x**.

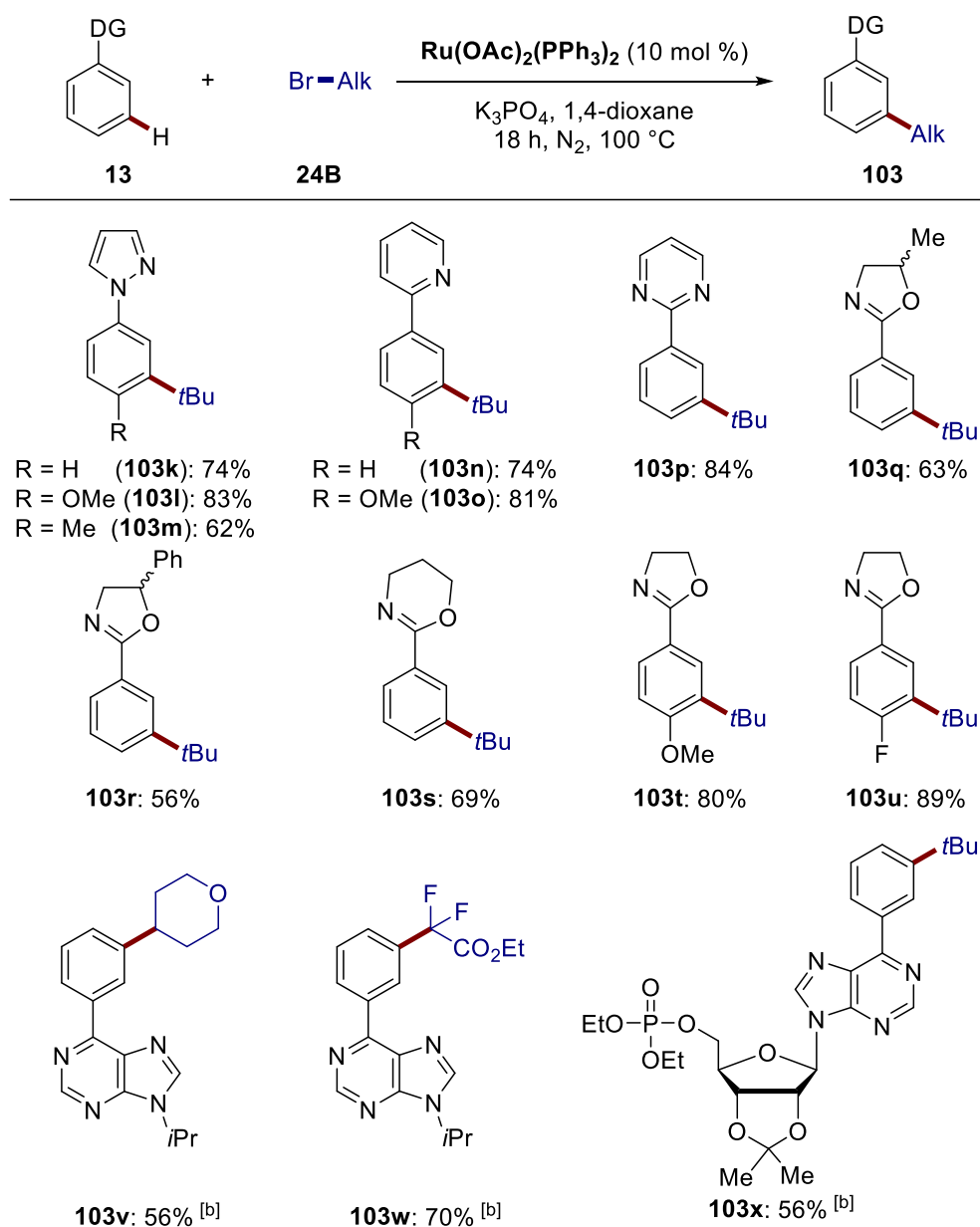


**Figure 3.2.3.** Scope of *meta*-C–H alkylation by arene-ligand-free ruthenium catalyst. <sup>[b]</sup> Performed by Fernando Fumagalli.

The mechanism of *meta*-C–H alkylation was well established,<sup>[66]</sup> as shown in **Figure 3.2.4**. After the coordination of ruthenium(II) biscalboxylate **104a** to the substrate bearing nitrogen atom, the key reversible C–H activation of substrate **13** took place in the presence of a base. Subsequently, an alkyl radical, generated from a single-electron transfer-type activation of the alkyl halide, underwent an electrophilic attack at the *para*-position of  $\sigma$ -C–Ru bond (**104c**) to give ruthenium intermediate **104d**. Finally, rearomatization occurred *via* SET and deprotonation to form a ruthenium(II) complex and the desired product **103** after proto-demetalation.

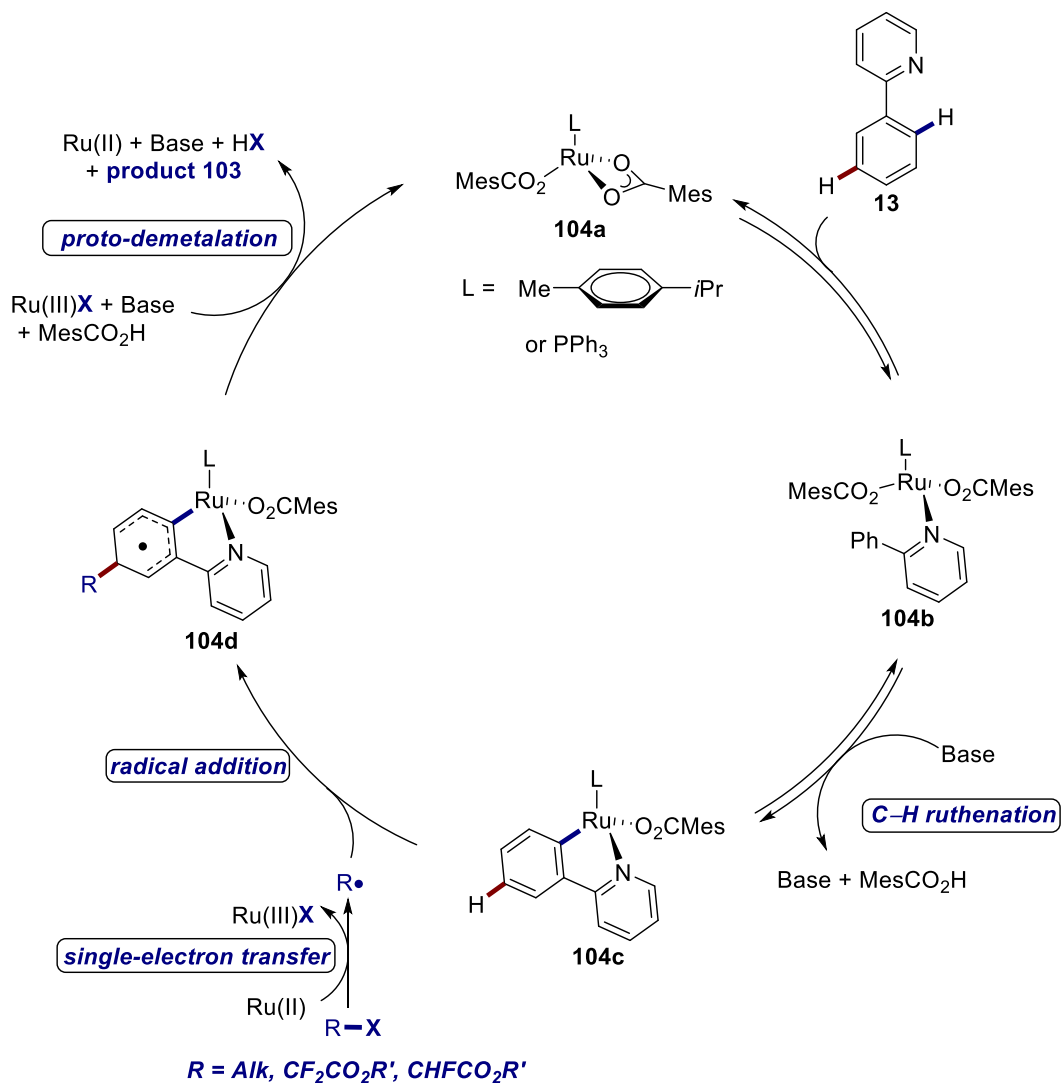


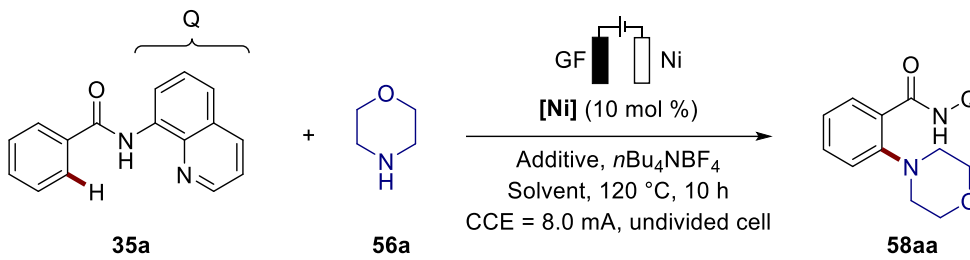
Figure 3.2.4. General mechanistic cycle of *meta*-C–H alkylation by ruthenium.

### 3.3 Nickela-Electrocatalyzed C–H Amination

Traditional metal-catalyzed C–H functionalization by electrocatalysis bears huge potential for constructing molecular complexity, avoiding stoichiometric amounts of toxic and expensive metal oxidants.<sup>[144]</sup> The use of storable, safe and waste-free electricity as formal oxidant for C–H activation is likewise attractive. Although this strategy considerably increased the resource-economy of C–H activation, advances were mainly focused on noble 4d and 5d transition metals, such as palladium,<sup>[146, 148c, 148d, 149e-k]</sup> ruthenium,<sup>[157, 158c]</sup> rhodium<sup>[150]</sup> and iridium.<sup>[160]</sup> In stark contrast, the inexpensive base metal cobalt has been very recently identified as efficient catalyst for electrochemical construction of C–C and C–Het bonds through C–H activation.<sup>[163, 164f-i, 165b, 165c]</sup> Despite the indisputable progress, less toxic and Earth-abundant nickel catalysis remained so far unexplored for electrocatalytic C–H activation.

#### 3.3.1 Optimization Studies

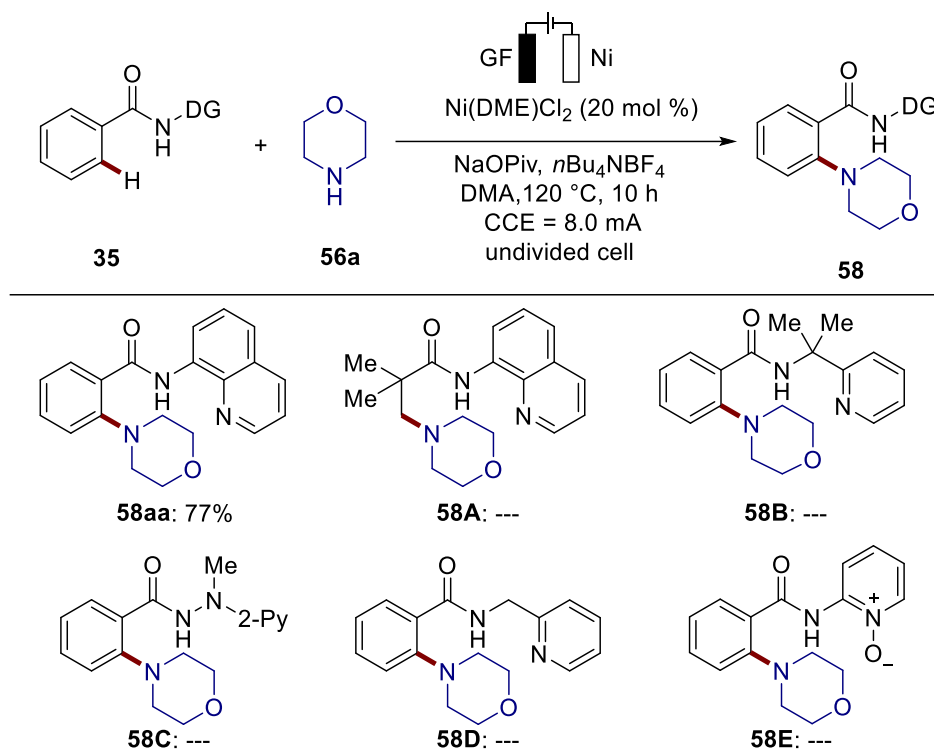
We started our studies by probing various reaction conditions for the nickela-electrocatalytic C–H amination (**Table 3.3.1**, entries 1–13). To our delight, the corresponding C–H amination product **58aa** was obtained with a yield of 10% when using Ni(OAc)<sub>2</sub>•4H<sub>2</sub>O as the electrocatalyst and DMA as the solvent in an undivided cell (entry 1). After testing various solvents and additives, DMA and NaOPiv emerged as being optimal, respectively (entries 2–8). Subsequent investigations of the reaction conditions, in terms of additive stoichiometry and reaction concentration, further improved the performance of the nickela-electrocatalysis (entries 9–11). The significant role of the electricity (entry 12) and the nickel catalyst (entry 13) were demonstrated by control experiments. Notably, an extra redox-mediator was not required to accomplish the nickela-electrooxidative C–H amination, which was different from a recent electrocatalytic C–H amination by copper catalysis.<sup>[166]</sup>

**Table 3.3.1.** Optimization of nickela-electrochemical C–H amination <sup>[a]</sup>


Entry	Solvent	Additive	[Ni]	<b>58aa</b> [%]
1	DMA	---	Ni(OAc) <sub>2</sub> •4H <sub>2</sub> O	10
2	DMA	PivOH	Ni(OAc) <sub>2</sub> •4H <sub>2</sub> O	35
3	DMA	NaOPiv	Ni(OAc) <sub>2</sub> •4H <sub>2</sub> O	55
4	DMA	Na <sub>2</sub> CO <sub>3</sub>	Ni(OAc) <sub>2</sub> •4H <sub>2</sub> O	24
5	GVL	NaOPiv	Ni(OAc) <sub>2</sub> •4H <sub>2</sub> O	---
6	NMP	NaOPiv	Ni(OAc) <sub>2</sub> •4H <sub>2</sub> O	44
7	DMF	NaOPiv	Ni(OAc) <sub>2</sub> •4H <sub>2</sub> O	22
8	DMA	NaOPiv	Ni(OAc) <sub>2</sub> •4H <sub>2</sub> O	20 <sup>[b]</sup>
9	DMA	NaOPiv	Ni(OAc) <sub>2</sub> •4H <sub>2</sub> O	61 <sup>[c]</sup>
10	DMA	NaOPiv	Ni(OAc) <sub>2</sub> •4H <sub>2</sub> O	72 <sup>[c, d]</sup>
<b>11</b>	<b>DMA</b>	NaOPiv	<b>Ni(DME)Cl<sub>2</sub></b>	<b>77</b> <sup>[c, d, e]</sup>
12	DMA	NaOPiv	Ni(DME)Cl <sub>2</sub>	--- <sup>[c, d, e, f]</sup>
13	DMA	NaOPiv	---	--- <sup>[d, e]</sup>

<sup>[a]</sup> Reaction conditions: **35a** (0.25 mmol), **56a** (0.50 mmol), **[Ni]** (10 mol %), Additive (0.50 mmol), *n*Bu<sub>4</sub>NBF<sub>4</sub> (0.50 mmol), Solvent (2.5 mL), constant current electrolysis (CCE) = 8.0 mA, 10 h, N<sub>2</sub>, 120 °C, graphite felt (GF) anode and nickel-foam cathode. <sup>[b]</sup> under air. <sup>[c]</sup> [Ni] (20 mol%). <sup>[d]</sup> PivONa (0.25 mmol). <sup>[e]</sup> DMA (3.0 mL). <sup>[f]</sup> no current. DMA = *N,N*-dimethylacetamide, GVL =  $\gamma$ -valerolactone, NMP = *N*-methyl-2-pyrrolidinone, DMF = *N,N*-dimethylformamide.

With the optimized reaction conditions in hand, we next probed the influence exerted by the *N*-substituent of benzamides **35** (Table 3.3.2). Hence, various *N,N*-chelation groups and an *N,O*-bidentate chelation failed to enable the desired C–N transformation, compared with the cobalt manifold.<sup>[163, 164f, 164h, 164i]</sup>

**Table 3.3.2.** Optimization of directing groups <sup>[a]</sup>

<sup>[a]</sup> Reaction conditions: Undivided cell, **35** (0.25 mmol), **56a** (0.50 mmol), NaOPiv (0.25 mmol), Ni(DME)Cl<sub>2</sub> (20 mol %),  $n\text{Bu}_4\text{NBF}_4$  (0.50 mmol), DMA (3.0 mL), 120 °C, 8.0 mA, 10 h, graphite felt (GF) anode, nickel-foam cathode.

### 3.3.2 Scope of Nickela-Electrocatalyzed C–H Amination

Having established 8-aminoquinoline-assisted electrochemical C–H nitration by nickel catalyst, we tested its versatility with diversely decorated benzamides **35** (Figure 3.3.1). Arenes bearing both electron-donating and electron-withdrawing substituents could be successfully converted to access the desired aryl amines **58aa–58qa**. Various valuable functional groups, including halo, cyano, sulfide or ester substituents **35g–35j**, were well tolerated. Intramolecular competition experiments with *meta*-substituted substrates were fully governed by steric interactions, delivering the products **58ka–58oa** with an excellent level of regioselectivity. Moreover, the heteroarenes **35p**, **35q** were identified as amenable substrates likewise to furnish the C–N transformation.

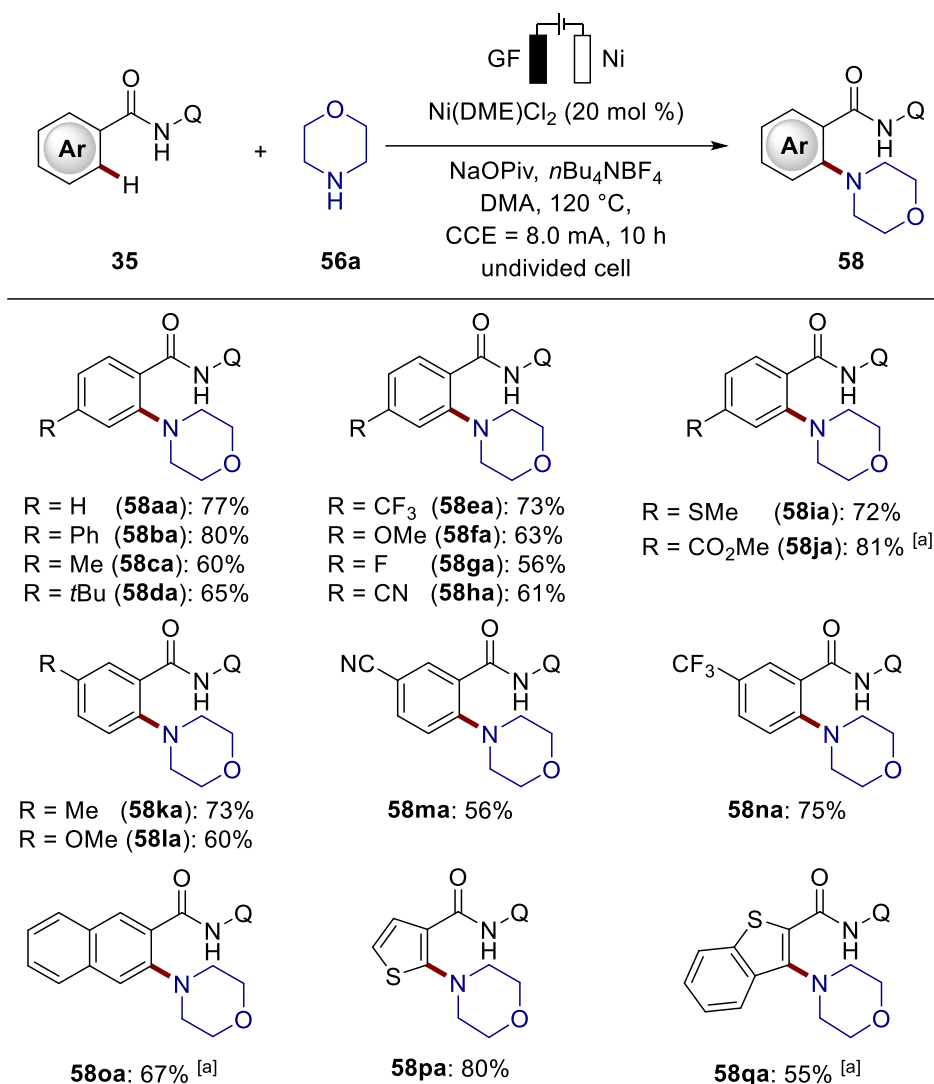


**Figure 3.3.1.** Nickela-electrocatalyzed C–H amination of arenes **35**.<sup>[a]</sup> Performed by Dr. Ramesh C. Samanta.

Furthermore, the robustness of the nickelaelectro-catalysis was proven by electrochemical C–H aminations with differently substituted secondary amines **56**, like piperazine and thiazine derivatives (**Figure 3.3.2**). Thereby, the substrates with valuable functional groups were well tolerated, featuring among others ester **56c** and cyano substituents **56f**. Remarkably, even more challenging acyclic secondary amine **56i** could be efficiently converted to corresponding aromatic amide **58ji**.





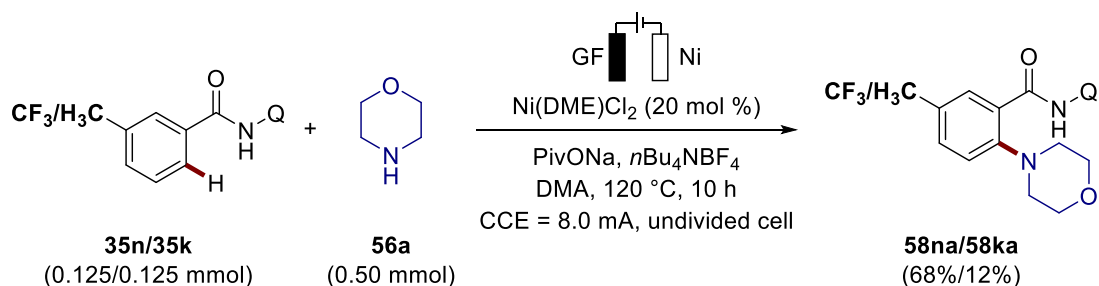


**Figure 3.3.3.** Competition experiment between electronically different arenes **35**. The ratio was determined by  $^1\text{H}$  NMR conversion using 1,3,5-(OMe) $_3\text{C}_6\text{H}_3$  as the internal standard.

### 3.3.3.2 Experiments with Isotopically Labelled Solvent

The optimized reaction was conducted in the presence of the cosolvent  $\text{D}_3\text{COD}$ . No H/D scrambling was found in the reisolated substrate and the desired product (**Figure 3.3.4**).

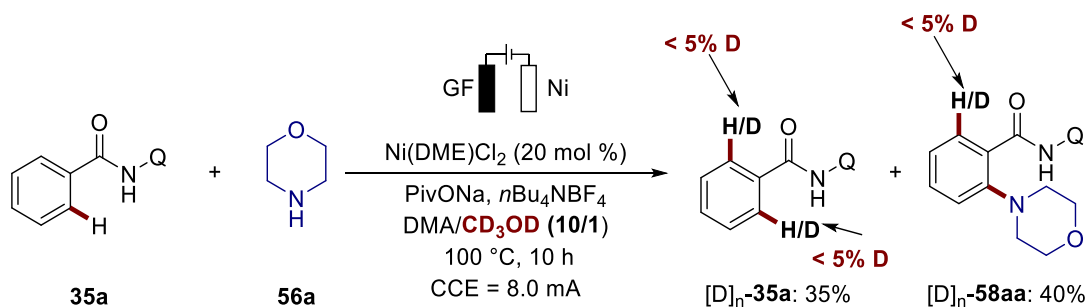


**Figure 3.3.4.** Deuteration experiment using  $\text{CD}_3\text{OD}$  as the cosolvent.

### 3.3.3.3 Reaction Profile

A kinetic profile was measured by means of *in-operando* React-IR by Dr. Nicolas Sauermann in the Ackermann group, showing the consumption of benzamide **35a** as well as the formation of C–H amination product **58aa** (**Figure 3.3.5**). These results revealed that there was no sign of initiation period during the nickel-electrooxidative C–H transformation.

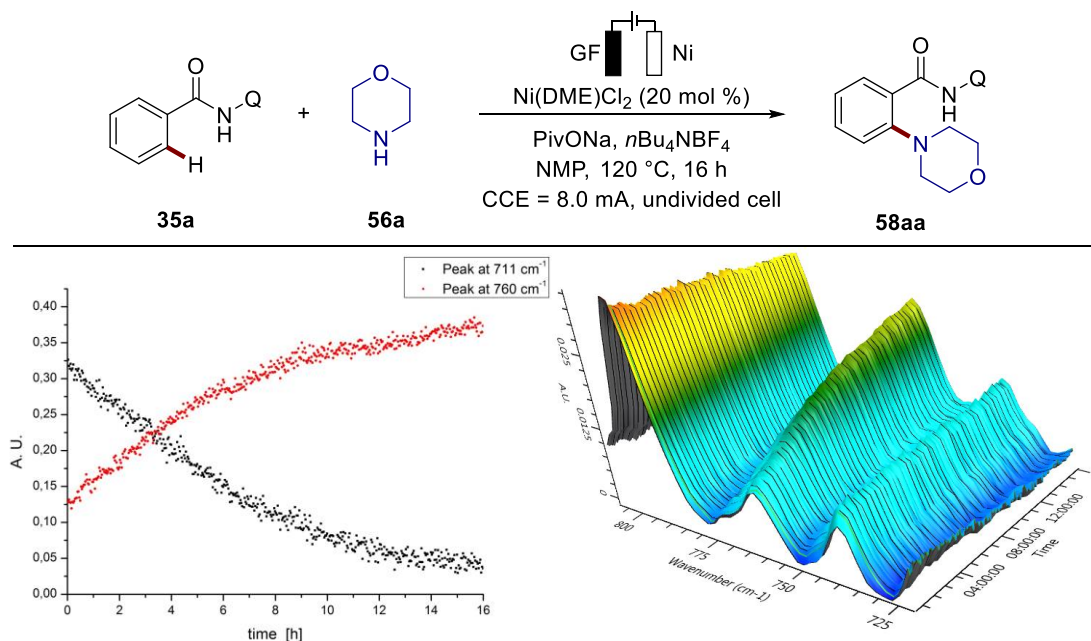


Figure 3.3.5. Reaction profile monitored by *in-operando* React-IR. Performed by Dr. Nicolas Sauermann.

### 3.3.3.4 KIE Studies

Two independent experiments between substrates **35a** and  $[\text{D}_5]\text{-35a}$  were conducted under the modified optimization condition (Figure 3.3.6). A kinetic isotope effect (KIE) of  $k_{\text{H}}/k_{\text{D}} \approx 1.1$  was recorded by Dr. Nicolas Sauermann by *in-operando* React-IR, which showed that the C–H bond cleavage was not the rate-limiting step.

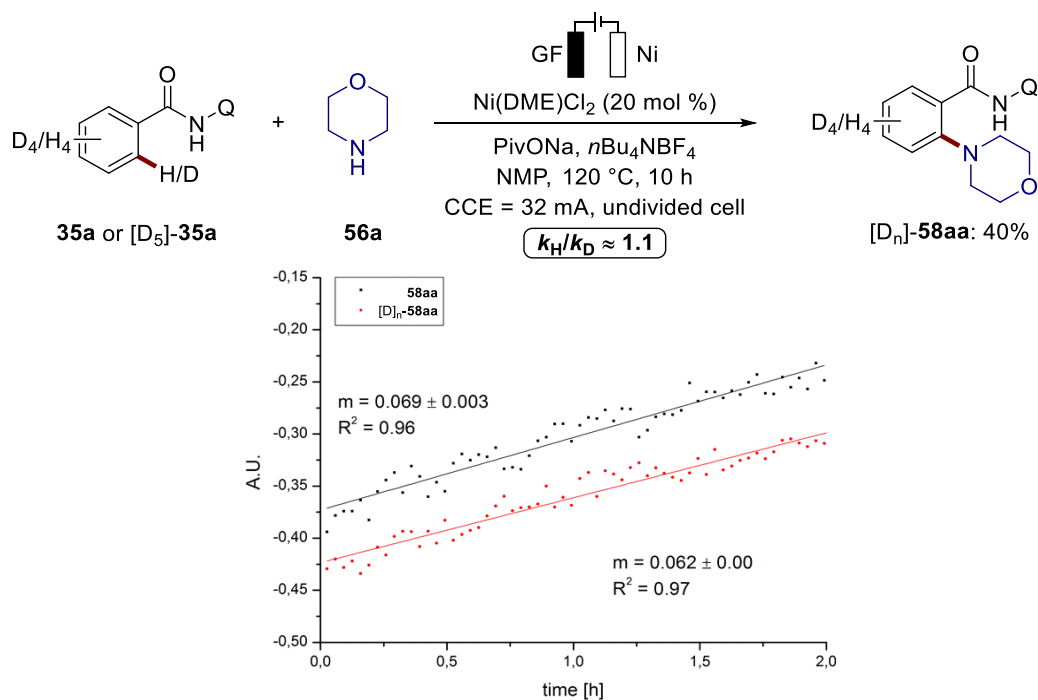


Figure 3.3.6. KIE studies by *in-operando* React-IR. Performed by Dr. Nicolas Sauermann.

3.3.3.5 H<sub>2</sub>-Detection

In order to prove the generation of molecular hydrogen, the atmosphere after the electrocatalytic C–H amination was collected and analyzed by Headspace GC-analysis (Figure 3.3.7). The byproduct H<sub>2</sub> was detected eventually.

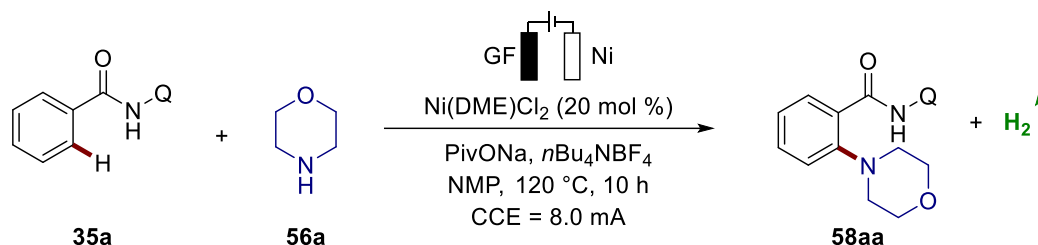


Figure 3.3.7. Headspace GC-analysis. Performed by Dr. Nicolas Sauermann.

## 3.3.3.6 Cyclic Voltammetry

Finally, we conducted detailed studies by means of cyclic voltammetry (Figure 3.3.8). Thereby, the electrode potential for the nickel(II/III) event was found by Dr. Nicolas Sauermann to be strongly influenced by the addition of both the substrate **35a** and NaOPiv, which was thus observed at  $E_p = +0.26$  V vs.  $Fc^{+/0}$  (orange) (Figure 3.3.8a). By increasing the reaction temperature, a reversible oxidation wave was significantly shifted to  $E_p = -0.18$  V vs.  $Fc^{+/0}$  (dark red), which could be rationalized by the generation of cyclometalated nickel(III) catalyst (Figure 3.3.8b). Moreover, an additional reversible oxidation wave at  $E_p = +0.49$  V vs.  $Fc^{+/0}$  was observed (Figure 3.3.8b), which was furthermore indicative of an oxidation to a nickel(IV) species.<sup>[174]</sup>

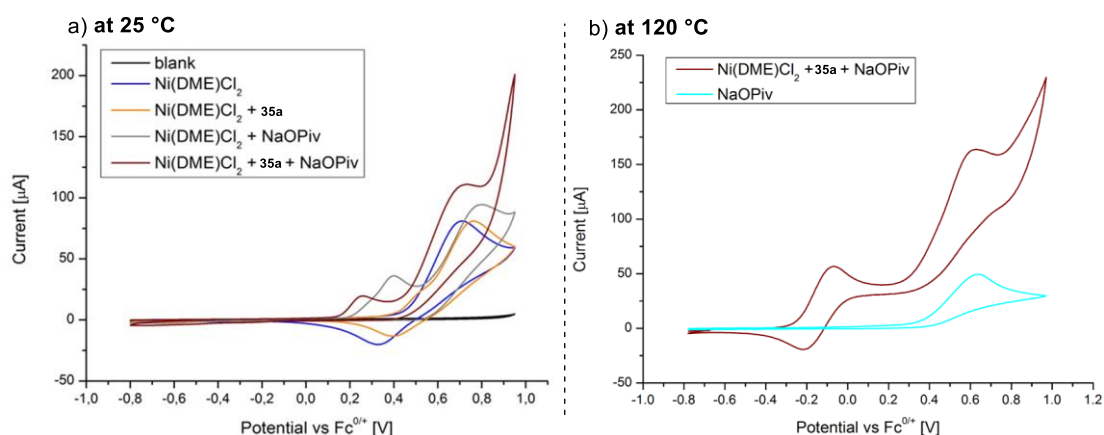
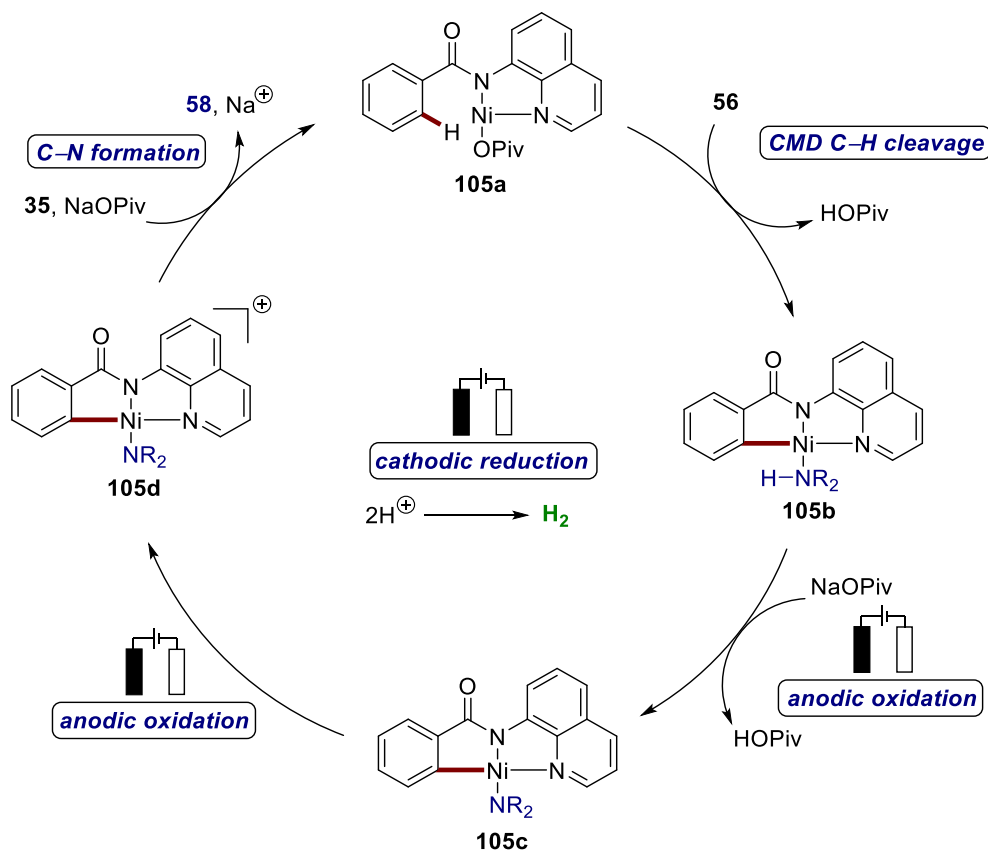


Figure 3.3.8. CV data (DMA, 5 mM *n*Bu<sub>4</sub>NBF<sub>4</sub>, 100 mVs<sup>-1</sup>) for a) Ni(DME)Cl<sub>2</sub> with the individual components of the catalysis. b) Ni(DME)Cl<sub>2</sub>, NaOPiv and **35a** after preheating at 120 °C for 30 min. Performed by Dr. Nicolas Sauermann.

## 3.3.4 Proposed Mechanism

Based on these results, we propose a plausible reaction pathway, as shown in **Figure 3.3.9**. The carboxylate-assisted C–H nickelation was commenced to deliver the nickel(II) complex **105b**, which was converted to nickel(III) species **105c** through an anodic oxidation. Amide-nickel(IV) **105d** was obtained through an anodic oxidation that induced the subsequent reductive elimination to release the desired C–N formation of **58** induced reductive elimination at nickel(III) **105c**. Thereby, the desired product **58** was formed, along with the regeneration of catalytically relevant competent **105a**. As the byproduct molecular hydrogen was formed at the cathode.



**Figure 3.3.9.** Proposed catalytic cycle for nickela-electrooxidative C–H amination.

### 3.4 Nickela-Electrocatalyzed C–H Alkoxylation with Secondary Alcohols

Traditional approaches for the construction of C–O bonds, such as Buchwald–Hartwig,<sup>[10]</sup> Ullmann–Goldberg<sup>[11]</sup> or Chan–Evans–Lam reactions,<sup>[12]</sup> mainly required to prefunctionalized substrates, the preparation and use of which increase the cost of organic syntheses. Cross dehydrogenative functionalization of C–H bonds was increasingly considered as a sustainable method for the improvement of atom- and step-economy of organic syntheses.<sup>[18]</sup> Despite the indisputable progress, dehydrogenative C–H alkoxylation were less investigated than hydroxylations,<sup>[123]</sup> acetoxylation<sup>[122, 165a]</sup> and phenoxylation,<sup>[124]</sup> mainly because aliphatic alcohols are prone to suffer from  $\beta$ -hydride elimination and overoxidation. Particularly, sterically encumbered secondary alcohols were underutilized for the C–O formations, compared to the previous reports on the use of primary alcohols.<sup>[124b, 125b-q, 126, 128, 129b-e, 130]</sup>

Although tremendous advances have been achieved by the cross dehydrogenative couplings, stoichiometric amounts of expensive and toxic chemical oxidants, such as silver(I) or copper(II) salts, were required, which disobey the principle of atom-economy.<sup>[121]</sup> Electrosynthesis has gained increasingly considerable attention through the use of waste-free and inexpensive electric current as green oxidant. As mentioned in **chapter 3.3**, studies of electrocatalytic C–H activations have mainly focused on precious 4d and 5d transition metals, recently with 3d transition metals, for instance, cobalt,<sup>[163, 164c-i, 165]</sup> copper,<sup>[166-168]</sup> iron and manganese.<sup>[169]</sup> Despite the indisputable advances, such Earth-abundant and cost-effective nickela-electrocatalysis has proven elusive until very recently, when we established electrocatalytic C–H aminations with diverse amines.<sup>[175]</sup> Furthermore, we have now found that robust nickel catalysts were highly effective for challenging electrooxidative C–H alkoxylation with sterically encumbered secondary alcohols **66**.

### 3.4.1 Optimization Studies

We commenced our investigations by optimizing the reaction conditions for the nickel-electrocatalytic C–H alkoxylation of benzamide **106a** with secondary alcohol **66a** in an undivided cell (Table 3.4.1). After considerable experimentation, the corresponding product **107a** was obtained in high yield using Ni(DME)Cl<sub>2</sub> as the catalyst, bulky carboxylate NaO<sub>2</sub>CAd as the additive and DMA as the solvent (entries 1–6). The performance of the nickel catalysts was improved by verifying the concentration of alcohols (entries 2, 5). The essential roles of electricity, the nickel complex and the carboxylate for the electrocatalytic C–H alkoxylation were confirmed by control experiments (entries 7–9). Other nickel complexes, e.g. Ni(cod)<sub>2</sub> and Ni(OAc)<sub>2</sub> successfully realized the formation of aryl ether **107a** (entries 10, 11). It is particularly noteworthy that the nickel catalysts proved uniquely effective for the challenging electrooxidative C–H alkoxylation, while other transition metals, like cobalt, copper, manganese and even precious palladium, iridium, ruthenium, or rhodium, failed to accomplish the C–H transformation under otherwise identical reaction conditions (entries 12–18).

**Table 3.4.1.** Optimization of nickela-electrooxidative C–H alkoxylation <sup>[a]</sup>

Entry	[TM]	Additive	<b>107a</b> [%]
1	Ni(DME)Cl <sub>2</sub>	NaOPiv	45 <sup>[b]</sup>
2	Ni(DME)Cl <sub>2</sub>	NaO <sub>2</sub> CAd	55 <sup>[b]</sup>
3	Ni(DME)Cl <sub>2</sub>	KOAc	24 <sup>[b]</sup>
4	Ni(DME)Cl <sub>2</sub>	K <sub>2</sub> HPO <sub>4</sub>	--- <sup>[b]</sup>
<b>5</b>	<b>Ni(DME)Cl<sub>2</sub></b>	<b>NaO<sub>2</sub>CAd</b>	<b>74</b>
6	Ni(DME)Cl <sub>2</sub>	NaO <sub>2</sub> CAd	69 <sup>[c]</sup>
7	---	NaO <sub>2</sub> CAd	---
8	Ni(DME)Cl <sub>2</sub>	---	---
9	Ni(DME)Cl <sub>2</sub>	NaO <sub>2</sub> CAd	--- <sup>[d]</sup>

### 3. Results and Discussion

10	Ni(cod) <sub>2</sub>	NaO <sub>2</sub> CAd	67
11	Ni(OAc) <sub>2</sub> ·4H <sub>2</sub> O	NaO <sub>2</sub> CAd	49 <sup>[b]</sup>
12	Co(OAc) <sub>2</sub> ·4H <sub>2</sub> O	NaO <sub>2</sub> CAd	---
13	Mn(OAc) <sub>2</sub>	NaO <sub>2</sub> CAd	---
14	Cu(OAc) <sub>2</sub> ·H <sub>2</sub> O	NaO <sub>2</sub> CAd	---
15	Ru(OAc) <sub>2</sub> (PPh <sub>3</sub> ) <sub>2</sub>	NaO <sub>2</sub> CAd	---
16	[Cp* <sup>+</sup> RhCl <sub>2</sub> ] <sub>2</sub>	NaO <sub>2</sub> CAd	--- <sup>[e]</sup>
17	Pd(OAc) <sub>2</sub>	NaO <sub>2</sub> CAd	---
18	[Cp* <sup>+</sup> IrCl <sub>2</sub> ] <sub>2</sub>	NaO <sub>2</sub> CAd	--- <sup>[e]</sup>

<sup>[a]</sup> Reaction conditions: **106a** (0.25 mmol), **66a** (2.5 mmol), 1-AdCO<sub>2</sub>H (20 mol %), [TM] (10 mol %), Additive (1.0 equiv), *n*Bu<sub>4</sub>NClO<sub>4</sub> (0.5 mmol), DMA (3.0 mL), CCE = 8.0 mA, 12 h, N<sub>2</sub>, GF Anode and nickel-foam Cathode, isolated yield. <sup>[b]</sup> 1.25 mmol of **66a**. <sup>[c]</sup> DMPU as solvent. <sup>[d]</sup> Without current. <sup>[e]</sup> [TM] (5.0 mol %). DMPU = 1,3-dimethyltetrahydropyrimidin-2(1*H*)-one.

The substitution pattern of the quinoline moiety has considerably affected the efficacy of nickel-electrochemical C–H oxygenation. Computation details performed by Dr. Lianrui Hu at the PEB0/Def2TZVP level of theory<sup>[176]</sup> uncovered that the elevated electron density at the quinolinyl nitrogen and decreased electron density at the amide nitrogen, which was beneficial for this C–H alkoxylation (**Table 3.4.2**). These results revealed the importance of increased  $\sigma$ -donation at the sp<sup>2</sup>-hybridized quinolinyl nitrogen in concert with an anionic amide nitrogen.

**Table 3.4.2.** The influence of the electronically-distinct quinoline moiety <sup>[a]</sup>

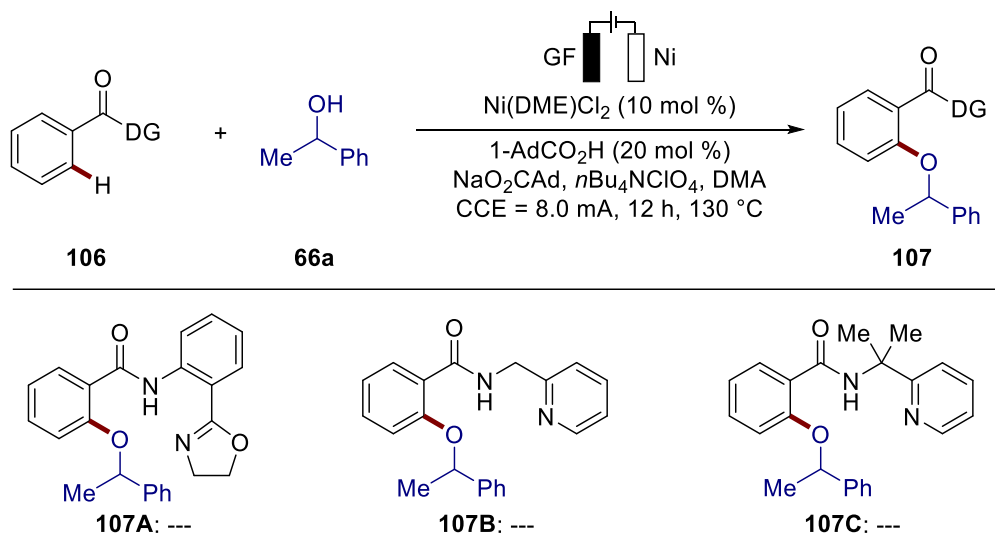
	<b>35a or 106</b>		<b>66a</b>	<b>107</b>		
	6-Me ( <b>106a</b> )	6-OMe ( <b>106b</b> )		5-Me ( <b>106c</b> )	H ( <b>35a</b> )	5-OMe ( <b>106e</b> )
<b>N2</b>	-0.33113	-0.33106		-0.32977	-0.32840	-0.32737
<b>N12</b>	-0.14754	-0.14863		-0.15310	-0.15201	-0.15529
<b>107</b>	<b>107a</b> 74% (15%)	<b>107b</b> 67% (19%)		<b>107c</b> 61% (21%)	<b>107d</b> 53% (37%)	<b>107e</b> 28% (64%)

<sup>[a]</sup> Calculation of electron density of *N,N*-coordinate atoms from modified 8-aminoquinoline (PBE0 Method): Recovered starting materials are in parentheses. **N2** = net atomic charges of the **N2** atom. **N12** = net atomic charges of the **N12** atom. Performed by Dr. Lianrui Hu.



Other *N,N*-bidentate assisted systems were also tested for the challenging C–H secondary alkoxylation (Table 3.4.3). The unsuccessful transformative C–O constructions furthermore illustrated the introduction of proper chelation system was important to accomplish highly-efficient electrosynthesis of aryl ether.

**Table 3.4.3.** Directing group power for nickela-electrooxidative alkoxylation <sup>[a]</sup>



<sup>[a]</sup> Reaction conditions: **106a** (0.25 mmol), **66a** (2.5 mmol), 1-AdCO<sub>2</sub>H (20 mol %), [TM] (10 mol %), Additive (1.0 equiv), *n*Bu<sub>4</sub>NClO<sub>4</sub> (0.5 mmol), DMA (3.0 mL), CCE = 8.0 mA, 12 h, N<sub>2</sub>, GF Anode and nickel-foam Cathode, isolated yield.

The clear benefits of electricity for this transformation were not restricted to act as a waste-free and inexpensive oxidant. In fact, the electricity-assisted C–H activation by nickel catalysis was highlighted by the outstanding levels of performance in comparison to the commonly used chemical oxidants, such as AgOAc, Cu(OAc)<sub>2</sub>, molecular oxygen, PhI(OAc)<sub>2</sub>, or K<sub>2</sub>S<sub>2</sub>O<sub>8</sub> (Figure 3.4.1).

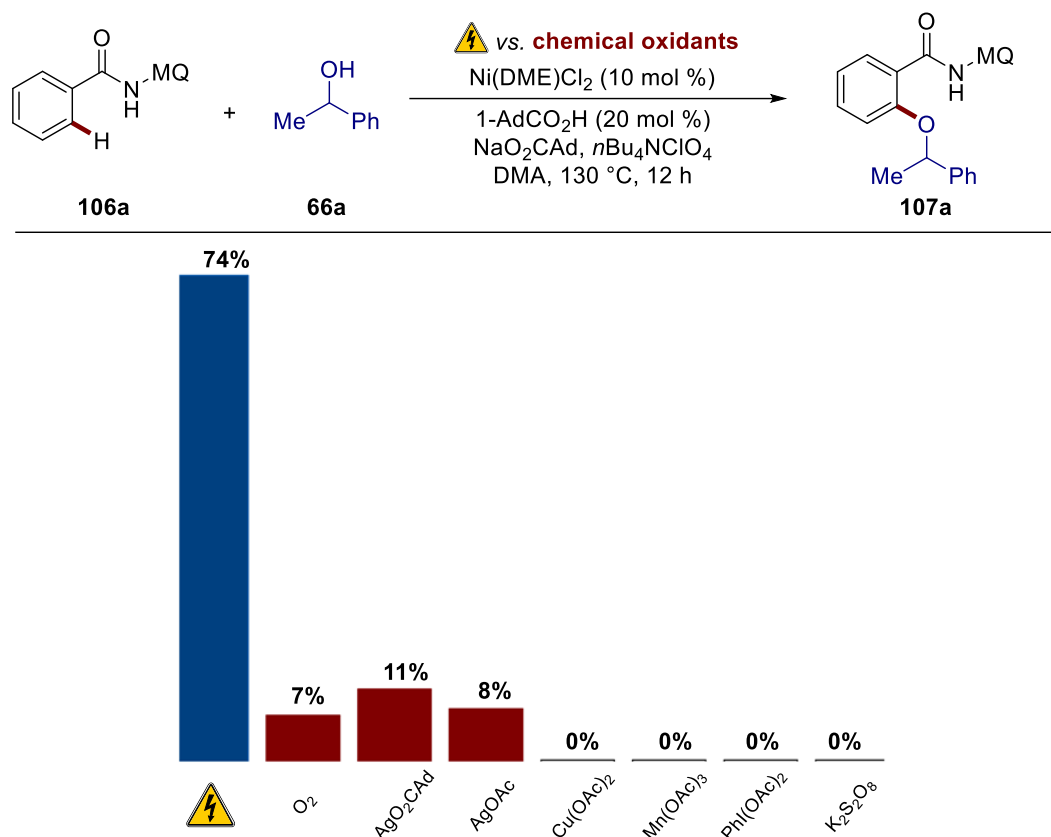
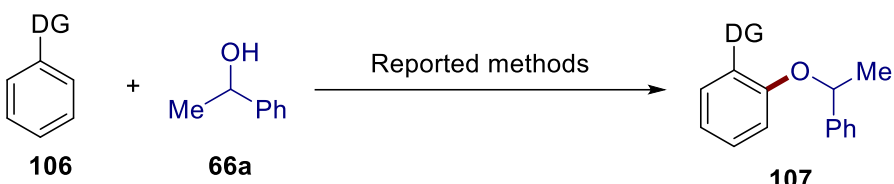


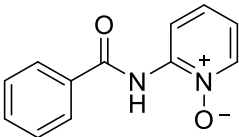
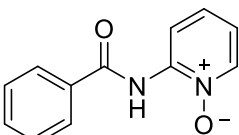
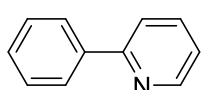
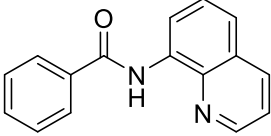
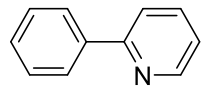
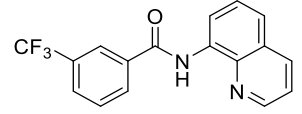
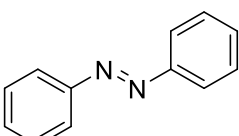
Figure 3.4.1. Electrochemical versus chemical oxidants.

### 3.4.2 Testing of Secondary Alcohols Following Reported Methods

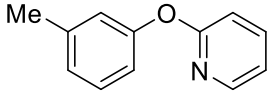
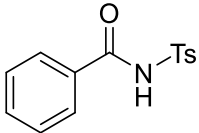
Most of the previous reports on transition metal-catalyzed C–H alkoxylation were limited to the use of primary alcohols or simply secondary alcohols, such as HFIP or *i*PrOH. To compare the efficiency of C–H alkoxylation between these known optimized reaction conditions and this nickel-electrocatalytic conditions, we next explored the performance of secondary alcohol **66a** with the previously developed methods (Table 3.4.4). Although palladium, copper, and cobalt catalysts showed high levels of performance for primary alcohols, no or minor conversions were observed with the sterically encumbered alcohol **66a** (entries 1–2, 5–9). In addition, the failure of known chemical oxidative C–H alkoxylation with nickel catalysis (entries 3–4) further highlighted the robustness and efficiency of the electrooxidative conditions we have established.

**Table 3.4.4.** Testing reaction of reported methods for alkoxylation with alcohol **66a**



Entry	Substrate	Usage of alcohol <b>66a</b>	[TM]	Isolated Yield
1 [129e]	 <b>106D</b> (0.20 mmol)	1.5 mL <b>(62 equiv)</b>	Co(OAc) <sub>2</sub>	<b>107D</b> : 10%
2 [163]	 <b>106D</b> (0.25 mmol)	2.3 mL <b>(76 equiv)</b>	Co(OAc) <sub>2</sub>	<b>107D</b> : n.r.
3 [130a]	 <b>13a</b> (0.50 mmol)	2.0 mL <b>(33 equiv)</b>	Ni(acac) <sub>2</sub>	<b>107E</b> : n.r.
4 [130b]	 <b>35a</b> (0.15 mmol)	0.9 mL <b>(50 equiv)</b>	Ni(OAc) <sub>2</sub>	<b>107F</b> : 18%
5 [126c]	 <b>13a</b> (1.0 mmol)	3.0 mL <b>(30 equiv)</b>	Cu(OAc) <sub>2</sub>	<b>107E</b> : n.r.
6 [124b]	 <b>35n</b> (0.50 mmol)	0.3 mL <b>(5.0 equiv)</b>	Cu <sub>2</sub> (OH) <sub>2</sub> CO <sub>3</sub>	<b>107G</b> : 19%
7 [125]	 <b>106H</b> (0.50 mmol)	2.0 mL <b>(33 equiv)</b>	Pd(OAc) <sub>2</sub>	<b>107H</b> : n.r. [a]

### 3. Results and Discussion

8 [125g]		2.2 mL (36 equiv)	Pd(OAc) <sub>2</sub>	107I: n.r. [a]
<hr/>				
9 [125j]		1.7 mL (70 equiv)	Pd(OAc) <sub>2</sub>	107J: n.r. [a]

The reactions were carried out according to the optimized reaction conditions of the literature methods, only by replacing the reported alcohol with the secondary alcohol **66a**. [a] **66a** was oxidized to acetophenone.

#### 3.4.3 Scope of Nickela-Electrocatalyzed C–H Alkoxylation

Having established the optimized reaction conditions, we probed the versatility of the nickela-electrocatalytic C–H oxygenation with diverse secondary alcohols **66** (Figure 3.4.2). Not only benzylic alcohols were converted efficiently (**107f**, **107g**), but also alicyclic, cyclic, and heterocyclic alcohols were identified as viable substrates, providing the desired products **107i–107t** with moderate to excellent yields. It is noteworthy that the naturally occurring alcohols, e.g., menthol, cholesterol, and  $\beta$ -estradiol were selectively transformed to the natural product hybrids **107u–107w**. Importantly, no racemization at the stereogenic centers occurred during this transformative electrosynthesis (**107u**, 99% ee).



### 3. Results and Discussion

heteroarene **106an**. Remarkably, the competition of strongly coordinating pyridine and 8-amininoquinoline chelation group afforded the unique amide-guided C–H activated product **107ao**. Additionally, the scale-up electrosynthesis was carried out without comprising the efficacy (**107aa**).

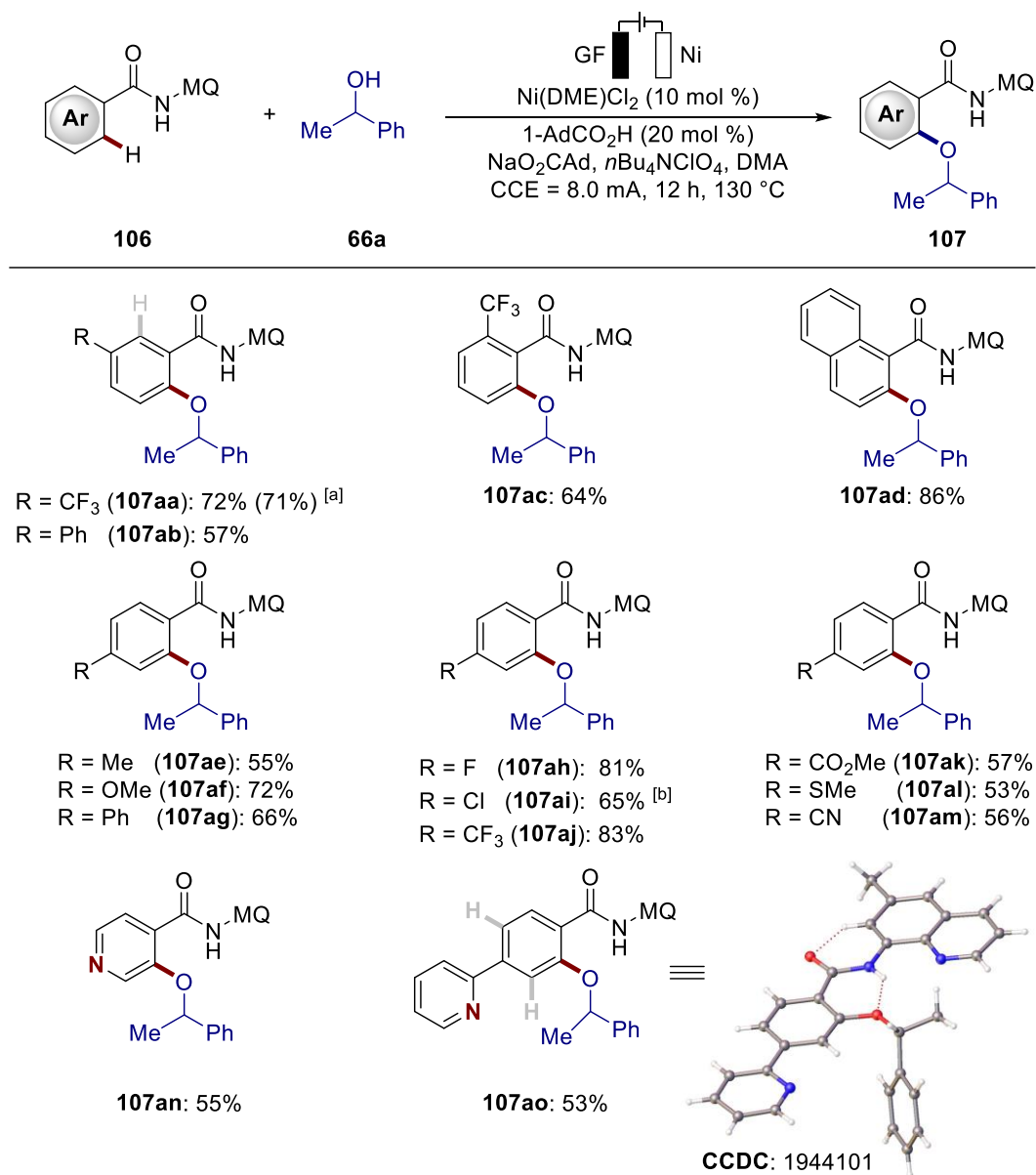


**Figure 3.4.3.** Electrooxidative C–H alkoxylation of arenes **106**. <sup>[a]</sup> Gram-scale testing with **106aa** (4.0 mmol, 1.32 g). <sup>[b]</sup> 3.0 mA, 32 h.

### 3.4.4 Mechanistic Studies

#### 3.4.4.1 Competition Experiments Between Distinct Arenes

In order to gain insights into the reaction mechanism of the robust nickela-electrocatalytic C–H alkoxylation, a series of mechanistic experiments were implemented. The intermolecular competition experiment was first performed between electronically-different *para*-substituted arenes **106aj** and **106ae**, with the electron-poor substrate proceeding faster (Figure 3.4.4a). And the same result was found when using *meta*-substrates **106aa** and **106a** (Figure 3.4.4b). In sharp contrast with the previous electrocatalytic C–H activations by palladium,<sup>[146, 148c, 148d, 149e-k]</sup> ruthenium,<sup>[157, 158c]</sup> rhodium<sup>[150]</sup>, iridium<sup>[160]</sup> or cobalt catalysis,<sup>[163, 164f-i, 165b, 165c]</sup> these findings suggested a concerted metalation deprotonation (CMD) pathway.<sup>[26, 173]</sup>

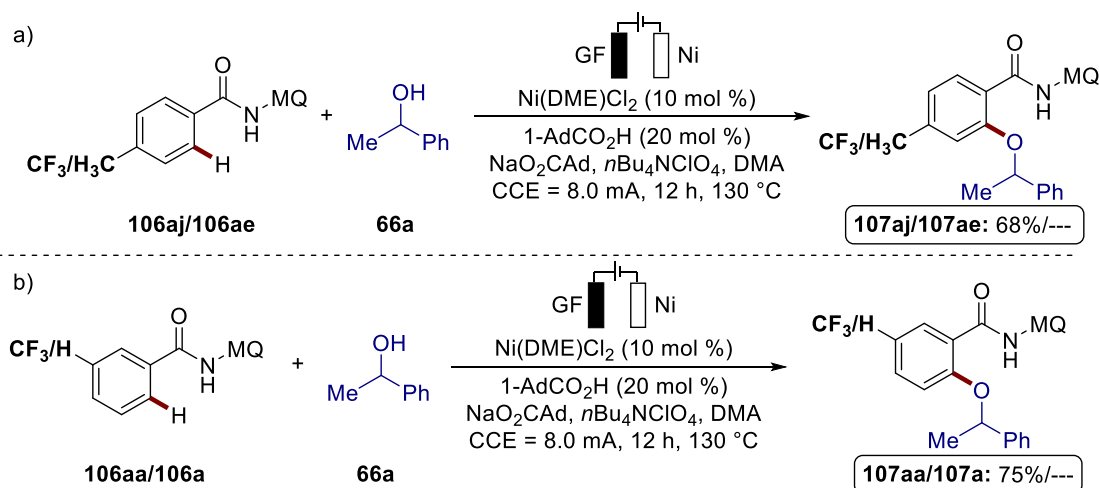


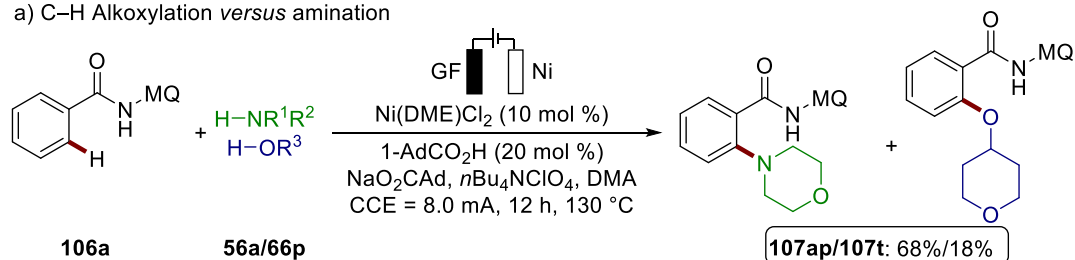
**Figure 3.4.4.** Competition experiments between arenes **106**. Conversions were determined by <sup>1</sup>H NMR analysis with 1,3,5-(MeO)<sub>3</sub>C<sub>6</sub>H<sub>3</sub> as the internal standard.

#### 3.4.4.2 Competition Experiments Between Different Nucleophiles

Competition experiments between secondary amine **56a** and alcohol **66p** showed that the C–O transformation was more challenging in comparison to the established nickela-electrocatalytic C–H amination (Figure 3.4.5a). Moreover, C–H alkoxylation occurred faster with primary alcohol **66t** than with secondary alcohol **66a**, further highlighting the power of the established nickela-electrosynthesis (Figure 3.4.5b).

### 3. Results and Discussion

#### a) C–H Alkoxylation *versus* amination



#### b) Primary *versus* secondary alcohol

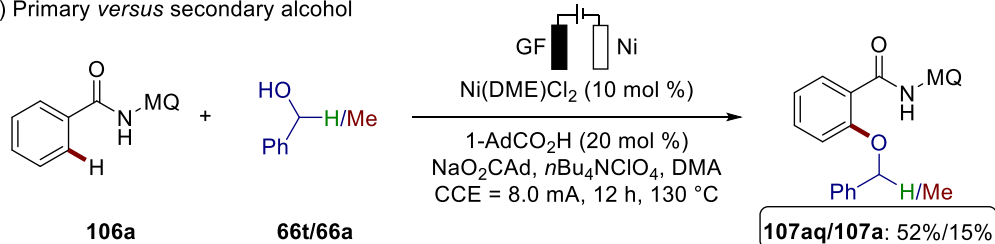
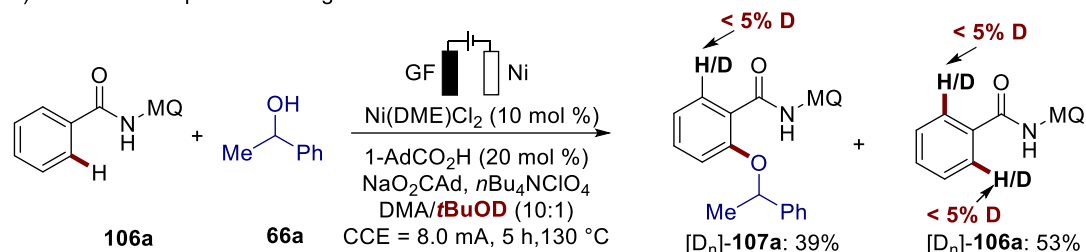


**Figure 3.4.5.** Competition experiment between different nucleophiles. Conversion determined by  $^1\text{H}$  NMR analysis with 1,3,5-(MeO) $_3\text{C}_6\text{H}_3$  as the internal standard.

#### 3.4.4.3 Experiments with Isotopically Labelled Solvent

No H/D scrambling was observed when using isotopically labelled *t*BuOD as the additive or using the deuterated substrate  $[\text{D}_5]\text{-}106a$ , supporting a plausible irreversible C–H activation (**Figure 3.4.6**).

#### a) Deuteration experiment using *t*BuOD as cosolvent



#### b) Deuteration experiment with $[\text{D}_5]\text{-}106a$

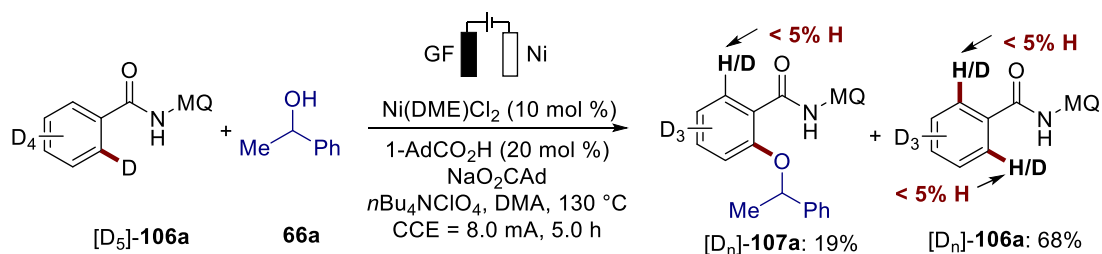


**Figure 3.4.6.** Deuteration experiments.



## 3.4.4.4 KIE Studies

A minor kinetic isotope effect (KIE) of  $k_H/k_D \approx 1.4$  as measured by independent experiments was suggestive of a facile C–H scission (**Figure 3.4.7**).

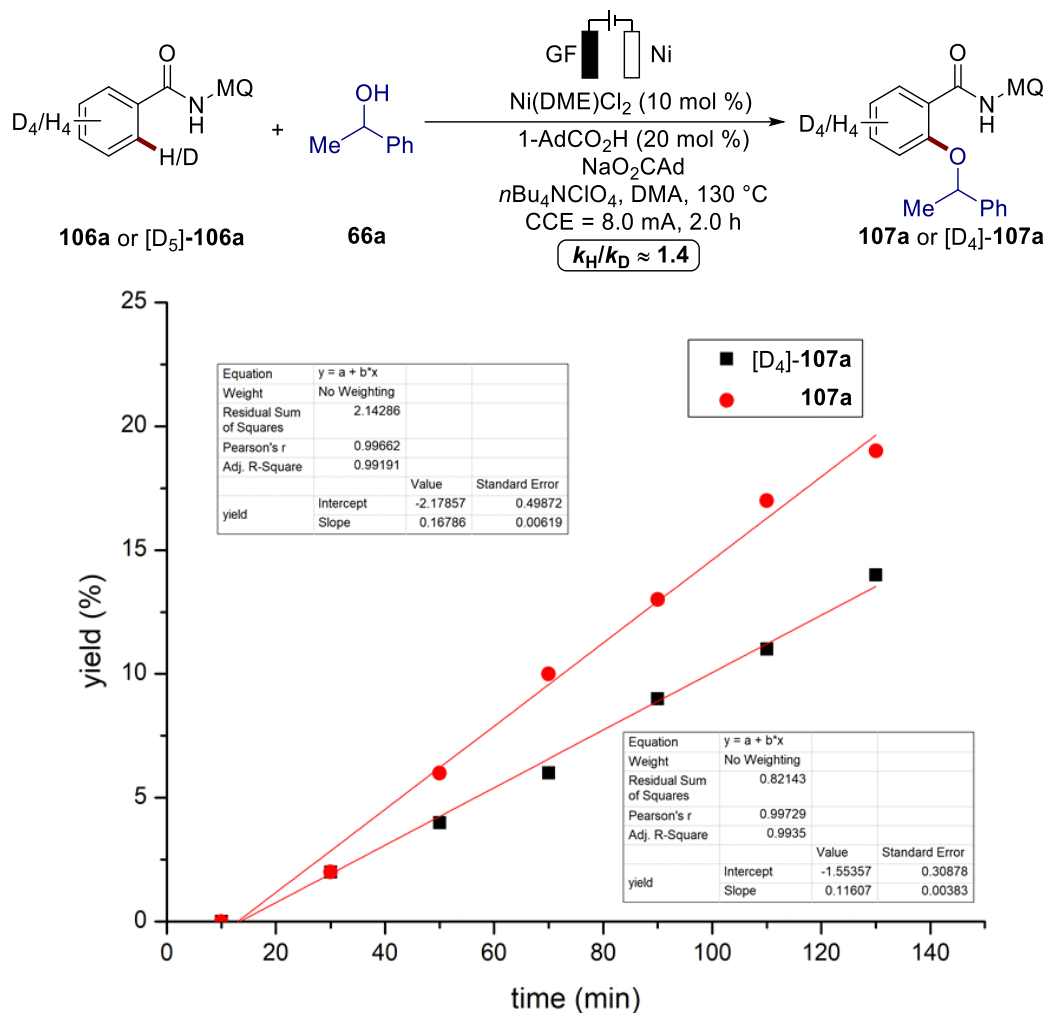


**Figure 3.4.7.** KIE studies by two parallel reactions.

## 3.4.4.5 Headspace GC-Analysis

Head-space gas-chromatographic analysis performed by Julia Struwe in the Ackermann group showed molecular hydrogen as the single stoichiometric byproduct (Figure 3.4.8).

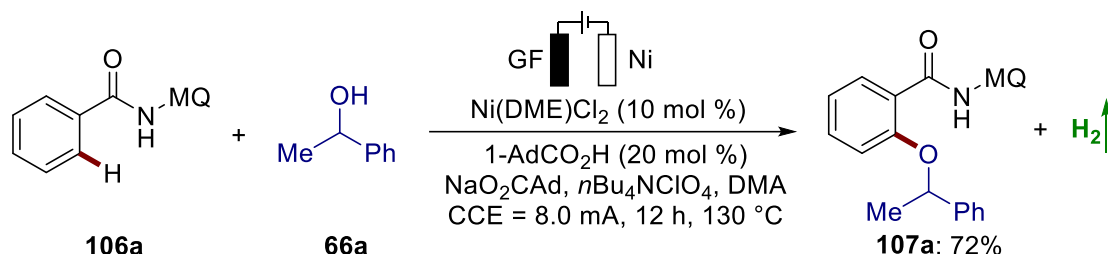


Figure 3.4.8. Headspace GC-analysis. Performed by Julia Struwe.

## 3.4.4.6 Radical Trapping Experiments

This electrocatalytic C–O formations were prevented through the independent addition of several typical radical scavengers, for example, TEMPO, BHT, or BQ, indicating a single-electron transfer (SET) step involved in the electrosynthesis (Figure 3.4.9).

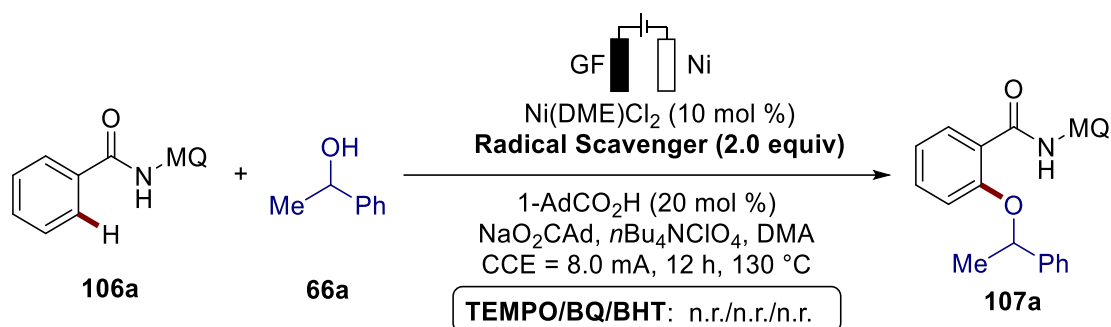


Figure 3.4.9. Radical trapping experiment with typical radical scavengers. TEMPO = (2,2,6,6-tetramethylpiperidin-1-yl)oxyl, BQ = benzoquinone, BHT = 2,6-di-*tert*-butyl-4-methylphenol.

## 3.4.5.7 Switch On-Off experiments

Additionally, we conducted electricity on-off experiments to investigate a radical-chain scenario (Figure 3.4.10). The C–H alkoxylation was inhibited without the electricity, however, the transformation continued after switching on the electric current again, thus ruling out a radical-chain process.

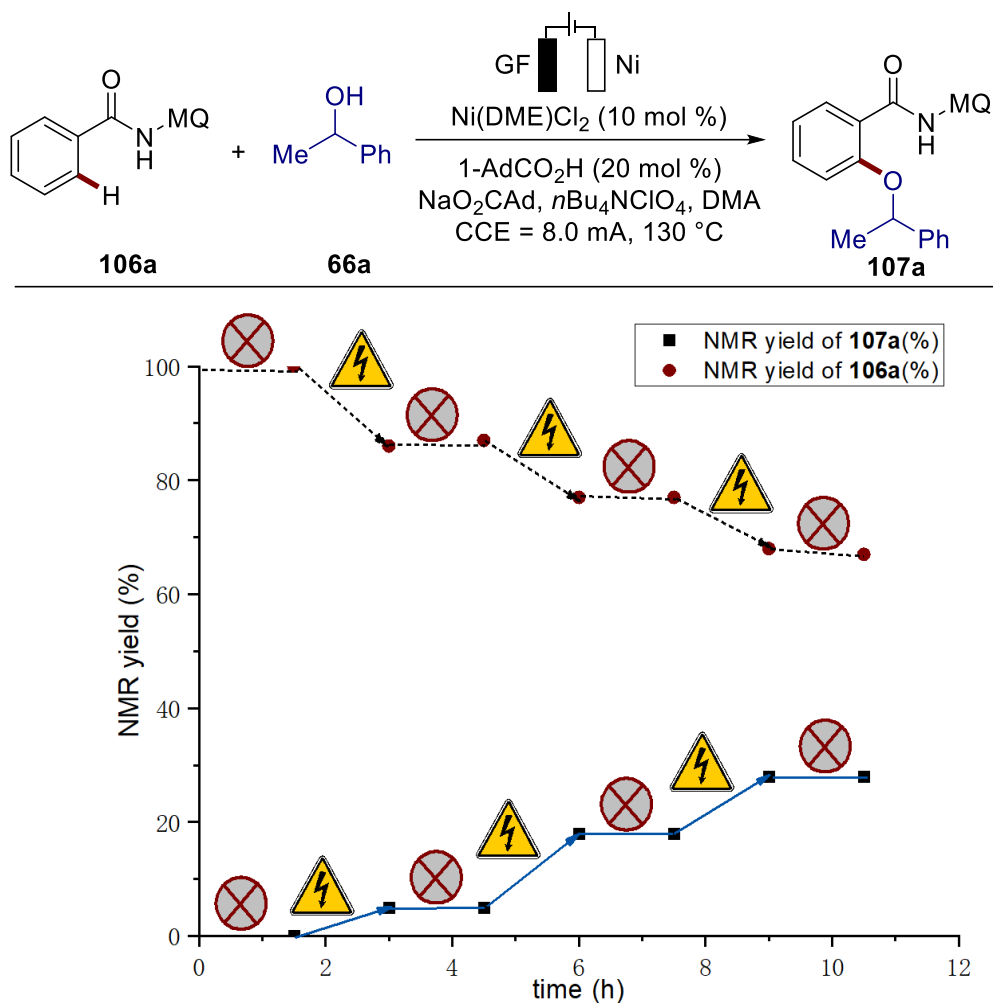
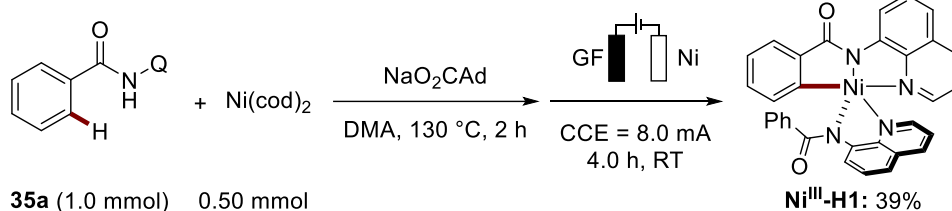
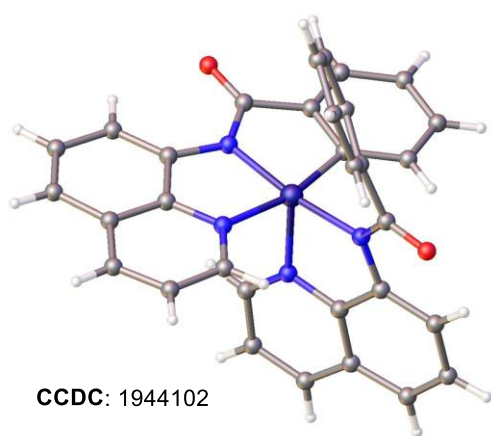
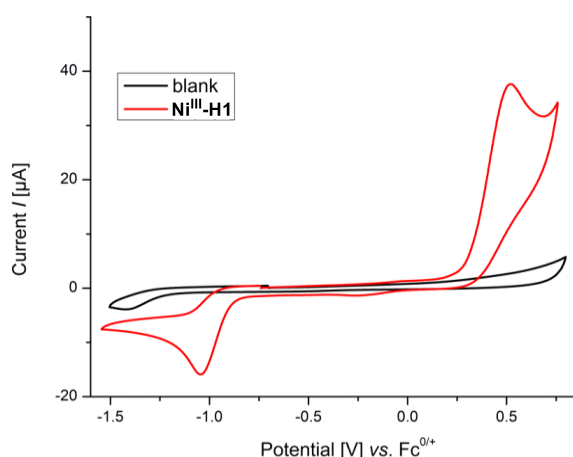


Figure 3.4.10. Switch on-off experiment of C–H alkoxylation.

## 3.4.4.8 Isolation and Characterization of Nickel(III) Intermediate

To rationalize the elementary process of C–O formation, the well-defined nickel(III) compound **Ni<sup>III</sup>-H1** was independently prepared through electrosynthesis, and fully characterized by X-ray diffraction analysis (**Figure 3.4.11a, b**).<sup>[177]</sup> Cyclic voltammetric studies of **Ni<sup>III</sup>-H1** by Julia Struwe showed a facile oxidation at the potential of +0.50 V vs. Fc<sup>+0</sup> (red, **Figure 3.4.11c**), revealing the generation of a formal nickel(IV) complex.

a) Synthesis of **Ni<sup>III</sup>-H1**b) X-ray of **Ni<sup>III</sup>-H1**c) CV of **Ni<sup>III</sup>-H1**

**Figure 3.4.11.** Isolation and characterization of nickel(III) complex. a) Synthesis of **Ni<sup>III</sup>-H1**. b) X-ray diffraction analysis of **Ni<sup>III</sup>-H1**. c) CV data of **Ni<sup>III</sup>-H1** (DMA, 0.1 M [nBu<sub>4</sub>NBF<sub>4</sub>], 100 mV/s). CV was performed by Julia Struwe.

With the well-defined nickel(III) complex **Ni<sup>III</sup>-H1** in hand, we thus probed its performance in catalytic (**Figure 3.4.12a, b**) and stoichiometric settings (**Figure 3.4.12c**). These results clearly manifested that **Ni<sup>III</sup>-H1** was the catalytically relevant species in the presence of electricity.

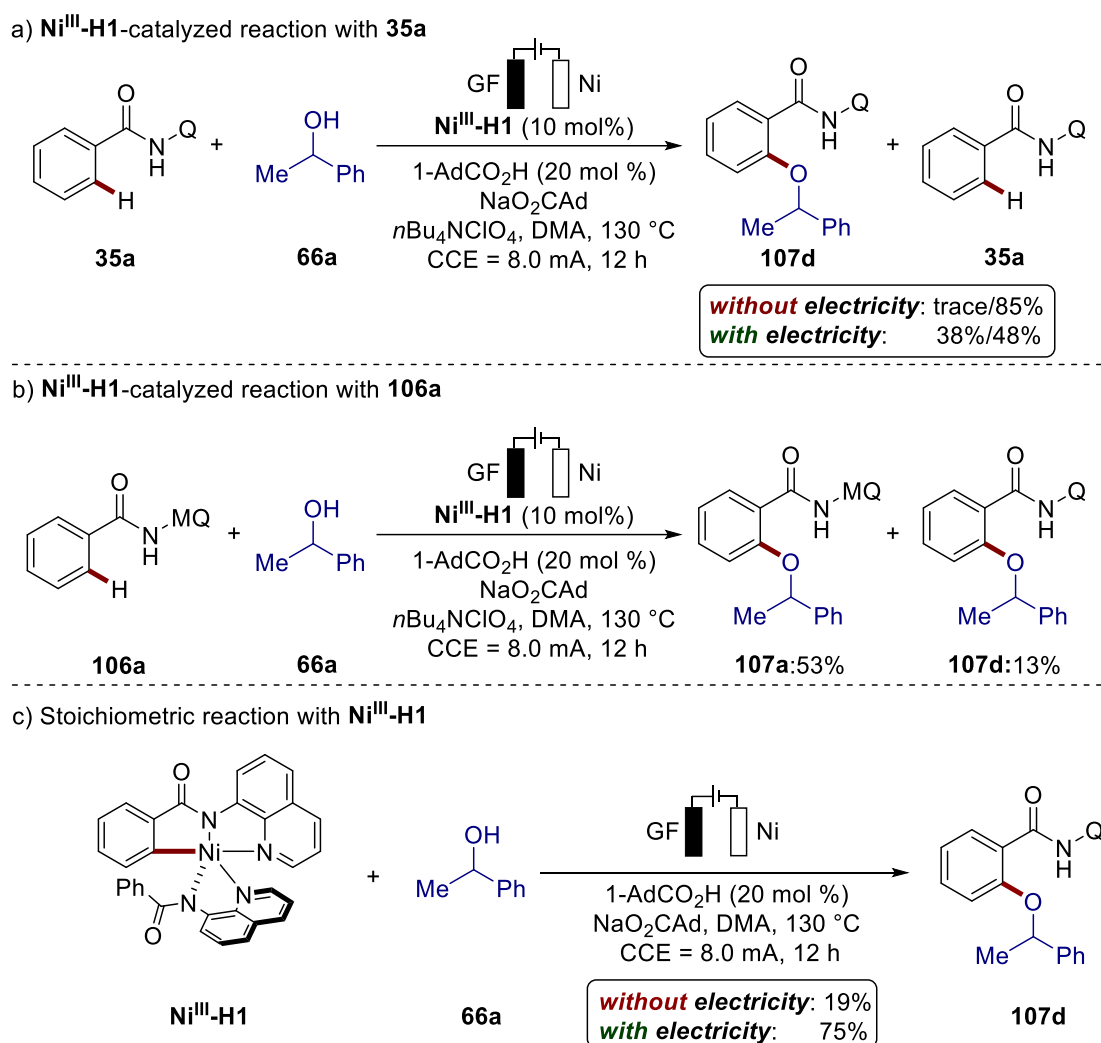


**Figure 3.4.12.** Catalytic and stoichiometric reaction using **Ni<sup>III</sup>-H1**. Conversion determined by <sup>1</sup>H NMR analysis with 1,3,5-(MeO)<sub>3</sub>C<sub>6</sub>H<sub>3</sub> as the internal standard.

## 3.4.4.9 DFT Calculations

In good agreement with these results, DFT calculations that were performed by Dr. Lianrui Hu indicated a non-innocent ligand phenomenon in the oxidation process to deliver a formal nickel(IV) species (**Figure 3.4.13**). The oxidation was thus best identified as a ligand-centered process.

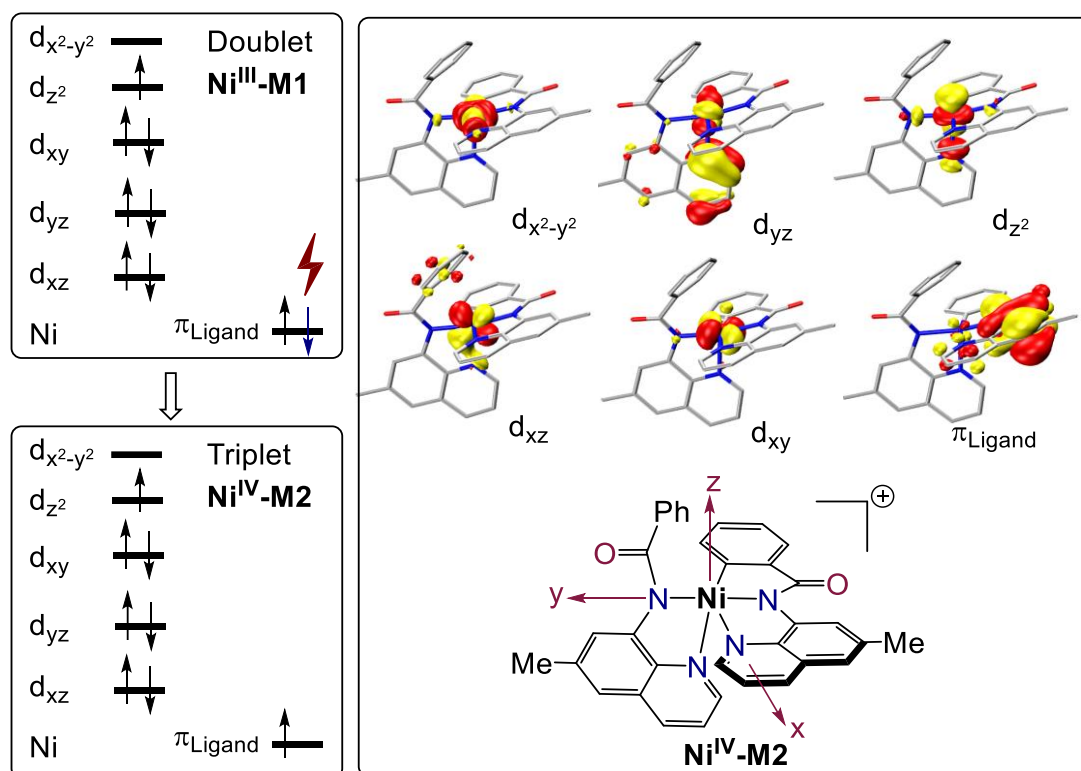


**Figure 3.4.13.** Calculated electronic configuration of **Ni<sup>IV</sup>-M2** ground triplet state. Performed by Dr. Lianrui Hu.

### 3.4.5 Proposed Mechanism

Based on these results, we proposed a catalytic C–H alkoxylation by nickel-electrocatalysis (Figure 3.4.14). The initial fast C–H nickelation occurred with the assistance of the carboxylate in a CMD manner to generate **108b**, which underwent anodic oxidation to form the catalytically competent **108c**. Finally, high-valent intermediate nickel(IV) complex  $\text{Ni}^{\text{IV}}\text{-M2}$  from the oxidized **108c** was coordinated by the alcohol **66**, along with subsequent deprotonation and reductive elimination to furnish the desired product **107** and the regenerated nickel(II) **108a** (Figure 3.4.14).

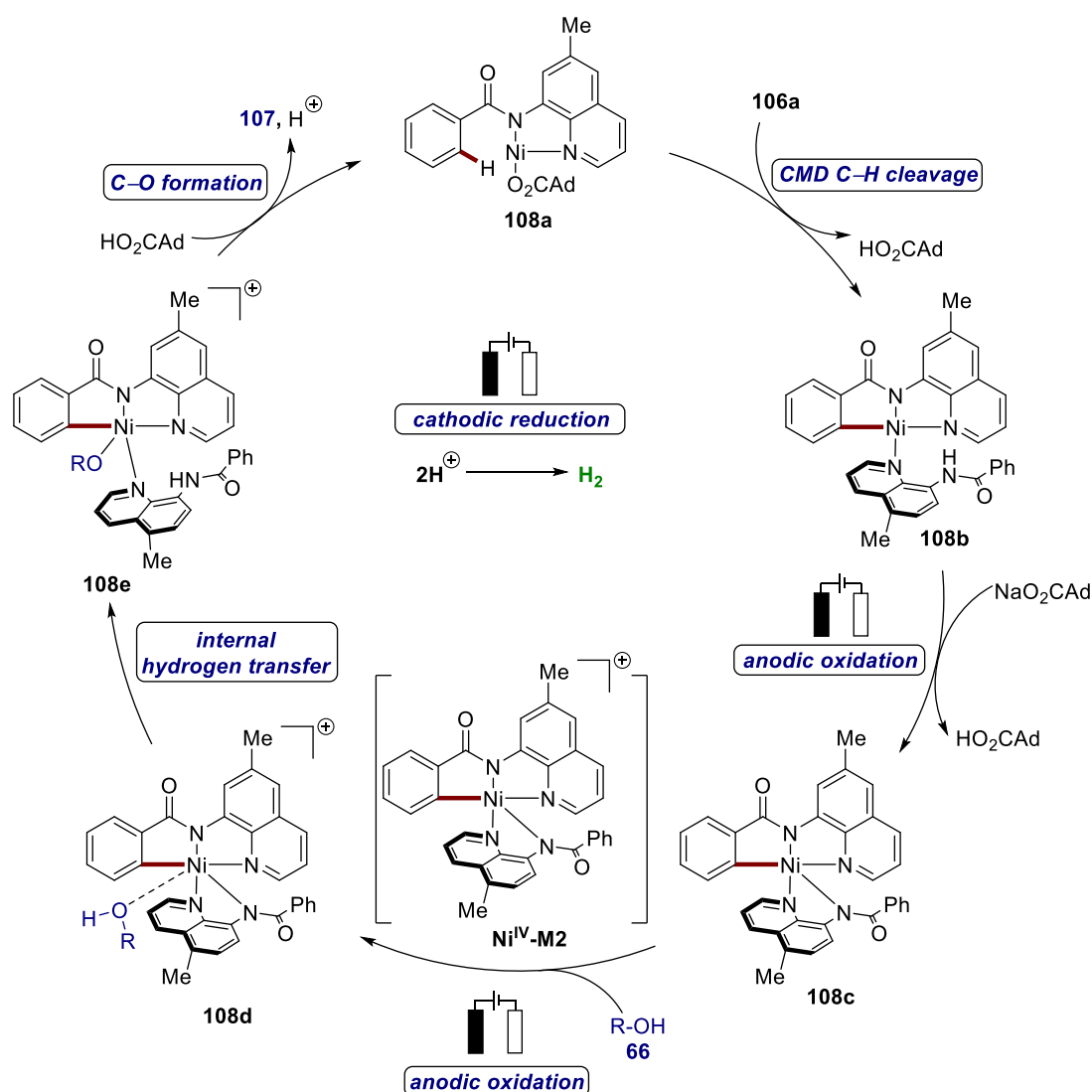
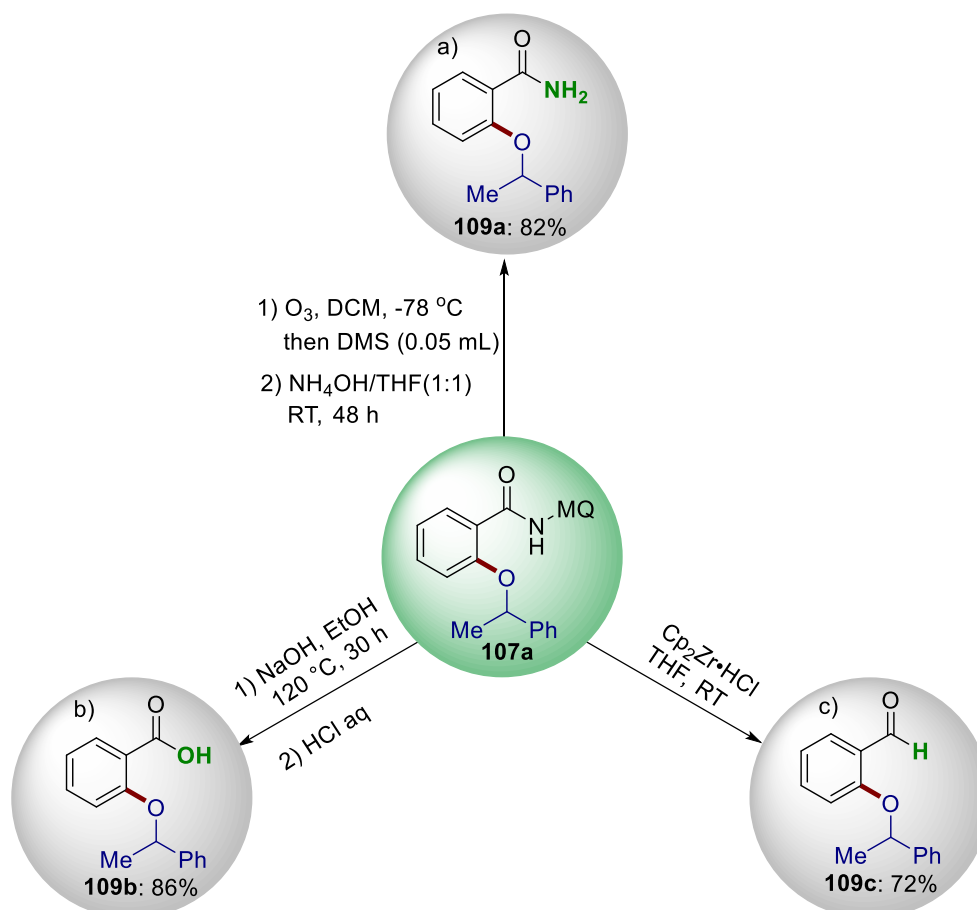


Figure 3.4.14. Proposed mechanism of nickel-electrooxidative C–H alkoxylation.

### 3.4.6 Removal of the Directing Group

As to the synthetic utility of this method, the 6-methylquinuoline was easily removed in a traceless manner to provide efficient access to benzamide **109a**, benzoic acid **109b**, or aromatic aldehyde **109c** (Figure 3.4.15).



**Figure 3.4.15.** Removal of the directing group to obtain a) primary amide **109a**; b) benzoic acid **109b**; c) aromatic aldehyde **109c**.



### 3.5 Nickela-Electrocatalyzed C–H Phosphorylation

Molecular synthesis with phosphorus-containing compound is of significance to access bioactive compounds and materials.<sup>[132-134]</sup> In a concept of step- and atom-economy, transition metal-catalyzed C–H phosphorylation without prefunctionalization represents a more attractive perspective over the classic Hirao cross-coupling reactions.<sup>[134]</sup> Due to the inherent strong coordination of phosphorus to the metal center, the few reports on C–P formation were so far restricted to the method of adding phosphonating reagents slowly or sequentially, or using masked substrates.<sup>[136-139]</sup>

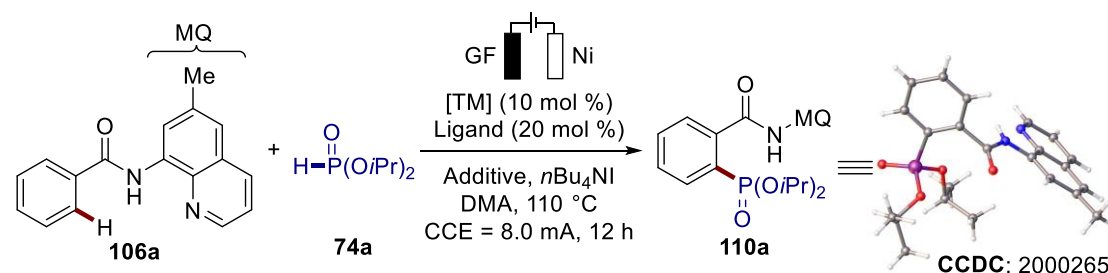
As mentioned in **chapter 1.4**, electrosynthesis has emerged as an increasingly powerful and useful tool for transition metal-catalyzed C–C and C–Het bond formation due to the replacement of toxic and costly chemical oxidants and reductants by safe and environmentally-benign electric current as redox mediator. To the best of our knowledge, nickel-catalyzed C–H phosphorylation using chemical oxidants are not described. We hence became attracted to the challenging C–P construction by cost-efficient electric current as the redox equivalent.

#### 3.5.1 Optimization Studies

We commenced our investigations by testing reaction conditions for the nickela-electrooxidative C–H phosphorylation of arene **106a** in presence of an unmasked phosphonating reagent **74a**, added in a non-sequential manner (**Table 3.5.1**). After additive and ligand optimization (entries 1–9), the desired product **110a** was isolated in high yield when the organic base TMG was employed as additive and (4-CF<sub>3</sub>C<sub>6</sub>H<sub>4</sub>)<sub>3</sub>P or [3,5-(CF<sub>3</sub>)<sub>2</sub>C<sub>6</sub>H<sub>3</sub>]<sub>3</sub>P as ligand (entries 1–9). Control experiments confirmed the essential role of the base, the nickel catalyst and the current for the C–H phosphorylation (entries 10–12). The use of other nickel complex like Ni(cod)<sub>2</sub> led to the C–P transformation as well, albeit with slightly reduced efficacy (entry 13). It is particularly noteworthy that Earth-abundant nickel catalysis proved to be more effective for the 8-aminoquinoline-assisted electrocatalytic C–H phosphorylation than other 3d

metals, such as cobalt, copper, manganese and iron, and precious metals likewise palladium, rhodium and iridium (entries 14–20).

**Table 3.5.1.** Optimization of nickela-electrooxidative C–H phosphorylation <sup>[a]</sup>



Entry	Additive	Ligand	[TM]	<b>110a</b> [%]
1	NaO <sub>2</sub> CAd	(4-CF <sub>3</sub> C <sub>6</sub> H <sub>4</sub> ) <sub>3</sub> P	Ni(DME)Cl <sub>2</sub>	62
2	NaOAc	(4-CF <sub>3</sub> C <sub>6</sub> H <sub>4</sub> ) <sub>3</sub> P	Ni(DME)Cl <sub>2</sub>	(35) <sup>[b]</sup>
3	DBU	(4-CF <sub>3</sub> C <sub>6</sub> H <sub>4</sub> ) <sub>3</sub> P	Ni(DME)Cl <sub>2</sub>	(51) <sup>[b]</sup>
4	DBN	(4-CF <sub>3</sub> C <sub>6</sub> H <sub>4</sub> ) <sub>3</sub> P	Ni(DME)Cl <sub>2</sub>	(60) <sup>[b]</sup>
5	<b>TMG</b>	<b>(4-CF<sub>3</sub>C<sub>6</sub>H<sub>4</sub>)<sub>3</sub>P</b>	<b>Ni(DME)Cl<sub>2</sub></b>	<b>72 (74) <sup>[b]</sup></b>
6	<b>TMG</b>	<b>[3,5-(CF<sub>3</sub>)<sub>2</sub>C<sub>6</sub>H<sub>3</sub>]<sub>3</sub>P</b>	<b>Ni(DME)Cl<sub>2</sub></b>	<b>73 (74) <sup>[b]</sup></b>
7	TMG	XPhos	Ni(DME)Cl <sub>2</sub>	67 <sup>[e]</sup>
8	TMG	---	Ni(DME)Cl <sub>2</sub>	45 (50) <sup>[b]</sup>
9	TMG	dtbpy	Ni(DME)Cl <sub>2</sub>	---
10	---	[3,5-(CF <sub>3</sub> ) <sub>2</sub> C <sub>6</sub> H <sub>3</sub> ] <sub>3</sub> P	Ni(DME)Cl <sub>2</sub>	---
11	TMG	[3,5-(CF <sub>3</sub> ) <sub>2</sub> C <sub>6</sub> H <sub>3</sub> ] <sub>3</sub> P	--	---
12	TMG	[3,5-(CF <sub>3</sub> ) <sub>2</sub> C <sub>6</sub> H <sub>3</sub> ] <sub>3</sub> P	Ni(DME)Cl <sub>2</sub>	--- <sup>[c]</sup>
13	TMG	[3,5-(CF <sub>3</sub> ) <sub>2</sub> C <sub>6</sub> H <sub>3</sub> ] <sub>3</sub> P	Ni(cod) <sub>2</sub>	66
14	TMG	[3,5-(CF <sub>3</sub> ) <sub>2</sub> C <sub>6</sub> H <sub>3</sub> ] <sub>3</sub> P	Cu(OAc) <sub>2</sub> ·H <sub>2</sub> O	(<5) <sup>[b]</sup>
15	TMG	[3,5-(CF <sub>3</sub> ) <sub>2</sub> C <sub>6</sub> H <sub>3</sub> ] <sub>3</sub> P	Co(OAc) <sub>2</sub> ·4H <sub>2</sub> O	(<5) <sup>[b]</sup>
16	TMG	[3,5-(CF <sub>3</sub> ) <sub>2</sub> C <sub>6</sub> H <sub>3</sub> ] <sub>3</sub> P	Mn(OAc) <sub>2</sub>	(8) <sup>[b]</sup>
17	TMG	[3,5-(CF <sub>3</sub> ) <sub>2</sub> C <sub>6</sub> H <sub>3</sub> ] <sub>3</sub> P	Fe(acac) <sub>3</sub>	(<5) <sup>[b]</sup>
18	TMG	[3,5-(CF <sub>3</sub> ) <sub>2</sub> C <sub>6</sub> H <sub>3</sub> ] <sub>3</sub> P	PdCl <sub>2</sub>	---
19	TMG	[3,5-(CF <sub>3</sub> ) <sub>2</sub> C <sub>6</sub> H <sub>3</sub> ] <sub>3</sub> P	[Cp* <i>Rh</i> Cl <sub>2</sub> ] <sub>2</sub>	--- <sup>[d]</sup>
20	TMG	[3,5-(CF <sub>3</sub> ) <sub>2</sub> C <sub>6</sub> H <sub>3</sub> ] <sub>3</sub> P	[Cp* <i>Ir</i> Cl <sub>2</sub> ] <sub>2</sub>	--- <sup>[d]</sup>

<sup>[a]</sup> Reaction conditions: **106a** (0.25 mmol), **74a** (0.50 mmol), [TM] (10 mol %), phosphine (20 mol %), Additive (1.0 equiv), TBAI (0.125 mmol), DMA (3.0 mL), CCE = 8.0 mA, 12 h, N<sub>2</sub>, graphite felt (GF) anode and nickel-foam cathode, isolated yield. <sup>[b]</sup> Yields were determined by <sup>1</sup>H NMR analysis with 1,3,5-(MeO)<sub>3</sub>C<sub>6</sub>H<sub>3</sub> as the internal standard. <sup>[c]</sup> Without current. <sup>[d]</sup> [TM] (5.0 mol %). DBU = 1,8-diazabicyclo[5.4.0]undec-7-ene; DBN = 1,5-diazabicyclo[4.3.0]non-5-ene; TMG = tetramethylguanidine; dtbpy = 4,4'-di-*tert*-butyl-2,2'-dipyridyl. <sup>[e]</sup> Performed by Dr. Antonio Del Vecchio.

A series of experiments was conducted by Dr. Antonio Del Vecchio with various typical chemical oxidants, such as AgOAc, Cu(OAc)<sub>2</sub>, Mn(OAc)<sub>3</sub>, K<sub>2</sub>S<sub>2</sub>O<sub>8</sub>, PhI(OAc)<sub>2</sub>, or molecular oxygen in the absence of electricity, furnishing the arylphosphonates with very low or even no conversions (**Figure 3.5.1**). These results clearly highlighted that electricity not only acted as a waste-free and cost-efficient oxidant, but also provided a unique efficacy for electron transfer during the C–H phosphorylation.

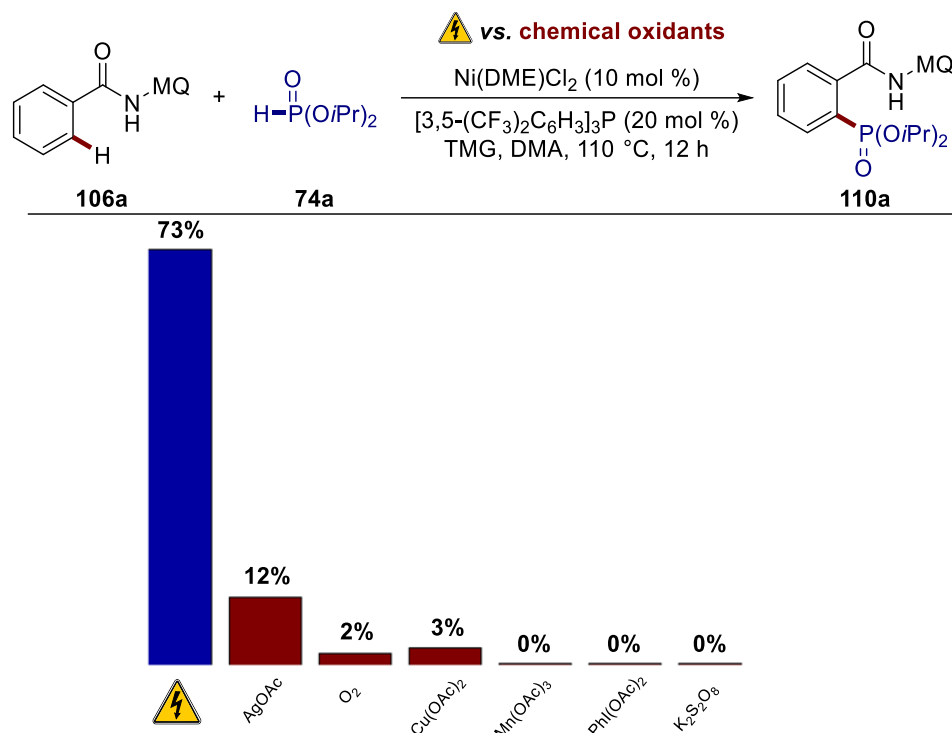


**Figure 3.5.1.** Electrochemical vs. chemical oxidants. Reaction conditions: **106a** (0.15 mmol), **74a** (0.30 mmol, 2.0 equiv), phosphine (0.030 mmol, 20 mol %), Ni(DME)Cl<sub>2</sub> (0.015 mmol, 10 mol %), TMG (0.15 mmol, 1.0 equiv), DMA (1.8 mL), chemical oxidants such as AgOAc (1.3 equiv, 0.20 mmol), Cu(OAc)<sub>2</sub> (1.3 equiv, 0.20 mmol), Mn(OAc)<sub>3</sub> (1.3 equiv, 0.20 mmol), K<sub>2</sub>S<sub>2</sub>O<sub>8</sub> (1.3 equiv, 0.20 mmol), PhI(OAc)<sub>2</sub> (1.3 equiv, 0.20 mmol), or O<sub>2</sub> (1.0 atm). <sup>1</sup>H NMR conversion with 1,3,5-(MeO)<sub>3</sub>C<sub>6</sub>H<sub>3</sub> as the internal standard. Performed by Dr. Antonio Del Vecchio.

### 3.5.2 Scope of the Nickela-Electrocatalyzed C–H Phosphorylation

Having the optimized electrocatalytic conditions in hand, we next investigated the effect of monodentate and bidentate directing groups (**Figure 3.5.2**). These findings emphasized the importance of the 8-aminoquinoline coordinating moiety towards the substrate for construction the C–P bond.

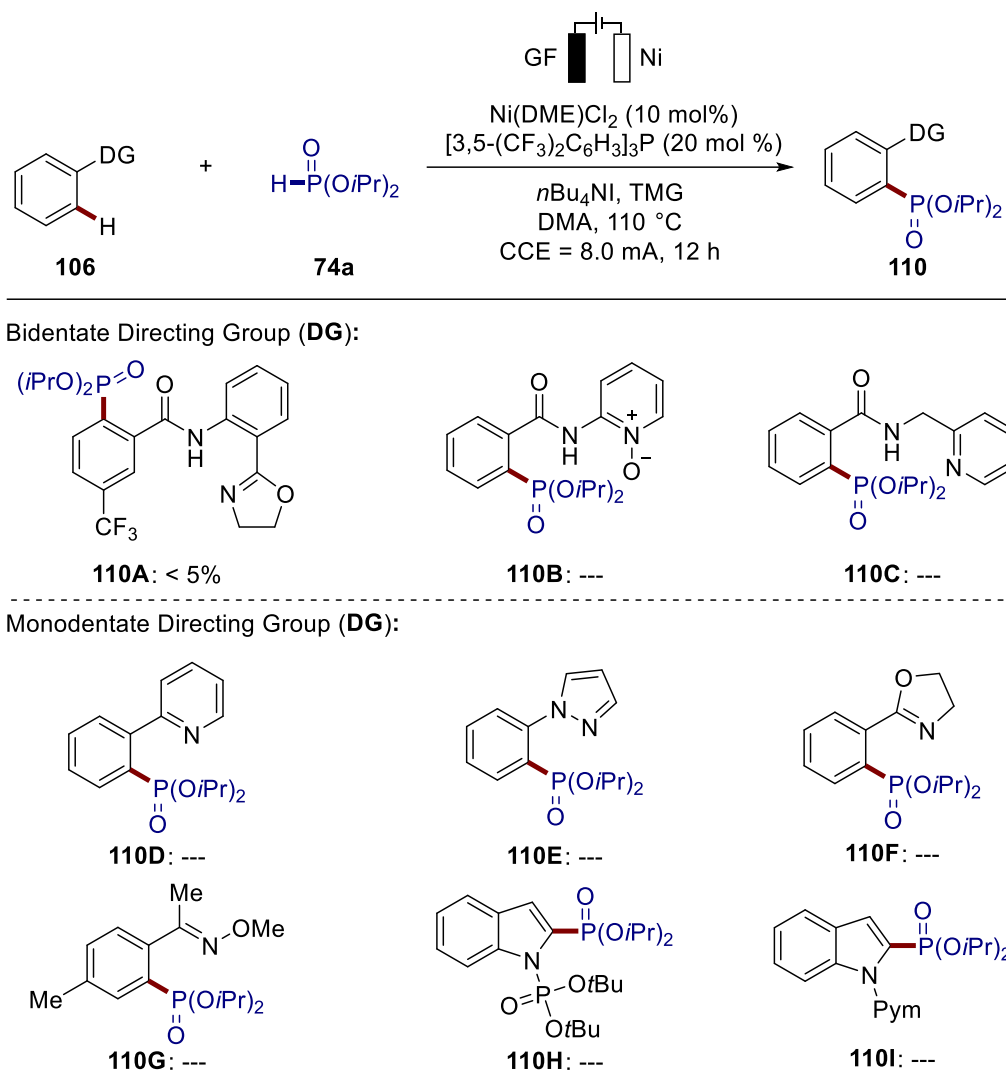


**Figure 3.5.2.** Investigation of the effect of the directing groups. The experiments with **110D–110I** were performed by Dr. Antonio Del Vecchio.

Moreover, it was observed that the efficacy of the nickela-catalytic C–H phosphorylation was affected by the substitution pattern of the quinoline moiety (**Figure 3.5.3**, **110a–110f**). We continued to probe the versatility of the nickela-electrooxidative C–H phosphorylation with diversely decorated arenes **106**. Thereby, substrates with different valuable functional groups including halo, ester or amine substituent, were transferred efficiently into aromatic phosponates **110l–110n**. The excellent regioselectivity of nickela-electrocatalysis regime was shown with *meta*-substituent benzamides **106n–106o** to deliver the sole product **110q–110u**. The electrocatalytic C–P formation was not restrained to arenes, but also heteroarenes furnished the corresponding arylphosponates **110v–110w** even in a shorter reaction time. Remarkably, the competition between the aminoquinoline directing group and the monodentate pyridine group exclusively produced the amide-guided C–H phosphorylated product **110x**. Benzamide containing the protected chiral amino acid was well tolerated for providing peptide **110y** without notable racemization. The strategy of versatile nickela-electrochemical C–H transformation was successfully applied to alkenes **106v** to give desired product **110z**. The efficiency of guanidine-assisted nickela-electrooxidative C–H phosphorylation was also proven by gram-scale experiment with a negligible difference in isolated yields (**110o**, 1.31 g).

### 3. Results and Discussion

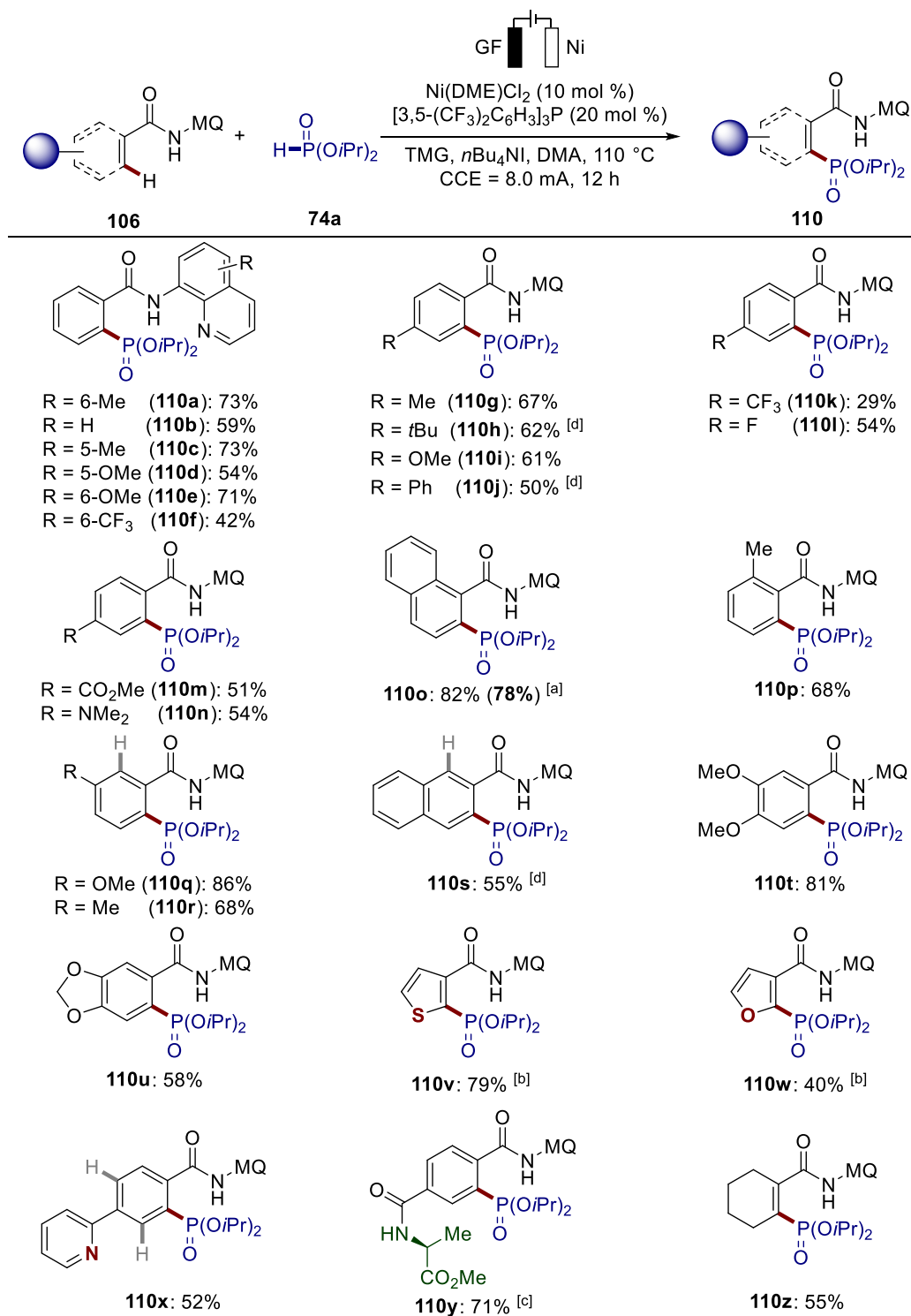


**Figure 3.5.3.** Nickela-electrooxidative C(sp<sup>2</sup>)-H phosphorylation of heteroarenes and olefins **106** with **74a**.

<sup>[a]</sup> Gram-scale reaction with benzamide (1.31 g of **17**); <sup>[b]</sup> 8.0 mA, 5.0 h; <sup>[c]</sup> Ni(DME)Cl<sub>2</sub> (20 mol %), [3,5-(CF<sub>3</sub>)<sub>2</sub>C<sub>6</sub>H<sub>3</sub>]<sub>3</sub>P (40 mol %), **74a** (3.0 equiv). <sup>[d]</sup> Performed by Dr. Antonio Del Vecchio.

Subsequently, the robustness of nickela-electrocatalytic C-H functionalization was highlighted by the synthesis of target products with valuable phosphonates, phosphine oxides and other substrates **74** (**Figure 3.5.4**, **110ab–110al**). Product **110af** derived

from the bulky natural *D*-menthol was acquired in a high yield. Six- and seven-membered cyclic phosphonates **74g–74i** were effectively converted. To our delight, the scope of phosphonating reagents could be extended to include mono- and dialkylphosphine oxides, delivering the desired arylphosphonates **110aj** and **110ak** with satisfactory yields. It is noteworthy that the sterically encumbered diaminophosphine oxide was efficiently converted into the corresponding product **110al**, establishing an alternative path for the synthesis of potentially exploitable compounds as flame-retardants for epoxy resins.<sup>[178]</sup>

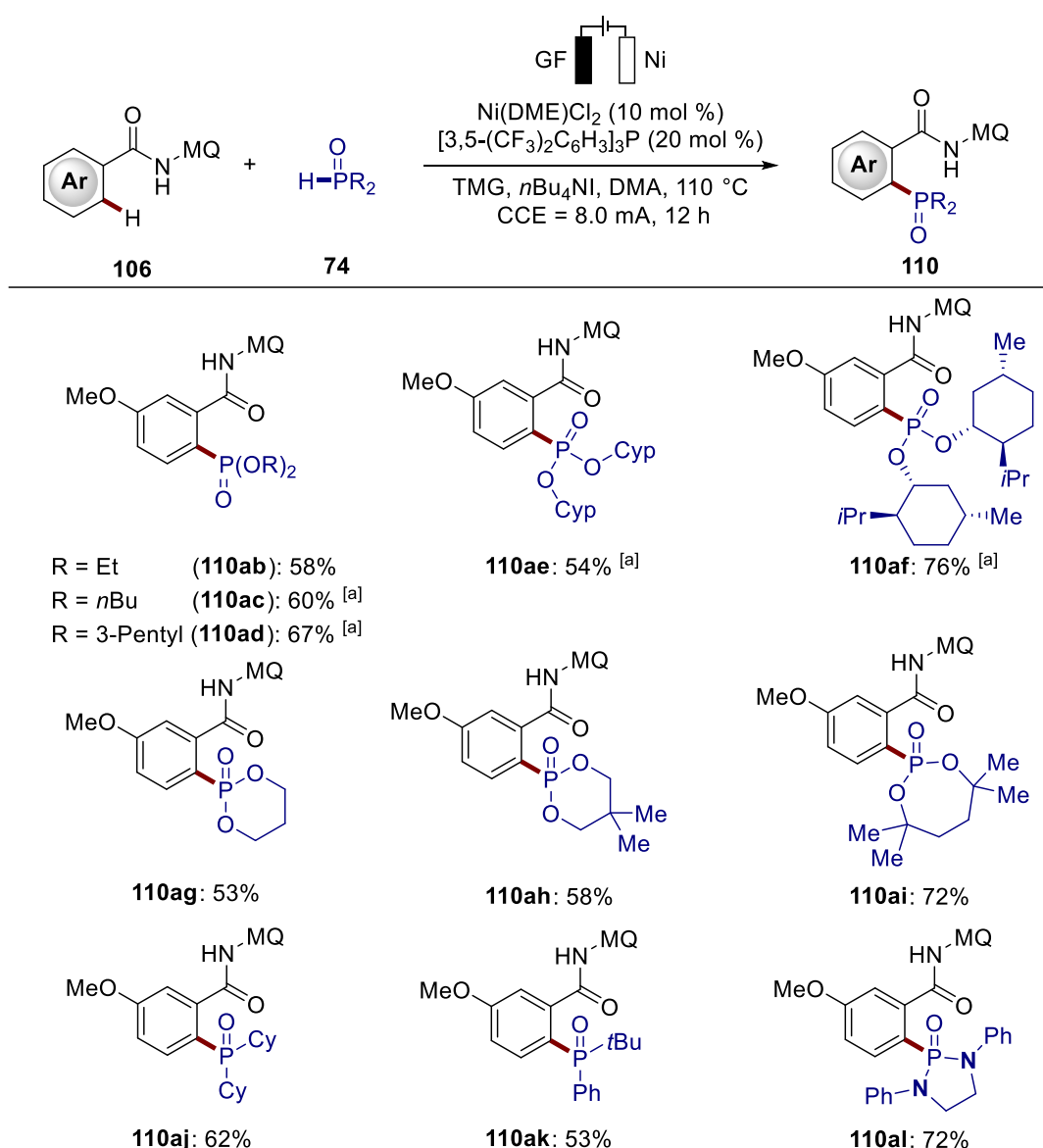


**Figure 3.5.4.** Nickela-electrooxidative C–H phosphorylation with phosphonating reagents **74**.  
<sup>[a]</sup> Performed by Dr. Antonio Del Vecchio.

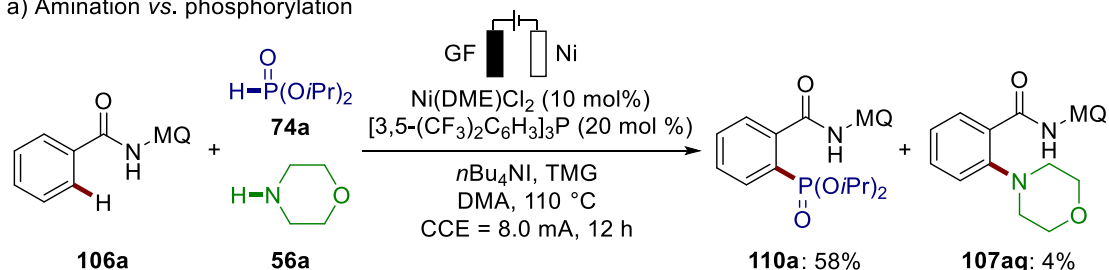
### 3.5.3 Mechanistic Studies

Intrigued by the unique performance of the nickel-electrocatalytic C–H phosphorylation, we became attracted to probing its *modus operandi*.

#### 3.5.3.1 Competition Experiment Between Phosphite and Amine

Intermolecular competition experiments between diisopropyl phosphonate (**74a**) and morpholine (**56a**) clearly showed that the optimized conditions were particularly suitable for forming C–P bonds (Figure 3.5.5a). In addition, the conditions for the C–H phosphorylation also resulted in excellent yields for C–N formation (Figure 3.5.5b).

a) Amination vs. phosphorylation



b) Electrooxidative amination

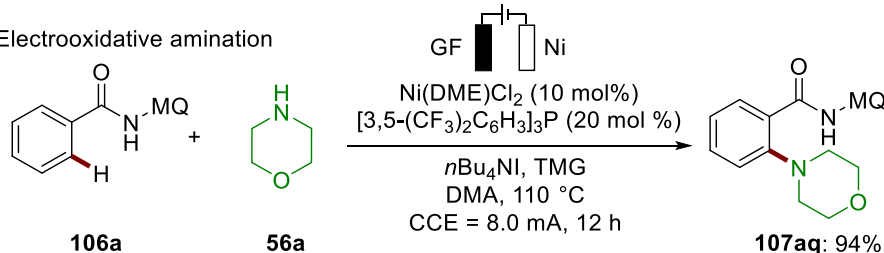


Figure 3.5.5. Competition experiment between amine **56a** and phosphite **74a**.

#### 3.5.3.2 Experiments with Isotopically Labelled Solvent

H/D exchange was not observed in both the product [D<sub>n</sub>]-**110a** and the reisolated benzamide [D<sub>n</sub>]-**106a**, when utilizing isotopically labelled *t*BuOD as a co-solvent (Figure 3.5.6).

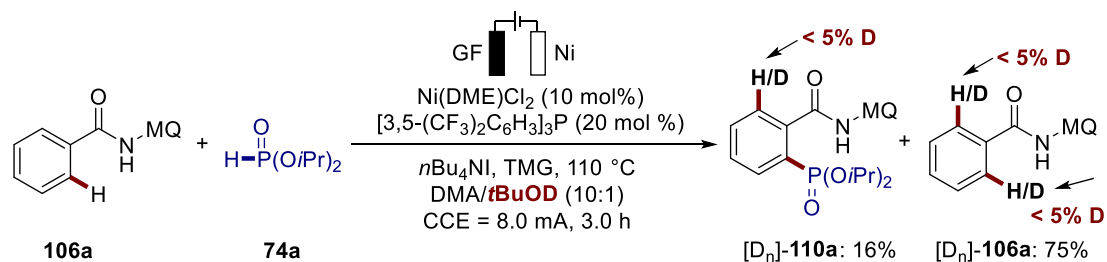
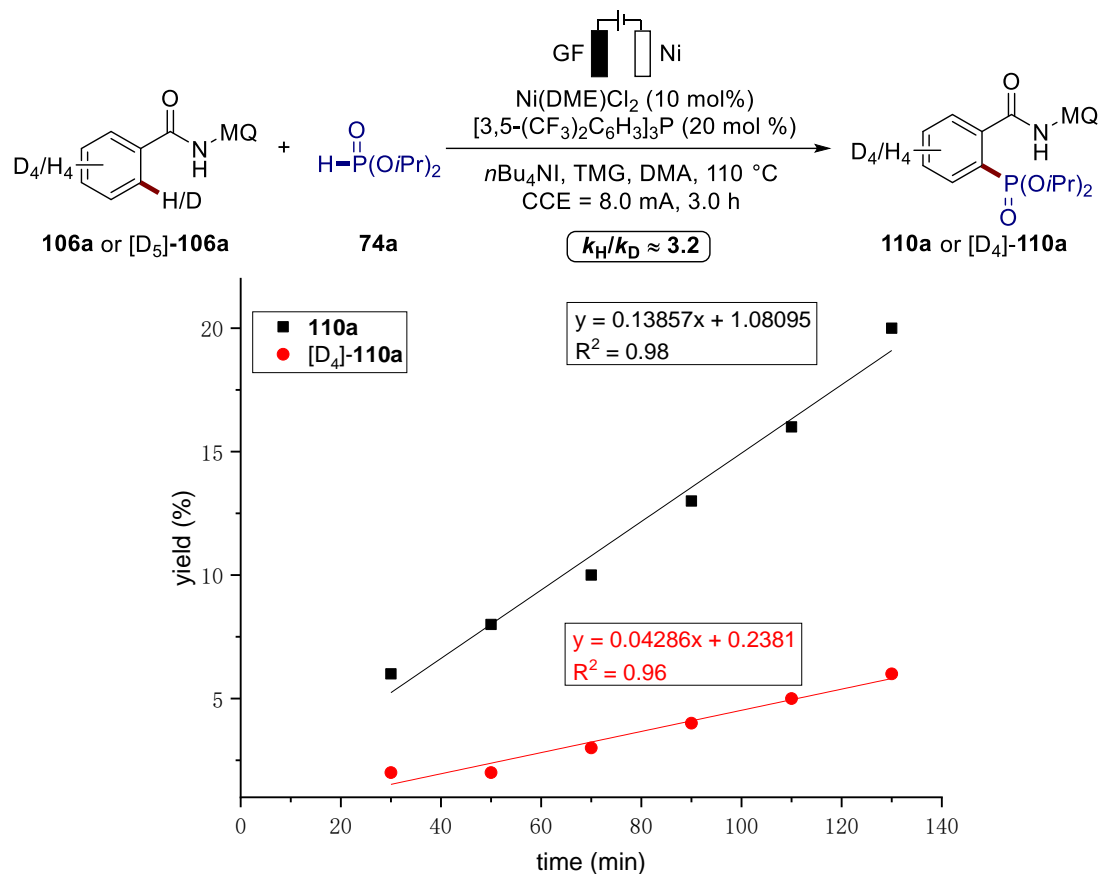


Figure 3.5.6. Deuteration experiment using *t*BuOD as the co-solvent.



## 3.5.3.3 KIE Studies

A high kinetic isotope effect (KIE) of  $k_H/k_D \approx 3.2$  was found by independent experiments, which was indicative of the C–H activation to be the rate-limiting step (**Figure 3.5.7**).



**Figure 3.5.7.** KIE studies by two parallel experiments.

## 3.5.3.4 Headspace GC-Analysis

Molecular hydrogen was generated as the sole byproduct, which was observed by Headspace GC-analysis (**Figure 3.5.8**).

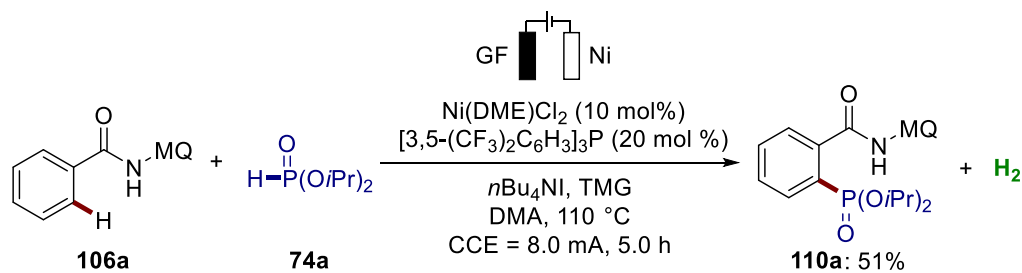


**Figure 3.5.8.** Headspace GC-analysis.

## 3.5.3.5 Switch On-Off Experiments

The on-off experiments showed the electrocatalytic C–P transformation rate was faster when heating for a period of time before getting through current (Figure 3.5.9a). The reason could be that the C–H nickelated species affecting the reaction rate accumulated, and then slowly enabled the transformation. The C–H phosphorylation was halted in the absence of electricity and continued after switching the electric current back on, thus ruling out a radical-chain process (Figure 3.5.9b).

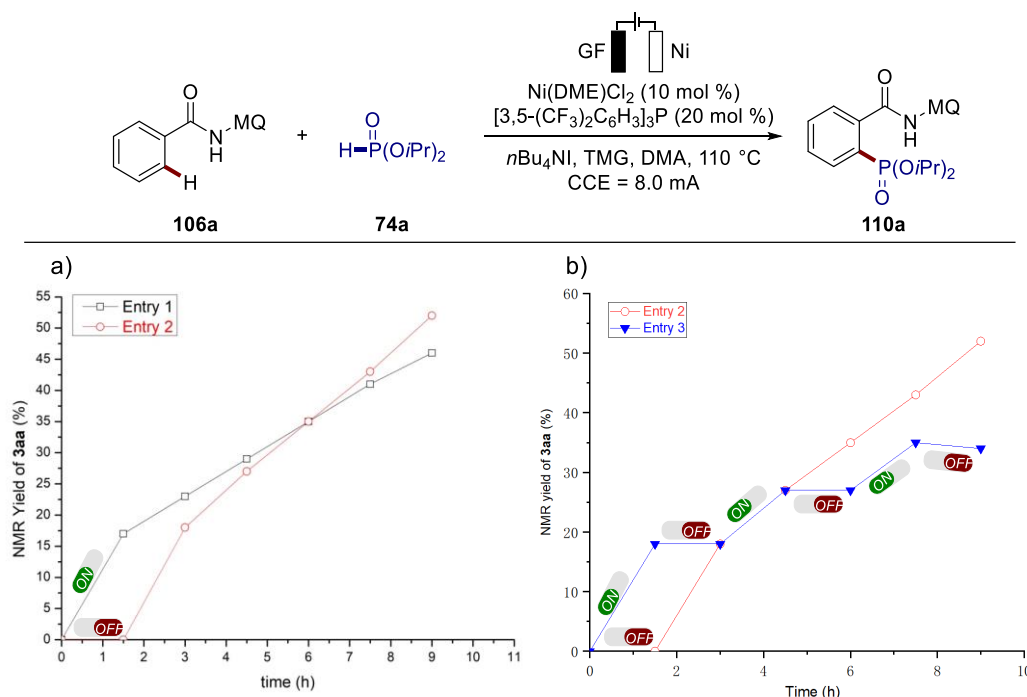


Figure 3.5.9. On-off experiments. a) L1 (in black) standard condition and L2 (in red) with a period without electricity for 1.5 h. b) L3 (in blue) with incontinuous current.

## 3.5.3.6 Radical Trapping Experiment

The typical radical scavenger TEMPO, even with up to four equivalents, failed to prevent the electrocatalytic C–H transformation, excluding the possible generation of radicals (Figure 3.5.10).

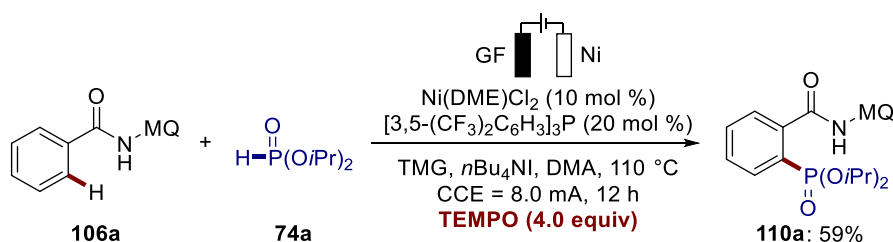


Figure 3.5.10. Radical trapping experiment. Performed by Dr. Antonio Del Vecchio.

### 3.5.3.7 Monitoring of the Electrocatalytic Reaction

The nickela-electrooxidative C–H phosphorylation was monitored by  $^1\text{H}$  NMR spectroscopy, where the consumption of benzamide **106a** together with the generation of phosphonated product **110a** was observed with no sign of an induction period (Figure 3.5.11). For the details, please see Figure 5.3.64.

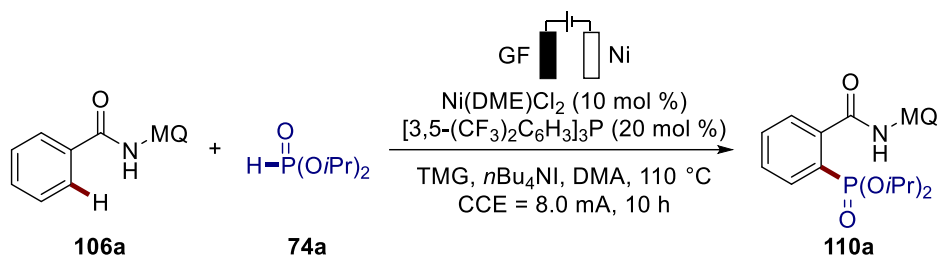
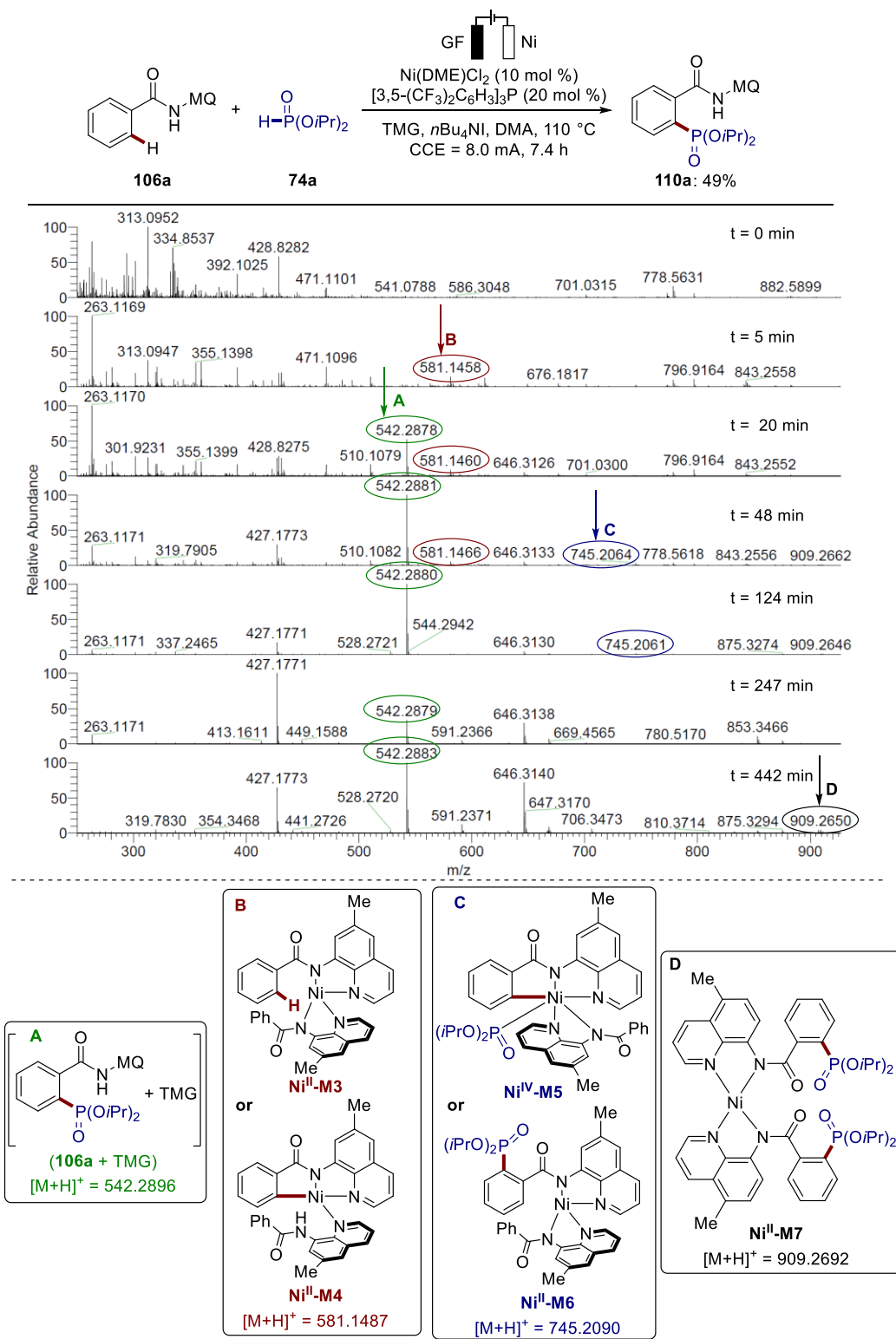


Figure 3.5.11. Monitoring electrocatalytic reaction monitoring between **106a** and **74a**.

The C–P transformation was monitored by *in-operando* high-resolution electrospray ionization-mass spectrometry (HR-ESI-MS), where two catalytically competent nickel intermediates were detected (Figure 3.5.12, performed by Dr. Antonis M. Messinis in Ackermann group). The peak at 581 ( $m/z$ ) corresponds to the nickel(II) species **Ni<sup>II</sup>-M3** or **Ni<sup>II</sup>-M4**, whereas **Ni<sup>IV</sup>-M5** or **Ni<sup>II</sup>-M6** from the elimination step was observed at 745 ( $m/z$ ) (Figure 3.5.12, box B,C). The nickel-amide dimer **Ni<sup>II</sup>-M7** (Figure 3.5.12, box D) could finally be observed after approximately seven hours.

### 3. Results and Discussion



**Figure 3.5.12.** HESI high resolution mass spectrometric monitoring of the reaction. Performed by Dr. Antonis M. Messinis.

## 3.5.3.8 DFT Calculations

In order to understand the reaction mechanism of nickel-electrooxidative C–H phosphorylation, DFT studies of the key steps were carried out by Dr. Rositha Kuniyil at the PBE0-D3(BJ)/def2-TZVP+SMD(DMA)//PBE0-D3(BJ)/def2-SVP level of theory.<sup>[176, 179]</sup> The calculations indicated that C–H activations at the guanidine-coordinated nickel species **Ni<sup>II</sup>-H2** (Figure 3.5.13a, barrier of 27.6 kcal/mol) as well as at the Ni(III) species **Ni<sup>III</sup>-H4** (Figure 3.5.13b, barrier of 27.3 kcal/mol) are favourable.

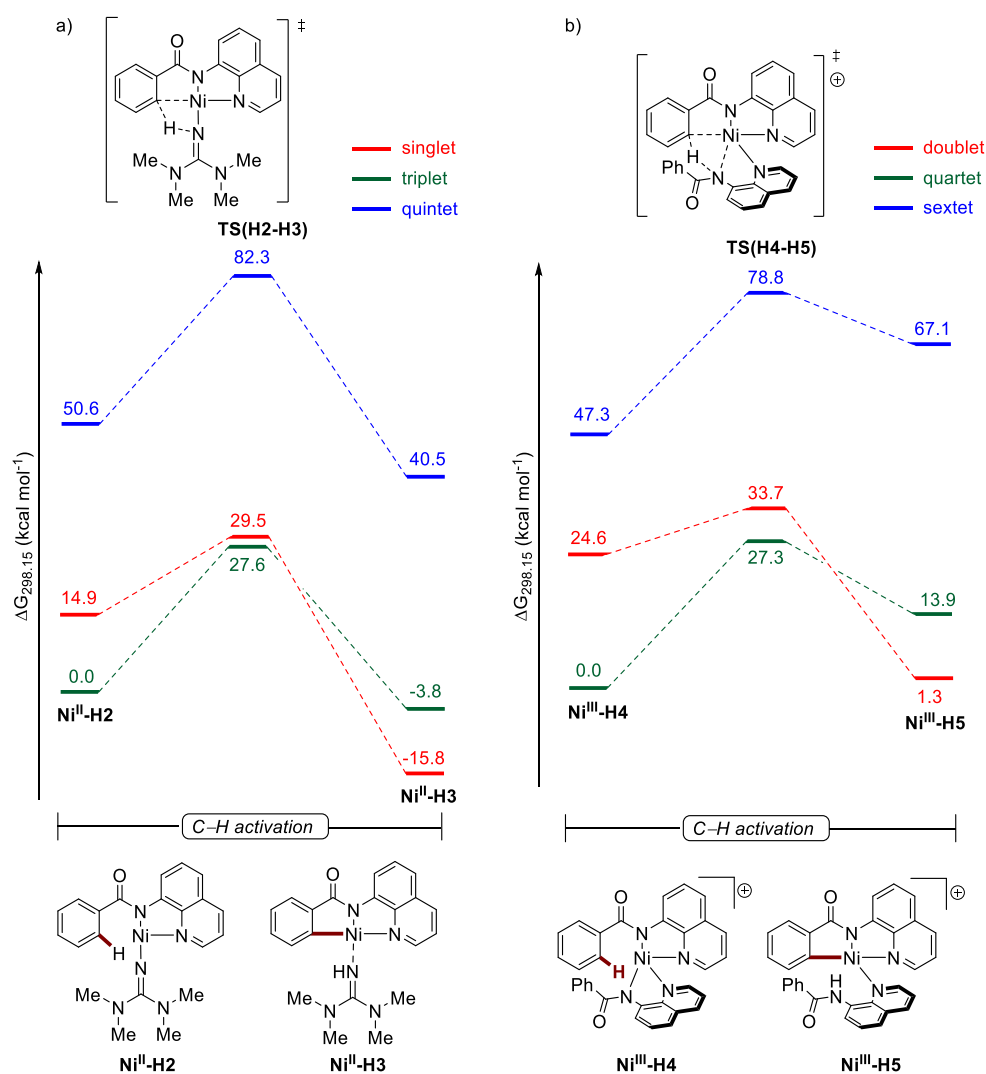


**Figure 3.5.13.** Gibbs free energy profile in kcal mol<sup>-1</sup> for the C–H activation elementary step. a), C–H activation from the guanidine-coordinated nickel(II) intermediate **Ni<sup>II</sup>-H2**; b), C–H activation from electron-positive nickel(III) intermediate **Ni<sup>III</sup>-H4** at the PBE0-D3(BJ)/def2-TZVP+SMD(DMA)//PBE0-D3(BJ)/def2-SVP level of theory. All DFT calculations of C–P formations were performed by Dr. Rositha Kuniyil. For details, see our publications.<sup>[180]</sup>

### 3.5.3.9 Synthesis, Characterization, and Catalytic Performance of Nickel(II) and Nickel(III)

The nickel (II) species **Ni<sup>II</sup>-M0** could not be observed when using bulky carboxylate NaO<sub>2</sub>CAd, while nickel(III) intermediate **Ni<sup>III</sup>-M1** was isolated under electricity (Figure 3.5.14a). Noteworthily, TMG was found to be a better coordinating reagent, stabilizing the initially-formed C–H nickelation complex by formation of a stable intermediate **Ni<sup>II</sup>-H3**, which was isolated and fully characterized by X-ray analysis (Figure 3.5.14b, c). **Ni<sup>II</sup>-H3** could be further transformed into the cyclonickelated complex **Ni<sup>III</sup>-H1** through anodic oxidation, assisted by the aminoquinoline substrate **35a** (Figure 3.5.14b). Furthermore, cyclic voltammetric studies by Zhipeng Lin of nickel complex **Ni<sup>II</sup>-H3** showed two oxidation waves at the potential of -0.20 V vs. Fc<sup>+0</sup> and +0.50 V vs. Fc<sup>+0</sup>, providing strong evidence for a Ni(II/III) and Ni(III/IV) redox events (Figure 3.5.14d).

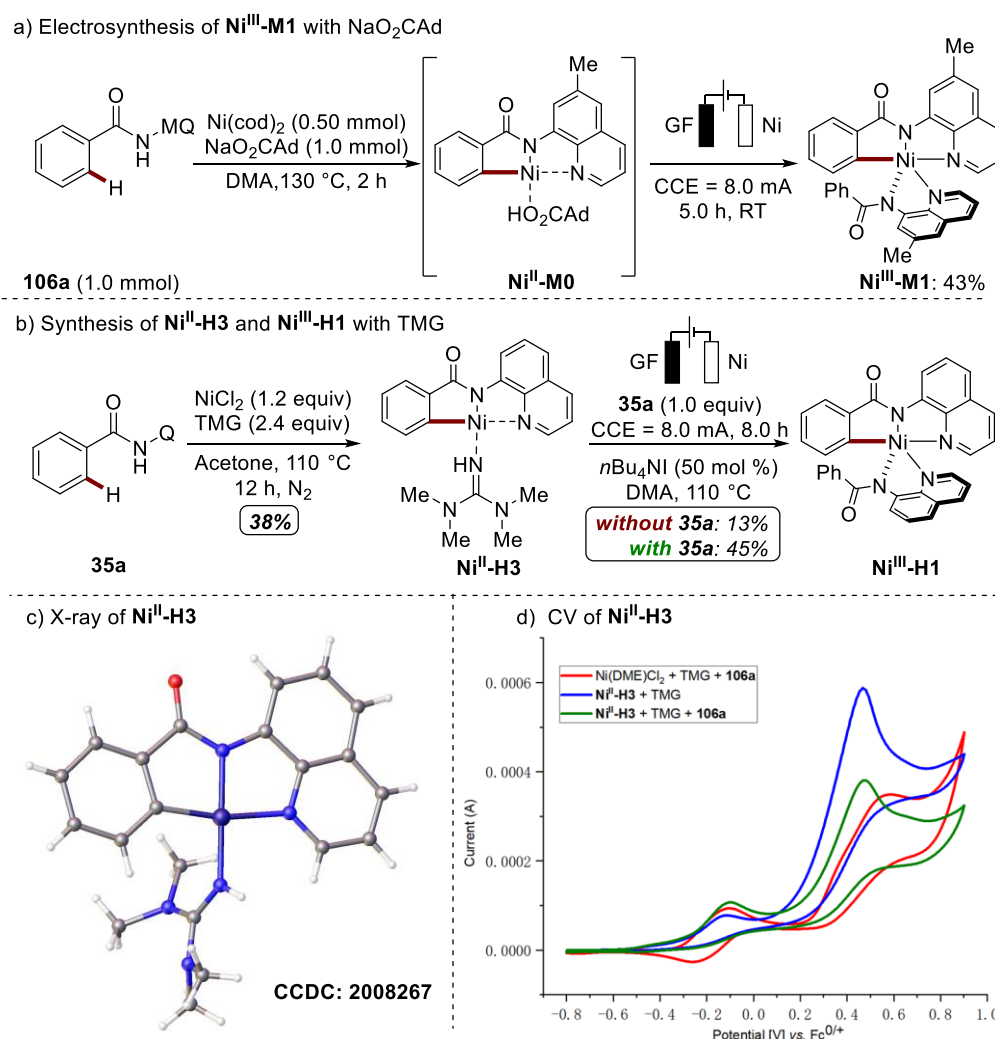


**Figure 3.5.14.** Synthesis, characterization and catalytic performance of nickel(II) and nickel(III) complexes. a) Electrosynthesis of **Ni<sup>III</sup>-M1** with NaO<sub>2</sub>CAd, isolated yield based on Ni(cod)<sub>2</sub> (0.5 mmol). b) Synthesis 100

of **Ni<sup>II</sup>-H3** with TMG, isolated yield based on **35a** (2.0 mmol); Electrosynthesis of **Ni<sup>III</sup>-H1** from **Ni<sup>II</sup>-H3** with or without benzamide **35a**, isolated yields based on **Ni<sup>II</sup>-H3** (0.20 mmol). c) X-ray analysis of **Ni<sup>II</sup>-H3** and the CCDC number is 2008267. d) Cyclic voltammograms at 100 mV/s. *n*Bu<sub>4</sub>NPF<sub>6</sub> (0.1 M in DMA); concentration of substrates 5 mM; at 110 °C. Ni(DME)Cl<sub>2</sub> + TMG + **106a** (red); **Ni<sup>II</sup>-H3** + TMG (blue); **Ni<sup>II</sup>-H3** + TMG + **106a** (green). CV studies were performed by Zhipeng Lin.

Electricity-mediated oxidation of **Ni<sup>II</sup>-H3** with a different benzamide **106o** clearly resulted in the formation of several dimeric nickel(III) complexes **Ni<sup>III</sup>-H1**, **Ni<sup>III</sup>-M8**, **Ni<sup>III</sup>-M9** and **Ni<sup>III</sup>-M10**. These nickel(III) complexes were collected together by column and analysed with HR-HESI-MS by IOBC department, being suggestive of a reversible C–H activation (**Figure 3.5.15** and **Figure 3.5.16**).

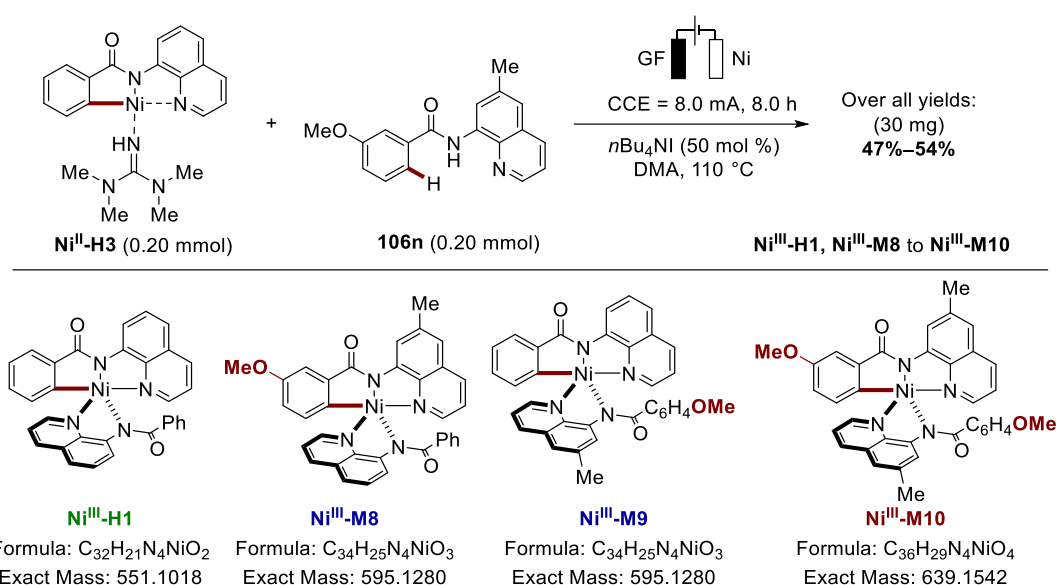


**Figure 3.5.15.** The reaction of **Ni<sup>II</sup>-H2** with benzamide **106n**.

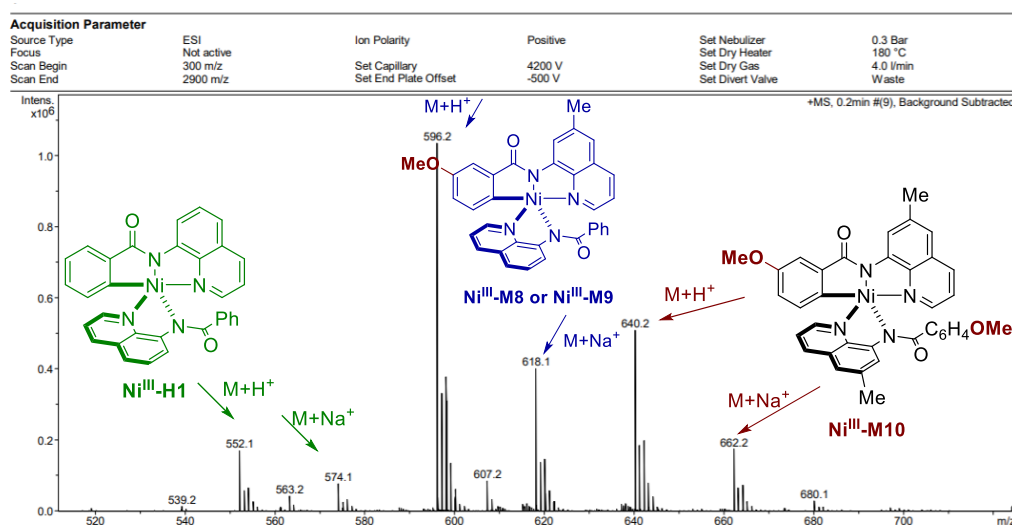
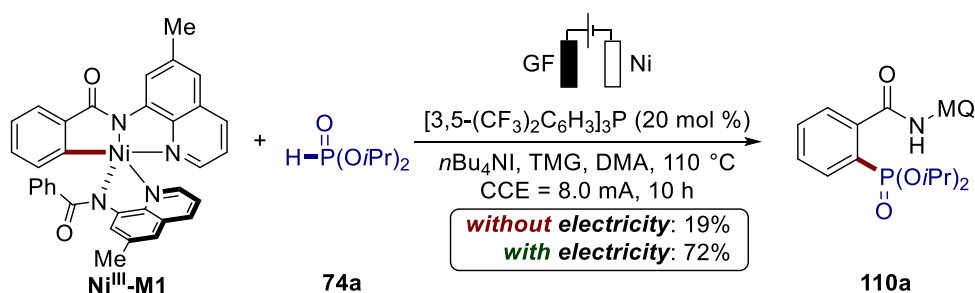


**Figure 3.5.16.** The HR-MS spectrum of the mixture from the reaction of **Ni<sup>II</sup>-H3** with benzamide **106n**. The mixture of products was analyzed by the IOBC department.

To highlight the performance of the nickel(III) complex **Ni<sup>III</sup>-M1** in the electrocatalytic C–H phosphorylation with **74a**, both stoichiometric and catalytic experiments were independently conducted with or without electricity in the presence of **Ni<sup>III</sup>-M1**, confirming the involvement of **Ni<sup>III</sup>-M1** in the electrosynthesis of C–P bond (**Figure 3.5.17**).

a) Stoichiometric reaction of **Ni<sup>III</sup>-M1** complex with **74a**



b) Catalytic reaction of **Ni<sup>III</sup>-M1** complex with **74a**

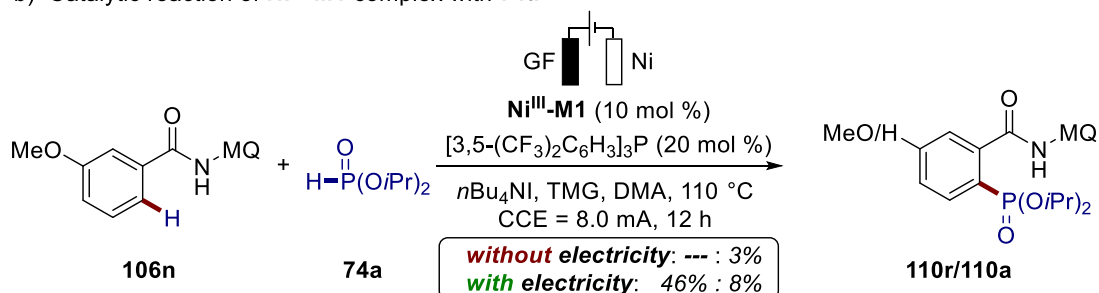


**Figure 3.5.17.** a) Stoichiometric reaction with **Ni<sup>III</sup>-M1**. b) Catalytic reaction with **Ni<sup>III</sup>-M1**. Conversion determined by  $^1\text{H}$  NMR analysis with 1,3,5-(MeO) $_3\text{C}_6\text{H}_3$  as the internal standard.

### 3.5.4 Proposed Mechanism

Based on our findings, a plausible catalytic cycle of C–H phosphorylation has been depicted in **Figure 3.5.18**. Initial C–H activation occurs upon coordination of substrate **106**, anodic oxidation and internal hydrogen transfer to produce nickel(III) **111b**. Subsequent coordination of phosphonate **74** sets the stage for an oxidation-induced reductive elimination at nickel(III) **111d**. The TMG additive is proposed to facilitate to obtain the desired product **110** and the TMG-coordinated nickel(II) complex **111g**, which undergoes a protodemetalation to regenerate **111a**. The thus-formed protons deliver molecular hydrogen through cathodic reduction.



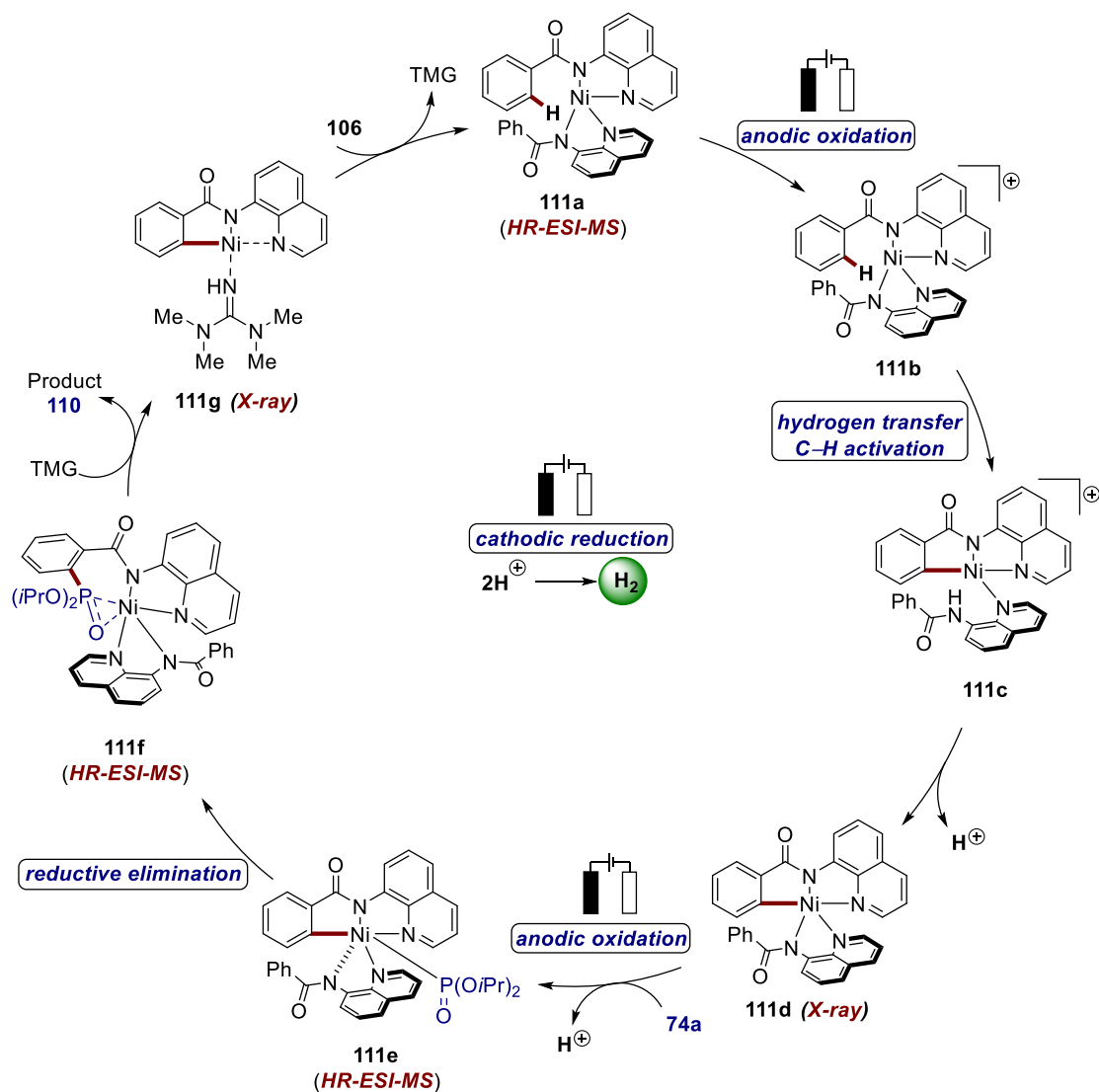


**Figure 3.5.18.** Proposed catalytic cycle of nickel-electrooxidative C-H phosphorylation.

## 4. Summary and Outlook

The development of highly step- and atom-economical C–H activations by inexpensive and Earth-abundant metals streamlines organic synthesis and offers new tools to construct C–C and C–Het bonds for *inter alia* pharmaceutical, agrochemical chemistry, and material sciences. The selective functionalization of inert C–H bonds remains a big challenge due to the omnipresent C–H bonds in organic compounds. In this thesis, several new synthetic methods have been devised to sustainable selective C–H activation by cost-effective ruthenium and nickel electro-catalysis.

In the first part, cost-effective ruthenium-catalyzed *ortho*- or *meta*-C–H activation of decorated arenes were achieved using orienting directing groups. Ruthenium-catalyzed *ortho*-C–H alkylation of diverse benzoic acids **98** through weak coordination was achieved, providing step-economical access to aromatic alkynes **99** (Figure 4.1). With the assistance of various nitrogen-containing directing groups, *meta*-C–H activations including mono- or difluoromethylation and alkylation through the  $\sigma$ -activation of the cyclometallated intermediate were efficiently developed by ruthenium catalysis (Figure 4.1).

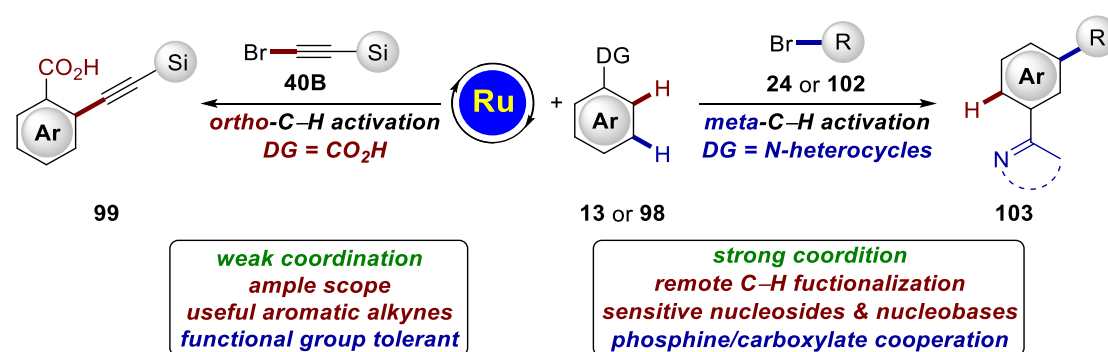
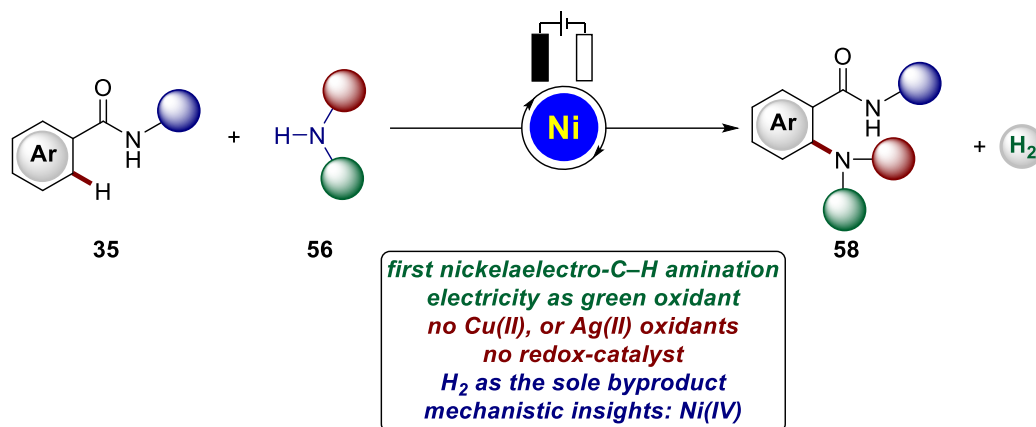


Figure 4.1. Ruthenium-catalyzed site-selective C–H activation with by assistances.

Compared with the chemical oxidative C–H functionalizations, electrocatalytic C–H activations employ safe, waste-free and cost-efficient electricity as the redox reagent to replace toxic and expensive chemical oxidants, which are closely related to the trend of atom- and step-economy.

In the second project, we developed the first nickela-electrochemical C–H activation in a dehydrogenative manner employing green and cheap electricity as the oxidant, providing an expedient approach to arylamines **58** (Figure 4.2). Moreover, the mechanism involving a Ni(III/IV/II) catalysis was distinct from the commonly suggested C–H amination with a Ni(II/III/I) pathway.<sup>[115]</sup>



**Figure 4.2.** Nickela-electrocatalyzed C–H amination.

In the third project, we developed a carboxylate-enabled nickela-electrocatalytic C–H alkoxylation of ample arene derivatives **106** with challenging secondary alcohols **66**, producing H<sub>2</sub> as the sole byproduct (Figure 4.3). The C–H alkoxylation was more effective with electricity than with any other chemical oxidants, showing a high level of both chemo-selectivity and position-selectivity. Detailed mechanistic studies including the isolation of catalytically relevant nickel(III) complex, cyclic voltammetry, and computation provided strong support for an oxidation-induced reductive elimination at nickel(III).

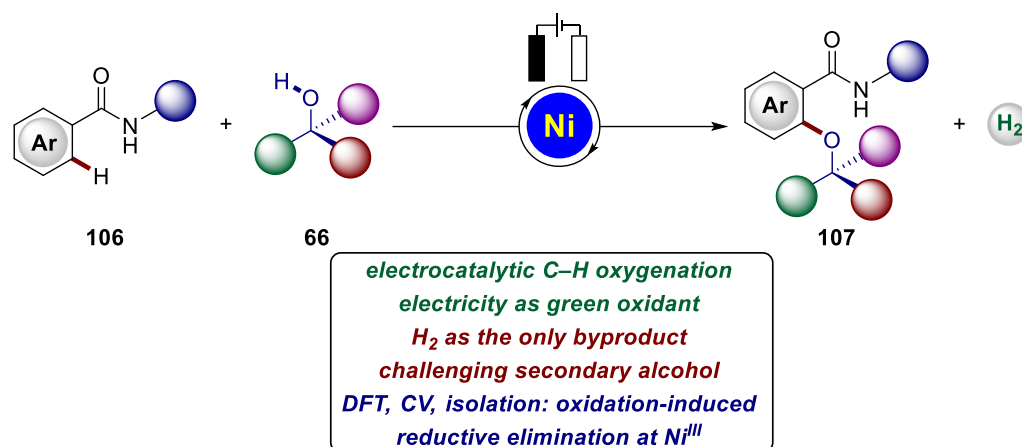


**Figure 4.3.** Nickela-electrocatalyzed C–H alkoxylation with secondary alcohols.

In the fourth project, we continued to work on electrocatalysis for the first C–H phosphorylation by cost-effective nickel using an operationally-simple non-sequential manifold, generating molecular hydrogen as the only waste (**Figure 4.4**). The robust electrooxidative C–P transformations allowed for a broad reaction manifold, featuring a plethora of heteroarenes and olefins **106** with diverse unmasked phosphorous reagents **74** to furnish arylphosphonates, phenylphosphine oxides and diazaphospholidine oxides **110**. Catalytically competent cyclometallic nickel(II) and nickel(III) intermediates were isolated and characterized. Experimental studies and cyclovoltammetric analysis were among others strongly suggestive of an oxidation-induced reductive elimination nickel(III/IV) manifold.

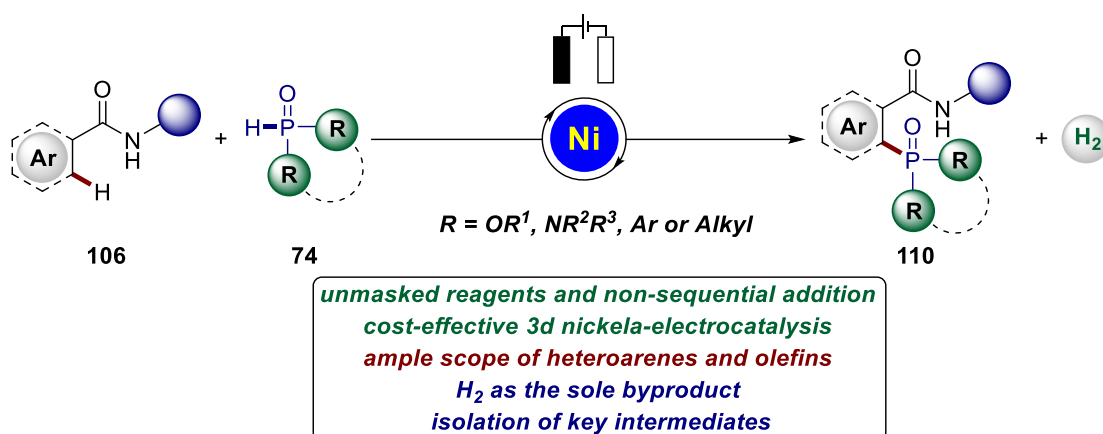


**Figure 4.4.** Nickela-electrocatalyzed C–H phosphorylation.

## 5. Experimental Section

### 5.1 General Remarks

Catalysis reactions under an atmosphere of air were conducted in the sealed tubes or Schlenk tubes. Unless otherwise noted, other reactions were performed under N<sub>2</sub> atmosphere using pre-dried glassware and standard Schlenk techniques.

If not otherwise noted, yields refer to isolated compounds, estimated to be >95% pure as determined by <sup>1</sup>H NMR.

#### Vacuum

The following pressures were measured on the used vacuum pump and were not corrected: membrane pump vacuum (MPV): 0.5 mbar, oil pump vacuum (OPV): 0.1 mbar.

#### Melting Points (M.p.)

Melting points were measured using a *Stuart*<sup>®</sup> Melting Point Apparatus *SMP3* from BARLOWORLD SCIENTIFIC. The reported values are uncorrected.

#### Chromatography

Analytical thin layer chromatography (TLC) was performed on 0.25 mm silica gel 60F-plates (MACHEREY-NAGEL) with 254 nm fluorescent indicator from MERCK. Plates were visualized under UV-light. Chromatographic purification of products was accomplished by flash column chromatography on MERCK silica gel, grade 60 (0.040–0.063 mm and 0.063–0.200 mm).

#### Gas Chromatography (GC)

The conversions of the reactions were monitored by applying coupled gas chromatography/mass spectrometry using G1760C GCDplus with mass detector *HP 5971, 5890 Series II* with mass detector *HP 5972* from HEWLETT-PACKARD and 7890A GC-System with mass detector *5975C (Triplex-Axis-Detector)* from AGILENT TECHNOLOGIES equipped with *HP-5MS* columns (30 m × 0.25 mm × 0.25 m).

### **Gel Permeation Chromatography (GPC)**

GPC purifications were performed on a JAI system (JAI-LC-9260 II NEXT) equipped with two sequential columns (JAIGEL-2HR, gradient rate: 5.000; JAIGEL-2.5HR, gradient rate: 20.000; internal diameter = 20 mm; length = 600 mm; Flush rate = 10.0 mL/min and chloroform (HPLC-quality with 0.6% ethanol as stabilizer) was used as the eluent.

### **Infrared Spectroscopy**

Infrared spectra were recorded with a BRUKER *Alpha-P ATR FT-IR* spectrometer. Liquid samples were measured as a film, solid samples neat. The analysis of the spectra was carried out using the software from BRUKER *OPUS 6*. The absorption was given in wave numbers ( $\text{cm}^{-1}$ ) and the spectra were recorded in the range of 4000–400  $\text{cm}^{-1}$ . *In situ*-IR studies were performed on METTLER TOLEDO *ReactIR™ 15* with an *iC IR 4.3* software.

### **Mass Spectrometry**

Electron-ionization (EI) mass spectra were recorded on a Jeol AccuTOF instrument at 70 eV. Electrospray-ionization (ESI) mass spectra were obtained on Bruker micrOTOF and maXis instruments. All systems were equipped with time-of-flight (TOF) analyzers. The ratios of mass to charge ( $m/z$ ) were reported and the intensity relative to the base peak ( $I = 100$ ) is given in parenthesis.

### **Nuclear Magnetic Resonance Spectroscopy (NMR)**

Nuclear magnetic resonance (NMR) spectra were recorded on VARIAN *Inova 500, 600*, VARIAN *Mercury 300, VX 300*, VARIAN *Avance 300*, VARIAN *VNMRS 300* and BRUKER *Avance III 300, 400* and *HD 500* spectrometers. All chemical shifts were given as  $\delta$ -values in ppm relative to the residual proton peak of the deuterated solvent or its carbon atom, respectively.  $^1\text{H}$  and  $^{13}\text{C}$  NMR spectra were referenced using the residual proton or solvent carbon peak (see table), respectively.  $^{13}\text{C}$  and  $^{19}\text{F}$  NMR were measured as proton-decoupled spectra.

	<sup>1</sup> H NMR	<sup>13</sup> C NMR
CDCl <sub>3</sub>	7.26	77.16
[D] <sub>6</sub> -DMSO	2.50	39.52

The observed resonance-multiplicities were described by the following abbreviations: s (singlet), d (doublet), t (triplet), q (quartet), hept (heptet), m (multiplet) or analogous representations. The coupling constants *J* were reported in Hertz (Hz). Analysis of the recorded spectra was carried out with *MestReNova 10* software.

### Electrochemistry

Nickel foam (Ni) electrodes (10 mm × 15 mm × 1.4 mm, RCM-Ni5763; obtained from Recemat BV, Germany) and graphite felt (GF) electrodes (10 mm × 15 mm × 6 mm, SIGRACELL®GFA 6 EA, obtained from SGL Carbon, Wiesbaden, Germany) were connected using stainless steel adapters. Electrolysis was conducted using an AXIOMET AX-3003P potentiostat in constant current mode, CV studies were performed using a Metrohm Autolab PGSTAT204 workstation and Nova 2.0 software. Divided cells separated by a P4-glassfrit were obtained from Glasgerätebau Ochs Laborfachhandel e. K. (Bovenden, Germany).

### Solvents

All solvents for reactions involving moisture-sensitive reagents were dried, distilled and stored under inert atmosphere (N<sub>2</sub>) according to the following standard procedures.

Purified by solvent purification system (SPS-800, M. Braun): **CH<sub>2</sub>Cl<sub>2</sub>**, **toluene**, **tetrahydrofuran**, **dimethylformamide**, **diethylether**. **1,2-dichloroethane**, **N-methyl-2-pyrrolidone (NMP)**, **N,N-dimethylacetamide (DMA)**, **dimethylsulfoxide (DMSO)** and **γ-valerolactone (GVL)** was dried over CaH<sub>2</sub> for 8 h, degassed and distilled under reduced pressure. **1,2-dimethoxyethane (DME)** was dried over sodium and freshly distilled under N<sub>2</sub>. **1,1,1,3,3,3-hexafluoropropan-2-ol (HFIP)** was distilled from 3 Å molecular sieves. **2,2,2-trifluoroethanol (TFE)** was stirred over CaSO<sub>4</sub> and distilled under reduced pressure. **Water** was degassed by repeated *Freeze-Pump-Thaw* degassing procedure. **1,4-dioxane** and **di-n-butyl-ether (nBu<sub>2</sub>O)** were distilled

from sodium benzophenone ketyl.

### Reagents

Chemicals obtained from commercial sources with purity above 95% were used without further purification. The following compounds were known and were synthesized according to previously described methods.

Nitrogen-containing arenes (**13a–13t**),<sup>[181]</sup> indole **106H–106I**,<sup>[182]</sup> benzamides derivatives (**35a–35q**, **106a–106v**, **106aa–106am**, **106A–106J**)<sup>[129e, 183]</sup>.

The following compounds were synthesized and provided by the persons listed below:

Karsten Rauch: [RuCl<sub>2</sub>(*p*-cymene)]<sub>2</sub>, [Cp\*RhCl<sub>2</sub>]<sub>2</sub>, [Cp\*IrCl<sub>2</sub>]<sub>2</sub>, [Ru(O<sub>2</sub>CMe)<sub>2</sub>(*p*-cymene)], [Ru(OAc)<sub>2</sub>(*p*-cymene)].

Fernando Fumagalli: Ru(OAc)<sub>2</sub>(PPh<sub>3</sub>)<sub>2</sub>

### Cooperation clarify:

In the project of nickela-electrocatalytic C–H amination, Dr. Ramesh C. Samanta and Dr. Nicolas Sauermann carried out some experiments for the scope. GC-Headspace analysis, KIE studies and reaction profile by *in-operando* React-IR, and CV studies were performed by Dr. Nicolas Sauermann.

In the project of nickela-electrocatalytic C–H alkoxylation, GC-Headspace analysis and CV studies were performed by Julia Struwe. DFT calculations were performed by Dr. Lianrui Hu.

In the project of nickela-electrocatalytic C–H phosphorylation, Dr. Antonio Del Vecchio carried out some experiments for the optimization and scope, experiments with chemical oxidants and radical trapping experiment. Dr. Antonis M. Messinis monitored the reaction by HR-HESI-MS. Dr. Rositha Kuniyil carried out all the DFT calculations. Zhipeng Lin performed all the CV studies.

Dr. Christopher Golz analyzed all the X-ray data in thesis thesis.



## 5.2 General Procedures

### General Procedure A: Ruthenium(II)-Catalyzed C–H Alkylation of Benzoic Acids: Access to Free Acids **99**

A suspension of  $[\text{RuCl}_2(\textit{p}\text{-cymene})]_2$  (15.3 mg, 5.0 mol %),  $\text{K}_2\text{CO}_3$  (138 mg, 1.0 mmol), benzoic acid **98** (0.50 mmol), and alkynyl bromide **40B** (0.65 mmol, 1.3 equiv) in 1,4-dioxane (1.0 mL) was stirred under  $\text{N}_2$  for 16 h at 120 °C. At ambient temperature, AcOH (2.0 mL) was added, the mixture was dry-loaded onto silica gel and purified by column chromatography (*n*hexane/EtOAc/AcOH) to give the products **99**.

### General Procedure B: Ruthenium(II)-Catalyzed *meta*-C–H Mono- and Difluoromethylation

To a solution of substrates **13** (0.50 mmol),  $[\text{Ru}(\text{O}_2\text{CMes})_2(\textit{p}\text{-cymene})]$  (28.1 mg, 10 mol %),  $\text{P}(\text{4-C}_6\text{H}_4\text{CF}_3)_3$  (46.7 mg, 20 mol %) or  $\text{Ni}(\text{PPh}_3)_2\text{Cl}_2$  (32.7 mg, 10 mol %) and  $\text{Na}_2\text{CO}_3$  (106 mg, 1.0 mmol) in 1,4-dioxane (2.0 mL), bromodifluoroester **102a** (304 mg, 1.5 mmol) or bromofluoroester **102b** (278 mg, 1.5 mmol) was added. The mixture was stirred at 60 °C for 18 h. After completion of the reaction,  $\text{CH}_2\text{Cl}_2$  (3.0 mL) was added at ambient temperature and the volatiles were removed *in vacuo*. Purification by chromatography on silica gel afforded the desired products **103**.

### General Procedure C: Ruthenium(II)-Catalyzed *meta*-Alkylation

Heteroarene **13** (0.50 mmol),  $[\text{Ru}(\text{OAc})_2(\text{PPh}_3)_2]$  (37.2 mg, 50  $\mu\text{mol}$ , 10 mol %), and  $\text{K}_3\text{PO}_4$  (212 mg, 1.0 mmol) were placed in a pre-dried 25 mL Ace pressure tube. The mixture was evacuated and purged with  $\text{N}_2$  for three times. Alkyl bromide **24B** (1.5 mmol) and 1,4-dioxane (2.0 mL) were added and the mixture was stirred at 100 °C. After 18 h, the resulting mixture was concentrated *in vacuo*. Purification of the residue by column chromatography (*n*hexane/EtOAc) yielded *meta*-product **103**.

#### **General Procedure D: Nickela-Electrocatalytic C–H Amination**

The electrolysis was carried out in an undivided cell, with a graphite felt (GF) anode (10 mm × 15 mm × 6 mm) and a nickel-foam cathode (10 mm × 15 mm × 1.4 mm). Ni(DME)Cl<sub>2</sub> (11 mg, 0.050 mmol, 20 mol %), PivONa (31 mg, 0.25 mmol, 1.0 equiv), *n*Bu<sub>4</sub>NBF<sub>4</sub> (0.50 mmol) and benzamide **35** (0.25 mmol, 1.0 equiv) were dissolved in DMA (3.0 mL), and then the amine **56** (0.50 mmol, 2.0 equiv) was added. At 120 °C, electrolysis was started with a constant current of 8.0 mA which was then maintained for 10 h. At ambient temperature, the mixture was transferred into a separating funnel and electrodes were rinsed with EtOAc (10 mL). The mixture was washed with H<sub>2</sub>O (10 mL) and the organic layer was separated. The aqueous layer was extracted with EtOAc (2 × 5.0 mL). Evaporation of the collected organic layer and subsequent column chromatography on silica gel (*n*hexane/EtOAc) yielded the desired product **58**.

#### **General Procedure E: Nickela-Electrocatalytic C–H Amination**

The electrolysis was carried out in an undivided cell, with a graphite felt (GF) anode (10 mm × 15 mm × 6 mm) and a nickel-foam cathode (10 mm × 15 mm × 1.4 mm). Ni(DME)Cl<sub>2</sub> (11 mg, 0.050 mmol, 20 mol %), PivONa (31 mg, 0.25 mmol, 1.0 equiv), *n*Bu<sub>4</sub>NBF<sub>4</sub> (0.50 mmol) and benzamide **35** (0.25 mmol, 1.0 equiv) were dissolved in DMA (3.0 mL), and then the amine **56** (1.25 mmol, 5.0 equiv) was added. At 130 °C, electrolysis was started with a constant current of 8.0 mA which was then maintained for 10 h. At ambient temperature, the mixture was transferred into a separating funnel and electrodes were rinsed with EtOAc (10 mL). The mixture was washed with H<sub>2</sub>O (10 mL) and the organic layer was separated. The aqueous layer was extracted with EtOAc (2 × 5.0 mL). Evaporation of the collected organic layer and subsequent column chromatography on silica gel (*n*hexane/EtOAc) yielded the desired product **58**.

#### **General Procedure F: Nickela-Electrocatalytic C–H Alkoxylation**

The electrolysis was carried out in an undivided cell, with a graphite felt (GF) anode (10 mm × 15 mm × 6 mm) and a nickel-foam cathode (10 mm × 15 mm × 1.4 mm). Ni(DME)Cl<sub>2</sub> (5.5 mg, 0.025 mmol, 10 mol %), 1-AdCO<sub>2</sub>H (9.0 mg, 0.050 mmol),

NaO<sub>2</sub>CAd (51 mg, 0.25 mmol), *n*Bu<sub>4</sub>NClO<sub>4</sub> (0.50 mmol) and benzamide **106** (0.25 mmol, 1.0 equiv) were dissolved in DMA (3.0 mL), and then the alcohol **66** (2.5 mmol) was added. At 130 °C, electrolysis was started with a constant current of 8.0 mA which was then maintained for 12 h under N<sub>2</sub>. At ambient temperature, the mixture was transferred into a separating funnel and electrodes were rinsed with EtOAc (10.0 mL). The mixture was washed with H<sub>2</sub>O (10.0 mL) and the organic layer was separated. The aqueous layer was extracted with EtOAc (2 × 5.0 mL). Evaporation of the combined organic layer and subsequent column chromatography on silica gel (eluent: *n*hexane/EtOAc, *n*hexane/acetone or CH<sub>2</sub>Cl<sub>2</sub>/acetone) yielded the desired product **107**.

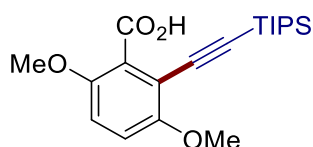
#### General Procedure G: Nickel-Electrocatalytic C–H Phosphorylation

The electrolysis was carried out in an undivided cell, with a graphite felt (GF) anode (10 mm × 15 mm × 6 mm) and a nickel-foam cathode (10 mm × 15 mm × 1.4 mm). Benzamide **106** (0.25 mmol, 1.0 equiv), Ni(DME)Cl<sub>2</sub> (5.5 mg, 0.025 mmol, 10 mol %), [3,5-(CF<sub>3</sub>)<sub>2</sub>C<sub>6</sub>H<sub>3</sub>]<sub>3</sub>P (33.5 mg, 0.050 mmol, 20 mol %), TMG (28.8 mg, 0.25 mmol, 1.0 equiv), *n*Bu<sub>4</sub>NI (0.125 mmol) and phosphonating reagents **74** were dissolved in DMA (3.0 mL). Electrolysis was conducted with a constant current of 8.0 mA which was maintained at 110 °C for 12 h under N<sub>2</sub>. At ambient temperature, the mixture was transferred into a separating funnel and electrodes were rinsed with EtOAc (10 mL). Subsequently, H<sub>2</sub>O (10 mL) was added to the mixture and the organic layer was collected. The aqueous layer was extracted with EtOAc (2 × 5.0 mL). Evaporation of the combined organic layers and subsequent column chromatography on silica gel (eluent: *n*hexane/EtOAc) yielded the desired product **110**.

## 5.3 Experimental Procedures and Analytical Data

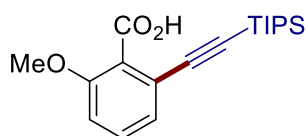
### 5.3.1 Ruthenium-Catalyzed *ortho*-C–H Alkynylation

#### 5.3.1.1 Characterization Data



#### 3,6-Dimethoxy-2-[(triisopropylsilyl)ethynyl]benzoic acid (**99a**)

The general procedure **A** was followed using benzoic acid **98a** (91 mg, 0.50 mmol) and (bromoethynyl)triisopropylsilane (**40B**) (170 mg, 0.65 mmol, 1.30 equiv). Purification by column chromatography on silica gel (*n*hexane/EtOAc: 4/1) yielded **99a** (174 mg, 96%) as a white solid. **M.p.**: 183–184 °C. **<sup>1</sup>H NMR** (300 MHz, CDCl<sub>3</sub>)  $\delta$  = 6.80 (s, 1H), 6.80 (s, 1H), 3.76 (s, 3H), 3.74 (s, 3H), 1.11–1.05 (m, 21H). **<sup>13</sup>C NMR** (75 MHz, CDCl<sub>3</sub>)  $\delta$  = 171.4 (C<sub>q</sub>), 155.2 (C<sub>q</sub>), 150.1 (C<sub>q</sub>), 126.5 (C<sub>q</sub>), 114.0 (CH), 112.7 (CH), 112.5 (C<sub>q</sub>), 100.9 (C<sub>q</sub>), 99.1 (C<sub>q</sub>), 57.0 (CH<sub>3</sub>), 56.6 (CH<sub>3</sub>), 18.6 (CH<sub>3</sub>), 11.3 (CH). **IR** (neat): 2939, 2863, 2154, 1703, 1258, 1061, 881, 660, 457 cm<sup>-1</sup>. **MS** (ESI) *m/z* (relative intensity) 385 (55) [M+Na]<sup>+</sup>, 363 (100) [M+H]<sup>+</sup>. **HR-MS** (ESI) *m/z* calcd for C<sub>20</sub>H<sub>31</sub>O<sub>4</sub>Si [M+H]<sup>+</sup>: 363.1986, found: 363.1987.

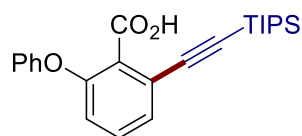


#### 2-Methoxy-6-[(triisopropylsilyl)ethynyl]benzoic acid (**99b**)

The general procedure **A** was followed using benzoic acid **98b** (76 mg, 0.50 mmol) and (bromoethynyl)triisopropylsilane (**40B**) (170 mg, 0.65 mmol, 1.30 equiv). Purification by column chromatography on silica gel (*n*hexane/EtOAc: 4/1) yielded **99b** (151 mg, 91%) as a white solid. **M.p.**: 146–147 °C. **<sup>1</sup>H NMR** (300 MHz, CDCl<sub>3</sub>)  $\delta$  = 7.24 (dd, *J* = 8.4, 7.7 Hz, 1H), 7.08 (dd, *J* = 7.7, 1.0 Hz, 1H), 6.85 (dd, *J* = 8.5, 1.0 Hz, 1H), 3.80 (s, 3H), 1.09–1.04 (m, 21H). **<sup>13</sup>C NMR** (75 MHz, CDCl<sub>3</sub>)  $\delta$  = 171.5 (C<sub>q</sub>), 156.4 (C<sub>q</sub>), 130.8 (CH), 125.4 (CH), 125.1 (C<sub>q</sub>), 122.9 (C<sub>q</sub>), 111.5 (CH), 103.3 (C<sub>q</sub>), 96.0 (C<sub>q</sub>), 56.0 (CH<sub>3</sub>), 18.6 (CH<sub>3</sub>), 11.3 (CH). **IR** (neat): 2940, 2863, 2148, 1697, 1463, 1278, 1080, 114

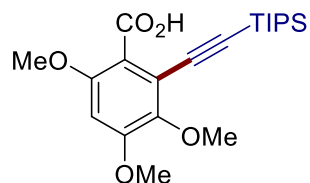
881, 665  $\text{cm}^{-1}$ . **MS** (ESI)  $m/z$  (relative intensity) 355 (100)  $[\text{M}+\text{Na}]^+$ , 333 (70)  $[\text{M}+\text{H}]^+$ .

**HR-MS** (ESI)  $m/z$  calcd for  $\text{C}_{19}\text{H}_{29}\text{O}_3\text{Si}$   $[\text{M}+\text{H}]^+$ : 333.1880, found: 333.1885.



### 2-Phenoxy-6-[(triisopropylsilyl)ethynyl]benzoic acid (**99c**)

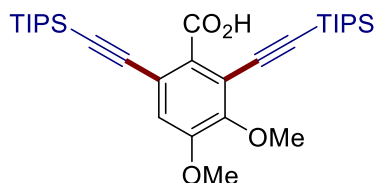
The general procedure **A** was followed using benzoic acid **98c** (107 mg, 0.50 mmol) and (bromoethynyl)triisopropylsilane (**40B**) (170 mg, 0.65 mmol, 1.30 equiv). Purification by column chromatography on silica gel (*n*hexane/EtOAc: 4/1) yielded **99c** (181 mg, 92%) as a white solid. **M.p.**: 127–128 °C. **<sup>1</sup>H NMR** (300 MHz,  $\text{CDCl}_3$ )  $\delta$  = 7.31–7.23 (m, 2H), 7.19 (s, 1H), 7.17 (d,  $J$  = 1.9 Hz, 1H), 7.10–7.02 (m, 1H), 6.98 (t,  $J$  = 1.0 Hz, 1H), 6.96 (dd,  $J$  = 2.0, 0.9 Hz, 1H), 6.73 (dd,  $J$  = 5.6, 3.8 Hz, 1H), 1.01–0.95 (m, 21H). **<sup>13</sup>C NMR** (75 MHz,  $\text{CDCl}_3$ )  $\delta$  = 171.4 ( $\text{C}_q$ ), 156.4 ( $\text{C}_q$ ), 154.7 ( $\text{C}_q$ ), 130.8 (CH), 129.8 (CH), 127.5 (CH), 127.4 ( $\text{C}_q$ ), 124.2 (CH), 123.1 ( $\text{C}_q$ ), 119.8 (CH), 118.3 (CH), 102.8 ( $\text{C}_q$ ), 96.6 ( $\text{C}_q$ ), 18.5 ( $\text{CH}_3$ ), 11.2 (CH). **IR** (neat): 2940, 2863, 2158, 1703, 1571, 1456, 1238, 997, 654  $\text{cm}^{-1}$ . **MS** (ESI)  $m/z$  (relative intensity) 417 (100)  $[\text{M}+\text{Na}]^+$ , 395 (80)  $[\text{M}+\text{H}]^+$ . **HR-MS** (ESI)  $m/z$  calcd for  $\text{C}_{24}\text{H}_{31}\text{O}_3\text{Si}$   $[\text{M}+\text{H}]^+$ : 395.2037, found: 395.2030.



### 3,4,6-Trimethoxy-2-[(triisopropylsilyl)ethynyl]benzoic acid (**99d**)

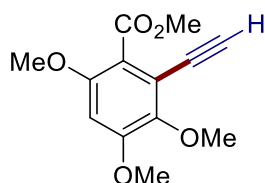
The general procedure **A** was followed using benzoic acid **98d** (106 mg, 0.50 mmol) and (bromoethynyl)triisopropylsilane (**40B**) (170 mg, 0.65 mmol, 1.30 equiv). Purification by column chromatography on silica gel (*n*hexane/EtOAc: 4/1) yielded **99d** (161 mg, 82%) as a white solid. **M. p.**: 177–178 °C. **<sup>1</sup>H NMR** (400 MHz,  $\text{CDCl}_3$ )  $\delta$  = 6.48 (s, 1H), 3.88 (s, 3H), 3.85 (s, 3H), 3.83 (s, 3H), 1.12–1.11 (m, 21H). **<sup>13</sup>C NMR** (101 MHz,  $\text{CDCl}_3$ )  $\delta$  = 169.6 ( $\text{C}_q$ ), 155.2 ( $\text{C}_q$ ), 153.8 ( $\text{C}_q$ ), 145.5 ( $\text{C}_q$ ), 118.3 ( $\text{C}_q$ ), 116.5 ( $\text{C}_q$ ), 101.5 ( $\text{C}_q$ ), 98.9 ( $\text{C}_q$ ), 97.9 (CH), 60.9 ( $\text{CH}_3$ ), 56.8 ( $\text{CH}_3$ ), 56.2 ( $\text{CH}_3$ ), 18.6 ( $\text{CH}_3$ ), 11.3 (CH). **IR** (neat): 2942, 2864, 2163, 1699, 1583, 1209, 1096, 691  $\text{cm}^{-1}$ . **MS** (ESI)  $m/z$  (relative intensity) 415 (30)  $[\text{M}+\text{Na}]^+$ , 393 (100)  $[\text{M}+\text{H}]^+$ . **HR-MS** (ESI)  $m/z$  calcd for

$C_{21}H_{33}O_5Si$   $[M+H]^+$ : 393.2092, found: 393.2092.



### 3,5-Dimethoxy-4-methyl-2,6-bis[(triisopropylsilyl)ethynyl]benzoic acid (**99e**)

The general procedure **A** was followed using benzoic acid **98e** (98 mg, 0.50 mmol) (bromoethynyl)triisopropylsilane (**40B**) (326 mg, 1.25 mmol, 2.50 equiv) and  $K_2CO_3$  (207 mg, 1.50 mmol, 3.0 equiv). Purification by column chromatography on silica gel (*n*hexane/EtOAc: 4/1) yielded **99e** (197 mg, 71%) as a pale yellow solid. **M. p.**: 198–199 °C.  **$^1H$  NMR** (300 MHz,  $CDCl_3$ )  $\delta$  = 3.94 (s, 6H), 2.23 (s, 3H), 1.17–1.10 (m, 42H).  **$^{13}C$  NMR** (75 MHz,  $CDCl_3$ )  $\delta$  = 170.5 ( $C_q$ ), 161.1 ( $C_q$ ), 137.6 ( $C_q$ ), 127.9 ( $C_q$ ), 112.1 ( $C_q$ ), 100.2 ( $C_q$ ), 99.0 ( $C_q$ ), 60.7 ( $CH_3$ ), 18.6 ( $CH_3$ ), 11.3 (CH), 9.6 ( $CH_3$ ). **IR** (neat): 2942, 2865, 2153, 1703, 1450, 1389, 994, 882, 661  $cm^{-1}$ . **MS** (EI)  $m/z$  (relative intensity) 557  $[M+H]^+$  (3), 556 (5), 537 (10), 515 (15), 514 (40), 513 (100), 455 (5). **HR-MS** (EI)  $m/z$  calcd for  $C_{32}H_{52}O_4Si_2$   $[M]^+$ : 556.3404, found: 556.3420.



### Methyl 2-ethynyl-3,4,6-trimethoxybenzoate (**100d**)

Colourless solid. **M.p.**: 90–91 °C.  **$^1H$  NMR** (300 MHz,  $CDCl_3$ )  $\delta$  = 6.54 (s, 1H), 3.91 (s, 3H), 3.90 (s, 3H), 3.87 (s, 3H), 3.84 (s, 3H), 3.39 (s, 1H).  **$^{13}C$  NMR** (75 MHz,  $CDCl_3$ )  $\delta$  = 166.7 ( $C_q$ ), 154.0 ( $C_q$ ), 153.2 ( $C_q$ ), 145.0 ( $C_q$ ), 118.7 ( $C_q$ ), 115.8 ( $C_q$ ), 98.7 (CH), 84.8 (CH), 61.2 ( $CH_3$ ), 56.6 ( $CH_3$ ), 56.2 ( $CH_3$ ), 52.4 ( $CH_3$ ). **IR** (neat): 3265, 2950, 1721, 1585, 1269, 1208, 1027, 814, 650  $cm^{-1}$ . **MS** (ESI)  $m/z$  (relative intensity) 273 (60)  $[M+Na]^+$ , 251 (100)  $[M+H]^+$ . **HR-MS** (ESI)  $m/z$  calcd for  $C_{13}H_{15}O_5$   $[M+H]^+$  251.0914, found: 251.0922.

## 5.3.1.2 Radical Trapping Experiment

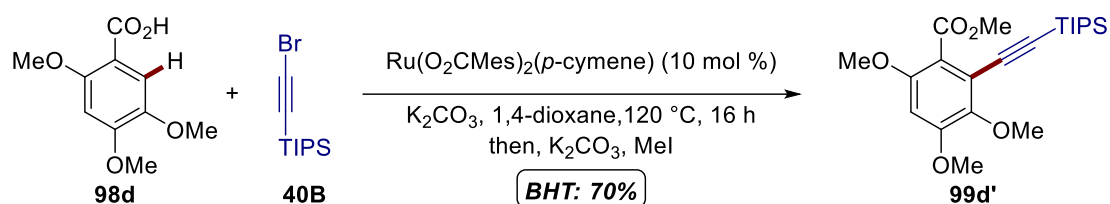


**Figure 5.3.1.** Radical trapping experiment.

Substrate **98d** (106 mg, 0.5 mmol, 1.0 equiv), (bromoethynyl)triisopropylsilane (**40B**) (170 mg, 1.3 equiv),  $[\text{Ru}(\text{O}_2\text{CMes})_2(\textit{p}\text{-cymene})]$  (28.1 mg, 10 mol %),  $\text{K}_2\text{CO}_3$  (138 mg, 1.0 mmol) and 2,6-bis(1,1-dimethylethyl)-4-methylphenol (110 mg, 0.5 mmol, 1.0 equiv) were placed into a 25 mL Schlenk tube equipped with a septum under  $\text{N}_2$  atmosphere. 1,4-dioxane (2.0 mL) was introduced via cannula. The reaction mixture was stirred at 120 °C for 16 h. At ambient temperature, MeCN (3.0 mL),  $\text{K}_2\text{CO}_3$  (207 mg, 1.50 mmol) and MeI (355 mg, 2.5 mmol) were added and the mixture was stirred at 50 °C for another 2.0 h. At ambient temperature, the mixture was dry loaded onto silica gel and purified by column chromatography on silica gel (*n*hexane/EtOAc: 4/1) to yield **99d'** (142 mg, 70%) as an off-white solid.

## 5.3.1.3 Removal of Silyl Group

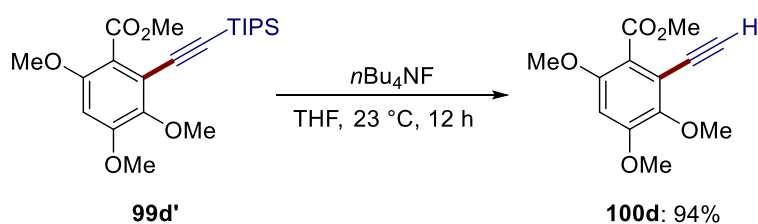
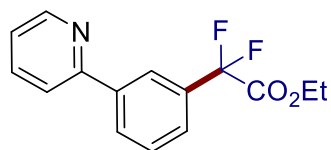


**Figure 5.3.2.** Traceless removal to access terminal aromatic alkynes.

Compound **99d'** (203 mg, 0.50 mmol) was dissolved in THF (3 mL) and TBAF (1.0 M in THF, 1.50 mL) was then added at ambient temperature with constant stirring for 12 hours, the mixture was concentrated *in vacuo*. The residue was dissolved in  $\text{H}_2\text{O}$  (30 mL) was extracted with EtOAc (3 × 5 mL), and the combined organic layers were washed with brine (10 mL), dried over  $\text{Na}_2\text{SO}_4$ , filtered and evaporated *in vacuo*. The obtained crude product was purified by column chromatography to afford the desired terminal alkyne **100d** (118 mg, 94% yield) as a white solid.

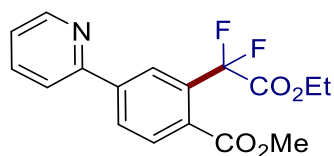
### 5.3.2 Ruthenium-Catalyzed *meta*-C–H Mono- and Difluoromethylation

#### 5.3.2.1 Characterization Data



#### Ethyl 2,2-difluoro-2-[3-(pyridin-2-yl)phenyl]acetate (**103a**)

The general procedure **B** was followed using substrate **13a** (78 mg, 0.50 mmol) and **102a** (304 mg, 1.5 mmol). Isolation by column chromatography (*n*hexane/EtOAc: 9/1) yielded **103a** (99 mg, 71%) as a colorless oil. A reaction using Ni(PPh<sub>3</sub>)<sub>2</sub>Cl<sub>2</sub> (10 mol %) instead of P(4-C<sub>6</sub>H<sub>4</sub>CF<sub>3</sub>)<sub>3</sub> yielded **103a** (100 mg, 72%). **<sup>1</sup>H NMR** (300 MHz, CDCl<sub>3</sub>) δ = 8.71 (ddd, *J* = 4.8, 1.6, 1.1 Hz, 1H), 8.24 (ddt, *J* = 1.9, 1.3, 0.7 Hz, 1H), 8.16 (dddt, *J* = 7.6, 1.9, 1.4, 0.7 Hz, 1H), 7.83–7.73 (m, 2H), 7.66 (ddd, *J* = 7.8, 1.9, 1.3 Hz, 1H), 7.57 (dd, *J* = 7.8, 7.6 Hz, 1H), 7.30–7.25 (m, 1H), 4.31 (q, *J* = 7.1 Hz, 2H), 1.31 (t, *J* = 7.1 Hz, 3H). **<sup>13</sup>C NMR** (125 MHz, CDCl<sub>3</sub>) δ = 164.0 (t, <sup>2</sup>*J*<sub>C–F</sub> = 35.2 Hz, C<sub>q</sub>), 156.0 (C<sub>q</sub>), 149.7 (CH), 139.8 (C<sub>q</sub>), 136.8 (CH), 133.3 (t, <sup>2</sup>*J*<sub>C–F</sub> = 25.5 Hz, C<sub>q</sub>), 129.4 (t, <sup>4</sup>*J*<sub>C–F</sub> = 1.7 Hz, CH), 129.1 (CH), 125.8 (t, <sup>3</sup>*J*<sub>C–F</sub> = 6.0 Hz, CH), 123.9 (t, <sup>3</sup>*J*<sub>C–F</sub> = 6.3 Hz, CH), 122.6 (CH), 120.6 (CH), 113.3 (t, <sup>1</sup>*J*<sub>C–F</sub> = 252.0 Hz, C<sub>q</sub>), 63.2 (CH<sub>2</sub>), 14.0 (CH<sub>3</sub>). **<sup>19</sup>F NMR** (282 MHz, CDCl<sub>3</sub>) δ = -103.7 (s). **IR** (neat): 2986, 1761, 1585, 1463, 1290, 1100, 777 cm<sup>-1</sup>. **MS** (ESI) *m/z* (relative intensity) 278 (100) [M+H]<sup>+</sup>. **HR-MS** (ESI) *m/z* calcd for C<sub>15</sub>H<sub>14</sub>F<sub>2</sub>NO<sub>2</sub> [M+H]<sup>+</sup>: 278.0987, found: 278.0994.

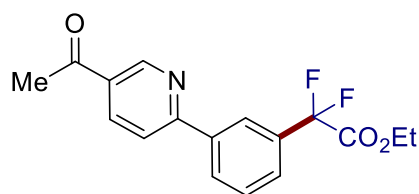


#### Methyl 2-(2-ethoxy-1,1-difluoro-2-oxoethyl)-4-(pyridin-2-yl)benzoate (**103b**)

The general procedure **B** was followed using substrate **13c** (107 mg, 0.50 mmol) and **102a** (304 mg, 1.5 mmol). Isolation by column chromatography (*n*hexane/EtOAc: 6/1) yielded **103b** (137 mg, 82%) as a colorless oil. A reaction using Ni(PPh<sub>3</sub>)<sub>2</sub>Cl<sub>2</sub> (10 mol %) instead of P(4-C<sub>6</sub>H<sub>4</sub>CF<sub>3</sub>)<sub>3</sub> yielded **103b** (106 mg, 63%). **<sup>1</sup>H NMR** (600 MHz, CDCl<sub>3</sub>) δ = 8.72 (ddd, *J* = 4.8, 1.8, 1.1 Hz, 1H), 8.47 (d, *J* = 1.8 Hz, 1H), 8.21 (dd, *J* = 8.1, 1.8 Hz, 1H), 8.10 (d, *J* = 8.1 Hz, 1H), 7.87–7.70 (m, 2H), 7.30 (ddd, *J* = 7.0, 4.8, 1.6 Hz, 1H), 118

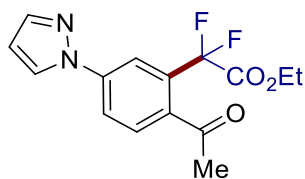


4.32 (q,  $J = 7.1$  Hz, 2H), 3.87 (s, 3H), 1.29 (t,  $J = 7.1$  Hz, 3H).  $^{13}\text{C}$  NMR (125 MHz,  $\text{CDCl}_3$ )  $\delta = 166.1$  ( $\text{C}_q$ ), 163.1 (t,  $^2J_{\text{C-F}} = 33.6$  Hz,  $\text{C}_q$ ), 155.0 ( $\text{C}_q$ ), 149.8 (CH), 143.0 ( $\text{C}_q$ ), 137.0 (CH), 134.1 (t,  $^2J_{\text{C-F}} = 23.7$  Hz,  $\text{C}_q$ ), 131.6 (CH), 128.7 (CH), 128.6 ( $\text{C}_q$ ), 125.2 (t,  $^3J_{\text{C-F}} = 10.5$  Hz, CH), 123.2 (CH), 121.0 (CH), 113.1 (t,  $^1J_{\text{C-F}} = 249.6$  Hz,  $\text{C}_q$ ), 62.8 ( $\text{CH}_2$ ), 52.4 ( $\text{CH}_3$ ), 13.9 ( $\text{CH}_3$ ).  $^{19}\text{F}$  NMR (282 MHz,  $\text{CDCl}_3$ )  $\delta = -99.0$  (s). IR (neat): 2987, 1757, 1721, 1566, 1281, 1080, 753  $\text{cm}^{-1}$ . MS (ESI)  $m/z$  (relative intensity) 358 (50)  $[\text{M}+\text{Na}]^+$ , 336 (100)  $[\text{M}+\text{H}]^+$ . HR-MS (ESI)  $m/z$  calcd for  $\text{C}_{17}\text{H}_{15}\text{F}_2\text{NO}_4$   $[\text{M}+\text{H}]^+$ : 336.1042, found: 336.1040.



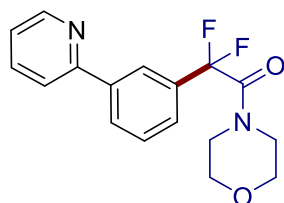
### Ethyl 2-[3-(5-acetylpyridin-2-yl)phenyl]-2,2-difluoroacetate (**103c**)

The general procedure **B** was followed using substrate **13d** (99 mg, 0.50 mmol) and **102a** (304 mg, 1.5 mmol). Isolation by column chromatography (*n*hexane/EtOAc: 5/1) yielded **103c** (123 mg, 77%) as a colorless oil. A reaction using  $\text{Ni}(\text{PPh}_3)_2\text{Cl}_2$  (10 mol %) instead of  $\text{P}(4\text{-C}_6\text{H}_4\text{CF}_3)_3$  yielded **103c** (125 mg, 78%).  $^1\text{H}$  NMR (600 MHz,  $\text{CDCl}_3$ )  $\delta = 9.22$  (d,  $J = 2.3$  Hz, 1H), 8.30 (s, 1H), 8.29 (dd,  $J = 8.2, 2.3$  Hz, 1H), 8.20 (dd,  $J = 7.8, 1.8$  Hz, 1H), 7.85 (dd,  $J = 8.2$  Hz, 1H), 7.70 (dd,  $J = 7.8, 1.9$  Hz, 1H), 7.58 (d,  $J = 7.8, 7.8$  Hz, 1H), 4.30 (q,  $J = 7.1$  Hz, 2H), 2.65 (s, 3H), 1.30 (t,  $J = 7.1$  Hz, 3H).  $^{13}\text{C}$  NMR (125 MHz,  $\text{CDCl}_3$ )  $\delta = 196.0$  ( $\text{C}_q$ ), 163.8 (t,  $^2J_{\text{C-F}} = 35.0$  Hz,  $\text{C}_q$ ), 159.2 ( $\text{C}_q$ ), 149.9 (CH), 138.6 ( $\text{C}_q$ ), 136.4 (CH), 133.5 (t,  $^2J_{\text{C-F}} = 25.6$  Hz,  $\text{C}_q$ ), 130.9 ( $\text{C}_q$ ), 129.7 (t,  $^4J_{\text{C-F}} = 1.8$  Hz, CH), 129.2 (CH), 126.8 (t,  $^3J_{\text{C-F}} = 6.0$  Hz, CH), 124.3 (t,  $^4J_{\text{C-F}} = 6.3$  Hz, CH), 120.1 (CH), 113.1 (t,  $^1J_{\text{C-F}} = 252.2$  Hz,  $\text{C}_q$ ), 63.2 ( $\text{CH}_2$ ), 26.7 ( $\text{CH}_3$ ), 13.9 ( $\text{CH}_3$ ).  $^{19}\text{F}$  NMR (282 MHz,  $\text{CDCl}_3$ )  $\delta = -103.8$ . IR (neat): 2986, 1761, 1685, 1588, 1276, 1224, 1100, 806  $\text{cm}^{-1}$ . MS (ESI)  $m/z$  (relative intensity) 342 (30)  $[\text{M}+\text{Na}]^+$ , 320 (100)  $[\text{M}+\text{H}]^+$ . HR-MS (ESI)  $m/z$  calcd for  $\text{C}_{17}\text{H}_{16}\text{F}_2\text{NO}_3$   $[\text{M}+\text{H}]^+$ : 320.1093, found: 320.1093.



### Ethyl 2-(2-acetyl-5-(1H-pyrazol-1-yl)phenyl)-2,2-difluoroacetate (**103d**)

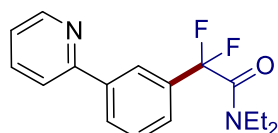
The general procedure **B** was followed using substrate **13e** (93 mg, 0.50 mmol) and **102a** (304 mg, 1.5 mmol). Isolation by column chromatography (*n*hexane/EtOAc: 4/1) yielded **103d** (43 mg, 28%) as a brown solid. A reaction using Ni(PPh<sub>3</sub>)<sub>2</sub>Cl<sub>2</sub> (10 mol %) instead of P(4-C<sub>6</sub>H<sub>4</sub>CF<sub>3</sub>)<sub>3</sub> yielded **103d** (83 mg, 53%). **M.p.**: 106–107 °C. **<sup>1</sup>H NMR** (600 MHz, CDCl<sub>3</sub>) δ = 8.18 (d, *J* = 1.9 Hz, 1H), 8.04 (d, *J* = 2.7 Hz, 1H), 7.99–7.93 (m, 2H), 7.77 (d, *J* = 1.7 Hz, 1H), 6.52 (dd, *J* = 2.6, 1.7 Hz, 1H), 4.35 (q, *J* = 7.1 Hz, 2H), 2.60 (s, 3H), 1.33 (t, *J* = 7.1 Hz, 3H). **<sup>13</sup>C NMR** (125 MHz, CDCl<sub>3</sub>) δ = 197.9 (C<sub>q</sub>), 162.7 (t, <sup>2</sup>*J*<sub>C-F</sub> = 32.9 Hz, C<sub>q</sub>), 142.6 (C<sub>q</sub>), 142.4 (CH), 134.6 (t, <sup>2</sup>*J*<sub>C-F</sub> = 23.7 Hz, C<sub>q</sub>), 133.0 (t, <sup>3</sup>*J*<sub>C-F</sub> = 2.8 Hz, C<sub>q</sub>), 131.9 (CH), 126.9 (CH), 119.8 (CH), 117.3 (t, <sup>3</sup>*J*<sub>C-F</sub> = 11.4 Hz, CH), 112.9 (t, <sup>1</sup>*J*<sub>C-F</sub> = 250.5 Hz, C<sub>q</sub>), 109.0 (CH), 62.8 (CH<sub>2</sub>), 28.0 (CH<sub>3</sub>), 13.9 (CH<sub>3</sub>). **<sup>19</sup>F NMR** (282 MHz, CDCl<sub>3</sub>) δ = -99.8. **IR** (neat): 3130, 2923, 1762, 1387, 1268, 1120, 1006, 742 cm<sup>-1</sup>. **MS** (ESI) *m/z* (relative intensity) 331 (85) [M+Na]<sup>+</sup>, 309 (100) [M+H]<sup>+</sup>. **HR-MS** (ESI) *m/z* calcd for C<sub>15</sub>H<sub>15</sub>F<sub>2</sub>N<sub>2</sub>O<sub>3</sub> [M+H]<sup>+</sup>: 309.1045, found: 309.1048.



### 2,2-Difluoro-1-morpholino-2-[3-(pyridin-2-yl)phenyl]ethan-1-one (**103e**)

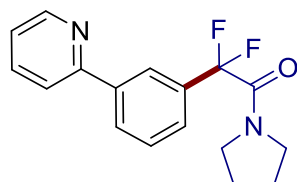
The general procedure **B** was followed using substrate **13a** (78 mg, 0.50 mmol) and **102b** (366 mg, 1.5 mmol). Isolation by column chromatography (*n*hexane/EtOAc: 8/1) yielded **103e** (49 mg, 31%) as a colorless oil. A reaction using Ni(PPh<sub>3</sub>)<sub>2</sub>Cl<sub>2</sub> (10 mol %) instead of P(4-C<sub>6</sub>H<sub>4</sub>CF<sub>3</sub>)<sub>3</sub> yielded **103e** (132 mg, 83%). **<sup>1</sup>H NMR** (400 MHz, CDCl<sub>3</sub>) δ = 8.69 (ddd, *J* = 4.8, 1.6, 1.1 Hz, 1H), 8.20 (d, *J* = 1.6 Hz, 1H), 8.16–8.08 (m, 1H), 7.81–7.69 (m, 2H), 7.58–7.51 (m, 2H), 7.26 (ddd, *J* = 6.7, 4.8, 1.7 Hz, 1H), 3.69–3.68 (m, 4H), 3.50–3.49 (m, 4H). **<sup>13</sup>C NMR** (101 MHz, CDCl<sub>3</sub>) δ = 162.0 (t, <sup>2</sup>*J*<sub>C-F</sub> = 30.3 Hz, C<sub>q</sub>), 155.9 (C<sub>q</sub>), 149.7 (CH), 140.0 (C<sub>q</sub>), 137.1 (CH), 134.0 (t, <sup>2</sup>*J*<sub>C-F</sub> = 24.9 Hz, C<sub>q</sub>), 129.4 (t,

$^4J_{C-F} = 1.7$  Hz, CH), 129.3 (CH), 125.6 (t,  $^3J_{C-F} = 5.6$  Hz, CH), 123.7 (t,  $^3J_{C-F} = 5.8$  Hz, CH), 122.8 (CH), 120.7 (CH), 115.6 (t,  $^1J_{C-F} = 251.2$  Hz, C<sub>q</sub>), 66.7 (CH<sub>2</sub>), 66.4 (CH<sub>2</sub>), 46.7 (t,  $^4J_{C-F} = 4.1$  Hz, CH<sub>2</sub>), 43.5 (CH<sub>2</sub>).  **$^{19}F$  NMR** (376 MHz, CDCl<sub>3</sub>)  $\delta = -94.5$  (s). **IR** (neat): 2918, 2856, 1666, 1435, 1225, 1114, 995, 729 cm<sup>-1</sup>. **MS** (ESI)  $m/z$  (relative intensity) 341 (15) [M+Na]<sup>+</sup>, 319 (100) [M+H]<sup>+</sup>. **HR-MS** (ESI)  $m/z$  calcd for C<sub>17</sub>H<sub>16</sub>F<sub>2</sub>N<sub>2</sub>O<sub>2</sub> [M+H]<sup>+</sup>: 319.1253, found: 319.1257.



### ***N,N*-Diethyl-2,2-difluoro-2-[3-(pyridin-2-yl)phenyl]acetamide (103f)**

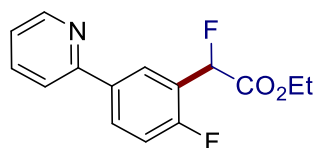
The general procedure **B** was followed using substrate **13a** (78 mg, 0.50 mmol) and **102c** (345 mg, 1.5 mmol). Isolation by column chromatography (*n*hexane/EtOAc: 8/1) yielded **103f** (81 mg, 53%) as a colorless oil. A reaction using Ni(PPh<sub>3</sub>)<sub>2</sub>Cl<sub>2</sub> (10 mol %) instead of P(4-C<sub>6</sub>H<sub>4</sub>CF<sub>3</sub>)<sub>3</sub> yielded **103f** (62 mg, 41%).  **$^1H$  NMR** (300 MHz, CDCl<sub>3</sub>)  $\delta = 8.63$  (dd,  $J = 4.8, 1.5$  Hz, 1H), 8.12 (dd,  $J = 1.7, 0.9$  Hz, 1H), 8.10–8.03 (m, 1H), 7.76–7.65 (m, 2H), 7.55–7.43 (m, 2H), 7.24–7.13 (m, 1H), 3.37 (q,  $J = 7.1$  Hz, 2H), 3.22 (qt,  $J = 7.0, 1.4$  Hz, 2H), 1.11 (t,  $J = 7.1$  Hz, 3H), 1.00 (t,  $J = 7.0$  Hz, 3H).  **$^{13}C$  NMR** (101 MHz, CDCl<sub>3</sub>)  $\delta = 162.7$  (t,  $^2J_{C-F} = 29.9$  Hz, C<sub>q</sub>), 156.1 (C<sub>q</sub>), 149.7 (CH), 140.0 (C<sub>q</sub>), 137.0 (CH), 134.6 (t,  $^2J_{C-F} = 25.1$  Hz, C<sub>q</sub>), 129.2 (CH), 125.7 (t,  $^3J_{C-F} = 5.6$  Hz, CH), 123.7 (t,  $^3J_{C-F} = 5.8$  Hz, CH), 122.7 (CH), 120.7 (CH), 115.6 (t,  $^1J_{C-F} = 250.6$  Hz, C<sub>q</sub>), 42.2 (t,  $^4J_{C-F} = 4.2$  Hz, CH<sub>2</sub>), 41.5 (CH<sub>2</sub>), 13.9 (CH<sub>3</sub>), 12.3 (CH<sub>3</sub>).  **$^{19}F$  NMR** (282 MHz, CDCl<sub>3</sub>)  $\delta = -94.7$ . **IR** (neat): 2977, 1661, 1461, 1431, 1242, 777, 700 cm<sup>-1</sup>. **MS** (ESI)  $m/z$  (relative intensity) 327 (20) [M+Na]<sup>+</sup>, 305 (100) [M+H]<sup>+</sup>. **HR-MS** (ESI)  $m/z$  calcd for C<sub>17</sub>H<sub>19</sub>F<sub>2</sub>N<sub>2</sub>O [M+H]<sup>+</sup>: 305.1460, found: 305.1460.



### **2,2-Difluoro-2-[3-(pyridin-2-yl)phenyl]-1-(pyrrolidin-1-yl)ethan-1-one (103g)**

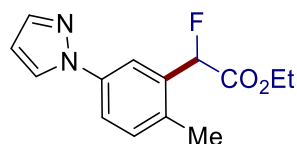
The general procedure **B** was followed using substrate **13a** (78 mg, 0.50 mmol) and **102d** (342 mg, 1.5 mmol). Isolation by column chromatography (*n*hexane/EtOAc: 8/1)

yielded **103g** (65 mg, 43%) as a colorless oil. A reaction using Ni(PPh<sub>3</sub>)<sub>2</sub>Cl<sub>2</sub> (10 mol %) instead of P(4-C<sub>6</sub>H<sub>4</sub>CF<sub>3</sub>)<sub>3</sub> yielded **103g** (116 mg, 77%). **<sup>1</sup>H NMR** (300 MHz, CDCl<sub>3</sub>) δ = 8.68 (dd, *J* = 4.9, 1.4 Hz, 1H), 8.19 (s, 1H), 8.12 (d, *J* = 7.7 Hz, 1H), 7.82–7.69 (m, 2H), 7.64–7.48 (m, 2H), 7.28–7.21 (m, 1H), 3.67–3.27 (m, 4H), 1.92–1.70 (m, 4H). **<sup>13</sup>C NMR** (75 MHz, CDCl<sub>3</sub>) δ = 162.1 (t, <sup>2</sup>*J*<sub>C-F</sub> = 31.1 Hz, C<sub>q</sub>), 156.2 (C<sub>q</sub>), 149.7 (CH), 139.8 (C<sub>q</sub>), 137.0 (CH), 133.9 (t, <sup>2</sup>*J*<sub>C-F</sub> = 25.8 Hz, C<sub>q</sub>), 129.2 (t, <sup>4</sup>*J*<sub>C-F</sub> = 1.8 Hz, CH), 129.1 (CH), 125.9 (t, <sup>3</sup>*J*<sub>C-F</sub> = 5.9 Hz, CH), 123.9 (t, <sup>3</sup>*J*<sub>C-F</sub> = 6.0 Hz, CH), 122.6 (CH), 120.8 (CH), 115.4 (t, <sup>1</sup>*J*<sub>C-F</sub> = 251.2 Hz, C<sub>q</sub>), 47.5 (CH<sub>2</sub>), 46.8 (t, <sup>1</sup>*J*<sub>C-F</sub> = 5.0 Hz, CH<sub>2</sub>), 26.4 (CH<sub>2</sub>), 23.2 (CH<sub>2</sub>). **<sup>19</sup>F NMR** (282 MHz, CDCl<sub>3</sub>) δ = -98.5 (s). **IR** (neat): 2976, 2884, 1657, 1434, 1223, 1064, 776 cm<sup>-1</sup>. **MS** (ESI) *m/z* (relative intensity) 325 (30) [M+Na]<sup>+</sup>, 303 (100) [M+H]<sup>+</sup>. **HR-MS** (ESI) *m/z* calcd for C<sub>17</sub>H<sub>17</sub>F<sub>2</sub>N<sub>2</sub>O [M+H]<sup>+</sup>: 303.1303, found: 303.1307.



#### Ethyl 2-fluoro-2-[3-(pyrimidin-2-yl)phenyl]acetate (**103i**)

The general procedure **B** was followed using substrate **13g** (87 mg, 0.50 mmol) and **102e** (278 mg, 1.5 mmol). Isolation by column chromatography (*n*hexane/EtOAc: 8/1) yielded **103i** (86 mg, 62%) as a colorless oil. **<sup>1</sup>H NMR** (300 MHz, CDCl<sub>3</sub>) δ = 8.60 (ddd, *J* = 4.9, 1.8, 1.0 Hz, 1H), 8.11–7.94 (m, 2H), 7.77–7.54 (m, 2H), 7.29–7.02 (m, 2H), 6.02 (d, *J* = 46.8 Hz, 1H), 4.29–4.11 (m, 2H), 1.19 (t, *J* = 7.1 Hz, 3H). **<sup>13</sup>C NMR** (101 MHz, CDCl<sub>3</sub>) δ = 167.9 (dd, <sup>2,4</sup>*J*<sub>C-F</sub> = 27.7, 1.0 Hz, C<sub>q</sub>), 160.9 (dd, <sup>1,3</sup>*J*<sub>C-F</sub> = 252.8, 4.4 Hz, C<sub>q</sub>), 155.5 (C<sub>q</sub>), 149.7 (CH), 137.0 (CH), 136.1 (dd, <sup>4,4</sup>*J*<sub>C-F</sub> = 3.4, 1.0 Hz, C<sub>q</sub>), 130.2 (dd, <sup>3,3</sup>*J*<sub>C-F</sub> = 8.6, 2.5 Hz, CH), 127.5 (dd, <sup>3,5</sup>*J*<sub>C-F</sub> = 5.5, 3.3 Hz, CH), 122.4 (CH), 122.2 (dd, <sup>2,2</sup>*J*<sub>C-F</sub> = 21.2, 14.5 Hz, C<sub>q</sub>), 120.3 (CH), 116.3 (d, <sup>2,4</sup>*J*<sub>C-F</sub> = 21.6, 1.2 Hz, CH), 83.7 (dd, <sup>1,3</sup>*J*<sub>C-F</sub> = 185.0, 3.3 Hz, CH), 62.1 (CH<sub>2</sub>), 14.0 (CH<sub>3</sub>). **<sup>19</sup>F NMR** (282 MHz, CDCl<sub>3</sub>) δ = -117.4 (s), -181.5 (s). **IR** (neat): 2986, 1761, 1711, 1467, 1220, 1055, 782 cm<sup>-1</sup>. **MS** (ESI) *m/z* (relative intensity) 300 (30) [M+Na]<sup>+</sup>, 278 (100) [M+H]<sup>+</sup>. **HR-MS** (ESI) *m/z* calcd for C<sub>15</sub>H<sub>14</sub>F<sub>2</sub>NO<sub>2</sub> [M+H]<sup>+</sup>: 278.0987, found: 278.0993.



### Ethyl 2-fluoro-2-[2-methyl-5-(1*H*-pyrazol-1-yl)phenyl]acetate (**103j**)

The general procedure **B** was followed using 1-(*p*-tolyl)-1*H*-pyrazole (**13h**) (79 mg, 0.50 mmol) and **102e** (278 mg, 1.5 mmol). Isolation by column chromatography (*n*hexane/EtOAc: 8/1) yielded **103j** (79 mg, 60%) as a colorless oil. **<sup>1</sup>H NMR** (300 MHz, CDCl<sub>3</sub>)  $\delta$  = 7.89 (dd,  $J$  = 2.5, 0.6 Hz, 1H), 7.71 (d,  $J$  = 2.5 Hz, 1H), 7.68 (dd,  $J$  = 1.8, 0.6 Hz, 1H), 7.63 (dd,  $J$  = 8.2, 2.5 Hz, 1H), 7.26 (d,  $J$  = 8.2 Hz, 1H), 6.43 (dd,  $J$  = 2.5, 1.8 Hz, 1H), 5.97 (d,  $J$  = 46.8 Hz, 1H), 4.42–4.08 (m, 2H), 2.43 (s, 3H), 1.23 (t,  $J$  = 7.1 Hz, 3H). **<sup>13</sup>C NMR** (125 MHz, CDCl<sub>3</sub>)  $\delta$  = 168.1 (d,  $^2J_{C-F}$  = 27.7 Hz, C<sub>q</sub>), 140.9 (CH), 138.5 (C<sub>q</sub>), 134.3 (d,  $^3J_{C-F}$  = 3.8 Hz, C<sub>q</sub>), 133.8 (d,  $^2J_{C-F}$  = 19.3 Hz, C<sub>q</sub>), 131.8 (CH), 126.6 (CH), 120.1 (d,  $^4J_{C-F}$  = 2.2 Hz, CH), 117.7 (d,  $^3J_{C-F}$  = 7.8 Hz, CH), 107.6 (CH), 87.0 (d,  $^1J_{C-F}$  = 185.0 Hz, CH), 61.9 (CH<sub>2</sub>), 18.7 (CH<sub>3</sub>), 14.1 (CH<sub>3</sub>). **<sup>19</sup>F NMR** (282 MHz, CDCl<sub>3</sub>)  $\delta$  = -181.2 (dd,  $J$  = 47.2, 1.2 Hz). **IR** (neat): 2983, 1923, 1756, 1522, 1393, 1323, 1043, 751 cm<sup>-1</sup>. **MS** (ESI)  $m/z$  (relative intensity) 285 (80) [M+Na]<sup>+</sup>, 263 (100) [M+H]<sup>+</sup>. **HR-MS** (ESI)  $m/z$  calcd for C<sub>14</sub>H<sub>16</sub>FN<sub>2</sub>O<sub>2</sub> [M+H]<sup>+</sup>: 263.1190, found: 263.1194.

#### 5.3.2.2 Hydrolysis of Ethyl Ester **103**

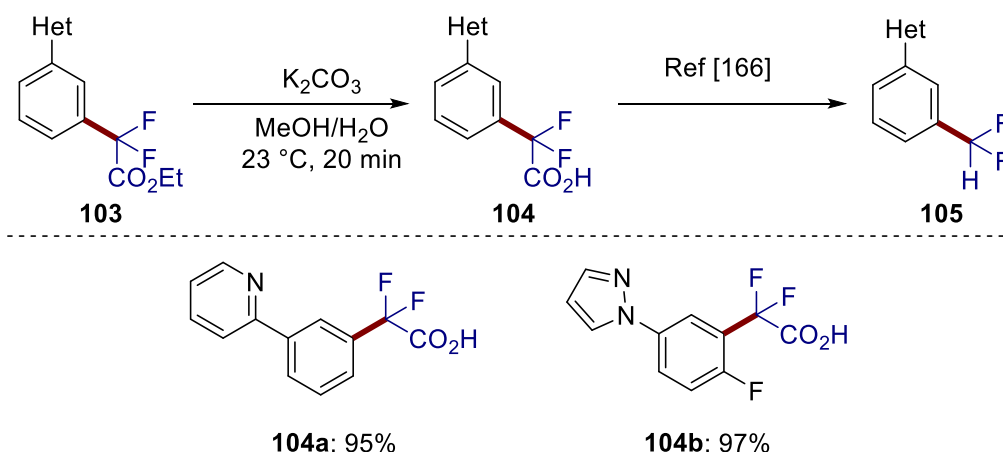


**Figure 5.3.3.** Traceless removal ethyl ester.

**2,2-Difluoro-2-[3-(pyridin-2-yl)phenyl]acetic acid (**104a**):** To a solution of **103a** (277 mg, 1.0 mmol) in MeOH (3 mL) was added K<sub>2</sub>CO<sub>3</sub> (3.0 mL, 1N) at 23 °C. The

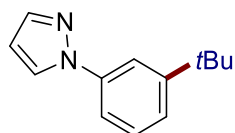
mixture was stirred at 23 °C for 20 min and poured into 5% HCl (3.0 mL), and successively extracted with EtOAc (10 mL × 3). The combined organic phase was washed with brine and dried over anhydrous Na<sub>2</sub>SO<sub>4</sub>. After removal of the solvents *in vacuo*, the residue was purified by column chromatography (CH<sub>2</sub>Cl<sub>2</sub>/MeOH: 5/1) to give **104a** (237 mg, 95%) as colorless solid. **M.p.**: 134–135 °C. **<sup>1</sup>H NMR** (300 MHz, DMSO-*d*<sub>6</sub>) δ = 8.71 (ddd, *J* = 4.8, 1.8, 1.0 Hz, 1H), 8.34 (s, 1H), 8.30–8.20 (m, 1H), 8.03 (dd, *J* = 8.0, 1.1 Hz, 1H), 7.92 (ddd, *J* = 8.1, 7.4, 1.8 Hz, 1H), 7.75–7.59 (m, 2H), 7.41 (ddd, *J* = 7.5, 4.8, 1.1 Hz, 1H), 3.18 (s, 1H). **<sup>13</sup>C NMR** (101 MHz, DMSO-*d*<sub>6</sub>) δ = 165.4 (t, <sup>2</sup>*J*<sub>C-F</sub> = 33.3 Hz, C<sub>q</sub>), 155.0 (C<sub>q</sub>), 150.1 (CH), 139.6 (C<sub>q</sub>), 138.0 (C<sub>q</sub>), 134.1 (t, <sup>2</sup>*J*<sub>C-F</sub> = 25.6 Hz, C<sub>q</sub>), 130.0 (CH), 129.4 (CH), 126.1 (t, <sup>3</sup>*J*<sub>C-F</sub> = 6.0 Hz, CH), 123.7 (CH), 123.5 (t, <sup>3</sup>*J*<sub>C-F</sub> = 6.2 Hz, CH), 121.0 (CH), 114.1 (t, <sup>1</sup>*J*<sub>C-F</sub> = 250.3 Hz, C<sub>q</sub>). **<sup>19</sup>F NMR** (282 MHz, DMSO-*d*<sub>6</sub>) δ = -102.3 (s). **IR** (neat): 3000, 1710, 1358, 1419, 1219, 1092, 899, 528 cm<sup>-1</sup>. **MS** (ESI) *m/z* (relative intensity) 272 (20) [M+Na]<sup>+</sup>, 250 (100) [M+H]<sup>+</sup>. **HR-MS** (ESI) *m/z* calcd for C<sub>13</sub>H<sub>10</sub>F<sub>2</sub>NO<sub>2</sub> [M+H]<sup>+</sup>: 250.0674, found: 250.0685.

**2,2-Difluoro-2-[2-fluoro-5-(1*H*-pyrazol-1-yl)]phenyl]acetic acid (104b):** To a solution of **103k** (284 mg, 1.0 mmol) in MeOH (3.0 mL) was added K<sub>2</sub>CO<sub>3</sub> (3.0 mL, 1N) at 23 °C. The mixture was stirred at 23 °C for 20 min and poured into 5% HCl (3.0 mL), and successively extracted with EtOAc (10 mL × 3). The combined organic phase was washed with brine and dried over anhydrous Na<sub>2</sub>SO<sub>4</sub>. After removal of the solvents *in vacuo*, the residue was purified by column chromatography (CH<sub>2</sub>Cl<sub>2</sub>/MeOH: 5/1) to give **104b** (275 mg, 97%) as colorless solid. **M.p.**: 119–120 °C. **<sup>1</sup>H NMR** (300 MHz, DMSO-*d*<sub>6</sub>) δ = 8.53 (dd, *J* = 2.6, 0.6 Hz, 1H), 7.98 (dd, *J* = 6.3, 2.8 Hz, 1H), 7.95–7.87 (m, 1H), 7.76 (dd, *J* = 1.7, 0.6 Hz, 1H), 7.38 (dd, *J* = 10.1, 8.9 Hz, 1H), 6.55 (dd, *J* = 2.6, 1.7 Hz, 1H). **<sup>13</sup>C NMR** (101 MHz, DMSO-*d*<sub>6</sub>) δ = 164.0 (t, <sup>2</sup>*J*<sub>C-F</sub> = 26.5 Hz, C<sub>q</sub>), 157.6 (dt, <sup>1,3</sup>*J*<sub>C-F</sub> = 249.7, 3.8 Hz, C<sub>q</sub>), 141.6 (CH), 136.1 (d, <sup>4</sup>*J*<sub>C-F</sub> = 2.9 Hz, C<sub>q</sub>), 128.5 (CH), 126.4 (dt, <sup>2,2</sup>*J*<sub>C-F</sub> = 26.5, 13.1 Hz, C<sub>q</sub>), 121.3 (d, <sup>3</sup>*J*<sub>C-F</sub> = 8.6 Hz, CH), 118.1 (td, <sup>3,3</sup>*J*<sub>C-F</sub> = 7.6, 3.3 Hz, CH), 117.6 (d, <sup>2</sup>*J*<sub>C-F</sub> = 23.0 Hz, CH), 114.2 (t, <sup>1</sup>*J*<sub>C-F</sub> = 254.4 Hz, C<sub>q</sub>), 108.5 (CH). **<sup>19</sup>F NMR** (282 MHz, DMSO-*d*<sub>6</sub>) δ = -98.4 (d, *J* = 11.2 Hz, 2F), -117.9 (t, *J* = 11.2 Hz, 1F). **IR** (neat): 3148, 1708, 1663, 1522, 1505, 1405, 1225, 1040, 753 cm<sup>-1</sup>. **MS** (ESI) *m/z*

(relative intensity) 279 (20)  $[M+Na]^+$ , 257 (100)  $[M+H]^+$ . **HR-MS** (ESI)  $m/z$  calcd for  $C_{11}H_6F_3N_2O_2$   $[M-H]^+$ : 255.0387, found: 255.0391.

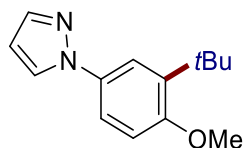
### 5.3.3 Ruthenium-Catalyzed *meta*-C–H Alkylation

#### 5.3.3.1 Characterization Data



#### 1-[3-(*tert*-Butyl)phenyl]-1*H*-pyrazole (103k)

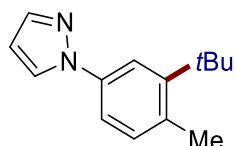
The general procedure **C** was followed using substrate **13i** (72.0 mg, 0.50 mmol) and bromide **24B** (206 mg, 1.5 mmol). Purification by column chromatography (*n*hexane/EtOAc: 10/1) yielded **103k** (74.0 mg, 74%) as a colorless oil. **<sup>1</sup>H NMR** (300 MHz,  $CDCl_3$ )  $\delta$  = 7.90 (dd,  $J$  = 2.5, 0.6 Hz, 1H), 7.75 (ddd,  $J$  = 2.2, 1.7, 0.6 Hz, 1H), 7.72 (dd,  $J$  = 1.8, 0.6 Hz, 1H), 7.43 (ddd,  $J$  = 7.5, 2.2, 1.7 Hz, 1H), 7.36 (ddd,  $J$  = 8.1, 7.5, 0.6 Hz, 1H), 7.31 (dd,  $J$  = 8.1, 1.7, 1.7 Hz, 1H), 6.44 (dd,  $J$  = 2.5, 1.8 Hz, 1H) **<sup>13</sup>C NMR** (126 MHz,  $CDCl_3$ )  $\delta$  = 152.8 ( $C_q$ ), 140.7 (CH), 140.0 ( $C_q$ ), 128.9 (CH), 126.8 (CH), 123.5 (CH), 116.7 (CH), 116.4 (CH), 107.3 (CH), 35.0 ( $C_q$ ), 31.3 ( $CH_3$ ). **IR** (ATR): 2963, 2867, 1589, 1519, 1391, 1043, 947, 787, 745, 698  $cm^{-1}$ . **MS** (EI)  $m/z$  (relative intensity) 200 (40)  $[M]^+$ , 185 (100), 157 (20). **HR-MS** (EI)  $m/z$  calcd for  $C_{13}H_{16}N_2$   $[M]^+$ : 200.1308, found: 200.1312.



#### 1-[3-(*tert*-Butyl)-4-methoxyphenyl]-1*H*-pyrazole (103l)

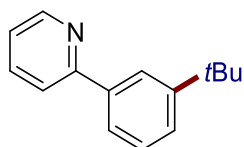
The general procedure **C** was followed using substrate **13j** (87.0 mg, 0.50 mmol) and bromide **24B** (206 mg, 1.5 mmol). Purification by column chromatography (*n*hexane/EtOAc: 10/1) yielded **103l** (95.9 mg, 83%) as a colorless oil. **<sup>1</sup>H NMR** (300 MHz,  $CDCl_3$ )  $\delta$  = 7.80 (dd,  $J$  = 2.4, 0.7 Hz, 1H), 7.68 (dd,  $J$  = 1.8, 0.7 Hz, 1H), 7.59 (d,  $J$  = 2.7 Hz, 1H), 7.40 (dd,  $J$  = 8.7, 2.7 Hz, 1H), 6.90 (d,  $J$  = 8.7 Hz, 1H), 6.41 (dd,  $J$  = 2.4, 1.8 Hz, 1H), 3.85 (s, 3H), 1.40 (s, 9H). **<sup>13</sup>C NMR** (126 MHz,  $CDCl_3$ )  $\delta$  =

157.1 (C<sub>q</sub>), 140.3 (CH), 139.4 (C<sub>q</sub>), 133.4 (C<sub>q</sub>), 126.9 (CH), 119.0 (CH), 118.1 (CH), 111.8 (CH), 106.8 (CH), 55.3 (CH<sub>3</sub>), 35.1 (C<sub>q</sub>), 29.6 (CH<sub>3</sub>). **IR** (ATR): 2954, 2867, 1516, 1493, 1234, 1045, 1028, 809, 746, 640 cm<sup>-1</sup>. **MS** (ESI) *m/z* (relative intensity) 231 (100) [M+H]<sup>+</sup>, 253 (25) [M+Na]<sup>+</sup>. **HR-MS** (ESI) *m/z* calcd for C<sub>14</sub>H<sub>19</sub>N<sub>2</sub>O [M+H]<sup>+</sup>: 231.1492, found: 231.1492. The spectral data are in accordance with those reported in the literature.<sup>[62c]</sup>



### 1-[3-(*tert*-Butyl)-4-methylphenyl]-1*H*-pyrazole (103m)

The general procedure **C** was followed using substrate **13h** (79.0 mg, 0.50 mmol) and bromide **24B** (206 mg, 1.5 mmol). Purification by column chromatography (*n*hexane/EtOAc: 10/1) yielded **103m** (66.7 mg, 62%) as a colorless oil. **<sup>1</sup>H NMR** (300 MHz, CDCl<sub>3</sub>)  $\delta$  = 7.88 (dd, *J* = 2.5, 0.7 Hz, 1H), 7.74 (d, *J* = 2.4 Hz, 1H), 7.72 (d, *J* = 1.6 Hz, 1H), 7.35 (dd, *J* = 8.2, 2.4 Hz, 1H), 7.18 (d, *J* = 8.2 Hz, 1H), 6.52–6.40 (m, 1H), 2.57 (s, 3H), 1.46 (s, 9H). **<sup>13</sup>C NMR** (101 MHz, CDCl<sub>3</sub>)  $\delta$  = 149.4 (C<sub>q</sub>), 140.6 (CH), 138.1 (C<sub>q</sub>), 134.7 (C<sub>q</sub>), 133.4 (CH), 126.8 (CH), 117.7 (CH), 116.6 (CH), 107.1 (CH), 36.0 (C<sub>q</sub>), 30.6 (CH<sub>3</sub>), 22.7 (CH<sub>3</sub>). **IR** (ATR): 2957, 2871, 1610, 1517, 1395, 1045, 950, 747, 611 cm<sup>-1</sup>. **MS** (EI) *m/z* (relative intensity) 214 (60) [M]<sup>+</sup>, 199 (100). **HR-MS** (EI) *m/z* calcd for C<sub>14</sub>H<sub>18</sub>N<sub>2</sub> [M]<sup>+</sup>: 214.1465, found: 214.1472.

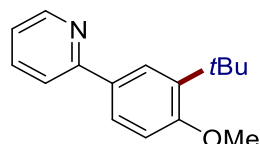


### 2-[3-(*tert*-butyl)phenyl]pyridine (103n)

The general procedure **C** was followed using substrate **13a** (77.5 mg, 0.50 mmol) and bromide **24B** (206 mg, 1.5 mmol). Purification by column chromatography (*n*hexane/EtOAc: 10/1) yielded **103n** (78.1mg, 74%) as a colorless oil. **<sup>1</sup>H NMR** (300 MHz, CDCl<sub>3</sub>)  $\delta$  = 8.78–8.70 (m, 1H), 8.07 (ddd, *J* = 1.6, 1.6, 0.6 Hz, 1H), 7.79 (ddd, *J* = 7.3, 1.6, 1.6 Hz, 1H), 7.76 (dd, *J* = 3.3, 1.4 Hz, 1H), 7.75 (d, *J* = 1.4 Hz, 1H), 7.53–7.47 (m, 1H), 7.45 (dd, *J* = 7.3, 0.6 Hz, 1H), 7.30–7.20 (m, 1H), 1.42 (s, 9H).

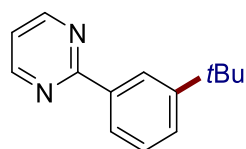


$^{13}\text{C}$  NMR (75 MHz,  $\text{CDCl}_3$ )  $\delta$  = 158.1 ( $\text{C}_q$ ), 151.6 ( $\text{C}_q$ ), 149.6 (CH), 139.2 ( $\text{C}_q$ ), 136.6 (CH), 128.4 (CH), 126.1 (CH), 124.2 (CH), 124.0 (CH), 121.9 (CH), 120.8 (CH), 34.9 ( $\text{C}_q$ ), 31.4 ( $\text{CH}_3$ ). IR (ATR): 2960, 2865, 1584, 1565, 1461, 1252, 774, 700, 614 $\text{cm}^{-1}$ . MS (EI)  $m/z$  (relative intensity) 212 (5)  $[\text{M}+\text{H}]^+$ , 211 (20)  $[\text{M}]^+$ , 196 (100). HR-MS (EI)  $m/z$  calcd for  $\text{C}_{15}\text{H}_{17}\text{N}$   $[\text{M}]^+$ : 211.1356, found: 211.1367. The spectral data are in accordance with those reported in the literature.<sup>[62c]</sup>



### 2-[3-(*tert*-Butyl)-4-methoxyphenyl]pyridine (103o)

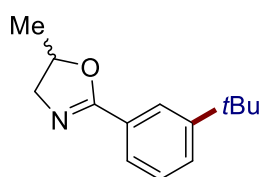
The general procedure **C** was followed using substrate **13b** (92.5 mg, 0.50 mmol) and bromide **24B** (206 mg, 1.5 mmol). Purification by column chromatography (*n*hexane/EtOAc: 10/1) yielded **103o** (97.7 mg, 81 %) as a colorless oil.  $^1\text{H}$  NMR (400 MHz,  $\text{CDCl}_3$ )  $\delta$  = 8.64 (ddd,  $J$  = 4.9, 1.6, 1.0 Hz, 1H), 7.95 (d,  $J$  = 2.4 Hz, 1H), 7.79 (dd,  $J$  = 8.5, 2.4 Hz, 1H), 7.71–7.61 (m, 2H), 7.14 (ddd,  $J$  = 7.0, 4.9, 1.6 Hz, 1H), 6.95 (d,  $J$  = 8.5 Hz, 1H), 3.88 (s, 3H), 1.43 (s, 9H).  $^{13}\text{C}$  NMR (101 MHz,  $\text{CDCl}_3$ )  $\delta$  = 159.4 ( $\text{C}_q$ ), 157.8 ( $\text{C}_q$ ), 149.5 (CH), 138.4 ( $\text{C}_q$ ), 136.5 (CH), 131.4 ( $\text{C}_q$ ), 125.7 (CH), 125.4 (CH), 121.1 (CH), 119.9 (CH), 111.6 (CH), 55.1 ( $\text{CH}_3$ ), 35.0 ( $\text{C}_q$ ), 29.7 ( $\text{CH}_3$ ). IR (ATR): 2954, 2864, 1586, 1463, 1235, 1092, 1027, 780, 742, 610  $\text{cm}^{-1}$ . MS (ESI)  $m/z$  (relative intensity) 242 (100)  $[\text{M}+\text{H}]^+$ , 165 (15), 151 (10), 119 (15). HR-MS (ESI)  $m/z$  calcd for  $\text{C}_{16}\text{H}_{20}\text{NO}$   $[\text{M}+\text{H}]^+$ : 242.1539, found: 242.1536. The spectral data are in accordance with those reported in the literature.<sup>[62c]</sup>



### 2-[3-(*tert*-Butyl)phenyl]pyrimidine (103p)

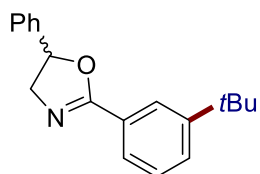
The general procedure **C** was followed using substrate **13k** (78.0 mg, 0.50 mmol) and bromide **24B** (206 mg, 1.5 mmol). Purification by column chromatography (*n*hexane/EtOAc: 9/1) yielded **103p** (89.1 mg, 84%) as a colorless solid. **M.p.**: 78–79 °C.  $^1\text{H}$  NMR (300 MHz,  $\text{CDCl}_3$ )  $\delta$  = 8.80 (d,  $J$  = 4.8 Hz, 2H), 8.53 (dd,  $J$  = 1.7, 1.7 Hz,

1H), 8.28 (dd,  $J = 7.7, 3.0, 3.0$  Hz, 1H), 7.55 (ddd,  $J = 7.7, 2.0, 1.3$  Hz, 1H), 7.44 (dd,  $J = 7.7, 7.7$  Hz, 1H), 7.15 (dd,  $J = 4.8, 4.8$  Hz, 1H), 1.42 (s, 9H).  $^{13}\text{C}$  NMR (75 MHz,  $\text{CDCl}_3$ )  $\delta = 165.1$  ( $\text{C}_q$ ), 157.2 (CH), 151.5 ( $\text{C}_q$ ), 137.3 ( $\text{C}_q$ ), 128.4 (CH), 127.9 (CH), 125.5 (CH), 125.1 (CH), 119.0 (CH), 34.9 ( $\text{C}_q$ ), 31.5 ( $\text{CH}_3$ ). IR (ATR): 3070, 2953, 1567, 1553, 1417, 1404, 1259, 781, 696, 623  $\text{cm}^{-1}$ . MS (ESI)  $m/z$  (relative intensity): 235 (3)  $[\text{M}+\text{Na}]^+$ , 213 (100)  $[\text{M}+\text{H}]^+$ . HR-MS (ESI):  $m/z$  calcd for  $\text{C}_{14}\text{H}_{17}\text{N}_2$   $[\text{M}+\text{H}]^+$ : 213.1386, found: 213.1389. The spectral data are in accordance with those reported in the literature.<sup>[62c]</sup>



### 2-[3-(*tert*-Butyl)phenyl]-5-methyl-4,5-dihydrooxazole (103q)

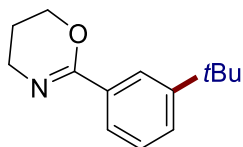
The general procedure **C** was followed using substrate **13l** (80.5 mg, 0.50 mmol) and bromide **24B** (206 mg, 1.5 mmol). Purification by column chromatography (*n*hexane/EtOAc: 10/1) yielded **103q** (69.0 mg, 63%) as a colorless oil.  $^1\text{H}$  NMR (400 MHz,  $\text{CDCl}_3$ )  $\delta = 7.97$  (ddd,  $J = 2.2, 1.6, 0.6$  Hz, 1H), 7.72 (ddd,  $J = 7.8, 1.6, 1.2$  Hz, 1H), 7.49 (ddd,  $J = 7.8, 2.2, 1.2$  Hz, 1H), 7.32 (ddd,  $J = 7.8, 7.8, 0.6$  Hz, 1H), 4.83 (ddq,  $J = 9.4, 7.4, 6.2$  Hz, 1H), 4.13 (dd,  $J = 14.4, 9.4$  Hz, 1H), 3.59 (dd,  $J = 14.4, 7.4$  Hz, 1H), 1.41 (d,  $J = 6.2$  Hz, 3H), 1.33 (s, 9H).  $^{13}\text{C}$  NMR (101 MHz,  $\text{CDCl}_3$ )  $\delta = 164.3$  ( $\text{C}_q$ ), 151.3 ( $\text{C}_q$ ), 128.3 (CH), 128.0 (CH), 127.7 ( $\text{C}_q$ ), 125.3 (CH), 125.0 (CH), 76.2 (CH), 61.6 ( $\text{CH}_2$ ), 34.8 ( $\text{C}_q$ ), 31.2 ( $\text{CH}_3$ ), 21.1 ( $\text{CH}_3$ ). IR (ATR): 2963, 2866, 1646, 1331, 1243, 1070, 903, 804, 699, 582  $\text{cm}^{-1}$ . MS (EI)  $m/z$  (relative intensity) 218 (5), 217 (30)  $[\text{M}]^+$ , 202 (100), 173 (50), 145 (40). HR-MS (EI)  $m/z$  calcd for  $\text{C}_{14}\text{H}_{19}\text{NO}$   $[\text{M}]^+$ : 17.1461, found: 217.1468.



### 2-[3-(*tert*-Butyl)phenyl]-5-phenyl-4,5-dihydrooxazole (103r)

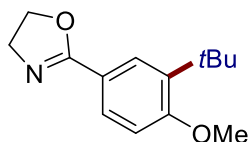
The general procedure **C** was followed using substrate **13m** (111.5 mg, 0.50 mmol)

and bromide **24B** (206 mg, 1.5 mmol). Purification by column chromatography (*n*hexane/EtOAc: 15/1) yielded **103r** (78.2 mg, 56%) as a pale yellow solid. **M.p.**: 94–96 °C. **<sup>1</sup>H NMR** (400 MHz, CDCl<sub>3</sub>)  $\delta$  = 8.07–8.06 (m, 1H), 7.81 (ddd, *J* = 7.8, 1.2, 1.2 Hz, 1H), 7.53 (ddd, *J* = 7.8, 2.1, 1.2 Hz, 1H), 7.40–7.37 (m, 1H), 7.36–7.34 (m, 3H), 7.34–7.29 (m, 2H), 5.65 (dd, *J* = 10.2, 8.0 Hz, 1H), 4.47 (dd, *J* = 14.7, 10.2 Hz, 1H), 3.98 (dd, *J* = 14.7, 8.0 Hz, 1H), 1.34 (s, 9H). **<sup>13</sup>C NMR** (101 MHz, CDCl<sub>3</sub>)  $\delta$  = 164.6 (C<sub>q</sub>), 151.5 (C<sub>q</sub>), 141.0 (C<sub>q</sub>), 128.8 (CH), 128.7 (CH), 128.3 (CH), 128.2 (CH), 127.2 (C<sub>q</sub>), 125.8 (CH), 125.6 (CH), 125.3 (CH), 81.1 (CH), 63.0 (CH<sub>2</sub>), 34.8 (C<sub>q</sub>), 31.3 (CH<sub>3</sub>). **IR** (ATR): 2962, 2869, 1649, 1334, 1242, 1067, 943, 805, 697, 541 cm<sup>-1</sup>. **MS** (ESI) *m/z* (relative intensity) 280 (100) [M+H]<sup>+</sup>, 201 (15), 139 (20), 117 (15). **HR-MS** (ESI) *m/z* calcd for C<sub>19</sub>H<sub>22</sub>NO [M+H]<sup>+</sup>: 280.1696, found: 280.1696.



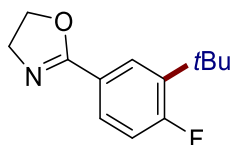
### 2-[3-(*tert*-Butyl)phenyl]-5,6-dihydro-4*H*-1,3-oxazine (**103s**)

The general procedure **C** was followed using substrate **13n** (80.5 mg, 0.50 mmol) and bromide **24B** (206 mg, 1.5 mmol). Purification by column chromatography (*n*hexane/EtOAc: 10/1) yielded **103s** (73.9 mg, 69%) as a colorless oil. **<sup>1</sup>H NMR** (300 MHz, CDCl<sub>3</sub>)  $\delta$  = 7.92 (ddd, *J* = 2.1, 1.7, 0.5 Hz, 1H), 7.68 (ddd, *J* = 7.8, 1.7, 1.2 Hz, 1H), 7.43 (ddd, *J* = 7.8, 2.1, 1.2 Hz, 1H), 7.27 (ddd, *J* = 7.8, 7.8, 0.5 Hz, 1H), 4.34 (tt, *J* = 5.5, 0.8 Hz, 2H), 3.60 (tt, *J* = 6.1, 0.8 Hz, 2H), 2.04–1.86 (m, 2H), 1.32 (s, 9H). **<sup>13</sup>C NMR** (126 MHz, CDCl<sub>3</sub>)  $\delta$  = 155.8 (C<sub>q</sub>), 150.7 (C<sub>q</sub>), 133.7 (C<sub>q</sub>), 127.6 (CH), 127.3 (CH), 124.0 (CH), 123.6 (CH), 65.1 (CH<sub>2</sub>), 42.7 (CH<sub>2</sub>), 34.8 (C<sub>q</sub>), 31.4 (CH<sub>3</sub>), 22.0 (CH<sub>2</sub>). **IR** (ATR): 2958, 2861, 1714, 1653, 1346, 1247, 1133, 804, 718, 530 cm<sup>-1</sup>. **MS** (EI) *m/z* (relative intensity) 217 (60) [M]<sup>+</sup>, 202 (100), 161 (65), 145 (60). **HR-MS** (EI) *m/z* calcd for C<sub>14</sub>H<sub>20</sub>NO [M+H]<sup>+</sup>: 218.1539, found: 218.1548.



### 2-[3-(*tert*-Butyl)-4-methoxyphenyl]-4,5-dihydrooxazole (**103t**)

The general procedure **C** was followed using substrate **13o** (88.5 mg, 0.50 mmol) and bromide **24B** (206 mg, 1.5 mmol). Purification by column chromatography (*n*hexane/EtOAc: 10/1) yielded **103t** (93.2 mg, 80%) as a pale yellow solid. **M.p.**: 100–102 °C. **<sup>1</sup>H NMR** (300 MHz, CDCl<sub>3</sub>)  $\delta$  = 7.87 (d, *J* = 2.2 Hz, 1H), 7.75 (dd, *J* = 8.5, 2.2 Hz, 1H), 6.85 (d, *J* = 8.5 Hz, 1H), 4.46–4.29 (m, 2H), 4.01 (td, *J* = 9.4, 0.8 Hz, 2H), 3.86 (s, 3H), 1.37 (s, 9H). **<sup>13</sup>C NMR** (126 MHz, CDCl<sub>3</sub>)  $\delta$  = 164.8 (C<sub>q</sub>), 160.9 (C<sub>q</sub>), 138.1 (C<sub>q</sub>), 127.5 (CH), 126.7 (CH), 119.5 (C<sub>q</sub>), 110.9 (CH), 67.4 (CH<sub>2</sub>), 55.1 (CH<sub>3</sub>), 54.9 (CH<sub>2</sub>), 35.0 (C<sub>q</sub>), 29.6 (CH<sub>3</sub>). **IR** (ATR): 2917, 2839, 1645, 1359, 1239, 1082, 830, 709, 634 cm<sup>-1</sup>. **MS** (ESI) *m/z* (relative intensity) 234 (5) [M+H]<sup>+</sup>, 233 (30) [M]<sup>+</sup>, 218 (100), 190 (20). **HR-MS** (ESI) *m/z* calcd for C<sub>14</sub>H<sub>19</sub>NO<sub>2</sub> [M]<sup>+</sup>: 233.1410, found: 233.1417.



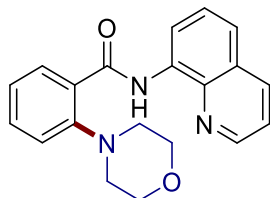
### 2-[3-(*tert*-Butyl)-4-fluorophenyl]-4,5-dihydrooxazole (**103u**)

The general procedure **C** was followed using substrate **13p** (82.5 mg, 0.50 mmol) and bromide **24B** (206 mg, 1.5 mmol). Purification by column chromatography (*n*hexane/EtOAc: 10/1) yielded **103u** (98.4 mg, 89%) as a pale yellow solid. **M.p.**: 65–66 °C. **<sup>1</sup>H NMR** (300 MHz, CDCl<sub>3</sub>)  $\delta$  = 7.90 (dd, *J* = 8.4, 2.2 Hz, 1H), 7.73 (ddd, *J* = 8.4, 4.6, 2.2 Hz, 1H), 6.99 (dd, *J* = 12.2, 8.4 Hz, 1H), 4.39 (td, *J* = 9.4, 0.8 Hz, 2H), 4.09–3.93 (m, 2H), 1.37 (d, *J* = 1.1 Hz, 9H). **<sup>13</sup>C NMR** (126 MHz, CDCl<sub>3</sub>)  $\delta$  = 164.0 (C<sub>q</sub>), 163.7 (d, <sup>1</sup>*J*<sub>C-F</sub> = 254.5 Hz, C<sub>q</sub>), 137.2 (d, <sup>2</sup>*J*<sub>C-F</sub> = 12.6 Hz, C<sub>q</sub>), 137.1 (C<sub>q</sub>), 127.7 (d, <sup>3</sup>*J*<sub>C-F</sub> = 10.1 Hz, CH), 127.5 (d, <sup>3</sup>*J*<sub>C-F</sub> = 7.6 Hz, CH), 123.4 (d, <sup>4</sup>*J*<sub>C-F</sub> = 3.8 Hz, C<sub>q</sub>), 116.3 (d, <sup>2</sup>*J*<sub>C-F</sub> = 25.2 Hz, CH), 67.6 (CH<sub>2</sub>), 55.0 (CH<sub>2</sub>), 34.4 (d, <sup>3</sup>*J*<sub>C-F</sub> = 2.5 Hz, C<sub>q</sub>), 29.8 (d, <sup>4</sup>*J*<sub>C-F</sub> = 2.5 Hz, CH<sub>3</sub>). **<sup>19</sup>F NMR** (282 MHz, CDCl<sub>3</sub>)  $\delta$  = -104.7 (s). **IR** (ATR): 2952, 2877, 1645, 1476, 1363, 1077, 948, 852, 707, 633 cm<sup>-1</sup>. **MS** (EI) *m/z* (relative intensity) 222 (10) [M+H]<sup>+</sup>, 221 (35) [M]<sup>+</sup>, 206 (100), 178 (40), 163.1 (30). **HR-MS** (EI) *m/z* calcd for

$C_{13}H_{16}FNO$   $[M]^+$ : 221.1210, found: 221.1213.

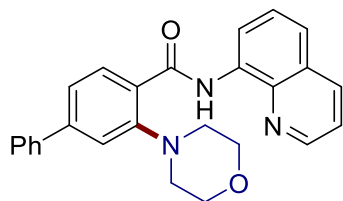
### 5.3.4 Nickela-Electrocatalyzed C–H Amination

#### 5.3.4.1 Characterization Data



#### 2-Morpholino-*N*-(quinolin-8-yl)benzamide (**58aa**)

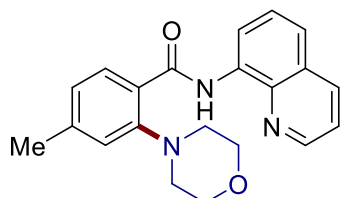
The general procedure **D** was followed using benzamide **35a** (62.0 mg, 0.25 mmol) and morpholine (**56a**) (43.5 mg, 0.50 mmol). Purification by column chromatography on silica gel (*n*hexane/EtOAc: 9/1→4/1) yielded **58aa** (64.2 mg, 77%) as a white solid. **M. p.**: 148–149 °C. **<sup>1</sup>H NMR** (400 MHz, CDCl<sub>3</sub>)  $\delta$  = 12.64 (s, 1H), 9.11 (dd,  $J$  = 7.6, 1.5 Hz, 1H), 8.85 (dd,  $J$  = 4.2, 1.7 Hz, 1H), 8.17 (dd,  $J$  = 8.3, 1.7 Hz, 2H), 7.60–7.56 (m, 1H), 7.54–7.50 (m, 1H), 7.49–7.43 (m, 2H), 7.25–7.21 (m, 2H), 4.03–3.88 (m, 4H), 3.27–2.95 (m, 4H). **<sup>13</sup>C NMR** (101 MHz, CDCl<sub>3</sub>)  $\delta$  = 165.7 (C<sub>q</sub>), 151.0 (C<sub>q</sub>), 148.0 (CH), 138.7 (C<sub>q</sub>), 136.4 (CH), 135.5 (C<sub>q</sub>), 132.3 (CH), 132.1 (CH), 128.9 (C<sub>q</sub>), 128.3 (C<sub>q</sub>), 127.6 (CH), 124.2 (CH), 121.7 (CH), 121.6 (CH), 119.2 (CH), 117.8 (CH), 66.1 (CH<sub>2</sub>), 53.9 (CH<sub>2</sub>). **IR** (ATR): 2958, 2829, 1656, 1515, 1112, 730, 696 cm<sup>-1</sup>. **MS** (ESI)  $m/z$  (relative intensity): 356 (25) [M+Na]<sup>+</sup>, 334 (100) [M+H]<sup>+</sup>. **HR-MS** (ESI)  $m/z$  calcd for C<sub>20</sub>H<sub>20</sub>N<sub>3</sub>O<sub>2</sub> [M+H]<sup>+</sup>: 334.1550, found: 334.1550. The analytical data correspond with those reported in the literature.<sup>[115]</sup>



#### 3-Morpholino-*N*-(quinolin-8-yl)-(1,1'-biphenyl)-4-carboxamide (**58ba**)

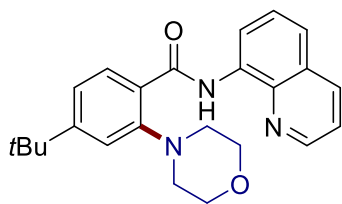
The general procedure **D** was followed using benzamide **35b** (81.0 mg, 0.25 mmol) and morpholine (**56a**) (43.5 mg, 0.50 mmol). Purification by column chromatography on silica gel (*n*hexane/EtOAc: 9/1→4/1) yielded **58ba** (81.8 mg, 80%) as a white solid. **M. p.**: 184–186 °C. **<sup>1</sup>H NMR** (300 MHz, CDCl<sub>3</sub>)  $\delta$  = 12.70 (s, 1H), 9.15 (dd,  $J$  = 7.6,

1.6 Hz, 1H), 8.89 (dd,  $J = 4.2, 1.7$  Hz, 1H), 8.27 (d,  $J = 8.0$  Hz, 1H), 8.21 (dd,  $J = 8.3, 1.7$  Hz, 1H), 7.65 (dd,  $J = 7.0, 2.1$  Hz, 2H), 7.61 (d,  $J = 7.6$  Hz, 1H), 7.56 (dd,  $J = 8.3, 1.6$  Hz, 1H), 7.51 (d,  $J = 4.2$  Hz, 1H), 7.50–7.45 (m, 4H), 7.44–7.38 (m, 1H), 4.02–3.99 (m, 4H), 3.25–3.22 (m, 4H).  $^{13}\text{C}$  NMR (125 MHz,  $\text{CDCl}_3$ )  $\delta = 165.3$  ( $\text{C}_q$ ), 151.3 ( $\text{C}_q$ ), 147.9 (CH), 145.2 ( $\text{C}_q$ ), 140.1 ( $\text{C}_q$ ), 138.7 ( $\text{C}_q$ ), 136.4 (CH), 135.5 ( $\text{C}_q$ ), 132.6 (CH), 128.8 (CH), 128.3 ( $\text{C}_q$ ), 128.0 (CH), 127.5 (CH), 127.5 ( $\text{C}_q$ ), 127.1 (CH), 122.9 (CH), 121.7 (CH), 121.5 (CH), 118.0 (CH), 117.8 (CH), 66.2 ( $\text{CH}_2$ ), 54.0 ( $\text{CH}_2$ ). IR (ATR): 2957, 2828, 1659, 1519, 1323, 1113, 760, 700  $\text{cm}^{-1}$ . MS (ESI)  $m/z$  (relative intensity): 432 (25)  $[\text{M}+\text{Na}]^+$ , 410 (100)  $[\text{M}+\text{H}]^+$ . HR-MS (ESI)  $m/z$  calcd for  $\text{C}_{26}\text{H}_{24}\text{N}_3\text{O}_2$   $[\text{M}+\text{H}]^+$ : 410.1863, found: 410.1868. The analytical data correspond with those reported in the literature.<sup>[115]</sup>



#### 4-Methyl-2-morpholino-*N*-(quinolin-8-yl)benzamide (**58ca**)

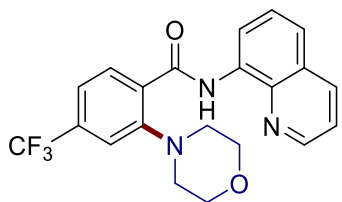
The general procedure **D** was followed using benzamide **35c** (65.5 mg, 0.25 mmol) and morpholine (**56a**) (43.5 mg, 0.50 mmol). Purification by column chromatography on silica gel (*n*hexane/EtOAc: 9/1→4/1→2/1) yielded **58ca** (52.1 mg, 60%) as a white solid. **M. p.**: 186–187 °C.  $^1\text{H}$  NMR (300 MHz,  $\text{CDCl}_3$ )  $\delta = 12.66$  (s, 1H), 9.11 (dd,  $J = 7.5, 1.6$  Hz, 1H), 8.85 (dd,  $J = 4.2, 1.7$  Hz, 1H), 8.16 (dd,  $J = 8.3, 1.7$  Hz, 1H), 8.12–8.01 (m, 1H), 7.62–7.54 (m, 1H), 7.51 (dd,  $J = 8.2, 1.6$  Hz, 1H), 7.46 (dd,  $J = 8.3, 4.2$  Hz, 1H), 7.07–7.02 (m, 2H), 4.02–3.86 (m, 4H), 3.23–3.03 (m, 4H), 2.40 (s, 3H).  $^{13}\text{C}$  NMR (125 MHz,  $\text{CDCl}_3$ )  $\delta = 165.6$  ( $\text{C}_q$ ), 151.0 ( $\text{C}_q$ ), 147.9 (CH), 142.8 ( $\text{C}_q$ ), 138.7 ( $\text{C}_q$ ), 136.3 (CH), 135.6 ( $\text{C}_q$ ), 132.1 (CH), 128.2 ( $\text{C}_q$ ), 127.5 (CH), 126.0 ( $\text{C}_q$ ), 125.0 (CH), 121.54 (CH), 121.50 (CH), 119.9 (CH), 117.7 (CH), 66.2 ( $\text{CH}_2$ ), 54.0 ( $\text{CH}_2$ ), 21.7 ( $\text{CH}_3$ ). IR (ATR): 2957, 2827, 1658, 1519, 1322, 1113, 826, 700  $\text{cm}^{-1}$ . MS (ESI)  $m/z$  (relative intensity): 370 (100)  $[\text{M}+\text{Na}]^+$ , 348 (60)  $[\text{M}+\text{H}]^+$ , 186 (10). HR-MS (ESI)  $m/z$  calcd for  $\text{C}_{21}\text{H}_{22}\text{N}_3\text{O}_2$   $[\text{M}+\text{H}]^+$ : 348.1707, found: 348.1709. The analytical data correspond with those reported in the literature.<sup>[115]</sup>



#### 4-(*tert*-Butyl)-2-morpholino-*N*-(quinolin-8-yl)benzamide (**58da**)

The general procedure **D** was followed using benzamide **35d** (76.0 mg, 0.25 mmol) and morpholine (**56a**) (43.5 mg, 0.50 mmol). Purification by column chromatography on silica gel (*n*hexane/EtOAc: 9/1→4/1) yielded **58da** (63.6 mg, 65%) as a white solid.

**M. p.:** 147–149 °C. **<sup>1</sup>H NMR** (400 MHz, CDCl<sub>3</sub>)  $\delta$  = 12.67 (s, 1H), 9.11 (dd,  $J$  = 7.6, 1.5 Hz, 1H), 8.85 (dd,  $J$  = 4.2, 1.7 Hz, 1H), 8.16 (dd,  $J$  = 8.3, 1.7 Hz, 1H), 8.12 (d,  $J$  = 8.8 Hz, 1H), 7.59–7.55 (m, 1H), 7.51 (dd,  $J$  = 8.3, 1.5 Hz, 1H), 7.46 (dd,  $J$  = 8.3, 4.2 Hz, 1H), 7.30–7.25 (m, 2H), 4.14–3.87 (m, 4H), 3.38–3.05 (m, 4H), 1.35 (s, 9H). **<sup>13</sup>C NMR** (101 MHz, CDCl<sub>3</sub>)  $\delta$  = 165.7 (C<sub>q</sub>), 156.0 (C<sub>q</sub>), 150.8 (C<sub>q</sub>), 148.0 (CH), 138.8 (C<sub>q</sub>), 136.4 (CH), 135.7 (C<sub>q</sub>), 131.9 (CH), 128.3 (C<sub>q</sub>), 127.6 (CH), 126.0 (C<sub>q</sub>), 121.6 (CH), 121.5 (CH), 121.5 (CH), 117.8 (CH), 116.2 (CH), 66.2 (CH<sub>2</sub>), 54.0 (CH<sub>2</sub>), 35.2 (C<sub>q</sub>), 31.2 (CH<sub>3</sub>). **IR** (ATR): 2959, 1661, 1519, 1323, 1114, 963, 826, 792, 606 cm<sup>-1</sup>. **MS** (ESI)  $m/z$  (relative intensity): 412 (75) [M+Na]<sup>+</sup>, 390 (100) [M+H]<sup>+</sup>. **HR-MS** (ESI)  $m/z$  calcd for C<sub>24</sub>H<sub>28</sub>N<sub>3</sub>O<sub>2</sub> [M+H]<sup>+</sup>: 390.2176, found: 390.2179. The analytical data correspond with those reported in the literature.<sup>[115]</sup>

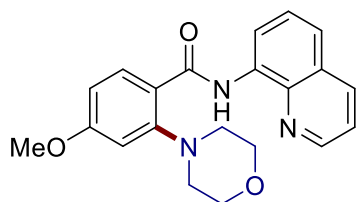


#### 2-Morpholino-*N*-(quinolin-8-yl)-4-(trifluoromethyl)benzamide (**58ea**)

The general procedure **D** was followed using benzamide **35e** (79.0 mg, 0.25 mmol) and morpholine (**56a**) (43.5 mg, 0.50 mmol). Purification by column chromatography on silica gel (*n*hexane/EtOAc: 9/1→4/1) yielded **58ea** (73.3 mg, 73%) as a white solid.

**M. p.:** 175–177 °C. **<sup>1</sup>H NMR** (500 MHz, CDCl<sub>3</sub>)  $\delta$  = 12.42 (s, 1H), 9.07 (dd,  $J$  = 7.4, 1.6 Hz, 1H), 8.84 (dd,  $J$  = 4.2, 1.7 Hz, 1H), 8.22 (dd,  $J$  = 8.1, 1.0 Hz, 1H), 8.18 (dd,  $J$  = 8.3, 1.7 Hz, 1H), 7.58 (dd,  $J$  = 8.2, 7.4 Hz, 1H), 7.55 (dd,  $J$  = 8.2, 1.6 Hz, 1H), 7.50–7.45 (m, 2H), 7.43 (d,  $J$  = 1.7 Hz, 1H), 3.96–3.89 (m, 4H), 3.21–3.13 (m, 4H). **<sup>13</sup>C NMR**

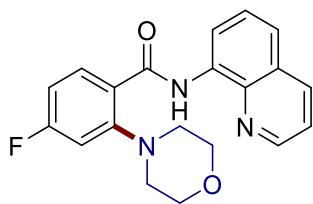
(125 MHz, CDCl<sub>3</sub>)  $\delta$  = 164.4 (C<sub>q</sub>), 151.2 (C<sub>q</sub>), 148.2 (CH), 138.5 (C<sub>q</sub>), 136.5 (CH), 134.9 (C<sub>q</sub>), 133.8 (q, <sup>2</sup>J<sub>C-F</sub> = 32.5 Hz, C<sub>q</sub>), 132.7 (CH), 131.9 (C<sub>q</sub>), 128.3 (C<sub>q</sub>), 127.5 (CH), 123.6 (q, <sup>1</sup>J<sub>C-F</sub> = 272.9 Hz, C<sub>q</sub>), 122.2 (CH), 121.7 (CH), 120.6 (q, <sup>3</sup>J<sub>C-F</sub> = 3.7 Hz, CH), 117.8 (CH), 115.9 (q, <sup>3</sup>J<sub>C-F</sub> = 3.6 Hz, CH), 65.9 (CH<sub>2</sub>), 53.6 (CH<sub>2</sub>). **<sup>19</sup>F NMR** (470 MHz, CDCl<sub>3</sub>)  $\delta$  = -62.9 (s). **IR** (ATR): 2960, 2833, 1666, 1522, 1310, 1114, 955, 736 cm<sup>-1</sup>. **MS** (ESI) *m/z* (relative intensity): 424 (100) [M+Na]<sup>+</sup>, 402 (30) [M+H]<sup>+</sup>, 382 (10). **HR-MS** (ESI) *m/z* calcd for C<sub>21</sub>H<sub>19</sub>F<sub>3</sub>N<sub>3</sub>O<sub>2</sub> [M+H]<sup>+</sup>: 402.1424, found: 402.1424. The analytical data correspond with those reported in the literature.<sup>[115]</sup>



#### 4-Methoxy-2-morpholino-*N*-(quinolin-8-yl)benzamide (**58fa**)

The general procedure **D** was followed using benzamide **35f** (69.5 mg, 0.25 mmol) and morpholine (**56a**) (43.5 mg, 0.50 mmol). Purification by column chromatography on silica gel (*n*hexane/EtOAc: 9/1→4/1) yielded **58fa** (57.0 mg, 63%) as a white solid. **M. p.**: 176–177 °C. **<sup>1</sup>H NMR** (400 MHz, CDCl<sub>3</sub>)  $\delta$  = 12.58 (s, 1H), 9.09 (dd, *J* = 7.6, 1.4 Hz, 1H), 8.85 (dd, *J* = 4.2, 1.7 Hz, 1H), 8.18 (d, *J* = 1.7 Hz, 1H), 8.16 (d, *J* = 1.6 Hz, 1H), 7.59–7.55 (m, 1H), 7.51 (dd, *J* = 8.2, 1.4 Hz, 1H), 7.46 (dd, *J* = 8.2, 4.2 Hz, 1H), 6.76–6.73 (m, 2H), 3.98–3.93 (m, 4H), 3.86 (s, 3H), 3.22–3.04 (m, 4H). **<sup>13</sup>C NMR** (101 MHz, CDCl<sub>3</sub>)  $\delta$  = 165.4 (C<sub>q</sub>), 162.8 (C<sub>q</sub>), 152.9 (C<sub>q</sub>), 147.9 (CH), 138.7 (C<sub>q</sub>), 136.5 (CH), 135.7 (C<sub>q</sub>), 134.0 (CH), 128.3 (C<sub>q</sub>), 127.6 (CH), 121.5 (CH), 121.5 (CH), 121.4 (C<sub>q</sub>), 117.8 (CH), 108.3 (CH), 106.1 (CH), 66.0 (CH<sub>2</sub>), 55.4 (CH<sub>2</sub>), 53.9 (CH<sub>3</sub>). **IR** (ATR): 2961, 2834, 1655, 1599, 1519, 1485, 1251, 1113, 825 cm<sup>-1</sup>. **MS** (ESI) *m/z* (relative intensity): 386 (100) [M+Na]<sup>+</sup>, 364 (80) [M+H]<sup>+</sup>, 220 (10). **HR-MS** (ESI) *m/z* calcd for C<sub>21</sub>H<sub>22</sub>N<sub>3</sub>O<sub>3</sub> [M+H]<sup>+</sup>: 364.1656, found: 364.1658. The analytical data correspond with those reported in the literature.<sup>[115]</sup>

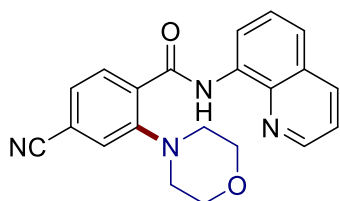




#### 4-Fluoro-2-morpholino-*N*-(quinolin-8-yl)benzamide (**58ga**)

The general procedure **D** was followed using benzamide **35g** (66.5 mg, 0.25 mmol) and morpholine (**56a**) (43.5 mg, 0.50 mmol). Purification by column chromatography on silica gel (*n*hexane/EtOAc: 9/1→4/1) yielded **58ga** (49.5 mg, 56%) as a white solid.

**M. p.:** 182–183 °C. **<sup>1</sup>H NMR** (400 MHz, CDCl<sub>3</sub>)  $\delta$  = 12.43 (s, 1H), 9.07 (dd,  $J$  = 7.5, 1.5 Hz, 1H), 8.85 (dd,  $J$  = 4.2, 1.7 Hz, 1H), 8.18 (dd,  $J$  = 8.3, 1.7 Hz, 1H), 8.17–8.12 (m, 1H), 7.61–7.56 (m, 1H), 7.53 (dd,  $J$  = 8.3, 1.5 Hz, 1H), 7.47 (dd,  $J$  = 8.3, 4.2 Hz, 1H), 6.97–6.87 (m, 2H), 4.00–3.80 (m, 4H), 3.19–2.96 (m, 4H). **<sup>13</sup>C NMR** (101 MHz, CDCl<sub>3</sub>)  $\delta$  = 165.1 (d,  $^1J_{C-F}$  = 256.0 Hz, C<sub>q</sub>), 164.8 (C<sub>q</sub>), 153.2 (d,  $^3J_{C-F}$  = 8.1 Hz, C<sub>q</sub>), 148.0 (CH), 138.6 (C<sub>q</sub>), 136.6 (CH), 135.3 (C<sub>q</sub>), 134.3 (d,  $^3J_{C-F}$  = 10.1 Hz, CH), 128.3 (C<sub>q</sub>), 127.6 (CH), 125.0 (d,  $^4J_{C-F}$  = 4.0 Hz, C<sub>q</sub>), 121.9 (CH), 121.6 (CH), 117.9 (CH), 110.9 (d,  $^2J_{C-F}$  = 21.2 Hz, CH), 106.6 (d,  $^2J_{C-F}$  = 23.2 Hz, CH), 66.0 (CH<sub>2</sub>), 53.7 (CH<sub>2</sub>). **<sup>19</sup>F NMR** (282 MHz, CDCl<sub>3</sub>)  $\delta$  = -106.5 (ddd,  $J$  = 10.5, 10.3, 7.3 Hz). **IR** (ATR): 2960, 2833, 1661, 1520, 1485, 1114, 987, 826, 607 cm<sup>-1</sup>. **MS** (ESI)  $m/z$  (relative intensity): 374 (100) [M+Na]<sup>+</sup>, 352 (40) [M+H]<sup>+</sup>. **HR-MS** (ESI)  $m/z$  calcd for C<sub>20</sub>H<sub>19</sub>FN<sub>3</sub>O<sub>2</sub> [M+H]<sup>+</sup>: 352.1456, found: 352.1456. The analytical data correspond with those reported in the literature.<sup>[115]</sup>

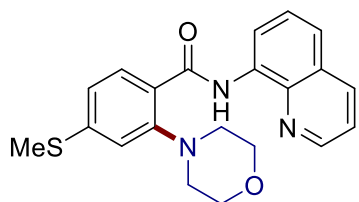


#### 4-Cyano-2-morpholino-*N*-(quinolin-8-yl)benzamide (**58ha**)

The general procedure **D** was followed using benzamide **35h** (68.3 mg, 0.25 mmol) and morpholine (**56a**) (43.5 mg, 0.50 mmol). Purification by column chromatography on silica gel (*n*hexane/EtOAc: 4/1→2/1) yielded **58ha** (54.7 mg, 61%) as a white solid.

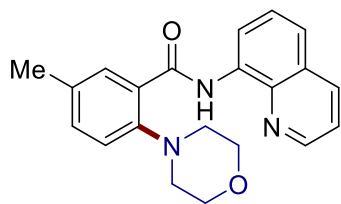
**M. p.:** 175–176 °C. **<sup>1</sup>H NMR** (400 MHz, CDCl<sub>3</sub>)  $\delta$  = 12.34 (s, 1H), 9.04 (dd,  $J$  = 6.6, 2.4 Hz, 1H), 8.85 (dd,  $J$  = 4.2, 1.7 Hz, 1H), 8.23–8.15 (m, 2H), 7.63–7.55 (m, 2H),

7.52–7.47 (m, 2H), 7.45 (d,  $J = 1.7$  Hz, 1H), 3.97–3.86 (m, 4H), 3.21–3.07 (m, 4H).  $^{13}\text{C}$  NMR (101 MHz,  $\text{CDCl}_3$ )  $\delta = 163.9$  ( $\text{C}_q$ ), 151.2 ( $\text{C}_q$ ), 148.3 (CH), 138.5 ( $\text{C}_q$ ), 136.6 (CH), 134.7 ( $\text{C}_q$ ), 133.0 ( $\text{C}_q$ ), 132.9 (CH), 128.3 ( $\text{C}_q$ ), 127.5 (CH), 127.3 (CH), 122.7 (CH), 122.4 (CH), 121.8 (CH), 118.1 ( $\text{C}_q$ ), 117.9 (CH), 115.5 ( $\text{C}_q$ ), 65.8 ( $\text{CH}_2$ ), 53.5 ( $\text{CH}_2$ ). IR (ATR): 2921, 2852, 2231, 1663, 1522, 1324, 1113, 827  $\text{cm}^{-1}$ . MS (ESI)  $m/z$  (relative intensity): 381 (95)  $[\text{M}+\text{Na}]^+$ , 359 (100)  $[\text{M}+\text{H}]^+$ . HR-MS (ESI)  $m/z$  calcd for  $\text{C}_{21}\text{H}_{19}\text{N}_4\text{O}_2$   $[\text{M}+\text{H}]^+$ : 359.1503, found: 359.1501. The analytical data correspond with those reported in the literature.<sup>[184]</sup>



#### 4-(Methylthio)-2-morpholino-*N*-(quinolin-8-yl)benzamide (**58ia**)

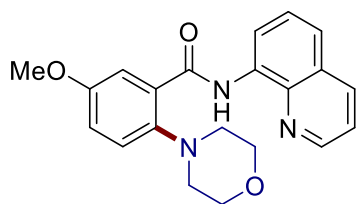
The general procedure **D** was followed using benzamide **35i** (73.5 mg, 0.25 mmol) and morpholine (**56a**) (43.5 mg, 0.50 mmol). Purification by column chromatography on silica gel (*n*hexane/EtOAc: 9/1→4/1) yielded **58ia** (67.8 mg, 72%) as a white solid. **M. p.**: 146–148 °C.  $^1\text{H}$  NMR (400 MHz,  $\text{CDCl}_3$ )  $\delta = 12.56$  (s, 1H), 9.08 (dd,  $J = 7.6$ , 1.5 Hz, 1H), 8.85 (dd,  $J = 4.2$ , 1.7 Hz, 1H), 8.17 (dd,  $J = 8.3$ , 1.7 Hz, 1H), 8.11 (d,  $J = 8.1$  Hz, 1H), 7.59–7.55 (m, 1H), 7.51 (dd,  $J = 8.2$ , 1.5 Hz, 1H), 7.46 (dd,  $J = 8.3$ , 4.2 Hz, 1H), 7.10–7.03 (m, 2H), 4.01–3.87 (m, 4H), 3.19–3.05 (m, 4H), 2.52 (s, 3H).  $^{13}\text{C}$  NMR (125 MHz,  $\text{CDCl}_3$ )  $\delta = 165.1$  ( $\text{C}_q$ ), 151.1 ( $\text{C}_q$ ), 147.9 (CH), 144.1 ( $\text{C}_q$ ), 138.6 ( $\text{C}_q$ ), 136.4 (CH), 135.4 ( $\text{C}_q$ ), 132.5 (CH), 128.2 ( $\text{C}_q$ ), 127.5 (CH), 125.1 ( $\text{C}_q$ ), 121.6 (CH), 121.5 (CH), 120.7 (CH), 117.8 (CH), 116.6 (CH), 66.0 ( $\text{CH}_2$ ), 53.9 ( $\text{CH}_2$ ), 15.1 ( $\text{CH}_3$ ). IR (ATR): 2957, 2829, 1657, 1520, 1322, 1113, 951, 825  $\text{cm}^{-1}$ . MS (ESI)  $m/z$  (relative intensity): 402 (40)  $[\text{M}+\text{Na}]^+$ , 380 (100)  $[\text{M}+\text{H}]^+$ , 334 (5), 236 (5), 186 (5). HR-MS (ESI)  $m/z$  calcd for  $\text{C}_{21}\text{H}_{22}\text{N}_3\text{O}_2\text{S}$   $[\text{M}+\text{H}]^+$ : 380.1427, found: 380.1433.



### 5-Methyl-2-morpholino-*N*-(quinolin-8-yl)benzamide (**58ka**)

The general procedure **D** was followed using benzamide **35k** (65.5 mg, 0.25 mmol) and morpholine (**56a**) (43.5 mg, 0.50 mmol). Purification by column chromatography on silica gel (*n*hexane/EtOAc: 9/1→4/1) yielded **58ka** (63.2 mg, 73%) as a white solid.

**M. p.:** 153–155 °C. **<sup>1</sup>H NMR** (500 MHz, CDCl<sub>3</sub>)  $\delta$  = 12.77 (s, 1H), 9.11 (dd,  $J$  = 7.7, 1.4 Hz, 1H), 8.85 (dd,  $J$  = 4.2, 1.7 Hz, 1H), 8.16 (dd,  $J$  = 8.3, 1.7 Hz, 1H), 8.01 (d,  $J$  = 2.3 Hz, 1H), 7.59–7.56 (m, 1H), 7.51 (dd,  $J$  = 8.2, 1.4 Hz, 1H), 7.45 (dd,  $J$  = 8.3, 4.2 Hz, 1H), 7.28 (ddd,  $J$  = 8.2, 2.3, 0.8 Hz, 1H), 7.14 (d,  $J$  = 8.1 Hz, 1H), 4.06–3.87 (m, 4H), 3.15–2.97 (m, 4H), 2.36 (s, 3H). **<sup>13</sup>C NMR** (125 MHz, CDCl<sub>3</sub>)  $\delta$  = 165.7 (C<sub>q</sub>), 148.7 (C<sub>q</sub>), 148.0 (CH), 138.8 (C<sub>q</sub>), 136.4 (CH), 135.6 (C<sub>q</sub>), 134.0 (C<sub>q</sub>), 132.8 (CH), 132.5 (CH), 128.4 (C<sub>q</sub>), 128.3 (C<sub>q</sub>), 127.5 (CH), 121.7 (CH), 121.5 (CH), 119.3 (CH), 117.8 (CH), 66.1 (CH<sub>2</sub>), 54.0 (CH<sub>2</sub>), 20.6 (CH<sub>3</sub>). **IR** (ATR): 2956, 2921, 1660, 1518, 1323, 1113, 824 cm<sup>-1</sup>. **MS** (ESI)  $m/z$  (relative intensity): 370 (100) [M+Na]<sup>+</sup>, 348 (80) [M+H]<sup>+</sup>. **HR-MS** (ESI)  $m/z$  calcd for C<sub>21</sub>H<sub>22</sub>N<sub>3</sub>O<sub>2</sub> [M+H]<sup>+</sup>: 348.1707, found: 348.1706. The analytical data correspond with those reported in the literature.<sup>[115]</sup>

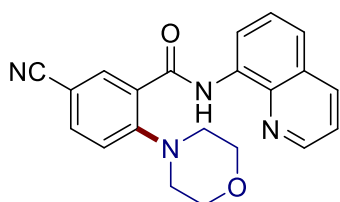


### 5-Methoxy-2-morpholino-*N*-(quinolin-8-yl)benzamide (**58la**)

The general procedure **D** was followed using benzamide **35I** (69.5 mg, 0.25 mmol) and morpholine (**56a**) (43.5 mg, 0.50 mmol). Purification by column chromatography on silica gel (*n*hexane/EtOAc: 9/1→4/1) yielded **58la** (54.8 mg, 60%) as a white solid.

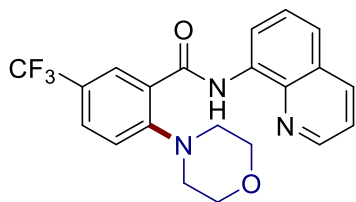
**M. p.:** 154–156 °C. **<sup>1</sup>H NMR** (400 MHz, CDCl<sub>3</sub>)  $\delta$  = 13.07 (s, 1H), 9.12 (dd,  $J$  = 7.5, 1.6 Hz, 1H), 8.87 (dd,  $J$  = 4.2, 1.7 Hz, 1H), 8.17 (dd,  $J$  = 8.3, 1.7 Hz, 1H), 7.81 (d,  $J$  = 3.2 Hz, 1H), 7.61–7.55 (m, 1H), 7.53 (dd,  $J$  = 8.3, 1.6 Hz, 1H), 7.46 (dd,  $J$  = 8.3, 4.2 Hz, 1H), 7.24 (d,  $J$  = 8.8 Hz, 1H), 7.04 (dd,  $J$  = 8.8, 3.2 Hz, 1H), 4.07–3.92 (m, 4H), 3.85

(s, 3H), 3.12–3.00 (m, 4H).  $^{13}\text{C}$  NMR (125 MHz,  $\text{CDCl}_3$ )  $\delta$  = 165.0 ( $\text{C}_q$ ), 156.4 ( $\text{C}_q$ ), 147.9 (CH), 144.4 ( $\text{C}_q$ ), 138.9 ( $\text{C}_q$ ), 136.3 (CH), 135.7 ( $\text{C}_q$ ), 129.8 ( $\text{C}_q$ ), 128.2 ( $\text{C}_q$ ), 127.4 (CH), 121.8 (CH), 121.5 (CH), 121.3 (CH), 118.9 (CH), 118.1 (CH), 115.6 (CH), 66.2 ( $\text{CH}_2$ ), 55.7 ( $\text{CH}_3$ ), 54.3 ( $\text{CH}_2$ ). IR (ATR): 2956, 2834, 1659, 1520, 1488, 1282, 1113, 825  $\text{cm}^{-1}$ . MS (ESI)  $m/z$  (relative intensity): 386 (100)  $[\text{M}+\text{Na}]^+$ , 364 (95)  $[\text{M}+\text{H}]^+$ , 345 (5). HR-MS (ESI)  $m/z$  calcd for  $\text{C}_{21}\text{H}_{22}\text{N}_3\text{O}_3$   $[\text{M}+\text{H}]^+$ : 364.1656, found: 364.1660. The analytical data correspond with those reported in the literature.<sup>[115]</sup>



#### 5-Cyano-2-morpholino-*N*-(quinolin-8-yl)benzamide (58ma)

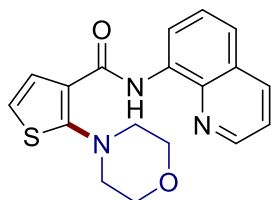
The general procedure **D** was followed using benzamide **35m** (68.3 mg, 0.25 mmol) and morpholine (**56a**) (43.5 mg, 0.50 mmol). Purification by column chromatography on silica gel (*n*hexane/EtOAc: 9/1→4/1) yielded **58ma** (49.8 mg, 56%) as a white solid. **M. p.**: 170–171 °C.  $^1\text{H}$  NMR (300 MHz,  $\text{CDCl}_3$ )  $\delta$  = 12.05 (s, 1H), 9.04 (dd,  $J$  = 6.6, 2.5 Hz, 1H), 8.86 (dd,  $J$  = 4.2, 1.7 Hz, 1H), 8.35 (d,  $J$  = 2.2 Hz, 1H), 8.23 (dd,  $J$  = 8.3, 1.7 Hz, 1H), 7.74 (dd,  $J$  = 8.5, 2.2 Hz, 1H), 7.67–7.56 (m, 2H), 7.52 (dd,  $J$  = 8.3, 4.2 Hz, 1H), 7.25–7.23 (m, 1H), 3.92–3.89 (m, 4H), 3.30–3.07 (m, 4H).  $^{13}\text{C}$  NMR (125 MHz,  $\text{CDCl}_3$ )  $\delta$  = 163.8 ( $\text{C}_q$ ), 154.0 ( $\text{C}_q$ ), 148.1 (CH), 138.2 ( $\text{C}_q$ ), 136.7 (CH), 136.1 (CH), 135.5 (CH), 134.5 ( $\text{C}_q$ ), 129.4 ( $\text{C}_q$ ), 128.2 ( $\text{C}_q$ ), 127.6 (CH), 122.3 (CH), 121.7 (CH), 119.3 (CH), 118.3 ( $\text{C}_q$ ), 117.8 (CH), 106.9 ( $\text{C}_q$ ), 65.8 ( $\text{CH}_2$ ), 53.2 ( $\text{CH}_2$ ). IR (ATR): 2964, 2227, 1664, 1523, 1486, 1113, 914, 827, 582  $\text{cm}^{-1}$ . MS (ESI)  $m/z$  (relative intensity): 381 (50)  $[\text{M}+\text{Na}]^+$ , 359 (100)  $[\text{M}+\text{H}]^+$ . HR-MS (ESI)  $m/z$  calcd for  $\text{C}_{21}\text{H}_{19}\text{N}_4\text{O}_2$   $[\text{M}+\text{H}]^+$ : 359.1503, found: 359.1507.



#### 2-Morpholino-*N*-(quinolin-8-yl)-5-(trifluoromethyl)benzamide (58na)

The general procedure **D** was followed using benzamide **35n** (79.0 mg, 0.25 mmol)

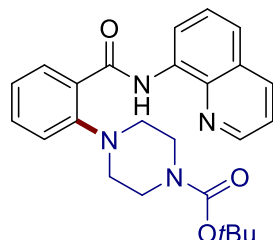
and morpholine (**56a**) (43.5 mg, 0.50 mmol). Purification by column chromatography on silica gel (*n*hexane/EtOAc: 9/1→4/1) yielded **58na** (75.4 mg, 75%) as a white solid. **M. p.**: 172–173 °C. **<sup>1</sup>H NMR** (400 MHz, CDCl<sub>3</sub>)  $\delta$  = 12.33 (s, 1H), 9.07 (dd,  $J$  = 7.3, 1.7 Hz, 1H), 8.84 (dd,  $J$  = 4.2, 1.7 Hz, 1H), 8.39 (dd,  $J$  = 2.4, 0.8 Hz, 1H), 8.18 (dd,  $J$  = 8.3, 1.7 Hz, 1H), 7.71 (ddd,  $J$  = 8.5, 2.4, 0.8 Hz, 1H), 7.59 (dd,  $J$  = 8.2, 7.3 Hz, 1H), 7.55 (dd,  $J$  = 8.2, 1.7 Hz, 1H), 7.48 (dd,  $J$  = 8.3, 4.2 Hz, 1H), 7.28 (dd,  $J$  = 8.5, 0.8 Hz, 1H), 3.99–3.82 (m, 4H), 3.27–3.10 (m, 4H). **<sup>13</sup>C NMR** (101 MHz, CDCl<sub>3</sub>)  $\delta$  = 164.4 (C<sub>q</sub>), 153.6 (C<sub>q</sub>), 148.2 (CH), 138.6 (C<sub>q</sub>), 136.5 (CH), 134.9 (C<sub>q</sub>), 129.5 (q,  $^3J_{C-F}$  = 3.8 Hz, CH), 129.1 (C<sub>q</sub>), 128.9 (q,  $^3J_{C-F}$  = 3.7 Hz, CH), 128.3 (C<sub>q</sub>), 127.6 (CH), 126.0 (q,  $^2J_{C-F}$  = 33.2 Hz, C<sub>q</sub>), 123.9 (q,  $^1J_{C-F}$  = 271.7 Hz, C<sub>q</sub>), 122.1 (CH), 121.7 (CH), 119.2 (CH), 117.7 (CH), 65.9 (CH<sub>2</sub>), 53.5 (CH<sub>2</sub>). **<sup>19</sup>F NMR** (282 MHz, CDCl<sub>3</sub>)  $\delta$  = –62.2 (s). **IR** (ATR): 2960, 2922, 1664, 1524, 1326, 1257, 1114, 826, 792 cm<sup>-1</sup>. **MS** (ESI)  $m/z$  (relative intensity): 424 (100) [M+Na]<sup>+</sup>, 402 (25) [M+H]<sup>+</sup>. **HR-MS** (ESI)  $m/z$  calcd for C<sub>21</sub>H<sub>19</sub>F<sub>3</sub>N<sub>3</sub>O<sub>2</sub> [M+H]<sup>+</sup>: 402.1424, found: 402.1420. The analytical data correspond with those reported in the literature.<sup>[183c]</sup>



### 2-Morpholino-*N*-(quinolin-8-yl)thiophene-3-carboxamide (**58pa**)

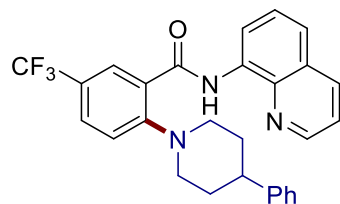
The general procedure **D** was followed using benzamide **35p** (63.5 mg, 0.25 mmol) and morpholine (**56a**) (43.5 mg, 0.50 mmol). Purification by column chromatography on silica gel (*n*hexane/EtOAc: 9/1→2/1) yielded **58pa** (68.0 mg, 80%) as a white solid. **M. p.**: 158–159 °C. **<sup>1</sup>H NMR** (600 MHz, CDCl<sub>3</sub>)  $\delta$  = 12.31 (s, 1H), 9.05 (dd,  $J$  = 7.7, 1.4 Hz, 1H), 8.89 (dd,  $J$  = 4.2, 1.7 Hz, 1H), 8.18 (dd,  $J$  = 8.2, 1.7 Hz, 1H), 7.58–7.55 (m, 1H), 7.57 (d,  $J$  = 5.8 Hz, 1H), 7.51 (dd,  $J$  = 8.2, 1.4 Hz, 1H), 7.48 (dd,  $J$  = 8.2, 4.2 Hz, 1H), 6.99 (d,  $J$  = 5.8 Hz, 1H), 4.21–4.00 (m, 4H), 3.26–3.08 (m, 4H). **<sup>13</sup>C NMR** (125 MHz, CDCl<sub>3</sub>)  $\delta$  = 161.0 (C<sub>q</sub>), 160.0 (C<sub>q</sub>), 147.8 (CH), 138.7 (C<sub>q</sub>), 136.4 (CH), 135.6 (C<sub>q</sub>), 128.1 (C<sub>q</sub>), 128.0 (CH), 127.5 (CH), 127.4 (C<sub>q</sub>), 121.5 (CH), 121.4 (CH), 118.5 (CH), 117.8 (CH), 66.3 (CH<sub>2</sub>), 56.4 (CH<sub>2</sub>). **IR** (ATR): 2921, 1659, 1522, 1488, 1324,

1262, 1113, 792, 700  $\text{cm}^{-1}$ . **MS** (ESI)  $m/z$  (relative intensity): 362 (100)  $[\text{M}+\text{Na}]^+$ , 340 (40)  $[\text{M}+\text{H}]^+$ , 340 (5). **HR-MS** (ESI)  $m/z$  calcd for  $\text{C}_{18}\text{H}_{18}\text{N}_3\text{O}_2\text{S}$   $[\text{M}+\text{H}]^+$ : 340.1114, found: 340.1114. The analytical data correspond with those reported in the literature.<sup>[165c]</sup>



**tert-Butyl 4-[2-(quinolin-8-ylcarbamoyl)phenyl]piperazine-1-carboxylate (58ab)**

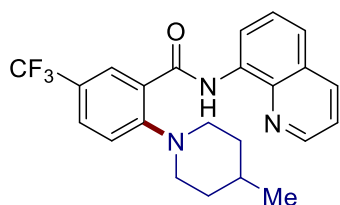
The general procedure **D** was followed using benzamide **35a** (62.0 mg, 0.25 mmol) and *tert*-butyl piperazine-1-carboxylate (**56b**) (93.1 mg, 0.50 mmol). Purification by column chromatography on silica gel (*n*hexane/EtOAc: 9/1→4/1) yielded **58ab** (81.0 mg, 75%) as a white solid. **M. p.**: 193–194 °C. **<sup>1</sup>H NMR** (400 MHz,  $\text{CDCl}_3$ )  $\delta$  = 12.67 (s, 1H), 9.10 (dd,  $J$  = 7.6, 1.5 Hz, 1H), 8.79 (dd,  $J$  = 4.2, 1.7 Hz, 1H), 8.20–8.17 (m, 2H), 7.61–7.57 (m, 1H), 7.53 (dd,  $J$  = 8.3, 1.5 Hz, 1H), 7.50–7.46 (m, 1H), 7.46–7.43 (m, 1H), 7.29–7.21 (m, 1H), 7.21 (dd,  $J$  = 8.3, 1.1 Hz, 1H), 3.70 (s, 4H), 3.09 (s, 4H), 1.41 (s, 9H). **<sup>13</sup>C NMR** (101 MHz,  $\text{CDCl}_3$ )  $\delta$  = 165.6 ( $\text{C}_q$ ), 154.8 ( $\text{C}_q$ ), 151.0 ( $\text{C}_q$ ), 147.8 (CH), 138.6 ( $\text{C}_q$ ), 136.7 (CH), 135.4 ( $\text{C}_q$ ), 132.3 (CH), 132.1 (CH), 128.9 ( $\text{C}_q$ ), 128.4 ( $\text{C}_q$ ), 127.7 (CH), 124.5 (CH), 121.8 (CH), 121.6 (CH), 119.5 (CH), 118.1 (CH), 79.8 ( $\text{C}_q$ ), 53.9 ( $\text{CH}_2$ ), 53.3 ( $\text{CH}_2$ ), 43.5 ( $\text{CH}_2$ ), 42.7 ( $\text{CH}_2$ ), 28.4 ( $\text{CH}_3$ ). **IR** (ATR): 2974, 2826, 1682, 1659, 1520, 1419, 1125, 792, 754  $\text{cm}^{-1}$ . **MS** (ESI)  $m/z$  (relative intensity): 455 (100)  $[\text{M}+\text{Na}]^+$ , 433 (30)  $[\text{M}+\text{H}]^+$ , 356 (10), 309 (10), 293 (35). **HR-MS** (ESI)  $m/z$  calcd for  $\text{C}_{25}\text{H}_{29}\text{N}_4\text{O}_3$   $[\text{M}+\text{H}]^+$ : 433.2234, found: 433.2223. The analytical data correspond with those reported in the literature.<sup>[115]</sup>



**2-(4-Phenylpiperidin-1-yl)-N-(quinolin-8-yl)-5-(trifluoromethyl)benzamide (58nd)**

The general procedure **E** was followed using benzamide **35n** (79.0 mg, 0.25 mmol)

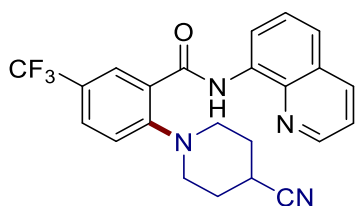
and 4-phenylpiperidine (**56d**) (201 mg, 1.25 mmol). Purification by column chromatography on silica gel (*n*hexane/EtOAc: 16/1→9/1) yielded **58nd** (73.0 mg, 61%) as a white solid. **M. p.**: 143–144 °C. **<sup>1</sup>H NMR** (400 MHz, CDCl<sub>3</sub>)  $\delta$  = 12.36 (s, 1H), 9.12 (dd, *J* = 7.4, 1.6 Hz, 1H), 8.83 (dd, *J* = 4.2, 1.7 Hz, 1H), 8.38 (dd, *J* = 2.4, 0.8 Hz, 1H), 8.22 (dd, *J* = 8.3, 1.7 Hz, 1H), 7.70 (ddd, *J* = 8.5, 2.4, 0.8 Hz, 1H), 7.64–7.59 (m, 1H), 7.57 (dd, *J* = 8.3, 1.6 Hz, 1H), 7.47 (dd, *J* = 8.3, 4.2 Hz, 1H), 7.31 (d, *J* = 8.5 Hz, 1H), 7.13–7.07 (m, 3H), 6.86–6.70 (m, 2H), 3.71–3.49 (m, 2H), 3.00–2.94 (m, 2H), 2.63–2.55 (m, 1H), 2.16–2.05 (m, 2H), 1.86–1.75 (m, 2H). **<sup>13</sup>C NMR** (101 MHz, CDCl<sub>3</sub>)  $\delta$  = 164.9 (C<sub>q</sub>), 154.6 (C<sub>q</sub>), 148.4 (CH), 145.4 (C<sub>q</sub>), 138.7 (C<sub>q</sub>), 136.6 (CH), 135.1 (C<sub>q</sub>), 129.2 (q, <sup>3</sup>*J*<sub>C-F</sub> = 3.8 Hz, CH), 129.1 (C<sub>q</sub>), 128.7 (q, <sup>3</sup>*J*<sub>C-F</sub> = 3.5 Hz, CH), 128.3 (C<sub>q</sub>), 128.2 (CH), 127.7 (CH), 126.6 (CH), 126.2 (CH), 125.2 (q, <sup>2</sup>*J*<sub>C-F</sub> = 33.2 Hz, C<sub>q</sub>), 124.1 (q, <sup>1</sup>*J*<sub>C-F</sub> = 272.7 Hz, C<sub>q</sub>), 122.0 (CH), 121.4 (CH), 119.2 (CH), 117.7 (CH), 54.6 (CH<sub>2</sub>), 42.0 (CH), 32.6 (CH<sub>2</sub>). **<sup>19</sup>F NMR** (376 MHz, CDCl<sub>3</sub>)  $\delta$  = –62.0 (s). **IR** (ATR): 2945, 2820, 1664, 1524, 1326, 1268, 1119, 825, 699 cm<sup>-1</sup>. **MS** (ESI) *m/z* (relative intensity): 498 (50) [M+Na]<sup>+</sup>, 476 (100) [M+H]<sup>+</sup>, 315 (20). **HR-MS** (ESI) *m/z* calcd for C<sub>28</sub>H<sub>25</sub>F<sub>3</sub>N<sub>3</sub>O [M+H]<sup>+</sup>: 476.1944, found: 476.1949.



### 2-(4-Methylpiperidin-1-yl)-N-(quinolin-8-yl)-5-(trifluoromethyl)benzamide (**58ne**)

The general procedure **E** was followed using benzamide **35n** (79.0 mg, 0.25 mmol) and 4-methylpiperidine (**56e**) (124 mg, 1.25 mmol). Purification by column chromatography on silica gel (*n*hexane/EtOAc: 16/1→9/1) yielded **58ne** (46.0 mg, 45%) as a white solid. **M. p.**: 174–175 °C. **<sup>1</sup>H NMR** (300 MHz, CDCl<sub>3</sub>)  $\delta$  = 12.41 (s, 1H), 9.12 (dd, *J* = 7.4, 1.7 Hz, 1H), 8.86 (dd, *J* = 4.2, 1.7 Hz, 1H), 8.39 (d, *J* = 2.3 Hz, 1H), 8.19 (dd, *J* = 8.3, 1.7 Hz, 1H), 7.68 (dd, *J* = 8.5, 2.3 Hz, 1H), 7.64–7.59 (m, 1H), 7.56 (dd, *J* = 8.3, 1.7 Hz, 1H), 7.48 (dd, *J* = 8.3, 4.2 Hz, 1H), 7.34–7.24 (m, 1H), 3.54–3.36 (m, 2H), 2.97–2.73 (m, 2H), 1.53–1.43 (m, 4H), 1.54–1.37 (m, 1H), 0.77 (d, *J* = 6.3 Hz, 3H). **<sup>13</sup>C NMR** (101 MHz, CDCl<sub>3</sub>)  $\delta$  = 164.9 (C<sub>q</sub>), 154.9 (C<sub>q</sub>), 147.9 (CH), 138.7 (C<sub>q</sub>), 136.4

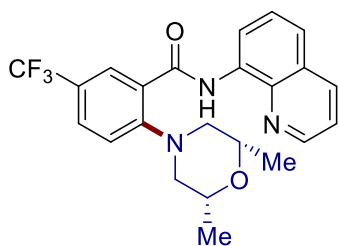
(CH), 135.3 (C<sub>q</sub>), 129.2 (q, <sup>3</sup>J<sub>C-F</sub> = 3.8 Hz, CH), 128.9 (C<sub>q</sub>), 128.7 (q, <sup>3</sup>J<sub>C-F</sub> = 3.6 Hz, CH), 128.3 (C<sub>q</sub>), 127.6 (CH), 125.1 (q, <sup>2</sup>J<sub>C-F</sub> = 33.1 Hz, C<sub>q</sub>), 124.1 (q, <sup>1</sup>J<sub>C-F</sub> = 271.6 Hz, C<sub>q</sub>), 121.9 (CH), 121.5 (CH), 119.3 (CH), 117.8 (CH), 54.3 (CH<sub>2</sub>), 33.2 (CH<sub>2</sub>), 30.3 (CH), 21.5 (CH<sub>3</sub>). **<sup>19</sup>F NMR** (376 MHz, CDCl<sub>3</sub>) δ = -62.1 (s). **IR** (ATR): 2951, 1663, 1522, 1327, 1267, 1119, 825, 792 cm<sup>-1</sup>. **MS** (ESI) *m/z* (relative intensity): 436 (40) [M+Na]<sup>+</sup>, 414 (100) [M+H]<sup>+</sup>, 191 (10). **HR-MS** (ESI) *m/z* calcd for C<sub>23</sub>H<sub>23</sub>F<sub>3</sub>N<sub>3</sub>O [M+H]<sup>+</sup>: 414.1788, found: 414.1786.



#### 2-(4-Cyanopiperidin-1-yl)-N-(quinolin-8-yl)-5-(trifluoromethyl)benzamide (**58nf**)

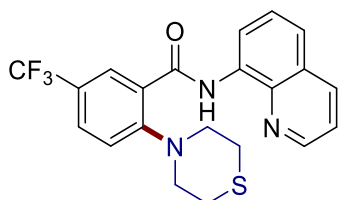
The general procedure **E** was followed using benzamide **35n** (79.0 mg, 0.25 mmol) and piperidine-4-carbonitrile (**56f**) (138 mg, 1.25 mmol). Purification by column chromatography on silica gel (*n*hexane/EtOAc: 9/1→4/1) yielded **58nf** (67.6 mg, 64%) as a white solid. **M. p.**: 193–195 °C. **<sup>1</sup>H NMR** (300 MHz, CDCl<sub>3</sub>) δ = 12.32 (s, 1H), 9.12 (dd, *J* = 7.0, 2.1 Hz, 1H), 8.86 (dd, *J* = 4.2, 1.7 Hz, 1H), 8.44 (d, *J* = 2.3 Hz, 1H), 8.21 (dd, *J* = 8.3, 1.7 Hz, 1H), 7.72 (dd, *J* = 8.5, 2.3 Hz, 1H), 7.65–7.55 (m, 2H), 7.51 (dd, *J* = 8.3, 4.2 Hz, 1H), 7.31 (d, *J* = 8.5 Hz, 1H), 3.54–3.30 (m, 2H), 3.12–3.04 (m, 2H), 2.73 (td, *J* = 7.5, 3.9 Hz, 1H), 2.29–2.16 (m, 4H). **<sup>13</sup>C NMR** (101 MHz, CDCl<sub>3</sub>) δ = 164.2 (C<sub>q</sub>), 153.7 (C<sub>q</sub>), 147.9 (CH), 138.5 (C<sub>q</sub>), 136.8 (CH), 134.9 (C<sub>q</sub>), 129.6 (q, <sup>3</sup>J<sub>C-F</sub> = 3.8 Hz, CH), 129.2 (C<sub>q</sub>), 129.0 (q, <sup>3</sup>J<sub>C-F</sub> = 3.6 Hz, CH), 128.4 (C<sub>q</sub>), 127.6 (CH), 126.3 (q, <sup>2</sup>J<sub>C-F</sub> = 33.1 Hz, C<sub>q</sub>), 123.8 (q, <sup>1</sup>J<sub>C-F</sub> = 272.0 Hz, C<sub>q</sub>), 122.3 (CH), 121.8 (CH), 121.1 (C<sub>q</sub>), 119.7 (CH), 118.0 (CH), 52.0 (CH<sub>2</sub>), 27.9 (CH<sub>2</sub>), 25.7 (CH). **<sup>19</sup>F NMR** (376 MHz, CDCl<sub>3</sub>) δ = -62.2 (s). **IR** (ATR): 3215, 2828, 2245, 1662, 1519, 1325, 1266, 1118, 826, 735 cm<sup>-1</sup>. **MS** (ESI) *m/z* (relative intensity): 447 (98) [M+Na]<sup>+</sup>, 425 (50) [M+H]<sup>+</sup>, 327 (10), 210 (10), 186 (100). **HR-MS** (ESI) *m/z* calcd for C<sub>23</sub>H<sub>20</sub>F<sub>3</sub>N<sub>4</sub>O [M+H]<sup>+</sup>: 425.1584, found: 425.1590.





**2-[(2R,6S)-2,6-Dimethylmorpholino]-N-(quinolin-8-yl)-5-(trifluoromethyl)benzamide (58ng)**

The general procedure **E** was followed using benzamide **35n** (79.0 mg, 0.25 mmol) and (2R,6S)-2,6-dimethylmorpholine (**56g**) (144 mg, 1.25 mmol). Purification by column chromatography on silica gel (*n*hexane/EtOAc: 9/1→4/1) yielded **58ng** (83.5 mg, 78%) as a white solid. **M. p.**: 150–151 °C. **<sup>1</sup>H NMR** (400 MHz, CDCl<sub>3</sub>) δ = 12.33 (s, 1H), 9.06 (dd, *J* = 7.4, 1.6 Hz, 1H), 8.78 (dd, *J* = 4.2, 1.7 Hz, 1H), 8.40 (dd, *J* = 2.4, 0.8 Hz, 1H), 8.17 (dd, *J* = 8.3, 1.7 Hz, 1H), 7.69 (ddd, *J* = 8.5, 2.4, 0.8 Hz, 1H), 7.59 (dd, *J* = 8.2, 7.4 Hz, 1H), 7.54 (dd, *J* = 8.2, 1.6 Hz, 1H), 7.47 (dd, *J* = 8.3, 4.2 Hz, 1H), 7.27 (dd, *J* = 8.5, 0.8 Hz, 1H), 4.10 (dq, *J* = 10.2, 6.3, 2.0 Hz, 2H), 3.25 (dt, *J* = 10.6, 1.6 Hz, 2H), 2.61 (dd, *J* = 11.7, 10.2 Hz, 2H), 1.12 (d, *J* = 6.3 Hz, 6H). **<sup>13</sup>C NMR** (125 MHz, CDCl<sub>3</sub>) δ = 164.3 (C<sub>q</sub>), 153.3 (C<sub>q</sub>), 148.0 (CH), 138.5 (C<sub>q</sub>), 136.4 (CH), 134.9 (C<sub>q</sub>), 129.4 (q, <sup>3</sup>*J*<sub>C-F</sub> = 3.9 Hz, CH), 129.1 (C<sub>q</sub>), 128.8 (q, <sup>3</sup>*J*<sub>C-F</sub> = 3.7 Hz, CH), 128.2 (C<sub>q</sub>), 127.5 (CH), 125.8 (q, <sup>2</sup>*J*<sub>C-F</sub> = 33.1 Hz, C<sub>q</sub>), 123.9 (q, <sup>1</sup>*J*<sub>C-F</sub> = 272.0 Hz, C<sub>q</sub>), 122.0 (CH), 121.6 (CH), 119.4 (CH), 117.7 (CH), 70.6 (CH), 59.0 (CH<sub>2</sub>), 19.0 (CH<sub>3</sub>). **<sup>19</sup>F NMR** (376 MHz, CDCl<sub>3</sub>) δ = -62.2 (s). **IR** (ATR): 2975, 1667, 1526, 1331, 1264, 1123, 827 cm<sup>-1</sup>. **MS** (ESI) *m/z* (relative intensity): 452 (40) [M+Na]<sup>+</sup>, 430 (100) [M+H]<sup>+</sup>. **HR-MS** (ESI) *m/z* calcd for C<sub>23</sub>H<sub>23</sub>F<sub>3</sub>N<sub>3</sub>O<sub>2</sub> [M+H]<sup>+</sup>: 430.1737, found: 430.1743.



**N-(Quinolin-8-yl)-2-thiomorpholino-5-(trifluoromethyl)benzamide (58nh)**

The general procedure **E** was followed using benzamide **35n** (79.0 mg, 0.25 mmol) and thiomorpholine (**56h**) (124 mg, 1.25 mmol). Purification by GPC using CHCl<sub>3</sub> yielded **58nh** (66.7 mg, 64%) as a white solid. **M. p.**: 182–184 °C. **<sup>1</sup>H NMR** (400 MHz,

CDCl<sub>3</sub>)  $\delta$  = 12.49 (s, 1H), 9.10 (dd,  $J$  = 7.3, 1.7 Hz, 1H), 8.90 (dd,  $J$  = 4.2, 1.7 Hz, 1H), 8.47 (dd,  $J$  = 2.4, 0.8 Hz, 1H), 8.19 (dd,  $J$  = 8.3, 1.7 Hz, 1H), 7.71 (ddt,  $J$  = 8.5, 2.4, 0.8 Hz, 1H), 7.59 (dd,  $J$  = 8.2, 7.3 Hz, 1H), 7.55 (dd,  $J$  = 8.2, 1.7 Hz, 1H), 7.49 (dd,  $J$  = 8.3, 4.2 Hz, 1H), 7.32 (dd,  $J$  = 8.5, 0.8 Hz, 1H), 3.52–3.32 (m, 4H), 3.00–2.94 (m, 4H). <sup>13</sup>C NMR (101 MHz, CDCl<sub>3</sub>)  $\delta$  = 164.1 (C<sub>q</sub>), 155.0 (C<sub>q</sub>), 147.9 (CH), 138.5 (C<sub>q</sub>), 136.6 (CH), 135.0 (C<sub>q</sub>), 129.6 (q, <sup>3</sup>J<sub>C-F</sub> = 3.7 Hz, CH), 129.4 (C<sub>q</sub>), 129.0 (q, <sup>3</sup>J<sub>C-F</sub> = 3.5 Hz, CH), 128.3 (C<sub>q</sub>), 127.5 (CH), 126.3 (q, <sup>2</sup>J<sub>C-F</sub> = 33.3 Hz, C<sub>q</sub>), 123.8 (q, <sup>1</sup>J<sub>C-F</sub> = 272.0 Hz, C<sub>q</sub>), 122.2 (CH), 121.8 (CH), 120.7 (CH), 118.2 (CH), 56.0 (CH<sub>2</sub>), 26.9 (CH<sub>2</sub>). <sup>19</sup>F NMR (376 MHz, CDCl<sub>3</sub>)  $\delta$  = -62.2 (s). IR (ATR): 3349, 2925, 2833, 1667, 1526, 1327, 1123, 826, 791 cm<sup>-1</sup>. MS (ESI)  $m/z$  (relative intensity): 440 (25) [M+Na]<sup>+</sup>, 418 (100) [M+H]<sup>+</sup>, 339 (20), 317 (80), 119 (20). HR-MS (ESI)  $m/z$  calcd for C<sub>23</sub>H<sub>19</sub>F<sub>3</sub>N<sub>3</sub>OS [M+H]<sup>+</sup>: 418.1195, found: 418.1199.

### 5.3.4.2 Competition Experiment

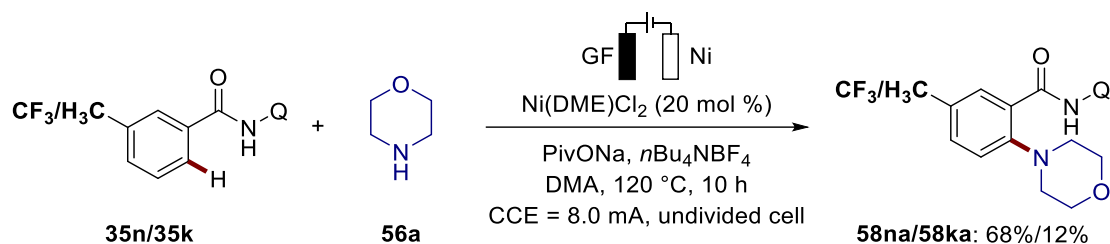


**Figure 5.3.4.** Competition experiment between electronically different arenes **35**.

The general procedure **D** was followed using benzamides **35k** (32.5 mg, 125  $\mu\text{mol}$ ) and **35n** (39.5 mg, 125  $\mu\text{mol}$ ) and morpholine (**56a**) (43.5 mg, 0.50 mmol). Electrolysis was carried out at 120 °C and a constant current of 8 mA was maintained for 10 h. After cooling to ambient temperature, purification by column chromatography (*n*hexane/EtOAc: 16/1→9/1→2/1) yielded the desired products **58na** (33.8 mg, 68%) and **58ka** (5.0 mg, 12%) as white solids.

## 5.3.4.3 Experiments with Isotopically Labelled Solvent

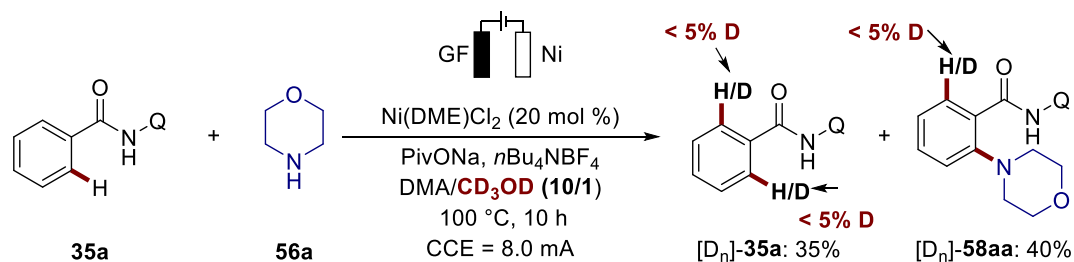


Figure 5.3.5. Experiments with isotopically labelled solvent  $\text{CD}_3\text{OD}$ .

The general procedure **D** was followed using benzamide **35a** (62.0 mg, 0.25 mmol) and morpholine (**56a**) (43.5 mg, 0.50 mmol) using a mixture of DMA and  $\text{CD}_3\text{OD}$  (10/1, 3.3 mL) as solvent. Electrolysis was carried out at 100 °C and a constant current of 8 mA was maintained for 10 h. Column chromatography (*n*hexane/EtOAc: 4/1) yielded the desired product  $[\text{D}_n]\text{-58aa}$  (33.2 mg, 40%) as a white solid and the reisolated starting material  $[\text{D}_n]\text{-35a}$  (22.1 mg, 35%) as a white solid. No deuteration could be detected in either compound as determined by  $^1\text{H}$  NMR spectroscopy.

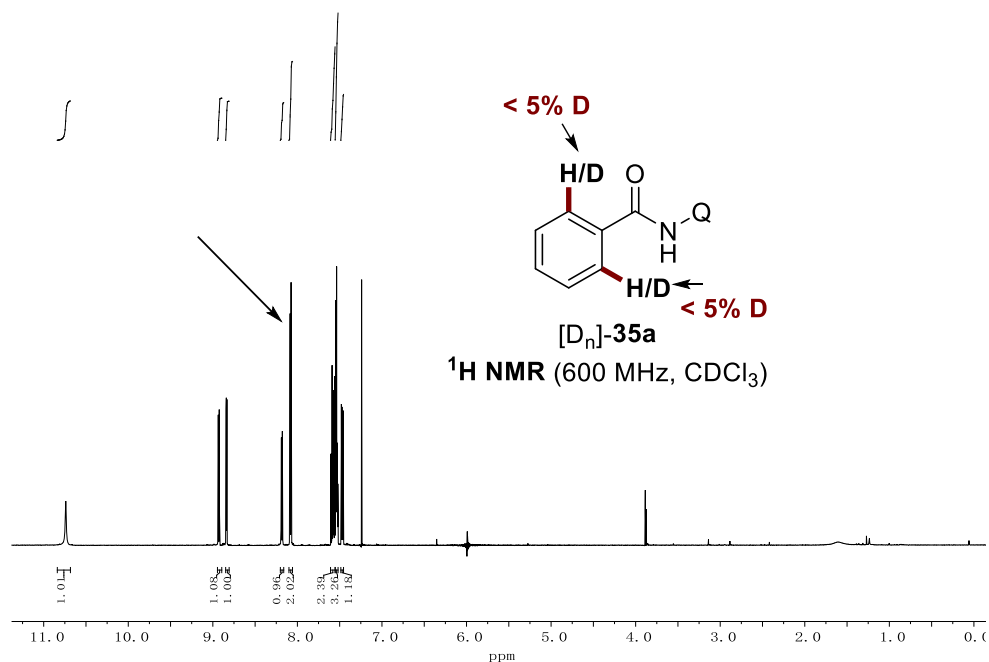


Figure 5.3.6.  $^1\text{H}$  NMR spectroscopy of reisolated  $[\text{D}_n]\text{-35a}$ .

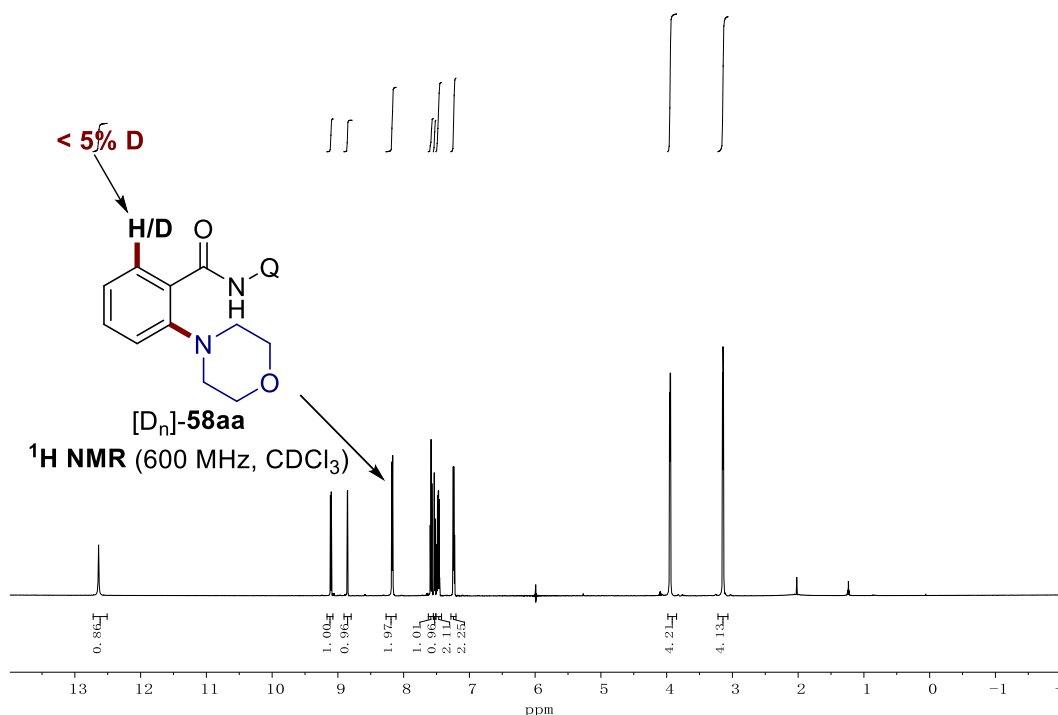


Figure 5.3.7.  $^1\text{H}$  NMR spectroscopy of  $[\text{D}_n]\text{-58aa}$ .

#### 5.3.4.4 Reaction Profile

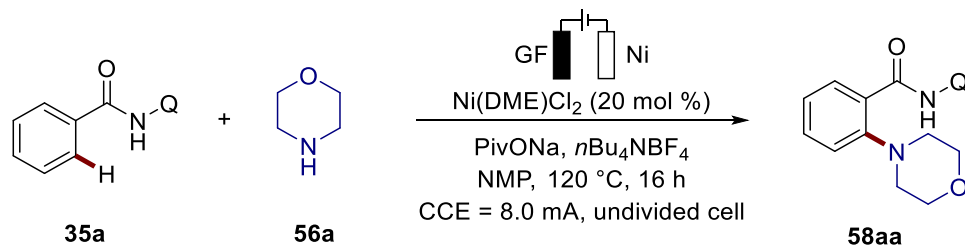
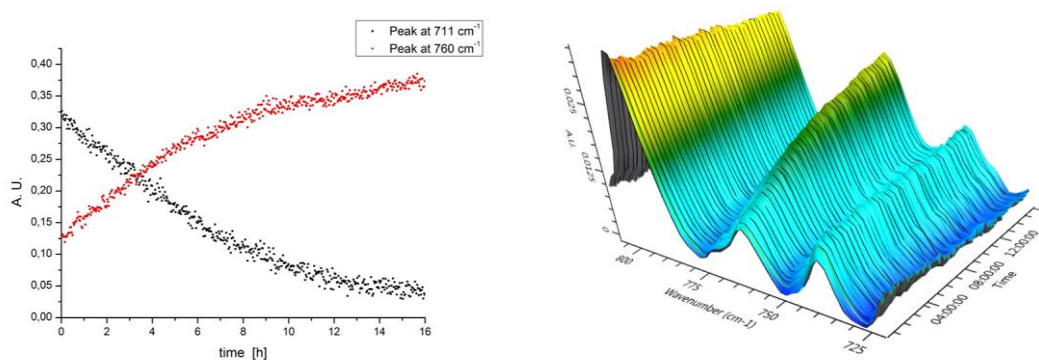


Figure 5.3.8. Reaction profile by *in situ* Rect-IR.

An undivided cell equipped with a GF anode (10 mm × 15 mm × 6 mm) and a nickel-foam cathode (10 mm × 15 mm × 1.4 mm) was charged under an atmosphere of  $\text{N}_2$  with benzamide **35a** (124 mg, 0.50 mmol, 1.00 equiv),  $\text{Ni(DME)Cl}_2$  (21.9 mg, 20 mol %),  $\text{NaOPiv}$  (62.0 mg, 0.50 mmol, 1.00 equiv) and  $n\text{Bu}_4\text{NBF}_4$  (329 mg, 0.50 mmol, 2.0 equiv), NMP (10.0 mL) and amine **56a** (84.0  $\mu\text{L}$ , 1.00 mmol, 2.0 equiv) and fitted with a diamond probe connected to a Mettler Toledo React-IR 15. After heating for 30 min to achieve a stable reaction temperature, electrolysis was started at a constant current of 8 mA for 16 h. An IR spectrum was recorded every 2 minutes. Peaks at  $711 \text{ cm}^{-1}$  and  $760 \text{ cm}^{-1}$  were identified to belong to the starting material and the product, respectively.



**Figure 5.3.9.** Reaction profile of **35a** and **58aa** by *in situ* Rect-IR. Performed by Dr. Nicolas Sauermann.

### 5.3.4.5 KIE studies

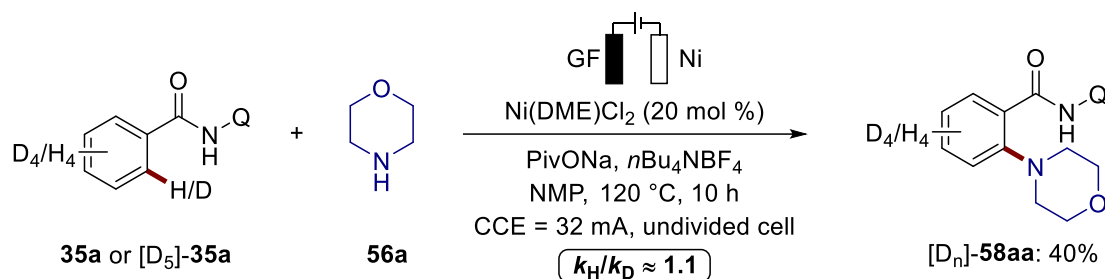


**Figure 5.3.10.** KIE studies of C–H amination.

Two parallel reactions were carried out with **35a** (248 mg, 1.0 mmol, 1.0 equiv) or [D<sub>5</sub>]-**35a** (253 mg, 1.0 mmol, 1.0 equiv) following the general procedure **D** for the React-IR studies (*vide supra*) using Ni(DME)Cl<sub>2</sub> (44 mg, 20 mol %), NaOPiv (124.0 mg, 1.0 mmol, 1.0 equiv), *n*Bu<sub>4</sub>NBF<sub>4</sub> (658 mg, 2.0 mmol, 2.0 equiv) and **56a** (166 μL, 2.0 mmol, 2.0 equiv) in NMP (10 mL). An IR spectrum was recorded every two minutes, and the KIE was determined by the analysis of the initial rates of the increase of the peak at 1117 cm<sup>-1</sup> as measured by the integration of the peak area between 1108 cm<sup>-1</sup> and 1124 cm<sup>-1</sup> after subtraction of the solvent spectrum.

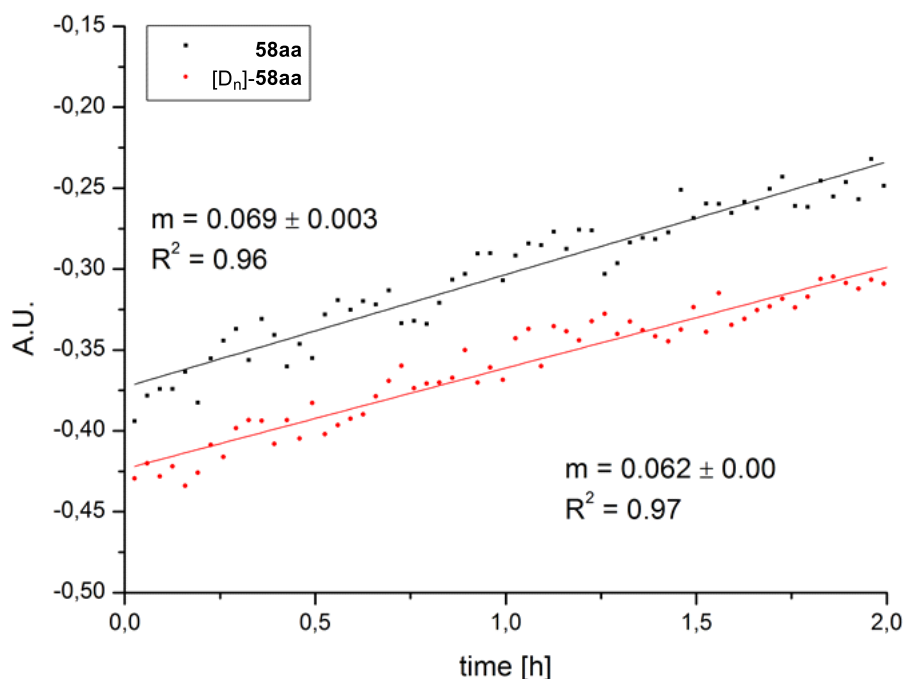


Figure 5.3.11. Initial rates for 58aa and [D<sub>4</sub>]-58aa.

#### 5.3.4.6 H<sub>2</sub>-Detection

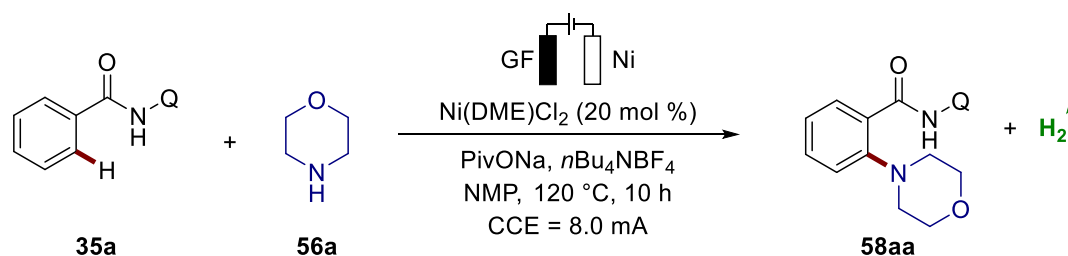
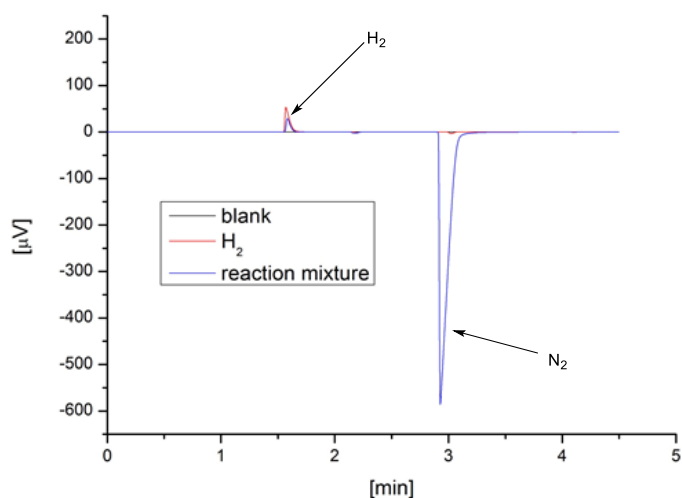


Figure 5.3.12. H<sub>2</sub>-detection under the optimized condition.

Following the general procedure **D**, a reaction was performed under N<sub>2</sub> atmosphere in a tightly closed flask. After 10 h, the gas-phase over the reaction mixture was analyzed by headspace GC analysis using an Agilent 7890B Chromatograph equipped with an Agilent CP-Molsieve 5Å column (length: 25 m, diameter: 0.32 mm, temperature 100 °C). Helium was used as the carrier gas (1.5 mL/min) and the sample was analyzed by a temperature conductivity detector at 110 °C. For comparison, also a blank sample of the carrier gas and a pure sample of hydrogen was obtained.



**Figure 5.3.13.** Headspace analysis of the reaction mixture. Performed by Dr. Nicolas Sauermann.

### 5.3.4.7 Cyclic Voltammetry

The cyclic voltammetry studies were carried out with a Metrohm Autolab PGSTAT204 workstation and following analysis was performed with Nova 2.0 software. A glassy carbon electrode (3 mm diameter, disc-electrode) was used as the working electrode, a Pt-Wire as auxiliary electrode and an Ag-Wire as pseudoreference. The measurements were then referenced using ferrocene. The measurements were carried out at a scan rate of 100 mV/s.

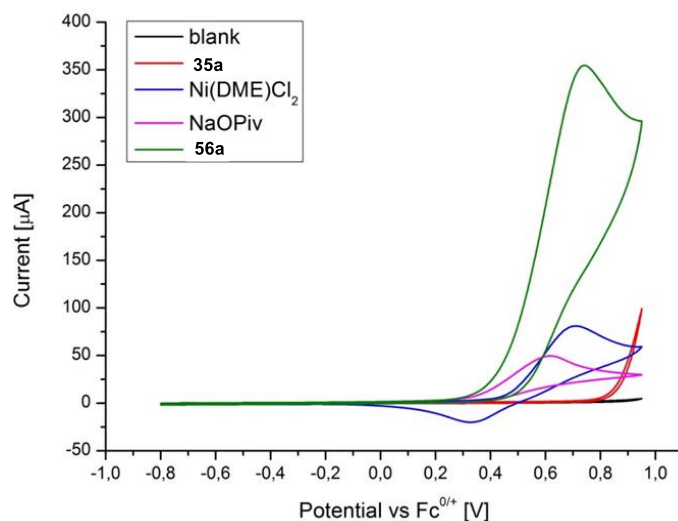


**Figure 5.3.14.** Cyclic voltammogram of the individual components at 100 mV/s. Cyclic voltammograms at 100 mV/s:  $n\text{Bu}_4\text{NBF}_4$  (0.05 M in DMA); concentration of substrates 5 mM. blank (black); **35a** (red);  $\text{Ni}(\text{DME})\text{Cl}_2$  (blue); NaOPiv (pink); **56a** (green). Performed by Dr. Nicolas Sauermann.

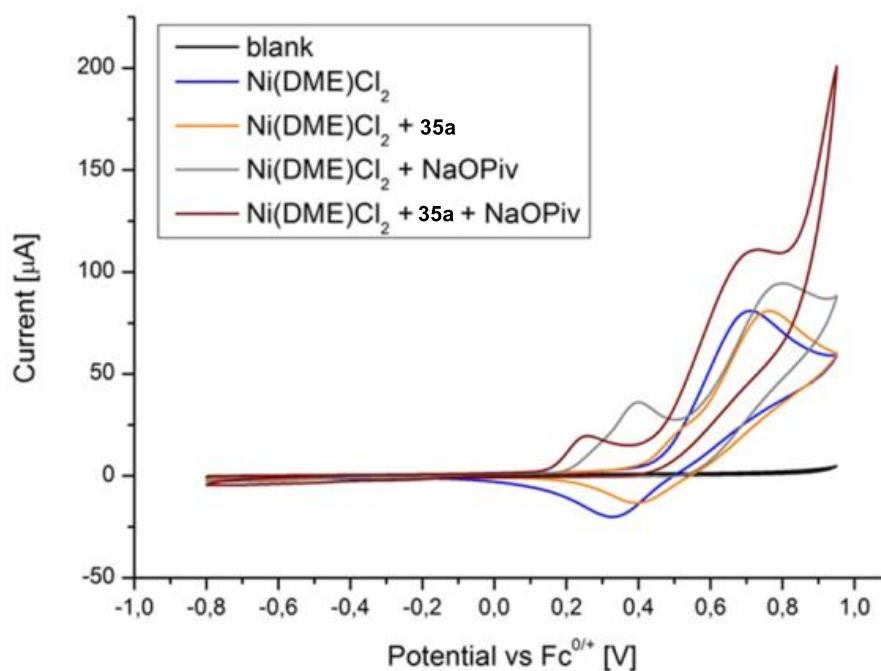


**Figure 5.3.15.** Cyclic voltammogram of Ni(DME)Cl<sub>2</sub> and the reaction components at ambient temperature at 100 mV/s: *n*Bu<sub>4</sub>NBF<sub>4</sub> (0.05 m in DMA); concentration of substrates 5 mM. blank (black); Ni(DME)Cl<sub>2</sub> (blue); Ni(DME)Cl<sub>2</sub> + **35a** (yellow); Ni(DME)Cl<sub>2</sub> + NaOPiv (grey); Ni(DME)Cl<sub>2</sub> + **35a** + NaOPiv (brown). Performed by Dr. Nicolas Sauermann.

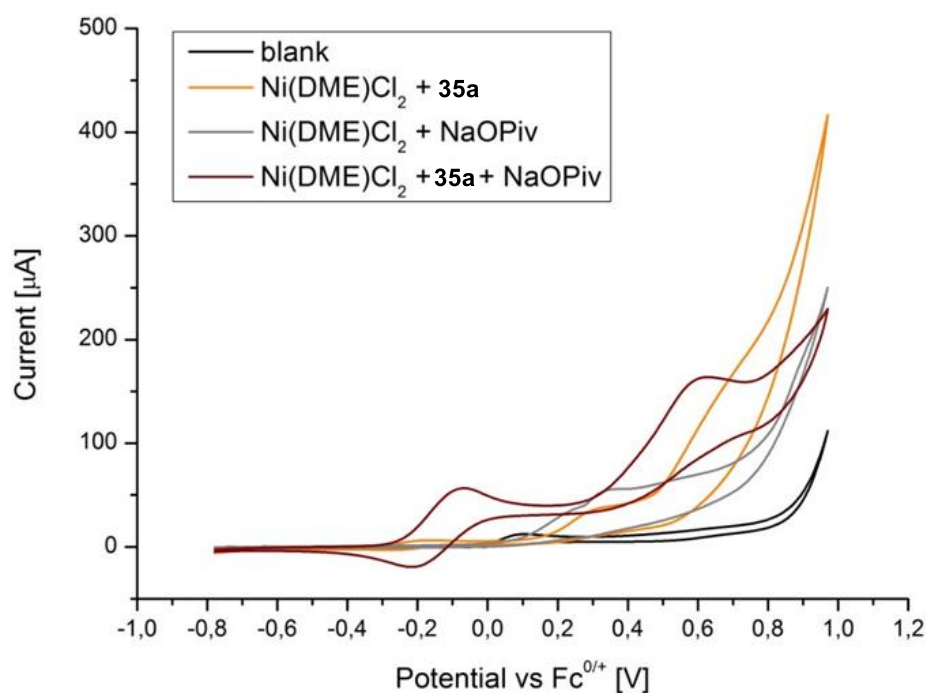
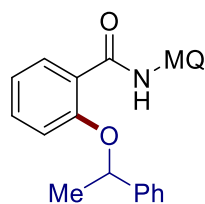


**Figure 5.3.16.** Cyclic voltammogram of Ni(DME)Cl<sub>2</sub> and the reaction components after heating to 120 °C for 30 min, spectra recorded after cooling to ambient temperature at 100 mV/s: *n*Bu<sub>4</sub>NBF<sub>4</sub> (0.05 m in DMA); concentration of substrates 5 mM. blank (black); Ni(DME)Cl<sub>2</sub> + **35a** (yellow); Ni(DME)Cl<sub>2</sub> + NaOPiv (grey); Ni(DME)Cl<sub>2</sub> + **35a** + NaOPiv (brown). Performed by Dr. Nicolas Sauermann.



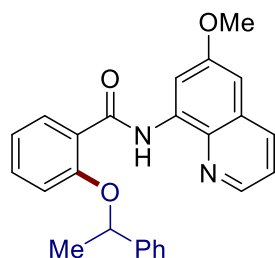
### 5.3.5 Nickela-Electrocatalyzed C–H Alkoxylation

#### 5.3.5.1 Characterization Data



#### ***N*-(6-Methylquinolin-8-yl)-2-(1-phenylethoxy)benzamide (107a)**

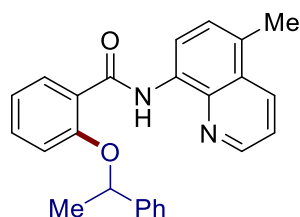
The general procedure **F** was followed using benzamide **106a** (0.25 mmol, 65.5 mg) and 1-phenylethan-1-ol (**66a**) (305 mg, 2.5 mmol). Purification by column chromatography on silica gel (*n*hexane/EtOAc: 16/1→9/1) yielded **107a** (70.7 mg, 74%) as a white solid. **M.p.**: 126–127 °C. **<sup>1</sup>H NMR** (400 MHz, CDCl<sub>3</sub>)  $\delta$  = 12.12 (s, 1H), 9.01 (d, *J* = 1.8 Hz, 1H), 8.69 (dd, *J* = 4.2, 1.7 Hz, 1H), 8.29 (dd, *J* = 7.8, 1.9 Hz, 1H), 8.07 (dd, *J* = 8.2, 1.7 Hz, 1H), 7.62–7.56 (m, 2H), 7.38 (dd, *J* = 8.2, 4.2 Hz, 1H), 7.35–7.29 (m, 3H), 7.29–7.22 (m, 2H), 7.02 (ddd, *J* = 8.3, 7.3, 1.0 Hz, 1H), 6.91–6.88 (m, 1H), 5.61 (q, *J* = 6.5 Hz, 1H), 2.58 (d, *J* = 1.0 Hz, 3H), 1.94 (d, *J* = 6.5 Hz, 3H). **<sup>13</sup>C NMR** (101 MHz, CDCl<sub>3</sub>)  $\delta$  = 164.1 (C<sub>q</sub>), 156.0 (C<sub>q</sub>), 146.8 (CH), 142.5 (C<sub>q</sub>), 137.9 (C<sub>q</sub>), 137.7 (C<sub>q</sub>), 135.5 (CH), 135.4 (C<sub>q</sub>), 132.7 (CH), 132.4 (CH), 128.8 (CH), 128.1 (C<sub>q</sub>), 127.7 (CH), 125.6 (CH), 123.1 (C<sub>q</sub>), 121.5 (CH), 121.0 (CH), 120.5 (CH), 119.9 (CH), 114.0 (CH), 77.9 (CH), 25.0 (CH<sub>3</sub>), 22.4 (CH<sub>3</sub>). **IR** (ATR): 3298, 2924, 1657, 1531, 1476, 1222, 855, 754, 696 cm<sup>-1</sup>. **MS** (ESI) *m/z* (relative intensity): 405 (40) [M+Na]<sup>+</sup>, 383 (100) [M+H]<sup>+</sup>. **HR-MS** (ESI) *m/z* calcd for C<sub>25</sub>H<sub>23</sub>N<sub>2</sub>O<sub>2</sub> [M+H]<sup>+</sup>: 383.1754, found: 383.1754.



#### ***N*-(6-Methoxyquinolin-8-yl)-2-(1-phenylethoxy)benzamide (107b)**

The general procedure **F** was followed using benzamide **106b** (0.25 mmol, 69.5 mg) and 1-phenylethan-1-ol (**66a**) (305 mg, 2.5 mmol). Purification by column chromatography on silica gel (*n*hexane/EtOAc: 12/1→6/1) yielded **107b** (66.5 mg, 67%)

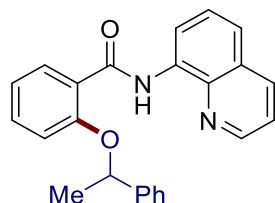
as a white solid and reisolated **106b** (13.0 mg, 19%). **M.p.**: 150–151 °C. **<sup>1</sup>H NMR** (400 MHz, CDCl<sub>3</sub>)  $\delta$  = 12.18 (s, 1H), 8.93 (d,  $J$  = 2.8 Hz, 1H), 8.63 (dd,  $J$  = 4.2, 1.7 Hz, 1H), 8.32 (dd,  $J$  = 7.9, 1.9 Hz, 1H), 8.08 (dd,  $J$  = 8.3, 1.7 Hz, 1H), 7.65–7.57 (m, 2H), 7.41 (dd,  $J$  = 8.3, 4.2 Hz, 1H), 7.39–7.33 (m, 2H), 7.33–7.27 (m, 2H), 7.05 (ddd,  $J$  = 8.1, 7.3, 1.0 Hz, 1H), 6.94 (dd,  $J$  = 8.5, 1.0 Hz, 1H), 6.88 (d,  $J$  = 2.8 Hz, 1H), 5.65 (q,  $J$  = 6.5 Hz, 1H), 4.00 (s, 3H), 1.99 (d,  $J$  = 6.5 Hz, 3H). **<sup>13</sup>C NMR** (101 MHz, CDCl<sub>3</sub>)  $\delta$  = 164.2 (C<sub>q</sub>), 158.6 (C<sub>q</sub>), 156.0 (C<sub>q</sub>), 145.1 (CH), 142.4 (C<sub>q</sub>), 136.8 (C<sub>q</sub>), 135.8 (C<sub>q</sub>), 134.9 (CH), 132.8 (CH), 132.5 (CH), 129.0 (C<sub>q</sub>), 128.8 (CH), 127.7 (CH), 125.6 (CH), 122.9 (C<sub>q</sub>), 121.9 (CH), 121.0 (CH), 114.0 (CH), 109.9 (CH), 100.0 (CH), 77.9 (CH), 55.6 (CH<sub>3</sub>), 25.0 (CH<sub>3</sub>). **IR** (ATR): 3230, 1656, 1520, 1477, 1222, 1157, 1067, 752, 700 cm<sup>-1</sup>. **MS** (ESI)  $m/z$  (relative intensity): 421 (35) [M+Na]<sup>+</sup>, 399 (100) [M+H]<sup>+</sup>, 295 (50). **HR-MS** (ESI)  $m/z$  calcd for C<sub>25</sub>H<sub>23</sub>N<sub>2</sub>O<sub>3</sub> [M+H]<sup>+</sup>: 399.1703, found: 399.1703.



#### ***N*-(5-Methylquinolin-8-yl)-2-(1-phenylethoxy)benzamide (107c)**

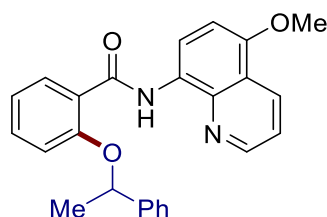
The general procedure **F** was followed using benzamide **106c** (0.25 mmol, 65.5 mg) and 1-phenylethan-1-ol (**66a**) (305 mg, 2.5 mmol). Purification by column chromatography on silica gel (*n*hexane/EtOAc: 16/1→9/1) yielded **107c** (57.8 mg, 61%) as a white solid and reisolated **106c** (13.9 mg, 21%). **M.p.**: 151–152 °C. **<sup>1</sup>H NMR** (300 MHz, CDCl<sub>3</sub>)  $\delta$  = 12.19 (s, 1H), 9.06 (d,  $J$  = 7.9 Hz, 1H), 8.81 (dd,  $J$  = 4.2, 1.6 Hz, 1H), 8.36 (ddd,  $J$  = 7.6, 5.9, 1.8 Hz, 2H), 7.67–7.60 (m, 2H), 7.53–7.45 (m, 2H), 7.43–7.25 (m, 4H), 7.10–7.03 (m, 1H), 6.94 (d,  $J$  = 8.2 Hz, 1H), 5.66 (q,  $J$  = 6.4 Hz, 1H), 2.69 (d,  $J$  = 0.8 Hz, 3H), 1.99 (d,  $J$  = 6.4 Hz, 3H). **<sup>13</sup>C NMR** (75 MHz, CDCl<sub>3</sub>)  $\delta$  = 164.0 (C<sub>q</sub>), 156.0 (C<sub>q</sub>), 147.3 (CH), 142.5 (C<sub>q</sub>), 139.5 (C<sub>q</sub>), 134.3 (C<sub>q</sub>), 132.9 (CH), 132.7 (CH), 132.5 (CH), 128.9 (CH), 128.2 (C<sub>q</sub>), 127.8 (CH), 127.7 (CH), 127.4 (C<sub>q</sub>), 125.7 (CH), 123.2 (C<sub>q</sub>), 121.1 (CH), 121.0 (CH), 117.5 (CH), 114.0 (CH), 77.8 (CH), 25.1 (CH<sub>3</sub>), 18.3 (CH<sub>3</sub>). **IR** (ATR): 3306, 1654, 1520, 1495, 1455, 1225, 753, 701 cm<sup>-1</sup>. **MS** (ESI)  $m/z$  (relative intensity): 405 (40) [M+Na]<sup>+</sup>, 383 (100) [M+H]<sup>+</sup>, 279 (85), 159 (50), 105 152

(40). **HR-MS** (ESI)  $m/z$  calcd for  $C_{25}H_{23}N_2O_2$   $[M+H]^+$ : 383.1754, found: 383.1755.



**2-(1-Phenylethoxy)-N-(quinolin-8-yl)benzamide (107d)**

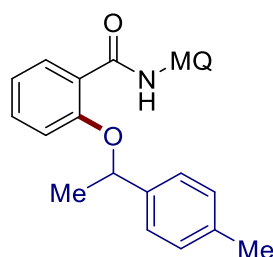
The general procedure **F** was followed using benzamide **35a** (0.25 mmol, 62.0 mg) and 1-phenylethan-1-ol (**66a**) (305 mg, 2.5 mmol). Purification by column chromatography on silica gel (*n*hexane/EtOAc: 16/1→9/1) yielded **107d** (48.9 mg, 53%) as a white solid and reisolated **35a** (23.0 mg, 37%). **M.p.**: 112–114 °C. **<sup>1</sup>H NMR** (400 MHz,  $CDCl_3$ )  $\delta$  = 12.22 (s, 1H), 9.18 (dd,  $J$  = 7.7, 1.4 Hz, 1H), 8.81 (dd,  $J$  = 4.2, 1.7 Hz, 1H), 8.35 (dd,  $J$  = 7.8, 1.9 Hz, 1H), 8.21 (dd,  $J$  = 8.2, 1.7 Hz, 1H), 7.68–7.61 (m, 3H), 7.58 (dd,  $J$  = 8.3, 1.4 Hz, 1H), 7.47 (dd,  $J$  = 8.2, 4.2 Hz, 1H), 7.42–7.32 (m, 2H), 7.34–7.27 (m, 2H), 7.06 (ddd,  $J$  = 8.0, 7.3, 1.0 Hz, 1H), 6.94 (dd,  $J$  = 8.5, 1.0 Hz, 1H), 5.66 (q,  $J$  = 6.5 Hz, 1H), 1.99 (d,  $J$  = 6.5 Hz, 3H). **<sup>13</sup>C NMR** (101 MHz,  $CDCl_3$ )  $\delta$  = 164.2 ( $C_q$ ), 156.0 ( $C_q$ ), 147.8 (CH), 142.5 ( $C_q$ ), 139.3 ( $C_q$ ), 136.3 (CH), 135.9 ( $C_q$ ), 132.8 (CH), 132.5 (CH), 128.9 (CH), 128.2 ( $C_q$ ), 127.8 (CH), 127.6 (CH), 125.7 (CH), 123.1 ( $C_q$ ), 121.6 (CH), 121.5 (CH), 121.0 (CH), 117.8 (CH), 114.1 (CH), 77.9 (CH), 25.1 ( $CH_3$ ). **IR** (ATR): 3304, 1655, 1519, 1324, 1221, 1066, 790, 750, 699  $cm^{-1}$ . **MS** (ESI)  $m/z$  (relative intensity): 391 (45)  $[M+Na]^+$ , 369 (90)  $[M+H]^+$ , 265 (100), 145 (70), 105 (30). **HR-MS** (ESI)  $m/z$  calcd for  $C_{24}H_{21}N_2O_2$   $[M+H]^+$ : 369.1598, found: 369.1597.



**N-(5-Methoxyquinolin-8-yl)-2-(1-phenylethoxy)benzamide (107e)**

The general procedure **F** was followed using benzamide **106e** (0.25 mmol, 69.5 mg) and 1-phenylethan-1-ol (**66a**) (305 mg, 2.5 mmol). Purification by column chromatography on silica gel (*n*hexane/EtOAc: 16/1→9/1) yielded **107e** (27.4 mg, 28%) as a white solid and reisolated **106e** (44.6 mg, 64%). **M.p.**: 147–148 °C. **<sup>1</sup>H NMR**

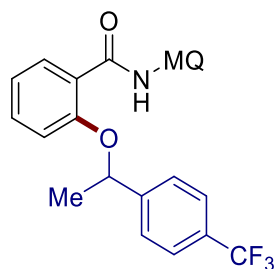
(400 MHz, CDCl<sub>3</sub>)  $\delta$  = 11.99 (s, 1H), 9.05 (d,  $J$  = 8.6 Hz, 1H), 8.77 (dd,  $J$  = 4.2, 1.7 Hz, 1H), 8.59 (dd,  $J$  = 8.4, 1.7 Hz, 1H), 8.30 (dd,  $J$  = 7.8, 1.9 Hz, 1H), 7.61–7.55 (m, 2H), 7.42 (dd,  $J$  = 8.4, 4.2 Hz, 1H), 7.35–7.29 (m, 2H), 7.31–7.20 (m, 2H), 7.01 (ddd,  $J$  = 8.1, 7.2, 1.0 Hz, 1H), 6.94–6.87 (m, 2H), 5.61 (q,  $J$  = 6.5 Hz, 1H), 4.01 (s, 3H), 1.95 (d,  $J$  = 6.5 Hz, 3H). **<sup>13</sup>C NMR** (101 MHz, CDCl<sub>3</sub>)  $\delta$  = 163.6 (C<sub>q</sub>), 155.9 (C<sub>q</sub>), 150.3 (C<sub>q</sub>), 148.2 (CH), 142.5 (C<sub>q</sub>), 139.9 (C<sub>q</sub>), 132.5 (CH), 132.4 (CH), 131.1 (CH), 129.3 (C<sub>q</sub>), 128.8 (CH), 127.7 (CH), 125.6 (CH), 123.1 (C<sub>q</sub>), 121.0 (CH), 120.6 (CH), 120.5 (C<sub>q</sub>), 117.9 (CH), 114.0 (CH), 104.6 (CH), 77.8 (CH), 55.8 (CH<sub>3</sub>), 25.1 (CH<sub>3</sub>). **IR** (ATR): 3311, 1644, 1526, 1269, 1222, 1089, 751, 701 cm<sup>-1</sup>. **MS** (ESI)  $m/z$  (relative intensity): 421 (30) [M+Na]<sup>+</sup>, 399 (100) [M+H]<sup>+</sup>, 295 (80), 175 (40), 105 (10). **HR-MS** (ESI)  $m/z$  calcd for C<sub>25</sub>H<sub>23</sub>N<sub>2</sub>O<sub>3</sub> [M+H]<sup>+</sup>: 399.1703, found: 399.1704.



#### ***N*-(6-Methylquinolin-8-yl)-2-[1-(*p*-tolyl)ethoxy]benzamide (107f)**

The general procedure **F** was followed using benzamide **106a** (0.25 mmol, 65.5 mg) and 1-(*p*-tolyl)ethan-1-ol (**66b**) (341 mg, 2.5 mmol). Purification by column chromatography on silica gel (*n*hexane/EtOAc: 16/1→9/1) yielded **107f** (54.4 mg, 55%) as a white solid. **M.p.**: 128–130 °C. **<sup>1</sup>H NMR** (300 MHz, CDCl<sub>3</sub>)  $\delta$  = 12.18 (s, 1H), 9.06 (d,  $J$  = 1.8 Hz, 1H), 8.79–8.74 (m, 1H), 8.34 (dd,  $J$  = 7.9, 1.9 Hz, 1H), 8.11 (dd,  $J$  = 8.2, 1.7 Hz, 1H), 7.56–7.49 (m, 2H), 7.42 (dd,  $J$  = 8.2, 4.2 Hz, 1H), 7.39–7.29 (m, 2H), 7.17 (d,  $J$  = 7.9 Hz, 2H), 7.09–7.03 (m, 1H), 7.00–6.94 (m, 1H), 5.63 (q,  $J$  = 6.4 Hz, 1H), 2.63 (d,  $J$  = 0.9 Hz, 3H), 2.34 (s, 3H), 1.97 (d,  $J$  = 6.4 Hz, 3H). **<sup>13</sup>C NMR** (75 MHz, CDCl<sub>3</sub>)  $\delta$  = 164.2 (C<sub>q</sub>), 156.1 (C<sub>q</sub>), 146.8 (CH), 139.5 (C<sub>q</sub>), 138.0 (C<sub>q</sub>), 137.7 (C<sub>q</sub>), 137.5 (C<sub>q</sub>), 135.5 (C<sub>q</sub>), 135.5 (CH), 132.8 (CH), 132.5 (CH), 129.5 (CH), 128.2 (C<sub>q</sub>), 125.7 (CH), 123.1 (C<sub>q</sub>), 121.5 (CH), 120.9 (CH), 120.5 (CH), 119.8 (CH), 114.1 (CH), 77.8 (CH), 25.1 (CH<sub>3</sub>), 22.4 (CH<sub>3</sub>), 21.2 (CH<sub>3</sub>). **IR** (ATR): 3302, 1657, 1527, 1476, 1422, 1291, 1221, 1067, 753 cm<sup>-1</sup>. **MS** (ESI)  $m/z$  (relative intensity): 419 (15) [M+Na]<sup>+</sup>, 397

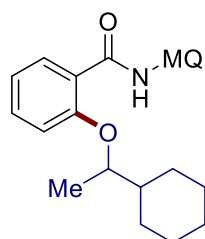
(100)  $[M+H]^+$ , 279 (90), 159 (50), 119 (100). **HR-MS** (ESI)  $m/z$  calcd for  $C_{26}H_{25}N_2O_2$   $[M+H]^+$ : 397.1911, found: 397.1913.



***N*-(6-Methylquinolin-8-yl)-2-{1-[4-(trifluoromethyl)phenyl]ethoxy}benzamide**

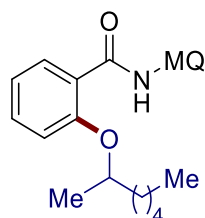
**(107g)**

The general procedure **F** was followed using benzamide **106a** (0.25 mmol, 65.5 mg) and 1-[4-(trifluoromethyl)phenyl]ethan-1-ol (**66c**) (475 mg, 2.5 mmol). Purification by column chromatography on silica gel (*n*hexane/EtOAc: 16/1→9/1) yielded **107g** (73.6 mg, 65%) as a white solid. **M.p.**: 138–139 °C. **<sup>1</sup>H NMR** (400 MHz,  $CDCl_3$ )  $\delta$  = 12.03 (s, 1H), 9.01 (d,  $J$  = 1.8 Hz, 1H), 8.63 (dd,  $J$  = 4.2, 1.7 Hz, 1H), 8.30 (dd,  $J$  = 7.8, 1.8 Hz, 1H), 8.07 (dd,  $J$  = 8.2, 1.7 Hz, 1H), 7.75–7.66 (m, 2H), 7.64–7.53 (m, 2H), 7.38 (dd,  $J$  = 8.2, 4.2 Hz, 1H), 7.33–7.27 (m, 2H), 7.06 (ddd,  $J$  = 8.2, 7.3, 1.0 Hz, 1H), 6.83 (dd,  $J$  = 8.5, 1.0 Hz, 1H), 5.66 (q,  $J$  = 6.5 Hz, 1H), 2.58 (d,  $J$  = 0.9 Hz, 3H), 1.93 (d,  $J$  = 6.5 Hz, 3H). **<sup>13</sup>C NMR** (101 MHz,  $CDCl_3$ )  $\delta$  = 163.9 ( $C_q$ ), 155.5 ( $C_q$ ), 146.7 (CH), 146.5 ( $C_q$ ), 137.8 ( $C_q$ ), 137.7 ( $C_q$ ), 135.6 (CH), 135.2 ( $C_q$ ), 132.8 (CH), 132.6 (CH), 130.0 (q,  $^2J_{C-F}$  = 32.4 Hz,  $C_q$ ), 128.1 ( $C_q$ ), 126.0 (CH), 125.9 (q,  $^3J_{C-F}$  = 3.8 Hz, CH), 123.9 (q,  $^1J_{C-F}$  = 272.3 Hz,  $C_q$ ), 123.3 ( $C_q$ ), 121.5 (CH), 121.4 (CH), 120.6 (CH), 119.8 (CH), 113.7 (CH), 77.1 (CH), 24.7 ( $CH_3$ ), 22.4 ( $CH_3$ ). **<sup>19</sup>F NMR** (282 MHz,  $CDCl_3$ )  $\delta$  = -62.5 (s). **IR** (ATR): 3312, 2926, 1658, 1531, 1478, 1325, 1125, 1069, 753  $cm^{-1}$ . **MS** (ESI)  $m/z$  (relative intensity): 473 (15)  $[M+Na]^+$ , 451 (100)  $[M+H]^+$ . **HR-MS** (ESI)  $m/z$  calcd for  $C_{26}H_{22}F_3N_2O_2$   $[M+H]^+$ : 451.1628, found: 451.1636.



**2-(1-Cyclohexylethoxy)-*N*-(6-methylquinolin-8-yl)benzamide (107h)**

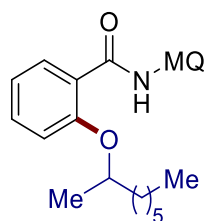
The general procedure **F** was followed using benzamide **106a** (0.25 mmol, 65.5 mg) and 1-cyclohexylethan-1-ol (**66d**) (320 mg, 2.5 mmol). Purification by column chromatography on silica gel (*n*hexane/acetone: 16/1→9/1) yielded **107h** (77.9 mg, 80%) as a colourless oil. **<sup>1</sup>H NMR** (400 MHz, CDCl<sub>3</sub>)  $\delta$  = 11.95 (s, 1H), 8.98 (d, *J* = 1.9 Hz, 1H), 8.76 (dd, *J* = 4.2, 1.7 Hz, 1H), 8.32 (dd, *J* = 7.9, 1.9 Hz, 1H), 8.05 (dd, *J* = 8.2, 1.7 Hz, 1H), 7.45 (ddd, *J* = 8.4, 7.3, 1.9 Hz, 1H), 7.40 (dd, *J* = 8.2, 4.2 Hz, 1H), 7.28 (dq, *J* = 1.9, 1.0 Hz, 1H), 7.12–7.03 (m, 2H), 4.46 (p, *J* = 6.2 Hz, 1H), 2.56 (d, *J* = 1.0 Hz, 3H), 2.16–2.05 (m, 1H), 2.02 (ddt, *J* = 11.7, 3.7, 1.9 Hz, 1H), 1.92–1.84 (m, 1H), 1.77–1.68 (m, 1H), 1.69–1.56 (m, 2H), 1.47 (d, *J* = 6.2 Hz, 3H), 1.21–1.00 (m, 5H). **<sup>13</sup>C NMR** (101 MHz, CDCl<sub>3</sub>)  $\delta$  = 164.3 (C<sub>q</sub>), 156.7 (C<sub>q</sub>), 146.7 (CH), 138.0 (C<sub>q</sub>), 137.6 (C<sub>q</sub>), 135.5 (C<sub>q</sub>), 135.4 (CH), 132.9 (CH), 132.6 (CH), 128.1 (C<sub>q</sub>), 123.5 (C<sub>q</sub>), 121.4 (CH), 120.8 (CH), 120.5 (CH), 119.8 (CH), 113.8 (CH), 80.6 (CH), 42.3 (CH), 29.8 (CH<sub>2</sub>), 28.1 (CH<sub>2</sub>), 26.4 (CH<sub>2</sub>), 26.1 (CH<sub>2</sub>), 25.9 (CH<sub>2</sub>), 22.3 (CH<sub>3</sub>), 16.9 (CH<sub>3</sub>). **IR** (ATR): 3295, 2923, 2851, 1656, 1521, 1475, 1420, 1286, 854, 752 cm<sup>-1</sup>. **MS** (ESI) *m/z* (relative intensity): 411 (90) [M+Na]<sup>+</sup>, 389 (100) [M+H]<sup>+</sup>. **HR-MS** (ESI) *m/z* calcd for C<sub>25</sub>H<sub>29</sub>N<sub>2</sub>O<sub>2</sub> [M+H]<sup>+</sup>: 389.2224, found: 389.2217



### 2-[(Heptan-2-yl)oxy]-*N*-(6-methylquinolin-8-yl)benzamide (**107i**)

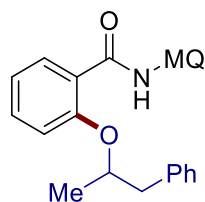
The general procedure **F** was followed using benzamide **106a** (0.25 mmol, 65.5 mg) and heptan-2-ol (**66e**) (290 mg, 2.5 mmol). Purification by column chromatography on silica gel (*n*hexane/EtOAc: 16/1→9/1) yielded **107i** (75.0 mg, 80%) as a colourless oil. **<sup>1</sup>H NMR** (400 MHz, CDCl<sub>3</sub>)  $\delta$  = 12.00 (s, 1H), 8.98 (d, *J* = 1.9 Hz, 1H), 8.74 (dd, *J* = 4.2, 1.7 Hz, 1H), 8.34 (dd, *J* = 7.8, 1.9 Hz, 1H), 8.05 (dd, *J* = 8.2, 1.7 Hz, 1H), 7.45 (ddd, *J* = 8.3, 7.2, 1.9 Hz, 1H), 7.39 (dd, *J* = 8.2, 4.2 Hz, 1H), 7.28 (dq, *J* = 1.9, 0.9 Hz, 1H), 7.12–7.04 (m, 2H), 4.71 (h, *J* = 6.2 Hz, 1H), 2.55 (d, *J* = 0.9 Hz, 3H), 2.17 (dddd, *J* = 13.6, 10.1, 6.5, 5.6 Hz, 1H), 1.79 (ddt, *J* = 13.6, 9.8, 6.0 Hz, 1H), 1.53 (d, *J* = 6.2 Hz, 3H), 1.51–1.44 (m, 1H), 1.44–1.35 (m, 1H), 1.31–1.15 (m, 4H), 0.78 (t, *J* = 7.0 Hz, 3H). 156

**<sup>13</sup>C NMR** (101 MHz, CDCl<sub>3</sub>)  $\delta$  = 164.2 (C<sub>q</sub>), 156.5 (C<sub>q</sub>), 146.7 (CH), 138.0 (C<sub>q</sub>), 137.6 (C<sub>q</sub>), 135.5 (C<sub>q</sub>), 135.4 (CH), 132.9 (CH), 132.6 (CH), 128.1 (C<sub>q</sub>), 123.4 (C<sub>q</sub>), 121.4 (CH), 120.9 (CH), 120.4 (CH), 119.8 (CH), 113.8 (CH), 76.2 (CH), 36.0 (CH<sub>2</sub>), 31.7 (CH<sub>2</sub>), 25.4 (CH<sub>2</sub>), 22.5 (CH<sub>2</sub>), 22.3 (CH<sub>3</sub>), 19.8 (CH<sub>3</sub>), 13.9 (CH<sub>3</sub>). **IR** (ATR): 3295, 2929, 1656, 1525, 1476, 1421, 1288, 752 cm<sup>-1</sup>. **MS** (ESI) *m/z* (relative intensity): 399 (98) [M+Na]<sup>+</sup>, 377 (100) [M+H]<sup>+</sup>. **HR-MS** (ESI) *m/z* calcd for C<sub>24</sub>H<sub>29</sub>N<sub>2</sub>O<sub>2</sub> [M+H]<sup>+</sup>: 377.2224, found: 377.2225.

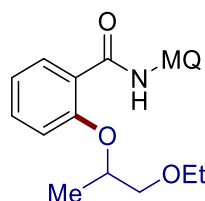


***N*-(6-Methylquinolin-8-yl)-2-[(octan-2-yl)oxy]benzamide (107j)**

The general procedure **F** was followed using benzamide **106a** (0.25 mmol, 65.5 mg) and octan-2-ol (**66f**) (325 mg, 2.5 mmol). Purification by column chromatography on silica gel (*n*hexane/acetone: 16/1→9/1) yielded **107j** (89.6 mg, 92%) as a white solid. **M.p.**: 133–134 °C. **<sup>1</sup>H NMR** (400 MHz, CDCl<sub>3</sub>)  $\delta$  = 12.00 (s, 1H), 8.97 (d, *J* = 1.9 Hz, 1H), 8.75 (dd, *J* = 4.2, 1.7 Hz, 1H), 8.33 (dd, *J* = 7.8, 1.9 Hz, 1H), 8.05 (dd, *J* = 8.2, 1.7 Hz, 1H), 7.45 (ddd, *J* = 8.2, 7.2, 1.9 Hz, 1H), 7.40 (dd, *J* = 8.2, 4.2 Hz, 1H), 7.28 (dq, *J* = 1.9, 1.0 Hz, 1H), 7.15–7.01 (m, 2H), 4.71 (h, *J* = 6.2 Hz, 1H), 2.56 (d, *J* = 1.0 Hz, 3H), 2.17 (dddd, *J* = 13.6, 10.1, 6.6, 5.5 Hz, 1H), 1.79 (ddt, *J* = 13.6, 9.9, 5.9 Hz, 1H), 1.53 (d, *J* = 6.2 Hz, 3H), 1.51–1.33 (m, 2H) 1.33–1.09 (m, 6H), 0.77 (t, *J* = 6.9 Hz, 3H). **<sup>13</sup>C NMR** (101 MHz, CDCl<sub>3</sub>)  $\delta$  = 164.2 (C<sub>q</sub>), 156.5 (C<sub>q</sub>), 146.7 (CH), 138.0 (C<sub>q</sub>), 137.7 (C<sub>q</sub>), 135.5 (C<sub>q</sub>), 135.4 (CH), 132.9 (CH), 132.6 (CH), 128.1 (C<sub>q</sub>), 123.5 (C<sub>q</sub>), 121.4 (CH), 120.9 (CH), 120.4 (CH), 119.8 (CH), 113.8 (CH), 76.3 (CH), 36.1 (CH<sub>2</sub>), 31.7 (CH<sub>2</sub>), 29.2 (CH<sub>2</sub>), 25.7 (CH<sub>2</sub>), 22.5 (CH<sub>2</sub>), 22.4 (CH<sub>3</sub>), 19.9 (CH<sub>3</sub>), 14.0 (CH<sub>3</sub>). **IR** (ATR): 3299, 2927, 1659, 1530, 1477, 753 cm<sup>-1</sup>. **MS** (EI) *m/z* (relative intensity): 391 (10) [M+H]<sup>+</sup>, 390 (30) [M]<sup>+</sup>, 158 (100), 121 (50). **HR-MS** (EI) *m/z* calcd for C<sub>25</sub>H<sub>30</sub>N<sub>2</sub>O<sub>2</sub> [M]<sup>+</sup>: 390.2302, found: 390.2311.

***N*-(6-Methylquinolin-8-yl)-2-[(1-phenylpropan-2-yl)oxy]benzamide (107k)**

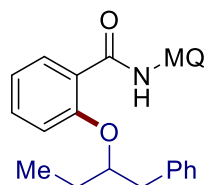
The general procedure **F** was followed using benzamide **106a** (0.25 mmol, 65.5 mg) and 1-phenylpropan-2-ol (**66g**) (340 mg, 2.5 mmol). Purification by column chromatography on silica gel (*n*hexane/EtOAc: 16/1→9/1) yielded **107k** (84.7 mg, 86%) as a colourless oil. **<sup>1</sup>H NMR** (400 MHz, CDCl<sub>3</sub>)  $\delta$  = 12.07 (s, 1H), 9.01 (d, *J* = 1.9 Hz, 1H), 8.76 (dd, *J* = 4.2, 1.7 Hz, 1H), 8.35 (dd, *J* = 7.9, 1.9 Hz, 1H), 8.06 (dd, *J* = 8.2, 1.7 Hz, 1H), 7.43 (ddd, *J* = 8.3, 7.2, 1.9 Hz, 1H), 7.40 (dd, *J* = 8.2, 4.2 Hz, 1H), 7.30 (dq, *J* = 1.9, 1.0 Hz, 1H), 7.28–7.25 (m, 2H), 7.25–7.20 (m, 2H), 7.18–7.13 (m, 1H), 7.09 (ddd, *J* = 8.1, 7.2, 1.0 Hz, 1H), 7.02 (dd, *J* = 8.3, 0.8 Hz, 1H), 4.99–4.85 (m, 1H), 3.59 (dd, *J* = 13.6, 6.3 Hz, 1H), 3.08 (dd, *J* = 13.6, 6.7 Hz, 1H), 2.58 (d, *J* = 1.0 Hz, 3H), 1.55 (d, *J* = 6.1 Hz, 3H). **<sup>13</sup>C NMR** (101 MHz, CDCl<sub>3</sub>)  $\delta$  = 164.0 (C<sub>q</sub>), 156.0 (C<sub>q</sub>), 146.8 (CH), 138.1 (C<sub>q</sub>), 137.9 (C<sub>q</sub>), 137.7 (C<sub>q</sub>), 135.5 (CH), 135.4 (C<sub>q</sub>), 132.9 (CH), 132.6 (CH), 129.3 (CH), 128.4 (CH), 128.1 (C<sub>q</sub>), 126.4 (CH), 123.6 (C<sub>q</sub>), 121.4 (CH), 121.2 (CH), 120.5 (CH), 119.8 (CH), 113.9 (CH), 77.3 (CH), 42.4 (CH<sub>2</sub>), 22.3 (CH<sub>3</sub>), 19.5 (CH<sub>3</sub>). **IR** (ATR): 3230, 2925, 1655, 1524, 1476, 1422, 1288, 750, 698 cm<sup>-1</sup>. **MS** (EI) *m/z* (relative intensity): 397 (5) [M+H]<sup>+</sup>, 396 (15) [M]<sup>+</sup>, 158 (100), 120 (50), 91 (50). **HR-MS** (EI) *m/z* calcd for C<sub>26</sub>H<sub>24</sub>N<sub>2</sub>O<sub>2</sub> [M]<sup>+</sup>: 396.1832, found: 396.1848.

**2-[(1-Ethoxypropan-2-yl)oxy]-*N*-(6-methylquinolin-8-yl)benzamide (107l)**

The general procedure **F** was followed using benzamide **106a** (0.25 mmol, 65.5 mg) and 1-ethoxypropan-2-ol (**66h**) (260 mg, 2.5 mmol). Purification by column chromatography on silica gel (*n*hexane/EtOAc: 16/1→9/1) yielded **107l** (48.5 mg, 54%) as a colourless oil. **<sup>1</sup>H NMR** (400 MHz, CDCl<sub>3</sub>)  $\delta$  = 11.95 (s, 1H), 8.96 (d, *J* = 1.9 Hz, 1H), 8.77 (dd, *J* = 4.2, 1.7 Hz, 1H), 8.32 (dd, *J* = 7.9, 1.9 Hz, 1H), 8.06 (dd, *J* = 8.2,



1.7 Hz, 1H), 7.46 (ddd,  $J = 8.4, 7.2, 1.9$  Hz, 1H), 7.41 (dd,  $J = 8.2, 4.2$  Hz, 1H), 7.28 (dq,  $J = 1.9, 1.0$  Hz, 1H), 7.16 (ddd,  $J = 8.4, 1.0, 0.5$  Hz, 1H), 7.11 (ddd,  $J = 7.9, 7.2, 1.0$  Hz, 1H), 4.89 (tdd,  $J = 6.1, 5.4, 0.7$  Hz, 1H), 4.03 (dd,  $J = 10.1, 6.1$  Hz, 1H), 3.71 (dd,  $J = 10.1, 5.4$  Hz, 1H), 3.49 (q,  $J = 7.0$  Hz, 2H), 2.55 (d,  $J = 1.0$  Hz, 3H), 1.56 (d,  $J = 6.3$  Hz, 3H), 1.09 (t,  $J = 7.0$  Hz, 3H).  $^{13}\text{C NMR}$  (101 MHz,  $\text{CDCl}_3$ )  $\delta = 164.0$  ( $\text{C}_q$ ), 156.3 ( $\text{C}_q$ ), 146.7 (CH), 138.0 ( $\text{C}_q$ ), 137.7 ( $\text{C}_q$ ), 135.6 (CH), 135.4 ( $\text{C}_q$ ), 132.9 (CH), 132.5 (CH), 128.1 ( $\text{C}_q$ ), 123.7 ( $\text{C}_q$ ), 121.4 (CH), 121.4 (CH), 120.5 (CH), 119.8 (CH), 114.4 (CH), 75.5 (CH), 73.6 ( $\text{CH}_2$ ), 66.9 ( $\text{CH}_2$ ), 22.3 ( $\text{CH}_3$ ), 17.4 ( $\text{CH}_3$ ), 15.1 ( $\text{CH}_3$ ). **IR** (ATR): 3300, 2976, 1655, 1523, 1475, 1219, 1109, 854, 751, 692  $\text{cm}^{-1}$ . **MS** (ESI)  $m/z$  (relative intensity): 387 (30)  $[\text{M}+\text{Na}]^+$ , 365 (100)  $[\text{M}+\text{H}]^+$ . **HR-MS** (ESI)  $m/z$  calcd for  $\text{C}_{22}\text{H}_{25}\text{N}_2\text{O}_3$   $[\text{M}+\text{H}]^+$ : 365.1860, found: 365.1861.

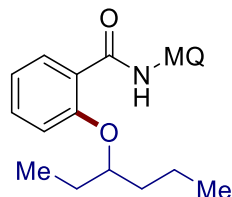


#### ***N*-(6-Methylquinolin-8-yl)-2-[(1-phenylbutan-2-yl)oxy]benzamide (107m)**

The general procedure **F** was followed using benzamide **106a** (0.25 mmol, 65.5 mg) and 1-phenylbutan-2-ol (**66i**) (375 mg, 2.5 mmol). Purification by column chromatography on silica gel (*n*hexane/acetone: 30/1→15/1) yielded **107m** (58.5 mg, 57%) as a colourless oil.  $^1\text{H NMR}$  (400 MHz,  $\text{CDCl}_3$ )  $\delta = 12.12$  (s, 1H), 9.03 (d,  $J = 1.9$  Hz, 1H), 8.74 (dd,  $J = 4.2, 1.7$  Hz, 1H), 8.36 (dd,  $J = 7.9, 1.9$  Hz, 1H), 8.06 (dd,  $J = 8.3, 1.7$  Hz, 1H), 7.44–7.38 (m, 2H), 7.30 (dq,  $J = 1.9, 1.0$  Hz, 1H), 7.28–7.23 (m, 2H), 7.22–7.17 (m, 2H), 7.15–7.10 (m, 1H), 7.08 (ddd,  $J = 7.9, 7.2, 1.0$  Hz, 1H), 6.99 (d,  $J = 8.4, 1.9$  Hz, 1H), 4.85–4.72 (m, 1H), 3.50 (dd,  $J = 13.8, 6.8$  Hz, 1H), 3.11 (dd,  $J = 13.8, 5.8$  Hz, 1H), 2.58 (d,  $J = 1.0$  Hz, 3H), 2.10 (ddd,  $J = 14.2, 7.5, 6.8$  Hz, 1H), 1.98–1.86 (m, 1H), 1.04 (t,  $J = 7.5$  Hz, 3H).  $^{13}\text{C NMR}$  (101 MHz,  $\text{CDCl}_3$ )  $\delta = 164.0$  ( $\text{C}_q$ ), 156.7 ( $\text{C}_q$ ), 146.6 (CH), 138.1 ( $\text{C}_q$ ), 138.0 ( $\text{C}_q$ ), 137.6 ( $\text{C}_q$ ), 135.5 ( $\text{C}_q$ ), 135.5 (CH), 132.9 (CH), 132.7 (CH), 129.3 (CH), 128.4 (CH), 128.1 ( $\text{C}_q$ ), 126.3 (CH), 123.3 ( $\text{C}_q$ ), 121.4 (CH), 121.0 (CH), 120.5 (CH), 119.8 (CH), 113.7 (CH), 82.5 (CH), 40.0 ( $\text{CH}_2$ ), 26.4 ( $\text{CH}_2$ ), 22.3 ( $\text{CH}_3$ ), 9.9 ( $\text{CH}_3$ ). **IR** (ATR): 3295, 2968, 1654, 1521, 1475, 1419, 1219, 854, 747,

692  $\text{cm}^{-1}$ . **MS** (ESI)  $m/z$  (relative intensity): 433 (50)  $[\text{M}+\text{Na}]^+$ , 411 (100)  $[\text{M}+\text{H}]^+$ .

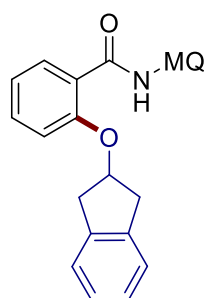
**HR-MS** (ESI)  $m/z$  calcd for  $\text{C}_{27}\text{H}_{27}\text{N}_2\text{O}_2$   $[\text{M}+\text{H}]^+$ : 411.2067, found: 411.2067.



### 2-[(Hexan-3-yl)oxy]-*N*-(6-methylquinolin-8-yl)benzamide (**107n**)

The general procedure **F** was followed using benzamide **106a** (0.25 mmol, 65.5 mg) and hexan-3-ol (**66j**) (255 mg, 2.5 mmol). Purification by column chromatography on silica gel (*n*hexane/EtOAc: 20/1→9/1) yielded **107n** (45.5 mg, 50%) as a colourless oil.

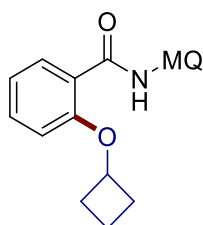
**$^1\text{H}$  NMR** (400 MHz,  $\text{CDCl}_3$ )  $\delta$  = 12.05 (s, 1H), 8.99 (d,  $J$  = 1.9 Hz, 1H), 8.74 (dd,  $J$  = 4.2, 1.7 Hz, 1H), 8.47–8.26 (m, 1H), 8.05 (dd,  $J$  = 8.2, 1.7 Hz, 1H), 7.49–7.42 (m, 1H), 7.40 (dd,  $J$  = 8.2, 4.2 Hz, 1H), 7.28 (dd,  $J$  = 1.9, 1.0 Hz, 1H), 7.12–7.05 (m, 2H), 4.65–4.48 (m, 1H), 2.56 (d,  $J$  = 1.0 Hz, 3H), 2.19–2.00 (m, 2H), 1.96–1.73 (m, 2H), 1.63–1.38 (m, 2H), 1.01 (t,  $J$  = 7.4 Hz, 3H), 0.87 (t,  $J$  = 7.4 Hz, 3H).  **$^{13}\text{C}$  NMR** (101 MHz,  $\text{CDCl}_3$ )  $\delta$  = 164.2 ( $\text{C}_q$ ), 157.1 ( $\text{C}_q$ ), 146.6 (CH), 138.1 ( $\text{C}_q$ ), 137.6 ( $\text{C}_q$ ), 135.6 ( $\text{C}_q$ ), 135.4 (CH), 132.9 (CH), 132.7 (CH), 128.1 ( $\text{C}_q$ ), 123.1 ( $\text{C}_q$ ), 121.4 (CH), 120.7 (CH), 120.5 (CH), 119.9 (CH), 113.6 (CH), 81.2 (CH), 35.6 ( $\text{CH}_2$ ), 26.7 ( $\text{CH}_2$ ), 22.4 ( $\text{CH}_3$ ), 18.8 ( $\text{CH}_2$ ), 14.1 ( $\text{CH}_3$ ), 10.0 ( $\text{CH}_3$ ). **IR** (ATR): 3293, 2960, 1654, 1522, 1475, 1287, 949, 854, 752, 692  $\text{cm}^{-1}$ . **MS** (ESI)  $m/z$  (relative intensity): 385 (30)  $[\text{M}+\text{Na}]^+$ , 363 (100)  $[\text{M}+\text{H}]^+$ . **HR-MS** (ESI)  $m/z$  calcd for  $\text{C}_{23}\text{H}_{27}\text{N}_2\text{O}_2$   $[\text{M}+\text{H}]^+$ : 363.2067, found: 363.2068.



### 2-[(2,3-Dihydro-1*H*-inden-2-yl)oxy]-*N*-(6-methylquinolin-8-yl)benzamide (**107o**)

The general procedure **F** was followed using benzamide **106a** (0.25 mmol, 65.5 mg) and 2,3-dihydro-1*H*-inden-2-ol (**66k**) (335 mg, 2.5 mmol). Purification by column chromatography on silica gel (*n*hexane/acetone: 16/1→9/1) yielded **107o** (70.7 mg,

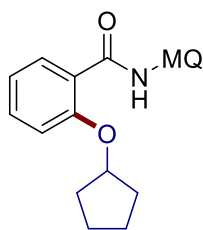
72%) as a white solid. **M.p.:** 157–158 °C. **<sup>1</sup>H NMR** (300 MHz, CDCl<sub>3</sub>)  $\delta$  = 11.77 (s, 1H), 8.91 (d,  $J$  = 1.9 Hz, 1H), 8.41 (dd,  $J$  = 4.2, 1.7 Hz, 1H), 8.34 (dd,  $J$  = 8.0, 1.9 Hz, 1H), 8.00 (dd,  $J$  = 8.2, 1.7 Hz, 1H), 7.54–7.46 (m, 1H), 7.31 (dd,  $J$  = 8.2, 4.2 Hz, 1H), 7.26–7.23 (m, 1H), 7.18–7.09 (m, 6H), 5.59–5.39 (m, 1H), 3.73 (dd,  $J$  = 16.7, 4.6 Hz, 2H), 3.54 (dd,  $J$  = 16.7, 7.2 Hz, 2H), 2.53 (d,  $J$  = 0.9 Hz, 3H). **<sup>13</sup>C NMR** (126 MHz, CDCl<sub>3</sub>)  $\delta$  = 163.7 (C<sub>q</sub>), 155.8 (C<sub>q</sub>), 146.6 (CH), 140.1 (C<sub>q</sub>), 137.7 (C<sub>q</sub>), 137.4 (C<sub>q</sub>), 135.3 (CH), 135.1 (C<sub>q</sub>), 132.8 (CH), 132.7 (CH), 127.9 (C<sub>q</sub>), 126.6 (CH), 124.5 (CH), 123.4 (C<sub>q</sub>), 121.3 (CH), 121.2 (CH), 120.4 (CH), 119.6 (CH), 113.5 (CH), 79.4 (CH), 39.6 (CH<sub>2</sub>), 22.4 (CH<sub>3</sub>). **IR** (ATR): 3300, 1651, 1531, 1475, 1290, 1028, 860, 744, 684, 591 cm<sup>-1</sup>. **MS** (ESI)  $m/z$  (relative intensity): 417 (30) [M+Na]<sup>+</sup>, 395 (100) [M+H]<sup>+</sup>. **HR-MS** (ESI)  $m/z$  calcd for C<sub>26</sub>H<sub>23</sub>N<sub>2</sub>O<sub>2</sub> [M+H]<sup>+</sup>: 395.1754, found: 395.1755.



### 2-Cyclobutoxy-*N*-(6-methylquinolin-8-yl)benzamide (107p)

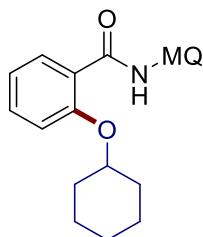
The general procedure **F** was followed using benzamide **106a** (0.25 mmol, 65.5 mg) and cyclobutanol (**66I**) (188 mg, 2.5 mmol). Purification by column chromatography on silica gel (*n*hexane/acetone: 16/1→9/1) yielded **107p** (61.8 mg, 74%) as a white solid. **M.p.:** 86–87 °C. **<sup>1</sup>H NMR** (300 MHz, CDCl<sub>3</sub>)  $\delta$  = 12.01 (s, 1H), 8.98 (d,  $J$  = 1.9 Hz, 1H), 8.74 (dd,  $J$  = 4.2, 1.7 Hz, 1H), 8.35 (dd,  $J$  = 7.9, 1.8 Hz, 1H), 8.04 (dd,  $J$  = 8.3, 1.7 Hz, 1H), 7.43 (ddd,  $J$  = 8.4, 7.2, 1.8 Hz, 1H), 7.38 (dd,  $J$  = 8.3, 4.2 Hz, 1H), 7.28 (dq,  $J$  = 1.9, 1.0 Hz, 1H), 7.09 (ddd,  $J$  = 7.9, 7.2, 1.0 Hz, 1H), 6.88 (dd,  $J$  = 8.4, 1.0 Hz, 1H), 4.94 (pd,  $J$  = 7.2, 1.0 Hz, 1H), 2.76–2.57 (m, 4H), 2.55 (d,  $J$  = 1.0 Hz, 3H), 2.11–1.91 (m, 1H), 1.85–1.72 (m, 1H). **<sup>13</sup>C NMR** (126 MHz, CDCl<sub>3</sub>)  $\delta$  = 163.8 (C<sub>q</sub>), 155.7 (C<sub>q</sub>), 146.7 (CH), 137.9 (C<sub>q</sub>), 137.5 (C<sub>q</sub>), 135.5 (C<sub>q</sub>), 135.4 (CH), 132.9 (CH), 132.5 (CH), 128.0 (C<sub>q</sub>), 122.3 (C<sub>q</sub>), 121.3 (CH), 120.9 (CH), 120.4 (CH), 119.8 (CH), 112.9 (CH), 72.9 (CH), 30.7 (CH<sub>2</sub>), 22.4 (CH<sub>3</sub>), 13.6 (CH<sub>2</sub>). **IR** (ATR): 3298, 2937, 1654, 1524, 1476, 1290, 1219, 854, 750, 689 cm<sup>-1</sup>. **MS** (ESI)  $m/z$  (relative intensity): 355 (80) [M+Na]<sup>+</sup>, 333 (100) [M+H]<sup>+</sup>. **HR-MS** (ESI)  $m/z$  calcd for C<sub>21</sub>H<sub>21</sub>N<sub>2</sub>O<sub>2</sub> [M+H]<sup>+</sup>: 333.1598,

found: 333.1601.



### 2-(Cyclopentyloxy)-*N*-(6-methylquinolin-8-yl)benzamide (107q)

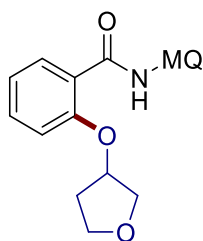
The general procedure **F** was followed using benzamide **106a** (0.25 mmol, 65.5 mg) and cyclopentanol (**66m**) (215 mg, 2.5 mmol). Purification by column chromatography on silica gel (*n*hexane/acetone: 16/1→9/1) yielded **107q** (68.4 mg, 79%) as a white solid. **M.p.**: 96–98 °C. **<sup>1</sup>H NMR** (300 MHz, CDCl<sub>3</sub>)  $\delta$  = 11.80 (s, 1H), 9.03 (d,  $J$  = 1.9 Hz, 1H), 8.77 (dd,  $J$  = 4.2, 1.7 Hz, 1H), 8.36 (dd,  $J$  = 7.8, 1.9 Hz, 1H), 8.09 (dd,  $J$  = 8.2, 1.7 Hz, 1H), 7.49 (ddd,  $J$  = 8.2, 7.3, 1.9 Hz, 1H), 7.43 (dd,  $J$  = 8.2, 4.2 Hz, 1H), 7.33 (dq,  $J$  = 1.9, 1.0 Hz, 1H), 7.16–7.06 (m, 2H), 5.13 (tt,  $J$  = 6.1, 2.9 Hz, 1H), 2.60 (d,  $J$  = 1.0 Hz, 3H), 2.45–2.33 (m, 2H), 2.22–2.02 (m, 2H), 1.98–1.80 (m, 2H), 1.67 (tdd,  $J$  = 10.9, 8.2, 5.2 Hz, 2H). **<sup>13</sup>C NMR** (101 MHz, CDCl<sub>3</sub>)  $\delta$  = 164.3 (C<sub>q</sub>), 156.3 (C<sub>q</sub>), 146.6 (CH), 138.0 (C<sub>q</sub>), 137.6 (C<sub>q</sub>), 135.5 (CH), 135.4 (C<sub>q</sub>), 132.8 (CH), 132.7 (CH), 128.1 (C<sub>q</sub>), 123.1 (C<sub>q</sub>), 121.4 (CH), 120.6 (CH), 120.5 (CH), 120.0 (CH), 113.6 (CH), 81.2 (CH), 32.9 (CH<sub>2</sub>), 24.4 (CH<sub>2</sub>), 22.3 (CH<sub>3</sub>). **IR** (ATR): 3305, 2960, 1656, 1528, 1478, 1421, 1289, 753 cm<sup>-1</sup>. **MS** (ESI)  $m/z$  (relative intensity): 369 (100) [M+Na]<sup>+</sup>, 347 (90) [M+H]<sup>+</sup>. **HR-MS** (ESI)  $m/z$  calcd for C<sub>22</sub>H<sub>23</sub>N<sub>2</sub>O<sub>2</sub> [M+H]<sup>+</sup>: 347.1754, found: 347.1756.



### 2-(Cyclohexyloxy)-*N*-(6-methylquinolin-8-yl)benzamide (107r)

The general procedure **F** was followed using benzamide **106a** (0.25 mmol, 65.5 mg) and cyclohexanol (**66n**) (251 mg, 2.5 mmol). Purification by column chromatography on silica gel (*n*hexane/acetone: 20/1) yielded **107r** (68.4 mg, 76%) as a white solid. **M.p.**: 121–123 °C. **<sup>1</sup>H NMR** (300 MHz, CDCl<sub>3</sub>)  $\delta$  = 11.97 (s, 1H), 9.01 (d,  $J$  = 1.9 Hz, 1H), 8.78 (dd,  $J$  = 4.2, 1.7 Hz, 1H), 8.34 (dd,  $J$  = 8.1, 1.9 Hz, 1H), 8.09 (dd,  $J$  = 8.2, 1.62

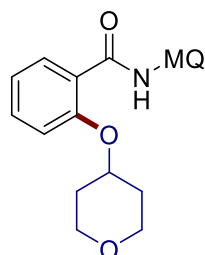
1.7 Hz, 1H), 7.48 (ddd,  $J = 8.4, 7.3, 1.9$  Hz, 1H), 7.44 (dd,  $J = 8.2, 4.2$  Hz, 1H), 7.32 (dq,  $J = 1.9, 1.0$  Hz, 1H), 7.16–7.06 (m, 2H), 4.59 (tt,  $J = 9.8, 4.0$  Hz, 1H), 2.60 (d,  $J = 1.0$  Hz, 3H), 2.29–2.20 (m, 2H), 2.03–1.92 (m, 2H), 1.88 (dt,  $J = 7.3, 3.3$  Hz, 2H), 1.74–1.65 (m, 1H), 1.51–1.26 (m, 3H).  $^{13}\text{C}$  NMR (101 MHz,  $\text{CDCl}_3$ )  $\delta = 164.3$  ( $\text{C}_q$ ), 156.0 ( $\text{C}_q$ ), 146.7 (CH), 137.9 ( $\text{C}_q$ ), 137.6 ( $\text{C}_q$ ), 135.4 (CH), 135.4 ( $\text{C}_q$ ), 132.7 (CH), 132.5 (CH), 128.1 ( $\text{C}_q$ ), 123.6 ( $\text{C}_q$ ), 121.4 (CH), 120.9 (CH), 120.4 (CH), 119.8 (CH), 113.9 (CH), 77.9 (CH), 31.9 ( $\text{CH}_2$ ), 25.6 ( $\text{CH}_2$ ), 24.4 ( $\text{CH}_2$ ), 22.3 ( $\text{CH}_3$ ). IR (ATR): 3293, 2936, 2857, 1656, 1527, 1476, 1289, 1221, 753  $\text{cm}^{-1}$ . MS (ESI)  $m/z$  (relative intensity): 383 (25)  $[\text{M}+\text{Na}]^+$ , 361 (100)  $[\text{M}+\text{H}]^+$ . HR-MS (ESI)  $m/z$  calcd for  $\text{C}_{23}\text{H}_{25}\text{N}_2\text{O}_2$   $[\text{M}+\text{H}]^+$ : 361.1911, found: 361.1913.



#### ***N*-(6-Methylquinolin-8-yl)-2-[(tetrahydrofuran-3-yl)oxy]benzamide (107s)**

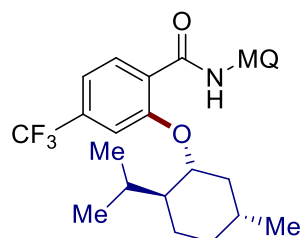
The general procedure **F** was followed using benzamide **106a** (0.25 mmol, 65.5 mg) and tetrahydrofuran-3-ol (**66o**) (220 mg, 2.5 mmol). Purification by column chromatography on silica gel (*n*hexane/EtOAc: 16/1→9/1) yielded **107s** (70.2 mg, 81%) as a white solid. **M.p.**: 113–114 °C.  $^1\text{H}$  NMR (400 MHz,  $\text{CDCl}_3$ )  $\delta = 11.76$  (s, 1H), 8.96 (d,  $J = 1.9$  Hz, 1H), 8.79 (dd,  $J = 4.2, 1.7$  Hz, 1H), 8.36 (dd,  $J = 7.9, 1.9$  Hz, 1H), 8.04 (dd,  $J = 8.2, 1.7$  Hz, 1H), 7.47 (ddd,  $J = 8.4, 7.3, 1.9$  Hz, 1H), 7.39 (dd,  $J = 8.2, 4.2$  Hz, 1H), 7.28 (dq,  $J = 1.9, 1.0$  Hz, 1H), 7.13 (ddd,  $J = 7.9, 7.3, 1.0$  Hz, 1H), 6.98 (dd,  $J = 8.4, 1.0$  Hz, 1H), 5.26–5.17 (m, 1H), 4.54 (dd,  $J = 10.3, 2.3$  Hz, 1H), 4.21 (dd,  $J = 10.3, 5.4$  Hz, 1H), 4.09 (td,  $J = 8.8, 6.3$  Hz, 1H), 3.96 (td,  $J = 8.2, 3.6$  Hz, 1H), 2.55 (d,  $J = 1.0$  Hz, 3H), 2.59–3.53 (m, 1H), 2.32 (dddd,  $J = 13.4, 9.0, 8.0, 6.4$  Hz, 1H).  $^{13}\text{C}$  NMR (101 MHz,  $\text{CDCl}_3$ )  $\delta = 163.7$  ( $\text{C}_q$ ), 155.5 ( $\text{C}_q$ ), 146.9 (CH), 137.9 ( $\text{C}_q$ ), 137.6 ( $\text{C}_q$ ), 135.5 (CH), 135.2 ( $\text{C}_q$ ), 133.1 (CH), 132.9 (CH), 128.1 ( $\text{C}_q$ ), 123.1 ( $\text{C}_q$ ), 121.6 (CH), 121.4 (CH), 120.6 (CH), 119.9 (CH), 112.9 (CH), 79.1 (CH), 72.9 ( $\text{CH}_2$ ), 67.3 ( $\text{CH}_2$ ), 33.2 ( $\text{CH}_2$ ), 22.3 ( $\text{CH}_3$ ). IR (ATR): 3307, 1653, 1525, 1477, 1421, 1290, 1220, 855, 752, 688  $\text{cm}^{-1}$ . MS (ESI)  $m/z$  (relative intensity): 371 (70)  $[\text{M}+\text{Na}]^+$ , 349 (100)  $[\text{M}+\text{H}]^+$ . HR-  
163

**MS** (ESI)  $m/z$  calcd for  $C_{21}H_{21}N_2O_3$   $[M+H]^+$ : 349.1547, found: 349.1550.



***N*-(6-Methylquinolin-8-yl)-2-[(tetrahydro-2*H*-pyran-4-yl)oxy]benzamide (107t)**

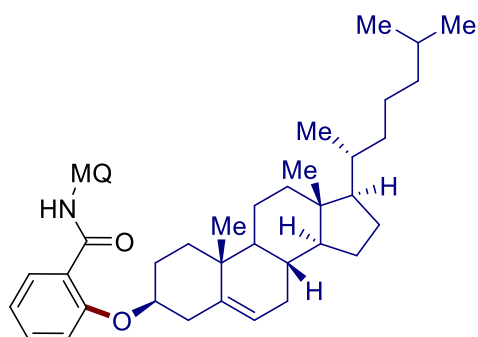
The general procedure **F** was followed using benzamide **106a** (0.25 mmol, 65.5 mg) and tetrahydro-2*H*-pyran-4-ol (**66p**) (255 mg, 2.5 mmol). Purification by column chromatography on silica gel (*n*hexane/EtOAc: 4/1→2/1) yielded **107t** (73.4 mg, 81%) as a white solid. **M.p.**: 145–147 °C. **<sup>1</sup>H NMR** (400 MHz, CDCl<sub>3</sub>)  $\delta$  = 11.81 (s, 1H), 8.94 (d,  $J$  = 1.7 Hz, 1H), 8.76 (dd,  $J$  = 4.3, 1.6 Hz, 1H), 8.28 (dd,  $J$  = 7.8, 1.9 Hz, 1H), 8.05 (dd,  $J$  = 8.3, 1.6 Hz, 1H), 7.45 (ddd,  $J$  = 8.9, 7.5, 1.9 Hz, 1H), 7.40 (dd,  $J$  = 8.3, 4.3 Hz, 1H), 7.30–7.27 (m, 1H), 7.14–7.05 (m, 2H), 4.79 (tt,  $J$  = 8.9, 4.3 Hz, 1H), 4.03 (dt,  $J$  = 11.9, 4.3 Hz, 2H), 3.52 (ddd,  $J$  = 12.1, 9.9, 2.8 Hz, 2H), 2.55 (s, 3H), 2.27 (dtd,  $J$  = 13.5, 9.3, 4.3 Hz, 2H), 2.18–2.09 (m, 2H). **<sup>13</sup>C NMR** (101 MHz, CDCl<sub>3</sub>)  $\delta$  = 164.0 (C<sub>q</sub>), 155.2 (C<sub>q</sub>), 146.9 (CH), 137.8 (C<sub>q</sub>), 137.7 (C<sub>q</sub>), 135.5 (CH), 135.1 (C<sub>q</sub>), 132.8 (CH), 132.7 (CH), 128.1 (C<sub>q</sub>), 124.0 (C<sub>q</sub>), 121.6 (CH), 121.4 (CH), 120.6 (CH), 119.7 (CH), 113.8 (CH), 74.0 (CH), 65.7 (CH<sub>2</sub>), 31.8 (CH<sub>2</sub>), 22.4 (CH<sub>3</sub>). **IR** (ATR): 3295, 2960, 1649, 1524, 1477, 980, 857, 753, 590 cm<sup>-1</sup>. **MS** (EI)  $m/z$  (relative intensity): 363 (5)  $[M+H]^+$ , 362 (15)  $[M]^+$ , 158 (100), 121 (50). **HR-MS** (EI)  $m/z$  calcd for  $C_{22}H_{22}N_2O_3$   $[M]^+$ : 362.1625, found: 362.1632.



**2-[[1*R*,2*S*,5*R*]-2-isopropyl-5-methylcyclohexyl]oxy-*N*-(quinolin-8-yl)-4-(trifluoromethyl)benzamide (107u)**

The general procedure **F** was followed using benzamide **106aj** (0.25 mmol, 82.5 mg) and (1*S*,2*R*,5*S*)-menthol (**66q**) (391 mg, 2.5 mmol). Purification by column

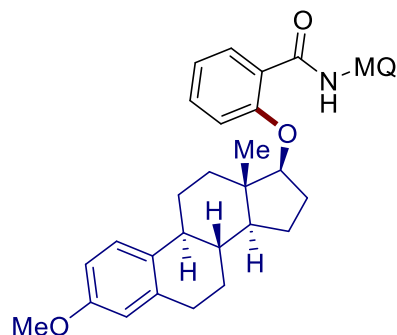
chromatography on silica gel (*n*hexane/acetone: 30/1) yielded **107u** (64.0 mg, 53%) as a white solid. **M.p.**: 87–89 °C. **<sup>1</sup>H NMR** (300 MHz, CDCl<sub>3</sub>)  $\delta$  = 12.07 (s, 1H), 9.00 (d, *J* = 1.7 Hz, 1H), 8.81 (dd, *J* = 4.2, 1.6 Hz, 1H), 8.50 (d, *J* = 8.1 Hz, 1H), 8.12 (dd, *J* = 8.3, 1.6 Hz, 1H), 7.47 (dd, *J* = 8.3, 4.2 Hz, 1H), 7.40–7.35 (m, 3H), 4.50 (td, *J* = 10.2, 4.3 Hz, 1H), 2.61 (s, 3H), 2.36–2.11 (m, 3H), 1.86 (tt, *J* = 10.2, 3.0 Hz, 2H), 1.64 (dt, *J* = 9.0, 5.6 Hz, 2H), 1.34–1.05 (m, 2H), 1.01 (d, *J* = 5.8 Hz, 3H), 0.77 (dd, *J* = 8.6, 6.9 Hz, 6H). **<sup>13</sup>C NMR** (101 MHz, CDCl<sub>3</sub>)  $\delta$  = 162.8 (C<sub>q</sub>), 156.6 (C<sub>q</sub>), 146.9 (CH), 138.0 (C<sub>q</sub>), 137.7 (C<sub>q</sub>), 135.6 (CH), 135.1 (C<sub>q</sub>), 134.5 (q, <sup>2</sup>*J*<sub>C-F</sub> = 32.4 Hz, C<sub>q</sub>), 133.5 (CH), 128.1 (C<sub>q</sub>), 126.3 (C<sub>q</sub>), 123.6 (q, <sup>1</sup>*J*<sub>C-F</sub> = 272.9 Hz, C<sub>q</sub>), 121.6 (CH), 120.9 (CH), 120.0 (CH), 117.4 (q, <sup>3</sup>*J*<sub>C-F</sub> = 3.8 Hz, CH), 110.1 (q, <sup>3</sup>*J*<sub>C-F</sub> = 3.8 Hz, CH), 80.3 (CH), 47.0 (CH), 40.1 (CH<sub>2</sub>), 34.6 (CH<sub>2</sub>), 31.5 (CH), 26.1 (CH), 23.6 (CH<sub>2</sub>), 22.3 (CH<sub>3</sub>), 22.1 (CH<sub>3</sub>), 20.6 (CH<sub>3</sub>), 16.5 (CH<sub>3</sub>). **<sup>19</sup>F NMR** (376 MHz, CDCl<sub>3</sub>)  $\delta$  = -62.9 (s). **IR** (ATR): 3300, 2956, 2927, 1665, 1532, 1325, 1127, 984, 855, 696 cm<sup>-1</sup>. **MS** (ESI) *m/z* (relative intensity): 507 (8) [M+Na]<sup>+</sup>, 485 (100) [M+H]<sup>+</sup>, 347 (10). **HR-MS** (ESI) *m/z* calcd for C<sub>28</sub>H<sub>32</sub>F<sub>3</sub>N<sub>2</sub>O<sub>2</sub> [M+H]<sup>+</sup>: 485.2410, found: 485.2401.



**2-[[[(3*S*,8*S*,10*R*,13*R*,14*S*,17*R*)-10,13-Dimethyl-17-[(*R*)-6-methylheptan-2-yl]-2,3,4,7,8,9,10,11,12,13,14,15,16,17-tetradecahydro-1*H*-cyclopenta-*a*]phenanthren-3-yl]-oxy}-*N*-(6-methylquinolin-8-yl)benzamide (107v)**

The general procedure **F** was followed using benzamide **106a** (0.25 mmol, 65.5 mg) and cholesterol (**66r**) (966 mg, 2.5 mmol). Purification by column chromatography on silica gel (*n*hexane/EtOAc: 20/1→9/1) yielded **107v** (98.6 mg, 61%) as a white solid. **M.p.**: 227–229 °C. **<sup>1</sup>H NMR** (400 MHz, CDCl<sub>3</sub>)  $\delta$  = 11.93 (s, 1H), 8.99 (d, *J* = 1.8 Hz, 1H), 8.75 (dd, *J* = 4.2, 1.7 Hz, 1H), 8.33 (dd, *J* = 7.8, 1.9 Hz, 1H), 8.05 (dd, *J* = 8.2, 1.7 Hz, 1H), 7.44 (ddd, *J* = 8.3, 7.3, 1.9 Hz, 1H), 7.39 (dd, *J* = 8.2, 4.2 Hz, 1H), 7.28

(dq,  $J = 1.8, 1.0$  Hz, 1H), 7.11–7.04 (m, 2H), 5.43 (dt,  $J = 5.5, 1.9$  Hz, 1H), 4.44 (tt,  $J = 11.2, 4.6$  Hz, 1H), 2.90 (tq,  $J = 11.4, 2.7$  Hz, 1H), 2.70–2.64 (m, 1H), 2.55 (d,  $J = 1.0$  Hz, 3H), 2.19 (dt,  $J = 11.0, 3.6$  Hz, 1H), 2.11 (ddd,  $J = 14.4, 11.0, 3.8$  Hz, 1H), 2.06–1.91 (m, 3H), 1.91–1.77 (m, 1H), 1.64–1.41 (m, 8H), 1.45–1.21 (m, 4H), 1.22–1.07 (m, 5H), 1.06 (s, 3H), 1.07–0.91 (m, 3H), 0.91 (d,  $J = 6.5$  Hz, 3H), 0.85 (dd,  $J = 6.6, 1.8$  Hz, 6H), 0.67 (s, 3H).  **$^{13}\text{C}$  NMR** (101 MHz,  $\text{CDCl}_3$ )  $\delta = 164.2$  ( $\text{C}_q$ ), 156.1 ( $\text{C}_q$ ), 146.8 (CH), 140.2 ( $\text{C}_q$ ), 138.0 ( $\text{C}_q$ ), 137.7 ( $\text{C}_q$ ), 135.5 ( $\text{C}_q$ ), 135.5 (CH), 132.9 (CH), 132.7 (CH), 128.2 ( $\text{C}_q$ ), 123.4 ( $\text{C}_q$ ), 122.6 (CH), 121.4 (CH), 121.0 (CH), 120.5 (CH), 119.9 (CH), 114.0 (CH), 79.3 (CH), 56.7 (CH), 56.1 (CH), 50.1 (CH), 42.3 ( $\text{C}_q$ ), 39.7 ( $\text{CH}_2$ ), 39.5 ( $\text{CH}_2$ ), 38.7 ( $\text{CH}_2$ ), 37.3 ( $\text{CH}_2$ ), 36.9 ( $\text{C}_q$ ), 36.2 ( $\text{CH}_2$ ), 35.8 (CH), 32.0 ( $\text{CH}_2$ ), 31.9 (CH), 28.2 ( $\text{CH}_2$ ), 28.1 ( $\text{CH}_2$ ), 28.0 (CH), 24.3 ( $\text{CH}_2$ ), 23.8 ( $\text{CH}_2$ ), 22.8 ( $\text{CH}_3$ ), 22.6 ( $\text{CH}_3$ ), 22.4 ( $\text{CH}_3$ ), 21.1 ( $\text{CH}_2$ ), 19.6 ( $\text{CH}_3$ ), 18.7 ( $\text{CH}_3$ ), 11.8 ( $\text{CH}_3$ ). **IR** (ATR): 3331, 2946, 1655, 1535, 1477, 1221, 1019, 858, 746, 675  $\text{cm}^{-1}$ . **MS** (ESI)  $m/z$  (relative intensity): 669 (15)  $[\text{M}+\text{Na}]^+$ , 647 (100)  $[\text{M}+\text{H}]^+$ . **HR-MS** (ESI)  $m/z$  calcd for  $\text{C}_{44}\text{H}_{59}\text{N}_2\text{O}_2$   $[\text{M}+\text{H}]^+$ : 647.4571, found: 647.4569.

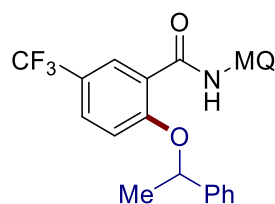


**2-[[*(8R,9S,13S,14S,17S)*-3-Methoxy-13-methyl-7,8,9,11,12,13,14,15,16,17-decahydro-6*H*-cyclopenta[*a*]phenanthren-17-yl]oxy]-*N*-(6-methylquinolin-8-yl)benzamide (107w)**

The general procedure **F** was followed using benzamide **106a** (0.25 mmol, 65.5 mg) and  $\beta$ -estradiol 3-methyl ether (**66s**) (716 mg, 2.5 mmol). Purification by column chromatography on silica gel (*n*hexane/EtOAc: 16/1→9/1) yielded **107w** (88.2 mg, 65%) as a white solid. **M.p.**: 193–195 °C.  **$^1\text{H}$  NMR** (300 MHz,  $\text{CDCl}_3$ )  $\delta = 11.52$  (s, 1H), 9.02 (d,  $J = 1.7$  Hz, 1H), 8.75 (dd,  $J = 4.2, 1.7$  Hz, 1H), 8.27 (dd,  $J = 7.8, 1.9$  Hz, 1H), 8.09 (dd,  $J = 8.3, 1.7$  Hz, 1H), 7.52–7.46 (m, 1H), 7.43 (dd,  $J = 8.3, 4.2$  Hz, 1H), 7.34



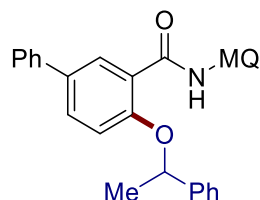
(dq,  $J = 1.9, 1.0$  Hz, 1H), 7.21 (dd,  $J = 8.4, 6.9$  Hz, 2H), 7.16–7.09 (m, 1H), 6.72 (dd,  $J = 8.6, 2.8$  Hz, 1H), 6.64 (d,  $J = 2.8$  Hz, 1H), 4.76 (t,  $J = 8.2$  Hz, 1H), 3.79 (s, 3H), 2.91–2.83 (m, 2H), 2.61 (s, 3H), 2.52–2.21 (m, 4H), 2.17 (dt,  $J = 11.7, 2.7$  Hz, 1H), 1.99–1.78 (m, 1H), 1.63–1.28 (m, 7H), 0.91 (s, 3H).  $^{13}\text{C}$  NMR (101 MHz,  $\text{CDCl}_3$ )  $\delta = 164.6$  ( $\text{C}_q$ ), 157.4 ( $\text{C}_q$ ), 157.0 ( $\text{C}_q$ ), 146.7 (CH), 137.8 ( $\text{C}_q$ ), 137.7 ( $\text{C}_q$ ), 137.6 ( $\text{C}_q$ ), 135.5 (CH), 135.1 ( $\text{C}_q$ ), 132.6 (CH), 132.4 (CH), 132.3 ( $\text{C}_q$ ), 128.2 ( $\text{C}_q$ ), 126.3 (CH), 123.7 ( $\text{C}_q$ ), 121.4 (CH), 120.9 (CH), 120.6 (CH), 120.1 (CH), 114.2 (CH), 113.8 (CH), 111.4 (CH), 87.8 (CH), 55.2 ( $\text{CH}_3$ ), 50.3 (CH), 44.1 ( $\text{C}_q$ ), 43.7 (CH), 38.6 (CH), 38.1 ( $\text{CH}_2$ ), 29.7 ( $\text{CH}_2$ ), 27.9 ( $\text{CH}_2$ ), 27.2 ( $\text{CH}_2$ ), 26.3 ( $\text{CH}_2$ ), 23.4 ( $\text{CH}_2$ ), 22.3 ( $\text{CH}_3$ ), 12.3 ( $\text{CH}_3$ ). IR (ATR): 3273, 2921, 1651, 1530, 1475, 1423, 1252, 760, 696  $\text{cm}^{-1}$ . MS (EI)  $m/z$  (relative intensity): 547 (10)  $[\text{M}+\text{H}]^+$ , 546 (30)  $[\text{M}]^+$ , 262 (10), 158 (100). HR-MS (EI)  $m/z$  calcd for  $\text{C}_{36}\text{H}_{38}\text{N}_2\text{O}_3$   $[\text{M}]^+$ : 546.2877, found: 546.2879.



***N*-(6-Methylquinolin-8-yl)-2-(1-phenylethoxy)-5-(trifluoromethyl)benzamide (107aa)**

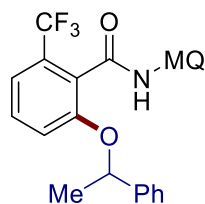
The general procedure **F** was followed using benzamide **106aa** (0.25 mmol, 82.5 mg) and 1-phenylethan-1-ol (**66a**) (305 mg, 2.5 mmol). Purification by column chromatography on silica gel (*n*hexane/EtOAc: 16/1) yielded **107aa** (81.5 mg, 72%) as a white solid. **M.p.**: 136–137 °C.  $^1\text{H}$  NMR (400 MHz,  $\text{CDCl}_3$ )  $\delta = 12.08$  (s, 1H), 8.99 (d,  $J = 1.7$  Hz, 1H), 8.70 (dd,  $J = 4.2, 1.7$  Hz, 1H), 8.60 (dd,  $J = 2.5, 0.8$  Hz, 1H), 8.08 (dd,  $J = 8.3, 1.7$  Hz, 1H), 7.62–7.56 (m, 2H), 7.52 (ddd,  $J = 8.7, 2.5, 0.8$  Hz, 1H), 7.40 (dd,  $J = 8.3, 4.2$  Hz, 1H), 7.37–7.32 (m, 3H), 7.30–7.25 (m, 1H), 6.98 (d,  $J = 8.7$  Hz, 1H), 5.66 (q,  $J = 6.4$  Hz, 1H), 2.59 (d,  $J = 0.9$  Hz, 3H), 1.99 (d,  $J = 6.4$  Hz, 3H).  $^{13}\text{C}$  NMR (101 MHz,  $\text{CDCl}_3$ )  $\delta = 162.6$  ( $\text{C}_q$ ), 158.1 ( $\text{C}_q$ ), 146.9 (CH), 141.6 ( $\text{C}_q$ ), 137.8 ( $\text{C}_q$ ), 137.7 ( $\text{C}_q$ ), 135.6 (CH), 135.0 ( $\text{C}_q$ ), 130.1 (q,  $^3J_{\text{C-F}} = 3.8$  Hz, CH), 129.6 (q,  $^3J_{\text{C-F}} = 3.5$  Hz, CH), 129.0 (CH), 128.1 (CH), 128.1 ( $\text{C}_q$ ), 125.5 (CH), 123.9 (q,  $^1J_{\text{C-F}} = 271.7$  Hz,  $\text{C}_q$ ), 123.4 ( $\text{C}_q$ ), 123.3 (q,  $^2J_{\text{C-F}} = 33.3$  Hz,  $\text{C}_q$ ), 121.6 (CH), 120.9 (CH), 120.0 (CH), 114.3

(CH), 78.6 (CH), 25.0 (CH<sub>3</sub>), 22.4 (CH<sub>3</sub>). **<sup>19</sup>F NMR** (282 MHz, CDCl<sub>3</sub>)  $\delta$  = -61.9 (s). **IR** (ATR): 3307, 1660, 1529, 1329, 1270, 1114, 1066, 738, 700 cm<sup>-1</sup>. **MS** (ESI) *m/z* (relative intensity): 473 (10) [M+Na]<sup>+</sup>, 451 (100) [M+H]<sup>+</sup>, 347 (45), 105 (40). **HR-MS** (ESI) *m/z* calcd for C<sub>26</sub>H<sub>22</sub>F<sub>3</sub>N<sub>2</sub>O<sub>2</sub> [M+H]<sup>+</sup>: 451.1628, found: 451.1640.



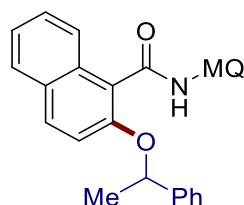
***N*-(6-methylquinolin-8-yl)-4-(1-phenylethoxy)-[1,1'-biphenyl]-3-carboxamide (107ab)**

The general procedure **F** was followed using benzamide **106ab** (0.25 mmol, 84.5 mg) and 1-phenylethan-1-ol (**66a**) (305 mg, 2.5 mmol). Purification by column chromatography on silica gel (*n*hexane/acetone: 20/1) yielded **107ab** (65.5 mg, 57%) as a white solid. **M.p.**: 120–122 °C. **<sup>1</sup>H NMR** (400 MHz, CDCl<sub>3</sub>)  $\delta$  = 12.22 (s, 1H), 9.09 (d, *J* = 1.8 Hz, 1H), 8.75 (dd, *J* = 4.2, 1.7 Hz, 1H), 8.63 (d, *J* = 2.6 Hz, 1H), 8.12 (dd, *J* = 8.2, 1.7 Hz, 1H), 7.67–7.61 (m, 4H), 7.57 (dd, *J* = 8.6, 2.6 Hz, 1H), 7.47–7.43 (m, 2H), 7.43–7.36 (m, 4H), 7.36–7.29 (m, 2H), 7.02 (d, *J* = 8.6 Hz, 1H), 5.70 (q, *J* = 6.5 Hz, 1H), 2.64 (d, *J* = 0.9 Hz, 3H), 2.02 (d, *J* = 6.5 Hz, 3H). **<sup>13</sup>C NMR** (101 MHz, CDCl<sub>3</sub>)  $\delta$  = 164.1 (C<sub>q</sub>), 155.5 (C<sub>q</sub>), 146.9 (CH), 142.5 (C<sub>q</sub>), 139.8 (C<sub>q</sub>), 138.0 (C<sub>q</sub>), 137.8 (C<sub>q</sub>), 135.6 (CH), 135.5 (C<sub>q</sub>), 133.9 (C<sub>q</sub>), 131.1 (CH), 131.0 (CH), 128.9 (CH), 128.8 (CH), 128.2 (C<sub>q</sub>), 127.9 (CH), 127.0 (CH), 126.7 (CH), 125.7 (CH), 123.2 (C<sub>q</sub>), 121.6 (CH), 120.6 (CH), 119.9 (CH), 114.5 (CH), 78.1 (CH), 25.1 (CH<sub>3</sub>), 22.4 (CH<sub>3</sub>). **IR** (ATR): 3303, 2924, 1656, 1525, 1422, 1266, 1067, 760, 735, 698 cm<sup>-1</sup>. **MS** (ESI) *m/z* (relative intensity): 481 (15) [M+Na]<sup>+</sup>, 459 (100) [M+H]<sup>+</sup>, 352 (30). **HR-MS** (ESI) *m/z* calcd for C<sub>31</sub>H<sub>27</sub>N<sub>2</sub>O<sub>2</sub> [M+H]<sup>+</sup>: 459.2067, found: 459.2069.



***N*-(6-Methylquinolin-8-yl)-2-(1-phenylethoxy)-6-(trifluoromethyl)benzamide (107ac)**

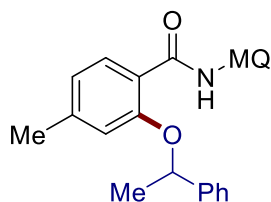
The general procedure **F** was followed using benzamide **106ac** (0.25 mmol, 82.5 mg) and 1-phenylethan-1-ol (**66a**) (305 mg, 2.5 mmol). Purification by column chromatography on silica gel (*n*hexane/acetone: 16/1) yielded **107ac** (72.2 mg, 64%) as a white solid. **M.p.**: 126–128 °C. **<sup>1</sup>H NMR** (400 MHz, CDCl<sub>3</sub>)  $\delta$  = 10.11 (s, 1H), 8.88 (d,  $J$  = 1.7 Hz, 1H), 8.72 (dd,  $J$  = 4.2, 1.6 Hz, 1H), 8.11 (dd,  $J$  = 8.3, 1.6 Hz, 1H), 7.46–7.39 (m, 3H), 7.37 (td,  $J$  = 2.0, 1.0 Hz, 1H), 7.34 (dd,  $J$  = 8.1, 1.0 Hz, 1H), 7.31–7.26 (m, 3H), 7.26–7.21 (m, 1H), 7.03 (d,  $J$  = 8.1 Hz, 1H), 5.40 (q,  $J$  = 6.5 Hz, 1H), 2.64 (d,  $J$  = 1.0 Hz, 3H), 1.53 (d,  $J$  = 6.5 Hz, 3H). **<sup>13</sup>C NMR** (101 MHz, CDCl<sub>3</sub>)  $\delta$  = 163.6 (C<sub>q</sub>), 155.2 (C<sub>q</sub>), 147.2 (CH), 142.1 (C<sub>q</sub>), 137.8 (C<sub>q</sub>), 137.2 (C<sub>q</sub>), 135.6 (CH), 134.1 (C<sub>q</sub>), 130.4 (CH), 129.2 (q,  $^2J_{C-F}$  = 31.8 Hz, C<sub>q</sub>), 128.7 (CH), 128.1 (C<sub>q</sub>), 127.7 (CH), 126.2 (q,  $^3J_{C-F}$  = 2.2 Hz, C<sub>q</sub>), 125.5 (CH), 123.5 (q,  $^1J_{C-F}$  = 274.2 Hz, C<sub>q</sub>), 121.7 (CH), 120.9 (CH), 119.0 (CH), 118.2 (q,  $^3J_{C-F}$  = 5.0 Hz, CH), 117.6 (CH), 77.5 (CH), 24.5 (CH<sub>3</sub>), 22.4 (CH<sub>3</sub>). **<sup>19</sup>F NMR** (376 MHz, CDCl<sub>3</sub>)  $\delta$  = -59.2 (s). **IR** (ATR): 3343, 1684, 1527, 1318, 1268, 1131, 701 cm<sup>-1</sup>. **MS** (ESI)  $m/z$  (relative intensity): 473 (90) [M+Na]<sup>+</sup>, 451 (100) [M+H]<sup>+</sup>. **HR-MS** (ESI)  $m/z$  calcd for C<sub>26</sub>H<sub>22</sub>F<sub>3</sub>N<sub>2</sub>O<sub>2</sub> [M+H]<sup>+</sup>: 451.1628, found: 451.1625.



#### ***N*-(6-Methylquinolin-8-yl)-2-(1-phenylethoxy)-1-naphthamide (107ad)**

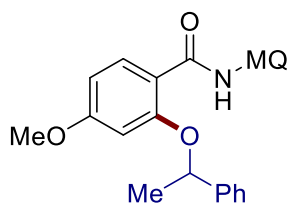
The general procedure **F** was followed using benzamide **106ad** (0.25 mmol, 78.0 mg) and 1-phenylethan-1-ol (**66a**) (305 mg, 2.5 mmol). Purification by column chromatography on silica gel (*n*hexane/EtOAc: 16/1→9/1) yielded **107ad** (92.3 mg, 86%) as a white solid. **M.p.**: 155–157 °C. **<sup>1</sup>H NMR** (400 MHz, CDCl<sub>3</sub>)  $\delta$  = 10.47 (s, 1H), 9.05 (d,  $J$  = 1.8 Hz, 1H), 8.65 (dd,  $J$  = 4.2, 1.7 Hz, 1H), 8.19 (dq,  $J$  = 8.6, 1.0 Hz, 1H), 8.07 (dd,  $J$  = 8.3, 1.7 Hz, 1H), 7.77–7.72 (m, 2H), 7.51–7.44 (m, 3H), 7.40–7.31 (m, 3H), 7.27–7.21 (m, 2H), 7.21–7.14 (m, 2H), 5.52 (q,  $J$  = 6.4 Hz, 1H), 2.64 (d,  $J$  = 1.0 Hz, 3H), 1.57 (d,  $J$  = 6.4 Hz, 3H). **<sup>13</sup>C NMR** (101 MHz, CDCl<sub>3</sub>)  $\delta$  = 165.9 (C<sub>q</sub>), 152.4 (C<sub>q</sub>), 147.1 (CH), 142.8 (C<sub>q</sub>), 137.7 (C<sub>q</sub>), 137.3 (C<sub>q</sub>), 135.5 (CH), 134.6 (C<sub>q</sub>), 131.9 (C<sub>q</sub>),

131.2 (CH), 128.9 (C<sub>q</sub>), 128.6 (CH), 128.1 (C<sub>q</sub>), 127.9 (CH), 127.5 (CH), 127.4 (CH), 125.7 (CH), 124.7 (CH), 124.2 (CH), 121.7 (C<sub>q</sub>), 121.6 (CH), 120.6 (CH), 118.7 (CH), 115.6 (CH), 77.8 (CH), 24.5 (CH<sub>3</sub>), 22.4 (CH<sub>3</sub>). **IR** (ATR): 3351, 1669, 1525, 1424, 1246, 1070, 701 cm<sup>-1</sup>. **MS** (ESI) *m/z* (relative intensity): 455 (10) [M+Na]<sup>+</sup>, 433 (100) [M+H]<sup>+</sup>, 329 (45), 159 (50). **HR-MS** (ESI) *m/z* calcd for C<sub>29</sub>H<sub>25</sub>N<sub>2</sub>O<sub>2</sub> [M+H]<sup>+</sup>: 433.1911, found: 433.1907.



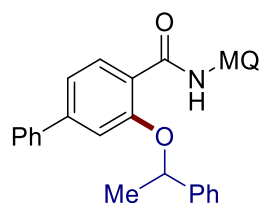
#### 4-Methyl-*N*-(6-methylquinolin-8-yl)-2-(1-phenylethoxy)benzamide (107ae)

The general procedure **F** was followed using benzamide **106ae** (0.25 mmol, 69.0 mg) and 1-phenylethan-1-ol (**66a**) (305 mg, 2.5 mmol). Purification by column chromatography on silica gel (*n*hexane/EtOAc: 16/1→9/1) yielded **107ae** (54.4 mg, 55%) as a white solid. **M.p.**: 160–162 °C. **<sup>1</sup>H NMR** (400 MHz, CDCl<sub>3</sub>) δ = 12.12 (s, 1H), 9.01 (d, *J* = 1.8 Hz, 1H), 8.67 (dd, *J* = 4.2, 1.7 Hz, 1H), 8.19 (d, *J* = 8.0 Hz, 1H), 8.05 (dd, *J* = 8.2, 1.7 Hz, 1H), 7.62–7.57 (m, 2H), 7.37 (dd, *J* = 8.2, 4.2 Hz, 1H), 7.35–7.30 (m, 2H), 7.30–7.29 (m, 1H), 7.28–7.20 (m, 1H), 6.84 (ddd, *J* = 8.0, 1.5, 0.8 Hz, 1H), 6.77–6.68 (m, 1H), 5.62 (q, *J* = 6.5 Hz, 1H), 2.58 (d, *J* = 1.0 Hz, 3H), 2.25 (d, *J* = 0.8 Hz, 3H), 1.94 (d, *J* = 6.5 Hz, 3H). **<sup>13</sup>C NMR** (101 MHz, CDCl<sub>3</sub>) δ = 164.2 (C<sub>q</sub>), 156.0 (C<sub>q</sub>), 146.7 (CH), 143.5 (C<sub>q</sub>), 142.5 (C<sub>q</sub>), 138.0 (C<sub>q</sub>), 137.7 (C<sub>q</sub>), 135.6 (C<sub>q</sub>), 135.4 (CH), 132.4 (CH), 128.8 (CH), 128.1 (C<sub>q</sub>), 127.7 (CH), 125.7 (CH), 122.0 (CH), 121.4 (CH), 120.4 (C<sub>q</sub>), 120.4 (CH), 119.7 (CH), 114.7 (CH), 77.7 (CH), 25.0 (CH<sub>3</sub>), 22.4 (CH<sub>3</sub>), 21.7 (CH<sub>3</sub>). **IR** (ATR): 3305, 1655, 1528, 1423, 1286, 1258, 1067, 762, 701 cm<sup>-1</sup>. **MS** (ESI) *m/z* (relative intensity): 419 (10) [M+Na]<sup>+</sup>, 397 (100) [M+H]<sup>+</sup>, 293 (70), 159 (40). **HR-MS** (ESI) *m/z* calcd for C<sub>26</sub>H<sub>25</sub>N<sub>2</sub>O<sub>2</sub> [M+H]<sup>+</sup>: 397.1911, found: 397.1909.



#### 4-Methoxy-*N*-(6-methylquinolin-8-yl)-2-(1-phenylethoxy)benzamide (107af)

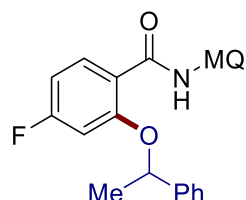
The general procedure **F** was followed using benzamide **106af** (0.25 mmol, 73.0 mg) and 1-phenylethan-1-ol (**66a**) (305 mg, 2.5 mmol). Purification by column chromatography on silica gel (*n*hexane/EtOAc: 16/1→9/1) yielded **107af** (74.4 mg, 72%) as a white solid. **M.p.**: 130–131 °C. **<sup>1</sup>H NMR** (300 MHz, CDCl<sub>3</sub>)  $\delta$  = 12.10 (s, 1H), 9.05 (d, *J* = 1.8 Hz, 1H), 8.72 (dd, *J* = 4.2, 1.7 Hz, 1H), 8.31 (d, *J* = 8.8 Hz, 1H), 8.09 (dd, *J* = 8.3, 1.7 Hz, 1H), 7.68–7.59 (m, 2H), 7.41 (dd, *J* = 7.7, 3.7 Hz, 1H), 7.38 (d, *J* = 5.7 Hz, 1H), 7.37–7.32 (m, 2H), 7.32–7.26 (m, 1H), 6.59 (dd, *J* = 8.8, 2.3 Hz, 1H), 6.47 (d, *J* = 2.3 Hz, 1H), 5.62 (q, *J* = 6.4 Hz, 1H), 3.74 (s, 3H), 2.61 (d, *J* = 0.9 Hz, 3H), 2.01 (d, *J* = 6.4 Hz, 3H). **<sup>13</sup>C NMR** (101 MHz, CDCl<sub>3</sub>)  $\delta$  = 164.0 (C<sub>q</sub>), 163.3 (C<sub>q</sub>), 157.4 (C<sub>q</sub>), 146.7 (CH), 142.4 (C<sub>q</sub>), 138.1 (C<sub>q</sub>), 137.7 (C<sub>q</sub>), 135.7 (C<sub>q</sub>), 135.5 (CH), 134.1 (CH), 128.9 (CH), 128.2 (C<sub>q</sub>), 127.9 (CH), 125.7 (CH), 121.5 (CH), 120.3 (CH), 119.7 (CH), 116.0 (C<sub>q</sub>), 105.7 (CH), 100.9 (CH), 78.0 (CH), 55.3 (CH<sub>3</sub>), 25.1 (CH<sub>3</sub>), 22.4 (CH<sub>3</sub>). **IR** (ATR): 3308, 1651, 1523, 1476, 1261, 1247, 1168, 701 cm<sup>-1</sup>. **MS** (ESI) *m/z* (relative intensity): 435 (10) [M+Na]<sup>+</sup>, 413 (100) [M+H]<sup>+</sup>, 309 (30). **HR-MS** (ESI) *m/z* calcd for C<sub>26</sub>H<sub>25</sub>N<sub>2</sub>O<sub>3</sub> [M+H]<sup>+</sup>: 413.1860, found: 413.1865.



***N*-(6-Methylquinolin-8-yl)-3-(1-phenylethoxy)-(1,1'-biphenyl)-4-carboxamide  
(107ag)**

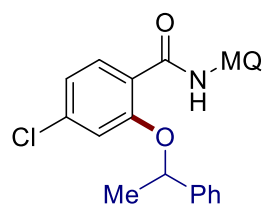
The general procedure **F** was followed using benzamide **106ag** (0.25 mmol, 84.5 mg) and 1-phenylethan-1-ol (**66a**) (305 mg, 2.5 mmol). Purification by column chromatography on silica gel (*n*hexane/acetone: 16/1→9/1) yielded **107ag** (75 mg, 66%) as a white solid. **M.p.**: 161–162 °C. **<sup>1</sup>H NMR** (400 MHz, CDCl<sub>3</sub>)  $\delta$  = 12.21 (s, 1H), 9.07 (d, *J* = 1.7 Hz, 1H), 8.75 (dd, *J* = 4.2, 1.7 Hz, 1H), 8.39 (d, *J* = 8.1 Hz, 1H), 8.12 (dd, *J* = 8.3, 1.7 Hz, 1H), 7.73–7.61 (m, 2H), 7.47–7.42 (m, 5H), 7.40–7.35 (m, 4H), 7.36–7.26 (m, 2H), 7.18 (d, *J* = 1.5 Hz, 1H), 5.75 (q, *J* = 6.4 Hz, 1H), 2.63 (d, *J* = 0.9 Hz, 3H), 2.04 (d, *J* = 6.4 Hz, 3H). **<sup>13</sup>C NMR** (101 MHz, CDCl<sub>3</sub>)  $\delta$  = 164.0 (C<sub>q</sub>), 156.3 (C<sub>q</sub>), 146.8 (CH), 145.6 (C<sub>q</sub>), 142.5 (C<sub>q</sub>), 140.1 (C<sub>q</sub>), 138.1 (C<sub>q</sub>), 137.8 (C<sub>q</sub>), 135.5 (CH), 135.5 (C<sub>q</sub>), 133.0 (CH), 128.9 (CH), 128.8 (CH), 128.2 (C<sub>q</sub>), 128.0 (CH), 127.9 (CH),

127.1 (CH), 125.8 (CH), 121.8 (C<sub>q</sub>), 121.5 (CH), 120.6 (CH), 119.9 (CH), 119.8 (CH), 113.0 (CH), 78.1 (CH), 25.0 (CH<sub>3</sub>), 22.4 (CH<sub>3</sub>). **IR** (ATR): 3305, 1655, 1529, 1475, 1422, 1199, 854, 756, 697 cm<sup>-1</sup>. **MS** (ESI) *m/z* (relative intensity): 481 (15) [M+Na]<sup>+</sup>, 459 (100) [M+H]<sup>+</sup>. **HR-MS** (ESI) *m/z* calcd for C<sub>31</sub>H<sub>27</sub>N<sub>2</sub>O<sub>2</sub> [M+H]<sup>+</sup>: 459.2067, found: 459.2067.



#### 4-Fluoro-*N*-(6-methylquinolin-8-yl)-2-(1-phenylethoxy)benzamide (107ah)

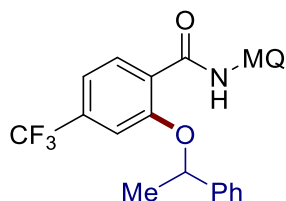
The general procedure **F** was followed using benzamide **106ah** (0.25 mmol, 70.0 mg) and 1-phenylethan-1-ol (**66a**) (305 mg, 2.5 mmol). Purification by column chromatography on silica gel (*n*hexane/EtOAc: 16/1→9/1) yielded **107ah** (81.1 mg, 81%) as a white solid. **M.p.**: 157–159 °C. **<sup>1</sup>H NMR** (400 MHz, CDCl<sub>3</sub>) δ = 12.08 (s, 1H), 9.02 (d, *J* = 1.8 Hz, 1H), 8.73 (dd, *J* = 4.2, 1.7 Hz, 1H), 8.35 (dd, *J* = 8.8, 7.1 Hz, 1H), 8.11 (dd, *J* = 8.2, 1.7 Hz, 1H), 7.65–7.60 (m, 2H), 7.43 (dd, *J* = 8.2, 4.2 Hz, 1H), 7.41–7.34 (m, 3H), 7.34–7.29 (m, 1H), 6.76 (ddd, *J* = 8.8, 7.6, 2.4 Hz, 1H), 6.66 (dd, *J* = 10.9, 2.4 Hz, 1H), 5.59 (q, *J* = 6.4 Hz, 1H), 2.62 (d, *J* = 0.9 Hz, 3H), 2.01 (d, *J* = 6.4 Hz, 3H). **<sup>13</sup>C NMR** (101 MHz, CDCl<sub>3</sub>) δ = 165.3 (d, <sup>1</sup>*J*<sub>C-F</sub> = 252.0 Hz, C<sub>q</sub>), 163.2 (C<sub>q</sub>), 157.4 (d, <sup>3</sup>*J*<sub>C-F</sub> = 10.7 Hz, C<sub>q</sub>), 146.9 (CH), 141.7 (C<sub>q</sub>), 138.0 (C<sub>q</sub>), 137.7 (C<sub>q</sub>), 135.6 (CH), 135.4 (C<sub>q</sub>), 134.4 (d, <sup>3</sup>*J*<sub>C-F</sub> = 10.7 Hz, CH), 129.0 (CH), 128.2 (C<sub>q</sub>), 128.1 (CH), 125.7 (CH), 121.6 (CH), 120.6 (CH), 119.9 (CH), 119.4 (d, <sup>4</sup>*J*<sub>C-F</sub> = 3.0 Hz, C<sub>q</sub>), 108.1 (d, <sup>2</sup>*J*<sub>C-F</sub> = 21.4 Hz, CH), 102.0 (d, <sup>2</sup>*J*<sub>C-F</sub> = 26.4 Hz, CH), 78.6 (CH), 25.0 (CH<sub>3</sub>), 22.4 (CH<sub>3</sub>). **<sup>19</sup>F NMR** (376 MHz, CDCl<sub>3</sub>) δ = -105.3 (s). **IR** (ATR): 3309, 1657, 1528, 1477, 1428, 1261, 997, 836, 701 cm<sup>-1</sup>. **MS** (ESI) *m/z* (relative intensity): 423 (15) [M+Na]<sup>+</sup>, 401 (100) [M+H]<sup>+</sup>, 297 (75), 159 (35), 105 (30). **HR-MS** (ESI) *m/z* calcd for C<sub>25</sub>H<sub>22</sub>FN<sub>2</sub>O<sub>2</sub> [M+H]<sup>+</sup>: 401.1660, found: 401.1660.



#### 4-Chloro-*N*-(6-methylquinolin-8-yl)-2-(1-phenylethoxy)benzamide (107ai)

The general procedure **F** was followed using benzamide **106ai** (0.25 mmol, 74.0 mg)

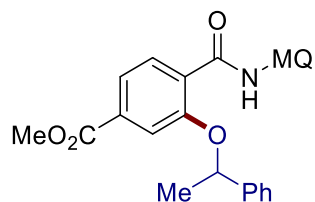
and 1-phenylethan-1-ol (**66a**) (305 mg, 2.5 mmol) at 3 mA for 32 h. Purification by column chromatography on silica gel (*n*hexane/EtOAc: 16/1→9/1) yielded **107ai** (67.3 mg, 65%) as a white solid. **M.p.**: 115–117 °C. **<sup>1</sup>H NMR** (400 MHz, CDCl<sub>3</sub>) δ = 12.08 (s, 1H), 9.01 (d, *J* = 1.8 Hz, 1H), 8.72 (dd, *J* = 4.2, 1.7 Hz, 1H), 8.27 (d, *J* = 8.5 Hz, 1H), 8.11 (dd, *J* = 8.3, 1.7 Hz, 1H), 7.68–7.60 (m, 2H), 7.43 (dd, *J* = 8.3, 4.2 Hz, 1H), 7.41–7.35 (m, 3H), 7.34–7.29 (m, 1H), 7.05 (dd, *J* = 8.5, 1.9 Hz, 1H), 6.95 (d, *J* = 1.9 Hz, 1H), 5.63 (q, *J* = 6.4 Hz, 1H), 2.62 (d, *J* = 0.9 Hz, 3H), 2.00 (d, *J* = 6.4 Hz, 3H). **<sup>13</sup>C NMR** (101 MHz, CDCl<sub>3</sub>) δ = 163.2 (C<sub>q</sub>), 156.4 (C<sub>q</sub>), 146.9 (CH), 141.7 (C<sub>q</sub>), 138.4 (C<sub>q</sub>), 138.0 (C<sub>q</sub>), 137.7 (C<sub>q</sub>), 135.6 (CH), 135.3 (C<sub>q</sub>), 133.6 (CH), 129.0 (CH), 128.2 (C<sub>q</sub>), 128.1 (CH), 125.7 (CH), 121.7 (C<sub>q</sub>), 121.6 (CH), 121.5 (CH), 120.8 (CH), 119.9 (CH), 114.6 (CH), 78.5 (CH), 25.0 (CH<sub>3</sub>), 22.4 (CH<sub>3</sub>). **IR** (ATR): 3306, 1662, 1531, 1475, 1426, 1229, 948, 855, 701 cm<sup>-1</sup>. **MS** (ESI) *m/z* (relative intensity): 439 (5) [M+Na]<sup>+</sup>, 417 (100) [M+H]<sup>+</sup>, 313 (30), 263 (30). **HR-MS** (ESI) *m/z* calcd for C<sub>25</sub>H<sub>22</sub>ClN<sub>2</sub>O<sub>2</sub> [M+H]<sup>+</sup>: 417.1364, found: 417.1372.



***N*-(6-Methylquinolin-8-yl)-2-(1-phenylethoxy)-4-(trifluoromethyl)benzamide  
(107aj)**

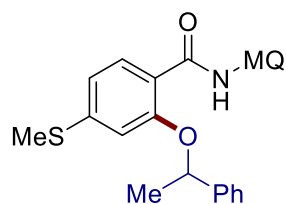
The general procedure **F** was followed using benzamide **106aj** (0.25 mmol, 82.5 mg) and 1-phenylethan-1-ol (**66a**) (305 mg, 2.5 mmol). Purification by column chromatography on silica gel (*n*hexane/acetone: 16/1) yielded **107aj** (93.5 mg, 83%) as a white solid. **M.p.**: 153–154 °C. **<sup>1</sup>H NMR** (400 MHz, CDCl<sub>3</sub>) δ = 12.13 (s, 1H), 9.02 (d, *J* = 1.7 Hz, 1H), 8.75 (dd, *J* = 4.2, 1.7 Hz, 1H), 8.43 (dd, *J* = 8.2, 1.0 Hz, 1H), 8.13 (dd, *J* = 8.2, 1.7 Hz, 1H), 7.68–7.61 (m, 2H), 7.45 (dd, *J* = 8.2, 4.2 Hz, 1H), 7.41–7.35 (m, 3H), 7.35–7.29 (m, 2H), 7.22 (d, *J* = 1.5 Hz, 1H), 5.70 (q, *J* = 6.4 Hz, 1H), 2.63 (d, *J* = 0.9 Hz, 3H), 2.02 (d, *J* = 6.4 Hz, 3H). **<sup>13</sup>C NMR** (101 MHz, CDCl<sub>3</sub>) δ = 162.8 (C<sub>q</sub>), 155.9 (C<sub>q</sub>), 147.0 (CH), 141.4 (C<sub>q</sub>), 137.9 (C<sub>q</sub>), 137.7 (C<sub>q</sub>), 135.6 (CH), 135.0 (C<sub>q</sub>), 134.0 (q, <sup>2</sup>*J*<sub>C-F</sub> = 32.4 Hz, C<sub>q</sub>), 133.2 (CH), 129.0 (CH), 128.2 (CH), 128.2 (C<sub>q</sub>), 126.3

(C<sub>q</sub>), 125.8 (CH), 123.4 (q, <sup>1</sup>J<sub>C-F</sub> = 272.8 Hz, C<sub>q</sub>), 121.7 (CH), 121.0 (CH), 120.0 (CH), 117.7 (q, <sup>3</sup>J<sub>C-F</sub> = 3.8 Hz, CH), 111.2 (q, <sup>3</sup>J<sub>C-F</sub> = 3.9 Hz, CH), 78.7 (CH), 24.8 (CH<sub>3</sub>), 22.4 (CH<sub>3</sub>). **<sup>19</sup>F NMR** (376 MHz, CDCl<sub>3</sub>) δ = -63.2 (s). **IR** (ATR): 3297, 1655, 1531, 1424, 1320, 1163, 1116, 952, 852, 702 cm<sup>-1</sup>. **MS** (ESI) *m/z* (relative intensity): 473 (10) [M+Na]<sup>+</sup>, 451 (100) [M+H]<sup>+</sup>, 347 (50), 105 (20). **HR-MS** (ESI) *m/z* calcd for C<sub>26</sub>H<sub>22</sub>F<sub>3</sub>N<sub>2</sub>O<sub>2</sub> [M+H]<sup>+</sup>: 451.1628, found: 451.1628.



#### Methyl 4-[(6-methylquinolin-8-yl)carbamoyl]-3-(1-phenylethoxy)benzoate (**107ak**)

The general procedure **F** was followed using benzamide **106ak** (0.25 mmol, 80.0 mg) and 1-phenylethan-1-ol (**66a**) (305 mg, 2.5 mmol). Purification by column chromatography on silica gel (*n*hexane/acetone: 10/1) yielded **107ak** (62.3 mg, 57%) as a white solid. **M.p.**: 178–180 °C. **<sup>1</sup>H NMR** (400 MHz, CDCl<sub>3</sub>) δ = 12.18 (s, 1H), 9.03 (d, *J* = 1.8 Hz, 1H), 8.74 (dd, *J* = 4.2, 1.7 Hz, 1H), 8.37 (d, *J* = 8.5 Hz, 1H), 8.12 (dd, *J* = 8.2, 1.7 Hz, 1H), 7.77–7.60 (m, 4H), 7.44 (dd, *J* = 8.2, 4.2 Hz, 1H), 7.38–7.32 (m, 3H), 7.32–7.26 (m, 1H), 5.77 (q, *J* = 6.4 Hz, 1H), 3.91 (s, 3H), 2.63 (s, 3H), 2.01 (d, *J* = 6.4 Hz, 3H). **<sup>13</sup>C NMR** (101 MHz, CDCl<sub>3</sub>) δ = 166.2 (C<sub>q</sub>), 163.2 (C<sub>q</sub>), 155.7 (C<sub>q</sub>), 147.0 (CH), 141.8 (C<sub>q</sub>), 138.0 (C<sub>q</sub>), 137.7 (C<sub>q</sub>), 135.6 (CH), 135.2 (C<sub>q</sub>), 133.8 (C<sub>q</sub>), 132.6 (CH), 128.9 (CH), 128.2 (C<sub>q</sub>), 128.0 (CH), 127.0 (C<sub>q</sub>), 125.9 (CH), 121.8 (CH), 121.6 (CH), 120.9 (CH), 120.0 (CH), 115.3 (CH), 78.2 (CH), 52.4 (CH<sub>3</sub>), 24.8 (CH<sub>3</sub>), 22.4 (CH<sub>3</sub>). **IR** (ATR): 3292, 1721, 1656, 1529, 1434, 1283, 1216, 1009, 738, 704 cm<sup>-1</sup>. **MS** (ESI) *m/z* (relative intensity): 463 (10) [M+Na]<sup>+</sup>, 441 (100) [M+H]<sup>+</sup>, 337 (55), 159 (15), 105 (10). **HR-MS** (ESI) *m/z* calcd for C<sub>27</sub>H<sub>25</sub>N<sub>2</sub>O<sub>4</sub> [M+H]<sup>+</sup>: 441.1809, found: 441.1810.

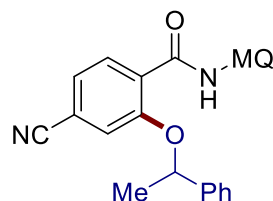


#### *N*-(6-Methylquinolin-8-yl)-4-(methylthio)-2-(1-phenylethoxy)benzamide (**107al**)

The general procedure **F** was followed using benzamide **106al** (0.25 mmol, 77.0 mg)



and 1-phenylethan-1-ol (**66a**) (305 mg, 2.5 mmol). Purification by column chromatography on silica gel (*n*hexane/acetone: 10/1) yielded **107aI** (56.2 mg, 53%) as a white solid. **M.p.**: 120–122 °C. **<sup>1</sup>H NMR** (400 MHz, CDCl<sub>3</sub>)  $\delta$  = 12.10 (s, 1H), 9.03 (d, *J* = 1.8 Hz, 1H), 8.73 (dd, *J* = 4.2, 1.7 Hz, 1H), 8.25 (d, *J* = 8.3 Hz, 1H), 8.10 (dd, *J* = 8.2, 1.7 Hz, 1H), 7.67–7.59 (m, 2H), 7.42 (dd, *J* = 8.2, 4.2 Hz, 1H), 7.38 (dd, *J* = 8.3, 6.7 Hz, 2H), 7.34 (d, *J* = 1.4 Hz, 1H), 7.33–7.29 (m, 1H), 6.90 (dd, *J* = 8.3, 1.7 Hz, 1H), 6.76 (d, *J* = 1.8 Hz, 1H), 5.63 (q, *J* = 6.5 Hz, 1H), 2.61 (d, *J* = 0.9 Hz, 3H), 2.37 (s, 3H), 2.00 (d, *J* = 6.5 Hz, 3H). **<sup>13</sup>C NMR** (101 MHz, CDCl<sub>3</sub>)  $\delta$  = 163.8 (C<sub>q</sub>), 156.1 (C<sub>q</sub>), 146.8 (CH), 144.8 (C<sub>q</sub>), 142.3 (C<sub>q</sub>), 138.0 (C<sub>q</sub>), 137.7 (C<sub>q</sub>), 135.5 (CH), 135.5 (C<sub>q</sub>), 132.7 (CH), 129.0 (CH), 128.2 (C<sub>q</sub>), 128.0 (CH), 125.7 (CH), 121.5 (CH), 120.5 (CH), 119.8 (CH), 119.5 (C<sub>q</sub>), 118.0 (CH), 111.0 (CH), 78.2 (CH), 25.0 (CH<sub>3</sub>), 22.4 (CH<sub>3</sub>), 14.9 (CH<sub>3</sub>). **IR** (ATR): 3307, 1655, 1528, 1478, 1423, 1222, 950, 702 cm<sup>-1</sup>. **MS** (ESI) *m/z* (relative intensity): 451 (10) [M+Na]<sup>+</sup>, 429 (100) [M+H]<sup>+</sup>, 325 (20). **HR-MS** (ESI) *m/z* calcd for C<sub>26</sub>H<sub>25</sub>N<sub>2</sub>O<sub>2</sub>S [M+H]<sup>+</sup>: 429.1631, found: 429.1637.

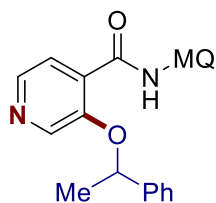


#### 4-Cyano-*N*-(6-methylquinolin-8-yl)-2-(1-phenylethoxy)benzamide (**107am**)

The general procedure **F** was followed using benzamide **106am** (0.25 mmol, 71.8 mg) and 1-phenylethan-1-ol (**66a**) (305 mg, 2.5 mmol). Purification by column chromatography on silica gel (*n*hexane/EtOAc: 16/1→9/1) yielded **107am** (57.0 mg, 56%) as a white solid. **M.p.**: 214–216 °C. **<sup>1</sup>H NMR** (400 MHz, CDCl<sub>3</sub>)  $\delta$  = 12.10 (s, 1H), 8.99 (d, *J* = 1.7 Hz, 1H), 8.74 (dd, *J* = 4.2, 1.7 Hz, 1H), 8.40 (d, *J* = 8.0 Hz, 1H), 8.13 (dd, *J* = 8.2, 1.7 Hz, 1H), 7.65–7.60 (m, 2H), 7.45 (dd, *J* = 8.2, 4.2 Hz, 1H), 7.43–7.37 (m, 3H), 7.36–7.31 (m, 2H), 7.18 (d, *J* = 1.3 Hz, 1H), 5.64 (q, *J* = 6.4 Hz, 1H), 2.63 (d, *J* = 0.9 Hz, 3H), 2.01 (d, *J* = 6.4 Hz, 3H). **<sup>13</sup>C NMR** (101 MHz, CDCl<sub>3</sub>)  $\delta$  = 162.2 (C<sub>q</sub>), 155.8 (C<sub>q</sub>), 147.0 (CH), 141.1 (C<sub>q</sub>), 137.9 (C<sub>q</sub>), 137.7 (C<sub>q</sub>), 135.7 (CH), 134.8 (C<sub>q</sub>), 133.4 (CH), 129.2 (CH), 128.4 (CH), 128.2 (C<sub>q</sub>), 127.4 (C<sub>q</sub>), 125.6 (CH), 124.6 (CH), 121.7 (CH), 121.2 (CH), 120.1 (CH), 118.1 (C<sub>q</sub>), 117.5 (CH), 115.7 (C<sub>q</sub>), 79.0 (CH),

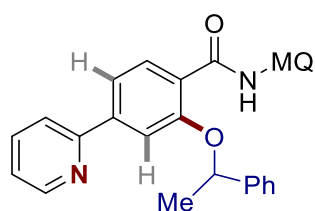
25.0 (CH<sub>3</sub>), 22.4 (CH<sub>3</sub>). **IR** (ATR): 3306, 2230, 1664, 1533, 1426, 1282, 854, 702 cm<sup>-1</sup>.

**MS** (ESI) *m/z* (relative intensity): 430 (10) [M+Na]<sup>+</sup>, 408 (100) [M+H]<sup>+</sup>, 117 (50). **HR-MS** (ESI) *m/z* calcd for C<sub>26</sub>H<sub>22</sub>N<sub>3</sub>O<sub>2</sub> [M+H]<sup>+</sup>: 408.1707, found: 408.1710.



#### ***N*-(6-Methylquinolin-8-yl)-3-(1-phenylethoxy)isonicotinamide (107an)**

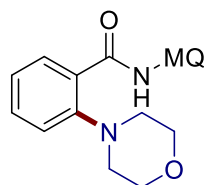
The general procedure **F** was followed using benzamide **106an** (0.25 mmol, 65.8 mg) and 1-phenylethan-1-ol (**66a**) (305 mg, 2.5 mmol). Purification by column chromatography on silica gel (*n*hexane/EtOAc: 9/1→4/1) yielded **107an** (52.5 mg, 55%) as a white solid. **M.p.**: 156–158 °C. **<sup>1</sup>H NMR** (400 MHz, CDCl<sub>3</sub>) δ = 12.13 (s, 1H), 9.00 (d, *J* = 1.9 Hz, 1H), 8.76 (dd, *J* = 4.2, 1.7 Hz, 1H), 8.43 (s, 1H), 8.36 (d, *J* = 4.9 Hz, 1H), 8.18–8.09 (m, 2H), 7.62 (dd, *J* = 7.4, 1.9 Hz, 2H), 7.45 (dd, *J* = 8.2, 4.2 Hz, 1H), 7.42–7.34 (m, 3H), 7.33–7.25 (m, 1H), 5.79 (q, *J* = 6.4 Hz, 1H), 2.62 (s, 3H), 2.04 (d, *J* = 6.4 Hz, 3H). **<sup>13</sup>C NMR** (101 MHz, CDCl<sub>3</sub>) δ = 162.0 (C<sub>q</sub>), 150.9 (C<sub>q</sub>), 147.1 (CH), 143.0 (CH), 141.4 (C<sub>q</sub>), 137.9 (C<sub>q</sub>), 137.7 (C<sub>q</sub>), 137.6 (CH), 135.6 (CH), 134.8 (C<sub>q</sub>), 129.3 (C<sub>q</sub>), 129.1 (CH), 128.3 (CH), 128.2 (C<sub>q</sub>), 125.7 (CH), 124.7 (CH), 121.7 (CH), 121.3 (CH), 120.1 (CH), 78.8 (CH), 25.1 (CH<sub>3</sub>), 22.4 (CH<sub>3</sub>). **IR** (ATR): 3298, 1663, 1528, 1424, 1224, 1064, 844, 734, 696 cm<sup>-1</sup>. **MS** (ESI) *m/z* (relative intensity): 406 (40) [M+Na]<sup>+</sup>, 384 (100) [M+H]<sup>+</sup>. **HR-MS** (ESI) *m/z* calcd for C<sub>24</sub>H<sub>22</sub>N<sub>3</sub>O<sub>2</sub> [M+H]<sup>+</sup>: 384.1707, found: 384.1706.



#### ***N*-(6-Methylquinolin-8-yl)-2-(1-phenylethoxy)-4-(pyridin-2-yl)benzamide (107ao)**

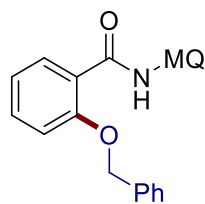
The general procedure **F** was followed using benzamide **106ao** (0.25 mmol, 84.8 mg) and 1-phenylethan-1-ol (**66a**) (305 mg, 2.5 mmol). Purification by column chromatography on silica gel (*n*hexane/EtOAc: 9/1) yielded **107ao** (61.0 mg, 53%) as a white solid. **M.p.**: 165–167 °C. **<sup>1</sup>H NMR** (400 MHz, CDCl<sub>3</sub>) δ = 12.25 (s, 1H), 9.07 (d,

$J = 1.8$  Hz, 1H), 8.73 (dd,  $J = 4.2, 1.7$  Hz, 1H), 8.71 (ddd,  $J = 4.8, 1.9, 0.9$  Hz, 1H), 8.43 (d,  $J = 8.2$  Hz, 1H), 8.11 (dd,  $J = 8.3, 1.7$  Hz, 1H), 7.77 (d,  $J = 1.5$  Hz, 1H), 7.74 (dd,  $J = 7.9, 6.1$  Hz, 1H), 7.72 (d,  $J = 1.5$  Hz, 1H), 7.70 (t,  $J = 1.2$  Hz, 1H), 7.64 (dd,  $J = 8.2, 1.6$  Hz, 1H), 7.61 (dt,  $J = 8.0, 1.1$  Hz, 1H), 7.43 (dd,  $J = 8.2, 4.2$  Hz, 1H), 7.38–7.32 (m, 3H), 7.31–7.21 (m, 2H), 5.90 (q,  $J = 6.4$  Hz, 1H), 2.63 (d,  $J = 0.9$  Hz, 3H), 2.03 (d,  $J = 6.4$  Hz, 3H).  **$^{13}\text{C}$  NMR** (101 MHz,  $\text{CDCl}_3$ )  $\delta = 163.9$  ( $\text{C}_q$ ), 156.4 ( $\text{C}_q$ ), 156.1 ( $\text{C}_q$ ), 149.7 (CH), 146.9 (CH), 143.5 ( $\text{C}_q$ ), 142.4 ( $\text{C}_q$ ), 138.1 ( $\text{C}_q$ ), 137.7 ( $\text{C}_q$ ), 136.8 (CH), 135.5 (CH), 135.5 ( $\text{C}_q$ ), 133.0 (CH), 128.8 (CH), 128.2 ( $\text{C}_q$ ), 127.8 (CH), 125.9 (CH), 123.3 ( $\text{C}_q$ ), 122.7 (CH), 121.5 (CH), 120.8 (CH), 120.6 (CH), 119.9 (CH), 119.3 (CH), 112.8 (CH), 77.9 (CH), 24.8 ( $\text{CH}_3$ ), 22.4 ( $\text{CH}_3$ ). **IR** (ATR): 3230, 2909, 1655, 1525, 1438, 1422, 1199, 763, 732, 700  $\text{cm}^{-1}$ . **MS** (ESI)  $m/z$  (relative intensity): 482 (35)  $[\text{M}+\text{Na}]^+$ , 460 (100)  $[\text{M}+\text{H}]^+$ , 356 (45). **HR-MS** (ESI)  $m/z$  calcd for  $\text{C}_{30}\text{H}_{26}\text{N}_3\text{O}_2$   $[\text{M}+\text{H}]^+$ : 460.2020, found: 460.2020.



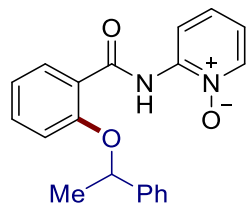
#### ***N*-(6-Methylquinolin-8-yl)-2-morpholinobenzamide (107ap)**

**107ap**: White solid. **M.p.**: 168–170 °C.  **$^1\text{H}$  NMR** (400 MHz,  $\text{CDCl}_3$ )  $\delta = 12.64$  (s, 1H), 9.03 (d,  $J = 1.7$  Hz, 1H), 8.82 (dd,  $J = 4.2, 1.7$  Hz, 1H), 8.20 (dd,  $J = 8.0, 1.8$  Hz, 1H), 8.11 (dd,  $J = 8.2, 1.7$  Hz, 1H), 7.56–7.50 (m, 1H), 7.46 (dd,  $J = 8.2, 4.2$  Hz, 1H), 7.35–7.34 (m, 1H), 7.32–7.23 (m, 2H), 4.03–3.92 (m, 4H), 3.26–3.12 (m, 4H), 2.61 (d,  $J = 0.9$  Hz, 3H).  **$^{13}\text{C}$  NMR** (101 MHz,  $\text{CDCl}_3$ )  $\delta = 165.7$  ( $\text{C}_q$ ), 151.1 ( $\text{C}_q$ ), 147.2 (CH), 137.7 ( $\text{C}_q$ ), 137.6 ( $\text{C}_q$ ), 135.7 (CH), 135.1 ( $\text{C}_q$ ), 132.3 (CH), 132.1 (CH), 128.9 ( $\text{C}_q$ ), 128.4 ( $\text{C}_q$ ), 124.3 (CH), 121.7 (CH), 120.8 (CH), 119.8 (CH), 119.2 (CH), 66.2 ( $\text{CH}_2$ ), 53.9 ( $\text{CH}_2$ ), 22.4 ( $\text{CH}_3$ ). **IR** (ATR): 2958, 2830, 1659, 1521, 1478, 1114, 919, 763, 704  $\text{cm}^{-1}$ . **MS** (ESI)  $m/z$  (relative intensity): 370 (45)  $[\text{M}+\text{Na}]^+$ , 348 (100)  $[\text{M}+\text{H}]^+$ . **HR-MS** (ESI)  $m/z$  calcd for  $\text{C}_{21}\text{H}_{22}\text{N}_3\text{O}_2$   $[\text{M}+\text{H}]^+$ : 348.1707, found: 348.1711.



### 2-(Benzyloxy)-*N*-(6-methylquinolin-8-yl)benzamide (**107aq**)

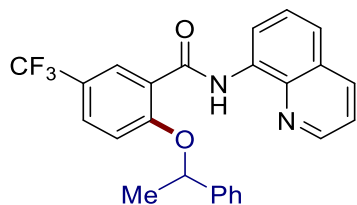
**107aq**: White solid. **M.p.**: 104–106 °C. **<sup>1</sup>H NMR** (400 MHz, CDCl<sub>3</sub>)  $\delta$  = 12.22 (s, 1H), 8.92 (d,  $J$  = 1.8 Hz, 1H), 8.40 (dd,  $J$  = 4.2, 1.7 Hz, 1H), 8.32 (dd,  $J$  = 7.8, 1.8 Hz, 1H), 8.01 (dd,  $J$  = 8.2, 1.7 Hz, 1H), 7.57–7.52 (m, 2H), 7.40 (ddd,  $J$  = 8.3, 7.3, 1.9 Hz, 1H), 7.33–7.24 (m, 5H), 7.13–7.07 (m, 1H), 7.05 (dd,  $J$  = 8.4, 1.0 Hz, 1H), 5.49 (s, 2H), 2.56 (d,  $J$  = 1.0 Hz, 3H). **<sup>13</sup>C NMR** (101 MHz, CDCl<sub>3</sub>)  $\delta$  = 163.8 (C<sub>q</sub>), 156.6 (C<sub>q</sub>), 147.0 (CH), 137.7 (C<sub>q</sub>), 137.6 (C<sub>q</sub>), 136.3 (C<sub>q</sub>), 135.4 (CH), 135.1 (C<sub>q</sub>), 132.8 (CH), 132.3 (CH), 128.6 (CH), 128.0 (CH), 128.0 (C<sub>q</sub>), 127.5 (CH), 123.2 (C<sub>q</sub>), 121.5 (CH), 121.3 (CH), 120.4 (CH), 119.5 (CH), 113.4 (CH), 71.1 (CH<sub>2</sub>), 22.3 (CH<sub>3</sub>). **IR** (ATR): 3277, 1655, 1526, 1475, 1424, 1209, 1001, 853, 732, 691 cm<sup>-1</sup>. **MS** (ESI)  $m/z$  (relative intensity): 391 (10) [M+Na]<sup>+</sup>, 369 (10) [M+H]<sup>+</sup>. **HR-MS** (ESI)  $m/z$  calcd for C<sub>24</sub>H<sub>21</sub>N<sub>2</sub>O<sub>2</sub> [M+H]<sup>+</sup>: 369.1598, found: 369.1599.



### 2-[2-(1-Phenylethoxy)benzamido]pyridine 1-oxide (**107D**)

**107D** was prepared according to the known method<sup>[129e]</sup> using benzamide **106D** (0.20 mmol, 1.0 equiv, 42.8 mg) and 1-phenylethan-1-ol (**66a**) (1.5 mL, 12.4 mmol). Purification by column chromatography on silica gel (CH<sub>2</sub>Cl<sub>2</sub>/acetone: 10/1) yielded **107D** (6.7 mg, 10%) as a white solid. **M.p.**: 179–180 °C. **<sup>1</sup>H NMR** (400 MHz, CDCl<sub>3</sub>)  $\delta$  = 12.39 (s, 1H), 8.77 (d,  $J$  = 8.6 Hz, 1H), 8.30 (s, 1H), 8.23 (dd,  $J$  = 7.9, 1.9 Hz, 1H), 7.53–7.41 (m, 2H), 7.43–7.26 (m, 4H), 7.23 (t,  $J$  = 7.3 Hz, 1H), 6.99 (t,  $J$  = 7.6 Hz, 2H), 6.89 (d,  $J$  = 8.4 Hz, 1H), 5.58 (q,  $J$  = 6.5 Hz, 1H), 1.97 (d,  $J$  = 6.5 Hz, 3H). **<sup>13</sup>C NMR** (101 MHz, CDCl<sub>3</sub>)  $\delta$  = 164.1 (C<sub>q</sub>), 156.4 (C<sub>q</sub>), 145.4 (C<sub>q</sub>), 141.8 (C<sub>q</sub>), 137.4 (CH), 134.0 (CH), 132.6 (CH), 128.9 (CH), 127.9 (CH), 127.7 (CH), 125.7 (CH), 121.0 (CH), 120.9 (C<sub>q</sub>), 118.5 (CH), 115.9 (CH), 114.3 (CH), 78.2 (CH), 24.8 (CH<sub>3</sub>). **IR** (ATR): 3214, 1668, 178

1562, 1504, 1477, 1426, 1234, 752, 701  $\text{cm}^{-1}$ . **MS** (ESI)  $m/z$  (relative intensity): 357 (75)  $[\text{M}+\text{Na}]^+$ , 335 (100)  $[\text{M}+\text{H}]^+$ , 231 (90). **HR-MS** (ESI)  $m/z$  calcd for  $\text{C}_{20}\text{H}_{19}\text{N}_2\text{O}_3$   $[\text{M}+\text{H}]^+$ : 335.1390, found: 335.1395.



### 2-(1-Phenylethoxy)-N-(quinolin-8-yl)-5-(trifluoromethyl)benzamide (**107G**)

**107G** was prepared according to the known method<sup>[124b]</sup> using benzamide **35n** (0.5 mmol, 1.0 equiv, 158 mg) and 1-phenylethan-1-ol (**66a**) (305 mg, 2.5 mmol). Purification by column chromatography on silica gel (*n*hexane/acetone: 16/1→9/1) yielded **107G** (42.0 mg, 19%) as a white solid. **M.p.**: 118–120 °C. **<sup>1</sup>H NMR** (400 MHz,  $\text{CDCl}_3$ )  $\delta$  = 12.13 (s, 1H), 9.10 (dd,  $J$  = 7.5, 1.5 Hz, 1H), 8.78 (dd,  $J$  = 4.2, 1.7 Hz, 1H), 8.60 (dd,  $J$  = 2.5, 0.8 Hz, 1H), 8.19 (dd,  $J$  = 8.3, 1.7 Hz, 1H), 7.66–7.55 (m, 4H), 7.52 (ddd,  $J$  = 8.7, 2.5, 0.8 Hz, 1H), 7.45 (dd,  $J$  = 8.3, 4.2 Hz, 1H), 7.39–7.32 (m, 2H), 7.31–7.25 (m, 1H), 6.98 (d,  $J$  = 8.7 Hz, 1H), 5.67 (q,  $J$  = 6.4 Hz, 1H), 2.00 (d,  $J$  = 6.4 Hz, 3H). **<sup>13</sup>C NMR** (101 MHz,  $\text{CDCl}_3$ )  $\delta$  = 162.6 ( $\text{C}_q$ ), 158.1 ( $\text{C}_q$ ), 147.8 (CH), 141.6 ( $\text{C}_q$ ), 139.2 ( $\text{C}_q$ ), 136.4 (CH), 135.5 ( $\text{C}_q$ ), 130.2 (q,  $^3J_{\text{C-F}}$  = 3.8 Hz, CH), 129.6 (q,  $^3J_{\text{C-F}}$  = 3.6 Hz, CH), 129.1 (CH), 128.2 (CH), 128.1 ( $\text{C}_q$ ), 127.6 (CH), 125.5 (CH), 123.9 (d,  $^1J_{\text{C-F}}$  = 271.7 Hz,  $\text{C}_q$ ), 123.4 ( $\text{C}_q$ ), 123.4 (q,  $^2J_{\text{C-F}}$  = 33.5 Hz,  $\text{C}_q$ ), 122.0 (CH), 121.6 (CH), 117.9 (CH), 114.3 (CH), 78.6 (CH), 25.1 ( $\text{CH}_3$ ). **<sup>19</sup>F NMR** (282 MHz,  $\text{CDCl}_3$ )  $\delta$  = -61.9 (s). **IR** (ATR): 3308, 1662, 1529, 1325, 1271, 1120, 824, 701  $\text{cm}^{-1}$ . **MS** (ESI)  $m/z$  (relative intensity): 459 (10)  $[\text{M}+\text{Na}]^+$ , 437 (100)  $[\text{M}+\text{H}]^+$ , 333 (35). **HR-MS** (ESI)  $m/z$  calcd for  $\text{C}_{25}\text{H}_{20}\text{F}_3\text{N}_2\text{O}_2$   $[\text{M}+\text{H}]^+$ : 437.1471, found: 437.1477.

## 5.3.5.2 Mechanistic Studies

## Competitive Experiment

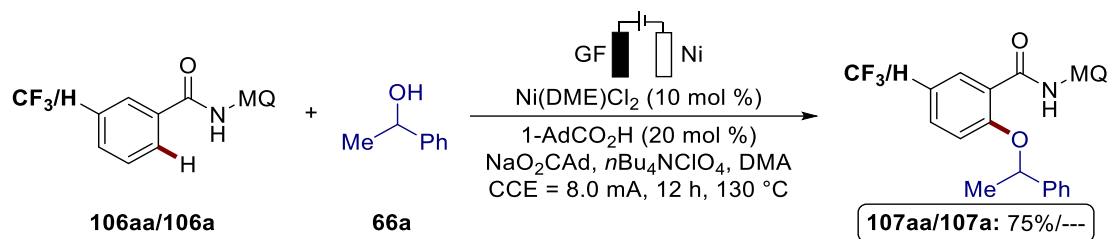


**Figure 5.3.17.** Competitive experiment between arenes **106**.

The general procedure **F** was followed using benzamides **106a** (65.5 mg, 0.25 mmol) and **106aa** (82.5 mg, 0.25 mmol) and 1-phenylethanol (**66a**) (305 mg, 2.5 mmol). Electrolysis was carried out at 130 °C and a constant current of 8.0 mA was maintained for 12 h. After cooling to ambient temperature, 1,3,5-trimethoxybenzene (0.25 mmol) was added as the internal standard to determine the  $^1\text{H}$  NMR yield.

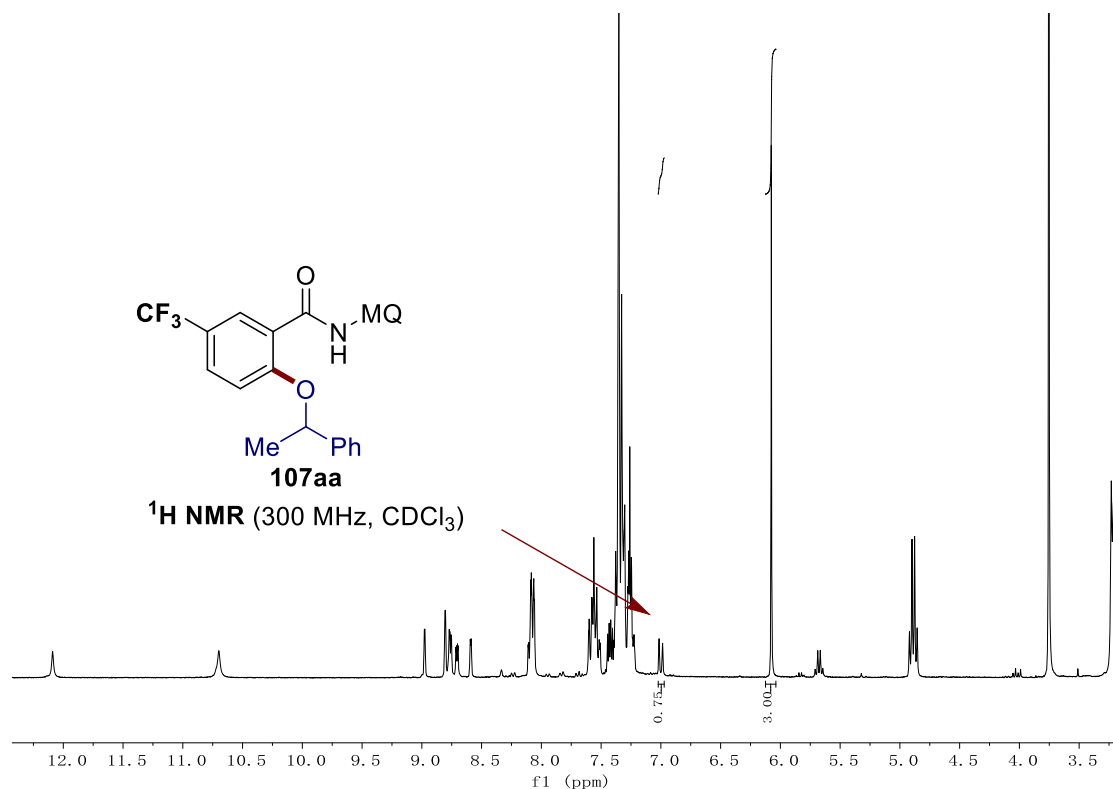


**Figure 5.3.18.** Crude  $^1\text{H}$  NMR spectroscopy of competition experiment between arene **106a** and **106aa**.

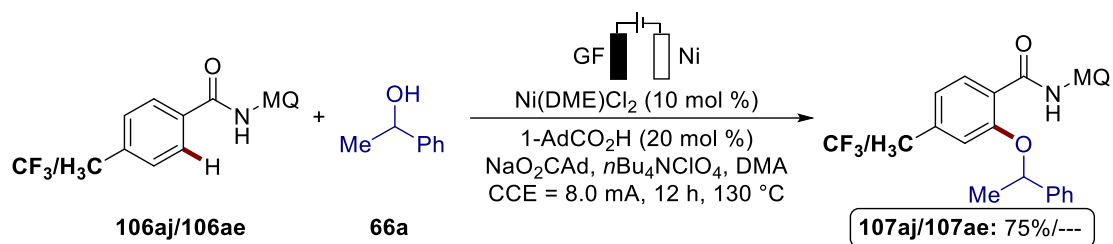


**Figure 5.3.19.** Competition experiment between arene **106aj** and **106ae**.

The general procedure **F** was followed using benzamides **106ae** (69.5 mg, 0.25 mmol) and **106aj** (82.5 mg, 0.25 mmol) and 1-phenylethan-1-ol (**66a**) (305 mg, 2.5 mmol). Electrolysis was carried out at 130 °C and a constant current of 8.0 mA was maintained for 12 h. After cooling to ambient temperature, 1,3,5-trimethoxybenzene (0.25 mmol) was added as the internal standard to determine the <sup>1</sup>H NMR yield.

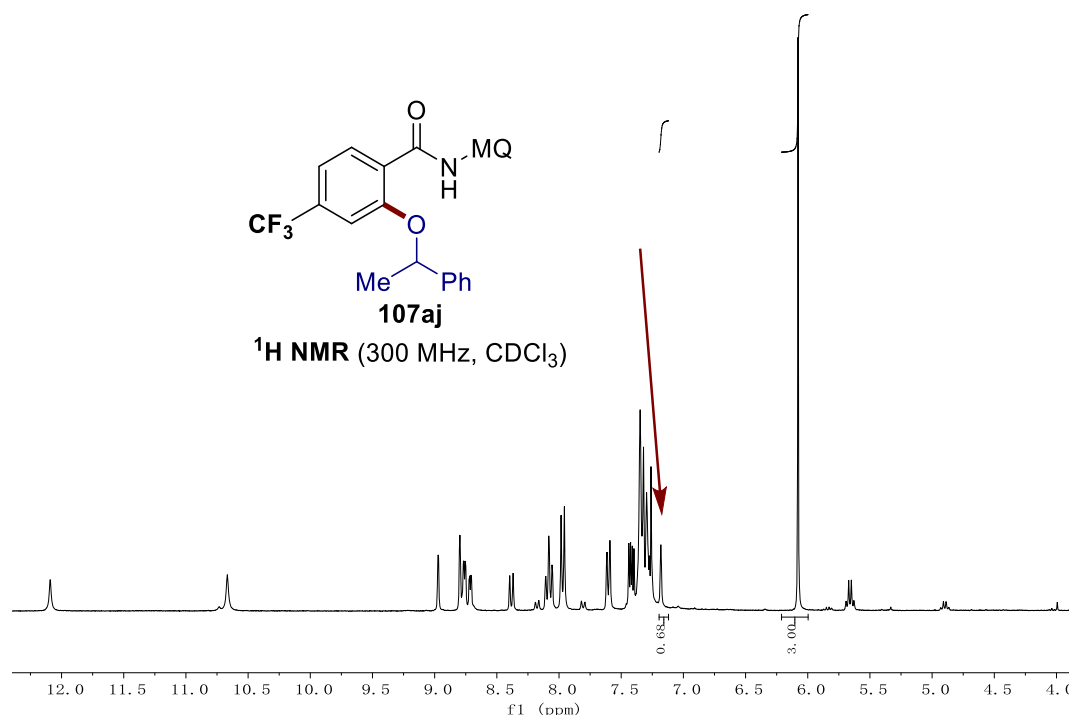


**Figure 5.3.20.** Crude <sup>1</sup>H NMR spectroscopy of competition experiment between arene **106aj** and **106ae**.

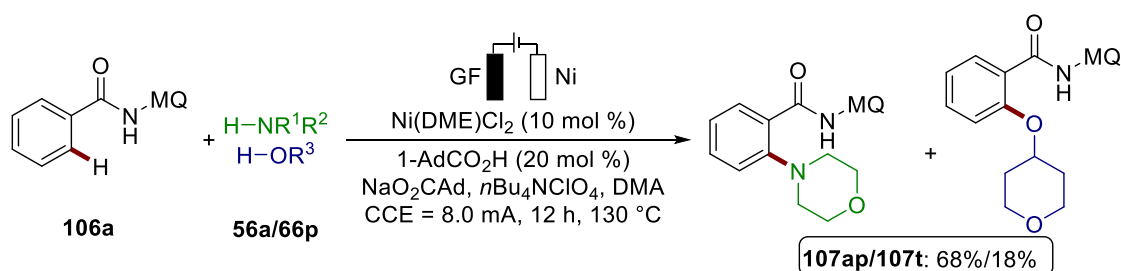


**Figure 5.3.21.** Competition experiment between alcohol **66p** and amine **56a**.

## 5. Experimental Section

The general procedure **F** was followed using benzamide **106a** (65.5 mg, 0.25 mmol), tetrahydro-2*H*-pyran-4-ol (**66p**) (128 mg, 1.25 mmol) and morpholine (**56a**) (109 mg, 1.25 mmol). Electrolysis was carried out at 130 °C and a constant current of 8.0 mA was maintained for 12 h. After cooling to ambient temperature, 1,3,5-trimethoxybenzene (0.25 mmol) was added as the internal standard to determine the <sup>1</sup>H NMR yield. **107ap** and **107t** were purified by column chromatography on silica gel (*n*hexane/EtOAc: 10/1→4/1) yielded **107t** (15.6 mg, 17%) as a white solid and **107ap** (52.9 mg, 61%) as a white solid.

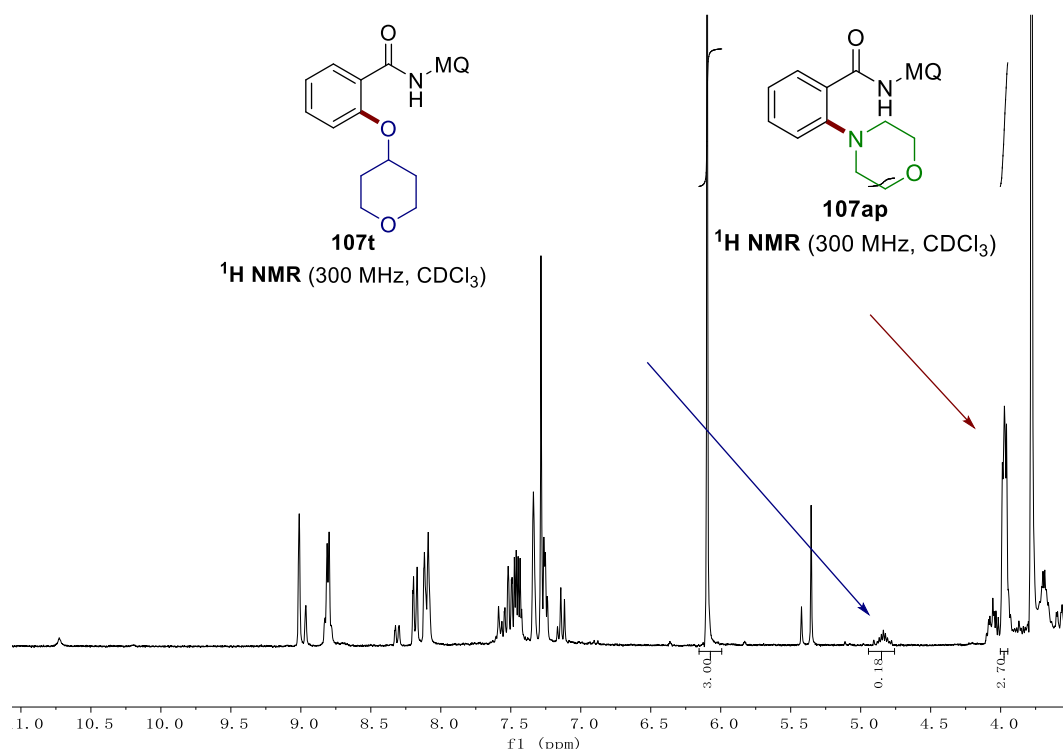


**Figure 5.3.22.** Crude <sup>1</sup>H NMR spectroscopy of competition experiment between alcohol **66p** and amine **56a**.

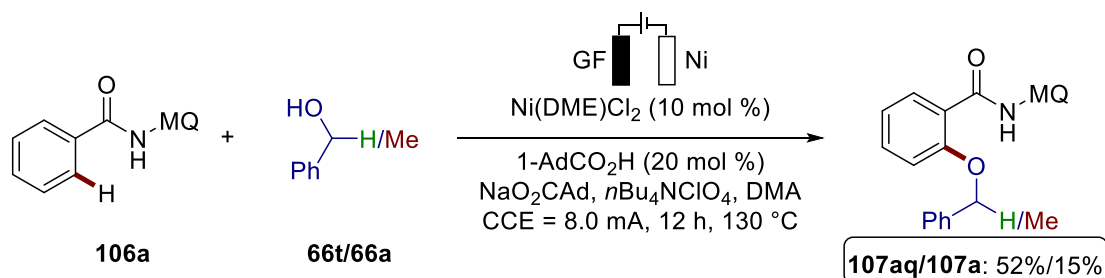


**Figure 5.3.23.** Competition experiment between primary alcohol **66** and secondary alcohol **106**.

The general procedure **F** was followed using benzamides **106a** (65.5 mg, 0.25 mmol), 1-phenylethan-1-ol (**66a**) (153 mg, 1.25 mmol) and phenylmethanol (**66t**) (135 mg, 182



1.25 mmol). Electrolysis was carried out at 130 °C and a constant current of 8.0 mA was maintained for 12 h. After cooling to ambient temperature, CH<sub>2</sub>Br<sub>2</sub> (0.25 mmol) was added as the internal standard to determine the <sup>1</sup>H NMR yield.

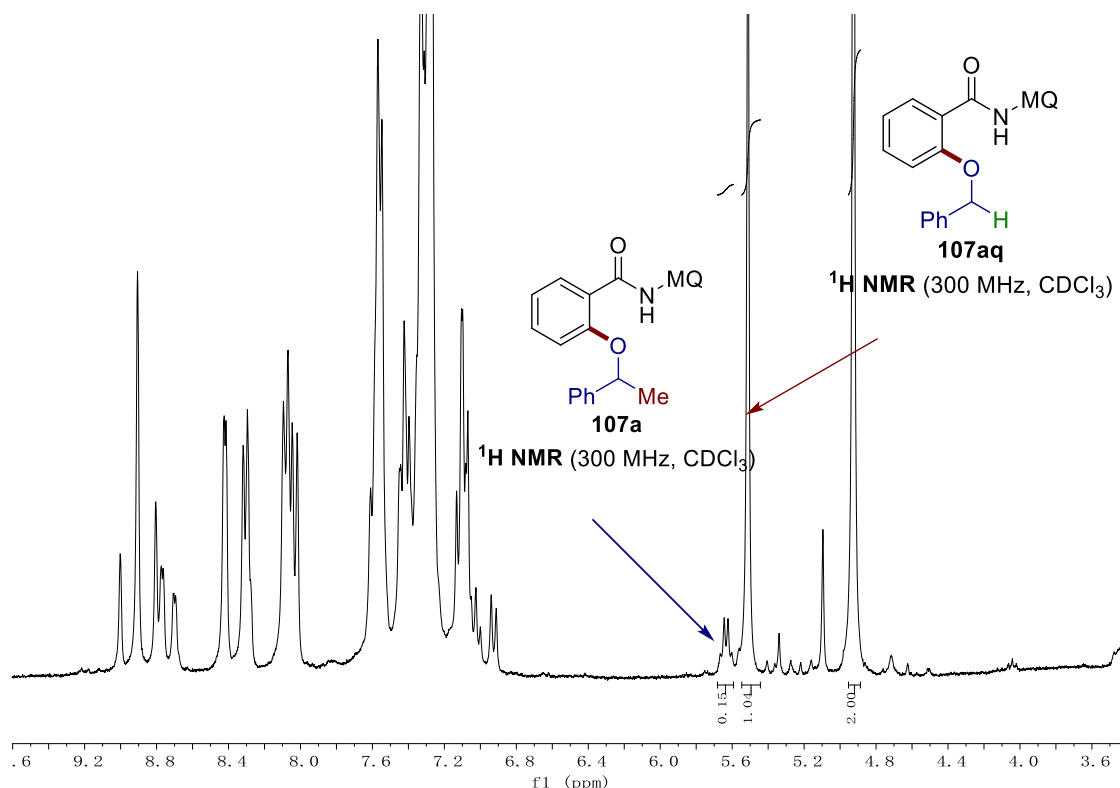


**Figure 5.3.24.** Crude <sup>1</sup>H NMR spectroscopy of competition experiment between secondary alcohol **66a** and primary alcohol **66t**.

### Experiments with Isotopically Labeled Solvent

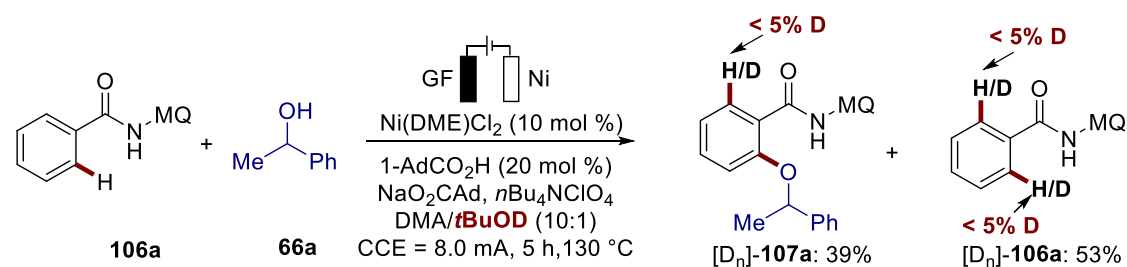


**Figure 5.3.25.** Deuteration experiment with *t*BuOD.

The general procedure **F** was followed using benzamide **106a** (65.5 mg, 0.25 mmol) and 1-phenylethan-1-ol (**66a**) (305 mg, 2.5 mmol) using a mixture of DMA and *t*BuOD (3.0/0.3 mL) as solvent with a balloon. Electrolysis was carried out at 130 °C and a constant current of 8.0 mA was maintained for 5.0 h. Column chromatography (*n*hexane/EtOAc: 16/1) yielded **[D<sub>n</sub>]-107a** (36.8 mg, 39%) as a white solid and

## 5. Experimental Section

reisolated starting material  $[D_n]$ -**106a** (34.5 mg, 53%) as a white solid. No deuteration was detected in either compound as determined by  $^1\text{H}$  NMR spectroscopy.

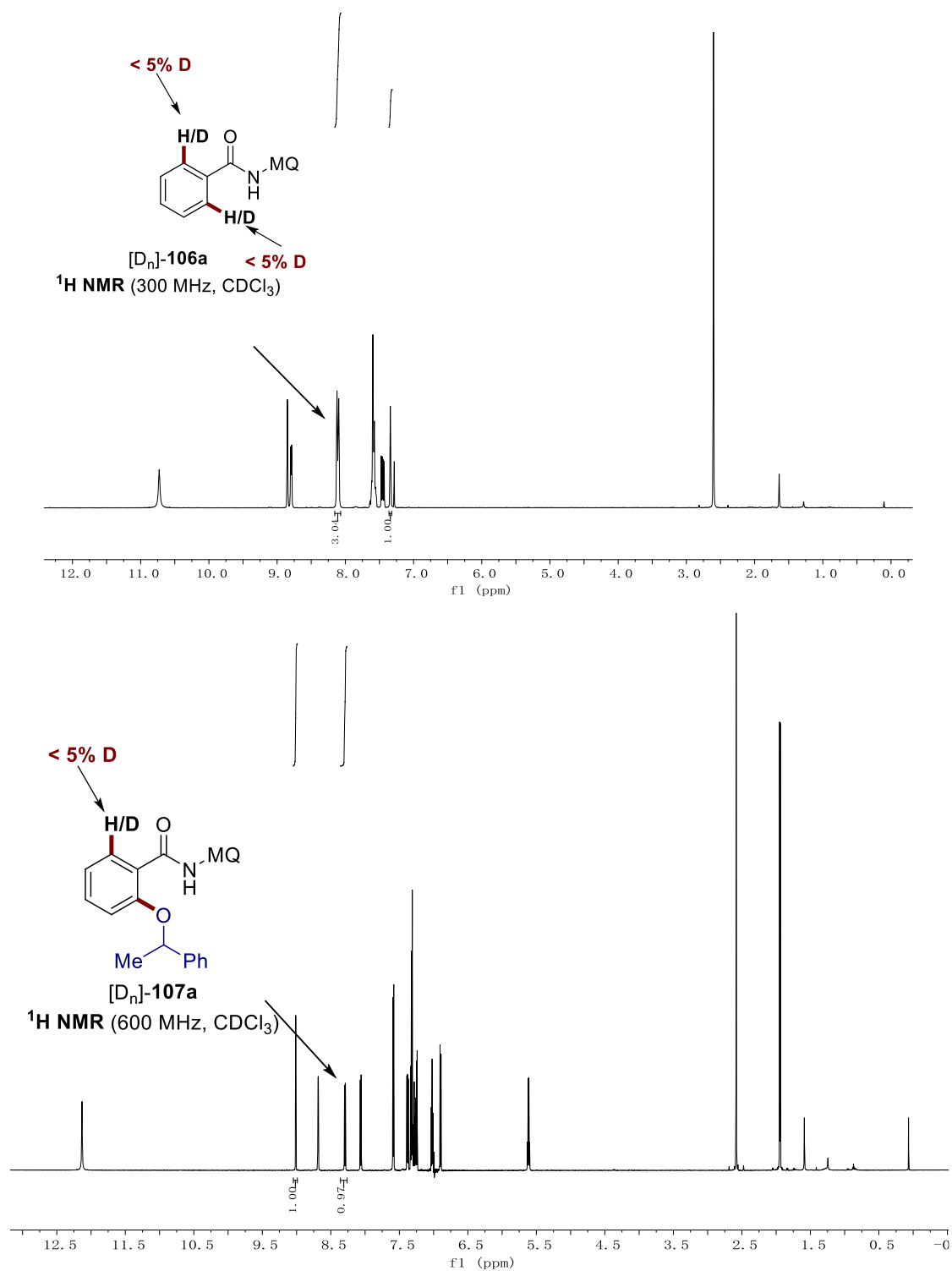


**Figure 5.3.26.** Experiments with isotopically labelled solvent  $t\text{BuOD}$ .

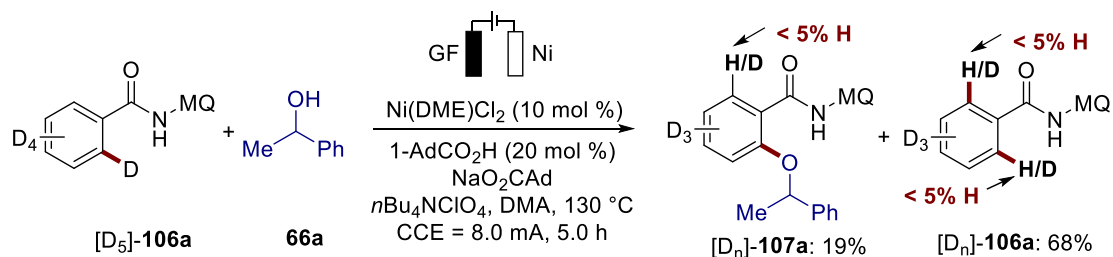


**Figure 5.3.27.** Deuteration experiment with  $[D_5]-106a$ .

The general procedure **F** was followed using benzamide  $[D_5]-106a$  (66.8 mg, 0.25 mmol) and 1-phenylethan-1-ol (**66a**) (305 mg, 2.5 mmol) in DMA (3.0 mL). Electrolysis was carried out at 130 °C and a constant current of 8.0 mA was maintained for 5.0 h. Column chromatography (*n*hexane/EtOAc: 4/1) yielded  $[D_n]-107a$  (18.5 mg, 19%) as a white solid and reisolated starting material  $[D_n]-106a$  (45.2 mg, 68%) as a white solid.

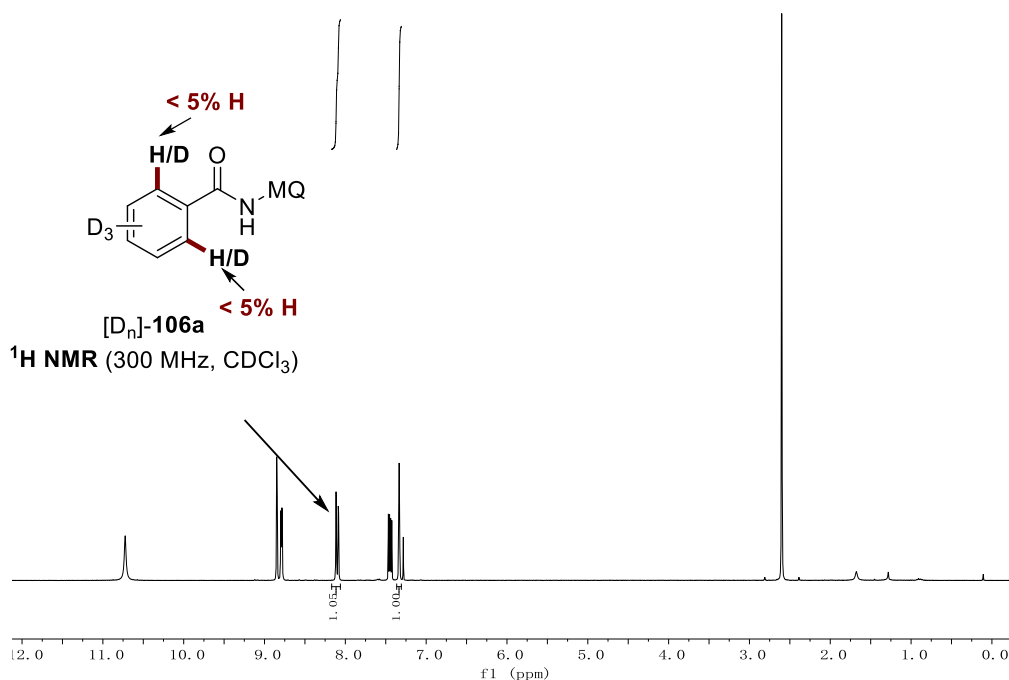


**Figure 5.3.28.** Deuteration experiment with reisolated substrate  $[D_5]-106a$ .

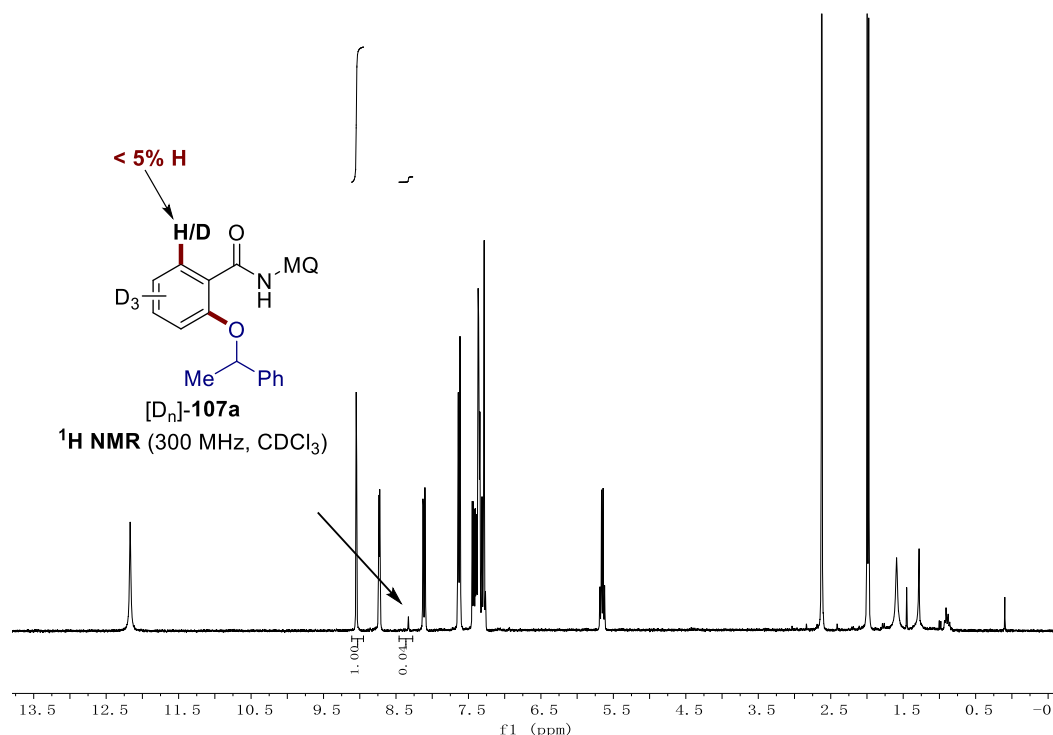


**Figure 5.3.29.** Deuteration experiment with [D<sub>5</sub>]-107a.

### KIE Studies

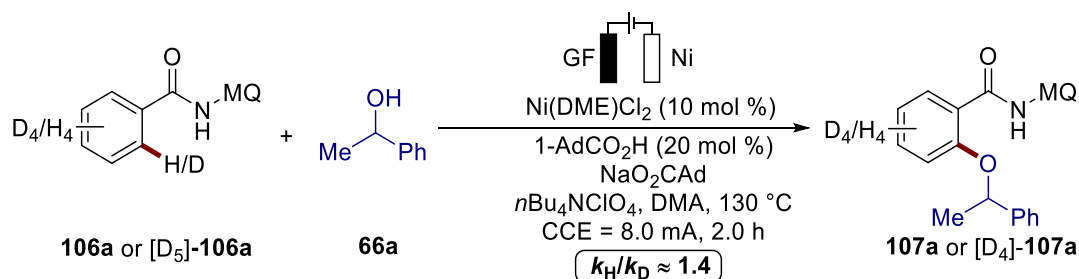


**Figure 5.3.30.** KIE studies by two parallel reactions.

Two parallel reactions were carried out with **106a** (196 mg, 0.75 mmol, 1.0 equiv) or [D<sub>5</sub>]-**106a** (200 mg, 0.75 mmol, 1.0 equiv) following the general procedure **F** using Ni(DME)Cl<sub>2</sub> (15.9 mg, 10 mol %), 1-AdCO<sub>2</sub>H (27.0 mg, 20 mol %), NaO<sub>2</sub>CAAd (151 mg, 0.75 mmol, 1.0 equiv), *n*Bu<sub>4</sub>NClO<sub>4</sub> (511 mg, 1.5 mmol, 2.0 equiv) and **66a** (0.90 mL, 7.5 mmol, 10 equiv) in DMA (6.0 mL). 1,3,5-trimethoxybenzene (0.25 mmol) was added as an internal standard. After 10 minutes to reach a stable constant current of 8.0 mA, aliquots of 0.40 mL were removed from the cell every twenty minutes. The mixture was extracted with EtOAc (3.0 mL). After evaporation of the solvent, the crude mixture was analyzed by <sup>1</sup>H NMR spectroscopy. The KIE was determined by the

analysis of the initial rates.

**Table 5.3.1.** KIE studies

Time [min]	10	30	50	70	90	110	130
<b>107a</b> [%]	0	2	6	10	13	17	19
<b>[D<sub>4</sub>]-107a</b> [%]	0	2	4	6	9	11	14

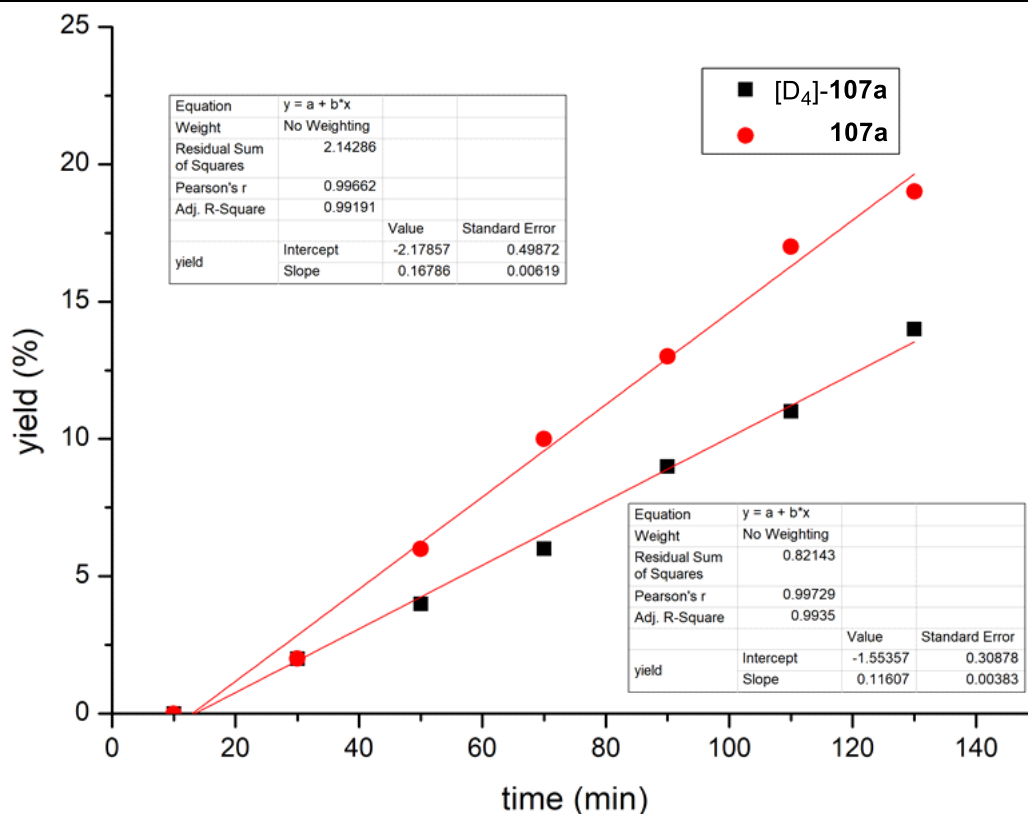


**Figure 5.3.31.** KIE studies by <sup>1</sup>H NMR spectroscopy.

### Headspace GC-Analysis

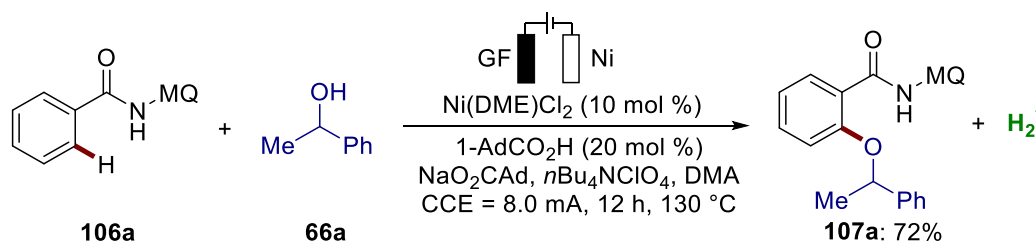


**Figure 5.3.32.** Headspace GC-analysis.

Following the general procedure **F**, after 12 h, the gas-phase over the reaction mixture was analyzed by headspace GC analysis using an Agilent 7890B chromatograph

## 5. Experimental Section

equipped with an Agilent CP–Molsieve 5Å column (length: 25 m, diameter: 0.32 mm, temperature 10 °C). Helium was used as the carrier gas (1.5 mL/min) and the sample was analyzed by a temperature conductivity detector at 110 °C. For comparison, also a blank sample of the carrier gas and a pure sample of hydrogen were obtained.

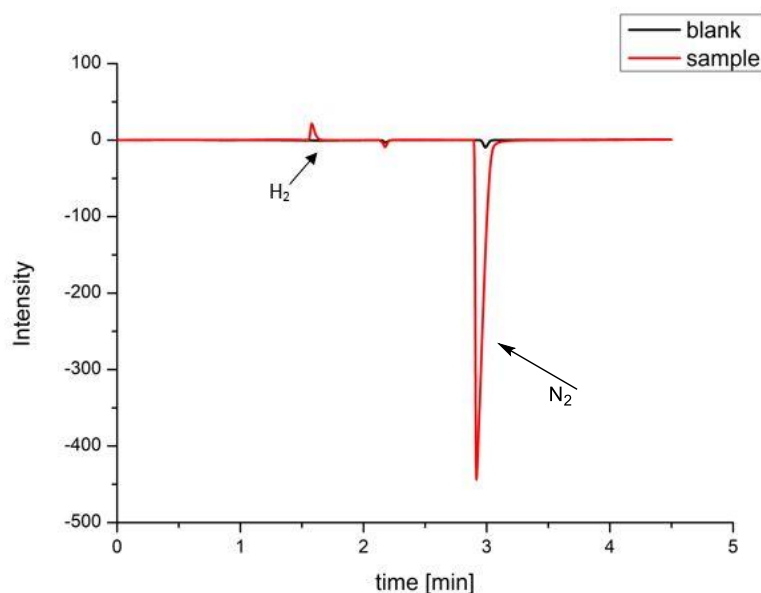


Figure 5.3.33. Headspace analysis of the reaction mixture.

### Radical Trapping Experiment

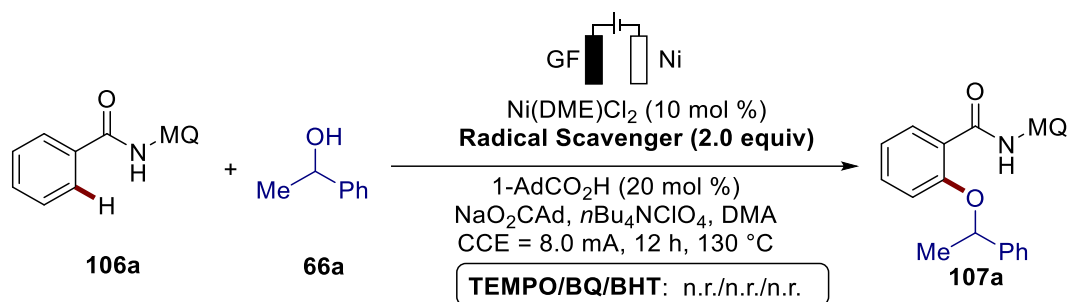


Figure 5.3.34. Radical trapping experiment with typical radical scavengers.

The electrolysis was carried out in an undivided cell, with a GF anode (10 mm × 15 mm × 6 mm) and a nickel-foam cathode (10 mm × 15 mm × 1.4 mm).  $\text{Ni(DME)Cl}_2$  (5.5 mg, 0.025 mmol, 10 mol %), 1-AdCO<sub>2</sub>H (9.0 mg, 0.050 mmol), NaO<sub>2</sub>CAd (50.5 mg, 0.25 mmol), *n*Bu<sub>4</sub>NCIO<sub>4</sub> (0.50 mmol), benzamide **106a** (0.25 mmol, 1.0 equiv) and 2.0 equiv of radical scavenger (TEMPO, benzoquinone or 2,6-di-*tert*-butyl-4-methylphenol) was dissolved in DMA (3.0 mL) and then the 1-phenylethan-1-ol (**66a**) (2.5 mmol) was added. At 130 °C, electrolysis was started with a constant current of 188

8.0 mA which was then maintained for 12 h. At ambient temperature, the mixture was transferred into a separating funnel and the electrodes were rinsed with EtOAc (10 mL). Then, H<sub>2</sub>O (10 mL) was added to the reaction mixture and the organic layer was separated. The aqueous layer was extracted with EtOAc (2 × 5.0 mL). After evaporation of the collected organic layer, the mixture was checked by TLC and GC-MS, and no desired products were found.

### Switch On-Off Experiment

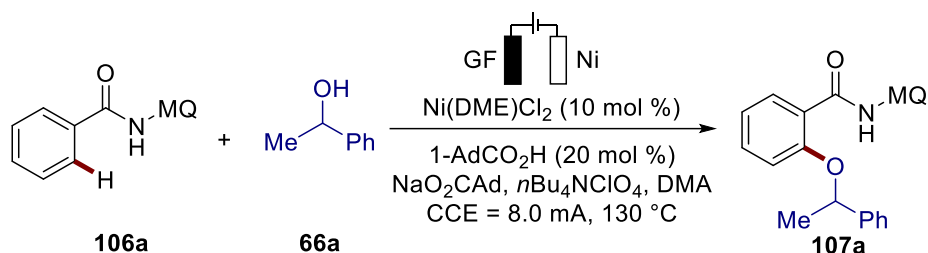


Figure 5.3.35. Switch on-off experiment.

“Switch off-on” reactions were carried out with **106a** (196 mg, 0.75 mmol, 1.0 equiv) following the procedure **H** using Ni(DME)Cl<sub>2</sub> (15.9 mg, 10 mol %), 1-AdCO<sub>2</sub>H (27.0 mg, 20 mol %), NaO<sub>2</sub>CAAd (152 mg, 0.75 mmol, 1.0 equiv), *n*Bu<sub>4</sub>NClO<sub>4</sub> (512 mg, 1.5 mmol, 2.0 equiv) and 1-phenylethan-1-ol (**66a**) (0.90 mL, 7.5 mmol, 10 equiv) in DMA (6.0 mL). 1,3,5-trimethoxybenzene (0.25 mmol) was added as an internal standard. Aliquots of 0.40 mL were removed from the cell every 1.5 hours. The mixture was extracted with EtOAc (3.0 mL). After evaporation of solvent, the crude mixture was analyzed by <sup>1</sup>H NMR spectroscopy.

Time [h]	1.5	3.0	4.5	6.0	7.5	9.0	10.5
<b>106a</b> [%]	100	86	87	77	77	68	67
<b>107a</b> [%]	0	5	5	18	18	28	28

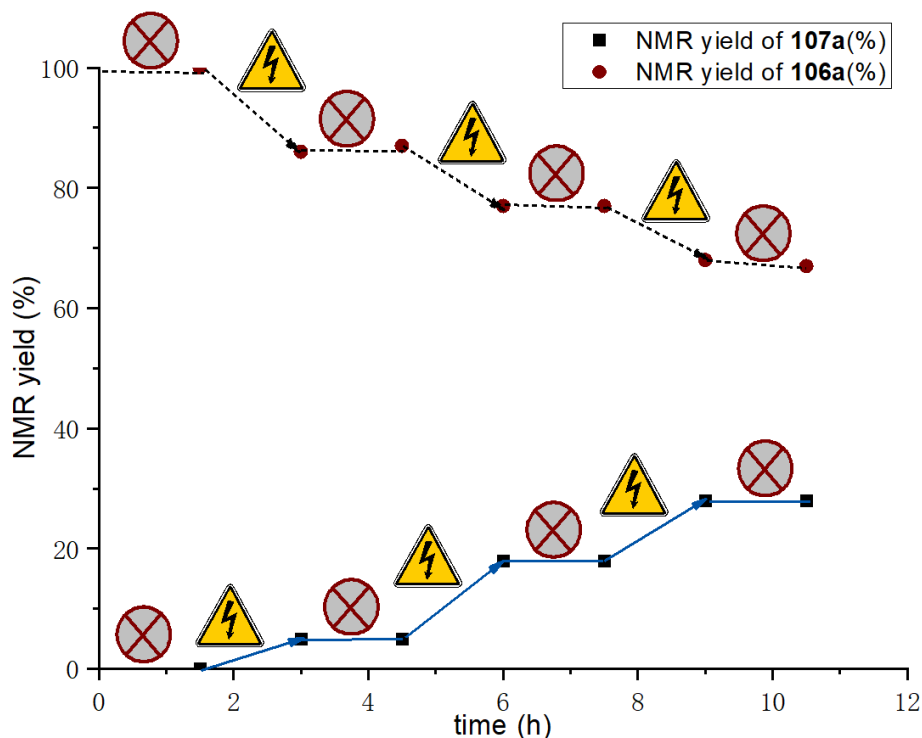


Figure 5.3.36. Switch off-on experiment.

### 5.3.5.3 Isolation and Characterization of Nickel(III) Intermediate

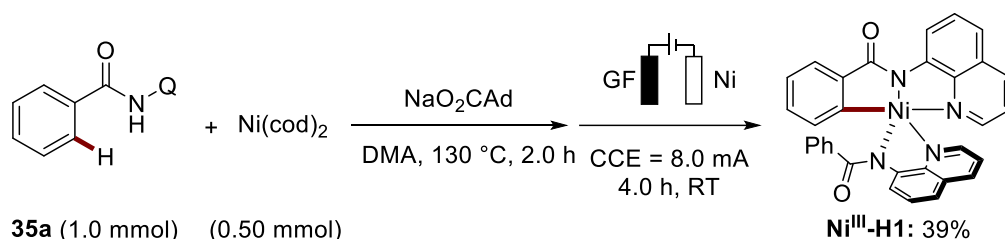
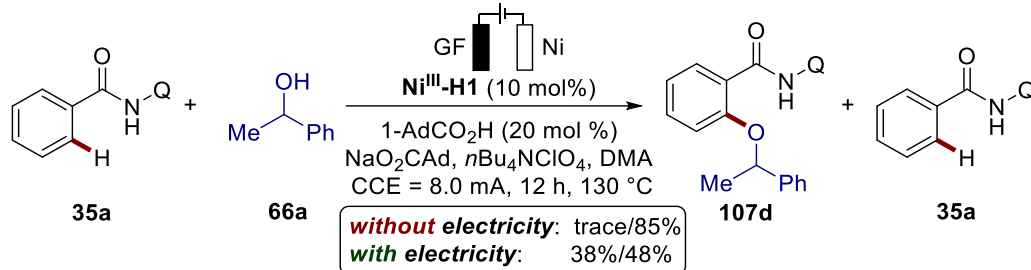


Figure 5.3.37. Synthesis and its X-ray analysis of  $\text{Ni}^{\text{III}}\text{-H1}$ .

According to a reported method,<sup>[177]</sup> an oven-dried 10 mL undivided electrochemical cell was charged with *N*-(quinolin-8-yl)benzamide (**35a**) (248 mg, 1.0 mmol),  $\text{Na}_2\text{OCAd}$  (202 mg, 1.0 mmol),  $\text{Ni}(\text{cod})_2$  (138 mg, 0.50 mmol) and dry DMA (3.0 mL) in a glovebox. The reaction vessel was capped and heated in an oil bath at 130 °C for 2.0 h. Upon cooling to room temperature, the cap of the undivided cell was exchanged by a GF anode and a nickel-foam cathode. Electrolysis was continued with a constant current of 8.0 mA which was then maintained for 4.0 h at ambient temperature under  $\text{N}_2$ . Then the reaction mixture was diluted with EtOAc (10 mL) and washed with  $\text{H}_2\text{O}$  (10 mL). The aqueous layer was extracted with EtOAc (2 x 10 mL). The combined organic phase was dried over  $\text{Na}_2\text{SO}_4$ , filtered and evaporated in vacuum. The residue was 190



purified by silica gel column chromatography at low temperature (eluent: *n*hexane/EtOAc = 4/1, then EtOAc) to afford **Ni<sup>III</sup>-H1** (108 mg, 39%) as a dark red solid. The product was crystallized using CH<sub>2</sub>Cl<sub>2</sub> and *n*hexane.



**Figure 5.3.38.** Catalytic reaction of substrate **35a** with **Ni<sup>III</sup>-H1**.

The electrolysis was carried out in an undivided cell, with a GF anode (10 mm × 15 mm × 6 mm) and a nickel-foam cathode (10 mm × 15 mm × 1.4 mm). **Ni<sup>III</sup>-H1** (27.6 mg, 0.025 mmol, 10 mol %), 1-AdCO<sub>2</sub>H (9.0 mg, 0.050 mmol), NaO<sub>2</sub>CAd (50.5 mg, 0.25 mmol), *n*Bu<sub>4</sub>NClO<sub>4</sub> (0.50 mmol) and benzamide **1s** (62.0 mg, 0.25 mmol, 1.0 equiv) were dissolved in DMA (3.0 mL), and then the 1-phenylethanol (**66a**) (2.5 mmol) was added. At 130 °C, electrolysis was started with a constant current of 8.0 mA (or without current) which was then maintained for 12 h. At ambient temperature, the mixture was transferred into a separating funnel and the electrodes were rinsed with EtOAc (10 mL). Then, H<sub>2</sub>O (10 mL) was added to the reaction mixture and the organic layer was separated. The aqueous layer was extracted with EtOAc (2 × 5.0 mL). Evaporation of the collected organic layer and subsequent column chromatography on silica gel (*n*hexane/EtOAc: 16/1) yielded the desired product **107d** (with electricity: 41.6 mg, 0.113 mmol, 38%; without electricity: trace) and recovered **35a** (with electricity: 36.0 mg, 0.145 mmol, 48%; without electricity: 63.2 mg, 0.255 mmol, 85%).

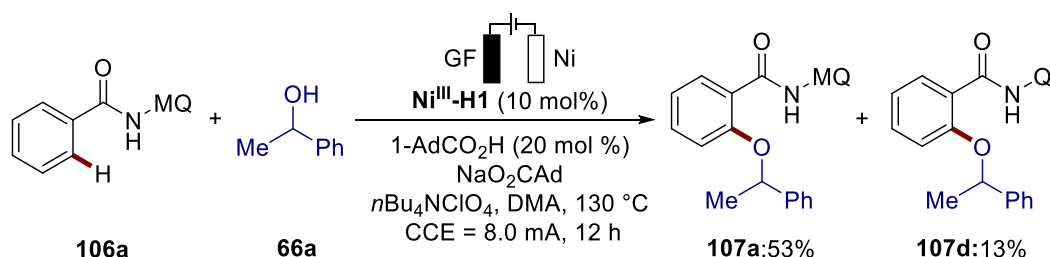


**Figure 5.3.39.** Catalytic reaction of substrate **106a** with **Ni<sup>III</sup>-H1**.

## 5. Experimental Section

The electrolysis was carried out in an undivided cell, with a GF anode (10 mm × 15 mm × 6 mm) and a nickel-foam cathode (10 mm × 15 mm × 1.4 mm). **Ni<sup>III</sup>-H1** (27.6 mg, 0.025 mmol, 10 mol %), 1-AdCO<sub>2</sub>H (9.0 mg, 0.050 mmol), NaO<sub>2</sub>CAd (50.5 mg, 0.25 mmol), *n*Bu<sub>4</sub>NClO<sub>4</sub> (0.50 mmol) and benzamide **106a** (65.5 mg, 0.25 mmol, 1.0 equiv) were dissolved in DMA (3.0 mL), and then the 1-phenylethan-1-ol (**66a**) (2.5 mmol) was added. At 130 °C, electrolysis was started with a constant current of 8.0 mA which was then maintained for 12 h. After cooling to ambient temperature, 1,3,5-trimethoxybenzene (0.25 mmol) was added as the internal standard to determine the <sup>1</sup>H NMR yield.

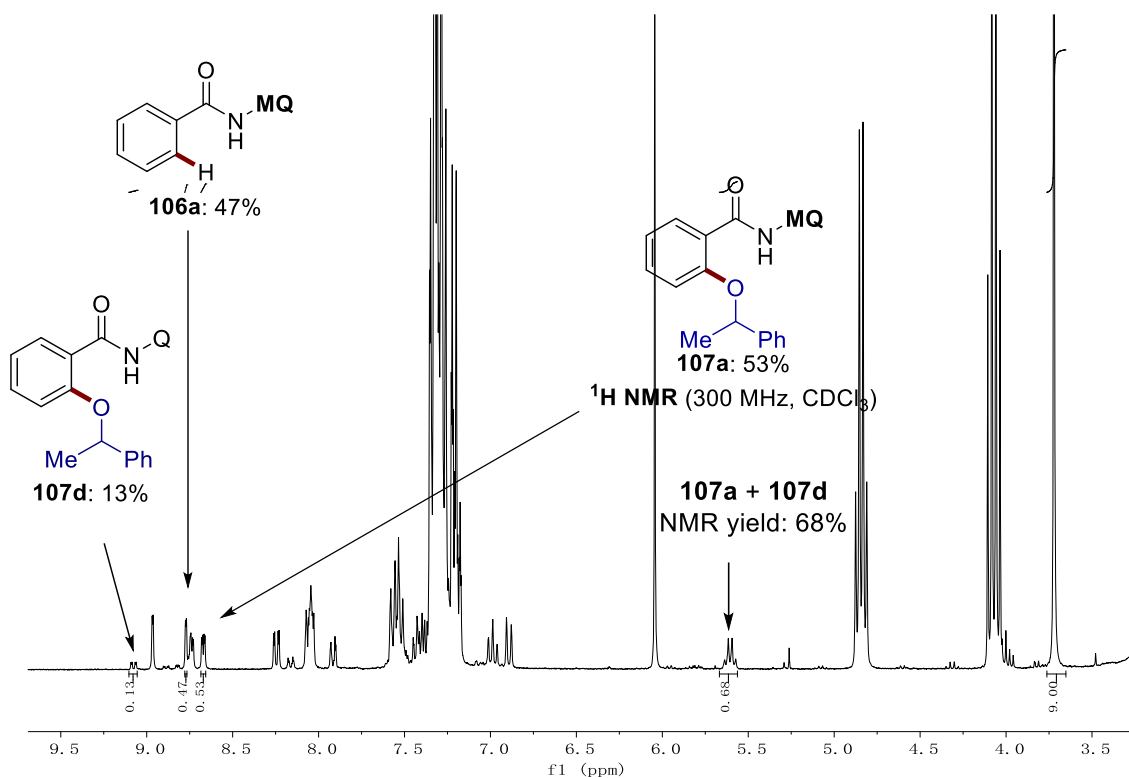


**Figure 5.3.40.** Ni<sup>III</sup>-H1 catalyzed reaction of substrate **106a**.

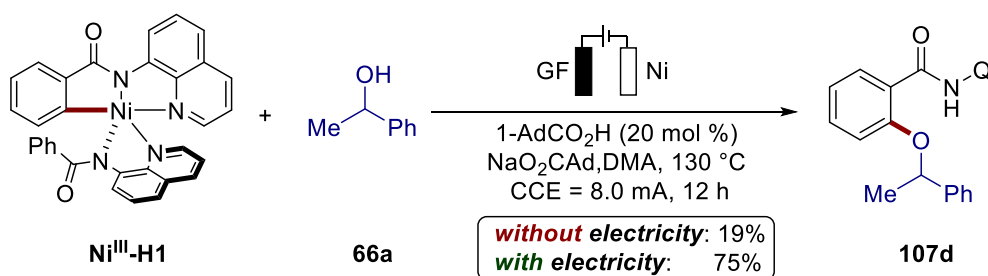


**Figure 5.3.41.** Stoichiometric reaction using nickel(III) complex.

The electrolysis was carried out in an undivided cell, with a GF anode (10 mm × 15 mm × 6 mm) and a nickel-foam cathode (10 mm × 15 mm × 1.4 mm). **Ni<sup>III</sup>-H1** (55.2 mg, 0.10 mmol), 1-AdCO<sub>2</sub>H (3.6 mg, 0.020 mmol), NaO<sub>2</sub>CAd (20.2 mg, 0.10 mmol) and *n*Bu<sub>4</sub>NClO<sub>4</sub> (0.20 mmol) were dissolved in DMA (1.5 mL), and then alcohol **66a** (1.0 mmol) was added. Then the reaction was carried out without or with electricity at 130 °C for 12 h. After cooling to ambient temperature, 1,3,5-trimethoxybenzene (0.10 mmol) was added as the internal standard to determine the <sup>1</sup>H NMR yield.

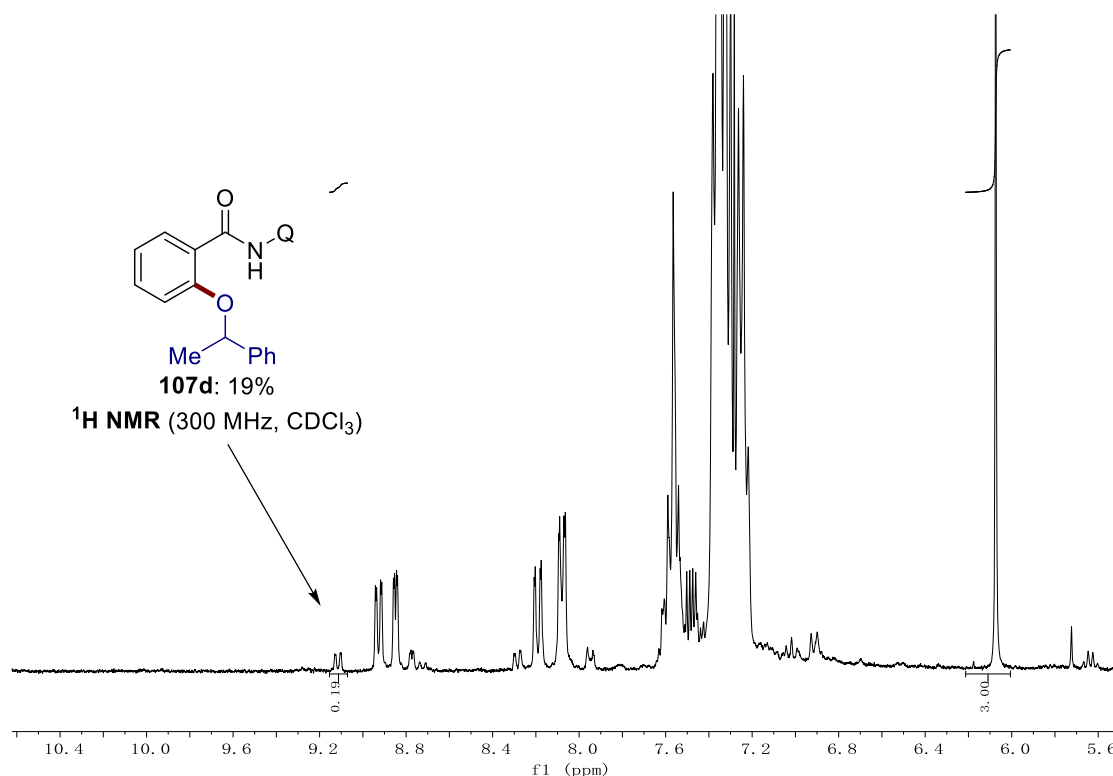


**Figure 5.3.42.** **Ni<sup>III</sup>-H1** reacted with the alcohol **66a** without electricity.

The electrolysis was carried out in an undivided cell, with a GF anode (10 mm × 15 mm × 6 mm) and a nickel-foam cathode (10 mm × 15 mm × 1.4 mm). **Ni<sup>III</sup>-H1** (110.4 mg, 0.20 mmol), 1-AdCO<sub>2</sub>H (7.2 mg, 0.040 mmol), NaO<sub>2</sub>CAd (40.4 mg, 0.20 mmol) and *n*Bu<sub>4</sub>NClO<sub>4</sub> (0.50 mmol) were dissolved in DMA (3.0 mL), and then alcohol **66a** (2.0 mmol) was added. At 130 °C, electrolysis was started with a constant current of 8.0 mA which was then maintained for 12 h. After cooling to ambient temperature, 1,3,5-trimethoxybenzene (0.20 mmol) was added as the internal standard to determine the <sup>1</sup>H NMR yield.

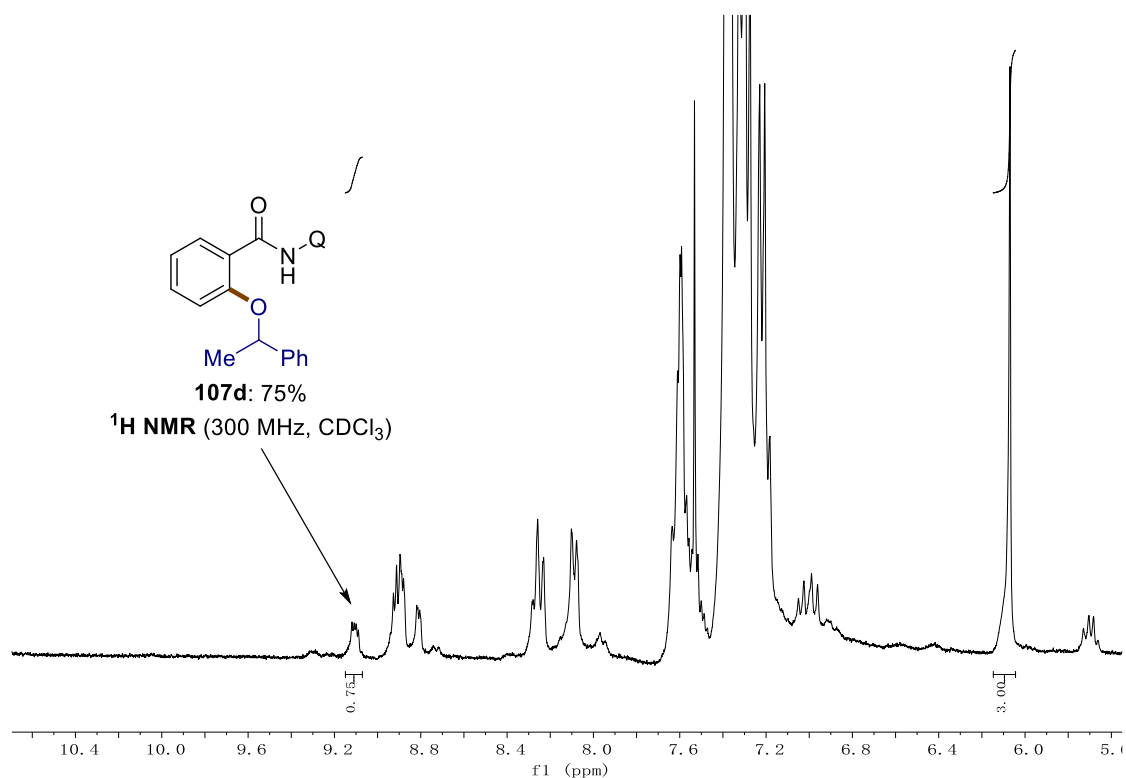


**Figure 5.3.43.**  $\text{Ni}^{\text{III}}$ -H1 reacted with the alcohol **66a** with electricity.

### 5.3.5.4 Gram-Scale Experiment

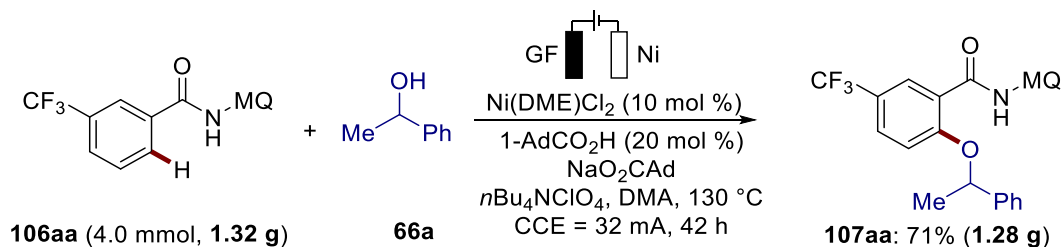


**Figure 5.3.44.** Gram-scale experiment with **106aa**.

The electrolysis was carried out in 100 mL Schlenk flask, with a GF anode (20 mm × 30 mm × 6 mm) and a nickel-foam cathode (20 mm × 30 mm × 1.4 mm).  $\text{Ni}(\text{DME})\text{Cl}_2$  (87.6 mg, 0.40 mmol, 10 mol %), 1-AdCO<sub>2</sub>H (144 mg, 0.80 mmol), NaO<sub>2</sub>CAd (808 mg, 4.0 mmol), *n*Bu<sub>4</sub>NClO<sub>4</sub> (7.0 mmol, 2.39 g) and benzamide **106aa** (4.0 mmol, 1.32 g) were dissolved in DMA (40.0 mL), and then the 1-phenylethan-1-ol (**66a**) (40 mmol) was added. At 130 °C, electrolysis was started with a constant current of 32.0 mA which was then maintained for 42 h. At ambient temperature, the mixture was transferred into a separating funnel and the electrodes were rinsed with EtOAc (50 mL). Then, the mixture was washed with H<sub>2</sub>O (50 mL) and the organic layer was separated.

The aqueous layer was extracted with EtOAc (2 × 50 mL). Evaporation of the collected organic layer and subsequent column chromatography on silica gel (*n*hexane/acetone:16/1→9/1) yielded the desired product **107aa** (1.28 g, 71%).

### 5.3.5.5 Traceless Removal of the Directing Group

As to the synthetic utility of this method, it is noteworthy that the 6-methylquinuoline was easily removed in a traceless fashion to provide efficient access to benzamide **109a**, benzoic acid **109b**, or aromatic aldehyde **109c** (Figure 3.4.17).

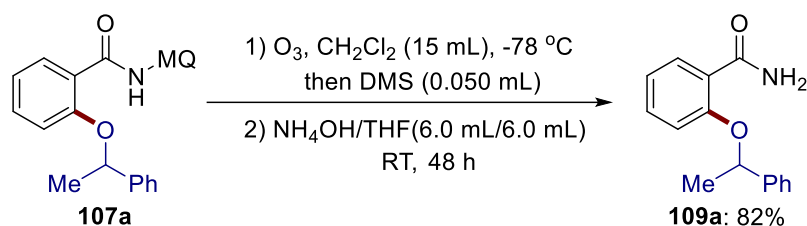


**Figure 5.3.45.** Traceless removal of the directing group to obtain primary amide **109a**.

According to the literature,<sup>[185]</sup> a stream of O<sub>3</sub> was passed through a solution of *N*-(6-methylquinolin-8-yl)-2-(1-phenylethoxy)benzamide (**107a**) (76.4 mg, 0.20 mmol) in CH<sub>2</sub>Cl<sub>2</sub> (15 mL) at -78 °C until the characteristic blue color appeared. A stream of oxygen was passed through until decolorization occurred and the mixture was quenched with dimethylsulfide (0.050 mL). After stirring at room temperature for 2.0 h, the mixture was concentrated under reduced pressure. The residue was redissolved in NH<sub>4</sub>OH (25%)/THF (6.0 mL, 1/1) and stirred for 48 h at ambient temperature. The mixture was diluted with CH<sub>2</sub>Cl<sub>2</sub> (20.0 mL) and washed with aqueous HCl (1N, 2 × 10 mL), and subsequently 1N NaOH (2 × 10 mL). The organic layer was dried with MgSO<sub>4</sub> and concentrated to dryness to give the primary amide **109a** (39.7 mg, 82%).

**M.p.:** 134–135 °C. **<sup>1</sup>H NMR** (400 MHz, CDCl<sub>3</sub>) δ = 8.23 (dd, *J* = 7.9, 1.9 Hz, 1H), 8.06–7.99 (m, 1H), 7.38 (d, *J* = 4.3 Hz, 4H), 7.35–7.28 (m, 2H), 7.02 (td, *J* = 7.5, 1.0 Hz, 1H), 6.85 (dd, *J* = 8.4, 1.0 Hz, 1H), 6.31 (s, 1H), 5.52 (q, *J* = 6.4 Hz, 1H), 1.77 (d, *J* = 6.4 Hz, 3H). **<sup>13</sup>C NMR** (101 MHz, CDCl<sub>3</sub>) δ = 167.3 (C<sub>q</sub>), 156.2 (C<sub>q</sub>), 141.6 (C<sub>q</sub>), 133.1 (CH), 132.5 (CH), 129.0 (CH), 128.1 (CH), 125.4 (CH), 121.4 (C<sub>q</sub>), 121.2 (CH), 114.3 (CH), 77.6 (CH), 24.4 (CH<sub>3</sub>). **IR** (ATR): 3455, 1663, 1592, 1454, 1374, 1229, 1066, 755,

701  $\text{cm}^{-1}$ . **MS** (ESI)  $m/z$  (relative intensity): 264 (100)  $[\text{M}+\text{Na}]^+$ , 242 (10)  $[\text{M}+\text{H}]^+$ , 138 (50), 117 (60). **HR-MS** (ESI)  $m/z$  calcd for  $\text{C}_{15}\text{H}_{16}\text{NO}_2$   $[\text{M}+\text{H}]^+$ : 242.1176, found: 242.1184.

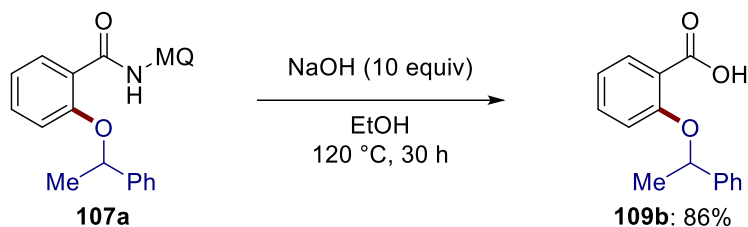


**Figure 5.3.46.** Traceless removal of the directing group to obtain benzoic acid **109b**.

An oven-dried 25 mL sealed tube equipped with a stir bar was charged with *N*-(6-methylquinolin-8-yl)-2-(1-phenylethoxy)benzamide (**107a**) (95.5 mg, 0.25 mmol), NaOH (100 mg, 2.5 mmol) and EtOH (2.0 mL). The resulting mixture was stirred at 120 °C for 24 h. After completion, the reaction mixture was cooled down to room temperature, diluted by 20.0 mL ethyl acetate and washed by HCl (3 × 10 mL of 0.5 N aqueous solution). The aqueous layers were combined and extracted with EtOAc (3 × 10 mL). Combined organic layers were dried over  $\text{MgSO}_4$ . Evaporation to remove organic solvent gave the pure acid **109b** (52.0 mg, 86%) as a colorless gummy.  **$^1\text{H NMR}$**  (400 MHz,  $\text{CDCl}_3$ )  $\delta$  = 11.13 (s, 1H), 8.15 (dd,  $J$  = 7.8, 1.8 Hz, 1H), 7.42–7.27 (m, 6H), 7.06–7.02 (m, 1H), 6.88 (dd,  $J$  = 8.4, 0.9 Hz, 1H), 5.57 (q,  $J$  = 6.4 Hz, 1H), 1.79 (d,  $J$  = 6.4 Hz, 3H).  **$^{13}\text{C NMR}$**  (101 MHz,  $\text{CDCl}_3$ )  $\delta$  = 165.5 ( $\text{C}_q$ ), 156.5 ( $\text{C}_q$ ), 140.4 ( $\text{C}_q$ ), 134.7 (CH), 133.7 (CH), 129.1 (CH), 128.5 (CH), 125.4 (CH), 122.2 (CH), 118.3 ( $\text{C}_q$ ), 114.4 (CH), 79.3 (CH), 24.0 ( $\text{CH}_3$ ). **IR** (ATR): 3252, 2979, 1732, 1692, 1600, 1455, 1241, 1065, 753, 700  $\text{cm}^{-1}$ . **MS** (ESI)  $m/z$  (relative intensity): 265 (100)  $[\text{M}+\text{Na}]^+$ . **HR-MS** (ESI)  $m/z$  calcd for  $\text{C}_{15}\text{H}_{14}\text{O}_3\text{Na}^+$   $[\text{M}+\text{Na}]^+$ : 265.0835, found: 265.0834. The analytical data correspond with those reported in the literature.<sup>[186]</sup>

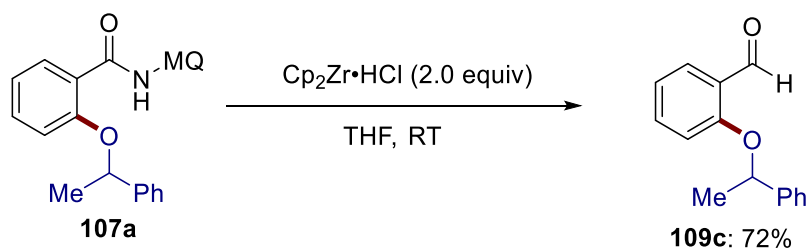
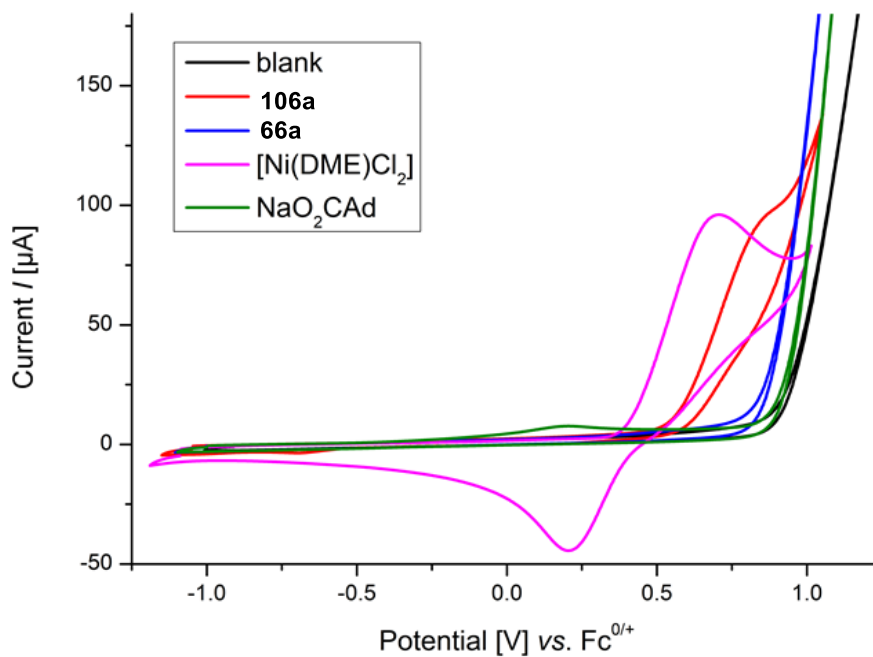


**Figure 5.3.47.** Traceless removal of the directing group to gain aromatic aldehyde **109c**.

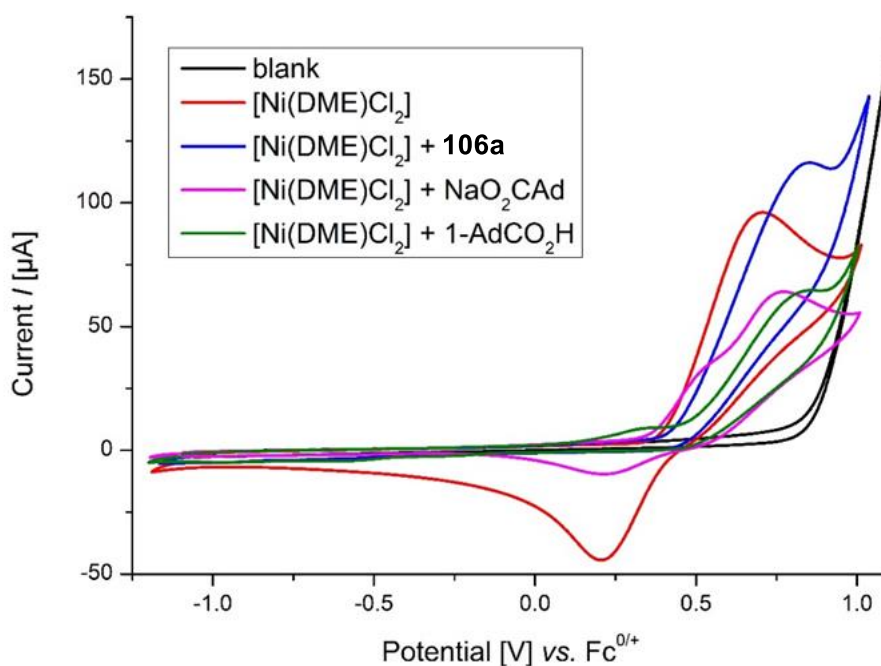
According to the literature,<sup>[97a]</sup> *N*-(6-methylquinolin-8-yl)-2-(1-phenylethoxy)benzamide (**107a**) (95.5 mg, 0.25 mmol), Cp<sub>2</sub>ZrHCl (0.50 mmol, 125 mg), and THF (2.0 mL) were charged to a 25 mL Schlenk tube under N<sub>2</sub>. The reaction mixture was stirred at room temperature for 6 hrs before carefully being quenched by saturated ammonium chloride at 0 °C. After being extracted with CH<sub>2</sub>Cl<sub>2</sub> (3 × 25.0 mL), the combined organic extract was washed with brine, dried over Na<sub>2</sub>SO<sub>4</sub>, and concentrated in vacuum. The residue was purified by column chromatography on silica gel (eluent: *n*hexane/EtOAc: 20/1) to afford aromatic aldehyde **109c** as a colorless oil (40.7 mg, 72%). **<sup>1</sup>H NMR** (400 MHz, CDCl<sub>3</sub>) δ = 10.64 (d, *J* = 0.8 Hz, 1H), 7.80 (dd, *J* = 7.7, 1.8 Hz, 1H), 7.41–7.29 (m, 5H), 7.30–7.24 (m, 1H), 7.00–6.87 (m, 1H), 6.82 (dd, *J* = 8.5, 0.8 Hz, 1H), 5.42 (q, *J* = 6.4 Hz, 1H), 1.69 (d, *J* = 6.4 Hz, 3H). **<sup>13</sup>C NMR** (101 MHz, CDCl<sub>3</sub>) δ = 189.9 (CH), 160.4 (C<sub>q</sub>), 142.1 (C<sub>q</sub>), 135.6 (CH), 128.8 (CH), 128.2 (CH), 127.8 (CH), 125.4 (CH), 125.4 (C<sub>q</sub>), 120.7 (CH), 114.5 (CH), 77.0 (CH), 24.2 (CH<sub>3</sub>). **IR** (ATR): 2979, 1683, 1596, 1478, 1455, 1235, 1067, 755, 699 cm<sup>-1</sup>. **MS** (ESI) *m/z* (relative intensity): 249 (100) [M+Na]<sup>+</sup>, 105 (25). **HR-MS** (ESI) *m/z* calcd for C<sub>15</sub>H<sub>14</sub>O<sub>2</sub>Na [M+Na]<sup>+</sup>: 249.0886, found: 249.08867. The analytical data correspond with those reported in the literature.<sup>[186]</sup>

### 5.3.5.6 Cyclic Voltammetry

A glassy-carbon electrode (3 mm diameter, disc-electrode) was used as the working electrode, a Pt-wire as auxiliary electrode and an Ag-wire as pseudoreference. The measurements were then referenced using ferrocene. The measurements were carried out at a scan rate of 100 mV/s.



**Figure 5.3.48.** Cyclic voltammograms at 100 mV/s.  $n\text{Bu}_4\text{NPF}_6$  (0.1 M in DMA); concentration of substrates 5 mM. blank (black); **106a** (red); **66a** (blue);  $[\text{Ni}(\text{DME})\text{Cl}_2]$  (purple);  $\text{NaO}_2\text{CAd}$  (green). Performed by Julia Struwe.

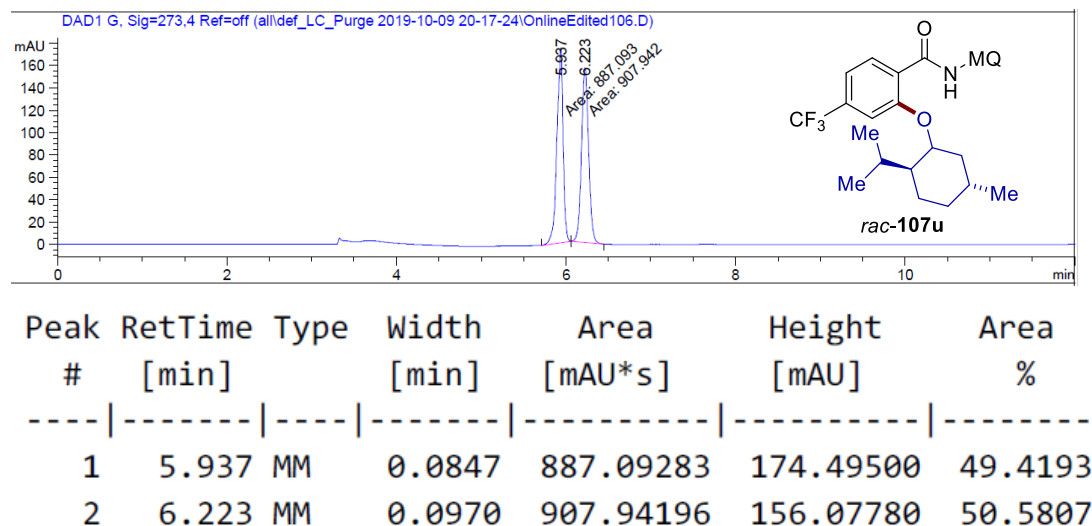
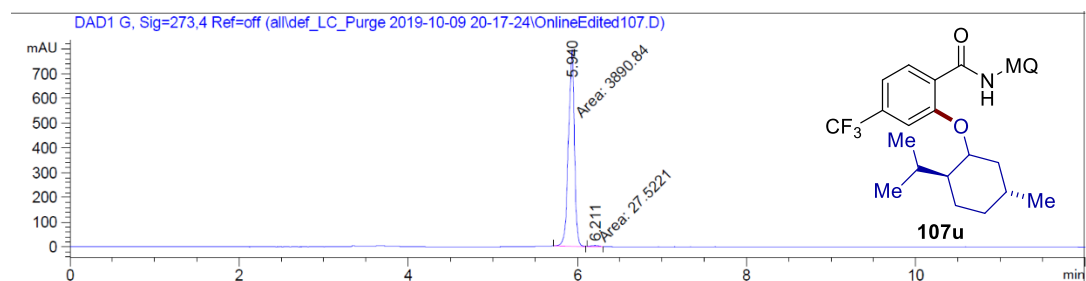


**Figure 5.3.49.** Cyclic voltammograms at 100 mV/s.  $n\text{Bu}_4\text{NPF}_6$  (0.1 M in DMA); concentration of substrates 5 mM. blank (black);  $[\text{Ni}(\text{DME})\text{Cl}_2]$  (red);  $[\text{Ni}(\text{DME})\text{Cl}_2] + \mathbf{106a}$  (blue);  $[\text{Ni}(\text{DME})\text{Cl}_2] + \text{NaO}_2\text{CAd}$  (purple);  $[\text{Ni}(\text{DME})\text{Cl}_2] + 1\text{-AdCO}_2\text{H}$  (green). Performed by Julia Struwe.



5.3.5.7 Studies on the Potential Racemization of **107u**

A racemic sample of **rac-107u** was synthesized following the general procedure using *L*-Menthol/*D*-Menthol (1.25 mmol/1.25 mmol). Analysis by chiral HPLC showed that racemization did not take place. HPLC chromatograms were recorded on an Agilent 1290 Infinity instrument using CHIRALPAK® IA-1 column and *n*hexane/*i*PrOH (98/2, 1.0 mL/min, detection at 273 nm, 99% ee)

Figure 5.3.50. HPLC–Chromatogram of **rac-107u**.

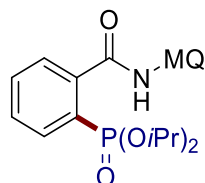
Signal 2: DAD1 G, Sig=273,4 Ref=off

Peak #	RetTime [min]	Type	Width [min]	Area [mAU*s]	Height [mAU]	Area %
1	5.940	MM	0.0814	3890.83911	796.27783	99.2976
2	6.211	MM	0.0993	27.52212	4.62122	0.7024

Figure 5.3.51. HPLC–Chromatogram of **107u**.

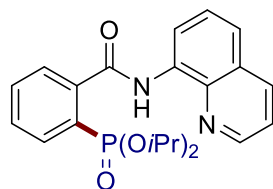
### 5.3.6 Nickela-Electrocatalyzed C–H Phosphorylation

#### 5.3.6.1 Characterization Data



#### Diisopropyl {2-[(6-methylquinolin-8-yl)carbamoyl]phenyl}phosphonate (**110a**)

The general procedure **G** was followed using benzamide **106a** (65.5 mg, 1.0 equiv, 0.25 mmol) and diisopropyl phosphonate (**74a**) (83.0 mg, 2.0 equiv, 0.50 mmol). Purification by column chromatography on silica gel (*n*hexane/EtOAc: 4/1→1/1) yielded **110a** (78.2 mg, 73%) as a white solid. **M.p.**: 127–129 °C. **<sup>1</sup>H NMR** (300 MHz, CDCl<sub>3</sub>)  $\delta$  = 10.12 (s, 1H), 8.83 (d, *J* = 1.8 Hz, 1H), 8.70 (dd, *J* = 4.2, 1.6 Hz, 1H), 8.17–8.05 (m, 2H), 7.76–7.55 (m, 3H), 7.41 (ddd, *J* = 8.2, 4.2, 1.0 Hz, 1H), 7.36–7.31 (m, 1H), 4.77 (dhept, *J* = 7.8, 6.2 Hz, 2H), 2.61 (s, 3H), 1.26 (d, *J* = 6.2 Hz, 6H), 1.18 (d, *J* = 6.2 Hz, 6H). **<sup>13</sup>C NMR** (101 MHz, CDCl<sub>3</sub>)  $\delta$  = 167.4 (d, <sup>3</sup>*J*<sub>C–P</sub> = 4.6 Hz, C<sub>q</sub>), 147.2 (CH), 140.9 (d, <sup>2</sup>*J*<sub>C–P</sub> = 9.3 Hz, C<sub>q</sub>), 137.5 (C<sub>q</sub>), 137.4 (C<sub>q</sub>), 135.5 (CH), 134.3 (C<sub>q</sub>), 133.4 (d, <sup>3</sup>*J*<sub>C–P</sub> = 9.3 Hz, CH), 132.3 (d, <sup>4</sup>*J*<sub>C–P</sub> = 2.9 Hz, CH), 129.4 (d, <sup>2</sup>*J*<sub>C–P</sub> = 14.2 Hz, CH), 128.6 (d, <sup>3</sup>*J*<sub>C–P</sub> = 13.0 Hz, CH), 128.0 (C<sub>q</sub>), 127.4 (d, <sup>1</sup>*J*<sub>C–P</sub> = 188.0 Hz, C<sub>q</sub>), 121.6 (CH), 120.9 (CH), 119.2 (CH), 71.5 (d, <sup>2</sup>*J*<sub>C–P</sub> = 6.0 Hz, CH), 23.8 (d, <sup>3</sup>*J*<sub>C–P</sub> = 4.2 Hz, CH<sub>3</sub>), 23.7 (d, <sup>3</sup>*J*<sub>C–P</sub> = 4.8 Hz, CH<sub>3</sub>), 22.3 (CH<sub>3</sub>). **<sup>31</sup>P{<sup>1</sup>H} NMR** (162 MHz, CDCl<sub>3</sub>)  $\delta$  = 14.4 (dd, *J* = 14.1, 7.2 Hz). **IR** (ATR): 3357, 2979, 1677, 1523, 1237, 979, 869, 670, 603 cm<sup>-1</sup>. **MS** (ESI) *m/z* (relative intensity): 449 (35) [M+Na]<sup>+</sup>, 427 (100) [M+H]<sup>+</sup>. **HR-MS** (ESI) *m/z* calcd for C<sub>23</sub>H<sub>28</sub>N<sub>2</sub>O<sub>4</sub>P [M+H]<sup>+</sup>: 427.1781, found: 427.1783.

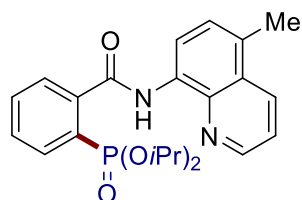


#### Diisopropyl [2-(quinolin-8-ylcarbamoyl)phenyl]phosphonate (**110b**)

The general procedure **G** was followed using benzamide **35a** (62.0 mg, 1.0 equiv, 0.25 mmol) and diisopropyl phosphonate (**74a**) (83.0 mg, 2.0 equiv, 0.50 mmol).

Purification by column chromatography on silica gel (*n*hexane/EtOAc: 4/1→1/1) yielded **110b** (61.2 mg, 59%) as a white solid. **M.p.**: 105–107 °C. **<sup>1</sup>H NMR** (400 MHz, CDCl<sub>3</sub>) δ = 10.18 (s, 1H), 8.96 (dd, *J* = 7.5, 1.6 Hz, 1H), 8.79 (dd, *J* = 4.2, 1.7 Hz, 1H), 8.19 (dd, *J* = 8.3, 1.7 Hz, 1H), 8.15–8.07 (m, 1H), 7.76–7.70 (m, 1H), 7.69–7.55 (m, 4H), 7.46 (dd, *J* = 8.3, 4.2 Hz, 1H), 4.77 (dhept, *J* = 7.8, 6.2 Hz, 2H), 1.26 (d, *J* = 6.2 Hz, 6H), 1.17 (d, *J* = 6.2 Hz, 6H). **<sup>13</sup>C NMR** (101 MHz, CDCl<sub>3</sub>) δ = 167.5 (d, <sup>3</sup>*J*<sub>C-P</sub> = 4.5 Hz, C<sub>q</sub>), 148.2 (CH), 140.8 (d, <sup>2</sup>*J*<sub>C-P</sub> = 9.3 Hz, C<sub>q</sub>), 138.7 (C<sub>q</sub>), 136.3 (CH), 134.7 (C<sub>q</sub>), 133.5 (d, <sup>3</sup>*J*<sub>C-P</sub> = 9.4 Hz, CH), 132.3 (d, <sup>4</sup>*J*<sub>C-P</sub> = 3.0 Hz, CH), 129.5 (d, <sup>2</sup>*J*<sub>C-P</sub> = 14.2 Hz, CH), 128.6 (d, <sup>3</sup>*J*<sub>C-P</sub> = 13.1 Hz, CH), 128.0 (C<sub>q</sub>), 127.4 (CH), 127.4 (d, <sup>1</sup>*J*<sub>C-P</sub> = 188.4 Hz, C<sub>q</sub>), 122.0 (CH), 121.6 (CH), 117.3 (CH), 71.5 (d, <sup>3</sup>*J*<sub>C-P</sub> = 6.0 Hz, CH), 23.8 (d, <sup>3</sup>*J*<sub>C-P</sub> = 4.2 Hz, CH<sub>3</sub>), 23.8 (d, <sup>3</sup>*J*<sub>C-P</sub> = 4.8 Hz, CH<sub>3</sub>). **<sup>31</sup>P{<sup>1</sup>H} NMR** (121 MHz, CDCl<sub>3</sub>) δ = 14.5–14.3 (m). **IR** (ATR): 3331, 2978, 1674, 1523, 1243, 969, 768, 567, 543 cm<sup>-1</sup>. **MS** (ESI) *m/z* (relative intensity): 435 (100) [M+Na]<sup>+</sup>, 413 (35) [M+H]<sup>+</sup>. **HR-MS** (ESI) *m/z* calcd for C<sub>22</sub>H<sub>26</sub>N<sub>2</sub>O<sub>4</sub>P [M+H]<sup>+</sup>: 413.1625, found: 413.1629.

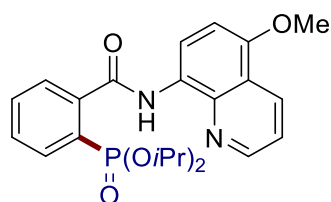
The analytical data correspond with those reported in the literature.<sup>[139]</sup>



#### Diisopropyl {2-[(5-methylquinolin-8-yl)carbamoyl]phenyl}phosphonate (**110c**)

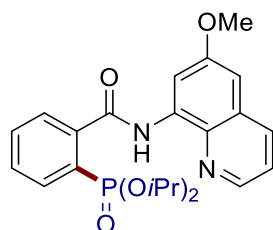
The general procedure **G** was followed using benzamide **106c** (65.5 mg, 1.0 equiv, 0.25 mmol) and diisopropyl phosphonate (**74a**) (83.0 mg, 2.0 equiv, 0.50 mmol). Purification by column chromatography on silica gel (*n*hexane/EtOAc: 4/1→1/1) yielded **110c** (77.9 mg, 73%) as a white solid. **M.p.**: 125–127 °C. **<sup>1</sup>H NMR** (400 MHz, CDCl<sub>3</sub>) δ = 10.14 (s, 1H), 8.83 (d, *J* = 7.8 Hz, 1H), 8.77 (dd, *J* = 3.9, 1.8 Hz, 1H), 8.33 (dq, *J* = 8.5, 1.5 Hz, 1H), 8.14–8.07 (m, 1H), 7.74–7.69 (m, 1H), 7.63 (td, *J* = 7.6, 1.5 Hz, 1H), 7.56 (tdd, *J* = 7.5, 3.0, 1.4 Hz, 1H), 7.47 (ddt, *J* = 8.5, 4.2, 1.1 Hz, 1H), 7.42 (d, *J* = 7.8 Hz, 1H), 4.76 (dhept, *J* = 7.8, 6.2 Hz, 2H), 2.74–2.60 (m, 3H), 1.25 (d, *J* = 6.2 Hz, 6H), 1.16 (d, *J* = 6.2 Hz, 6H). **<sup>13</sup>C NMR** (101 MHz, CDCl<sub>3</sub>) δ = 167.3 (d, <sup>3</sup>*J*<sub>C-P</sub> = 4.4 Hz, C<sub>q</sub>), 147.6 (CH), 141.0 (d, <sup>2</sup>*J*<sub>C-P</sub> = 9.3 Hz, C<sub>q</sub>), 139.0 (C<sub>q</sub>), 133.5 (d,

$^3J_{C-P} = 9.4$  Hz, CH), 133.1 (C<sub>q</sub>), 132.9 (CH), 132.2 (d,  $^4J_{C-P} = 3.0$  Hz, CH), 129.4 (d,  $^2J_{C-P} = 14.3$  Hz, CH), 128.7 (C<sub>q</sub>), 128.6 (d,  $^3J_{C-P} = 13.0$  Hz, CH), 127.5 (CH), 127.3 (d,  $^1J_{C-P} = 188.3$  Hz, C<sub>q</sub>), 127.3 (C<sub>q</sub>), 121.1 (CH), 117.0 (CH), 71.5 (d,  $^2J_{C-P} = 6.1$  Hz, CH), 23.8 (d,  $^3J_{C-P} = 4.3$  Hz, CH<sub>3</sub>), 23.8 (d,  $^3J_{C-P} = 4.9$  Hz, CH<sub>3</sub>), 18.3 (CH<sub>3</sub>).  **$^{31}P\{^1H\}$  NMR** (121 MHz, CDCl<sub>3</sub>)  $\delta = 14.4$  (ddq,  $J = 11.9, 7.7, 4.0$  Hz). **IR** (ATR): 3336, 2976, 1671, 1522, 1243, 974, 769, 567, 544 cm<sup>-1</sup>. **MS** (ESI)  $m/z$  (relative intensity): 449 (100) [M+Na]<sup>+</sup>, 427 (50) [M+H]<sup>+</sup>, 369 (5). **HR-MS** (ESI)  $m/z$  calcd for C<sub>23</sub>H<sub>28</sub>N<sub>2</sub>O<sub>4</sub>P [M+H]<sup>+</sup>: 427.1781, found: 427.1784.



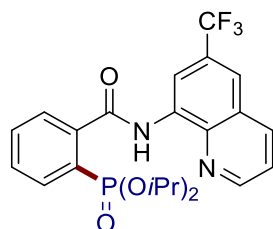
#### Diisopropyl {2-[(5-methoxyquinolin-8-yl)carbamoyl]phenyl}phosphonate (**110d**)

The general procedure **G** was followed using benzamide **106e** (69.5 mg, 1.0 equiv, 0.25 mmol) and diisopropyl phosphonate (**74a**) (83.0 mg, 2.0 equiv, 0.50 mmol). Purification by column chromatography on silica gel (*n*hexane/EtOAc: 4/1→1/1) yielded **110d** (79.0 mg, 71%) as a white solid. **M.p.**: 155–157 °C.  **$^1H$  NMR** (300 MHz, CDCl<sub>3</sub>)  $\delta = 9.94$  (s, 1H), 8.87 (d,  $J = 8.6$  Hz, 1H), 8.79 (dd,  $J = 4.2, 1.7$  Hz, 1H), 8.60 (dd,  $J = 8.4, 1.7$  Hz, 1H), 8.16–8.05 (m, 1H), 7.76–7.70 (m, 1H), 7.67–7.61 (m, 1H), 7.57 (tdd,  $J = 7.4, 3.4, 1.5$  Hz, 1H), 7.44 (dd,  $J = 8.4, 4.2$  Hz, 1H), 6.92 (d,  $J = 8.6$  Hz, 1H), 4.76 (dhept,  $J = 7.6, 6.2$  Hz, 2H), 4.03 (s, 3H), 1.26 (d,  $J = 6.2$  Hz, 6H), 1.17 (d,  $J = 6.2$  Hz, 6H).  **$^{13}C$  NMR** (101 MHz, CDCl<sub>3</sub>)  $\delta = 167.0$  (d,  $^3J_{C-P} = 4.6$  Hz, C<sub>q</sub>), 150.6 (C<sub>q</sub>), 148.6 (CH), 141.0 (d,  $^2J_{C-P} = 9.4$  Hz, C<sub>q</sub>), 139.5 (C<sub>q</sub>), 133.4 (d,  $^3J_{C-P} = 9.4$  Hz, CH), 132.2 (d,  $^4J_{C-P} = 2.9$  Hz, CH), 131.2 (CH), 129.3 (d,  $^2J_{C-P} = 14.3$  Hz, CH), 128.7 (d,  $^3J_{C-P} = 13.0$  Hz, CH), 128.2 (C<sub>q</sub>), 127.3 (d,  $^1J_{C-P} = 188.5$  Hz, C<sub>q</sub>), 120.7 (CH), 120.5 (C<sub>q</sub>), 117.5 (CH), 104.4 (CH), 71.5 (d,  $^2J_{C-P} = 6.1$  Hz, CH), 55.8 (CH<sub>3</sub>), 23.8 (d,  $^3J_{C-P} = 4.1$  Hz, CH<sub>3</sub>), 23.8 (d,  $^3J_{C-P} = 4.8$  Hz, CH<sub>3</sub>).  **$^{31}P\{^1H\}$  NMR** (121 MHz, CDCl<sub>3</sub>)  $\delta = 14.6$  (td,  $J = 8.2, 4.4$  Hz). **IR** (ATR): 3344, 2978, 1665, 1532, 1272, 1247, 974, 786, 552, 539 cm<sup>-1</sup>. **MS** (ESI)  $m/z$  (relative intensity): 465 (100) [M+Na]<sup>+</sup>, 443 (35) [M+H]<sup>+</sup>. **HR-MS** (ESI)  $m/z$  calcd for C<sub>23</sub>H<sub>28</sub>N<sub>2</sub>O<sub>5</sub>P [M+H]<sup>+</sup>: 443.1730, found: 443.1734.



**Diisopropyl {2-[(6-methoxyquinolin-8-yl)carbamoyl]phenyl}phosphonate (110e)**

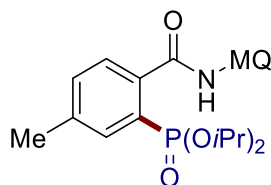
The general procedure **G** was followed using benzamide **106b** (69.5 mg, 1.0 equiv, 0.25 mmol) and diisopropyl phosphonate (**74a**) (83.0 mg, 2.0 equiv, 0.50 mmol). Purification by column chromatography on silica gel (*n*hexane/EtOAc: 4/1→1/1) yielded **110e** (60.0 mg, 54%) as a white solid. **M.p.**: 100–102 °C. **<sup>1</sup>H NMR** (300 MHz, CDCl<sub>3</sub>) δ = 10.13 (s, 1H), 8.70 (d, *J* = 2.7 Hz, 1H), 8.61 (dd, *J* = 4.2, 1.6 Hz, 1H), 8.17–8.02 (m, 2H), 7.76–7.53 (m, 3H), 7.39 (dd, *J* = 8.3, 4.2 Hz, 1H), 6.85 (d, *J* = 2.7 Hz, 1H), 4.76 (dhept, *J* = 7.6, 6.2 Hz, 2H), 3.97 (s, 3H), 1.26 (d, *J* = 6.2 Hz, 6H), 1.17 (d, *J* = 6.2 Hz, 6H). **<sup>13</sup>C NMR** (101 MHz, CDCl<sub>3</sub>) δ = 167.5 (d, <sup>3</sup>*J*<sub>C-P</sub> = 4.5 Hz, C<sub>q</sub>), 158.5 (C<sub>q</sub>), 145.6 (CH), 140.7 (d, <sup>2</sup>*J*<sub>C-P</sub> = 9.2 Hz, C<sub>q</sub>), 135.6 (C<sub>q</sub>), 135.3 (C<sub>q</sub>), 134.9 (CH), 133.4 (d, <sup>3</sup>*J*<sub>C-P</sub> = 9.4 Hz, CH), 132.3 (d, <sup>4</sup>*J*<sub>C-P</sub> = 2.9 Hz, CH), 129.5 (d, <sup>2</sup>*J*<sub>C-P</sub> = 14.2 Hz, CH), 129.0 (C<sub>q</sub>), 128.6 (d, <sup>3</sup>*J*<sub>C-P</sub> = 12.9 Hz, CH), 127.3 (d, <sup>1</sup>*J*<sub>C-P</sub> = 188.3 Hz, C<sub>q</sub>), 122.1 (CH), 109.7 (CH), 100.1 (CH), 71.5 (d, <sup>2</sup>*J*<sub>C-P</sub> = 6.0 Hz, CH), 55.6 (CH<sub>3</sub>), 23.8 (d, <sup>3</sup>*J*<sub>C-P</sub> = 4.1 Hz, CH<sub>3</sub>), 23.8 (d, <sup>3</sup>*J*<sub>C-P</sub> = 4.9 Hz, CH<sub>3</sub>). **<sup>31</sup>P{<sup>1</sup>H} NMR** (121 MHz, CDCl<sub>3</sub>) δ = 14.3 (td, *J* = 9.0, 4.9 Hz). **IR** (ATR): 3341, 2978, 1688, 1524, 1452, 1234, 983, 832, 566, 544 cm<sup>-1</sup>. **MS** (ESI) *m/z* (relative intensity): 465 (100) [M+Na]<sup>+</sup>, 443 (40) [M+H]<sup>+</sup>, 369 (5). **HR-MS** (ESI) *m/z* calcd for C<sub>23</sub>H<sub>28</sub>N<sub>2</sub>O<sub>5</sub>P [M+H]<sup>+</sup>: 443.1730, found: 443.1734.



**Diisopropyl {2-[(6-(trifluoromethyl)quinolin-8-yl)carbamoyl]phenyl}phosphonate (110f)**

The general procedure **G** was followed using benzamide **106i** (79.0 mg, 1.0 equiv, 0.25 mmol) and diisopropyl phosphonate (**74a**) (83.0 mg, 2.0 equiv, 0.50 mmol). Purification by column chromatography on silica gel (*n*hexane/EtOAc: 4/1→1/1)

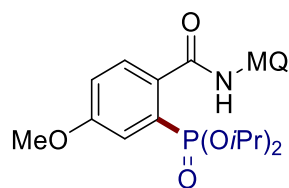
yielded **110f** (50.2 mg, 42%) as a white solid. **M.p.**: 104–106 °C. **<sup>1</sup>H NMR** (300 MHz, CDCl<sub>3</sub>)  $\delta$  = 10.23 (s, 1H), 9.20 (d,  $J$  = 1.9 Hz, 1H), 8.91 (dd,  $J$  = 4.2, 1.7 Hz, 1H), 8.29 (dd,  $J$  = 8.3, 1.7 Hz, 1H), 8.20–8.05 (m, 1H), 7.90 (dd,  $J$  = 1.9, 1.0 Hz, 1H), 7.77–7.54 (m, 4H), 4.78 (dhept,  $J$  = 7.7, 6.2 Hz, 2H), 1.26 (d,  $J$  = 6.2 Hz, 6H), 1.18 (d,  $J$  = 6.2 Hz, 6H). **<sup>13</sup>C NMR** (101 MHz, CDCl<sub>3</sub>)  $\delta$  = 167.7 (d,  $^3J_{C-P}$  = 4.5 Hz, C<sub>q</sub>), 150.2 (CH), 140.3 (d,  $^2J_{C-P}$  = 9.2 Hz, C<sub>q</sub>), 139.5 (C<sub>q</sub>), 137.3 (CH), 135.8 (C<sub>q</sub>), 133.4 (d,  $^3J_{C-P}$  = 9.2 Hz, CH), 132.3 (d,  $^4J_{C-P}$  = 3.0 Hz, CH), 129.7 (d,  $^2J_{C-P}$  = 14.3 Hz, CH), 129.3 (q,  $^2J_{C-F}$  = 32.5 Hz, C<sub>q</sub>), 128.6 (d,  $^3J_{C-P}$  = 12.9 Hz, CH), 127.5 (d,  $^1J_{C-P}$  = 188.4 Hz, C<sub>q</sub>), 127.0 (C<sub>q</sub>), 123.9 (q,  $^1J_{C-F}$  = 272.8 Hz, C<sub>q</sub>), 122.8 (CH), 119.4 (q,  $^3J_{C-F}$  = 4.6 Hz, CH), 112.8 (d,  $^3J_{C-F}$  = 3.3 Hz, CH), 71.6 (d,  $^2J_{C-P}$  = 6.1 Hz, CH), 23.8 (d,  $^3J_{C-P}$  = 4.2 Hz, CH<sub>3</sub>), 23.7 (d,  $^3J_{C-P}$  = 4.9 Hz, CH<sub>3</sub>). **<sup>31</sup>P{<sup>1</sup>H} NMR** (121 MHz, CDCl<sub>3</sub>)  $\delta$  = 14.2 (d,  $J$  = 13.0 Hz). **<sup>19</sup>F NMR** (376 MHz, CDCl<sub>3</sub>)  $\delta$  = -62.7. **IR** (ATR): 3363, 2987, 1682, 1523, 1244, 1115, 977, 661, 567, 538 cm<sup>-1</sup>. **MS** (ESI)  $m/z$  (relative intensity): 503 (100) [M+Na]<sup>+</sup>, 481 (20) [M+H]<sup>+</sup>, 369 (40). **HR-MS** (ESI)  $m/z$  calcd for C<sub>23</sub>H<sub>25</sub>F<sub>3</sub>N<sub>2</sub>O<sub>4</sub>P [M+H]<sup>+</sup>: 481.1499, found: 481.1500.



**Diisopropyl {5-methyl-2-[(6-methylquinolin-8-yl)carbamoyl]phenyl}phosphonate (110g)**

The general procedure **G** was followed using benzamide **106ae** (69.0 mg, 1.0 equiv, 0.25 mmol) and diisopropyl phosphonate (**74a**) (83.0 mg, 2.0 equiv, 0.50 mmol). Purification by column chromatography on silica gel (*n*hexane/EtOAc: 4/1→1/1) yielded **110g** (73.5 mg, 67%) as a white solid. **M.p.**: 119–121 °C. **<sup>1</sup>H NMR** (400 MHz, CDCl<sub>3</sub>)  $\delta$  = 10.09 (s, 1H), 8.81 (d,  $J$  = 1.9 Hz, 1H), 8.69 (dd,  $J$  = 4.3, 1.7 Hz, 1H), 8.08 (dd,  $J$  = 8.3, 1.7 Hz, 1H), 7.93 (dd,  $J$  = 14.6, 1.8 Hz, 1H), 7.62 (dd,  $J$  = 7.8, 5.3 Hz, 1H), 7.45 (d,  $J$  = 7.8 Hz, 1H), 7.40 (dd,  $J$  = 8.3, 4.3 Hz, 1H), 7.35–7.32 (m, 1H), 4.76 (dhept,  $J$  = 7.7, 6.2 Hz, 2H), 2.60 (s, 3H), 2.47 (s, 3H), 1.26 (d,  $J$  = 6.2 Hz, 6H), 1.17 (d,  $J$  = 6.2 Hz, 6H). **<sup>13</sup>C NMR** (101 MHz, CDCl<sub>3</sub>)  $\delta$  = 167.6 (d,  $^3J_{C-P}$  = 4.4 Hz, C<sub>q</sub>), 147.2 (CH),

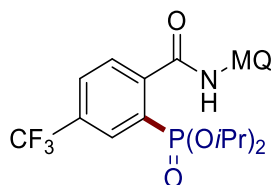
139.7 (d,  $^2J_{C-P} = 14.2$  Hz, C<sub>q</sub>), 138.2 (d,  $^3J_{C-P} = 9.1$  Hz, C<sub>q</sub>), 137.6 (C<sub>q</sub>), 137.5 (C<sub>q</sub>), 135.5 (CH), 134.4 (C<sub>q</sub>), 134.0 (d,  $^3J_{C-P} = 9.6$  Hz, CH), 132.8 (d,  $^4J_{C-P} = 3.1$  Hz, CH), 128.7 (d,  $^2J_{C-P} = 13.7$  Hz, CH), 128.0 (C<sub>q</sub>), 127.1 (d,  $^1J_{C-P} = 186.9$  Hz, C<sub>q</sub>), 121.6 (CH), 120.8 (CH), 119.2 (CH), 71.4 (d,  $^2J_{C-P} = 6.0$  Hz, CH), 23.8 (d,  $^3J_{C-P} = 4.4$  Hz, CH<sub>3</sub>), 23.8 (d,  $^3J_{C-P} = 5.1$  Hz, CH<sub>3</sub>), 22.4 (CH<sub>3</sub>), 21.3 (CH<sub>3</sub>).  **$^{31}P\{^1H\}$  NMR** (162 MHz, CDCl<sub>3</sub>)  $\delta = 14.9$  (dd,  $J = 14.2, 6.9$  Hz). **IR** (ATR): 3355, 2980, 1675, 1525, 1236, 975, 600, 571 cm<sup>-1</sup>. **MS** (ESI)  $m/z$  (relative intensity): 463 (10) [M+Na]<sup>+</sup>, 441 (100) [M+H]<sup>+</sup>. **HR-MS** (ESI)  $m/z$  calcd for C<sub>24</sub>H<sub>30</sub>N<sub>2</sub>O<sub>4</sub>P [M+H]<sup>+</sup>: 441.1938, found: 441.1938.



**Diisopropyl {5-methoxy-2-[(6-methylquinolin-8-yl)carbamoyl]phenyl} phosphonate (110i)**

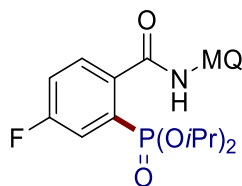
The general procedure **G** was followed using benzamide **106af** (73.0 mg, 1.0 equiv, 0.25 mmol) and diisopropyl phosphonate (**74a**) (83.0 mg, 2.0 equiv, 0.50 mmol). Purification by column chromatography on silica gel (*n*hexane/EtOAc: 4/1→1/1) yielded **110i** (70.0 mg, 61%) as a white solid. **M.p.**: 151–153 °C.  **$^1H$  NMR** (300 MHz, CDCl<sub>3</sub>)  $\delta = 10.11$  (s, 1H), 8.79 (d,  $J = 1.8$  Hz, 1H), 8.70 (dd,  $J = 4.2, 1.7$  Hz, 1H), 8.07 (dd,  $J = 8.3, 1.7$  Hz, 1H), 7.74–7.57 (m, 2H), 7.39 (dd,  $J = 8.3, 4.2$  Hz, 1H), 7.34–7.30 (m, 1H), 7.13 (ddd,  $J = 8.5, 2.7, 0.8$  Hz, 1H), 4.76 (dhept,  $J = 7.6, 6.2$  Hz, 2H), 3.91 (s, 3H), 2.61–2.56 (m, 3H), 1.27 (d,  $J = 6.2$  Hz, 6H), 1.17 (d,  $J = 6.2$  Hz, 6H).  **$^{13}C$  NMR** (101 MHz, CDCl<sub>3</sub>)  $\delta = 167.3$  (d,  $^3J_{C-P} = 4.2$  Hz, C<sub>q</sub>), 160.1 (d,  $^2J_{C-P} = 17.8$  Hz, C<sub>q</sub>), 147.2 (CH), 137.5 (C<sub>q</sub>), 137.5 (C<sub>q</sub>), 135.5 (CH), 134.4 (C<sub>q</sub>), 133.4 (d,  $^3J_{C-P} = 8.7$  Hz, C<sub>q</sub>), 130.6 (d,  $^2J_{C-P} = 15.3$  Hz, CH), 129.1 (d,  $^1J_{C-P} = 186.5$  Hz, C<sub>q</sub>), 128.1 (C<sub>q</sub>), 121.6 (CH), 120.8 (CH), 119.2 (CH), 118.4 (d,  $^3J_{C-P} = 10.6$  Hz, CH), 117.8 (d,  $^4J_{C-P} = 3.0$  Hz, CH), 71.6 (d,  $^2J_{C-P} = 6.1$  Hz, CH), 55.6 (CH<sub>3</sub>), 23.8 (d,  $^3J_{C-P} = 4.2$  Hz, CH<sub>3</sub>), 23.7 (d,  $^3J_{C-P} = 4.9$  Hz, CH<sub>3</sub>), 22.3 (CH<sub>3</sub>).  **$^{31}P\{^1H\}$  NMR** (121 MHz, CDCl<sub>3</sub>)  $\delta = 14.3$  (dq,  $J = 14.7, 7.3$  Hz). **IR** (ATR): 3336, 2975, 1674, 1526, 1250, 970, 874, 682, 584, 559 cm<sup>-1</sup>. **MS** (ESI)  $m/z$  (relative intensity): 479 (100) [M+Na]<sup>+</sup>, 457 (35) [M+H]<sup>+</sup>. **HR-MS** (ESI)  $m/z$

calcd for  $C_{24}H_{30}N_2O_5P$   $[M+H]^+$ : 457.1887, found: 457.1892.



**Diisopropyl {2-[(6-methylquinolin-8-yl)carbamoyl]-5-(trifluoromethyl)phenyl} phosphonate (110k)**

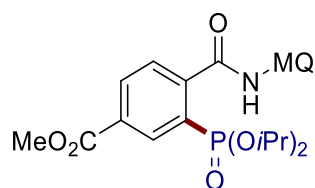
The general procedure **G** was followed using benzamide **106aj** (82.5 mg, 1.0 equiv, 0.25 mmol) and diisopropyl phosphonate (**74a**) (83.0 mg, 2.0 equiv, 0.50 mmol). Purification by column chromatography on silica gel (*n*hexane/EtOAc: 4/1→1/1) yielded **110k** (36.0 mg, 29%) as a white solid. **M.p.**: 139–140 °C. **<sup>1</sup>H NMR** (300 MHz,  $CDCl_3$ )  $\delta$  = 10.16 (s, 1H), 8.80 (d,  $J$  = 1.7 Hz, 1H), 8.71 (dd,  $J$  = 4.3, 1.7 Hz, 1H), 8.47–8.30 (m, 1H), 8.11 (dd,  $J$  = 8.3, 1.7 Hz, 1H), 7.96–7.89 (m, 1H), 7.85 (dd,  $J$  = 8.1, 4.5 Hz, 1H), 7.43 (dd,  $J$  = 8.3, 4.3 Hz, 1H), 7.39–7.36 (m, 1H), 4.80 (dhept,  $J$  = 7.7, 6.2 Hz, 2H), 2.61 (d,  $J$  = 0.9 Hz, 3H), 1.27 (d,  $J$  = 6.2 Hz, 6H), 1.21 (d,  $J$  = 6.2 Hz, 6H). **<sup>13</sup>C NMR** (126 MHz,  $CDCl_3$ )  $\delta$  = 166.1 (d,  $^3J_{C-P}$  = 4.2 Hz,  $C_q$ ), 147.3 (CH), 143.9 (d,  $^2J_{C-P}$  = 9.0 Hz,  $C_q$ ), 137.5 ( $C_q$ ), 137.3 ( $C_q$ ), 135.6 (CH), 133.9 ( $C_q$ ), 131.6 (qd,  $^2J_{C-F}$ ,  $^3J_{C-P}$  = 33.2, 14.8 Hz,  $C_q$ ), 130.4 (dq,  $^2J_{C-P}$ ,  $^3J_{C-F}$  = 10.9, 3.6 Hz, CH), 129.2 (d,  $^3J_{C-P}$  = 13.0 Hz, CH), 129.0 (q,  $^3J_{C-F}$  = 3.5 Hz, CH), 128.9 (d,  $^1J_{C-P}$  = 189.6 Hz,  $C_q$ ), 128.0 ( $C_q$ ), 123.3 (qd,  $^1J_{C-F}$ ,  $^4J_{C-P}$  = 272.8, 2.1 Hz,  $C_q$ ), 121.7 (CH), 121.3 (CH), 119.3 (CH), 72.2 (d,  $^2J_{C-P}$  = 6.1 Hz, CH), 23.8 (d,  $^3J_{C-P}$  = 4.1 Hz,  $CH_3$ ), 23.7 (d,  $^3J_{C-P}$  = 4.9 Hz,  $CH_3$ ), 22.3 ( $CH_3$ ). **<sup>31</sup>P{<sup>1</sup>H} NMR** (121 MHz,  $CDCl_3$ )  $\delta$  = 12.1 (dd,  $J$  = 14.1, 6.7 Hz). **<sup>19</sup>F NMR** (470 MHz,  $CDCl_3$ )  $\delta$  = -62.9. **IR** (ATR): 3343, 2981, 1681, 1538, 1329, 1127, 979, 853, 653, 562  $cm^{-1}$ . **MS** (ESI)  $m/z$  (relative intensity): 517 (40)  $[M+Na]^+$ , 495 (100)  $[M+H]^+$ . **HR-MS** (ESI)  $m/z$  calcd for  $C_{24}H_{27}F_3N_2O_4P$   $[M+H]^+$ : 495.1655, found: 495.1656.



**Diisopropyl {5-fluoro-2-[(6-methylquinolin-8-yl)carbamoyl]phenyl} phosphonate (110l)**



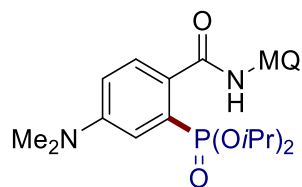
The general procedure **G** was followed using benzamide **106ah** (70.0 mg, 1.0 equiv, 0.25 mmol) and diisopropyl phosphonate (**74a**) (83.0 mg, 2.0 equiv, 0.50 mmol). Purification by column chromatography on silica gel (*n*hexane/EtOAc: 4/1→1/1) yielded **110i** (60.0 mg, 54%) as a colourless oil. **<sup>1</sup>H NMR** (300 MHz, CDCl<sub>3</sub>)  $\delta$  = 10.12 (s, 1H), 8.79 (d,  $J$  = 1.8 Hz, 1H), 8.71 (dd,  $J$  = 4.2, 1.7 Hz, 1H), 8.09 (dd,  $J$  = 8.3, 1.7 Hz, 1H), 7.86–7.69 (m, 2H), 7.41 (dd,  $J$  = 8.3, 4.2 Hz, 1H), 7.37–7.29 (m, 2H), 4.78 (dhept,  $J$  = 7.7, 6.2 Hz, 2H), 2.60 (d,  $J$  = 0.9 Hz, 3H), 1.27 (d,  $J$  = 6.2 Hz, 6H), 1.19 (d,  $J$  = 6.2 Hz, 6H). **<sup>13</sup>C NMR** (101 MHz, CDCl<sub>3</sub>)  $\delta$  = 166.5 (d,  $^3J_{C-P}$  = 4.2 Hz, C<sub>q</sub>), 162.6 (dd,  $^1J_{C-F}$ ,  $^3J_{C-P}$  = 252.4, 20.2 Hz, C<sub>q</sub>), 147.3 (CH), 137.5 (C<sub>q</sub>), 137.4 (C<sub>q</sub>), 137.1 (dd,  $^2J_{C-P}$ ,  $^4J_{C-F}$  = 8.6, 3.9 Hz, C<sub>q</sub>), 135.5 (CH), 134.2 (C<sub>q</sub>), 131.1 (dd,  $^3J_{C-F}$ ,  $^3J_{C-P}$  = 15.3, 7.9 Hz, CH), 130.5 (dd,  $^1J_{C-P}$ ,  $^3J_{C-F}$  = 187.9, 6.3 Hz, C<sub>q</sub>), 128.1 (C<sub>q</sub>), 121.7 (CH), 121.0 (CH), 120.4 (dd,  $^2J_{C-F}$ ,  $^4J_{C-P}$  = 23.2, 9.8 Hz, CH), 119.3 (CH), 119.2 (dd,  $^2J_{C-F}$ ,  $^2J_{C-P}$  = 15.3, 7.9 Hz, CH), 72.0 (d,  $^2J_{C-P}$  = 6.1 Hz, CH), 23.8 (d,  $^3J_{C-P}$  = 4.1 Hz, CH<sub>3</sub>), 23.7 (d,  $^3J_{C-P}$  = 4.9 Hz, CH<sub>3</sub>), 22.4 (CH<sub>3</sub>). **<sup>31</sup>P{<sup>1</sup>H} NMR** (121 MHz, CDCl<sub>3</sub>)  $\delta$  = 12.3 (dp,  $J$  = 14.4, 7.3 Hz). **<sup>19</sup>F NMR** (376 MHz, CDCl<sub>3</sub>)  $\delta$  = -109.4 (ddt,  $J$  = 13.9, 9.5, 4.4 Hz). **IR** (ATR): 3346, 2980, 1677, 1528, 1426, 1249, 978, 855, 690, 567 cm<sup>-1</sup>. **MS** (ESI)  $m/z$  (relative intensity): 467 (100) [M+Na]<sup>+</sup>, 445 (20) [M+H]<sup>+</sup>, 381 (10). **HR-MS** (ESI)  $m/z$  calcd for C<sub>23</sub>H<sub>27</sub>FN<sub>2</sub>O<sub>4</sub>P [M+H]<sup>+</sup>: 445.1687, found: 445.1686.



**Methyl 3-(diisopropoxyphosphoryl)-4-[(6-methylquinolin-8-yl)carbamoyl]benzoate (110m)**

The general procedure **G** was followed using benzamide **106k** (80.0 mg, 1.0 equiv, 0.25 mmol) and diisopropyl phosphonate (**74a**) (83.0 mg, 2.0 equiv, 0.50 mmol). Purification by column chromatography on silica gel (*n*hexane/EtOAc: 4/1→1/1) yielded **110m** (61.8 mg, 51%) as a white solid. **M.p.**: 129–130 °C. **<sup>1</sup>H NMR** (300 MHz, CDCl<sub>3</sub>)  $\delta$  = 10.15 (s, 1H), 8.81 (d,  $J$  = 1.7 Hz, 1H), 8.79–8.67 (m, 2H), 8.31 (dt,  $J$  = 8.0, 1.5 Hz, 1H), 8.09 (dd,  $J$  = 8.3, 1.7 Hz, 1H), 7.80 (dd,  $J$  = 8.0, 4.7 Hz, 1H), 7.42 (dd,  $J$  =

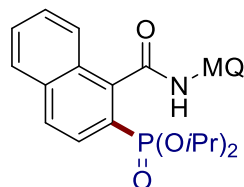
8.3, 4.2 Hz, 1H), 7.38–7.34 (m, 1H), 4.79 (dhept,  $J = 7.7, 6.2$  Hz, 2H), 3.99 (s, 3H), 2.62–2.59 (m, 3H), 1.26 (d,  $J = 6.2$  Hz, 6H), 1.20 (d,  $J = 6.2$  Hz, 6H).  $^{13}\text{C NMR}$  (101 MHz,  $\text{CDCl}_3$ )  $\delta = 166.6$  (d,  $^3J_{\text{C-P}} = 4.4$  Hz,  $\text{C}_q$ ), 165.7 (d,  $^4J_{\text{C-P}} = 1.8$  Hz,  $\text{C}_q$ ), 147.3 (CH), 144.5 (d,  $^3J_{\text{C-P}} = 9.5$  Hz,  $\text{C}_q$ ), 137.6 ( $\text{C}_q$ ), 137.4 ( $\text{C}_q$ ), 135.6 (CH), 134.5 (d,  $^3J_{\text{C-P}} = 10.3$  Hz, CH), 134.0 ( $\text{C}_q$ ), 133.3 (d,  $^4J_{\text{C-P}} = 2.9$  Hz, CH), 131.1 (d,  $^2J_{\text{C-P}} = 14.4$  Hz,  $\text{C}_q$ ), 128.9 (d,  $^2J_{\text{C-P}} = 13.1$  Hz, CH), 128.2 (d,  $^1J_{\text{C-P}} = 189.3$  Hz,  $\text{C}_q$ ), 128.1 ( $\text{C}_q$ ), 121.7 (CH), 121.2 (CH), 119.4 (CH), 71.9 (d,  $^2J_{\text{C-P}} = 6.1$  Hz, CH), 52.5 ( $\text{CH}_3$ ), 23.8 (d,  $^3J_{\text{C-P}} = 4.2$  Hz,  $\text{CH}_3$ ), 23.7 (d,  $^3J_{\text{C-P}} = 4.9$  Hz,  $\text{CH}_3$ ), 22.4 ( $\text{CH}_3$ ).  $^{31}\text{P}\{^1\text{H}\}$  NMR (121 MHz,  $\text{CDCl}_3$ )  $\delta = 12.9$  (dq,  $J = 13.1, 6.8$  Hz). IR (ATR): 3353, 2983, 1720, 1683, 1530, 1244, 978, 755, 654, 545  $\text{cm}^{-1}$ . MS (ESI)  $m/z$  (relative intensity): 507 (100)  $[\text{M}+\text{Na}]^+$ , 485 (40)  $[\text{M}+\text{H}]^+$ , 381 (10). HR-MS (ESI)  $m/z$  calcd for  $\text{C}_{25}\text{H}_{30}\text{N}_2\text{O}_6\text{P}$   $[\text{M}+\text{H}]^+$ : 485.1836, found: 485.1839.



**Diisopropyl {5-(dimethylamino)-2-[(6-methylquinolin-8-yl)carbamoyl]phenyl} phosphonate (110n)**

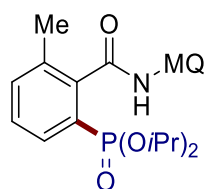
The general procedure **G** was followed using benzamide **106l** (76.3 mg, 1.0 equiv, 0.25 mmol) and diisopropyl phosphonate (**74a**) (83.0 mg, 2.0 equiv, 0.50 mmol). Purification by column chromatography on silica gel (*n*hexane/EtOAc: 4/1→1/1) yielded **110n** (63.0 mg, 54%) as a white solid. **M.p.**: 160–162 °C.  $^1\text{H NMR}$  (300 MHz,  $\text{CDCl}_3$ )  $\delta = 10.16$  (s, 1H), 8.79 (d,  $J = 1.8$  Hz, 1H), 8.71 (dd,  $J = 4.4, 1.6$  Hz, 1H), 8.08 (d,  $J = 8.2$  Hz, 1H), 7.65 (dd,  $J = 8.6, 6.3$  Hz, 1H), 7.46–7.36 (m, 2H), 7.34–7.30 (m, 1H), 6.88 (dd,  $J = 8.7, 2.7$  Hz, 1H), 4.86–4.65 (m, 2H), 3.09 (s, 6H), 2.59 (s, 3H), 1.28 (d,  $J = 6.2$  Hz, 6H), 1.18 (d,  $J = 6.2$  Hz, 6H).  $^{13}\text{C NMR}$  (101 MHz,  $\text{CDCl}_3$ )  $\delta = 168.0$  (d,  $^3J_{\text{C-P}} = 4.2$  Hz,  $\text{C}_q$ ), 150.6 (d,  $^2J_{\text{C-P}} = 16.4$  Hz,  $\text{C}_q$ ), 147.1 (CH), 137.6 ( $\text{C}_q$ ), 137.6 ( $\text{C}_q$ ), 135.5 (CH), 134.7 ( $\text{C}_q$ ), 130.5 (d,  $^2J_{\text{C-P}} = 14.9$  Hz, CH), 128.2 (d,  $^1J_{\text{C-P}} = 185.0$  Hz,  $\text{C}_q$ ), 128.1 ( $\text{C}_q$ ), 127.9 (d,  $^3J_{\text{C-P}} = 8.7$  Hz,  $\text{C}_q$ ), 121.5 (CH), 120.5 (CH), 119.3 (CH), 116.6 (d,  $^3J_{\text{C-P}} = 11.7$  Hz, CH), 114.3 (d,  $^4J_{\text{C-P}} = 2.9$  Hz, CH), 71.3 (d,  $^2J_{\text{C-P}} = 5.9$  Hz, CH), 40.2 ( $\text{CH}_3$ ), 23.9 (d,  $^3J_{\text{C-P}} = 4.0$  Hz,  $\text{CH}_3$ ), 23.8 (d,  $^3J_{\text{C-P}} = 4.9$  Hz,  $\text{CH}_3$ ), 22.4 ( $\text{CH}_3$ ).  $^{31}\text{P}\{^1\text{H}\}$  NMR (162 MHz,  $\text{CDCl}_3$ )  $\delta = 16.2$  (dd,  $J = 16.5, 7.9$  Hz). IR (ATR): 3345, 2984, 208

1664, 1527, 1233, 1003, 974, 672, 566  $\text{cm}^{-1}$ . **MS** (ESI)  $m/z$  (relative intensity): 492 (100)  $[\text{M}+\text{Na}]^+$ , 470 (40)  $[\text{M}+\text{H}]^+$ , 381 (10), 273 (10). **HR-MS** (ESI)  $m/z$  calcd for  $\text{C}_{25}\text{H}_{33}\text{N}_3\text{O}_4\text{P}$   $[\text{M}+\text{H}]^+$ : 470.2203, found: 470.2205.



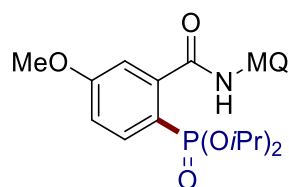
**Diisopropyl {1-[(6-methylquinolin-8-yl)carbamoyl]naphthalen-2-yl}phosphonate (110o)**

The general procedure **G** was followed using benzamide **106ad** (78.0 mg, 1.0 equiv, 0.25 mmol) and diisopropyl phosphonate (**74a**) (83.0 mg, 2.0 equiv, 0.50 mmol). Purification by column chromatography on silica gel (*n*hexane/EtOAc: 4/1→1/1) yielded **110o** (98.0 mg, 82%) as a white solid. **M.p.**: 139–141 °C.  **$^1\text{H NMR}$**  (400 MHz,  $\text{CDCl}_3$ )  $\delta$  = 10.17 (s, 1H), 9.04 (d,  $J$  = 2.0 Hz, 1H), 8.60 (dd,  $J$  = 4.2, 1.8 Hz, 1H), 8.18 (d,  $J$  = 8.4 Hz, 1H), 8.11–7.99 (m, 3H), 7.93 (d,  $J$  = 8.1 Hz, 1H), 7.67–7.51 (m, 2H), 7.39–7.36 (m, 2H), 5.00–4.52 (m, 2H), 2.65 (s, 3H), 1.33–1.07 (m, 12H).  **$^{13}\text{C NMR}$**  (101 MHz,  $\text{CDCl}_3$ )  $\delta$  = 166.5 (d,  $^3J_{\text{C-P}}$  = 5.9 Hz,  $\text{C}_q$ ), 147.1 (CH), 140.0 (d,  $^3J_{\text{C-P}}$  = 10.3 Hz,  $\text{C}_q$ ), 137.7 ( $\text{C}_q$ ), 137.3 ( $\text{C}_q$ ), 135.5 (CH), 135.0 (d,  $^4J_{\text{C-P}}$  = 2.5 Hz,  $\text{C}_q$ ), 134.4 ( $\text{C}_q$ ), 130.1 (d,  $^2J_{\text{C-P}}$  = 15.1 Hz,  $\text{C}_q$ ), 129.1 (d,  $^2J_{\text{C-P}}$  = 13.8 Hz, CH), 128.3 (CH), 128.1 ( $\text{C}_q$ ), 128.0 (CH), 127.7 (CH), 127.6 (d,  $^3J_{\text{C-P}}$  = 9.1 Hz, CH), 126.6 (CH), 124.3 (d,  $^1J_{\text{C-P}}$  = 186.9 Hz,  $\text{C}_q$ ), 121.6 (CH), 120.9 (CH), 119.1 (CH), 71.4 (d,  $^2J_{\text{C-P}}$  = 30.4 Hz, CH), 23.9 ( $\text{CH}_3$ ), 23.8 (d,  $^3J_{\text{C-P}}$  = 4.8 Hz,  $\text{CH}_3$ ), 22.4 ( $\text{CH}_3$ ).  **$^{31}\text{P}\{^1\text{H}\}$  NMR** (162 MHz,  $\text{CDCl}_3$ )  $\delta$  = 14.3 (dtd,  $J$  = 11.8, 7.4, 4.0 Hz). **IR** (ATR): 3335, 2975, 1668, 1524, 1245, 976, 868, 682, 530  $\text{cm}^{-1}$ . **MS** (ESI)  $m/z$  (relative intensity): 499 (5)  $[\text{M}+\text{Na}]^+$ , 477 (100)  $[\text{M}+\text{H}]^+$ . **HR-MS** (ESI)  $m/z$  calcd for  $\text{C}_{27}\text{H}_{30}\text{N}_2\text{O}_4\text{P}$   $[\text{M}+\text{H}]^+$ : 477.1938, found: 477.1939.



**Diisopropyl {3-methyl-2-[(6-methylquinolin-8-yl)carbamoyl]phenyl}phosphonate (110p)**

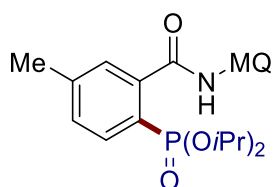
The general procedure **G** was followed using benzamide **106m** (69.0 mg, 1.0 equiv, 0.25 mmol) and diisopropyl phosphonate (**74a**) (83.0 mg, 2.0 equiv, 0.50 mmol). Purification by column chromatography on silica gel (*n*hexane/EtOAc: 4/1→1/1) yielded **110p** (75.0 mg, 68%) as a white solid. **M.p.**: 138–140 °C. **<sup>1</sup>H NMR** (300 MHz, CDCl<sub>3</sub>) δ = 9.93 (s, 1H), 8.90 (d, *J* = 1.8 Hz, 1H), 8.67 (dd, *J* = 4.2, 1.7 Hz, 1H), 8.08 (dd, *J* = 8.3, 1.7 Hz, 1H), 7.96–7.85 (m, 1H), 7.49–7.42 (m, 2H), 7.39 (dd, *J* = 8.3, 4.2 Hz, 1H), 7.35–7.32 (m, 1H), 4.71 (dhept, *J* = 7.6, 6.2 Hz, 2H), 2.60 (d, *J* = 0.9 Hz, 3H), 2.47 (s, 3H), 1.21 (d, *J* = 6.2 Hz, 6H), 1.13 (d, *J* = 6.2 Hz, 6H). **<sup>13</sup>C NMR** (101 MHz, CDCl<sub>3</sub>) δ = 166.9 (d, <sup>3</sup>*J*<sub>C-P</sub> = 4.9 Hz, C<sub>q</sub>), 147.1 (CH), 140.1 (d, <sup>3</sup>*J*<sub>C-P</sub> = 10.0 Hz, C<sub>q</sub>), 137.6 (C<sub>q</sub>), 137.3 (C<sub>q</sub>), 136.2 (d, <sup>2</sup>*J*<sub>C-P</sub> = 13.2 Hz, C<sub>q</sub>), 135.5 (CH), 134.3 (d, <sup>4</sup>*J*<sub>C-P</sub> = 3.0 Hz, CH), 134.3 (C<sub>q</sub>), 130.7 (d, <sup>3</sup>*J*<sub>C-P</sub> = 9.1 Hz, CH), 128.6 (d, <sup>2</sup>*J*<sub>C-P</sub> = 15.2 Hz, CH), 128.0 (C<sub>q</sub>), 127.1 (d, <sup>1</sup>*J*<sub>C-P</sub> = 187.3 Hz, C<sub>q</sub>), 121.6 (CH), 120.8 (CH), 119.0 (CH), 71.2 (d, <sup>2</sup>*J*<sub>C-P</sub> = 6.1 Hz, CH), 23.8 (d, <sup>3</sup>*J*<sub>C-P</sub> = 4.1 Hz, CH<sub>3</sub>), 23.7 (d, <sup>3</sup>*J*<sub>C-P</sub> = 4.8 Hz, CH<sub>3</sub>), 19.6 (d, <sup>4</sup>*J*<sub>C-P</sub> = 1.5 Hz, CH<sub>3</sub>). **<sup>31</sup>P{<sup>1</sup>H} NMR** (121 MHz, CDCl<sub>3</sub>) δ = 15.0–14.7 (m). **IR** (ATR): 3366, 2977, 1674, 1526, 1249, 967, 869, 659, 611 cm<sup>-1</sup>. **MS** (ESI) *m/z* (relative intensity): 463 (100) [M+Na]<sup>+</sup>, 441 (25) [M+H]<sup>+</sup>, 381 (20). **HR-MS** (ESI) *m/z* calcd for C<sub>24</sub>H<sub>30</sub>N<sub>2</sub>O<sub>4</sub>P [M+H]<sup>+</sup>: 441.1938, found: 441.1938.



**Diisopropyl {4-methoxy-2-[(6-methylquinolin-8-yl)carbamoyl]phenyl} phosphonate (110q)**

The general procedure **G** was followed using benzamide **106n** (73.0 mg, 1.0 equiv, 0.25 mmol) and diisopropyl phosphonate (**74a**) (83.0 mg, 2.0 equiv, 0.50 mmol). Purification by column chromatography on silica gel (*n*hexane/EtOAc: 4/1→1/1) yielded **110q** (98.0 mg, 86%) as a white solid. **M.p.**: 151–153 °C. **<sup>1</sup>H NMR** (300 MHz, CDCl<sub>3</sub>) δ = 10.11 (s, 1H), 8.80 (d, *J* = 1.9 Hz, 1H), 8.69 (dd, *J* = 4.2, 1.7 Hz, 1H), 8.11–7.96 (m, 2H), 7.39 (dd, *J* = 8.3, 4.2 Hz, 1H), 7.36–7.30 (m, 1H), 7.21 (dd, *J* = 4.1, 2.6 Hz, 1H), 7.05 (dt, *J* = 8.6, 2.6 Hz, 1H), 4.72 (dhept, *J* = 7.7, 6.2 Hz, 2H), 3.88 (s,

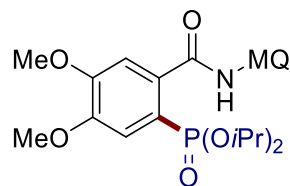
3H), 2.58 (d,  $J = 1.0$  Hz, 3H), 1.24 (d,  $J = 6.2$  Hz, 6H), 1.14 (d,  $J = 6.2$  Hz, 6H).  $^{13}\text{C}$  NMR (101 MHz,  $\text{CDCl}_3$ )  $\delta = 167.1$  (d,  $^3J_{\text{C-P}} = 4.2$  Hz,  $\text{C}_q$ ), 162.4 (d,  $^4J_{\text{C-P}} = 3.2$  Hz,  $\text{C}_q$ ), 147.3 (CH), 142.8 (d,  $^2J_{\text{C-P}} = 10.7$  Hz,  $\text{C}_q$ ), 137.5 ( $\text{C}_q$ ), 137.5 ( $\text{C}_q$ ), 135.6 (d,  $^3J_{\text{C-P}} = 10.7$  Hz, CH), 135.5 (CH), 134.2 ( $\text{C}_q$ ), 128.0 ( $\text{C}_q$ ), 121.6 (CH), 120.9 (CH), 119.3 (CH), 118.6 (d,  $^1J_{\text{C-P}} = 195.0$  Hz,  $\text{C}_q$ ), 115.0 (d,  $^2J_{\text{C-P}} = 15.2$  Hz, CH), 114.1 (d,  $^3J_{\text{C-P}} = 14.1$  Hz, CH), 71.2 (d,  $^2J_{\text{C-P}} = 5.9$  Hz, CH), 55.5 ( $\text{CH}_3$ ), 23.8 (d,  $^3J_{\text{C-P}} = 4.2$  Hz,  $\text{CH}_3$ ), 23.7 (d,  $^3J_{\text{C-P}} = 4.8$  Hz,  $\text{CH}_3$ ), 22.3 ( $\text{CH}_3$ ).  $^{31}\text{P}\{^1\text{H}\}$  NMR (121 MHz,  $\text{CDCl}_3$ )  $\delta = 15.2$ . IR (ATR): 3329, 2975, 1669, 1528, 1260, 973, 867, 556, 530  $\text{cm}^{-1}$ . MS (ESI)  $m/z$  (relative intensity): 479 (100)  $[\text{M}+\text{Na}]^+$ , 457 (35)  $[\text{M}+\text{H}]^+$ . HR-MS (ESI)  $m/z$  calcd for  $\text{C}_{24}\text{H}_{30}\text{N}_2\text{O}_5\text{P}$   $[\text{M}+\text{H}]^+$ : 457.1887, found: 457.1888.



**Diisopropyl {4-methyl-2-[(6-methylquinolin-8-yl)carbamoyl]phenyl}phosphonate (110r)**

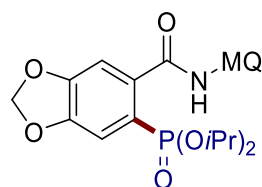
The general procedure **G** was followed using benzamide **106o** (69.0 mg, 1.0 equiv, 0.25 mmol) and diisopropyl phosphonate (**74a**) (83.0 mg, 2.0 equiv, 0.50 mmol). Purification by column chromatography on silica gel (*n*hexane/EtOAc: 4/1→1/1) yielded **110r** (75.2 mg, 68%) as a white solid. **M.p.**: 116–118 °C.  $^1\text{H}$  NMR (400 MHz,  $\text{CDCl}_3$ )  $\delta = 10.08$  (s, 1H), 8.82 (d,  $J = 1.8$  Hz, 1H), 8.70 (dd,  $J = 4.1, 1.6$  Hz, 1H), 8.08 (dt,  $J = 8.3, 1.4$  Hz, 1H), 8.02–7.94 (m, 1H), 7.52 (d,  $J = 4.7$  Hz, 1H), 7.45–7.36 (m, 2H), 7.35–7.31 (m, 1H), 4.78–4.70 (m, 2H), 2.60 (s, 3H), 2.46 (s, 3H), 1.24 (d,  $J = 6.2$  Hz, 6H), 1.16 (d,  $J = 6.2$  Hz, 6H).  $^{13}\text{C}$  NMR (101 MHz,  $\text{CDCl}_3$ )  $\delta = 167.6$  (d,  $^3J_{\text{C-P}} = 4.5$  Hz,  $\text{C}_q$ ), 147.2 (CH), 143.0 (d,  $^4J_{\text{C-P}} = 3.0$  Hz,  $\text{C}_q$ ), 140.9 (d,  $^2J_{\text{C-P}} = 9.7$  Hz,  $\text{C}_q$ ), 137.5 ( $\text{C}_q$ ), 137.5 ( $\text{C}_q$ ), 135.5 (CH), 134.3 ( $\text{C}_q$ ), 133.6 (d,  $^3J_{\text{C-P}} = 9.8$  Hz, CH), 130.1 (d,  $^2J_{\text{C-P}} = 14.6$  Hz, CH), 129.3 (d,  $^3J_{\text{C-P}} = 13.4$  Hz, CH), 128.0 ( $\text{C}_q$ ), 124.1 (d,  $^1J_{\text{C-P}} = 190.4$  Hz,  $\text{C}_q$ ), 121.6 (CH), 120.8 (CH), 119.2 (CH), 71.3 (d,  $^2J_{\text{C-P}} = 6.0$  Hz), 23.8 (d,  $^3J_{\text{C-P}} = 4.1$  Hz,  $\text{CH}_3$ ), 23.7 (d,  $^3J_{\text{C-P}} = 4.9$  Hz,  $\text{CH}_3$ ), 22.4 ( $\text{CH}_3$ ), 21.5 (d,  $^5J_{\text{C-P}} = 1.4$  Hz).  $^{31}\text{P}\{^1\text{H}\}$  NMR (162 MHz,  $\text{CDCl}_3$ )  $\delta = 15.0$  (d,  $J = 12.9$  Hz). IR (ATR): 3349, 2984, 1680, 1527, 1232, 1000, 975, 859, 661, 539  $\text{cm}^{-1}$ . MS (ESI)  $m/z$  (relative intensity): 463 (100)

$[M+Na]^+$ , 441 (30)  $[M+H]^+$ , 381 (5). **HR-MS** (ESI)  $m/z$  calcd for  $C_{24}H_{30}N_2O_4P$   $[M+H]^+$ : 441.1938, found: 441.1942.



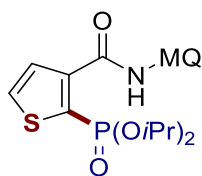
**Diisopropyl {4,5-dimethoxy-2-[(6-methylquinolin-8-yl)carbamoyl]phenyl} phosphonate (110t)**

The general procedure **G** was followed using benzamide **106q** (80.5 mg, 1.0 equiv, 0.25 mmol) and diisopropyl phosphonate (**74a**) (83.0 mg, 2.0 equiv, 0.50 mmol). Purification by column chromatography on silica gel (*n*hexane/EtOAc: 4/1→1/1) yielded **110t** (98.0 mg, 81%) as a white solid. **M.p.**: 153–155 °C. **<sup>1</sup>H NMR** (300 MHz,  $CDCl_3$ )  $\delta$  = 10.14 (s, 1H), 8.77 (d,  $J$  = 1.8 Hz, 1H), 8.70 (dd,  $J$  = 4.2, 1.7 Hz, 1H), 8.07 (dd,  $J$  = 8.3, 1.7 Hz, 1H), 7.55 (d,  $J$  = 14.7 Hz, 1H), 7.40 (dd,  $J$  = 8.3, 4.2 Hz, 1H), 7.36–7.30 (m, 1H), 7.22 (d,  $J$  = 4.9 Hz, 1H), 4.85–4.63 (m, 2H), 4.00 (s, 3H), 3.94 (s, 3H), 2.59 (s, 3H), 1.26 (d,  $J$  = 6.2 Hz, 6H), 1.12 (d,  $J$  = 6.2 Hz, 6H). **<sup>13</sup>C NMR** (101 MHz,  $CDCl_3$ )  $\delta$  = 167.3 (d,  $^3J_{C-P}$  = 4.2 Hz,  $C_q$ ), 151.7 (d,  $^4J_{C-P}$  = 2.9 Hz,  $C_q$ ), 149.3 (d,  $^2J_{C-P}$  = 17.6 Hz,  $C_q$ ), 147.3 (CH), 137.6 ( $C_q$ ), 137.5 ( $C_q$ ), 135.5 (CH), 134.7 (d,  $^3J_{C-P}$  = 9.3 Hz,  $C_q$ ), 134.3 ( $C_q$ ), 128.1 ( $C_q$ ), 121.6 (CH), 121.0 (CH), 119.3 (CH), 119.0 (d,  $^1J_{C-P}$  = 193.3 Hz,  $C_q$ ), 115.5 (d,  $^3J_{C-P}$  = 11.9 Hz, CH), 112.0 (d,  $^2J_{C-P}$  = 16.2 Hz, CH), 71.4 (d,  $^2J_{C-P}$  = 5.7 Hz, CH), 56.3 ( $CH_3$ ), 56.1 ( $CH_3$ ), 23.8 (d,  $^3J_{C-P}$  = 3.9 Hz,  $CH_3$ ), 22.4 ( $CH_3$ ). **<sup>31</sup>P{<sup>1</sup>H} NMR** (162 MHz,  $CDCl_3$ )  $\delta$  = 15.3 (dq,  $J$  = 14.0, 7.1 Hz). **IR** (ATR): 3345, 2977, 1671, 1530, 1510, 1268, 1213, 977, 575, 537  $cm^{-1}$ . **MS** (ESI)  $m/z$  (relative intensity): 509 (35)  $[M+Na]^+$ , 487 (100)  $[M+H]^+$ . **HR-MS** (ESI)  $m/z$  calcd for  $C_{25}H_{32}N_2O_6P$   $[M+H]^+$ : 487.1992, found: 487.1994.



**Diisopropyl {6-[(6-methylquinolin-8-yl)carbamoyl]benzo[d][1,3]dioxol-5-yl} phosphonate (110u)**

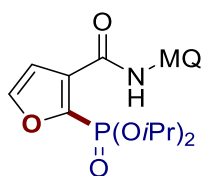
The general procedure **G** was followed using benzamide **106r** (76.5 mg, 1.0 equiv, 0.25 mmol) and diisopropyl phosphonate (**74a**) (83.0 mg, 2.0 equiv, 0.50 mmol). Purification by column chromatography on silica gel (*n*hexane/EtOAc: 4/1→1/1) yielded **110u** (67.8 mg, 58%) as a white solid. **M.p.**: 139–141 °C. **<sup>1</sup>H NMR** (400 MHz, CDCl<sub>3</sub>) δ = 10.09 (s, 1H), 8.77 (d, *J* = 1.8 Hz, 1H), 8.71 (dd, *J* = 4.2, 1.7 Hz, 1H), 8.08 (dd, *J* = 8.3, 1.7 Hz, 1H), 7.51 (d, *J* = 13.8 Hz, 1H), 7.41 (dd, *J* = 8.3, 4.2 Hz, 1H), 7.35–7.32 (m, 1H), 7.16 (d, *J* = 4.4 Hz, 1H), 6.11 (s, 2H), 4.73 (dhept, *J* = 7.6, 6.2 Hz, 2H), 2.59 (s, 3H), 1.26 (d, *J* = 6.2 Hz, 6H), 1.16 (d, *J* = 6.2 Hz, 6H). **<sup>13</sup>C NMR** (101 MHz, CDCl<sub>3</sub>) δ = 166.7 (d, <sup>3</sup>*J*<sub>C-P</sub> = 4.8 Hz, C<sub>q</sub>), 150.6 (d, <sup>4</sup>*J*<sub>C-P</sub> = 3.3 Hz, C<sub>q</sub>), 148.4 (d, <sup>2</sup>*J*<sub>C-P</sub> = 21.4 Hz, C<sub>q</sub>), 147.2 (CH), 137.5 (C<sub>q</sub>), 137.5 (C<sub>q</sub>), 136.7 (d, <sup>3</sup>*J*<sub>C-P</sub> = 10.4 Hz, C<sub>q</sub>), 135.5 (CH), 134.2 (C<sub>q</sub>), 128.1 (C<sub>q</sub>), 121.6 (CH), 121.3 (d, <sup>1</sup>*J*<sub>C-P</sub> = 192.3 Hz, C<sub>q</sub>), 120.9 (CH), 119.3 (CH), 112.9 (d, <sup>3</sup>*J*<sub>C-P</sub> = 11.4 Hz, CH), 109.4 (d, <sup>2</sup>*J*<sub>C-P</sub> = 16.5 Hz, CH), 102.2 (CH<sub>2</sub>), 71.5 (d, <sup>2</sup>*J*<sub>C-P</sub> = 6.0 Hz, CH), 23.8 (d, <sup>3</sup>*J*<sub>C-P</sub> = 3.8 Hz, CH<sub>3</sub>), 23.7 (d, <sup>3</sup>*J*<sub>C-P</sub> = 4.4 Hz, CH<sub>3</sub>), 22.3 (CH<sub>3</sub>). **<sup>31</sup>P{<sup>1</sup>H} NMR** (162 MHz, CDCl<sub>3</sub>) δ = 14.4 (dp, *J* = 12.4, 4.6, 4.0 Hz). **IR** (ATR): 3258, 2978, 1661, 1526, 1485, 1242, 967, 768, 581, 523 cm<sup>-1</sup>. **MS** (ESI) *m/z* (relative intensity): 493 (100) [M+Na]<sup>+</sup>, 471 (30) [M+H]<sup>+</sup>. **HR-MS** (ESI) *m/z* calcd for C<sub>24</sub>H<sub>28</sub>N<sub>2</sub>O<sub>6</sub>P [M+H]<sup>+</sup>: 471.1679, found: 471.1681.



**Diisopropyl {3-[(6-methylquinolin-8-yl)carbamoyl]thiophen-2-yl}phosphonate (110v)**

The general procedure **G** was followed using benzamide **106s** (67.0 mg, 1.0 equiv, 0.25 mmol) and diisopropyl phosphonate (**74a**) (83.0 mg, 2.0 equiv, 0.50 mmol) under a constant current of 8.0 mA for 5.0 h. Purification by column chromatography on silica gel (*n*hexane/EtOAc: 4/1→1/1) yielded **110v** (85.0 mg, 79%) as a white solid. **M.p.**: 119–120 °C. **<sup>1</sup>H NMR** (400 MHz, CDCl<sub>3</sub>) δ = 10.54 (s, 1H), 8.77 (dd, *J* = 4.2, 1.7 Hz, 1H), 8.73 (d, *J* = 1.8 Hz, 1H), 8.08 (dd, *J* = 8.3, 1.7 Hz, 1H), 7.69–7.64 (m, 1H), 7.63–7.59 (m, 1H), 7.42 (dd, *J* = 8.3, 4.2 Hz, 1H), 7.37–7.33 (m, 1H), 4.83 (dhept, *J* = 7.9,

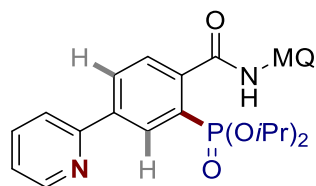
6.2 Hz, 2H), 2.59 (s, 3H), 1.32 (d,  $J = 6.3$  Hz, 6H), 1.30 (d,  $J = 6.3$  Hz, 8H).  $^{13}\text{C}$  NMR (101 MHz,  $\text{CDCl}_3$ )  $\delta = 161.9$  (d,  $^3J_{\text{C-P}} = 2.8$  Hz,  $\text{C}_q$ ), 147.5 (CH), 144.0 (d,  $^2J_{\text{C-P}} = 10.9$  Hz,  $\text{C}_q$ ), 137.9 ( $\text{C}_q$ ), 137.4 ( $\text{C}_q$ ), 135.5 (CH), 134.1 ( $\text{C}_q$ ), 131.9 (d,  $^3J_{\text{C-P}} = 7.6$  Hz, CH), 130.5 (d,  $^3J_{\text{C-P}} = 16.4$  Hz, CH), 130.2 (d,  $^1J_{\text{C-P}} = 206.4$  Hz,  $\text{C}_q$ ), 128.1 ( $\text{C}_q$ ), 121.7 (CH), 121.3 (CH), 120.0 (CH), 72.4 (d,  $^2J_{\text{C-P}} = 5.8$  Hz, CH), 24.0 (d,  $^3J_{\text{C-P}} = 4.1$  Hz,  $\text{CH}_3$ ), 23.6 (d,  $^3J_{\text{C-P}} = 5.0$  Hz,  $\text{CH}_3$ ), 22.2 ( $\text{CH}_3$ ).  $^{31}\text{P}\{^1\text{H}\}$  NMR (162 MHz,  $\text{CDCl}_3$ )  $\delta = 7.1$  (tt,  $J = 8.5, 4.6$  Hz). IR (ATR): 3077, 2980, 1662, 1533, 1250, 982, 854, 545, 529  $\text{cm}^{-1}$ . MS (ESI)  $m/z$  (relative intensity): 455 (100)  $[\text{M}+\text{Na}]^+$ , 433 (40)  $[\text{M}+\text{H}]^+$ . HR-MS (ESI)  $m/z$  calcd for  $\text{C}_{21}\text{H}_{26}\text{N}_2\text{O}_4\text{PS}$   $[\text{M}+\text{H}]^+$ : 433.1345, found: 433.1349.



#### Diisopropyl {3-[(6-methylquinolin-8-yl)carbamoyl]furan-2-yl}phosphonate (**110w**)

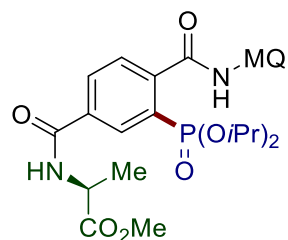
The general procedure **G** was followed using benzamide **106t** (63.0 mg, 1.0 equiv, 0.25 mmol) and diisopropyl phosphonate (**74a**) (83.0 mg, 2.0 equiv, 0.50 mmol) under a constant current of 8.0 mA for 5.0 h. Purification by column chromatography on silica gel (*n*hexane/EtOAc: 4/1→1/1) yielded **110w** (42.0 mg, 40%) as a white solid. **M.p.**: 94–96 °C.  $^1\text{H}$  NMR (400 MHz,  $\text{CDCl}_3$ )  $\delta = 11.21$  (s, 1H), 8.74 (dd,  $J = 4.2, 1.7$  Hz, 1H), 8.64 (d,  $J = 1.8$  Hz, 1H), 8.02 (dd,  $J = 8.3, 1.7$  Hz, 1H), 7.64 (dd,  $J = 2.8, 1.7$  Hz, 1H), 7.36 (dd,  $J = 8.3, 4.2$  Hz, 1H), 7.31 (dt,  $J = 1.8, 0.9$  Hz, 1H), 7.02 (dd,  $J = 2.4, 1.7$  Hz, 1H), 4.86 (dhept,  $J = 8.0, 6.2$  Hz, 2H), 2.53 (d,  $J = 0.9$  Hz, 3H), 1.37 (d,  $J = 6.2$  Hz, 6H), 1.27 (d,  $J = 6.2$  Hz, 6H).  $^{13}\text{C}$  NMR (101 MHz,  $\text{CDCl}_3$ )  $\delta = 159.9$  ( $\text{C}_q$ ), 147.6 (CH), 146.3 (CH), 146.2 (CH), 143.4 (d,  $^1J_{\text{C-P}} = 233.5$  Hz,  $\text{C}_q$ ), 138.4 ( $\text{C}_q$ ), 137.1 ( $\text{C}_q$ ), 135.3 (CH), 134.2 ( $\text{C}_q$ ), 133.1 (d,  $^2J_{\text{C-P}} = 23.8$  Hz,  $\text{C}_q$ ), 128.2 ( $\text{C}_q$ ), 121.5 (d,  $^3J_{\text{C-P}} = 5.3$  Hz, CH), 121.0 (CH), 113.0 (d,  $^3J_{\text{C-P}} = 10.1$  Hz, CH), 72.7 (d,  $^2J_{\text{C-P}} = 5.4$  Hz, CH,  $\text{CH}_3$ ), 24.0 (d,  $^3J_{\text{C-P}} = 4.1$  Hz), 23.6 (d,  $^3J_{\text{C-P}} = 5.0$  Hz,  $\text{CH}_3$ ), 22.2 ( $\text{CH}_3$ ).  $^{31}\text{P}\{^1\text{H}\}$  NMR (162 MHz,  $\text{CDCl}_3$ )  $\delta = 0.8$  (t,  $J = 8.2$  Hz). IR (ATR): 3115, 2982, 1667, 1537, 1255, 1001, 855, 748, 557, 530  $\text{cm}^{-1}$ . MS (ESI)  $m/z$  (relative intensity): 439 (100)  $[\text{M}+\text{Na}]^+$ , 417 (50)  $[\text{M}+\text{H}]^+$ . HR-MS (ESI)  $m/z$  calcd for  $\text{C}_{21}\text{H}_{26}\text{N}_2\text{O}_5\text{P}$   $[\text{M}+\text{H}]^+$ : 417.1574, found: 417.1576.





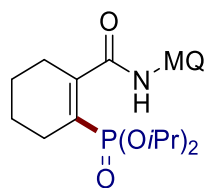
**Diisopropyl {2-[(6-methylquinolin-8-yl)carbamoyl]-5-(pyridin-2-yl)phenyl} phosphonate (110x)**

The general procedure **G** was followed using benzamide **106ao** (84.8 mg, 1.0 equiv, 0.25 mmol) and diisopropyl phosphonate (**74a**) (83.0 mg, 2.0 equiv, 0.50 mmol). Purification by column chromatography on silica gel (*n*hexane/EtOAc: 4/1→1/1) yielded **110x** (65.3 mg, 52%) as a white solid. **M.p.**: 166–168 °C. **<sup>1</sup>H NMR** (300 MHz, CDCl<sub>3</sub>)  $\delta$  = 10.18 (s, 1H), 8.84 (d, *J* = 1.8 Hz, 1H), 8.76 (ddd, *J* = 4.8, 1.8, 1.0 Hz, 1H), 8.72 (dd, *J* = 3.6, 1.8 Hz, 1H), 8.69 (dd, *J* = 7.1, 1.8 Hz, 1H), 8.43–8.32 (m, 1H), 8.09 (dd, *J* = 8.3, 1.8 Hz, 1H), 7.91–7.78 (m, 3H), 7.41 (dd, *J* = 8.3, 4.2 Hz, 1H), 7.35 (s, 1H), 7.32 (ddd, *J* = 7.3, 4.8, 1.4 Hz, 1H), 4.80 (dhept, *J* = 7.7, 6.2 Hz, 2H), 2.61 (d, *J* = 1.0 Hz, 3H), 1.28 (d, *J* = 6.2 Hz, 6H), 1.20 (d, *J* = 6.2 Hz, 6H). **<sup>13</sup>C NMR** (101 MHz, CDCl<sub>3</sub>)  $\delta$  = 167.2 (d, <sup>3</sup>*J*<sub>C-P</sub> = 4.3 Hz, C<sub>q</sub>), 155.5 (d, <sup>4</sup>*J*<sub>C-P</sub> = 1.4 Hz, C<sub>q</sub>), 149.9 (CH), 147.3 (CH), 141.0 (d, <sup>3</sup>*J*<sub>C-P</sub> = 9.3 Hz, C<sub>q</sub>), 140.4 (d, <sup>2</sup>*J*<sub>C-P</sub> = 14.2 Hz, C<sub>q</sub>), 137.5 (C<sub>q</sub>), 137.5 (C<sub>q</sub>), 136.9 (CH), 135.5 (CH), 134.3 (C<sub>q</sub>), 131.9 (d, <sup>3</sup>*J*<sub>C-P</sub> = 10.4 Hz, CH), 130.6 (d, <sup>4</sup>*J*<sub>C-P</sub> = 3.0 Hz, CH), 129.3 (d, <sup>2</sup>*J*<sub>C-P</sub> = 13.4 Hz, CH), 128.1 (C<sub>q</sub>), 127.9 (d, <sup>1</sup>*J*<sub>C-P</sub> = 188.0 Hz, C<sub>q</sub>), 122.9 (CH), 121.6 (CH), 120.9 (CH), 120.8 (CH), 119.2 (CH), 71.6 (d, <sup>2</sup>*J*<sub>C-P</sub> = 6.0 Hz, CH), 23.9 (d, <sup>3</sup>*J*<sub>C-P</sub> = 4.0 Hz, CH<sub>3</sub>), 23.8 (d, <sup>3</sup>*J*<sub>C-P</sub> = 4.9 Hz, CH<sub>3</sub>), 22.4 (CH<sub>3</sub>). **<sup>31</sup>P{<sup>1</sup>H} NMR** (121 MHz, CDCl<sub>3</sub>)  $\delta$  = 14.3 (dq, *J* = 13.9, 7.1 Hz). **IR** (ATR): 3342, 2982, 1665, 1528, 1234, 978, 852, 762, 654, 560 cm<sup>-1</sup>. **MS** (ESI) *m/z* (relative intensity): 526 (100) [M+Na]<sup>+</sup>, 504 (35) [M+H]<sup>+</sup>. **HR-MS** (ESI) *m/z* calcd for C<sub>28</sub>H<sub>31</sub>N<sub>3</sub>O<sub>4</sub>P [M+H]<sup>+</sup>: 504.2047, found: 504.2049.



**Methyl {3-(diisopropoxyphosphoryl)-4-[(6-methylquinolin-8-yl)carbamoyl]benzoyl}-L-alaninate (110y)**

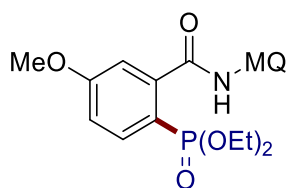
The general procedure **G** was followed using benzamide **106u** (97.8 mg, 1.0 equiv, 0.25 mmol), diisopropyl phosphonate (**74a**) (124 mg, 3.0 equiv, 0.75 mmol), Ni(DME)Cl<sub>2</sub> (11.0 mg, 20 mol %) and [3,5-(CF<sub>3</sub>)<sub>2</sub>C<sub>6</sub>H<sub>3</sub>]<sub>3</sub>P (67.0 mg, 40 mol %). Purification by column chromatography on silica gel (*n*hexane/EtOAc: 2/1→1/1→1/2) yielded **110y** (98.7 mg, 71%) as a white solid. **M.p.**: 70–72 °C. **<sup>1</sup>H NMR** (400 MHz, CDCl<sub>3</sub>) δ = 10.08 (s, 1H), 8.74 (d, *J* = 1.8 Hz, 1H), 8.64 (dd, *J* = 4.2, 1.7 Hz, 1H), 8.44 (dd, *J* = 14.4, 1.8 Hz, 1H), 8.13–8.09 (m, 1H), 8.04 (dd, *J* = 8.3, 1.7 Hz, 1H), 7.74 (dd, *J* = 8.0, 4.6 Hz, 1H), 7.36 (dd, *J* = 8.3, 4.2 Hz, 1H), 7.30 (dd, *J* = 1.8, 1.0 Hz, 1H), 7.01 (d, *J* = 7.2 Hz, 1H), 4.80 (q, *J* = 7.2 Hz, 1H), 4.77–4.65 (m, 2H), 3.76 (s, 3H), 2.55 (d, *J* = 1.0 Hz, 3H), 1.53 (d, *J* = 7.2 Hz, 3H), 1.21 (dd, *J* = 6.2, 1.9 Hz, 6H), 1.13 (dd, *J* = 6.2, 2.3 Hz, 6H). **<sup>13</sup>C NMR** (101 MHz, CDCl<sub>3</sub>) δ = 173.2 (C<sub>q</sub>), 166.4 (d, <sup>3</sup>*J*<sub>C-P</sub> = 4.2 Hz, C<sub>q</sub>), 165.2 (C<sub>q</sub>), 147.3 (CH), 143.5 (d, <sup>3</sup>*J*<sub>C-P</sub> = 9.2 Hz, C<sub>q</sub>), 137.5 (C<sub>q</sub>), 137.3 (C<sub>q</sub>), 135.5 (CH), 134.8 (d, <sup>2</sup>*J*<sub>C-P</sub> = 13.6 Hz, C<sub>q</sub>), 134.0 (C<sub>q</sub>), 131.6 (d, <sup>3</sup>*J*<sub>C-P</sub> = 10.3 Hz, CH), 131.4 (d, <sup>4</sup>*J*<sub>C-P</sub> = 2.8 Hz, CH), 129.1 (d, <sup>2</sup>*J*<sub>C-P</sub> = 13.0 Hz, CH), 128.0 (C<sub>q</sub>), 128.0 (d, <sup>1</sup>*J*<sub>C-P</sub> = 188.7 Hz, C<sub>q</sub>), 121.7 (CH), 121.1 (CH), 119.2 (CH), 71.9 (d, <sup>2</sup>*J*<sub>C-P</sub> = 6.1 Hz, CH), 52.5 (CH), 48.7 (CH<sub>3</sub>), 23.7 (d, <sup>3</sup>*J*<sub>C-P</sub> = 3.7 Hz, CH<sub>3</sub>), 23.6 (d, <sup>3</sup>*J*<sub>C-P</sub> = 2.4 Hz, CH<sub>3</sub>), 22.3 (CH<sub>3</sub>), 18.3 (CH<sub>3</sub>). **<sup>31</sup>P{<sup>1</sup>H} NMR** (121 MHz, CDCl<sub>3</sub>) δ = 13.1 (dt, *J* = 13.1, 6.8 Hz). **IR** (ATR): 3336, 2980, 1745, 1663, 1527, 1234, 982, 891, 856, 564 cm<sup>-1</sup>. **MS** (ESI) *m/z* (relative intensity): 578 (60) [M+Na]<sup>+</sup>, 556 (100) [M+H]<sup>+</sup>. **HR-MS** (ESI) *m/z* calcd for C<sub>28</sub>H<sub>35</sub>N<sub>3</sub>O<sub>7</sub>P [M+H]<sup>+</sup>: 556.2207, found: 556.2207.



**Diisopropyl {2-[(6-methylquinolin-8-yl)carbamoyl]cyclohex-1-en-1-yl} phosphonate (110z)**

The general procedure **G** was followed using benzamide **106v** (66.5 mg, 1.0 equiv, 0.25 mmol) and diisopropyl phosphonate (**74a**) (83.0 mg, 2.0 equiv, 0.50 mmol). Purification by column chromatography on silica gel (*n*hexane/EtOAc: 4/1→1/1) yielded **110z** (59.0 mg, 55%) as a white solid. **M.p.**: 113–115 °C. **<sup>1</sup>H NMR** (400 MHz,

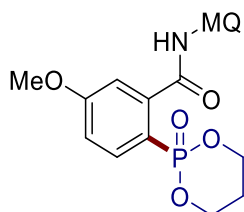
CDCl<sub>3</sub>)  $\delta$  = 9.85 (s, 1H), 8.78–8.70 (m, 2H), 8.06 (d,  $J$  = 8.2 Hz, 1H), 7.40 (dd,  $J$  = 8.2, 4.2 Hz, 1H), 7.29 (d,  $J$  = 3.2 Hz, 1H), 4.86–4.56 (m, 2H), 2.58 (dt,  $J$  = 7.2, 3.4 Hz, 2H), 2.55 (s, 3H), 2.40 (tt,  $J$  = 5.6, 3.0 Hz, 2H), 1.81–1.72 (m, 4H), 1.27 (d,  $J$  = 6.2 Hz, 6H), 1.18 (d,  $J$  = 6.2 Hz, 6H). **<sup>13</sup>C NMR** (101 MHz, CDCl<sub>3</sub>)  $\delta$  = 169.1 (d,  $^3J_{C-P}$  = 9.6 Hz, C<sub>q</sub>), 148.2 (d,  $^2J_{C-P}$  = 8.4 Hz, C<sub>q</sub>), 147.0 (CH), 137.6 (C<sub>q</sub>), 137.3 (C<sub>q</sub>), 135.5 (CH), 134.3 (C<sub>q</sub>), 128.1 (C<sub>q</sub>), 126.4 (d,  $^1J_{C-P}$  = 180.1 Hz, C<sub>q</sub>), 121.5 (CH), 120.6 (CH), 119.0 (CH), 70.6 (d,  $^2J_{C-P}$  = 6.0 Hz, CH), 29.1 (d,  $^2J_{C-P}$  = 15.9 Hz, CH<sub>2</sub>), 25.9 (d,  $^3J_{C-P}$  = 8.5 Hz, CH<sub>2</sub>), 23.9 (d,  $^3J_{C-P}$  = 4.0 Hz, CH<sub>3</sub>), 23.8 (d,  $^3J_{C-P}$  = 4.9 Hz, CH<sub>3</sub>), 22.3 (CH<sub>3</sub>), 21.6 (d,  $^3J_{C-P}$  = 9.3 Hz, CH<sub>2</sub>), 21.4 (d,  $^4J_{C-P}$  = 1.4 Hz, CH<sub>2</sub>). **<sup>31</sup>P{<sup>1</sup>H} NMR** (162 MHz, CDCl<sub>3</sub>)  $\delta$  = 14.0. **IR** (ATR): 3354, 2981, 1672, 1525, 1255, 974, 870, 665, 580 cm<sup>-1</sup>. **MS** (ESI)  $m/z$  (relative intensity): 453 (25) [M+Na]<sup>+</sup>, 431 (100) [M+H]<sup>+</sup>, 369 (10). **HR-MS** (ESI)  $m/z$  calcd for C<sub>23</sub>H<sub>32</sub>N<sub>2</sub>O<sub>4</sub>P [M+H]<sup>+</sup>: 431.2094, found: 431.2099.



**Diethyl {4-methoxy-2-[(6-methylquinolin-8-yl)carbamoyl]phenyl}phosphonate (110ab)**

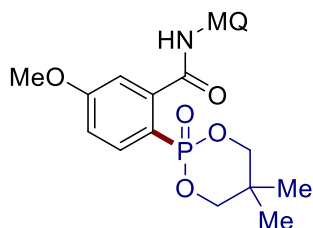
The general procedure **G** was followed using benzamide **106n** (73.0 mg, 1.0 equiv, 0.25 mmol) and diethyl phosphonate (**74b**) (69.0 mg, 2.0 equiv, 0.50 mmol). Purification by column chromatography on silica gel (*n*hexane/EtOAc: 2/1→1/1) yielded **110ab** (62.0 mg, 58%) as a white solid. **M.p.**: 132–134 °C. **<sup>1</sup>H NMR** (300 MHz, CDCl<sub>3</sub>)  $\delta$  = 10.17 (s, 1H), 8.82 (d,  $J$  = 1.8 Hz, 1H), 8.70 (dd,  $J$  = 4.2, 1.7 Hz, 1H), 8.19–7.94 (m, 2H), 7.41 (dd,  $J$  = 8.3, 4.2 Hz, 1H), 7.35 (dd,  $J$  = 1.8, 1.0 Hz, 1H), 7.24 (dd,  $J$  = 4.2, 2.6 Hz, 1H), 7.08 (dt,  $J$  = 8.6, 2.6 Hz, 1H), 4.16–3.99 (m, 4H), 3.91 (s, 3H), 2.60 (d,  $J$  = 1.0 Hz, 3H), 1.24–1.17 (m, 6H). **<sup>13</sup>C NMR** (101 MHz, CDCl<sub>3</sub>)  $\delta$  = 167.0 (d,  $^3J_{C-P}$  = 4.4 Hz, C<sub>q</sub>), 162.8 (d,  $^4J_{C-P}$  = 3.2 Hz, C<sub>q</sub>), 147.2 (CH), 142.9 (d,  $^2J_{C-P}$  = 11.0 Hz, C<sub>q</sub>), 137.6 (C<sub>q</sub>), 137.4 (C<sub>q</sub>), 136.1 (d,  $^3J_{C-P}$  = 10.6 Hz, CH), 135.6 (CH), 134.2 (C<sub>q</sub>), 128.1 (C<sub>q</sub>), 121.7 (CH), 121.0 (CH), 119.1 (CH), 116.9 (d,  $^1J_{C-P}$  = 193.6 Hz, C<sub>q</sub>), 115.1 (d,  $^2J_{C-P}$  = 15.2 Hz, CH), 114.1 (d,  $^3J_{C-P}$  = 14.1 Hz, CH), 62.4 (d,  $^2J_{C-P}$  = 5.6 Hz, CH<sub>2</sub>),

55.6 (CH<sub>3</sub>), 22.4 (CH<sub>3</sub>), 16.1 (d, <sup>3</sup>J<sub>C-P</sub> = 6.4 Hz, CH<sub>3</sub>). <sup>31</sup>P{<sup>1</sup>H} NMR (121 MHz, CDCl<sub>3</sub>) δ = 17.4 (ddp, J = 12.1, 7.9, 3.7 Hz). IR (ATR): 3300, 2984, 1656, 1533, 1252, 1023, 959, 819, 672, 554 cm<sup>-1</sup>. MS (ESI) m/z (relative intensity): 451 (80) [M+Na]<sup>+</sup>, 429 (100) [M+H]<sup>+</sup>. HR-MS (ESI) m/z calcd for C<sub>22</sub>H<sub>26</sub>N<sub>2</sub>O<sub>5</sub>P [M+H]<sup>+</sup>: 429.1574, found: 429.1578.



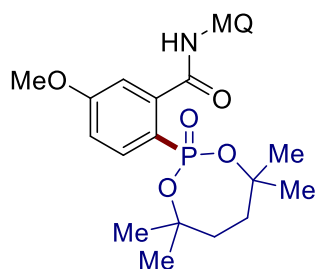
**5-Methoxy-N-(6-methylquinolin-8-yl)-2-(2-oxido-1,3,2-dioxaphosphinan-2-yl)benzamide (110ag)**

The general procedure **G** was followed using benzamide **106n** (73.0 mg, 1.0 equiv, 0.25 mmol) and 1,3,2-dioxaphosphinane 2-oxide (**74g**) (61.0 mg, 2.0 equiv, 0.50 mmol). Purification by column chromatography on silica gel (*n*hexane/EtOAc: 2/1→1/1) yielded **110ag** (54.7 mg, 53%) as a white solid. **M.p.**: 194–196 °C. <sup>1</sup>H NMR (300 MHz, CDCl<sub>3</sub>) δ = 10.29 (s, 1H), 8.82 (d, J = 1.8 Hz, 1H), 8.72 (dd, J = 4.3, 1.6 Hz, 1H), 8.07 (dd, J = 8.3, 1.6 Hz, 1H), 8.00 (dd, J = 13.6, 8.6 Hz, 1H), 7.40 (dd, J = 8.3, 4.2 Hz, 1H), 7.36–7.33 (s, 1H), 7.25 (dd, J = 4.2, 2.5 Hz, 1H), 7.09 (dt, J = 8.6, 2.5 Hz, 1H), 4.58–4.44 (m, 2H), 4.16 (tt, J = 11.3, 5.4 Hz, 2H), 3.90 (s, 3H), 2.59 (s, 3H), 1.92–1.82 (m, 2H). <sup>13</sup>C NMR (101 MHz, CDCl<sub>3</sub>) δ = 166.8 (d, <sup>3</sup>J<sub>C-P</sub> = 4.2 Hz, C<sub>q</sub>), 163.1 (d, <sup>4</sup>J<sub>C-P</sub> = 3.0 Hz, C<sub>q</sub>), 147.6 (CH), 143.0 (d, <sup>2</sup>J<sub>C-P</sub> = 11.2 Hz, C<sub>q</sub>), 137.4 (C<sub>q</sub>), 137.3 (C<sub>q</sub>), 136.1 (d, <sup>3</sup>J<sub>C-P</sub> = 10.8 Hz, CH), 135.5 (CH), 134.1 (C<sub>q</sub>), 128.1 (C<sub>q</sub>), 121.8 (CH), 121.3 (CH), 119.0 (CH), 115.4 (d, <sup>1</sup>J<sub>C-P</sub> = 194.7 Hz, C<sub>q</sub>), 115.2 (d, <sup>2</sup>J<sub>C-P</sub> = 15.5 Hz, CH), 114.4 (d, <sup>3</sup>J<sub>C-P</sub> = 14.2 Hz, CH), 66.8 (d, <sup>2</sup>J<sub>C-P</sub> = 6.2 Hz, CH<sub>2</sub>), 55.7 (CH<sub>3</sub>), 25.9 (d, <sup>3</sup>J<sub>C-P</sub> = 7.9 Hz, CH<sub>2</sub>), 22.4 (CH<sub>3</sub>). <sup>31</sup>P{<sup>1</sup>H} NMR (162 MHz, CDCl<sub>3</sub>) δ = 13.7. IR (ATR): 3330, 1673, 1524, 1268, 1057, 1046, 931, 819, 776, 681, 586, 525 cm<sup>-1</sup>. MS (ESI) m/z (relative intensity): 435 (50) [M+Na]<sup>+</sup>, 413 (100) [M+H]<sup>+</sup>. HR-MS (ESI) m/z calcd for C<sub>21</sub>H<sub>22</sub>N<sub>2</sub>O<sub>5</sub>P [M+H]<sup>+</sup>: 413.1261, found: 413.1263.



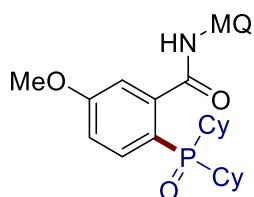
**2-(5,5-Dimethyl-2-oxido-1,3,2-dioxaphosphinan-2-yl)-5-methoxy-*N*-(6-methylquinolin-8-yl)benzamide (110ah)**

The general procedure **G** was followed using benzamide **106n** (73.0 mg, 1.0 equiv, 0.25 mmol) and 5,5-dimethyl-1,3,2-dioxaphosphinane 2-oxide (**74h**) (75.0 mg, 2.0 equiv, 0.50 mmol). Purification by column chromatography on silica gel (*n*hexane/EtOAc: 2/1→1/1) yielded **110ah** (63.8 mg, 58%) as a white solid. **M.p.**: 156–158 °C. **<sup>1</sup>H NMR** (400 MHz, CDCl<sub>3</sub>)  $\delta$  = 10.37 (s, 1H), 8.76 (d, *J* = 1.8 Hz, 1H), 8.73 (dd, *J* = 4.2, 1.6 Hz, 1H), 8.05 (dd, *J* = 8.3, 1.6 Hz, 1H), 7.83 (dd, *J* = 13.0, 8.6 Hz, 1H), 7.38 (dd, *J* = 8.3, 4.2 Hz, 1H), 7.35–7.31 (m, 1H), 7.30 (dt, *J* = 4.4, 2.2 Hz, 1H), 7.11 (dt, *J* = 8.6, 2.6 Hz, 1H), 4.09–4.01 (m, 2H), 3.91 (s, 3H), 3.94–3.84 (m, 2H), 2.57 (s, 3H), 1.18 (s, 3H), 0.87 (s, 3H). **<sup>13</sup>C NMR** (101 MHz, CDCl<sub>3</sub>)  $\delta$  = 166.7 (d, <sup>3</sup>*J*<sub>C-P</sub> = 4.4 Hz, C<sub>q</sub>), 162.8 (d, <sup>4</sup>*J*<sub>C-P</sub> = 3.2 Hz, C<sub>q</sub>), 147.5 (CH), 143.2 (d, <sup>2</sup>*J*<sub>C-P</sub> = 12.1 Hz, C<sub>q</sub>), 137.4 (C<sub>q</sub>), 137.3 (C<sub>q</sub>), 135.5 (CH), 134.6 (d, <sup>3</sup>*J*<sub>C-P</sub> = 10.1 Hz, CH), 134.0 (C<sub>q</sub>), 128.1 (C<sub>q</sub>), 121.7 (CH), 121.3 (CH), 119.4 (CH), 115.9 (d, <sup>2</sup>*J*<sub>C-P</sub> = 14.9 Hz, CH), 115.2 (d, <sup>1</sup>*J*<sub>C-P</sub> = 187.7 Hz, C<sub>q</sub>), 114.2 (d, <sup>3</sup>*J*<sub>C-P</sub> = 14.2 Hz, CH), 76.8 (d, <sup>2</sup>*J*<sub>C-P</sub> = 6.4 Hz, CH<sub>2</sub>), 55.7 (CH<sub>3</sub>), 32.4 (d, <sup>3</sup>*J*<sub>C-P</sub> = 6.4 Hz, C<sub>q</sub>), 22.3 (CH<sub>3</sub>), 21.9 (CH<sub>3</sub>), 21.0 (CH<sub>3</sub>). **<sup>31</sup>P{<sup>1</sup>H} NMR** (162 MHz, CDCl<sub>3</sub>)  $\delta$  = 11.8. **IR** (ATR): 3340, 2969, 1675, 1526, 1276, 1055, 1004, 788, 509, 471 cm<sup>-1</sup>. **MS** (ESI) *m/z* (relative intensity): 463 (35) [M+Na]<sup>+</sup>, 441 (100) [M+H]<sup>+</sup>. **HR-MS** (ESI) *m/z* calcd for C<sub>23</sub>H<sub>26</sub>N<sub>2</sub>O<sub>5</sub>P [M+H]<sup>+</sup>: 441.1574, found: 441.1575.



**5-Methoxy-*N*-(6-methylquinolin-8-yl)-2-(4,4,7,7-tetramethyl-2-oxido-1,3,2-dioxaphosphinan-2-yl)benzamide (110ai)**

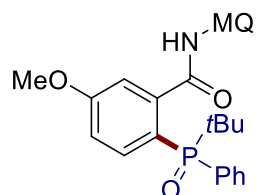
The general procedure **G** was followed using benzamide **106n** (73.0 mg, 1.0 equiv, 0.25 mmol) and 4,4,7,7-tetramethyl-1,3,2-dioxaphosphepane 2-oxide (**74i**) (96.0 mg, 2.0 equiv, 0.50 mmol). Purification by column chromatography on silica gel (*n*hexane/EtOAc: 2/1→1/1) yielded **110ai** (87.0 mg, 72%) as a white solid. **M.p.**: 189–191 °C. **<sup>1</sup>H NMR** (400 MHz, CDCl<sub>3</sub>)  $\delta$  = 10.09 (s, 1H), 8.83 (d,  $J$  = 1.9 Hz, 1H), 8.70 (dd,  $J$  = 4.2, 1.9 Hz, 1H), 8.08 (dt,  $J$  = 8.4, 2.0 Hz, 1H), 8.01–7.93 (m, 1H), 7.40 (ddd,  $J$  = 8.4, 4.2, 2.3 Hz, 1H), 7.34 (s, 1H), 7.16 (dt,  $J$  = 4.4, 2.5 Hz, 1H), 7.03 (dq,  $J$  = 8.3, 2.6 Hz, 1H), 3.87 (s, 3H), 2.61 (d,  $J$  = 2.6 Hz, 3H), 2.18–2.07 (m, 2H), 1.87–1.76 (m, 2H), 1.52 (t,  $J$  = 2.3 Hz, 6H), 1.18 (t,  $J$  = 1.9 Hz, 6H). **<sup>13</sup>C NMR (101 MHz, CDCl<sub>3</sub>)**  $\delta$  = 167.3 (d,  $^3J_{C-P}$  = 4.3 Hz, C<sub>q</sub>), 162.2 (d,  $^4J_{C-P}$  = 3.3 Hz, C<sub>q</sub>), 147.3 (CH), 142.4 (d,  $^2J_{C-P}$  = 10.6 Hz, C<sub>q</sub>), 137.5 (C<sub>q</sub>), 137.4 (C<sub>q</sub>), 135.6 (CH), 135.1 (d,  $^3J_{C-P}$  = 10.5 Hz, CH), 134.3 (C<sub>q</sub>), 128.1 (C<sub>q</sub>), 121.7 (CH), 121.0 (CH), 119.5 (CH), 118.9 (d,  $^1J_{C-P}$  = 206.9 Hz, C<sub>q</sub>), 114.9 (d,  $^2J_{C-P}$  = 15.5 Hz, CH), 113.7 (d,  $^3J_{C-P}$  = 14.4 Hz, CH), 83.3 (d,  $^2J_{C-P}$  = 8.2 Hz, C<sub>q</sub>), 55.5 (CH<sub>3</sub>), 36.5 (d,  $^3J_{C-P}$  = 1.7 Hz, CH<sub>2</sub>), 29.7 (d,  $^3J_{C-P}$  = 9.3 Hz, CH<sub>3</sub>), 28.4 (CH<sub>3</sub>), 22.4 (CH<sub>3</sub>). **<sup>31</sup>P{<sup>1</sup>H} NMR** (162 MHz, CDCl<sub>3</sub>)  $\delta$  = 12.6 (d,  $J$  = 13.5 Hz). **IR** (ATR): 3343, 2978, 1680, 1528, 1234, 982, 954, 677, 651, 572 cm<sup>-1</sup>. **MS** (ESI)  $m/z$  (relative intensity): 505 (45) [M+Na]<sup>+</sup>, 483 (100) [M+H]<sup>+</sup>. **HR-MS** (ESI)  $m/z$  calcd for C<sub>26</sub>H<sub>32</sub>N<sub>2</sub>O<sub>5</sub>P [M+H]<sup>+</sup>: 483.2043, found: 483.2045.



**2-(Dicyclohexylphosphoryl)-5-methoxy-N-(6-methylquinolin-8-yl)benzamide (110aj)**

The general procedure **G** was followed using benzamide **106n** (73.0 mg, 1.0 equiv, 0.25 mmol) and dicyclohexylphosphine oxide (**74j**) (107 mg, 2.0 equiv, 0.50 mmol). Purification by column chromatography on silica gel (*n*hexane/EtOAc: 2/1→1/1) yielded **110aj** (78.5 mg, 62%) as a white solid. **M.p.**: 230–232 °C. **<sup>1</sup>H NMR** (400 MHz, CDCl<sub>3</sub>)  $\delta$  = 10.15 (s, 1H), 8.76–8.71 (m, 1H), 8.68 (d,  $J$  = 4.3 Hz, 1H), 8.13–8.03 (m, 2H), 7.40 (dd,  $J$  = 8.3, 4.3 Hz, 1H), 7.36–8.30 (s, 1H), 7.27 (q,  $J$  = 3.4, 2.6 Hz, 1H),

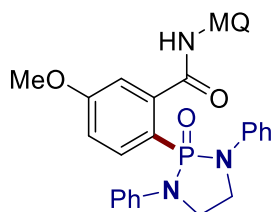
7.12 (dd,  $J = 8.6, 2.6$  Hz, 1H), 3.90 (s, 3H), 2.60 (s, 3H), 2.32–2.19 (m, 2H), 2.15–2.01 (m, 2H), 1.86–1.73 (m, 2H), 1.68–0.97 (m, 16H).  $^{13}\text{C NMR}$  (101 MHz,  $\text{CDCl}_3$ )  $\delta = 167.5$  ( $\text{C}_q$ ), 161.6 (d,  $^4J_{\text{C-P}} = 2.1$  Hz,  $\text{C}_q$ ), 147.4 (CH), 141.2 (d,  $^2J_{\text{C-P}} = 7.6$  Hz,  $\text{C}_q$ ), 137.5 ( $\text{C}_q$ ), 137.3 ( $\text{C}_q$ ), 136.4 (d,  $^3J_{\text{C-P}} = 6.6$  Hz, CH), 135.6 (CH), 134.0 ( $\text{C}_q$ ), 128.0 ( $\text{C}_q$ ), 121.8 (CH), 121.4 (d,  $^1J_{\text{C-P}} = 81.8$  Hz,  $\text{C}_q$ ), 121.1 (CH), 118.7 (CH), 114.6 (d,  $^2J_{\text{C-P}} = 10.2$  Hz, CH), 113.9 (d,  $^3J_{\text{C-P}} = 9.1$  Hz, CH), 55.5 ( $\text{CH}_3$ ), 37.6 (d,  $^1J_{\text{C-P}} = 67.3$  Hz, CH), 26.5 (d,  $^2J_{\text{C-P}} = 7.2$  Hz,  $\text{CH}_2$ ), 26.5 (d,  $^3J_{\text{C-P}} = 3.0$  Hz,  $\text{CH}_2$ ), 26.4 (d,  $^2J_{\text{C-P}} = 6.4$  Hz,  $\text{CH}_2$ ), 26.3 (d,  $^3J_{\text{C-P}} = 3.0$  Hz,  $\text{CH}_2$ ), 25.8 ( $\text{CH}_2$ ), 22.4 ( $\text{CH}_3$ ).  $^{31}\text{P}\{^1\text{H}\}$  NMR (162 MHz,  $\text{CDCl}_3$ )  $\delta = 49.1$ . IR (ATR): 3347, 2920, 2850, 1679, 1524, 1447, 1279, 1152, 848, 575, 491  $\text{cm}^{-1}$ . MS (ESI)  $m/z$  (relative intensity): 527 (100)  $[\text{M}+\text{Na}]^+$ , 505 (95)  $[\text{M}+\text{H}]^+$ , 401 (70), 379 (70). HR-MS (ESI)  $m/z$  calcd for  $\text{C}_{30}\text{H}_{38}\text{N}_2\text{O}_3\text{P}$   $[\text{M}+\text{H}]^+$ : 505.2615, found: 505.2605.



**2-[*tert*-Butyl(phenyl)phosphoryl]-5-methoxy-*N*-(6-methylquinolin-8-yl)benzamide (110ak)**

The general procedure **G** was followed using benzamide **106n** (73.0 mg, 1.0 equiv, 0.25 mmol) and *tert*-butyl(phenyl)phosphine oxide (**74k**) (91.0 mg, 2.0 equiv, 0.50 mmol). Purification by column chromatography on silica gel (*n*hexane/EtOAc: 2/1→1/1) yielded **110ak** (63.0 mg, 53%) as a white solid. **M.p.**: 263–265 °C.  $^1\text{H NMR}$  (300 MHz,  $\text{CDCl}_3$ )  $\delta = 10.01$  (s, 1H), 8.60 (dd,  $J = 4.2, 1.6$  Hz, 1H), 8.22 (d,  $J = 1.8$  Hz, 1H), 8.07–7.94 (m, 2H), 7.73–7.54 (m, 2H), 7.34 (dd,  $J = 8.3, 4.2$  Hz, 1H), 7.31–7.17 (m, 5H), 7.09 (dt,  $J = 8.6, 2.2$  Hz, 1H), 3.89 (s, 3H), 2.51 (s, 3H), 1.34 (d,  $J = 14.9$  Hz, 9H).  $^{13}\text{C NMR}$  (101 MHz,  $\text{CDCl}_3$ )  $\delta = 167.0$  ( $\text{C}_q$ ), 161.8 (d,  $^4J_{\text{C-P}} = 2.4$  Hz,  $\text{C}_q$ ), 147.3 (CH), 145.1 (d,  $^2J_{\text{C-P}} = 7.7$  Hz,  $\text{C}_q$ ), 137.6 ( $\text{C}_q$ ), 137.0 ( $\text{C}_q$ ), 135.1 (CH), 133.7 (d,  $^3J_{\text{C-P}} = 10.5$  Hz, CH), 133.7 ( $\text{C}_q$ ), 132.0 (d,  $^3J_{\text{C-P}} = 8.6$  Hz, CH), 131.5 (d,  $^1J_{\text{C-P}} = 91.4$  Hz,  $\text{C}_q$ ), 130.8 (d,  $^4J_{\text{C-P}} = 2.6$  Hz, CH), 127.9 ( $\text{C}_q$ ), 127.7 (d,  $^2J_{\text{C-P}} = 11.1$  Hz, CH), 121.3 (CH), 120.8 (CH), 120.2 (d,  $^1J_{\text{C-P}} = 90.4$  Hz,  $\text{C}_q$ ), 119.7 (CH), 115.1 (d,  $^3J_{\text{C-P}} = 9.7$  Hz, CH), 114.9 (d,  $^2J_{\text{C-P}} = 11.5$  Hz, CH), 55.5 ( $\text{CH}_3$ ), 34.4 (d,  $^1J_{\text{C-P}} = 71.2$  Hz,  $\text{C}_q$ ), 25.9 ( $\text{CH}_3$ ),

22.2 (CH<sub>3</sub>). <sup>31</sup>P{<sup>1</sup>H} NMR (121 MHz, CDCl<sub>3</sub>) δ = 41.2. IR (ATR): 3356, 2971, 1683, 1523, 1090, 757, 671, 535 cm<sup>-1</sup>. MS (ESI) *m/z* (relative intensity): 495 (5) [M+Na]<sup>+</sup>, 473 (45) [M+H]<sup>+</sup>, 401 (60), 379 (100). HR-MS (ESI) *m/z* calcd for C<sub>28</sub>H<sub>30</sub>N<sub>2</sub>O<sub>3</sub>P [M+H]<sup>+</sup>: 473.1989, found: 473.1988.



**5-Methoxy-N-(6-methylquinolin-8-yl)-2-(2-oxido-1,3-diphenyl-1,3,2-diazaphospholidin-2-yl)benzamide (110al)**

The general procedure **G** was followed using benzamide **106n** (73.0 mg, 1.0 equiv, 0.25 mmol) and 1,3-diphenyl-1,3,2-diazaphospholidine 2-oxide (**74I**) (129 mg, 2.0 equiv, 0.50 mmol). Purification by column chromatography on silica gel (*n*hexane/EtOAc: 2/1→1/1) yielded **110al** (98.8 mg, 72%) as a white solid. **M.p.**: 236–238 °C. <sup>1</sup>H NMR (400 MHz, CDCl<sub>3</sub>) δ = 9.51 (s, 1H), 8.76 (d, *J* = 1.8 Hz, 1H), 8.56–8.47 (m, 1H), 8.29 (dt, *J* = 5.1, 2.4 Hz, 1H), 8.03 (dd, *J* = 8.1, 1.7 Hz, 1H), 7.36–7.30 (m, 2H), 7.11 (dt, *J* = 8.8, 2.6 Hz, 1H), 7.04–6.96 (m, 9H), 6.81–6.75 (m, 2H), 3.93 (dt, *J* = 8.2, 3.9 Hz, 2H), 3.85 (s, 3H), 3.78–3.68 (m, 2H), 2.63 (s, 3H). <sup>13</sup>C NMR (101 MHz, CDCl<sub>3</sub>) δ = 167.2 (d, <sup>3</sup>*J*<sub>C-P</sub> = 4.3 Hz, C<sub>q</sub>), 162.6 (d, <sup>4</sup>*J*<sub>C-P</sub> = 3.2 Hz, C<sub>q</sub>), 147.1 (CH), 141.9 (d, <sup>2</sup>*J*<sub>C-P</sub> = 12.0 Hz, C<sub>q</sub>), 141.2 (d, <sup>2</sup>*J*<sub>C-P</sub> = 8.5 Hz, C<sub>q</sub>), 140.2 (d, <sup>3</sup>*J*<sub>C-P</sub> = 10.7 Hz, CH), 137.2 (C<sub>q</sub>), 136.6 (C<sub>q</sub>), 135.2 (CH), 134.0 (C<sub>q</sub>), 128.9 (CH), 127.8 (C<sub>q</sub>), 121.5 (CH), 121.2 (CH), 121.0 (CH), 119.0 (d, <sup>1</sup>*J*<sub>C-P</sub> = 162.9 Hz, C<sub>q</sub>), 117.7 (CH), 116.2 (d, <sup>3</sup>*J*<sub>C-P</sub> = 5.0 Hz, CH), 114.6 (d, <sup>2</sup>*J*<sub>C-P</sub> = 14.3 Hz, CH), 113.8 (d, <sup>3</sup>*J*<sub>C-P</sub> = 13.4 Hz, CH), 55.5 (CH<sub>3</sub>), 43.1 (d, <sup>2</sup>*J*<sub>C-P</sub> = 9.7 Hz, CH<sub>2</sub>), 22.5 (CH<sub>3</sub>). <sup>31</sup>P{<sup>1</sup>H} NMR (162 MHz, CDCl<sub>3</sub>) δ = 14.9. IR (ATR): 3343, 1684, 1598, 1526, 1252, 1231, 1092, 958, 745, 678, 557, 526 cm<sup>-1</sup>. MS (ESI) *m/z* (relative intensity): 571 (20) [M+Na]<sup>+</sup>, 549 (100) [M+H]<sup>+</sup>. HR-MS (ESI) *m/z* calcd for C<sub>32</sub>H<sub>30</sub>N<sub>4</sub>O<sub>3</sub>P [M+H]<sup>+</sup>: 549.2050, found: 549.2050.



## 5.3.6.2 Mechanistic Studies

## Competitive Experiment Between Different Nucleophiles

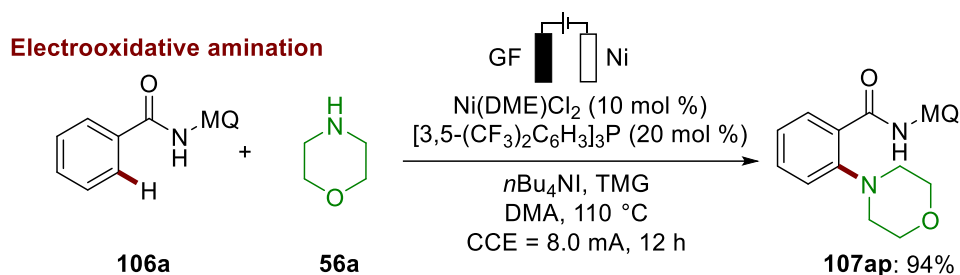


**Figure 5.3.52.** C–H Amination under optimized conditions.

Before the competitive experiment between amine and phosphonating reagent, C–H amination experiments were carried out independently. The general procedure **G** was followed using benzamides **106a** (65.5 mg, 0.25 mmol), amine **56a** (43.5 mg, 0.50 mmol, 2.0 equiv). Electrolysis was carried out at 110 °C and a constant current of 8.0 mA was maintained for 12 h. At ambient temperature, the mixture was transferred into a separating funnel and the electrodes were rinsed with EtOAc (10 mL). Subsequently, H<sub>2</sub>O (10 mL) was added to the mixture and the organic layer was collected. The aqueous layer was extracted with EtOAc (2 × 5.0 mL). Evaporation of the combined organic layers and subsequent column chromatography on silica gel (eluent: *n*hexane/EtOAc: 10/1 → 4/1) yielded the desired product **107ap** (81.6 mg, 94%).

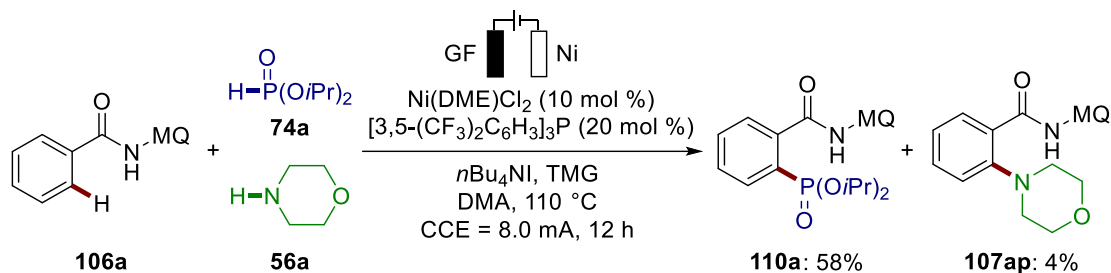


**Figure 5.3.53.** Competitive experiment between amine **56a** and phosphite **74a**.

The general procedure **G** was followed using benzamides **106a** (65.5 mg, 0.25 mmol), phosphonate **74a** (83.0 mg, 0.50 mmol, 2.0 equiv) and amine **56a** (43.5 mg, 0.50 mmol, 2.0 equiv). Electrolysis was carried out at 110 °C and a constant current of 8.0 mA was maintained for 12 h. After cooling to ambient temperature, 1,3,5-(MeO)<sub>3</sub>C<sub>6</sub>H<sub>3</sub> (0.25 mmol) was added as the internal standard to determine the <sup>1</sup>H NMR yield.

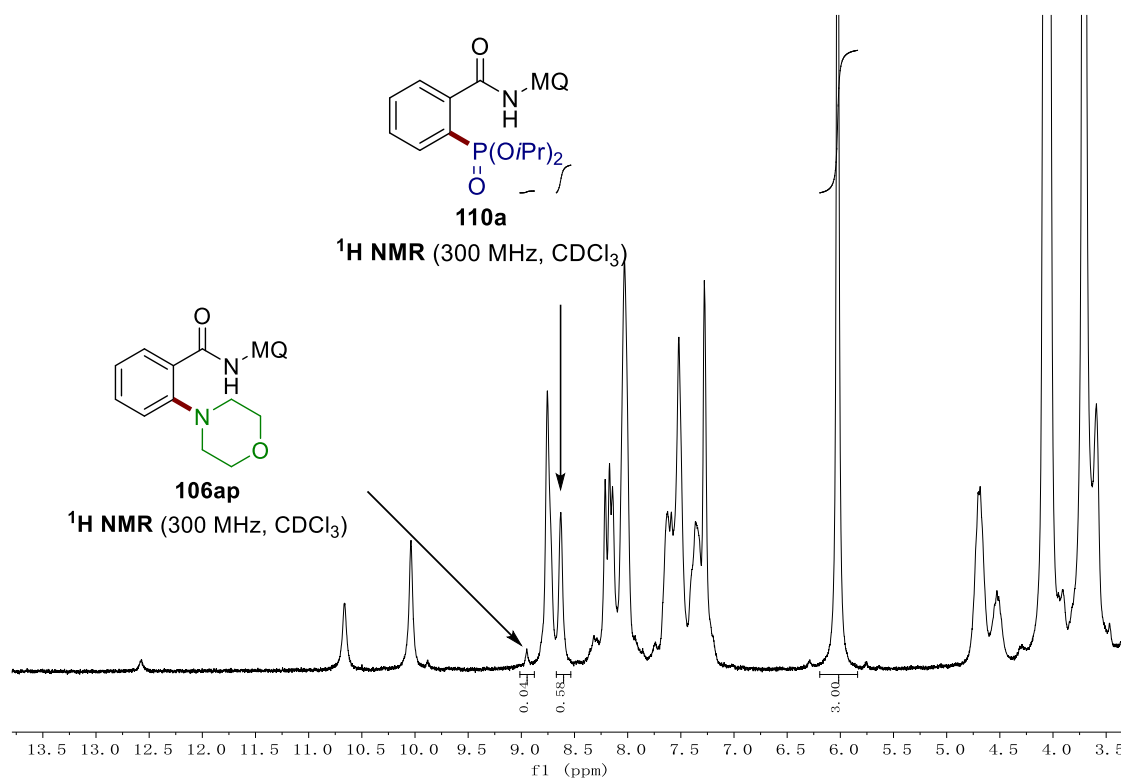


**Figure 5.3.54.** Crude  $^1\text{H}$  NMR spectrum of competitive experiments between phosphonate **74a** and amine **56a**.

### Experiments with Isotopically Labeled Solvent

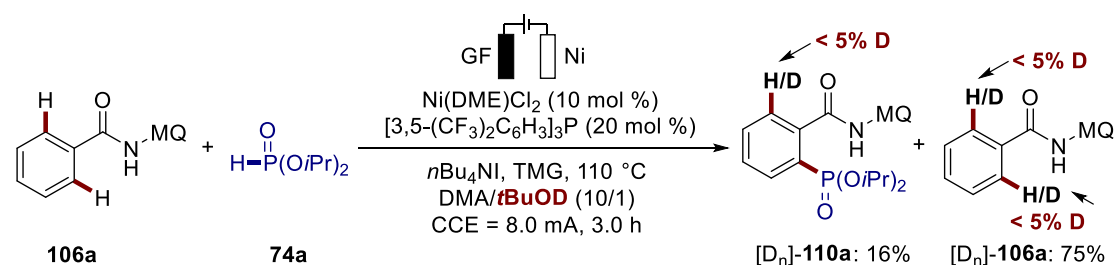


**Figure 5.3.55.** Deuteration experiment using  $t\text{BuOD}$  as the cosolvent.

The general procedure **G** was followed using  $\text{Ni}(\text{DME})\text{Cl}_2$  (5.5 mg, 0.025 mmol, 10 mol %),  $[3,5\text{-(CF}_3)_2\text{C}_6\text{H}_3]_3\text{P}$  (33.5 mg, 0.050 mmol, 20 mol %), TMG (38.4 mg, 0.25 mmol, 1.0 equiv),  $n\text{Bu}_4\text{NI}$  (40.3 mg, 0.125 mmol, 50 mol %) and **74a** (83.0 mg, 0.50 mmol, 2.0 equiv) in a mixture solvent of DMA and  $t\text{BuOD}$  (3.0/0.30 mL). Electrolysis was carried out at  $110\text{ }^\circ\text{C}$  and a constant current of 8.0 mA was maintained for 3.0 h. Column chromatography ( $n\text{hexane}/\text{EtOAc}$ : 8/1 $\rightarrow$ 1/1) yielded  $[\text{D}_n]\text{-110a}$  (17.2 mg, 16%) as a white solid and reisolated starting material  $[\text{D}_n]\text{-106a}$  (49.3 mg, 75%) as a white solid. No deuteration was detected in either compound as determined

by  $^1\text{H}$  NMR spectroscopy.

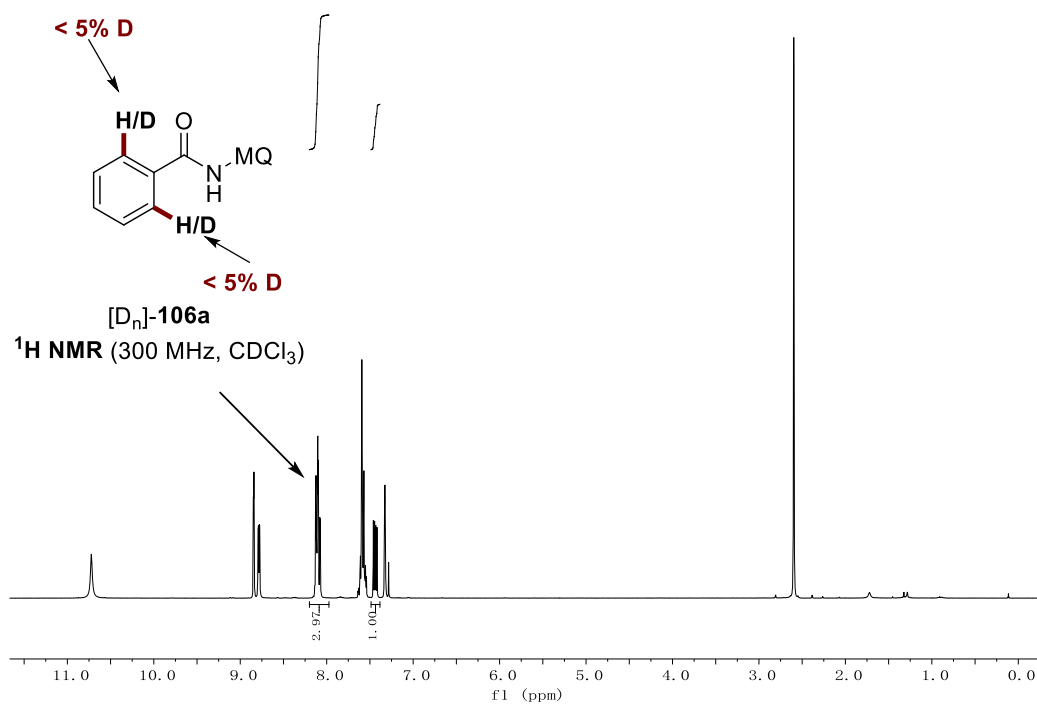


Figure 5.3.56.  $^1\text{H}$  NMR spectrum of the reisolated starting materials  $[\text{D}_n]\text{-106a}$ .

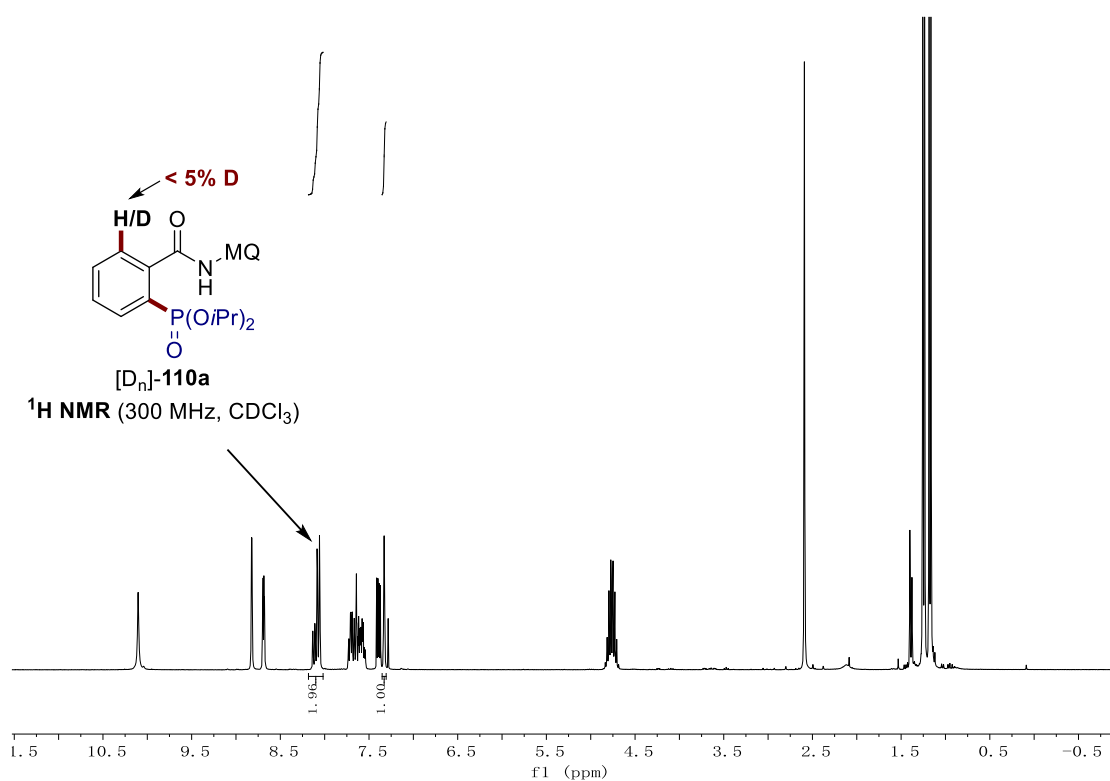
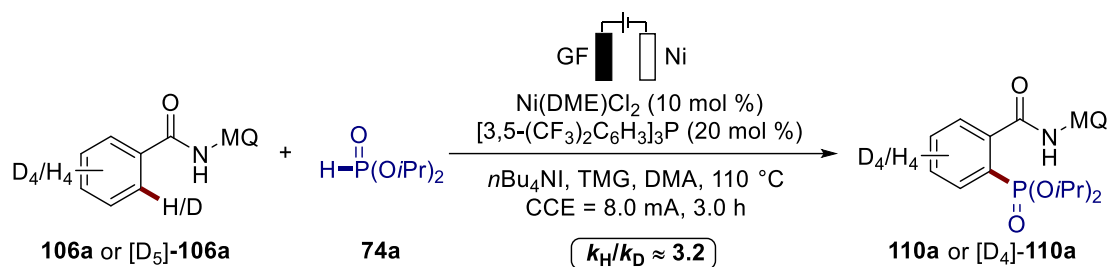


Figure 5.3.57.  $^1\text{H}$  NMR spectrum of the product  $[\text{D}_n]\text{-110a}$ .

## KIE Studies



**Figure 5.3.58.** KIE studies show a large KIE value ( $k_H/k_D \approx 3.2$ ).

Two parallel reactions were carried out with **106a** (196 mg, 0.75 mmol, 1.0 equiv) or **[D<sub>5</sub>]-106a** (200 mg, 0.75 mmol, 1.0 equiv) following The general procedure **G** using Ni(DME)Cl<sub>2</sub> (15.9 mg, 0.075 mmol, 10 mol %), [3,5-(CF<sub>3</sub>)<sub>2</sub>C<sub>6</sub>H<sub>3</sub>]<sub>3</sub>P (100 mg, 0.15 mmol, 20 mol %), TMG (86.4 mg, 0.75 mmol, 1.0 equiv), *n*Bu<sub>4</sub>NI (121 mg, 0.375 mmol, 50 mol %) and **74a** (249 mg, 1.5 mmol, 2.0 equiv) in DMA (7.0 mL). 1,3,5-trimethoxybenzene (42.0 mg, 0.25 mmol) was added as an internal standard. Aliquots of 0.40 mL were removed from the cell every twenty minutes. The reaction mixture was extracted with EtOAc (3.0 mL). After evaporation of the solvent, the mixture was analyzed by <sup>1</sup>H NMR spectroscopy. The KIE was determined by the analysis of the initial rates.

**Table 5.3.2.** Data collecting by NMR spectroscopy.

Time [min]	10	30	50	70	90	110	130
<b>110a</b> [%]	0	6	8	10	13	16	20
<b>[D<sub>4</sub>]-110a</b> [%]	0	2	2	3	4	5	6

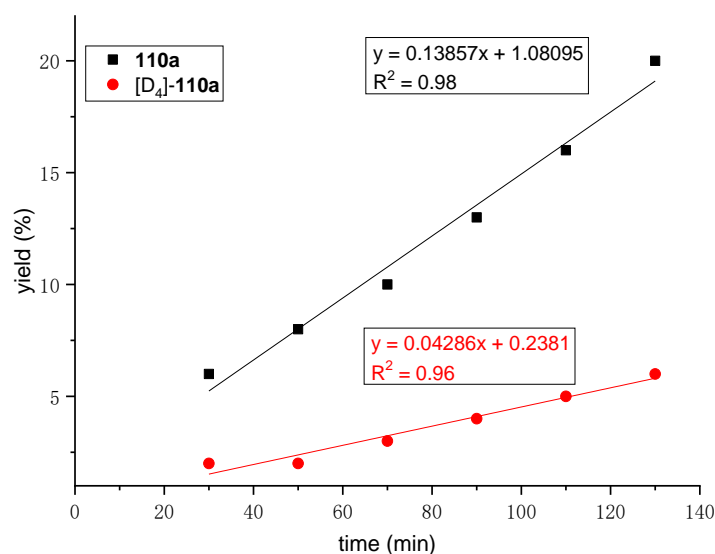


**Figure 5.3.59.** KIE studies show a large  $k_H/k_D$  value (KIE  $\approx 3.2$ ).

## Headspace GC-Analysis

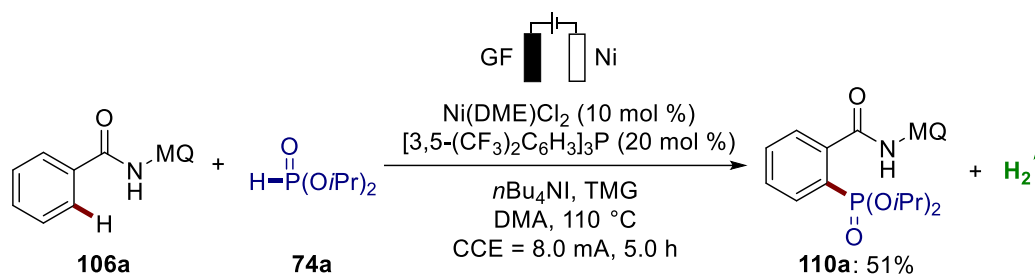


**Figure 5.3.60.** Headspace GC-analysis.

Following The general procedure **G**, after 5.0 h, the gas-phase over the reaction mixture was analyzed by headspace GC analysis using an Agilent 7890B chromatograph equipped with an Agilent CP-Molsieve 5Å column (length: 25 m, diameter: 0.32 mm, temperature 10 °C). Helium was used as the carrier gas (1.5 mL/min) and the sample was analyzed by a temperature conductivity detector at 110 °C. For comparison, also a blank sample of the carrier gas and a pure sample of hydrogen were obtained.

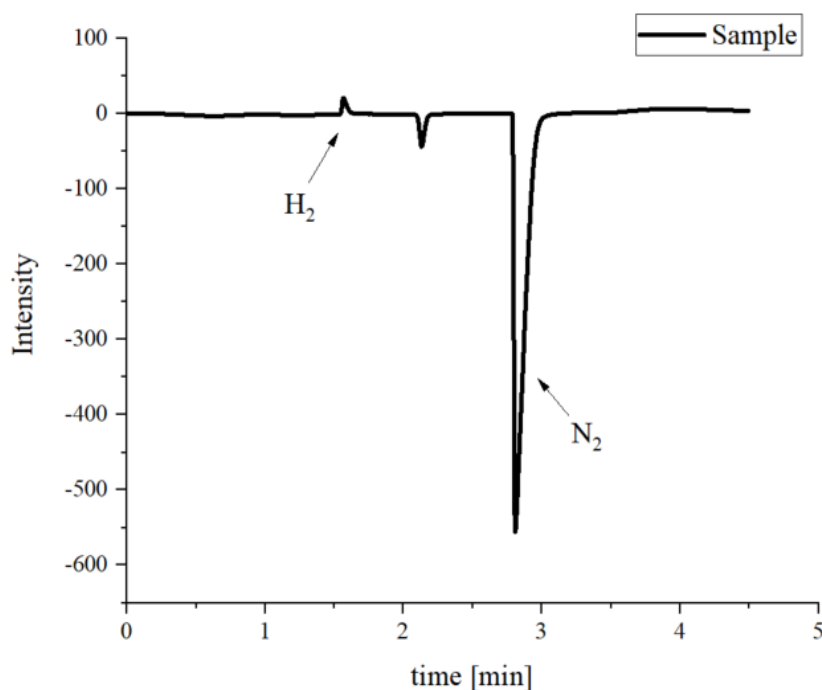


**Figure 5.3.61.** Headspace analysis of the reaction mixture showed the formation of  $\text{H}_2$ .

### Switch Off-On Experiment

“Switch off-on” reactions were carried out with benzamide **106a** (196 mg, 0.75 mmol, 1.0 equiv) following the general procedure **G** using Ni(DME)Cl<sub>2</sub> (15.9 mg, 0.075 mmol, 10 mol %), [3,5-(CF<sub>3</sub>)<sub>2</sub>C<sub>6</sub>H<sub>3</sub>]<sub>3</sub>P (100 mg, 0.15 mmol, 20 mol %), TMG (86.4 mg, 0.75 mmol, 1.0 equiv), *n*Bu<sub>4</sub>Ni (121 mg, 0.375 mmol, 50 mol %) and **74a** (249 mg, 1.5 mmol, 10.0 equiv) in DMA (6.0 mL) with 1,3,5-trimethoxybenzene (0.25 mmol) as an internal standard. Aliquots of 0.40 mL were removed from the cell one and a half hours, quenched by addition of H<sub>2</sub>O (2.0 mL) and extracted with EtOAc (2 x 3.0 mL). Subsequently, the solvent was evaporated from each sample and the resulted crude mixtures were analyzed by <sup>1</sup>H NMR spectroscopy.

**Table 5.3.3.** Data collecting by <sup>1</sup>H NMR spectroscopy

Entry	Time [h]	1.5	3.0	4.5	6.0	7.5	9.0
1	<b>110a</b> [%]-L1	17	23	29	35	41	46
2	<b>110a</b> [%]-L2	0	18	27	35	43	52
3	<b>110a</b> [%]-L3	18	18	27	27	35	34

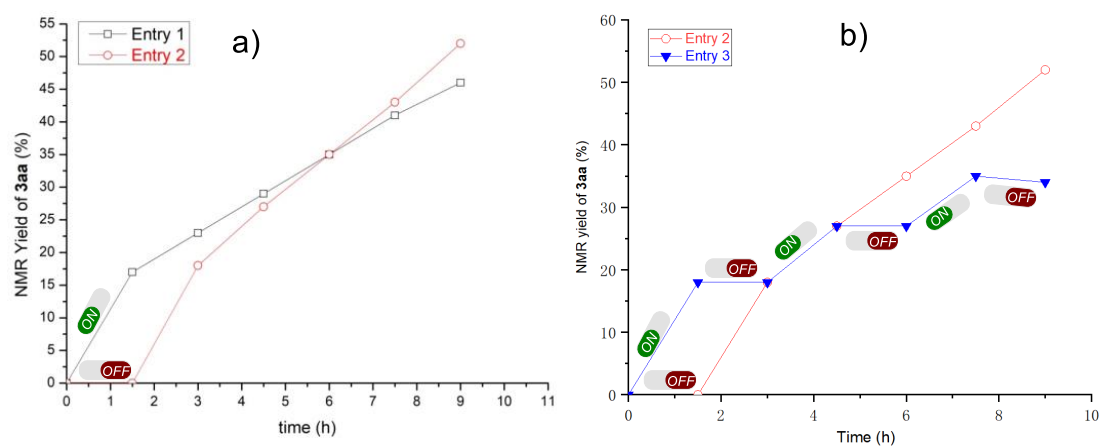


**Figure 5.3.62.** On-Off experiments. a), L1 (in black) got through current all the time and L2 (in red) without initial current for 1.5 h. b), L3 (in blue) with incontinuous current.

## Monitoring the Catalytic Reaction

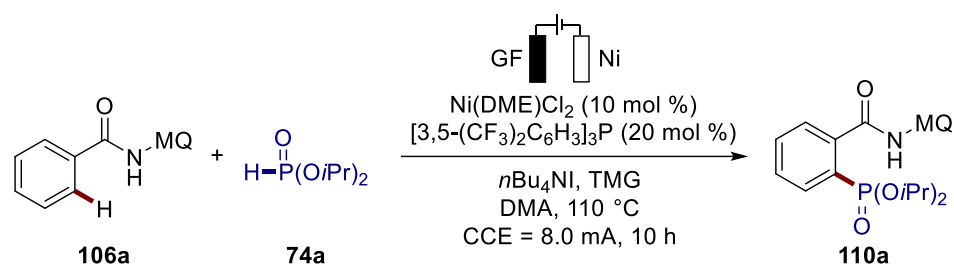


**Figure 5.3.63.** Catalytic reaction was monitored by HR-HESI-MS.

Experiments were carried out with **106a** (196 mg, 0.75 mmol, 1.0 equiv) following the general procedure **G** using Ni(DME)Cl<sub>2</sub> (15.9 mg, 0.075 mmol, 10 mol %), [3,5-(CF<sub>3</sub>)<sub>2</sub>C<sub>6</sub>H<sub>3</sub>]<sub>3</sub>P (100 mg, 0.15 mmol, 20 mol %), TMG (86.4 mg, 0.75 mmol, 1.0 equiv), *n*Bu<sub>4</sub>NI (121 mg, 0.375 mmol, 50 mol %), 1,3,5-trimethoxybenzene (0.25 mmol) and **74a** (249 mg, 1.5 mmol, 2.0 equiv) in DMA (7.5 mL). Aliquots of 0.10 mL were removed from the cell every twenty minutes, quenched by addition of H<sub>2</sub>O (2.0 mL) and extracted with EtOAc (2 x 2.0 mL). Subsequently, the solvent was evaporated from each sample and the resulted crude mixtures were analyzed by <sup>1</sup>H NMR spectroscopy resulting in the profile presented in **Figure 5.3.64**.

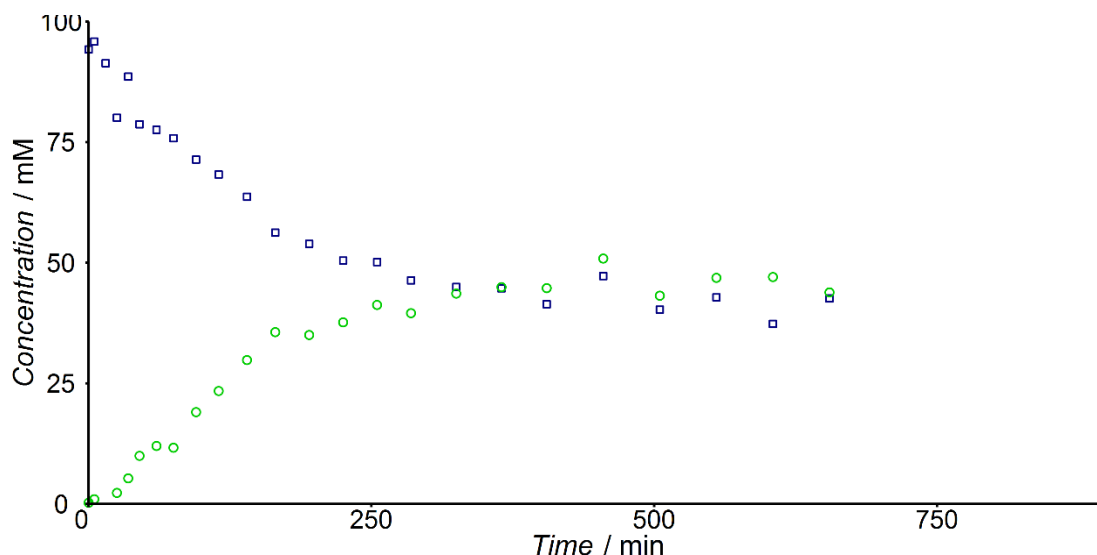


**Figure 5.3.64.** <sup>1</sup>H NMR spectroscopic monitoring of the reaction between **106a** (0.75 mmol) and **74a** (1.50 mmol) with Ni(DME)Cl<sub>2</sub> (10 mol %) as precatalyst at 110 °C in DMA (7.5 mL) under constant current electrolysis at 8.0 mA.

## Monitoring the Catalytic Reaction by HR-HESI-MS Spectrometry

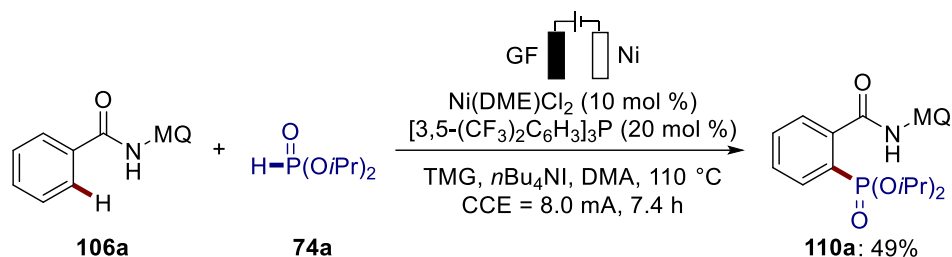


**Figure 5.3.65.** Catalytic reaction was monitored by HR-HESI-MS. Performed by Dr. Antonis M. Messinis.

Electrocatalysis was carried out in a nitrogen filled glove box with **106a** (196 mg, 0.75 mmol, 1.0 equiv) following the general procedure **G** using  $\text{Ni(DME)Cl}_2$  (15.9 mg, 0.075 mmol, 10 mol %),  $[3,5\text{-(CF}_3)_2\text{C}_6\text{H}_3]_3\text{P}$  (100 mg, 0.15 mmol, 20 mol %), TMG (86.4 mg, 0.75 mmol, 1.0 equiv),  $n\text{Bu}_4\text{NI}$  (121 mg, 0.375 mmol, 50 mol %), **74a** (249 mg, 1.5 mmol, 2.0 equiv) in DMA (7.5 mL) with 1,3,5-trimethoxybenzene (0.25 mmol) as an internal standard. During the course of the reaction, aliquots were collected, diluted with acetonitrile and analyzed by high resolution HESI mass spectrometry (**Figure 5.3.67**). The solution was quenched with  $\text{H}_2\text{O}$  after about seven hours and the yield was found to be 49% according to an  $^1\text{H}$  NMR spectroscopic analysis (**Figure 5.3.66**).

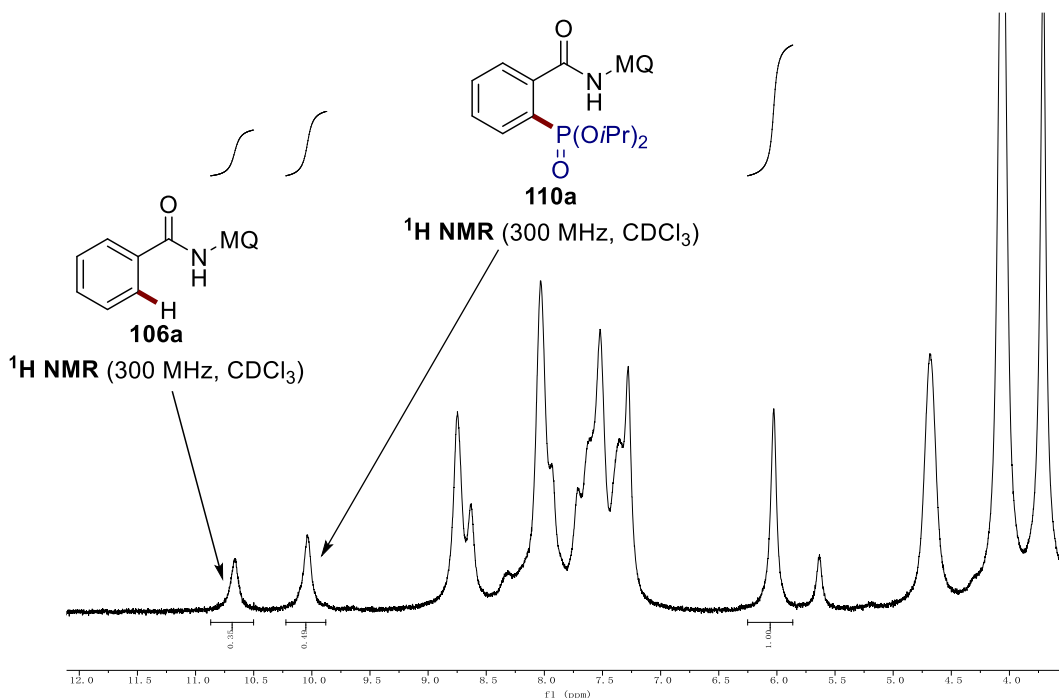


**Figure 5.3.66.** Crude  $^1\text{H}$  NMR spectroscopy after the reaction was carried out for about seven hours.



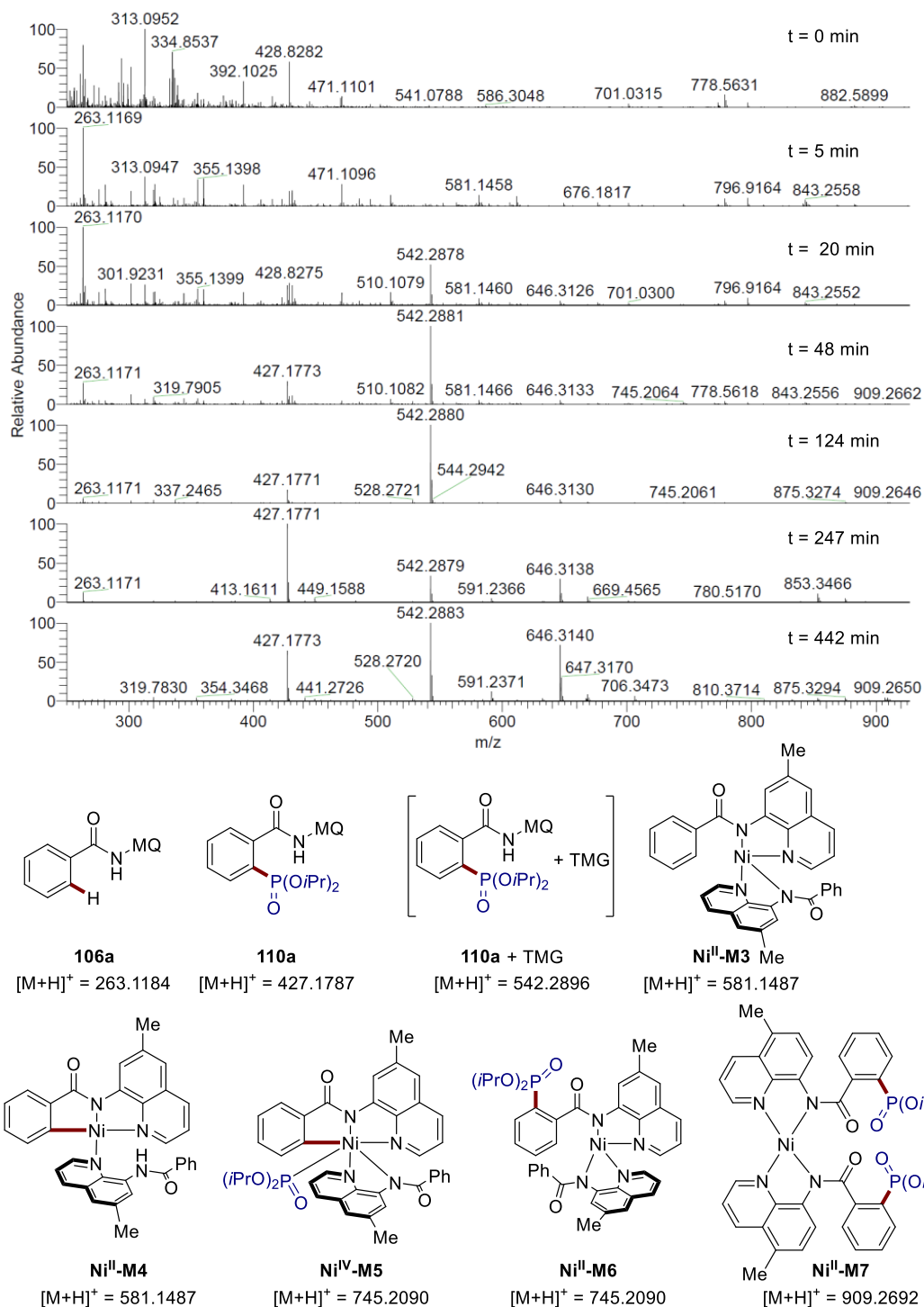


**Figure 5.3.67.** HESI high resolution mass spectrometric monitoring of the reaction. Performed by Dr. Antonis M. Messinis.

## 5. Experimental Section

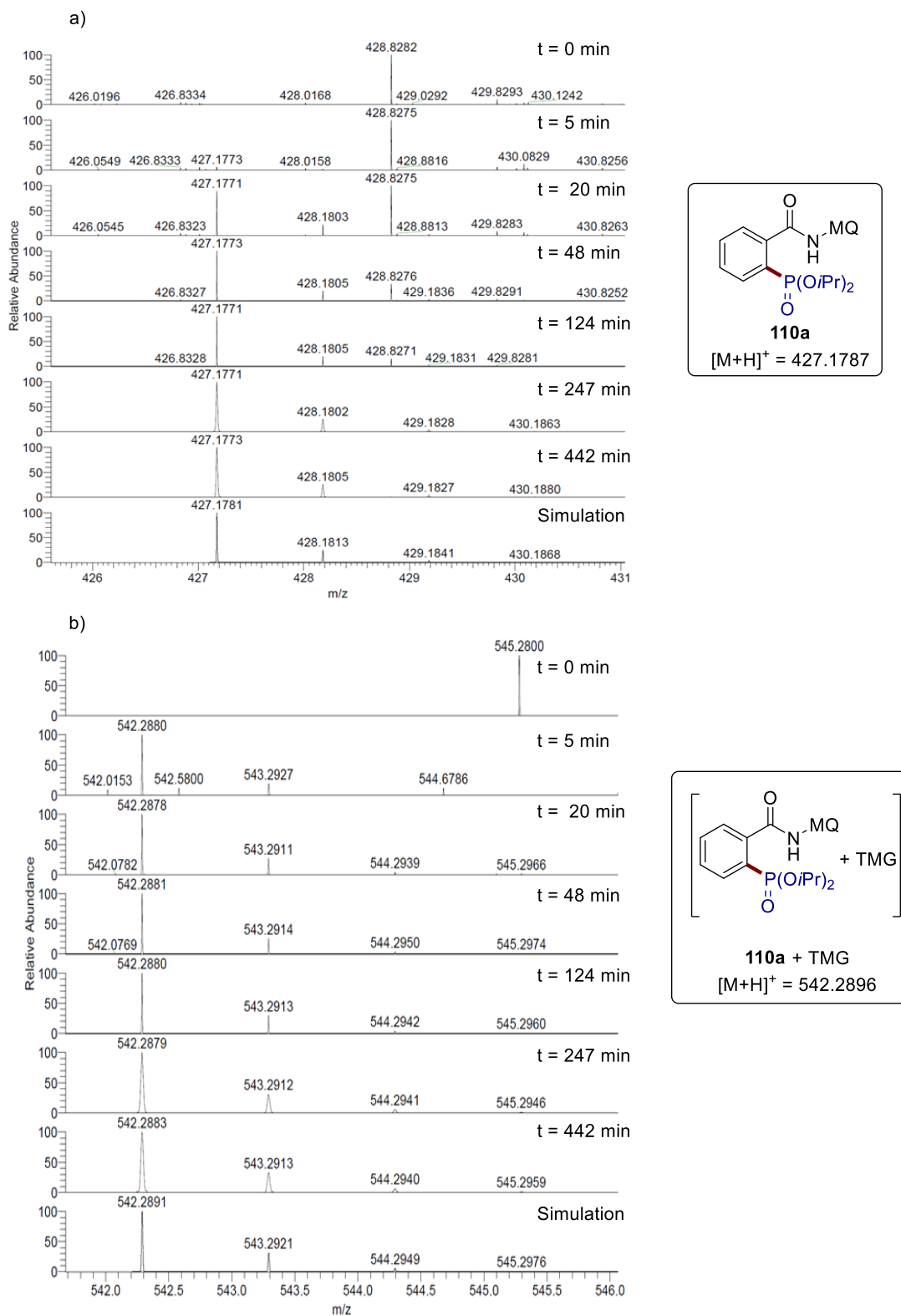


**Figure 5.3.68.** Comparison between the isotopic pattern of the experimentally observed species during catalysis (top spectra, expansion from [Figure 5.3.67](#)) and the simulated isotopic pattern (bottom spectrum) of the structures. a) product **110a**. b) product **110a + TMG**. Performed by Dr. Antonis M. Messinis.

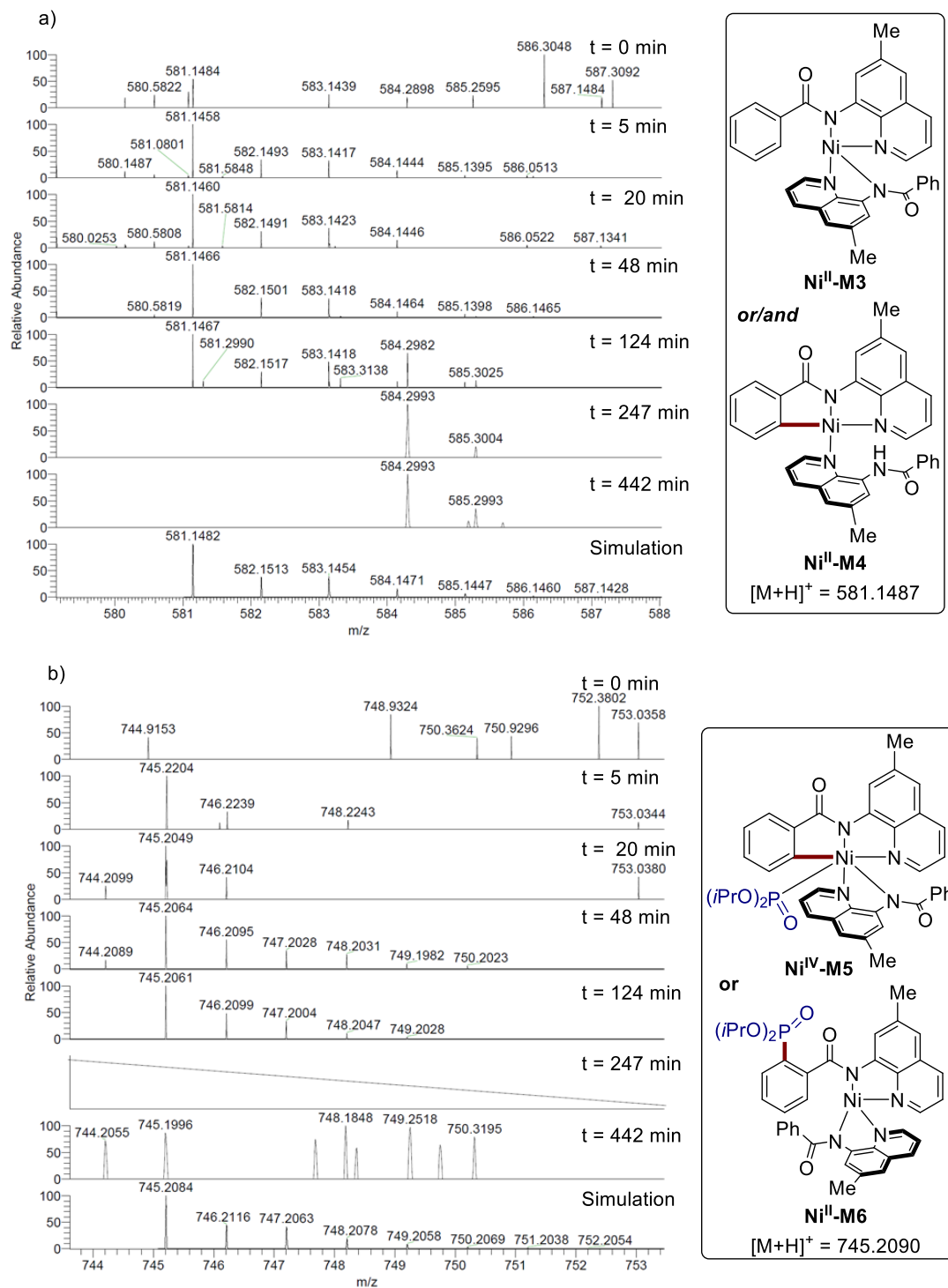


**Figure 5.3.69.** Comparison between the isotopic pattern of the experimentally observed species during catalysis (top spectra, expansion from [Figure 5.3.67](#)) and the simulated isotopic pattern (bottom spectrum) of the structures. a) **Ni<sup>II</sup>-M3** or/and **Ni<sup>II</sup>-M4**. b) **Ni<sup>IV</sup>-M5** or/and **Ni<sup>II</sup>-M6**. Performed by Dr. Antonis M. Messinis.

## 5. Experimental Section

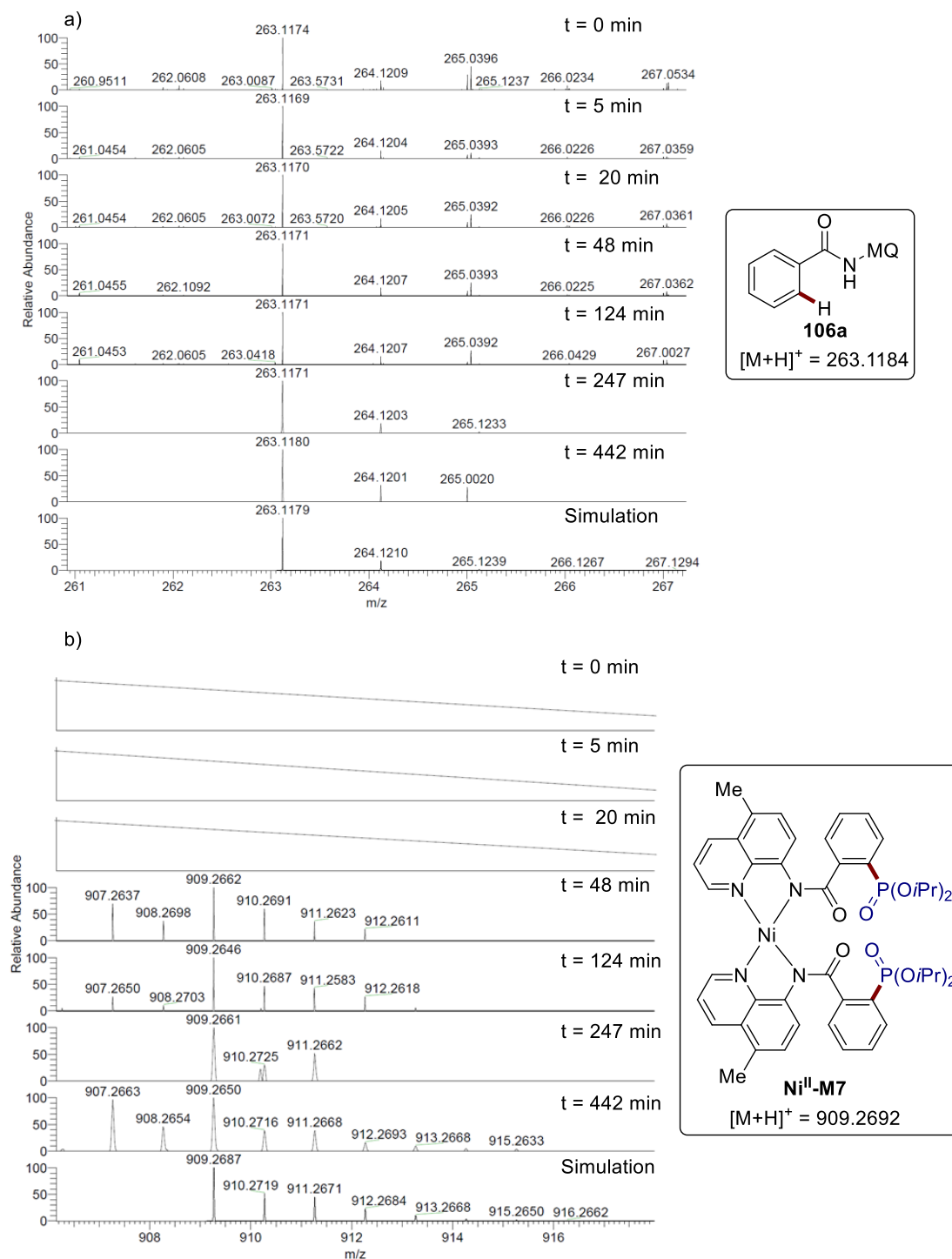


**Figure 5.3.70.** Comparison between the isotopic pattern of the experimentally observed species during catalysis (top spectra, expansion from [Figure 5.3.67](#)) and the simulated isotopic pattern (bottom spectrum) of the structures. a) benzamide **106a**. b) **Ni<sup>II</sup>-M7**. Performed by Dr. Antonis M. Messinis.

## 5.3.6.3 (Electro)synthesis of Nickel(II) and Nickel(III) Complex

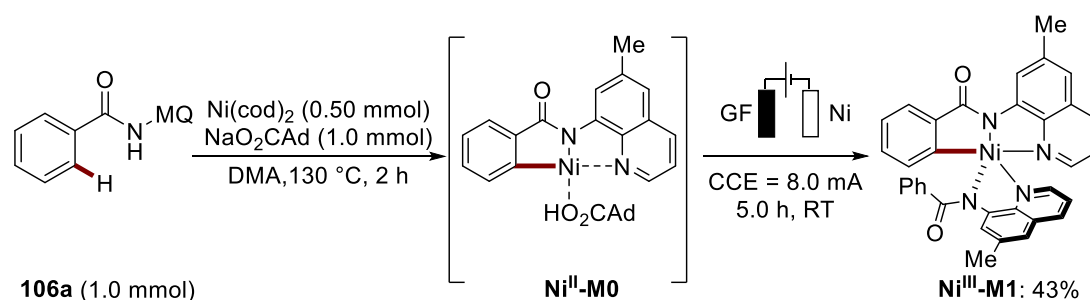


**Figure 5.3.71.** Electrosynthesis of  $\text{Ni}^{\text{III}}\text{-M1}$  with  $\text{NaO}_2\text{CAd}$ .

According to our previous work, an oven-dried 10 mL undivided electrochemical cell was charged with benzamide **106a** (262 mg, 1.0 mmol),  $\text{NaO}_2\text{CAd}$  (202 mg, 1.0 mmol),  $\text{Ni(cod)}_2$  (138 mg, 0.50 mmol) and dry DMA (3.0 mL) in a glovebox. The reaction vessel was capped and heated in an oil bath at 130 °C for 2.0 h. Upon cooling to room temperature, the cap of the undivided cell was exchanged by a GF anode and a Ni foam cathode. Electrolysis was continued with a constant current of 8.0 mA which was then maintained for 5.0 h at ambient temperature under  $\text{N}_2$ . Then, the reaction mixture was diluted with EtOAc (10 mL) and washed with  $\text{H}_2\text{O}$  (10 mL). The aqueous layer was extracted with EtOAc (2 x 10 mL). The combined organic phases were dried over  $\text{Na}_2\text{SO}_4$ , filtered and evaporated in vacuum. The residue was purified by silica gel column chromatography at low temperature (eluent: *n*hexane/EtOAc = 4/1  $\rightarrow$  EtOAc) to afford  $\text{Ni}^{\text{III}}\text{-M1}$  (125 mg, 43%) as a dark red solid. (The eluent was stored in the fridge for 2.0 hours before use to decrease the decomposition of nickel complex).  $\text{Ni}^{\text{III}}\text{-M1}$  was crystallized using  $\text{CH}_2\text{Cl}_2$  and *n*hexane.

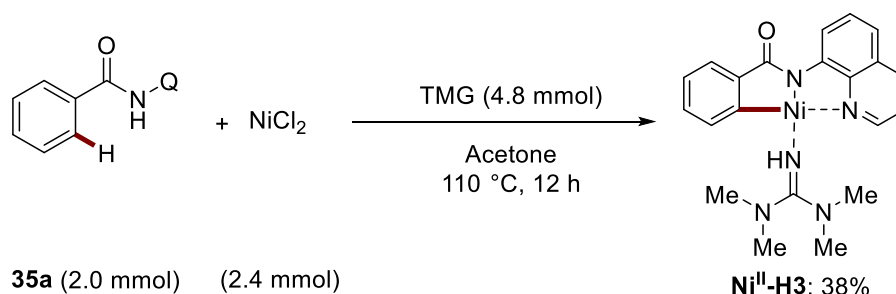


**Figure 5.3.72.** Synthesis of  $\text{Ni}^{\text{II}}\text{-H3}$  with TMG from the direct C–H phosphorylation.

The experiment was carried out using benzamide **35a** (496 mg, 2.0 mmol, 1.0 equiv), NiCl<sub>2</sub> (311 mg, 2.4 mg, 1.2 equiv), TMG (553 mg, 4.8 mmol, 2.4 equiv) in acetone (5.0 mL) under N<sub>2</sub>, at 110 °C for 12 h. After the completion of the reaction, the reaction mixture was cooled down to ambient temperature, followed by filtration and washed with acetone. The combined mixture was added with 1,3,5-trimethoxybenzene (0.67 mmol) as the internal standard to obtain the crude <sup>1</sup>H NMR spectrum. After removal of the solvent, the residue was purified by silica gel column chromatography at low temperature (eluent: *n*hexane/EtOAc 4:1→EtOAc) to reisolate benzamide **35a** (248mg, 50%) and afford Ni<sup>II</sup>-**H3** (320 mg, 38%) as a red solid. Ni<sup>II</sup>-**H3** was crystallized using CH<sub>2</sub>Cl<sub>2</sub> and *n*hexane in the glovebox. <sup>1</sup>H NMR (300 MHz, CDCl<sub>3</sub>) δ = 8.82 (d, *J* = 7.8 Hz, 1H), 7.86 (d, *J* = 8.2 Hz, 1H), 7.73 (d, *J* = 4.8 Hz, 1H), 7.42–7.31 (m, 2H), 7.11–6.79 (m, 4H), 6.41 (d, *J* = 7.2 Hz, 1H), 4.05 (s, 1H), 3.27 (s, 6H), 2.76 (s, 6H). <sup>13</sup>C NMR (101 MHz, CDCl<sub>3</sub>) δ = 177.5 (C<sub>q</sub>), 168.1 (C<sub>q</sub>), 148.3 (C<sub>q</sub>), 147.7 (C<sub>q</sub>), 147.1 (C<sub>q</sub>), 145.4 (C<sub>q</sub>), 144.6 (CH), 136.7 (CH), 133.3 (CH), 129.2 (CH), 129.0 (C<sub>q</sub>), 128.5 (CH), 125.0 (CH), 123.8 (CH), 120.8 (CH), 118.1 (CH), 115.9 (CH), 40.6 (CH<sub>3</sub>), 39.2 (CH<sub>3</sub>).

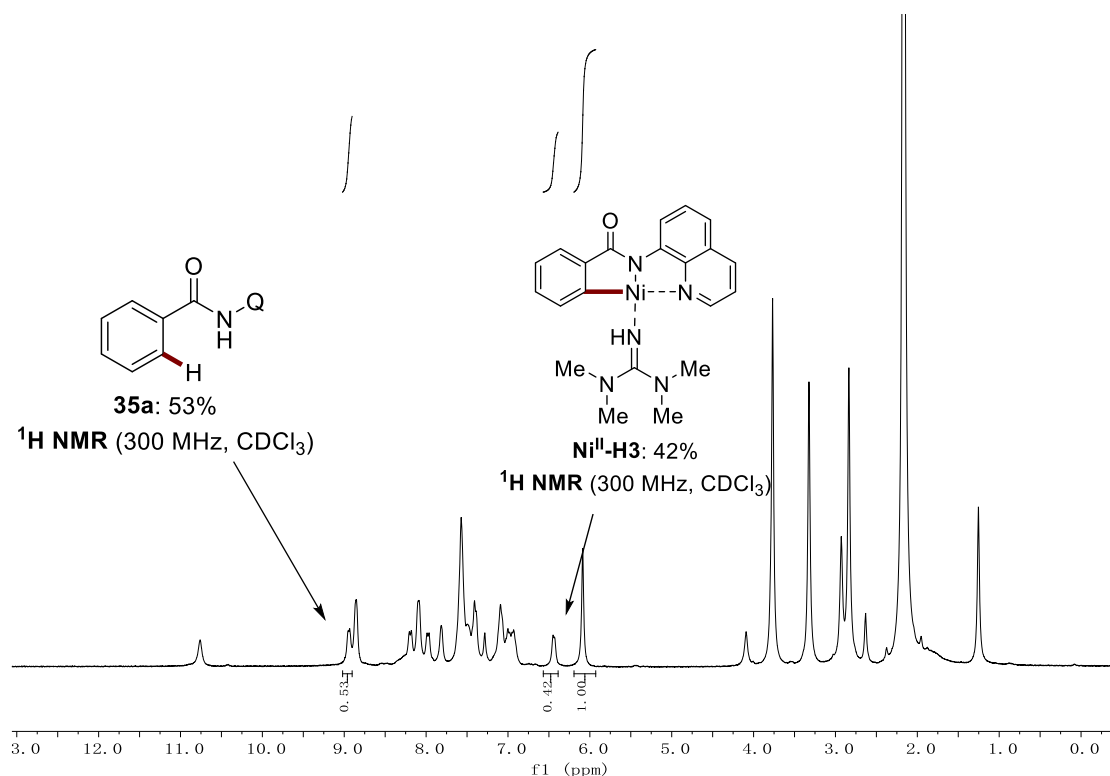


**Figure 5.3.73.** Crude <sup>1</sup>H NMR spectrum of TMG-assisted direct C–H phosphorylation.

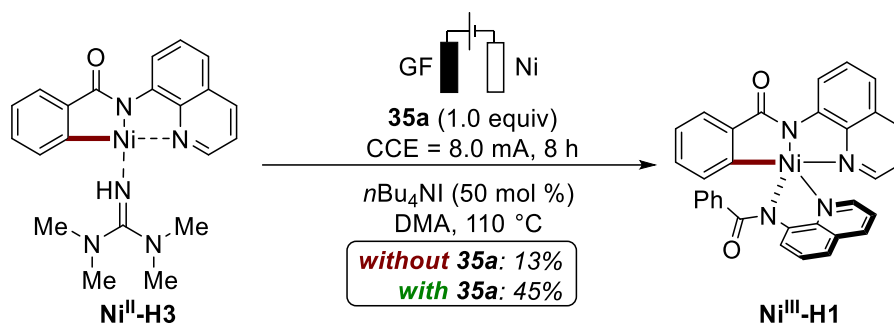


**Figure 5.3.74.** Electrosynthesis of **Ni<sup>III</sup>-H1** from **Ni<sup>II</sup>-H3**.

The electrolysis was carried out in an undivided cell, with a GF anode (10 mm × 15 mm × 6 mm) and a Ni foam cathode (10 mm × 15 mm × 1.4 mm). **Ni<sup>II</sup>-H3** (84.0 mg, 0.20 mmol, 1.0 equiv) and *n*Bu<sub>4</sub>NI (32.2 mg, 0.10 mmol) with or without benzamide **35a** (49.6 mg, 0.20 mmol, 1.0 equiv) were dissolved in DMA (2.5 mL). Electrolysis was started with a constant current of 8.0 mA at 110 °C, which was then maintained for 8.0 h under N<sub>2</sub>. At ambient temperature, the mixture was transferred into a separating funnel and the electrodes were rinsed with EtOAc (10 mL). Subsequently, H<sub>2</sub>O (10 mL) was added to the mixture and the organic layer was collected. The aqueous layer was extracted with EtOAc (2 × 5.0 mL). Evaporation of the combined organic layers and subsequent column chromatography on silica gel at low temperature (eluent: EtOAc) to afford **Ni<sup>III</sup>-H1** as a dark red solid (7.0 mg, 0.0127 mmol, 13%) or (25.0 mg, 0.045 mmol, 45%) when adding **35a**.

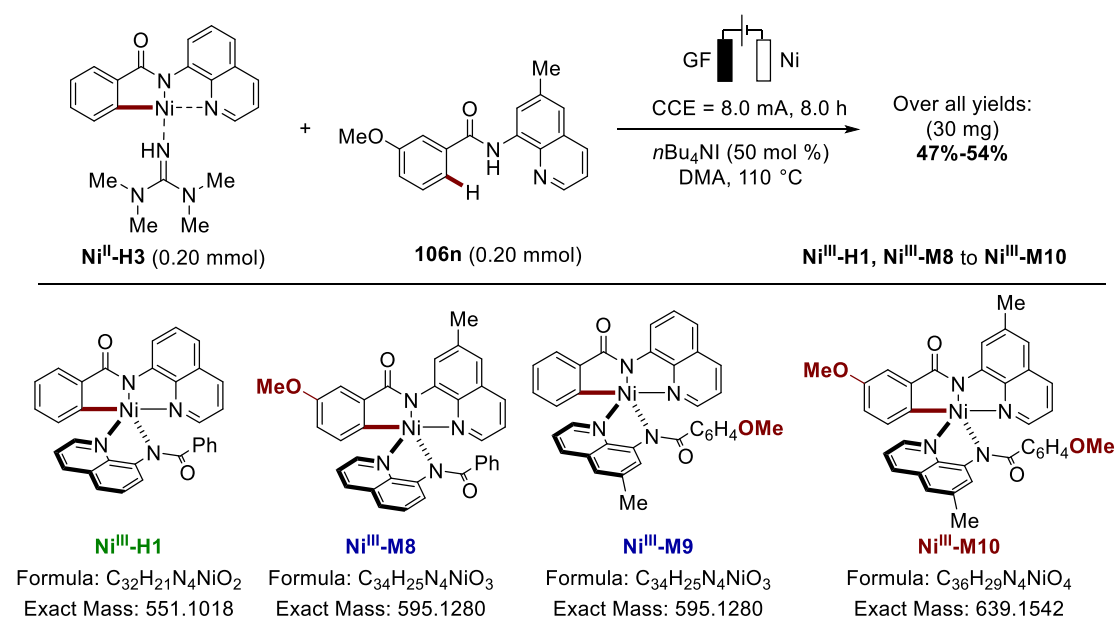


**Figure 5.3.75.** The reaction of **Ni<sup>II</sup>-H3** with benzamide **106n**.

## 5. Experimental Section

The electrolysis was carried out in an undivided cell, with a GF anode (10 mm × 15 mm × 6 mm) and a Ni foam cathode (10 mm × 15 mm × 1.4 mm). **Ni<sup>II</sup>-H3** (84.0 mg, 0.20 mmol, 1.0 equiv) and *n*Bu<sub>4</sub>Ni (32.2 mg, 0.10 mmol) with benzamide **106n** (58.4 mg, 0.20 mmol, 1.0 equiv) were dissolved in DMA (2.5 mL). Electrolysis was started with a constant current of 8.0 mA at 110 °C, which was then maintained for 8.0 h under N<sub>2</sub>. At ambient temperature, the mixture was transferred into a separating funnel and the electrodes were rinsed with EtOAc (10 mL). Subsequently, H<sub>2</sub>O (10 mL) was added to the mixture and the organic layer was collected. The aqueous layer was extracted with EtOAc (2 × 5.0 mL). Evaporation of the combined organic layers and subsequent column chromatography on silica gel at low temperature (eluent: EtOAc) to afford as a mixture of nickel (III) complex (30 mg) which gave the isolated yield range from 47%-54%. The mixture was tested by HR-MS as following.

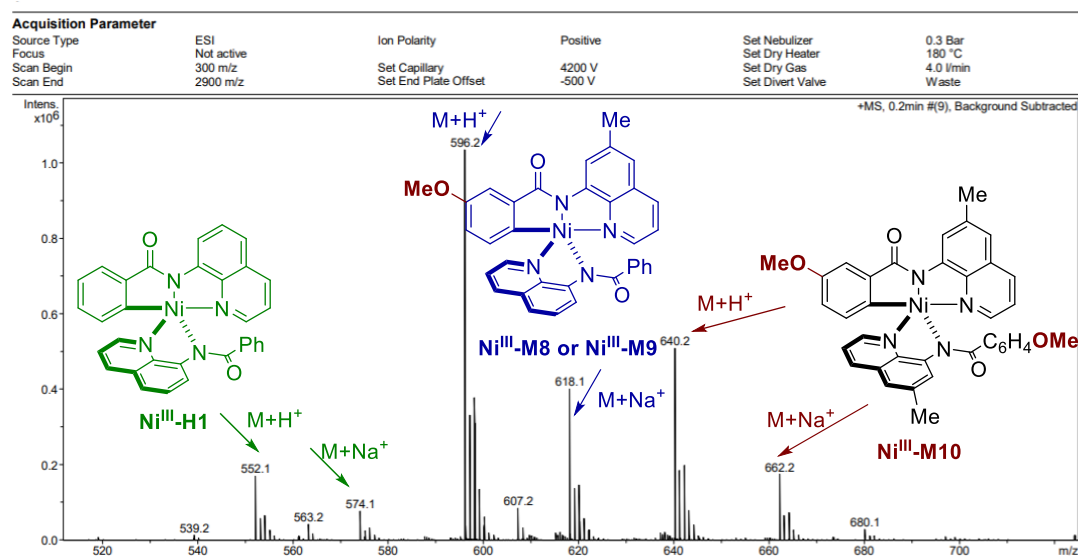
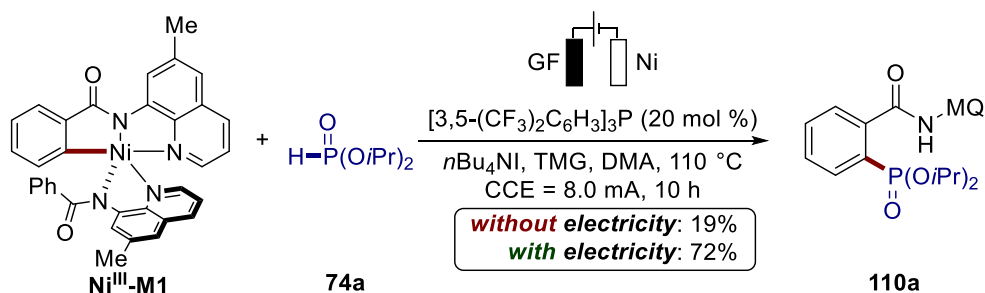


Figure 5.3.76. HR-ESI-MS spectrum analyzed by the IOBC department.



5.3.6.4 Catalytic and Stoichiometric Reaction Performance of Ni<sup>III</sup>-M1

**Figure 5.3.77.** Stoichiometric reaction performance of **Ni<sup>III</sup>-M1** without or with electricity.

The electrolysis was carried out in an undivided cell, with a GF anode (10 mm × 15 mm × 6 mm) and a Ni foam cathode (10 mm × 15 mm × 1.4 mm). **Ni<sup>III</sup>-M1** (58.0 mg, 0.10 mmol),  $[3,5-(\text{CF}_3)_2\text{C}_6\text{H}_3]_3\text{P}$  (13.4 mg, 0.020 mmol, 20 mol %), TMG (11.5 mg, 0.10 mmol, 1.0 equiv),  $n\text{Bu}_4\text{NI}$  (16.1 mg, 0.050 mmol, 50 mol %) and **74a** (33.2 mg, 0.20 mmol, 2.0 equiv) were dissolved in DMA (1.5 mL). Subsequently, the reaction was carried out without or with electricity at 110 °C for 12 h. After cooling to ambient temperature, triphenylphosphine oxide (0.10 mmol) was added as the internal standard to determine the  $^{31}\text{P}\{^1\text{H}\}$  NMR yield.

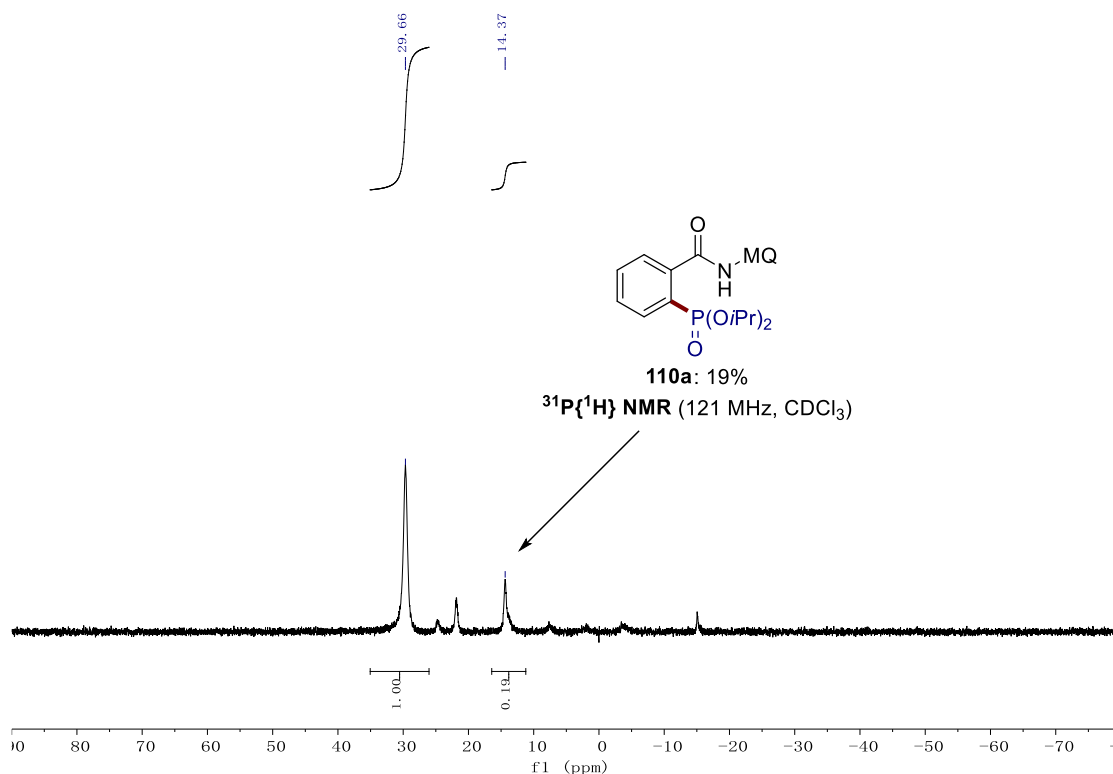


**Figure 5.3.78.** Crude  $^{31}\text{P}\{^1\text{H}\}$  NMR spectrum of stoichiometric reaction of **Ni<sup>III</sup>-M1** without electricity.

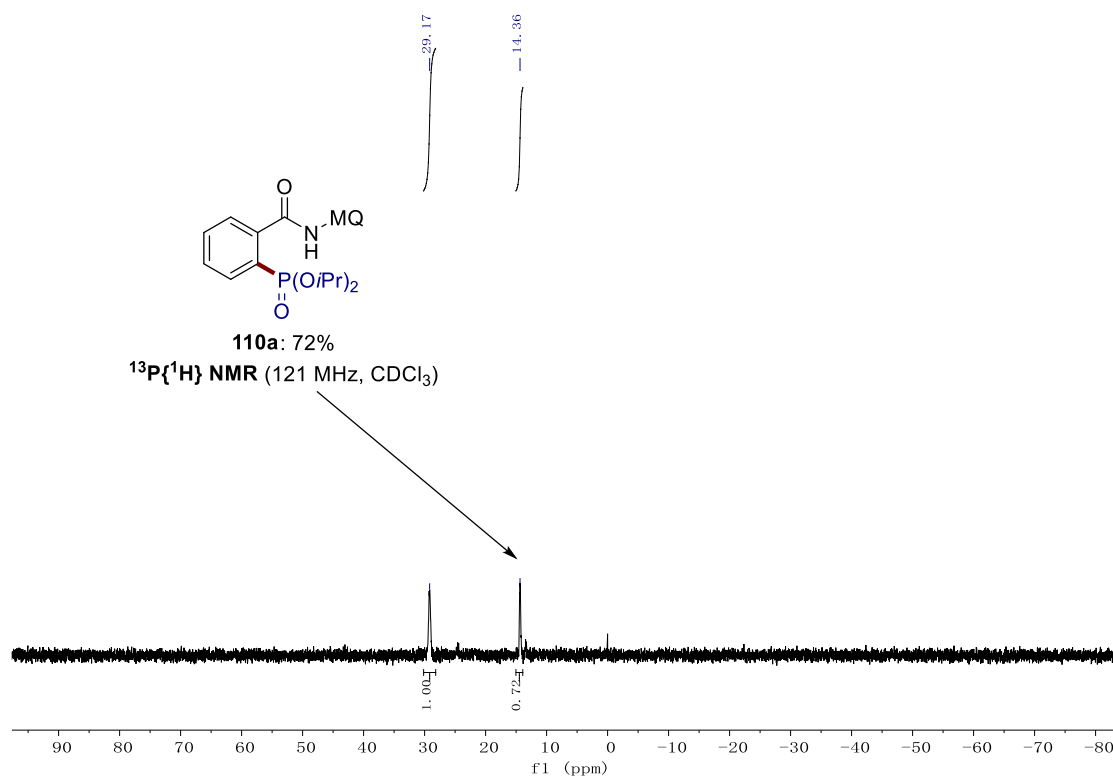


**Figure 5.3.79.** Crude  $^{31}\text{P}\{^1\text{H}\}$  NMR spectrum of stoichiometric reaction of  $\text{Ni}^{\text{III}}\text{-M1}$  with electricity.

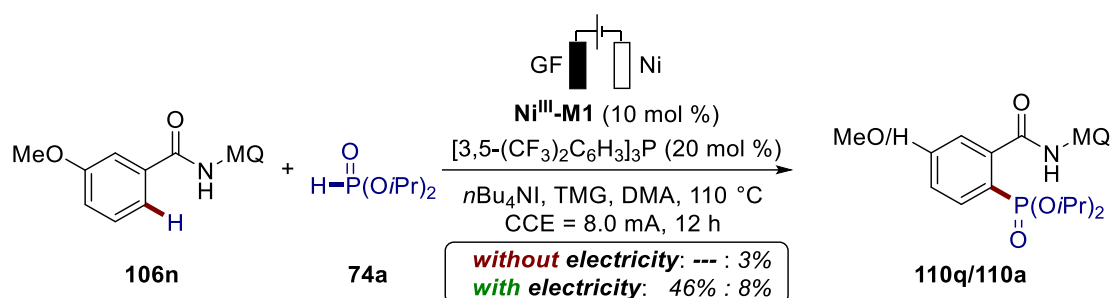


**Figure 5.3.80.** Catalytic reaction performance of  $\text{Ni}^{\text{III}}\text{-M1}$  without or with electricity.

The electrolysis was carried out in an undivided cell, with a GF anode (10 mm × 15 mm × 6 mm) and a Ni foam cathode (10 mm × 15 mm × 1.4 mm).  $\text{Ni}^{\text{III}}\text{-M1}$  (14.5 mg, 0.025 mmol),  $[\text{3,5-(CF}_3)_2\text{C}_6\text{H}_3]_3\text{P}$  (33.5 mg, 0.050 mmol, 20 mol %), TMG (28.8 mg, 0.25 mmol, 1.0 equiv),  $n\text{Bu}_4\text{NI}$  (40.3 mg, 0.125 mmol, 50 mol %) and **74a** (83.0 mg, 0.50 mmol, 2.0 equiv) were dissolved in DMA (3.0 mL). Subsequently, the reaction was carried out without or with electricity at 110 °C for 12 h. After cooling to ambient temperature, triphenylphosphine oxide (0.20 mmol) was added as the internal standard to determine the  $^{31}\text{P}\{^1\text{H}\}$  NMR yield.

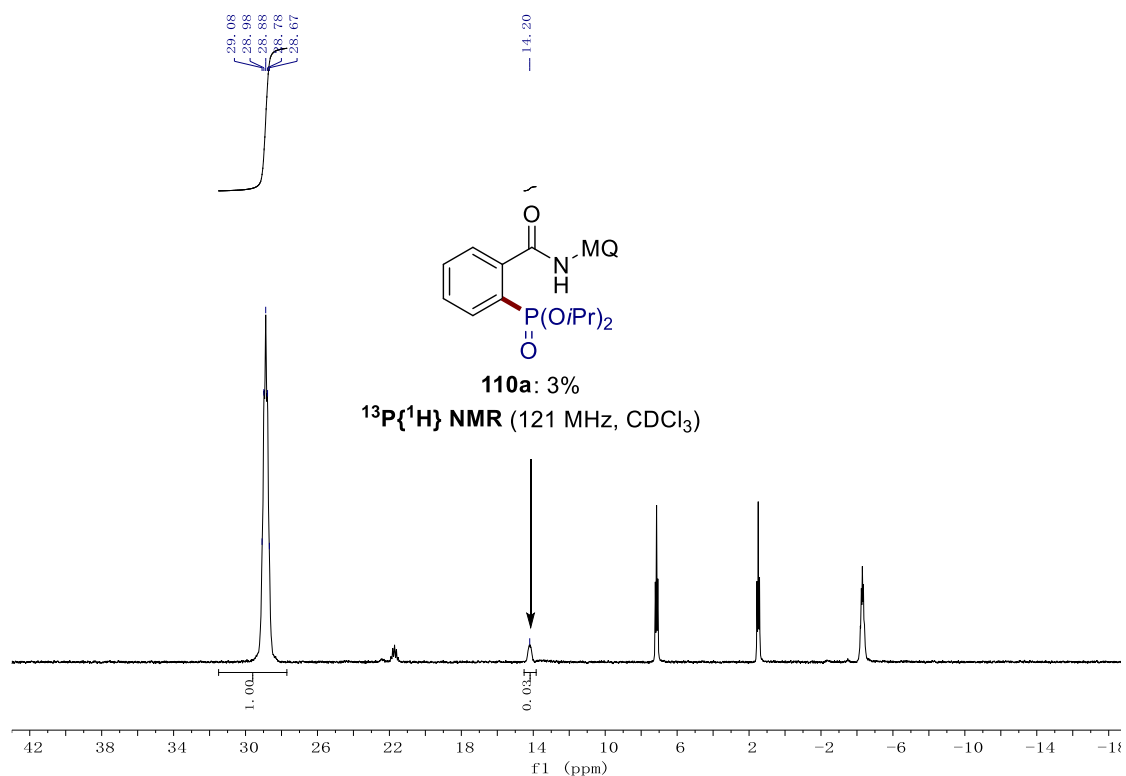


**Figure 5.3.81.** Crude  $^{31}\text{P}\{^1\text{H}\}$  NMR spectrum of catalytic reaction of  $\text{Ni}^{\text{III}}\text{-M1}$  without electricity.

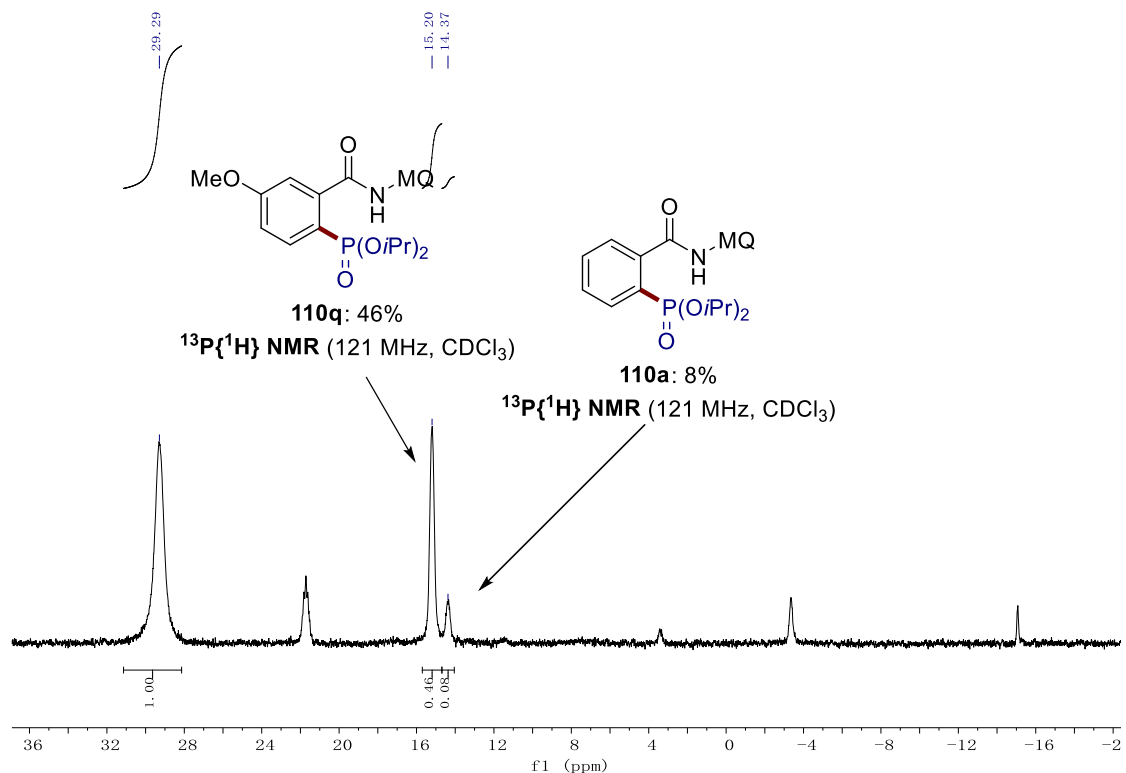


**Figure 5.3.82.** Crude  $^{31}\text{P}\{^1\text{H}\}$  NMR spectrum of catalytic reaction of  $\text{Ni}^{\text{III}}\text{-M1}$  with electricity.

## 5.3.6.5 Gram-Scale Experiment

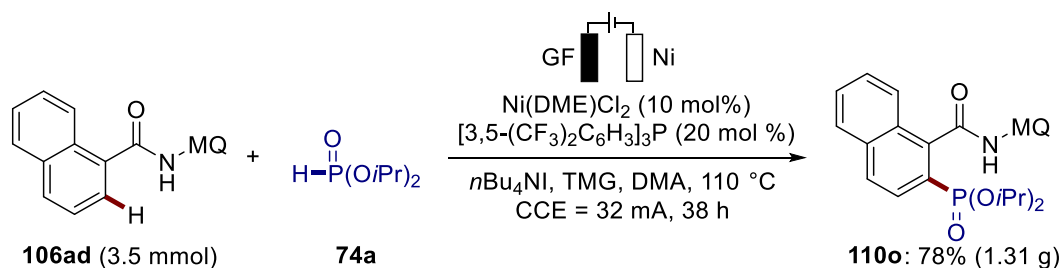
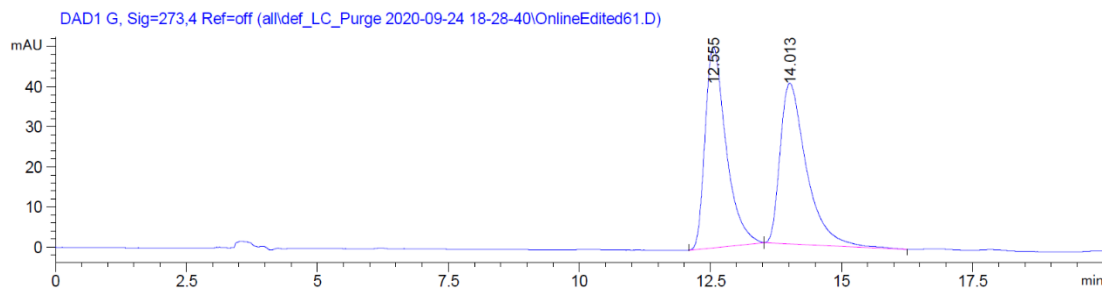


Figure 5.3.83. Gram-scale experiment with **106ad**.

The electrolysis was carried out in 100 mL Schlenk flask, with a GF anode (20 mm × 30 mm × 6 mm) and a Ni foam cathode (20 mm × 30 mm × 1.4 mm). Benzamide **106ad** (1.09 g, 3.5 mmol), Ni(DME)Cl<sub>2</sub> (76.7 mg, 0.35 mmol, 10 mol %), [3,5-(CF<sub>3</sub>)<sub>2</sub>C<sub>6</sub>H<sub>3</sub>]<sub>3</sub>P (469 mg, 0.70 mmol, 20 mol %), TMG (403 mg, 3.5 mmol, 1.0 equiv), *n*Bu<sub>4</sub>NI (564 mg, 1.75 mmol, 50 mol %) and **74a** (1.16 g, 7.0 mmol, 2.0 equiv) were dissolved in DMA (40 mL). Electrolysis was started with a constant current of 32 mA which was then maintained for 38 h at 110 °C. At ambient temperature, the mixture was transferred into a separating funnel and the electrodes were rinsed with EtOAc (50 mL). Subsequently, the mixture was washed with H<sub>2</sub>O (50 mL) and the organic layer was collected. The aqueous layer was extracted with EtOAc (2 × 50 mL). Evaporation of the collected organic layer and subsequent column chromatography on silica gel (*n*hexane/EtOAc: 4/1→1/1) yielded the desired product **110o** (1.31 g, 78%).

5.3.6.6 Studies on the Potential Racemization of **110y**

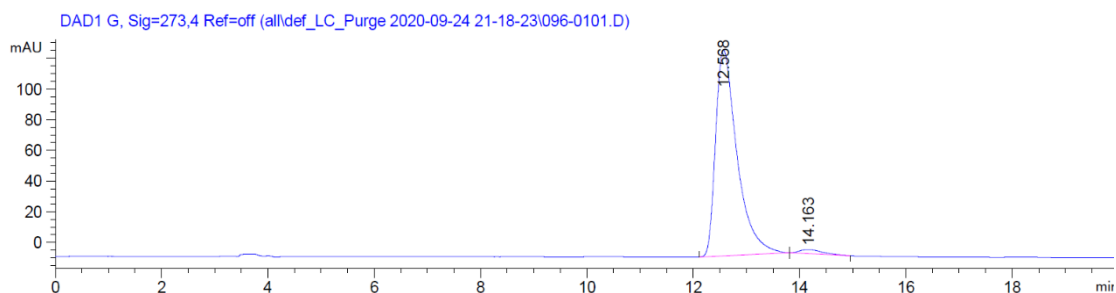
A racemic sample of *rac*-**110y** was synthesized following the general procedure **G**. Analysis by chiral HPLC showed that racemization did not take place. HPLC chromatograms were recorded on an Agilent 1290 Infinity instrument using CHIRALPAK® IF-3 column and *n*hexane/*i*PrOH (70/30, 1.0 mL/min, detection at 273 nm, 96% ee)



Signal 2: DAD1 G, Sig=273,4 Ref=off

Peak #	RetTime [min]	Type	Width [min]	Area [mAU*s]	Height [mAU]	Area %
1	12.555	BB	0.4186	1398.39465	50.11267	49.9708
2	14.013	BB	0.5084	1400.02734	40.09042	50.0292

Figure 5.3.84. HPLC–Chromatogram of *rac*-110y.



Signal 2: DAD1 G, Sig=273,4 Ref=off

Peak #	RetTime [min]	Type	Width [min]	Area [mAU*s]	Height [mAU]	Area %
1	12.568	BB	0.4190	3765.65771	134.35774	97.9104
2	14.163	BB	0.3561	80.36766	2.67073	2.0896

Figure 5.3.85. HPLC–Chromatogram of 110y.

### 5.3.6.7 Cyclic Voltammetry

A glassy-carbon electrode (3.0 mm diameter, disc-electrode) was used as the working electrode, a Pt-wire as auxiliary electrode and an Ag-wire as pseudoreference. The measurements were then referenced using ferrocene. The measurements were carried out at a scan rate of 100 mV/s.

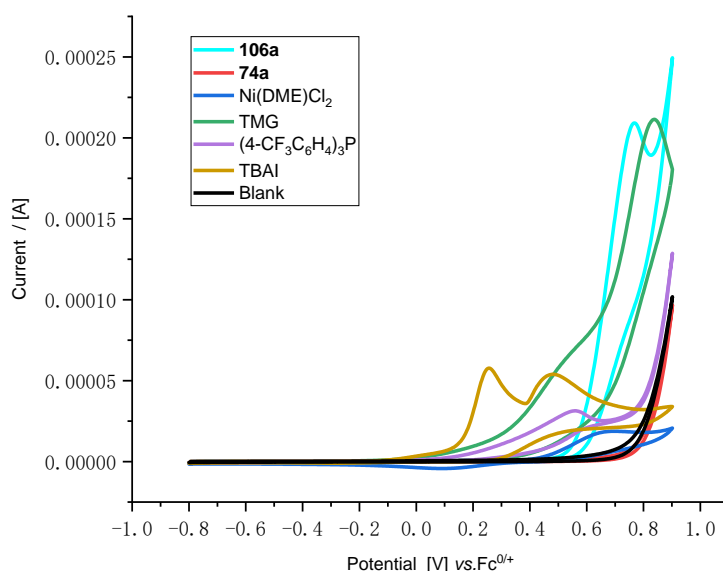


**Figure 5.3.86.** Cyclic voltammograms at 100 mV/s. *n*Bu<sub>4</sub>NPF<sub>6</sub> (0.1 M in DMA); concentration of substrates 5 mM. Performed by Zhipeng Lin.

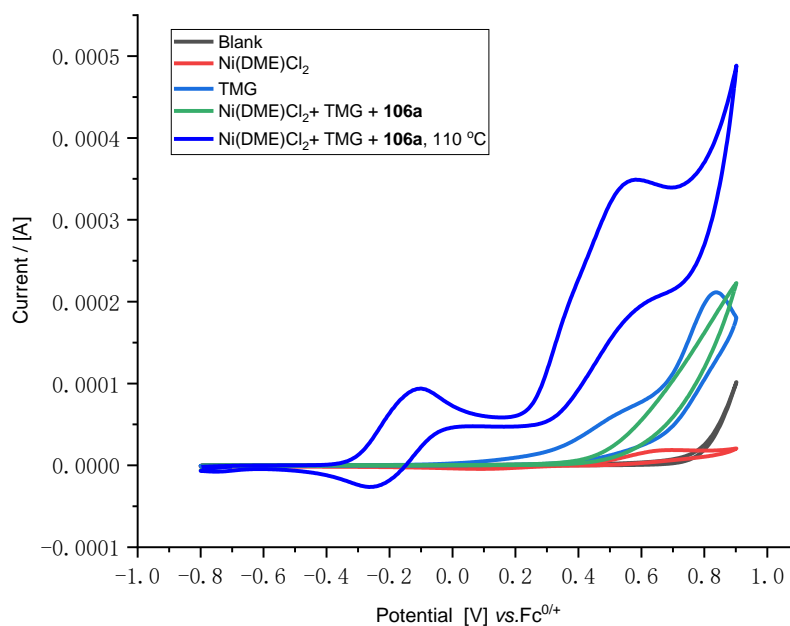


**Figure 5.3.87.** Cyclic voltammograms at 100 mV/s. *n*Bu<sub>4</sub>NPF<sub>6</sub> (0.1 M in DMA); concentration of substrates 5 mM. Blank (black); Ni(DME)Cl<sub>2</sub> + TMG + 106a (green); Ni(DME)Cl<sub>2</sub> + TMG + 106a at 110 °C (blue). Performed by Zhipeng Lin.

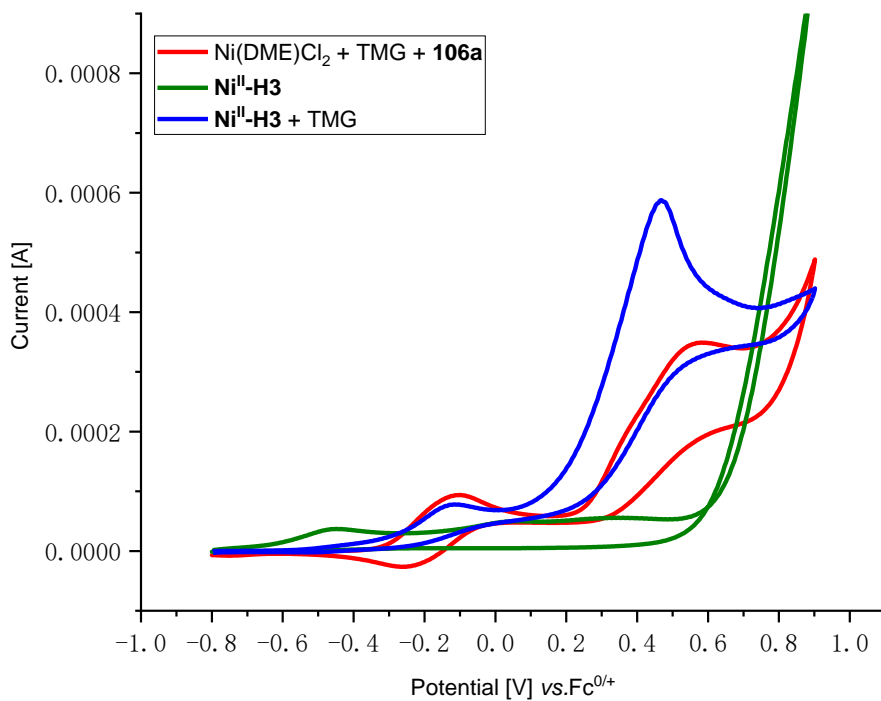


**Figure 5.3.88.** Cyclic voltammograms at 100 mV/s. *n*Bu<sub>4</sub>NPF<sub>6</sub> (0.1 M in DMA); concentration of substrates 5 mM; temperature (110 °C). Ni(DME)Cl<sub>2</sub> + TMG + **106a** (red); Ni<sup>II</sup>-H<sub>3</sub> complex (green); Ni<sup>II</sup>-H<sub>3</sub> + TMG (blue). Performed by Zhipeng Lin.

## 6. References

- [1] a) P. T. Anastas, J. C. Warner, *Green Chemistry: Theory and Practice*, Oxford Universal Press, Oxford, **1998**; b) P. T. Anastas, T. C. Williamson, *Green Chemistry: Designing Chemistry for the Environment*, American Chemical Society, Washington, D.C., **1996**.
- [2] A. de Meijere, F. Diederich, *Metal-Catalyzed Cross-Coupling Reactions 2nd ed.*, Wiley-VCH, Weinheim, **2004**.
- [3] The Nobel Prize in Chemistry 2010- Press Release, <https://www.nobelprize.org/prizes/chemistry/2010/press-release/>. accessed on **Sept. 05, 2020**.
- [4] a) R. F. Heck, *Synlett* **2006**, 2855–2860; b) R. F. Heck, *Acc. Chem. Res.* **1979**, *12*, 146–151; c) R. F. Heck, J. P. Nolley, *J. Org. Chem.* **1972**, *37*, 2320–2322; d) T. Mizoroki, K. Mori, A. Ozaki, *Bull. Chem. Soc. Jap.* **1971**, *44*, 581–581.
- [5] a) N. Miyaura, A. Suzuki, *Chem. Rev.* **1995**, *95*, 2457–2483; b) N. Miyaura, K. Yamada, A. Suzuki, *Tetrahedron Lett.* **1979**, *20*, 3437–3440.
- [6] a) J. K. Stille, *Angew. Chem. Int. Ed.* **1986**, *25*, 508–524; b) D. Milstein, J. K. Stille, *J. Am. Chem. Soc.* **1978**, *100*, 3636–3638; c) M. Kosugi, Y. Shimizu, T. Migita, *Chem. Lett.* **1977**, *6*, 1423–1424.
- [7] a) E. Negishi, *Acc. Chem. Res.* **1982**, *15*, 340–348; b) E. Negishi, A. O. King, N. Okukado, *J. Org. Chem.* **1977**, *42*, 1821–1823; c) S. Baba, E. Negishi, *J. Am. Chem. Soc.* **1976**, *98*, 6729–6731.
- [8] a) K. Sonogashira, *J. Organomet. Chem.* **2002**, *653*, 46–49; b) K. Sonogashira, Y. Tohda, N. Hagihara, *Tetrahedron Lett.* **1975**, *16*, 4467–4470.
- [9] a) T. Hiyama, in *Metal-Catalyzed Cross-Coupling Reactions* (Eds.: A. de Meijere, F. Diederich), Wiley-VCH, Weinheim, **1998**; b) M. Fujita, T. Hiyama, *J. Org. Chem.* **1988**, *53*, 5415–5421; c) T. Hiyama, M. Obayashi, I. Mori, H. Nozaki, *J. Org. Chem.* **1983**, *48*, 912–914.
- [10] a) J. F. Hartwig, *Nature* **2008**, *455*, 314–322; b) A. R. Muci, S. L. Buchwald, *Top. Curr. Chem.* **2002**, *219*, 131–209; c) J. F. Hartwig, *Angew. Chem. Int. Ed.* **1998**, *37*, 2046–2067.
- [11] a) H. Lin, D. Sun, *Org. Prep. Proced. Int.* **2013**, *45*, 341–394; b) F. Monnier, M. Taillefer, *Angew. Chem. Int. Ed.* **2009**, *48*, 6954–6971.
- [12] J. X. Qiao, P. Y. S. Lam, *Synthesis* **2011**, 829–856.
- [13] L. Ackermann, *Modern Arylation Methods*, Wiley-VCH, Weinheim, **2009**.
- [14] a) B. M. Trost, *Angew. Chem. Int. Ed.* **1995**, *34*, 259–281; b) B. Trost, *Science* **1991**, *254*, 1471–1477.
- [15] a) P. A. Wender, B. L. Miller, *Nature* **2009**, *460*, 197–201; b) P. A. Wender, M. P. Croatt, B. Witulski, *Tetrahedron* **2006**, *62*, 7505–7511.
- [16] a) F. Colobert, J. Wencel-Delord, *C–H Activation for Asymmetric Synthesis*, Wiley-VCH, Weinheim, **2019**; b) L. Ackermann, T. B. Gunnoe, L. Goji Habgood, *Catalytic Hydroarylation of Carbon-Carbon Multiple Bonds*, Wiley-VCH, Weinheim, **2017**; c) P. H. Dixneuf, H. Doucet, *C–H Bond Activation and Catalytic Functionalization II*, Springer International Publishing, Switzerland, **2016**; d) P. H.



- Dixneuf, H. Doucet, *C–H Bond Activation and Catalytic Functionalization I*, Springer International Publishing, Switzerland, **2016**; e) J. J. Li, *C–H Bond Activation in Organic Synthesis*, CRC press, Taylor & Francis Group, LLC, **2015**;  
f) X. Ribas, *C–H and C–X Bond Functionalization: Transition Metal Mediation*, Royal Society of Chemistry, Thomas Graham House, Cambridge, **2013**; g) J.-Q. Yu, Z. Shi, *C–H Activation*, Springer-Verlag Berlin, Heidelberg, **2010**.
- [17] a) R. C. Samanta, T. H. Meyer, I. Siewert, L. Ackermann, *Chem. Sci.* **2020**, *11*, 8657–8670; b) P. Gandeepan, L. H. Finger, T. H. Meyer, L. Ackermann, *Chem. Soc. Rev.* **2020**, *49*, 4254–4272; c) L. Ackermann, S.-L. You, M. Oestreich, S. Meng, D. MacFarlane, Y. Yin, *Trends Chem.* **2020**, *2*, 275–277; d) T. H. Meyer, L. H. Finger, P. Gandeepan, L. Ackermann, *Trends Chem.* **2019**, *1*, 63–76.
- [18] a) S. A. Girard, T. Knauber, C.-J. Li, *Angew. Chem. Int. Ed.* **2014**, *53*, 74–100; b) C. S. Yeung, V. M. Dong, *Chem. Rev.* **2011**, *111*, 1215–1292; c) C. J. Scheuermann, *Chem. Asian J.* **2010**, *5*, 436–451; d) C.-J. Li, Z. Li, *Pure Appl. Chem.* **2006**, *78*, 935–945.
- [19] a) J. Wencel-Delord, T. Dröge, F. Liu, F. Glorius, *Chem. Soc. Rev.* **2011**, *40*, 4740–4761; b) H. Lu, X. P. Zhang, *Chem. Soc. Rev.* **2011**, *40*, 1899–1909; c) L. Ackermann, *Chem. Rev.* **2011**, *111*, 1315–1345; d) D. Balcells, E. Clot, O. Eisenstein, *Chem. Rev.* **2010**, *110*, 749–823; e) H. M. L. Davies, J. R. Manning, *Nature* **2008**, *451*, 417–424; f) L. Ackermann, in *Directed Metallation* (Ed.: N. Chatani), Springer Berlin Heidelberg, Berlin, Heidelberg, **2007**, 35–60.
- [20] H. Yi, G. Zhang, H. Wang, Z. Huang, J. Wang, A. K. Singh, A. Lei, *Chem. Rev.* **2017**, *117*, 9016–9085.
- [21] J. R. Webb, S. A. Burgess, T. R. Cundari, T. B. Gunnoe, *Dalton Trans.* **2013**, *42*, 16646–16665.
- [22] J. Kua, X. Xu, R. A. Periana, W. A. Goddard, *Organometallics* **2002**, *21*, 511–525.
- [23] Z. Lin, *Coord. Chem. Rev.* **2007**, *251*, 2280–2291.
- [24] a) T. R. Cundari, T. R. Klinckman, P. T. Wolczanski, *J. Am. Chem. Soc.* **2002**, *124*, 1481–1487; b) J. L. Bennett, P. T. Wolczanski, *J. Am. Chem. Soc.* **1997**, *119*, 10696–10719.
- [25] a) J. C. Gaunt, B. L. Shaw, *J. Organomet. Chem.* **1975**, *102*, 511–516; b) J. M. Duff, B. E. Mann, B. L. Shaw, B. Turtle, *J. Chem. Soc., Dalton Trans.* **1974**, 139–145; c) J. M. Duff, B. L. Shaw, *J. Chem. Soc., Dalton Trans.* **1972**, 2219–2225.
- [26] S. I. Gorelsky, D. Lapointe, K. Fagnou, *J. Am. Chem. Soc.* **2008**, *130*, 10848–10849.
- [27] a) Y. Boutadla, D. L. Davies, S. A. Macgregor, A. I. Poblador-Bahamonde, *Dalton Trans.* **2009**, 5887–5893; b) D. L. Davies, S. M. A. Donald, S. A. Macgregor, *J. Am. Chem. Soc.* **2005**, *127*, 13754–13755.
- [28] a) D. Zell, M. Bursch, V. Müller, S. Grimme, L. Ackermann, *Angew. Chem. Int. Ed.* **2017**, *56*, 10378–10382; b) W. Ma, R. Mei, G. Tenti, L. Ackermann, *Chem. Eur. J.* **2014**, *20*, 15248–15251.
- [29] a) J. Wang, G. Dong, *Chem. Rev.* **2019**, *119*, 7478–7528; b) B. Niu, K. Yang, B. Lawrence, H. Ge, *ChemSusChem* **2019**, *12*, 2955–2969; c) C. Sambigioglio, D. Schönbauer, R. Blicke, T. Dao-Huy, G. Pototschnig, P. Schaaf, T. Wiesinger, M.

- F. Zia, J. Wencel-Delord, T. Besset, B. U. W. Maes, M. Schnürch, *Chem. Soc. Rev.* **2018**, *47*, 6603–6743; d) M. Ghosh, S. De Sarkar, *Asian J. Org. Chem.* **2018**, *7*, 1236–1255; e) P. Gandeepan, L. Ackermann, *Chem* **2018**, *4*, 199–222; f) J. A. Leitch, C. G. Frost, *Chem. Soc. Rev.* **2017**, *46*, 7145–7153; g) M. Font, J. M. Quibell, G. J. P. Perry, I. Larrosa, *Chem. Commun.* **2017**, *53*, 5584–5597; h) Z. Chen, B. Wang, J. Zhang, W. Yu, Z. Liu, Y. Zhang, *Org. Chem. Front.* **2015**, *2*, 1107–1295.
- [30] K. Shen, Y. Fu, J.-N. Li, L. Liu, Q.-X. Guo, *Tetrahedron* **2007**, *63*, 1568–1576.
- [31] a) J. Li, S. De Sarkar, L. Ackermann, *Top. Organomet. Chem.* **2016**, *55*, 217–257; b) G. Cera, L. Ackermann, *Top. Curr. Chem.* **2016**, *374*, 57; c) L. Ackermann, J. Li, *Nat. Chem.* **2015**, *7*, 686–687; d) L. Ackermann, R. Vicente, *Top. Curr. Chem.* **2010**, *292*, 211–229; e) L. Ackermann, R. Vicente, A. R. Kapdi, *Angew. Chem. Int. Ed.* **2009**, *48*, 9792–9826.
- [32] N. Y. P. Kumar, A. Bechtoldt, K. Raghuvanshi, L. Ackermann, *Angew. Chem. Int. Ed.* **2016**, *55*, 6929–6932.
- [33] a) S. I. Kozhushkov, L. Ackermann, *Chem. Sci.* **2013**, *4*, 886–896; b) P. B. Arockiam, C. Bruneau, P. H. Dixneuf, *Chem. Rev.* **2012**, *112*, 5879–5918; c) L. Ackermann, R. Vicente, in *C–H Activation* (Eds.: J.-Q. Yu, Z. Shi), Springer Berlin Heidelberg, Berlin, Heidelberg, **2010**, 211–229; d) The Prices of Precious Metals, <http://www.platinum.matthey.com/prices/price-charts>. accessed on Jul., 2020.
- [34] J. Chatt, J. M. Davidson, *J. Chem. Soc.* **1965**, 843–855.
- [35] L. N. Lewis, J. F. Smith, *J. Am. Chem. Soc.* **1986**, *108*, 2728–2735.
- [36] S. Murai, F. Kakiuchi, S. Sekine, Y. Tanaka, A. Kamatani, M. Sonoda, N. Chatani, *Nature* **1993**, *366*, 529–531.
- [37] H. Weissman, X. Song, D. Milstein, *J. Am. Chem. Soc.* **2001**, *123*, 337–338.
- [38] a) S. Oi, S. Fukita, N. Hirata, N. Watanuki, S. Miyano, Y. Inoue, *Org. Lett.* **2001**, *3*, 2579–2581; b) S. G. Ouellet, A. Roy, C. Molinaro, R. Angelaud, J.-F. Marcoux, P. D. O’Shea, I. W. Davies, *J. Org. Chem.* **2011**, *76*, 1436–1439.
- [39] L. Ackermann, R. Vicente, A. Althammer, *Org. Lett.* **2008**, *10*, 2299–2302.
- [40] a) L. Wang, L. Ackermann, *Org. Lett.* **2013**, *15*, 176–179; b) W. Ma, K. Graczyk, L. Ackermann, *Org. Lett.* **2012**, *14*, 6318–6321; c) B. Li, H. Feng, N. Wang, J. Ma, H. Song, S. Xu, B. Wang, *Chem. Eur. J.* **2012**, *18*, 12873–12879; d) L. Ackermann, L. Wang, A. V. Lygin, *Chem. Sci.* **2012**, *3*, 177–180; e) L. Ackermann, A. V. Lygin, *Org. Lett.* **2012**, *14*, 764–767; f) L. Ackermann, A. V. Lygin, N. Hofmann, *Org. Lett.* **2011**, *13*, 3278–3281; g) L. Ackermann, A. V. Lygin, N. Hofmann, *Angew. Chem. Int. Ed.* **2011**, *50*, 6379–6382.
- [41] a) M. Deponti, S. I. Kozhushkov, D. S. Yufit, L. Ackermann, *Org. Biomol. Chem.* **2013**, *11*, 142–148; b) V. S. Thirunavukkarasu, M. Donati, L. Ackermann, *Org. Lett.* **2012**, *14*, 3416–3419; c) R. K. Chinnagolla, M. Jeganmohan, *Chem. Commun.* **2012**, *48*, 2030–2032; d) L. Ackermann, J. Pospech, K. Graczyk, K. Rauch, *Org. Lett.* **2012**, *14*, 930–933.
- [42] L. Ackermann, *Acc. Chem. Res.* **2014**, *47*, 281–295.
- [43] L. Ackermann, J. Pospech, *Org. Lett.* **2011**, *13*, 4153–4155.
- [44] T. Ueyama, S. Mochida, T. Fukutani, K. Hirano, T. Satoh, M. Miura, *Org. Lett.*

- 2011**, *13*, 706–708.
- [45] a) C. Tirlir, L. Ackermann, *Tetrahedron* **2015**, *71*, 4543–4551; b) B. Li, K. Devaraj, C. Darcel, P. H. Dixneuf, *Green Chem.* **2012**, *14*, 2706–2709; c) H. Yuto, U. Takumi, F. Tatsuya, H. Koji, S. Tetsuya, M. Masahiro, *Chem. Lett.* **2011**, *40*, 1165–1166; d) P. B. Arockiam, C. Fischmeister, C. Bruneau, P. H. Dixneuf, *Green Chem.* **2011**, *13*, 3075–3078.
- [46] a) K. Padala, M. Jeganmohan, *Org. Lett.* **2012**, *14*, 1134–1137; b) K. Padala, M. Jeganmohan, *Org. Lett.* **2011**, *13*, 6144–6147.
- [47] a) K. Padala, S. Pimparkar, P. Madasamy, M. Jeganmohan, *Chem. Commun.* **2012**, *48*, 7140–7142; b) K. Graczyk, W. Ma, L. Ackermann, *Org. Lett.* **2012**, *14*, 4110–4113.
- [48] a) M. C. Reddy, M. Jeganmohan, *Eur. J. Org. Chem.* **2013**, 1150–1157; b) J. Li, C. Kornhaaß, L. Ackermann, *Chem. Commun.* **2012**, *48*, 11343–11345.
- [49] W. Ma, L. Ackermann, *Chem. Eur. J.* **2013**, *19*, 13925–13928.
- [50] a) L.-Q. Zhang, S. Yang, X. Huang, J. You, F. Song, *Chem. Commun.* **2013**, *49*, 8830–8832; b) B. Li, J. Ma, W. Xie, H. Song, S. Xu, B. Wang, *J. Org. Chem.* **2013**, *78*, 9345–9353.
- [51] a) J. Zhang, T.-P. Loh, *Chem. Commun.* **2012**, *48*, 11232–11234; b) Y. Hashimoto, T. Ortloff, K. Hirano, T. Satoh, C. Bolm, M. Miura, *Chem. Lett.* **2012**, *41*, 151–153; c) L. Ackermann, L. Wang, R. Wolfram, A. V. Lygin, *Org. Lett.* **2012**, *14*, 728–731.
- [52] a) F. Yang, L. Ackermann, *J. Org. Chem.* **2014**, *79*, 12070–12082; b) C. Kornhaaß, J. Li, L. Ackermann, *J. Org. Chem.* **2012**, *77*, 9190–9198; c) R. K. Chinnagolla, S. Pimparkar, M. Jeganmohan, *Org. Lett.* **2012**, *14*, 3032–3035; d) B. Li, H. Feng, S. Xu, B. Wang, *Chem. Eur. J.* **2011**, *17*, 12573–12577; e) L. Ackermann, S. Fenner, *Org. Lett.* **2011**, *13*, 6548–6551.
- [53] B. Li, J. Ma, N. Wang, H. Feng, S. Xu, B. Wang, *Org. Lett.* **2012**, *14*, 736–739.
- [54] a) K. Korvorapun, M. Moselage, J. Struwe, T. Rogge, A. M. Messinis, L. Ackermann, *Angew. Chem. Int. Ed.* **2020**, *59*, 18795–18803; b) L. Ackermann, P. Novák, R. Vicente, N. Hofmann, *Angew. Chem. Int. Ed.* **2009**, *48*, 6045–6048.
- [55] G. R. Clark, C. E. L. Headford, W. R. Roper, L. J. Wright, V. P. D. Yap, *Inorg. Chim. Acta* **1994**, *220*, 261–272.
- [56] J.-P. Sutter, D. M. Grove, M. Beley, J.-P. Collin, N. Veldman, A. L. Spek, J.-P. Sauvage, G. van Koten, *Angew. Chem. Int. Ed.* **1994**, *33*, 1282–1285.
- [57] C. Coudret, S. Fraysse, *Chem. Commun.* **1998**, 663–664.
- [58] A. M. Clark, C. E. F. Rickard, W. R. Roper, L. J. Wright, *Organometallics* **1999**, *18*, 2813–2820.
- [59] L. Ackermann, N. Hofmann, R. Vicente, *Org. Lett.* **2011**, *13*, 1875–1877.
- [60] O. Saidi, J. Marafie, A. E. W. Ledger, P. M. Liu, M. F. Mahon, G. Kociok-Köhn, M. K. Whittlesey, C. G. Frost, *J. Am. Chem. Soc.* **2011**, *133*, 19298–19301.
- [61] a) A. J. Paterson, C. J. Heron, C. L. McMullin, M. F. Mahon, N. J. Press, C. G. Frost, *Org. Biomol. Chem.* **2017**, *15*, 5993–6000; b) A. J. Paterson, S. St John-Campbell, M. F. Mahon, N. J. Press, C. G. Frost, *Chem. Commun.* **2015**, *51*, 12807–12810.
- [62] a) G. Li, D. Li, J. Zhang, D.-Q. Shi, Y. Zhao, *ACS Catal.* **2017**, *7*, 4138–4143; b)

- B. Li, S.-L. Fang, D.-Y. Huang, B.-F. Shi, *Org. Lett.* **2017**, *19*, 3950–3953; c) J. Li, S. Warratz, D. Zell, S. De Sarkar, E. E. Ishikawa, L. Ackermann, *J. Am. Chem. Soc.* **2015**, *137*, 13894–13901.
- [63] a) Q. Yu, L. a. Hu, Y. Wang, S. Zheng, J. Huang, *Angew. Chem. Int. Ed.* **2015**, *54*, 15284–15288; b) C. J. Teskey, A. Y. W. Lui, M. F. Greaney, *Angew. Chem. Int. Ed.* **2015**, *54*, 11677–11680.
- [64] Z. Fan, J. Ni, A. Zhang, *J. Am. Chem. Soc.* **2016**, *138*, 8470–8475.
- [65] S. Warratz, D. J. Burns, C. Zhu, K. Korvorapun, T. Rogge, J. Scholz, C. Jooss, D. Gelman, L. Ackermann, *Angew. Chem. Int. Ed.* **2017**, *56*, 1557–1560.
- [66] N. Hofmann, L. Ackermann, *J. Am. Chem. Soc.* **2013**, *135*, 5877–5884.
- [67] a) G. Li, X. Ma, C. Jia, Q. Han, Y. Wang, J. Wang, L. Yu, S. Yang, *Chem. Commun.* **2017**, *53*, 1261–1264; b) G. Li, X. Lv, K. Guo, Y. Wang, S. Yang, L. Yu, Y. Yu, J. Wang, *Org. Chem. Front.* **2017**, *4*, 1145–1148.
- [68] G. Li, P. Gao, X. Lv, C. Qu, Q. Yan, Y. Wang, S. Yang, J. Wang, *Org. Lett.* **2017**, *19*, 2682–2685.
- [69] a) J. Li, K. Korvorapun, S. De Sarkar, T. Rogge, D. J. Burns, S. Warratz, L. Ackermann, *Nat. Commun.* **2017**, *8*, 15430; b) Z. Fan, J. Li, H. Lu, D.-Y. Wang, C. Wang, M. Uchiyama, A. Zhang, *Org. Lett.* **2017**, *19*, 3199–3202.
- [70] S. Z. Tasker, E. A. Standley, T. F. Jamison, *Nature* **2014**, *509*, 299–309.
- [71] J. Montgomery, *Angew. Chem. Int. Ed.* **2004**, *43*, 3890–3908.
- [72] a) R. Shi, Z. Zhang, X. Hu, *Acc. Chem. Res.* **2019**, *52*, 1471–1483; b) N. Hazari, P. R. Melvin, M. M. Beromi, *Nat. Rev. Chem.* **2017**, *1*, 0025; c) F.-S. Han, *Chem. Soc. Rev.* **2013**, *42*, 5270–5298; d) B. M. Rosen, K. W. Quasdorf, D. A. Wilson, N. Zhang, A.-M. Resmerita, N. K. Garg, V. Percec, *Chem. Rev.* **2011**, *111*, 1346–1416.
- [73] a) S. M. Khake, N. Chatani, *Chem* **2020**, *6*, 1056–1081; b) Y. Liu, M. Bandini, *Chin. J. Chem.* **2019**, *37*, 431–441; c) S. M. Khake, N. Chatani, *Trends Chem.* **2019**, *1*, 524–539; d) P. Gandeepan, T. Müller, D. Zell, G. Cera, S. Warratz, L. Ackermann, *Chem. Rev.* **2019**, *119*, 2192–2452; e) V. Arun, K. Mahanty, S. De Sarkar, *ChemCatChem* **2019**, *11*, 2243–2259; f) J. Yamaguchi, K. Muto, K. Itami, *Top. Curr. Chem.* **2016**, *374*, 55; g) J. Yamaguchi, K. Muto, K. Itami, *Eur. J. Org. Chem.* **2013**, 19–30; h) Y. Nakao, *Chem. Rec.* **2011**, *11*, 242–251.
- [74] J. P. Kleiman, M. Dubeck, *J. Am. Chem. Soc.* **1963**, *85*, 1544–1545.
- [75] N. D. Clement, K. J. Cavell, *Angew. Chem. Int. Ed.* **2004**, *43*, 3845–3847.
- [76] L.-C. Liang, P.-S. Chien, Y.-L. Huang, *J. Am. Chem. Soc.* **2006**, *128*, 15562–15563.
- [77] a) H. Hachiya, K. Hirano, T. Satoh, M. Miura, *Org. Lett.* **2009**, *11*, 1737–1740; b) J. Canivet, J. Yamaguchi, I. Ban, K. Itami, *Org. Lett.* **2009**, *11*, 1733–1736.
- [78] T. Yamamoto, K. Muto, M. Komiyama, J. Canivet, J. Yamaguchi, K. Itami, *Chem. Eur. J.* **2011**, *17*, 10113–10122.
- [79] H. Hachiya, K. Hirano, T. Satoh, M. Miura, *Angew. Chem. Int. Ed.* **2010**, *49*, 2202–2205.
- [80] a) G.-R. Qu, P.-Y. Xin, H.-Y. Niu, D.-C. Wang, R.-F. Ding, H.-M. Guo, *Chem. Commun.* **2011**, *47*, 11140–11142; b) H. Hachiya, K. Hirano, T. Satoh, M. Miura,

- ChemCatChem* **2010**, *2*, 1403–1406.
- [81] M. Tobisu, I. Hyodo, N. Chatani, *J. Am. Chem. Soc.* **2009**, *131*, 12070–12071.
- [82] a) W. Song, L. Ackermann, *Angew. Chem. Int. Ed.* **2012**, *51*, 8251–8254; b) L. Ackermann, A. Althammer, S. Fenner, *Angew. Chem. Int. Ed.* **2009**, *48*, 201–204.
- [83] K. Muto, J. Yamaguchi, K. Itami, *J. Am. Chem. Soc.* **2012**, *134*, 169–172.
- [84] K. Muto, J. Yamaguchi, A. Lei, K. Itami, *J. Am. Chem. Soc.* **2013**, *135*, 16384–16387.
- [85] K. Muto, T. Hatakeyama, J. Yamaguchi, K. Itami, *Chem. Sci.* **2015**, *6*, 6792–6798.
- [86] a) K. Yang, P. Wang, C. Zhang, A. A. Kadi, H.-K. Fun, Y. Zhang, H. Lu, *Eur. J. Org. Chem.* **2014**, 7586–7589; b) K. Amaike, K. Muto, J. Yamaguchi, K. Itami, *J. Am. Chem. Soc.* **2012**, *134*, 13573–13576.
- [87] M. G. Hanson, N. M. Olson, Z. Yi, G. Wilson, D. Kalyani, *Org. Lett.* **2017**, *19*, 4271–4274.
- [88] a) S. Rej, Y. Ano, N. Chatani, *Chem. Rev.* **2020**, *120*, 1788–1887; b) O. Daugulis, J. Roane, L. D. Tran, *Acc. Chem. Res.* **2015**, *48*, 1053–1064; c) G. Rouquet, N. Chatani, *Angew. Chem. Int. Ed.* **2013**, *52*, 11726–11743.
- [89] A. Yokota, Y. Aihara, N. Chatani, *J. Org. Chem.* **2014**, *79*, 11922–11932.
- [90] B. Liu, Z.-Z. Zhang, X. Li, B.-F. Shi, *Org. Chem. Front.* **2016**, *3*, 897–900.
- [91] S. Zhao, B. Liu, B.-B. Zhan, W.-D. Zhang, B.-F. Shi, *Org. Lett.* **2016**, *18*, 4586–4589.
- [92] A. P. Honeycutt, J. M. Hoover, *ACS Catal.* **2017**, *7*, 4597–4601.
- [93] P. Li, G.-W. Wang, H. Chen, L. Wang, *Org. Biomol. Chem.* **2018**, *16*, 8783–8790.
- [94] Y. Cheng, Y. Wu, G. Tan, J. You, *Angew. Chem. Int. Ed.* **2016**, *55*, 12275–12279.
- [95] R. A. Jagtap, V. Soni, B. Punji, *ChemSusChem* **2017**, *10*, 2242–2248.
- [96] N. Matsuyama, K. Hirano, T. Satoh, M. Miura, *Org. Lett.* **2009**, *11*, 4156–4159.
- [97] a) V. G. Landge, C. H. Shewale, G. Jaiswal, M. K. Sahoo, S. P. Midya, E. Balaraman, *Catal. Sci. Technol.* **2016**, *6*, 1946–1951; b) Y.-J. Liu, Y.-H. Liu, S.-Y. Yan, B.-F. Shi, *Chem. Commun.* **2015**, *51*, 6388–6391.
- [98] Z. Ruan, S. Lackner, L. Ackermann, *ACS Catal.* **2016**, *6*, 4690–4693.
- [99] S. M. Khake, V. Soni, R. G. Gonnade, B. Punji, *Chem. Eur. J.* **2017**, *23*, 2907–2914.
- [100] a) Y.-H. Liu, Y.-J. Liu, S.-Y. Yan, B.-F. Shi, *Chem. Commun.* **2015**, *51*, 11650–11653; b) N. Matsuyama, M. Kitahara, K. Hirano, T. Satoh, M. Miura, *Org. Lett.* **2010**, *12*, 2358–2361.
- [101] L. Ackermann, *Chem. Commun.* **2010**, *46*, 4866–4877.
- [102] O. Vechorkin, V. Proust, X. Hu, *Angew. Chem. Int. Ed.* **2010**, *49*, 3061–3064.
- [103] T. Yao, K. Hirano, T. Satoh, M. Miura, *Chem. Eur. J.* **2010**, *16*, 12307–12311.
- [104] L. Ackermann, B. Punji, W. Song, *Adv. Synth. Catal.* **2011**, *353*, 3325–3329.
- [105] T. Yao, K. Hirano, T. Satoh, M. Miura, *Angew. Chem. Int. Ed.* **2012**, *51*, 775–779.
- [106] P.-Y. Xin, H.-Y. Niu, G.-R. Qu, R.-F. Ding, H.-M. Guo, *Chem. Commun.* **2012**, *48*, 6717–6719.
- [107] Y. Aihara, N. Chatani, *J. Am. Chem. Soc.* **2013**, *135*, 5308–5311.
- [108] W. Song, S. Lackner, L. Ackermann, *Angew. Chem. Int. Ed.* **2014**, *53*, 2477–2480.
- [109] T. Kubo, N. Chatani, *Org. Lett.* **2016**, *18*, 1698–1701.

- [110] V. Soni, R. A. Jagtap, R. G. Gonnade, B. Punji, *ACS Catal.* **2016**, *6*, 5666–5672.
- [111] Z. Ruan, D. Ghorai, G. Zanoni, L. Ackermann, *Chem. Commun.* **2017**, *53*, 9113–9116.
- [112] a) A. Ricci, *Amino Group Chemistry: From Synthesis to the Life Sciences*, Wiley-VCH, Weinheim, **2008**; b) Z. Rappoport, *The Chemistry of Anilines*, Wiley-VCH, Weinheim, **2007**; c) R. Hili, A. K. Yudin, *Nat. Chem. Biol.* **2006**, *2*, 284–287.
- [113] a) Y. Park, Y. Kim, S. Chang, *Chem. Rev.* **2017**, *117*, 9247–9301; b) J. Jiao, K. Murakami, K. Itami, *ACS Catal.* **2016**, *6*, 610–633; c) M.-L. Louillat, F. W. Patureau, *Chem. Soc. Rev.* **2014**, *43*, 901–910; d) F. Collet, C. Lescot, P. Dauban, *Chem. Soc. Rev.* **2011**, *40*, 1926–1936.
- [114] Y. Li, J. Liu, Y. Xie, R. Zhang, K. Jin, X. Wang, C. Duan, *Org. Biomol. Chem.* **2012**, *10*, 3715–3720.
- [115] Q. Yan, Z. Chen, W. Yu, H. Yin, Z. Liu, Y. Zhang, *Org. Lett.* **2015**, *17*, 2482–2485.
- [116] L. Yu, X. Chen, D. Liu, L. Hu, Y. Yu, H. Huang, Z. Tan, Q. Gui, *Adv. Synth. Catal.* **2018**, *360*, 1346–1351.
- [117] L. Yu, C. Yang, Y. Yu, D. Liu, L. Hu, Y. Xiao, Z.-N. Song, Z. Tan, *Org. Lett.* **2019**, *21*, 5634–5638.
- [118] a) M. Seki, *Org. Process Res. Dev.* **2016**, *20*, 867–877; b) T. Cernak, K. D. Dykstra, S. Tyagarajan, P. Vachal, S. W. Krska, *Chem. Soc. Rev.* **2016**, *45*, 546–576.
- [119] J. Alvarez-Builla, J. J. Vaquero, J. Barluenga, *Modern Heterocyclic Chemistry*, Wiley-VCH, Weinheim, **2011**.
- [120] a) J. Yamaguchi, A. D. Yamaguchi, K. Itami, *Angew. Chem. Int. Ed.* **2012**, *51*, 8960–9009; b) L. McMurray, F. O'Hara, M. J. Gaunt, *Chem. Soc. Rev.* **2011**, *40*, 1885–1898.
- [121] a) I. B. Krylov, V. A. Vil', A. O. Terent'ev, *Beilstein J. Org. Chem.* **2015**, *11*, 92–146; b) J. Le Bras, J. Muzart, *Chem. Soc. Rev.* **2014**, *43*, 3003–3040; c) G. Song, F. Wang, X. Li, *Chem. Soc. Rev.* **2012**, *41*, 3651–3678; d) E. M. Beccalli, G. Broggini, M. Martinelli, S. Sottocornola, *Chem. Rev.* **2007**, *107*, 5318–5365.
- [122] a) K. Raghuvanshi, D. Zell, L. Ackermann, *Org. Lett.* **2017**, *19*, 1278–1281; b) T. Okada, K. Nobushige, T. Satoh, M. Miura, *Org. Lett.* **2016**, *18*, 1150–1153; c) H. Zhang, R.-B. Hu, X.-Y. Zhang, S.-X. Li, S.-D. Yang, *Chem. Commun.* **2014**, *50*, 4686–4689; d) W. Yu, J. Chen, K. Gao, Z. Liu, Y. Zhang, *Org. Lett.* **2014**, *16*, 4870–4873; e) A. R. Dick, K. L. Hull, M. S. Sanford, *J. Am. Chem. Soc.* **2004**, *126*, 2300–2301.
- [123] a) Y. Wu, B. Zhou, *Org. Lett.* **2017**, *19*, 3532–3535; b) F. Yang, K. Rauch, K. Kettelhoit, L. Ackermann, *Angew. Chem. Int. Ed.* **2014**, *53*, 11285–11288; c) Y. Yan, P. Feng, Q.-Z. Zheng, Y.-F. Liang, J.-F. Lu, Y. Cui, N. Jiao, *Angew. Chem. Int. Ed.* **2013**, *52*, 5827–5831; d) V. S. Thirunavukkarasu, J. Hubrich, L. Ackermann, *Org. Lett.* **2012**, *14*, 4210–4213; e) F. Mo, L. J. Trzepakowski, G. Dong, *Angew. Chem. Int. Ed.* **2012**, *51*, 13075–13079; f) X. Chen, X.-S. Hao, C. E. Goodhue, J.-Q. Yu, *J. Am. Chem. Soc.* **2006**, *128*, 6790–6791.
- [124] a) X.-Q. Hao, L.-J. Chen, B. Ren, L.-Y. Li, X.-Y. Yang, J.-F. Gong, J.-L. Niu, M.-P. Song, *Org. Lett.* **2014**, *16*, 1104–1107; b) J. Roane, O. Daugulis, *Org. Lett.* **2013**,

- 15, 5842–5845; c) Y. Wei, N. Yoshikai, *Org. Lett.* **2011**, *13*, 5504–5507.
- [125] a) Y. Ren, Y. Liu, S. Gao, X. Dong, T. Xiao, Y. Jiang, *Tetrahedron* **2020**, *76*, 130985; b) F.-C. Qiu, Q. Xie, B.-T. Guan, *Asian J. Org. Chem.* **2018**, *7*, 107–110; c) S. Li, W. Zhu, F. Gao, C. Li, J. Wang, H. Liu, *J. Org. Chem.* **2017**, *82*, 126–134; d) M. Yu, Z. Wang, M. Tian, C. Lu, S. Li, H. Du, *J. Org. Chem.* **2016**, *81*, 3435–3442; e) P. Villuendas, E. Serrano, E. P. Urriolabeitia, *New J. Chem.* **2015**, *39*, 3077–3083; f) S. Kolle, S. Batra, *Org. Biomol. Chem.* **2015**, *13*, 10376–10385; g) C. Zhang, P. Sun, *J. Org. Chem.* **2014**, *79*, 8457–8461; h) S. Shi, C. Kuang, *J. Org. Chem.* **2014**, *79*, 6105–6112; i) F. Péron, C. Fossey, J. Sopkova-de Oliveira Santos, T. Cailly, F. Fabis, *Chem. Eur. J.* **2014**, *20*, 7507–7513; j) A. Kamal, V. Srinivasulu, M. Sathish, Y. Tangella, V. L. Nayak, M. P. N. Rao, N. Shankaraiah, N. Nagesh, *Asian J. Org. Chem.* **2014**, *3*, 68–76; k) T. Gao, P. Sun, *J. Org. Chem.* **2014**, *79*, 9888–9893; l) Z. Yin, X. Jiang, P. Sun, *J. Org. Chem.* **2013**, *78*, 10002–10007; m) B. V. Subba Reddy, N. Umadevi, G. Narasimhulu, J. S. Yadav, *Tetrahedron Lett.* **2012**, *53*, 6091–6094; n) W. Li, P. Sun, *J. Org. Chem.* **2012**, *77*, 8362–8366; o) T.-S. Jiang, G.-W. Wang, *J. Org. Chem.* **2012**, *77*, 9504–9509; p) G.-W. Wang, T.-T. Yuan, *J. Org. Chem.* **2010**, *75*, 476–479; q) L. V. Desai, H. A. Malik, M. S. Sanford, *Org. Lett.* **2006**, *8*, 1141–1144.
- [126] a) Y. Xiao, J. Li, Y. Liu, S. Wang, H. Zhang, H. Ding, *Eur. J. Org. Chem.* **2018**, 3306–3311; b) W. Lu, H. Xu, Z. Shen, *Org. Biomol. Chem.* **2017**, *15*, 1261–1267; c) S. Bhadra, C. Matheis, D. Katayev, L. J. Gooßen, *Angew. Chem. Int. Ed.* **2013**, *52*, 9279–9283.
- [127] a) Y. Zong, Y. Rao, *Org. Lett.* **2014**, *16*, 5278–5281; b) G. Shan, X. Yang, Y. Zong, Y. Rao, *Angew. Chem. Int. Ed.* **2013**, *52*, 13606–13610; c) F.-J. Chen, S. Zhao, F. Hu, K. Chen, Q. Zhang, S.-Q. Zhang, B.-F. Shi, *Chem. Sci.* **2013**, *4*, 4187–4192; d) S.-Y. Zhang, G. He, Y. Zhao, K. Wright, W. A. Nack, G. Chen, *J. Am. Chem. Soc.* **2012**, *134*, 7313–7316.
- [128] a) Y. Hu, M. Wang, P. Li, H. Li, L. Wang, *Asian J. Org. Chem.* **2019**, *8*, 171–178; b) L.-B. Zhang, X.-Q. Hao, S.-K. Zhang, K. Liu, B. Ren, J.-F. Gong, J.-L. Niu, M.-P. Song, *J. Org. Chem.* **2014**, *79*, 10399–10409.
- [129] a) M. Zhang, Z. Yang, R. Li, X. Huang, R. Feng, C. Qi, *Tetrahedron Lett.* **2020**, *61*, 151592; b) T. Zhang, H. Zhu, F. Yang, Y. Wu, Y. Wu, *Tetrahedron* **2019**, *75*, 1541–1547; c) S.-K. Liu, X.-F. Cui, X.-X. Liu, H.-J. Ma, D.-D. Wei, X.-L. Luo, G.-S. Huang, *ChemistrySelect* **2018**, *3*, 3989–3992; d) J.-N. Han, C. Du, X. Zhu, Z.-L. Wang, Y. Zhu, Z.-Y. Chu, J.-L. Niu, M.-P. Song, *Beilstein J. Org. Chem.* **2018**, *14*, 2090–2097; e) L.-B. Zhang, X.-Q. Hao, S.-K. Zhang, Z.-J. Liu, X.-X. Zheng, J.-F. Gong, J.-L. Niu, M.-P. Song, *Angew. Chem. Int. Ed.* **2015**, *54*, 272–275.
- [130] a) Z.-I. Li, K.-k. Sun, C. Cai, *Org. Chem. Front.* **2019**, *6*, 637–642; b) N. Rajesh, B. Sundararaju, *Asian J. Org. Chem.* **2018**, *7*, 1368–1371.
- [131] a) T. D. Baguley, H.-C. Xu, M. Chatterjee, A. C. Nairn, P. J. Lombroso, J. A. Ellman, *J. Med. Chem.* **2013**, *56*, 7636–7650; b) Q. Dang, Y. Liu, D. K. Cashion, S. R. Kasibhatla, T. Jiang, F. Taplin, J. D. Jacintho, H. Li, Z. Sun, Y. Fan, J. DaRe, F. Tian, W. Li, T. Gibson, R. Lemus, P. D. van Poelje, S. C. Potter, M. D. Erion, *J. Med. Chem.* **2011**, *54*, 153–165.

- [132] a) C. Queffelec, M. Petit, P. Janvier, D. A. Knight, B. Bujoli, *Chem. Rev.* **2012**, *112*, 3777–3807; b) K. J. Gagnon, H. P. Perry, A. Clearfield, *Chem. Rev.* **2012**, *112*, 1034–1054.
- [133] a) Y.-N. Ma, S.-X. Li, S.-D. Yang, *Acc. Chem. Res.* **2017**, *50*, 1480–1492; b) J. M. Bayne, D. W. Stephan, *Chem. Soc. Rev.* **2016**, *45*, 765–774; c) W. Tang, X. Zhang, *Chem. Rev.* **2003**, *103*, 3029–3070; d) G. Helmchen, A. Pfaltz, *Acc. Chem. Res.* **2000**, *33*, 336–345.
- [134] a) C. S. Demmer, N. Krogsgaard-Larsen, L. Bunch, *Chem. Rev.* **2011**, *111*, 7981–8006; b) T. Hirao, T. Masunaga, Y. Ohshiro, T. Agawa, *Synthesis* **1981**, 56–57.
- [135] L. Chen, X.-Y. Liu, Y.-X. Zou, *Adv. Synth. Catal.* **2020**, *362*, 1724–1818.
- [136] C.-G. Feng, M. Ye, K.-J. Xiao, S. Li, J.-Q. Yu, *J. Am. Chem. Soc.* **2013**, *135*, 9322–9325.
- [137] C. Li, T. Yano, N. Ishida, M. Murakami, *Angew. Chem. Int. Ed.* **2013**, *52*, 9801–9804.
- [138] M. Min, D. Kang, S. Jung, S. Hong, *Adv. Synth. Catal.* **2016**, *358*, 1296–1301.
- [139] S. Wang, R. Guo, G. Wang, S.-Y. Chen, X.-Q. Yu, *Chem. Commun.* **2014**, *50*, 12718–12721.
- [140] A. Volta, *Philos. Trans. R. Soc. London* **1800**, *90*, 403–431.
- [141] a) H. Kolbe, *Liebigs Ann. Chem.* **1849**, *69*, 257–294; b) H. Kolbe, *Liebigs Ann. Chem.* **1848**, *64*, 339–341.
- [142] M. Faraday, *Philos. Trans. R. Soc. London* **1825**, 440–466.
- [143] a) F. Wang, S. S. Stahl, *Acc. Chem. Res.* **2020**, *53*, 561–574; b) J. C. Siu, N. Fu, S. Lin, *Acc. Chem. Res.* **2020**, *53*, 547–560; c) P. Xiong, H.-C. Xu, *Acc. Chem. Res.* **2019**, *52*, 3339–3350; d) A. Wiebe, T. Gieshoff, S. Möhle, E. Rodrigo, M. Zirbes, S. R. Waldvogel, *Angew. Chem. Int. Ed.* **2018**, *57*, 5594–5619; e) Y. Jiang, K. Xu, C. Zeng, *Chem. Rev.* **2018**, *118*, 4485–4540; f) M. Yan, Y. Kawamata, P. S. Baran, *Chem. Rev.* **2017**, *117*, 13230–13319; g) R. Feng, J. A. Smith, K. D. Moeller, *Acc. Chem. Res.* **2017**, *50*, 2346–2352; h) E. J. Horn, B. R. Rosen, P. S. Baran, *ACS Cent. Sci.* **2016**, *2*, 302–308; i) R. Francke, R. D. Little, *Chem. Soc. Rev.* **2014**, *43*, 2492–2521; j) J.-i. Yoshida, K. Kataoka, R. Horcajada, A. Nagaki, *Chem. Rev.* **2008**, *108*, 2265–2299; k) A. Jutand, *Chem. Rev.* **2008**, *108*, 2300–2347; l) E. Duñach, D. Franco, S. Olivero, *Eur. J. Org. Chem.* **2003**, 1605–1622.
- [144] a) K.-J. Jiao, Y.-K. Xing, Q.-L. Yang, H. Qiu, T.-S. Mei, *Acc. Chem. Res.* **2020**, *53*, 300–310; b) L. Ackermann, *Acc. Chem. Res.* **2020**, *53*, 84–104; c) Y. Qiu, J. Struwe, L. Ackermann, *Synlett* **2019**, *30*, 1164–1173; d) Q.-L. Yang, P. Fang, T.-S. Mei, *Chin. J. Chem.* **2018**, *36*, 338–352; e) S. Tang, Y. Liu, A. Lei, *Chem* **2018**, *4*, 27–45; f) N. Sauermann, T. H. Meyer, Y. Qiu, L. Ackermann, *ACS Catal.* **2018**, *8*, 7086–7103; g) N. Sauermann, T. H. Meyer, L. Ackermann, *Chem. Eur. J.* **2018**, *24*, 16209–16217; h) C. Ma, P. Fang, T.-S. Mei, *ACS Catal.* **2018**, *8*, 7179–7189.
- [145] S.-K. Zhang, R. C. Samanta, A. Del Vecchio, L. Ackermann, *Chem. Eur. J.* **2020**, *26*, 10936–10947.
- [146] C. Amatore, C. Cammoun, A. Jutand, *Adv. Synth. Catal.* **2007**, *349*, 292–296.
- [147] a) Y. Fujiwara, I. Moritani, S. Danno, R. Asano, S. Teranishi, *J. Am. Chem. Soc.* **1969**, *91*, 7166–7169; b) Y. Fujiwara, I. Moritani, M. Matsuda, S. Teranishi,



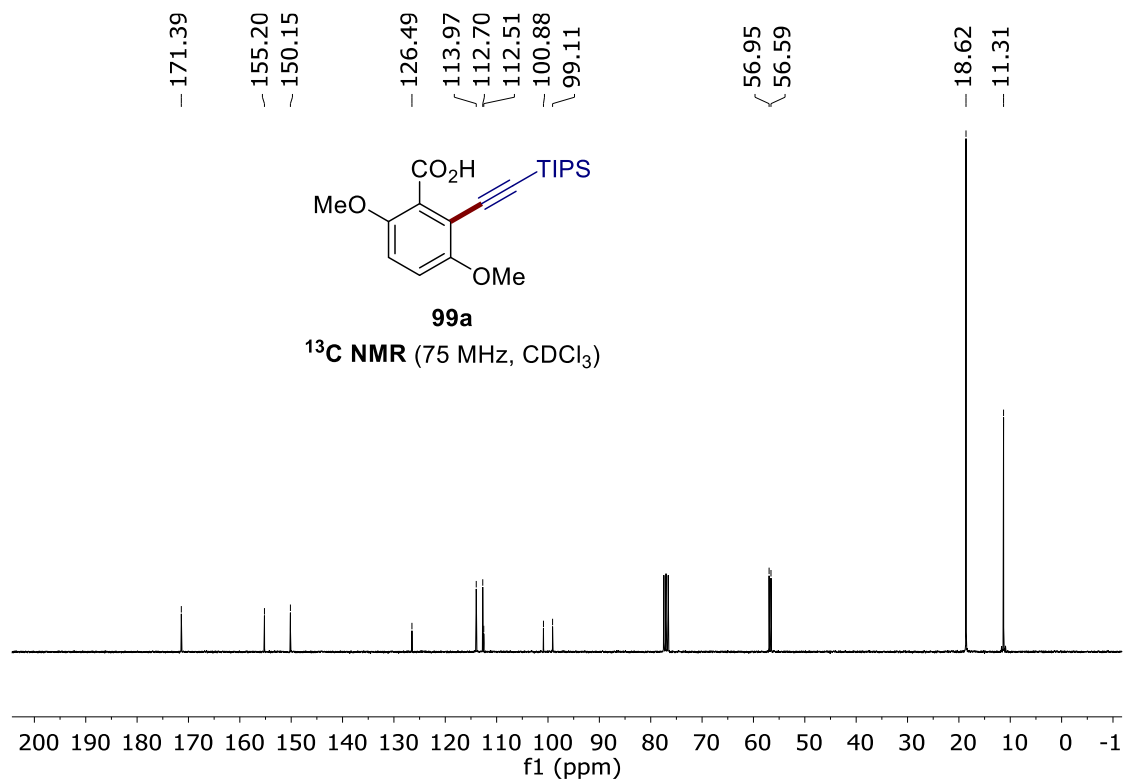
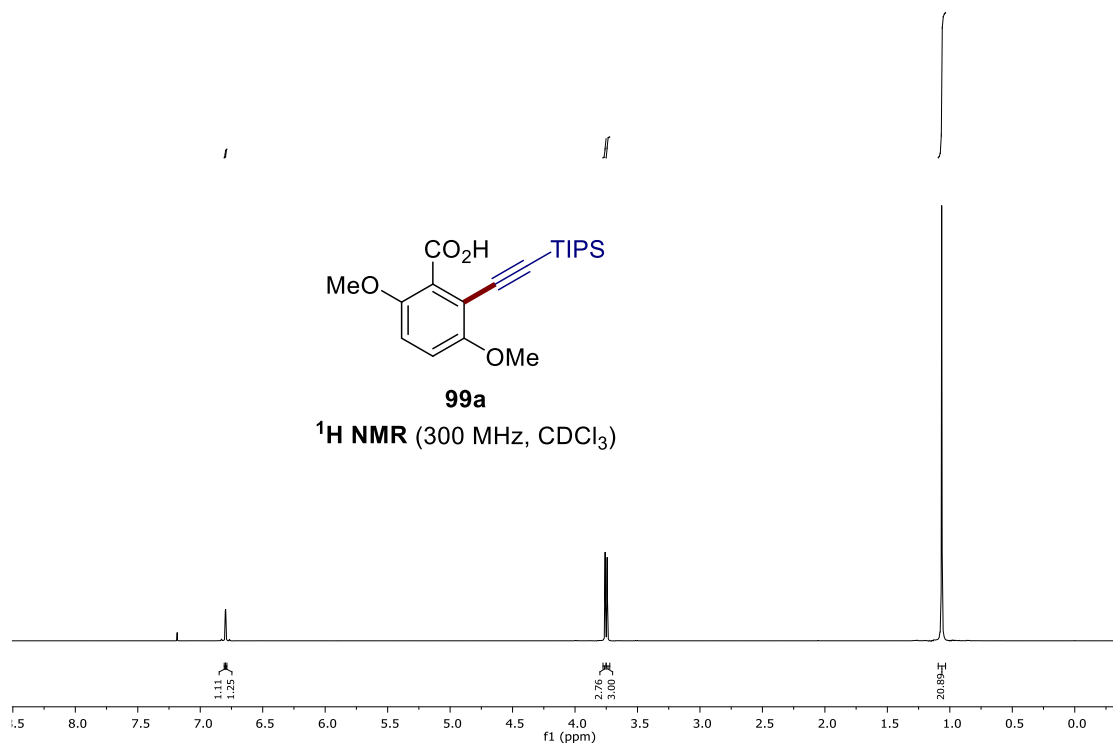
- Tetrahedron Lett.* **1968**, *9*, 633–636; c) I. Moritanl, Y. Fujiwara, *Tetrahedron Lett.* **1967**, *8*, 1119–1122.
- [148] a) U. Dhawa, C. Tian, T. Wdowik, J. C. A. Oliveira, J. Hao, L. Ackermann, *Angew. Chem. Int. Ed.* **2020**, *59*, 13451–13457; b) Q.-L. Yang, C.-Z. Li, L.-W. Zhang, Y.-Y. Li, X. Tong, X.-Y. Wu, T.-S. Mei, *Organometallics* **2019**, *38*, 1208–1212; c) C. Ma, C.-Q. Zhao, Y.-Q. Li, L.-P. Zhang, X.-T. Xu, K. Zhang, T.-S. Mei, *Chem. Commun.* **2017**, *53*, 12189–12192; d) F. Saito, H. Aiso, T. Kochi, F. Kakiuchi, *Organometallics* **2014**, *33*, 6704–6707.
- [149] a) Z. Duan, L. Zhang, W. Zhang, L. Lu, L. Zeng, R. Shi, A. Lei, *ACS Catal.* **2020**, *10*, 3828–3831; b) Q.-L. Yang, X.-Y. Wang, T.-L. Wang, X. Yang, D. Liu, X. Tong, X.-Y. Wu, T.-S. Mei, *Org. Lett.* **2019**, *21*, 2645–2649; c) A. Shrestha, M. Lee, A. L. Dunn, M. S. Sanford, *Org. Lett.* **2018**, *20*, 204–207; d) K. Sano, N. Kimura, T. Kochi, F. Kakiuchi, *Asian J. Org. Chem.* **2018**, *7*, 1311–1314; e) Q.-L. Yang, Y.-Q. Li, C. Ma, P. Fang, X.-J. Zhang, T.-S. Mei, *J. Am. Chem. Soc.* **2017**, *139*, 3293–3298; f) Y.-Q. Li, Q.-L. Yang, P. Fang, T.-S. Mei, D. Zhang, *Org. Lett.* **2017**, *19*, 2905–2908; g) M. Konishi, K. Tsuchida, K. Sano, T. Kochi, F. Kakiuchi, *J. Org. Chem.* **2017**, *82*, 8716–8724; h) T. V. Grayaznova, Y. B. Dudkina, D. R. Islamov, O. N. Kataeva, O. G. Sinyashin, D. A. Vicic, Y. H. Budnikova, *J. Organomet. Chem.* **2015**, *785*, 68–71; i) Y. B. Dudkina, T. V. Gryaznova, O. N. Kataeva, Y. H. Budnikova, O. G. Sinyashin, *Russ. Chem. Bull.* **2015**, *63*, 2641–2646; j) H. Aiso, T. Kochi, H. Mutsutani, T. Tanabe, S. Nishiyama, F. Kakiuchi, *J. Org. Chem.* **2012**, *77*, 7718–7724; k) F. Kakiuchi, T. Kochi, H. Mutsutani, N. Kobayashi, S. Urano, M. Sato, S. Nishiyama, T. Tanabe, *J. Am. Chem. Soc.* **2009**, *131*, 11310–11311.
- [150] Y. Qiu, W.-J. Kong, J. Struwe, N. Sauermann, T. Rogge, A. Scheremetjew, L. Ackermann, *Angew. Chem. Int. Ed.* **2018**, *57*, 5828–5832.
- [151] Y. Zhang, J. Struwe, L. Ackermann, *Angew. Chem. Int. Ed.* **2020**, *59*, 15076–15080.
- [152] Y. Qiu, A. Scheremetjew, L. Ackermann, *J. Am. Chem. Soc.* **2019**, *141*, 2731–2738.
- [153] W.-J. Kong, L. H. Finger, J. C. A. Oliveira, L. Ackermann, *Angew. Chem. Int. Ed.* **2019**, *58*, 6342–6346.
- [154] W.-J. Kong, Z. Shen, L. H. Finger, L. Ackermann, *Angew. Chem. Int. Ed.* **2020**, *59*, 5551–5556.
- [155] W.-J. Kong, L. H. Finger, A. M. Messinis, R. Kuniyil, J. C. A. Oliveira, L. Ackermann, *J. Am. Chem. Soc.* **2019**, *141*, 17198–17206.
- [156] Z.-J. Wu, F. Su, W. Lin, J. Song, T.-B. Wen, H.-J. Zhang, H.-C. Xu, *Angew. Chem. Int. Ed.* **2019**, *58*, 16770–16774.
- [157] a) F. Xu, Y.-J. Li, C. Huang, H.-C. Xu, *ACS Catal.* **2018**, *8*, 3820–3824; b) Y. Qiu, C. Tian, L. Massignan, T. Rogge, L. Ackermann, *Angew. Chem. Int. Ed.* **2018**, *57*, 5818–5822.
- [158] a) L. Yang, R. Steinbock, A. Scheremetjew, R. Kuniyil, L. H. Finger, A. M. Messinis, L. Ackermann, *Angew. Chem. Int. Ed.* **2020**, *59*, 11130–11135; b) M.-J. Luo, M. Hu, R.-J. Song, D.-L. He, J.-H. Li, *Chem. Commun.* **2019**, *55*, 1124–1127; c) R. Mei, J. Koeller, L. Ackermann, *Chem. Commun.* **2018**, *54*, 12879–12882.

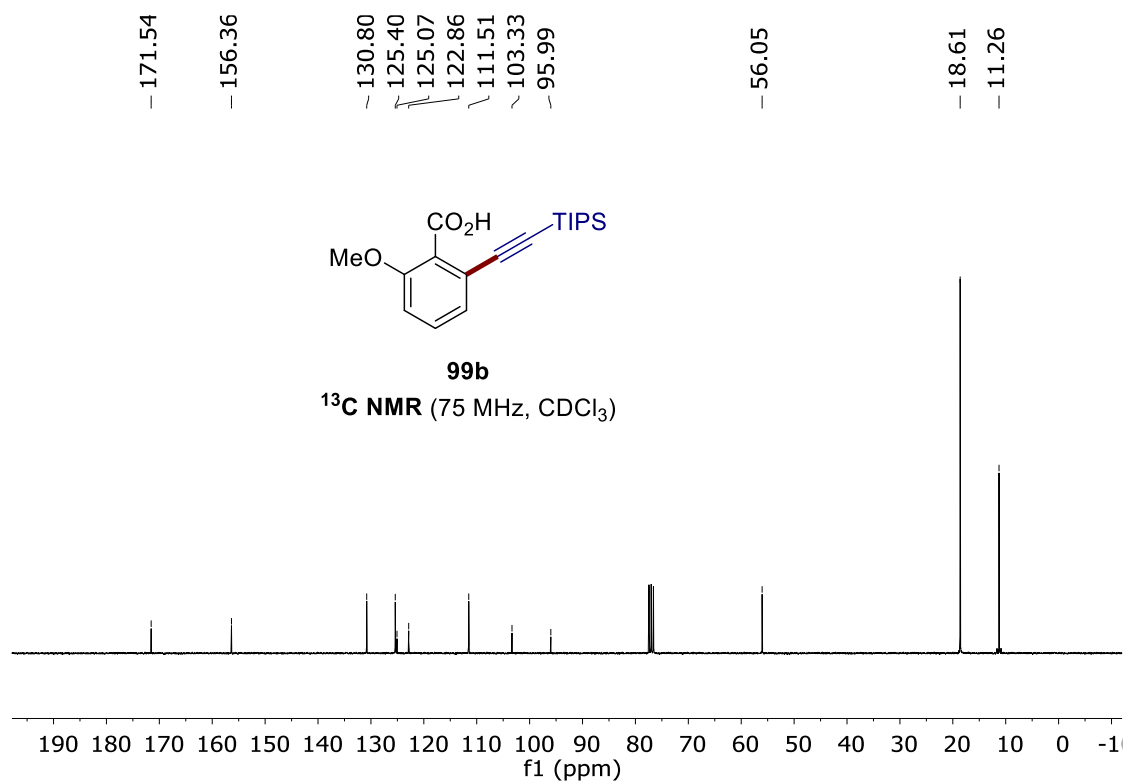
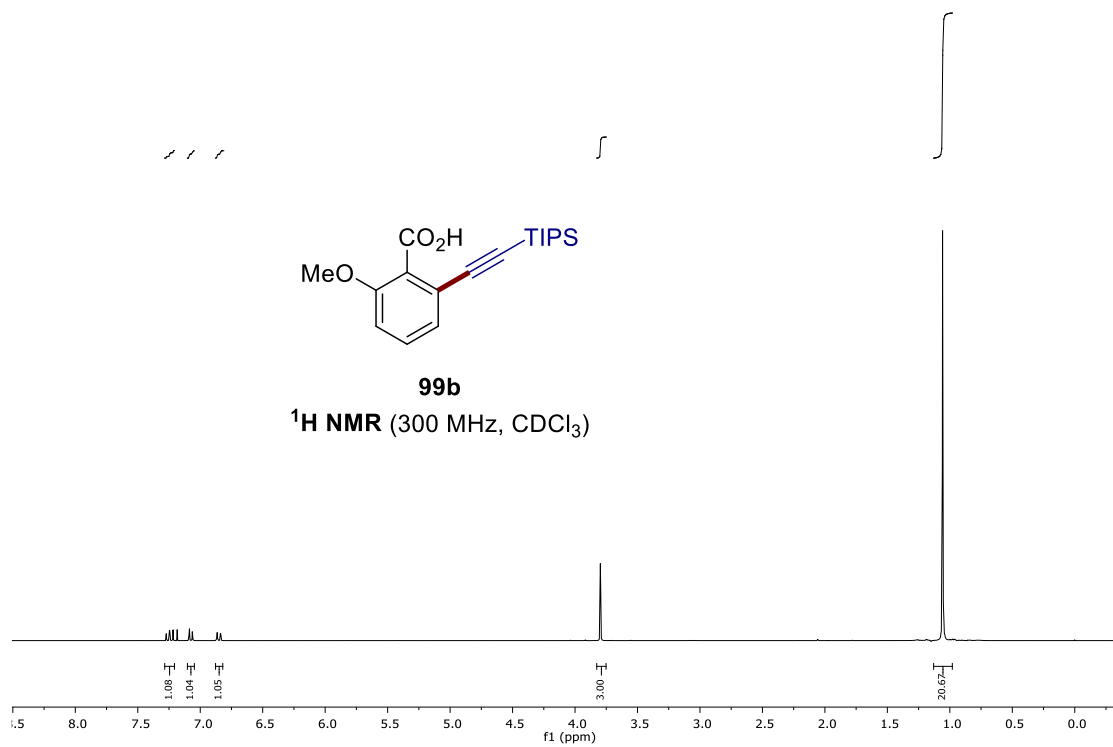
- [159] Z.-Q. Wang, C. Hou, Y.-F. Zhong, Y.-X. Lu, Z.-Y. Mo, Y.-M. Pan, H.-T. Tang, *Org. Lett.* **2019**, *21*, 9841–9845.
- [160] Y. Qiu, M. Stangier, T. H. Meyer, J. C. A. Oliveira, L. Ackermann, *Angew. Chem. Int. Ed.* **2018**, *57*, 14179–14183.
- [161] Q.-L. Yang, Y.-K. Xing, X.-Y. Wang, H.-X. Ma, X.-J. Weng, X. Yang, H.-M. Guo, T.-S. Mei, *J. Am. Chem. Soc.* **2019**, *141*, 18970–18976.
- [162] X. Ye, C. Wang, S. Zhang, J. Wei, C. Shan, L. Wojtas, Y. Xie, X. Shi, *ACS Catal.* **2020**, 11693–11699.
- [163] N. Sauermann, T. H. Meyer, C. Tian, L. Ackermann, *J. Am. Chem. Soc.* **2017**, *139*, 18452–18455.
- [164] a) R. Mei, X. Fang, L. He, J. Sun, L. Zou, W. Ma, L. Ackermann, *Chem. Commun.* **2020**, *56*, 1393–1396; b) U. Dhawa, C. Tian, W. Li, L. Ackermann, *ACS Catal.* **2020**, *10*, 6457–6462; c) S. C. Sau, R. Mei, J. Struwe, L. Ackermann, *ChemSusChem* **2019**, *12*, 3023–3027; d) R. Mei, W. Ma, Y. Zhang, X. Guo, L. Ackermann, *Org. Lett.* **2019**, *21*, 6534–6538; e) L. Zeng, H. Li, S. Tang, X. Gao, Y. Deng, G. Zhang, C.-W. Pao, J.-L. Chen, J.-F. Lee, A. Lei, *ACS Catal.* **2018**, *8*, 5448–5453; f) C. Tian, L. Massignan, T. H. Meyer, L. Ackermann, *Angew. Chem. Int. Ed.* **2018**, *57*, 2383–2387; g) S. Tang, D. Wang, Y. Liu, L. Zeng, A. Lei, *Nat. Commun.* **2018**, *9*, 798; h) T. H. Meyer, J. C. A. Oliveira, S. C. Sau, N. W. J. Ang, L. Ackermann, *ACS Catal.* **2018**, *8*, 9140–9147; i) R. Mei, N. Sauermann, J. C. A. Oliveira, L. Ackermann, *J. Am. Chem. Soc.* **2018**, *140*, 7913–7921.
- [165] a) C. Tian, U. Dhawa, J. Struwe, L. Ackermann, *Chin. J. Chem.* **2019**, *37*, 552–556; b) N. Sauermann, R. Mei, L. Ackermann, *Angew. Chem. Int. Ed.* **2018**, *57*, 5090–5094; c) X. Gao, P. Wang, L. Zeng, S. Tang, A. Lei, *J. Am. Chem. Soc.* **2018**, *140*, 4195–4199.
- [166] Q.-L. Yang, X.-Y. Wang, J.-Y. Lu, L.-P. Zhang, P. Fang, T.-S. Mei, *J. Am. Chem. Soc.* **2018**, *140*, 11487–11494.
- [167] S. Kathiravan, S. Suriyanarayanan, I. A. Nicholls, *Org. Lett.* **2019**, *21*, 1968–1972.
- [168] C. Tian, U. Dhawa, A. Scheremetjew, L. Ackermann, *ACS Catal.* **2019**, *9*, 7690–7696.
- [169] C. Zhu, M. Stangier, J. C. A. Oliveira, L. Massignan, L. Ackermann, *Chem. Eur. J.* **2019**, *25*, 16382–16389.
- [170] R. Mei, S.-K. Zhang, L. Ackermann, *Org. Lett.* **2017**, *19*, 3171–3174.
- [171] a) X. Li, S. Li, S. Sun, F. Yang, W. Zhu, Y. Zhu, Y. Wu, Y. Wu, *Adv. Synth. Catal.* **2016**, *358*, 1699–1704; b) M. Ke, Q. Song, *J. Org. Chem.* **2016**, *81*, 3654–3664; c) M.-C. Belhomme, T. Poisson, X. Pannecoucke, *J. Org. Chem.* **2014**, *79*, 7205–7211; d) K. Fujikawa, Y. Fujioka, A. Kobayashi, H. Amii, *Org. Lett.* **2011**, *13*, 5560–5563.
- [172] a) V. Gayakhe, Y. S. Sanghvi, I. J. S. Fairlamb, A. R. Kapdi, *Chem. Commun.* **2015**, *51*, 11944–11960; b) J. Štambaský, M. Hocek, P. Kočovský, *Chem. Rev.* **2009**, *109*, 6729–6764.
- [173] a) D. Lapointe, K. Fagnou, *Chem. Lett.* **2010**, *39*, 1118–1126; b) S. I. Gorelsky, D. Lapointe, K. Fagnou, *J. Am. Chem. Soc.* **2008**, *130*, 10848–10849.
- [174] a) M. B. Watson, N. P. Rath, L. M. Mirica, *J. Am. Chem. Soc.* **2017**, *139*, 35–38;

- b) M. Rovira, S. Roldán-Gómez, V. Martin-Diaconescu, C. J. Whiteoak, A. Company, J. M. Luis, X. Ribas, *Chem. Eur. J.* **2017**, *23*, 11662–11668; c) F. D'Accriscio, P. Borja, N. Saffon-Merceron, M. Fustier-Boutignon, N. Mézailles, N. Nebra, *Angew. Chem. Int. Ed.* **2017**, *56*, 12898–12902; d) W. Zhou, S. Zheng, J. W. Schultz, N. P. Rath, L. M. Mirica, *J. Am. Chem. Soc.* **2016**, *138*, 5777–5780; e) N. M. Camasso, M. S. Sanford, *Science* **2015**, *347*, 1218–1220.
- [175] S.-K. Zhang, R. C. Samanta, N. Sauermann, L. Ackermann, *Chem. Eur. J.* **2018**, *24*, 19166–19170.
- [176] a) F. Weigend, R. Ahlrichs, *Phys. Chem. Chem. Phys.* **2005**, *7*, 3297–3305; b) C. Adamo, V. Barone, *J. Chem. Phys.* **1999**, *110*, 6158–6170.
- [177] Z. He, Y. Huang, *ACS Catal.* **2016**, *6*, 7814–7823.
- [178] Z. Li, C. Liu, W. Cao, Q. Yao, *J. Appl. Polym. Sci.* **2020**, *137*, 47411.
- [179] a) S. Grimme, S. Ehrlich, L. Goerigk, *J. Comput. Chem.* **2011**, *32*, 1456–1465; b) S. Grimme, J. Antony, S. Ehrlich, H. Krieg, *J. Chem. Phys.* **2010**, *132*, 154104–154119; c) A. V. Marenich, C. J. Cramer, D. G. Truhlar, *J. Phys. Chem. B* **2009**, *113*, 6378–6396; d) F. Weigend, *Phys. Chem. Chem. Phys.* **2006**, *8*, 1057–1065; e) A. Schäfer, C. Huber, R. Ahlrichs, *J. Chem. Phys.* **1994**, *100*, 5829–5835; f) A. Schäfer, H. Horn, R. Ahlrichs, *J. Chem. Phys.* **1992**, *97*, 2571–2577.
- [180] S.-K. Zhang, J. Struwe, L. Hu, L. Ackermann, *Angew. Chem. Int. Ed.* **2020**, *59*, 3178–3183.
- [181] a) X. Zhou, S. Yu, L. Kong, X. Li, *ACS Catal.* **2016**, *6*, 647–651; b) R. Mei, J. Loup, L. Ackermann, *ACS Catal.* **2016**, *6*, 793–797.
- [182] Y. Yang, R. Li, Y. Zhao, D. Zhao, Z. Shi, *J. Am. Chem. Soc.* **2016**, *138*, 8734–8737.
- [183] a) D. Kalsi, N. Barsu, B. Sundararaju, *Chem. Eur. J.* **2018**, *24*, 2360–2364; b) L. Wan, K. Qiao, X. Yuan, M.-W. Zheng, B.-B. Fan, Z. C. Di, D. Zhang, Z. Fang, K. Guo, *Adv. Synth. Catal.* **2017**, *359*, 2596–2604; c) L. D. Tran, J. Roane, O. Daugulis, *Angew. Chem. Int. Ed.* **2013**, *52*, 6043–6046.
- [184] J. Roane, O. Daugulis, *J. Am. Chem. Soc.* **2016**, *138*, 4601–4607.
- [185] M. Berger, R. Chauhan, C. A. B. Rodrigues, N. Maulide, *Chem. Eur. J.* **2016**, *22*, 16805–16808.
- [186] a) S. E. Barber, K. E. S. Dean, A. J. Kirby, *Can. J. Chem.* **1999**, *77*, 792–801; b) W. Kirmse, W. Konrad, I. S. Özkir, *Tetrahedron* **1997**, *53*, 9935–9964; c) W. Kirmse, I. S. Özkir, *J. Am. Chem. Soc.* **1992**, *114*, 7590–7591.

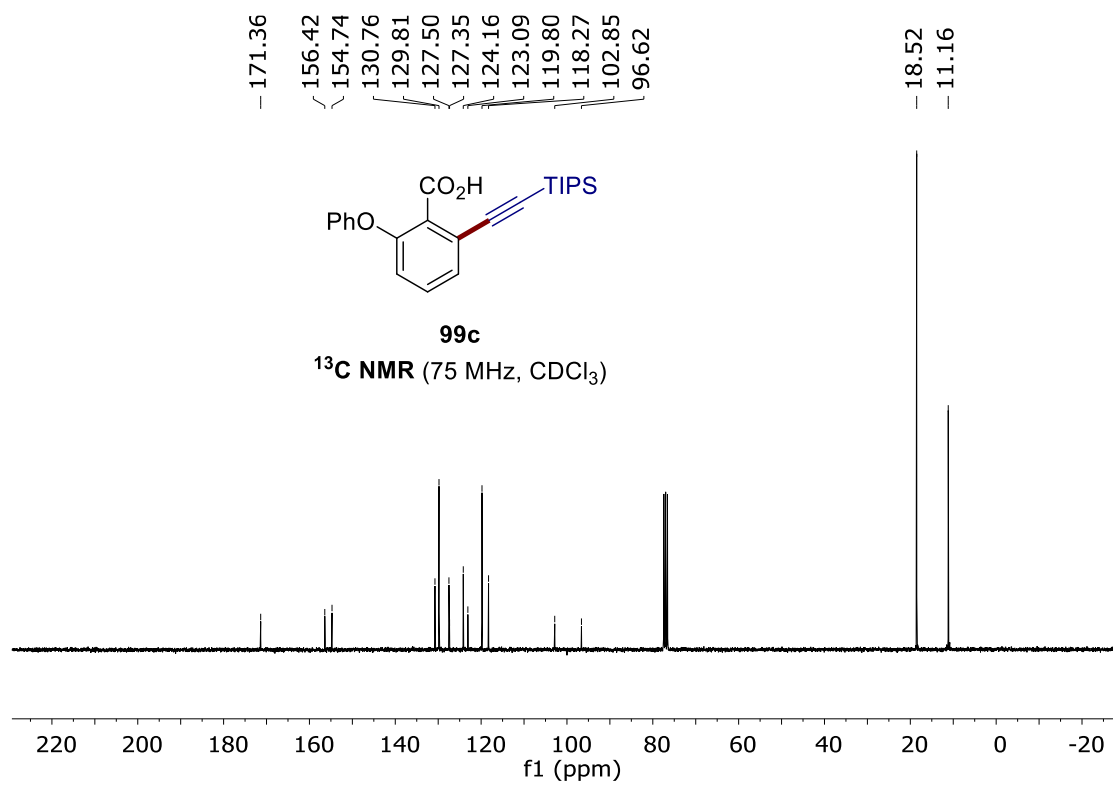
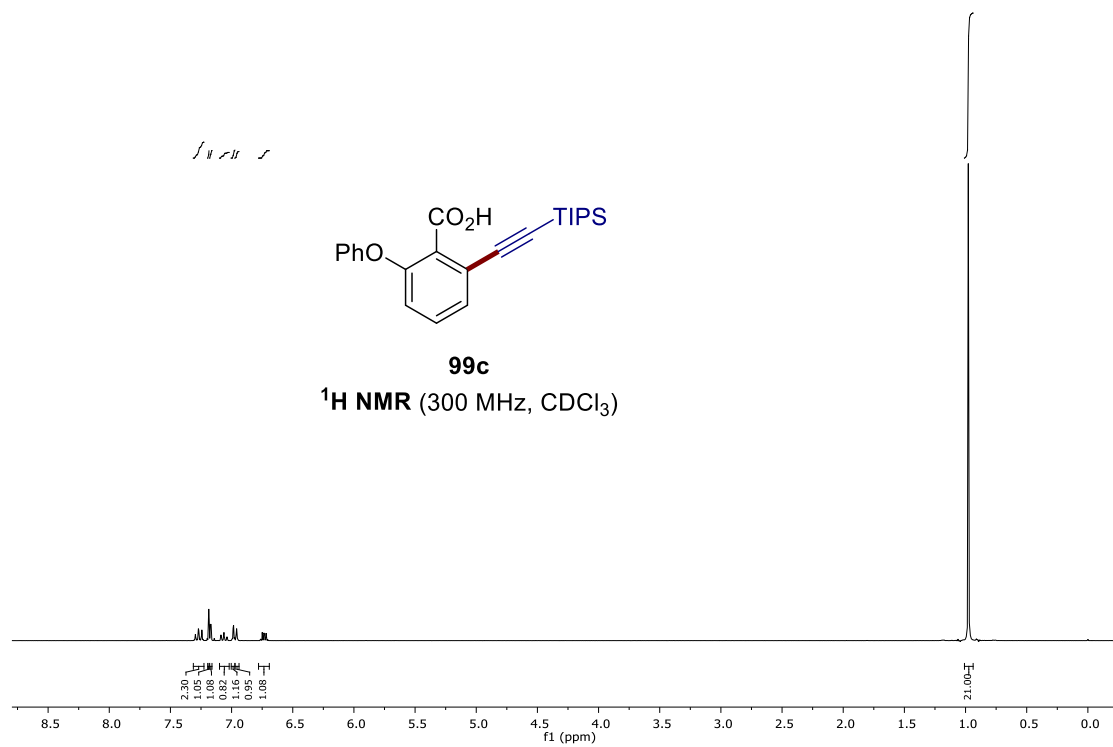
## 7. NMR Spectra

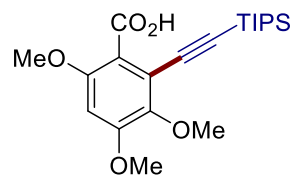
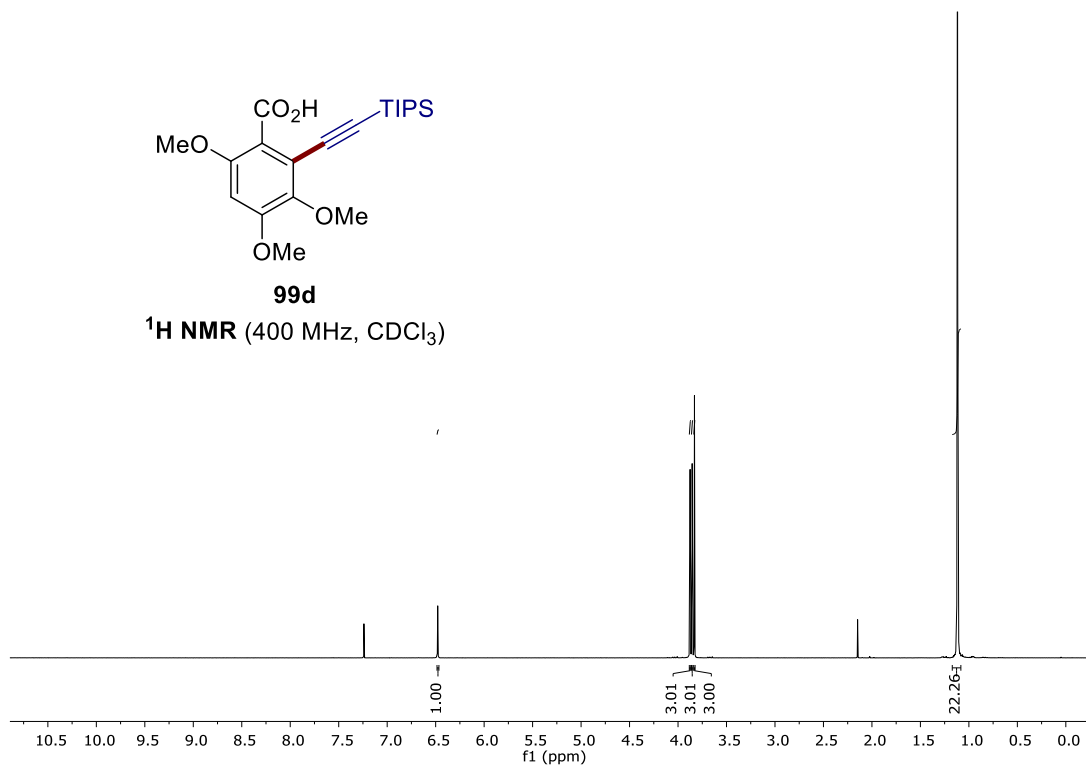
### 7.1 Ruthenium-Catalyzed *ortho*-C–H Alkynylation



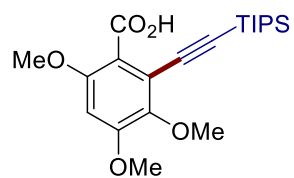
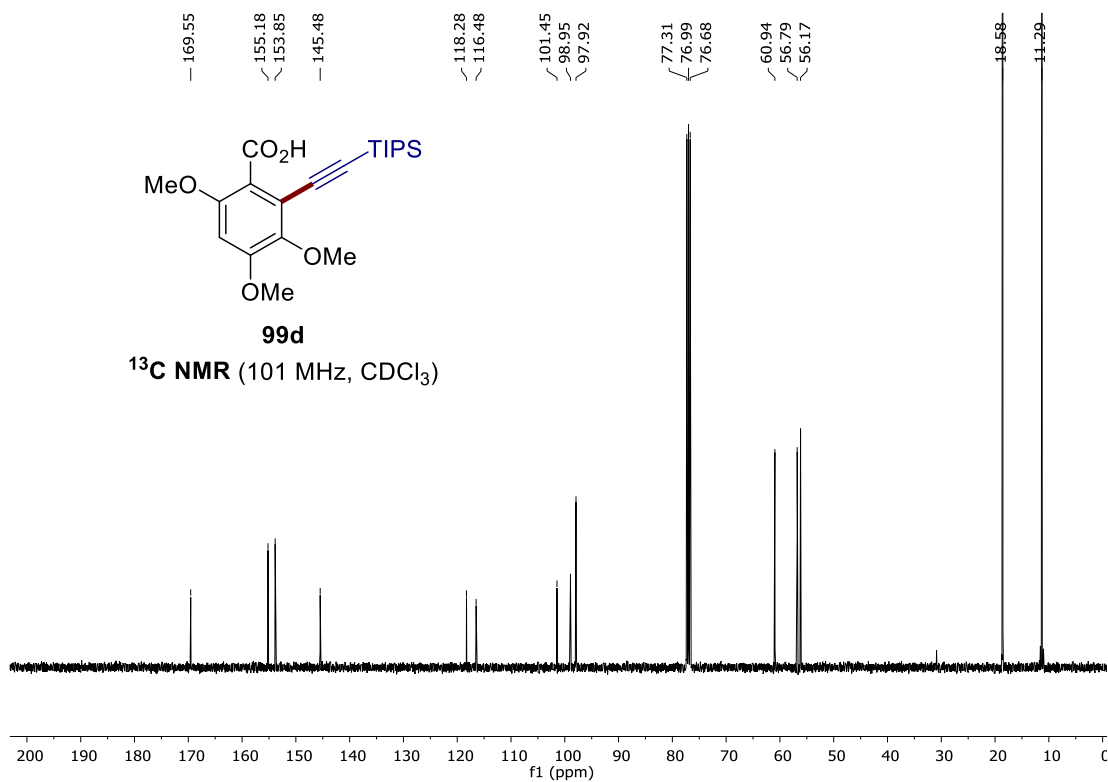


# 7. NMR Spectra

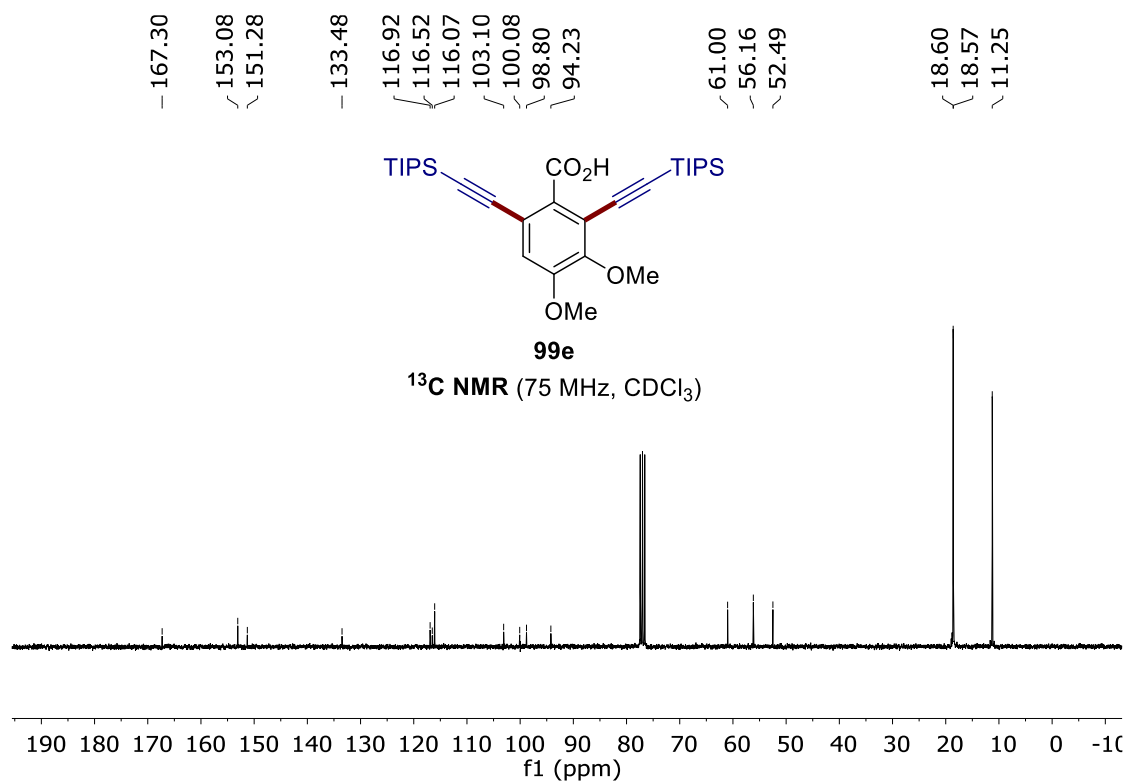
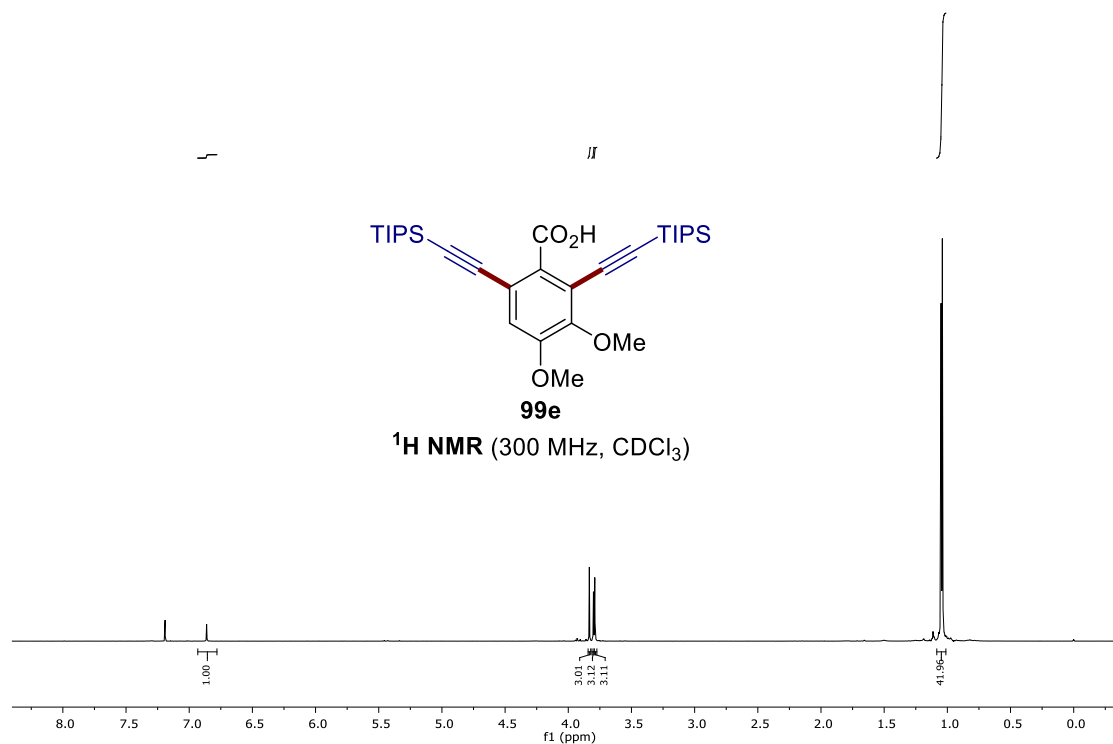


**99d**<sup>1</sup>H NMR (400 MHz, CDCl<sub>3</sub>)

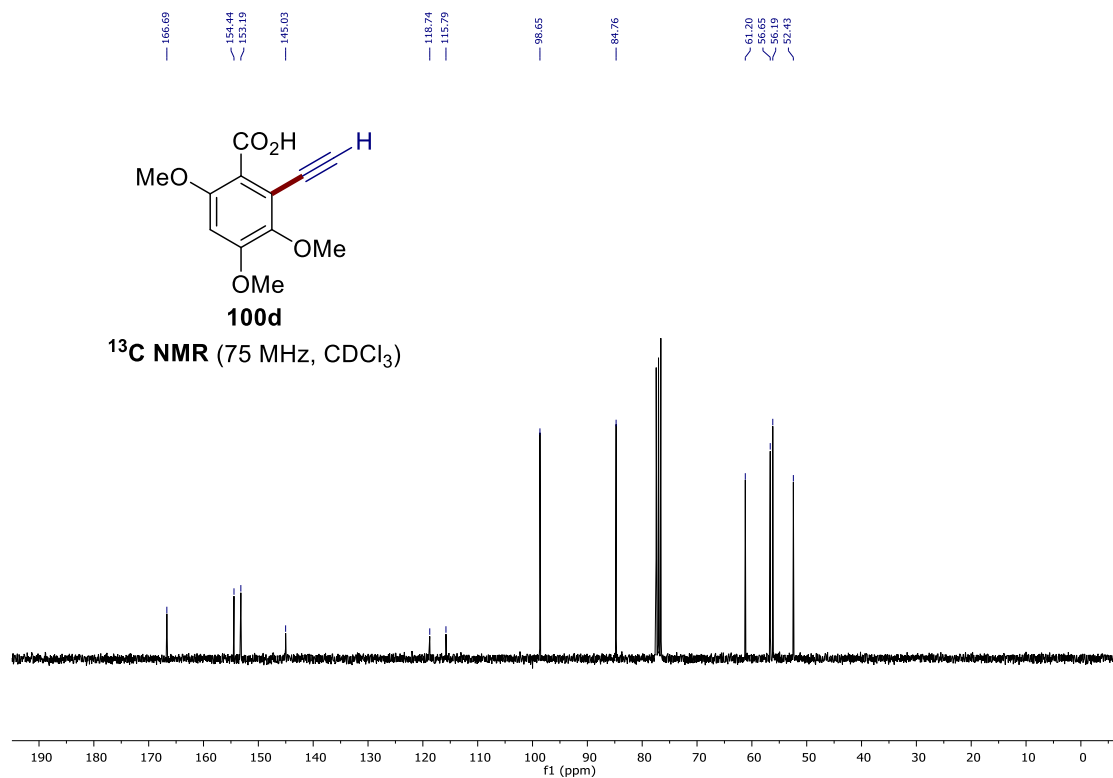
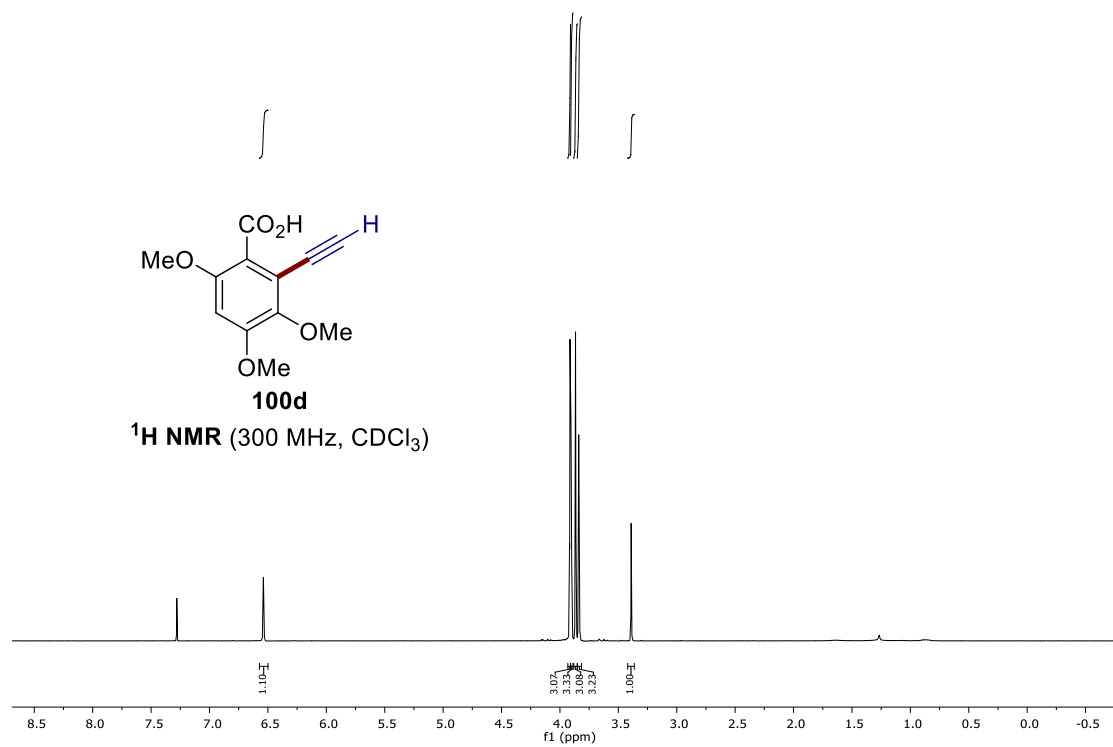
169.55  
155.18  
153.85  
145.48  
118.28  
116.48  
101.45  
98.95  
97.92  
77.31  
76.99  
76.68  
60.94  
56.79  
56.17

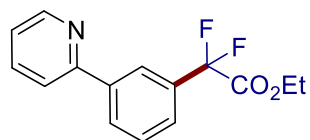
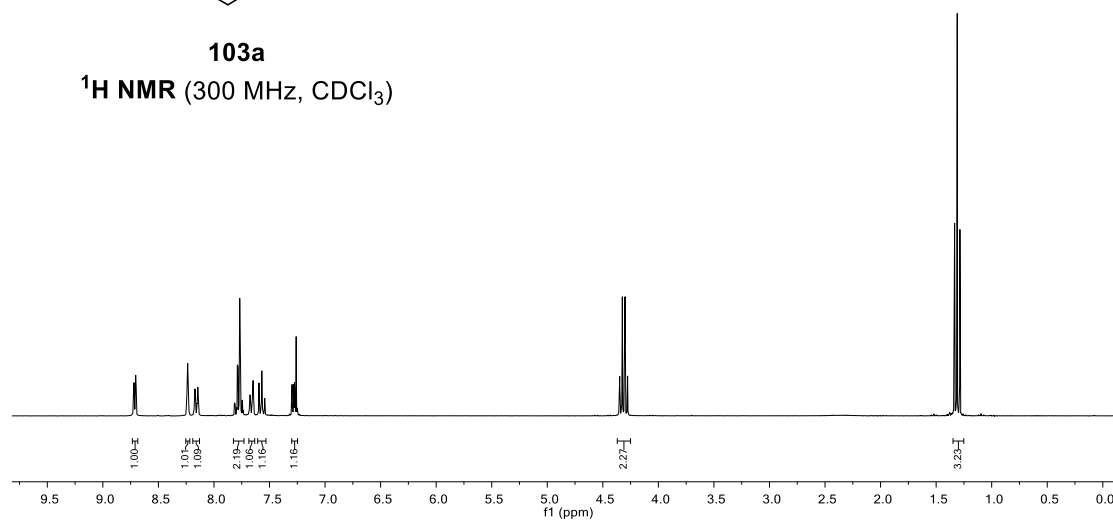
**99d**<sup>13</sup>C NMR (101 MHz, CDCl<sub>3</sub>)

7. NMR Spectra





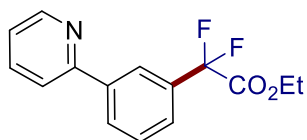
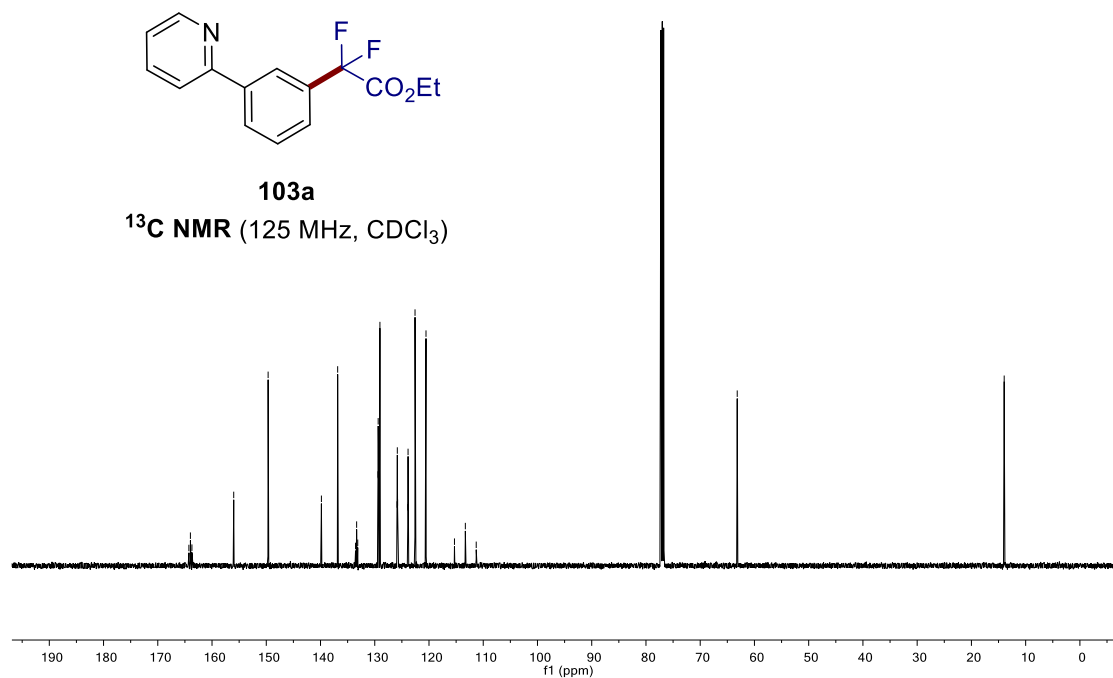


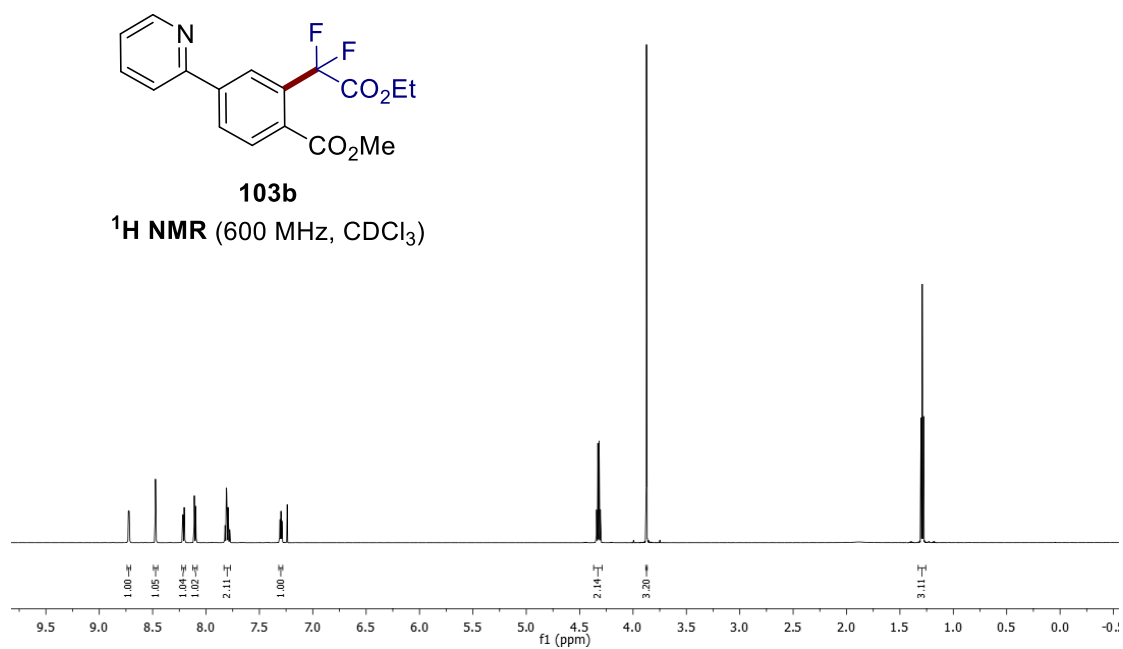
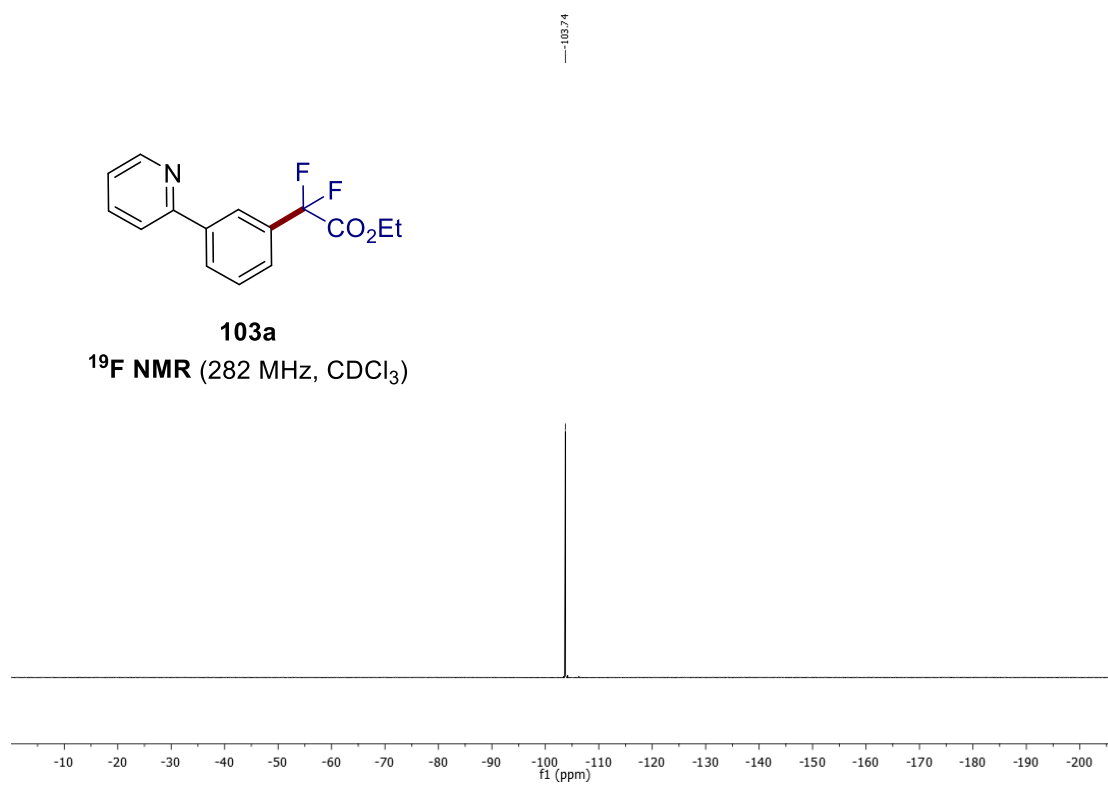
7.2 Ruthenium-Catalyzed *meta*-C–H Mono- and Difluoromethylation**103a** $^1\text{H NMR}$  (300 MHz,  $\text{CDCl}_3$ )

164.26  
163.99  
163.70  
156.00  
149.86  
138.84  
138.84  
133.54  
133.34  
133.14  
129.37  
129.35  
128.05  
122.89  
122.89  
122.70  
122.70  
122.86  
122.81  
122.81  
120.55  
115.30  
113.30  
111.29

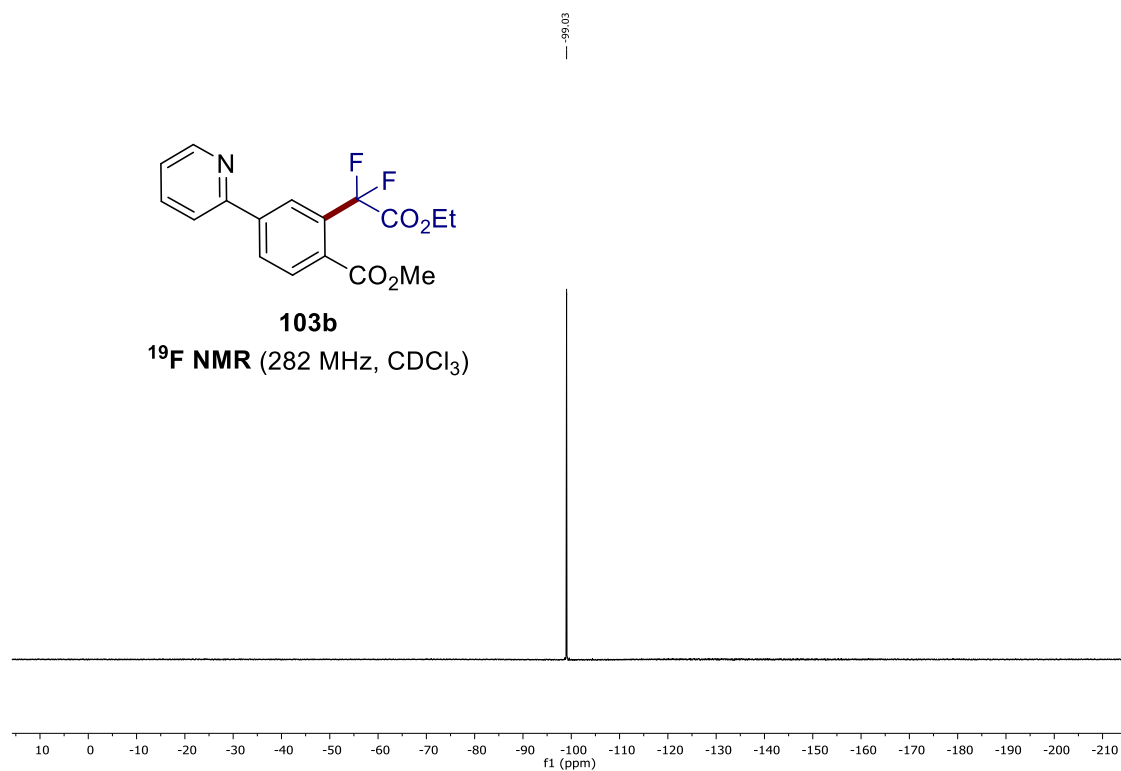
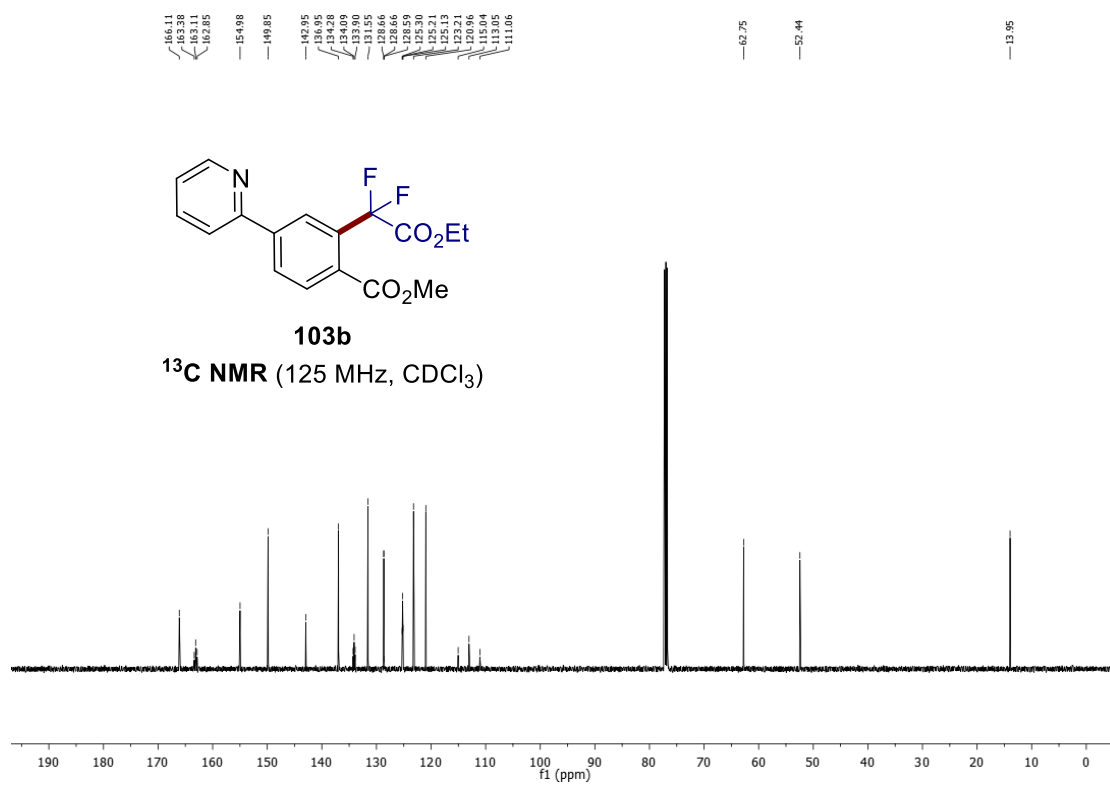
63.17

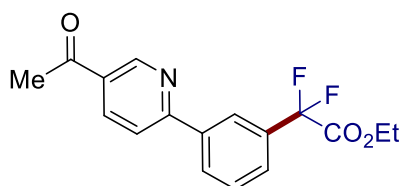
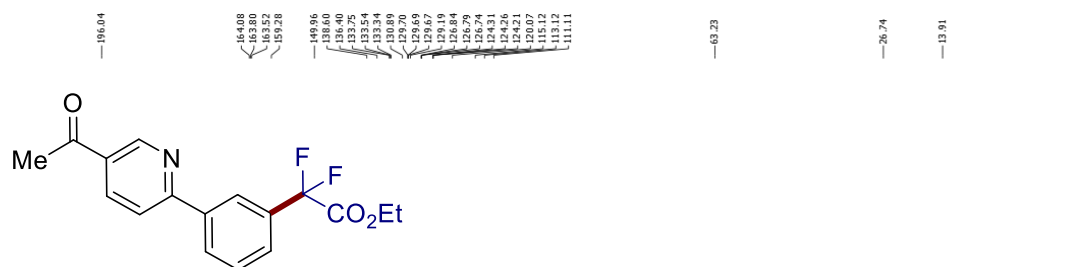
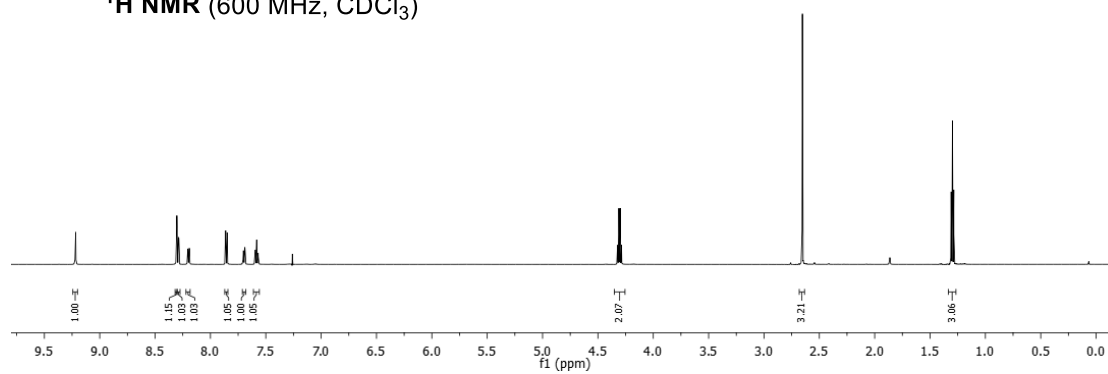
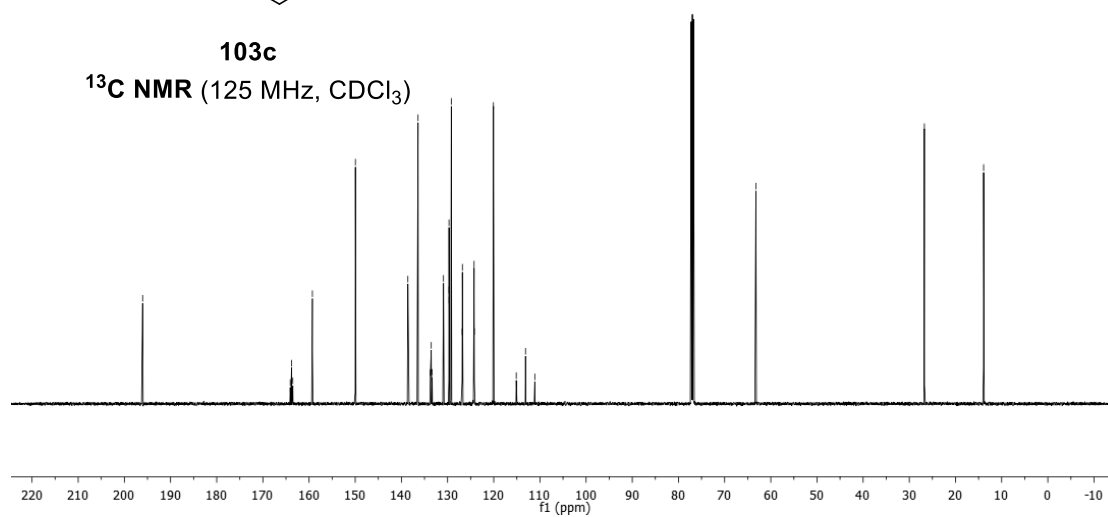
13.96

**103a** $^{13}\text{C NMR}$  (125 MHz,  $\text{CDCl}_3$ )

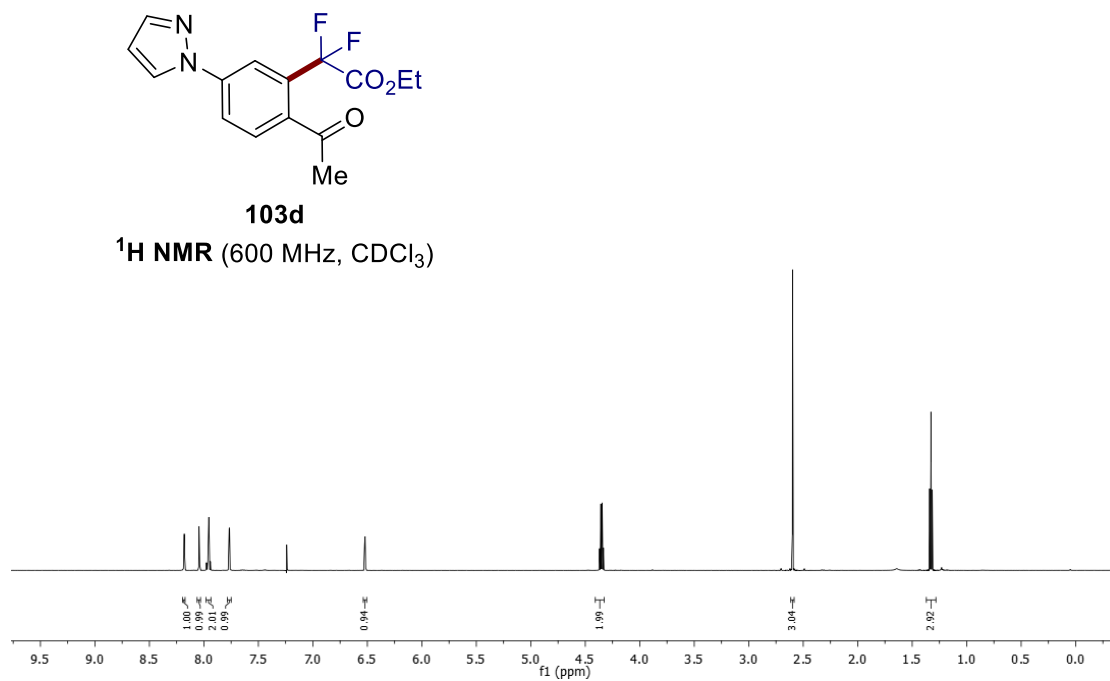
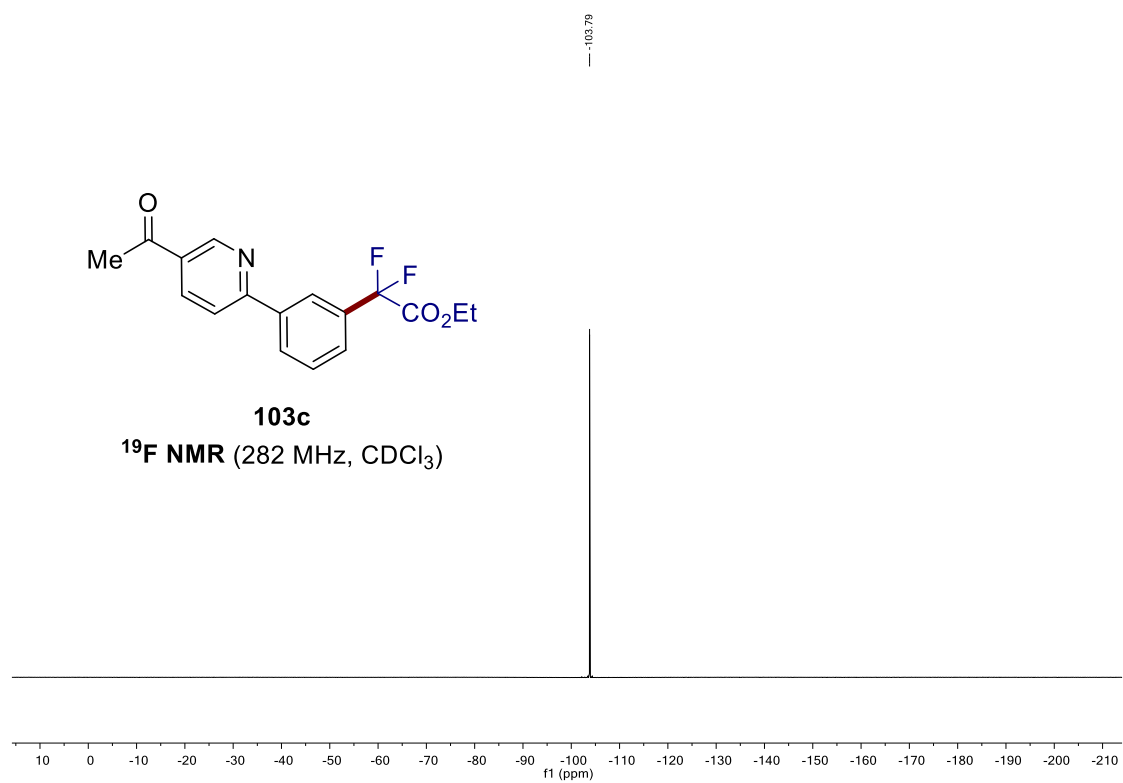


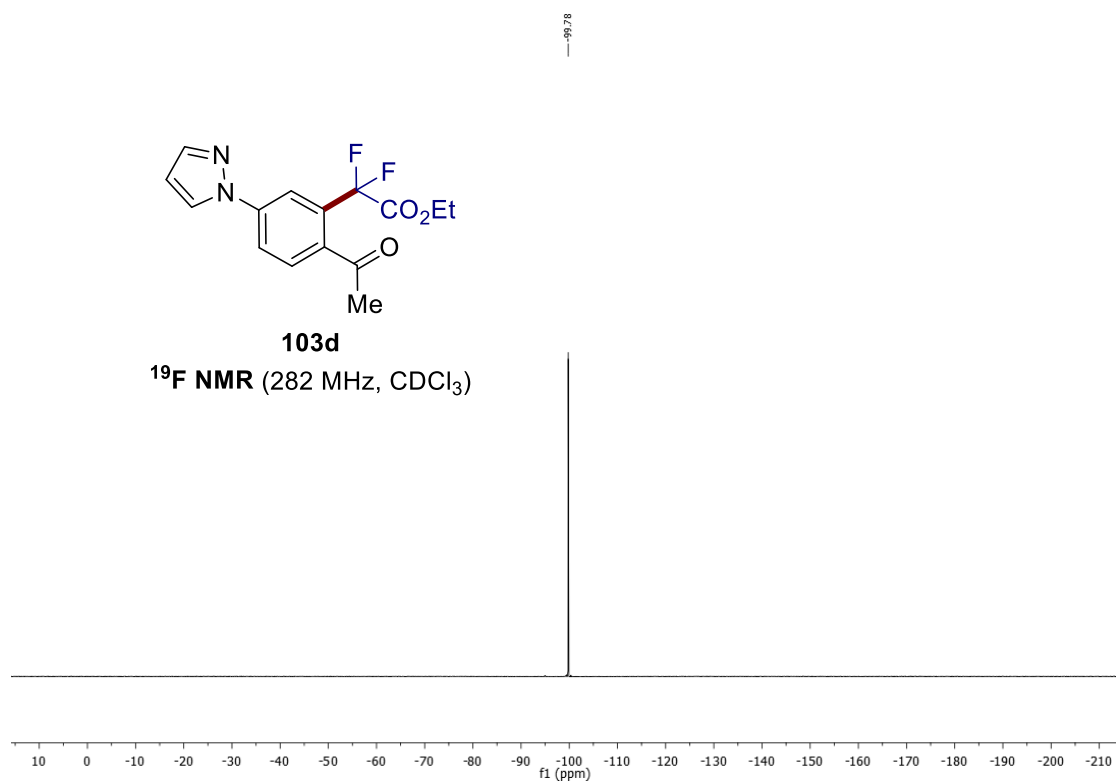
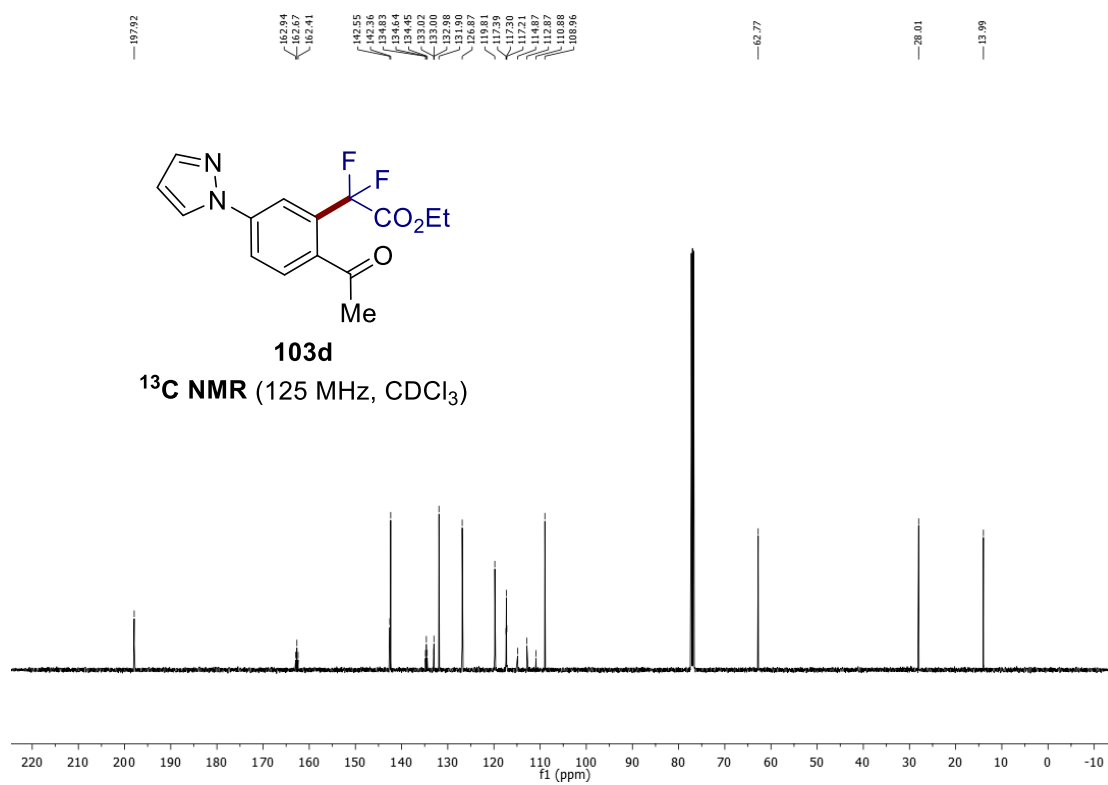
## 7. NMR Spectra



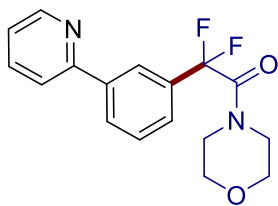
**103c** $^1\text{H NMR}$  (600 MHz,  $\text{CDCl}_3$ )**103c** $^{13}\text{C NMR}$  (125 MHz,  $\text{CDCl}_3$ )

## 7. NMR Spectra



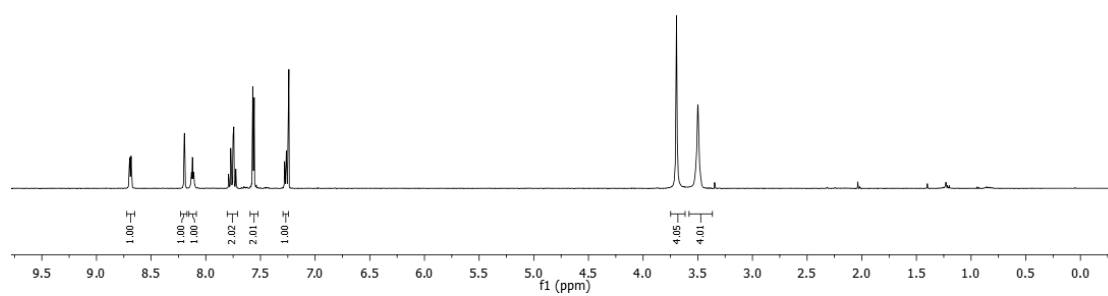


## 7. NMR Spectra

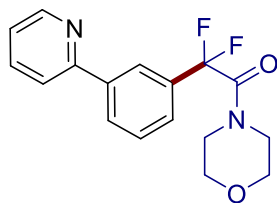


**103e**

$^1\text{H NMR}$  (400 MHz,  $\text{CDCl}_3$ )

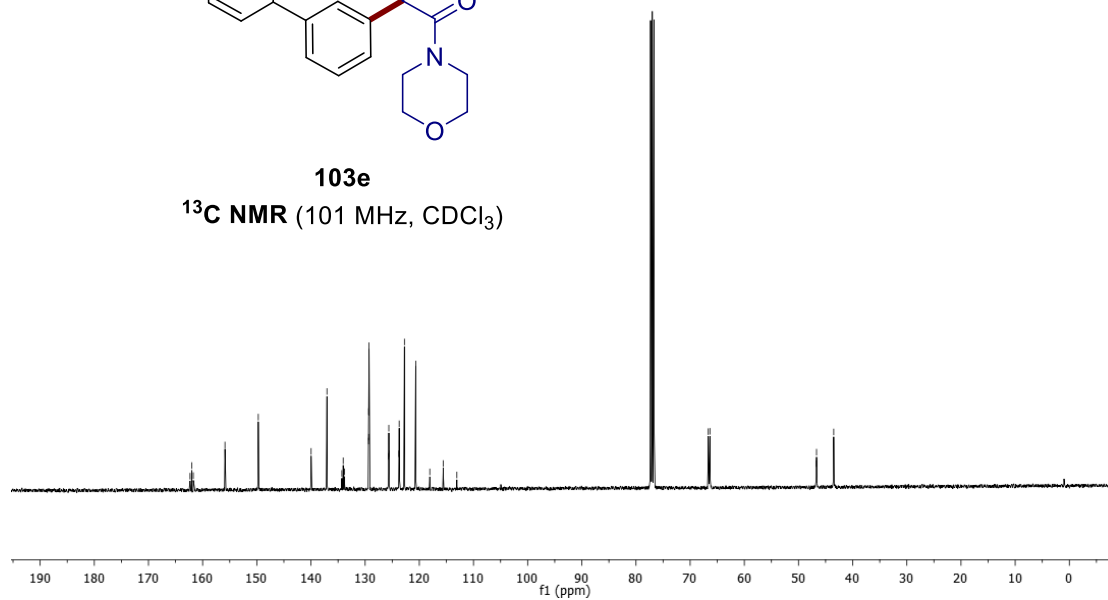


162.32, 162.02, 161.72, 155.87, 149.73, 139.97, 137.05, 136.46, 134.05, 133.81, 129.37, 129.35, 129.28, 125.28, 125.69, 125.63, 125.57, 123.72, 123.72, 123.66, 122.75, 120.67, 118.67, 118.57, 113.07, 66.66, 66.35, 46.72, 46.67, 46.50.

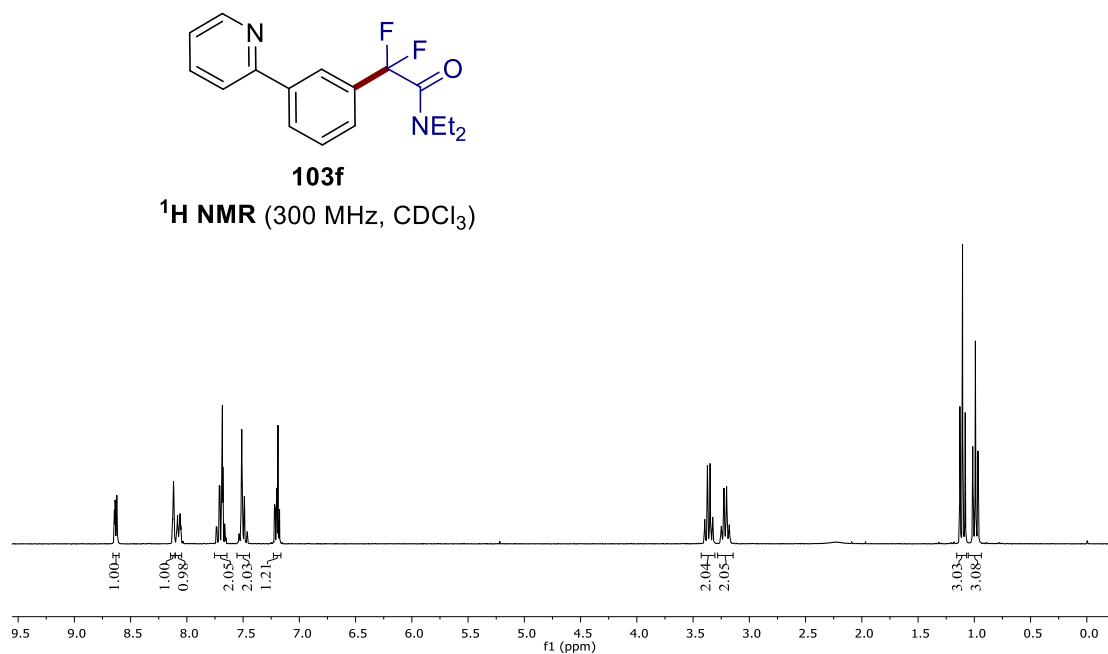
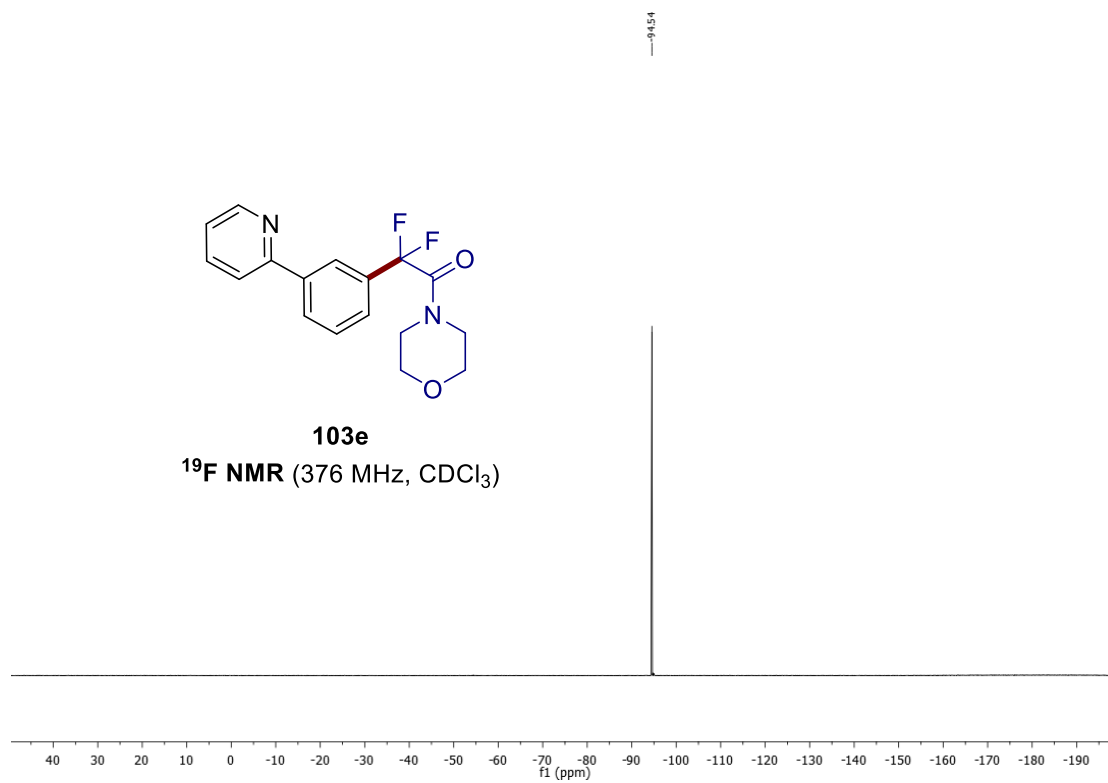


**103e**

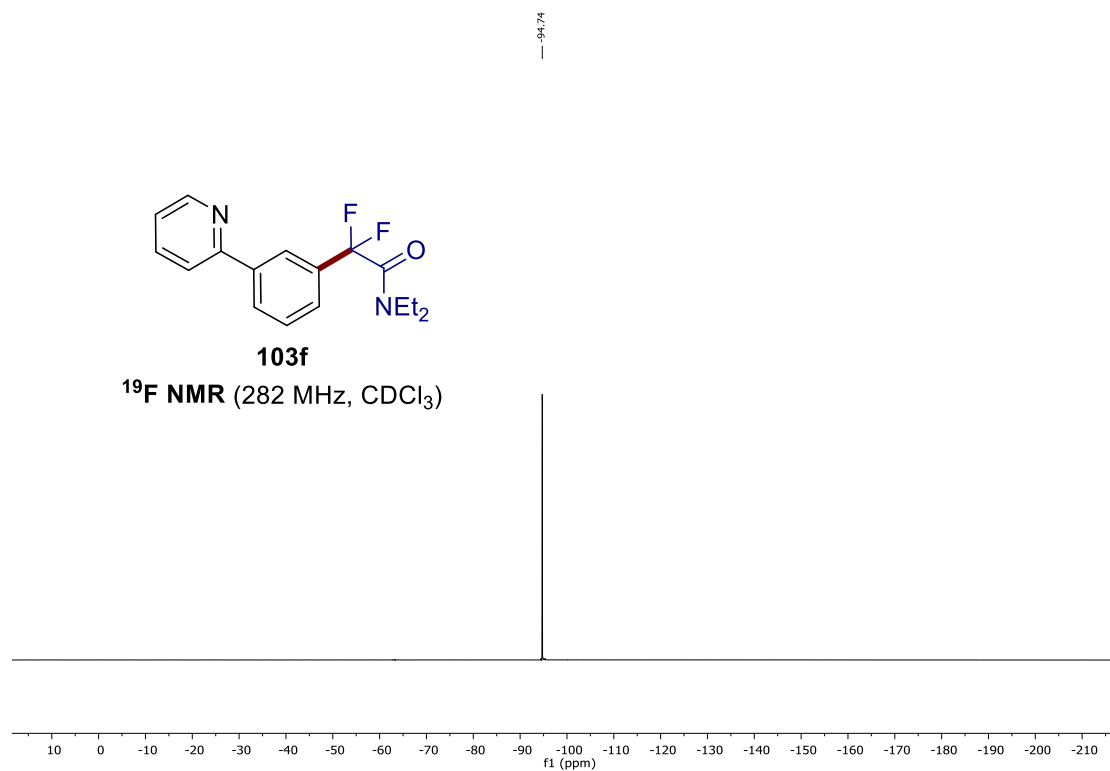
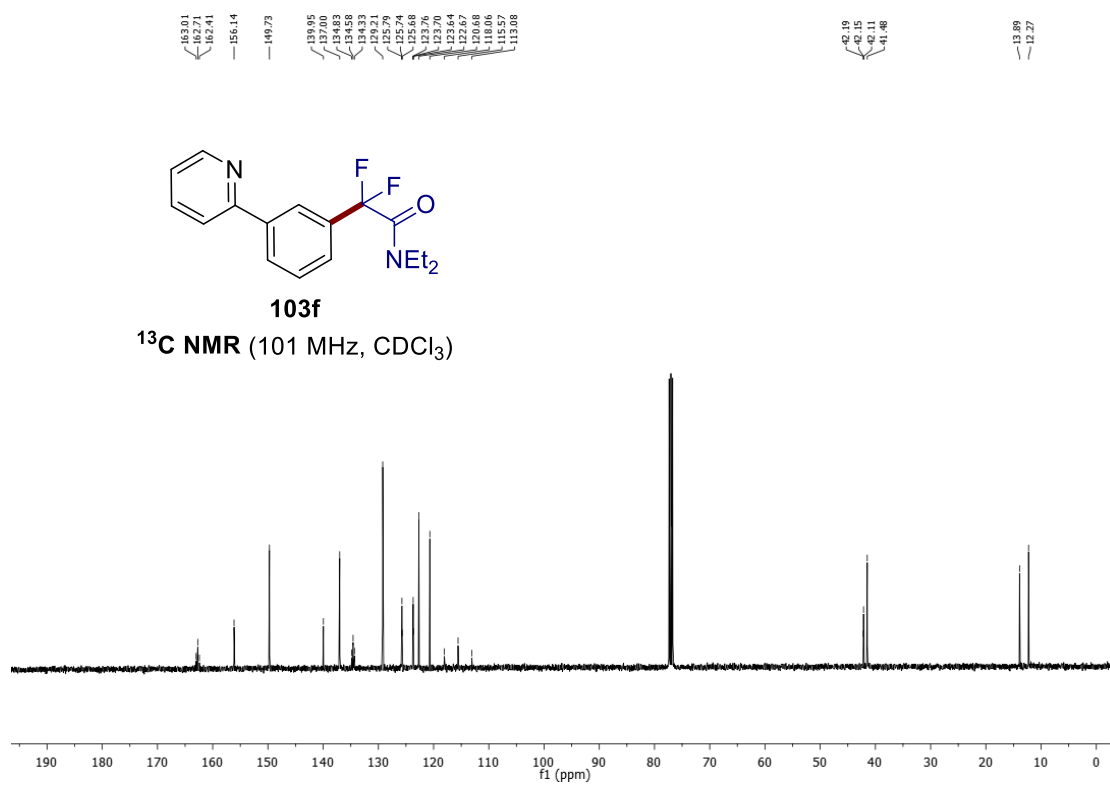
$^{13}\text{C NMR}$  (101 MHz,  $\text{CDCl}_3$ )

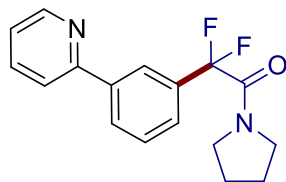
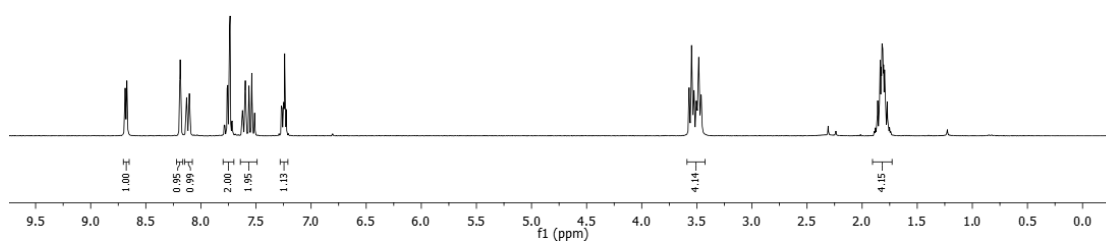






## 7. NMR Spectra

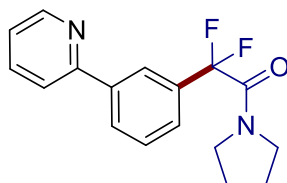
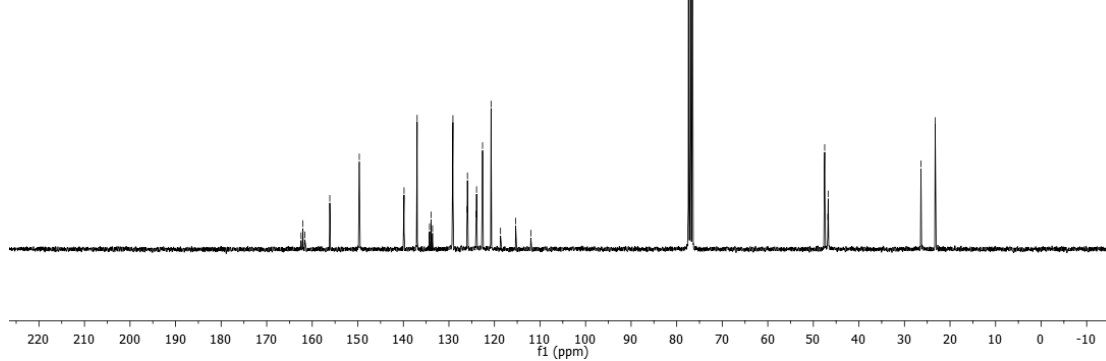


**103g****<sup>1</sup>H NMR (300 MHz, CDCl<sub>3</sub>)**

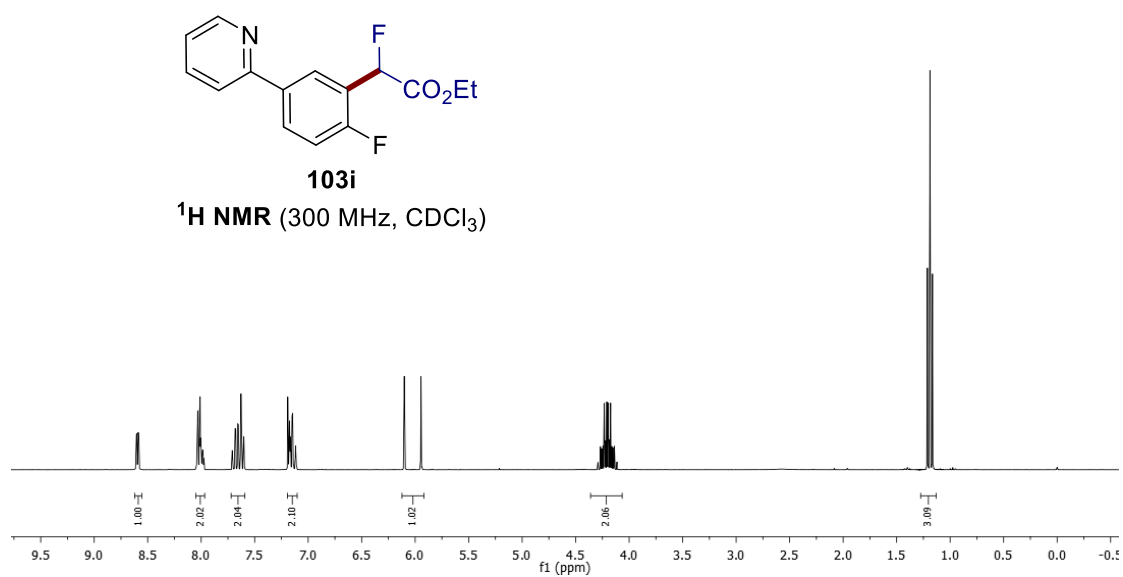
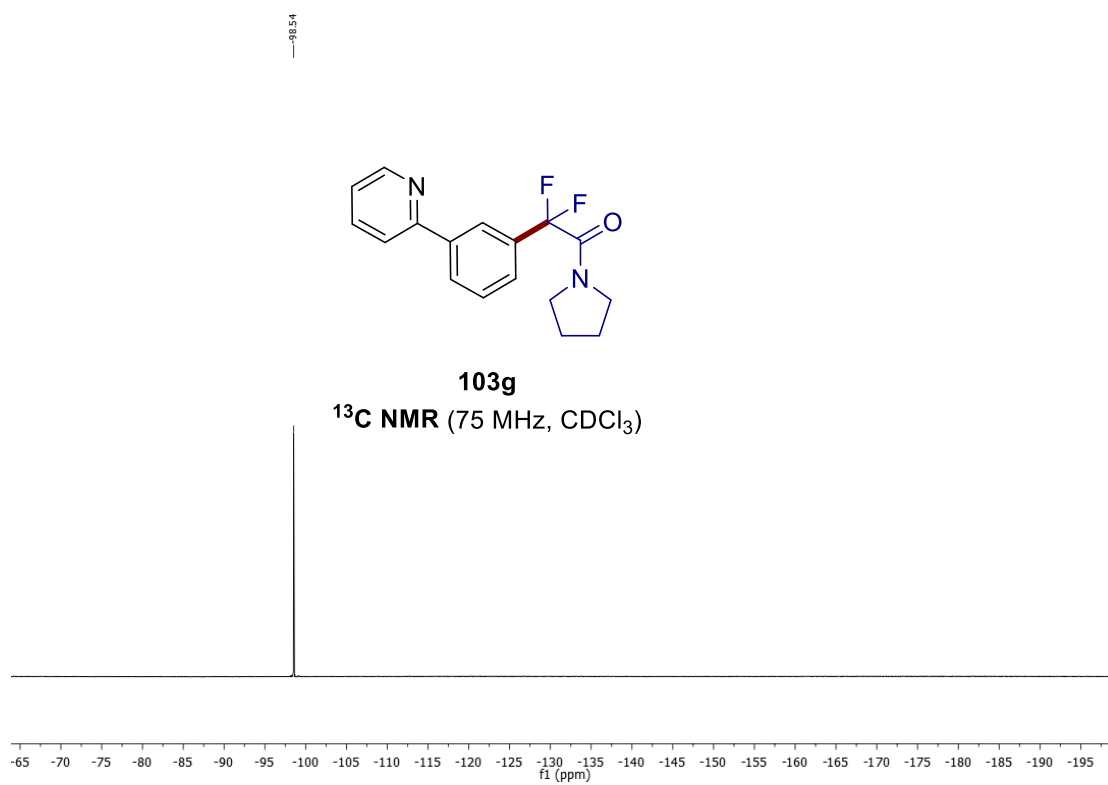
152.46  
152.46  
161.64  
156.15  
149.67  
139.86  
136.97  
134.25  
133.92  
133.92  
133.96  
129.21  
129.21  
129.12  
129.12  
129.01  
125.91  
125.85  
125.85  
124.01  
123.93  
123.85  
123.85  
120.75  
118.67  
115.35  
112.02

47.51  
46.32  
46.19

26.38  
23.25

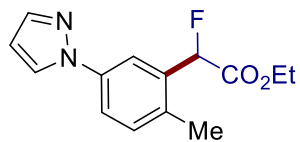
**103g****<sup>13</sup>C NMR (75 MHz, CDCl<sub>3</sub>)**

## 7. NMR Spectra



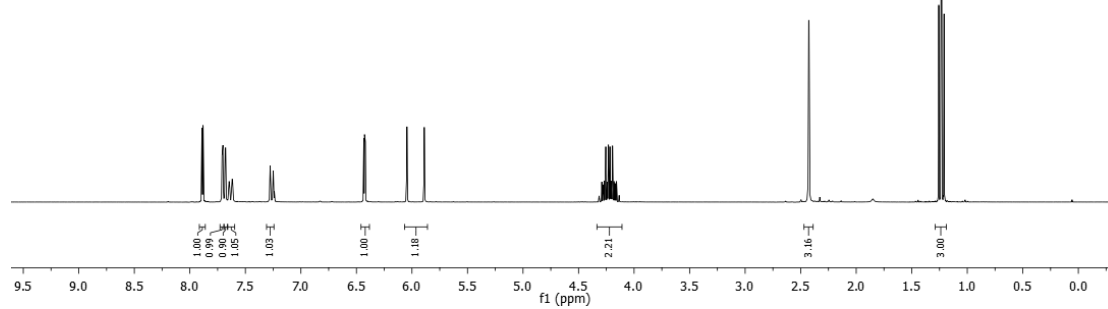


## 7. NMR Spectra

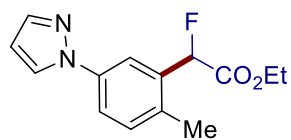


**103j**

<sup>1</sup>H NMR (300 MHz, CDCl<sub>3</sub>)

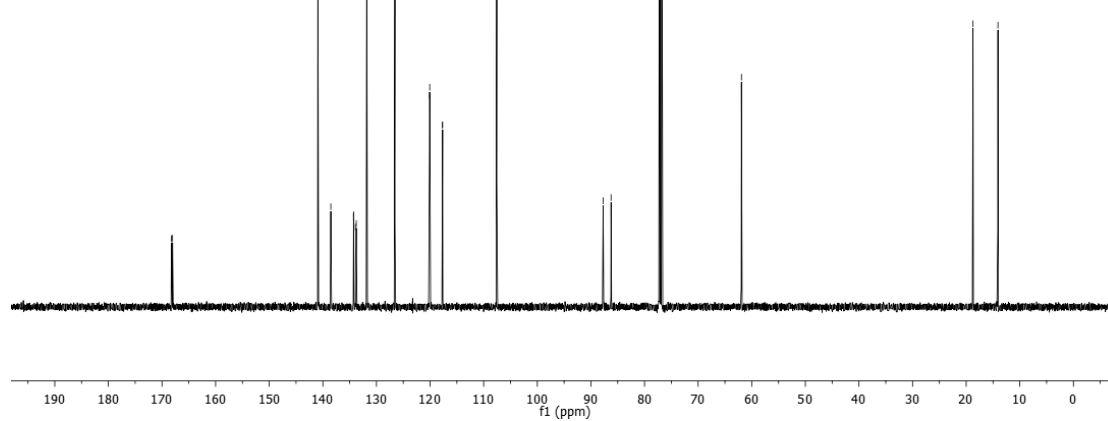


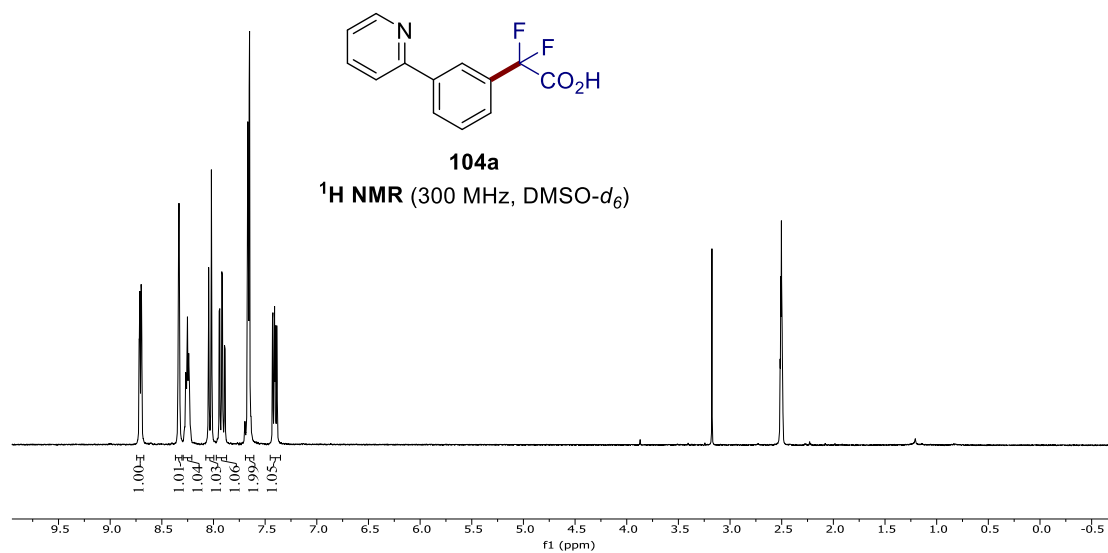
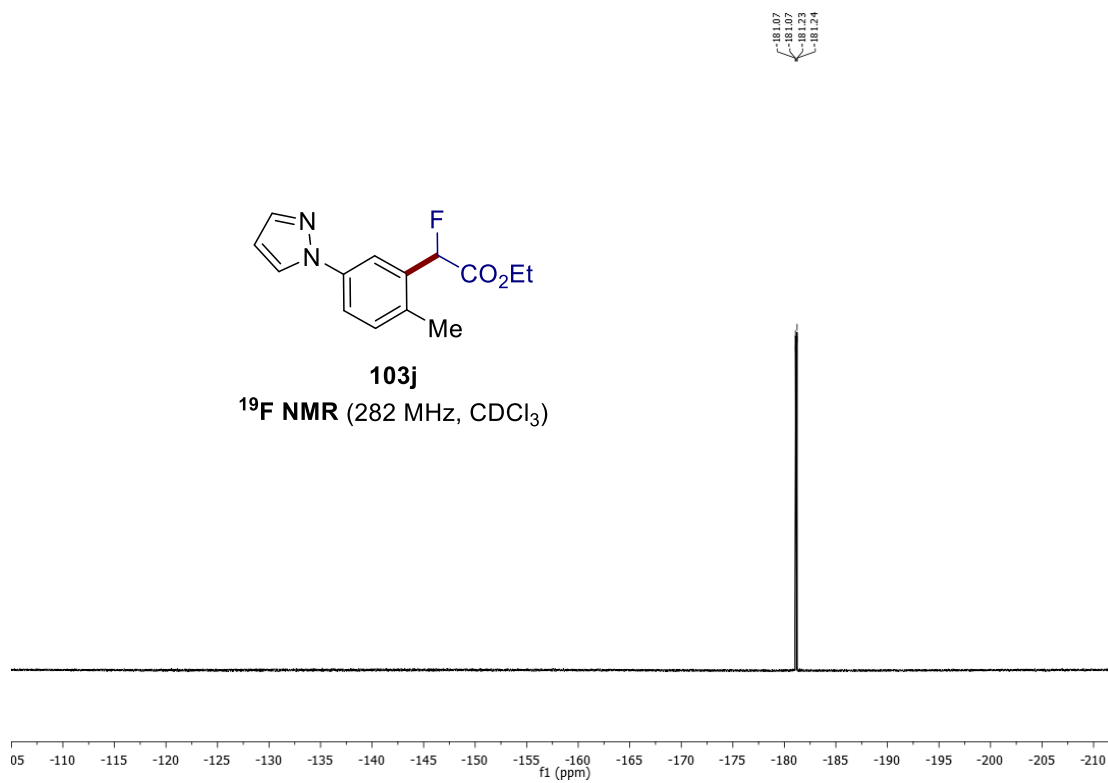
Chemical shift values (ppm): 168.25, 168.03, 140.93, 139.51, 138.90, 138.40, 133.92, 133.77, 131.81, 126.56, 120.08, 120.07, 117.72, 117.66, 107.56, 87.71, 86.24, 61.92, 18.73, 14.08.



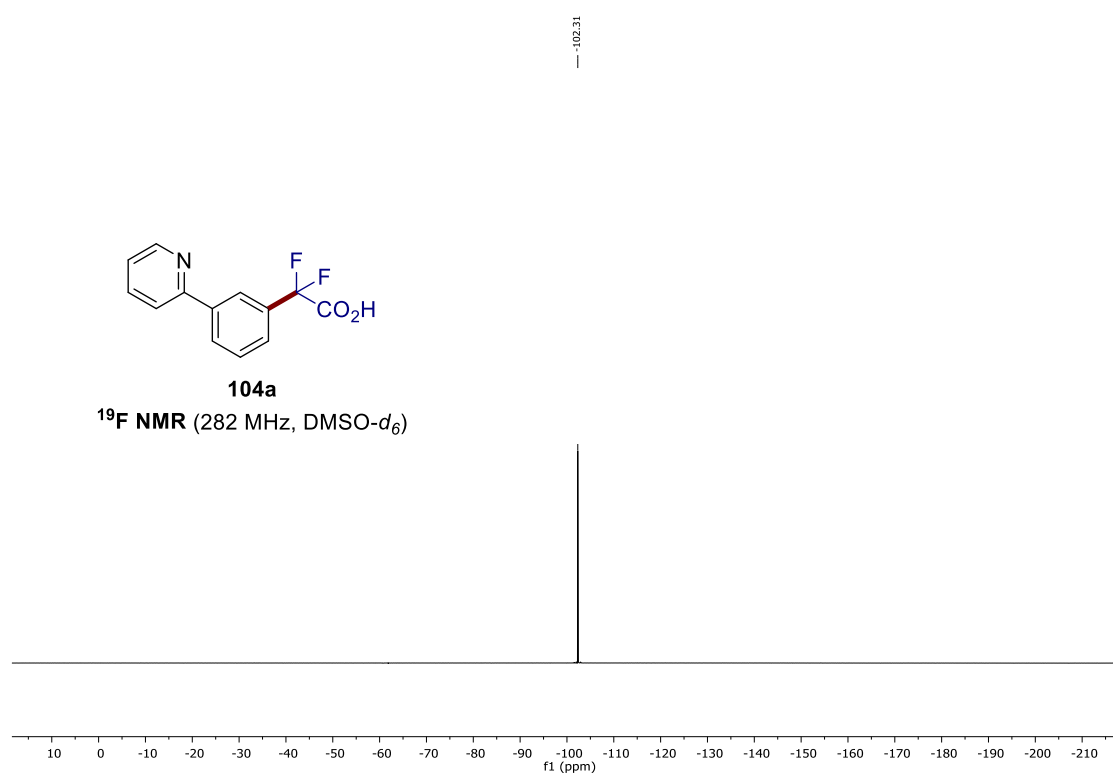
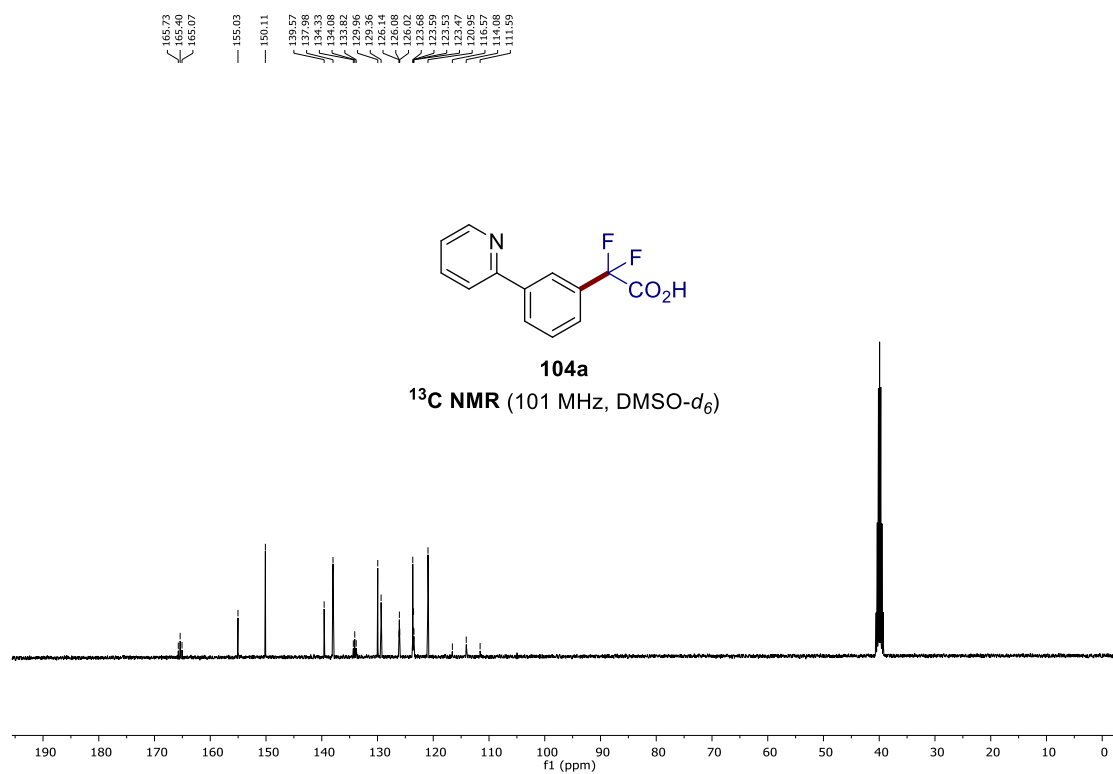
**103j**

<sup>13</sup>C NMR (125 MHz, CDCl<sub>3</sub>)

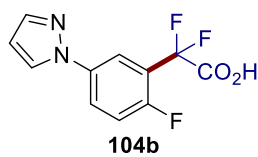




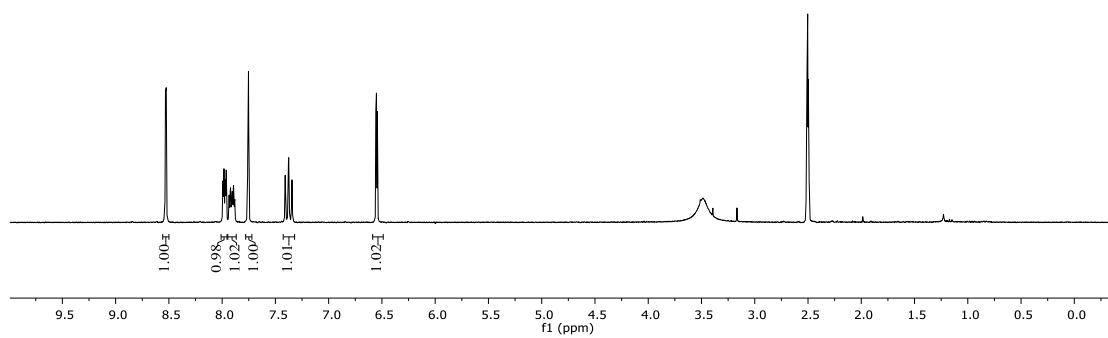
## 7. NMR Spectra



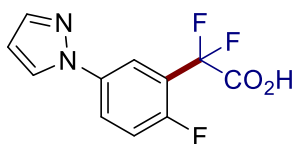




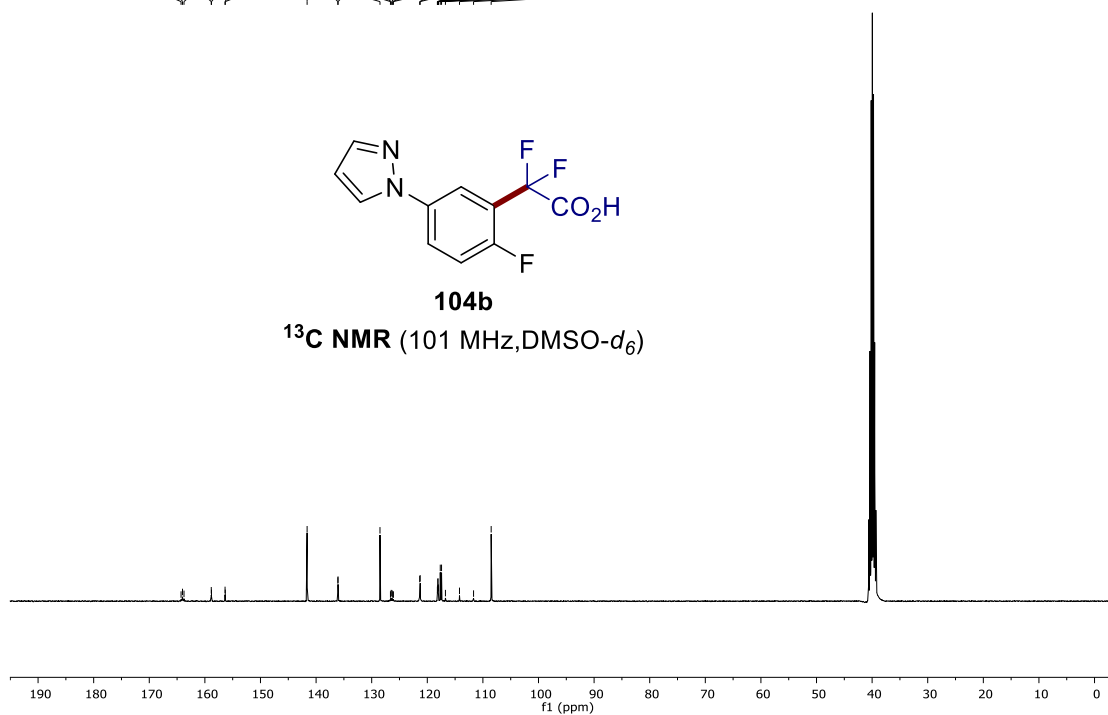
$^1\text{H NMR}$  (300 MHz,  $\text{DMSO-}d_6$ )



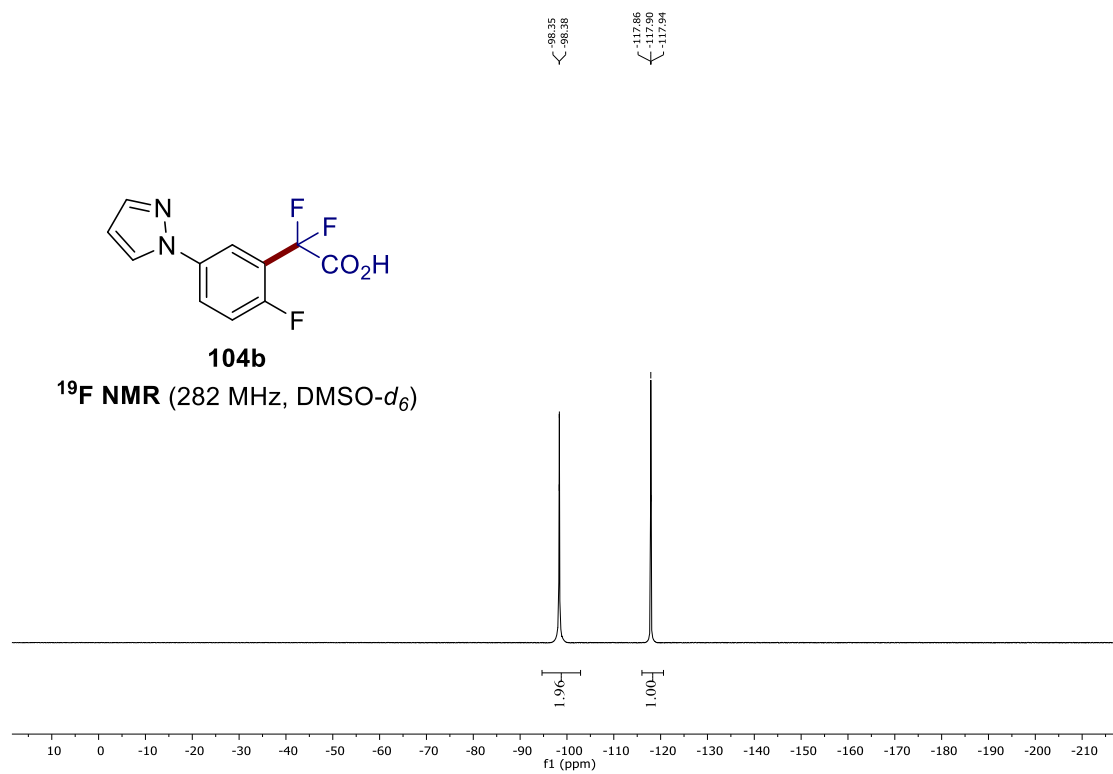
164.28  
164.02  
163.76  
159.85  
159.54  
158.37  
156.33  
141.61  
136.09  
135.85  
135.61  
126.62  
126.50  
126.36  
126.23  
126.09  
121.37  
121.28  
118.18  
118.15  
118.07  
118.07  
118.03  
118.00  
117.67  
116.74  
116.74  
114.21  
111.69  
108.51

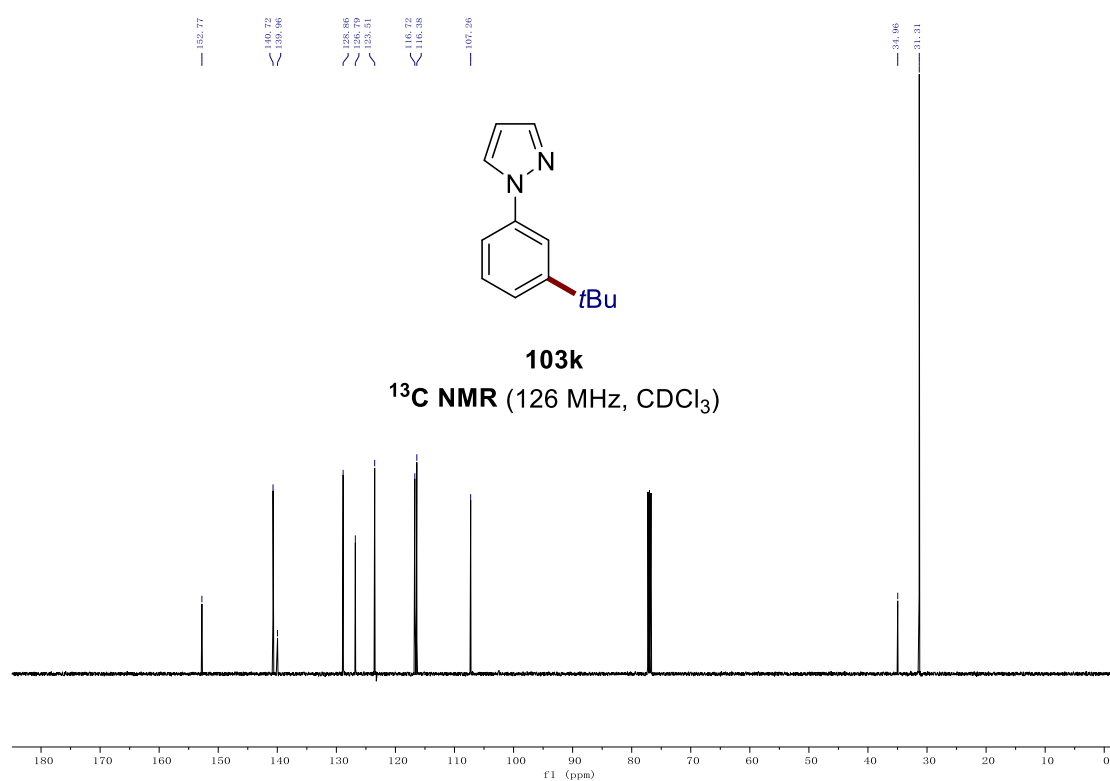
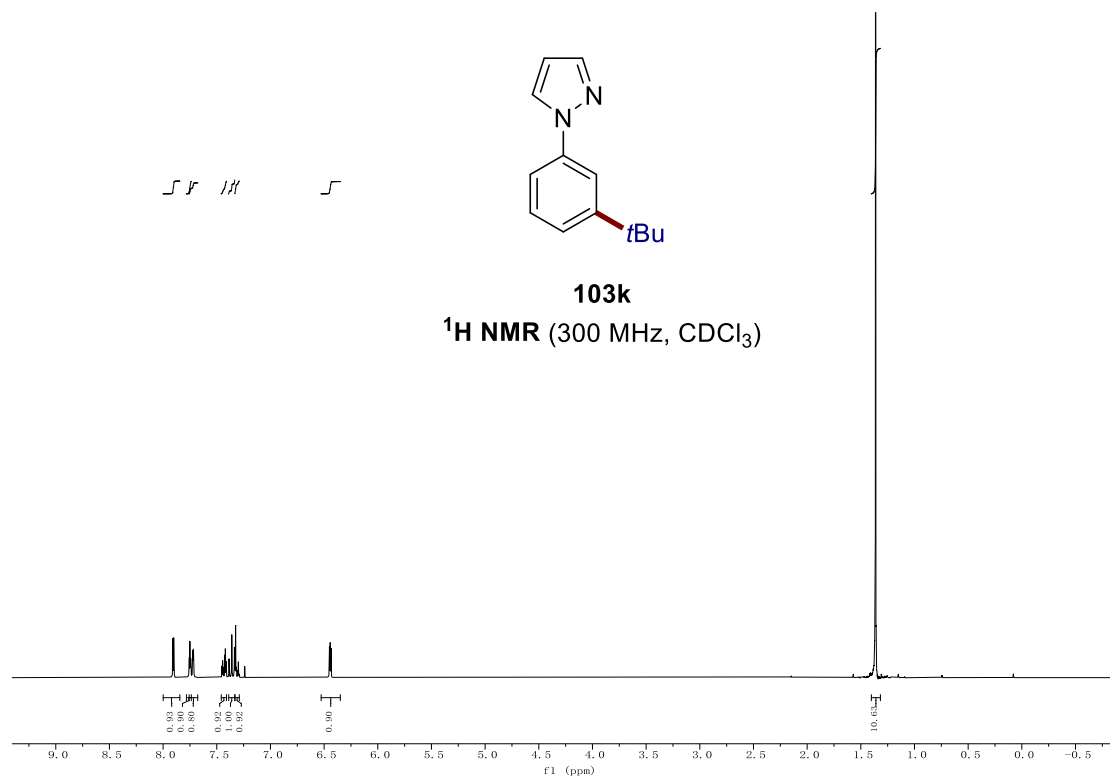


$^{13}\text{C NMR}$  (101 MHz,  $\text{DMSO-}d_6$ )

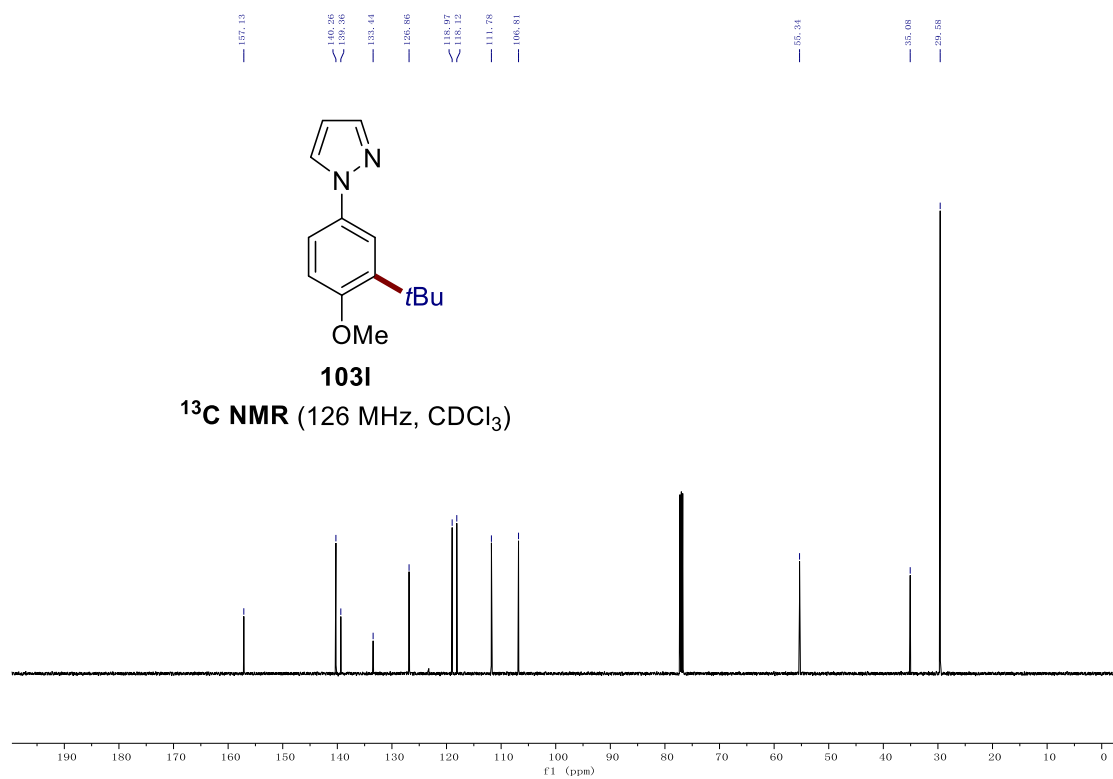
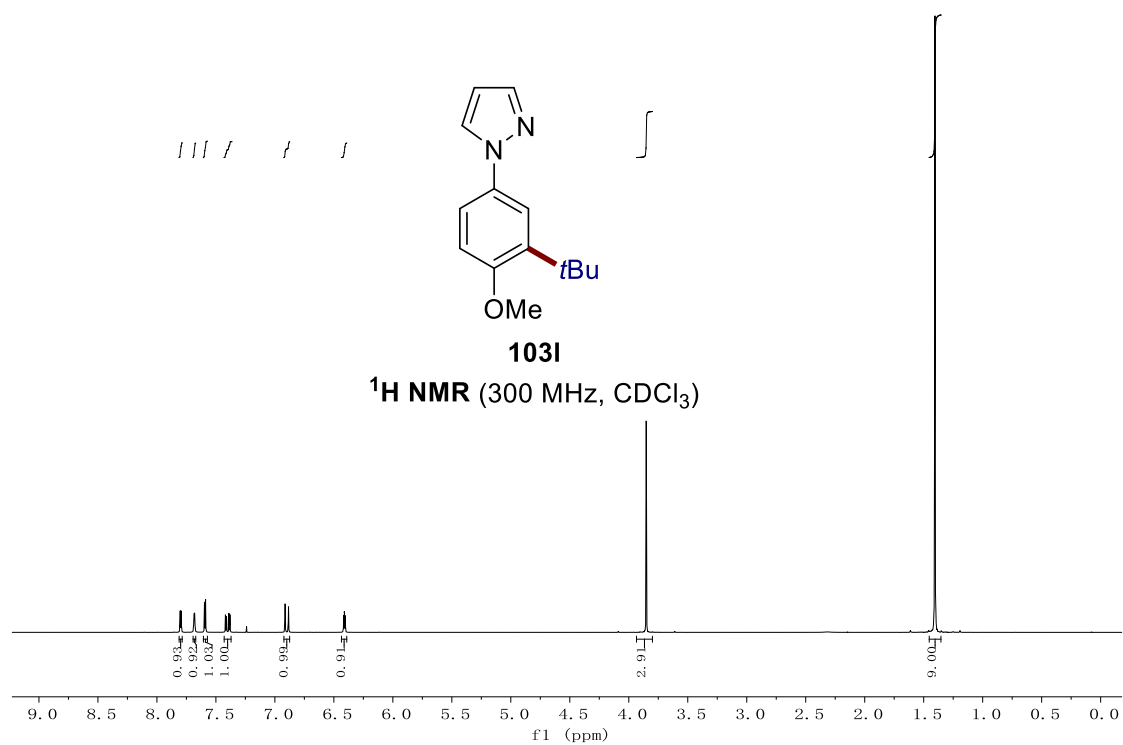


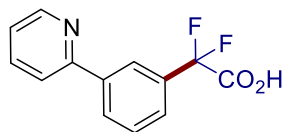
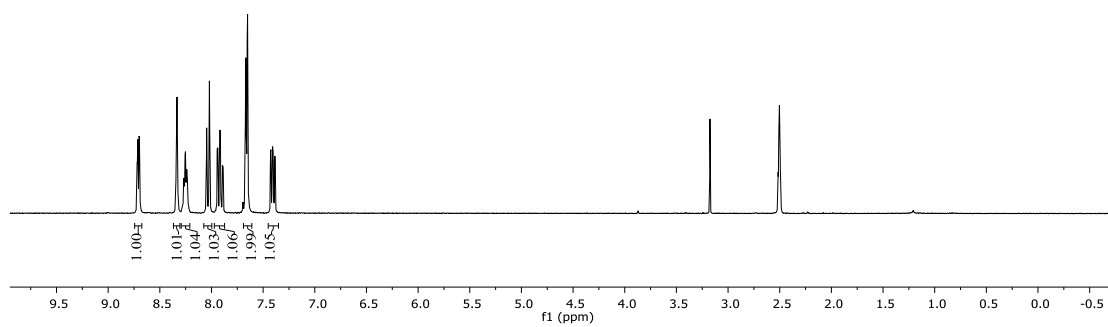
## 7. NMR Spectra



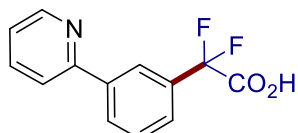
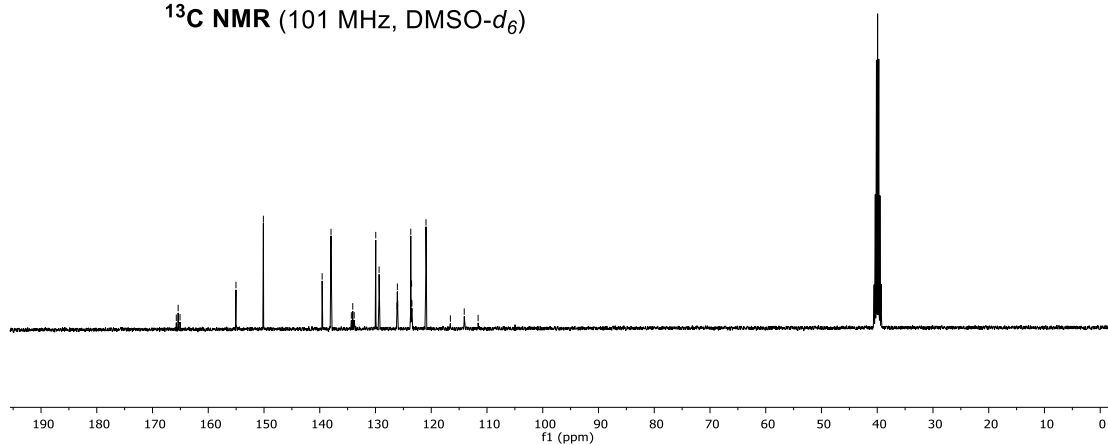
7.3 Ruthenium-Catalyzed *meta*-C–H Alkylation

## 7. NMR Spectra

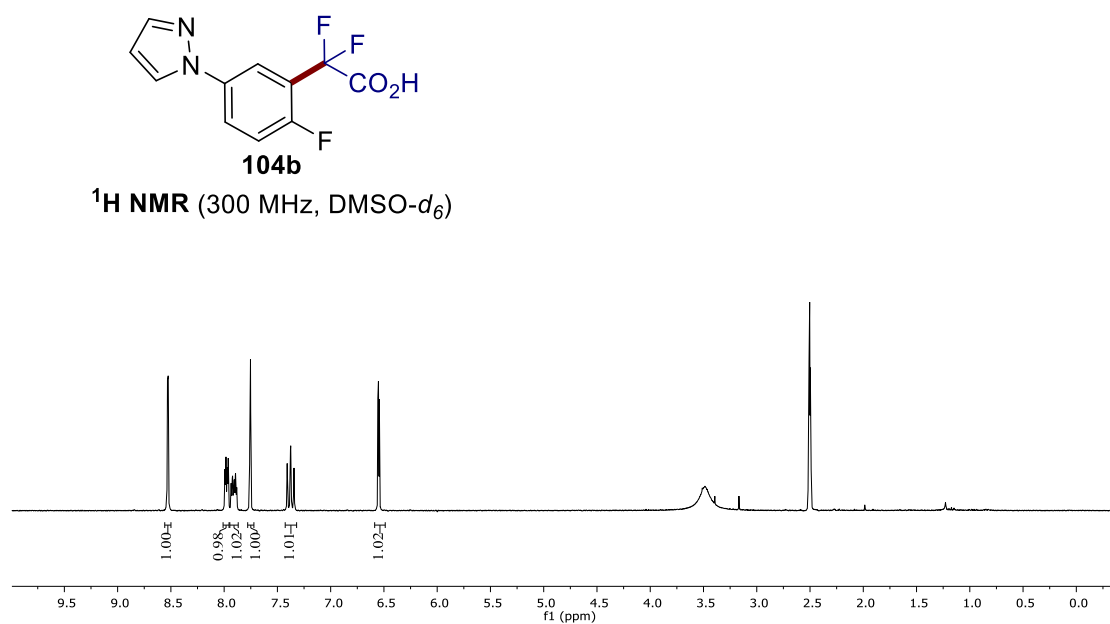
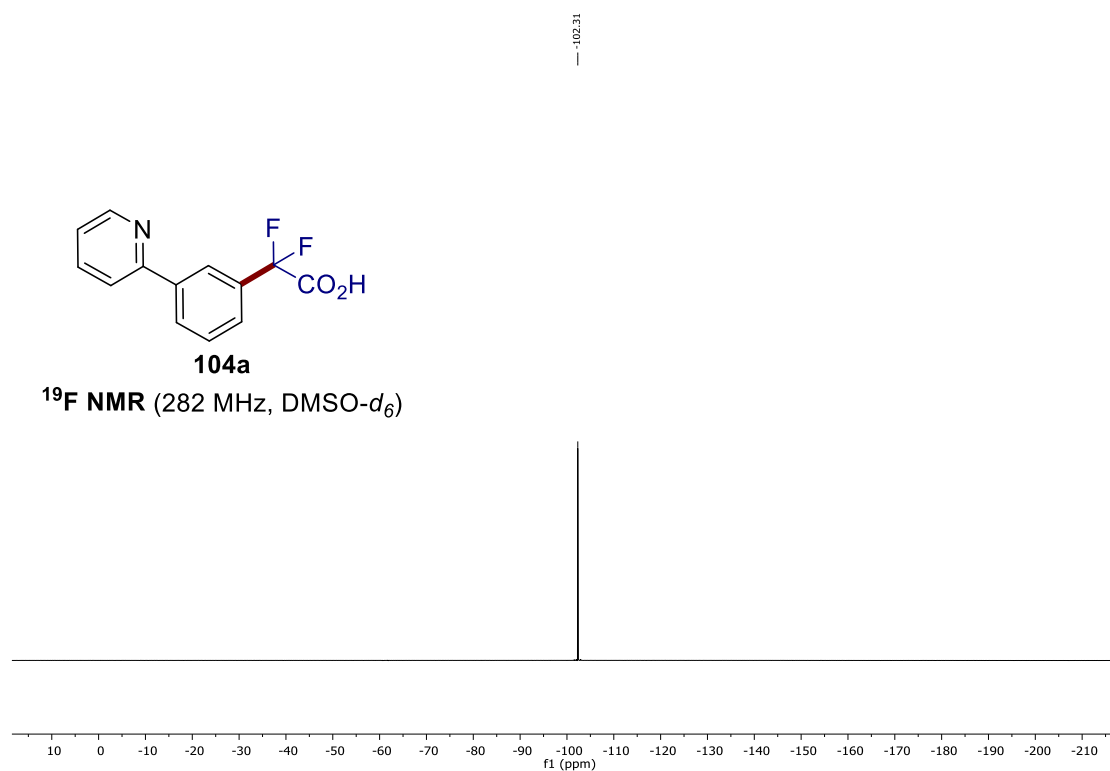


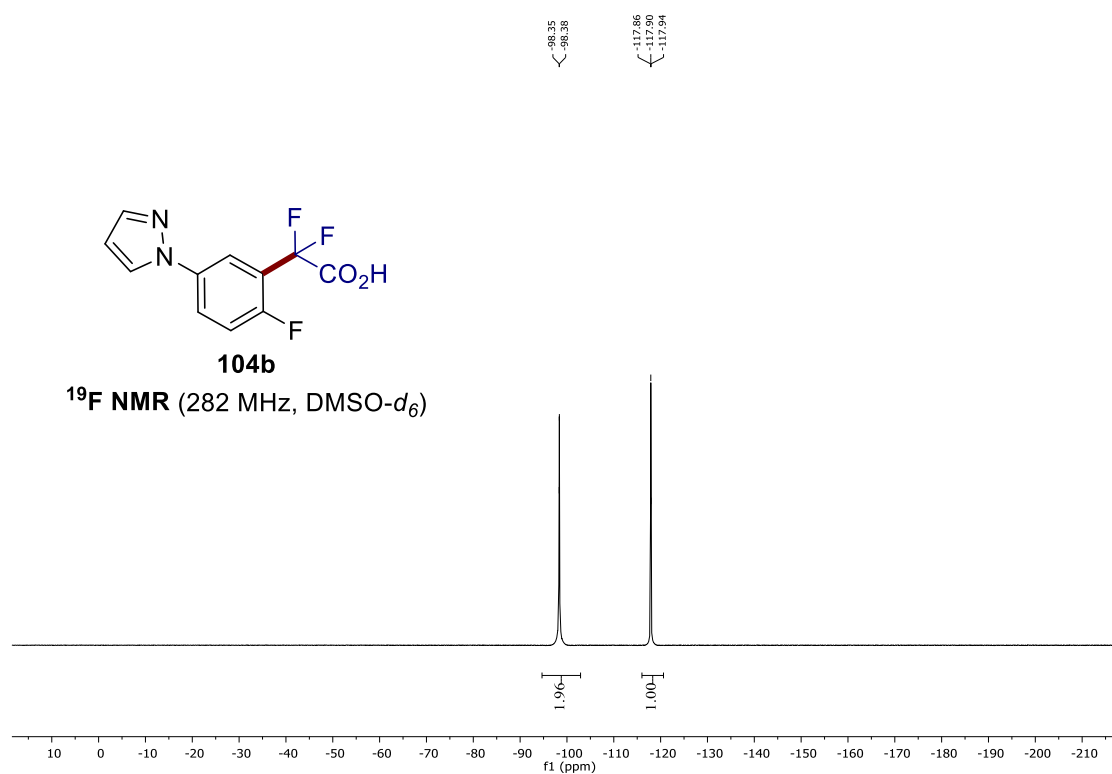
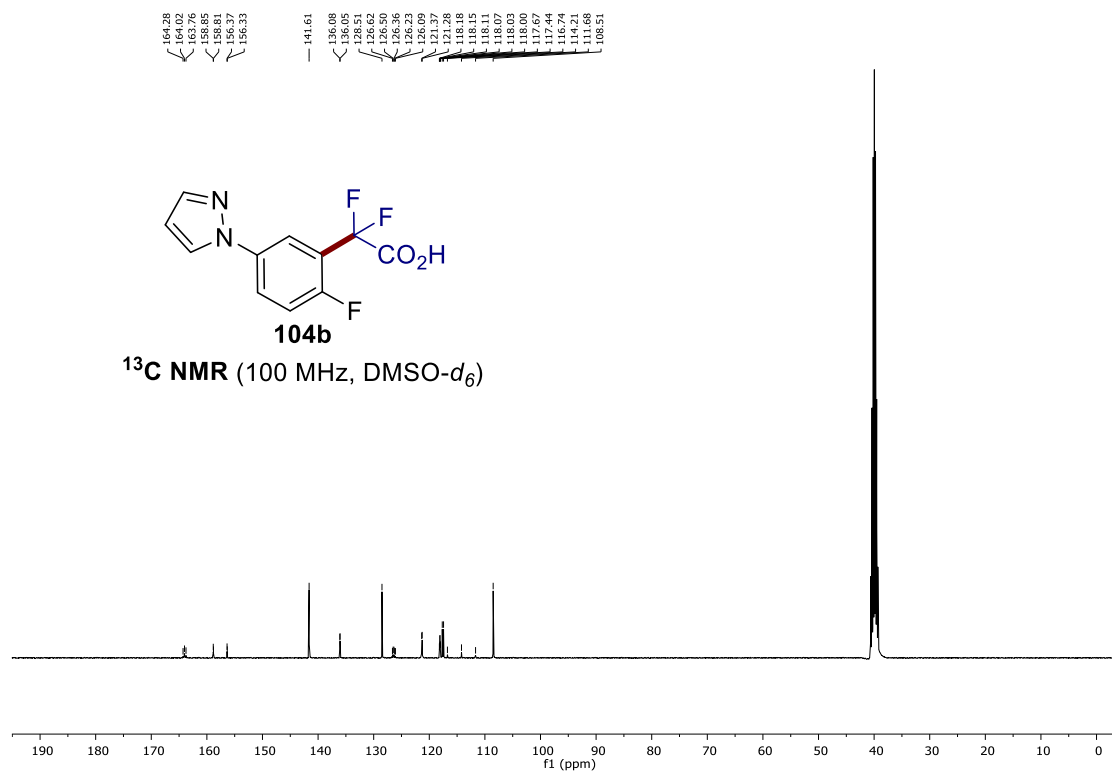
**104a**<sup>1</sup>H NMR (300 MHz, DMSO-*d*<sub>6</sub>)

165.73  
165.40  
165.07  
155.03  
150.11  
139.57  
137.98  
134.33  
134.08  
133.52  
129.86  
129.36  
126.14  
126.08  
125.22  
123.68  
123.59  
123.53  
123.47  
118.52  
114.67  
114.08  
111.59

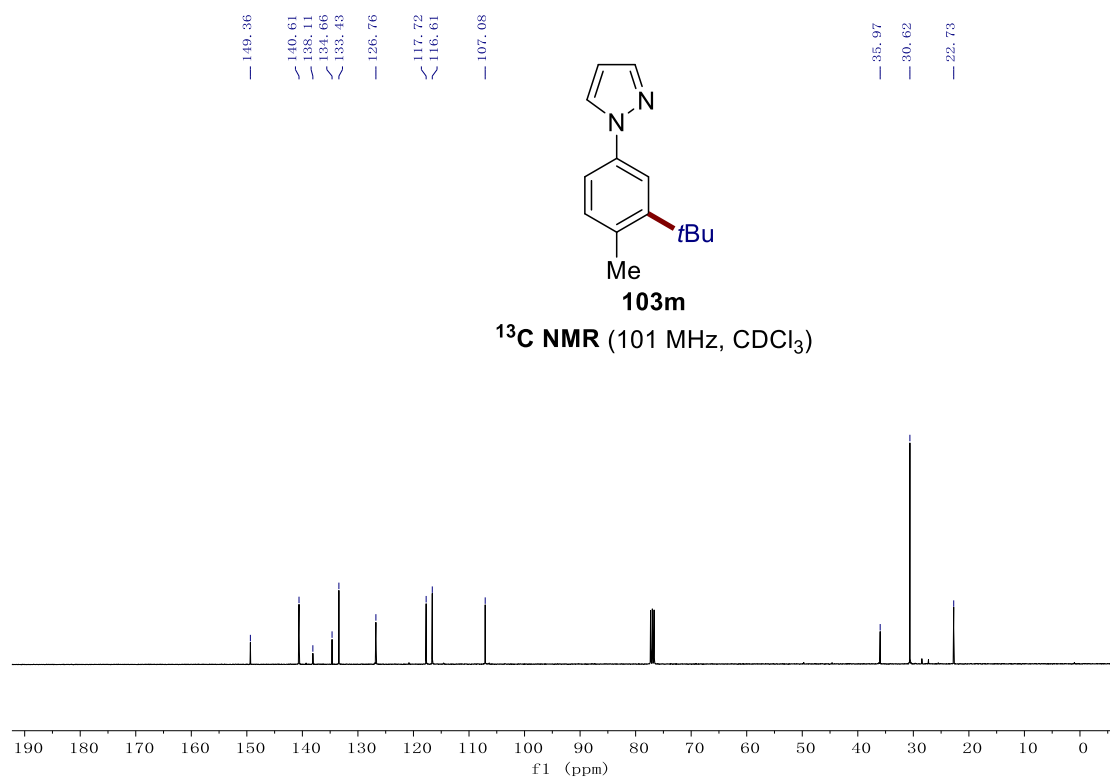
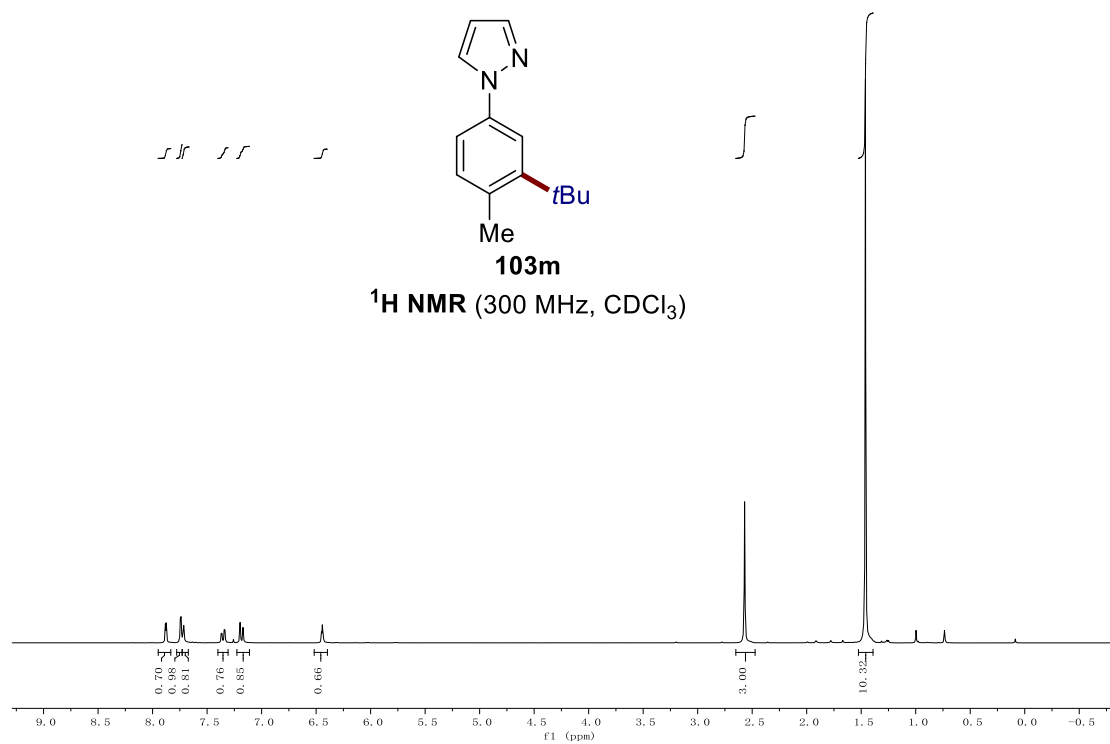
**104a**<sup>13</sup>C NMR (101 MHz, DMSO-*d*<sub>6</sub>)

## 7. NMR Spectra

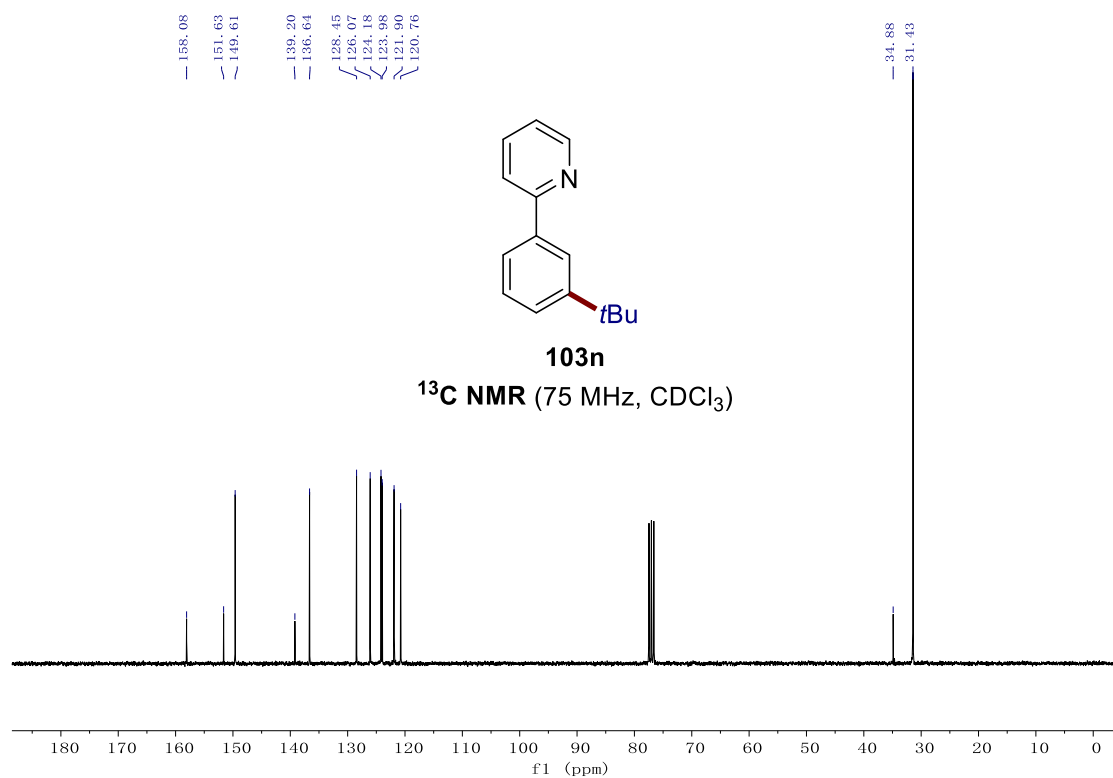
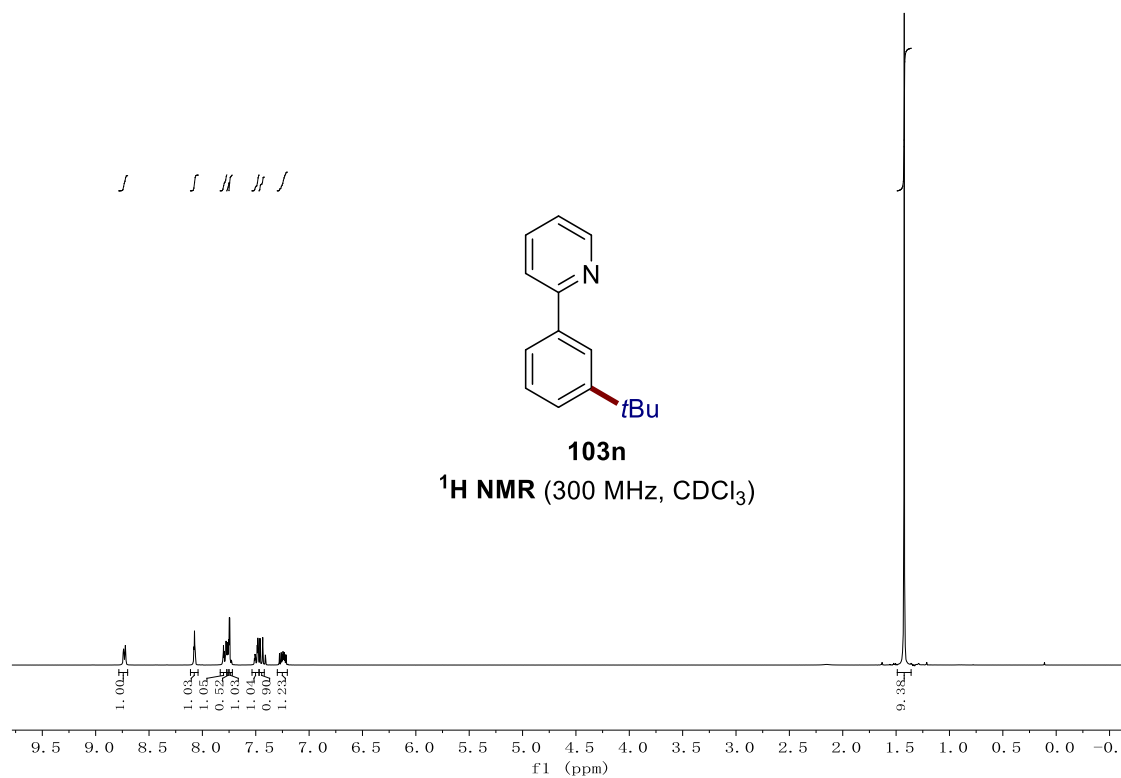




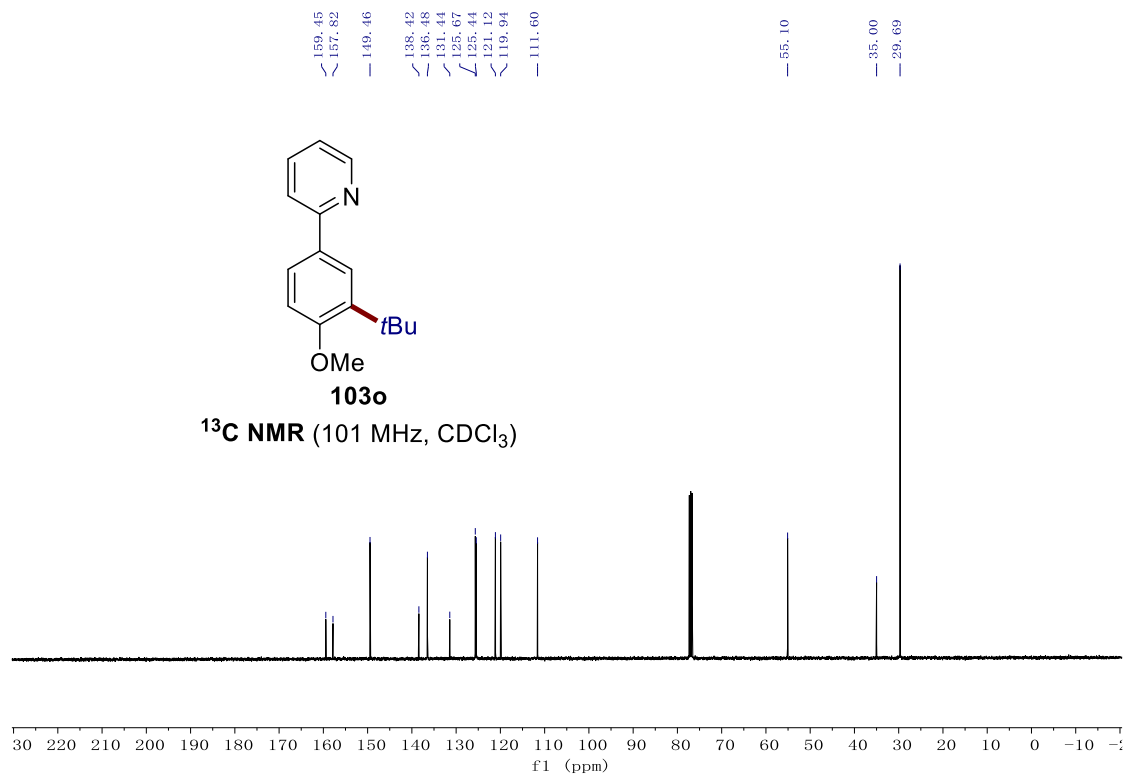
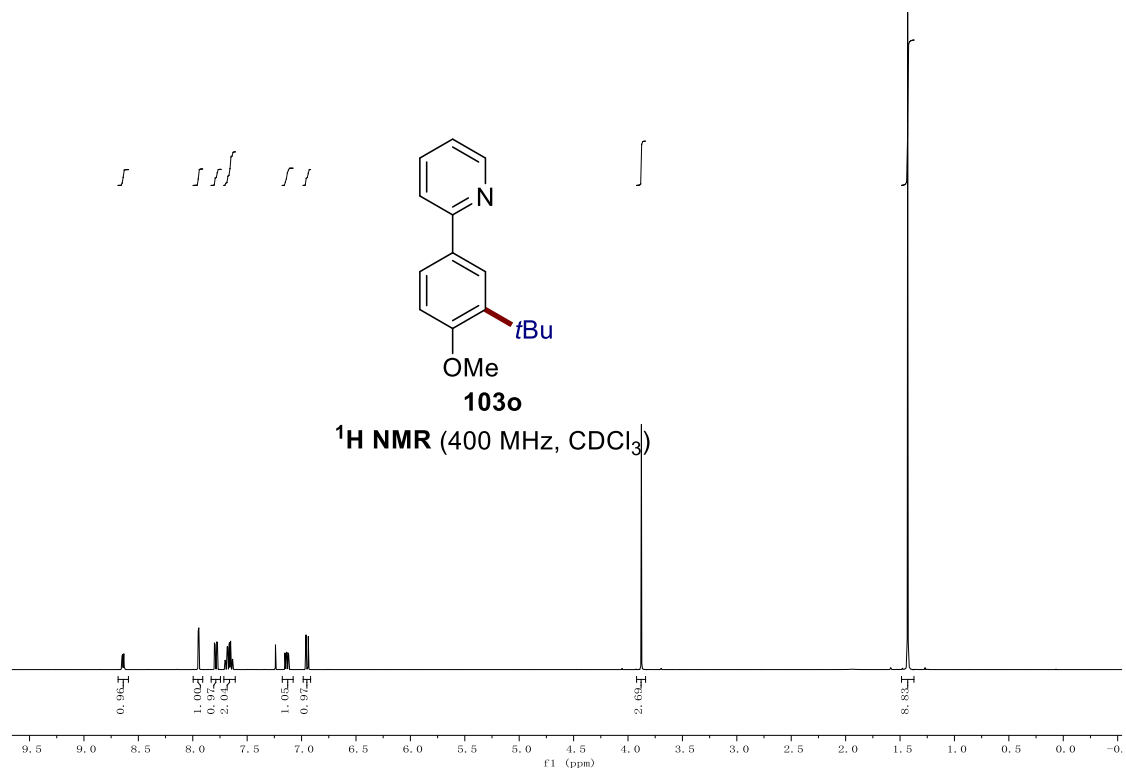
## 7. NMR Spectra

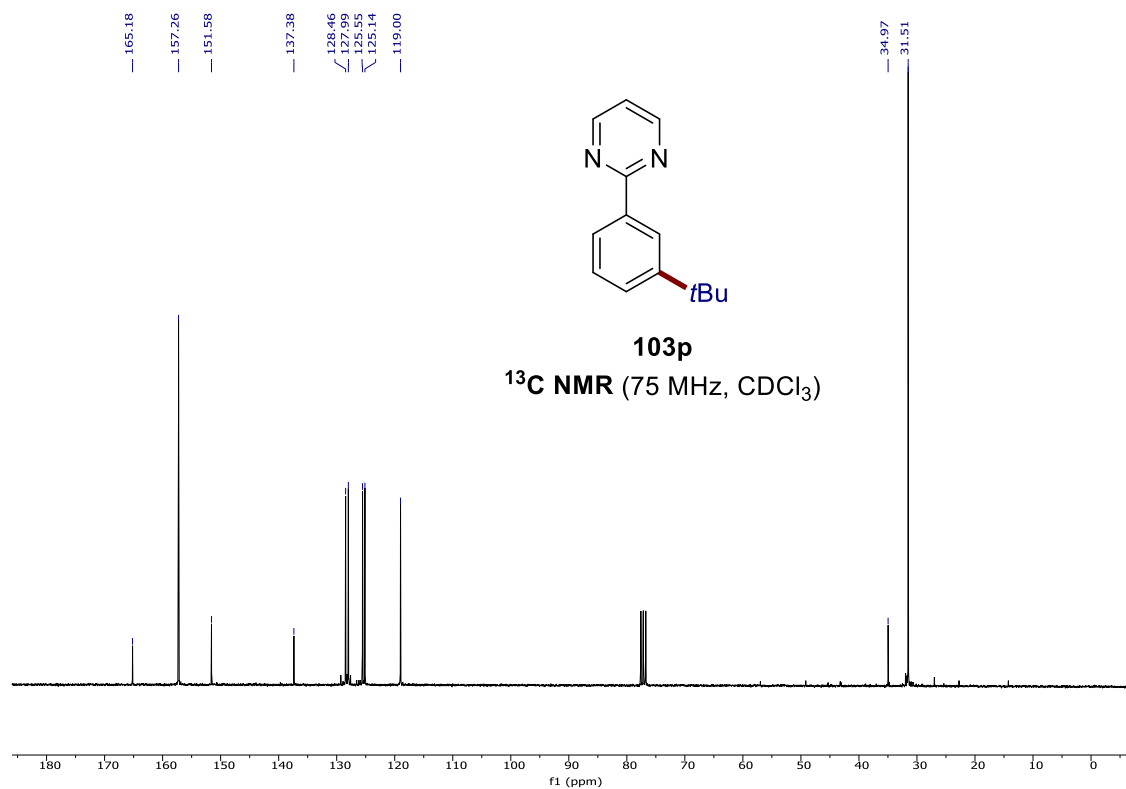
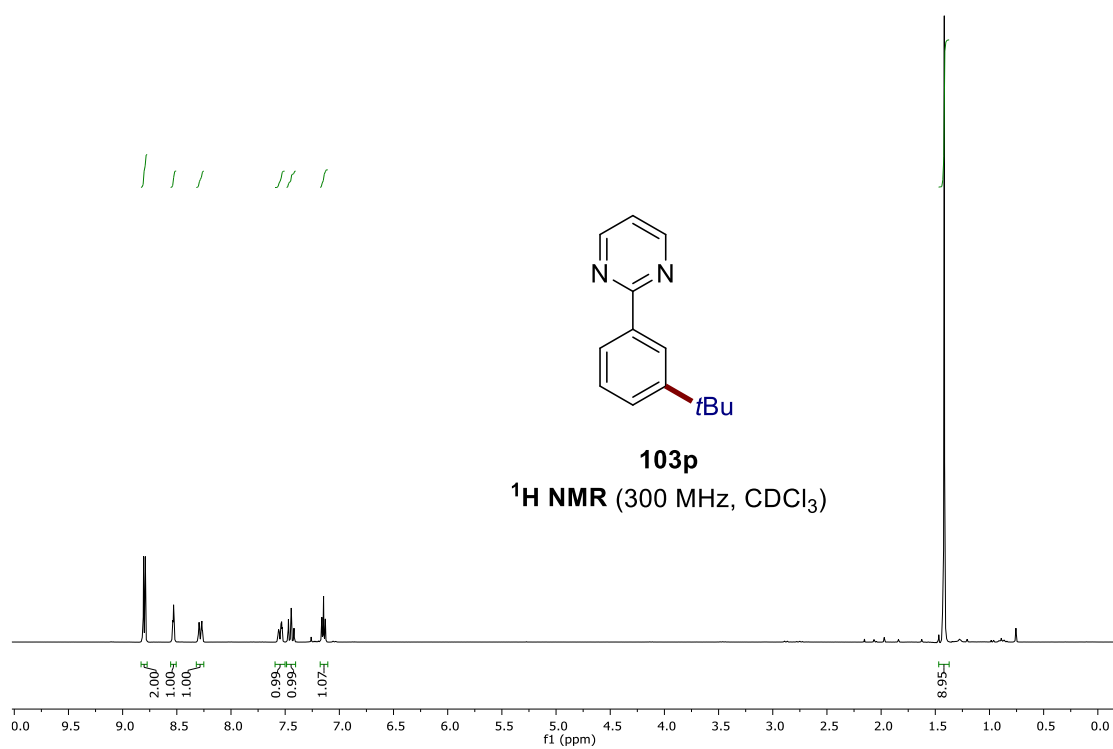




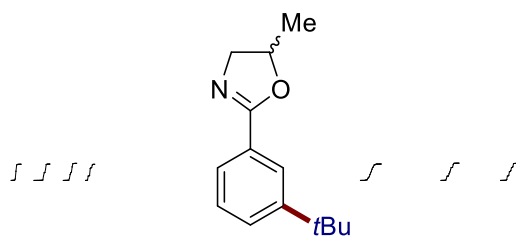


# 7. NMR Spectra

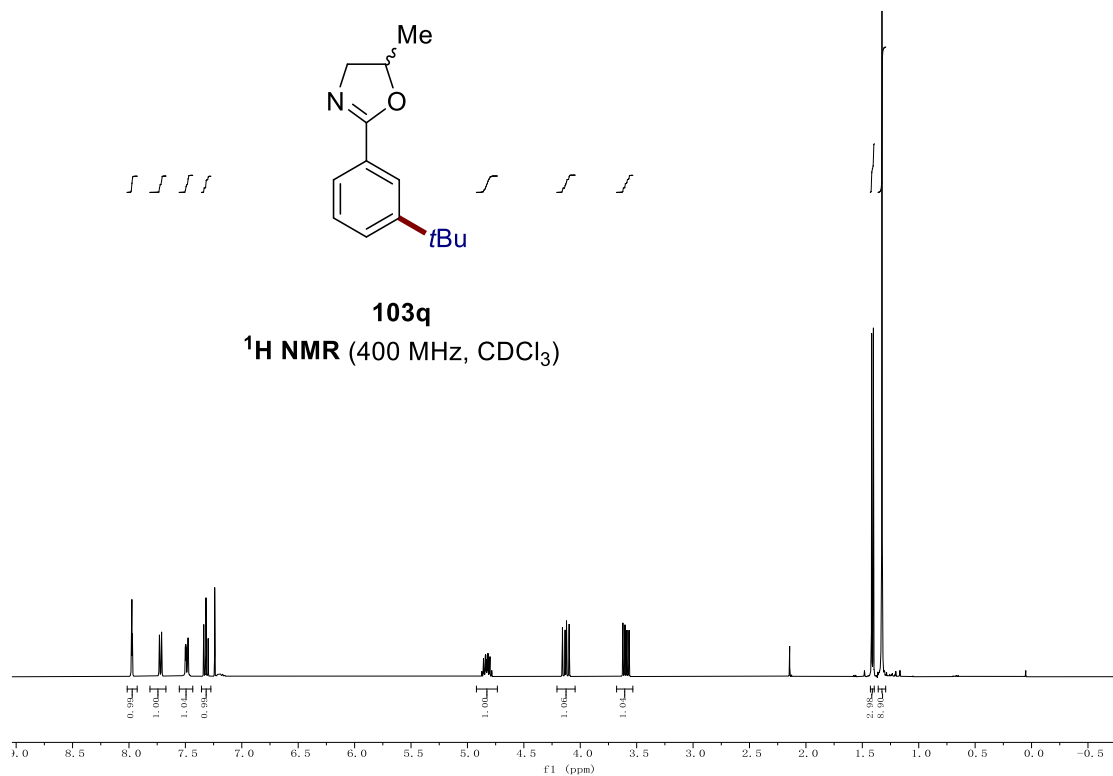




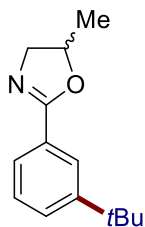
7. NMR Spectra



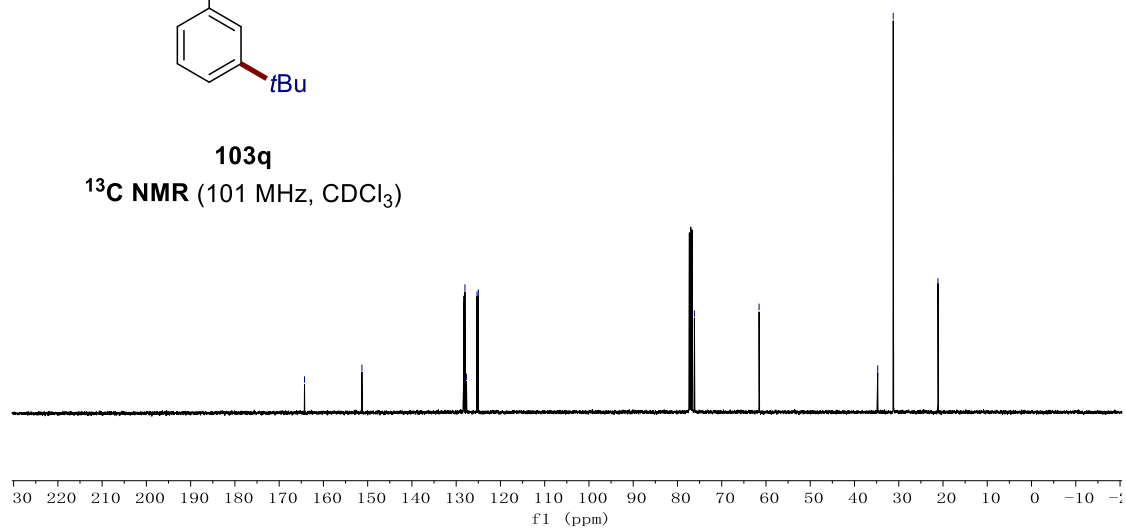
**103q**  
 $^1\text{H NMR}$  (400 MHz,  $\text{CDCl}_3$ )

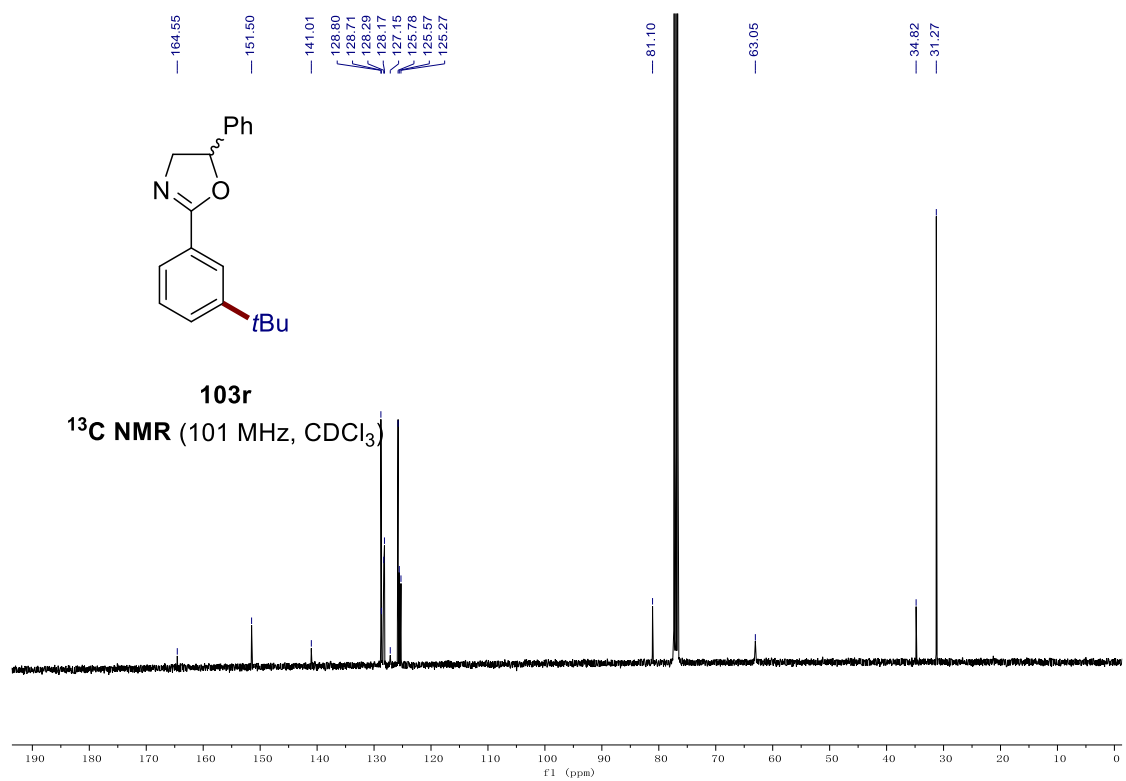
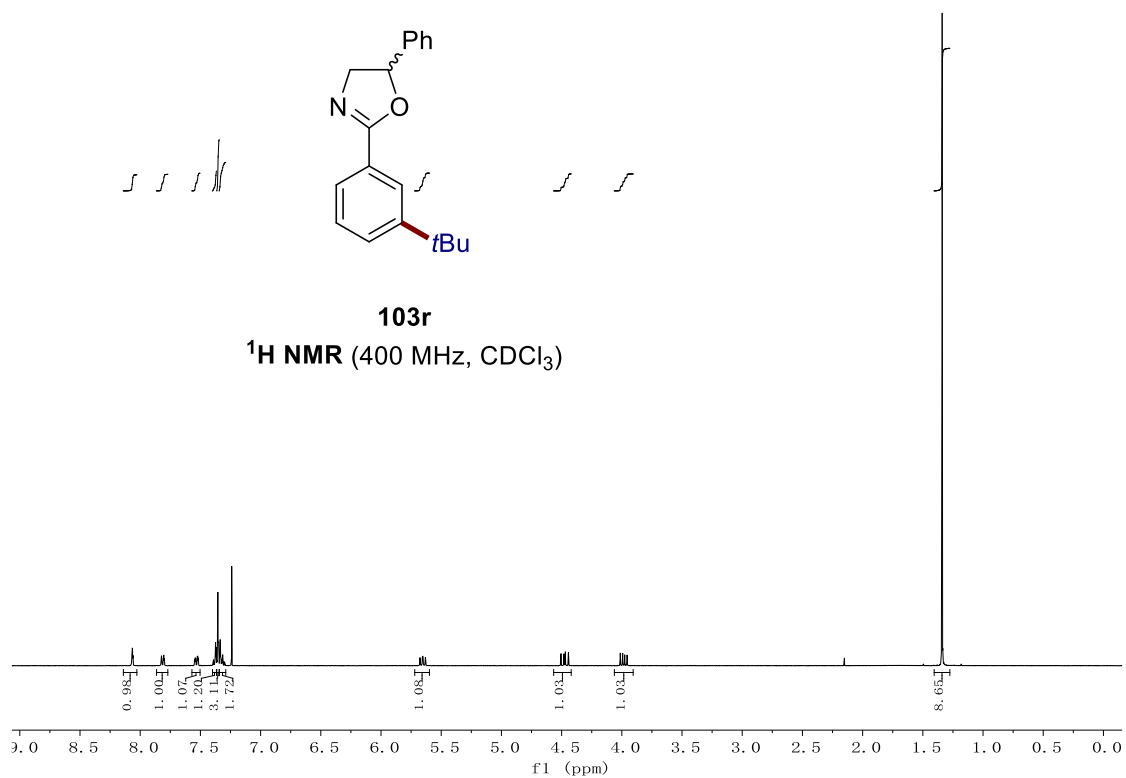


164.27  
 151.29  
 128.32  
 128.02  
 127.68  
 125.30  
 124.99  
 76.17  
 61.56  
 34.75  
 31.25  
 21.13

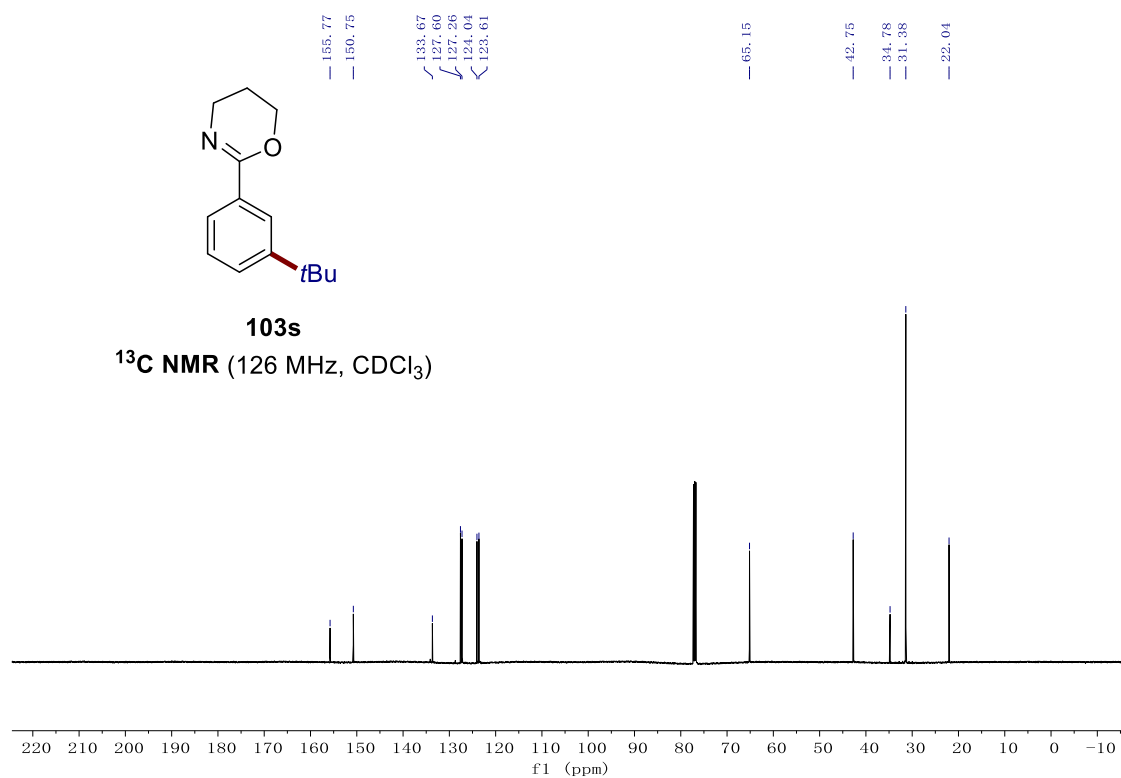
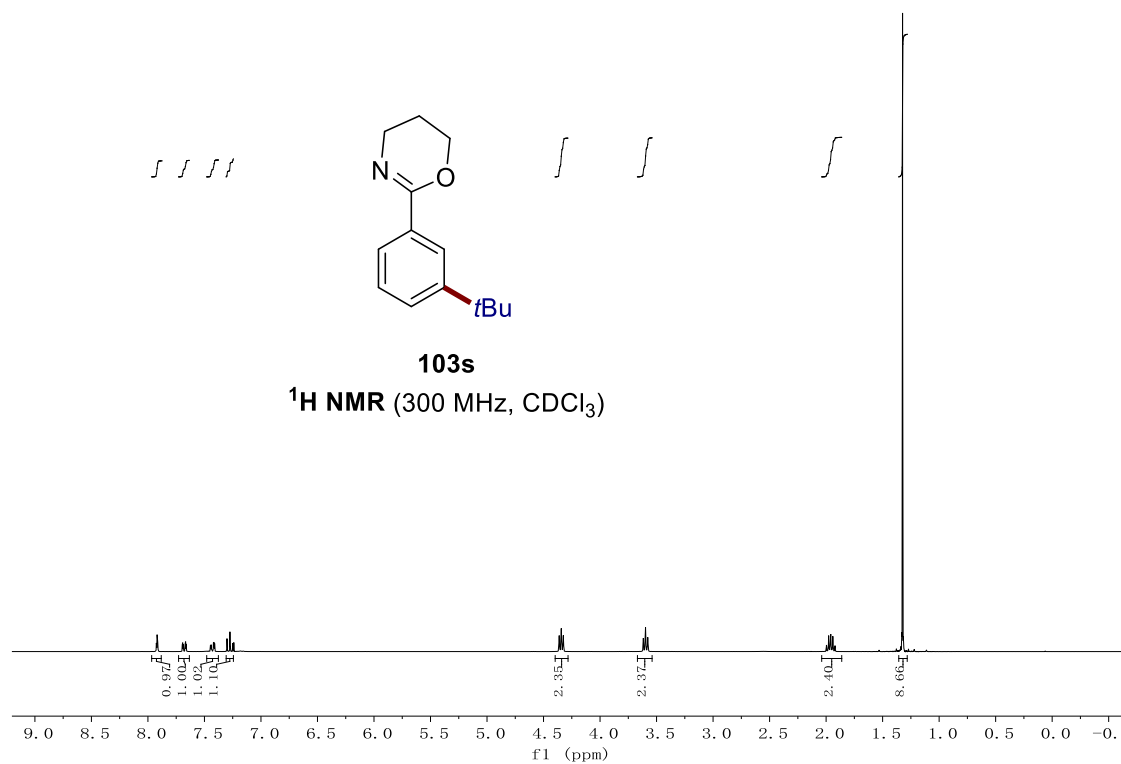


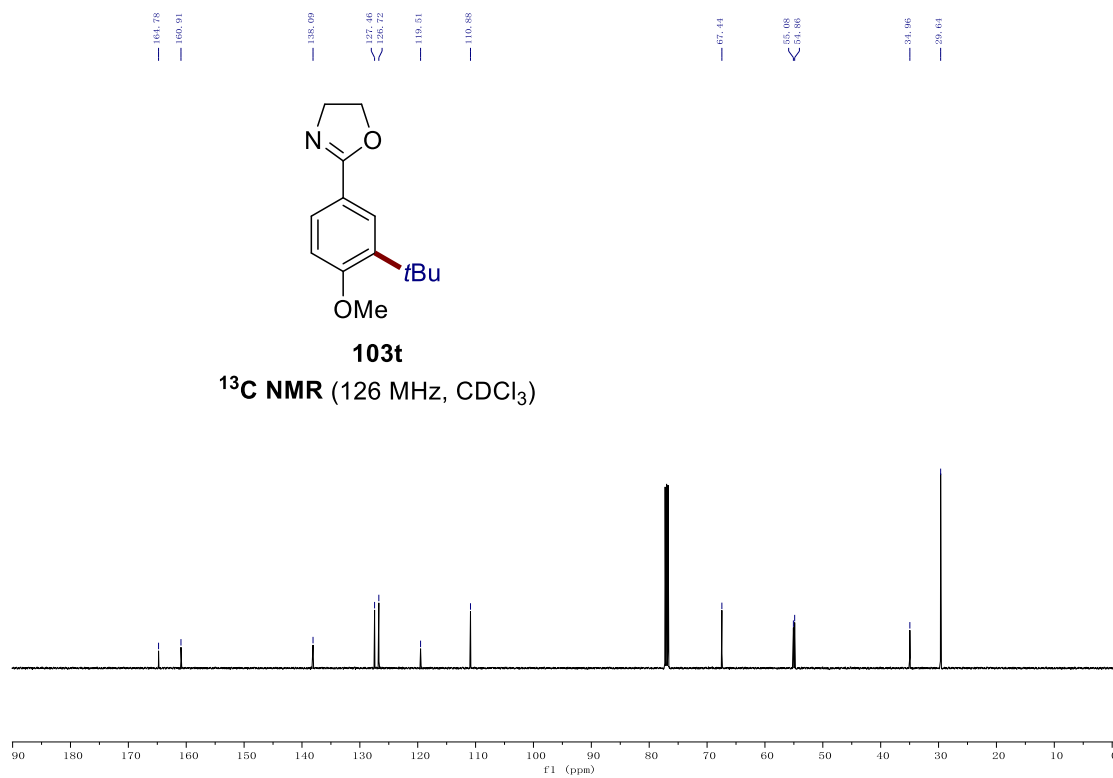
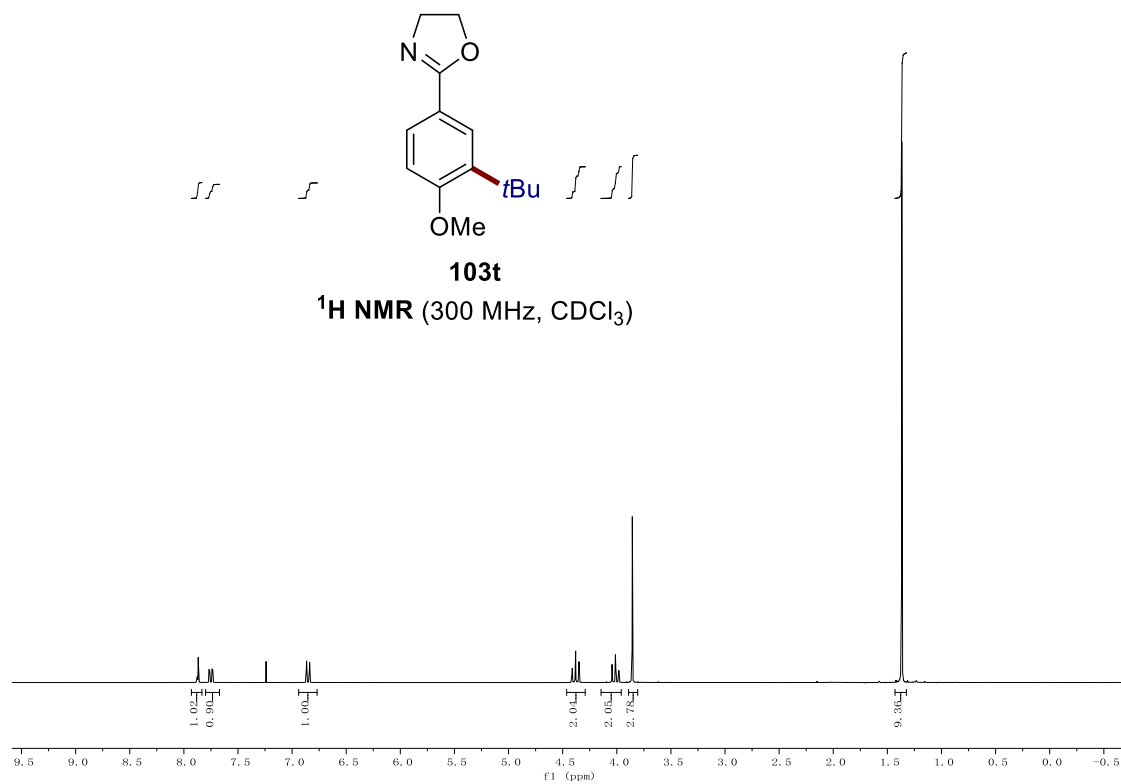
**103q**  
 $^{13}\text{C NMR}$  (101 MHz,  $\text{CDCl}_3$ )



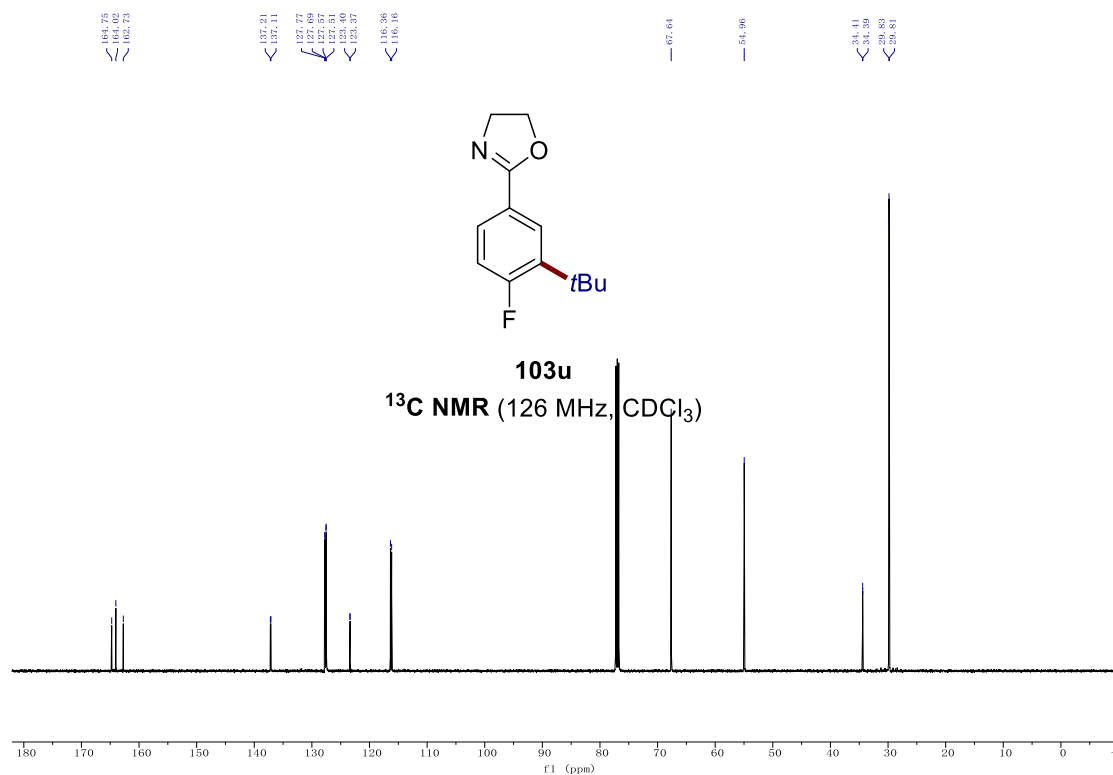
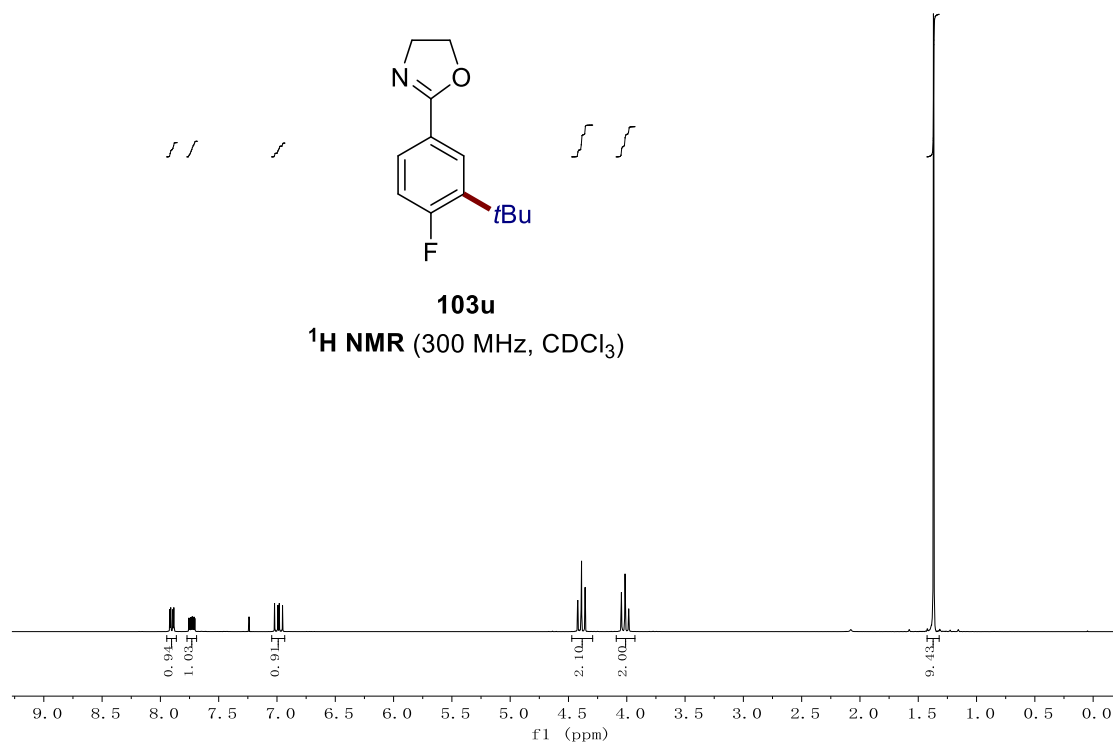


7. NMR Spectra

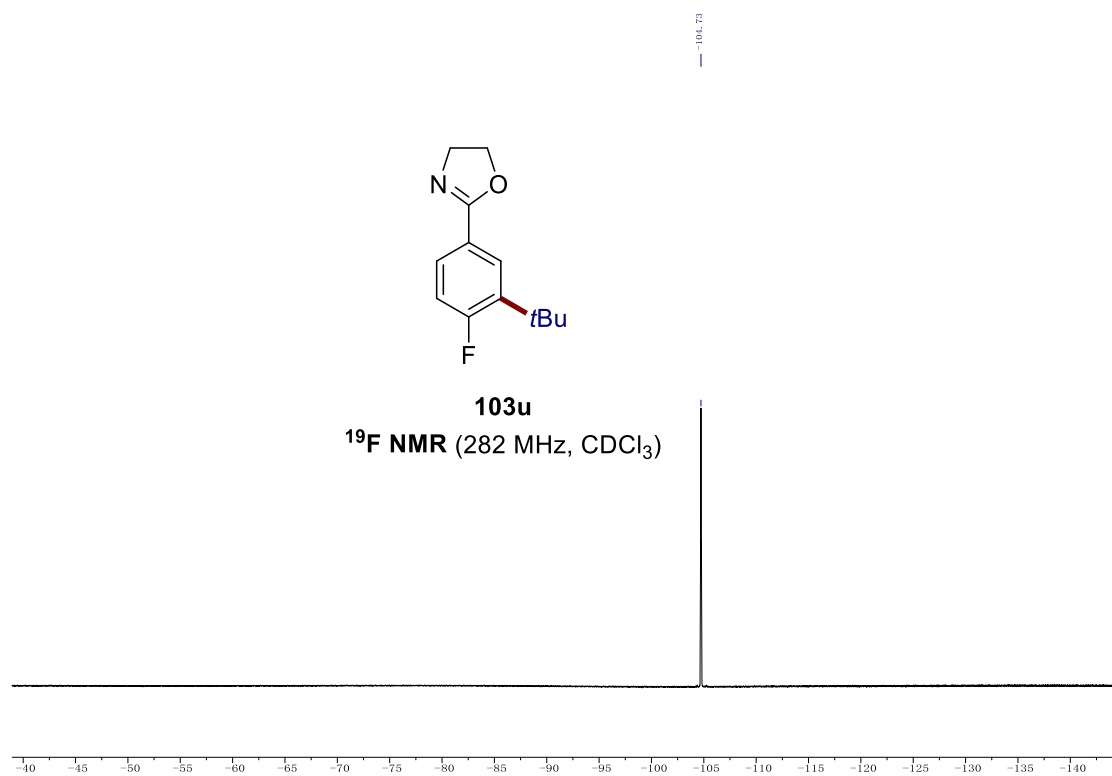




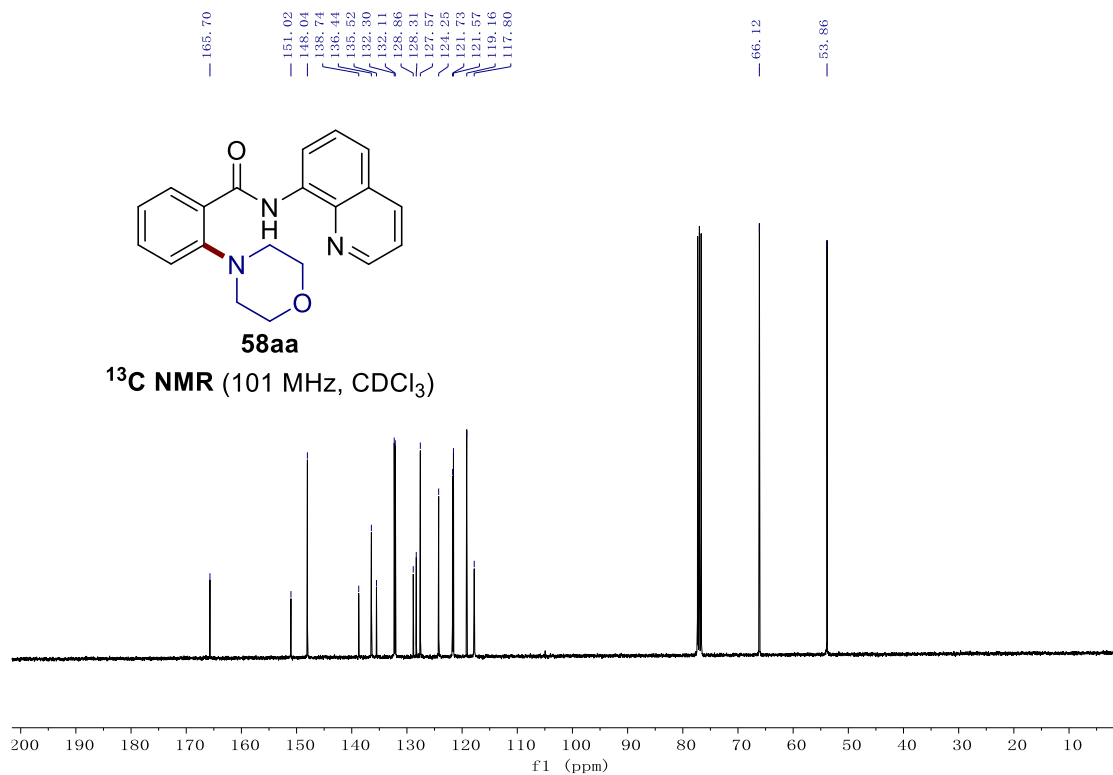
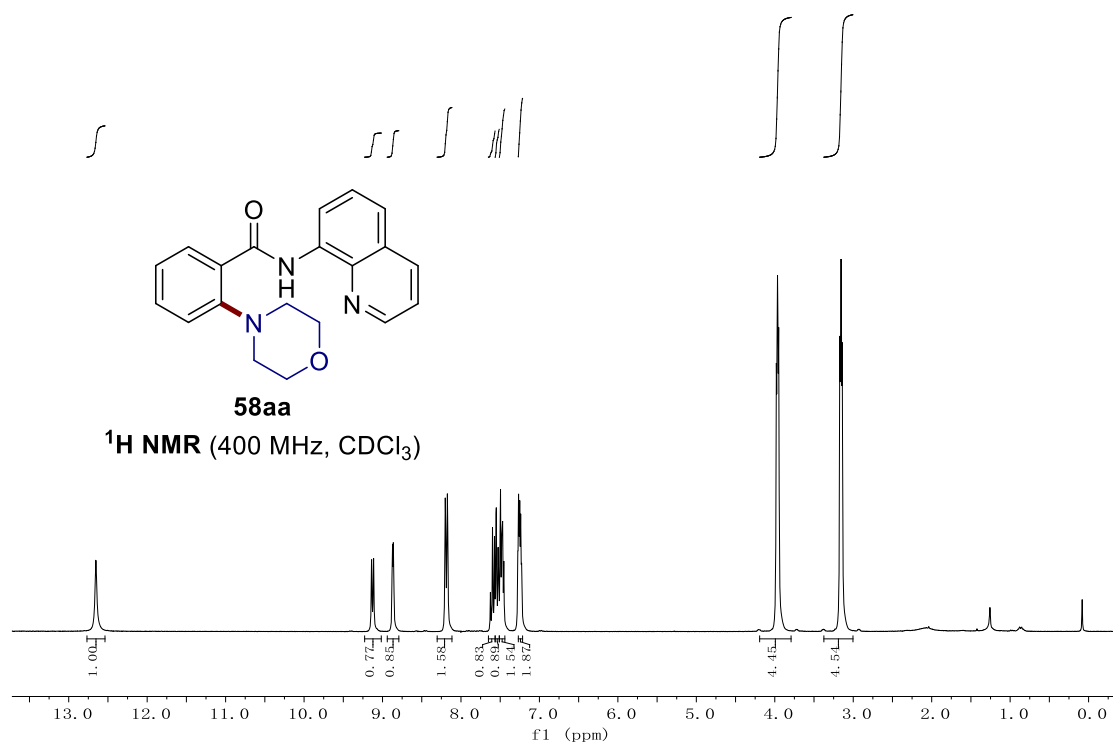
7. NMR Spectra

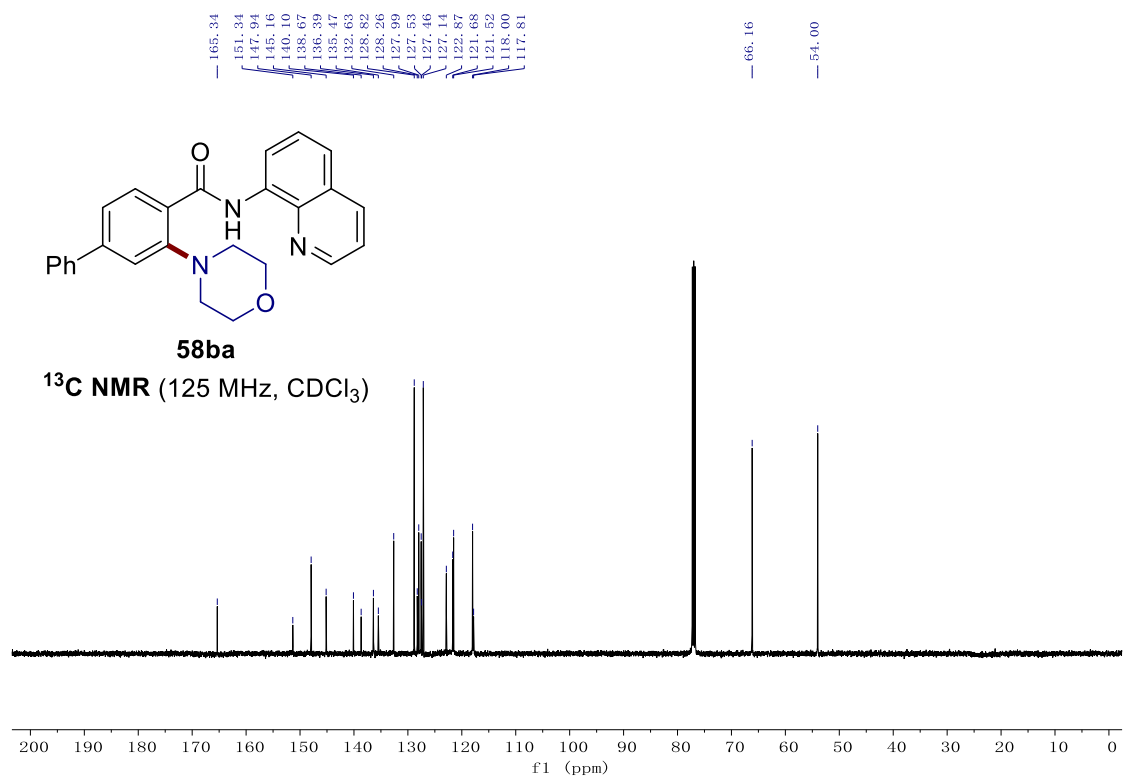
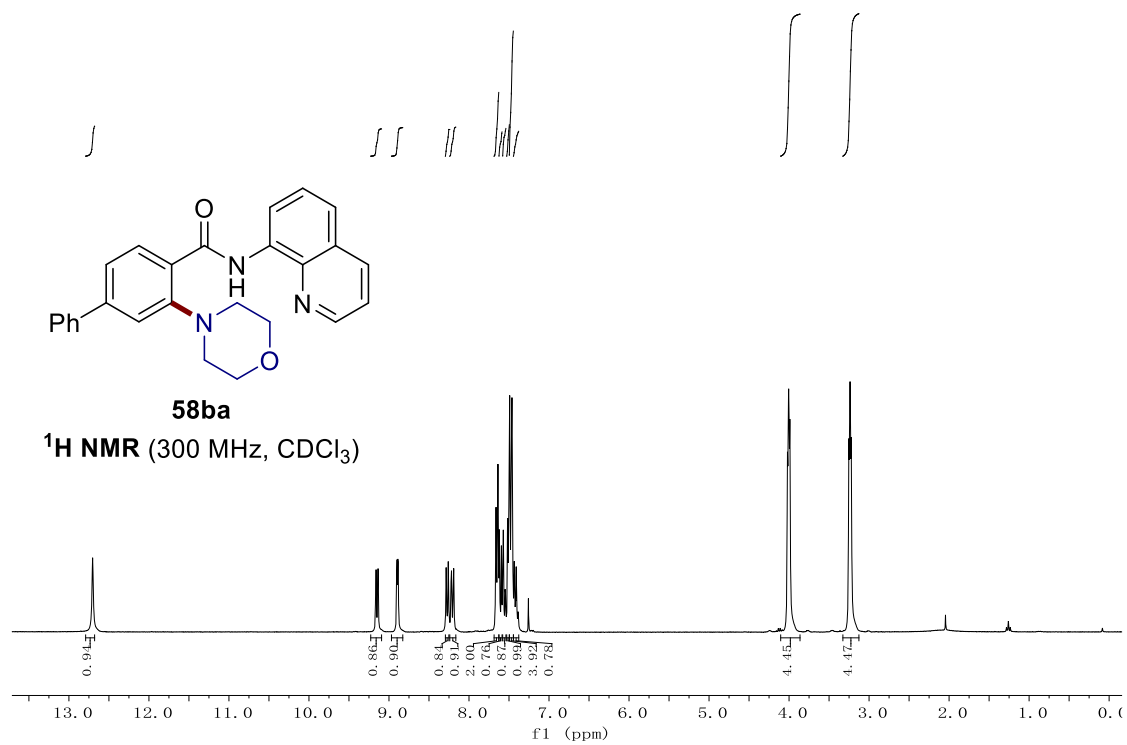




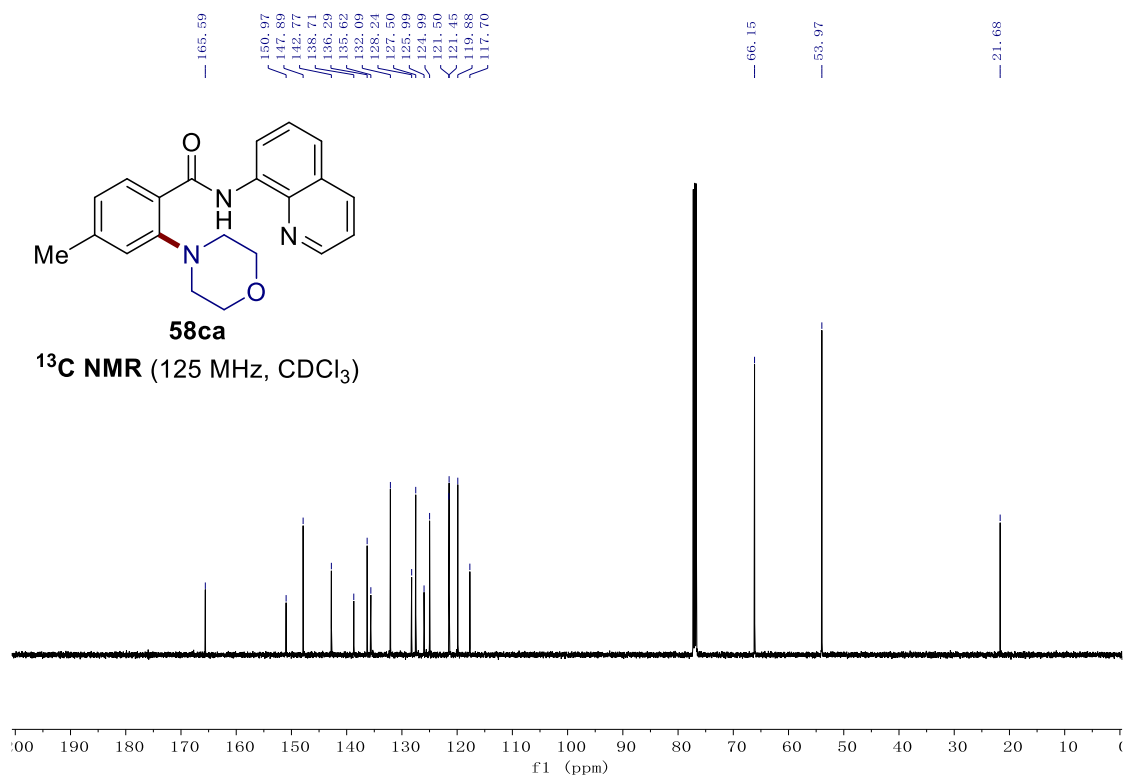
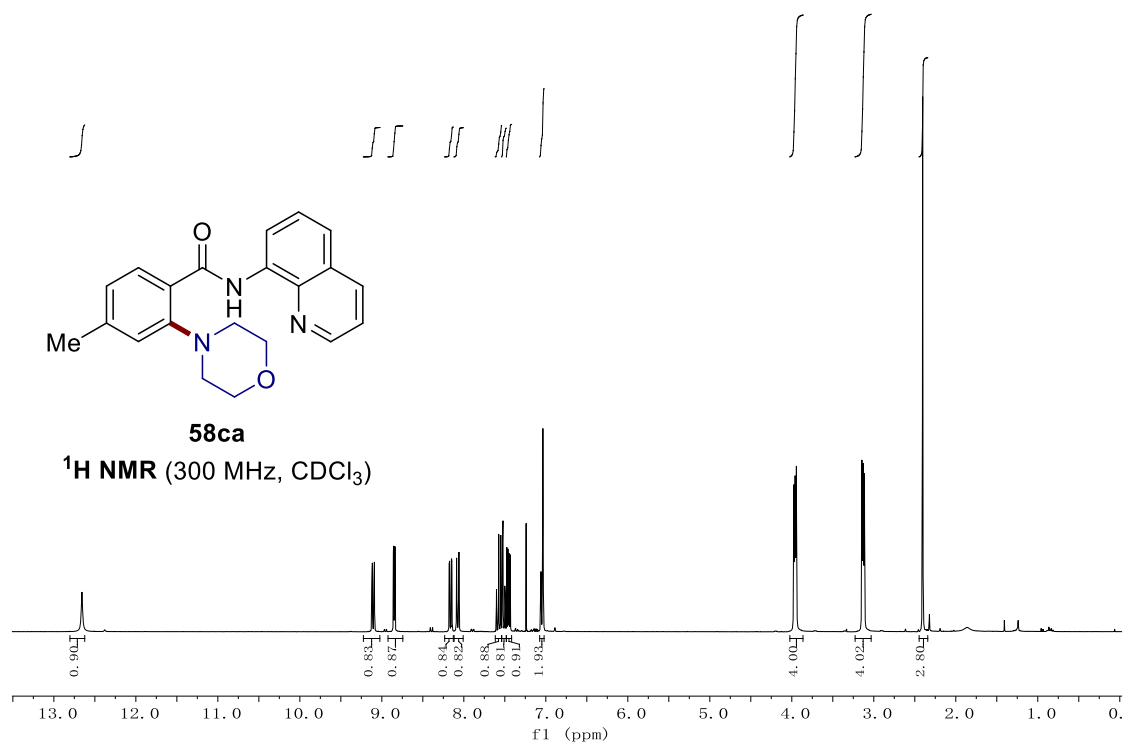


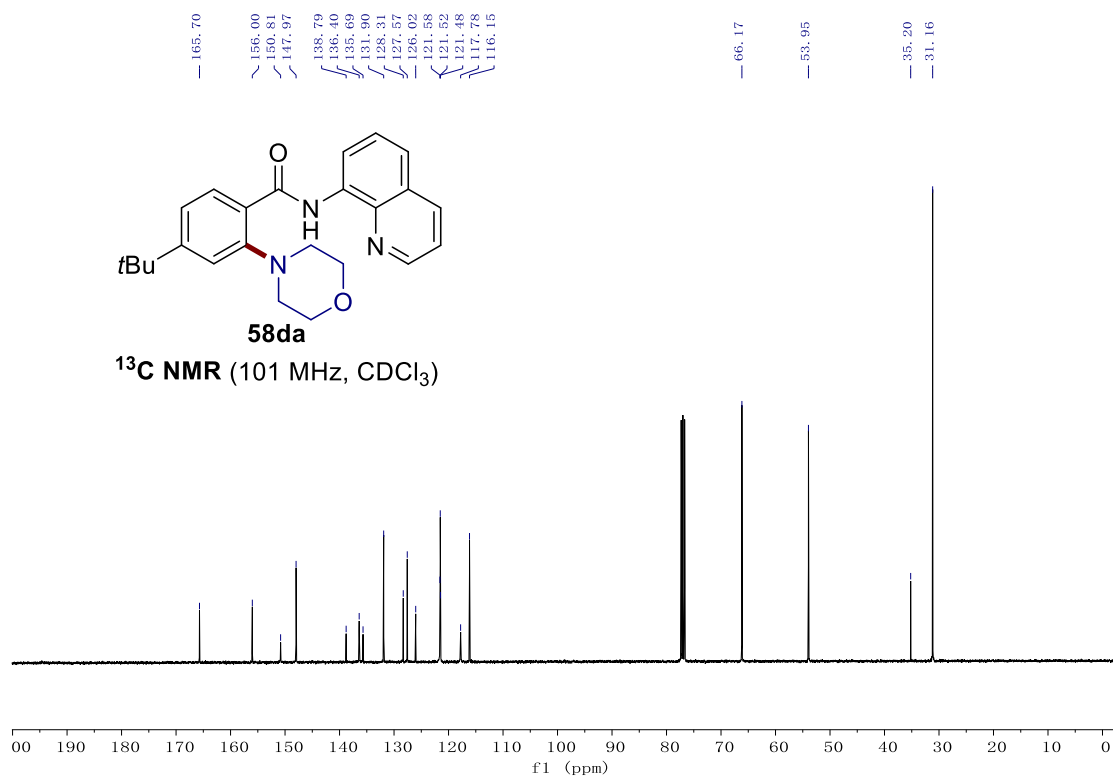
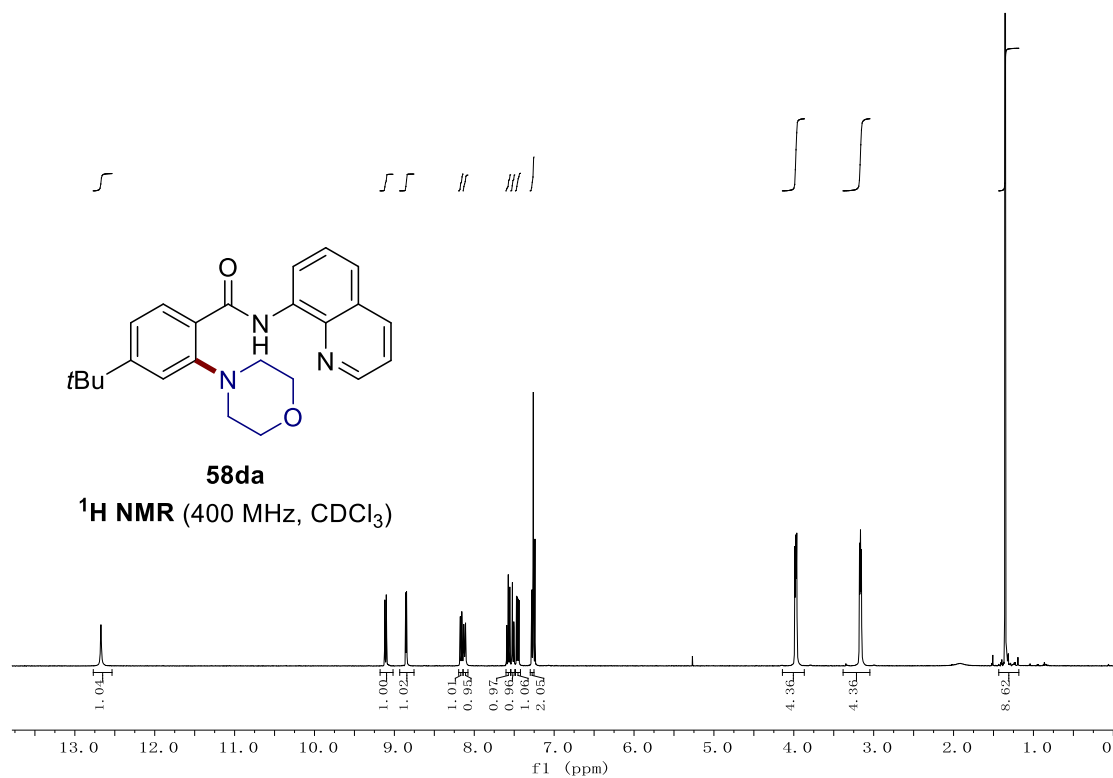
## 7.4 Nickela-Electrocatalyzed C–H Amination



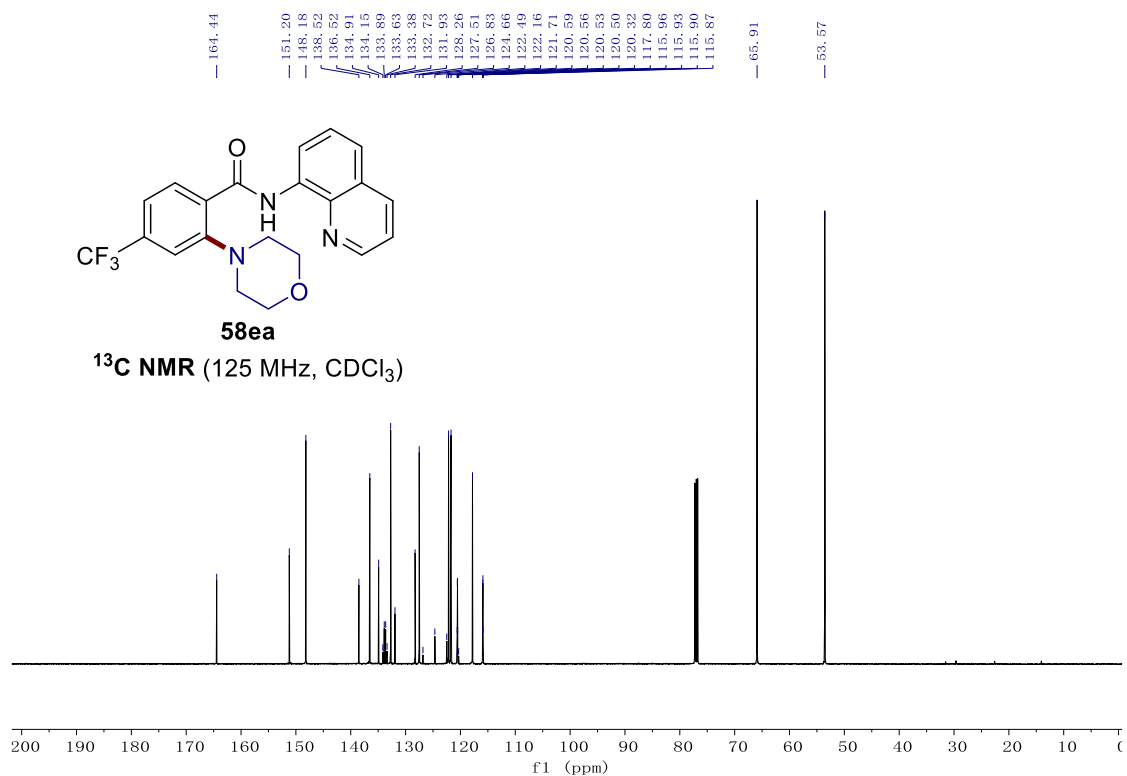
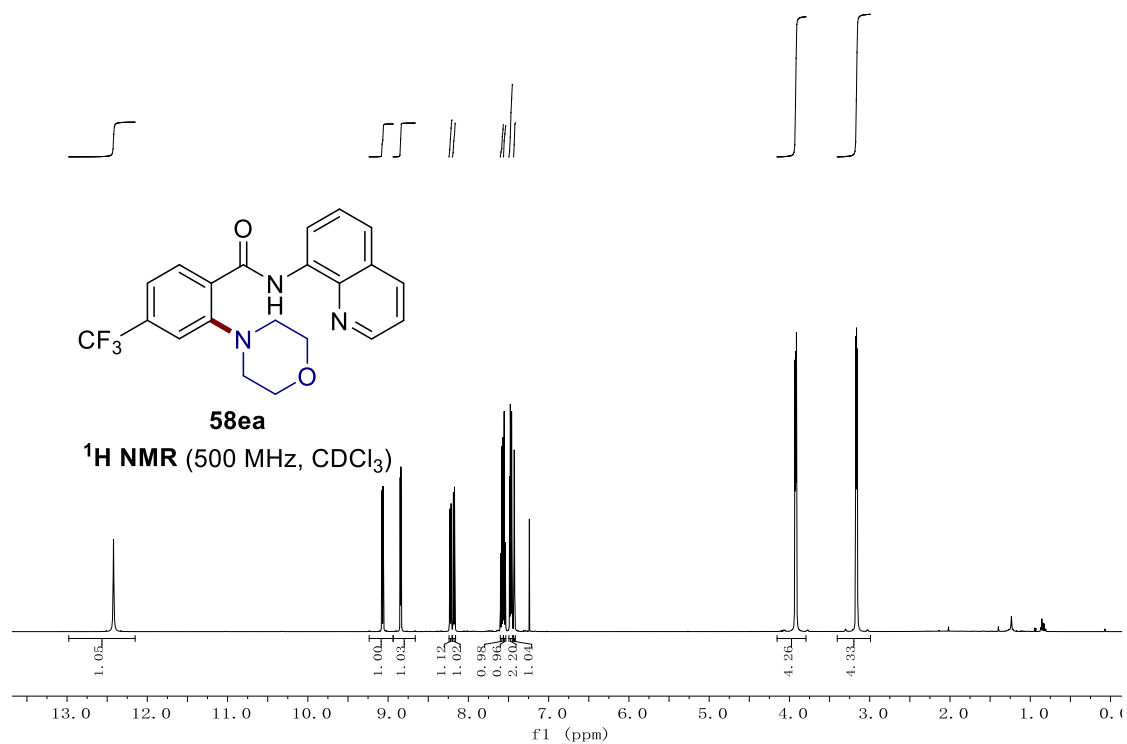


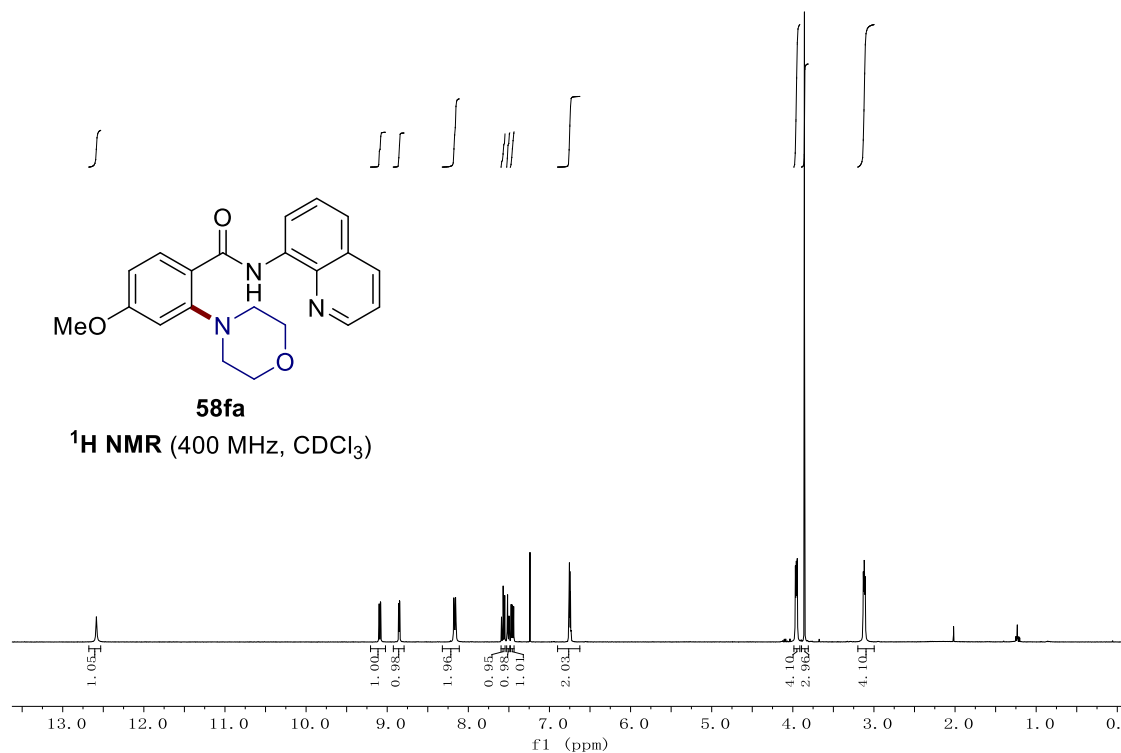
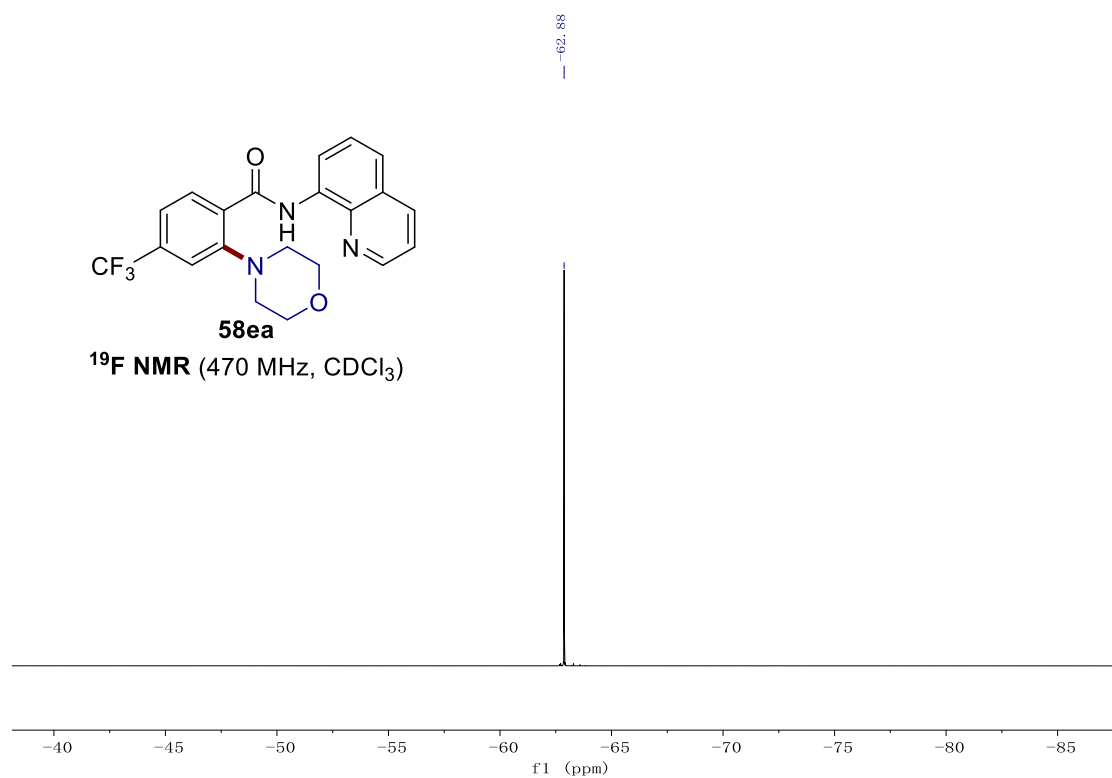
## 7. NMR Spectra



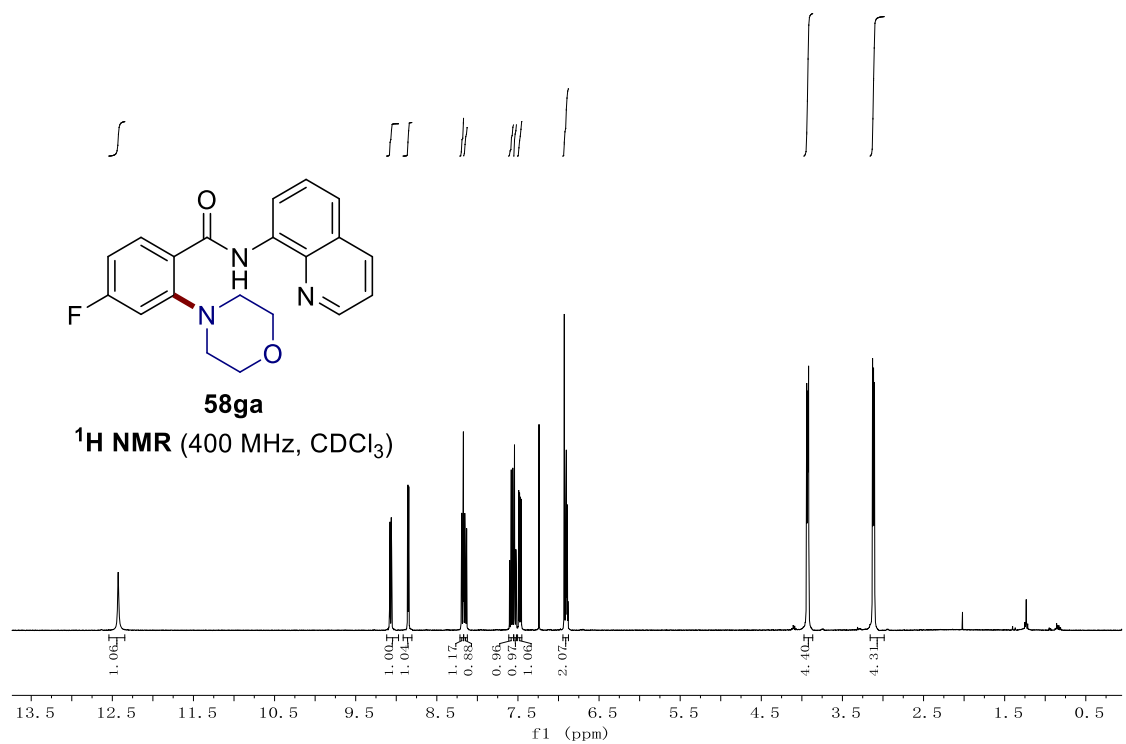
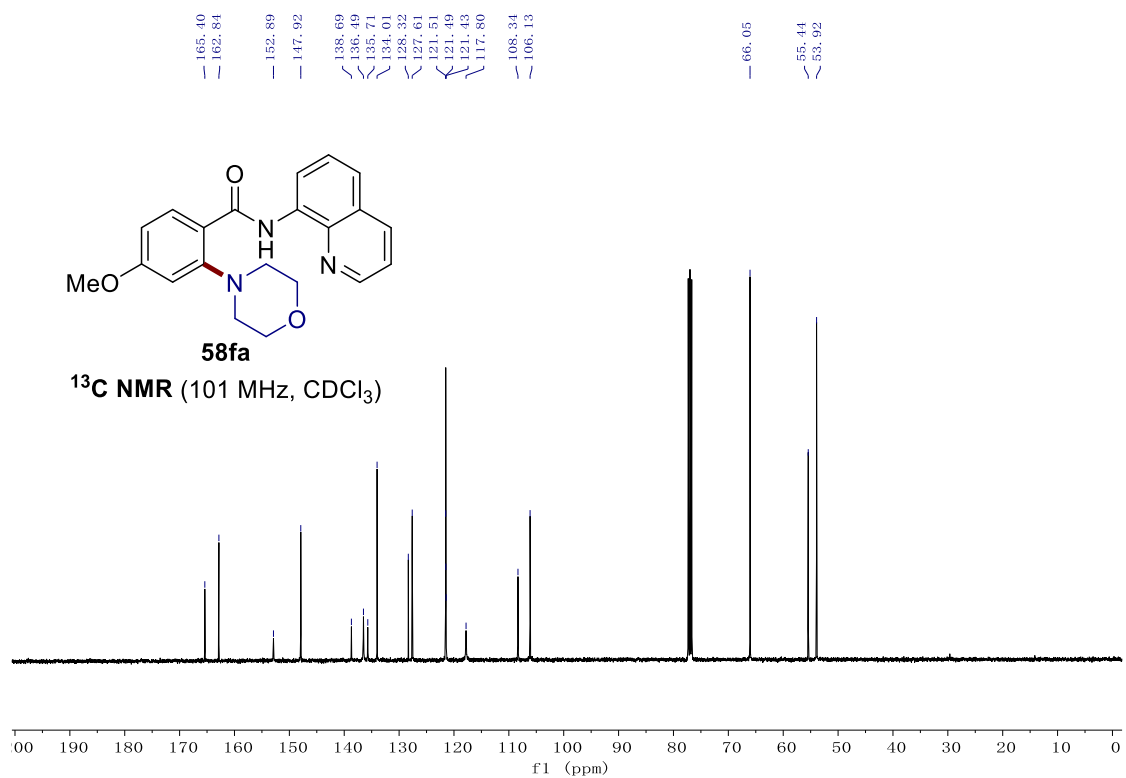


## 7. NMR Spectra

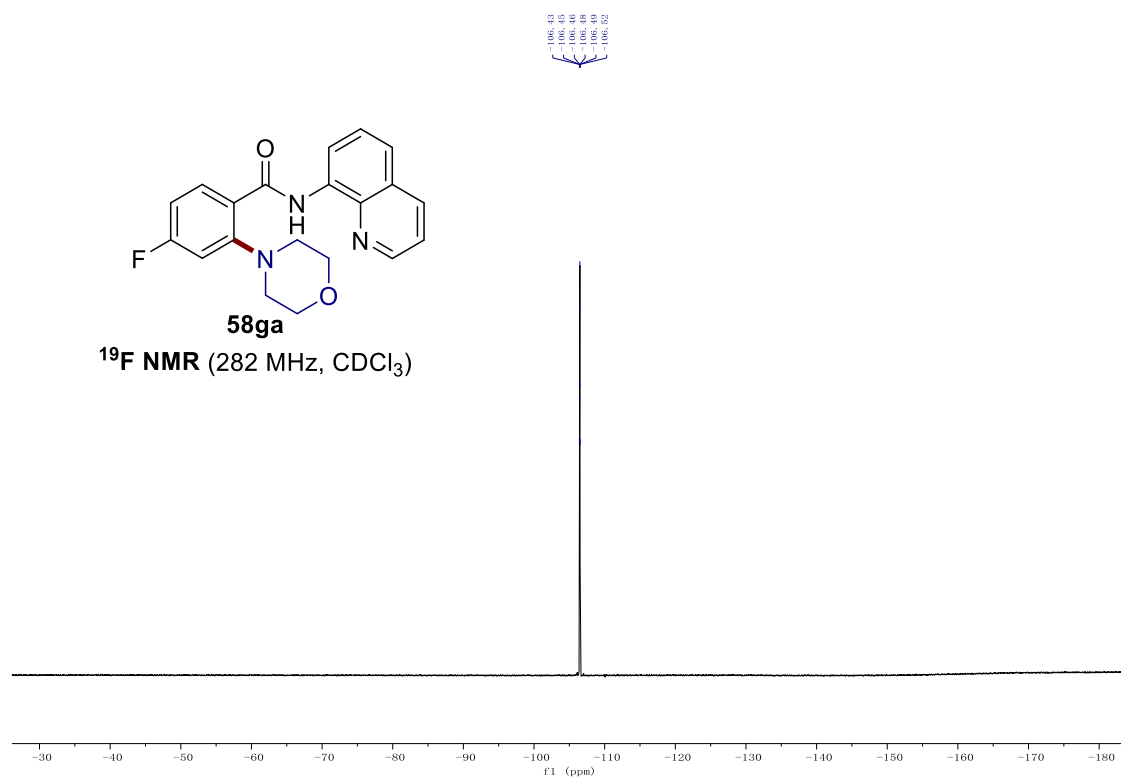
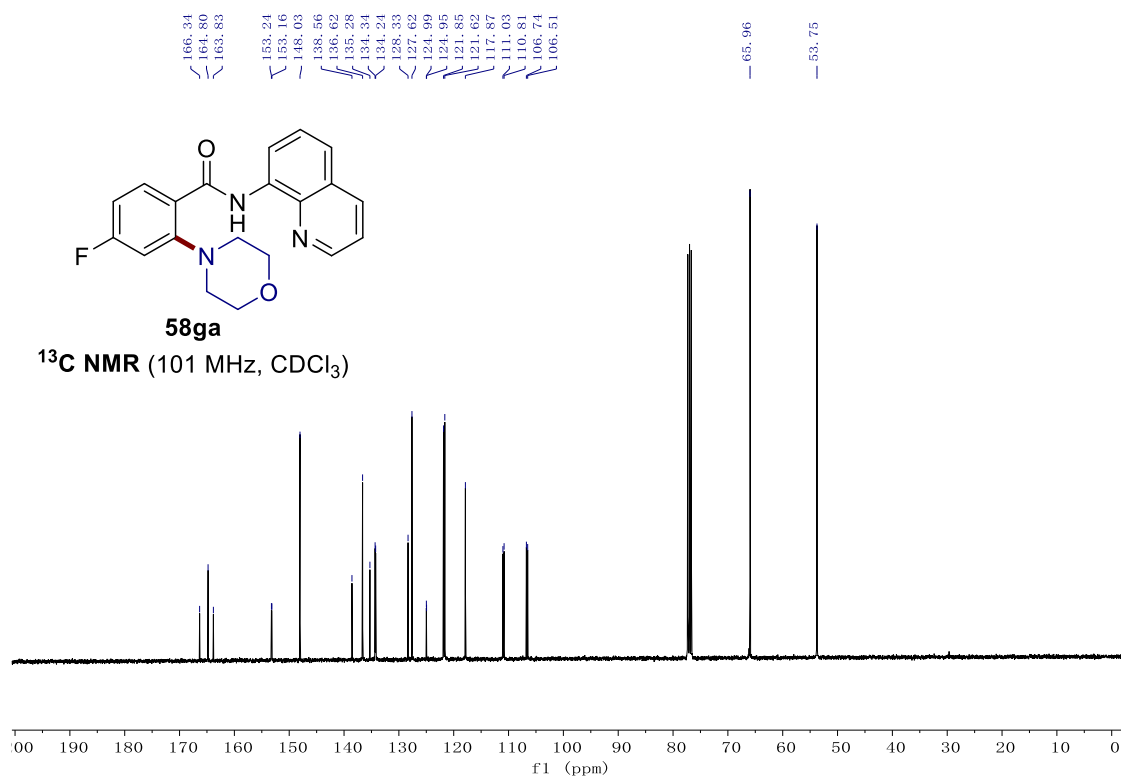




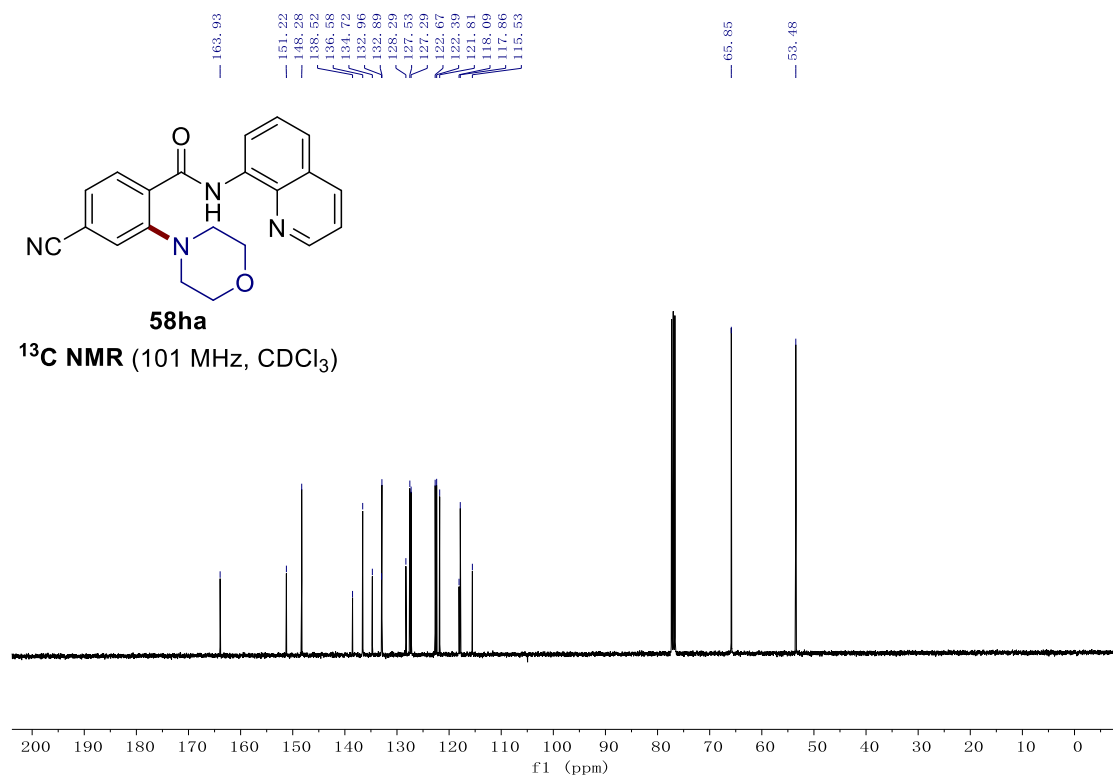
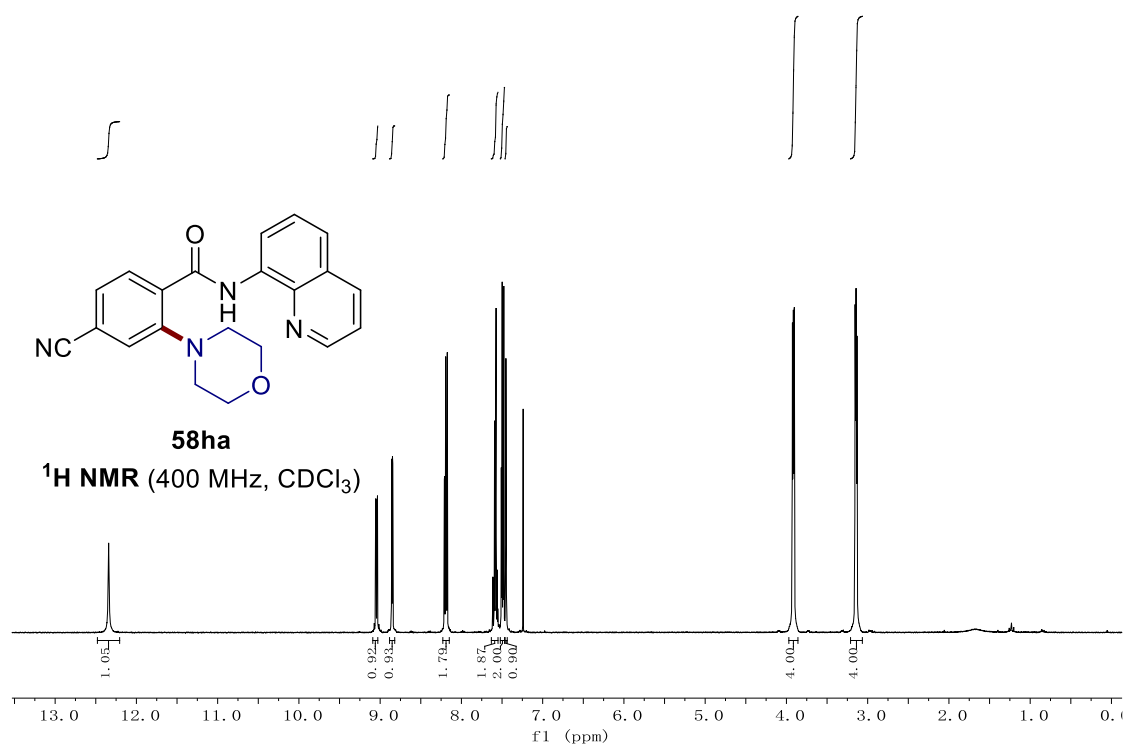
## 7. NMR Spectra

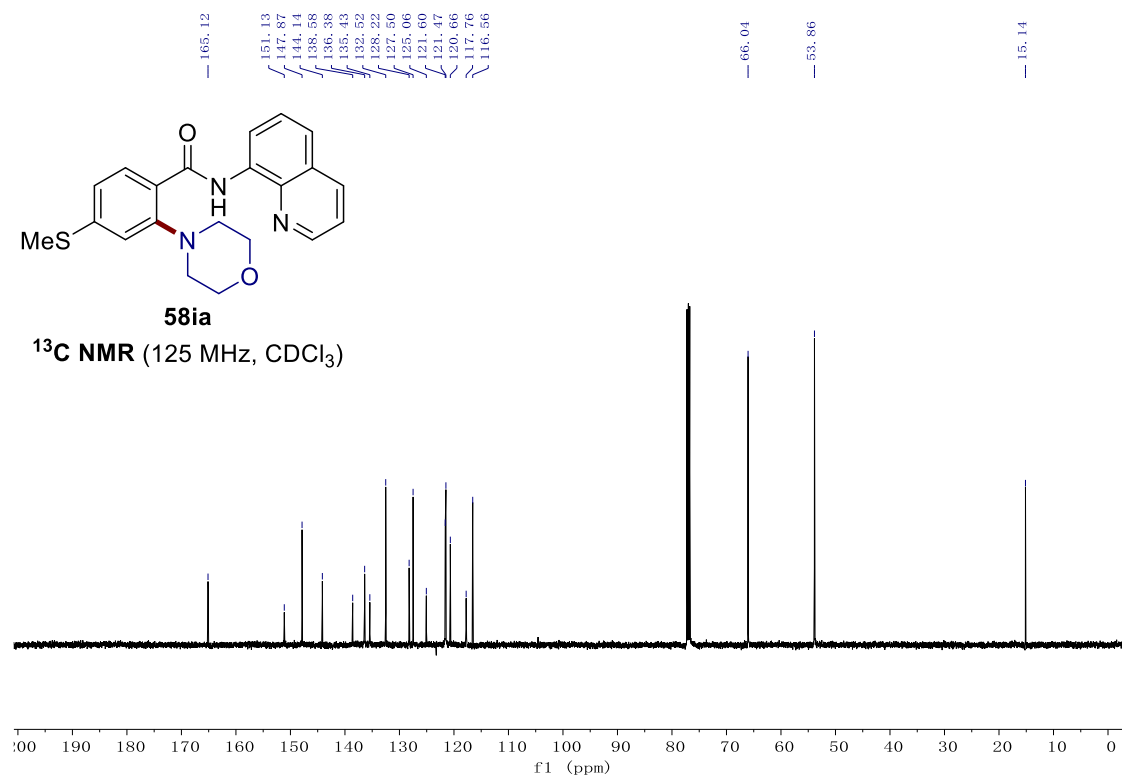
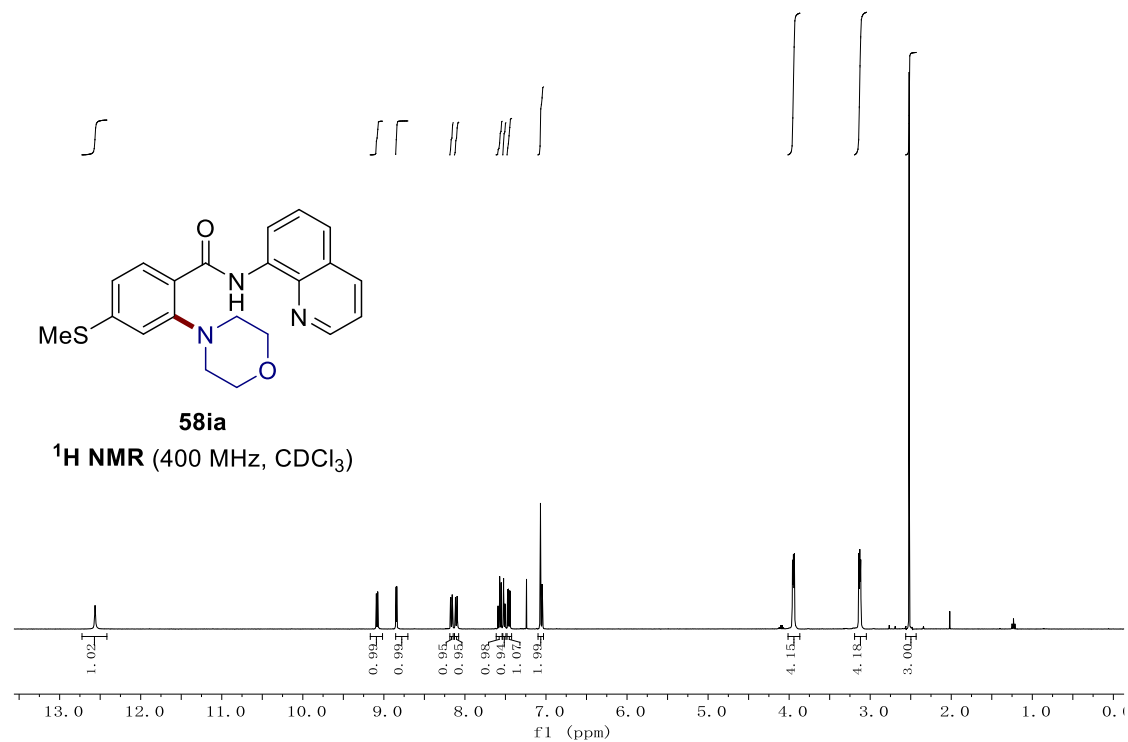




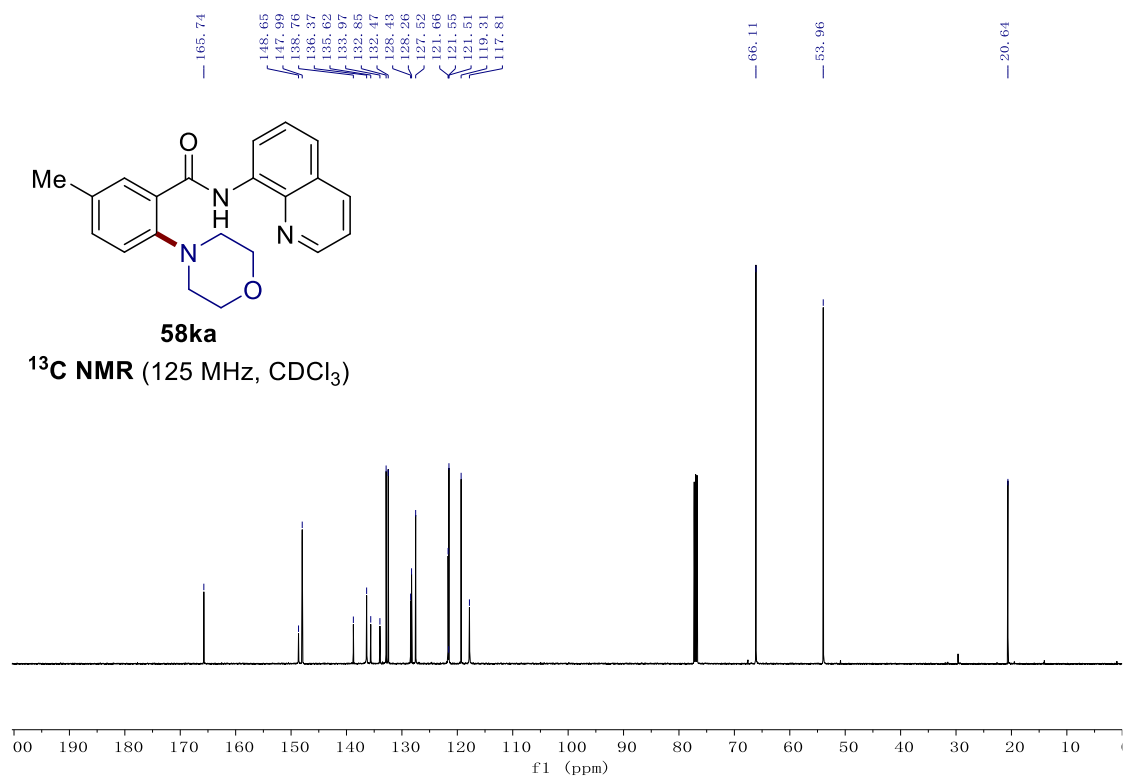
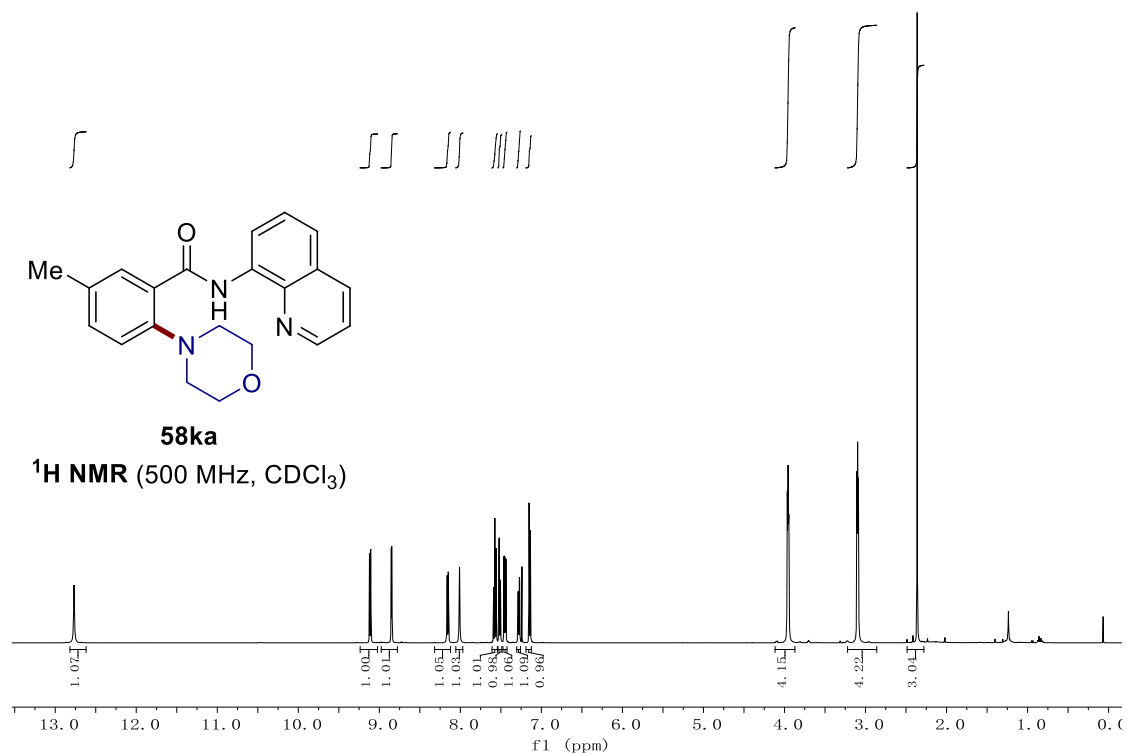


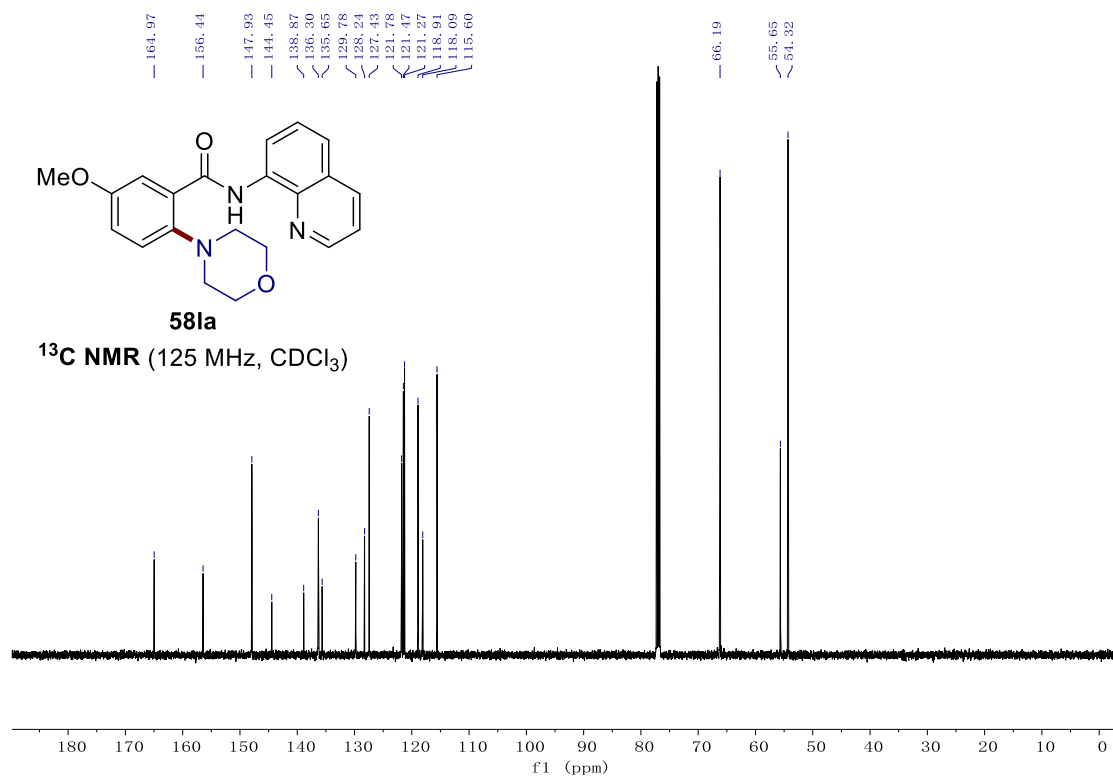
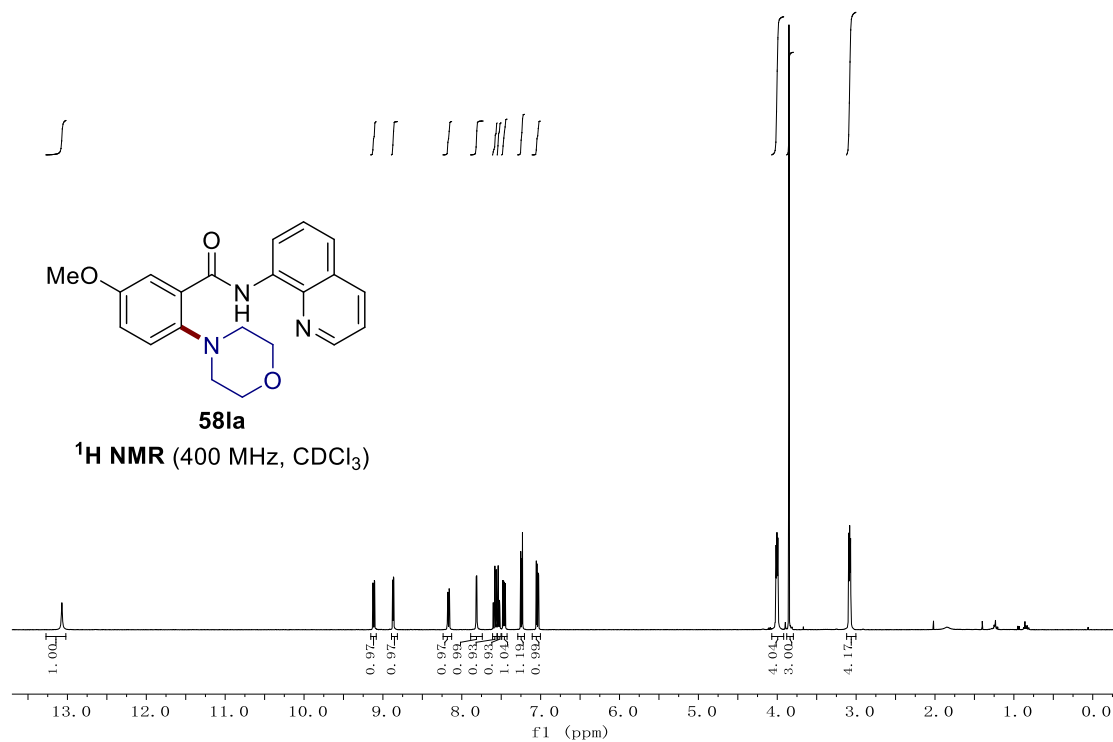
## 7. NMR Spectra



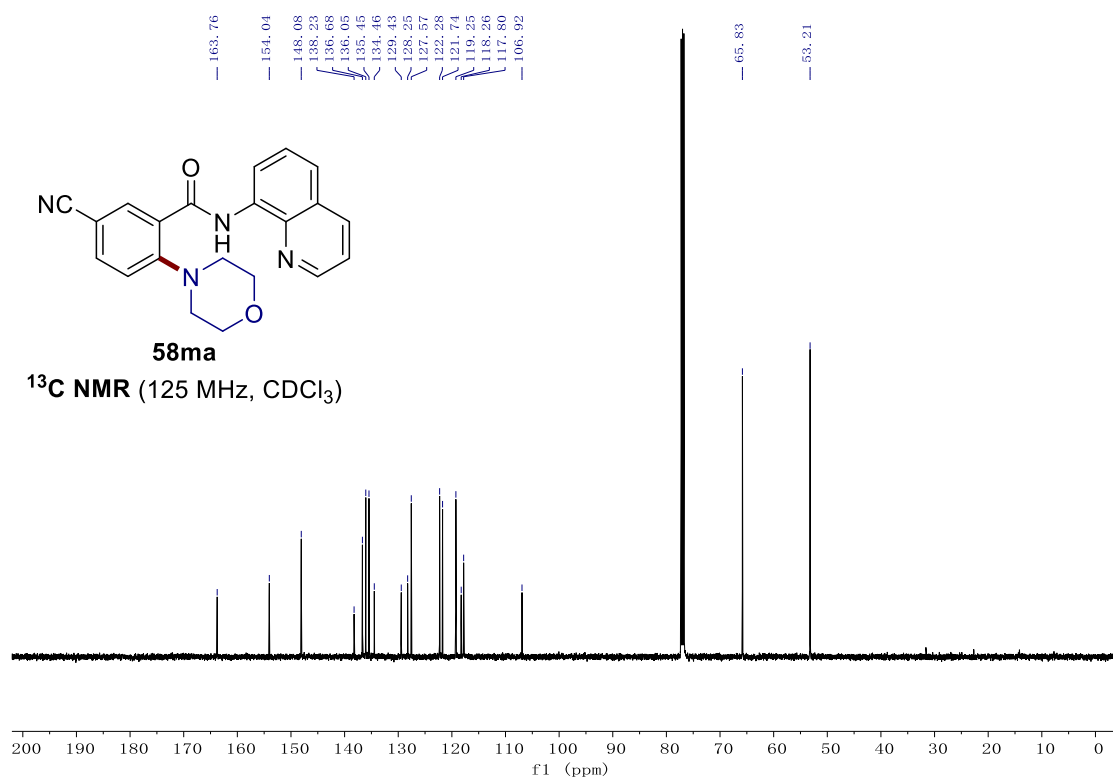
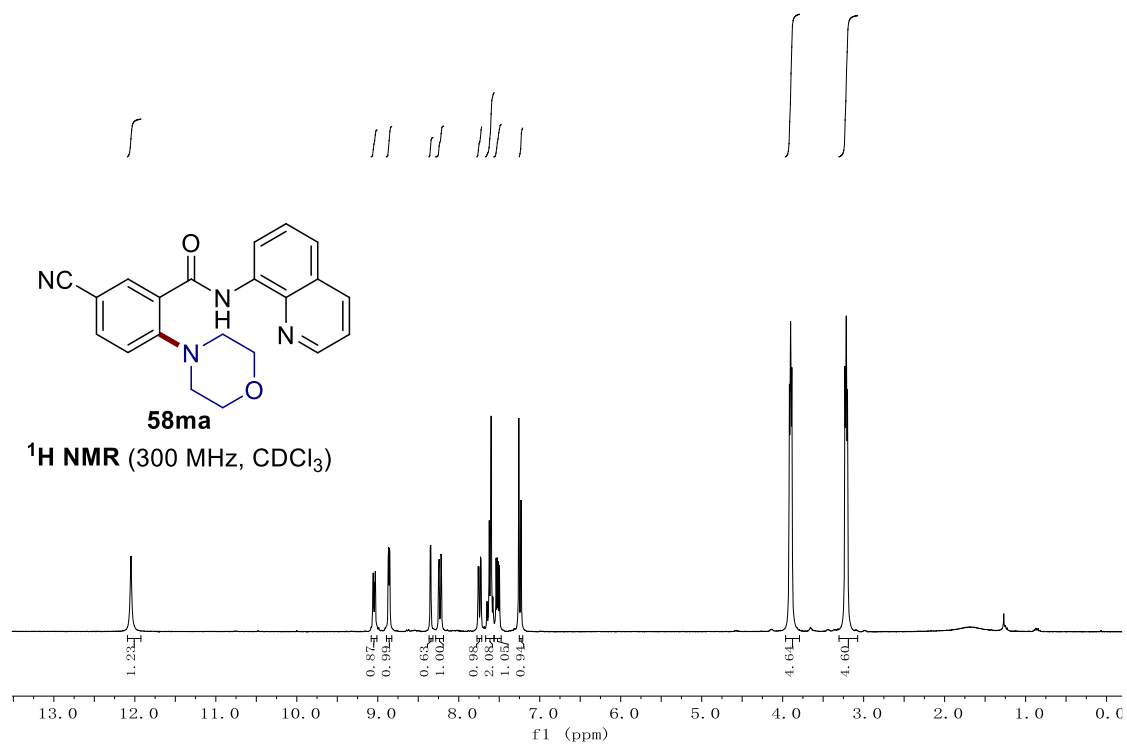


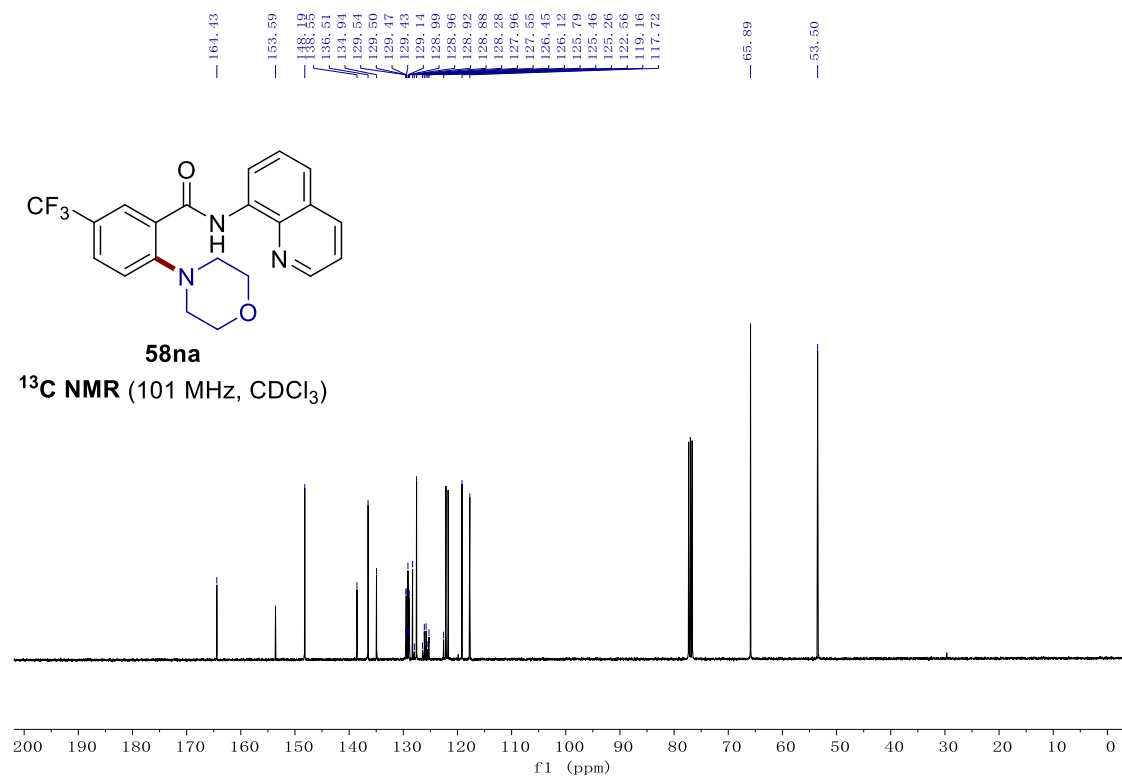
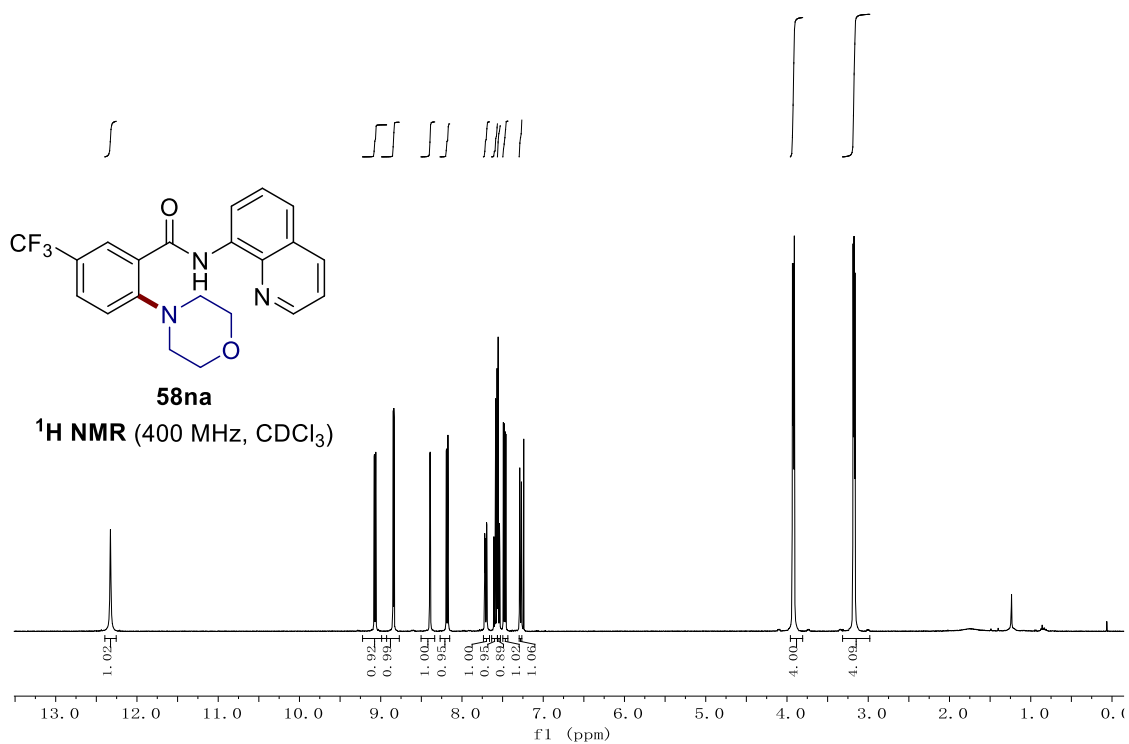
# 7. NMR Spectra



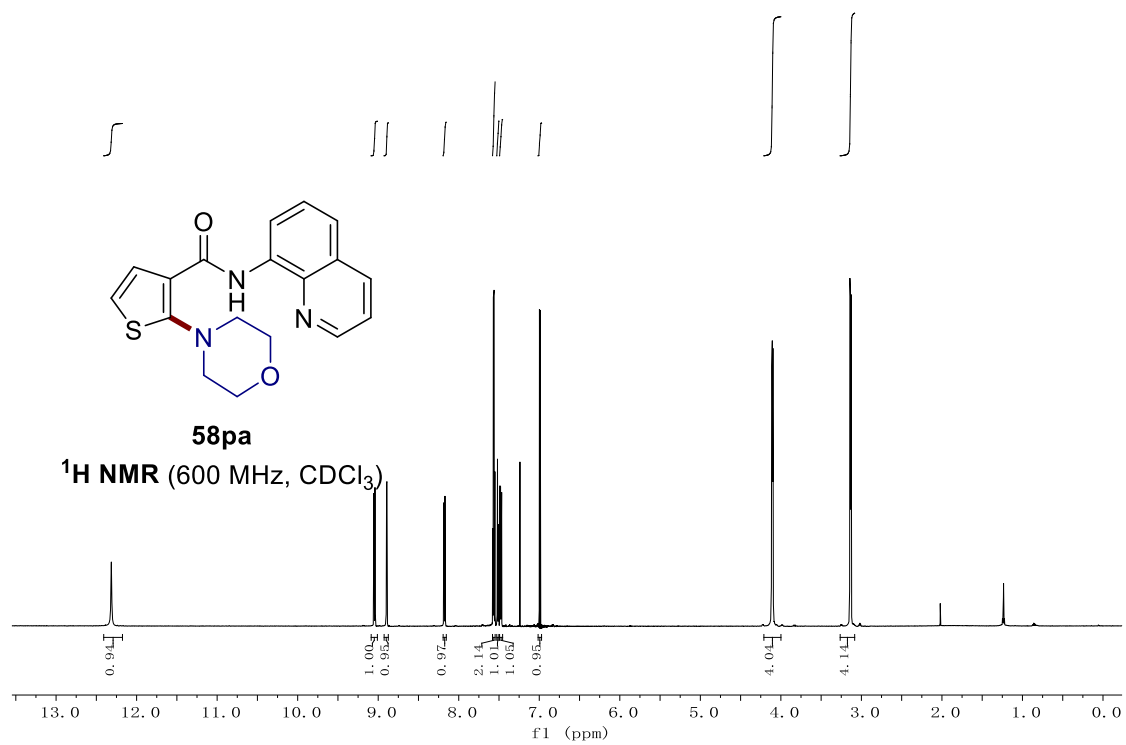
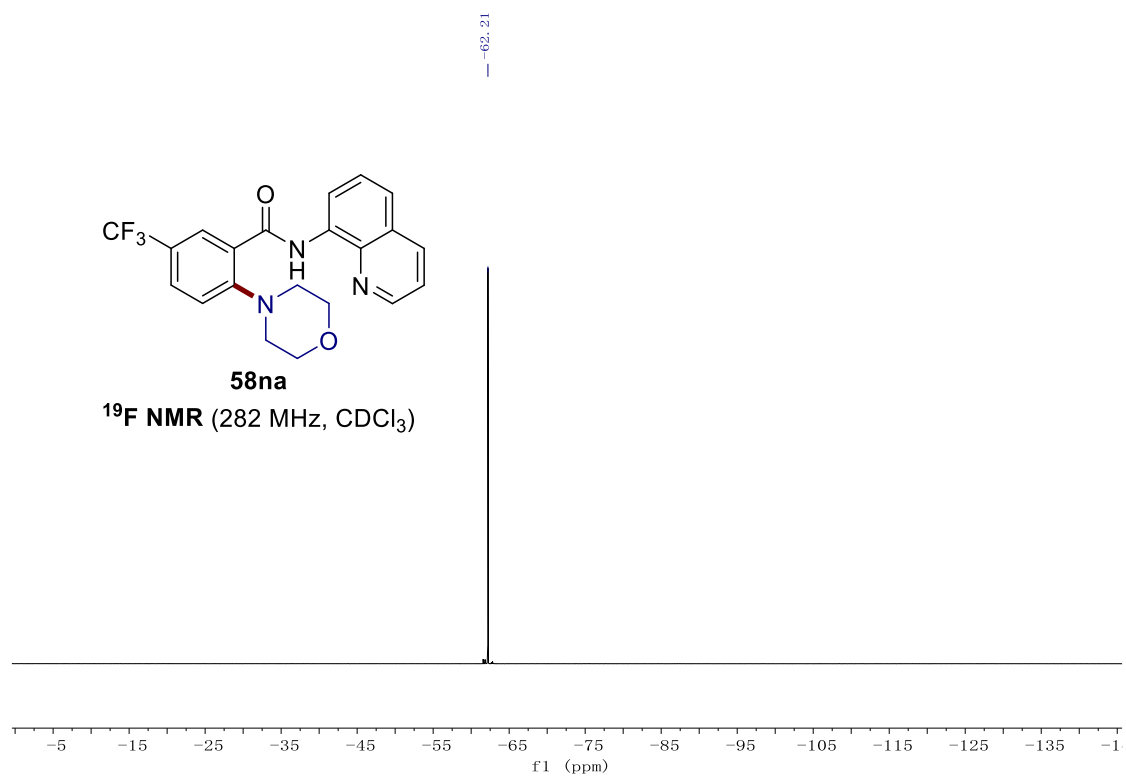


## 7. NMR Spectra

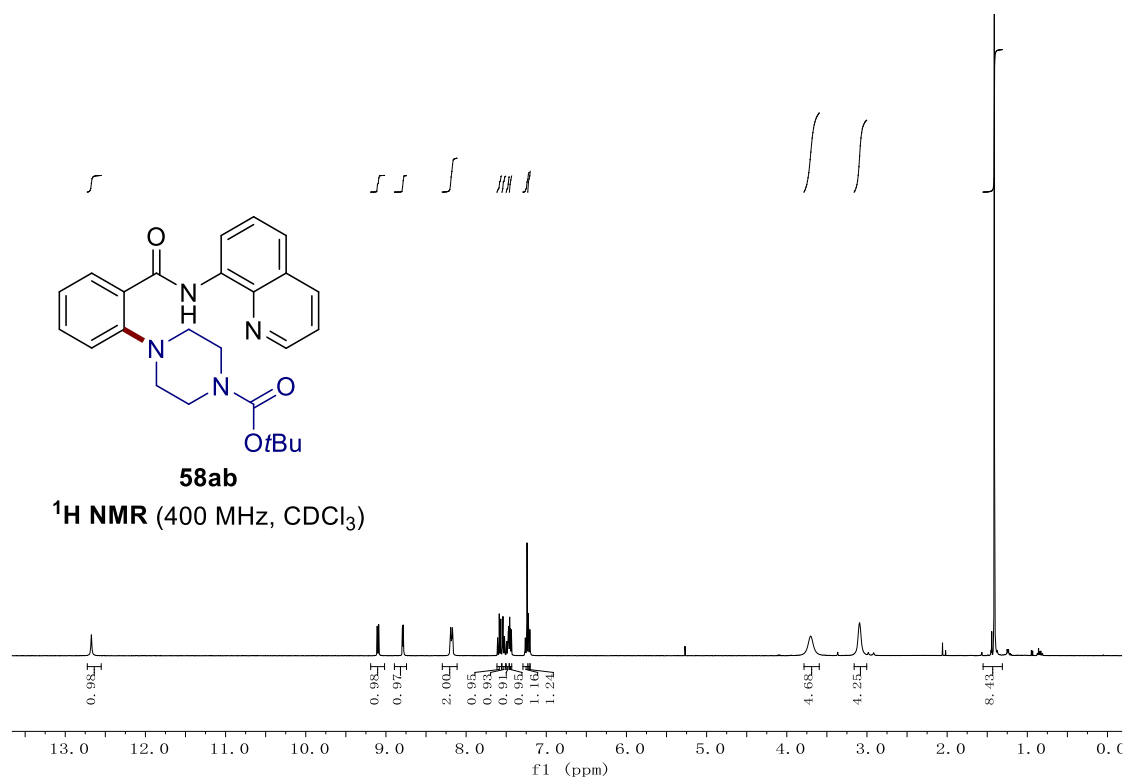
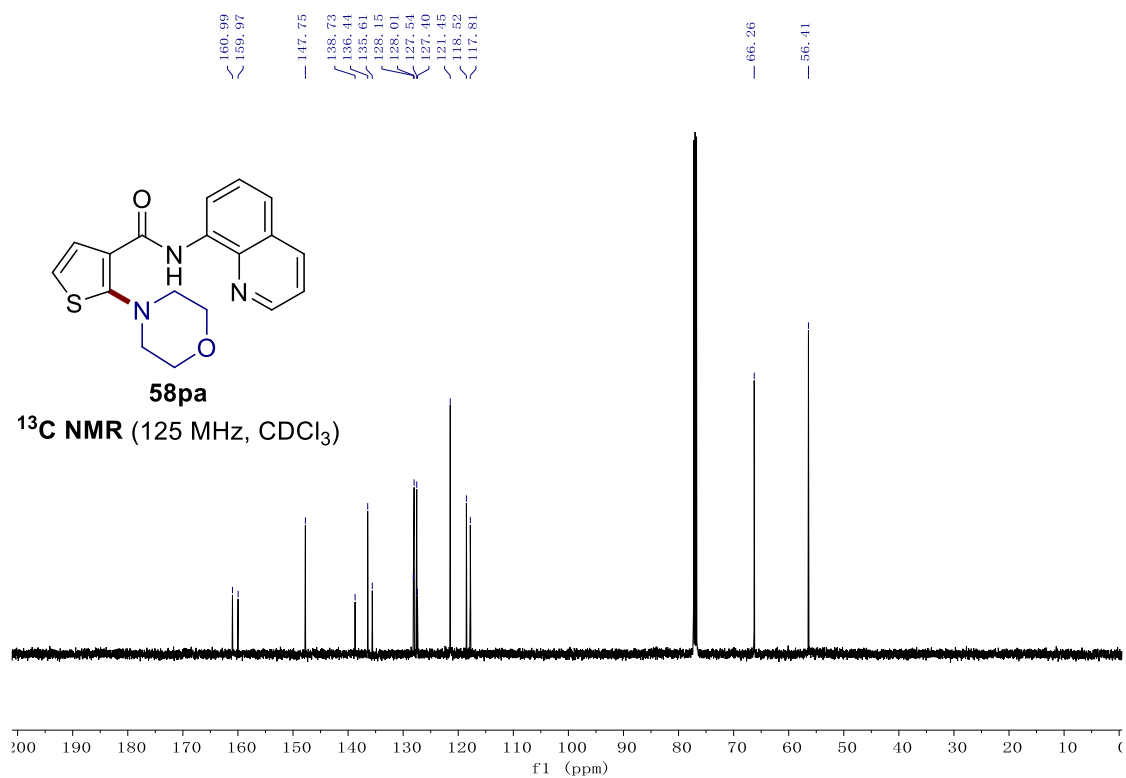




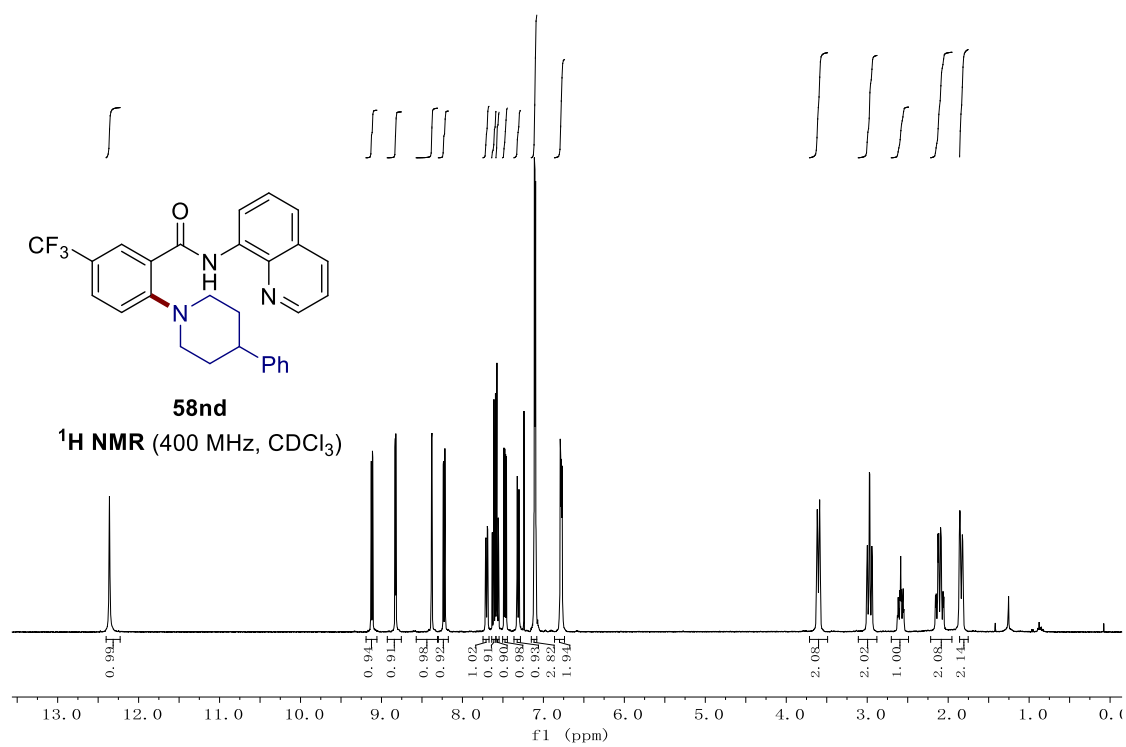
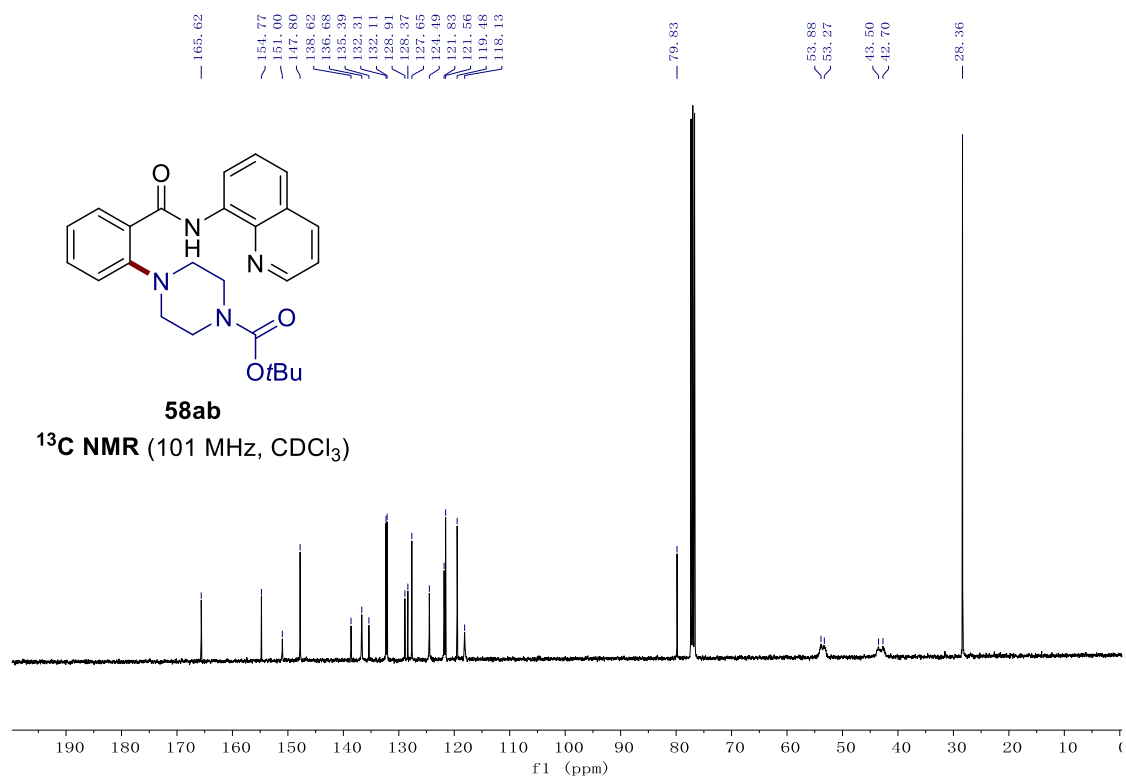
## 7. NMR Spectra



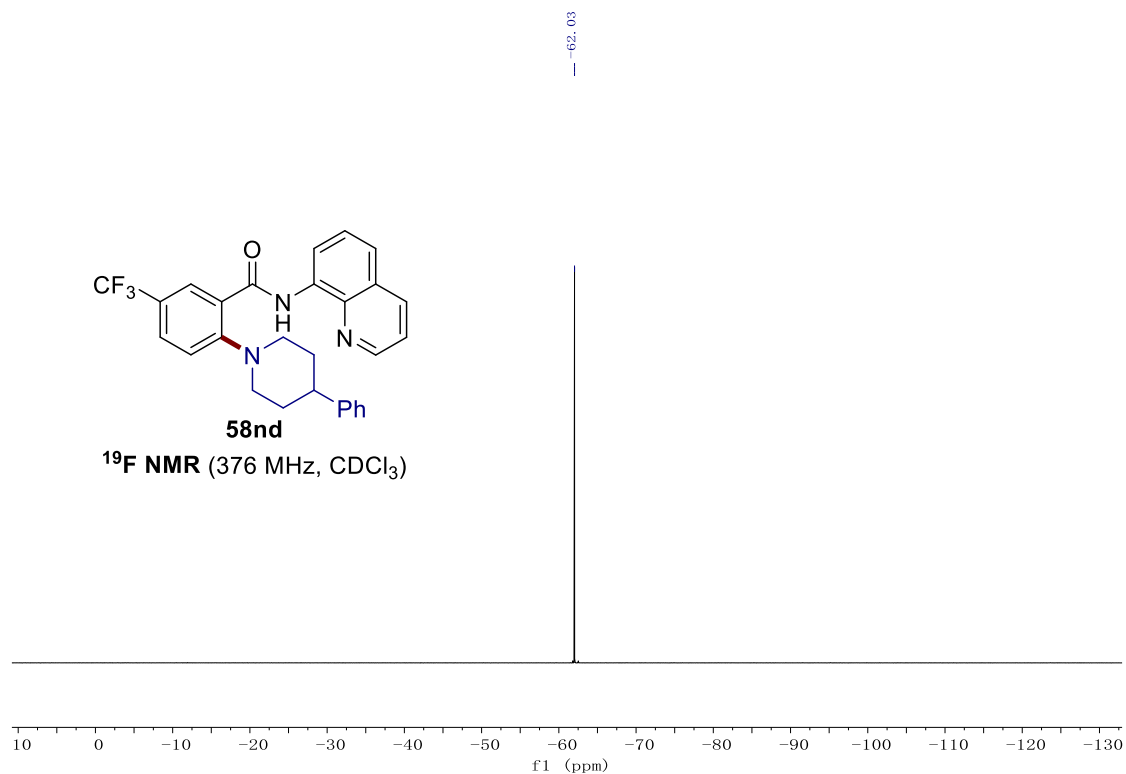
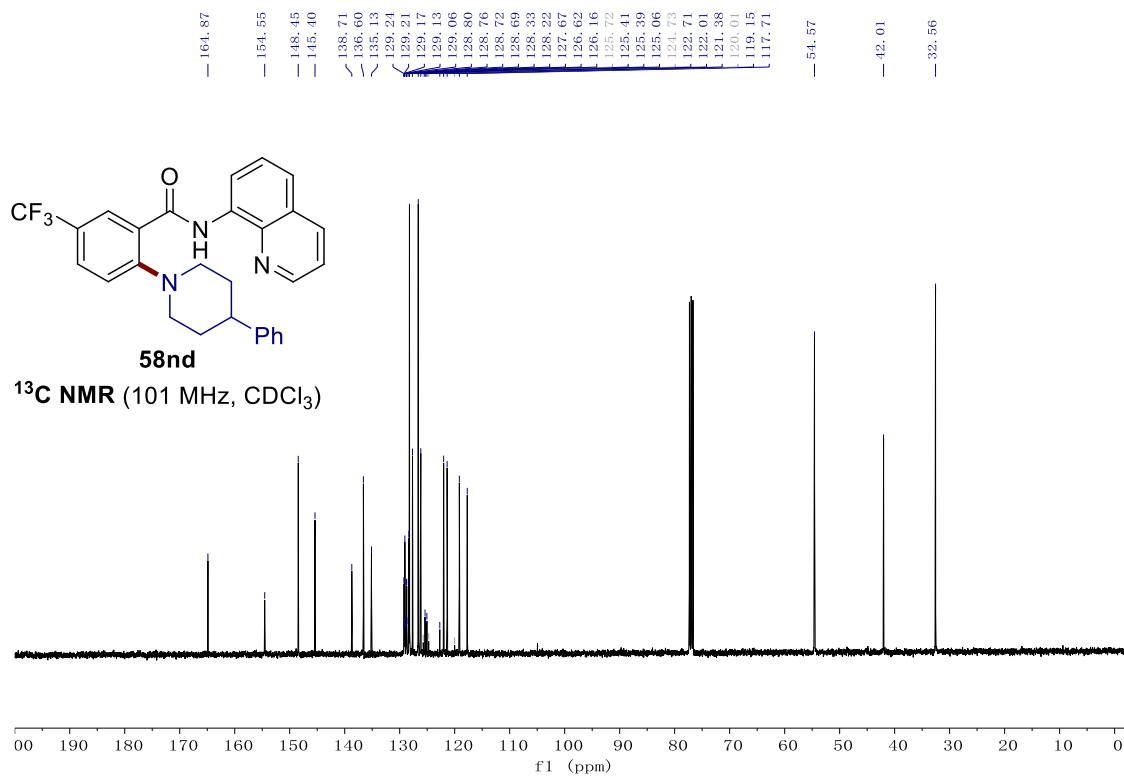




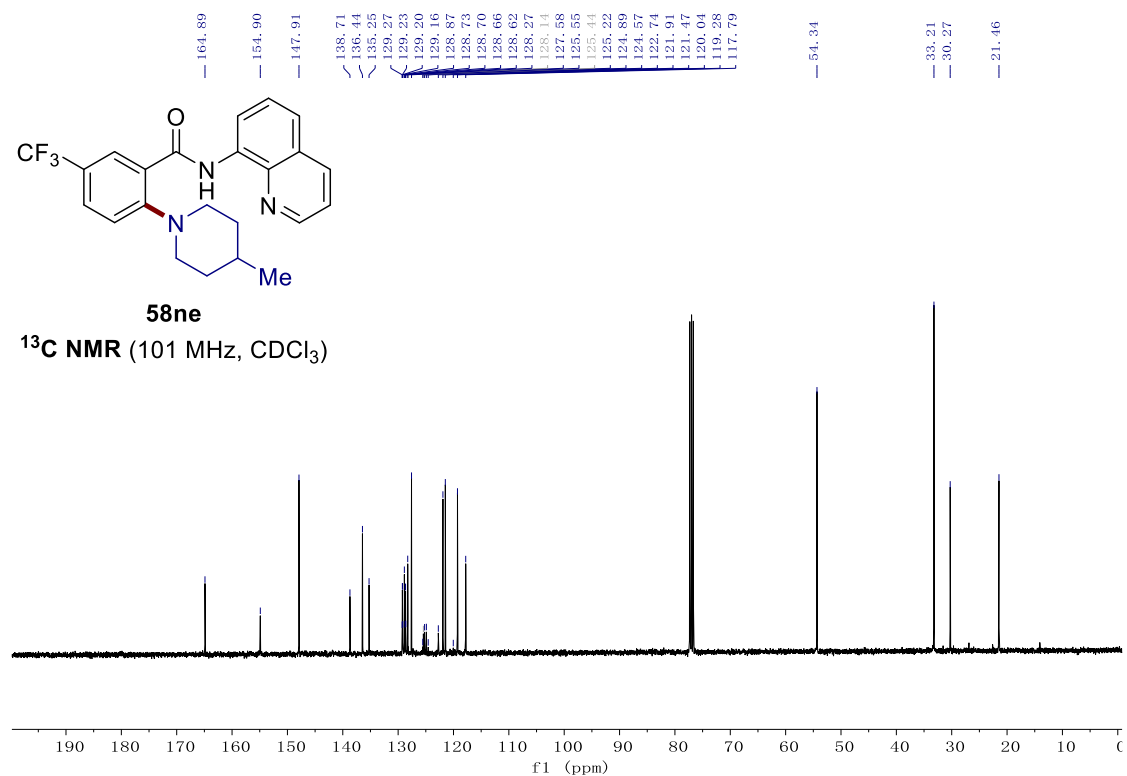
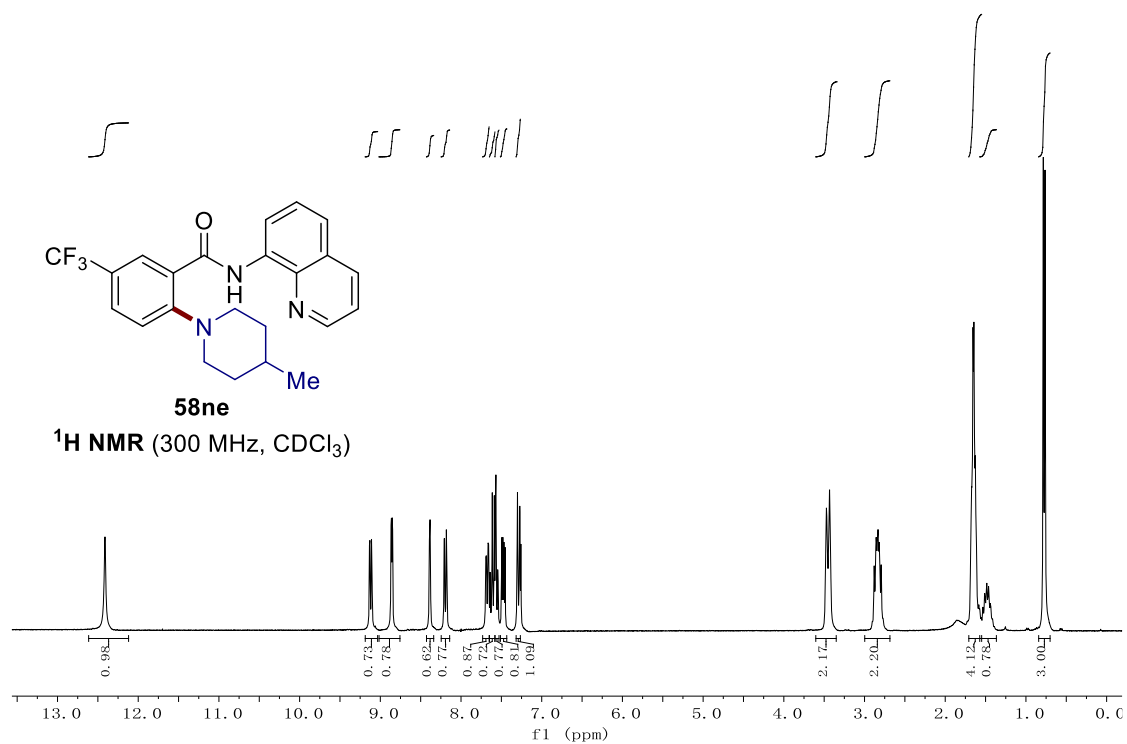
## 7. NMR Spectra

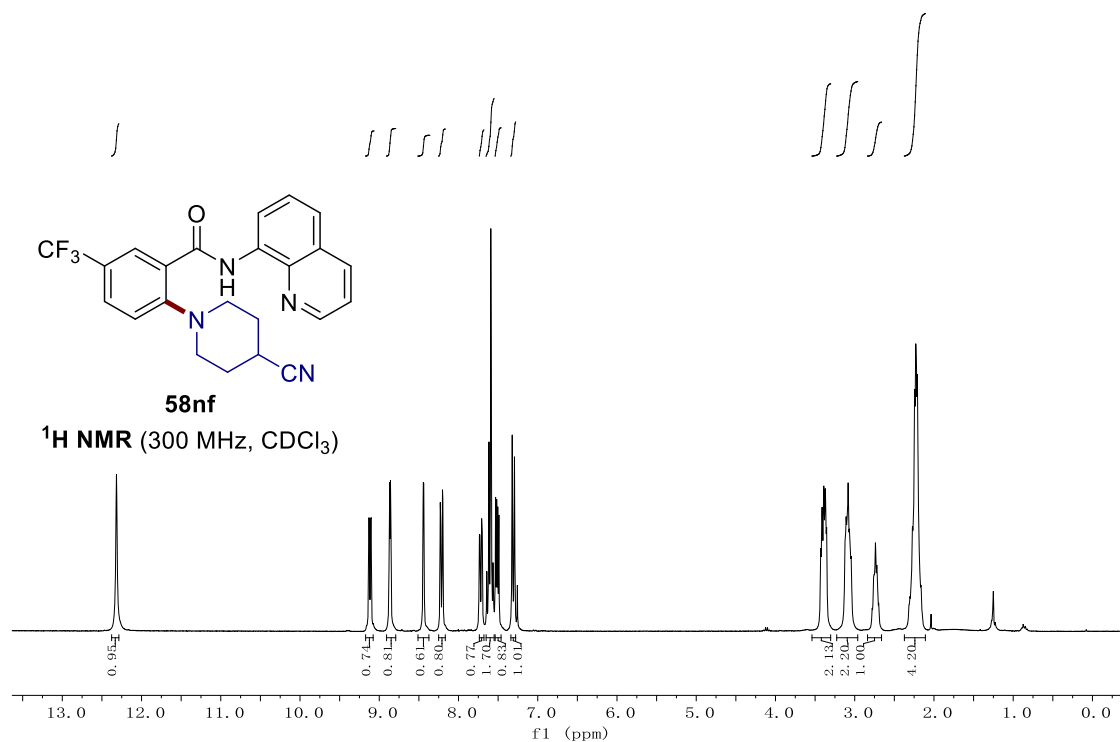
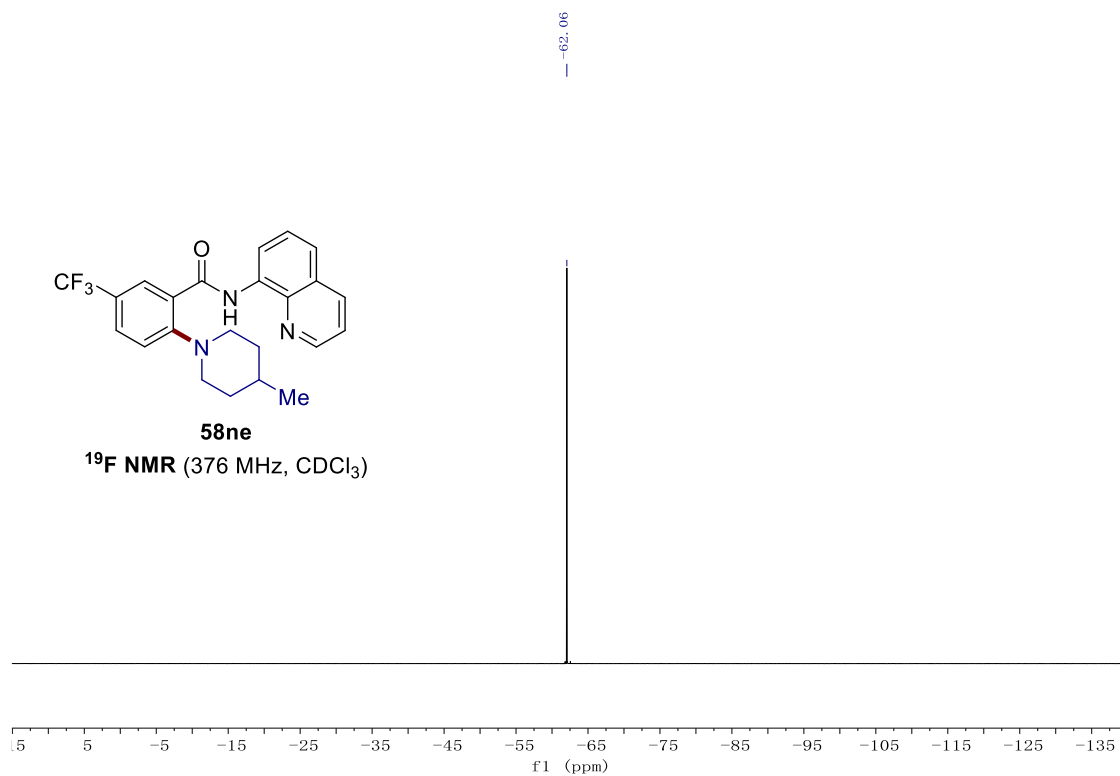


7. NMR Spectra

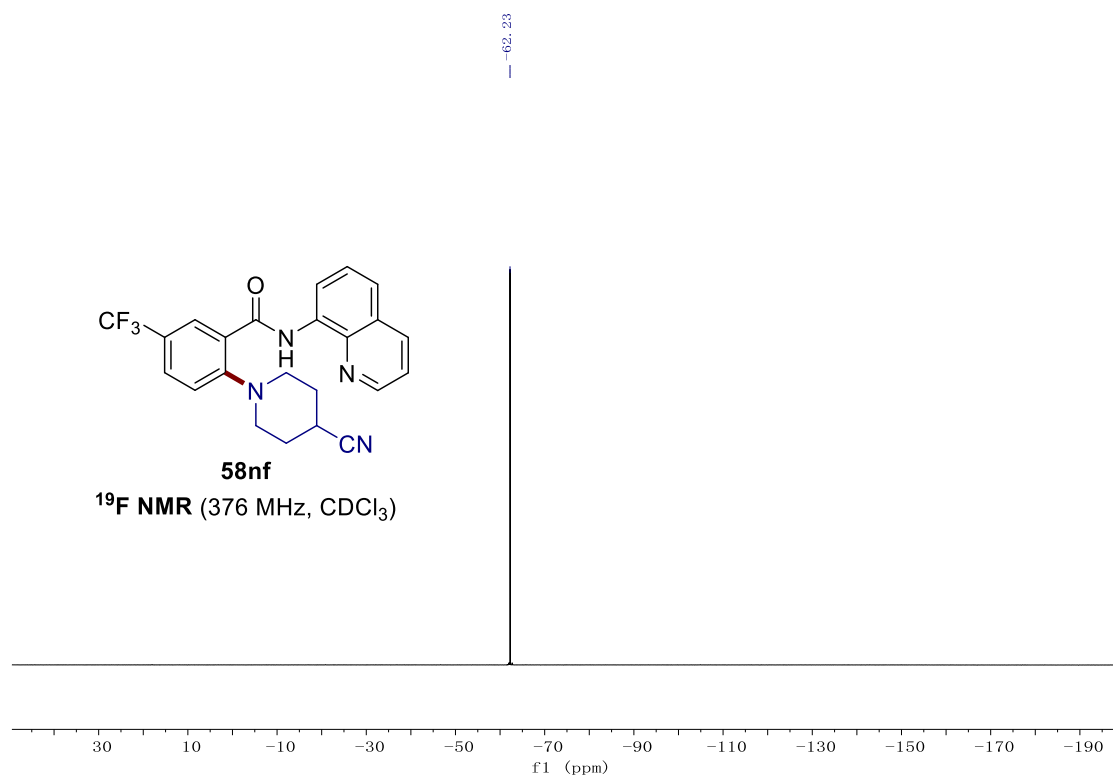
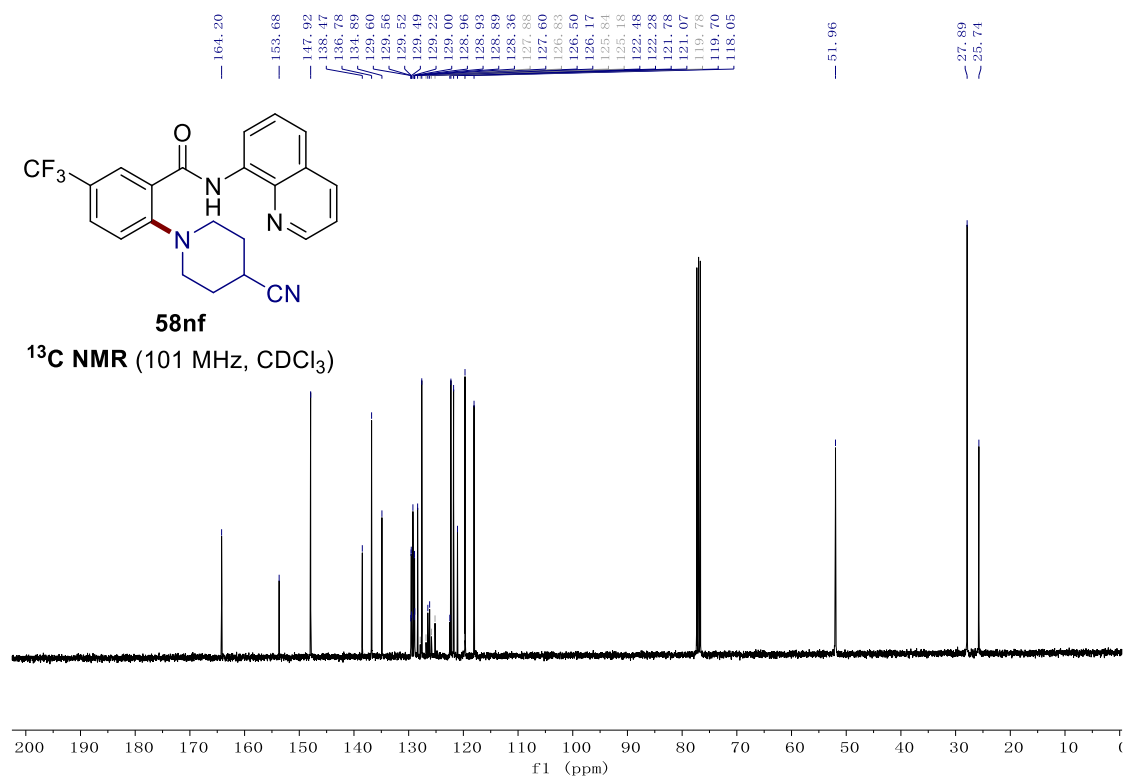


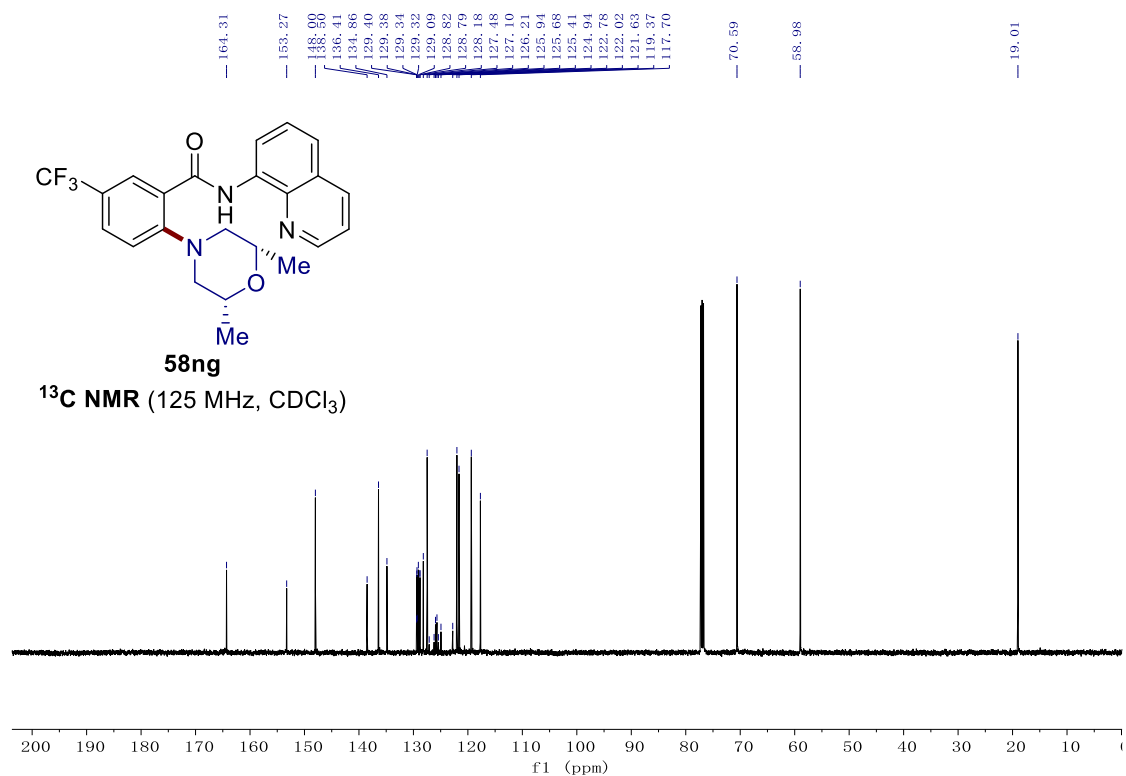
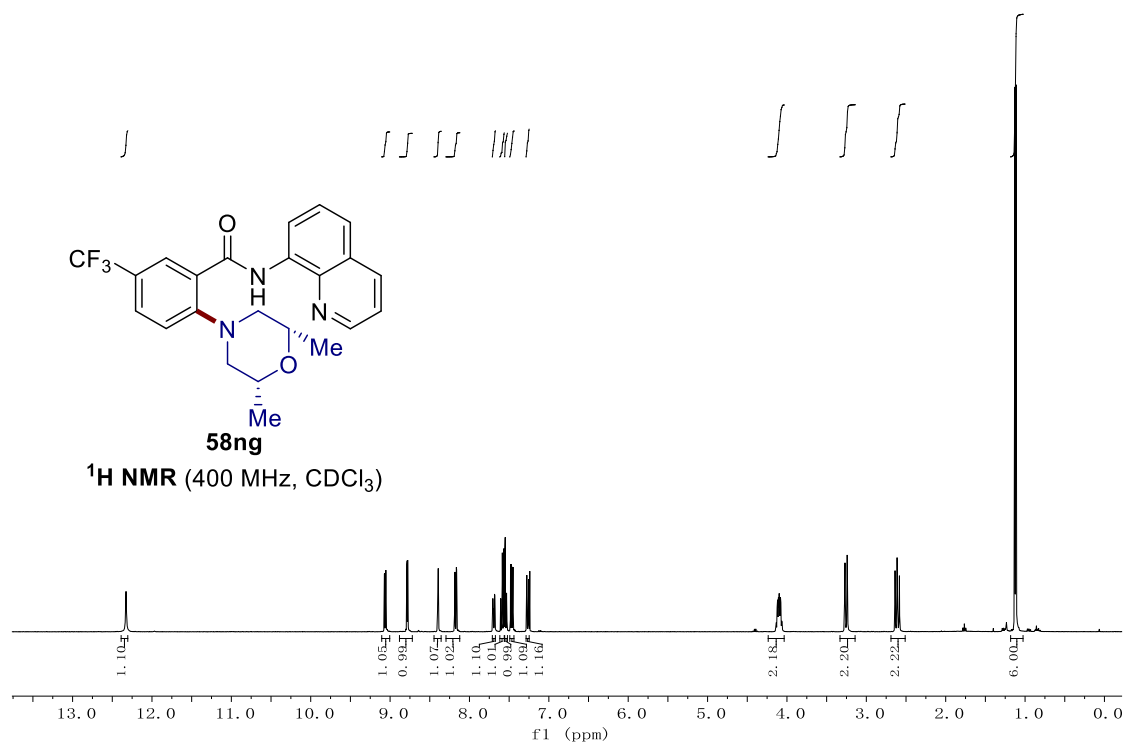
## 7. NMR Spectra



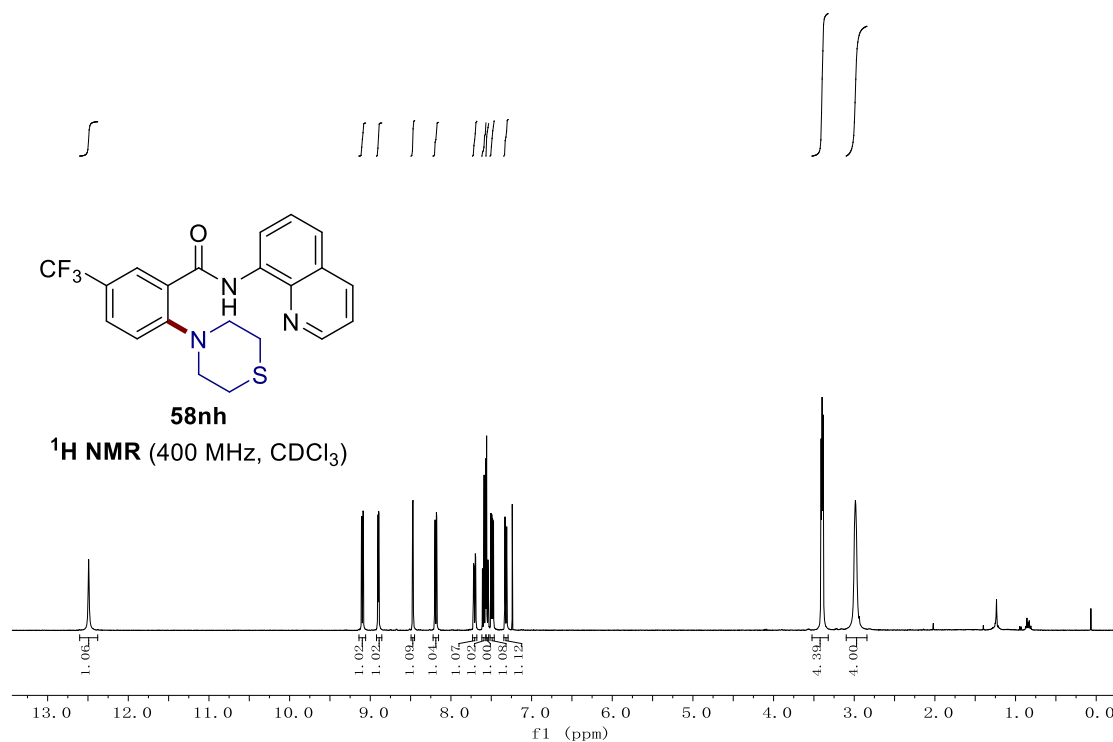
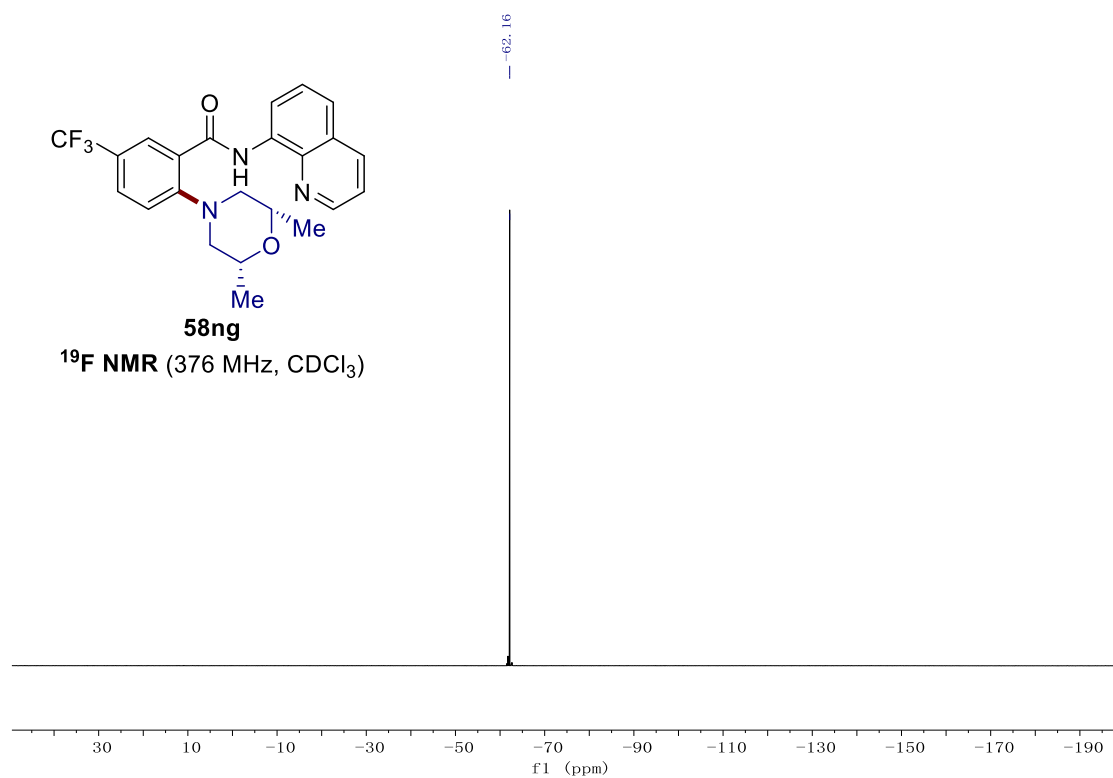


## 7. NMR Spectra

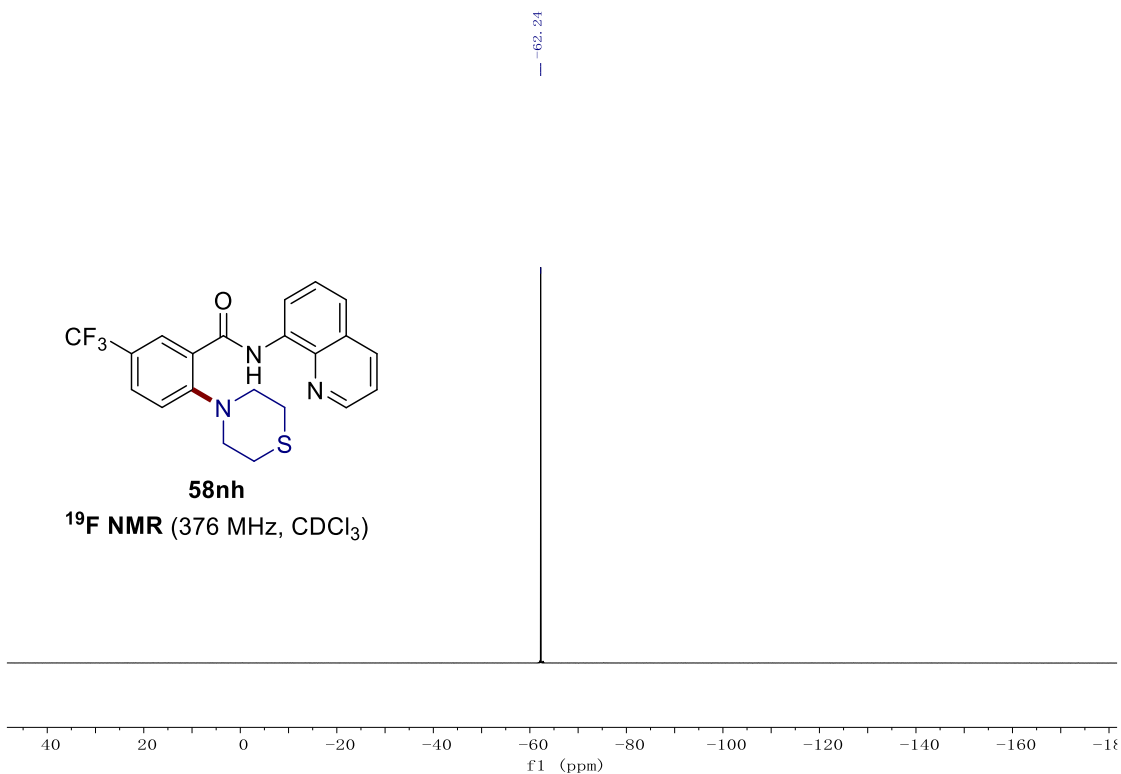
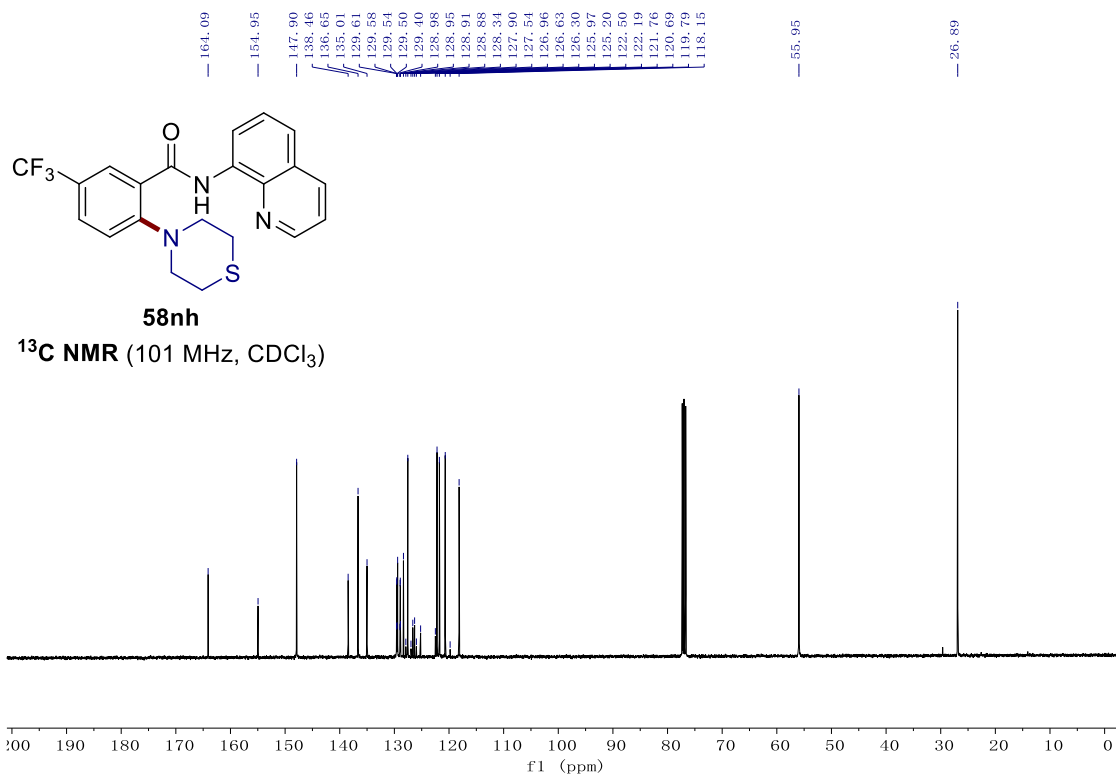




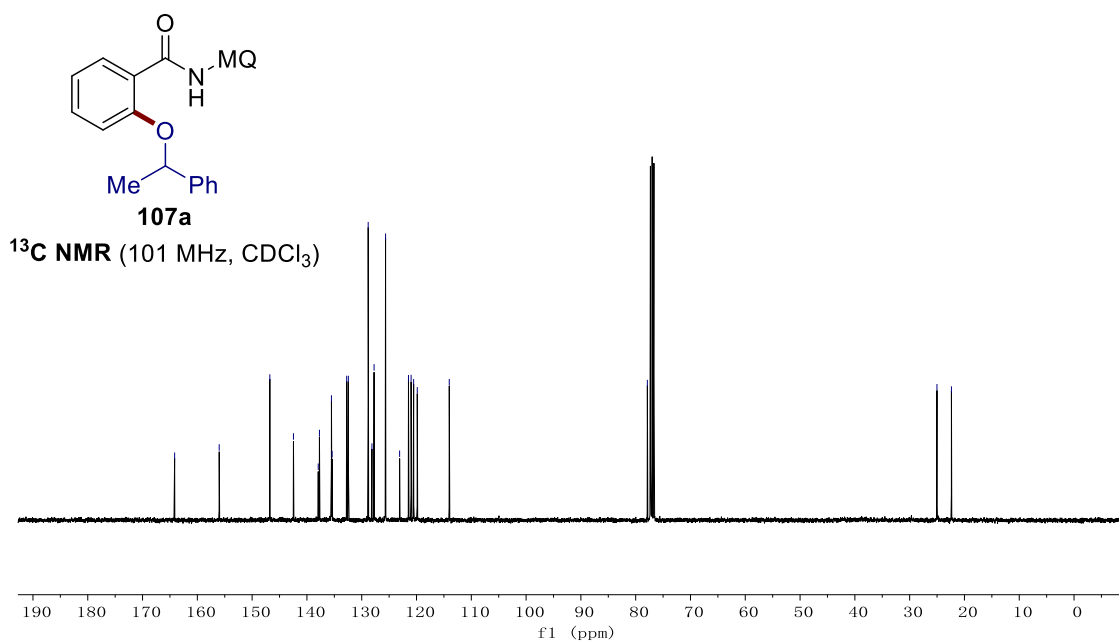
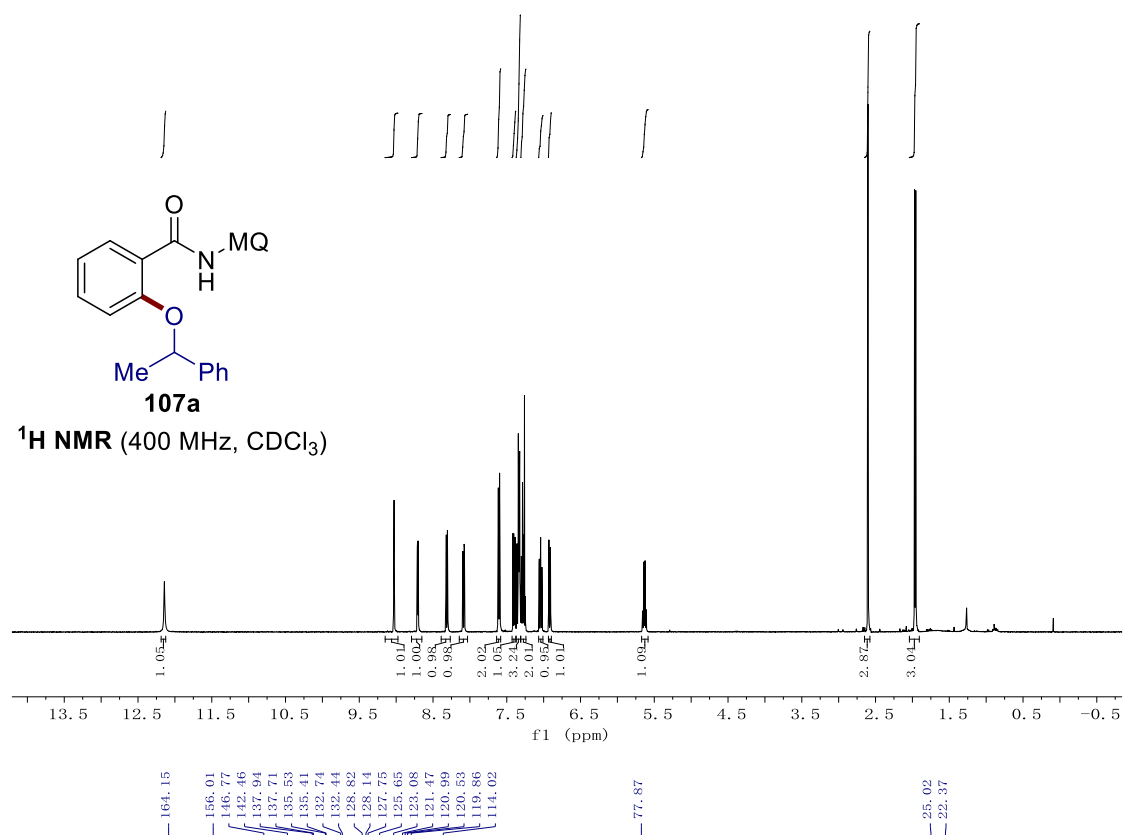
## 7. NMR Spectra

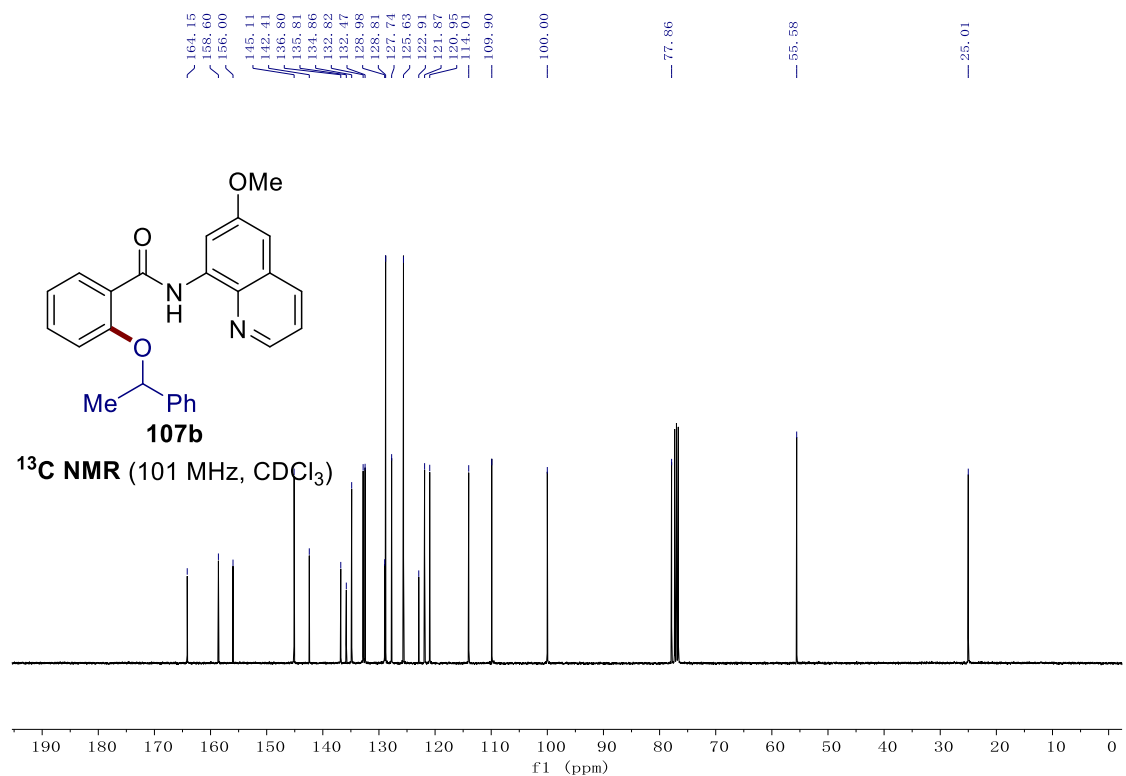
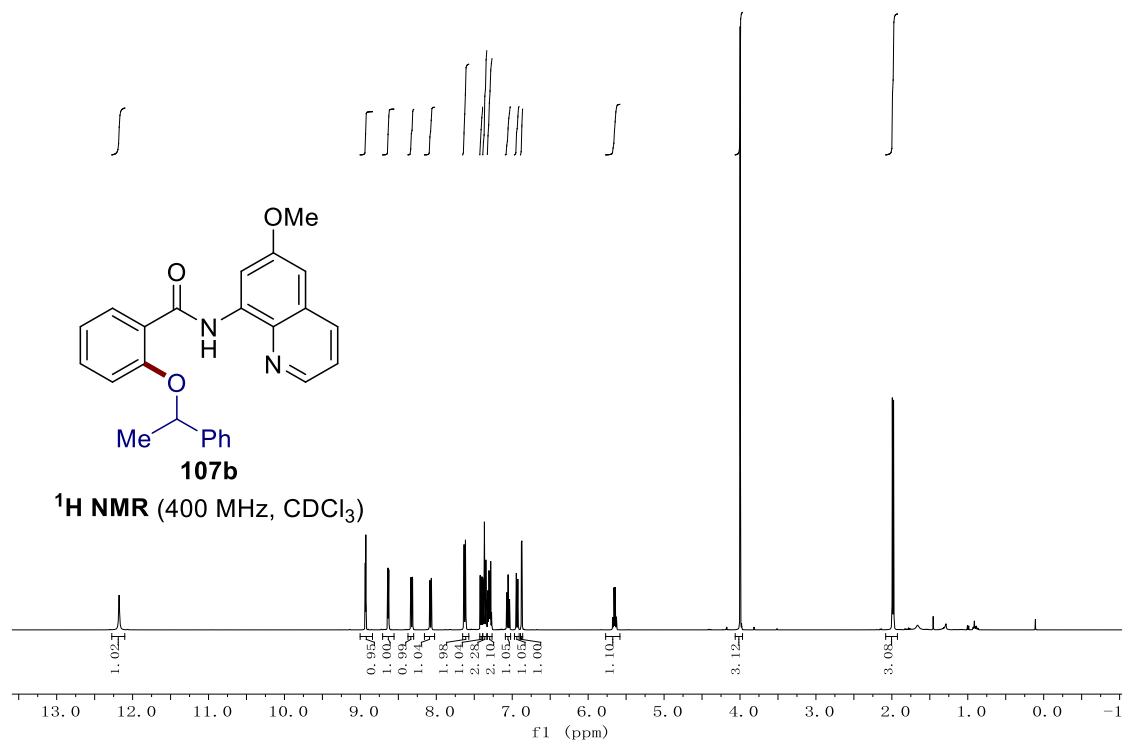




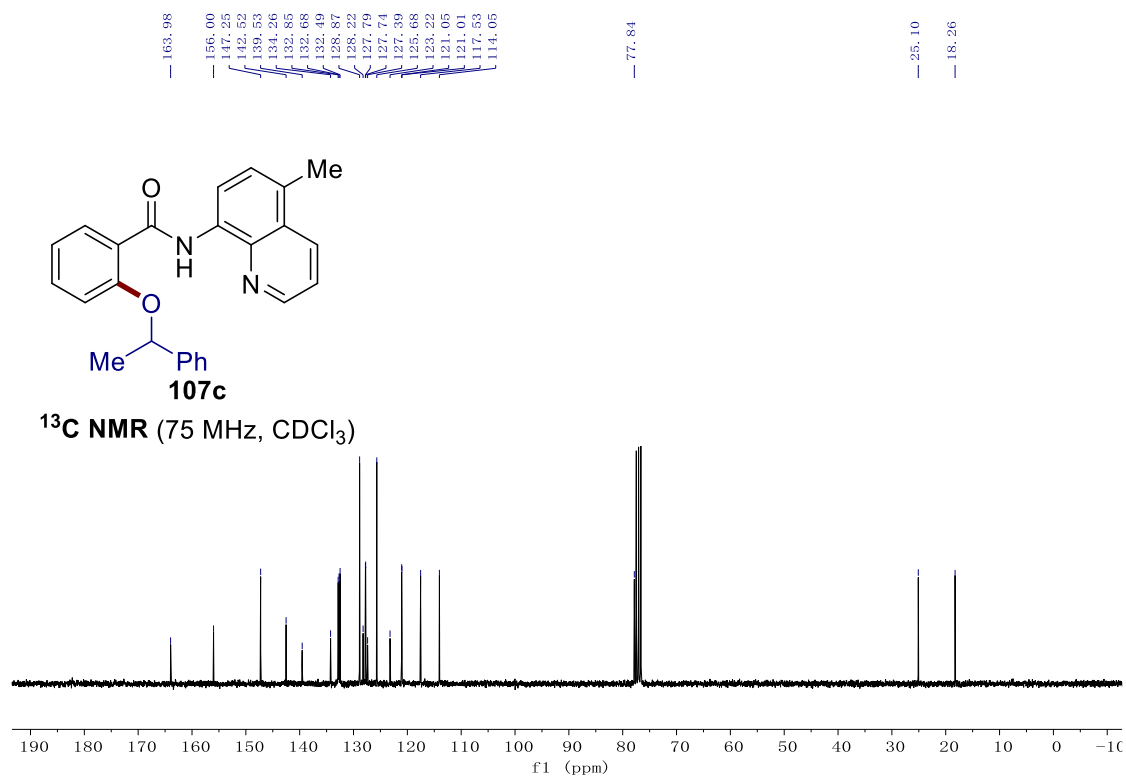
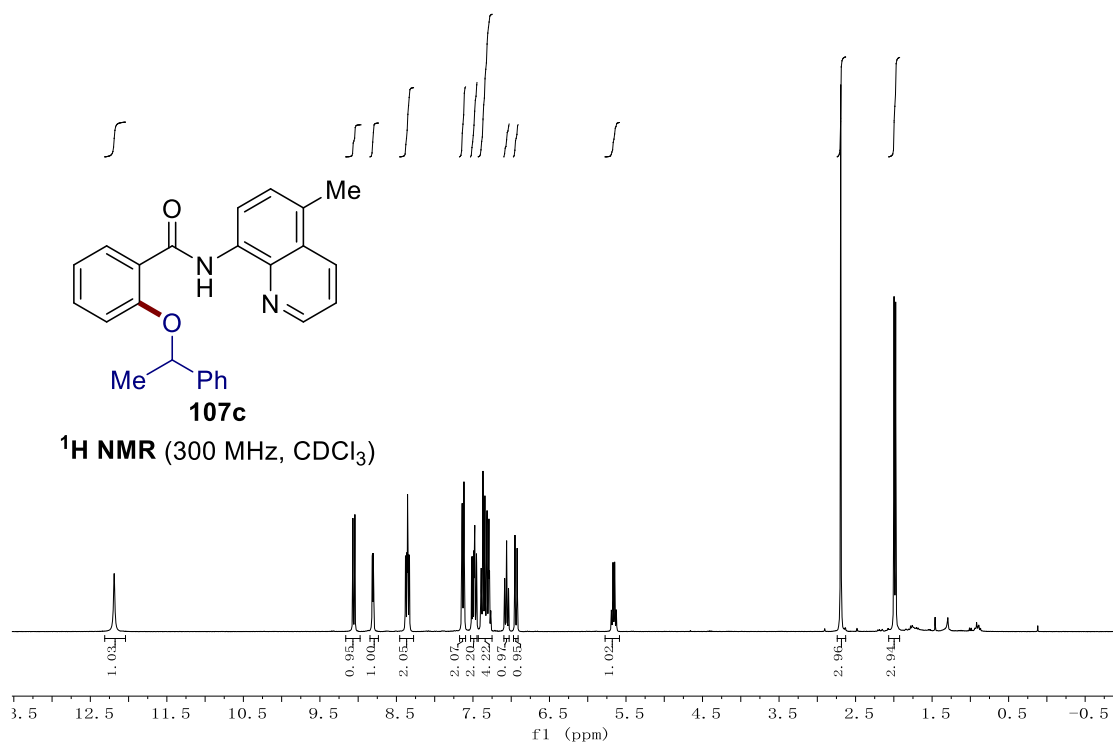


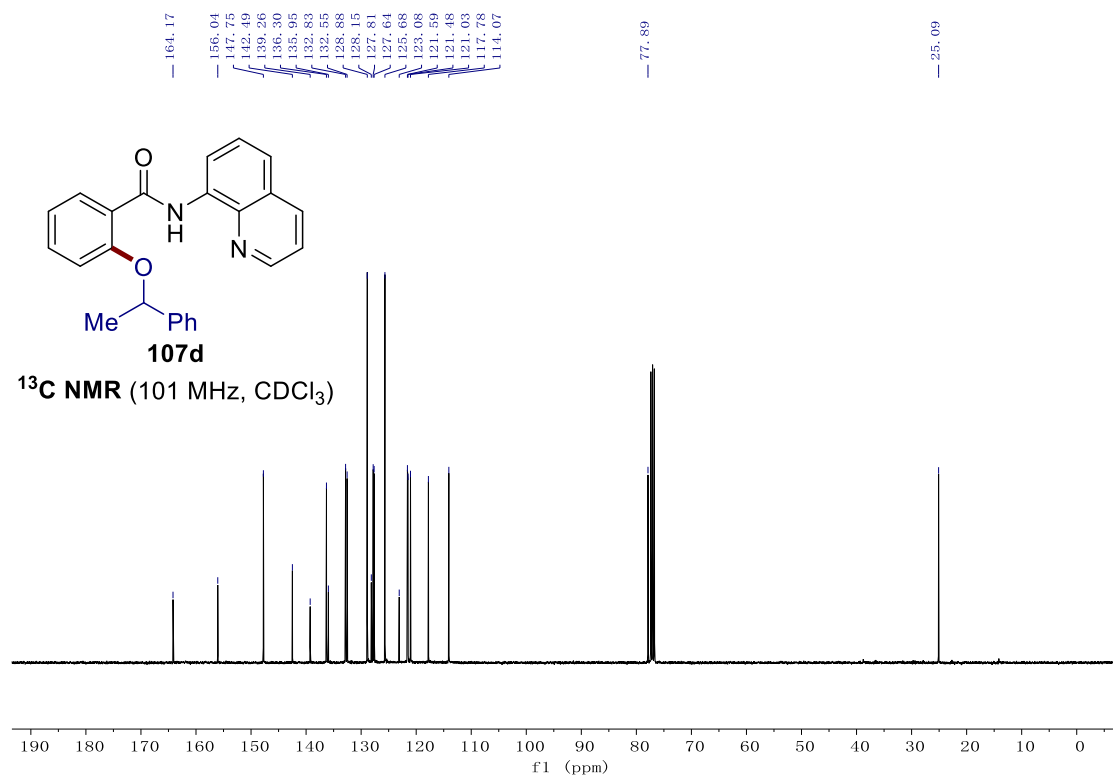
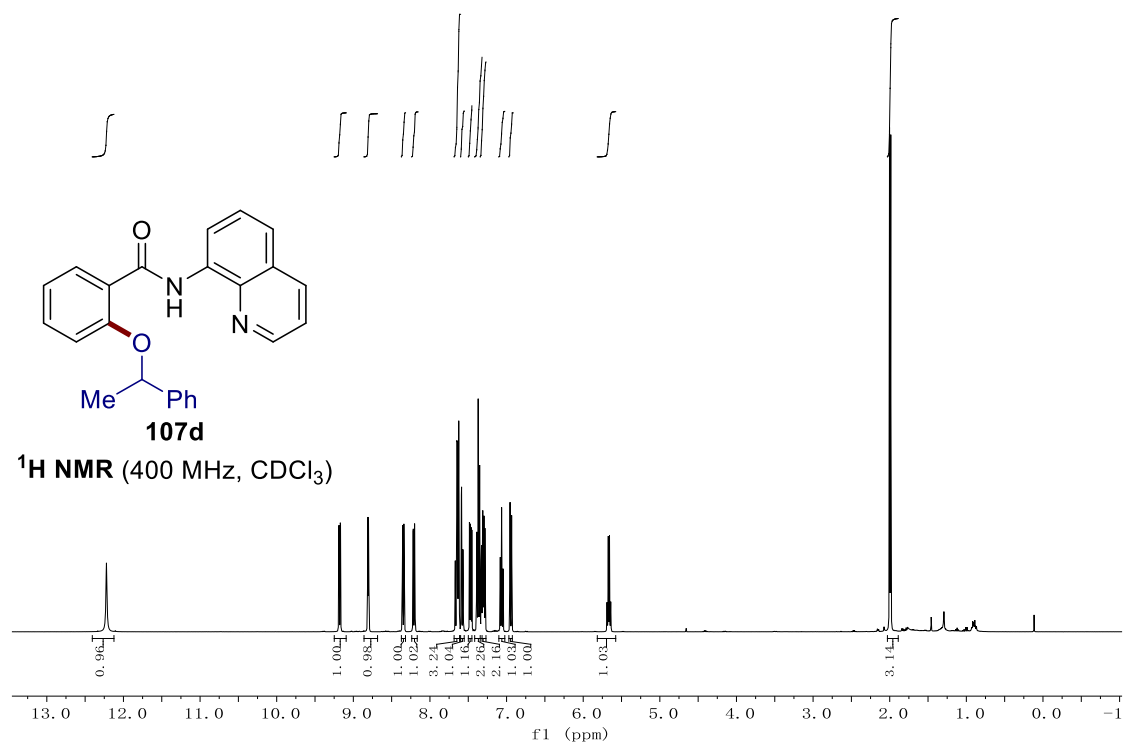
## 7.5 Nickel-Electrocatalyzed C–H Alkoxylation



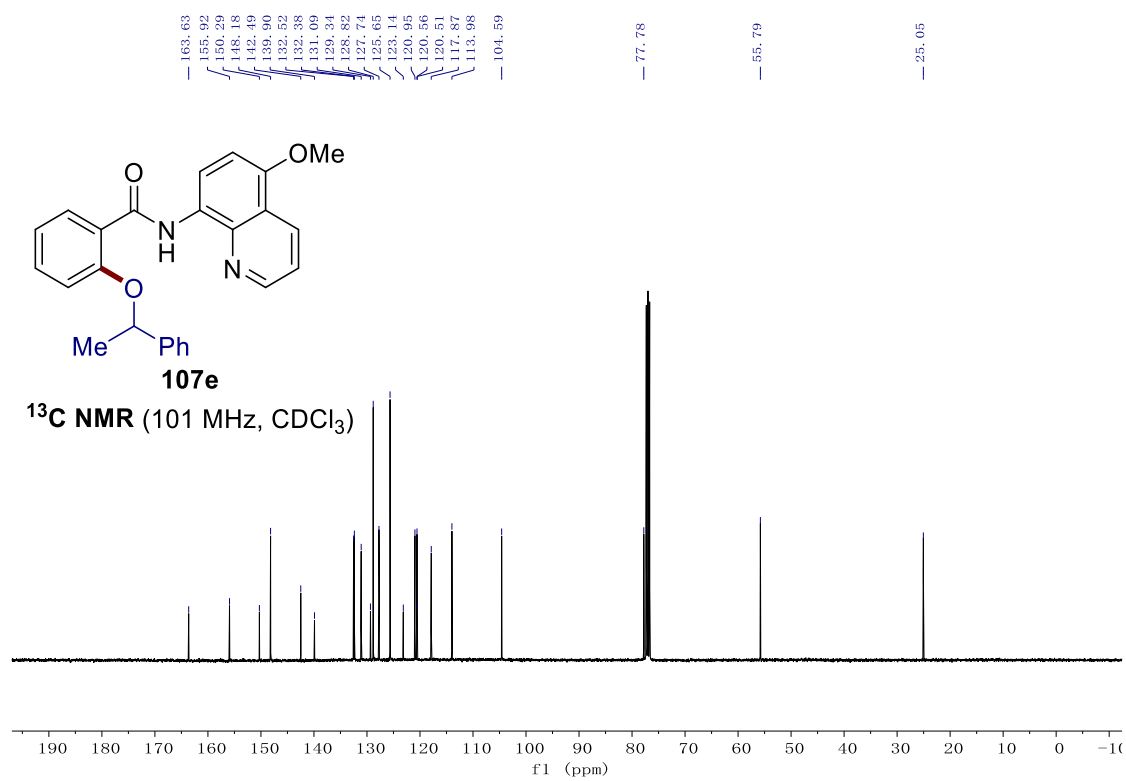
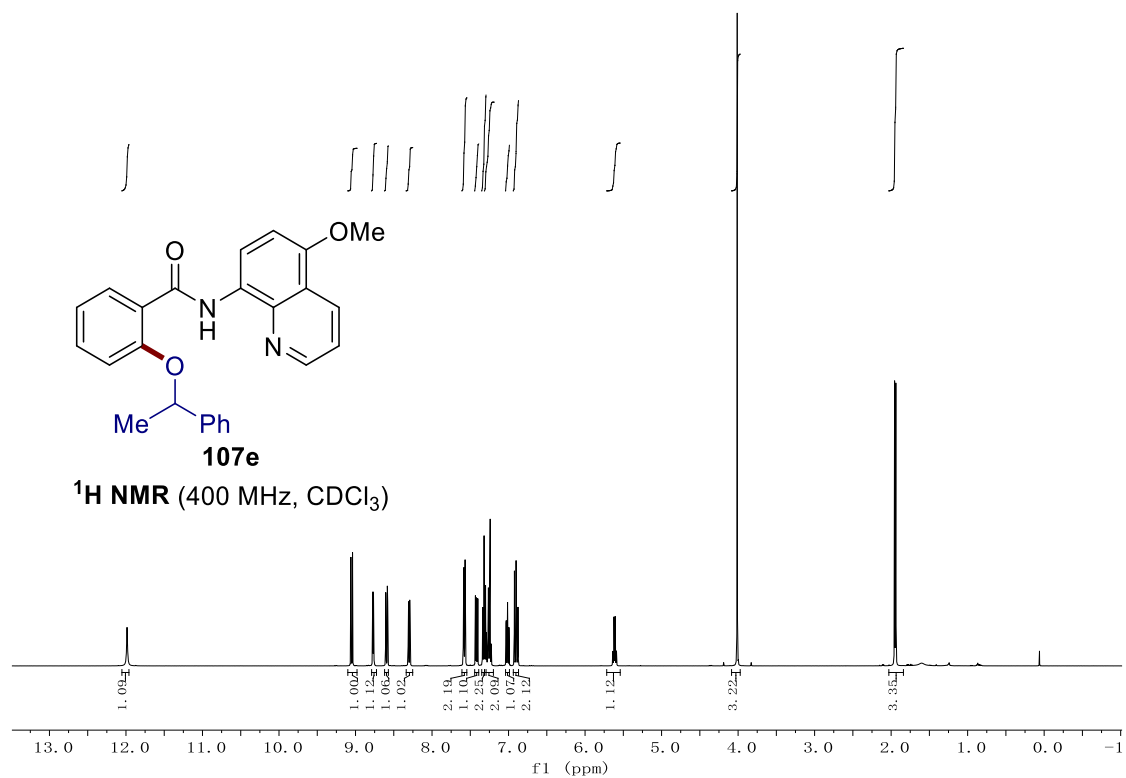


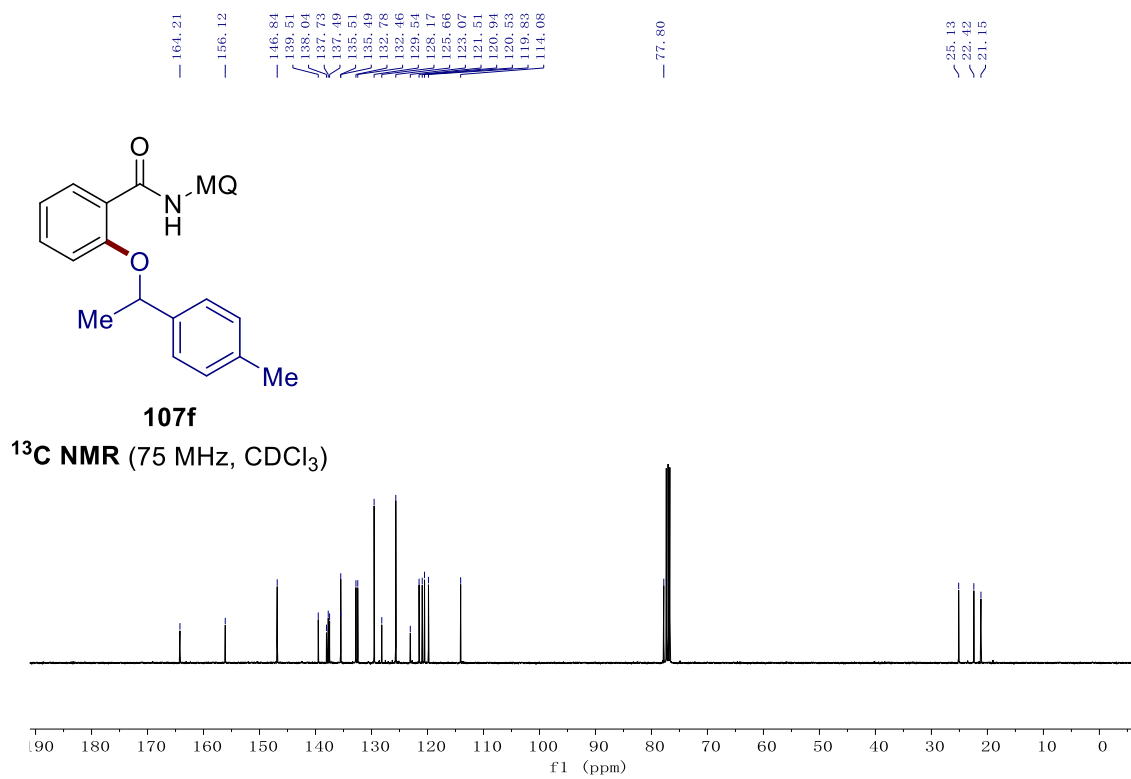
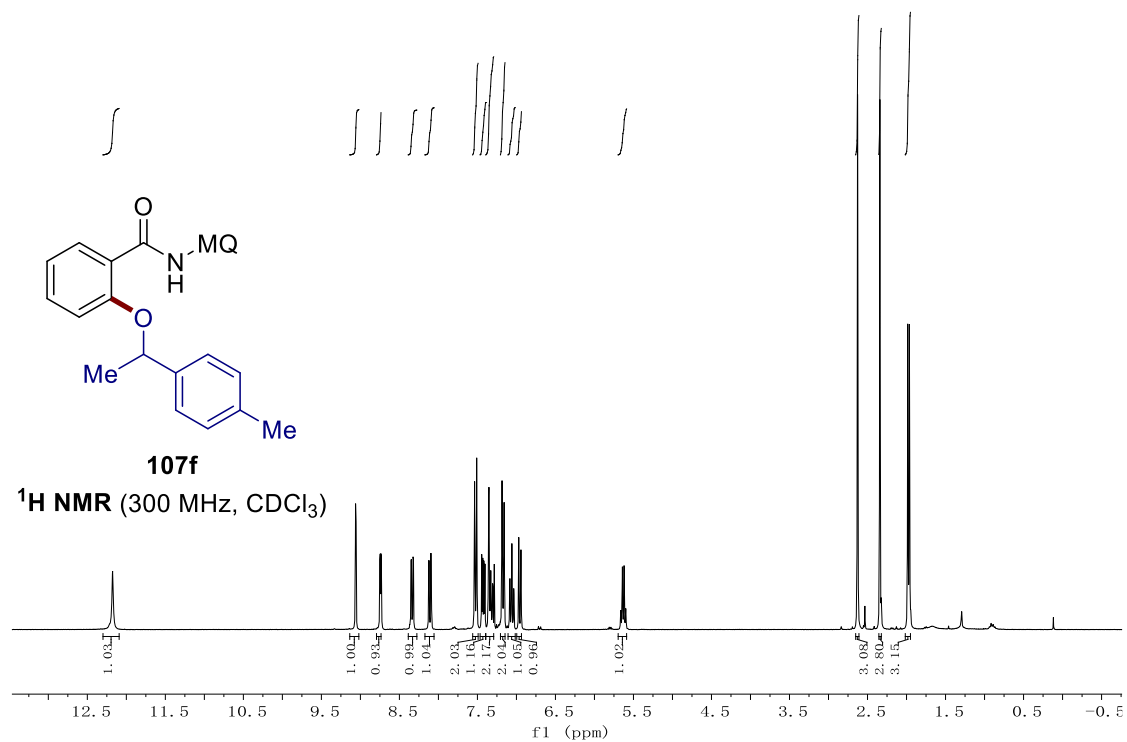
## 7. NMR Spectra



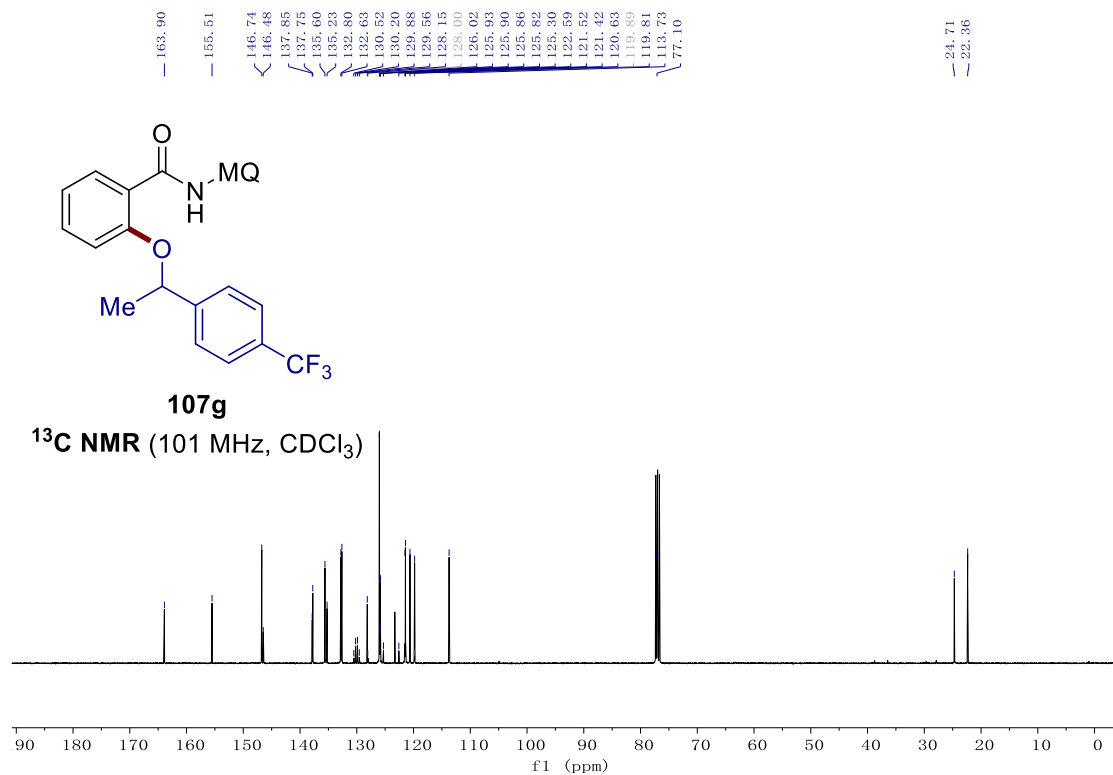
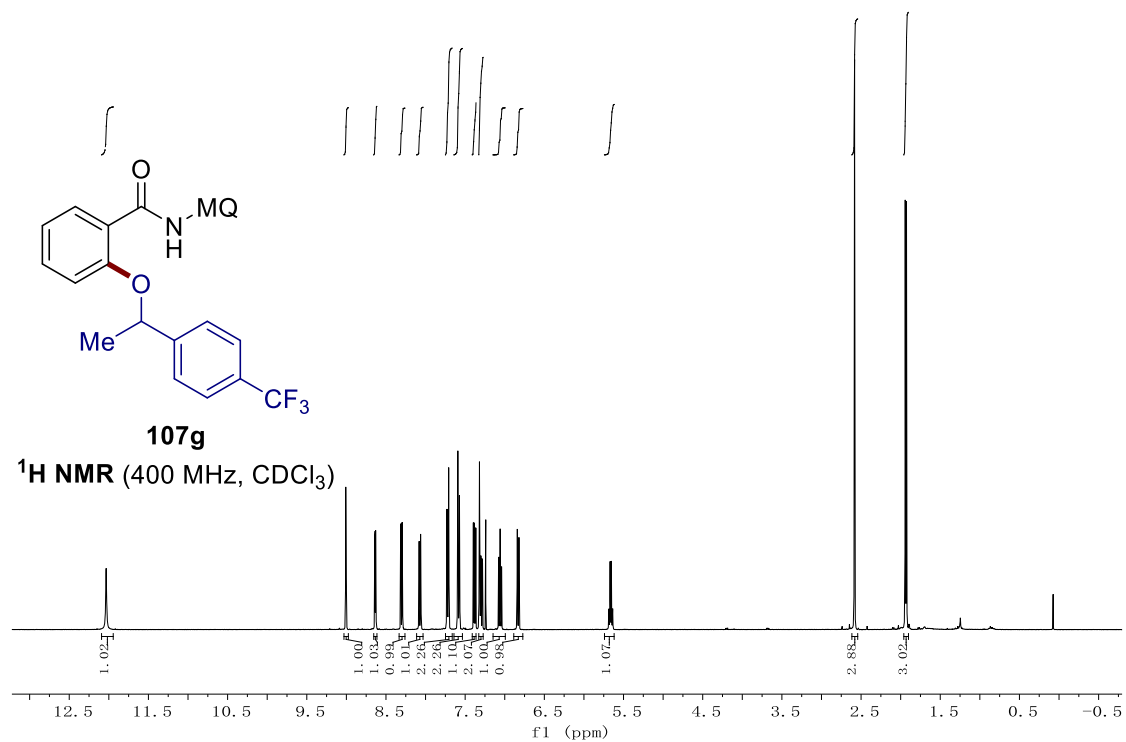


# 7. NMR Spectra

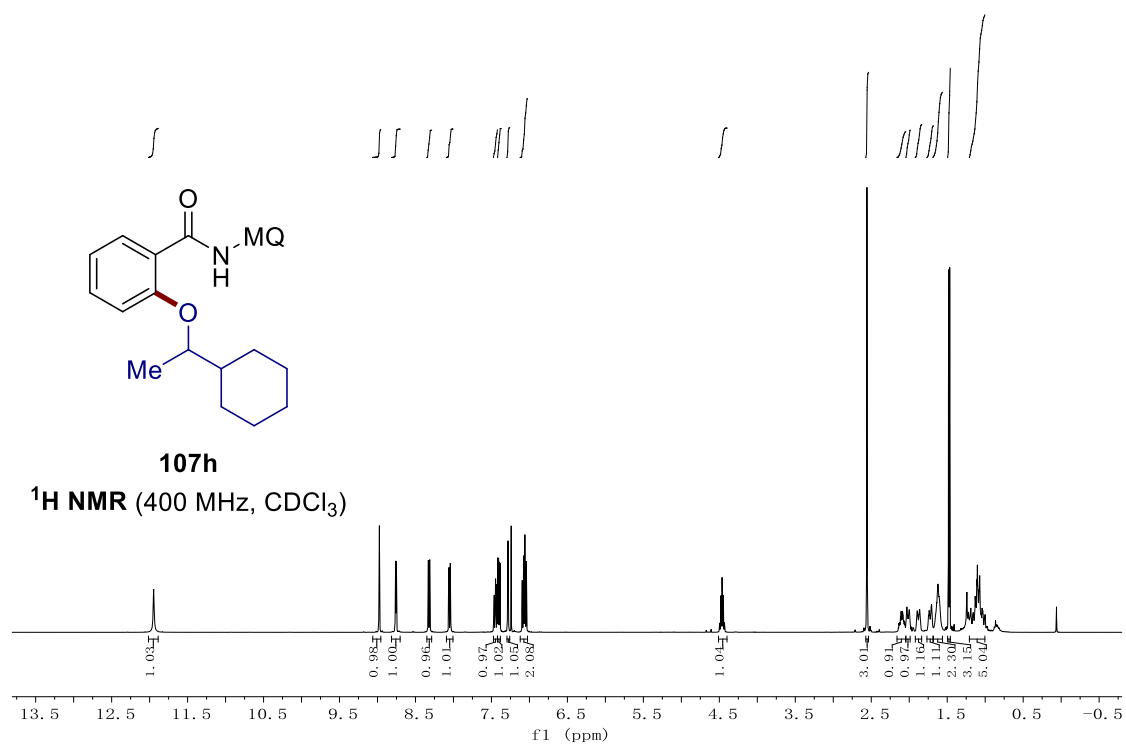
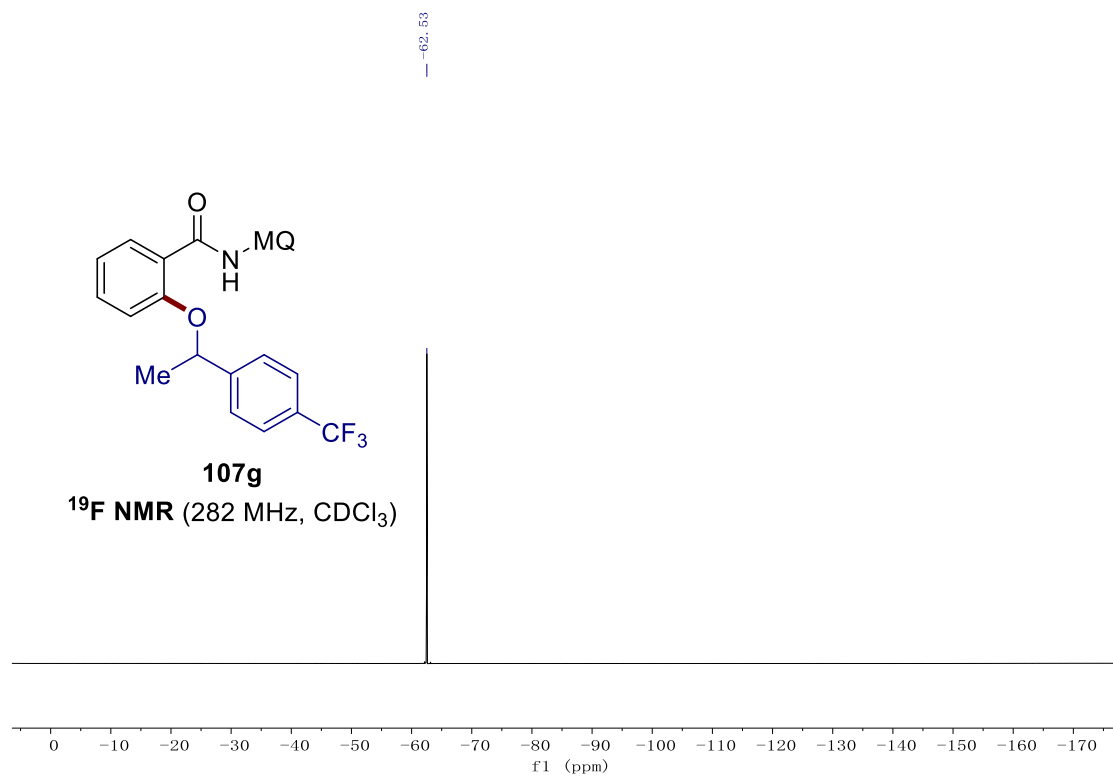




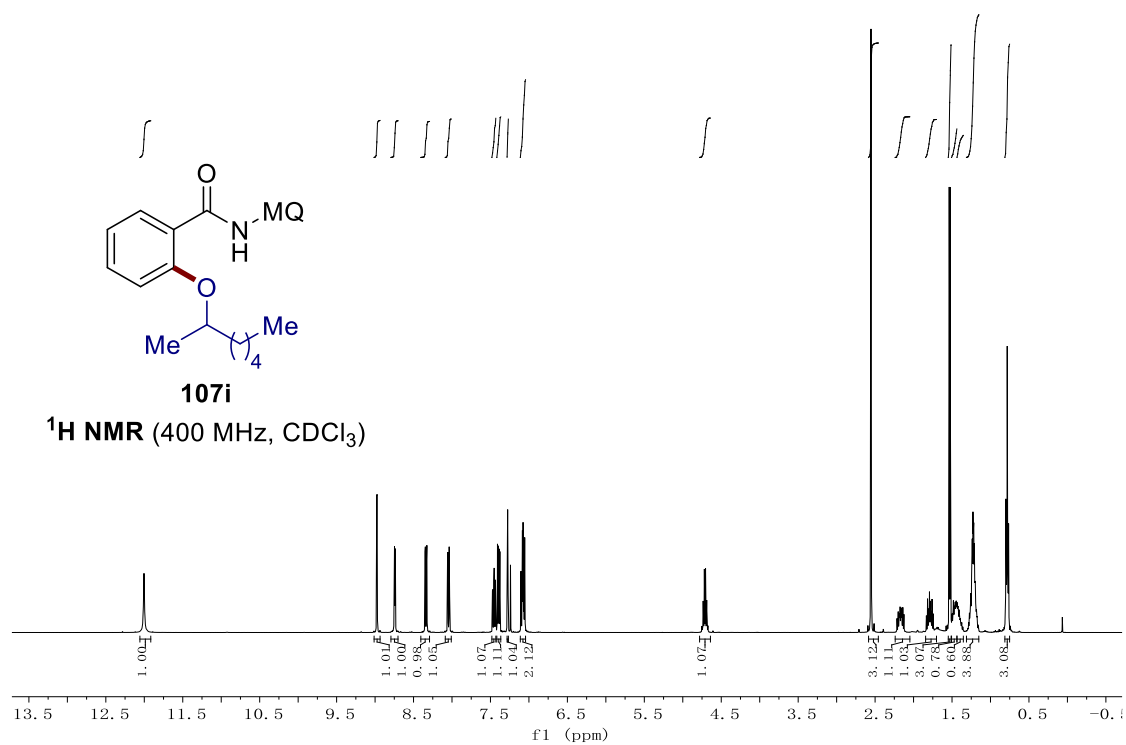
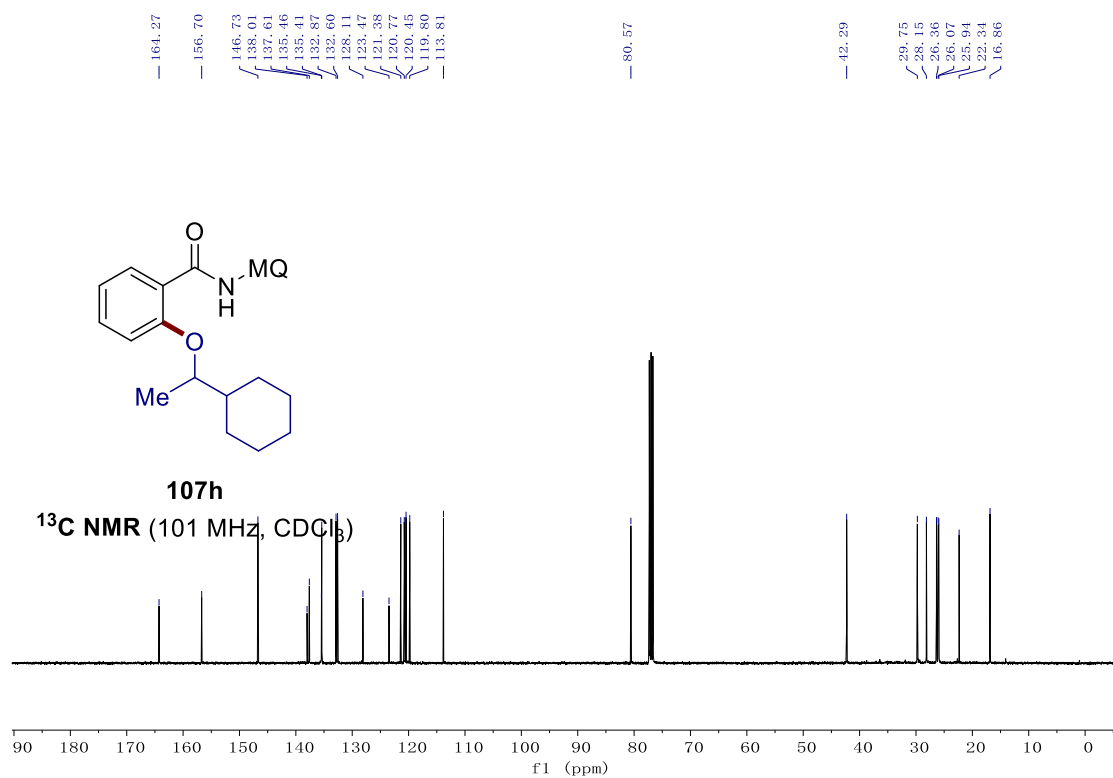
## 7. NMR Spectra

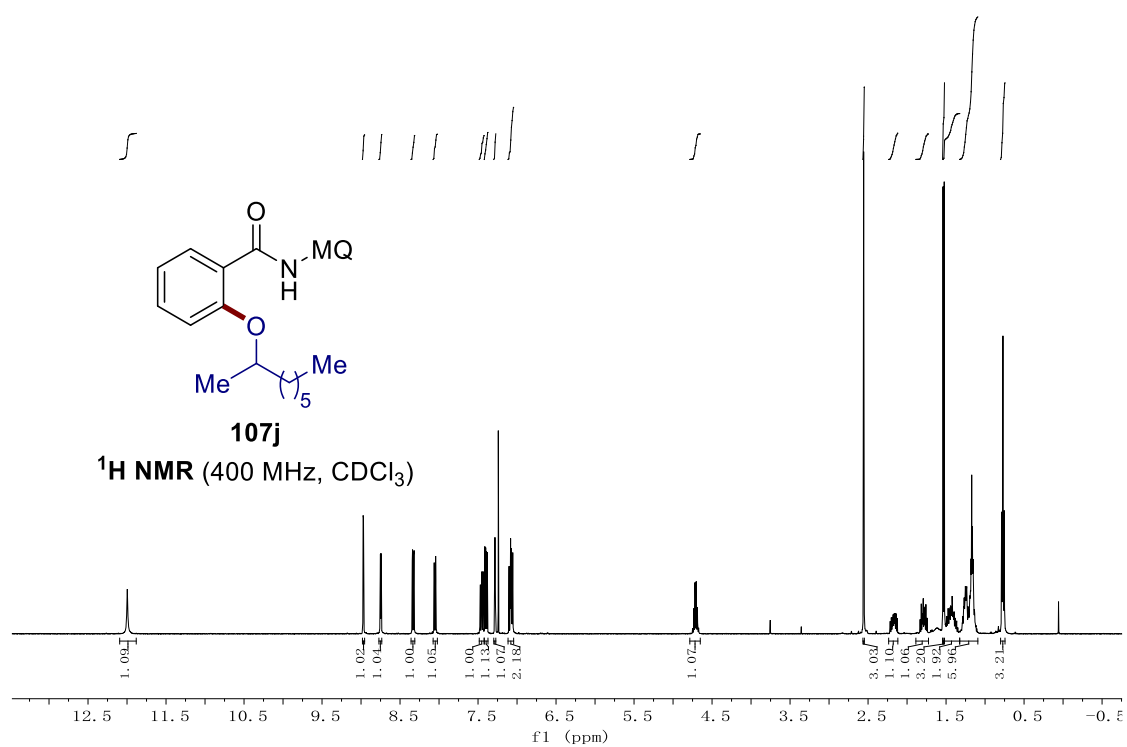
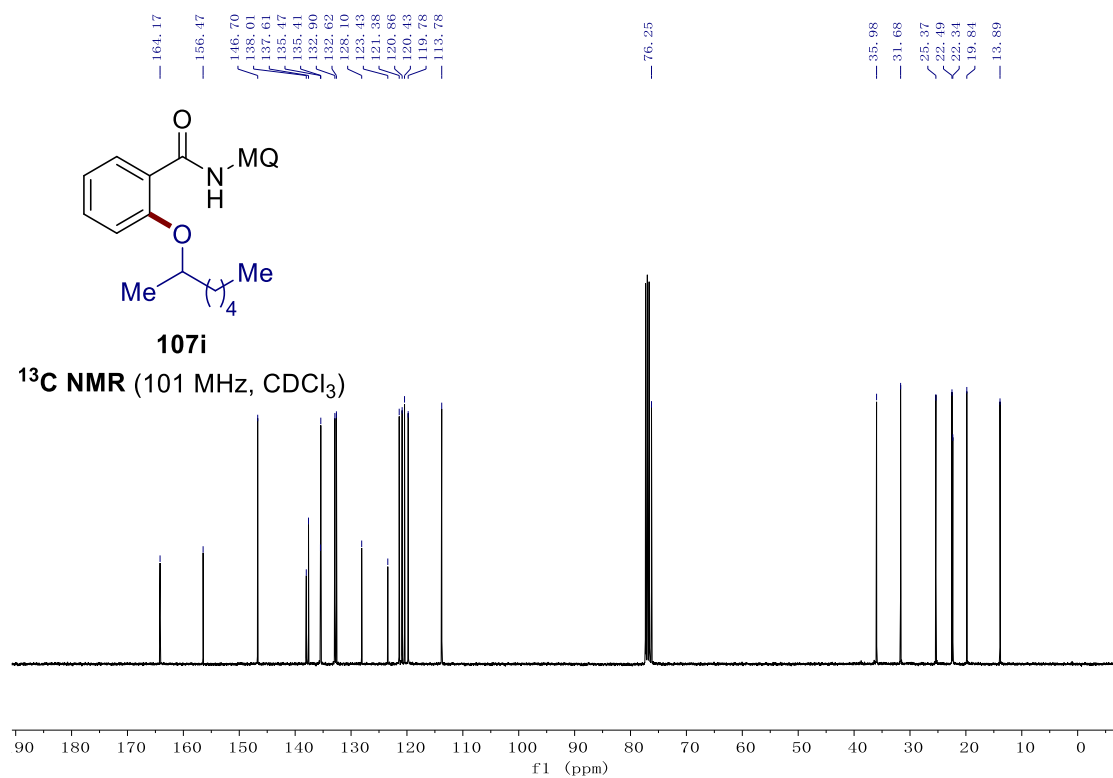




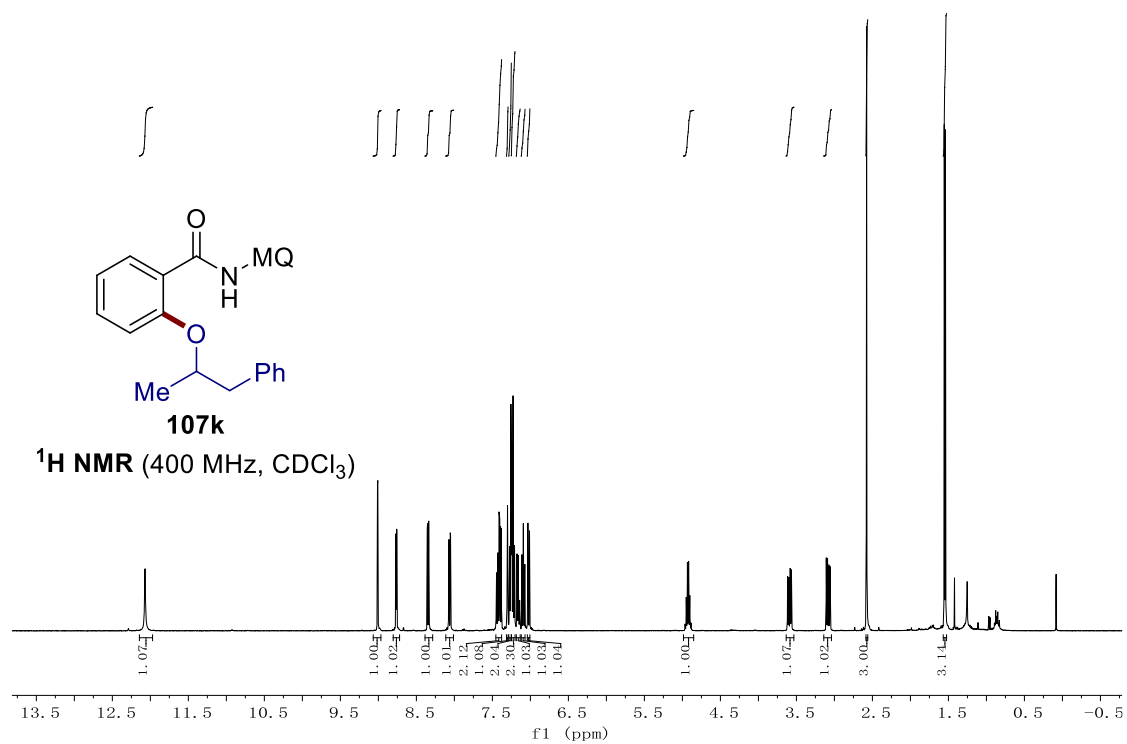
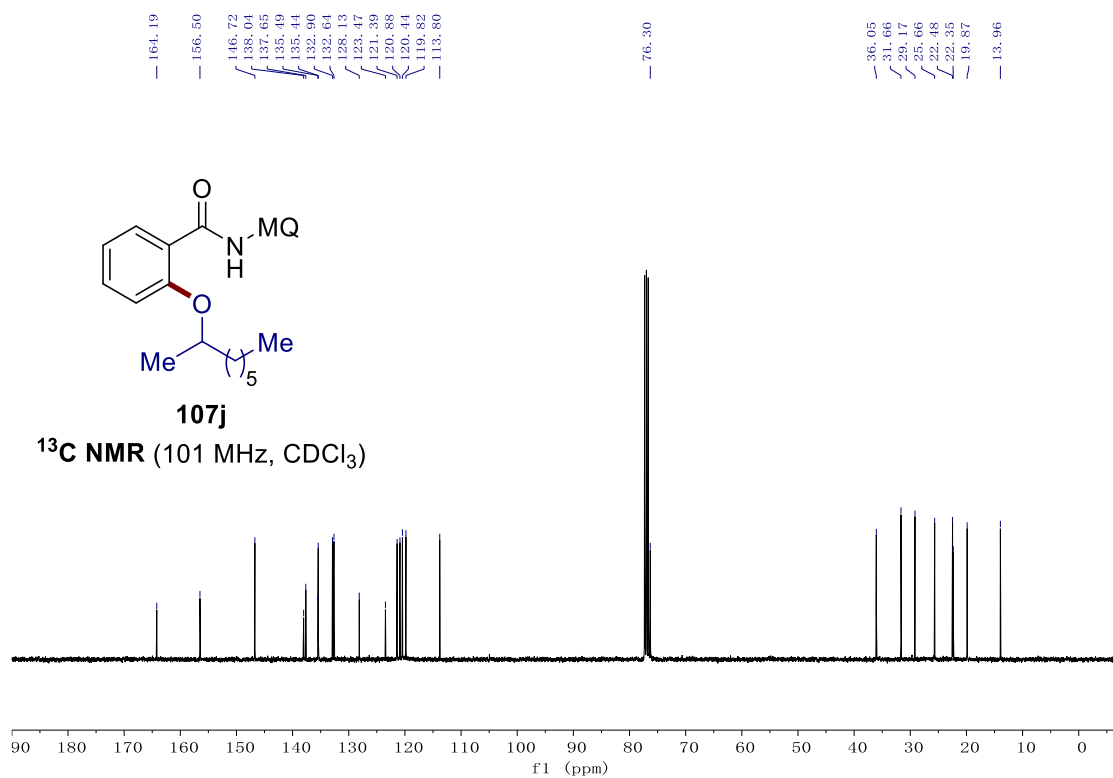


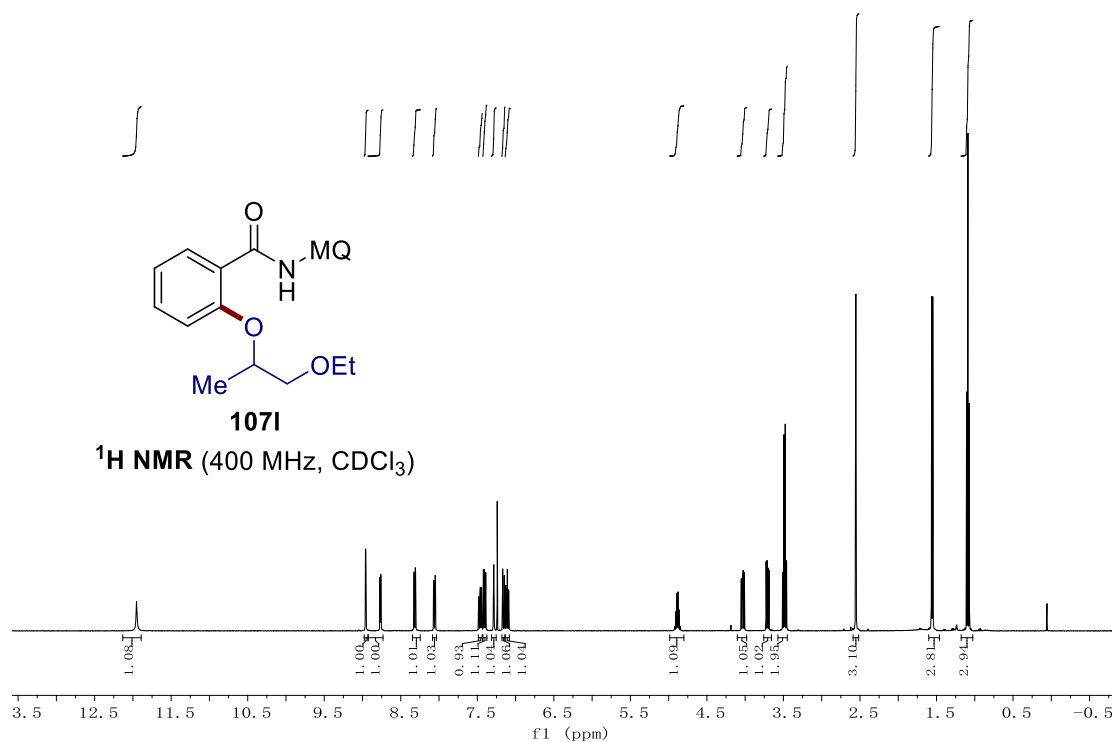
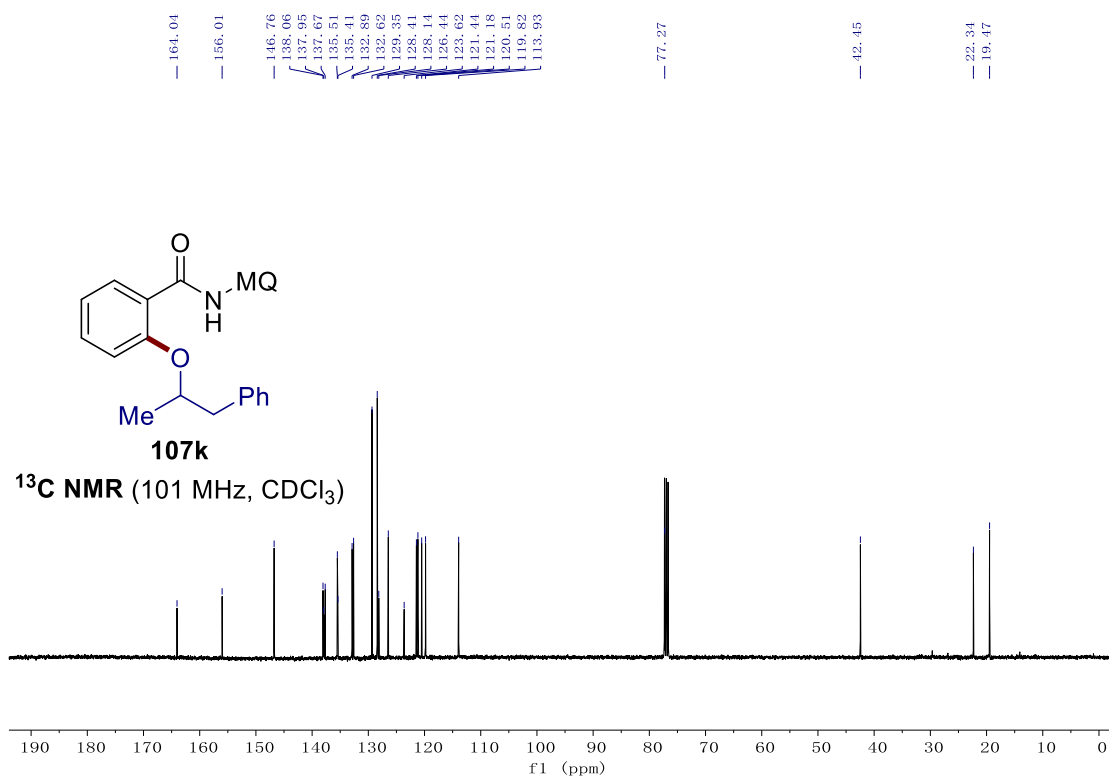
## 7. NMR Spectra



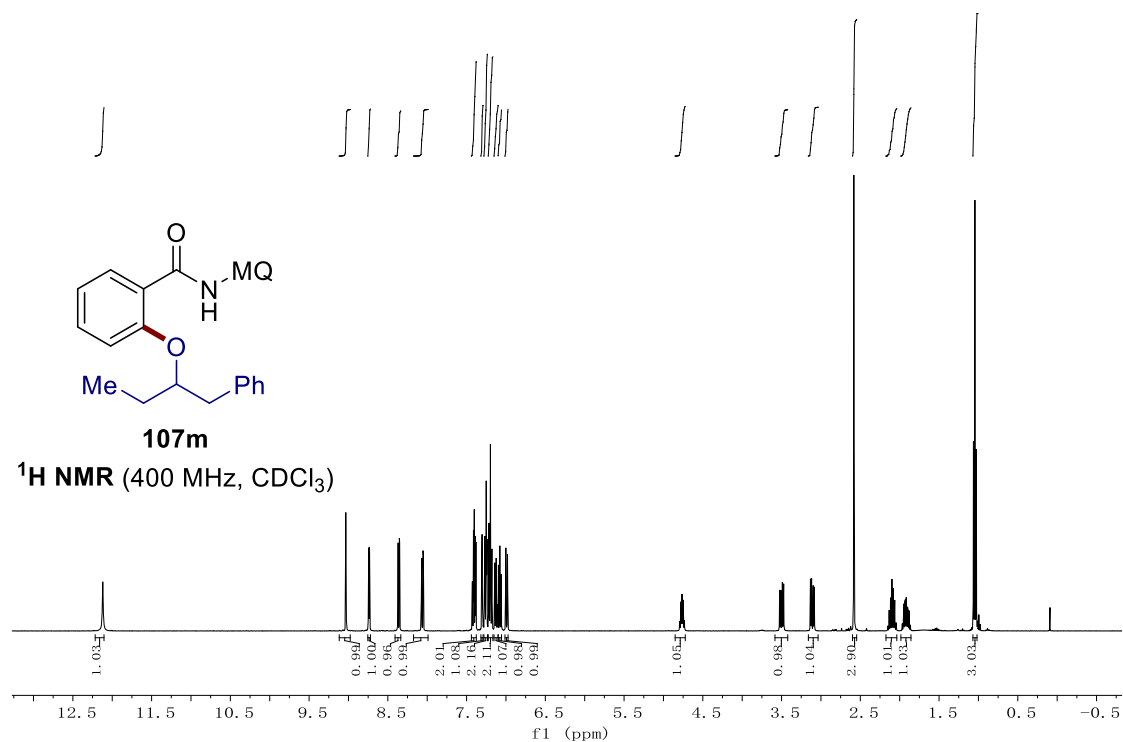
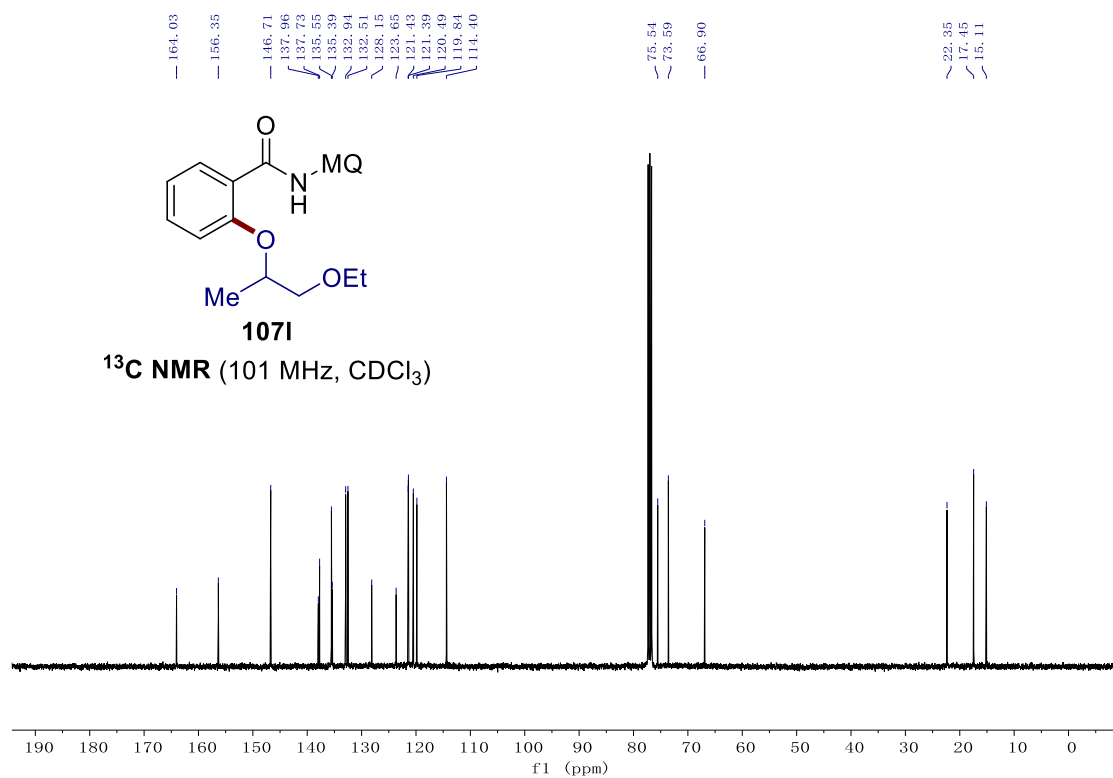


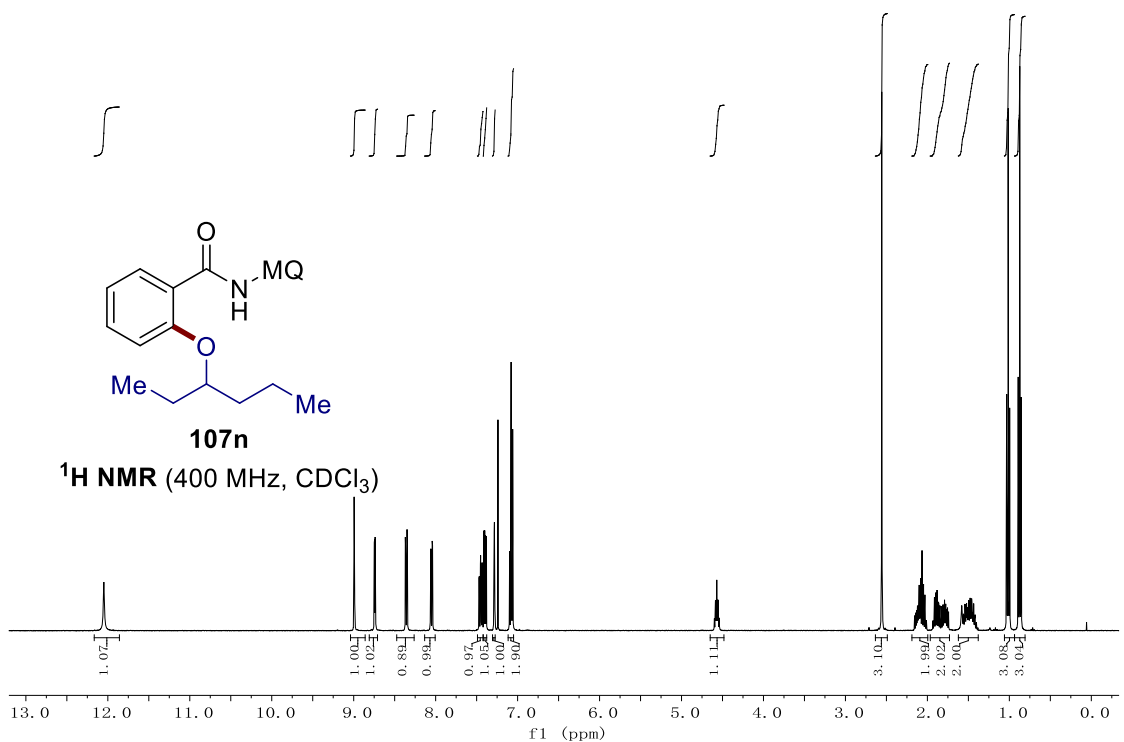
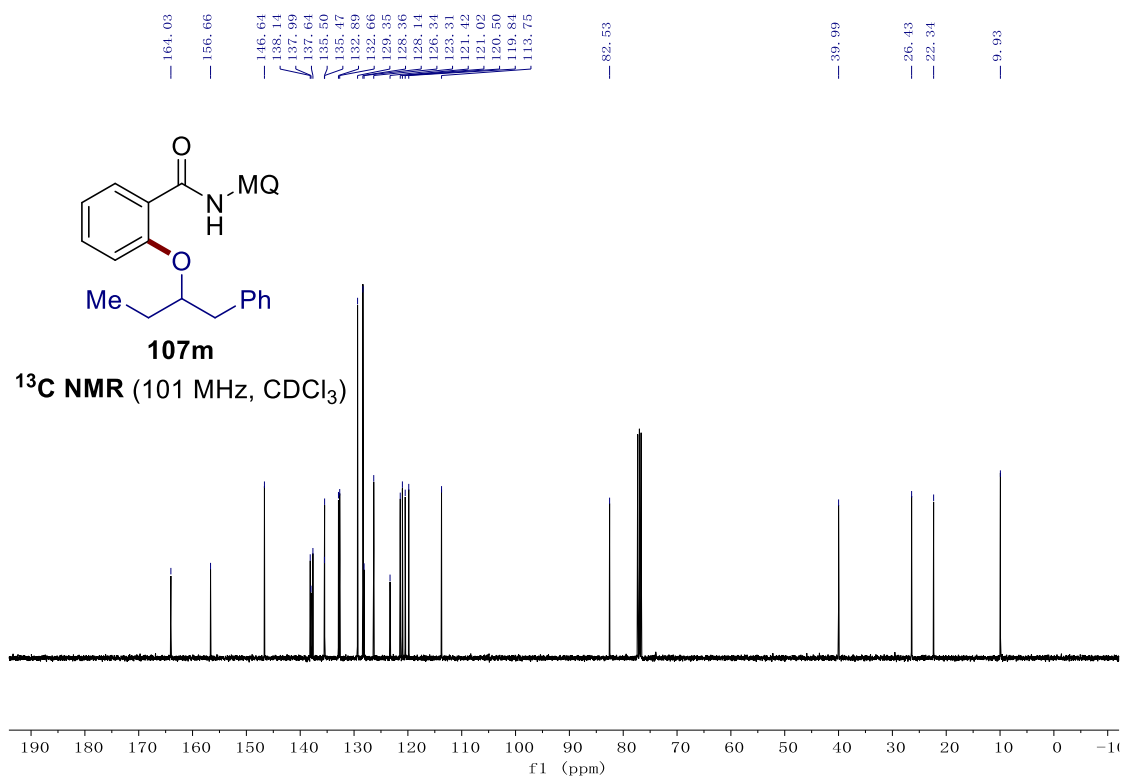
## 7. NMR Spectra



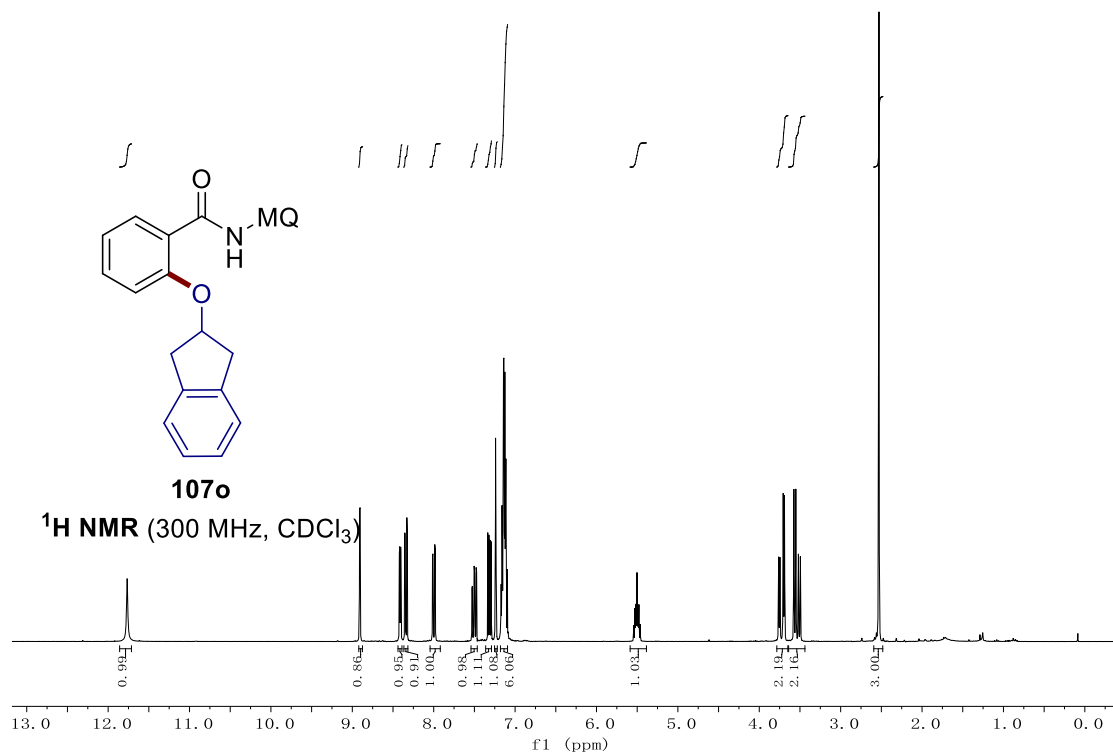
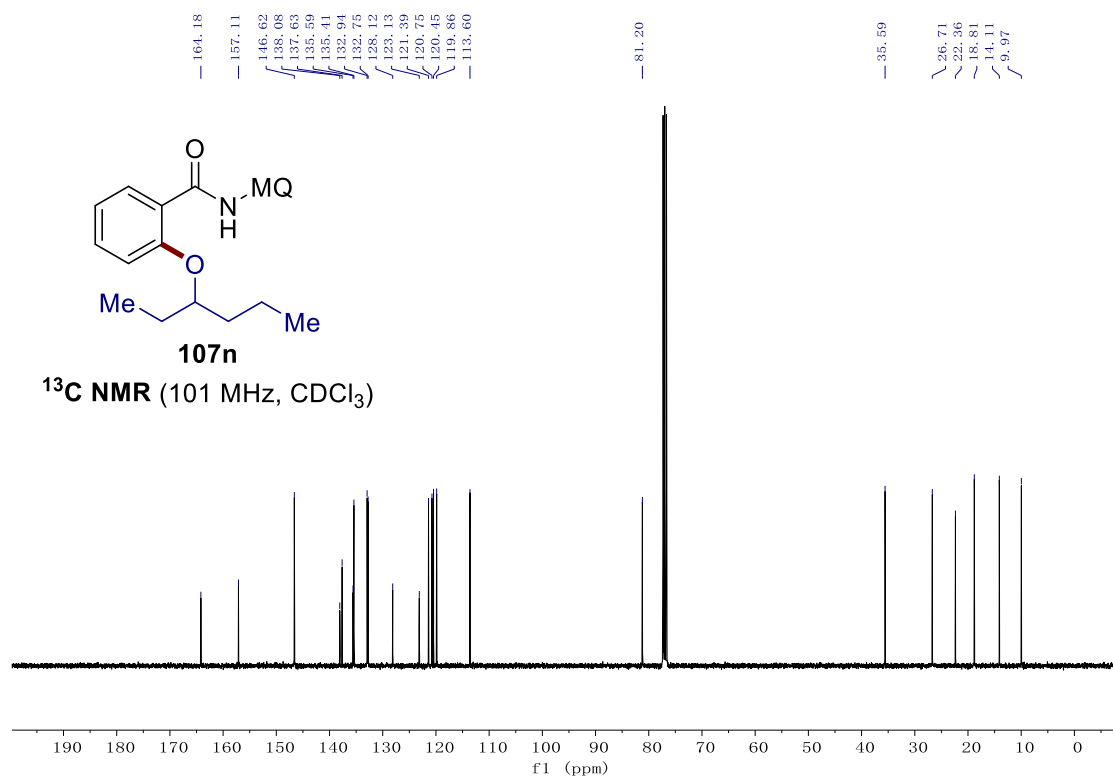


## 7. NMR Spectra

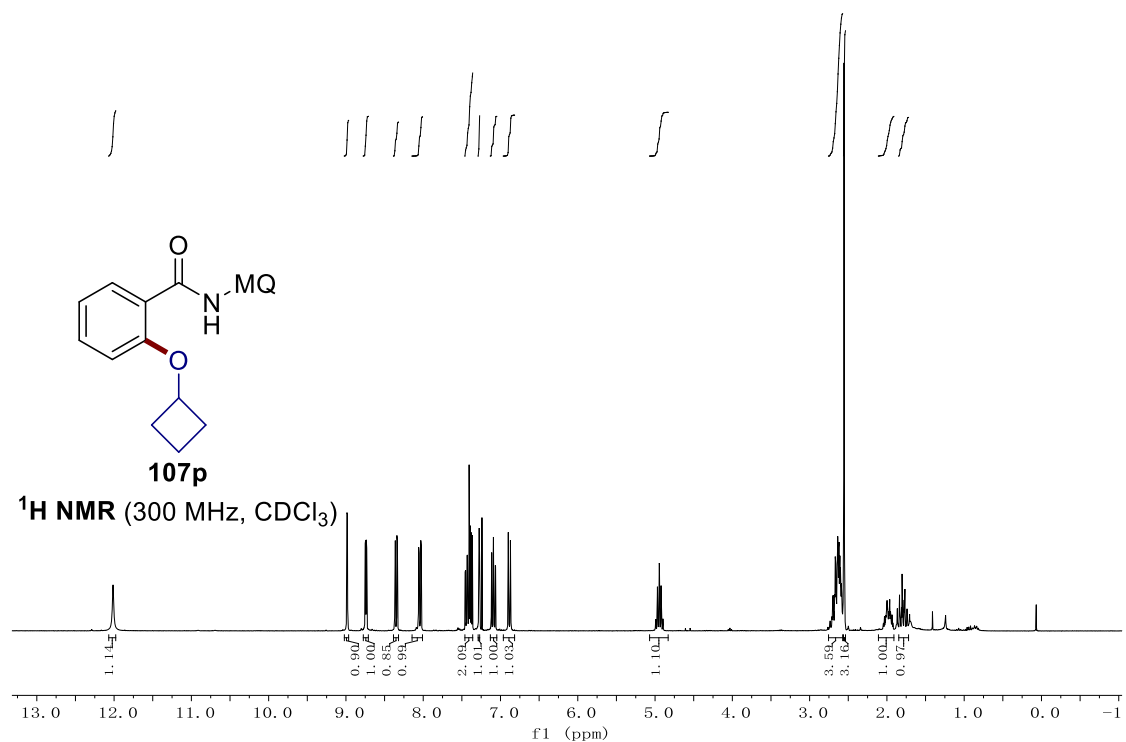
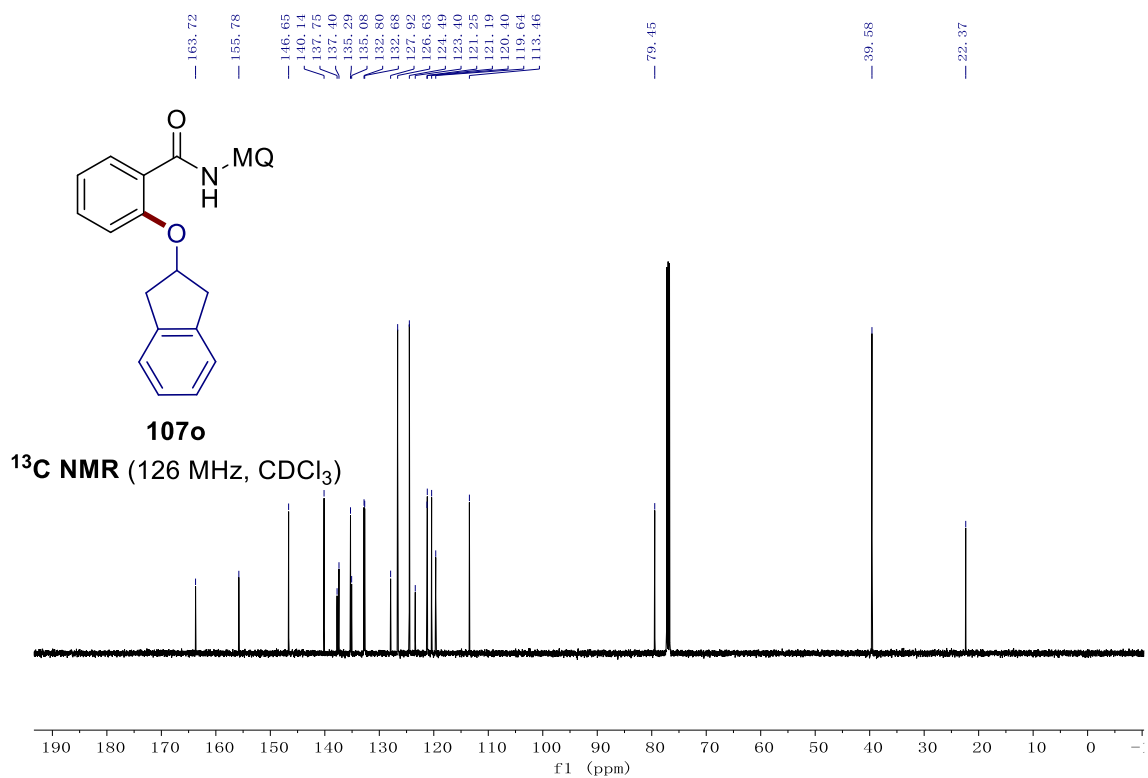




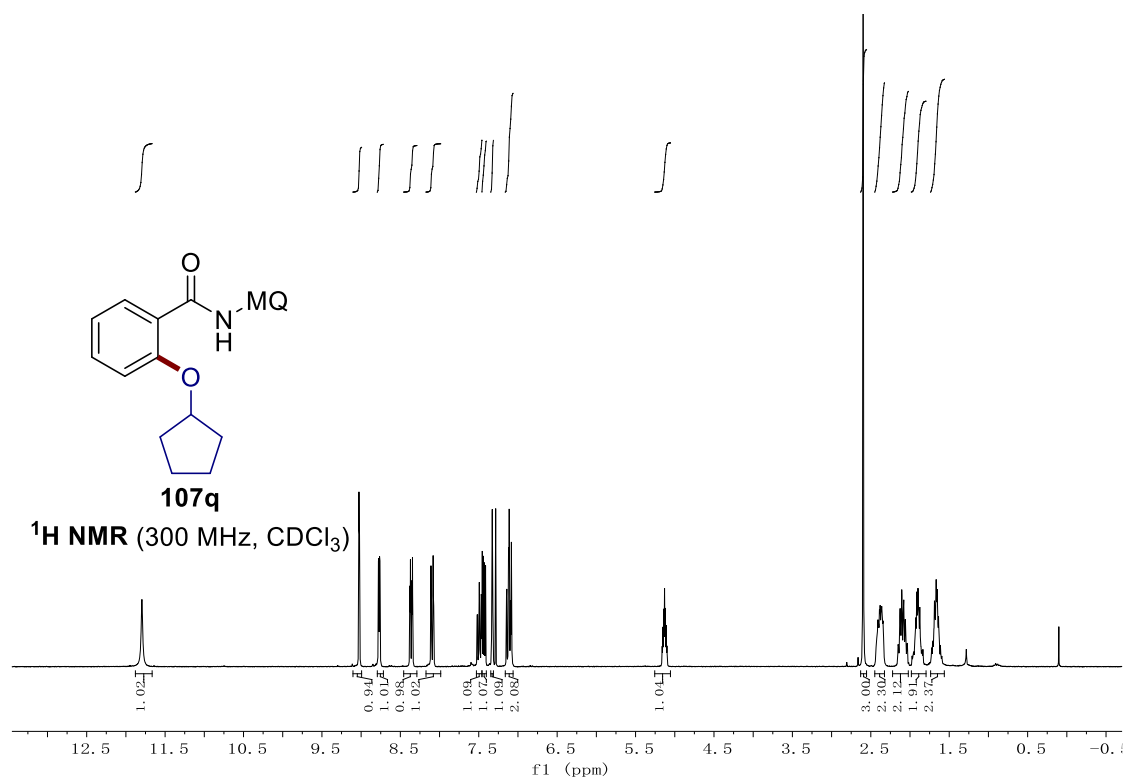
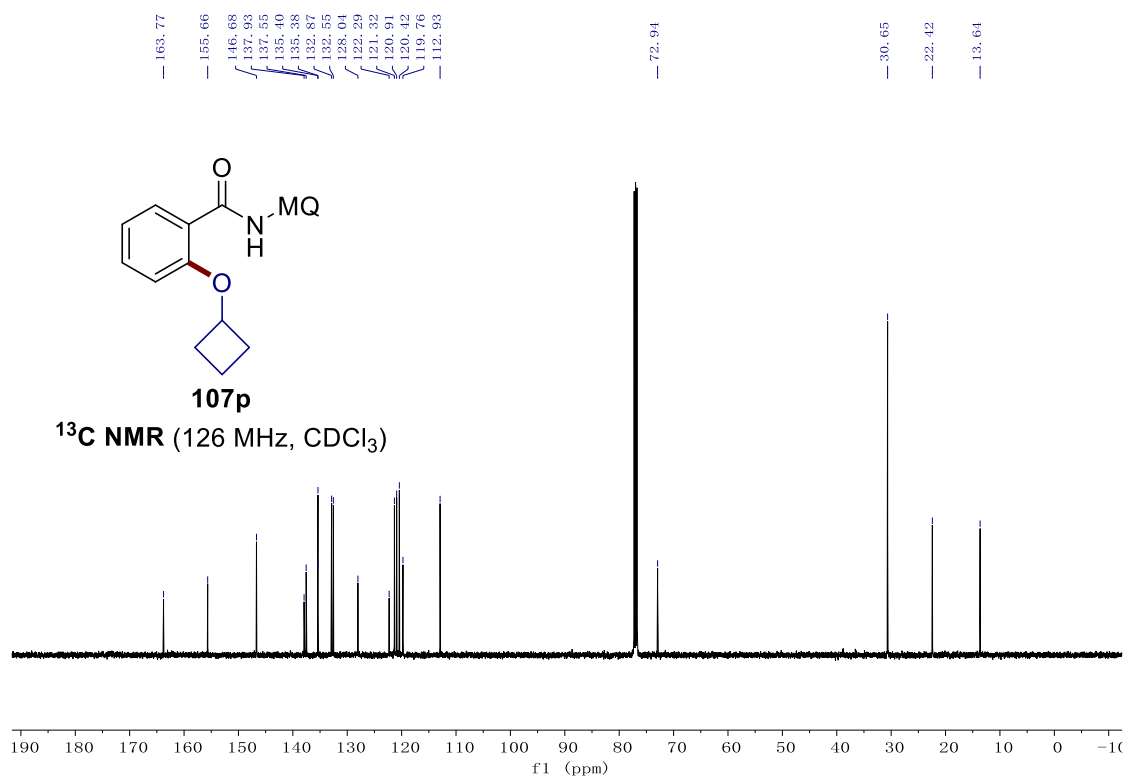
## 7. NMR Spectra

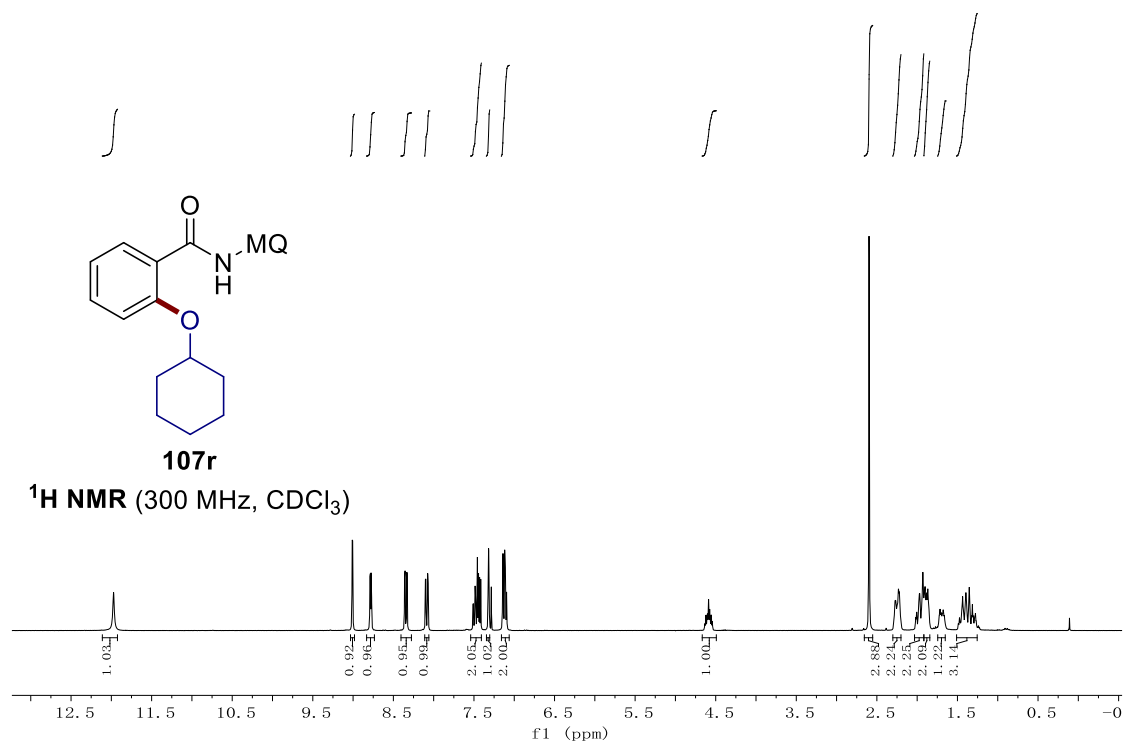
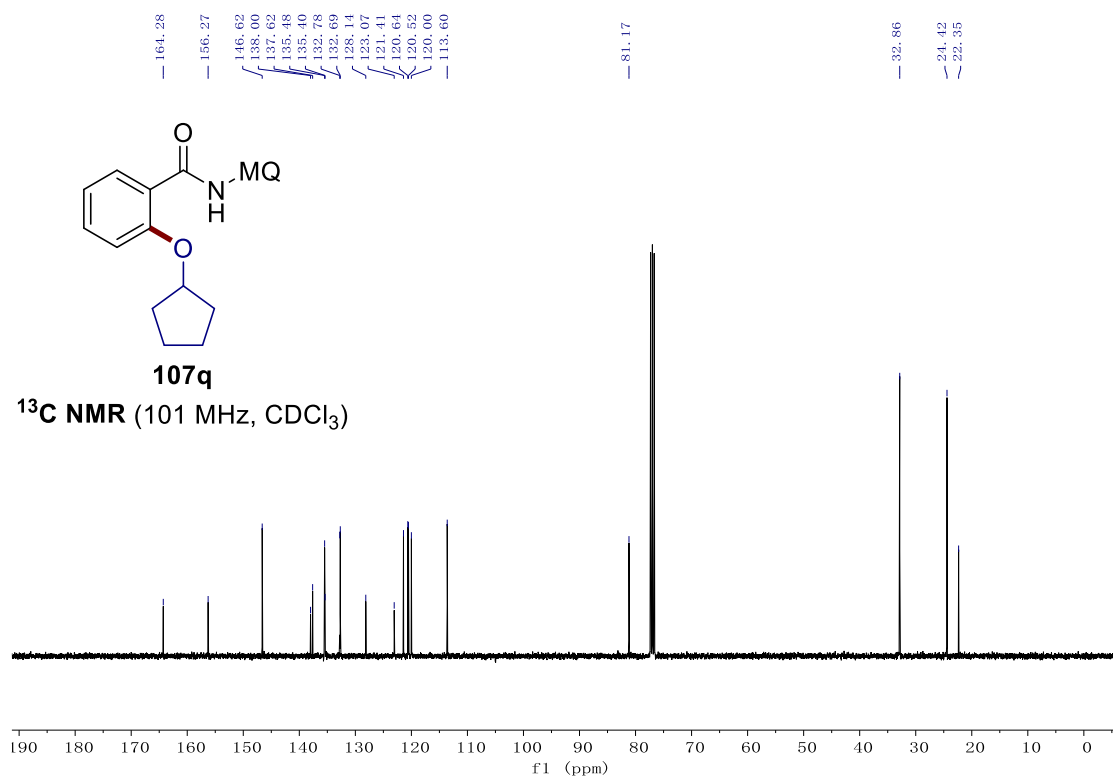




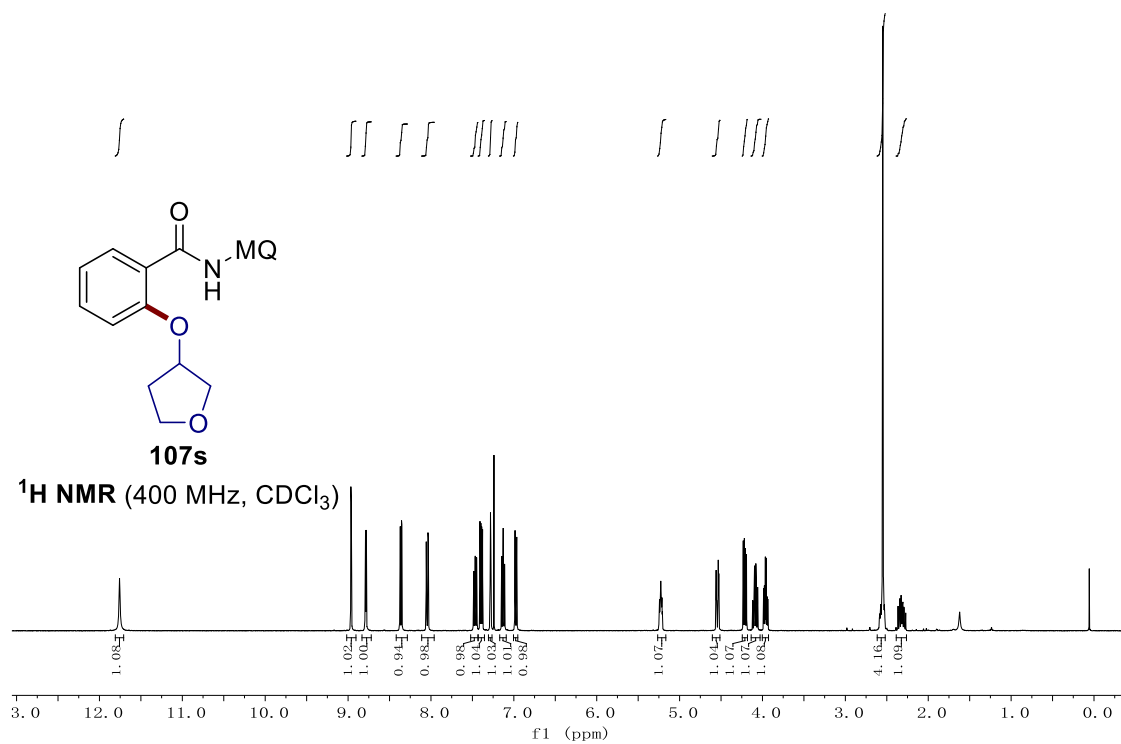
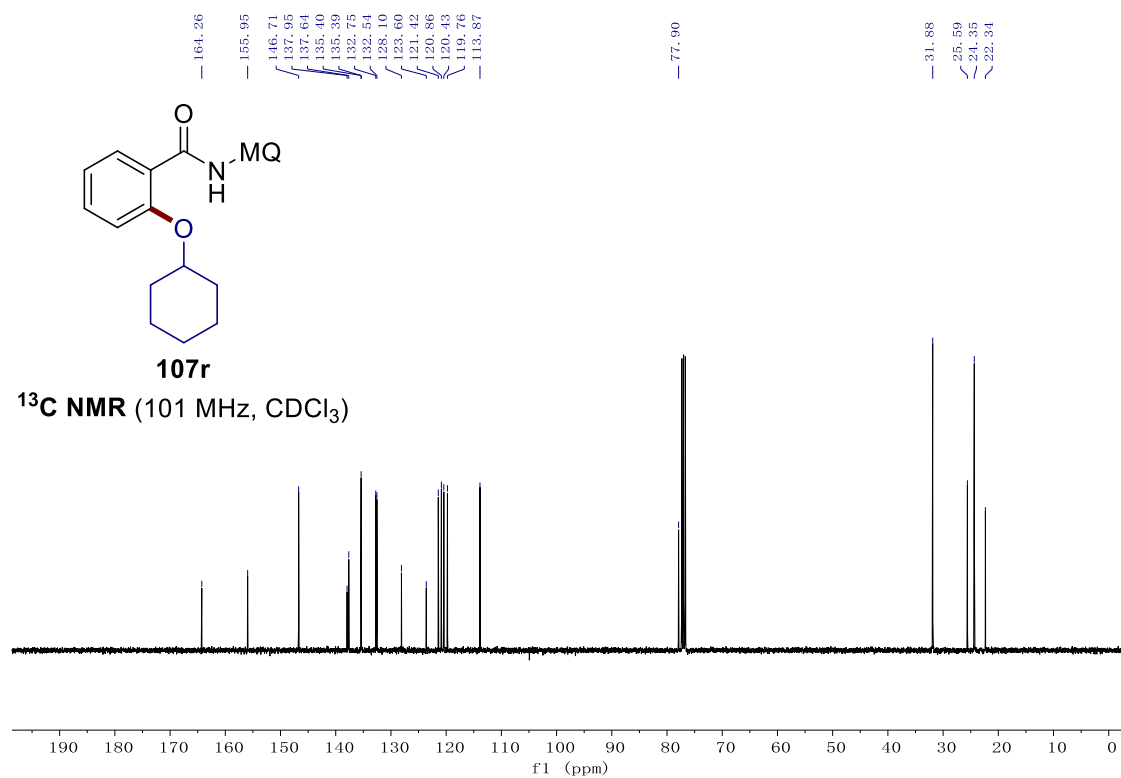


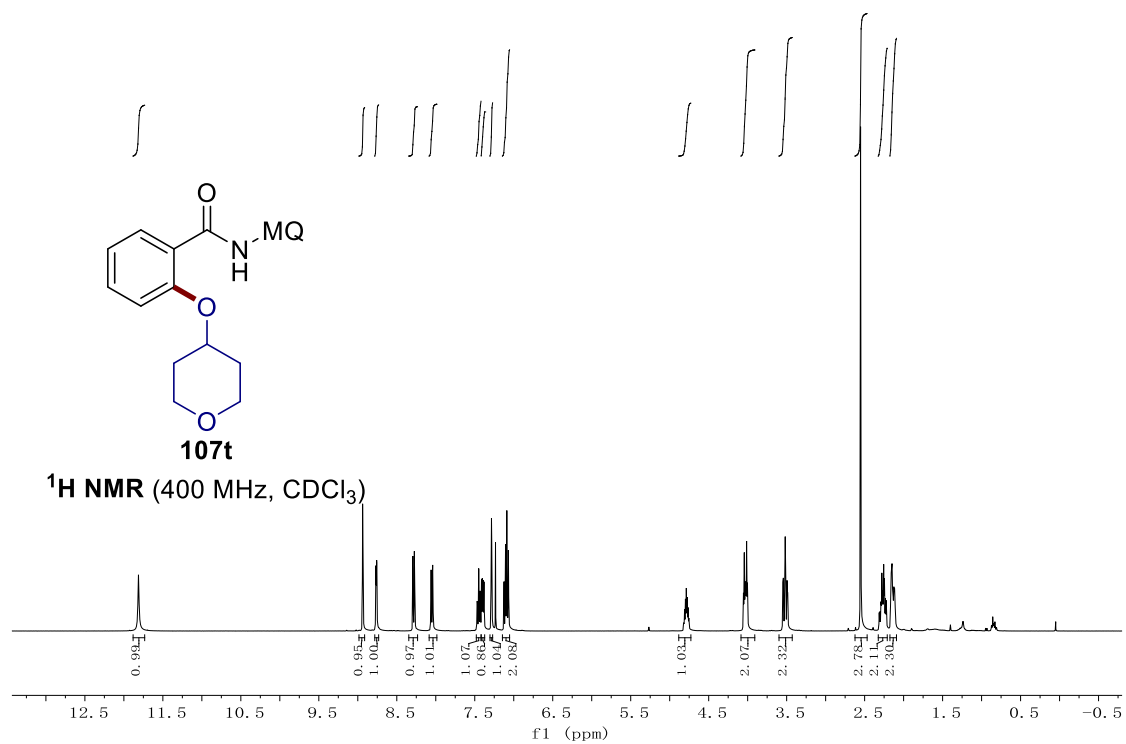
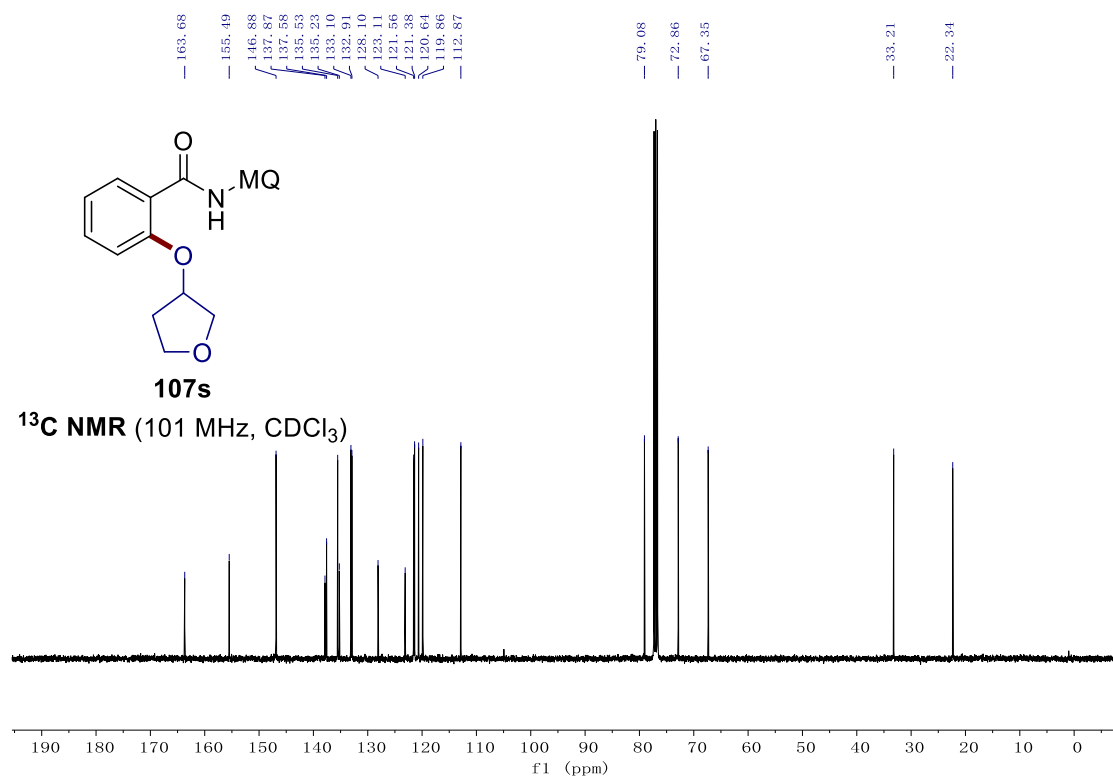
## 7. NMR Spectra



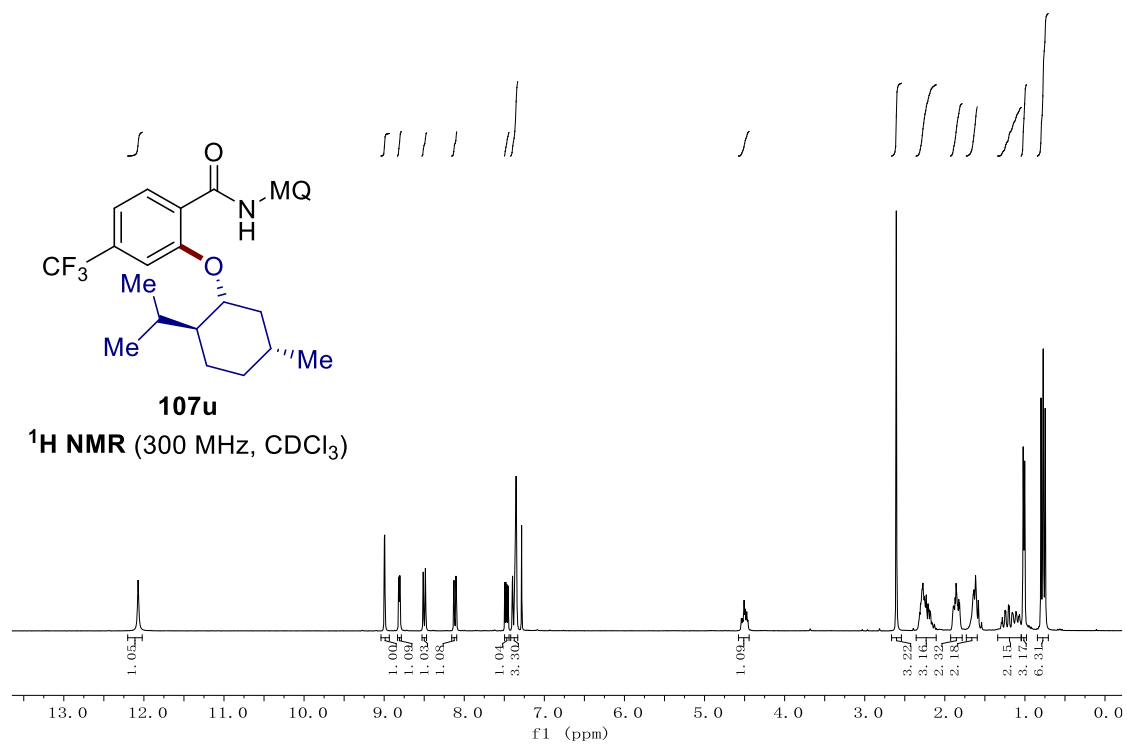
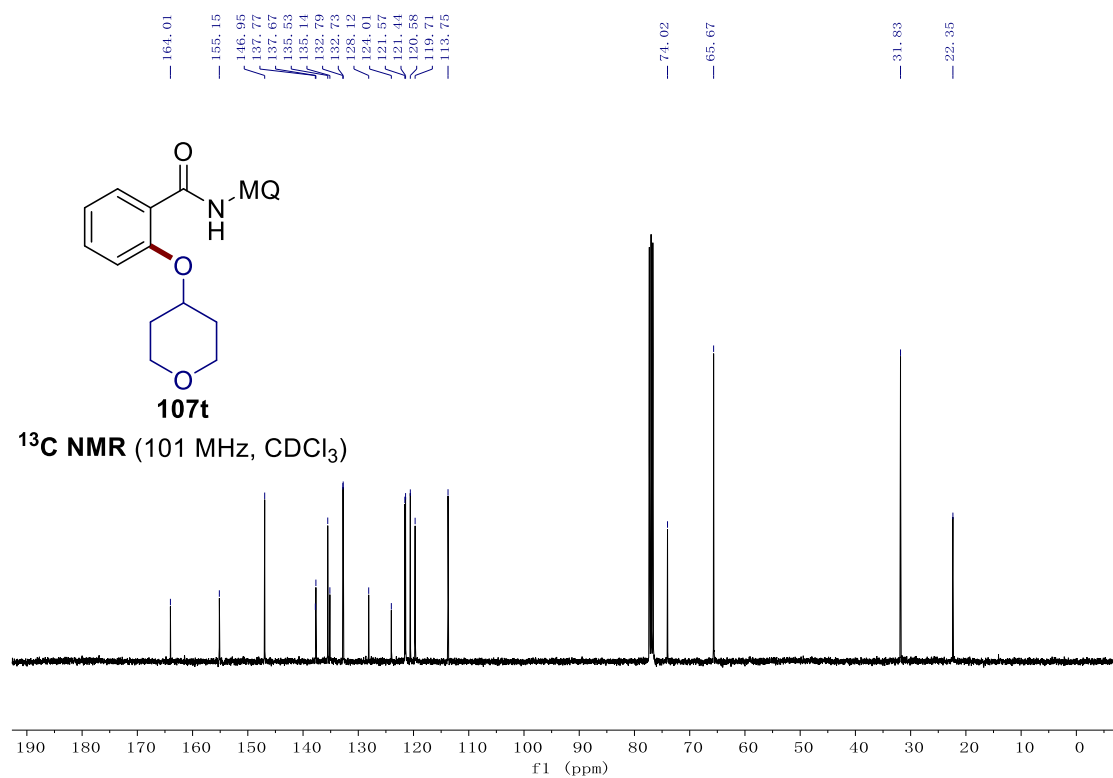


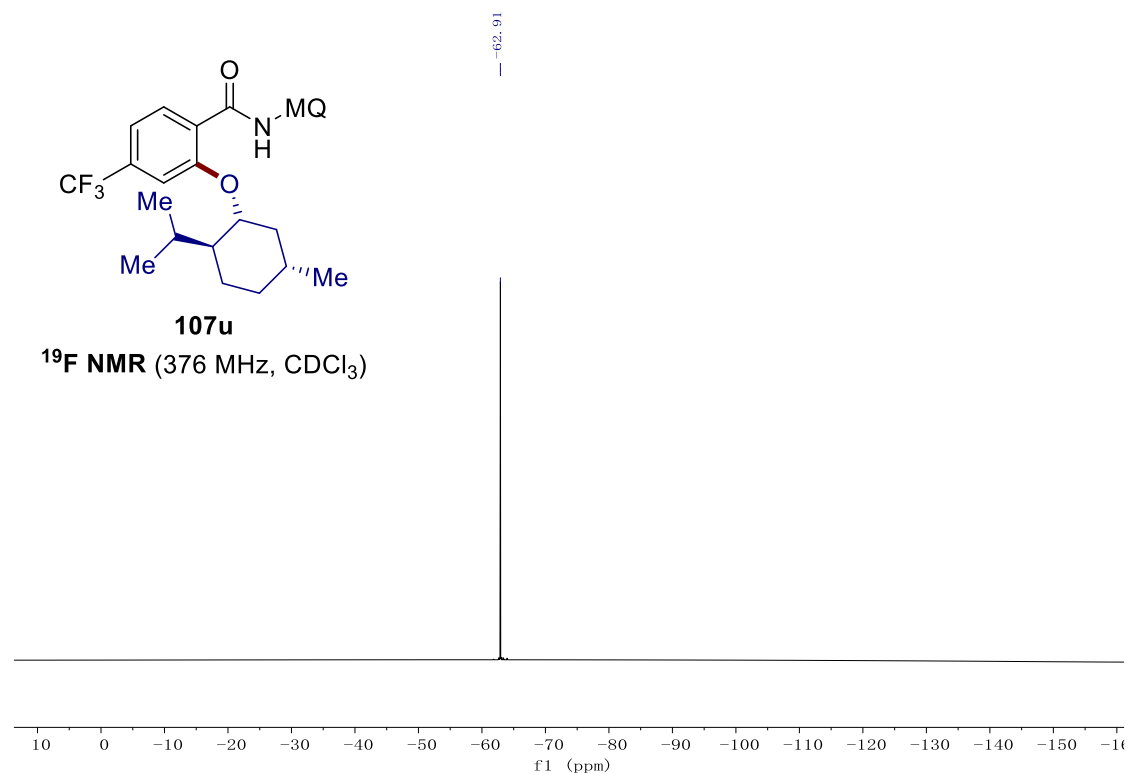
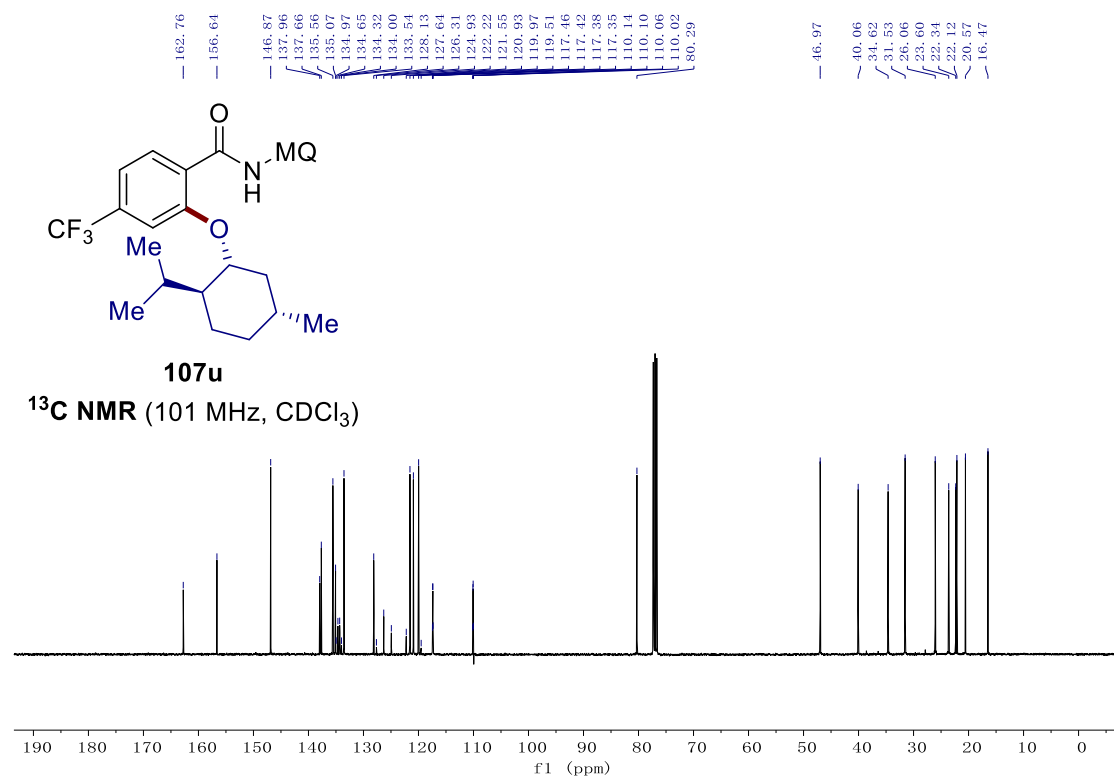
## 7. NMR Spectra





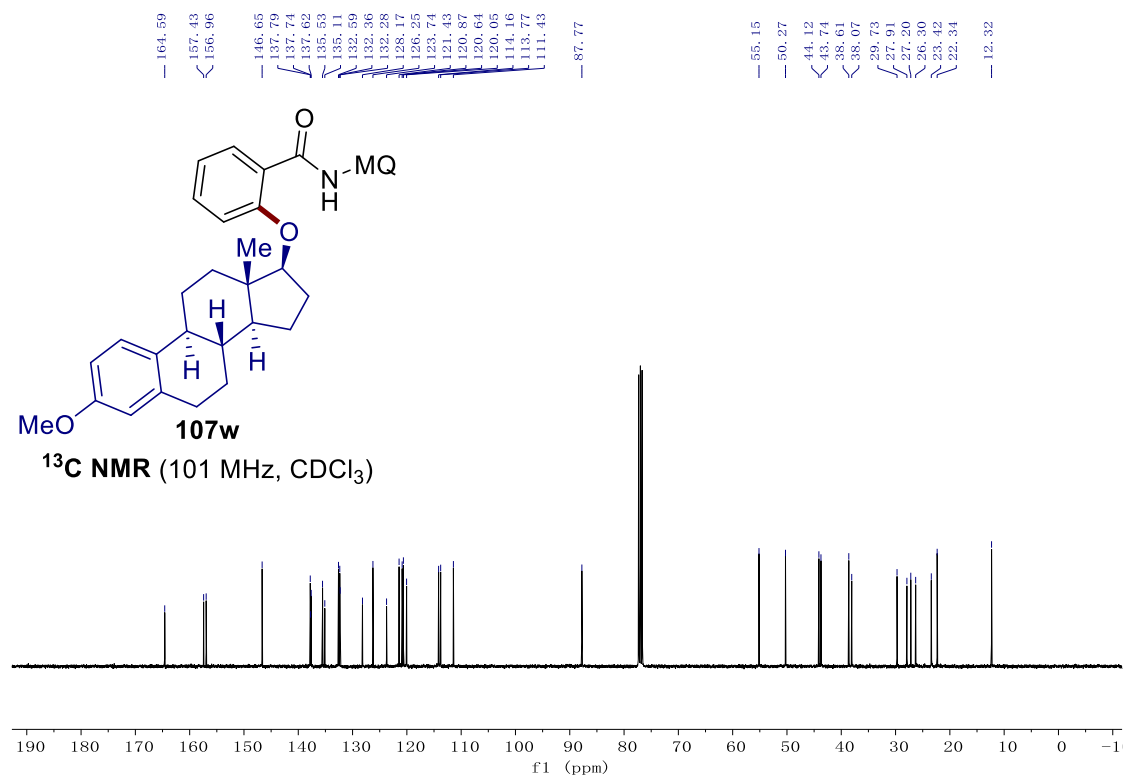
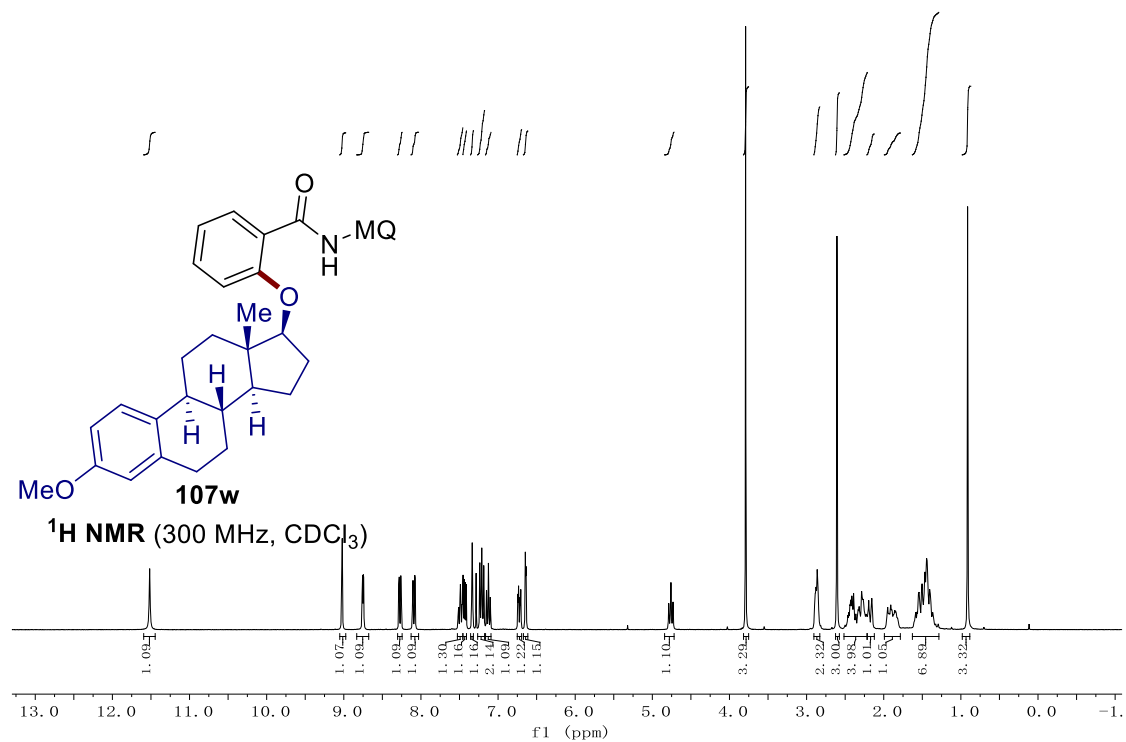
## 7. NMR Spectra



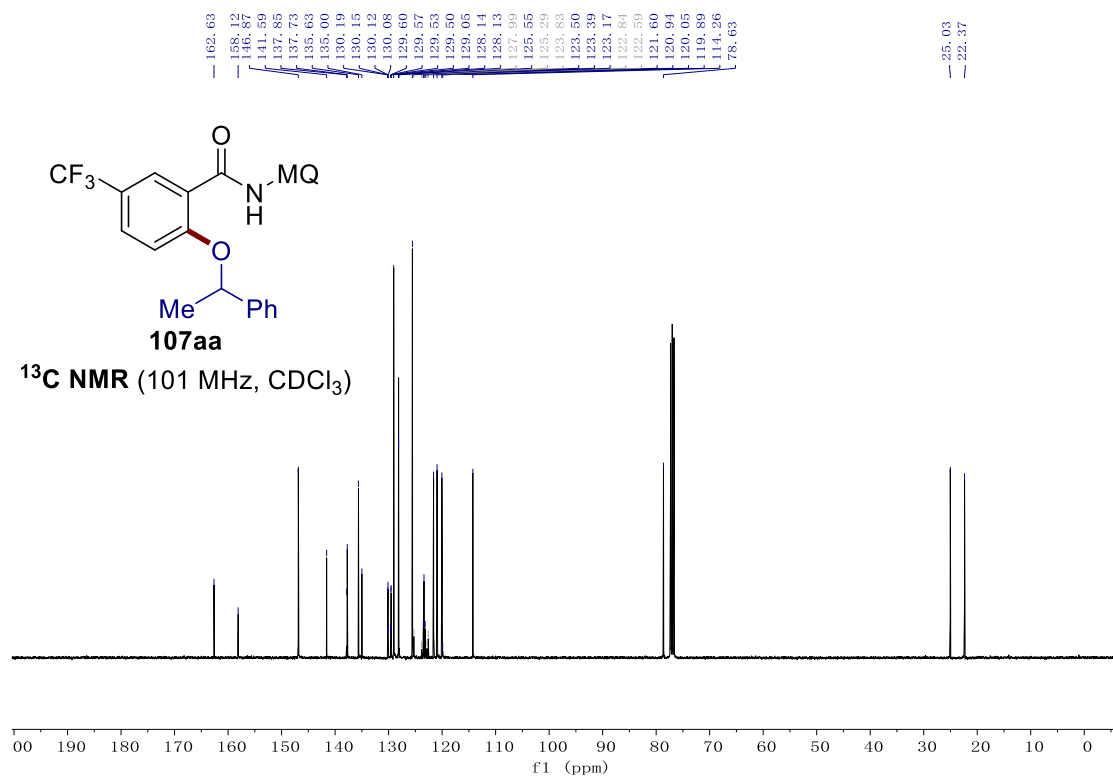
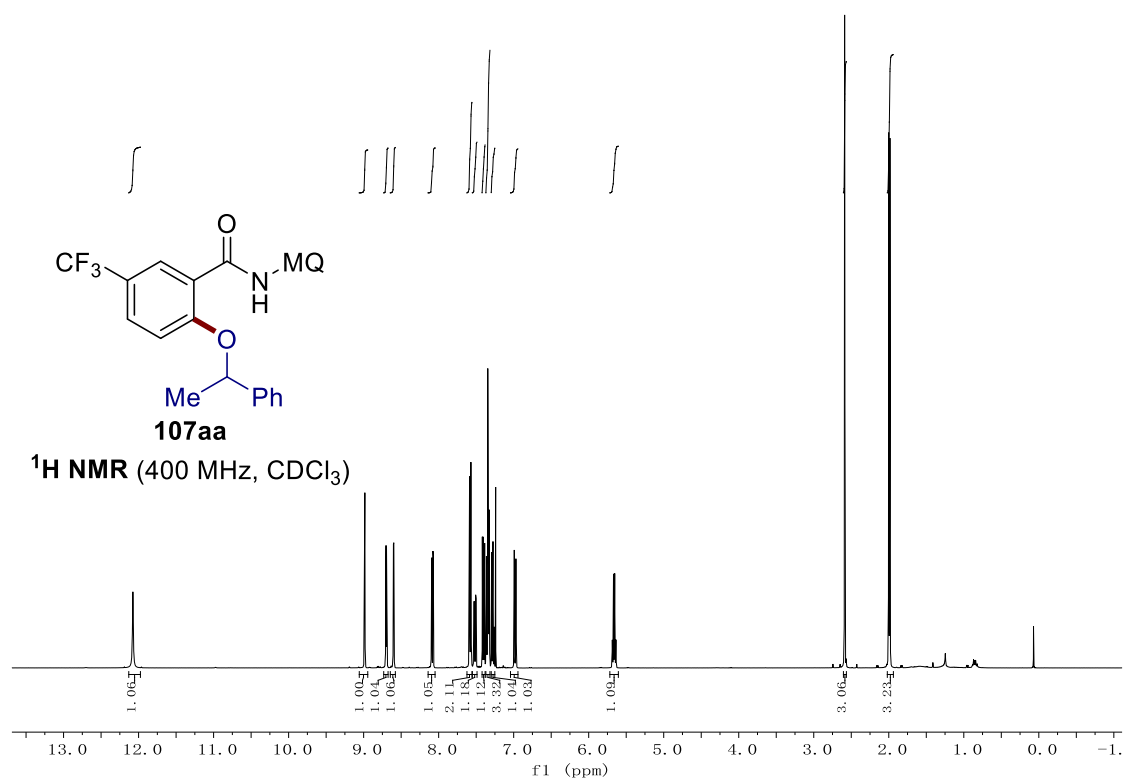


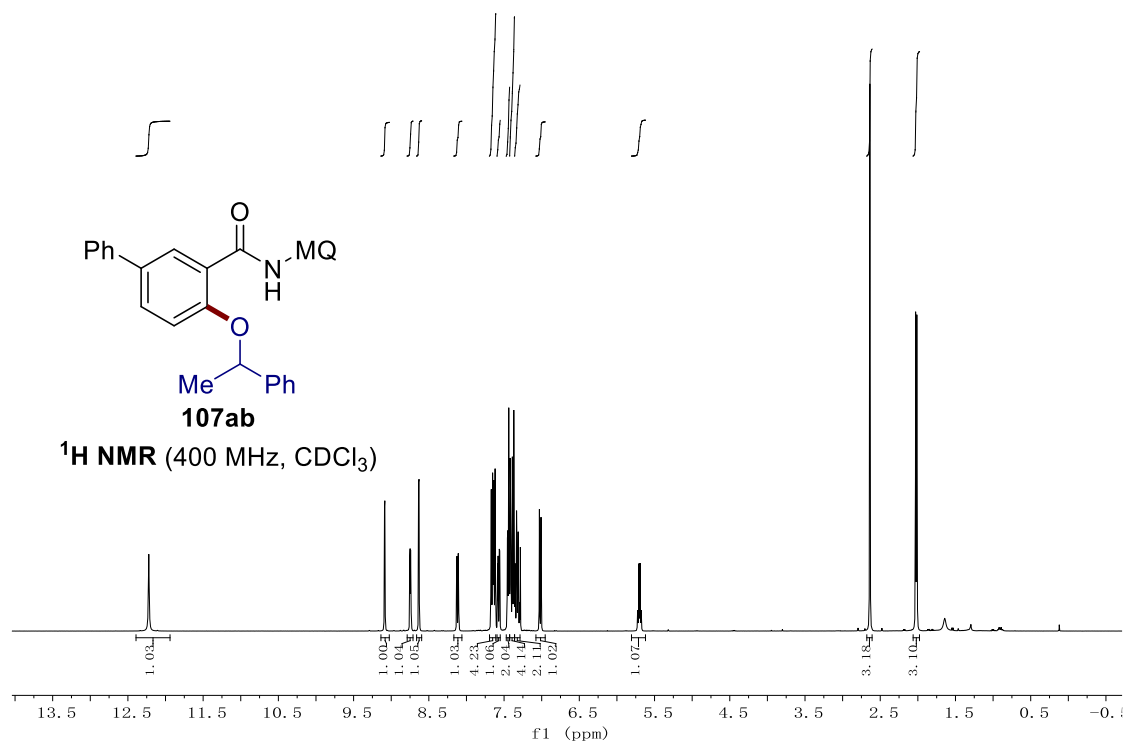
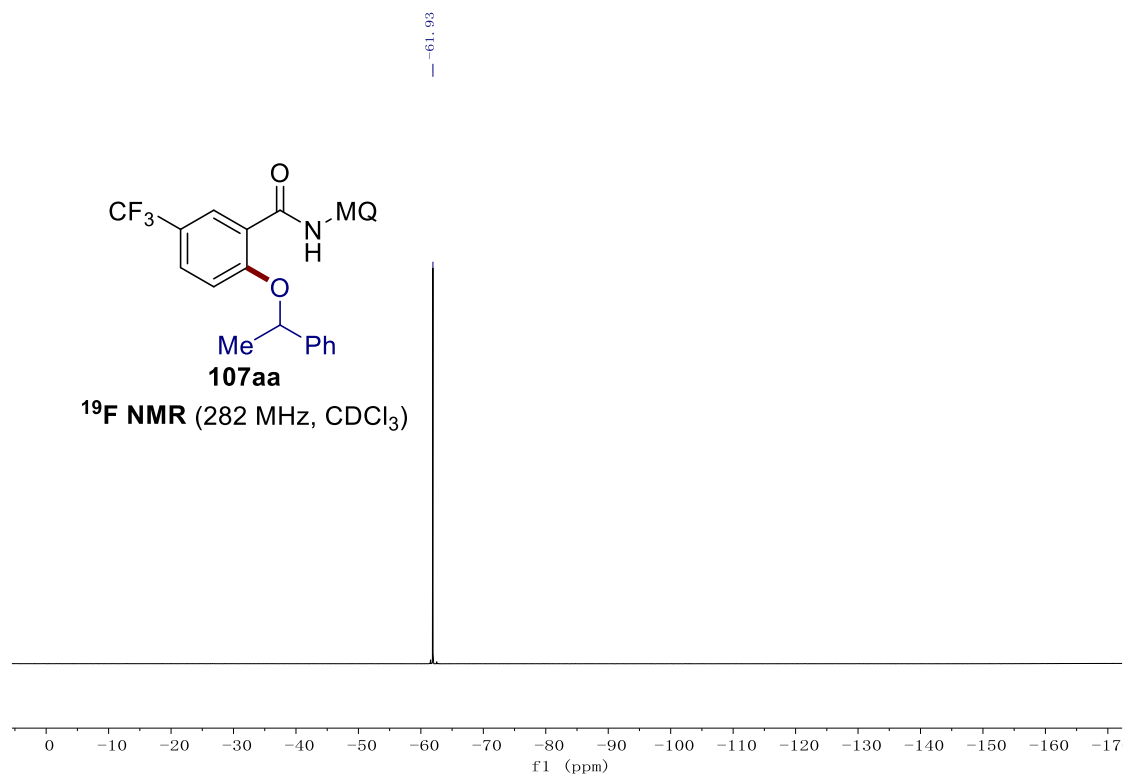




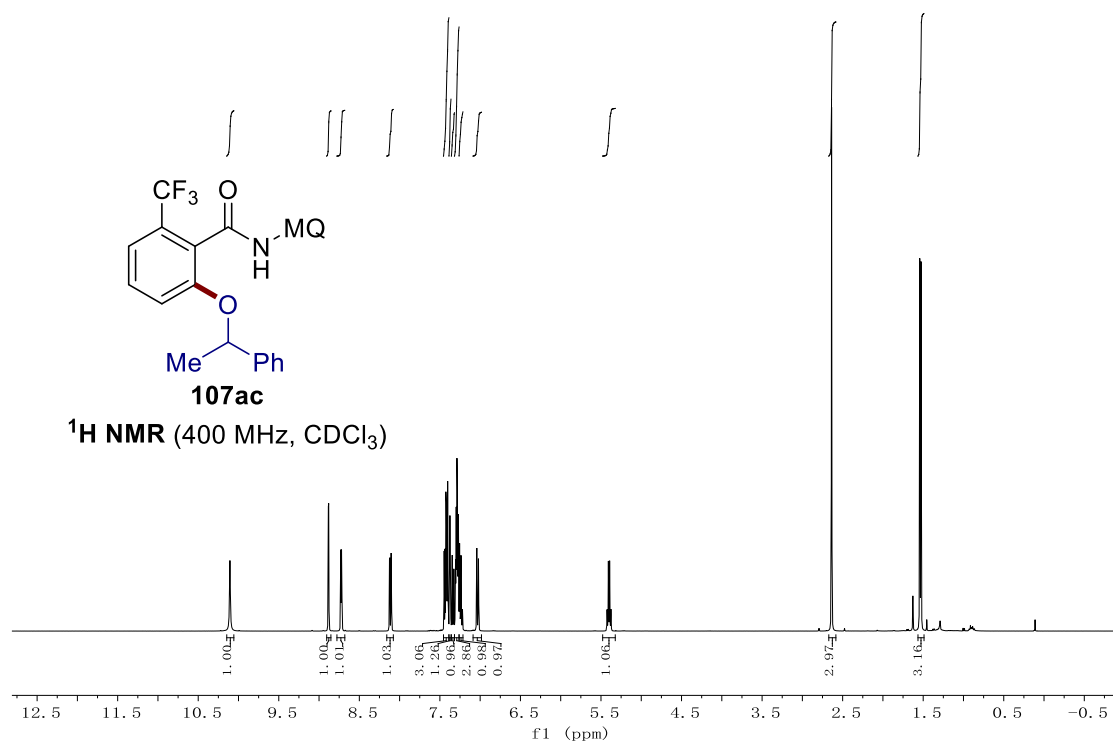
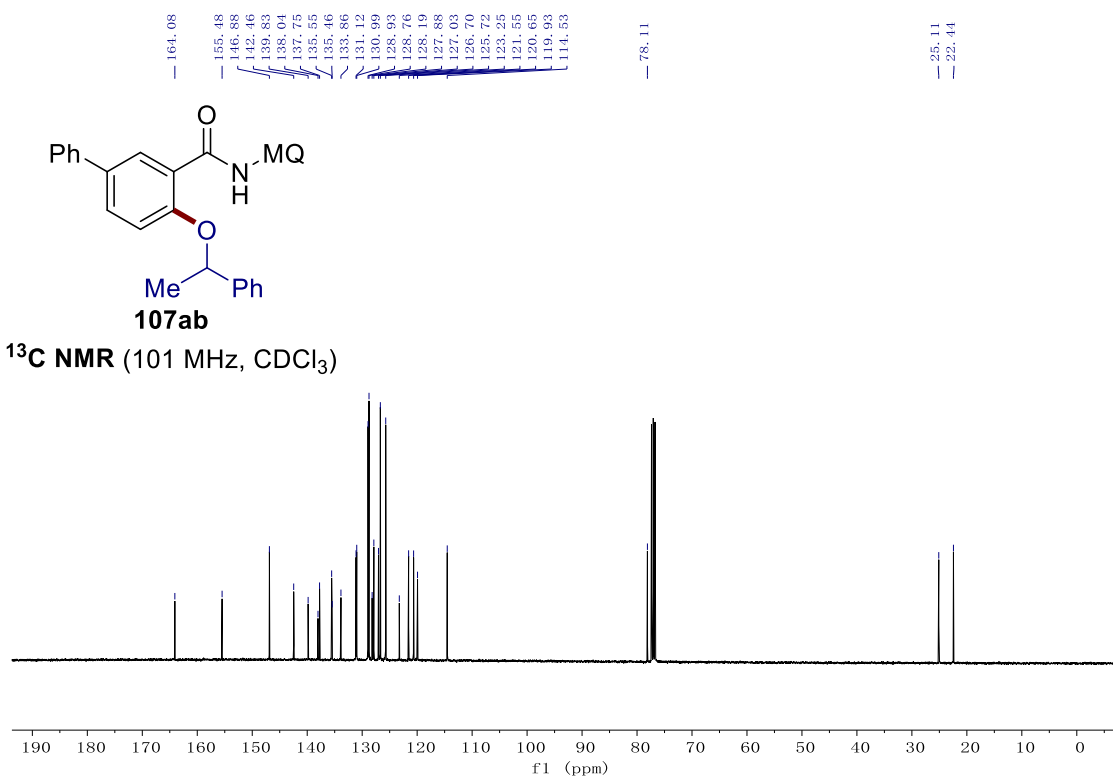


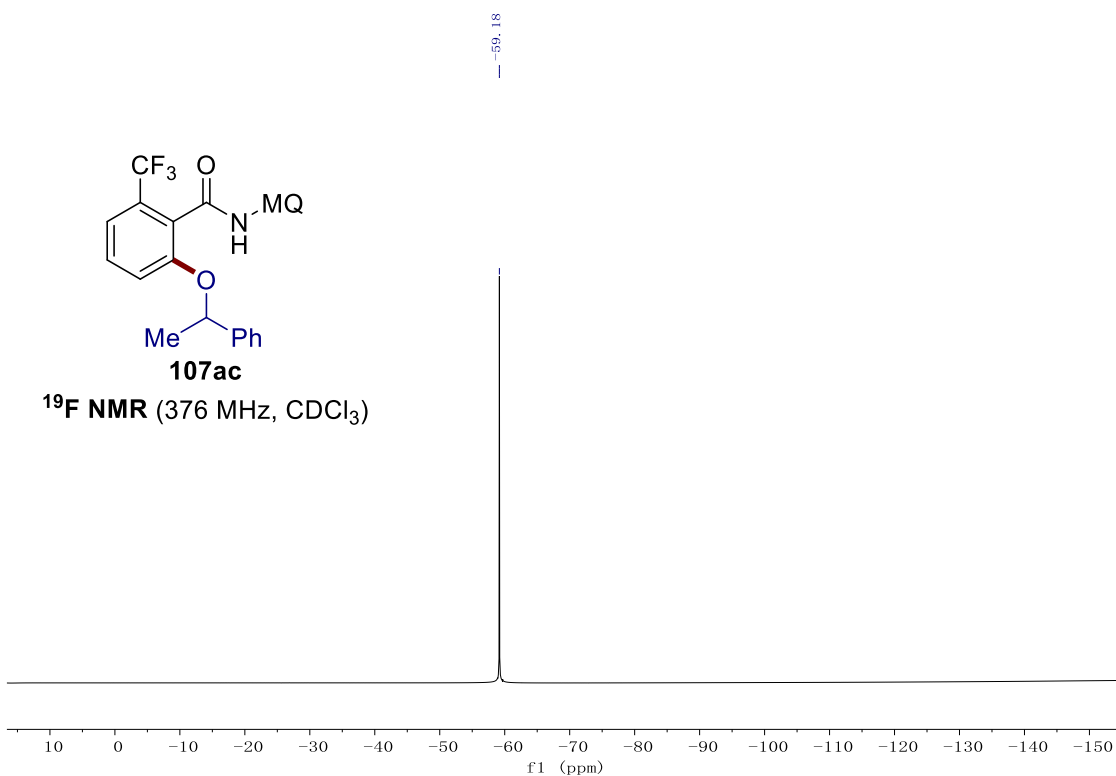
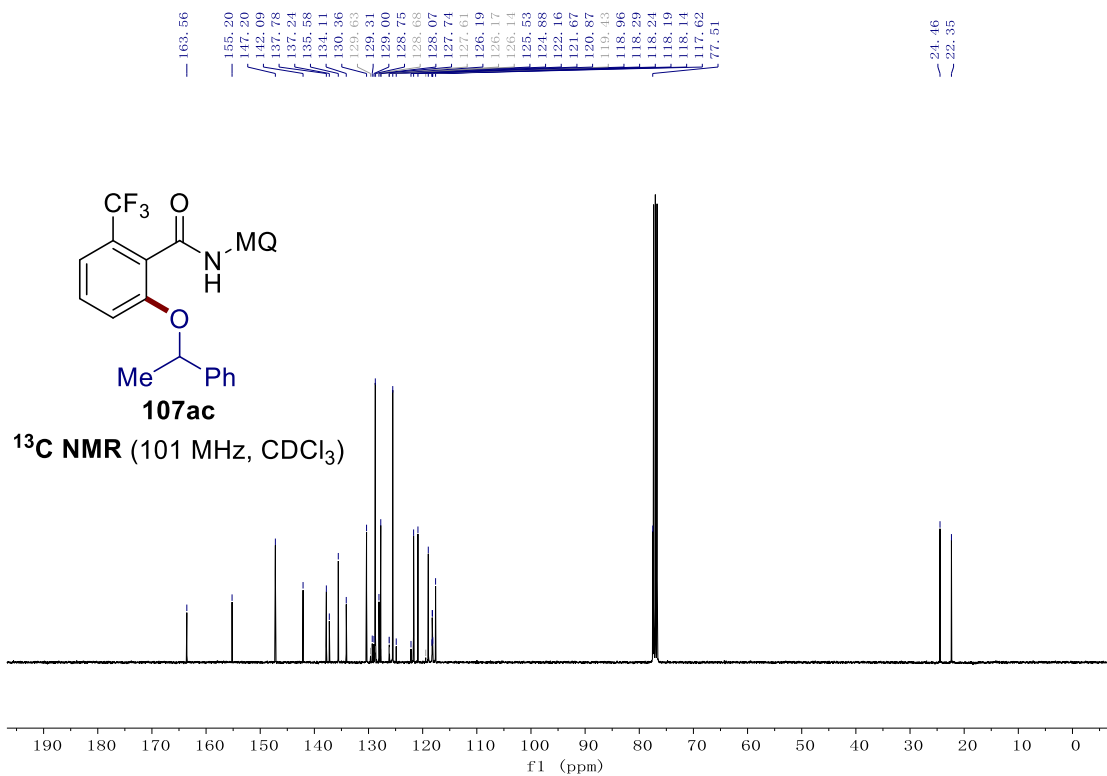
## 7. NMR Spectra



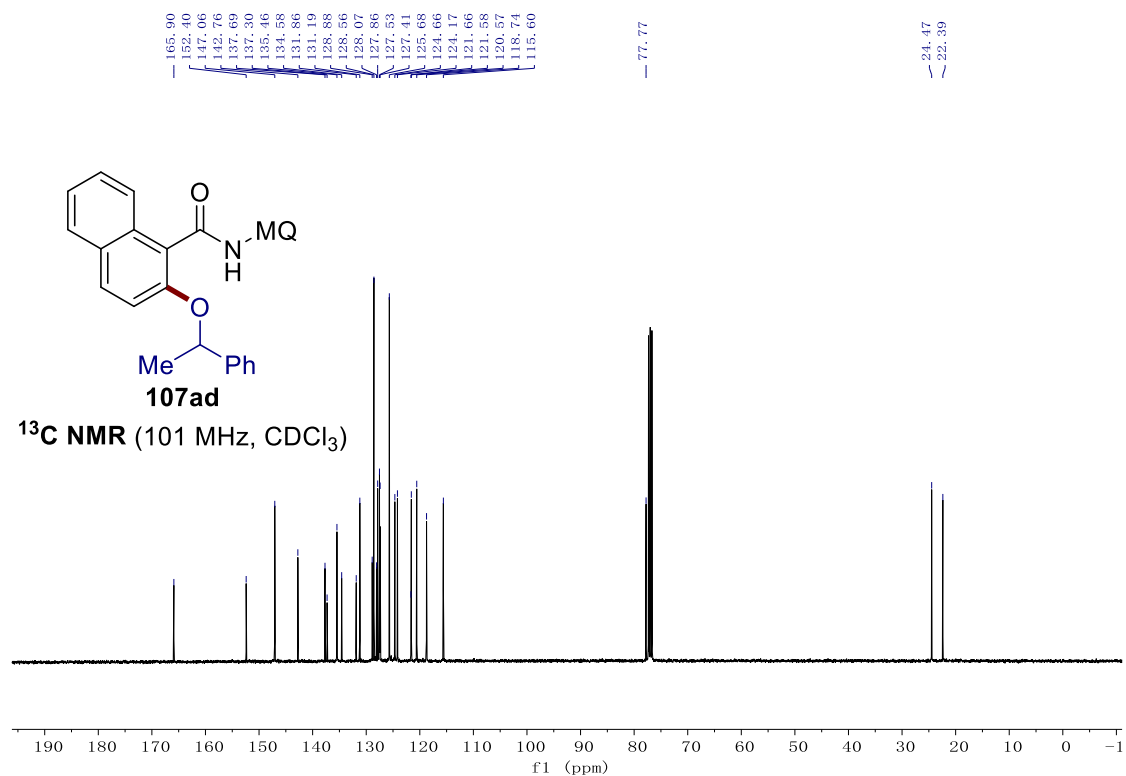
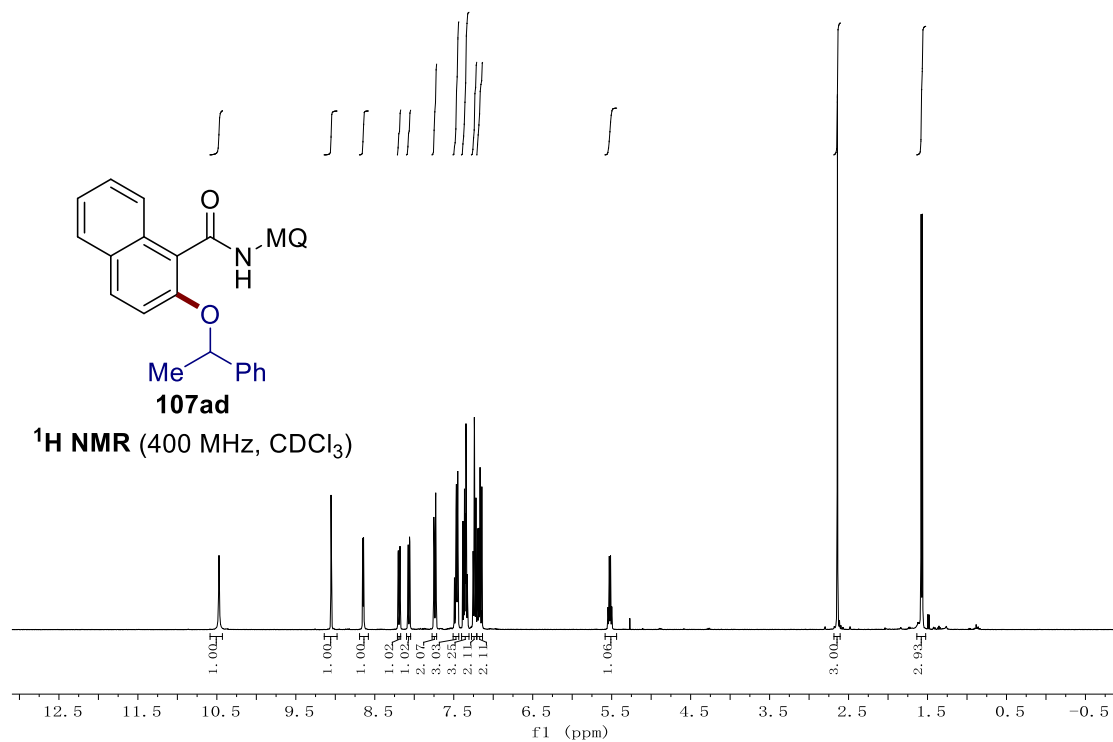


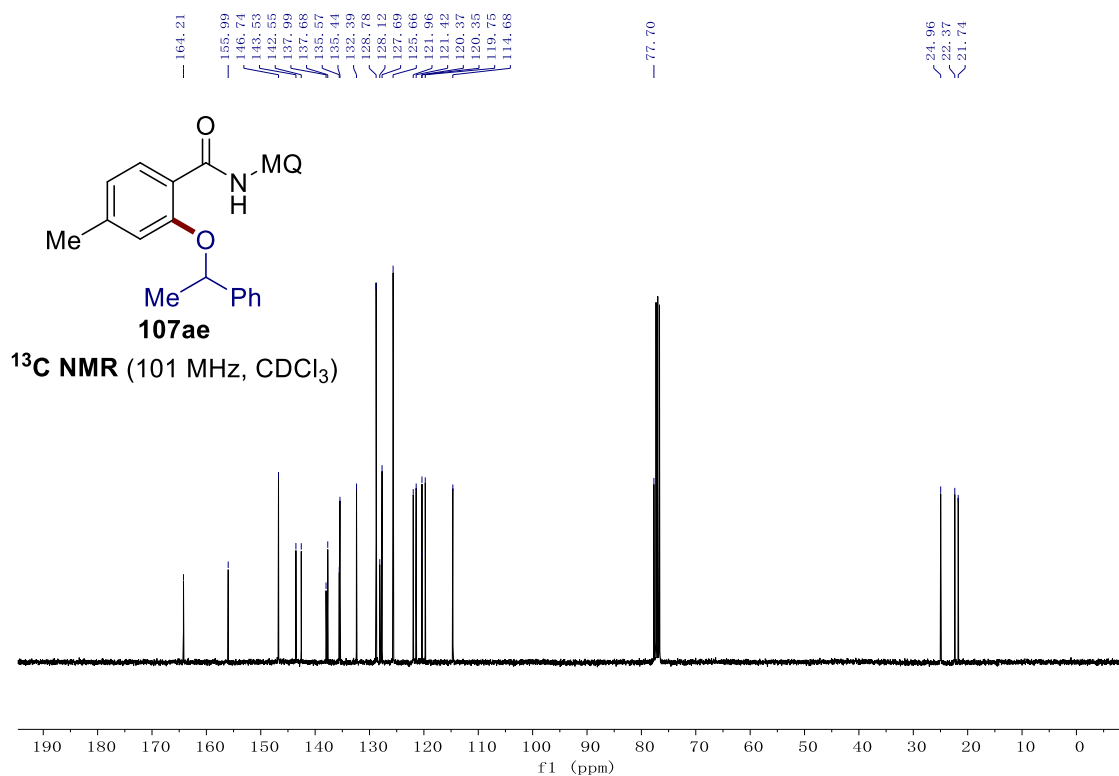
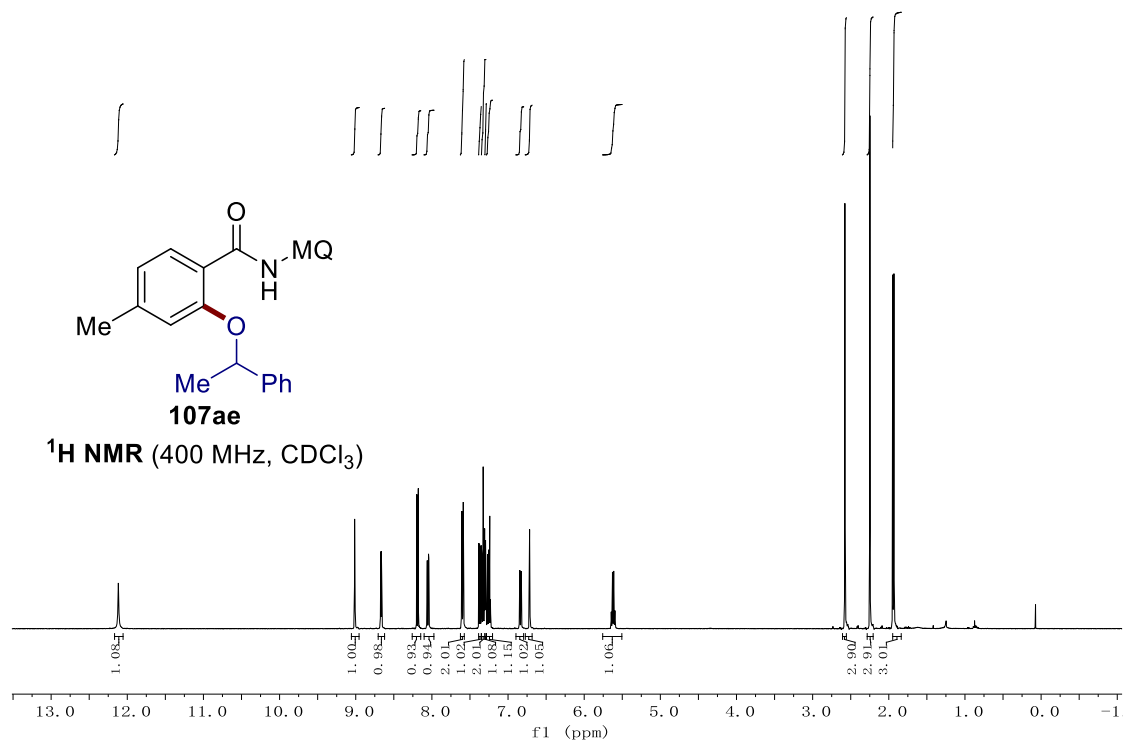
## 7. NMR Spectra



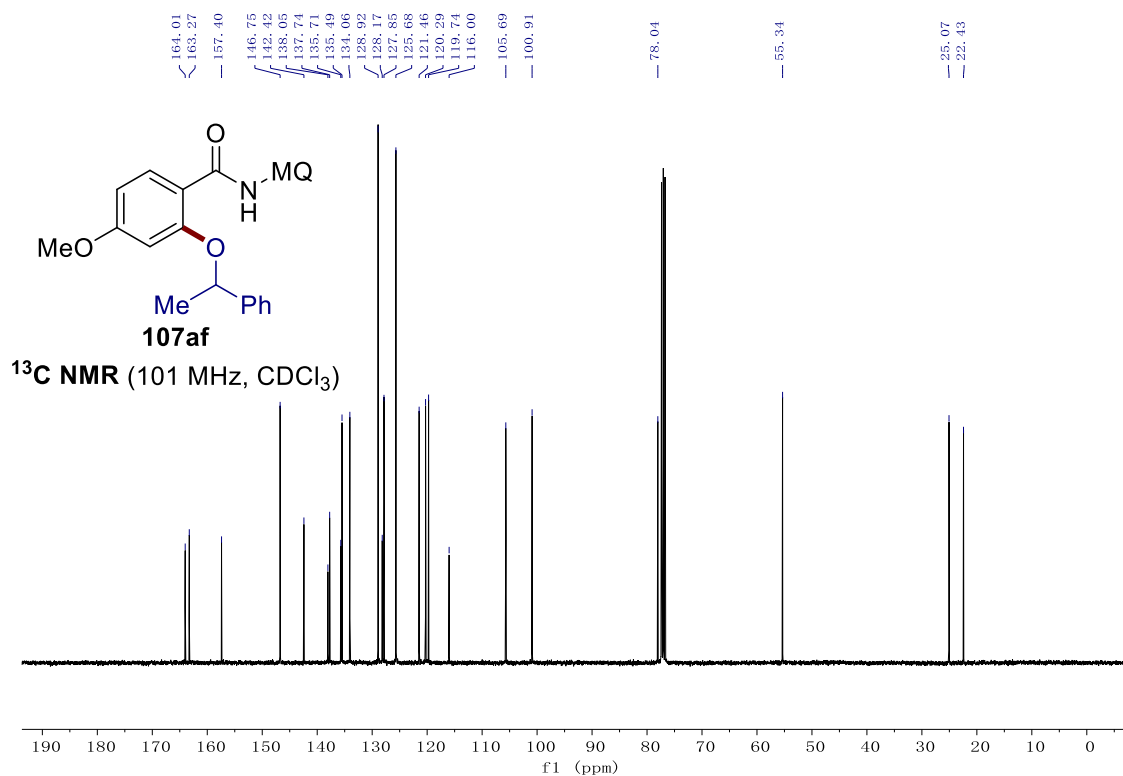
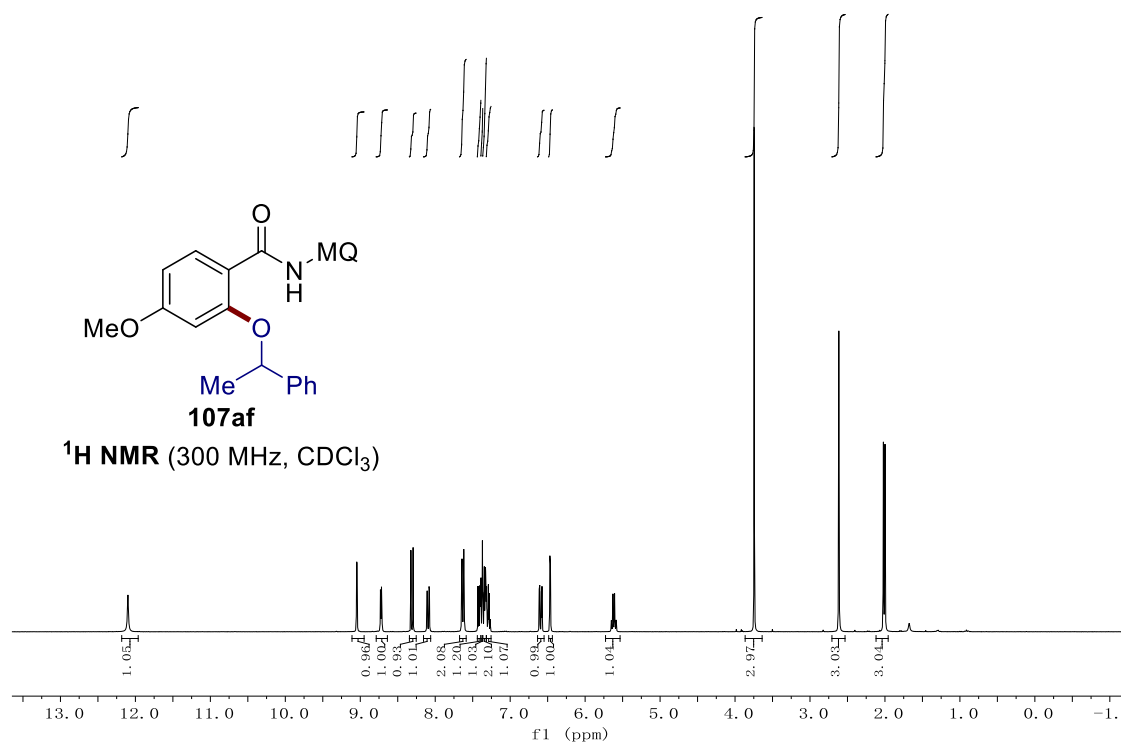


## 7. NMR Spectra

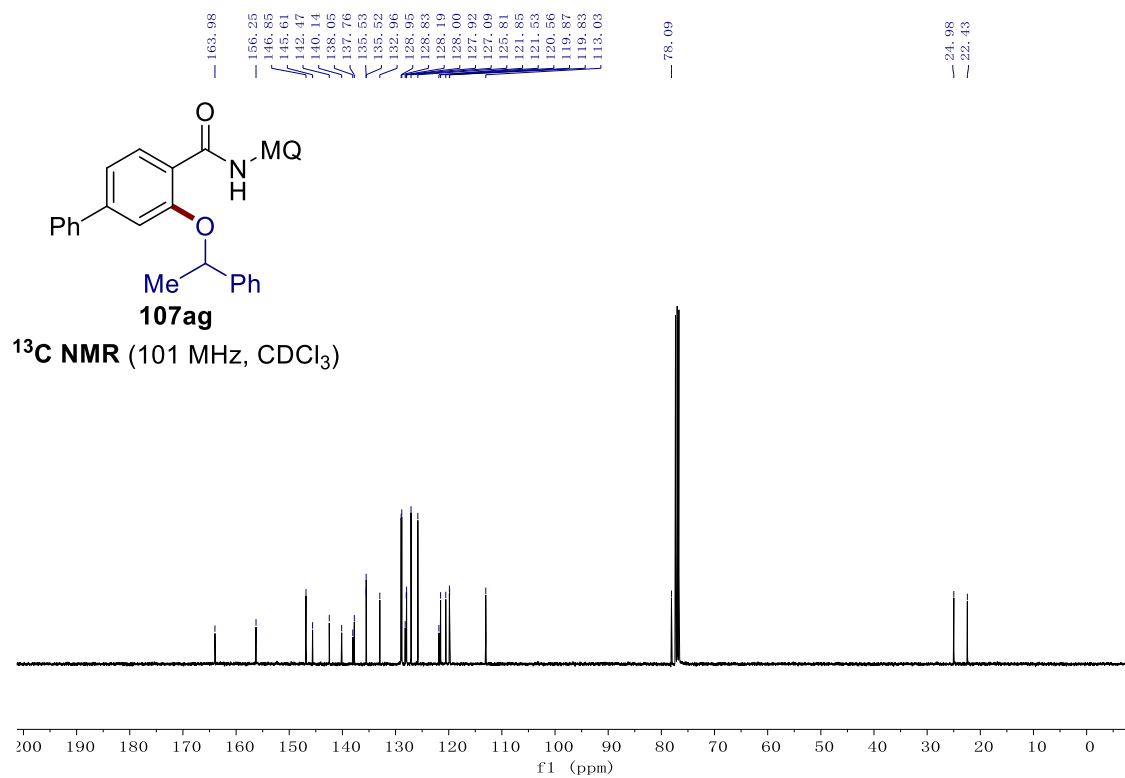
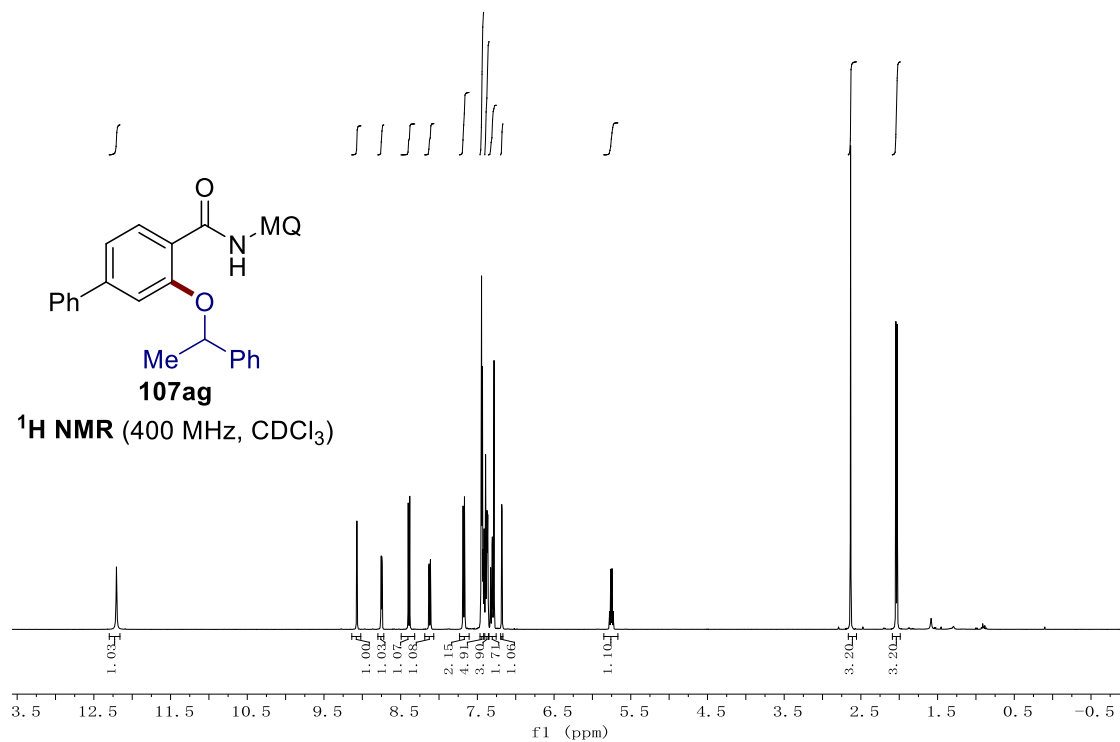




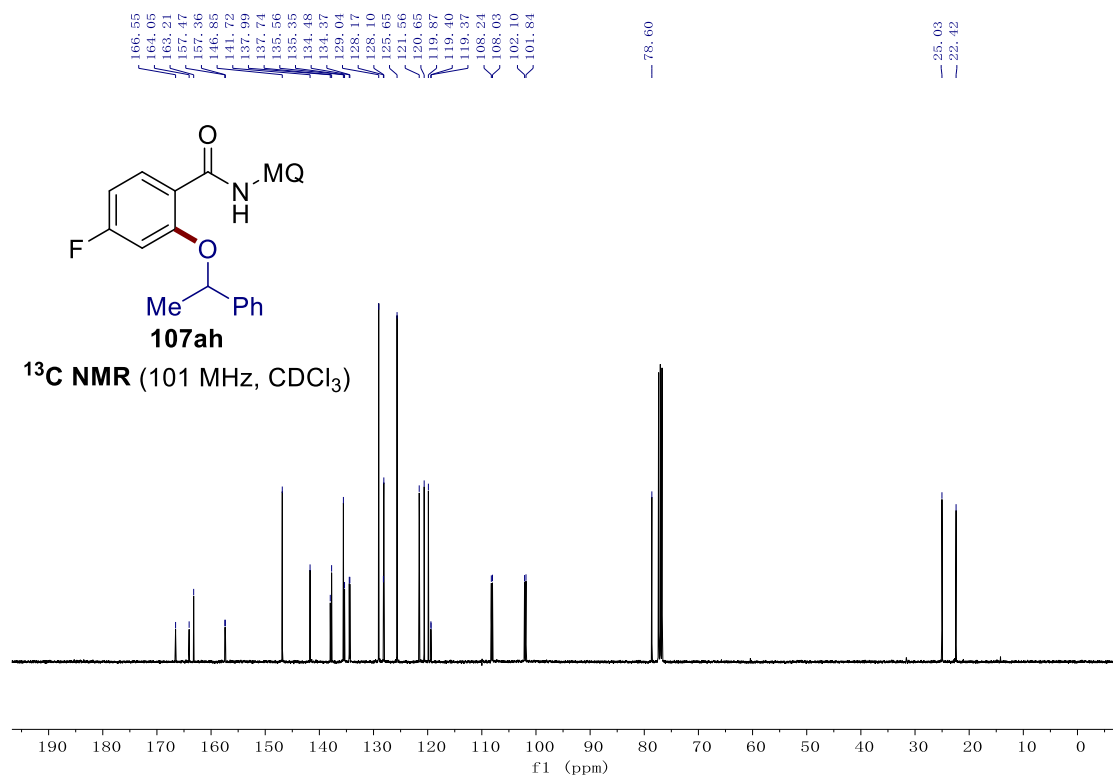
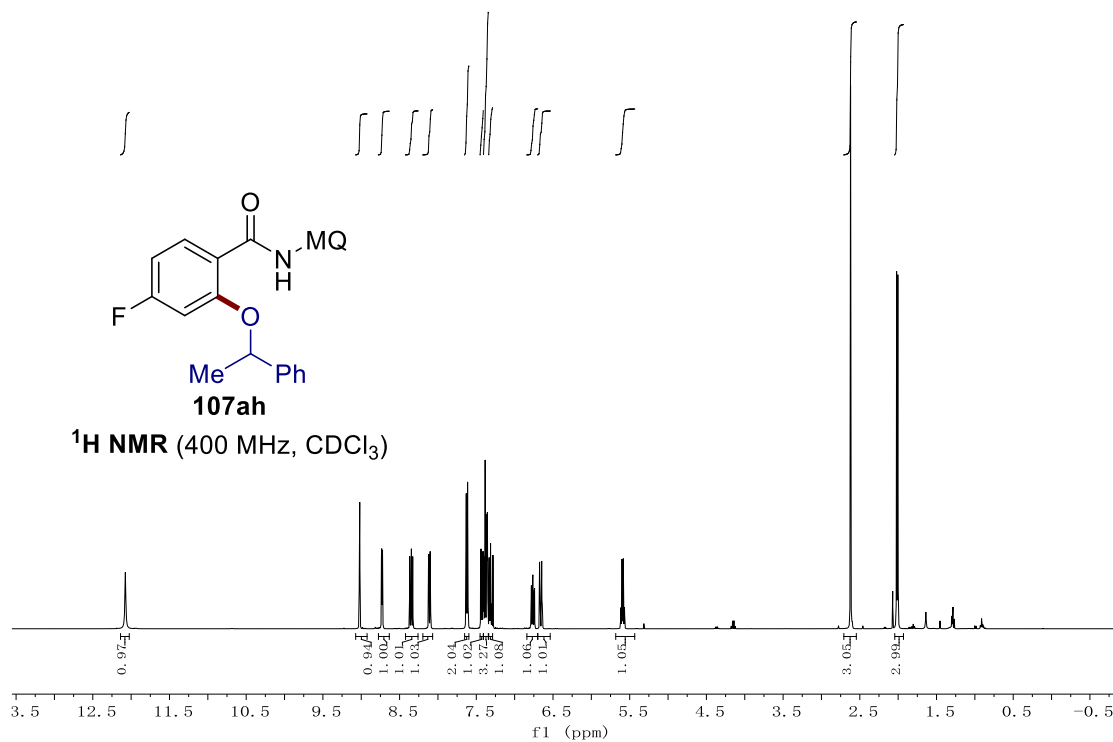
## 7. NMR Spectra

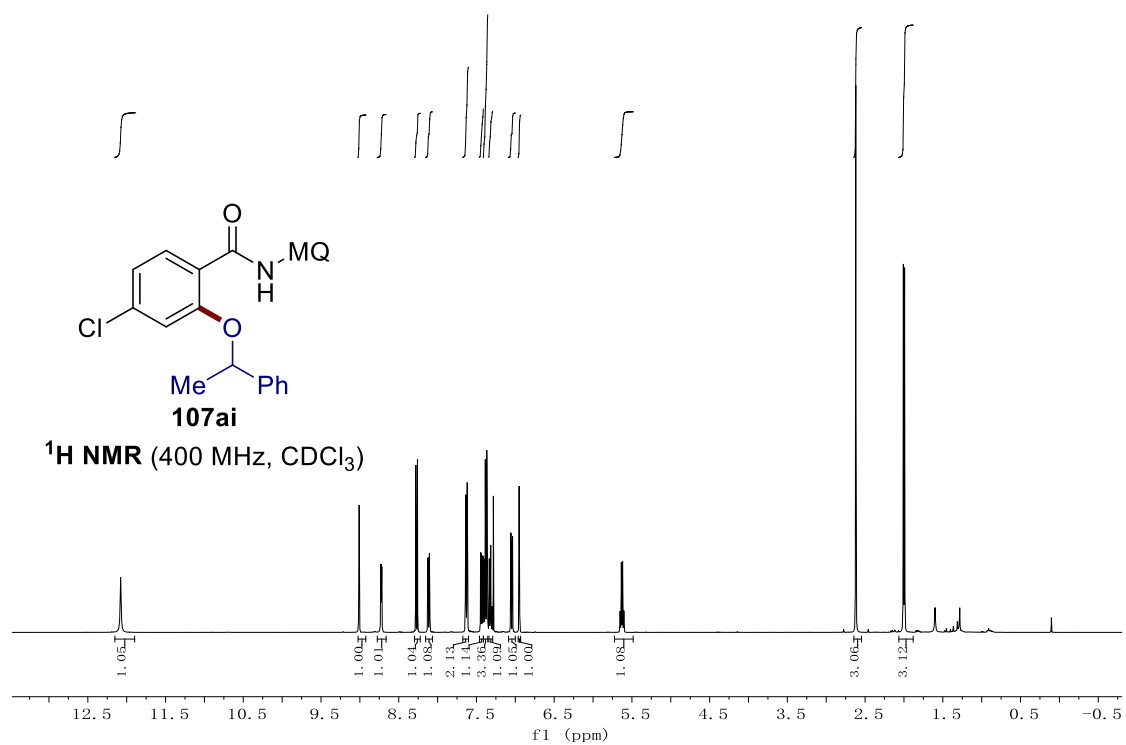
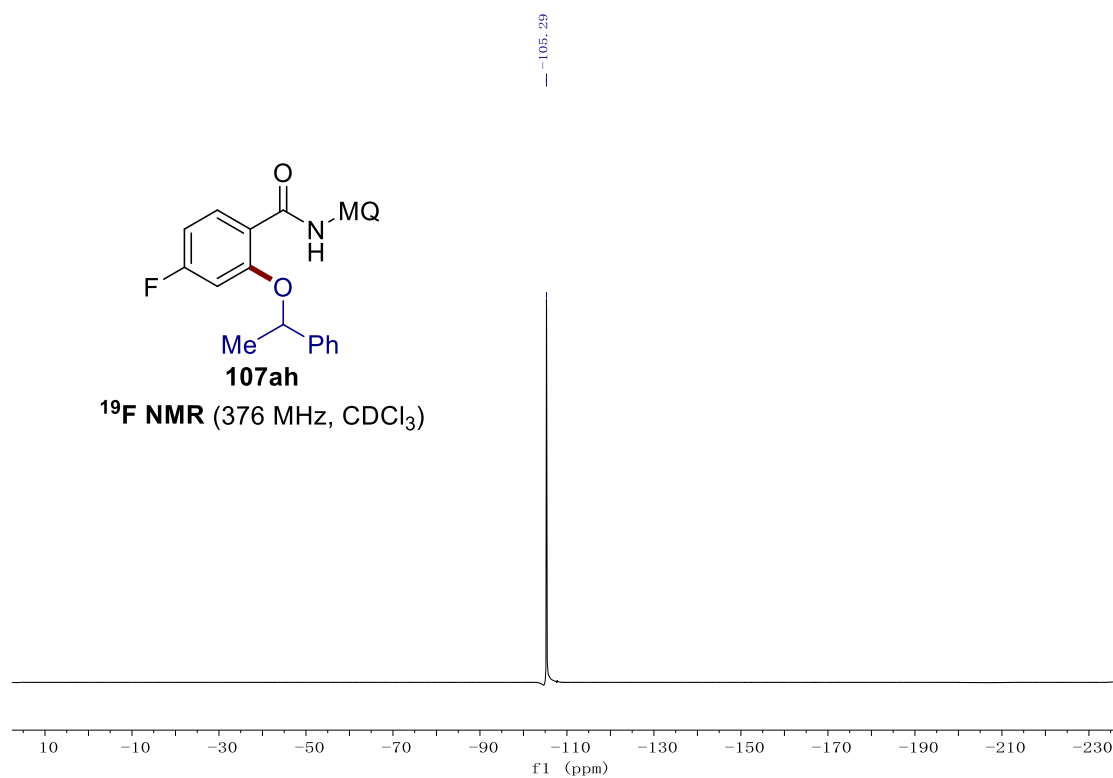




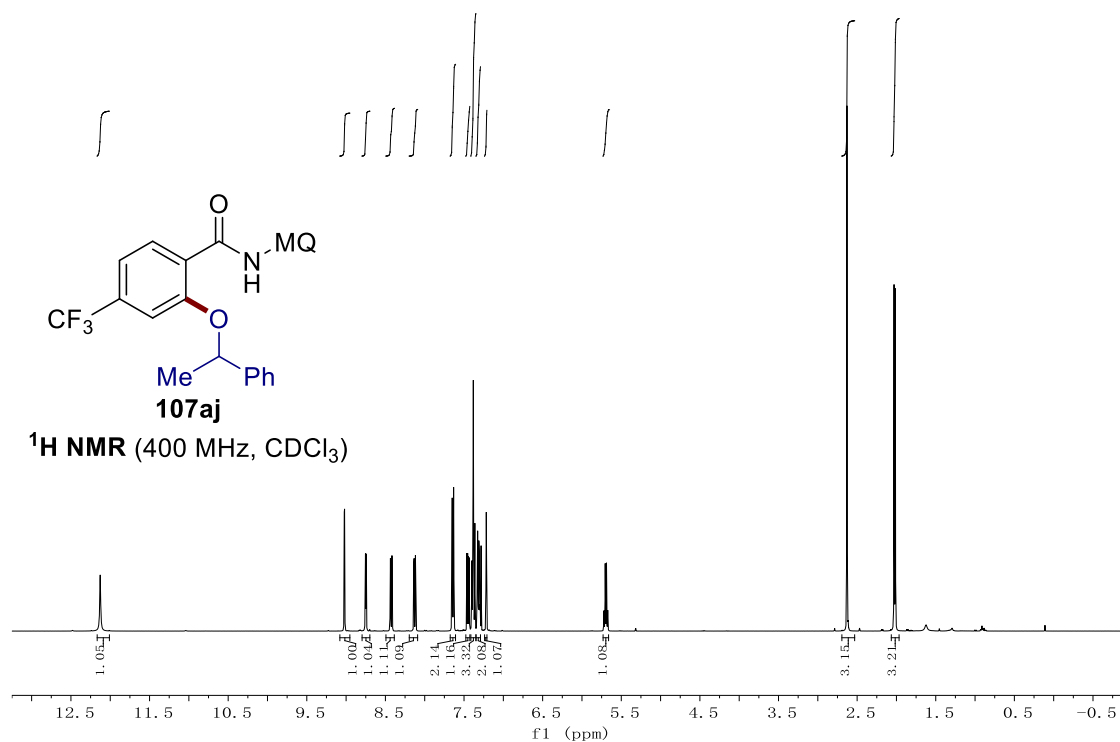
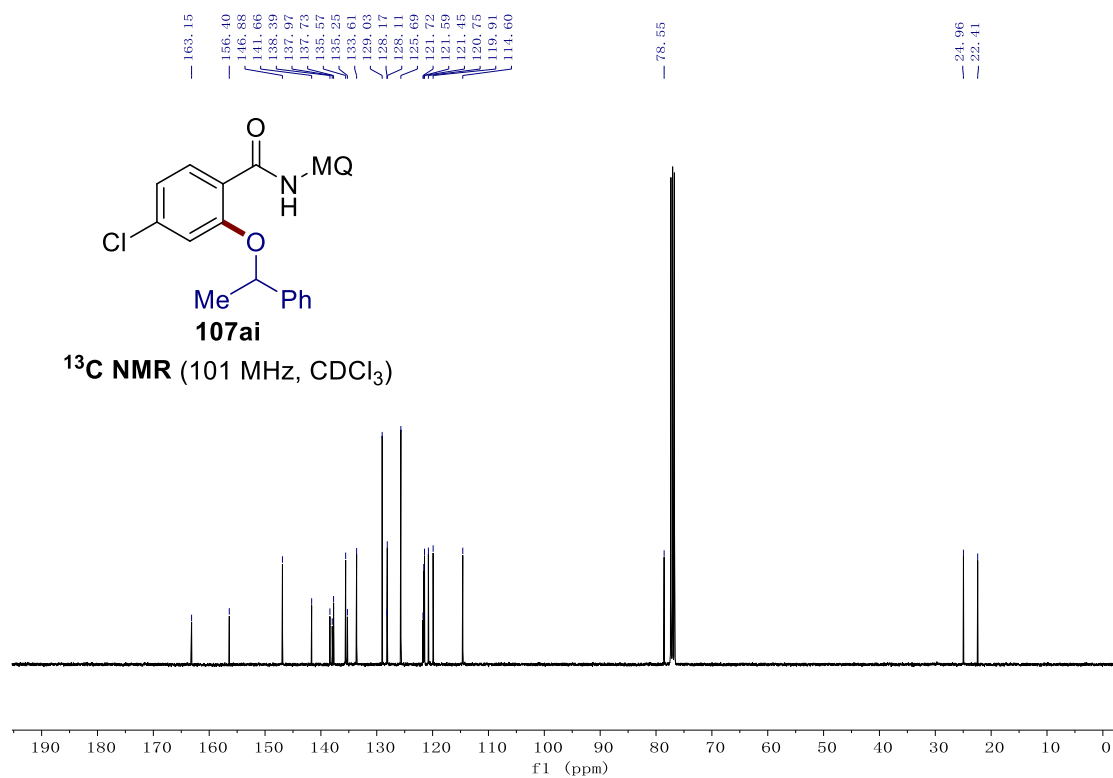


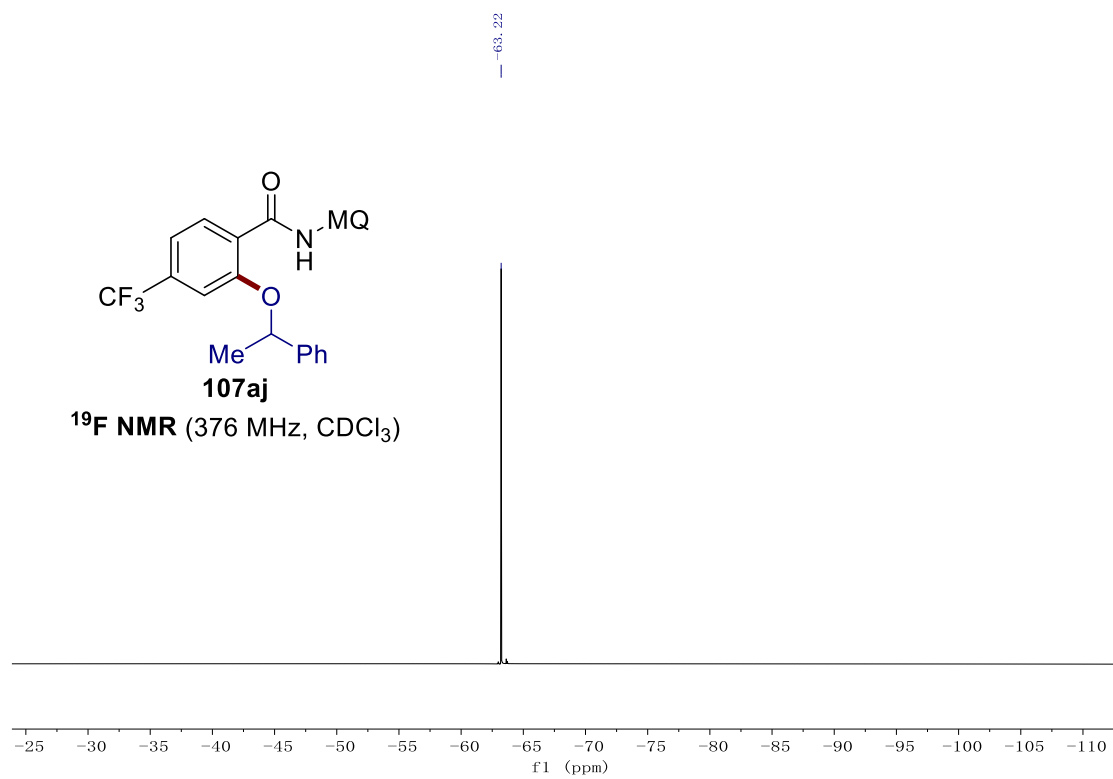
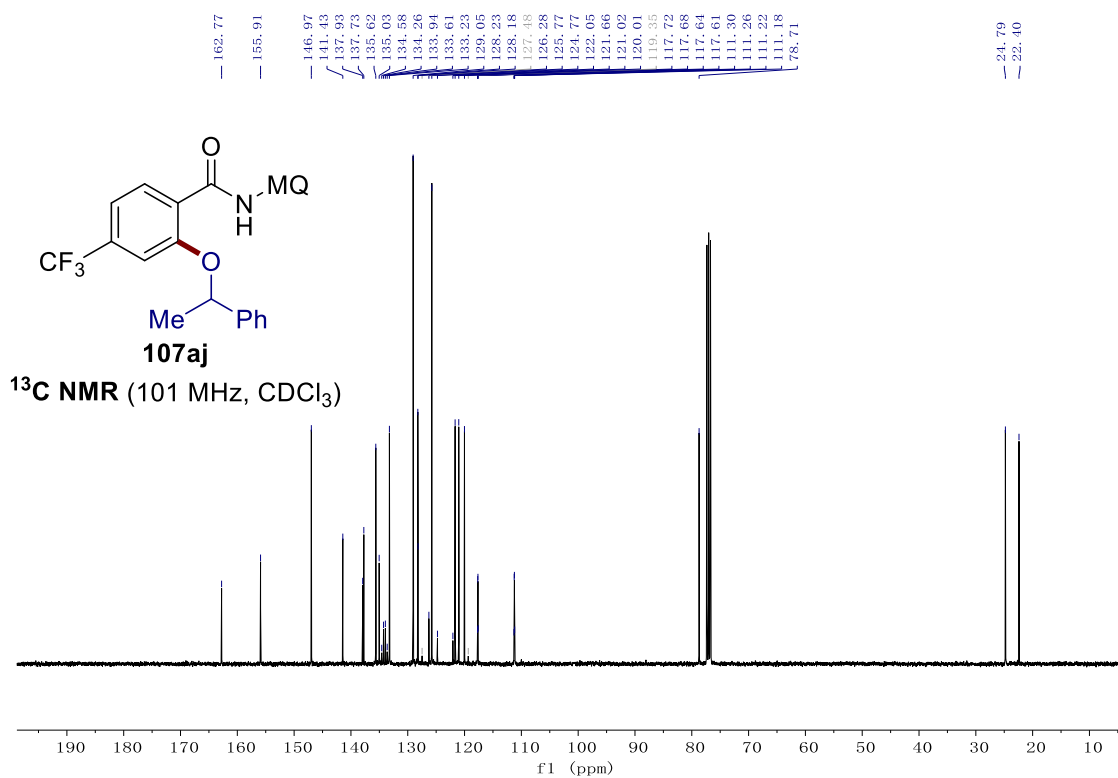
## 7. NMR Spectra



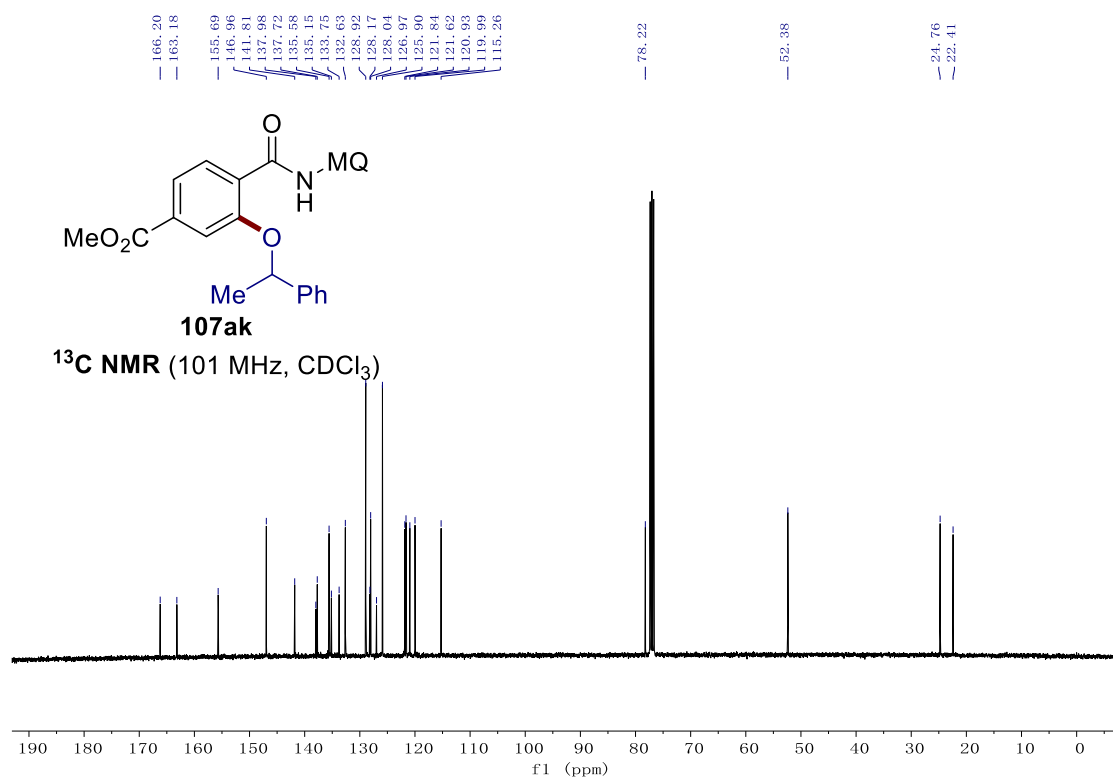
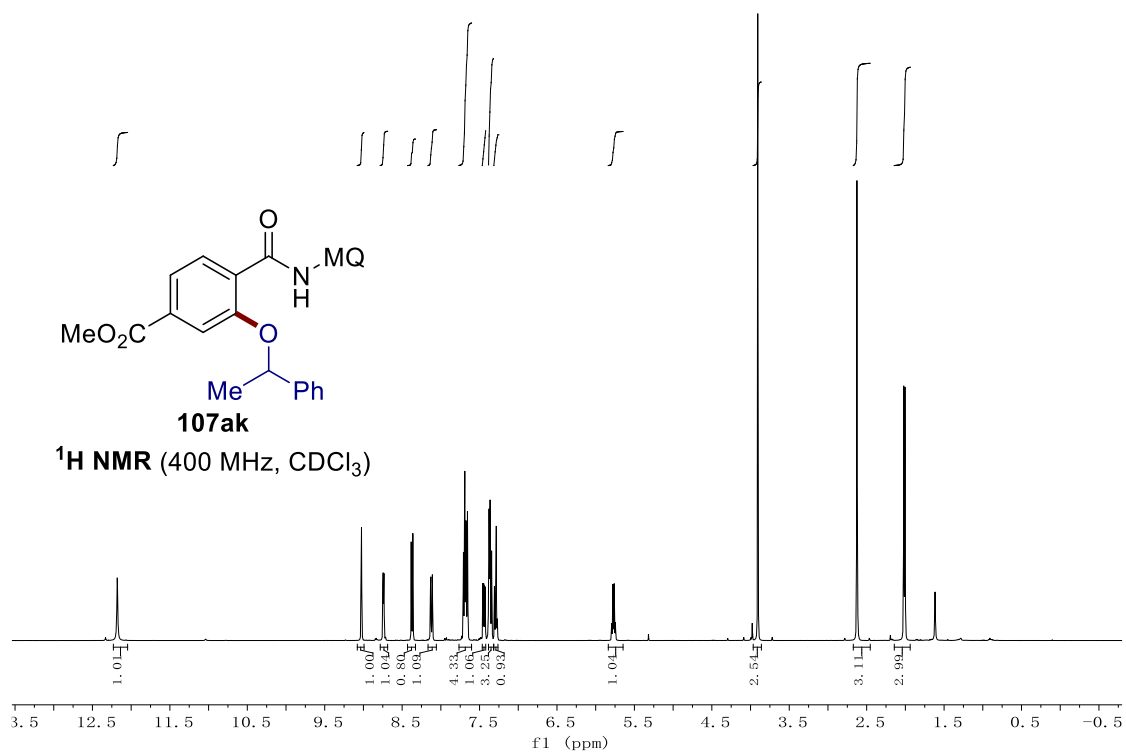


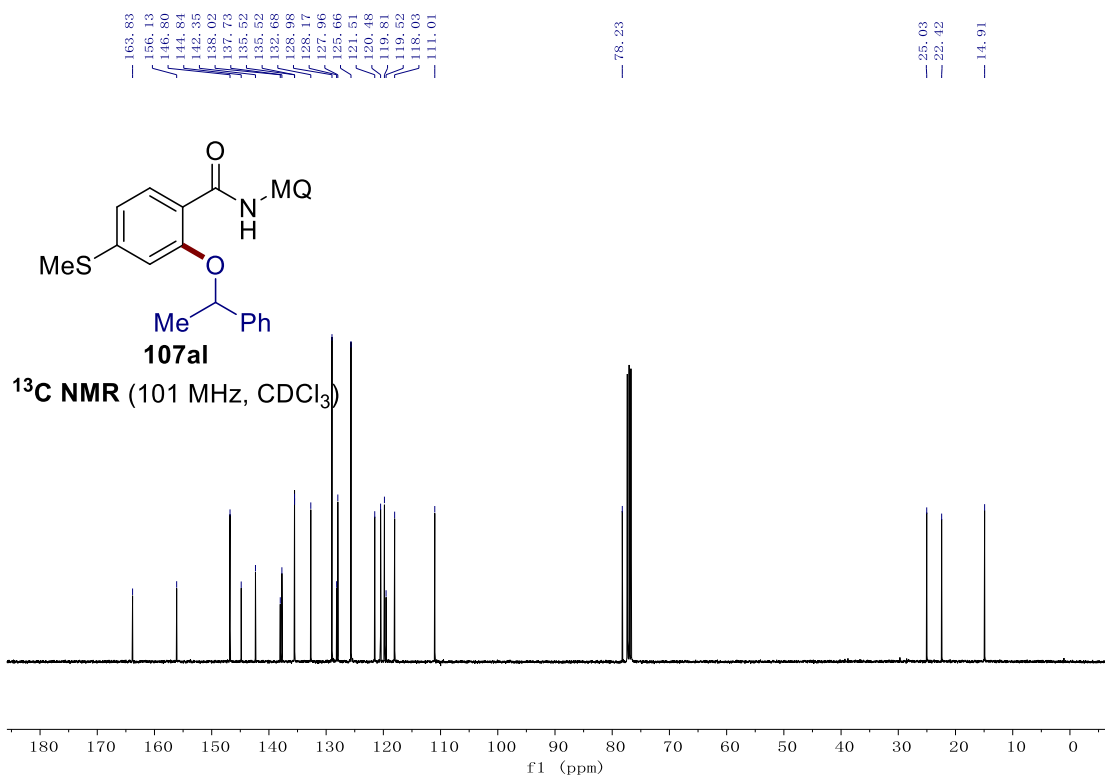
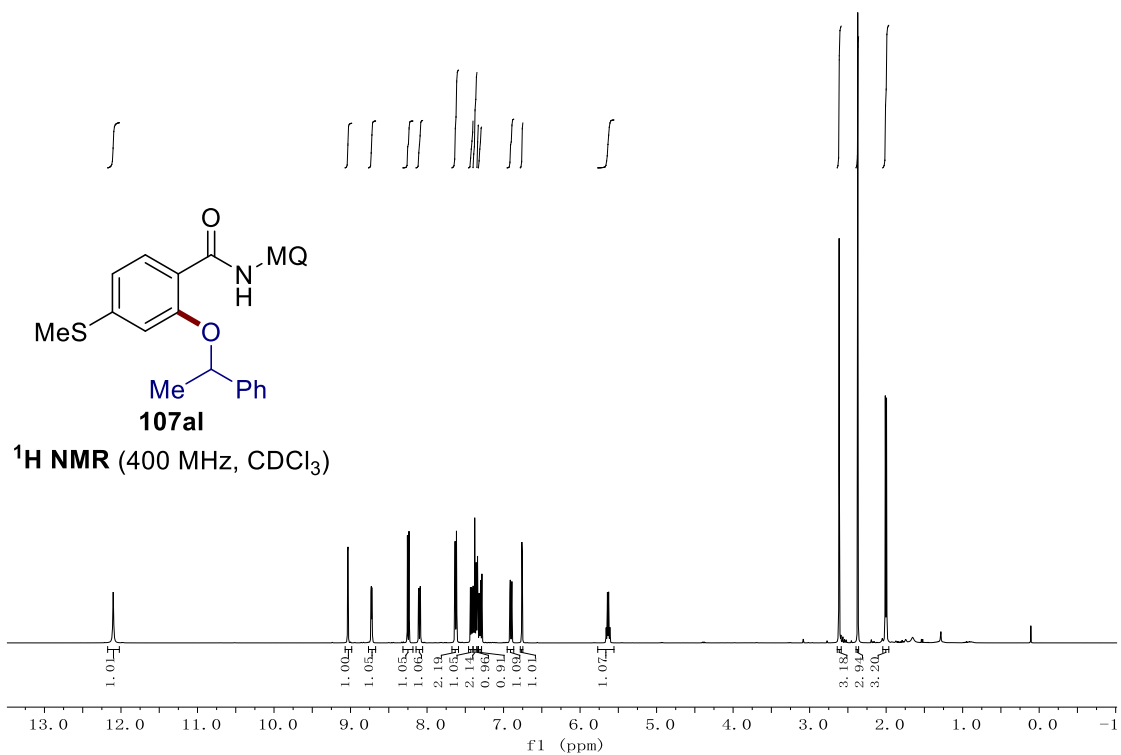
## 7. NMR Spectra



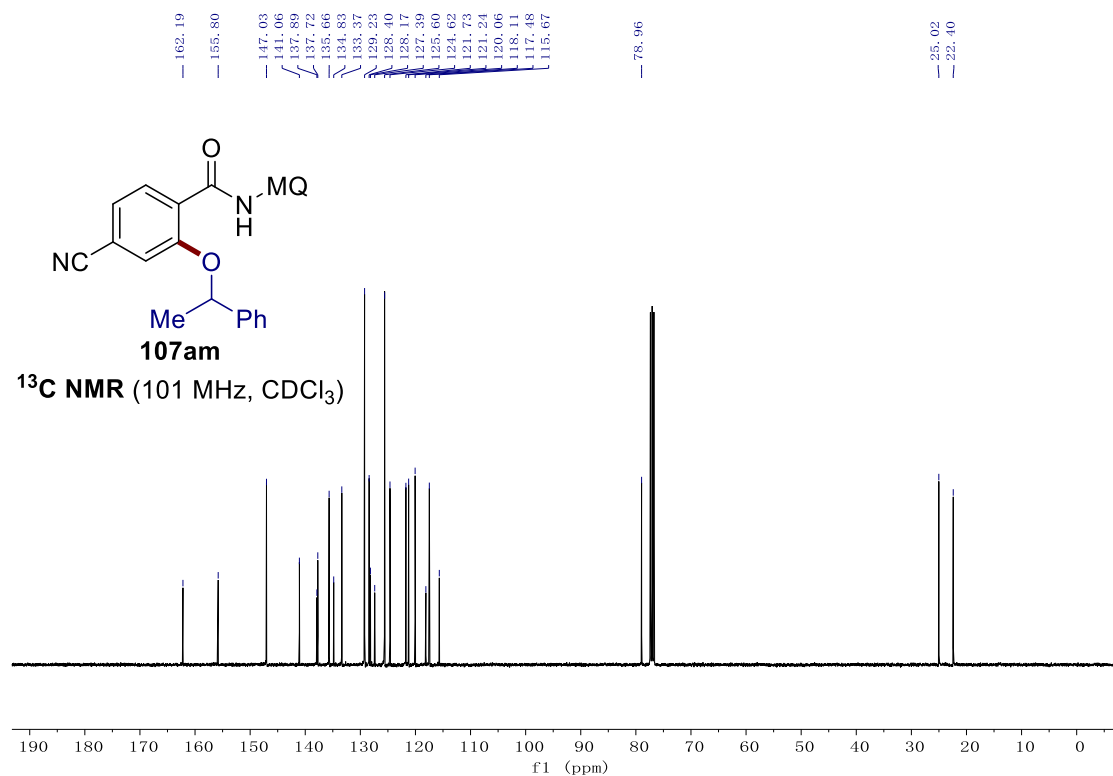
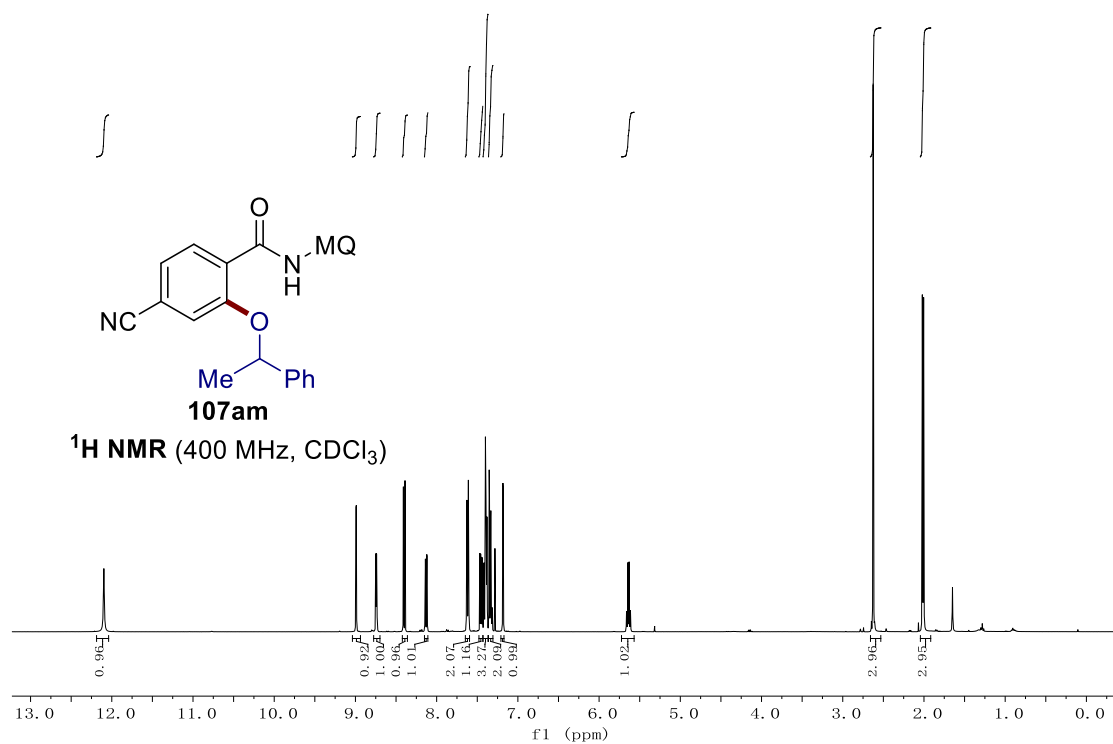


## 7. NMR Spectra

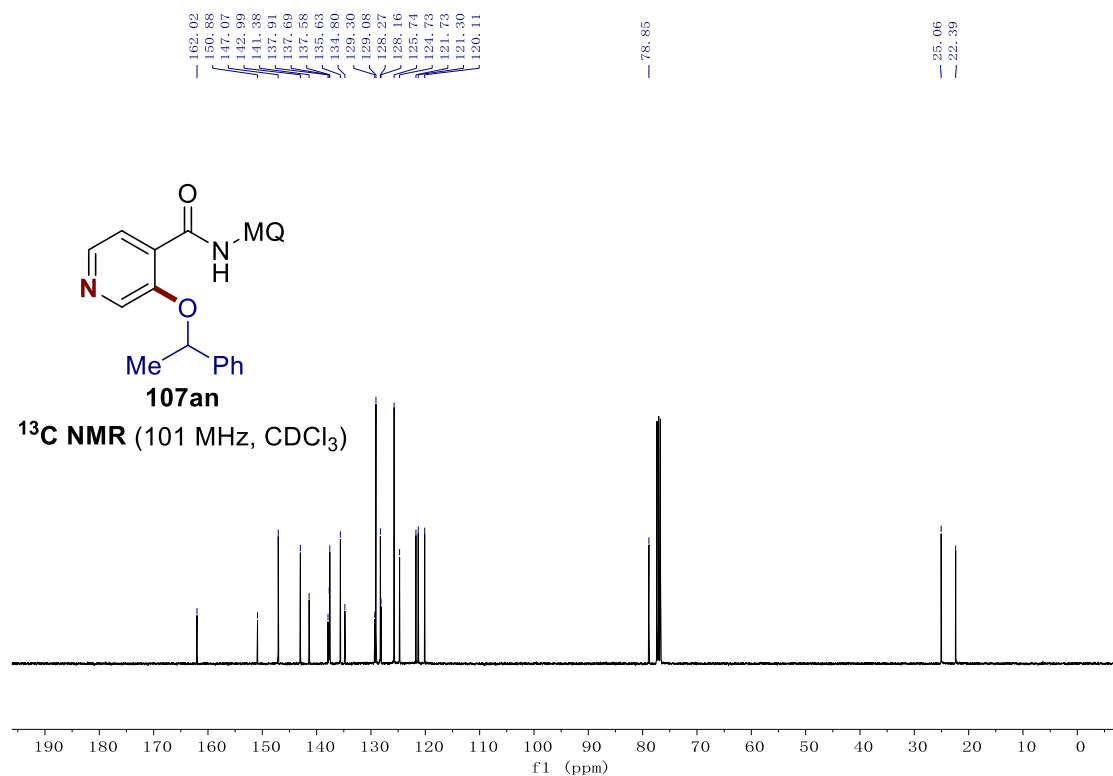
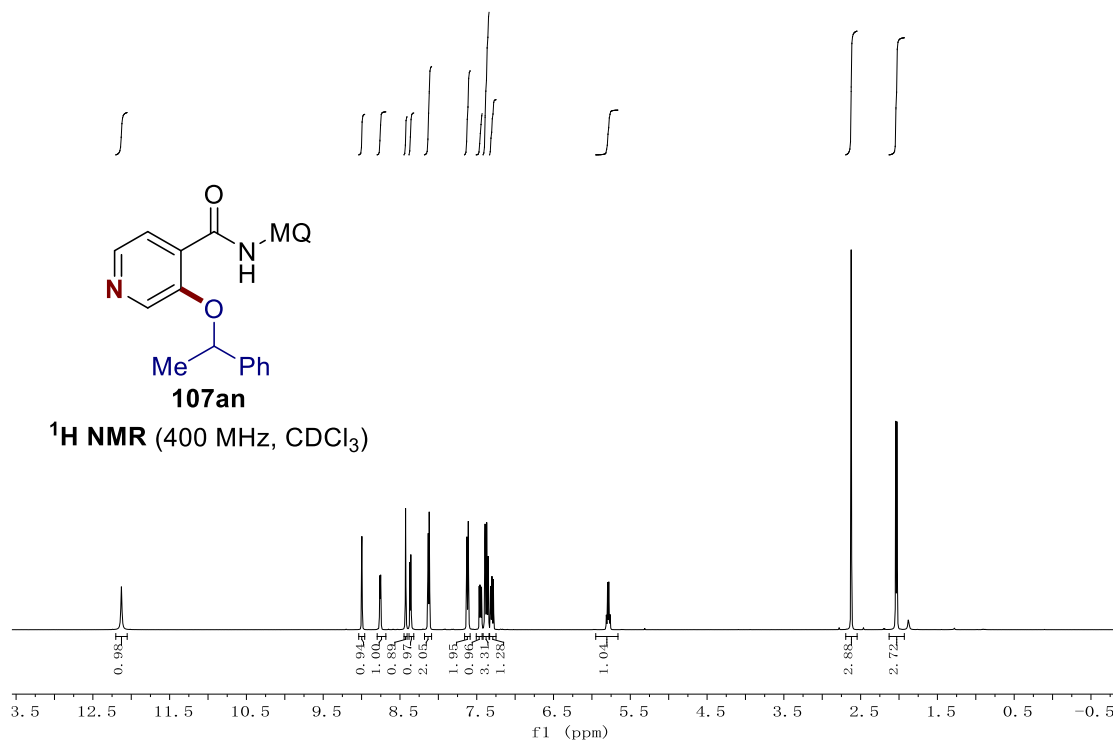




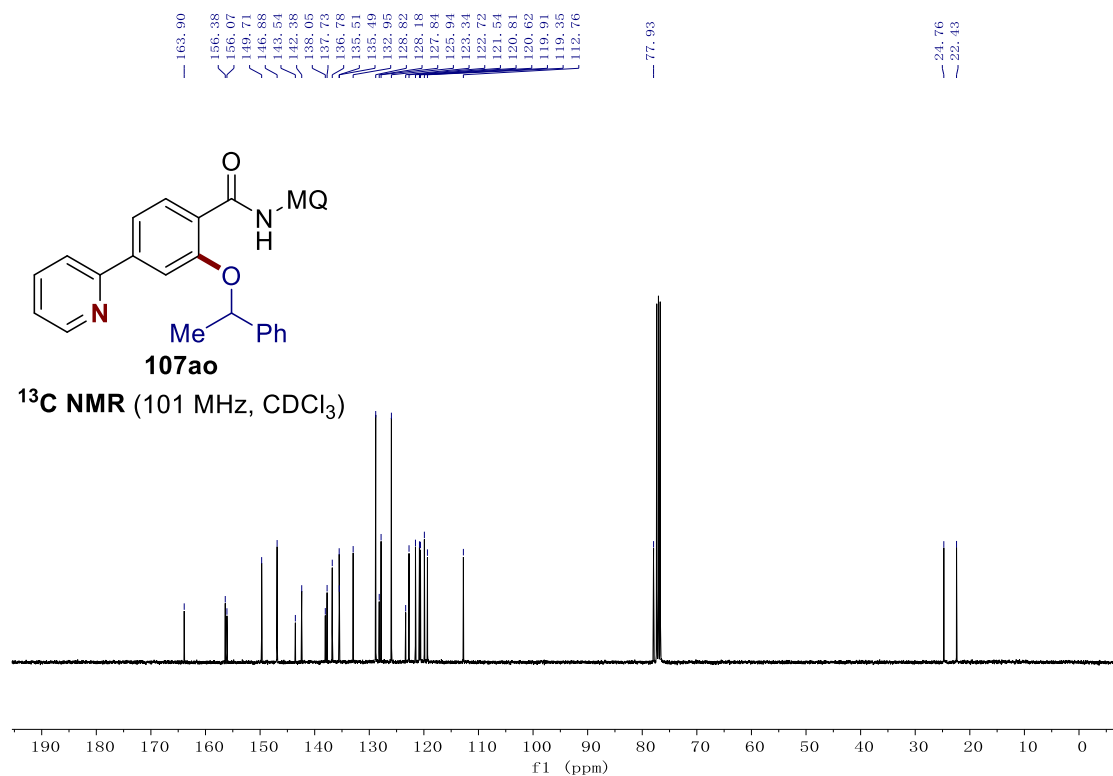
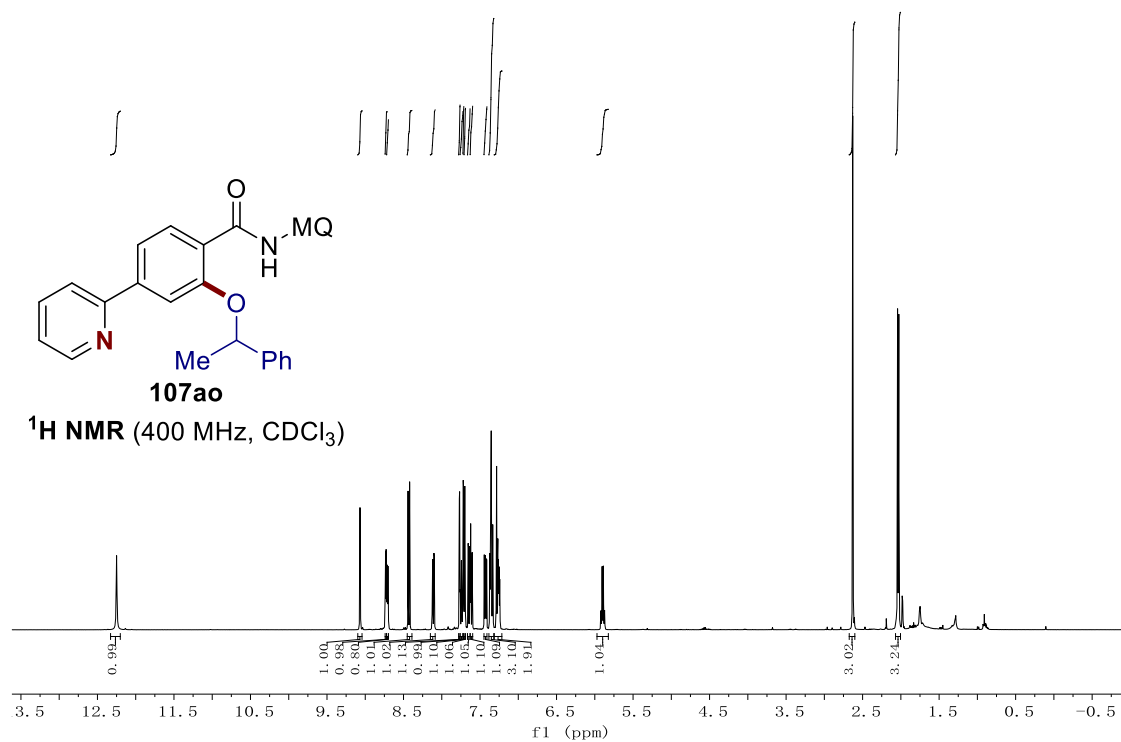
## 7. NMR Spectra

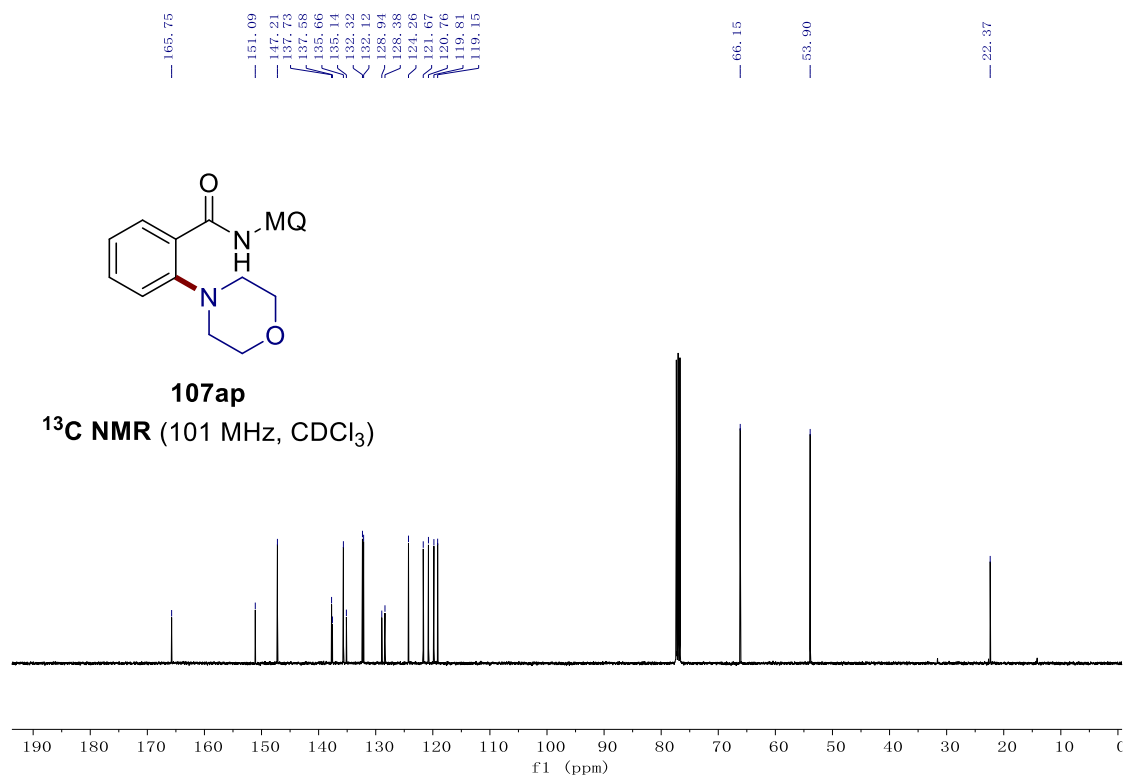
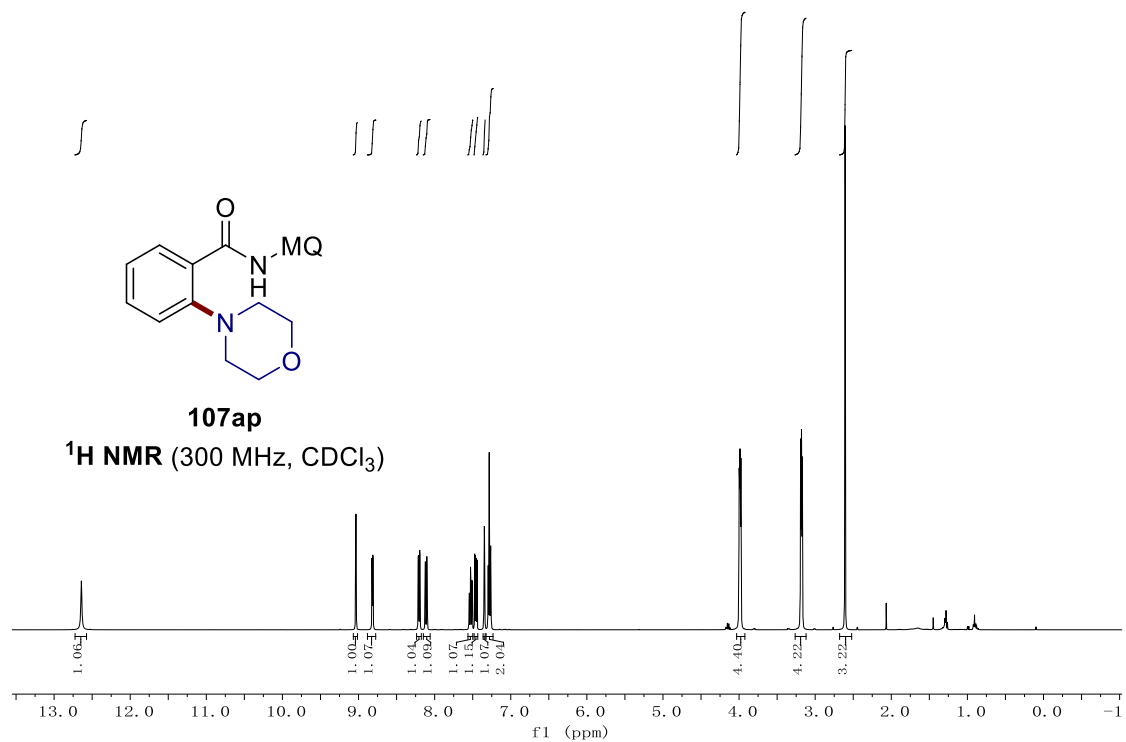




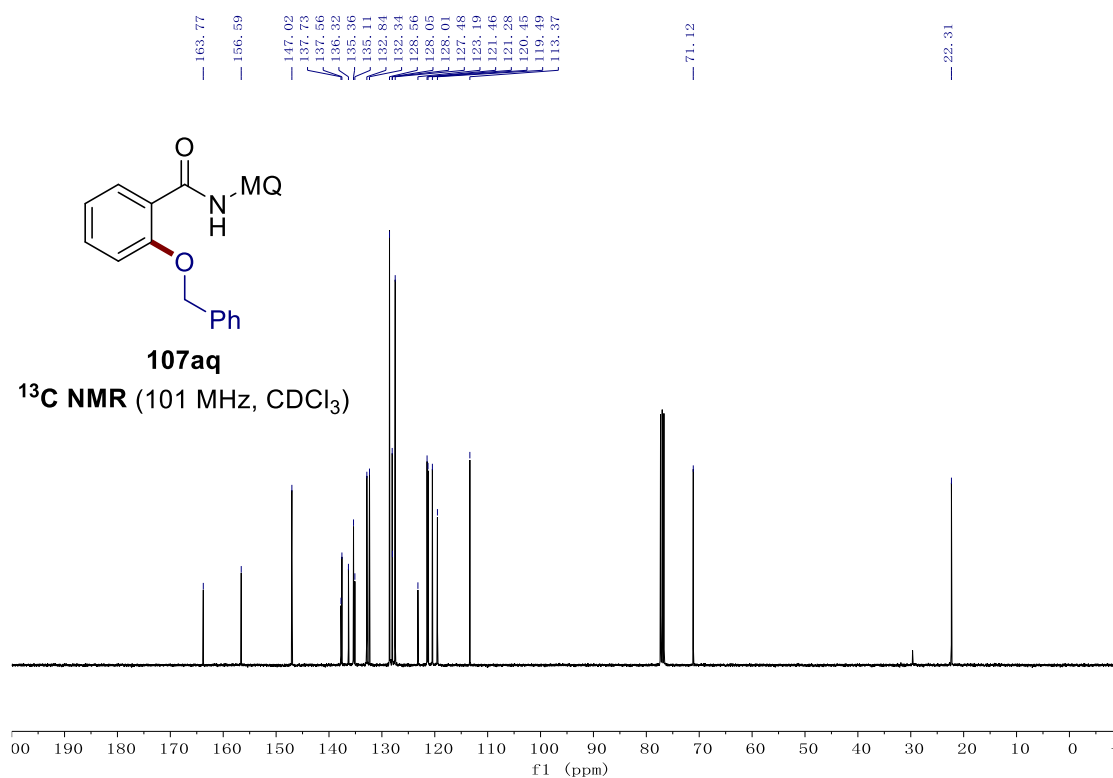
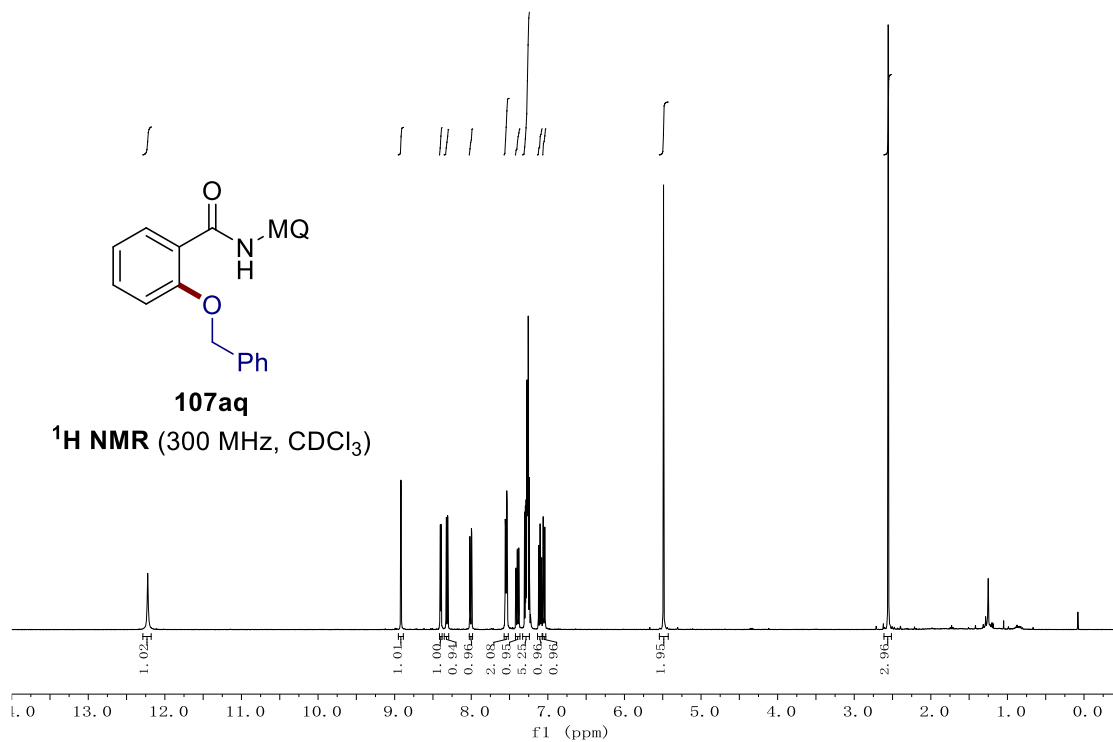


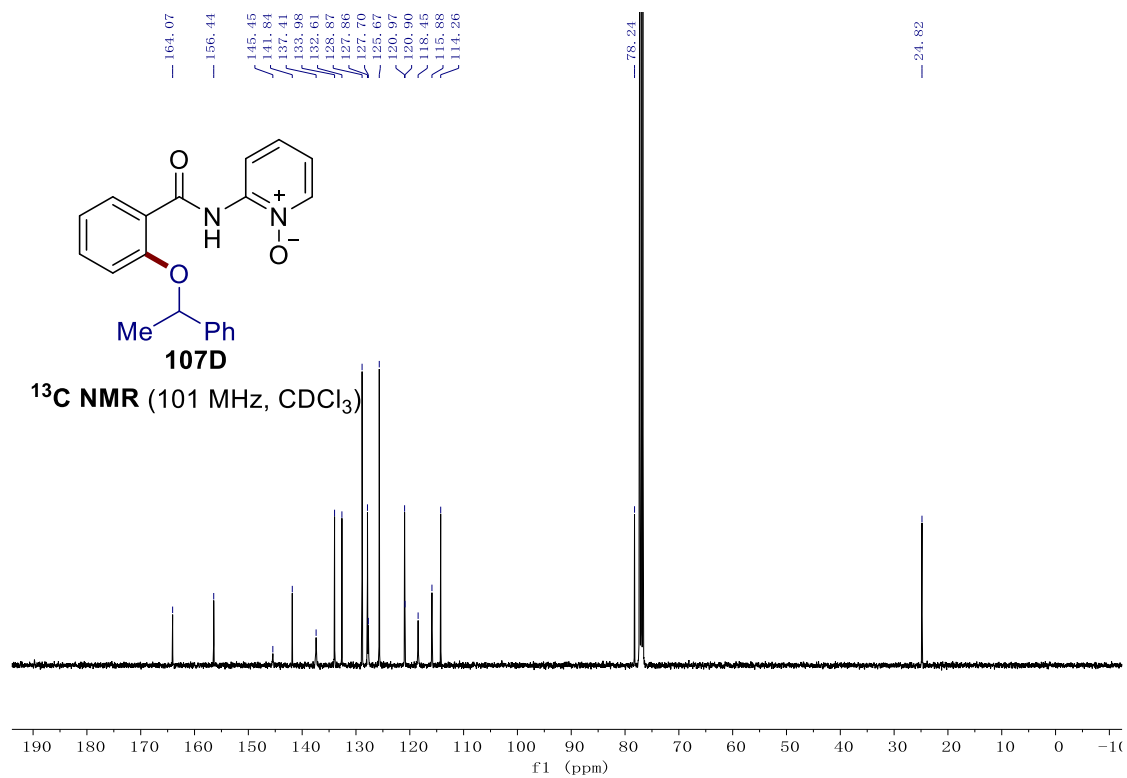
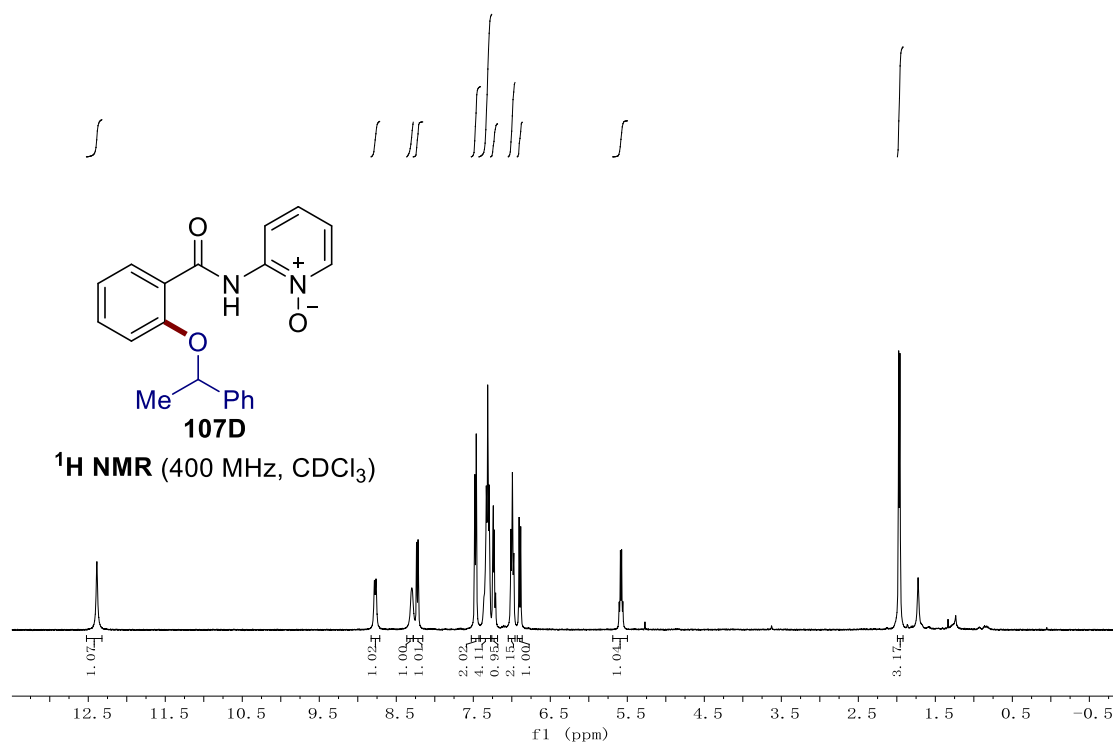
## 7. NMR Spectra



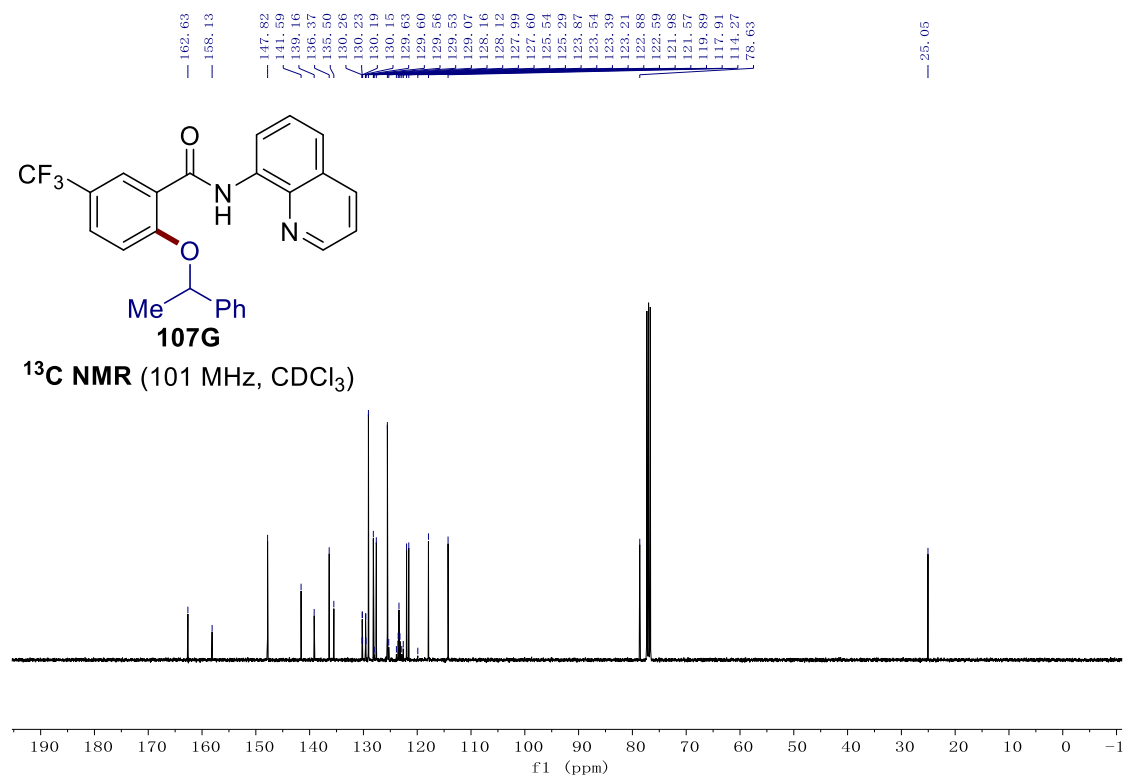
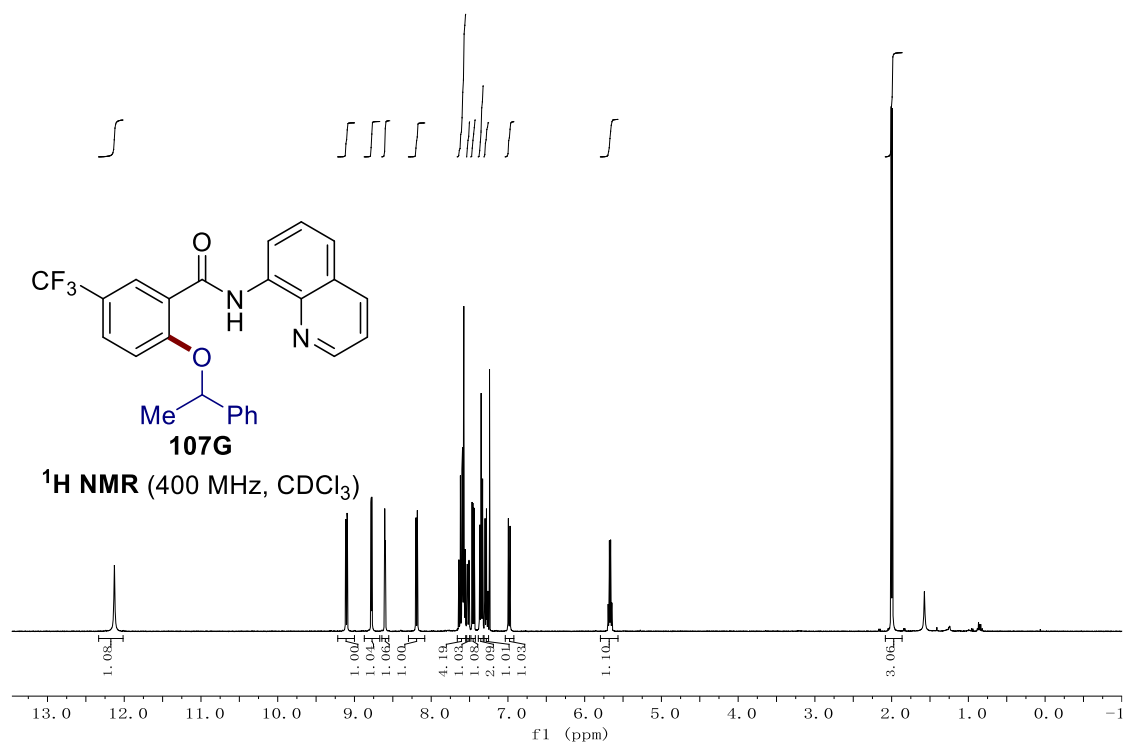


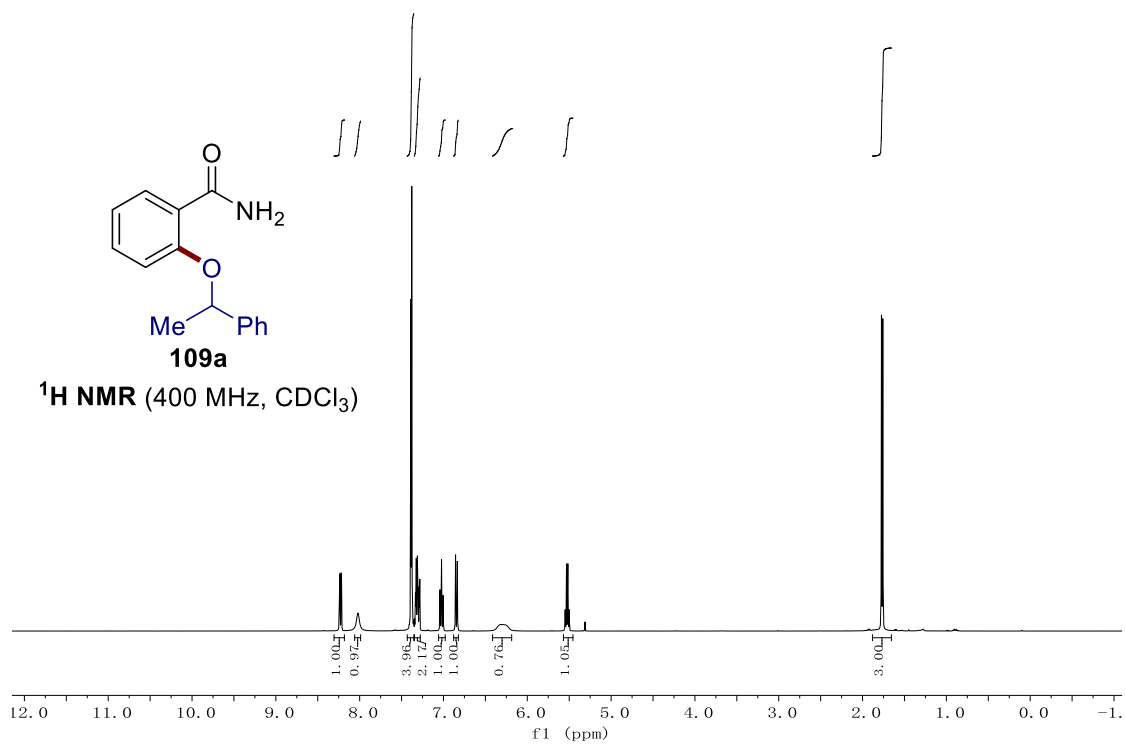
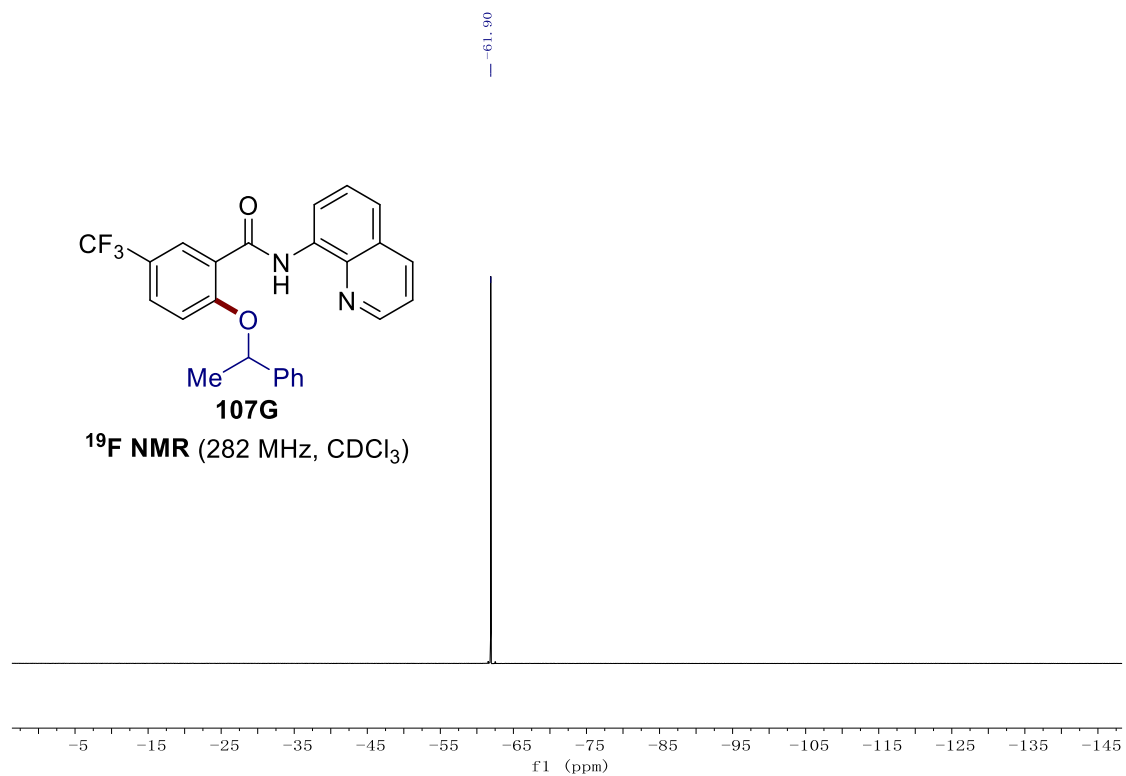
## 7. NMR Spectra



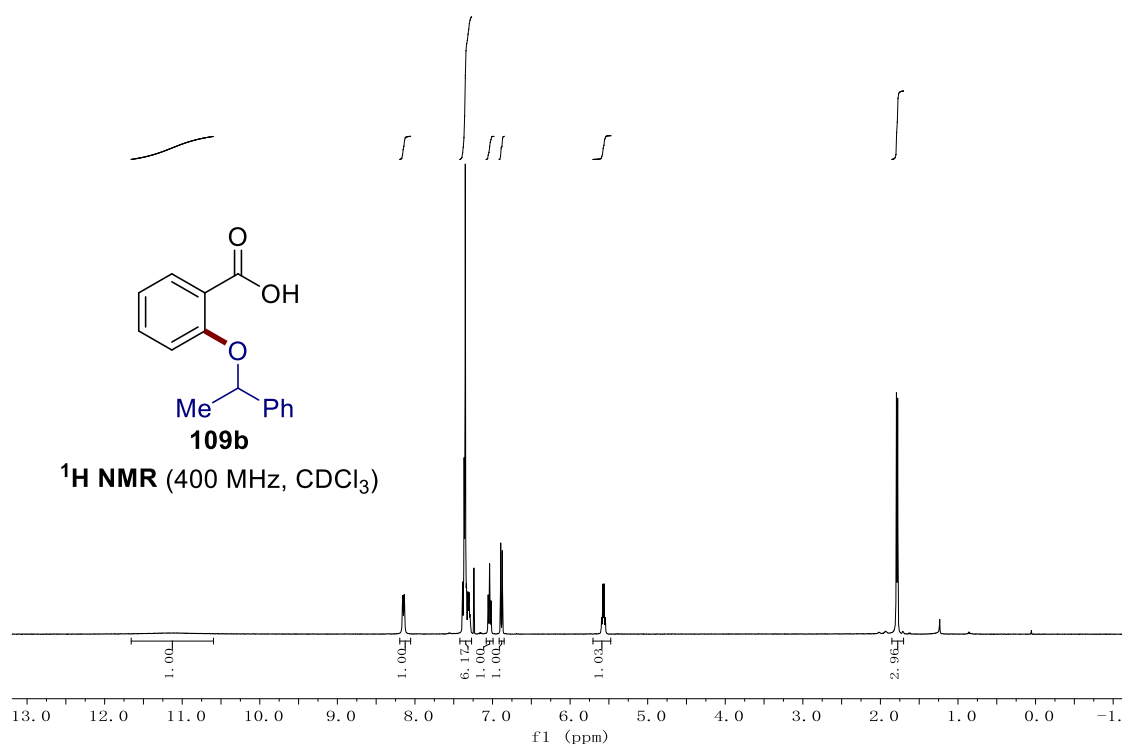
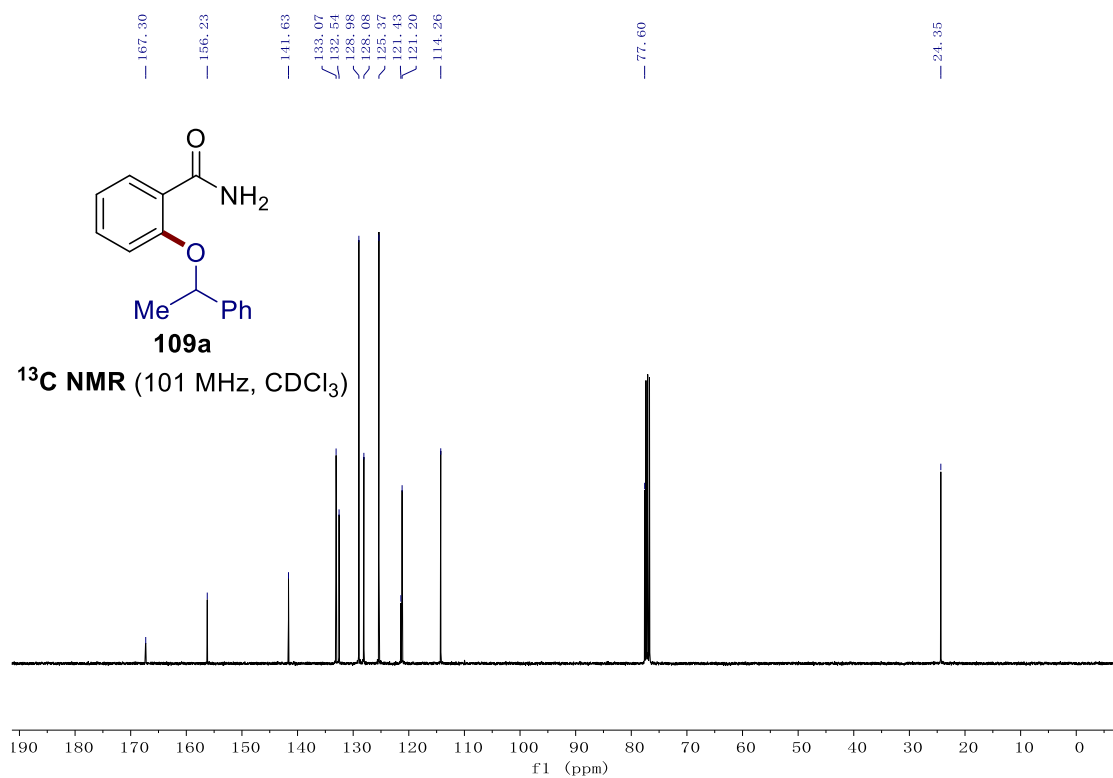


## 7. NMR Spectra

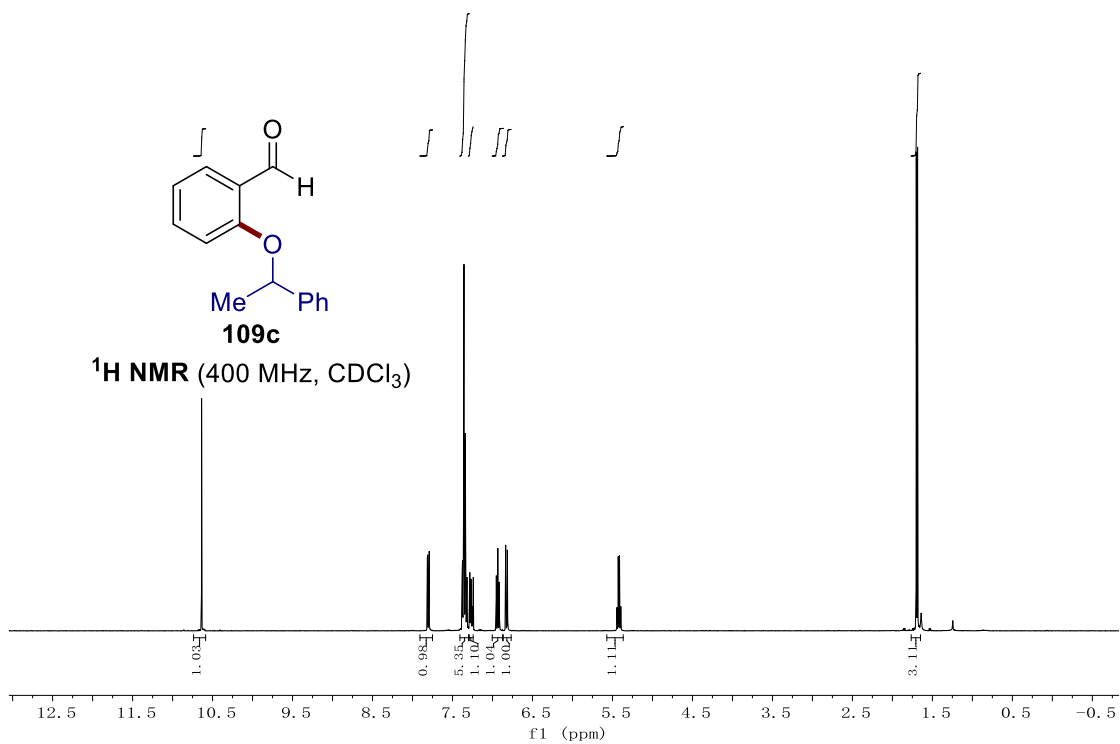
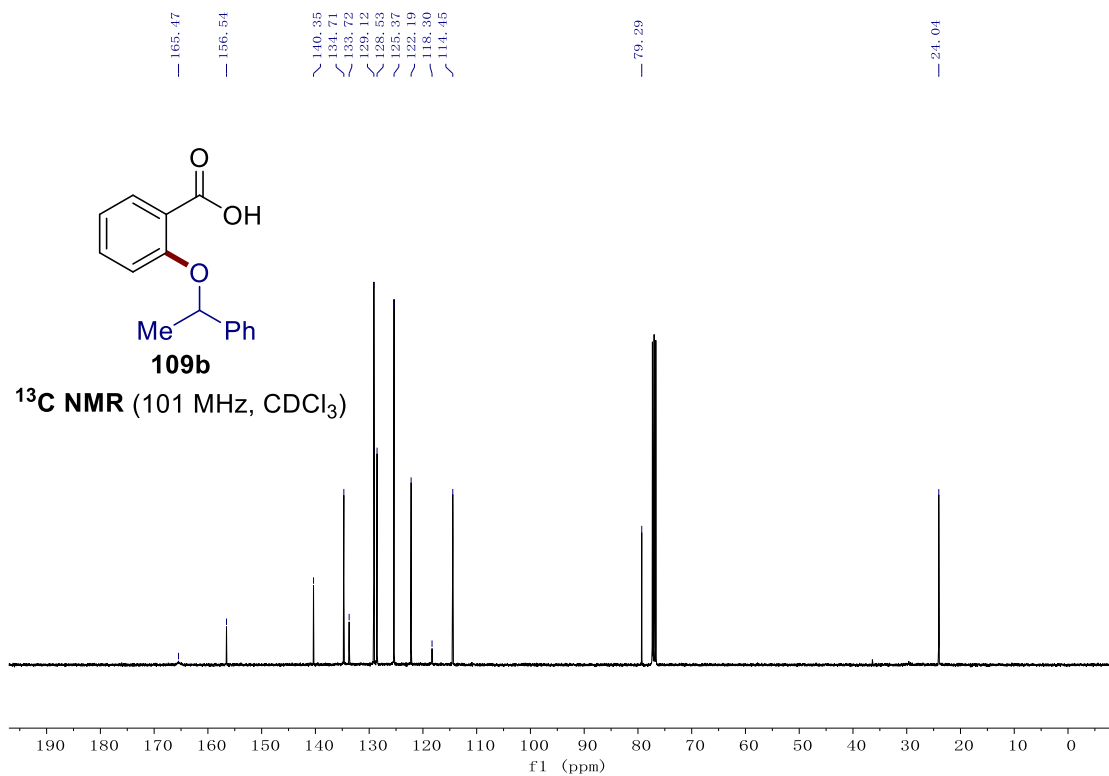




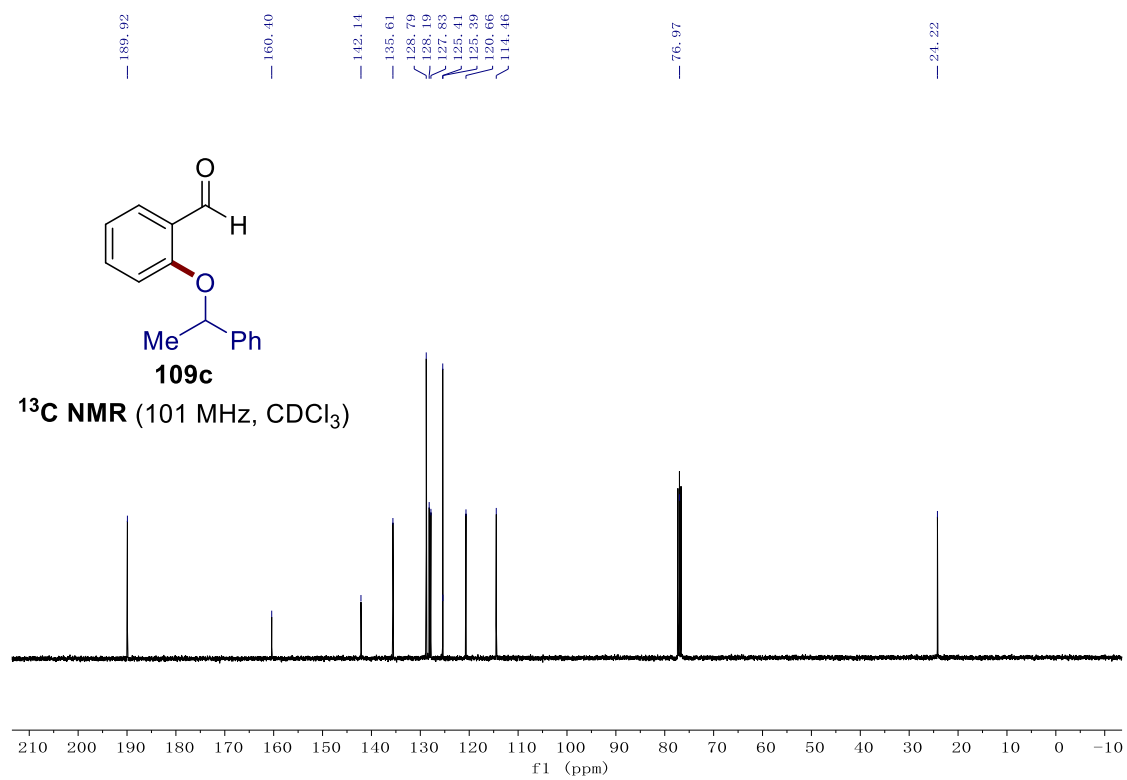
## 7. NMR Spectra



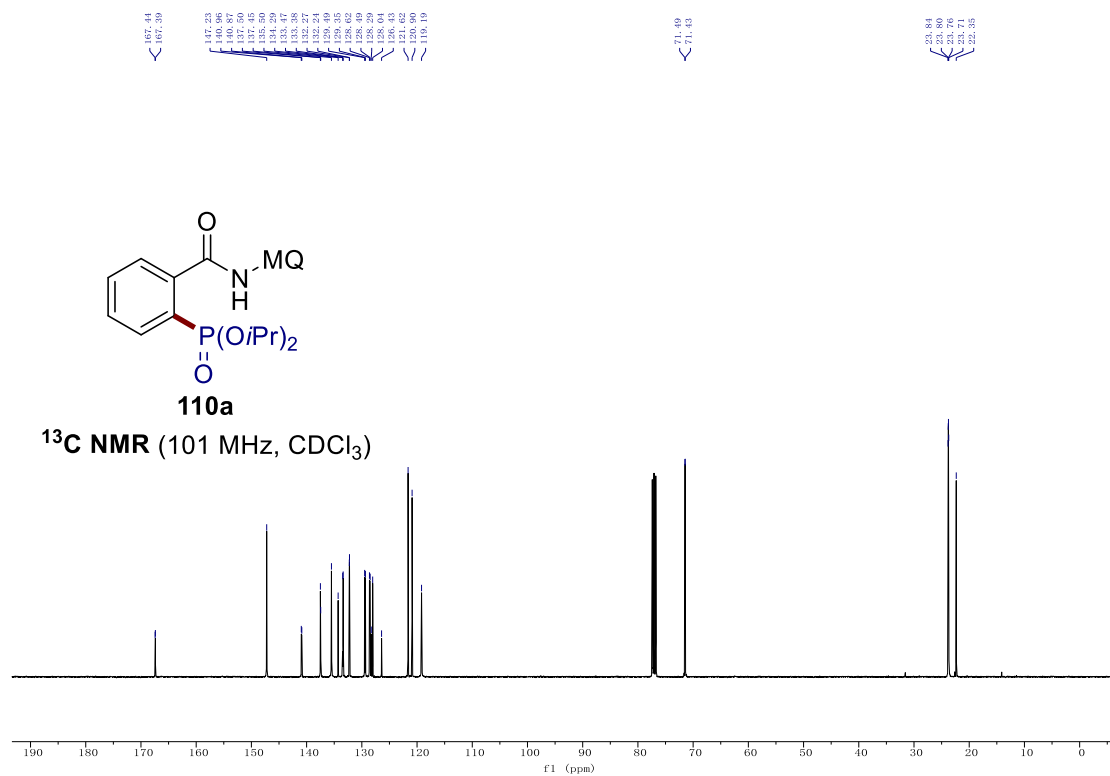
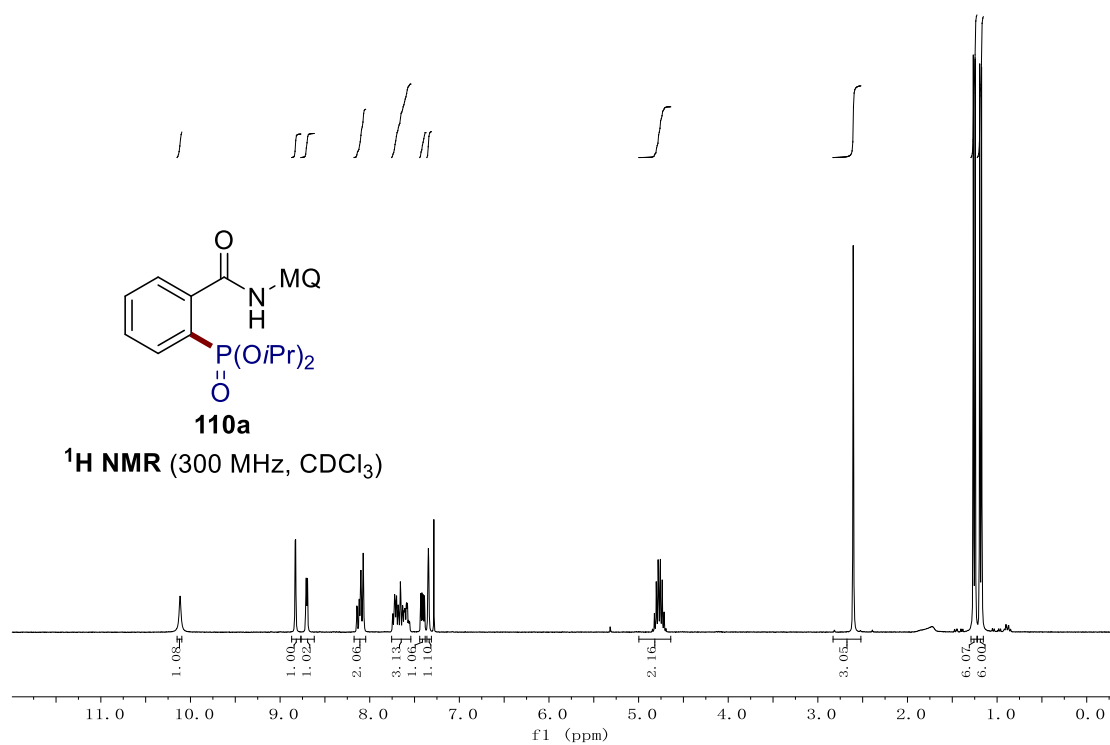




## 7. NMR Spectra

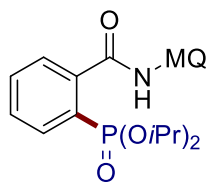


## 7.6 Nickela-Electrocatalyzed C–H Phosphorylation



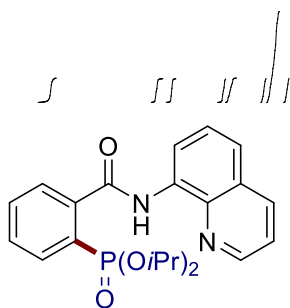
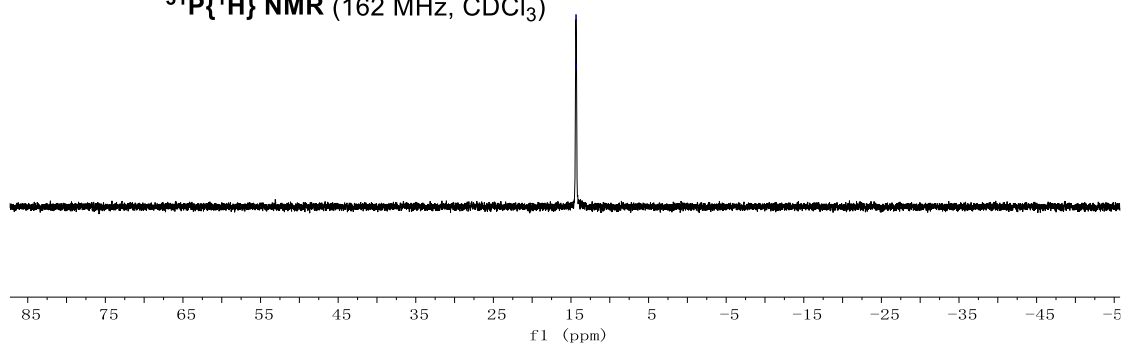
7. NMR Spectra

14.42  
14.37  
14.32  
14.28



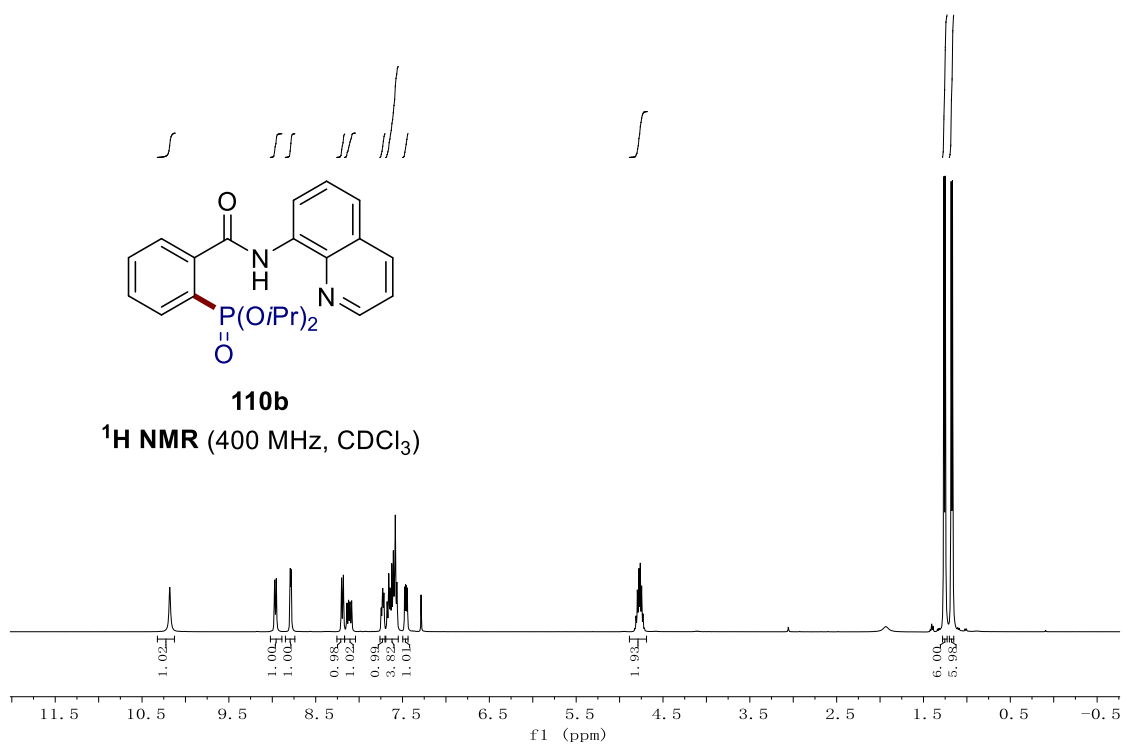
110a

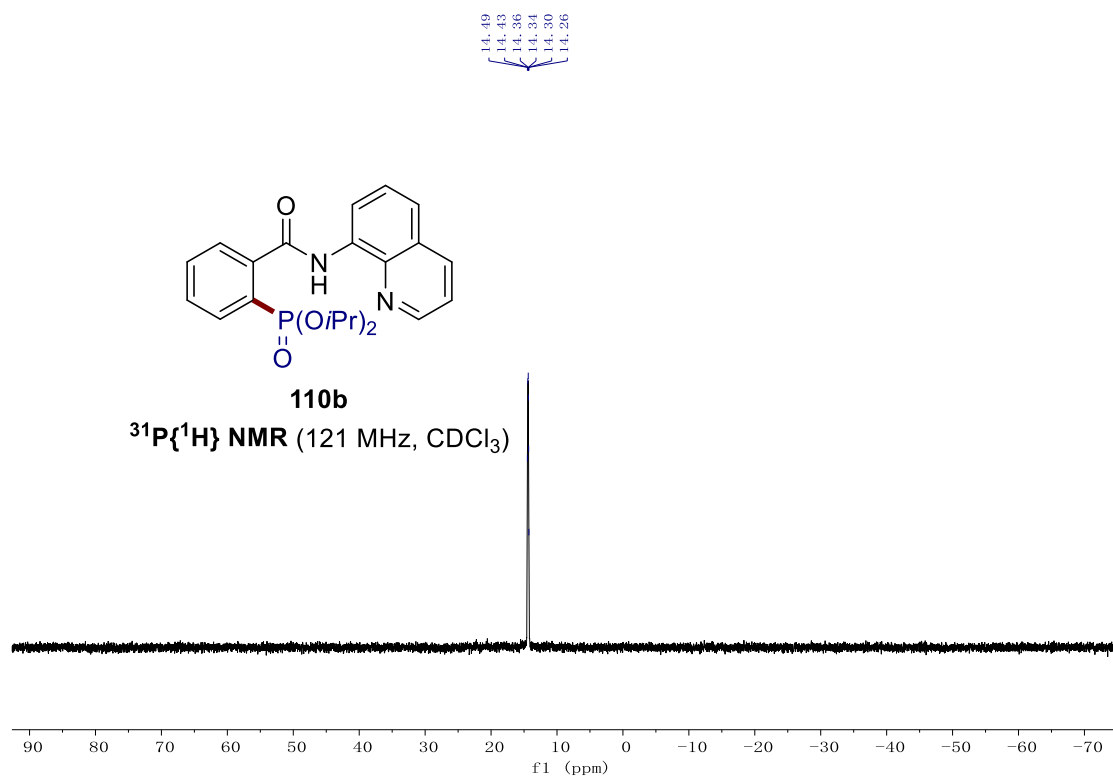
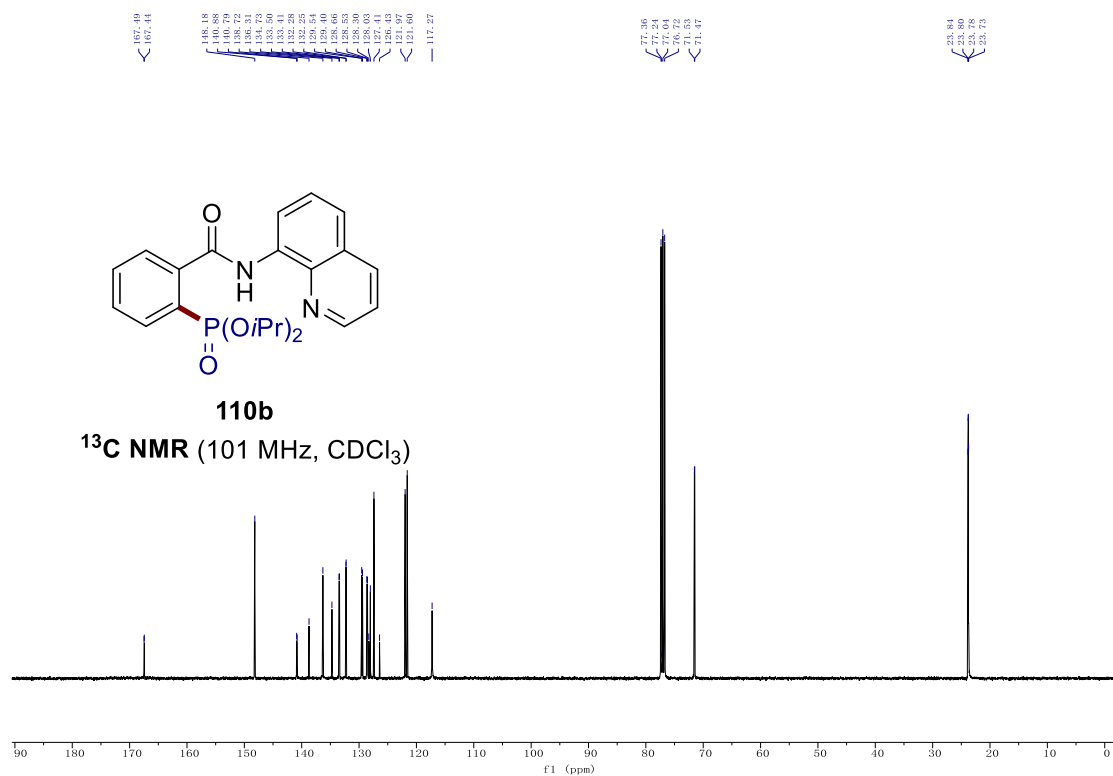
$^{31}\text{P}\{^1\text{H}\}$  NMR (162 MHz,  $\text{CDCl}_3$ )



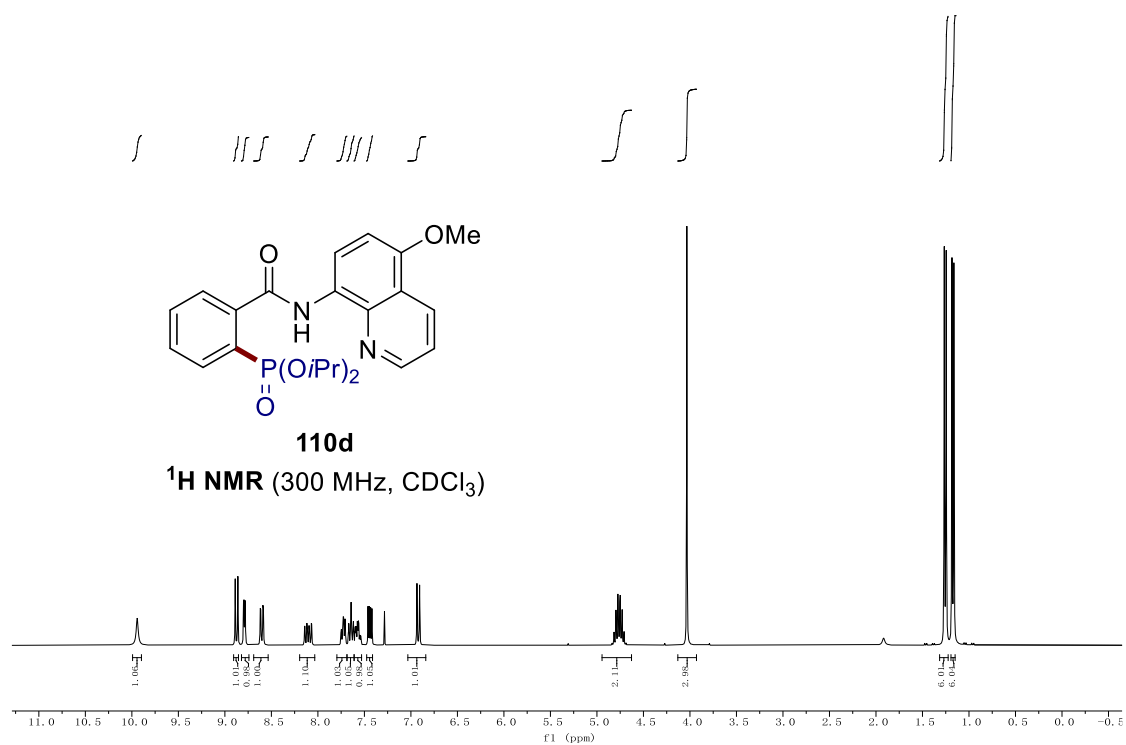
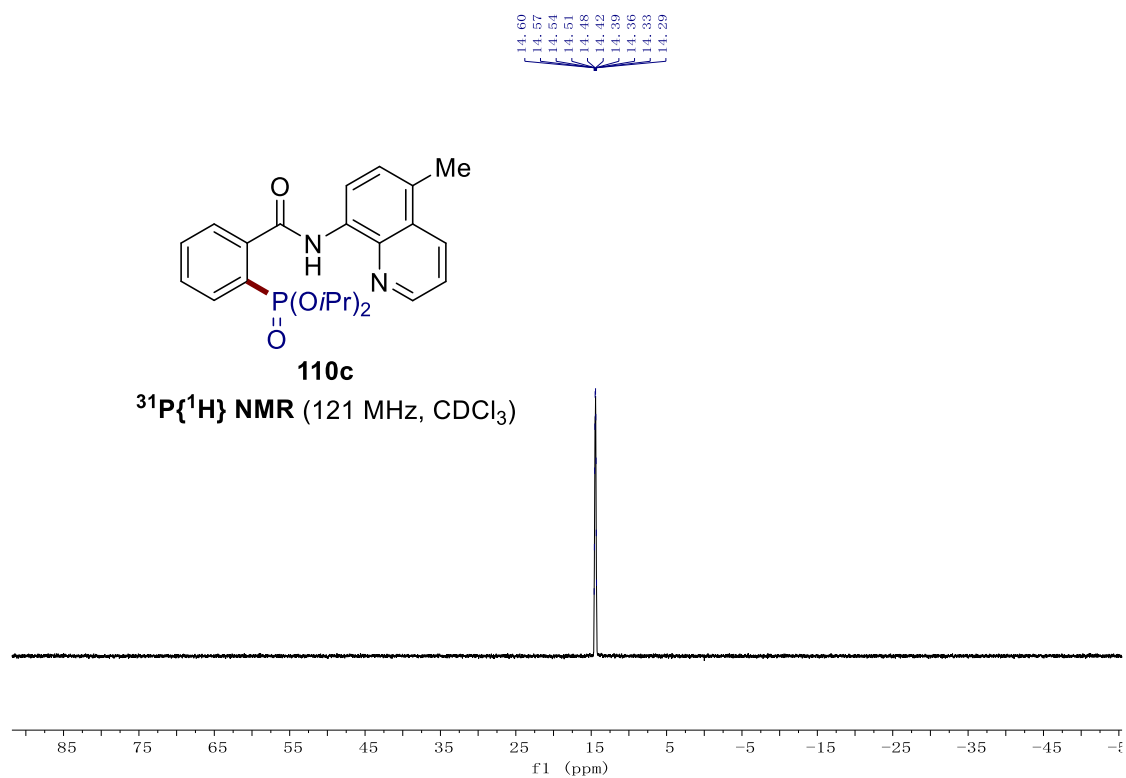
110b

$^1\text{H}$  NMR (400 MHz,  $\text{CDCl}_3$ )



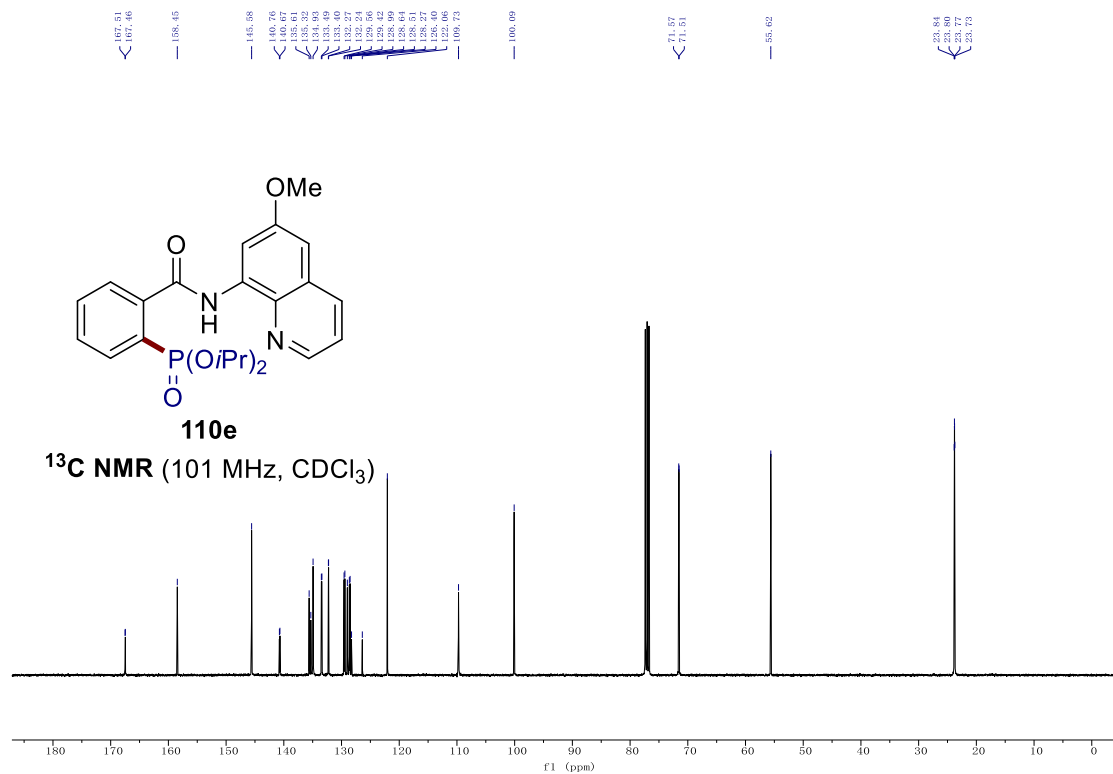
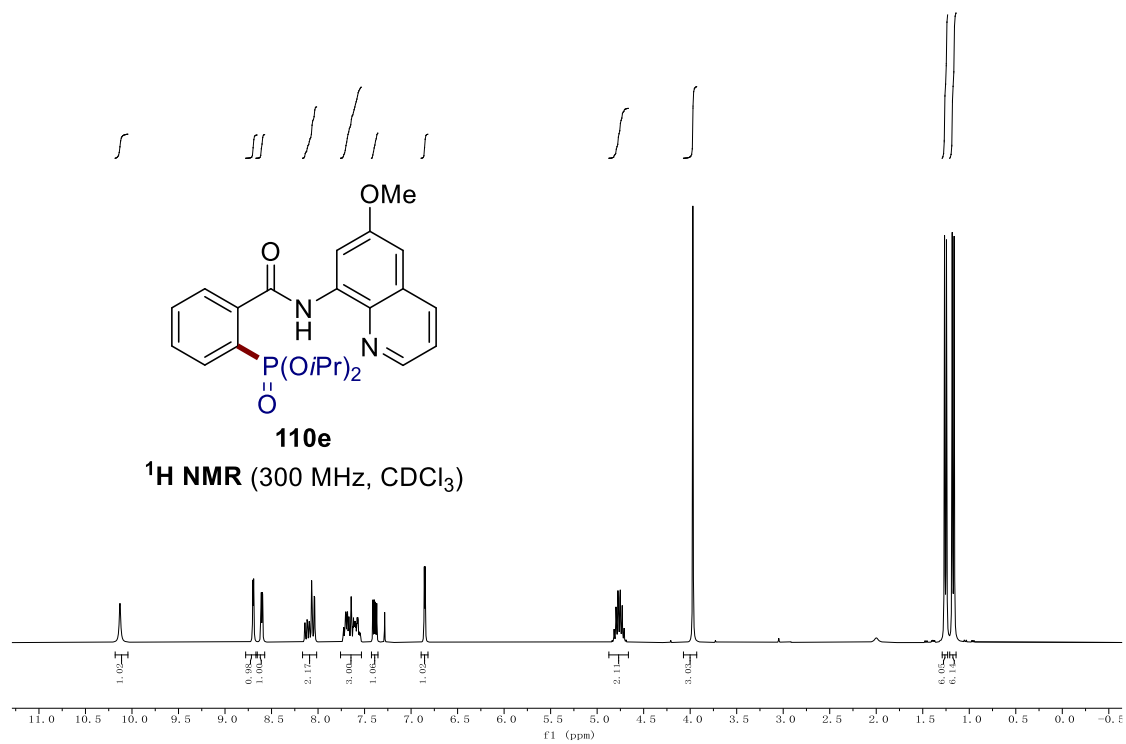




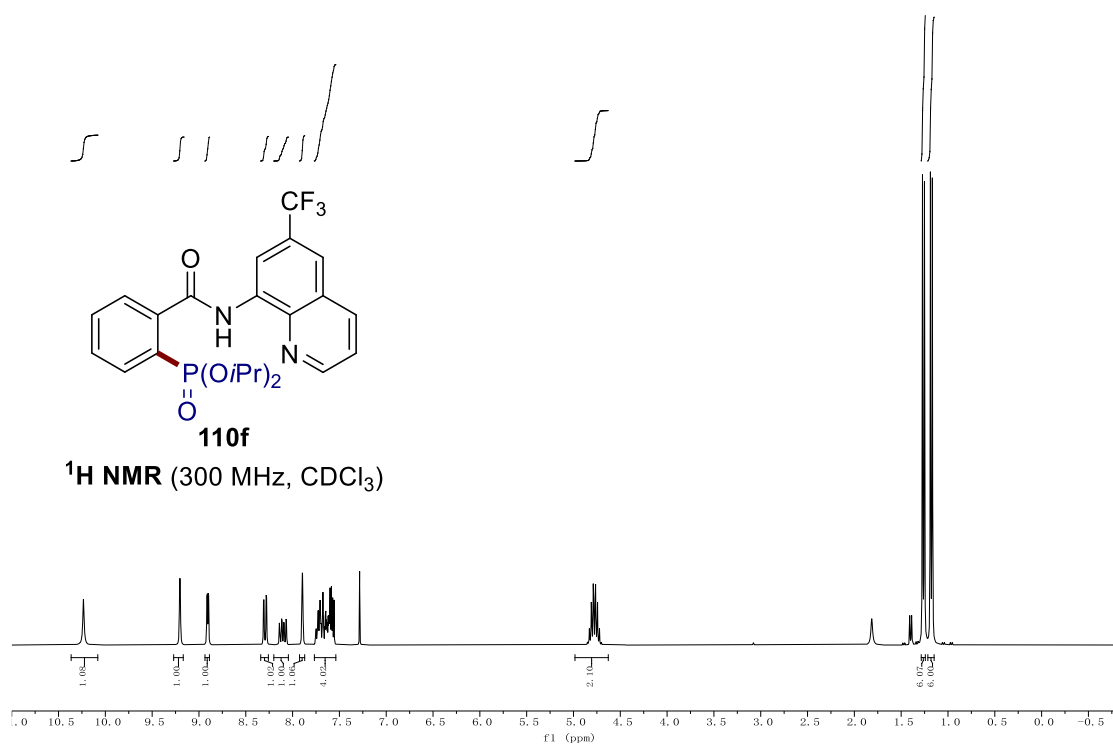
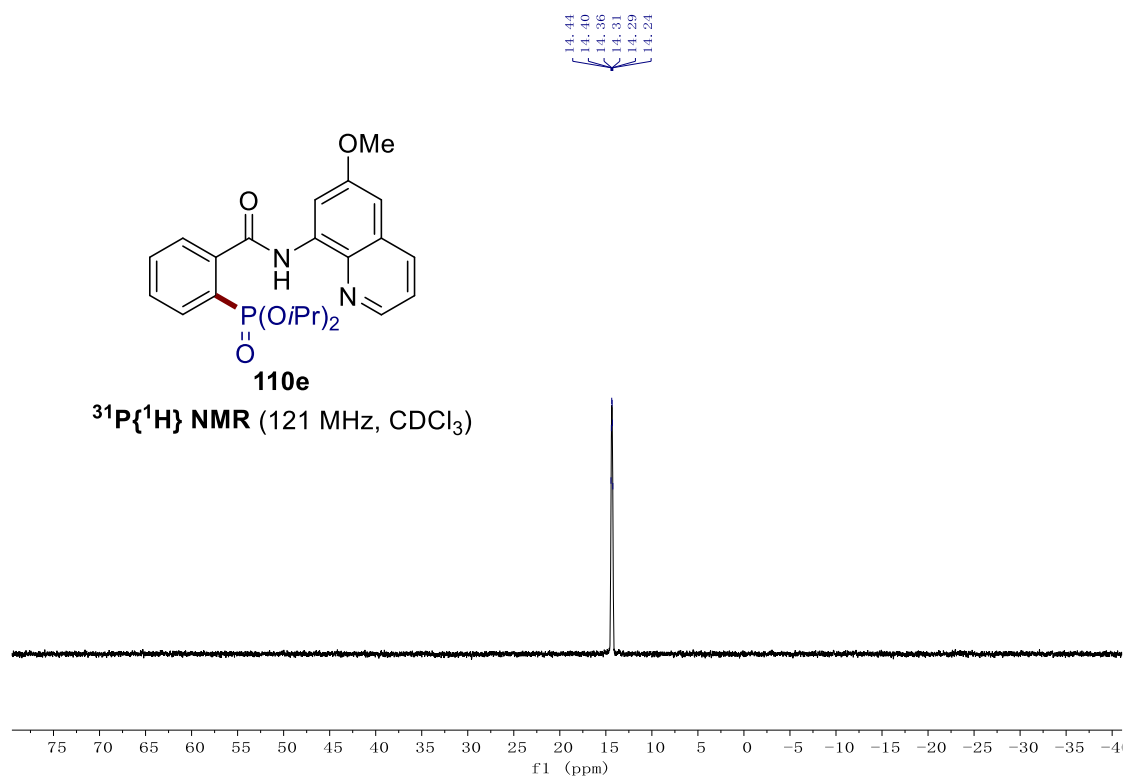


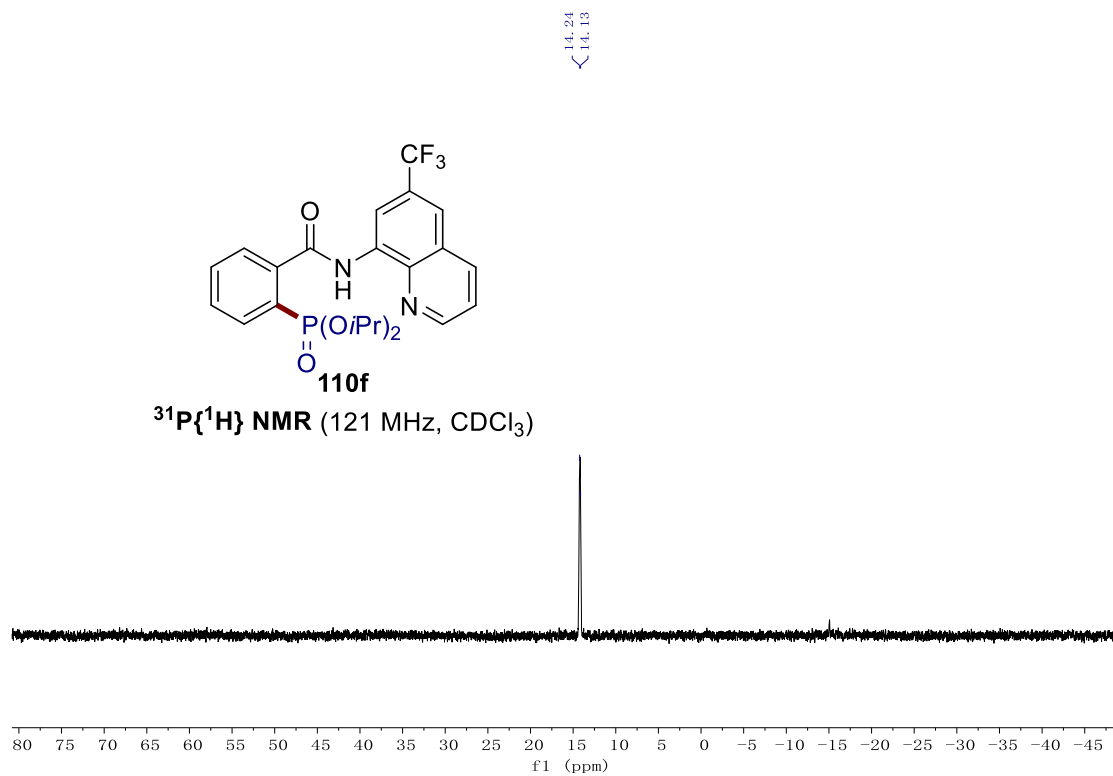
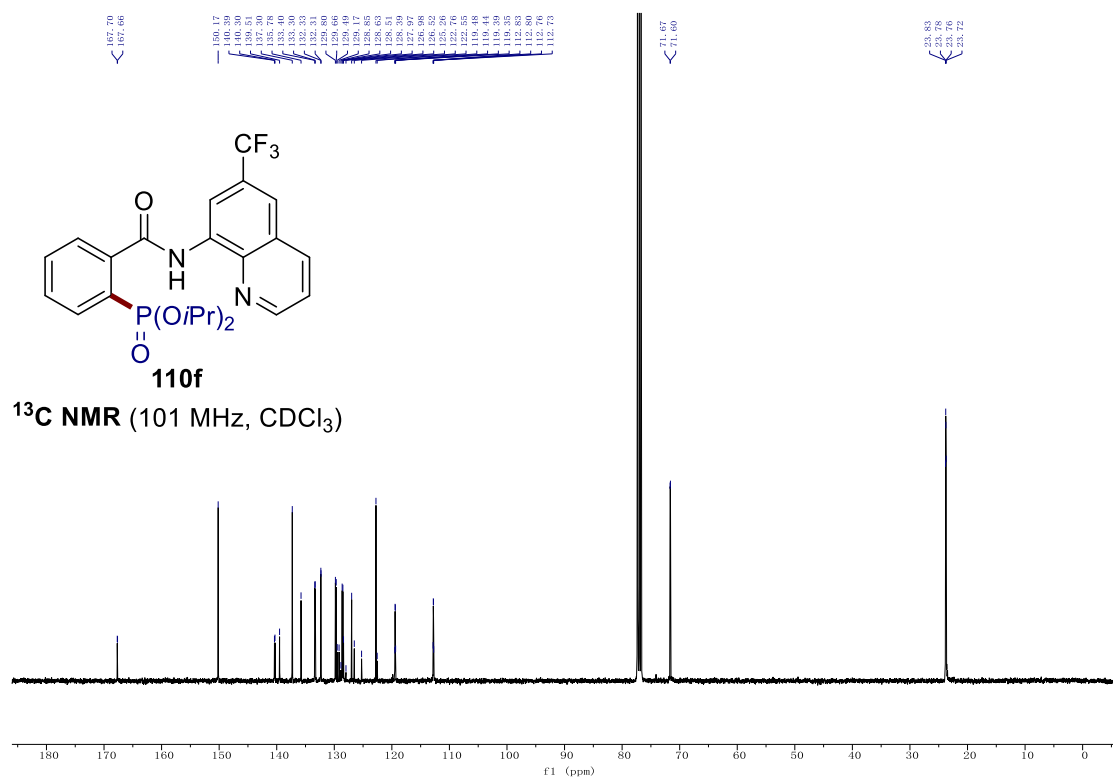




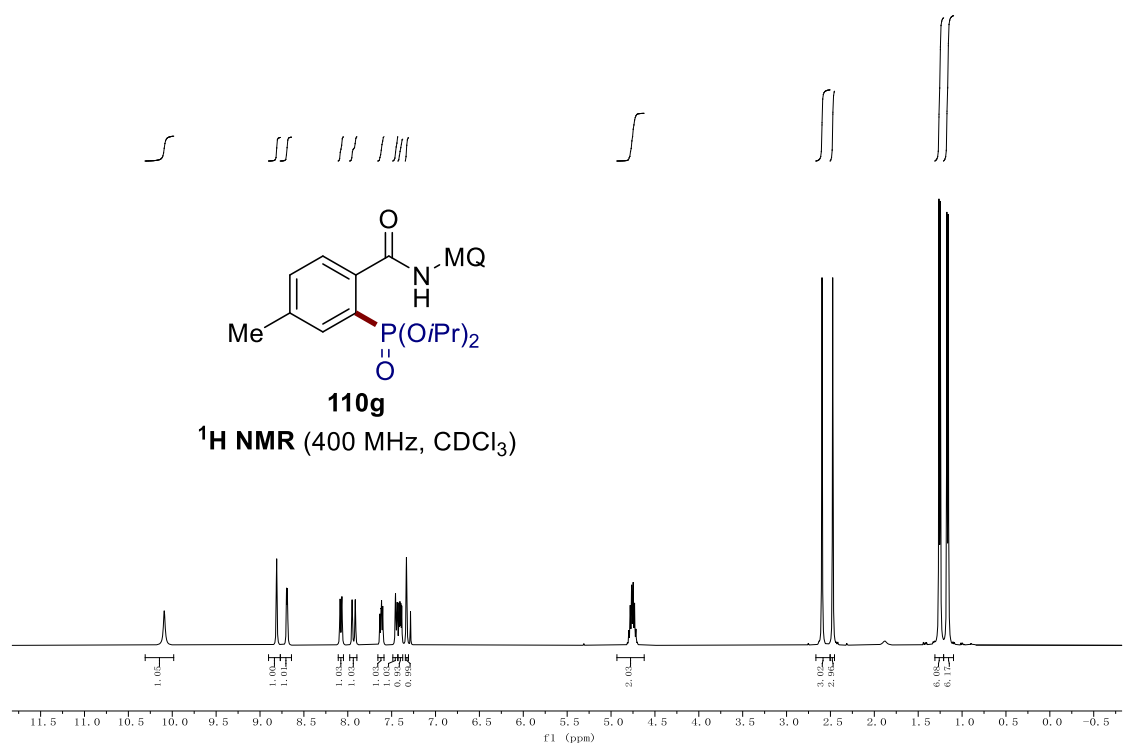
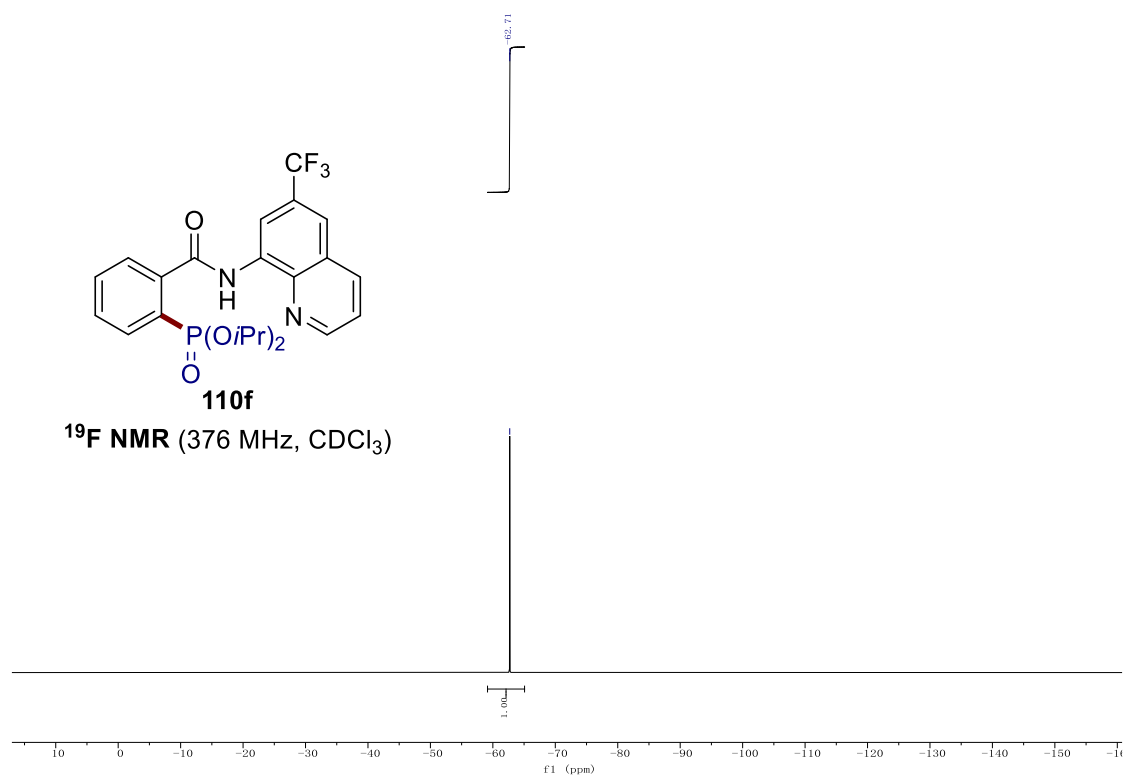


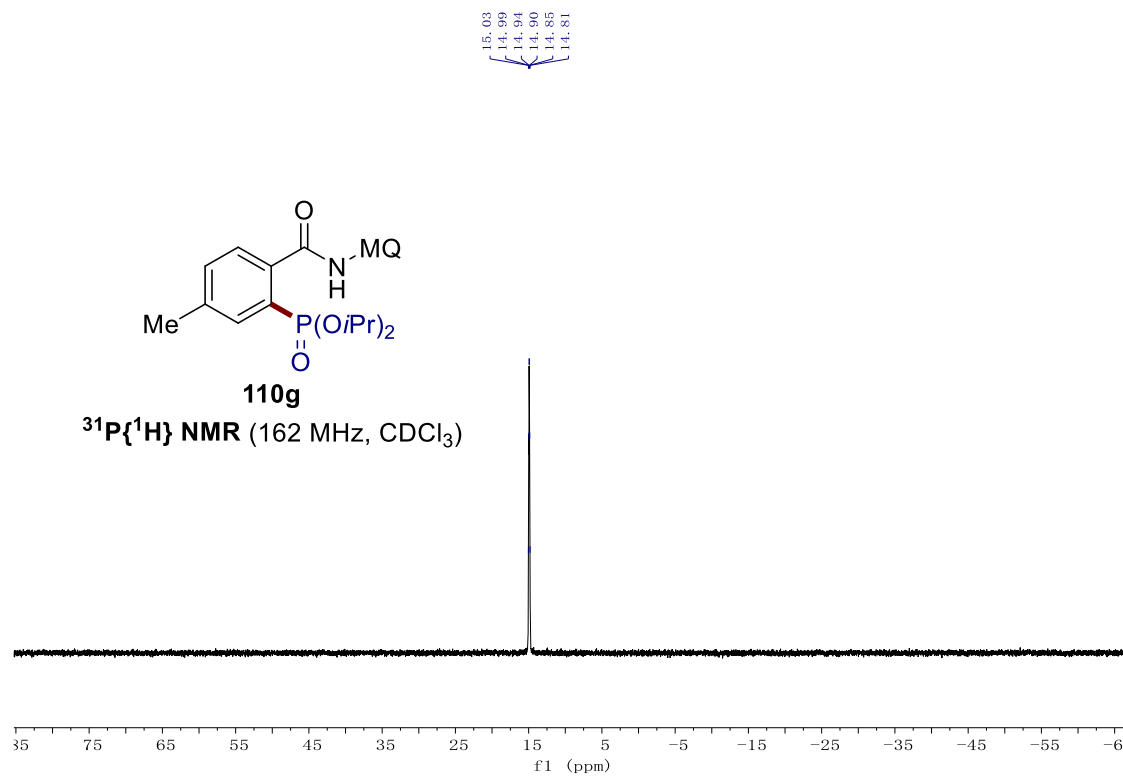
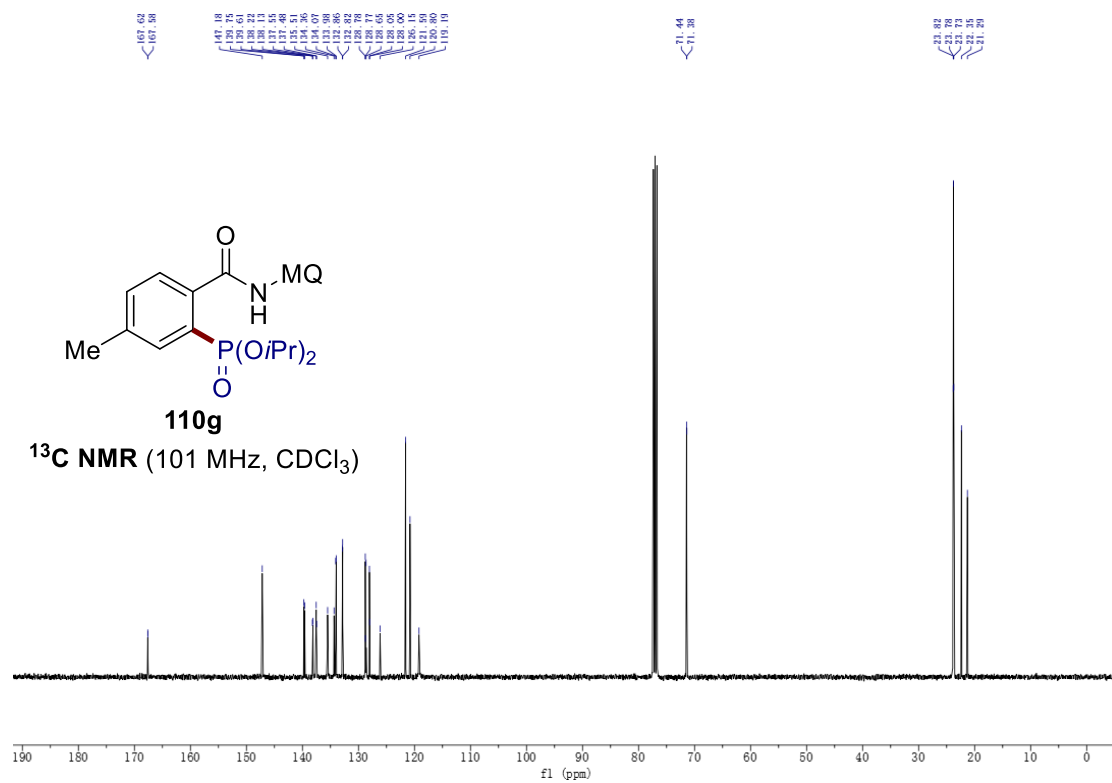
7. NMR Spectra



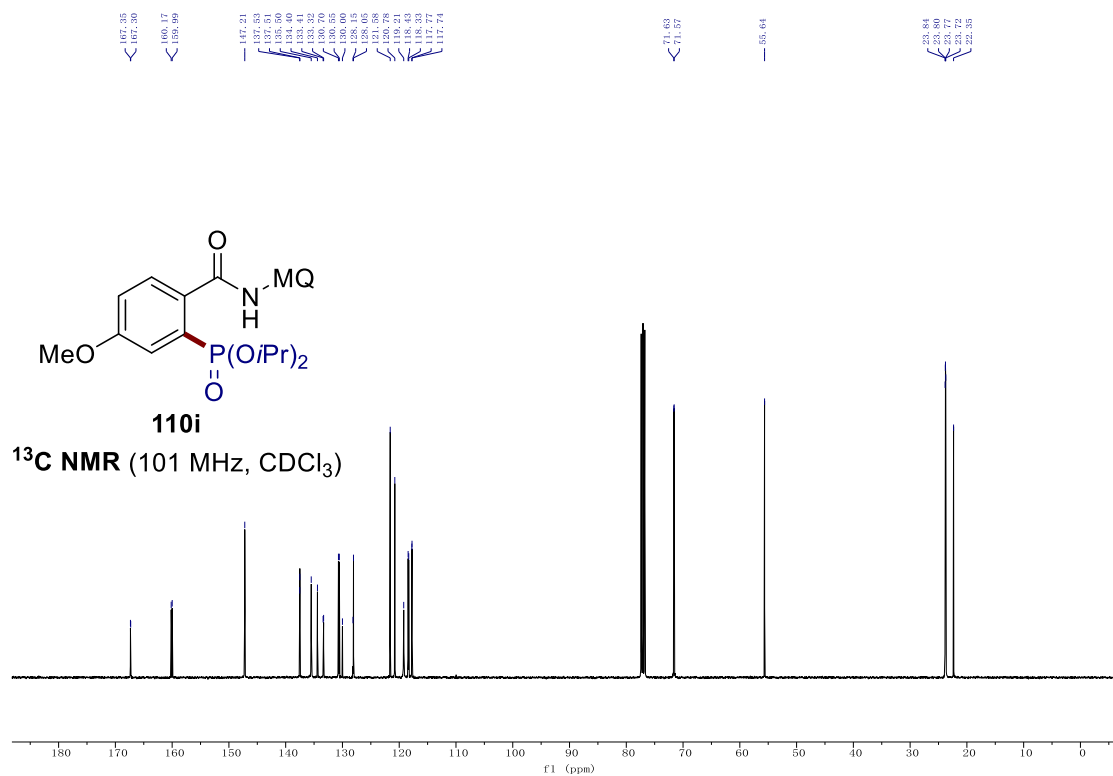
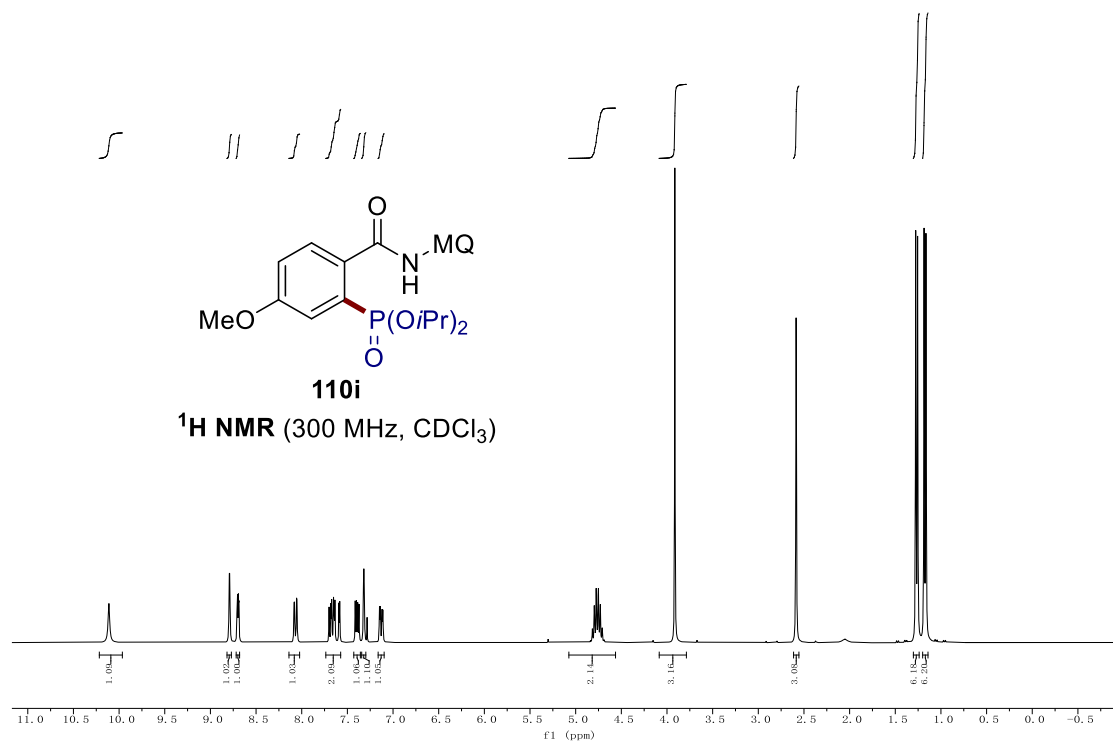


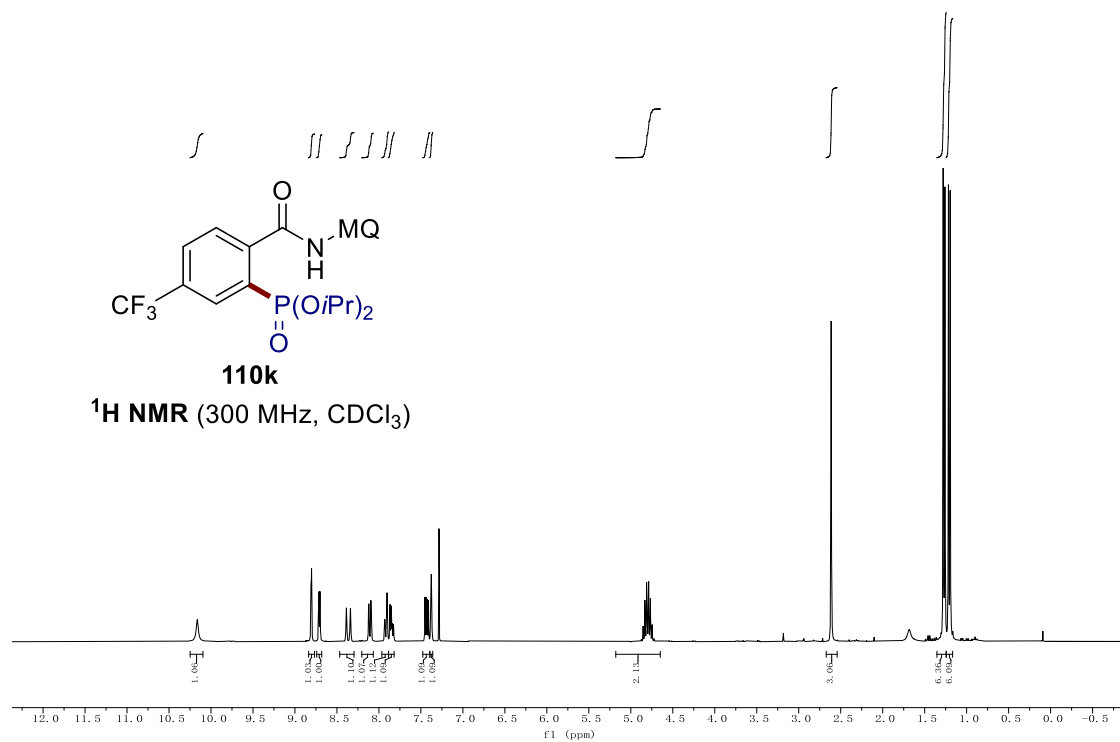
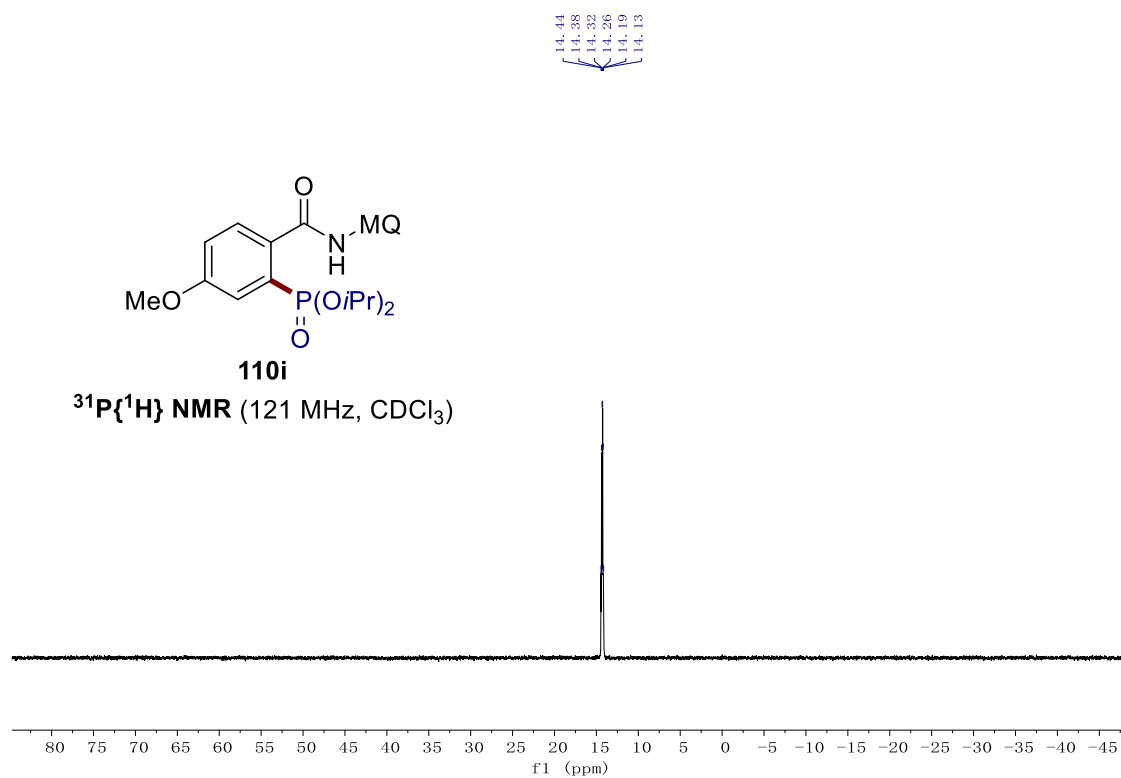
## 7. NMR Spectra



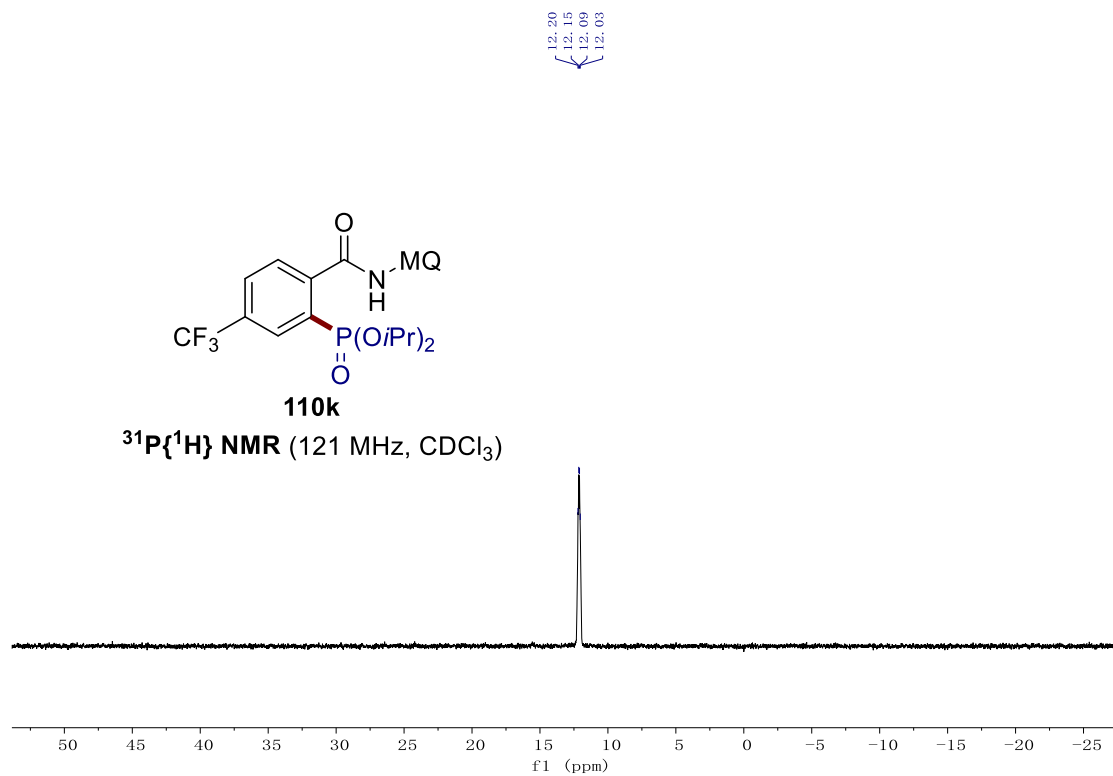
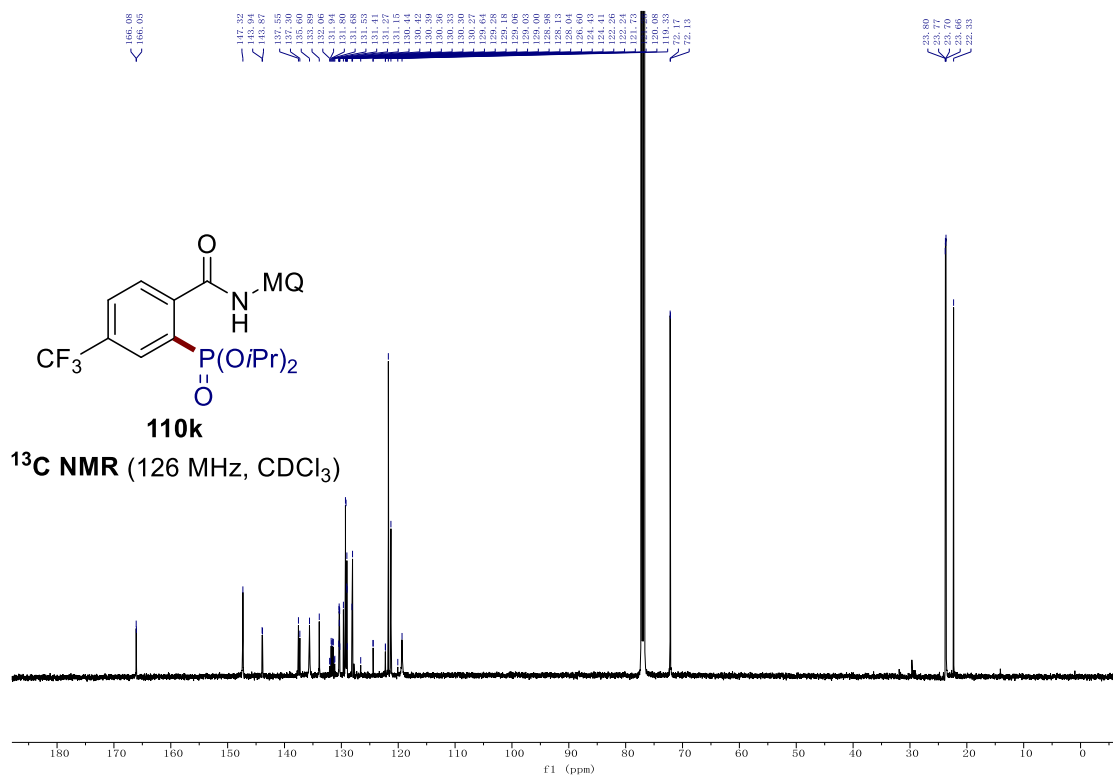


## 7. NMR Spectra

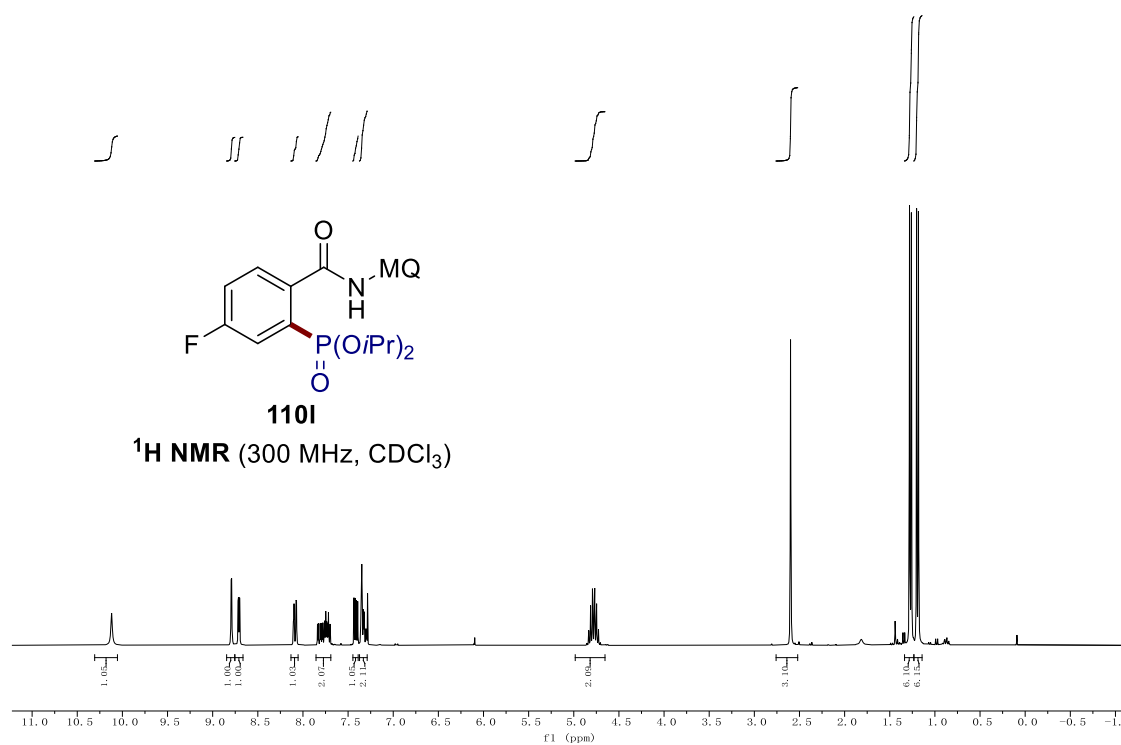
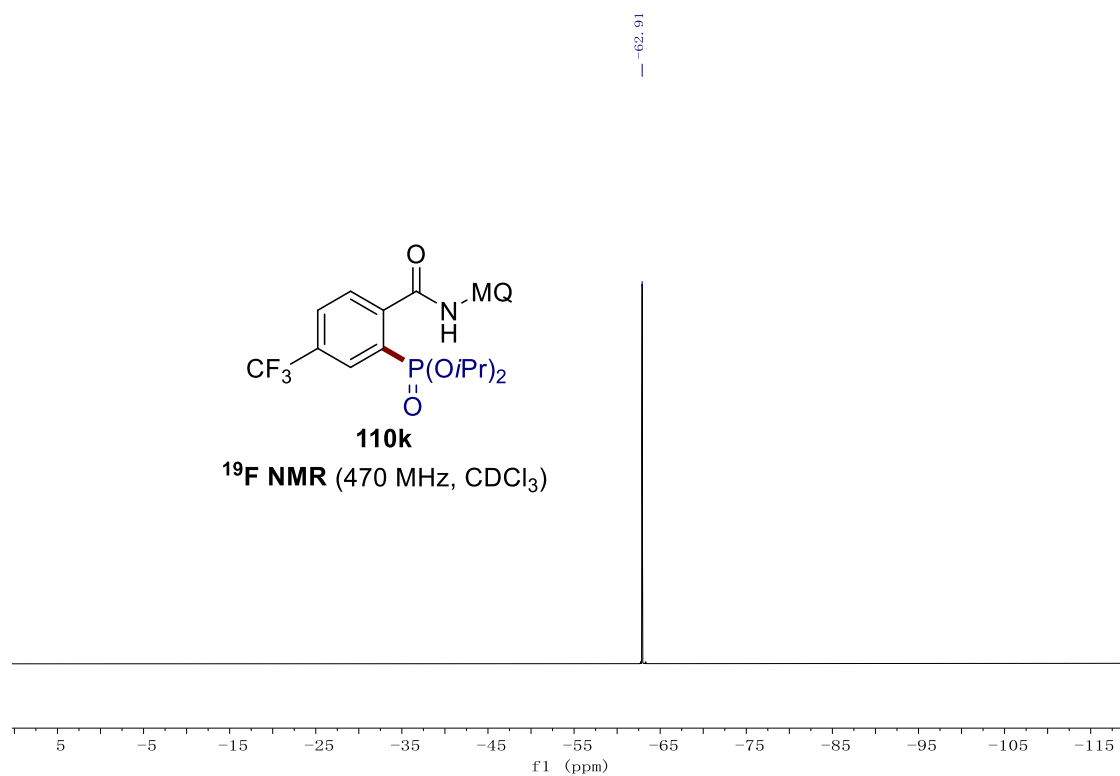




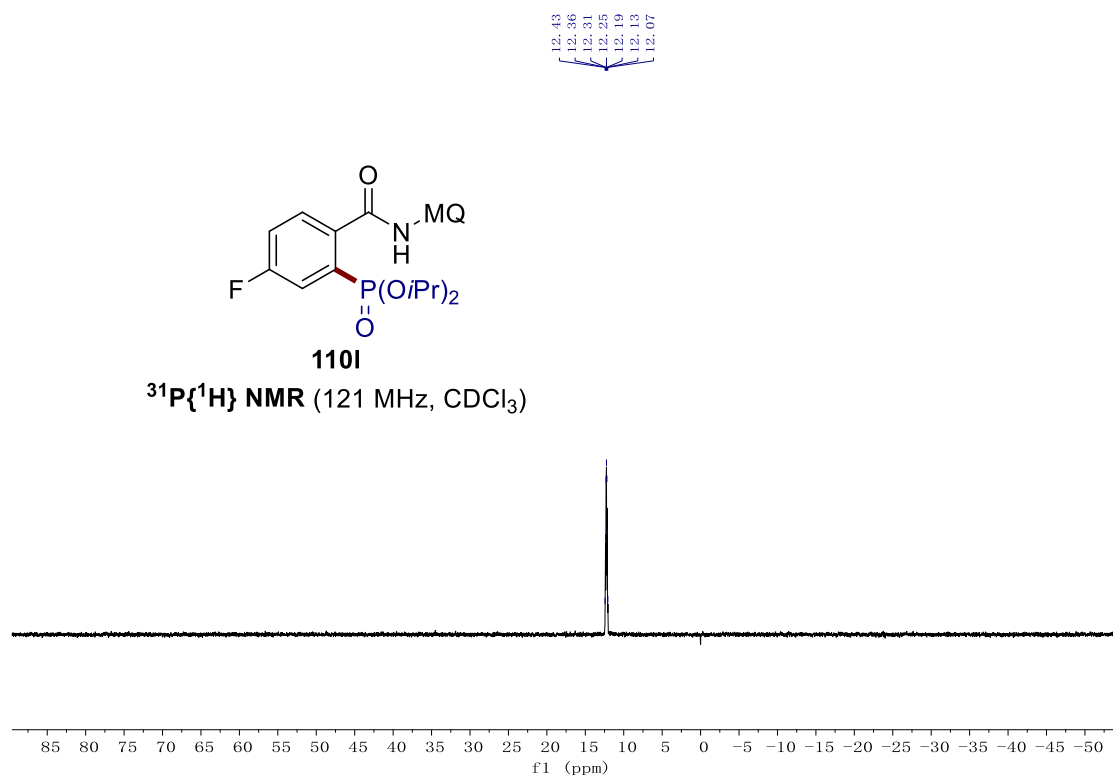
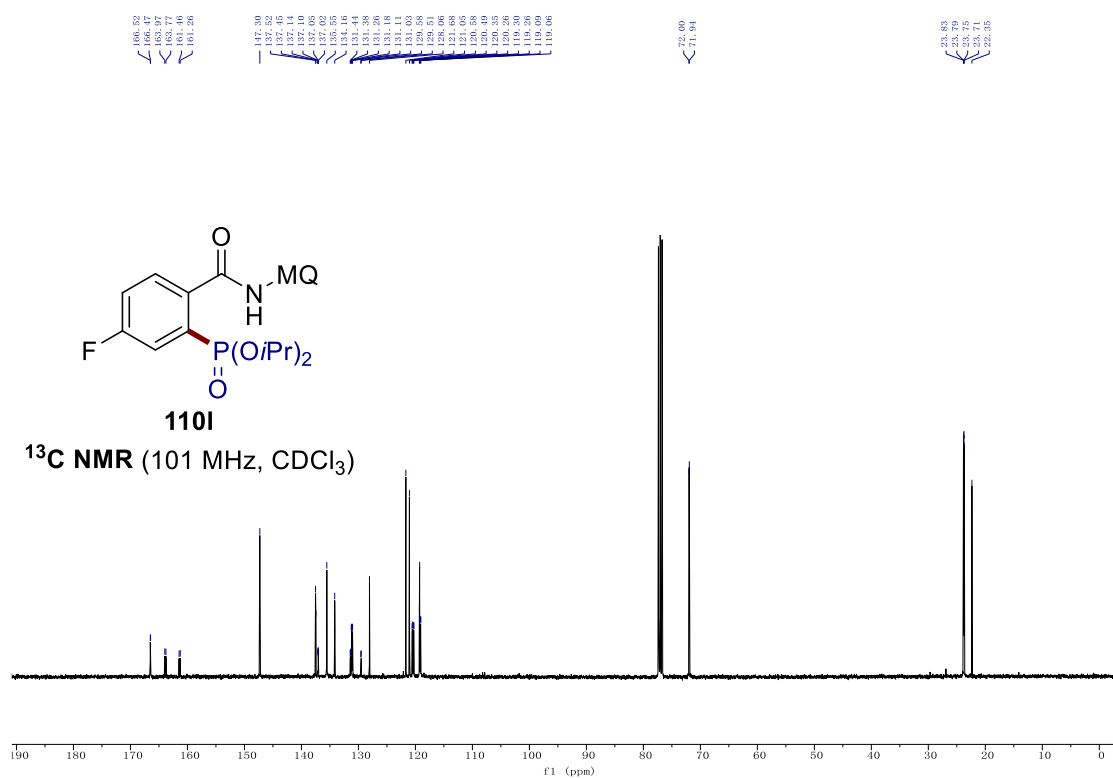
## 7. NMR Spectra

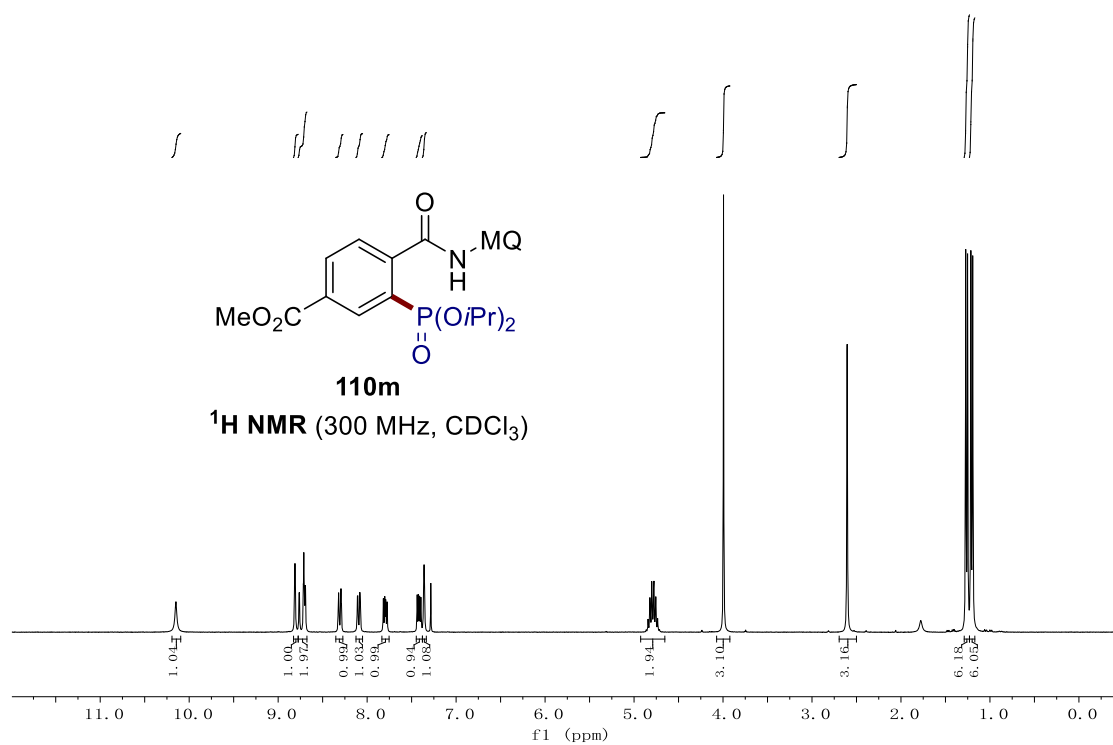
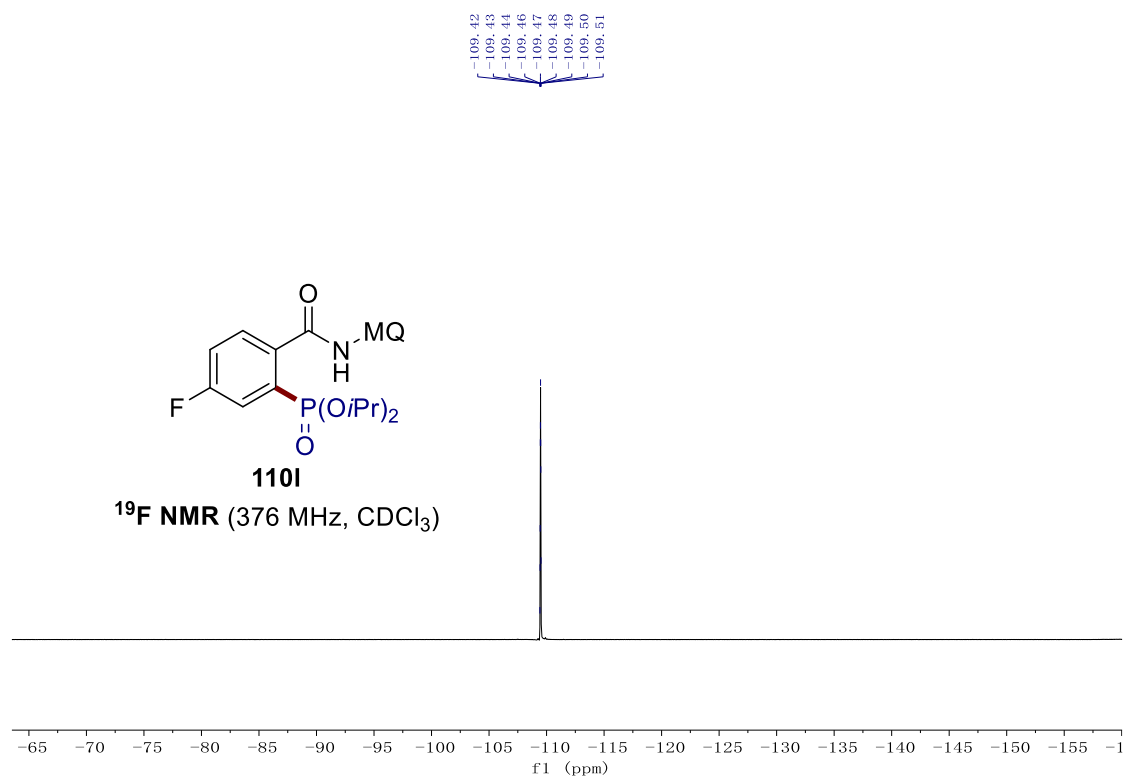




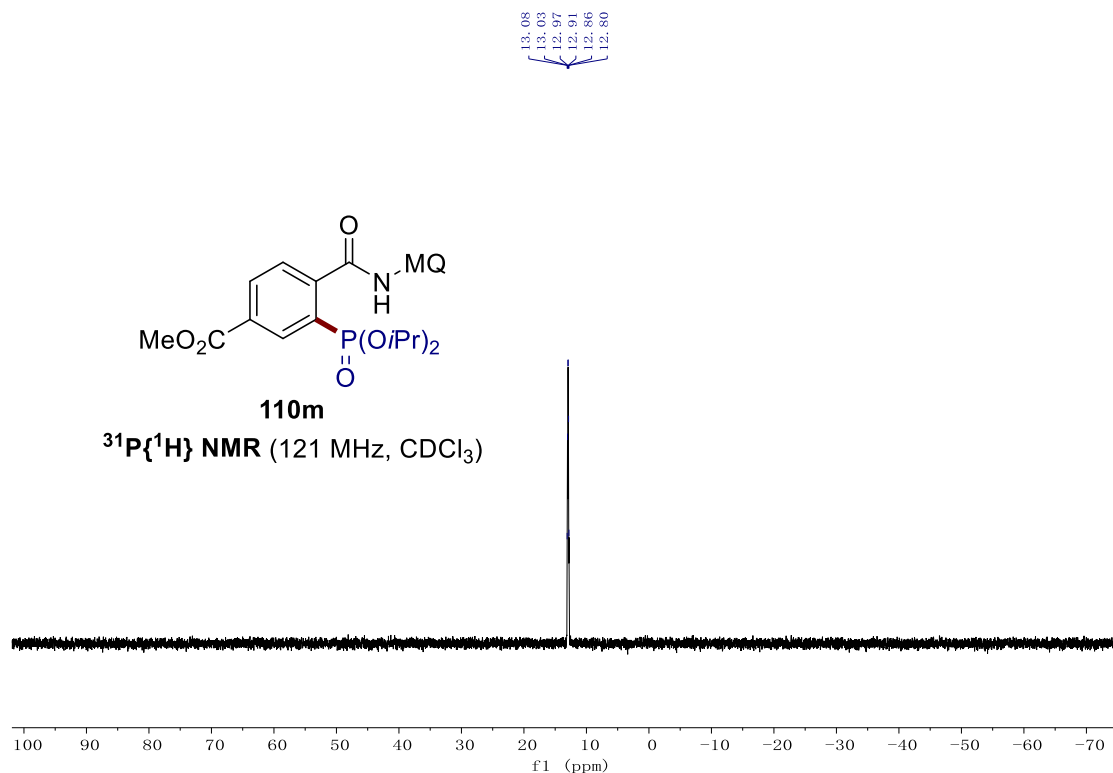
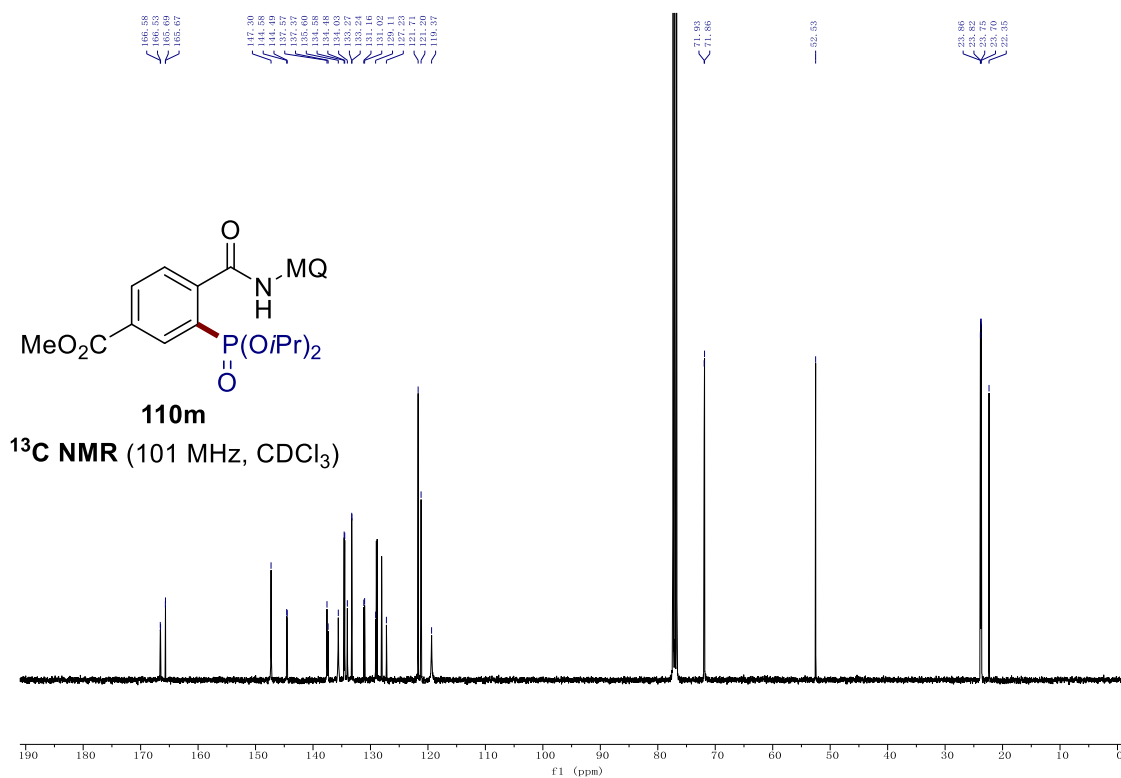


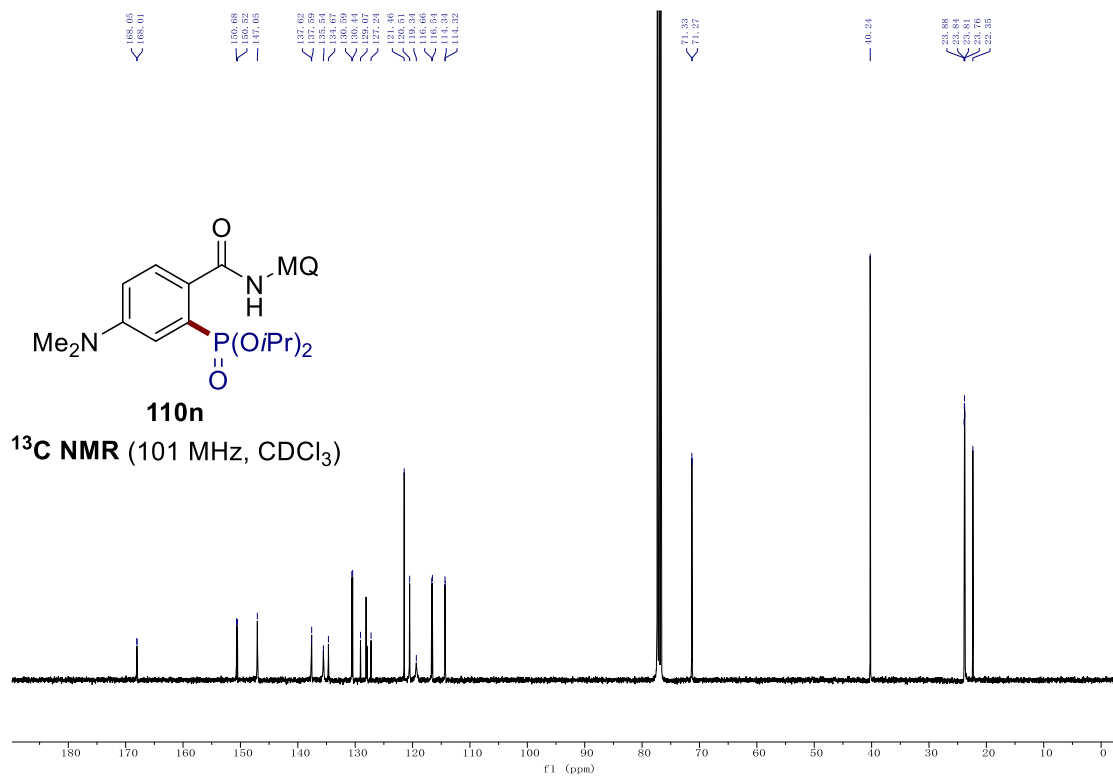
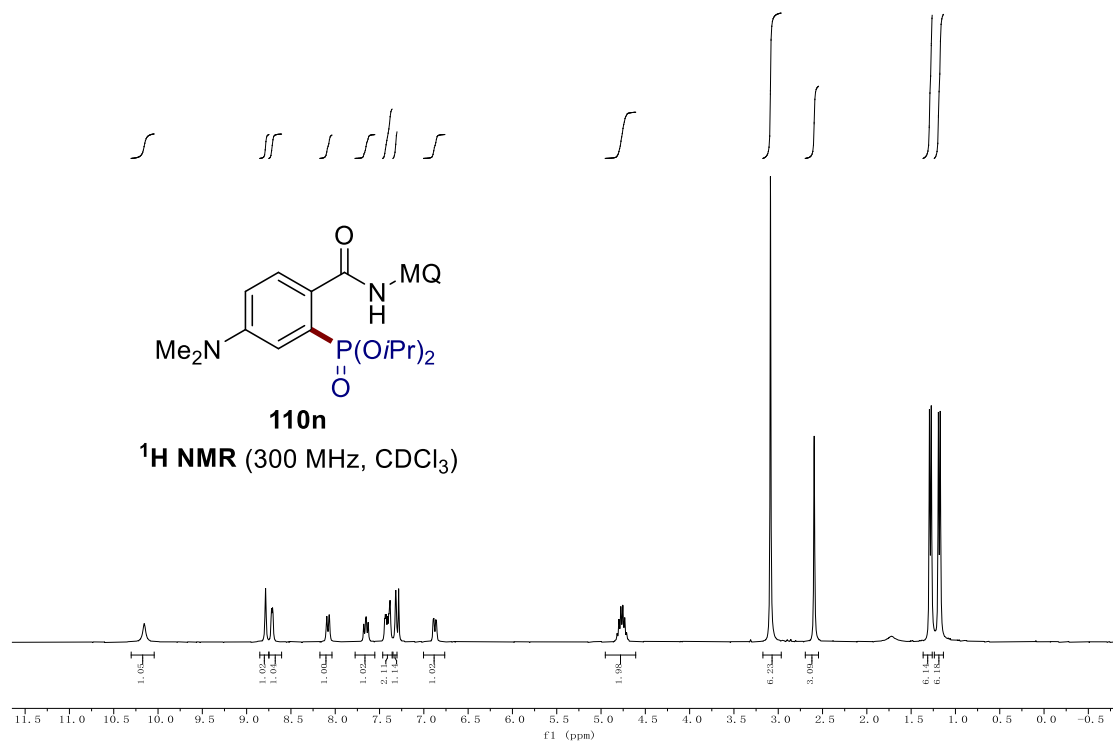
## 7. NMR Spectra



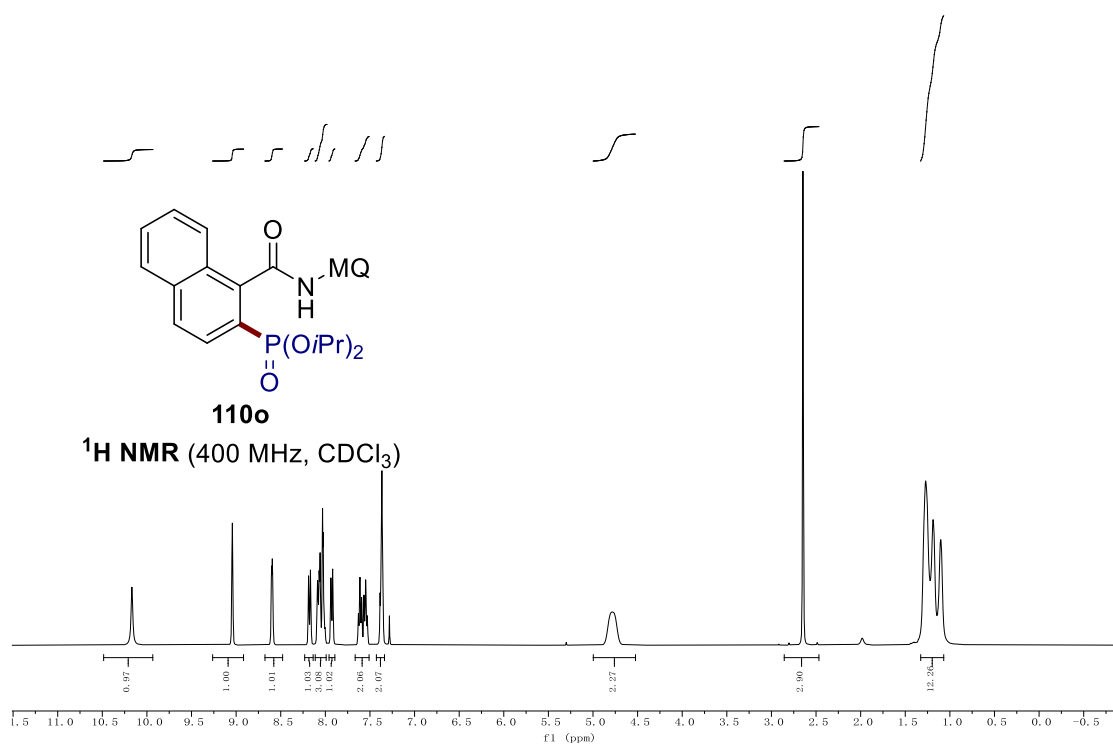
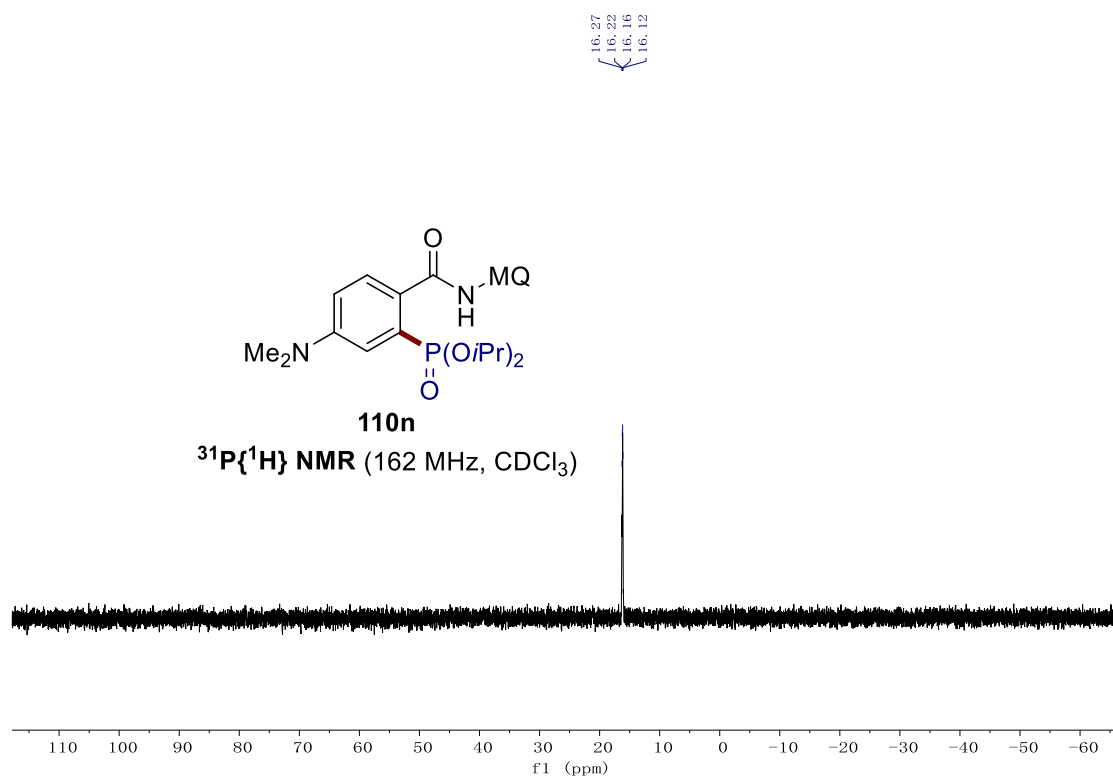


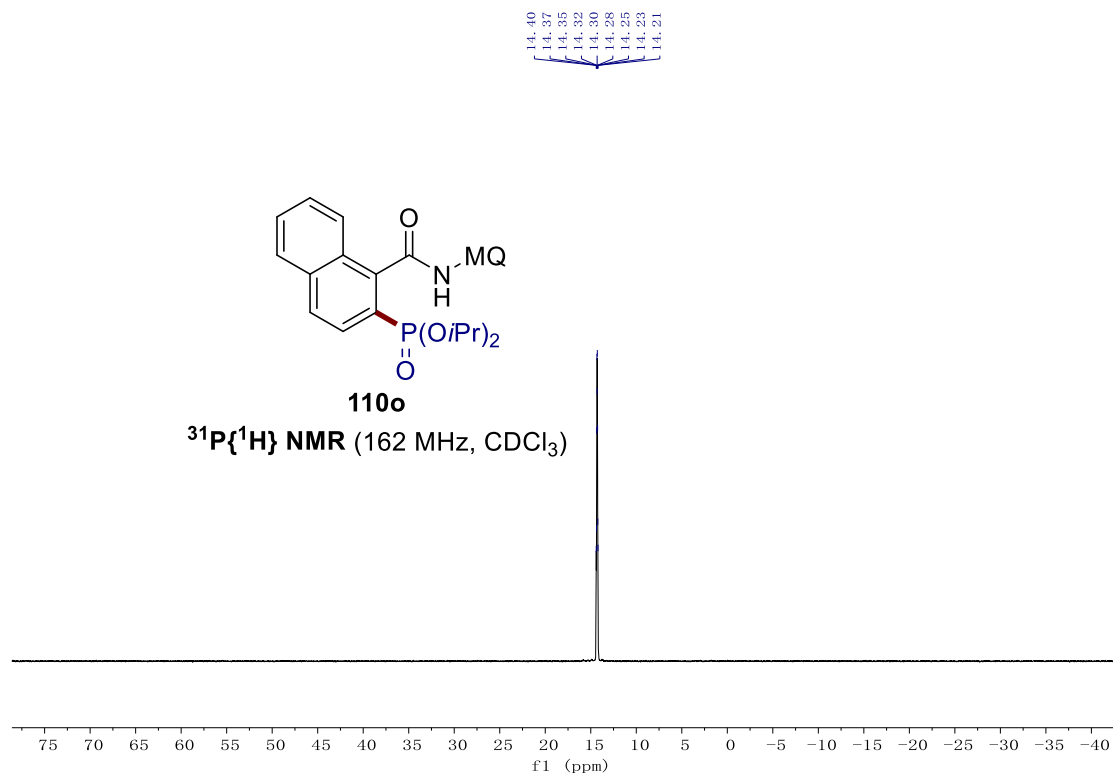
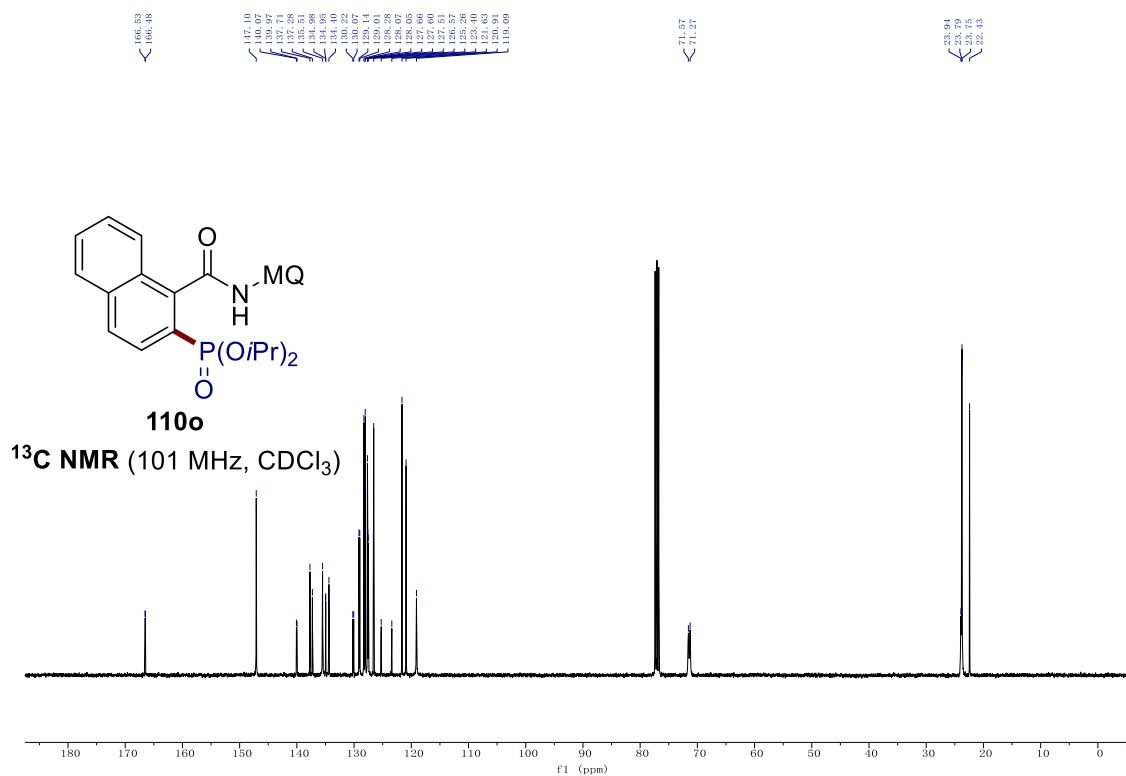
## 7. NMR Spectra



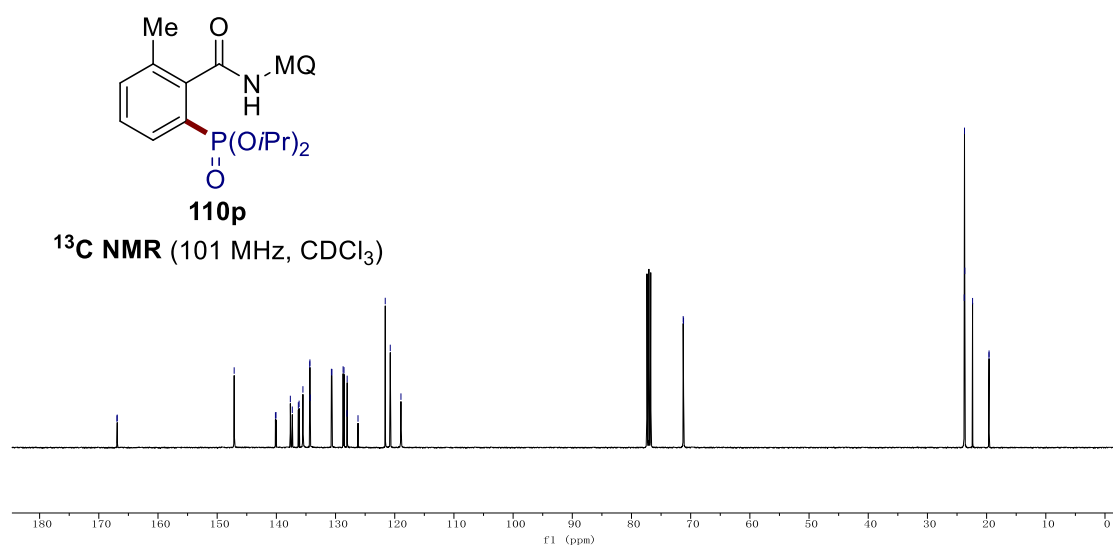
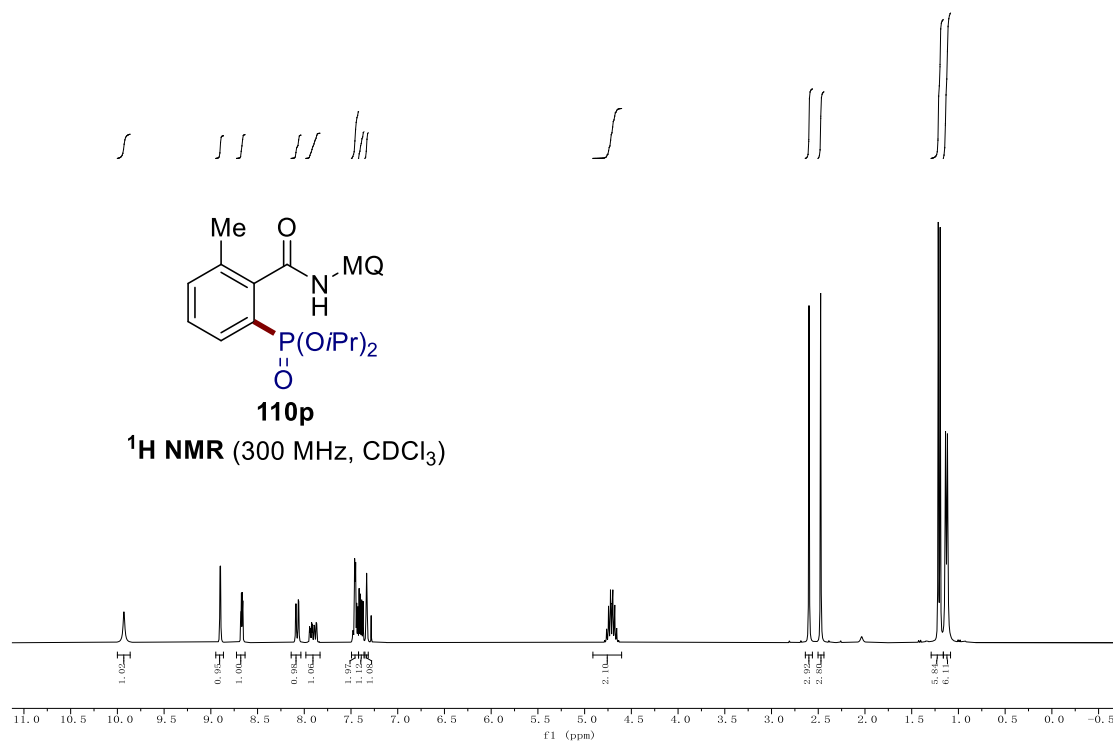


7. NMR Spectra

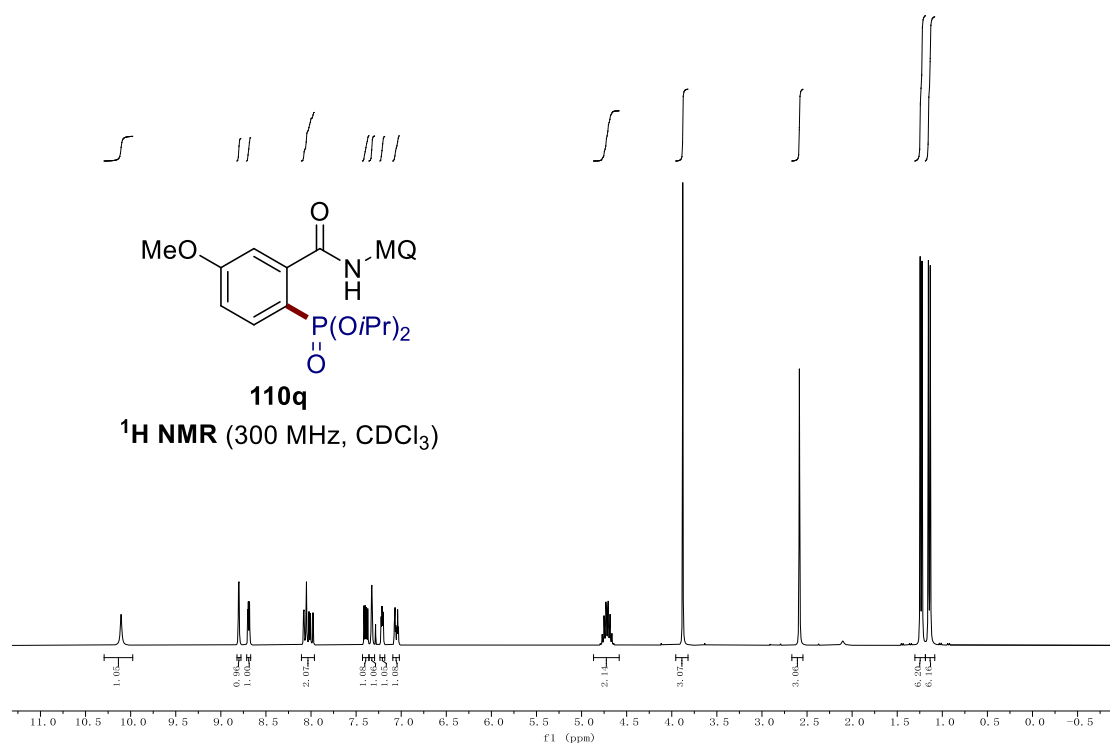
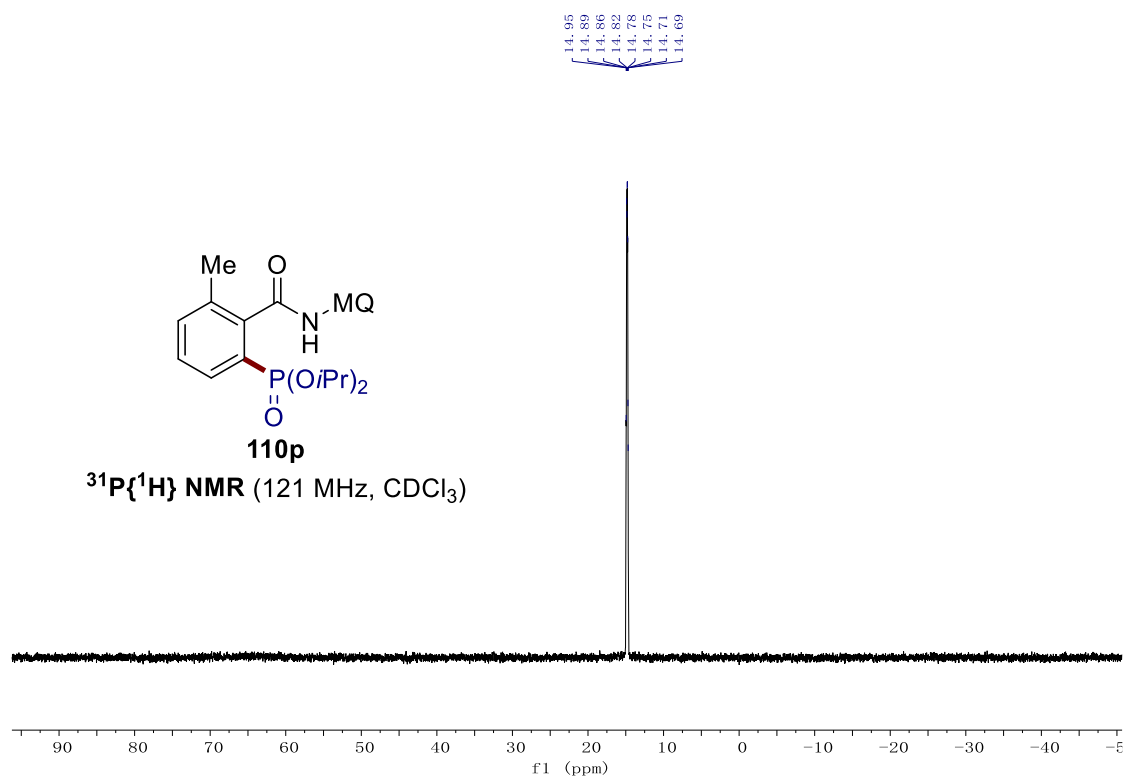




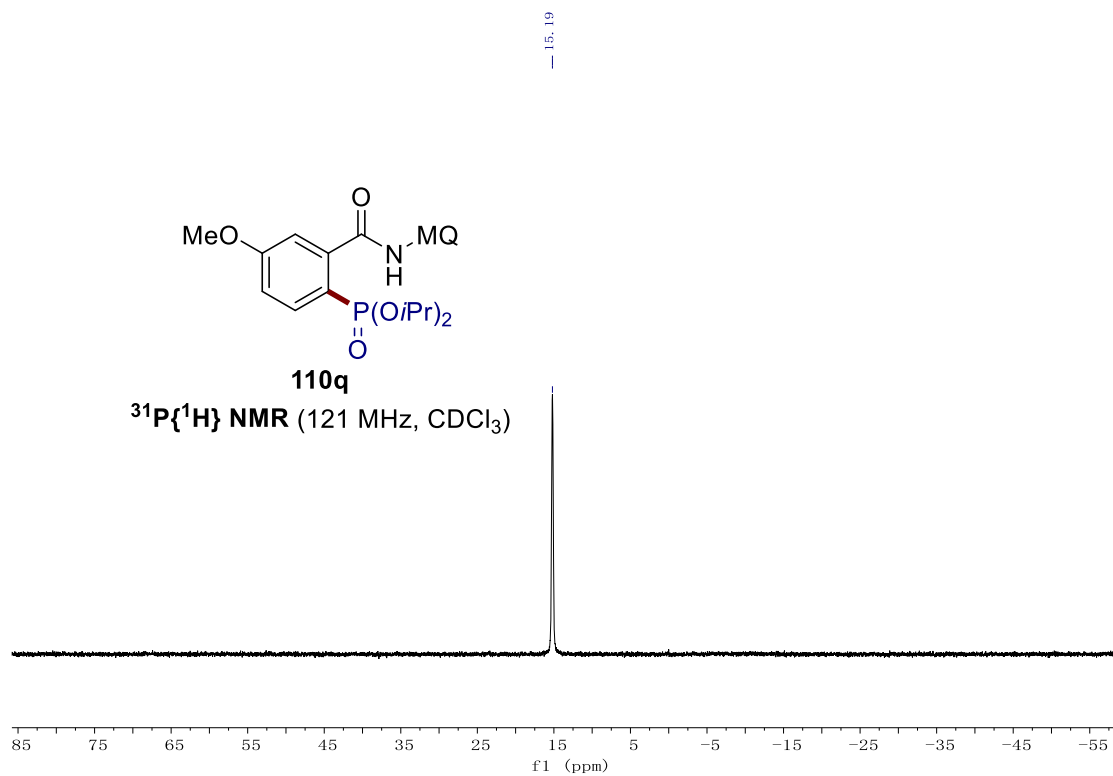
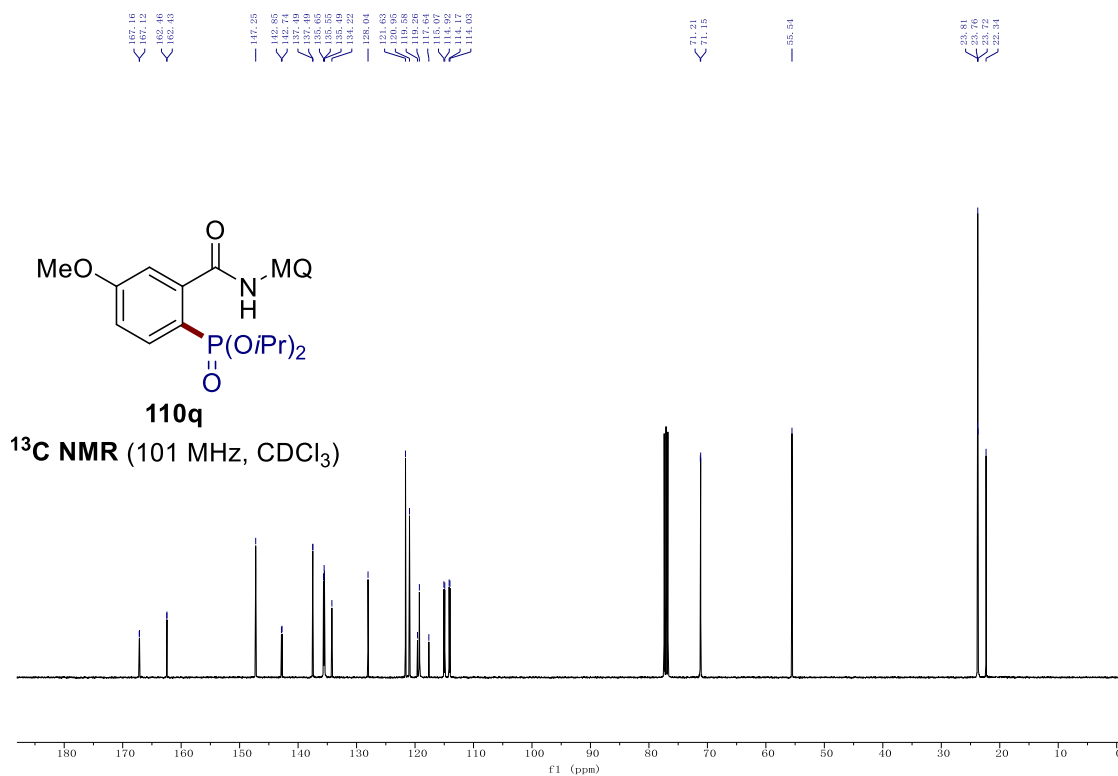
## 7. NMR Spectra

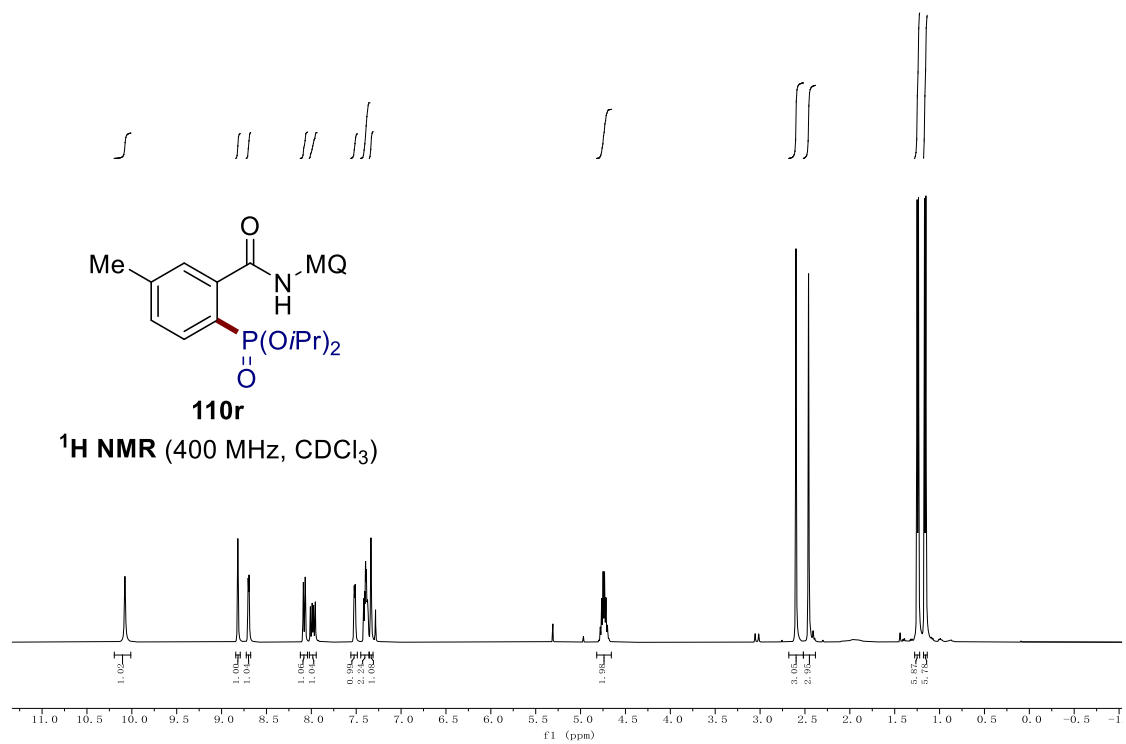
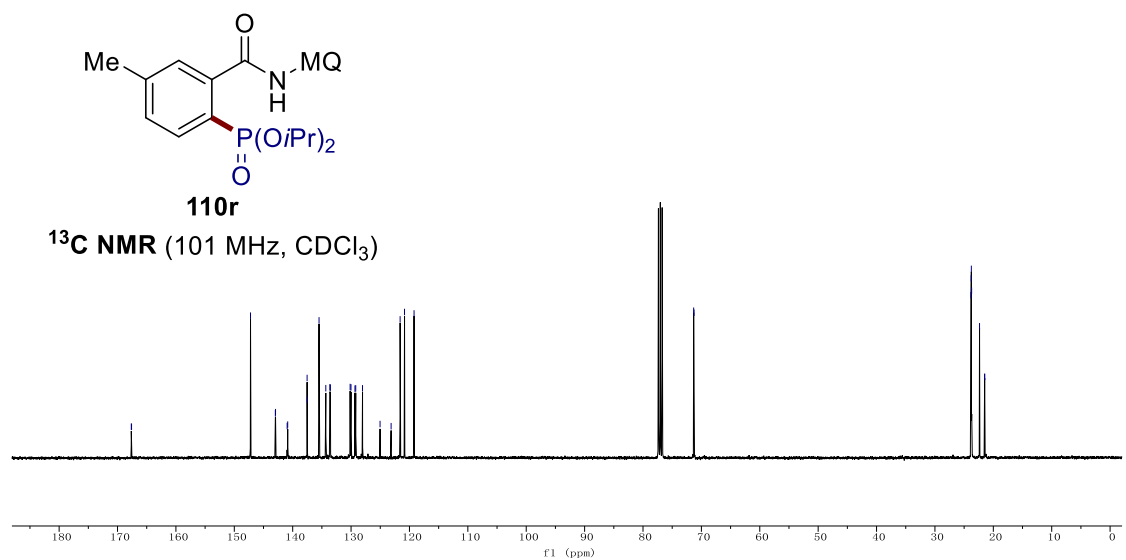




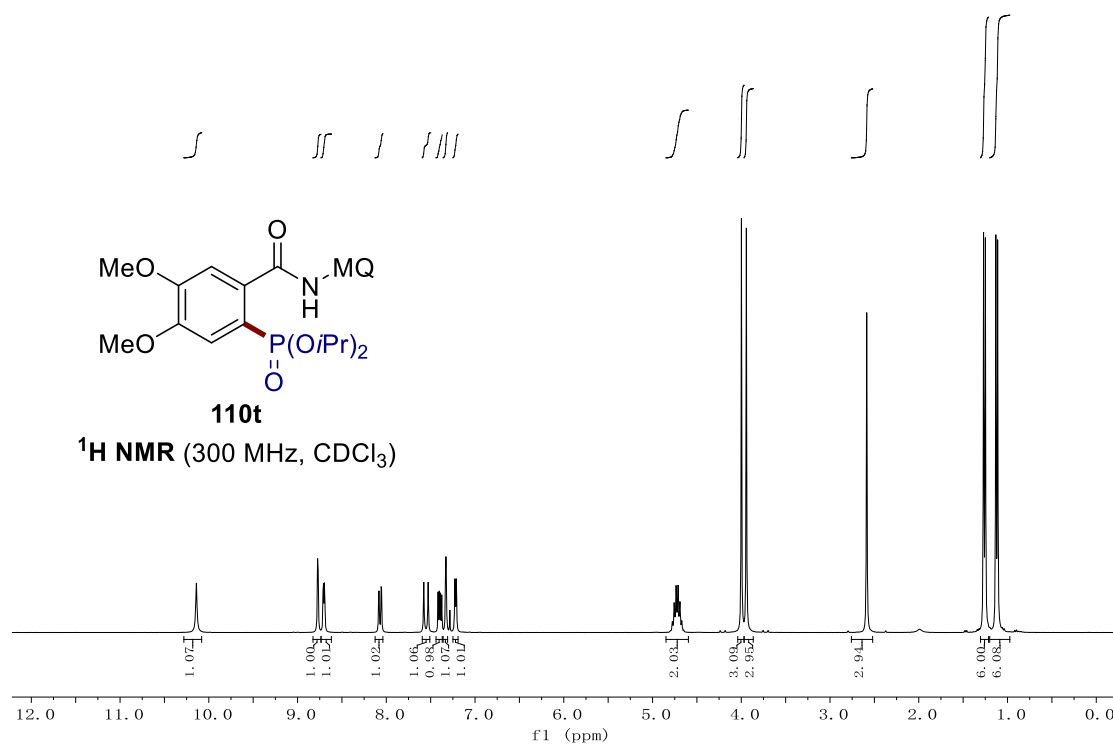
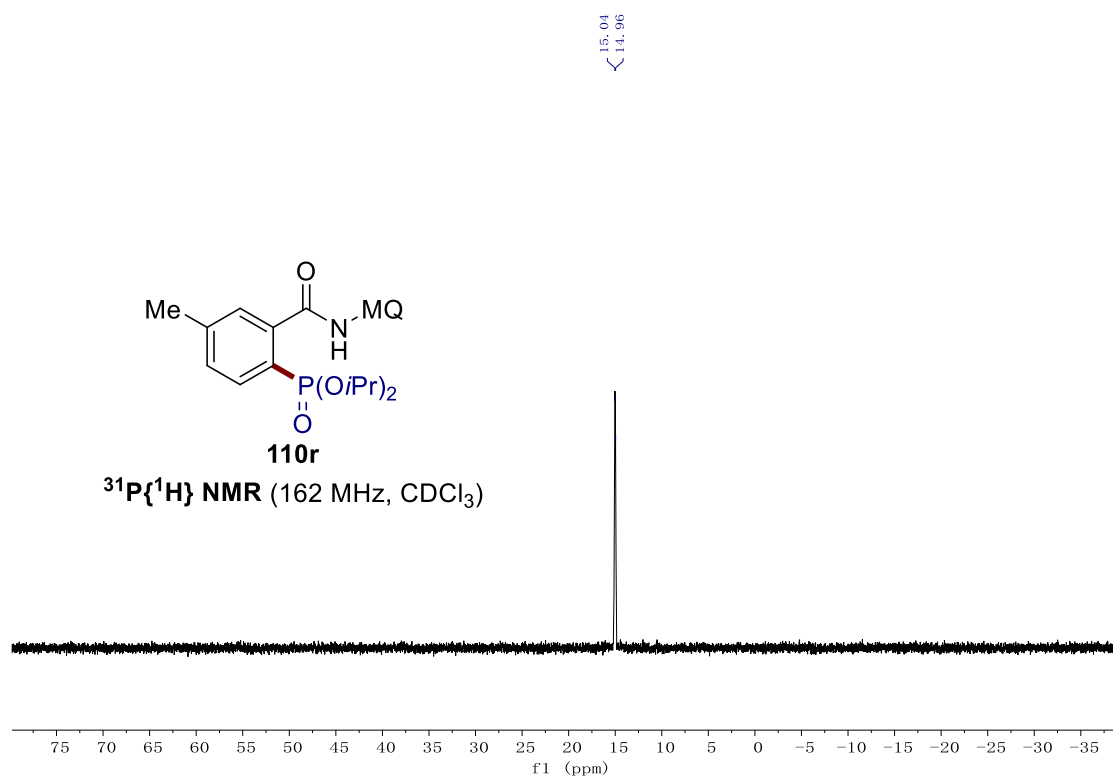


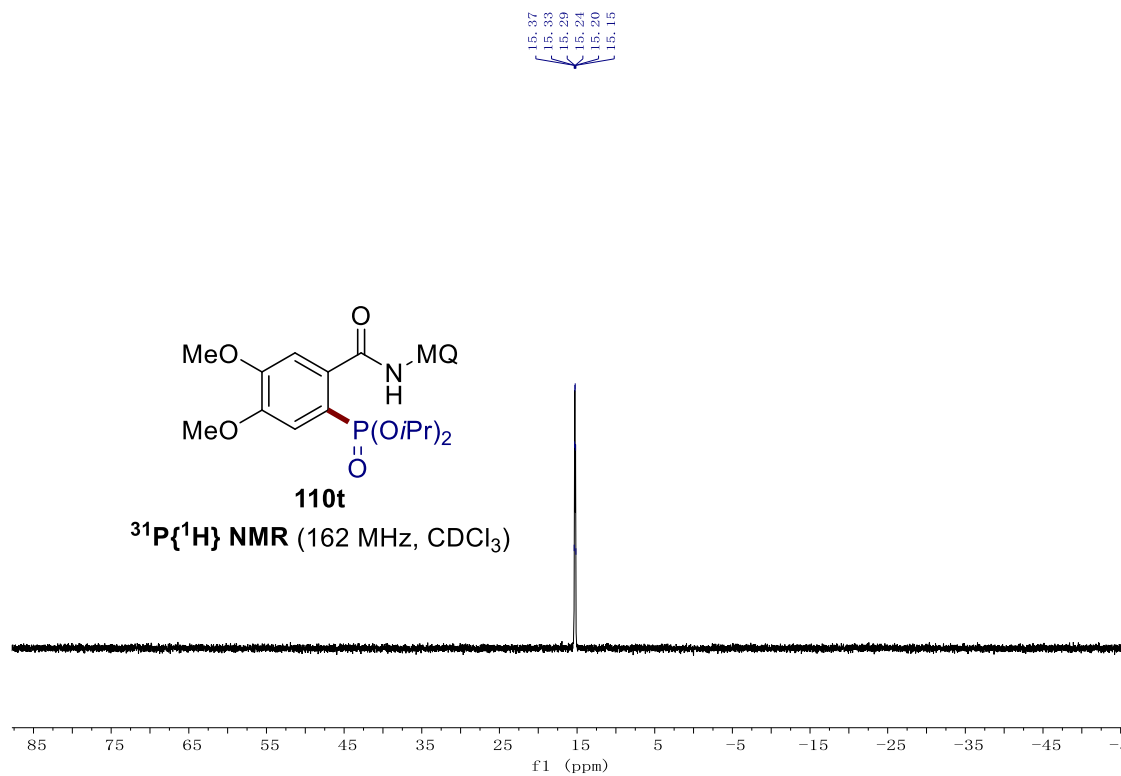
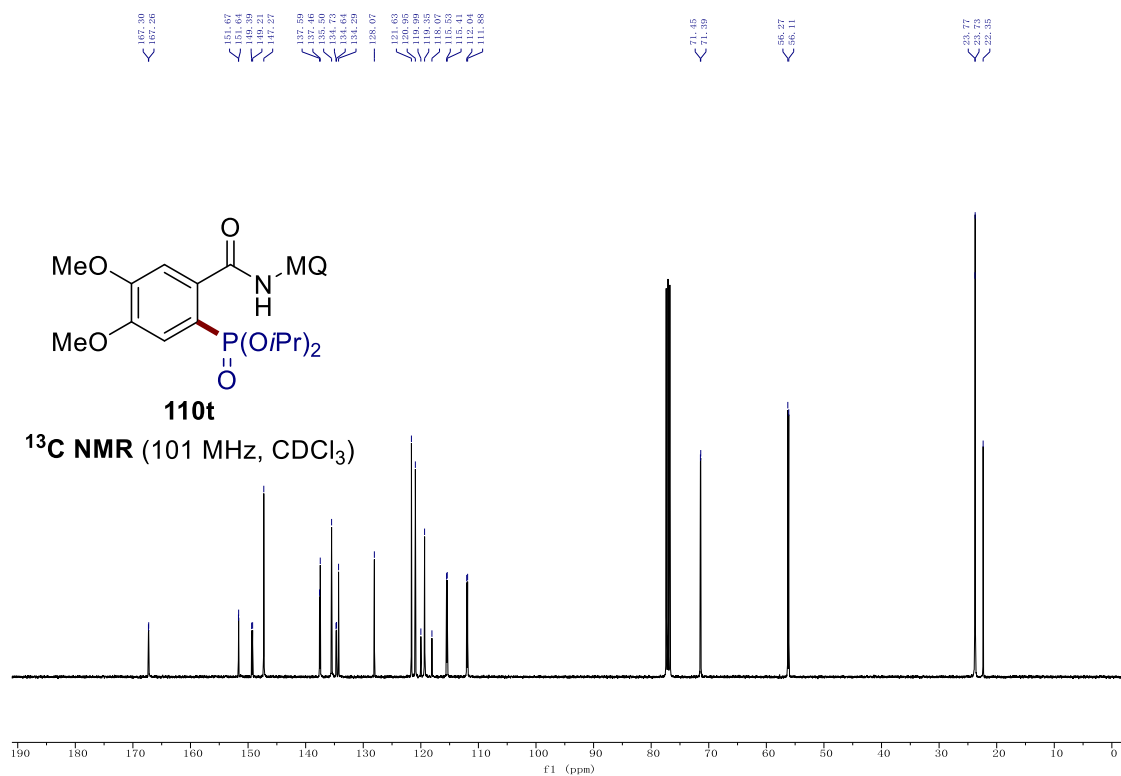
## 7. NMR Spectra



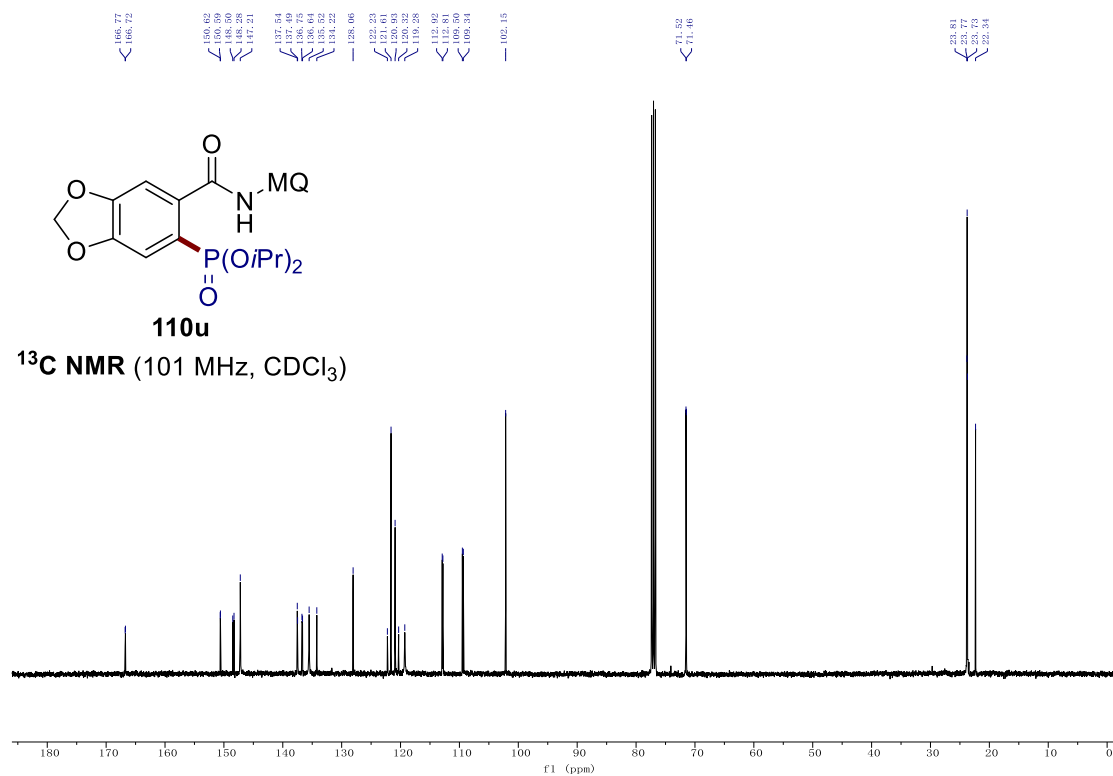
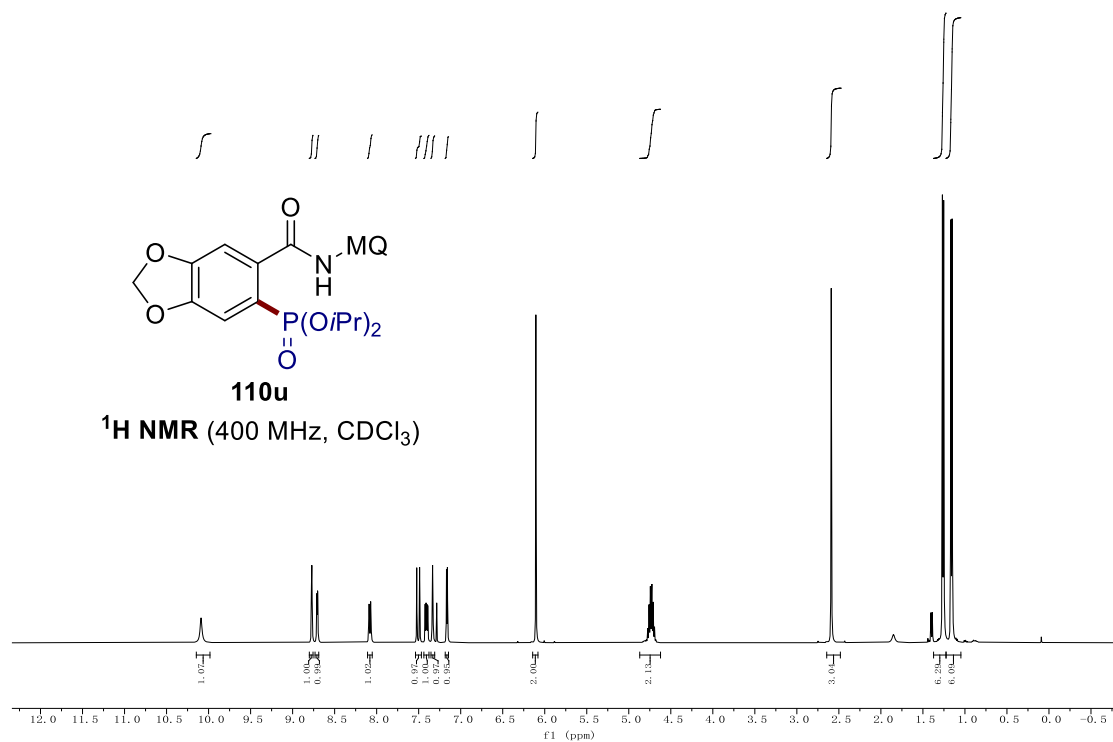
137.64  
137.36147.03  
142.97  
142.94  
140.85  
137.63  
135.89  
134.33  
133.94  
130.16  
129.92  
129.20  
128.04  
123.14  
121.09  
119.2171.32  
71.2623.82  
23.78  
23.77  
22.36  
21.49  
21.48

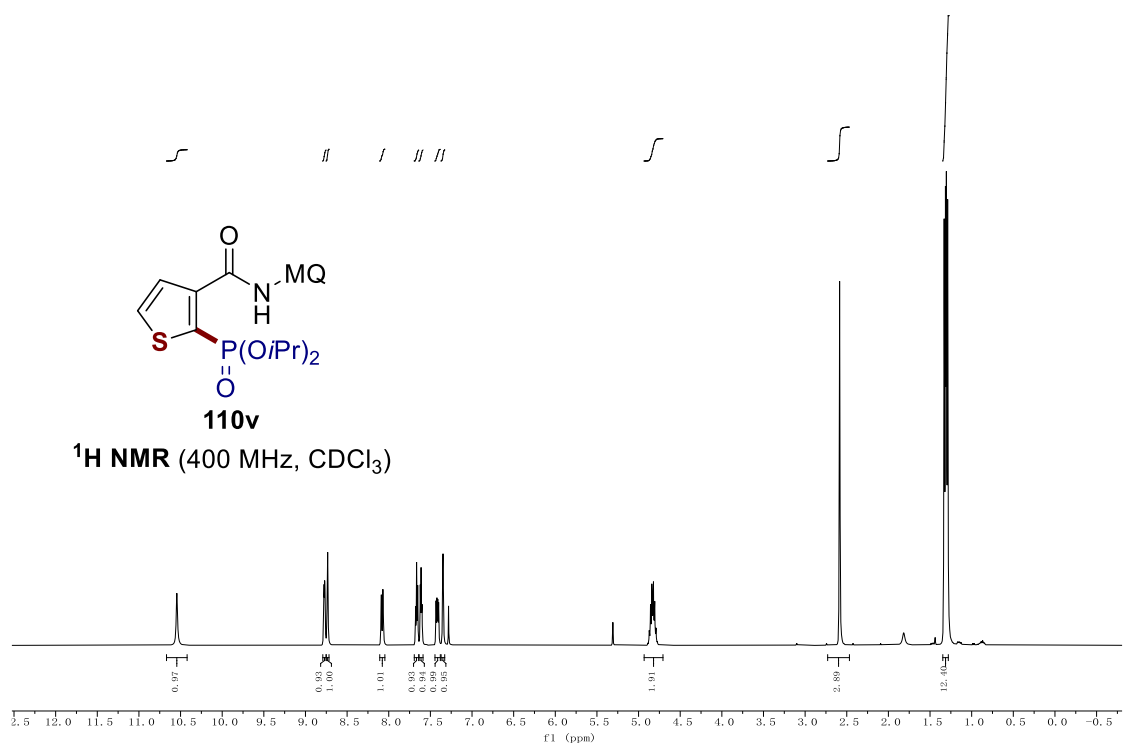
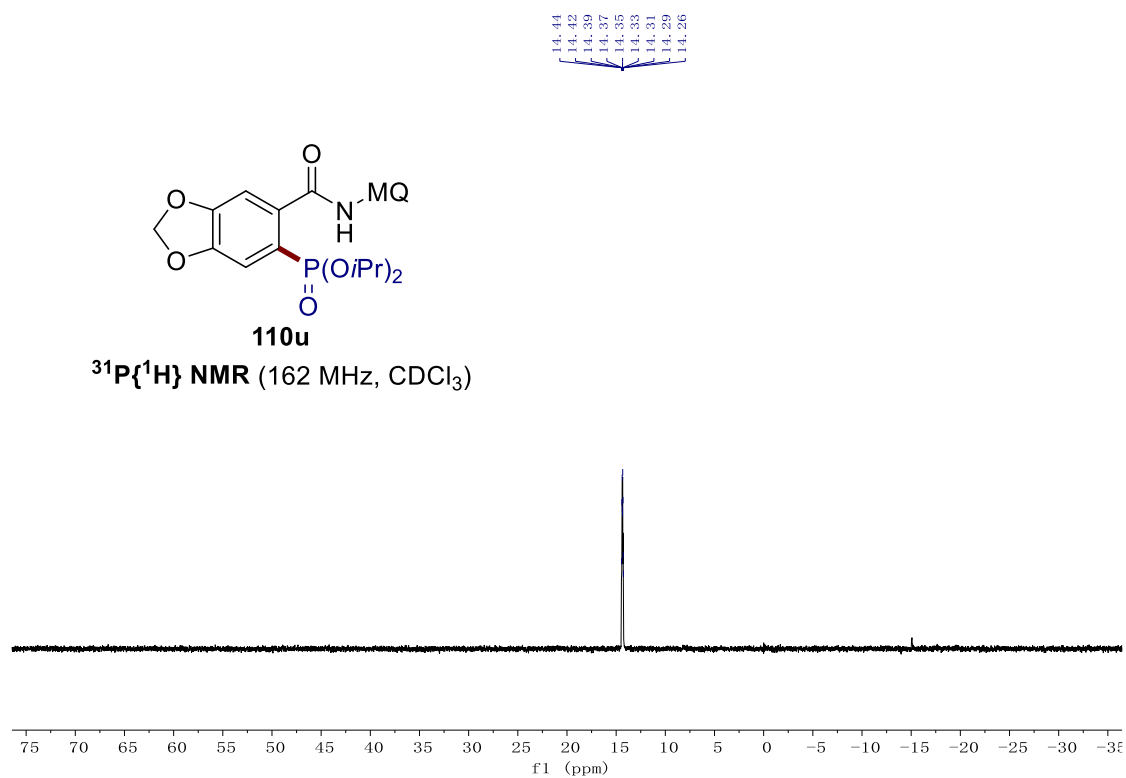
7. NMR Spectra



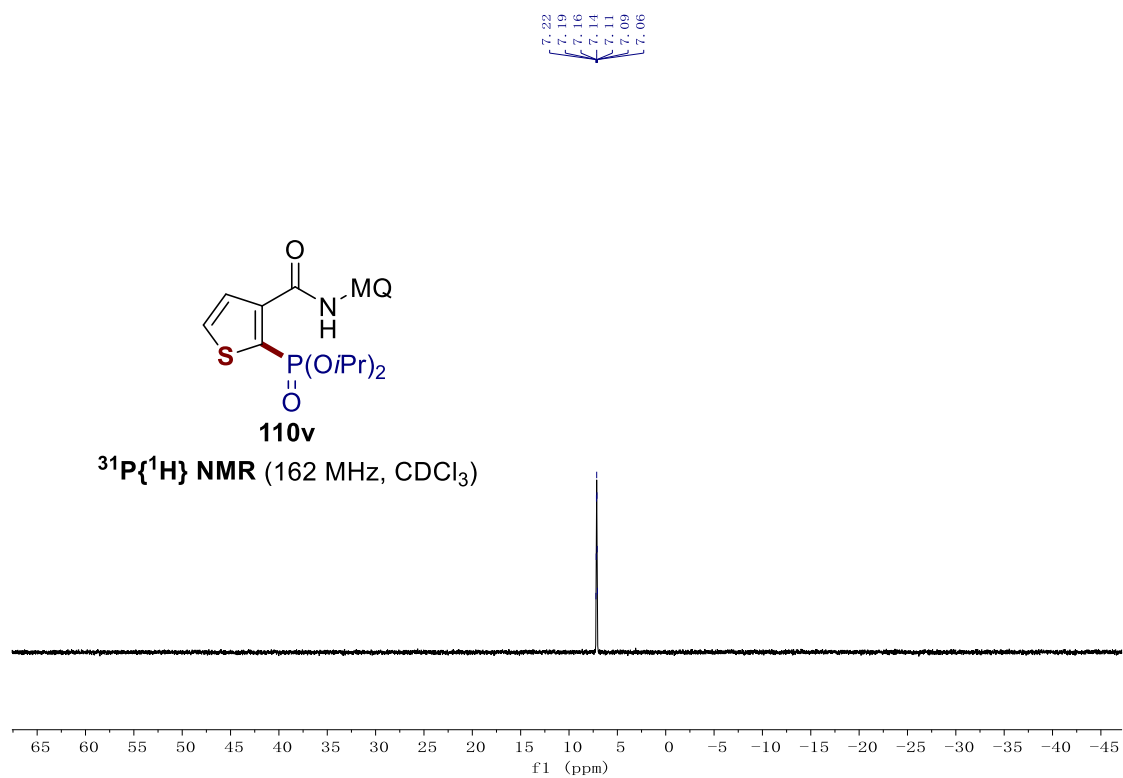
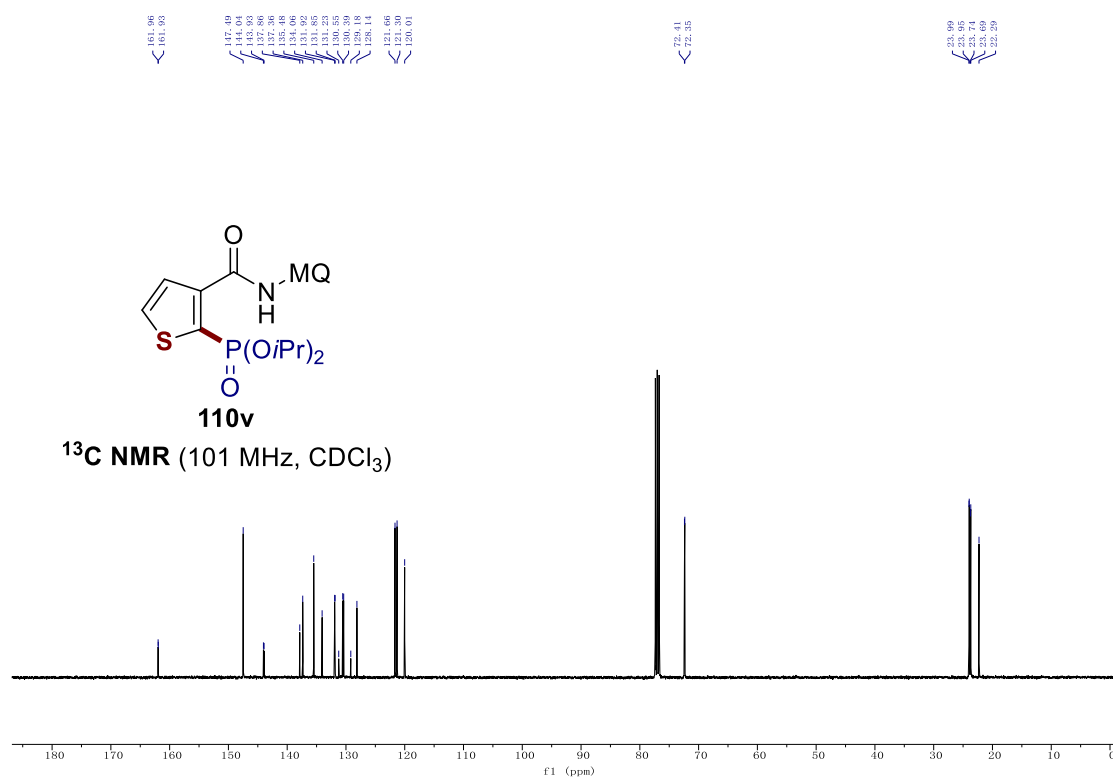


## 7. NMR Spectra

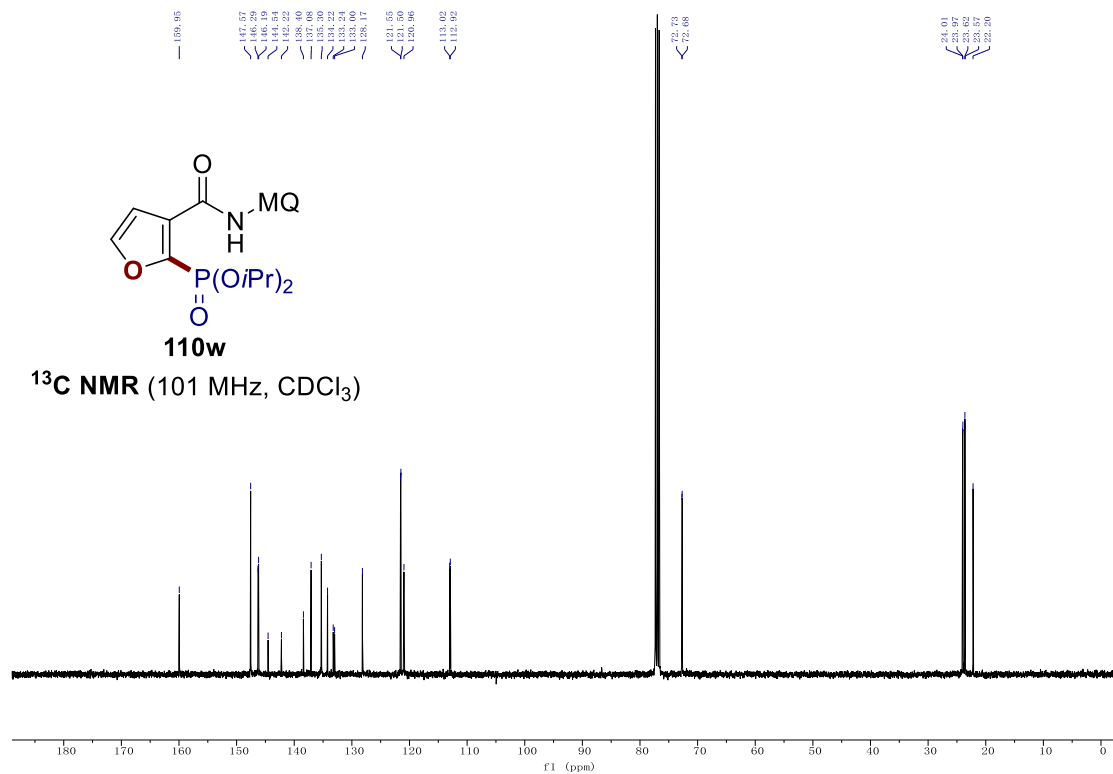
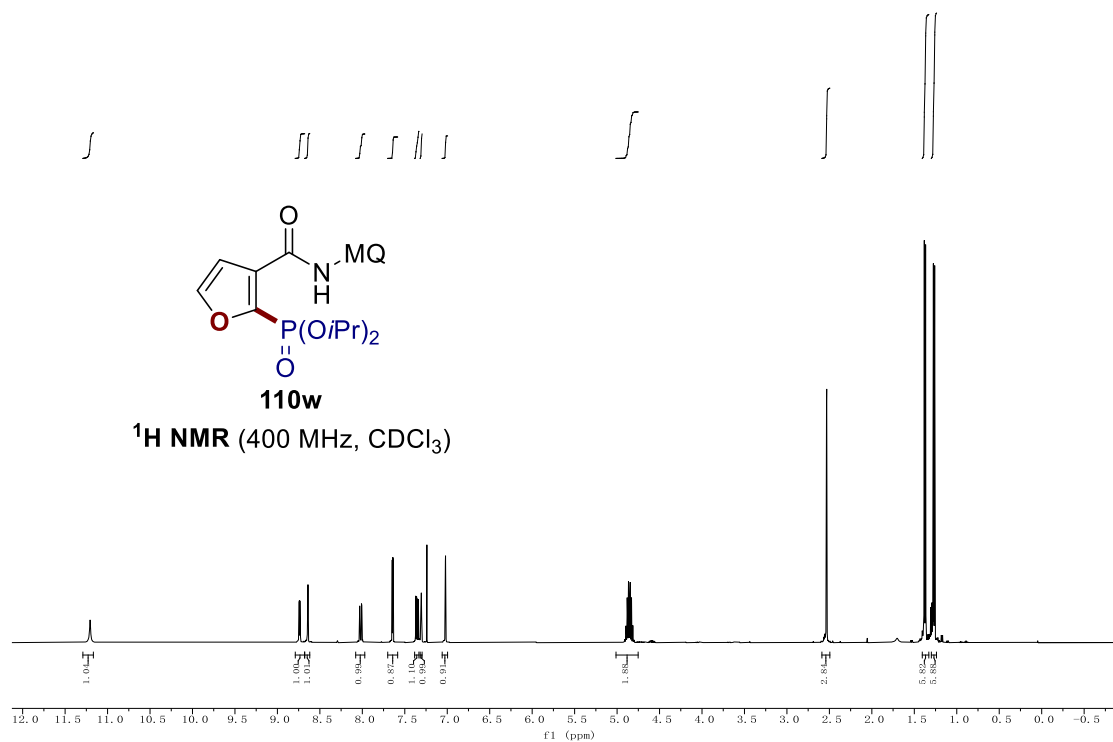




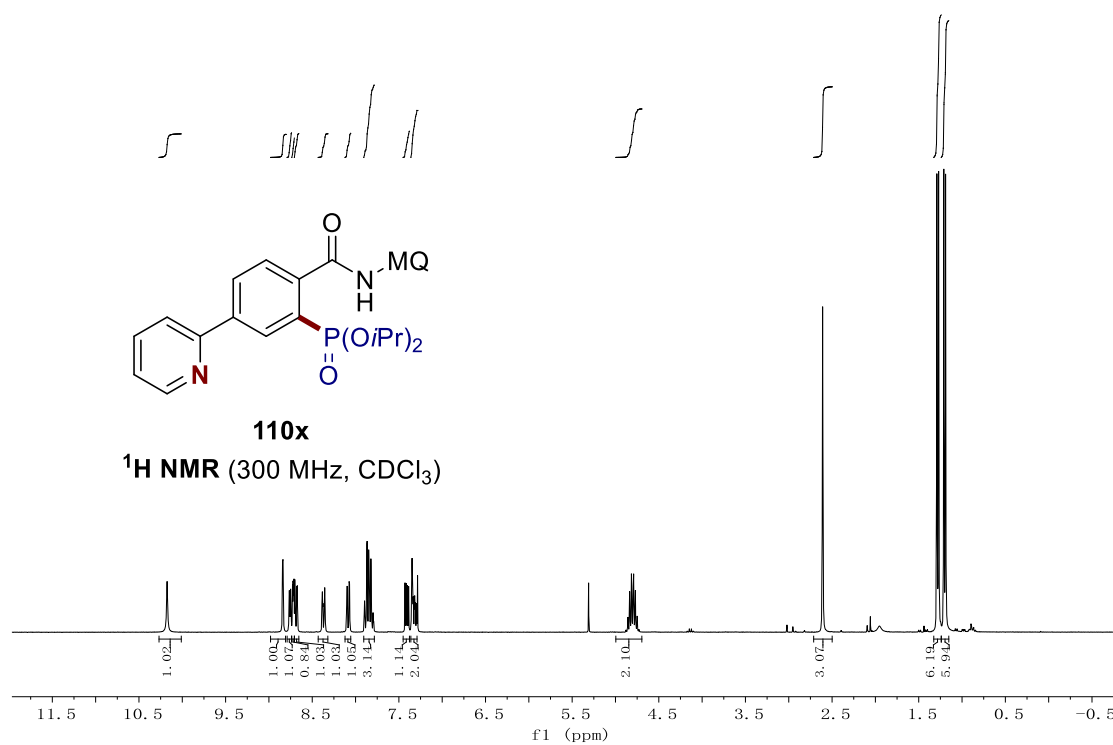
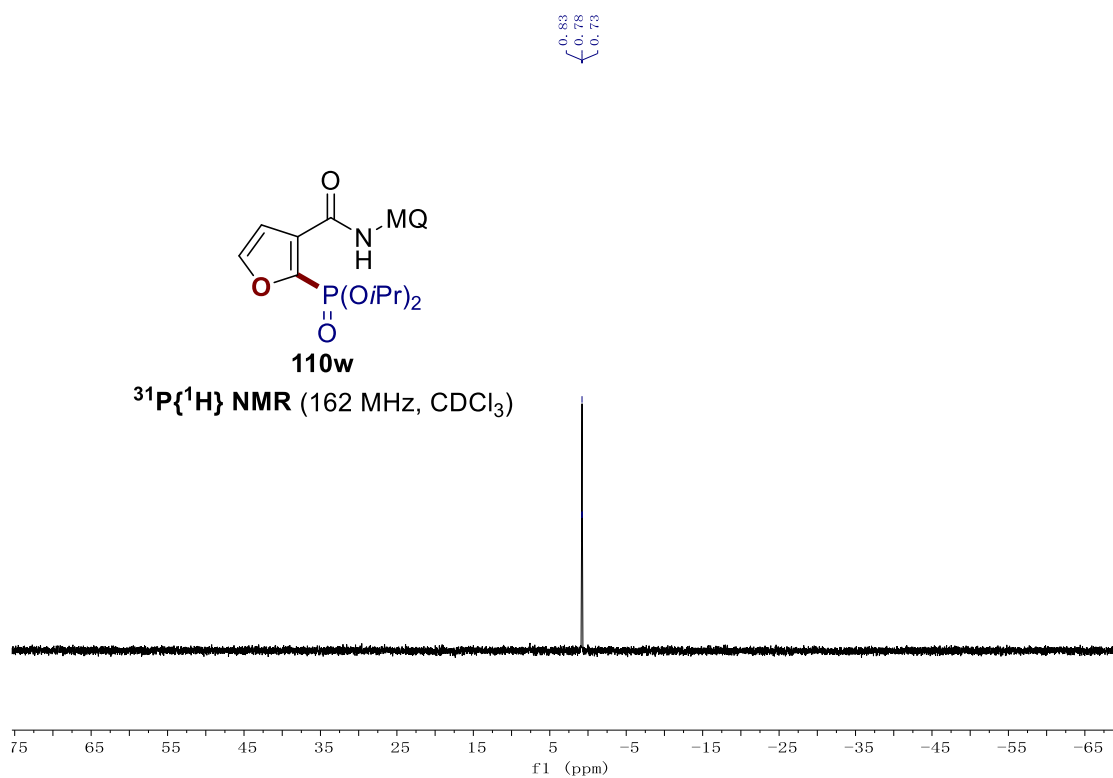
## 7. NMR Spectra

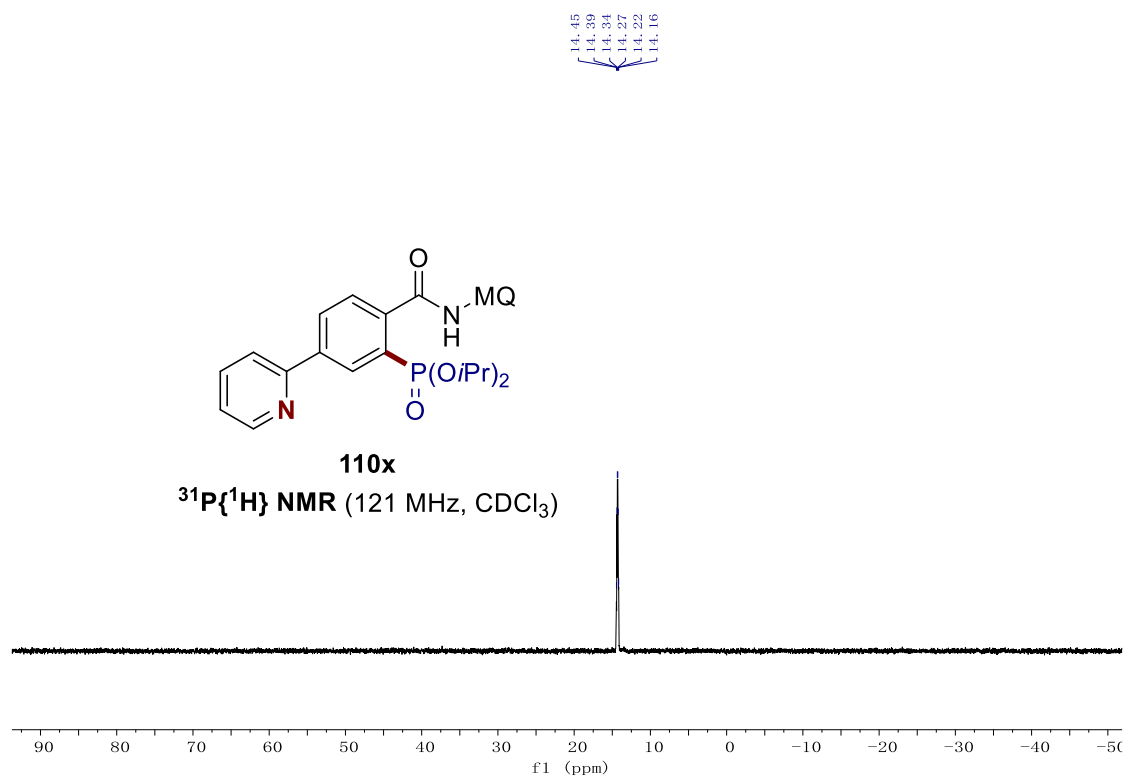
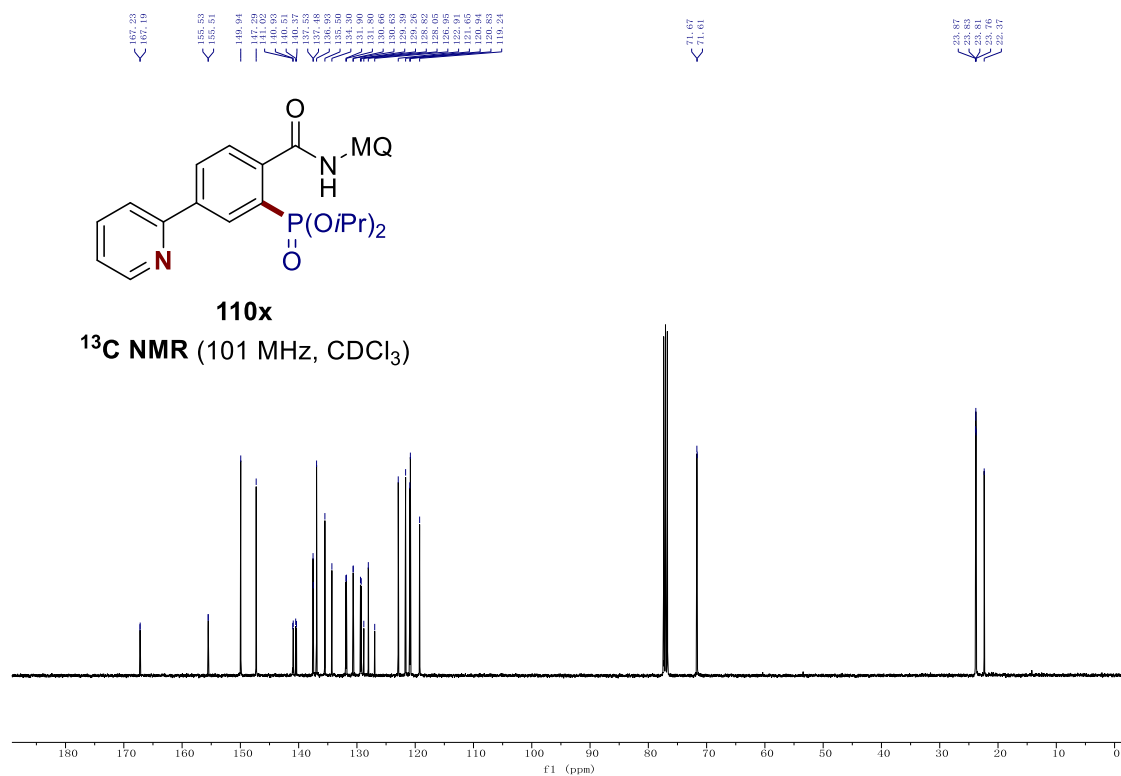




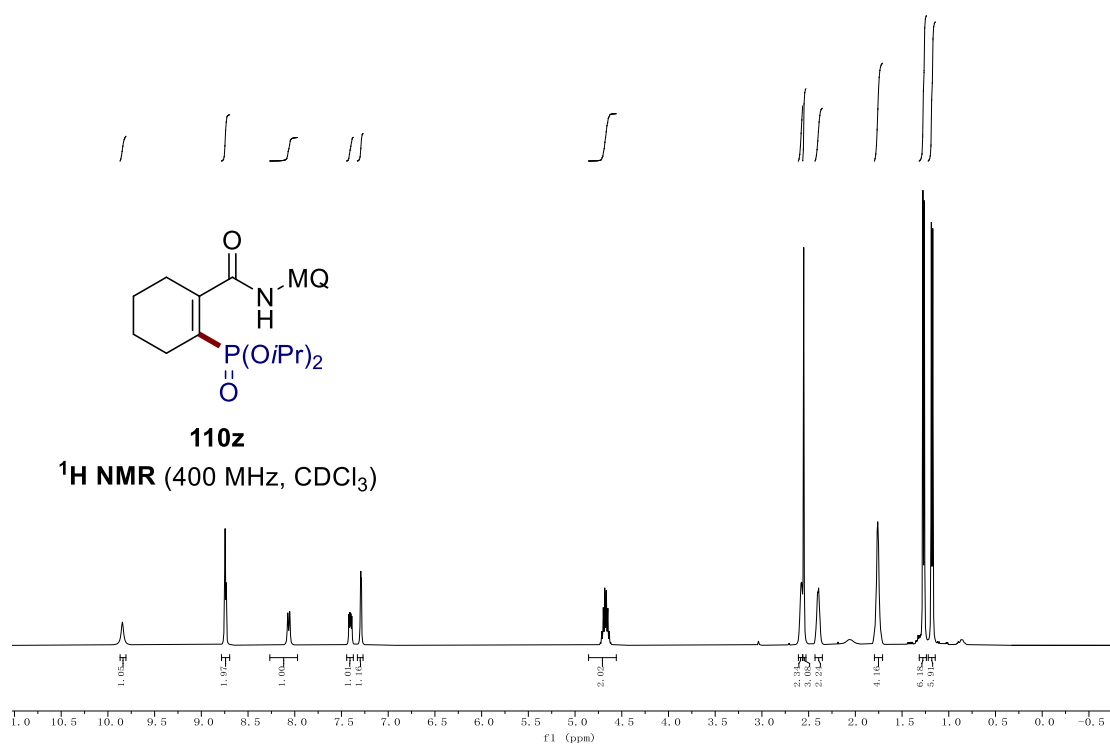
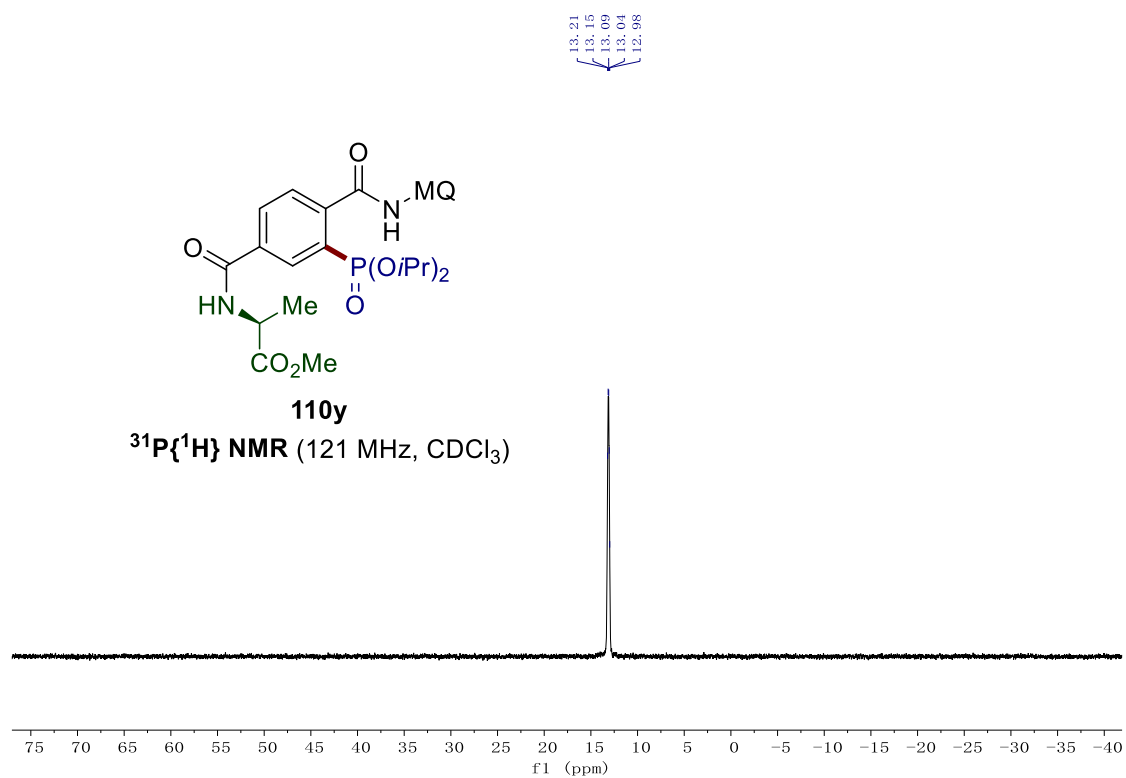


## 7. NMR Spectra

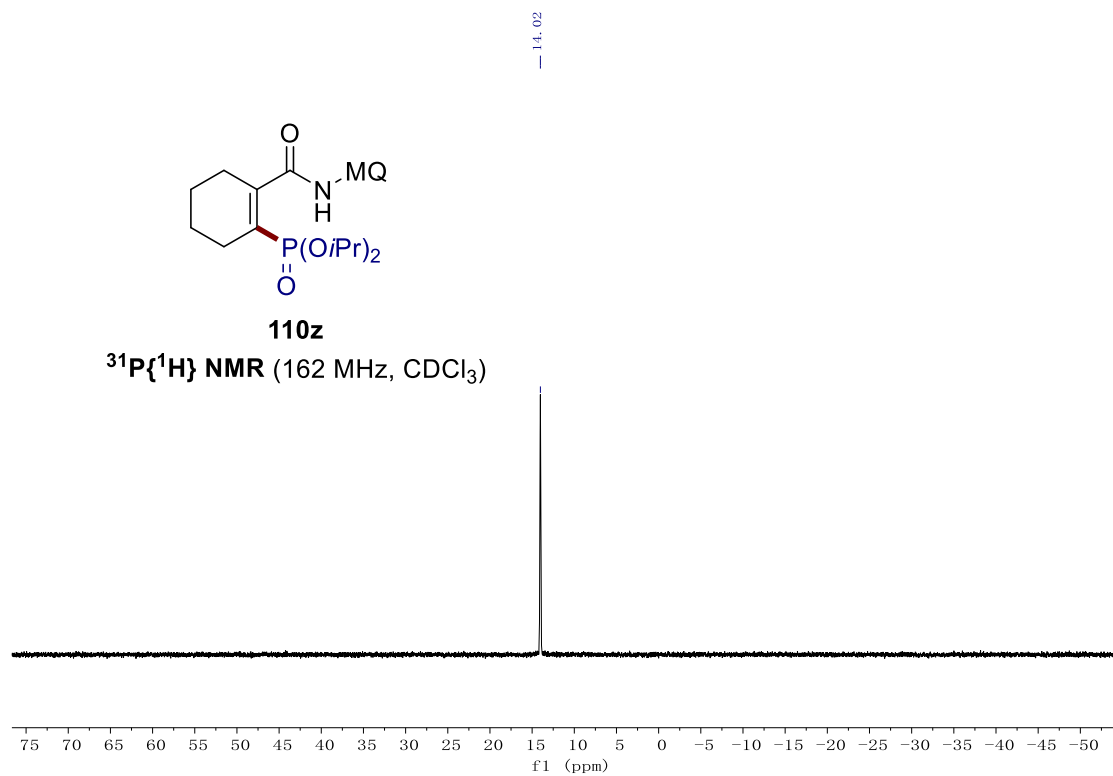
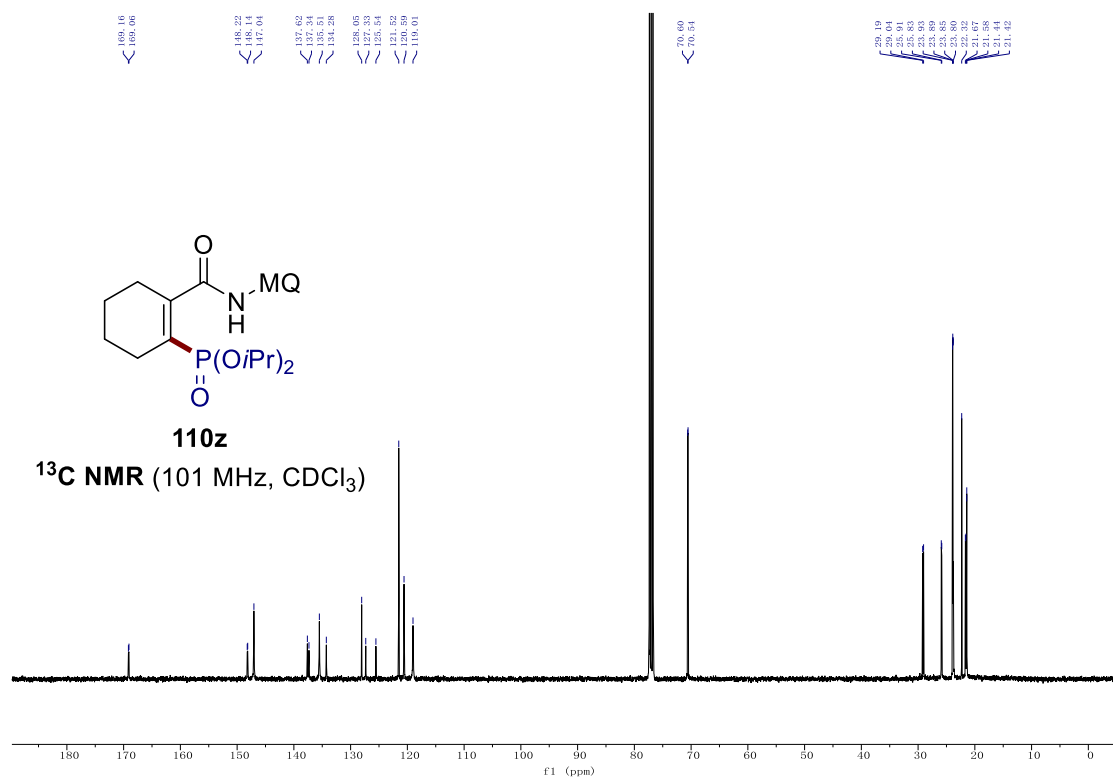


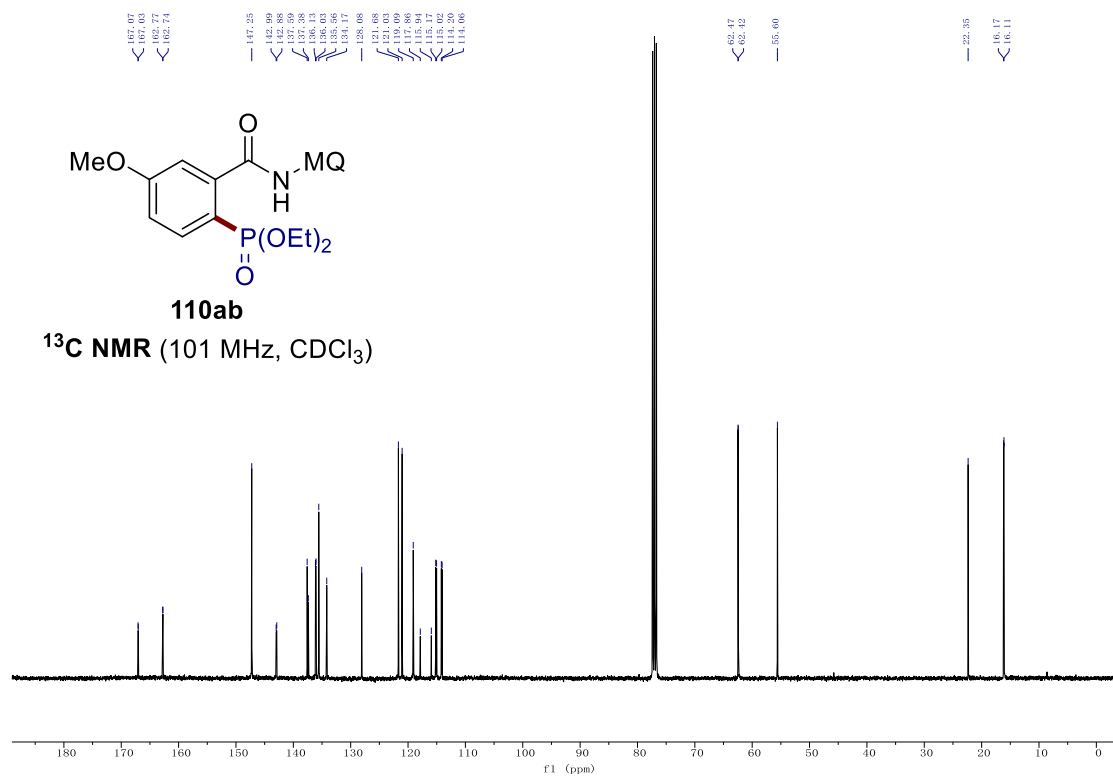
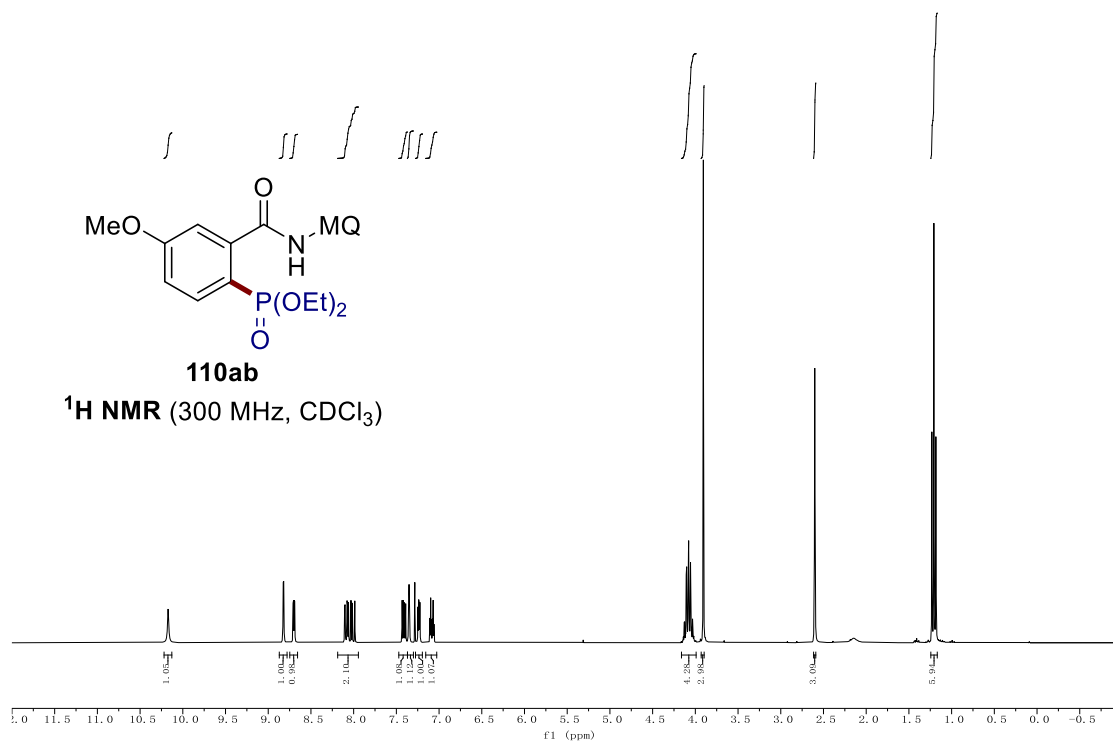




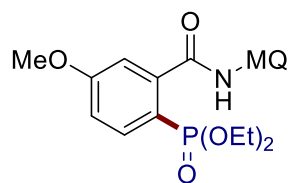


## 7. NMR Spectra



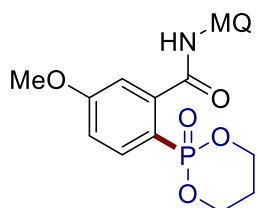
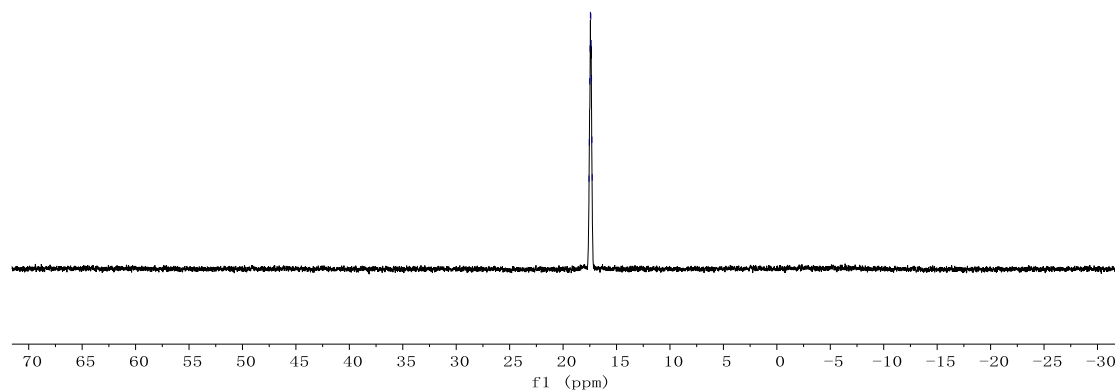


7. NMR Spectra



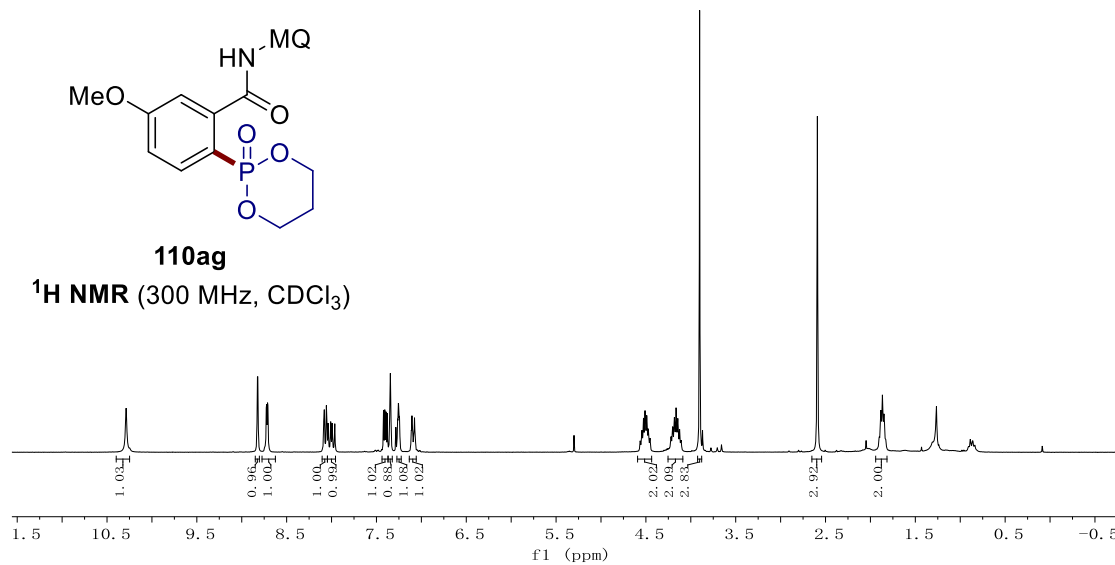
**110ab**

$^{31}\text{P}\{^1\text{H}\}$  NMR (121 MHz,  $\text{CDCl}_3$ )

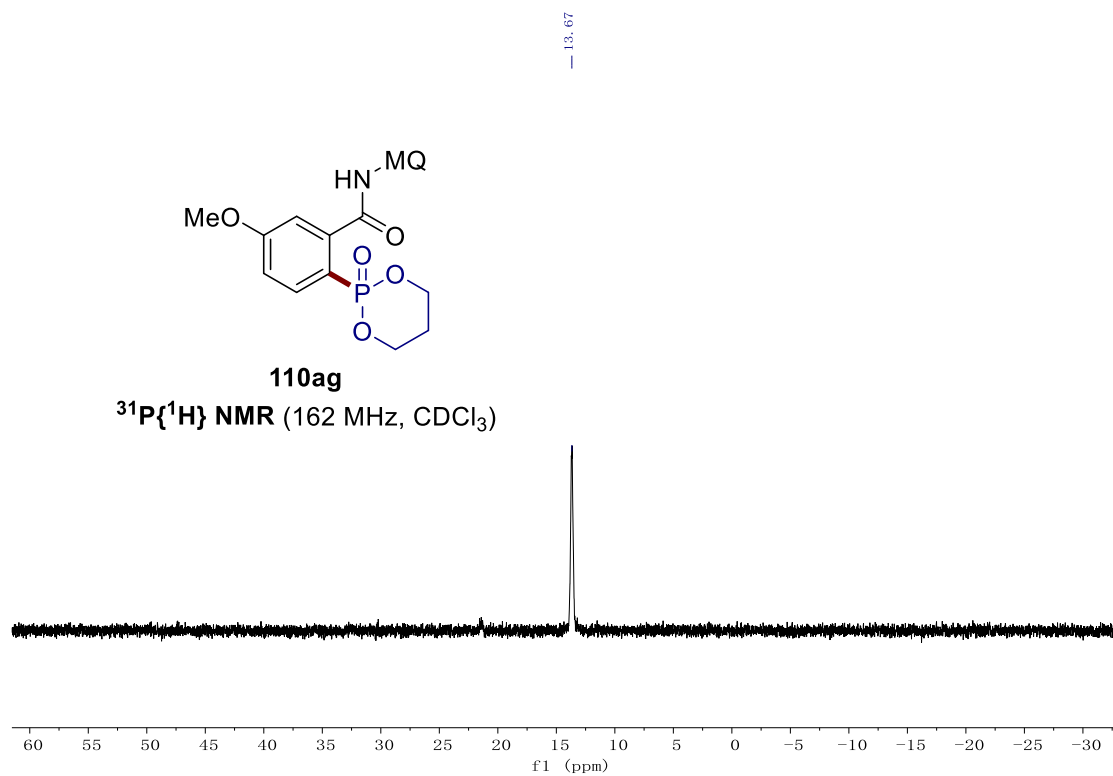
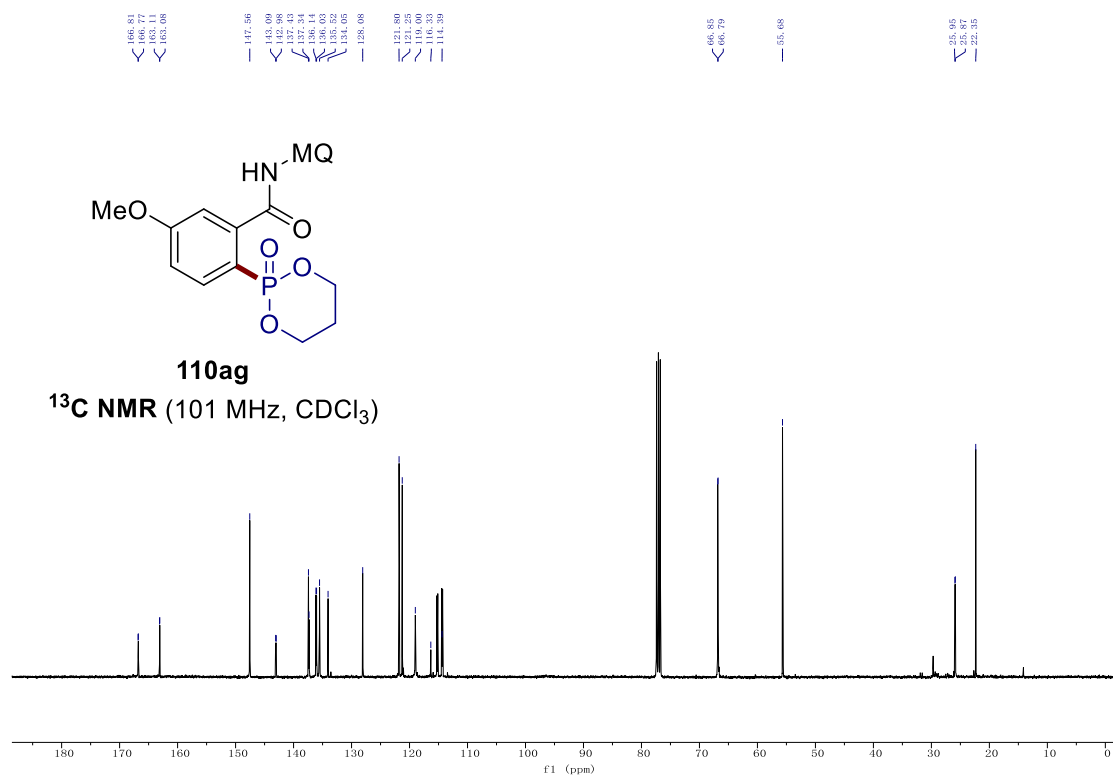


**110ag**

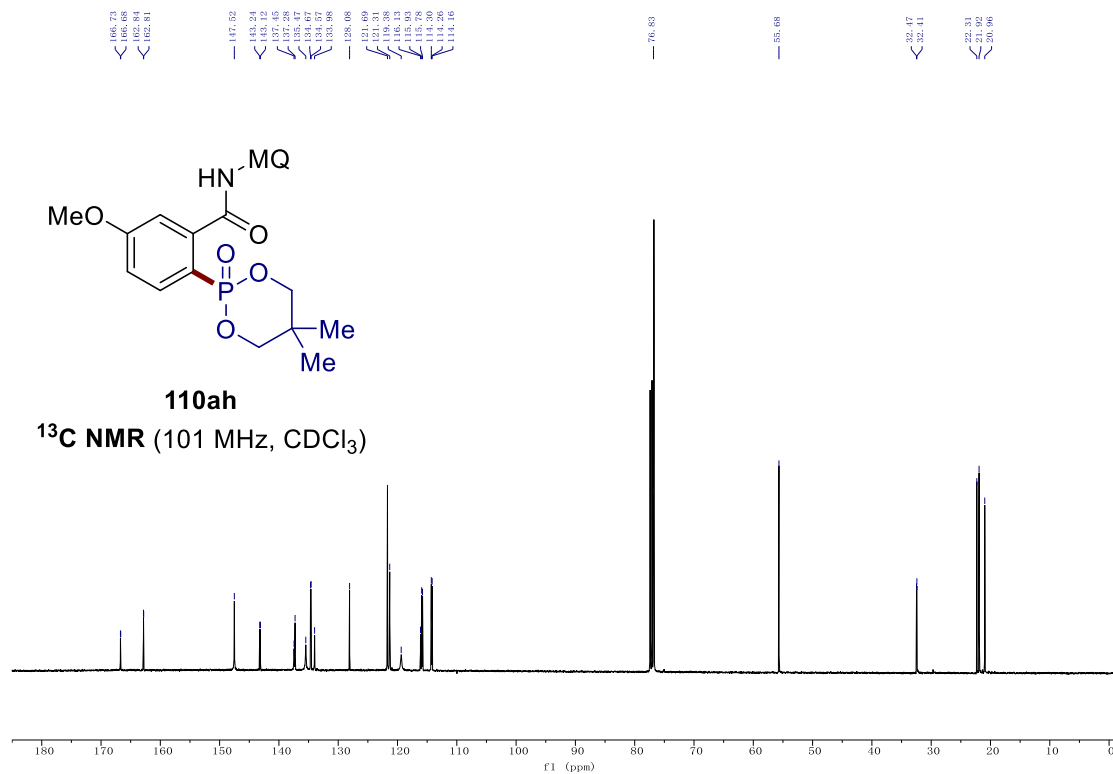
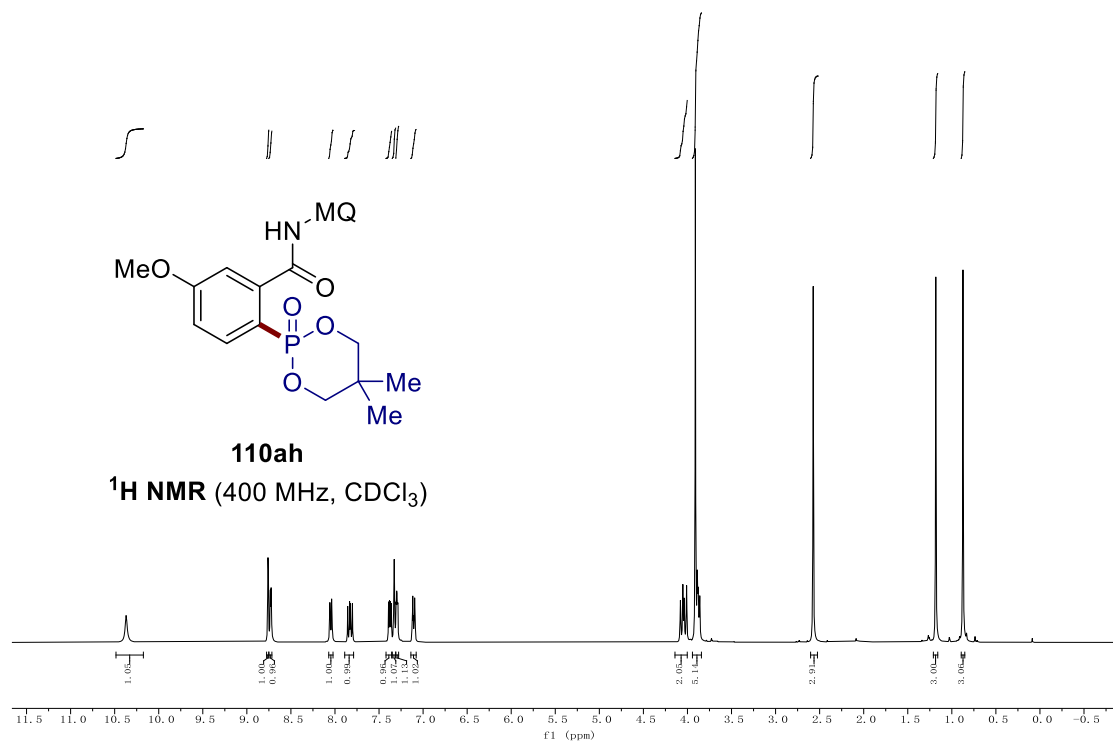
$^1\text{H}$  NMR (300 MHz,  $\text{CDCl}_3$ )

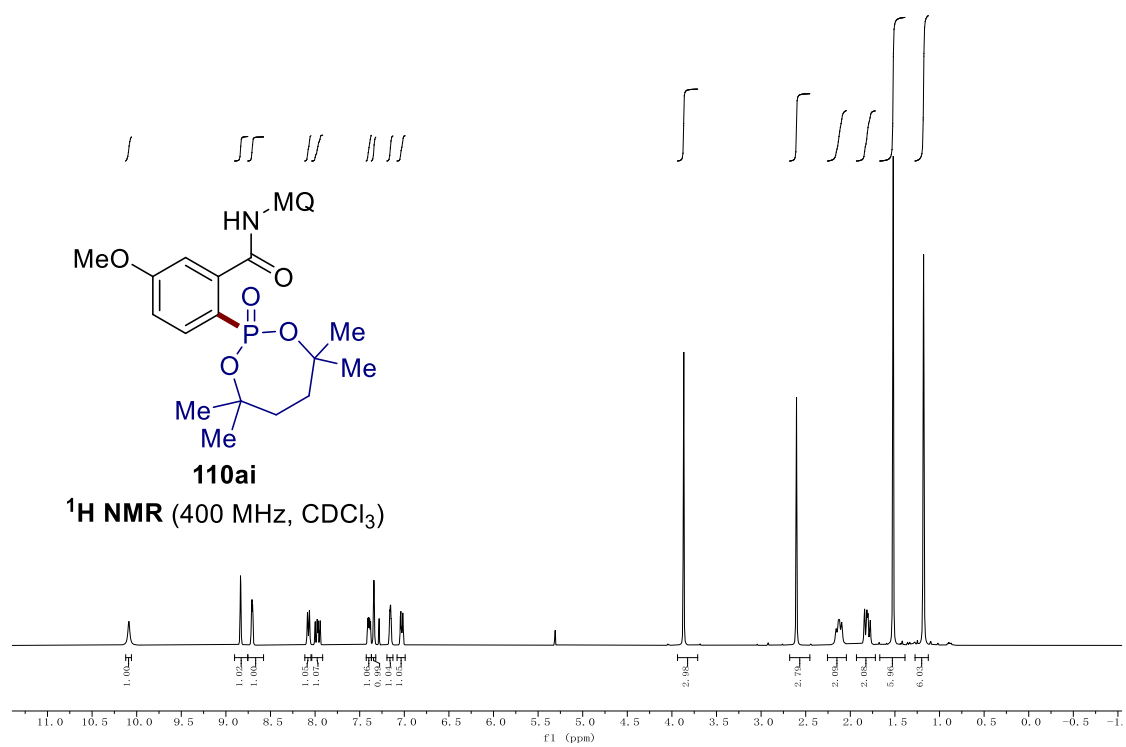
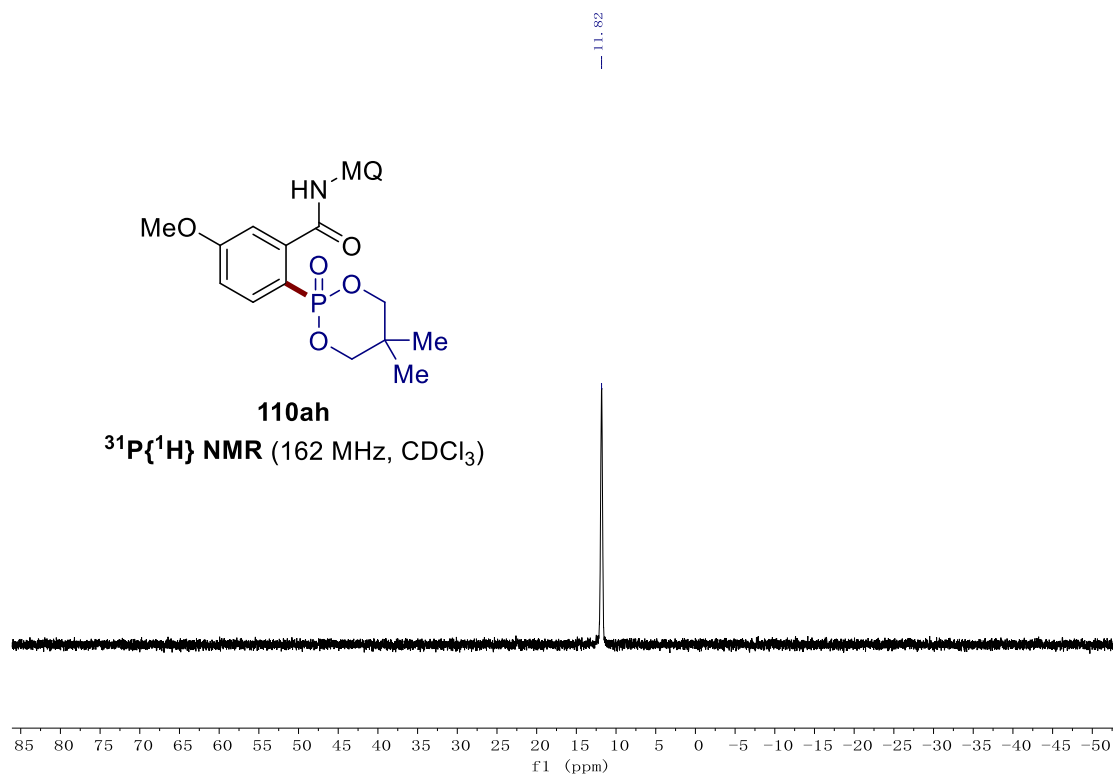




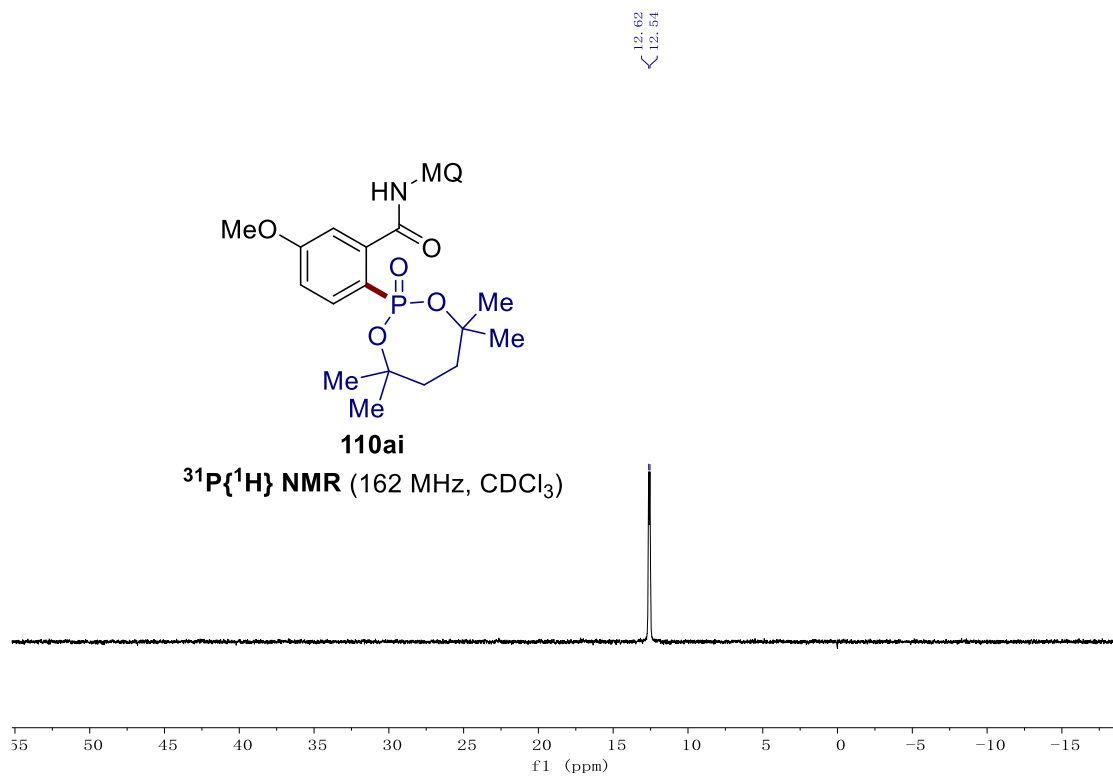
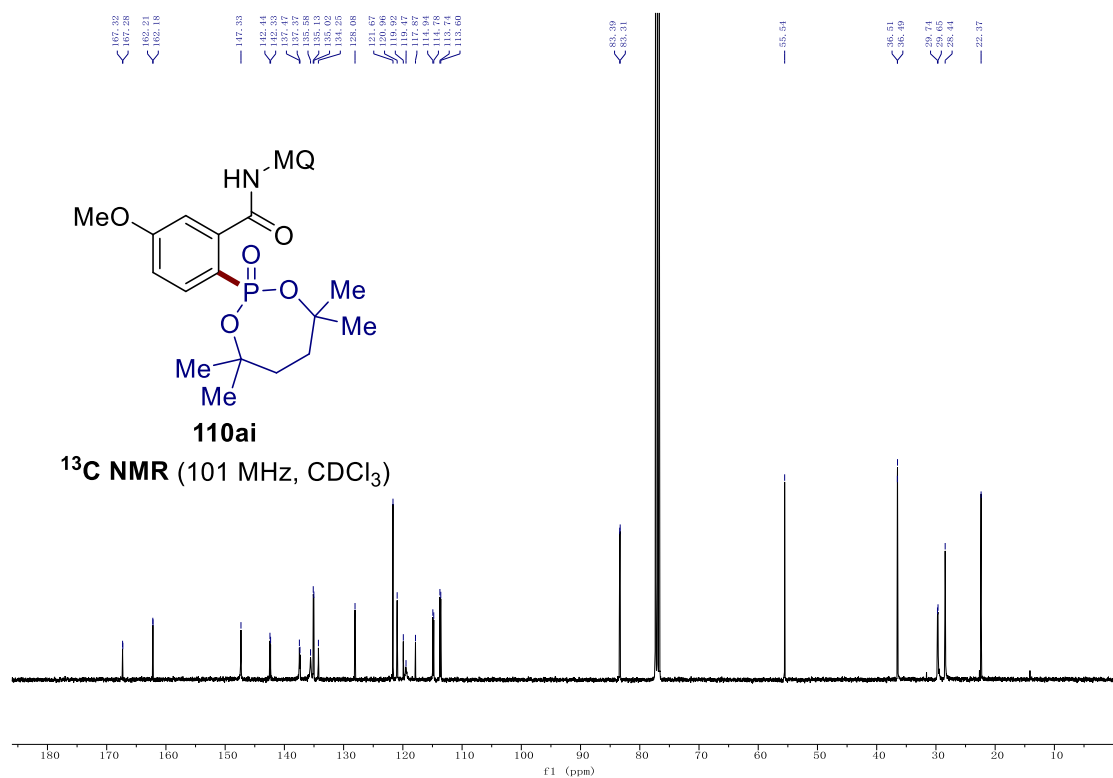


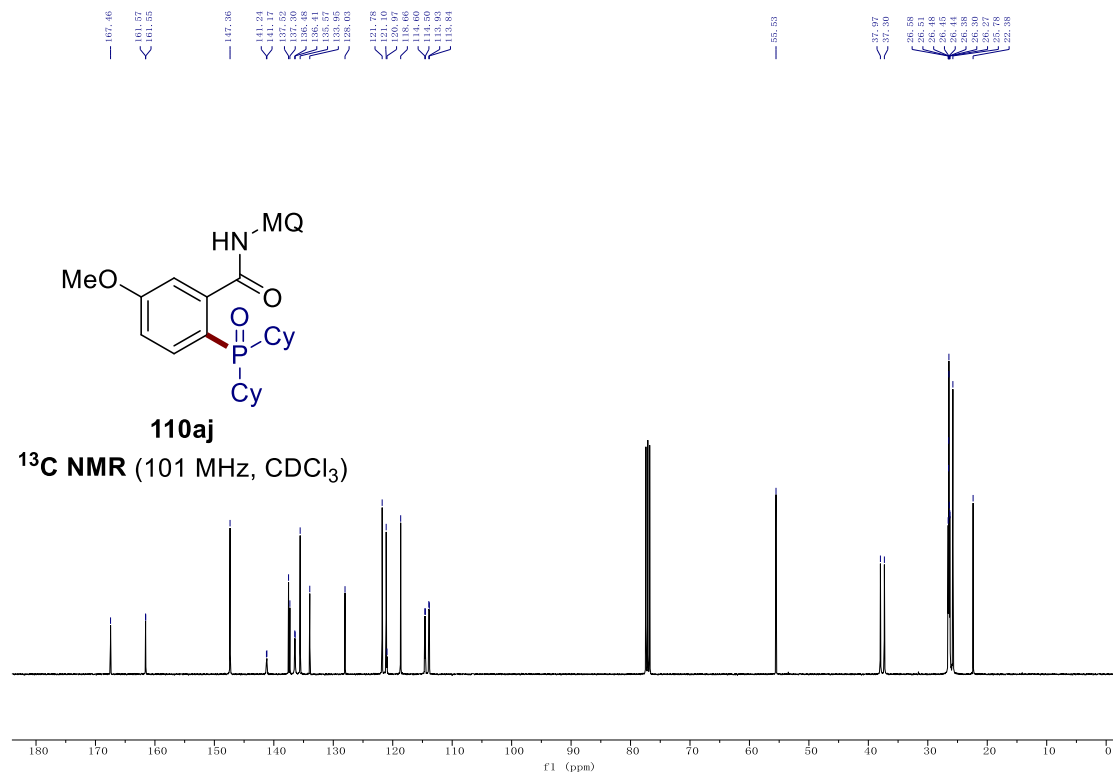
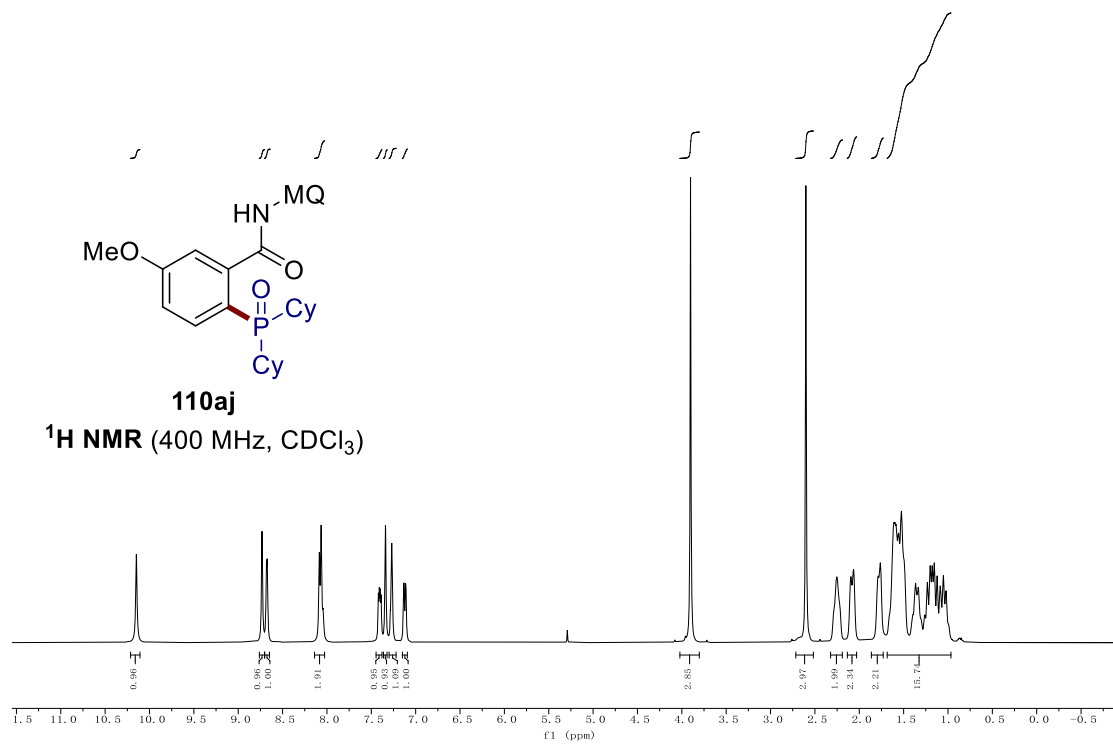
## 7. NMR Spectra





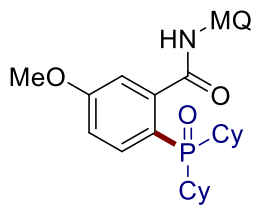
## 7. NMR Spectra



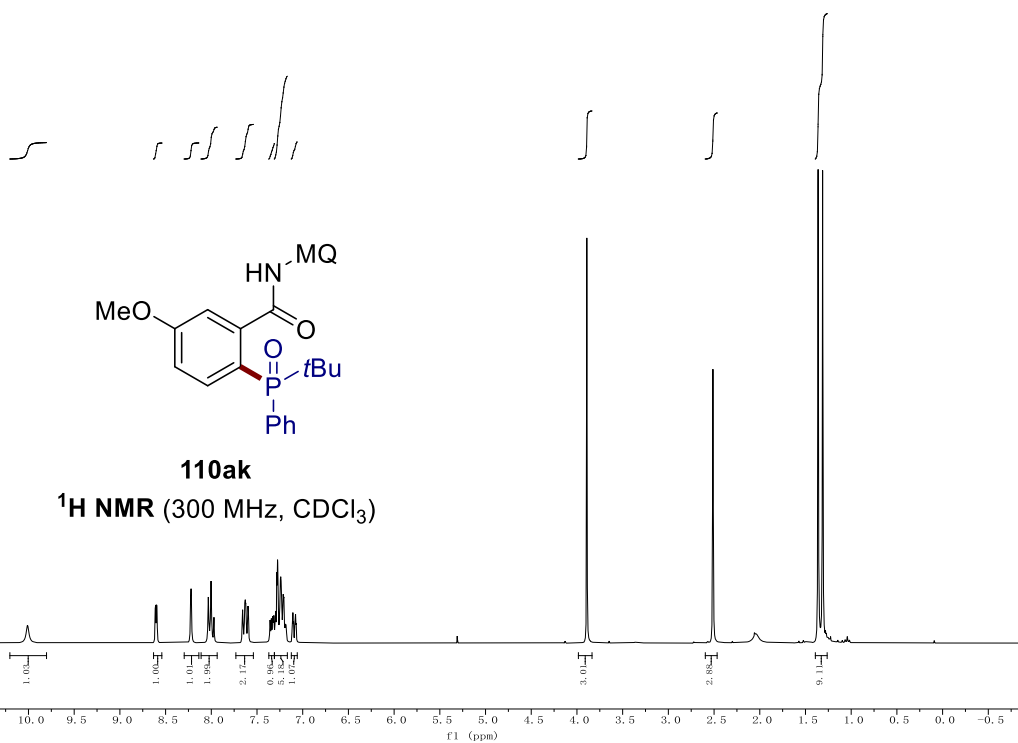
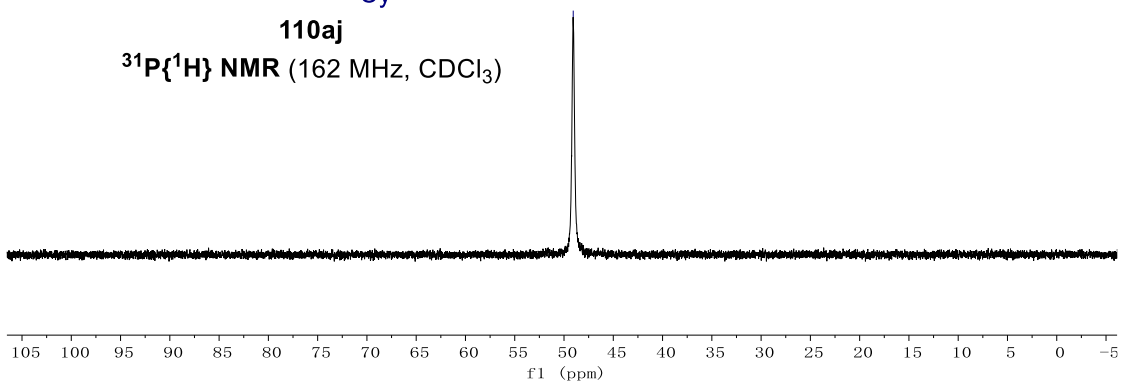


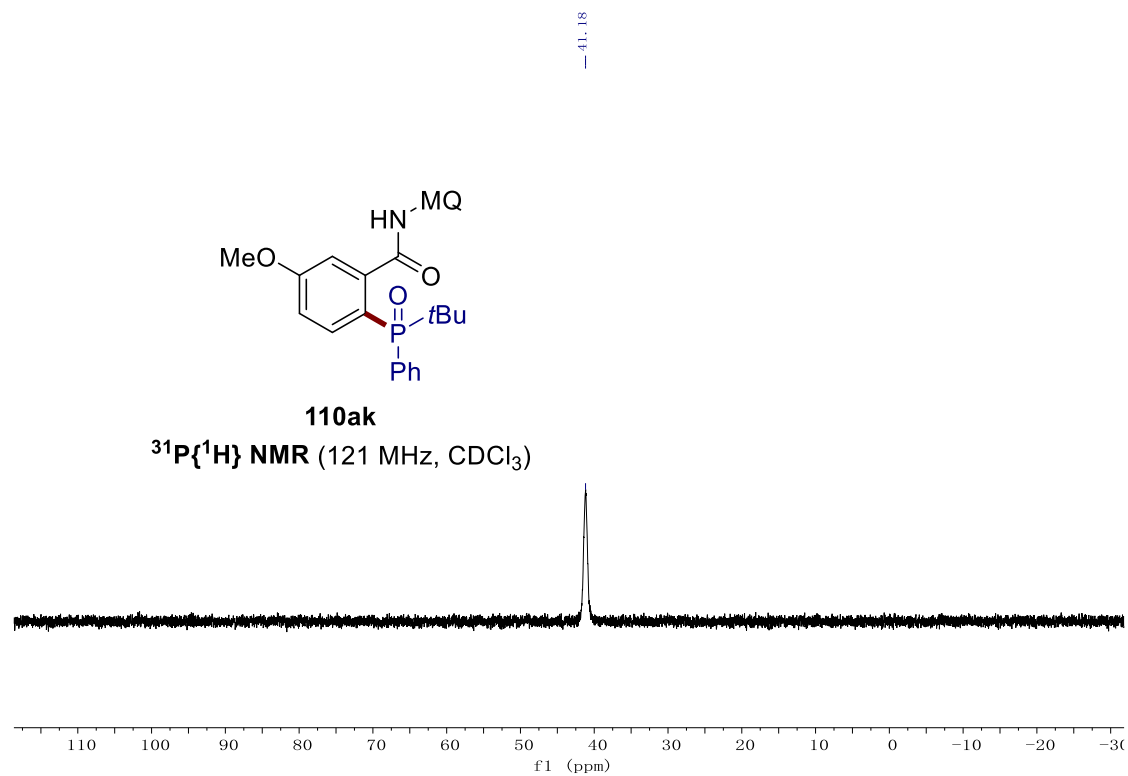
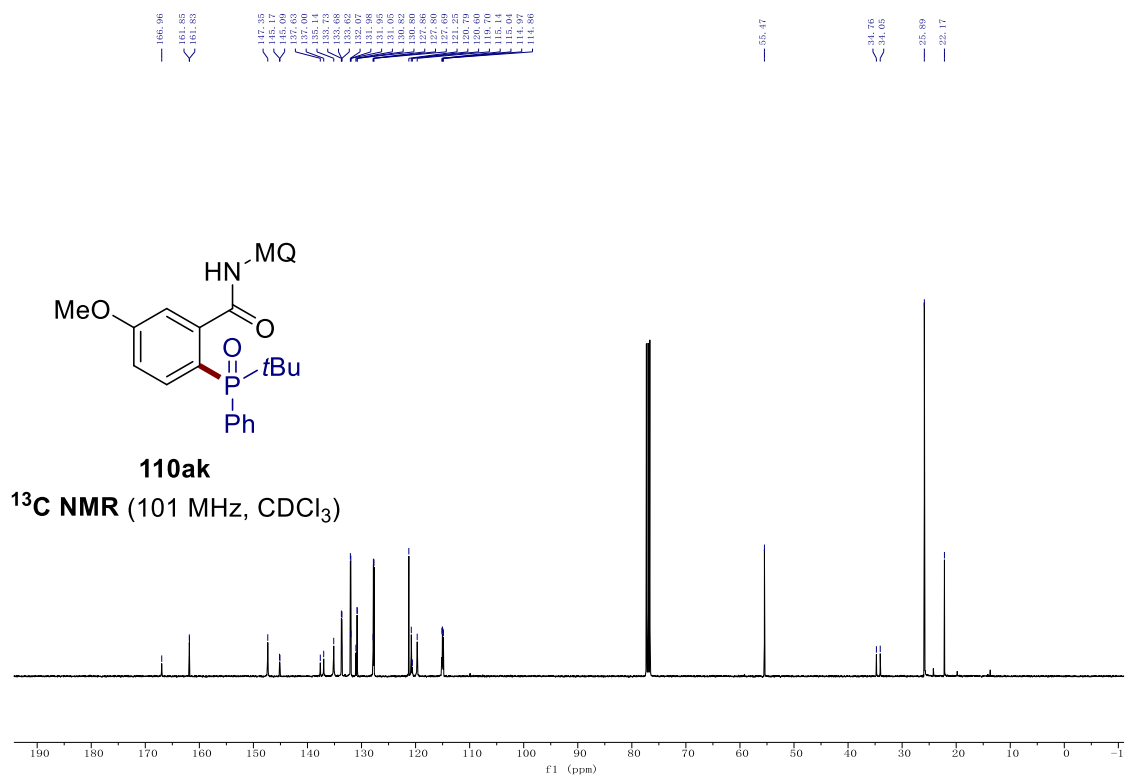
7. NMR Spectra

— 49.06

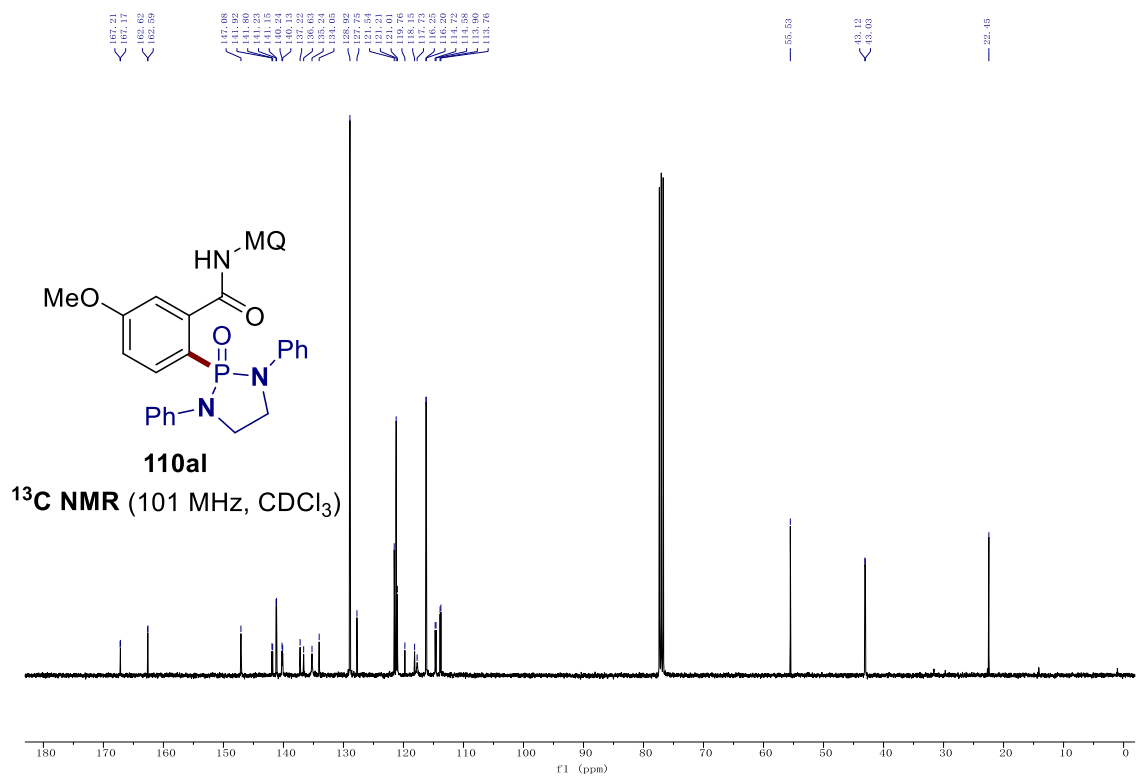
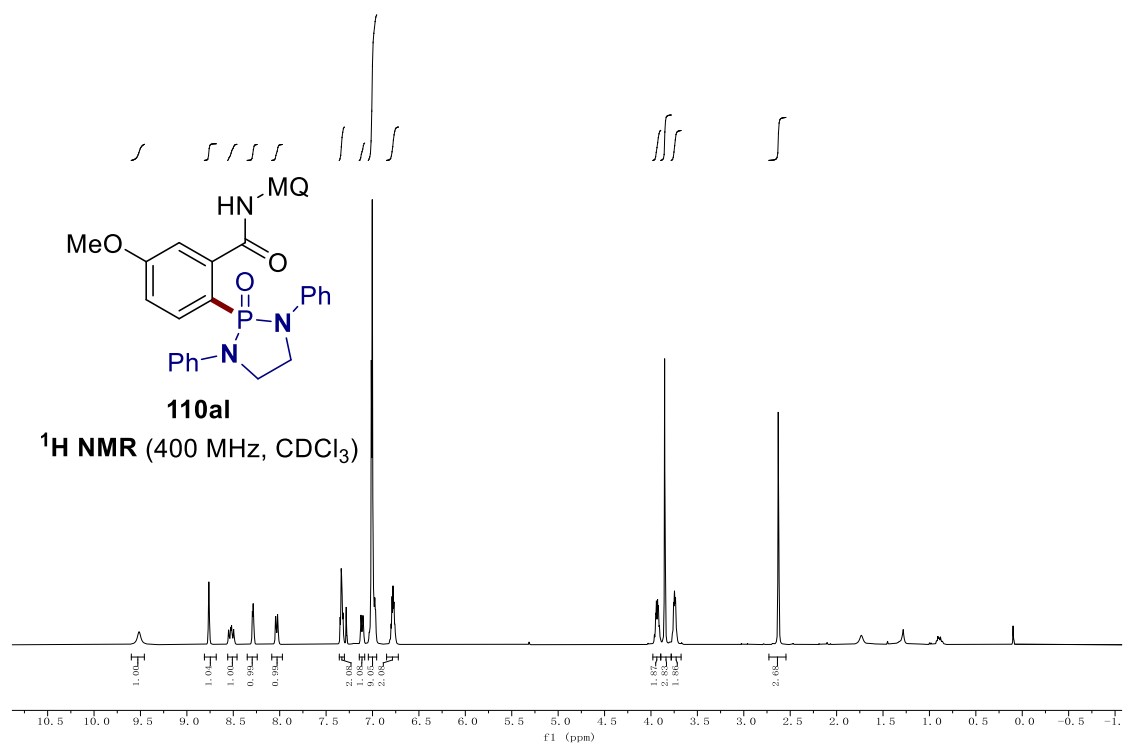


**110aj**  
 $^{31}\text{P}\{^1\text{H}\}$  NMR (162 MHz,  $\text{CDCl}_3$ )

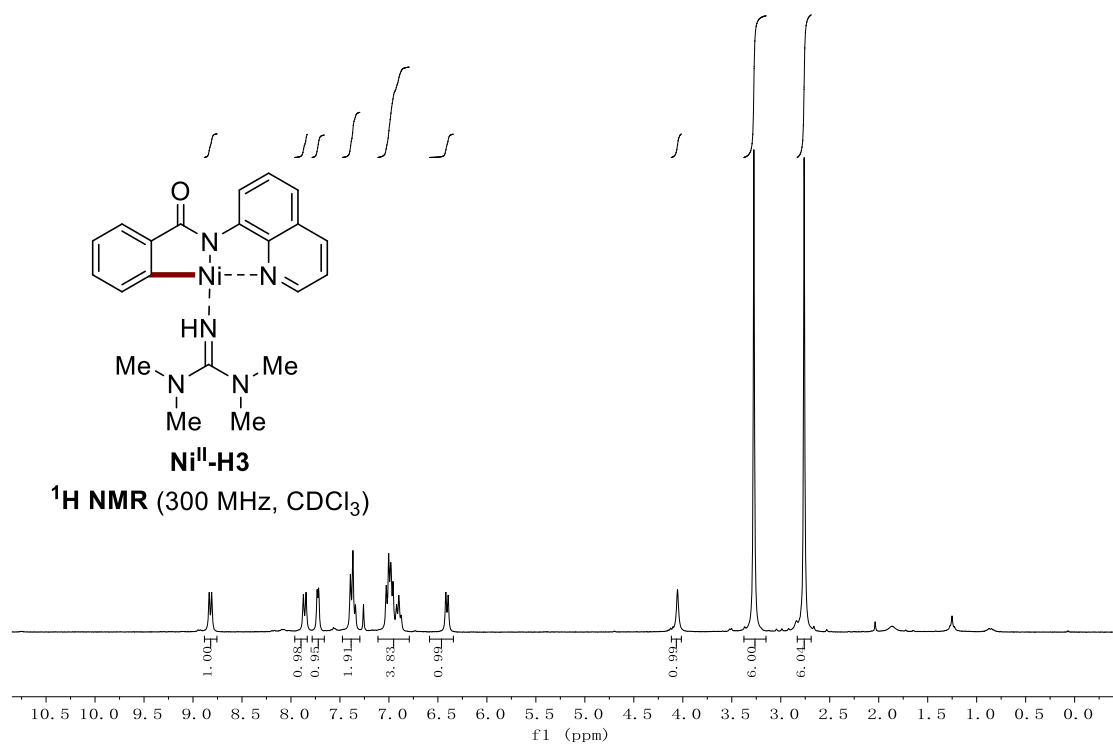
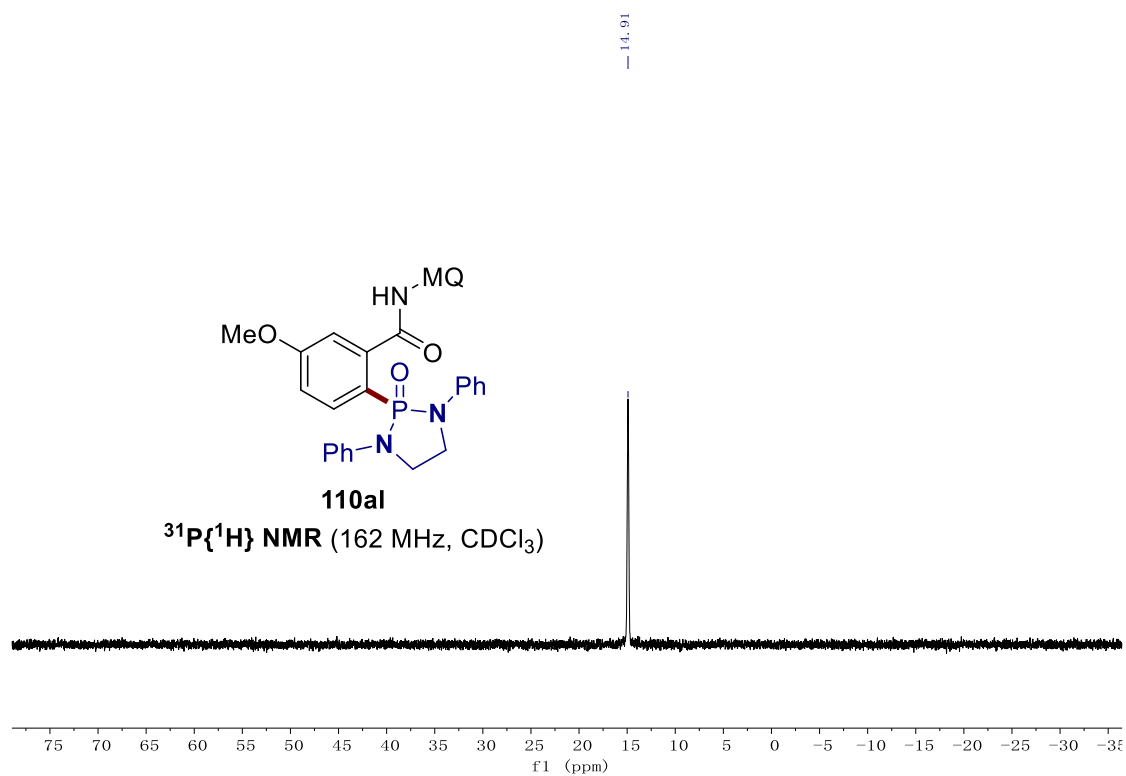




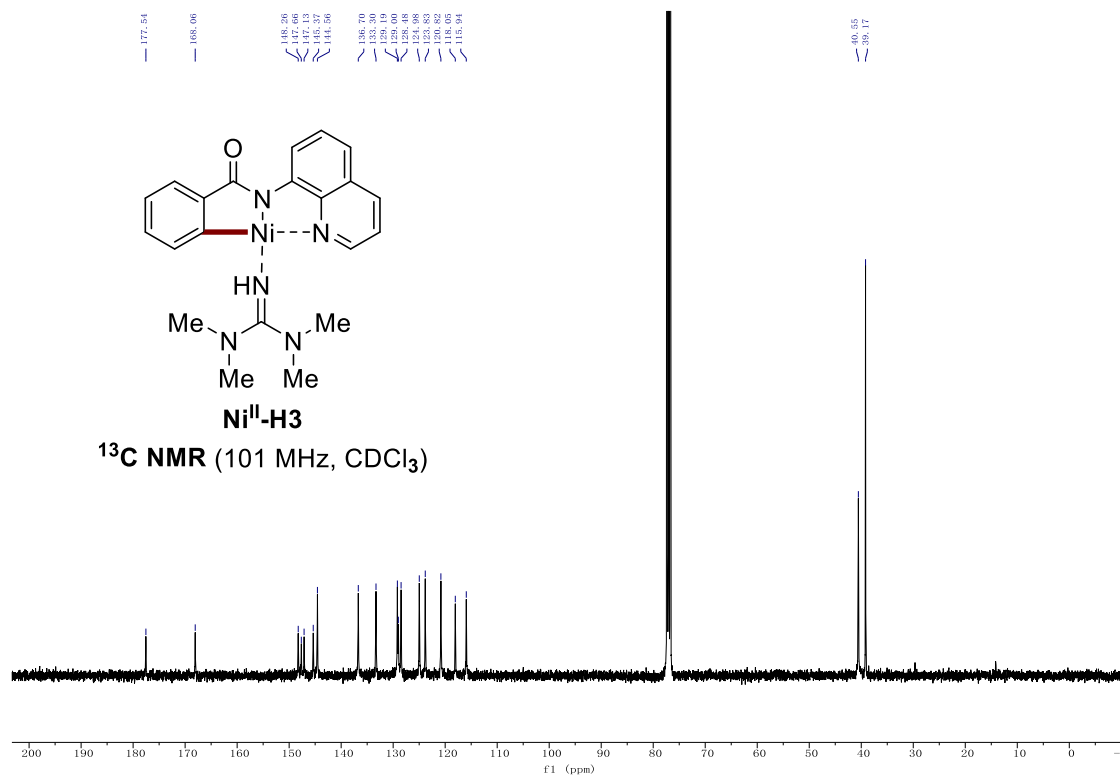
## 7. NMR Spectra







## 7. NMR Spectra



## Acknowledgement

I would like to take this opportunity to express my gratitude to all the people who have supported me during my PhD stay. First and foremost, many thanks go to my doctoral supervisor Prof. Dr. Lutz Ackermann for your countless guidance, valuable advice and constant encouragement. It is a great honor for me to work in this excellent international group.

I would like to thank my second supervisor Prof. Dr. Shoubhik Das. I truly appreciate your help and kind suggestion in chemistry as well as life. I also thank the other members of the examination committee, Prof. Dr. Manuel Alcarazo, Prof. Dr. Dietmar Stalke, Jun.-Prof. Dr. Johannes C. L. Walker, Dr. Michael John.

I am very grateful to have the chance to collaborate with all my co-workers: Dr. Zhixiong Ruan, Dr. Cuiju Zhu, Paul Niklas Ruth, Prof. Dr. Dietmar Stalke, Dr. Ruhuai Mei, Fernando Fumagalli, Dr. Svenja Warratz, Dr. Torben Rogge, Dr. A. Claudia Stückl, Dr. Ramesh C. Samanta, Dr. Nicolas Sauermann, Julia Struwe, Dr. Lianrui Hu, Dr. Antonio Del Vecchio, Dr. Rositha Kuniyil, Dr. Antonis M. Messinis, Zhipeng Lin.

I am thankful for all the people who helped me correct the doctoral thesis: Dr. Cong Tian, Dr. Torben Rogge, Dr. Ramesh C. Samanta, Nikolaos Kaplaneris, Becky Bongsuiru Jei, Dr. Xuefeng Tan, Jun Wu, Long Yang and Zhipeng Lin.

I would also like to thank all the people who have done a lot of favor with my previous publications including correcting manuscripts, giving kind suggestions, and the use of Headspace GC-Analysis, *in situ* NMR, HPLC, etc.: Dr. Torben Rogge, Dr. Hui Wang, Dr. Youai Qiu, Dr. Weiping Liu, Dr. Antonio Del Vecchio, Dr. Yu-Feng Liang, Dr. Wei-Jun Kong, Dr. Cong Tian, Dr. Wei Wang, Alexj Scheremetjew, Maximilian Stangier, Uttam Dhawa and Dr. Tomasz Wdowik.

I really enjoyed the football games and Great Barrier Run with Alexj Scheremetjew, Tjark Meyer, Maximilian Stangier, Dr. Ramesh C. Samanta, Dr. Youai Qiu, Leonardo Massignan, Dr. Wei-Jun Kong, Jun Wu, Dr. Thomas Müller, Dr. Antonis M. Messinis, Dr. João C. A. de Oliveira, Dr. Korkit Korvorapun, Dr. Wei Wang, Zhigao Shen, Long Yang, Ralf Alexander Steinbock, Dr. Elżbieta Gońka.

I am very happy to have a great time in Germany with all my friends. Nice BBQ, rafting, Cuxhaven traveling, Christmas market hiking, Goslar skiing, group parties, various excellent beers, bar experience, and so on, will stay in my memory forever.

Many thanks to Gabriele Keil-Knepel, Bianca Spitalieri, Stefan Beußhausen, Karsten Rauch for creating the great working conditions. I also want to thank the analytical departments of IOBC for their kind support in chemistry. I appreciate the help from Dr. Christopher Golz for the X-ray analysis.

Moreover, I truly appreciate the financial support from China Scholarship Council (CSC) during the last four years in Germany.

Last but not least, words are powerless to express my gratitude to my family for their understanding and constantly support.